Ontogeny and functional adaptation of trabecular bone in the human foot

Jacobus Petrus Paulus Saers

Downing College

PAVE Research Group

Division of Biological Anthropology

Department of Archaeology and Anthropology

University of Cambridge

This dissertation is submitted for the

degree of Doctor of Philosophy

July 2017

UNIVERSITY OF
CAMBRIDGE

Declaration

This dissertation is the result of my own work and includes nothing which is the outcome of work done in collaboration except as declared in the Preface and specified in the text. It is not substantially the same as any that I have submitted, or, is being concurrently submitted for a degree or diploma or other qualification at the University of Cambridge or any other University or similar institution. I further state that no substantial part of my dissertation has already been submitted, or, is being concurrently submitted for any such degree, diploma or other qualification at the University of Cambridge or any other University or similar institution except as declared in the Preface and specified in the text. It does not exceed the prescribed word limit of 80,000 words excluding references and appendices.

Jacobus Saers

July 2017

Summary

Trabecular bone forms the internal scaffolding of most bones, and consists of a microscopic lattice-like structure of interconnected bony struts. Experimental work has demonstrated that trabecular bone adapts its structural rigidity and orientation in response to the strains placed upon the skeleton during life, a concept popularly known as "Wolff's Law" or "bone functional adaptation". Anthropological work has focused on correlating variation in primate trabecular bone to locomotor and masticatory function, to provide a context for the interpretation of fossil morphology. However, intraspecies variation and its underlying mechanisms are still poorly understood. In this thesis, variation in trabecular bone structure is examined in the human foot in four archaeological populations. The aim is to tease apart the factors underlying variation in human trabecular microstructure to determine whether it may be a suitable proxy for inferring terrestrial mobility in past populations.

µCT scanning is used to image the three-dimensional trabecular structure of the talus, calcaneus, and first metatarsal in samples from four archaeological populations. Trabecular structure is quantified in seventeen volumes of interest placed throughout the foot.

Trabecular bone is influenced by a variety of factors including body mass, age, diet, temperature, genetics, sex, and mechanical loading. Before trabecular structure can be used to infer habitual behaviour, the effects of these factors need to be understood and ideally statistically accounted for. Therefore, the effects of variation in bone size and shape, body mass, age, and sex on human trabecular structure are examined in four populations. Significant effects of body mass and age are reported, but little sexual dimorphism was found within populations. Taking these results into account, variation in trabecular structure is compared between archaeological populations that were divided into high and low mobility categories. Results demonstrate that the four populations show similar patterns of trabecular variation throughout the foot, with a signal of terrestrial mobility level superimposed upon it. Terrestrial mobility is associated with greater bone volume fraction and thicker, more widely spaced, and less interconnected trabeculae.

Ontogeny of trabecular bone in the human calcaneus is investigated in two archaeological populations in the final chapter of the thesis. Results indicate that calcaneal trabecular bone adapts predictably to changes in loading associated with phases of gait maturation and increases in body mass. This opens the possibility of using trabecular structure to serve as a proxy of neuromuscular development in juvenile hominins.

This work demonstrates that trabecular bone may serve as a useful proxy of habitual behaviour in hominin fossils and past populations when all contributing factors are carefully considered and ideally statistically controlled for.

Acknowledgements

I am grateful to my supervisor, Jay Stock, without whom this project would not have been possible. I want to thank you for all your help, guidance, advice, and excellent tunage suggestions over the past four years. I came into this PhD knowing little about biological anthropology, let alone trabecular bone. Thank you for introducing me to the world of skeletal biomechanics and for supporting me when I needed it. There has not been a single meeting after which I was not excited and motivated to push on. The breadth and depth of your approach to human evolution and adaptation is unique and truly inspiring.

I want to deeply thank Colin Shaw and Tim Ryan, upon who's hard work many of the methods used in this thesis are built. Thanks to Colin for the energetic discussions in your giant chair, for teaching me how to use the CT scanner, and all your helpful advice. Tim, thank you for hosting me for a month in Pennsylvania, a delicious thanksgiving dinner, and generously scanning all those bones for me. Thank you both for all your advice along the way and for giving me the opportunity to publish my first paper. Between you guys and Jay I could not have asked for a better team of advisors.

I have Andrea Waters-Rist to thank for introducing me to Jay and encouraging me to pursue a PhD. Without her motivation and enthusiasm none of this would have happened.

I want to thank all the staff, post-docs, and graduate students from the Division of Biological Anthropology, and particularly all the members of PAVE who have been around over the past four years. Thanks to Tom, Emma, Danny, Alison, Marielle, Pere, Michelle, Tina, Devin, Sarah-Louise, Michael, Laura, Eóin, Kate, and Steph. We've had so many good times in the office and outside, you guys made coming in every day a real joy.

Thanks to everyone in the ceilidh band for introducing me to a whole new world of folk music. Over 50 gigs, 96 rehearsals, and countless sessions have shown that there is hope even for a rhythmically impaired chump like me. Special thanks to David, Harriet, and Clare with whom I've had so many memorable evenings over the past year.

I greatly appreciate all my friends and family from home who visited me over the years. You often provided some much-needed breaks and I loved every single visit. I am especially grateful to Lonieke for all her support throughout the years. I have met too many awesome people in Cambridge to list. I enjoyed living with everyone at Parkside, Devonshire road, Girton, and Mawson Road. Thanks to Nicky for teaching me all about America, Kyle for being the greatest pub-philosopher in Western Europe, and Eóin for the countless late nights jamming and listening to great tunes.

I am grateful to Terrance Martin at the Illinois State Museum, George Milner at Pennsylvania State University, Heather Lapham at the Center for Archaeological Investigations, Southern Illinois University, Maggie Bellatti and Marta Mirazón-Lahr at the Leverhulme Centre for Human

Evolutionary Studies, University of Cambridge, for providing me access to the skeletal collections under their care.

This PhD would not have been possible without generous financial support from numerous Dutch and British funding bodies and charities. My first year at Cambridge was funded with support from the VSB Fonds, Prins Bernhard Cultuurfonds, Hendrik Müller Vaderlandsch Fonds, and the Fundatie van Renswoude. The Arts and Humanities Research Council (award 1503975) funded my second and third year fees and provided me with the financial means to undertake a month-long trip to Pennsylvania State University. Funding for two conferences in the USA was generously provided by Downing College, the Department of Archaeology, and the School of the Humanities and Social Sciences, University of Cambridge. Further much appreciated financial assistance was provided by the Richard Stapley Trust, the Oon Khye Beng Ch'hia Tsio Scholarship, the Treherne Biological Sciences Scholarship, and the Lundgren Fund.

Finally, I want to thank my family who have always around for advice and encouragement. My parents supported me financially, emotionally, and in more ways than I could list. Hannah was always there for a chat whenever I lost sight of where I was going. Sander provided much needed relaxation during many late nights. Thank you for your unending support, your visits, and always being there. This dissertation is dedicated to them.

Table of Contents

List of figures

List of tables

Chapter 1 - Trabecular bone functional adaptation

Introduction

Trabecular bone is a porous, lattice-like structure of bone found predominantly in the epiphyseal ends of long bones, and other irregular bones such as vertebrae, the ilium, and the calcaneus. The three-dimensional microstructure of trabecular bone is seeing a rapid increase in research due to the increased availability of microtomography scanning and high-throughput computing. Experimental work has provided evidence that trabecular bone adapts rapidly to mechanical loading and may therefore be a useful proxy for inferring past habitual behaviour from skeletal morphology. Anthropological research has focused on correlating variation trabecular bone structure to locomotor mode in primates. The goal of such studies is to find anatomical correlates of behaviour and to provide a context for the interpretation of fossil morphology. Relatively little attention has been paid to within species variation. Before behaviour can be inferred from fossil morphology, the range of within species variation and the mechanisms underlying this variation must be understood. This thesis focuses on variation in trabecular bone structure in the human foot in four archaeological populations. The aim is to tease apart the factors underlying variation in human trabecular microstructure to determine whether it may be useful as a proxy for inferring behaviour in the past. The calcaneus, talus, and first metatarsal were chosen for their distinctive roles during bipedal gait. This is the first study to thoroughly examine variation in human trabecular bone and systematically assesses the factors underlying this variation.

Bone functional adaptation

Adaptation is defined as "*the evolutionary process whereby an organism becomes fitted to its environment, or a structure or habit fitted for some special environment or activity"* (Lawrence, 1995). Adaptation encompasses all aspects of the fit between an organism and its environment, both during an individual's life (phenotypic plasticity) or over generations by genetic adaptation through natural selection. Humans show a high degree of phenotypic variation, yet a relatively low degree of genetic diversity (Li et al., 2008). Phenotypic plasticity has been argued to have played a key role in the rapid dispersal of *Homo sapiens*, allowing humans to survive in a diverse range of climates and habitats (Wells and Stock, 2007). Wells and Stock (2007) modelled human adaptation as consisting of physiological plasticity, and cultural and behavioural buffering, leaving the residual stresses to be accommodated through natural selection. Famous examples of phenotypic adaptation to the environment are Bergmann's (Bergmann, 1847) and Allen's (Allen, 1877) rule. Bergmann's rule states that within geographically wide-ranging species, the larger bodied variants are found in the colder regions while smaller bodied variants are found in the warmer regions. Allen's rule states that individuals in cold climates possess shorter extremities than individuals in warmer climates. Both rules are products of thermoregulatory adaptations, reducing surface area to body volume ratio in colder environments to conserve heat, whilst increasing the ration in warmer climates to dispense of it more

quickly (Ruff, 1994; Kurki et al., 2008; Stock, 2009; Davies, 2012). The environment is not the only determinant of an individual's skeletal phenotype. Bone shape and size are highly variable and the observed phenotype is a combination of a number of interacting variables including: habitual loading (Trinkaus et al., 1994; Shaw and Stock, 2009 a; b; Warden et al., 2014), climate (Ruff, 1994; Holliday, 1997; Kurki et al., 2008; Stock, 2009; Davies, 2012), nutrition (Cowgill, 2010), health (Maat, 2005), and (epi-)genetics (Badyaev and Martin, 2000; Robling and Turner, 2002; Judex et al., 2004; Dubois et al., 2007; Morris et al., 2012; Wallace et al., 2012; 2017). Increased strain under mechanical loading placed upon a bone, for example through increased body mass or regular activity, results in the formation of new bone which stiffens the bone reducing the strain to its original level. Habitual inactivity on the other hand, causes bone to be resorbed which weakens the bone until it reaches the normalized strain levels (Frost, 2003; Christen et al., 2014).

The ability of bone to perform effectively under its function-specific loadings depends on the bone's material properties and its spatial arrangement (Currey, 2003). The term 'bone functional adaptation' is used to describe the general premise that bone tissue and structure adapts to the mechanical forces it experiences by altering bone shape and size (Ruff 2008). The mechanisms that control where and how bone cells are activated are complex and not fully understood (Wallace et al., 2017). Four types of bone cells are important in this process. Osteoblasts are cells that produce bone by synthesizing and calcifying collagen. Osteoclasts are cells that degrade bone matrix. Most bone cells are osteocytes and bone lining cells. Osteocytes lie within the bone matrix which in turn is surrounded by bone lining cells on the surface. Both osteocytes and lining cells derive from osteoblasts that have stopped producing bone matrix. When an osteoblast stops working it is replaced and buried by a new osteoblast, and turns into an osteocyte. When osteoblast recruitment has stopped, the last remaining osteoblasts flatten out into lining cells after they have stopped producing matrix (Burger and Klein-Nulend, 1999; Huiskes et al., 2000). Osteocytes are post-mitotic and imbedded in hard tissue, making them difficult to study. However, multiple studies have observed that mechanical loading activates several cellular processes in osteocytes including gene activation, growth factor production, and matrix synthesis (Inaoka et al., 1995; Lean et al., 1995; Burger and Klein-Nulend, 1999; Wallace et al., 2017). Osteocytes remain connected with bone surface cells and neighbouring osteocytes via a network of lacunae and canaliculi. This network of interconnected cells, filled with interstitial fluid is an ideal structure for the detection of mechanical inadequacies in the bone. One method through which bone adapts to mechanical forces is the strain-driven motion of interstitial fluid through the canaliculi and along the osteocytes which is subsequently sensed and transducted by the osteocytes (Burger and Klein-Nulend, 1999; Huiskes et al., 2000; Currey, 2002; Knothe Tate, 2003; Wallace et al., 2017). Strain causes the interstitial fluid to be squeezed through the small non-mineralized matrix surrounding osteocytes, producing shear stress at the cell membrane. This signals the osteocytes to increase their activities and recruit osteoblasts. When strains are normalized a balanced state is reached in which bone formation and removal are roughly equal, although a state of equilibrium is

never reached (Christen et al., 2014). When bone is disused the osteoclasts are no longer suppressed and start removing bone until a state of balance has yet again been established (Burger and Klein-Nulend, 1999).

Bone functional adaptation in anthropology

The principles of bone functional adaptation have been applied to the archaeological and fossil record mainly by studying variation in the cross-sectional shape of long bone diaphyses. Cross-sectional geometric analysis has been used by anthropologists to investigate long-term evolutionary trends (Churchill, 1994; Pearson, 1997; Trinkaus and Ruff, 2012) as well as differences in habitual activity within and between populations (Ruff and Hayes, 1983; Shaw and Stock, 2009 b; Sparacello et al., 2011; Stock et al., 2011). This type of research is used most often to distinguish between subsistence strategies (Ruff et al., 1984; Bridges, 1989), sexual division of labour (Pomeroy and Zakrzewski, 2009; Villotte et al., 2010), mobility levels (Ruff and Hayes, 1983; Holt, 2003; Shaw and Stock, 2013), and environmental contexts (Ruff, 1994; Stock and Pfeiffer, 2001; Marchi et al., 2006; Sparacello et al., 2011).

The relationships between bone morphology and habitual activities are not entirely straightforward (Lieberman et al., 2004; Wallace et al., 2014). Extracting relevant behavioural data from cortical bone morphology is complicated, as cross-sectional morphology is the combined result of not just habitual activity (Haapasalo et al., 2000; Wallace et al., 2007; Shaw and Stock, 2009a, 2009b; Wallace et al., 2017), but also diet (Cowgill, 2010), Climate (Pearson, 2000; Davies, 2012), environment (Marchi et al., 2006; Sparacello and Marchi, 2008), and (epi-) genetics (Badyaev and Martin, 2000; Judex et al., 2004; Dubois et al., 2007; Morris et al., 2012; Wallace et al., 2012). The remodeling rate of bone is high during growth but following this period the skeletal response is severely reduced (Forwood and Burr, 1993; Wallace et al., 2017). However, remodeling in mature bone does continue over a longer time frame with the possibility of cumulative long-term effects (Pearson and Lieberman, 2004). Despite the many factors influencing bone morphology, the study of cross-sectional geometry has led to significant insights into the habitual activities of past human populations that would otherwise be undetectable in the archaeological and fossil records (Ruff, 2008). The analysis of trabecular bone is a relatively new approach that is increasingly becoming available to researchers through computation improvements. Trabecular bone has different geometric, biological, and mechanical properties which may be able to provide a higher interpretive resolution reflective of physical activity during life when combined with analyses of diaphyseal cross-sectional geometry.

Trabecular bone

The study of the three-dimensional structure of trabecular bone has only recently become feasible due to the availability of high-resolution micro-CT scanning and high-throughput computing. Trabecular bone is a complex, porous three-dimensional structure consisting of interconnected bony struts called trabeculae, which is found inside joints across the skeleton. Trabecular bone combines strength and

stiffness with minimal weight for optimal load transfer, following the rules of mathematical design (Huiskes et al., 2000; Ruimerman et al., 2005; Reznikov et al., 2016). Due to their different structural organization and material composition, the mechanical properties of cortical and trabecular bone differ substantially. Cortical bone is stiffer than trabecular bone, being able to withstand greater stress, but substantially less strain before failure (Frankel and Nording, 2012). Trabeculae are thought to be oriented in line with principal loads, making them efficient at load bearing, a concept known as *Wolff's law* (Wolff, 1867; Gefen and Seliktar, 2004) or bone functional adaptation (Ruff, 2008). The principles of Wolff's law can be observed in the human foot where trabeculae are aligned to the principal directions of mechanical stress (Figure 1.1). This non-random structural optimization is accomplished through the removal of bone in unstrained areas and deposition of bone in strained areas (Currey, 1984, 2002; Rubin et al., 2002).

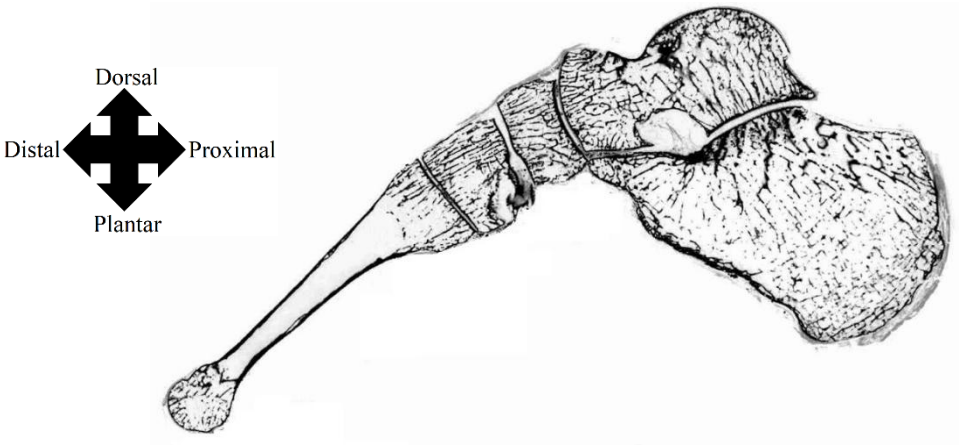

Figure 1.1. Sagittal cross-section of a mummified human foot demonstrating the alignment of the trabecular structure to principal loading directions.

The annual turnover rate of cortical bone in adult humans is about 2-3%, whereas the rate is approximately 25% in trabecular bone (Eriksen, 1986), although these percentages vary considerably based on anatomical location and local loading conditions (Menkes et al., 1993; Parfitt, 2002). Due to its complex structure and high remodeling rate, trabecular bone may be more dynamic in its response to mechanical loading than cortical bone (Huiskes et al., 2000; Ryan and Krovitz, 2006; Barak et al., 2011; Ryan and Shaw, 2012). Experimental and modelling data suggest a strong correlation between habitual mechanical loading and trabecular architectural properties, total bone volume, and elastic, yield, and strength properties (Odgaard et al., 1997; Huiskes et al., 2000; Pontzer et al., 2006; Fajardo et al., 2007; Rincón-Kohli and Zysset, 2009; Barak et al., 2011; Lazenby et al., 2011a; Ryan and Shaw, 2012; Zeininger, 2013; Tsegai et al., 2013; Saers et al., 2016). Theoretically, trabecular bone should be an effective proxy of behaviour in fossils and for distinguishing locomotor correlates from phylogenetic baggage (Macchiarelli et al., 1999; Fajardo and Müller, 2001; Ryan and Shaw, 2012; Zeininger, 2013; Skinner et al., 2015). External bone morphology can arguably be unused retentions of ancestral traits that are no longer functional and provide a false indication of habitual behaviour (Gould and Lewontin, 1979; Ward, 2002). The internal trabecular structure of bone may not be as

strictly bound by a genetic *bauplan* as the external features. Combined with its sensitivity to mechanical loading and high remodeling rates, the analysis of trabecular bone functional adaptation may provide a dynamic source of data reflecting the mechanical forces placed upon bones during life.

The three-dimensional structure of trabecular bone is often described using several trabecular structural properties which are summarized in Table 1.1.

Table 1.1. Definitions of trabecular structural properties discussed in this thesis.

Measurement	**Abv.**	**Units**	**Description**
Bone volume fraction	BV/TV	%	Ratio of bone volume to total volume of interest
Degree of anisotropy	DA	-	Extent to which trabeculae are similarly oriented
Trabecular thickness	Tb.Th	mm	Average trabecular strut thickness
Trabecular spacing	Tb.Sp	mm	Average distance between struts
Connectivity density	Conn.D	mm^{-3}	Number of interconnected trabeculae per volume

Trabecular structural properties vary within and between skeletal elements (Skedros and Baucom, 2007; Rincón-Kohli and Zysset, 2009). Trabecular bone structure is anisotropic and therefore its strength and stiffness depend on loading direction. Trabecular bone stiffness also depends on the type of loading it is subjected to, it is much stiffer in compression than tension, and least stiff in shear (Keaveny et al., 2001; Frankel and Nording, 2012). Combinations of structural properties and bone volume have been shown to accurately reflect the true elastic, yield, and strength properties of trabecular bone (Ulrich et al., 1999; Keaveny et al., 2001; Homminga et al., 2003; Rincón-Kohli and Zysset, 2009; Maquer et al., 2015). Rincón-Kohli and Zysset (2009) quantified the morphological and multi-axial strength properties of human trabecular bone cores taken from different skeletal sites. They used bone core samples aligned to the primary material direction and applied uni-axial traction, torsion, uni-axial compression, and three multi-axial compression tests. Afterwards, trabecular properties were correlated to the experimentally derived elastic, yield, and strength properties. They found that roughly 91% of the observed variation in measured mechanical properties could be explained by a composite measure of bone volume fraction and trabecular architectural properties. Maquer et al. (2015) found that BV/TV explained roughly 87% of variation in elastic properties of trabecular bone from multiple individuals and anatomical locations. They found that a combination of degree of anisotropy with BV/TV could predict 97% of bone elastic properties calculated using finite element analysis. Adding other properties such as trabecular thickness or connectivity created only marginal improvements (<1%). It is important to note that these structural properties are only an approximation of actual mechanical properties. Structural properties are only averages of bone properties within a selected volume of interest, and do not precisely reflect the geometry of the actual trabecular structure. Studies using nanoindentation to measure the tissue elastic modulus have demonstrated that the material composition of the trabecular bone varies within and between individuals (Zysset et al., 1999). Measures of trabecular structural properties are unaffected by subtle

damage within trabeculae and microcracks caused by material overloading. Several studies have demonstrated that this small damage significantly reduces the apparent modulus of trabecular bone (Zysset and Curnier, 1996; Kopperdahl et al., 2000). After many cyclic loadings, fatigue and creep will also decrease trabecular bone strength through the accumulation of microdamage and deformation, respectively. The exact creep and fatigue characteristics of trabecular bone are unknown as bone is actively repaired by remodeling (Keaveny et al., 2001). It should therefore be kept in mind that although trabecular bone structural properties are highly correlated to experimentally determined mechanical properties, they are only approximations of actual bone strength.

Experiments have demonstrated that variation in trabecular properties and orientation corresponds to variation in loading conditions within and amongst several animal species. Experimental studies on the knees of guinea fowl (Pontzer et al., 2006) and the tarsals of sheep (Barak et al., 2011) have demonstrated the functional response of trabecular bone architecture to the magnitude and the direction of mechanical loads experienced. Barak and colleagues (2011) studied three groups of sheep: one group was exercised daily on a horizontal treadmill, and one group was exercised daily on an inclined treadmill which caused tarsal joint extension by 3–4.5° during peak loading. Additionally, the tarsal joint angle of the incline group was maintained in a more extended posture throughout the day by placing elevated platform shoes on their forelimbs. A third control group did not run but wore platform shoes throughout the day. The sheep were obtained at the age of 3 weeks, and were exercised 15 minutes a day, 6 days a week, for 34 days. The exercised groups displayed significant differences in trabecular structural properties compared to the non-exercised groups, including significantly higher bone volume fraction (BV/TV), trabecular thickness (Tb.Th), trabecular number (Tb.N), lower trabecular spacing (Tb.Sp), and less rod-shaped trabeculae (higher structure model index, SMI). The orientation of trabeculae was 2.7 to 4.3° more obtuse in the incline group versus the horizontal group**.** The non-exercised control group did not show any change in directionality of trabecular bone (Barak et al., 2011). This suggests that the magnitude of forces placed upon the trabecular bone is an important factor in remodeling, and that trabecular bone only remodels when subjected to strains above a certain threshold. A similar study was conducted by Pontzer and colleagues on guinea fowl where one group ran on a horizontal treadmill and the other on a 20° inclined treadmill, and found similar differences in trabecular orientation within the knee (Pontzer et al., 2006).

Studies on inter-specific variation attempting to distinguish between locomotor modes of primates by examining trabecular bone architecture have produced mixed results depending on experimental design (Fajardo and Müller, 2001; Maga et al., 2006; Fajardo et al., 2007; Griffin et al., 2010; Ryan and Walker, 2010; Lazenby et al., 2011 a; Saparin et al., 2011; Shaw and Ryan, 2012; Ryan and Shaw, 2012, 2013; Tsegai et al., 2013; Scherf et al., 2013). Significant variation in trabecular structures between primates with different locomotor modes were found by Ryan and Shaw (2012). They used multivariate discriminant function analysis to compare suites of trabecular architectural properties rather than individual properties, which allowed them to accurately distinguish between locomotor

groups. Scherf et al. (2013) also adopted this approach in their study of the proximal humerus of humans, orangutans and chimpanzees. Principal component analysis distinguished between the three taxa and enabled a structural characterization of the humeral trabecular bone of each species. The authors attributed differences in trabecular organization to variation in loading patterns associated with different activity patterns. Maga et al. (2006) comapred the trabecular structure of the calcanei of a small sample of 2 humans, 2 chimpanzees, 1 gorilla and 1 orangutan. They found large differences between humans and the other primates, but were not able to determine the differences statistically due to low sample size. The most striking differences were in DA, conforming to the expectation that more humans load their calcanei in more uniform ways compared to the other primates in the sample (Maga et al., 2006). Griffin and colleagues (2010 b) investigated the presence of a locomotor signal in the metatarsals and phalanges of extant hominins. They observed that trabecular structures within the metatarsal head of humans were more anisotropic compared to the other primates. Differences were most prominent in the dorsal aspect of the metatarsal head, which they argues may be related to a propulsive function of the forefoot that is unique to humans (Griffin et al., 2010).

Several researchers have examined the trabecular bone morphology of fossil hominins compared to modern humans and other extant primates. Barak et al. (2013) investigated trabecular structural organization of the distal tibia to assess whether *Australopithecus africanus* walked with an extended knee like modern humans or a flexed knee like chimpanzees. They observed that human ankles were 10° more plantarflexed during midstance compared to chimpanzees. Results suggested that the trabecular orientation of the *Australopithecus* was similar to that of humans but not of chimpanzees. Trabecular structural properties were different in all three groups, with *Australopithecus* falling mostly between the values of humans and chimpanzees. Earlier work has demonstrated that the lateral part of the tibial distal articular surface bears the highest loads (Kimizuka et al., 1980). Barak and colleagues (2013) found this also to be reflected in the trabecular architecture of all three species, and suggest that this may be a primitive trait. DeSilva and Devlin (2012) compared the trabecular organization of human tali to other primates and fossil australopiths. They did not manage to find a specific locomotor signature between species and argue that talar trabecular structure is highly conservative. Alternatively, the lack of a clear locomotor signal may have been a consequence of their study design. The authors examined trabecular bone from four arbitrarily divided quadrants, possibly averaging out any variation in the process. They also did not investigate trabecular orientation. Su and colleagues (2013) investigated the talar trabecular bone orientation of humans, chimpanzees, gorillas, orang-utans and the KNM-ER 1464 Early Pleistocene hominin (typically assigned to *Paranthropus boisei*). They examined nine volumes of interest taken just below the talar trochlea, where a functional loading signal might be more readily indentified. The authors found that humans have more anisotropic trabeculae and higher inter regional variation in anisotropy than the comparative species. This conforms to expectations that humans load their tali in a uniform direction during bipedal terrestrial locomotion whereas other apes load their tali in more variable directions by combining terrestrial and

arboreal mobility. The fossil talus of KNM-ER 1464 showed a mix of similarities to both humans and non-human apes in different locations, conform to the current consensus that although habitually bipedal, its locomotion was likely different than that of modern humans and included a possible arboreal component. Macchiarelli and colleagues (1999) studied the pelvis of South African australopiths compared to humans and primates and also came to the conclusion that *Australopithecus* falls somewhere between modern humans and extant apes in pelvic trabecular morphology.

Numerous alleles have been associated with variation in trabecular structure and the norms of reaction to mechanical loading (Robling et al., 2003, 2007; Judex et al., 2004; Kesavan et al., 2006; Wallace et al., 2012, 2017). Growth must be canalized and regulated to a degree in order to ensure that normal development can proceed regardless of environmental conditions (Badyaev and Martin, 2000). As a result, many components of body size, shape, and bone morphology are genetically canalized to some extent (Lovejoy et al., 2003; Dubois et al., 2007; Wells and Stock, 2007, 2011; Morris et al., 2012; Wallace et al., 2012). Cunningham and Black (2009) found similar trabecular structures in the ilium of neonates and adults that were previously thought to be adaptive to bipedal locomotion. They argue that the observed trabecular patterning in the ilium may be indicative of a predetermined template upon which functional locomotor influences are superimposed at a later age. It has been suggested that certain genes control site-specific bone distribution (Turner et al., 2000; Judex et al., 2004). Turner et al. (2000) compared the cortical and trabecular bone structures in two strains of inbred mice in the femoral midshaft, femoral neck, and the lumber vertebrae. The C3H/HeJ group of mice are associated with high cortical bone strength, but possessed low trabecular bone strength compared to B6 mice. The lack of trabecular strengthening in the C3H strain may be caused by site specific genetic factors, but it may also be that the increased cortical bone buffers strains reducing the need for a strong trabecular structure. However, no correlation was found between cortical thickness and vertebral strength. This research does demonstrate that the observation of greater femoral bone strength does not imply greater bone strength across the entire skeleton. Judex et al. (2004) further examined the site specific effects of genes on cortical and trabecular bone structure in three distinct strains of mice who had been previously labeled low, medium, and high BMD based on whole bone density. Their results indicate that genetic control of bone structure is highly site-specific. Studies using exogenous limb loading have demonstrated that some inbred mouse strains require more diaphyseal deformation to prompt osteogenesis, and show lower increases with deformation (Akhter et al., 1998; Robling and Turner, 2002; Kesavan et al., 2005). Over eighty percent of genetic diversity in humans in found within populations (Li et al., 2008), and there is little evidence that alleles affecting bone mechano-responsiveness are unequally distributed between populations (Styrkarsdottir et al., 2010). Thus, there is little reason to believe that analyses that test differences in bone structure between large enough samples of populations should be biased by genetic factors (Wallace et al., 2017). However, recent research using outbred mice suggests that differences in the norms of reaction to loading may be found in separate populations (Wallace et al., 2015).

The effects of diet on trabecular bone structure are not well known. Jatkar et al. (2016) compared cortical and trabecular bone of mice fed for 15 weeks with a high-fat, high fructose, or control diets. They found that the high-fat diet increased osteoclastogenesis and leptin levels, and significantly decreased trabecular bone volume fraction and cortical thickness compared to the other two diets. Fructose consumption did not affect bone or fat mass, however, it did singificantly compromise bone stiffness (Jatkar et al., 2016). Minimal differences were found in body mass between the three categories of mice only at the end of the 15 week period. High-protein diets are also thought to be detrimental to bone mass. The effects of protein intake on bone are dose-dependent, and also depend on calcium intake and the intake of Vitamin D (Agarwal, 2007). Mixed results regarding the relationship between calcium intake and bone fragility are found in the clinical literature. Calcium supplementation has been demonstrated to be ineffective in preventing bone loss in older women (Elders et al., 1994), and in preventing fractures (Feskanich et al., 1994), or even promoting fractures (Abelow et al., 1992).

The effects of temperature on trabecular bone during growth and development are not well understood, but cold dwelling humans also have been demonstrated to possess lower cortical thickness than those from warmer environments (Wallace et al., 2014; Devlin et al., 2016). Devlin et al. (2016) tested the hypothesis that trabecular bone mass acquisition would reduce in groups of growing mice housed in habitats at different temperatures with ad libitum access to food and water. They found mice housed at 66-72 °F showed 43-66% lower BV/TV and 35-46% lower Tb.Th than mice held at 78 °F. These results indicate that temperature has a significant effect on bone structure, despite unrestricted access to energy and water.

Overall, the studies described here suggest that trabecular bone dynamically adjusts and realigns itself in relation to changes in peak loading direction of mechanical stress. While the effects of environmental variables such as climate, diet, health, age, and (epi-) genetics on cortical bone variation are relatively well studied, this is not yet the case for trabecular bone. Trabecular bone structure is clearly not exclusively shaped by mechanical loading. However, its apparent responsiveness to loading combined with its rapid remodeling rate and complex structure theoretically makes trabecular bone a suitable proxy for inferring behaviour in fossil and archaeological samples when all factors are carefully considered.

Trabecular bone ontogeny

Bone growth occurs via the transformation of growth plate cartilage into bone through a series of cell and matrix changes (Byers et al., 2000; Parfitt et al., 2000; Burr and Organ, 2017). The transformation from growth plate cartilage to trabecular bone is similar amongst mammals, indicating a highly conserved process (Frost and Jee, 1994 a; Byers et al., 2000). This process sets up a basic trabecular structure which is later modified through biological and mechanical factors (Ryan et al., 2017). Byers et al. (2000) found that BV/TV and Tb.Th increased and trabecular number decreased with age, and

that trabecular structure changed most rapidly during the first year of life. Frost and Jee (1994 b) argue that the effects of mechanical usage during this period of rapid bone growth explain many of the features observed during the ossification process. They propose a model which states that mechanical strain is the controlling mechanism for endochondral ossification, in which the underloaded elements of the dense bone structure during the first years of life are removed and bone is added in strained areas, resulting in a mechanically adapted state (Frost and Jee, 1994 b). This model correctly predicts observations of bone loss at early stages of ontogeny, and explains it as the result of the removal of redundant material based on mechanical loading. Most work on trabecular bone ontogeny has been performed on a range of mammal species (Nafei et al., 2000; Tanck et al., 2001; Wolschrijn and Weijs, 2004). In a study on pig vertebrae and tibiae Tanck et al. (2001) found that BV/TV and anisotropy increase with age and body mass, with a time-lag between increases in bone mass and anisotropy. They argue that bone mass is added first, and subsequently refined into an efficiently oriented structure. This process was also found in two studies of human trabecular ontogeny (Ryan and Krovitz, 2006; Gosman and Ketcham, 2009). Ryan and Krovitz (2006) examined femoral trabecular bone properties in humans. The authors analysed the trabecular structure of the femoral head of 15 children aged between 6 months and 3 years. The individuals belonged to a group of village agriculturalists from the Norris Farms #36 site from the Illinois River Valley, USA, dated to 1300AD. Gosman and Ketcham (2009) studied the proximal tibia of subadults from an archaeological skeletal sample from Sunwatch Village, also an agriculturalist site from the Late Prehistoric Ohio Valley. Both studies found similar patterns in the proximal tibia and the femoral head. At birth, trabecular architecture is dense and constructed of numerous small anisotropic trabeculae. During the first year of life bone volume, anisotropy, and trabecular number decrease. Trabecular bone is subsequently reorganized through biological and mechanical factors resulting in fewer, thicker, and more complexly organized systems of trabeculae (Ryan and Krovitz, 2006; Gosman and Ketcham, 2009). The results from studies on humans and other animals suggest a similarity in the developmental process of trabecular bone across species and anatomical sites. Primary trabecular bone is deposited dense and uniformly oriented across studies. However, these initial structures then appear to remodel rapidly into diverging morphologies under the influence of mechanical loading.

Allometry

Body size is a vital aspect of an animal's biology and it has important functional implications for an organism. If an organism scales isometrically, a two-fold increase length will result in a four-fold increase in surface area, and an eight-fold increase in mass and volume. Its body needs to support eight times more mass with bone and muscle strength that has only increased four times, creating a mismatch between scaling and physical demands. A scaling relationship is called allometric when traits scale in any other way than the above described isometry.

Research has demonstrated that trabecular properties scale to increases in body size in different ways (Swartz et al., 1998; Doube et al., 2011; Ryan and Shaw, 2013). Trabecular thickness scales negatively

or not at all with body size, thus trabeculae are relatively larger in small bodied taxa compared to larger ones (Fajardo and Müller, 2001). Smaller bodied taxa also have relatively fewer trabeculae, and they have a larger percentage of trabeculae that connect to cortical bone instead of other trabeculae (Swartz et al., 1998). Swartz and colleagues (1998) calculated trabecular lengths and diameters using cross-sections of humeral head trabecular bone of mammals ranging in size between 40000 and 0.004kg and found a strong negative allometry across the sample. However, in a sample containing only bats, Swartz and colleagues (1998) found an isometric scaling relationship between trabecular thickness and body size. This raised the possibility of a phylogenetic effect on this relationship or different relationships between trabecular structure and animals of different body sizes. The relationship between body mass and trabecular properties was further investigated recently using three-dimensional µCT scanning (Doube et al., 2011; Ryan and Shaw, 2013). Ryan and Shaw (2013) investigated scaling relationships in the humerus and the femur of a group of 34 genera of primates covering a range of body sizes between 0.06 and 230kg. The authors found that BV/TV, Tb.Th, and Tb.Sp. increased with body size whereas the ratio of bone surface area to volume decreased. Tb.N, DA, and Conn.D scaled inversely with body size. They found that most of these variables scaled with significant negative allometry except bone surface area to volume ratio which scaled with positive allometry. A slight positive relationship between BV/TV and body size was found in primates by Ryan and Shaw (2013) and in mammals and birds by Doube et al. (2011). This relationship approaches isometry but still significantly deviates from it. There are several possible avenues by which trabecular bone mass can increase with body size, such as by simply increasing trabecular thickness or number. Ryan and Shaw (2013) noted that larger primates possess absolutely larger and more widely spaced trabeculae but that they are relatively thinner and more closely packed when accounting for differences in body size. It thus appears that increased BV/TV with body size is reached by a combination of increased Tb.Th, Conn.D, and Tb.N. Theoretically the most efficient way of reducing strain would be to just increase Tb.Th, however trabecular thickness is constrained by osteocyte function. Osteocytes can only function at a distance of 0.230mm away from the bone surface (Lozupone and Favia, 1990). This constrains the maximum width of trabeculae to twice this size: 0.460mm. Shaw and Ryan (2013) suggest that this limitation to Tb.Th forces larger animals to compensate for the increased loading through other means such as cortical bone adaptation, and different postures and gait speeds.

Aims and structure of the thesis

Interest is rising in using trabecular structure as a potential proxy for inferring behaviour in the past. Over the last decade, anthropological work has focused on correlating variation in primate trabecular bone to locomotor and masticatory function, to provide a context for the interpretation of fossil morphology. The variation found within species and its underlying mechanisms are still poorly understood. To address this deficit, this thesis focuses on understanding variation in trabecular bone structure in the human foot.

The main aims of this project is to determine whether archaeologically inferred levels of terrestrial mobility (here defined as the sum of all lower limb locomotor loading) significantly correlate to variation in trabecular structure in the foot in past populations. The foot was chosen because the biomechanics of bipedal locomotion are similar across human populations, but the levels of terrestrial mobility differ. Population-wide estimates of terrestrial mobility can be inferred using archaeological data. Predictions can therefore be tested regarding how trabecular structure should respond to differences in terrestrial mobility based on the experimental literature.

There are numerous factors besides habitual loading that underlie trabecular bone morphology. Before the effects of behavioural variation can be examined, the contributions of non-behavioural factors must be understood. A large portion of this thesis is dedicated to elucidating the relationship between trabecular bone morphology and important variables such as body mass, bone size, age, and sex. This research assesses the suitability of trabecular bone as a proxy for inferring behaviour in the past by examining numerous factors underlying trabecular bone structure in past populations.

The materials and methods used in this dissertation are described in the remainder of this chapter. All following chapters will include a review of the relevant literature and an overview of the statistics used. In Chapter 2 the internal trabecular structure of the talus, calcaneus, and first metatarsal is explored in the context of mechanical loading during bipedal gait. Based on these findings 17 volumes of interest are placed for quantitative analysis of trabecular structure. Variation in body mass and external bone dimensions in four archaeological populations are explored in Chapter 3, followed by an examination of the correlations of these variables on trabecular structure. The relationship between trabecular properties and body mass is assessed in relation to the literature on interspecific trabecular bone allometry in Chapter 4. Results from this chapter are used to correct for the significant effects of body mass in subsequent analyses. In Chapter 5 sexual dimorphism in trabecular bone structure is examined in all four populations. Sexual dimorphism did not vary according to predictions based on sexual dimorphism in lower limb diaphyseal rigidity in most populations. Trabecular bone mass reduces significantly with age, leading to an epidemic of osteoporosis in modern industrial populations. Chapter 6 explores age-related bone loss in the archaeological populations. Trabecular structure is investigated in relation to terrestrial mobility levels in two mobile and two sedentary human populations in Chapter 7. Results indicate that all four populations have a similar distribution of trabecular properties throughout the foot with a signal of mobility superimposed upon it. Greater inferred mobility associated with greater bone volume fraction, thicker, more widely-spaced, and fewer trabeculae. The ontogeny of trabecular structure is described for the human calcaneus in Chapter 8. This chapter examines how the complex trabecular structures found in adult calcanei are established during growth and explores the roles of the development of bipedal gait and increases in body mass in shaping the calcaneus. The thesis is concluded with a summary of the results and future directions in Chapter 9.

Materials and methods

Populations

Five archaeological populations spanning three continents and roughly 4000 years are examined in the current study (Table 1.2). Populations were chosen based on levels of terrestrial mobility and availability for µCT scanning. The project was originally designed to focus on northeast Africa to minimise the potential effects of environmental, climatic, and genetic factors on trabecular bone variation. Unfortunately, it was logistically not possible to obtain access to additional mobile and sedentary populations housed at the British Museum in London. To obtain a suitable size of two sedentary and two mobile populations the Black Earth hunter gatherers and sedentary medieval St. Johns population were chosen. A total of eighty adult calcanei, tali and first metatarsals (Figure 1.2) were collected from four human archaeological populations, resulting in the largest intra-species sample published to date. Twenty-five juvenile calcanei from individuals aged between 0 and 20 years were studied from two populations. Bones were taken from the best-preserved side, preferentially all from the same side. Individuals showing evidence of movement impairing pathologies were excluded. Individuals showing signs of old age were not included unless no alternatives were available.

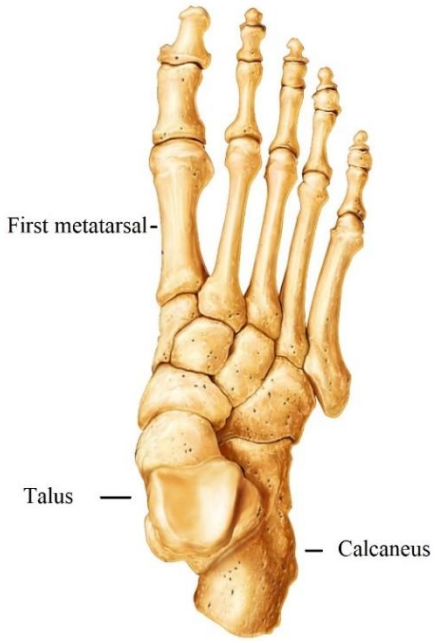

Figure 1.2. A human foot indicating the position of the calcaneus (heel), talus (ankle) and first metatarsal.

Table 1.2. Summary information of study populations used. M=male, F=female, I=indeterminate.

Population	Location	Date	Subsistence strategy	Demography	Relative mobility
Black Earth	Illinois, USA	3000 BC	Foragers	M=11, F=9	High
Jebel Moya	Sudan	100 BC AD 1000	Pastoralists	M=11, F=3, I=6	High

Norris Farms	Illinois, USA	AD 1300	Village agriculture and foraging	Juveniles: I=13	Intermediate
Kerma	Sudan	2100 BC 1500 BC	Agriculture	M=13, F=7	Low
St. Johns	Cambridge, UK	AD 1230 AD 1511	Urban	Adults: M=10, F=10 Juveniles: I=12	Low

Populations are assigned to either high or low mobility categories based on subsistence strategy and archaeological evidence. Mobility is defined here as the total sum of all locomotor activities using the lower limb (Pearson et al., 2014). The mobile Black Earth forager population is from southern Illinois, USA, and is dated to 3000 B.C. The site has been interpreted as a multi-season forager base camp (Jefferies and Avery, 1982; Jefferies, 2013). The Norris Farms #36 population hails from central Illinois, USA, and is associated with the Oneota culture. Dated to approximately 1300 A.D., the people from Norris Farms #36 practised a form of village agriculture supplemented with foraging (Birmingham and Eisenberg, 2000). The sedentary North African Kerma are from the ancient Nubian city of Kerma, one of the first urban centres that arose in eastern Africa, dated between 2100 and 1500 BC (Thompson et al., 2008; Nikita et al., 2011). The mobile Jebel Moya are a mobile Nubian pastoral population dated between 100 BC and AD 1000 (Mukherjee et al., 1955; Brass, 2015a). The sedentary urban St. Johns population comes from a hospital cemetery in medieval Cambridge, UK, that was used between 1230 and 1511 AD. The archaeological, behavioural, and biomechanical data available for these populations are described in detail in Appendix 1.1.

Chapters 2 to 7 examine variation in adult trabecular structure in four populations: Black Earth, Jebel Moya, Kerma, and St. Johns. In chapter 8 ontogeny is explored using juveniles from the Norris Farms and St. Johns populations.

Body mass, age, and sex estimation

Body mass (BM, in kg) was estimated from measures of femoral head diameter (FHD, in mm), measured to 0.01 mm using Mitutoyo digital callipers. Body mass was calculated as the average of three equations as recommended by Pomeroy and Stock (2012):

- BM = 2.2393 x FHD – 39.9 (McHenry, 1992)
- BM = 2.2683 x FHD – 36.5 (Grine et al., 1995)
- BM♂ = 2.7413 x FHD – 54.9; BM♀ = 2.426 x FHD – 35.1 (Ruff et al., 1991)

Individuals showing signs of old age were excluded during sample collection. Individuals were first selected based on preservation and excluded when general signs pathology or old age. Sex and age-at-death estimates for the Kerma, Norris Farms and Black Earth populations were taken from existing museum collection records while the ages for St. Johns were obtained from the archaeological site

report (Cessford, 2012). Age-at-death for the Black Earth individuals was estimated using the multifactorial method described in (Lovejoy et al., 1985), and transition analysis was used to estimate age-at-death for the Norris Farms (Milner and Smith, 1990). The mean ages in years for the Black Earth sample were 31.3 ± 4.39 for the males and 35 ± 9.51 for the females. The median ages (non-normal distribution) for the Norris Farms sample were 31.36 ± 4.39 for males and 26.9 ± 6.95 for the females. For St. Johns and Kerma, age was determined using pelvic traits (Brooks and Suchey, 1990) and molar wear (Brothwell, 1981). Three broad age categories were used: young adult 18-25, mature adult 26-45, old adult >46 (Brothwell, 1981; Brooks and Suchey, 1990; Buikstra and Ubelaker, 1994). The Jebel Moya could not be aged due to the fragmentary and incomplete nature of the collection. The Black Earth and Norris Farms were placed in the same broad categories as the Kerma and St. Johns. The sex of the all individuals was determined by pelvic and skull traits using the standards by Buikstra and Ubelaker (1994).

µCT scanning and analysis

The juvenile Norris Farms calcanei of the were scanned on the ONMI-X HD600 High-Resolution X-ray computed tomography (HRCT) scanner at the Center for Quantitative Imaging (CQI), Pennsylvania State University (Ryan and Krovitz, 2006; Shaw and Ryan, 2012; Macintosh et al., 2013; Ryan and Shaw, 2015). HRCT scans were made using optimised energy settings using source energy settings 180 kV, 110 µA, and between 2800 and 4800 views. The Black Earth talus, calcaneus, and first metatarsals were later scanned at the same facility using a GE v|tome|x L300 multi-scale nano/microCT system. Resolutions obtained are 43µm for the calcaneus, 39µm for the MT1 and 32µm for the talus, using 1080 views, and an exposure of 1 second. The Kerma, Jebel Moya, and St. Johns specimens were scanned using an identical protocol with a Nikon XTH 225 ST HRCT laboratory scanning system at the Cambridge Biotomography Centre, University of Cambridge. Scans were made using optimised energy settings (125 kV, 135 µA, 1080 views) with resolutions of 47µm in the calcaneus, 33µm in the talus, and 40µm in the first metatarsal. Each specimen was mounted inside an acrylic tube and secured using radio-translucent low-density polyethylene foam disks (Macintosh et al., 2013). Scans are saved as 16-bit TIFF greyscale images with a 2000×2000 pixel matrix.

Spherical volumes of interest (VOIs) were extracted from 3D models of scans using Avizo Fire 6.3. Detailed protocols for VOI placement are given in Chapter 2 after the biomechanical context of the calcaneus, talus, and first metatarsal is discussed. Once created, the spherical VOI was saved as a stack of dicom files and imported into ImageJ (http://rsbweb.nih.gov/ij/) to calculate the trabecular properties. Bone was separated from air using the optimise threshold function. Five trabecular bone morphometric variables were quantified using the BoneJ plugin (Doube, 2010) and are used throughout this thesis (Table 1.1). Bone volume fraction (BV/TV, %) is the volume of mineralised bone per unit volume. Mean trabecular thickness (Tb.Th, mm) and trabecular separation (Tb.Sp, mm) are calculated using model-independent distance transform methods (Hildebrand and Ruegsegger, 1997; Dougherty and Kunzelmann, 2007). Connectivity density (Conn.D, mm^{-3}) was calculated

following the topological approach of Odgaard and Gundersen (1993). Degree of anisotropy (DA) was determined using the mean intercept length (MIL) method and is calculated as 1 - primary eigenvalue/tertiary eigenvalue (Odgaard, 1997). Recent work has demonstrated that the widely used structure model index is unsuitable for use on real bone geometries and was thus excluded from the analysis (Salmon et al., 2015).

Sample size

The study was initially designed to contain 20 individuals from each population with a roughly equal ratio of males and females. Unfortunately, some of the specimens that looked good externally were found to contain taphonomic damage to the internal trabecular structure. Some individuals from the Black Earth and Jebel Moya had dense material that stuck to certain trabeculae (Figure 1.3). No method was found that could accurately remove the contamination. Volumes of interest that were affected by this phenomenon were removed, resulting in a lower sample size in the Jebel Moya and Black Earth.

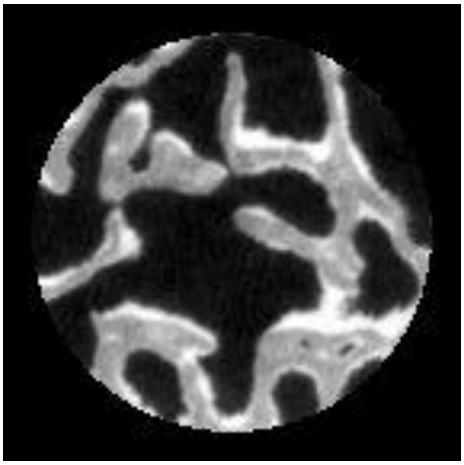

Figure 1.3. Dense (white) material stuck to the trabeculae of one Black Earth individual.

Chapter 2 - Trabecular bone structure throughout the foot

Introduction

In this chapter, the trabecular bone architecture in the calcaneus, talus, and first metatarsal is described qualitatively and quantitatively. Distinctive trabecular bone features are discussed in the context of mechanical loading during normal walking and running gait. The placement of volumes of interest in which trabecular structure is quantified throughout this thesis is described here. The mean values of trabecular properties in a pooled sex and pooled population sample are provided for each volume of interest. Predictions of trabecular structural variation in the pooled human sample are generated using biomechanical data from the literature.

Trabecular bone is adapted to effectively accommodate the strains to which is it habitually subjected (Mullender and Huiskes, 1995; Gefen and Seliktar, 2004; Skedros et al., 2004; Skedros and Baucom, 2007). Adaptation to loading conditions can be achieved through the addition of bone or an efficient organization of trabeculae in the primary direction of loading. Trabecular bone structure is highly correlated with the elastic properties of bone (Maquer et al., 2015). High BV/TV, Tb.Th, and low Conn.D are associated with high levels of mechanical strain (Hodgskinson and Currey, 1990; Goulet et al., 1994; Odgaard et al., 1997; Kabel et al., 1999; Ulrich et al., 1999; Rubin et al., 2002; Mittra et al., 2005; Rincón-Kohli and Zysset, 2009; Barak et al., 2011; Karim and Vashishth, 2011; Ryan and Shaw, 2015). Bone volume fraction is a common predictor of fracture risk in clinical settings and correlates strongly with ultimate bone strength and elastic modulus (Ulrich et al., 1999; Mittra et al., 2005; Maquer et al., 2015). Tb.Th, Tb.Sp, and Conn.D are strongly correlated to BV/TV, and after statistically removing the shared variance with BV/TV these properties have little predictive power of bone stiffness (Maquer et al., 2015). However, these properties are useful to describe how the trabecular bone is organized in different volumes of interest, and how bone structure changes with age, body mass, and under different loading conditions. In addition to BV/TV, fabric anisotropy is a good predictor of trabecular bone stiffness (Odgaard et al., 1997; Ulrich et al., 1999; Maquer et al., 2015), and has been found to correlate significantly to ultimate strength and elastic modulus (Mittra et al., 2005). Trabecular bone is stiffest when loaded in the primary direction in which struts are oriented (Odgaard et al., 1997). Maquer et al. (2015) found that BV/TV predicts 87% of variance in finite element calculated bone stiffness with an additional 10% further described by fabric anisotropy. Thus, using a combination of BV/TV and DA, they could account for 97% of variance in finite element calculated bone stiffness.

Foot loading during gait

The foot is a highly complex system of bones, muscles, and ligaments that changes in configuration during gait. The bones of the foot move into various positions during gait which affects the distribution of loading through the foot, and are described in detail in Appendix 2.1. Measuring joint loadings in vivo is difficult without affecting foot function. The complexity of foot motion and loading

during gait and the many factors which affect them (ligaments, muscles, bone shape, bone movement, trabecular architecture) makes the creation of an accurate finite element (FE) model challenging. Parr et al. (2013) demonstrated the importance of including trabecular structure into finite element analyses by showing that tali with modelled trabecular structures were significantly stiffer than tali modelled as solid bone with the same mass. This shows that the geometry of trabecular structure and its distribution throughout the bone increases stiffness while limiting bone mass, and that FE studies which include trabecular architecture provide more accurate models of bone strength and stiffness. Gefen et al. (2000) studied the distribution of stress in a finite element model of the whole foot during six phases of stance. They found elevated Von-Mises stress in the posterior-medial calcaneus and talar trochlea during initial impact and heel-strike. During midstance, high stresses are found in the talus, calcaneus, and medial metatarsals, with the greatest loading occurring in the subtalar joint, followed by the trochlea, the Achilles tendon attachment, and the dorsal part of the first three metatarsals. During midstance, the dorsal part of the foot experiences compression while the plantar aspect experiences mostly tensile stress. As the foot flattens, the plantar ligaments and plantar fascia stretch, subjecting the anterior/plantar calcaneus and the plantar metatarsal heads to tension. During forefoot-contact, push-off, and toe-off the highest stress was observed in the dorsal aspects of the first four metatarsals, shifting from the centre of the shaft to the metatarsal heads from forefoot contact to toe-off. Additionally, elevated levels of stress were found in the dorsal aspect of the talus and the posterior calcaneus (Gefen et al., 2000). The results from this FE simulation indicate that the talus, calcaneus, and first metatarsal play variable roles in load transmission during gait.

The internal trabecular architecture of the foot reflects the complex loading to which the foot is subjected during gait (Figure 2.1). In this chapter, the trabecular morphology and biomechanics of the calcaneus, talus, and first metatarsal are discussed, and the volumes of interest used throughout this thesis are determined. Trabecular structure is then quantified in volumes of interest and discussed in relation to predictions based on biomechanical analyses from the literature.

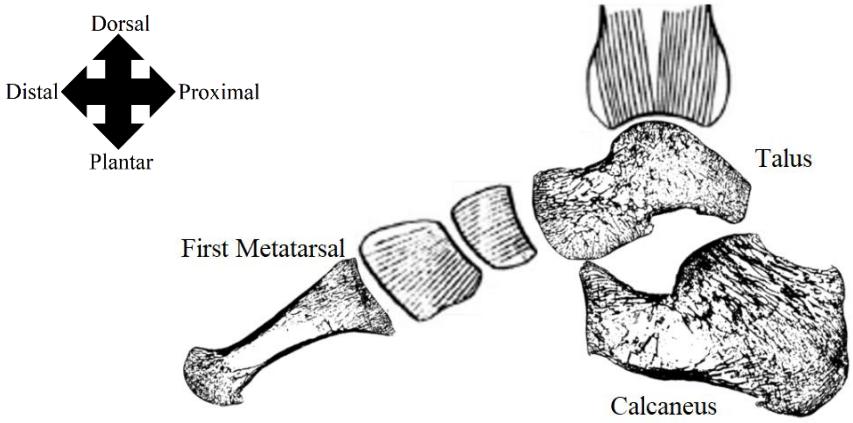

Figure 2.1. Sagittal slice through the foot and lower limb in which the main trabecular bands are shown. Illustration by von Meyer (1867) combined with orthoslices through the talus, calcaneus and first metatarsal.

Materials and methods

Trabecular bone structure throughout the calcaneus, talus, and first metatarsal is described qualitatively using 3D models and 2D images taken from µCT scans. The images are interpreted based on biomechanical data taken from the literature. After considering the mechanical context and internal trabecular architecture, the locations for placement of 17 volumes of interest (VOIs) are determined. Trabecular structure is then quantified in the 17 chosen VOIs which will be analysed in the rest of this thesis. Finally, trabecular structure will then be compared between all VOIs using repeated-measures one-way ANOVA, followed by pairwise comparisons with a Bonferroni correction. Adults from Black Earth, Jebel Moya, Kerma, and St. Johns are pooled for all analysis. α was set at .05 for all statistical tests.

Volume of interest placement: general considerations

The trabecular microstructural properties used throughout this thesis will be calculated within spherical volumes of interest (VOIs) placed in the calcaneus, talus, and first metatarsal. Correct and consistent placement of VOIs is crucial to obtain results that are reproducible and mechanically informative. The success of previous studies has largely depended on suitable placement of VOIs. For example, Desilva and Devlin (2012) divided the talus into large quadrants of trabecular bone. These large and somewhat arbitrarily placed VOIs averaged out trabecular bone structure within the quadrants, preventing significant variation between species from being found. Su et al. (2013) placed VOIs just deep to the talar trochlea of humans, primates, and *Paranthropus boisei* and managed to find significant locomotor signals in the trabecular structure. Thus, the location and size of volumes of interest are of critical importance to the robusticity of trabecular analyses. Kivell and colleagues (2011) argue that use of a VOI in differently sized individuals will inevitably bias the outcome because trabecular properties do not scale isometrically with body size. Placing a similarly sized VOI in large and small individuals results in a greater number of trabeculae sampled in the smaller

individuals (Kivell et al., 2011; Lazenby et al., 2011 b). In a paper testing the differences between using scaled and non-scaled VOIs, Lazenby et al. (2011 b) found that variation in VOI location by just a few millimetres within a bone greatly influences bone properties (Kivell et al., 2011). This problem is increased when analysing the trabecular properties of complex-shaped bones such as tarsals, compared to more regularly shaped long bone epiphyses (Maga et al., 2006; Griffin et al., 2010; Kivell et al., 2011). Trabecular properties are more susceptible to changes in VOI location than VOI size with Conn.D being greatly affected by both (Kivell et al., 2011). Great care should therefore be taken when comparing small and/or complex arthroses, and especially when comparing different species (Kivell et al., 2011). Harrigan et al. (1988) demonstrated that in order to accurately quantify trabecular structure, the dimensions of volumes of interest need to be at least 3 to 5 times larger than the trabecular lengths to satisfy the continuum assumption of trabecular structure. All VOIs used in this study meet this requirement. The sensitivity of trabecular properties to VOI size and location may be one of the reasons why studies on trabecular bone functional adaptation have sometimes yielded contrasting results (eg. Su et al. (2013) versus Desilva and Devlin (2012)). Variation in VOI size and location between studies also limits the potential of comparing data to previous findings in the literature, and prevents meta-analyses from being performed.

A volume of interest must meet two requirements: it should be in a functionally relevant region and it needs to be replicable between individuals and populations. VOIs should not be too large in order to avoid the risk of averaging out loading related variation, but large enough to include a minimum of five intertrabecular lengths in order to satisfy the continuum assumption (Harrigan et al., 1988). The VOIs used in this study will be placed using a systematic approach in order to produce VOIs that are homologous in relative size and location (Gosman and Ketcham, 2009; Ryan and Shaw, 2013). Stacks of TIFF images created from µCT scans are uploaded into Avizo Fire 6.3 and oriented in along clearly defined axes (for full protocols see Appendix 2.2). In the calcaneus and the talus a bounding box (xyz-grid) is placed around the maximum dimensions of the scanned bone with an x-axis orthogonal to the anteroposterior axis. In the first metatarsal, a bounding box is placed around the head and base. VOIs are scaled by bounding box dimensions. The VOIs will subsequently be placed in predetermined locations within the bounding box using a script. This results in the placement of homologous VOIs that are scaled to the size of the bone or joint being analysed. Volumes of interest are subsequently imported into ImageJ, and analysed with the BoneJ plugin to calculate the trabecular bone properties. Visual inspection ensures the correct and consistent placement of VOIs, and checks that only trabecular bone is sampled in VOIs close to articular surfaces. However, there is variation in bone morphology between individuals. If the automated scripts fail to place VOIs in the correct location, the VOI will be manually adjusted.

Qualitative description of trabecular structure and VOI placement

Calcaneus

Humans have a large calcaneus relative to their body size that is adapted to withstand the high cyclical loading associated with bipedal locomotion (Latimer and Lovejoy, 1989). The long axis of the calcaneus is directed anteriorly, laterally, and dorsally. The dorsal angle of inclination with the horizontal plane can vary between 10 and 30 degrees (Sarrafian and Kelikian, 2011a). There exists variation in calcaneal shape, including the inclination angle of the anterior and posterior talar facets, tuber shape, and the shape and number of talar facets (Sarrafian and Kelikian, 2011a). Human calcanei have a unique lateral plantar process which likely functions to increase the contact area between the calcaneus and the ground (Latimer and Lovejoy, 1989). The calcaneus articulates with the cuboid and the talus, and attached to it are the Achilles tendon, plantar ligaments, and the plantar fascia (Figure 2.2) (Giddings et al., 2000; Gefen and Seliktar, 2004). The plantar fascia originates from the calcaneus and is attached to each proximal phalanx (Erdemir et al., 2004). The plantar fascia maintains the longitudinal arch of the foot, transmits forces between the forefoot and the hindfoot during stance, and acts as an energy saving mechanism (Griffin et al., 2010a; Hagins and Pappas, 2012). Figure 2.2 shows a sagittal cross-section of the calcaneus, with vectors of tensile and compressive forces from tendons and joints at the most strenuous parts of the stance phase of running and walking, just prior to toe-off. It has been found that differences between static and dynamic loading states in the calcaneus are in the intensity of calcaneal stresses rather than differences in the directions or spatial distributions of stress flow (Gefen and Seliktar, 2004). Little variation is found in loading distributions between static (Gefen, 2002) and dynamic loading (Gefen et al., 2000). The greatest compressive loading is placed on the posterior talar facet (PTF), and the calcaneocuboid (CC) joint, while the largest tensile loading is placed on the Achilles tendon (Giddings et al., 2000). The internal architecture consists of three distinctive trabecular systems with a triangular zone of low-density in the centre (Figure 2.2). A trabecular system extends from the PTF towards the heel, and anteriorly from the superior aspect of the CC articulation. A third system of trabeculae extends along the plantar surface of the calcaneus (Giddings et al., 2000). Principal stress trajectories calculated from finite element analyses correspond to these three trabecular systems, with compressive trajectories extending posteriorly and anteriorly along the superior half of the calcaneus and tensile trajectories extending along the inferior half (Giddings et al., 2000).

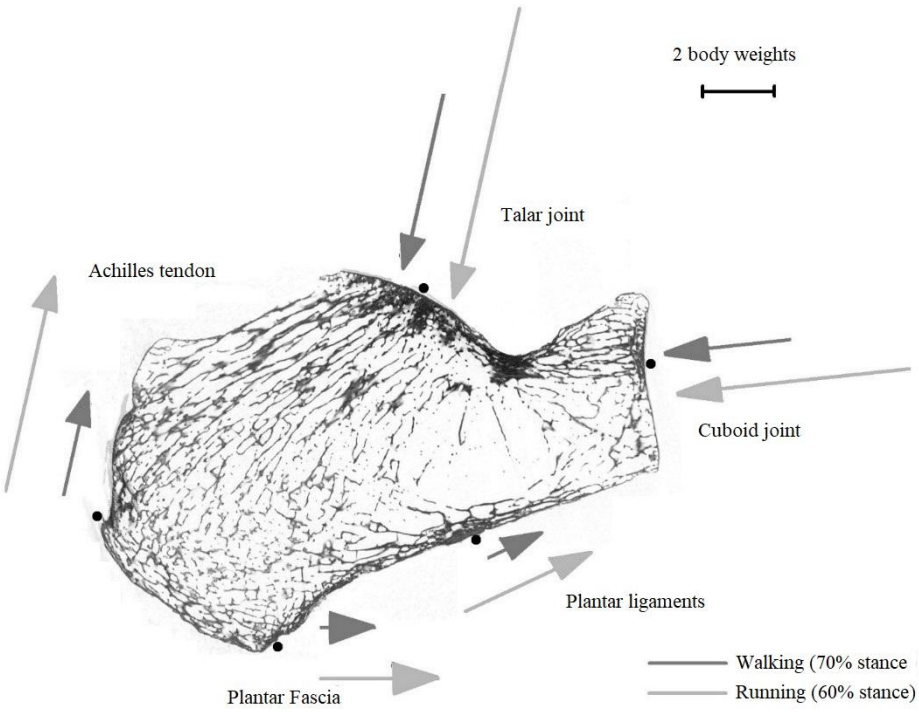

Figure 2.2. Sagittal cross-section of the calcaneus showing ligament, tendon, and joint forces at 70% of stance during walking and 60% of stance during running. Force vectors were adapted from Giddings et al. (2000, Figure 4). Dots indicate the location of force application.

Seven volumes of interest will be placed in the calcaneus, with each VOI associated with compressive stress associated with joint loading, or tensile stress associated with the pull of a tendon or ligament (Figure 2.3). The AutoVOI – calcaneus script for Avizo 6.3 was used to determine the size and location of each volume of interest. VOI diameter was calculated as a percentage of maximum calcaneal length which is strongly correlated to body mass (see Chapter 3). The protocol for VOI placement and size are provided in Appendix 2.2.

- Achilles tendon (AT): the triceps surae muscle pulls on the posterior portion of the calcaneal tuber where the Achilles tendon is attached. Substantial tension is produced by the triceps surae during toe-off (Levine et al., 2012), sometimes resulting in tensile fractures of the calcaneal tuber (Frankel and Nording, 2012). Aside from the pull of the triceps surae this VOI location is also expected to be influenced significantly by tensile stress produced by the plantar fascia during terminal stance (Figure 2.3, red).

- Posterior talar facet (PTF): the highest loading experienced by the calcaneus is at the posterior talocalcaneal joint. The direction and magnitude of loading at the joint changes throughout stance (Hagins and Pappas, 2012; Levine et al., 2012). Three volumes of interest will be placed just below the articular surface in order to capture variation in this region (Figure 2.3, posterior (PP, purple), central (PC, grey), anterior (PA, salmon)).

- Calcaneocuboid (CC): the superior aspect of the calcaneocuboid joint experiences strong compressive loading during toe-off as force is transmitted to the forefoot (Figure 2.3, green).

- Plantar ligaments (PL): the plantar ligaments attach to the plantar surface of the calcaneus and produce tension during regular standing and during gait. A volume of interest is placed just below the cortical shell and posterior to the low-density triangle (Figure 2.3, blue).

- Calcaneal tuber (CT): This volume of interest is the only one which is not placed directly near an articular surface or a muscle attachment. It measures trabeculae which transmit the compressive loading through the calcaneal tuber from the posterior talar facet. The volume of interest is placed just beneath the cortical shell, in the middle of the tuber between the most superior parts of the tuber and the posterior talar facet (Figure 2.3, cyan).

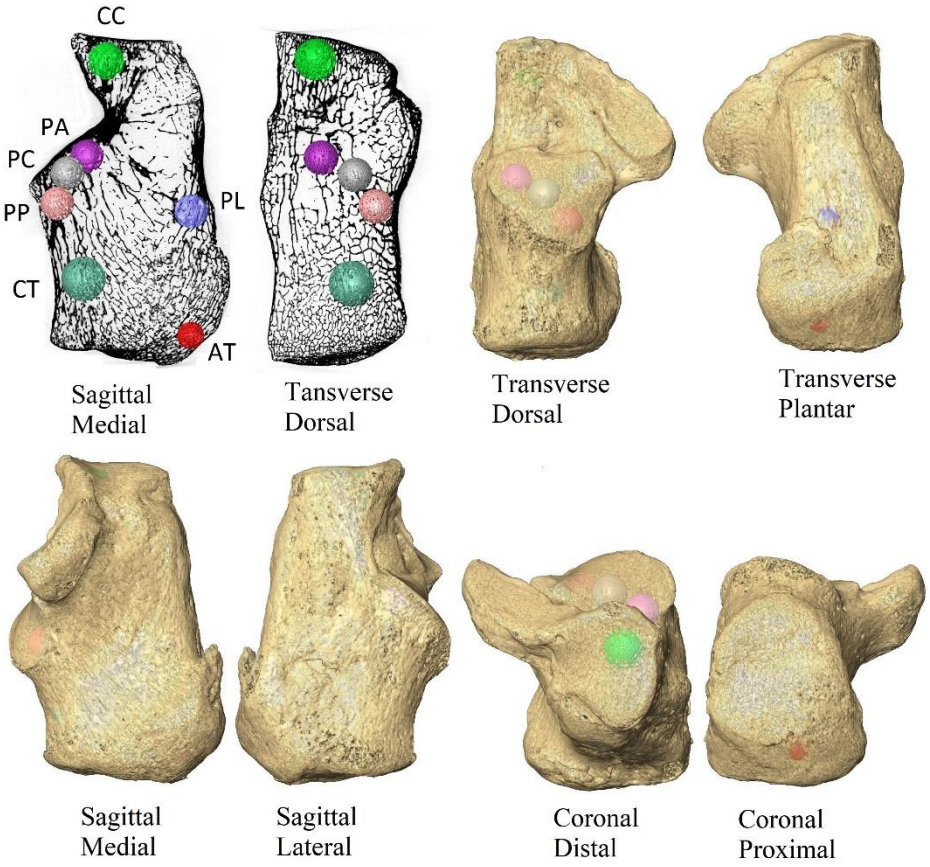

Figure 2.3. Volumes of interest in the calcaneus. Achilles tendon (AT, red), calcaneal tuber (CT, mint green), plantar ligaments (PL, blue), posterior talar facet (posterior (PP, salmon), central (PC, grey), anterior (PA, purple), calcaneocuboid (CC, green). Described below the bone is the anatomical plane and the direction from which the image is viewed.

Based on the finite element model of Giddings et al. (2000), it is predicted that the PTF VOIs are subjected to the highest levels of strain during gait. The PTF VOIs are predicted to contain the highest values of BV/TV and Tb.Th, and the lowest levels of Conn.D and Tb.Sp. Based on the loading magnitudes presented in Figure 2.2 it is predicted that that the PTF VOIs are followed by the calcaneocuboid and Achilles tendon VOIs who should have lower BV/TV and Tb.Th as a result of lower maximum loading magnitudes to which they are subjected during gait. The plantar ligament VOI is expected to contain the lowest BV/TV and Tb.Th, and the highest Conn.D and Tb.Sp as it is subjected to the lowest loading during stance (Giddings et al., 2000). However, trabecular bone

stiffness also depends on the type of loading it is subjected to. Trabecular bone is much stiffer in compression than tension (Keaveny et al., 2001; Frankel and Nording, 2012). Because the plantar ligaments and Achilles tendon are primarily loaded in tension, it is possible that because trabeculae fail quicker in tension, greater BV/TV is required despite the tensile forces being lower than the compressive forces on the dorsal side of the calcaneus. Based on the models of Giddings et al. (2000) it is difficult to predict BV/TV in the calcaneal tuber VOI. The region of the tuber where the VOI is placed is subjected to purely compression during stance and is not near any articular surface or muscle attachment, where stress is generally highest. Because the tuber VOI is subjected only to compressive stress from the direction of the PTF, it is predicted to contain lower BV/TV than the PTF VOIs, but highly anisotropic as it is not subjected to loadings from different directions. DA is also expected to be high in the calcaneocuboid, Achilles tendon, and plantar ligament VOIs, because they are primarily loaded from single directions.

Talus

The talus has no muscular attachments, consists of a body, head, and neck and 60% of its external surface is covered by articular cartilage (Dawe and Davis, 2011). There is significant variation in humans in certain osteological features of the talus such as the talar angle, the inclination and declination angles of the talar neck, the torsion of the talar head, and differences in the size and contour of the calcaneal articular surfaces (Sarrafian and Kelikian, 2011a). The talus receives the weight of the body through the trochlear surface and transmits it inferiorly towards the calcaneus and anteriorly into the navicular. The trochlea and the talar head are in two almost perpendicular planes. Thus, a change occurs in the direction of force within the bone when it is transmitted from the trochlea to the talar head. Similarly, the talus is subjected to various loading directions and magnitudes during walking as a result of the rolling of tibia over the trochlear surface, and with change in position of talus itself (Pal and Routal, 1998). Talar trabecular architecture is described below along with the varying loadings it is subjected to during stance.

At heel strike, all of the initial load is transmitted from the posterior half of the trochlear surface to the posterior calcaneal facet (Pal and Routal, 1998). During midstance, loadings are transmitted to the heel through the posterior and anterior calcaneal facets, and distally towards the navicular through the talar head. From heel rise to toe-off the weight of the body is transmitted to the forefoot while the talar neck and head are subjected to tensile forces. During heel rise, forces from the triceps surae are exerted on the calcaneus producing a proximal/anterior force on the plantar side of the talus (Pal and Routal, 1998).

Talar trabecular structure is complex and merits a detailed description. The complexity results from the talus' function in transmitting loads from different orientations during stance. The talus consists primarily of plate-like trabeculae, surrounded by a cortical shell. The cortical shell is thickest in the posterior calcaneal facet, around the talar neck, at the malleolar facets, and at the attachment sites of the deltoid and interosseous ligaments (Athavale et al., 2008). The medial side of the talar body

consists of sagittal plates which run through the talar neck into the talar head. The medial plates become less plate-like and more rod-like as they approach the posterior calcaneal facet. The plates under the lateral portion of the trochlea are a mix of medially, posteriorly, and anteriorly directed plates. The anterior third of the medially facing plates eventually curve anteriorly into the neck, becoming continuous with the curved plates of the talar head. The posterior two-thirds of the medially facing plates curve posteriorly in the sagittal plane (Athavale et al., 2008). The superior two thirds of the talar head consists of a stack of obliquely oriented plates connected by small rods. The inferior third of the talar head consists of thinner rods and plates oriented largely perpendicular to the anterior and middle calcaneal facets. The vertical plates in the talar body and the arched plates in the head are connected by a mass of irregularly shaped trabecular plates in the talar neck. Pal and Routal (1998) argue that this trabecular meshwork within the neck facilitates changes in direction of forces in the talus. The thickest plates are found in the talar neck, resulting from the effects of compressive and tensile forces acting on this region (Athavale et al., 2008).

The talar trochlea has a relatively large load-bearing surface area. The distribution of loads on the talus is determined by the position of the ankle and the condition of the relevant ligaments (Hagins and Pappas, 2012). Depending on foot position, between 77 and 90% of the load is transmitted through the talar dome, with the remaining loads being transmitted though the medial and lateral talar facets. In dorsiflexed position the anterior side of the trochlea is loaded, in plantarflexion the posterior side is loaded. When the ankle is inverted the medial facet is loaded and when the ankle is everted the lateral facet carries a higher load (Calhoun et al., 1994). As the ankle moves from plantarflexion into dorsiflexed position, the contact area centroid moves from posterior to the anterior talus. During inversion the centroid moves from medial to lateral (Calhoun et al., 1994).

The talus is a complex and irregularly shaped bone that consists largely of articular surfaces. Thus, many locations in the talus are interesting for placement of VOIs. A bounding box was placed around the anteroposterior length of the talus and the mediolateral breadth of the trochlea (Appendix 2.2). The AutoVOI – talus script for Avizo 6.3 was used to determine the size and location of each volume of interest. Talar length and trochlear breadth are highly correlated with body mass (see Chapter 3 and Jung et al., 2014). Six spherical VOIs were placed just beneath the cortical shell (Figure 2.4).

- Trochlea: a medial, lateral, and central VOI were placed just deep to the highest point of the trochlea in the sagittal plane (Figure 2.4, purple (medial), pale green (central), salmon (lateral)).
- Posterior calcaneal facet: a VOI was placed inferior to the lateral trochlea VOI in the centre of the breadth of the posterior calcaneal facet (Figure 2.4, red).
- Anterior calcaneal facet: a VOI was placed in the posterior third of the length of the anterior calcaneal facet, just beneath the cortex (Figure 2.4, green).

- Talar head: a VOI was placed in the centre of the talar head, in the most anterior part of the head, just beneath the cortex (Figure 2.4, blue).

In a finite element analysis of the trabecular structure of the talus, Parr et al. (2013) found that the areas with the highest Von Mises strain during three types of normal loading (neutral, inversion, eversion) were in the talar head, neck, and the posterior calcaneal facet. In a finite element analysis of the whole foot during different phases of stance, Gefen et al. (2000) found the highest concentrations of stress in the talar trochlea, the subtalar joints, and the dorsal talus in general. This dorsal concentration of compressive stress was again found in a subsequent FE analysis of the whole foot (Gefen, 2002). The results of Parr et al. (2013) and Gefen et al. (2000, 2002) do not agree completely, making it difficult to predict with certainty which of the VOIs is most likely to contain the highest BV/TV and Tb.Th. These studies indicate that most likely all VOIs will have a relatively high level of BV/TV, and Tb.Th, and low Conn.D and Tb.Sp, as all of them seem to be subjected to significant stress. The ACF VOI is predicted to have the lowest BV/TV, Tb.Th, and the highest Conn.D and Tb.Sp, as it plays a smaller role in transmitting stress to the forefoot compared to the dorsal side of the head, and a smaller role in transmitting stress to the calcaneus relative to the forces coming down from the trochlea and travelling straight downward into the posterior calcaneal facet. The thickest trabeculae have been observed in the talar neck by previous researchers, but no VOI is placed in the neck in the current study (Pal and Routal, 1998; Athavale et al., 2008). The most anisotropic structures are predicted in the talar head and posterior calcaneal facet VOIs as an adaptation to their largely unidirectional compressive loading. Lower DA is predicted for the trochlear VOIs, due to the changes in loading directionality as the tibia rotates around anteriorly and posteriorly during stance. Lower DA is also predicted for the anterior calcaneal facet as an adaptation to stress received plantarly from the calcaneus and anteriorly stress from the navicular. Finally, the lateral part of the articular surface of the distal tibia is most strongly loaded in humans (Kimizuka et al., 1980). It is thus predicted that the talus will thus also experience the highest loadings on the lateral side of the tibial articulation, resulting in greater BV/TV in the lateral VOI compared to the other two trochlear VOIs.

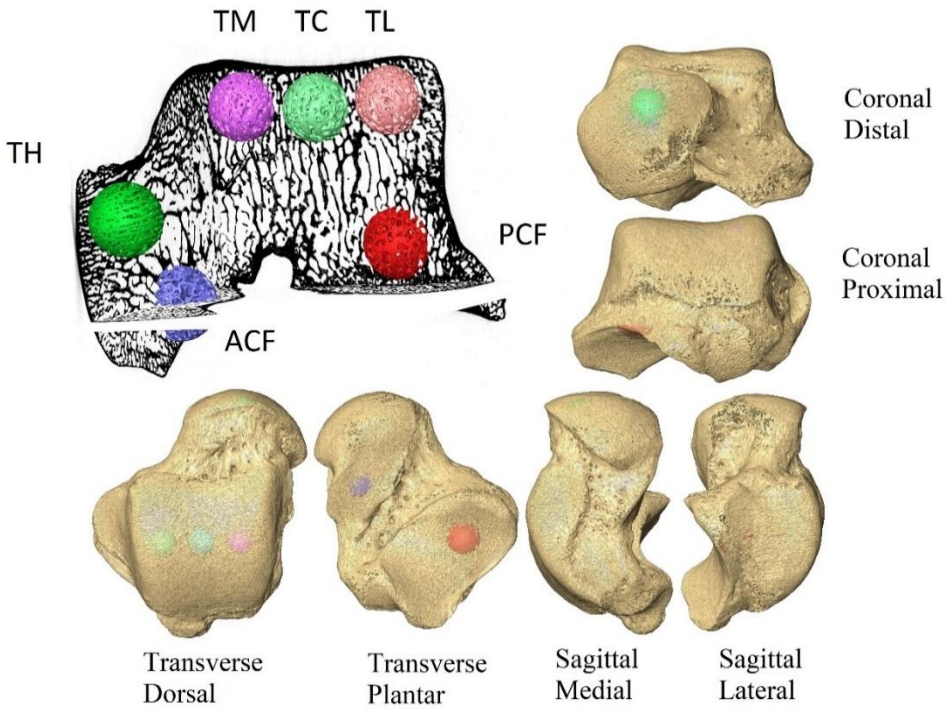

Figure 2.4. Volumes of interest in the talus. Talar head (TH, dark green), anterior calcaneal facet (ACF, blue), posterior calcaneal facet (PCF, red), medial trochlea (TM, purple), central trochlea (TC, mint green), lateral trochlea (TL, salmon). Described below the bone is the anatomical plane and the direction from which the image is viewed.

First Metatarsal

The anatomy of the first metatarsal consists of the base, the head, and the shaft. These regions are surrounded by a shell of cortical bone which is thick in the shaft and thin in the base and head. The first metatarsal is the shortest and thickest of the metatarsals, and is subjected to the highest loadings during gait (Jacob, 2001). Humans have a unique forefoot which plays a key role in leverage and weight transmission during gait. Humans are the only apes without an opposable hallux (Griffin et al., 2010b). The first metatarsal is part of the medial longitudinal arch which serves as the primary load-bearing structure in the foot during gait (Glasoe et al., 1999; Hagins and Pappas, 2012). Early stance pronation of the subtalar joint lowers the first metatarsal to the ground, dissipating the shock of heel strike (Glasoe et al., 1999). As the body moves anteriorly, supination of the foot stabilizes the medial longitudinal arch, preparing the foot as a rigid lever for toe-off (Glasoe et al., 1999; Hagins and Pappas, 2012). Two sesamoid bones lie dorsal to the head of the first metatarsal and are encased by tendons. Possible functions of the sesamoids are to enhance the load-bearing capacity of the first metatarsal, improve leverage for the attached muscles, or elevate the first metatarsal so that it can plantar flex during hallucal extension (Glasoe et al., 1999). The base of the first metatarsal has a medial, lateral and inferior joint surface. The base joint surface is concave with a dorsoplantar groove which roughly aligns to the metatarsocuneiform joint axis.

The first metatarsal contains three distinct trabecular patterns: superior longitudinal, inferior longitudinal, and proximal transverse (Sarrafian and Kelikian, 2011b). The longitudinal dorsal trabeculae are curved with inferior concavity. The longitudinal plantar trabeculae mirror the dorsal system but are slightly less curved. The transverse trabecular system crosses the longitudinal trabecular systems at almost 90 degrees (Sarrafian and Kelikian, 2011b). Trabecular bone is densest in the head and the base, and reduces within the shaft (Figure 2.5). Some predictions of trabecular architecture in the head and base of the first metatarsal can be based off of studies of forefoot function and loading. The first metatarsal head becomes the weight-bearing fulcrum of the foot during push-off (Erdemir et al., 2004). This results in greater compressive stress in the dorsal portion of the MT1 head as the body moves forward towards toe-off. The greater loading of the MT1 head is reflected in variation in bone mineral density which is found to be greater dorsally compared to plantarly in the human MT1 head and base (Muehleman et al., 1999; Griffin et al., 2010b). Griffin et al. (2010 b) compared the MT1 and MT2 heads of *Homo, Pongo, Pan,* and *Gorilla,* and found that trabecular bone volume fraction in humans was lower compared to extant apes. However, humans had more anisotropic trabeculae compared to the other apes, most notably in the dorsal metatarsal head. This matches with the prediction that humans load their feet more in a primary direction during propulsive gait, whereas the apes load their metatarsals in from more variable directions, particularly during arboreal locomotion. Muehleman et al. (1999) found significantly higher bone mineral density (BMD) in the base and head of males compared to females, and no significant bilateral asymmetry. This sexual dimorphism may be a result of the fact that they used an elderly sample, and elderly women are more severely affected by age related bone loss (Ruff, 2008; Ito, 2011). Muehleman et al. (1999) found significantly higher BMD in the dorsal regions of the head and base compared to the plantar regions. In both males and females the lateral portion of the MT1 head and base contained a higher density than the medial side (Muehleman et al., 1999). Finally, Muehleman et al. (1999) found that the head was significantly denser than the base in both sexes. During normal walking, loads are initially primarily distributed under the heel, and are transferred forward as the body moves over the foot. Maximum loading occurs during toe-off when the body weight is centred under the ball of the foot while the load at the midfoot is low. Thus, the head of the MT1 is subjected to greater peak loading compared to the base, which is reflected in the significant differences in BMD (Muehleman et al., 1999; Hagins and Pappas, 2012). In late stance weight is transferred from the lateral to the medial side of the foot (Hagins and Pappas, 2012). After this stage, all weight is supported by the ball of the foot as the MT1 is maximally loaded and it everts and plantar flexes (Muehleman et al., 1999; Hagins and Pappas, 2012). The hallux deviates laterally at this stage and places compressive forces on the lateral MT1 head. This explains significantly greater lateral BMD in the MT1 head found by Muehleman et al. (1999).

Griffin and colleagues (2010) used three VOIs placed in the MT1 head: on the dorsal aspect, the plantar aspect, and in the centre. In this study four VOIs are examined: one dorsal and one plantar VOI

are placed in the first metatarsal and base. The metatarsal was placed in anatomical position (Figure 2.5). A bounding box was placed around the head and base. VOI size and location was determined using the autoVOI-MT1 for Avizo 6.3. The head VOIs were placed in the centre of the mediolateral plane of the bounding box, just internal to the joint surface. Due to variation in joint morphology within and between populations, VOIs sometimes required manual movement anteriorly or posteriorly to ensure the VOI was placed just below the cortical shell. The dorsal base VOI is placed in the centre of the dorsal half of the articular facet. The plantar base VOI was placed in the centre of the plantar half of the articular facet. VOI size was determined by dorsoplantar height of the bounding box in the head and the base. The diameter of the VOIs was set to 35% of dorsoplantar head height for the first metatarsal head, and 25% of dorsoplantar base height for the two base VOIs.

Some predictions can be made based on the biomechanical data retrieved from the literature. Muehleman et al. (1999) found the highest BMD in the dorsal portions of the metatarsal head and base, and a higher BMD in the head compared to the base. From this it is predicted that BV/TV will be higher in the head compared to the base, and that the dorsal VOIs will contain higher BV/TV ratios compared to the plantar VOIs. Tb.Th is positively correlated with BV/TV and Conn.D and Tb.Sp are negatively correlated with BV/TV. From this is it predicted that Tb.Th will be higher, and Conn.D and Tb.Sp will be lower in the dorsal compared to the plantar VOIs, and in the head compared to the base. DA is predicted to be higher in the base compared to the head because the joint surface of the base has a flatter shape, making the joint significantly less mobile compared to the head, resulting in less predicted variation in loading directionality during gait.

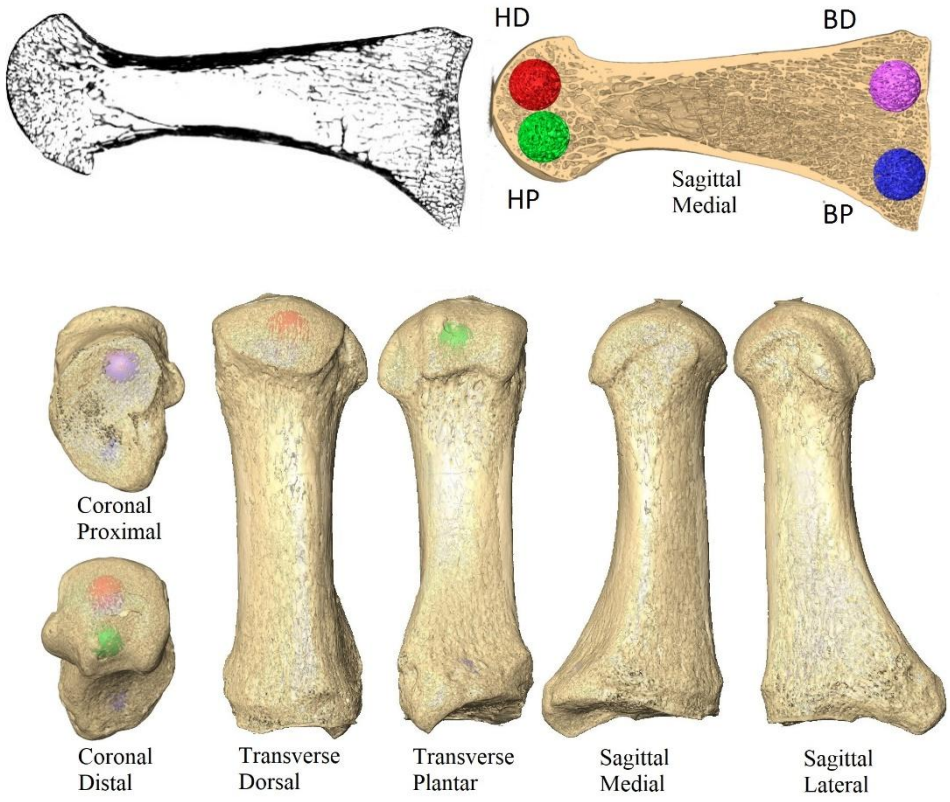

Figure 2.5. Volumes of interest in the first metatarsal head and base. Dorsal base (BD, purple), plantar base (BP, blue), dorsal head (HD, red), plantar head (HP, green). Described below the bone is the anatomical plane and the direction from which the image is viewed.

Trabecular bone properties are calculated in a pooled sex pooled population sample in each of the 17 volumes of interest. Sample size for each VOI is provided in Table 2.1.

Table 2.1. Sample size used in this chapter for each population and sex per VOI. Achilles tendon (AT), calcaneal tuber (CT), plantar ligaments (PL), posterior talar facet (PP: posterior, PC: central, PA: anterior), calcaneocuboid (CC), dorsal base (BD), plantar base (BP), dorsal head (HD), plantar head (HP), talar head (TH), anterior calcaneal facet (ACF), posterior calcaneal facet (PCF), trochlea (lateral: TL, central: TC, medial: TM).

		Black Earth		Jebel Moya			Kerma		St Johns		Total	All VOIs present
		Sex		**Sex**			**Sex**		**Sex**			
		M	**F**	**M**	**F**	**I**	**M**	**F**	**M**	**F**		
Calcaneus	AT	7	10	8	2	5	9	7	9	11	69	48
	CC	7	6	9	2	5	12	7	8	9	66	
	CT	7	9	10	2	5	12	7	8	10	71	
	PA	7	6	8	2	4	12	7	9	11	67	
	PC	6	7	8	2	4	12	6	9	11	66	
	PP	7	8	9	1	4	12	5	9	11	67	
	PL	6	6	5	1	5	11	7	8	10	60	
MT1	BD	7	8	5	2	2	9	5	9	9	56	44
	BP	6	7	2	2	1	9	4	9	9	49	
	HD	8	9	5	3	3	9	4	9	9	59	
	HP	7	7	4	2	2	9	4	9	9	53	
Talus	ACF	5	8	5	2	3	13	7	8	11	62	58
	PCF	5	7	7	4	4	12	6	6	11	62	
	TH	5	6	10	4	5	12	7	8	11	68	
	TL	7	8	10	4	5	10	5	7	11	67	
	TC	6	8	9	4	3	12	5	7	11	65	
	TM	7	8	9	3	3	10	5	7	11	63	

Quantitative description of trabecular structure

The calcaneus, talus, and first metatarsal have been thoroughly investigated in terms of bone mineral density, but the variation in three dimensional microstructure has not seen much detailed investigation until recently (Maga et al., 2006; Griffin et al., 2010b; DeSilva and Devlin, 2012; Su et al., 2013; Zeininger et al., 2016; Su and Carlson, 2017). Trabecular properties are calculated for each VOI and are discussed in a pooled sex and pooled population sample. The summary statistics of trabecular properties for the pooled sample of all populations and sexes are provided in Appendix 2.3. Repeated measures ANOVA was run to compare the VOIs to detect regional differences within each bone. Only individuals for whom all VOIs were present were included in the repeated-measures design. Pairwise comparisons were run with a Bonferroni adjustment after the initial ANOVA, but the corrected α remains at 0.05. Finally, Pearson correlations will be discussed between trabecular properties.

Result

Boxplots of the mean and standard deviation of trabecular properties in all VOIs are presented in Figure 2.6.

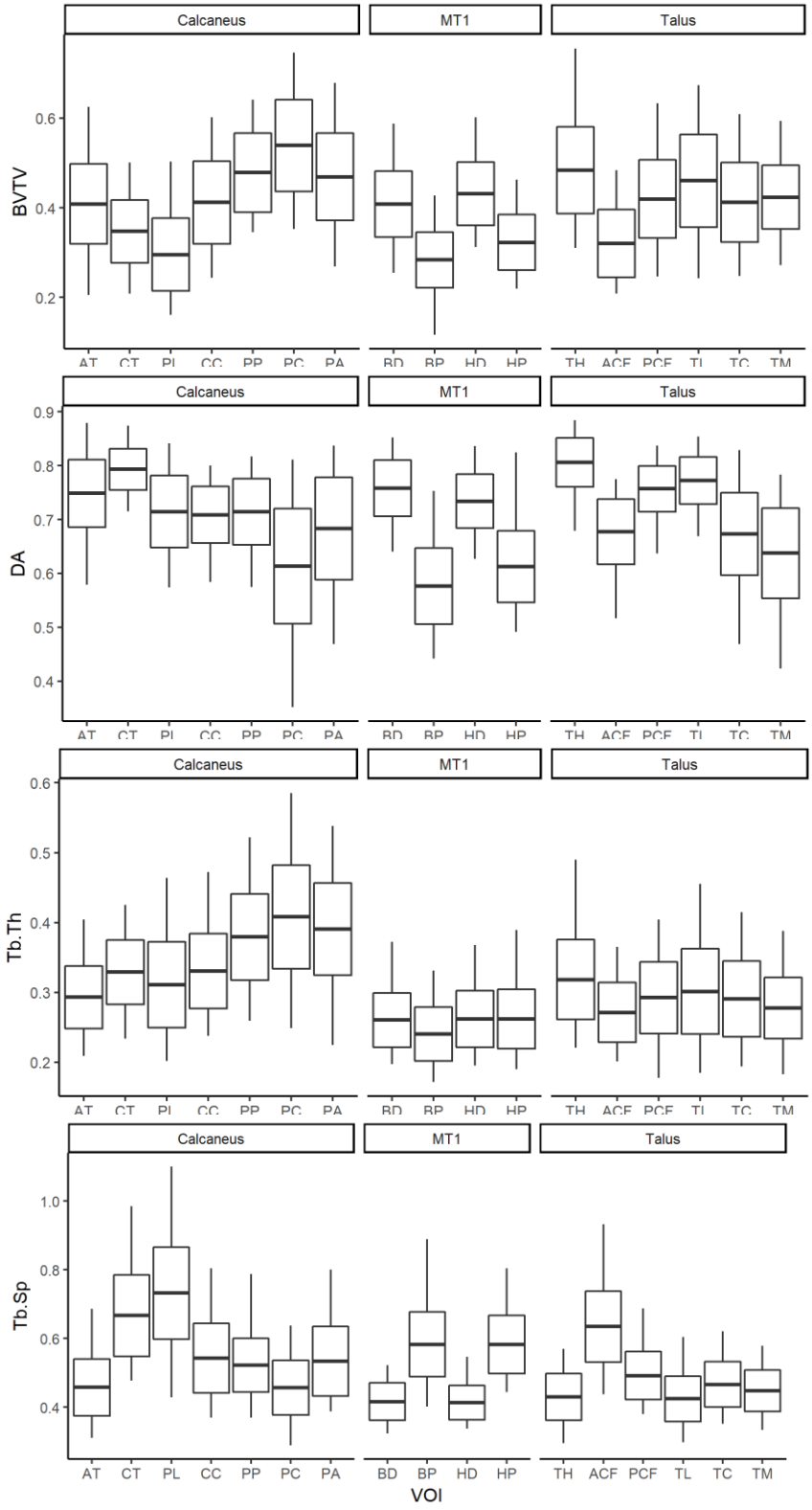

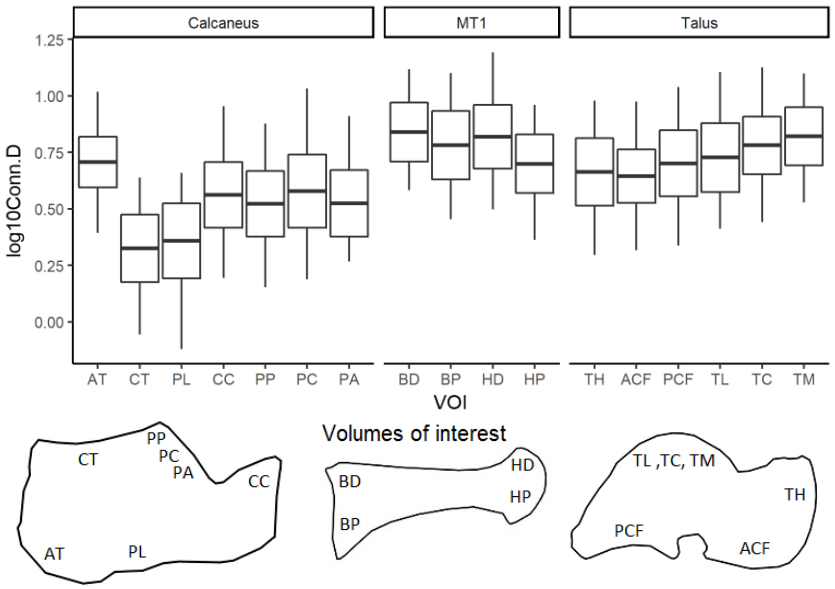

Figure 2.6. Boxplots of the mean and standard deviation of trabecular properties per volume of interest, whiskers represent maximum and minimum. Volumes of interest: Achilles tendon (AT), calcaneal tuber (CT), plantar ligaments (PL), posterior talar facet (PP: posterior, PC: central, PA: anterior), calcaneocuboid (CC), dorsal base (BD), plantar base (BP), dorsal head (HD), plantar head (HP), talar head (TH), anterior calcaneal facet (ACF), posterior calcaneal facet (PCF), trochlea (lateral: TL, central: TC, medial: TM).

Results of the repeated-measures ANOVA in the calcaneus are summarised in Table 2.2. There are substantial regional differences in BV/TV in the calcaneus. The highest BV/TV and Tb.Th are found in the posterior talar facet (PTF) VOIs with the central PTF having significantly greater BV/TV than all other VOIs. This is followed in BV/TV by the calcaneocuboid (CC) and Achilles tendon (AT) VOIs. The lowest BV/TV is found in the plantar ligament VOI which is significantly lower than all other VOIs. These results conform to predictions made in the previous section based on peak loading during gait. Peak forces during gait are highest in the PTF, followed by the CC and AT, and finally the PL.

The central posterior talar facet (PC) VOI has significantly higher BV/TV, thicker, and more isotropic trabeculae compared to all other calcaneal VOIs. It has the lowest Tb.Sp of all calcaneal VOIs, the only nonsignificant difference was with the Achilles tendon (AT) VOI. The three PTF VOIs contain significantly thicker trabeculae compared to the other VOIs. The three PTF VOIs have significantly higher Conn.D than the calcaneal tuber (CT) and plantar ligament (PL), and significantly lower Conn.D compared to the Achilles tendon. Trabecular in the central PTF are significantly more interconnected than those in the anterior or posterior PTF. No significant differences were found in any trabecular property between the anterior PTF (PA) and posterior PTF (PP) VOIs. Both VOIs contain the second highest BV/TV of the calcaneus and are significantly greater than all other VOIs except for the central PTF (PC).

The Achilles tendon (AT) VOI has an intermediate level of BV/TV which is significantly lower compared to the three PTF VOIs but higher compared to the calcaneal tuber and the plantar ligament

VOIS. The AT has the lowest Tb.Th of all calcaneal VOIs, significantly lower than all except the plantar ligament VOI. The Achilles tendon has a moderately anisotropic structure which is significantly more anisotropic than the PTF, PL and CC VOIs. The AT VOI has significantly higher Conn.D compared to all other VOIs and has trabecular separation that is significantly lower than all VOIs except for PC.

The calcaneocuboid (CC) has an intermediate level of BV/TV, similar to the AT VOI. The trabeculae are significantly thicker than those in the AT and thinner than those in the posterior talar facet. The CC VOI contains significantly more anisotropic trabeculae than the PC VOI and significantly less anisotropic than the AT and CT VOIs. The CC VOI has significantly widely spaced trabeculae compared to the AT and PC VOI and significantly more closely spaced and more interconnected than the CT and PL VOIs.

The plantar ligament (PL) VOI has significantly lower BV/TV than all other calcaneal VOIs, and significantly thinner struts compared to the PTF VOIs. The PL VOI contains significantly more anisotropic trabeculae than the PC and less than the CT. The PL VOI has the most highly separated trabeculae of all calcaneal VOIs, significantly different than all except for the calcaneal tuber. Trabecular in the PL are significantly less interconnected than all except for the CT VOI.

The calcaneal tuber (CT) has low BV/TV but the most anisotropic structure of all calcaneal VOIs. It contains significantly greater BV/TV than the PL but significantly lower BV/TV compared to all other calcaneal VOIs. Trabecular thickness is intermediate relative to other VOIs and significantly lower than the PTF. The trabeculae in the tuber are weakly interconnected and widely separated resulting in low BV/TV. Conn.D is significantly lower and Tb.Sp is significantly higher than all VOIs except for the PL.

Table 2.2. Repeated measures ANOVA of calcaneal trabecular properties between VOIs in a pooled sex, pooled population sample.

Calcaneus		N	Mean	SD	SE	F	Significant pairwise comparisons
BV/TV	Achilles tendon (AT)	48	0.408	0.087	.012	1287.248	>CT,PL <PA,PC,PP
	Calcaneocuboid (CC)	48	0.409	0.087	.013		>CT,PL <PA,PC,PP
	Calcaneal tuber (CT)	48	0.346	0.073	.010		>PL <AT,CC,PA,PC,PP
	PTF anterior (PA)	48	0.476	0.102	.015		>AT,CC,CT,PL <PC
	PTF central (PC)	48	0.546	0.107	.015		>AT,CC,CT,PA,PP,PL <
	PTF posterior (PP)	48	0.474	0.086	.012		>AT,CC,CT,PL <PC
	Plantar ligament (PL)	48	0.299	0.085	.012		> <AT,CC,CT,PA,PC,PP
Tb.Th	Achilles tendon (AT)	48	0.289	0.042	.006	2088.423	> < CC,CT,PA,PC,PP
	Calcaneocuboid (CC)	48	0.328	0.050	.007		>AT <PA,PC,PP
	Calcaneal tuber (CT)	48	0.332	0.046	.007		>AT <PA,PC,PP
	PTF anterior (PA)	48	0.393	0.071	.010		>AT,CC,CT,PL <PC
	PTF central (PC)	48	0.409	0.077	.011		>AT,CC,CT,PA,PP,PL <
	PTF posterior (PP)	48	0.374	0.061	.009		>AT,CC,CT, PL < PC
	Plantar ligament (PL)	48	0.314	0.063	.009		>AT <PA,PC,PP
DA	Achilles tendon (AT)	48	0.760	0.063	.009	15275.357	>CC,PA,PC,PP,PL <CT
	Calcaneocuboid (CC)	48	0.708	0.055	.008		>PC <AT,CT
	Calcaneal tuber (CT)	48	0.797	0.036	.005		>AT,CC,PA,PC,PP,PL <
	PTF anterior (PA)	48	0.686	0.099	.014		>PC <AT,CT,
	PTF central (PC)	48	0.610	0.106	.015		> <AT,CC,CT,PA,PP,PL
	PTF posterior (PP)	48	0.712	0.064	.009		>PC <AT,CT
	Plantar ligament (PL)	48	0.721	0.065	.009		>PC <AT,CT
Tb.Sp	Achilles tendon (AT)	47	.452	.083	.012	1758.159	> <CC,CT,PA,PP,PL
	Calcaneocuboid (CC)	47	.537	.100	.015		>AT,PC <CT,PL
	Calcaneal tuber (CT)	47	.667	.126	.018		>AT,CC,PA,PC,PP <PL
	PTF anterior (PA)	47	.525	.105	.015		>AT,PC <CT,PL
	PTF central	47	.449	.082	.012		>

	(PC)						<CC,CT,PA,PP,PL
	PTF posterior (PP)	47	.519	.082	.012		>AT,PC <CT,PL
	Plantar ligament (PL)	47	.731	.145	.021		>AT,CC,CT,PA,PC,PP <
Conn.D	Achilles tendon (AT)	48	5.230	1.423	.205	502.597	>CC,CT,PA,PC,PP,PL <
	Calcaneocuboid (CC)	48	3.926	1.492	.215		>CT,PL <AT
	Calcaneal tuber (CT)	48	2.226	0.830	.120		> <AT,CC,PA,PC,PP
	PTF anterior (PA)	48	3.572	1.423	.205		>CT,PL <AT
	PTF central (PC)	48	4.136	1.797	.259		>CT,PA,PP,PL <AT
	PTF posterior (PP)	48	3.661	1.278	.184		>CT,PL <AT,PC
	Plantar ligament (PL)	48	2.419	0.927	.134		> <AT,CC,PA,PC,PP

Results for the repeated-measures ANOVA in the first metatarsal are presented in Table 2.3. The dorsal VOI of the base (BD) has the second highest BV/TV, significantly greater than both plantar VOIs. The dorsal base contains significantly thicker trabeculae compared to the plantar base (BP), and significantly more widely spaced and more interconnected relative to both plantar VOIs.

The plantar base (BP) VOI contained significantly lower BV/TV, as well as thinner and more isotropic trabeculae compared to all other VOIs. Trabeculae are significantly more widely separated than both dorsal VOIs and significantly more interconnected than the plantar head (HP) and less interconnected than the dorsal base VOI.

The dorsal head (HD) VOI has the highest mean BV/TV of all VOIs, significantly greater than the plantar head and base VOIs. Trabeculae are significantly less anisotropic than both plantar VOIs. The struts are significantly thicker than those in the plantar base VOI. The HD trabeculae are significantly more interconnected than those in the plantar head and significantly less widely separated than those of the plantar base and head.

The plantar head (HP) has significantly higher BV/TV, Tb.Th, and DA than the plantar base, but significantly lower BV/TV and DA compared to the dorsal VOIs. Trabeculae in the plantar head are significantly more widely spaced apart compared to the dorsal VOIs and significantly less interconnected than all other VOIs.

Table 2.3. Repeated measures ANOVA of first metatarsal trabecular properties between VOIs in a pooled sex, pooled population sample.

First metatarsal		N	Mean	S.D.	S.E.	F	Significant pairwise comparisons
BV/TV	MT1 base dorsal (BD)	45	.398	.071	.011	160.926	>BP,HP
	MT1 base plantar (BP)	45	.280	.062	.009		<BD,HD,HP
	MT1 head dorsal (HD)	45	.408	.059	.009		>BP,HP
	MT1 head plantar (HP)	45	.313	.058	.009		>BP<BD,HD
Tb.Th	MT1 base dorsal (BD)	45	.253	.035	.005	9.233	>BP
	MT1 base plantar (BP)	45	.237	.038	.006		<BD,HD,HP
	MT1 head dorsal (HD)	45	.249	.031	.005		>BP
	MT1 head plantar (HP)	45	.253	.034	.005		>BP
DA	MT1 base dorsal (BD)	44	.757	.053	.008	142.051	>BP,HP
	MT1 base plantar (BP)	44	.577	.070	.011		<BD,HD,HP
	MT1 head dorsal (HD)	44	.744	.048	.007		>BP,HP
	MT1 head plantar (HP)	44	.616	.067	.010		>BP<BD,HD
Tb.Sp	MT1 base dorsal (BD)	45	.418	.056	.007	147.559	<BP,HP
	MT1 base plantar (BP)	45	.583	.097	.014		>BD,HD
	MT1 head dorsal (HD)	45	.421	.051	.007		<BP,HP
	MT1 head plantar (HP)	45	.587	.086	.012		>BD,HD
Conn.D	MT1 base dorsal (BD)	45	7.478	2.166	.323	23.851	>BP,HP
	MT1 base plantar (BP)	45	6.499	2.332	.348		>HP<BD
	MT1 head dorsal (HD)	45	7.151	2.371	.353		>HP
	MT1 head plantar (HP)	45	5.340	1.620	.242		<BD,BP,HD

Results for the repeated-measures ANOVA in the talus are presented in Table 2.4. The anterior calcaneal facet (ACF) has significantly lower BV/TV with more widely separated struts compared to all talar VOIs. The ACF has significantly thinner struts compared to the talar head (TH) and the lateral trochlea (TL), but thicker struts than the medial trochlea. The ACF has significantly more isotropic trabeculae than the posterior calcaneal facet (PCF), talar head (TH), and lateral trochlea (TL). The structure is significantly less interconnected than all but the talar head.

The posterior calcaneal facet (PCF) has significantly greater BV/TV than the ACF but significantly lower than the talar head (TH). The PCF has significantly thinner trabeculae than the talar head but thicker trabeculae compared to the medial trochlea. The PCF VOI contains a significantly more anisotropic structure than the ACF, TC, and TM, and significantly lower DA compared to the TH and TL. The PCF has significantly more widely spaced trabecular than the three trochlea VOIs, but less widely spaced compared to the ACF. Connectivity density is significantly lower in the PCF compared to the three trochlea VOIs, but significantly greater than the ACF and TH.

The talar head (TH) VOI contains the highest BV/TV, has significantly thicker trabeculae, and more anisotropic structure compared to all other VOIs. Trabeculae are significantly less widely spaced compared to the ACF, PCF and TC, and significantly less interconnected than the PCF and the three trochlear VOIs.

The lateral trochlea (TL) VOI has higher BV/TV than the ACF. The lateral trochlea has thicker trabeculae relative to the medial and central trochlea. The TL contains a significantly more anisotropic structure compared to the ACF, PCF, TM, and TC, but significantly more isotropic than the TH. Trabeculae in the TL are significantly less separated compared to the PCF, ACF, and the other two trochlear VOIs. The structure is significantly less interconnected than the TM, but significantly more interconnected compared the ACF, PCF, and TH.

The central trochlea (TC) has significantly greater BV/TV ratio than the ACF and significantly lower than the TH. The central trochlea has thicker struts than the medial trochlea, but thinner than the lateral trochlea and talar head. The TC VOI has significantly lower DA, but significantly greater Conn.D compared to the PCF, TH, and TL. It has significantly more widely spaced structure than the TH and TL VOIs, but significantly less so than the ACF and TC.

The medial trochlea (TM) VOI has significantly greater BV/TV than the ACF but significantly lower than the TH. The TM VOI contains significantly thinner struts compared to all other VOIs. It has a significantly more isotropic structure compared to the PCF, TH, and TL. The trabeculae are significantly less widely spaced than the ACF, PCF and TC, but more so than the TL. Trabeculae in the TM are significantly more interconnected than all other VOIs.

Table 2.4. Repeated measures ANOVA of talar trabecular properties between VOIs in a pooled sex, pooled population sample.

Talus		N	Mean	S.D.	S.E.	F	Significant pairwise comparisons
BVTV	Anterior calcaneal facet (ACF)	58	.345	.071	.009	53.70	> <PCF,TH,TL,TC,TM
	Posterior calcaneal facet (PCF)	58	.411	.079	.010		>ACF <TH
	Talus head (TH)	58	.466	.080	.011		>ACF,PCF,TC,TM <
	Trochlea lateral (TL)	58	.453	.087	.011		>ACF <
	Trochlea central (TC)	58	.400	.073	.010		>ACF <TH,
	Trochlea medial (TM)	58	.410	.060	.008		>ACF <TH
Tb.Th	Anterior calcaneal facet (ACF)	58	.285	.051	.007	16.94	>TM <TH,TL
	Posterior calcaneal facet (PCF)	58	.292	.053	.007		>TM <TH
	Talus head (TH)	58	.314	.056	.007		>ACF,PCF,TL,TC,TM <
	Trochlea lateral (TL)	58	.298	.054	.007		>ACF,TC,TM <TH
	Trochlea central (TC)	58	.285	.048	.006		>TM <TH,TL
	Trochlea medial (TM)	58	.274	.043	.006		> <ACF,PCF,TH,TL,TC
DA	Anterior calcaneal facet (ACF)	58	.674	.088	.012	40.64	>~~TM~~ <PCF,TH,TL
	Posterior calcaneal facet (PCF)	58	.719	.075	.010		>ACF,TC,TM <TH,TL
	Talus head (TH)	58	.786	.064	.008		>ACF,PCF,TL,TC,TM <
	Trochlea lateral (TL)	58	.740	.080	.010		>ACF,PCF,TC,TM <TH
	Trochlea central (TC)	58	.653	.091	.012		> <PCF,TH,TL
	Trochlea medial (TM)	58	.645	.074	.010		> <~~ACF,~~PCF,TH,TL
Tb.Sp	Anterior calcaneal facet (ACF)	58	.621	.095	.012	131.35	>PCF,TH,TL,TC,TM <
	Posterior calcaneal facet (PCF)	58	.514	.088	.012		>TH,TL,TM <ACF
	Talus head (TH)	58	.460	.090	.012		> <ACF,PCF,TC
	Trochlea lateral (TL)	58	.441	.076	.010		> <ACF,PCF,TC,TM
	Trochlea central (TC)	58	.494	.098	.013		>TH,TL <ACF,TC
	Trochlea medial (TM)	58	.475	.093	.012		>TL <ACF,PCF,TC
Conn.D	Anterior calcaneal facet (ACF)	58	4.353	1.605	.211	38.80	> <PCF,TL,TC,TM

	Posterior calcaneal facet (PCF)	58	5.208	2.140	.281	>ACF,TH <TL,TC,TM
	Talus head (TH)	58	4.526	1.836	.241	> <PCF,TL,TC,TM
	Trochlea lateral (TL)	58	5.670	2.371	.311	>ACF,PCF,TH <TM
	Trochlea central (TC)	58	5.982	2.341	.307	>ACF,PCF,TH <TM
	Trochlea medial (TM)	58	6.516	2.585	.339	>ACF,PCF,TH,TC,TL <

Discussion

Calcaneus

Overall, the results from the calcaneus conform to the predictions made based on biomechanical data and finite element analyses, where the VOIs placed in locations subjected to the highest strains also contained the highest BV/TV and Tb.Th. It was predicted that the PTF VOIs would contain the highest BV/TV and Tb.Th, as well as the lowest Tb.Sp and Conn.D. The highest BV/TV and Tb.Th, and low Tb.Sp were indeed found in the three PTF VOIs, but not the lowest level of Conn.D. The highest calcaneal BV/TV is found in the central PTF VOI. This can be explained by the observation that the PP VOI is more strongly loaded during plantarflexion, and the anterior PTF is more strongly loaded during dorsiflexion. However, the central PTF is loaded during the entire stance phase. This may also explain the significantly lower DA in PC compared to the PP and PA VOIs, as the PC is loaded from different directions during plantarflexion and dorsiflexion which results in a more generalized isotropic structure. The prediction that BV/TV and Tb.Th of the AT and CC VOIs would be lower than the PTF but higher than the PL was also correct. The relatively low BV/TV of the calcaneal tuber VOI was not predicted. The tuber VOI contains the highest DA and relatively thick struts, high trabecular separation, and low connectivity. This indicates that the structure of the tuber is adapted to loading from a single direction, which may reduce the need of a high BV/TV ratio, in this case transferring the load from the posterior talar facet to through the tuber.

The degree of anisotropy was generally very high in the calcaneus with all but the PC and PA VOIs falling between 0.7 and 0.8. This indicates that most of the trabecular inside the chosen VOIs are adapted to primarily resist unidirectional loadings. The posterior talar facet VOIs have the most isotropic structure, consistent with their more varied loading directions during gait.

Pearson correlation coefficients were calculated between all trabecular properties (Table 2.5). All properties are shown to correlate significantly with each other. These correlations were performed on a pooled sample of all calcaneal VOIs. The strongest correlations are found between BV/TV, and Tb.Th and Tb.Sp. The patterns seen throughout the calcaneal VOIs in BV/TV and Tb.Sp mirror one another (Figure 2.6), which is consistent with the strong negative correlation reported in Table 2.5. The patterns observed throughout the calcaneal VOIs of BV/TV and Tb.Th are very similar, except in the Achilles tendon which has low Tb.Th relative to BV/TV. Instead the high BV/TV in the AT is likely a

result of an increase in the number of trabeculae, as shown by the high level of Conn.D and low Tb.Sp. A strong correlation was also found between Conn.D and Tb.Sp indicating that as the number of connections per unit volume increases, the average distance between trabeculae decreases. This relationship is also clearly observed in the patterns throughout the calcaneus where Conn.D and Tb.Sp are almost mirror images (Figure 2.6). The weakest correlations were found between BV/TV, Conn.D, and DA. BV/TV and DA were negatively correlated indicating that in the calcaneus with increasing BV/TV comes a lower DA. It is likely that the results presented in Table 2.5 are not entirely representative as they are calculated by pooling different VOIs which experience different mechanical environments. As discussed before, the high BV/TV and low DA of the PC VOI can be explained through the loading imposed on the VOI. The same can be said for the high DA and low BV/TV in the CT and PL VOIs. When the correlations are run on individual VOIs correlations between BV/TV and DA are often not significant. Inspection of individual VOIs shows that this significant negative correlation is driven by local differences in loading conditions rather than underlying structural rules of bone modelling. BV/TV is high and DA low in the three posterior talar facet VOIs compared to the others because of joint function. However, strong correlations are repeatedly found between BV/TV and Tb.Th and Tb.Sp, as well as between Conn.D and Tb.Sp in pooled as well as individual VOIs.

Table 2.5. Pearson correlation coefficients between trabecular properties in a sample of pooled calcaneus VOIs and populations.

		BV/TV	Tb.Th	DA	Tb.Sp
Calcaneus					
Tb.Th	Pearson Correlation	.829			
	p (2-tailed)	.000			
	N	466			
DA	Pearson Correlation	-.310	-.225		
	p (2-tailed)	.000	.000		
	N	465	465		
Tb.Sp	Pearson Correlation	-.769	-.356	.294	
	p (2-tailed)	.000	.000	.000	
	N	465	465	464	
Conn.D	Pearson Correlation	.112	-.347	-.334	-.603
	p (2-tailed)	.015	.000	.000	.000
	N	466	466	465	465

Talus

It was predicted that in general all VOIs in the talus would contain high levels of BV/TV and Tb.Th, and low Tb.Sp and Conn.D, and that the ACF would contain the lowest BV/TV. The highest levels of DA were predicted to be in the TH and the PCF VOIs, and the lowest DA was predicted to be found in the trochlear VOIs and the ACF. It was predicted that of the three trochlear VOIs, the lateral VOI would contain the highest BV/TV ratio.

High levels of BV/TV were indeed found in all talar VOIs with ACF containing significantly lower BV/TV compared to the other VOIs. The highest BV/TV was found in the talar head which was significantly greater than all VOIs except the lateral trochlea. As predicted, the lateral trochlea contained higher mean BV/TV compared to the central and medial VOIs, but this difference was not significant.

The talar head has highest BV/TV and the highest DA of all the 17 foot VOIs, indicating that the talar head is subjected to high unidirectional loading. Following predictions, relatively isotropic trabeculae were found in the ACF as a result of multidirectional loading at this location. The lateral trochlea VOI contains significantly more anisotropic trabeculae compared to the medial and central VOI. DA in the medial and lateral trochlea is also more variable than in the lateral trochlea, shown by the substantially larger standard deviations. This suggests that loading is less varied in the lateral trochlea compared to the central and medial side.

Similarly to the calcaneus, Tb.Th follows the same pattern throughout the talus as BV/TV as a result of the high positive correlation between these two variables (Figure 2.6, Table 2.6). Tb.Sp mirrors the pattern of BV/TV and is strongly negatively correlated with BV/TV. This shows the predictable result than with increasing BV/TV comes through an increase in the thickness of trabeculae, which reduces the average distance between trabeculae. A strong negative correlation was observed between Tb.Th and Conn.D, but a substantially weaker negative correlation was found between BV/TV and Conn.D. Weak negative correlations were observed between DA and Conn.D and Tb.Sp, while weak positive correlations were found between DA and BV/TV and Tb.Th. This contradicts the results found in the calcaneus where DA was found to correlate negatively with BV/TV and Tb.Th, but positively with Tb.Sp. These contradictions likely result from the fact that they are calculated by pooling different VOIs which are under different mechanical adaptive pressures.

Table 2.6. Pearson correlation coefficients between trabecular properties in a sample of all talar VOIs in a pooled population sample.

Talus		**BV/TV**	**Tb.Th**	**DA**	**Tb.Sp**
Tb.Th	Pearson Correlation	.863			
	p (2-tailed)	.000			
	N	386			
DA	Pearson Correlation	.184	.136		
	p (2-tailed)	.000	.007		
	N	387	386		
Tb.Sp	Pearson Correlation	-.744	-.365	-.151	
	p (2-tailed)	.000	.000	.003	
	N	385	384	385	
Conn.D	Pearson Correlation	-.209	-.567	-.342	-.360
	p (2-tailed)	.000	.000	.000	.000
	N	387	386	387	385

First metatarsal

The dorsal first metatarsal VOIs of have significantly greater BV/TV and lower Tb.Sp than the plantar VOIs, conforming to predictions based on biomechanical data (Muehleman et al., 1999). Trabecular thickness was predicted to follow the same pattern throughout the MT1 as BV/TV., Instead, the plantar base VOI contained significantly thinner trabeculae compared to all other VOIs. Thus, in the MT1 the increase in BV/TV in the dorsal VOIs is not a result of thickening trabeculae but of decreasing the distance between trabeculae and an increase in Conn.D. It was additionally predicted that the VOIs in the head would contain greater BV/TV compared to the base. This prediction was met by the plantar head which contained significantly greater BV/TV than the plantar base. While the dorsal head did contain the highest mean BV/TV, it was not significantly different from the dorsal base.

It was predicted that the base would contain more anisotropic trabeculae due to its flat joint surface relative to the head, which was predicted to reduce possible variation in loading directions. The results did not meet this prediction as both dorsal VOIs contained significantly greater DA compared to the plantar VOIs, with the plantar base significantly being less anisotropic than all three other VOIs. Gefen (2002) showed in a finite element analysis of the whole foot during six stages of human gait and found that the dorsal portion of the metatarsals are most strenuously loaded during push-off. The highly anisotropic structure in the dorsal head may be the result of the short time frame during the push-off phase of gait where the metatarsal head is subjected to peak loading, resulting in high BV/TV in an anisotropic configuration.

Pearson correlation coefficients between first metatarsal trabecular properties are provided in Table 2.7. The strongest correlation was found between BV/TV and Tb.Sp, rather than Tb.Th as was found in the talus and calcaneus. When examining the patterns of variation throughout the MT1 (Figure 2.6), it can be seen that BV/TV and Tb.Sp are mirror images. Unlike in the talus and calcaneus, Tb.Th does not follow the same pattern as is found in BV/TV. The greater relative BV/TV in the dorsal compared to the plantar VOIs is driven by increases in the relative number of trabeculae (Conn.D) rather than increases in trabecular thickness. The strong correlation found between DA and BV/TV is a result of the pooling of all four VOIs. When examining VOIs individually the only significant correlation is found in the plantar head ($r=-.319$, $P=.02$, $N=53$) while the other VOIs are very poorly correlated.

Table 2.7. Pearson correlation coefficients between trabecular properties in a sample of pooled first metatarsal VOIs and populations.

MT1		BV/TV	Tb.Th	DA	Tb.Sp
Tb.Th	Pearson Correlation	.685			
	p (2-tailed)	.000			
	N	217			
DA	Pearson Correlation	.455	.120		
	p (2-tailed)	.000	.078		
	N	216	216		
Tb.Sp	Pearson Correlation	-.797	-.192	-.518	
	p (2-tailed)	.000	.004	.000	
	N	217	217	216	
Conn.D	Pearson Correlation	.096	-.504	-.004	-.534
	p (2-tailed)	.157	.000	.951	.000
	N	217	217	216	217

Relationships between trabecular properties throughout the foot

To assess how strongly trabecular properties are correlated in throughout the foot, coefficients of determination calculated as the mean of 17 VOIs are presented in Figure 2.7. If trabecular properties are strongly correlated, they would be expected to show similar patterns of variation throughout the foot. Coefficients of determination indicate that there is a very strong correlation between BV/TV and Tb.Th and Tb.Sp, but a very weak correlation with DA and Conn.D. Tb.Th is strongly correlated with Conn.D but not with DA or Tb.Sp. DA correlates only very weakly with all other trabecular properties, and most strongly with Conn.D. Tb.Sp correlates very strongly with BV/TV and less strongly with Conn.D. Conn.D Shows intermediate to weak correlations with all trabecular properties, the weakest correlation is found with BV/TV.

The strong coefficients of determination presented in Figure 2.7 suggest that BV/TV and Tb.Th should show similar patterns throughout all VOIs, while Tb.Sp should be a mirror image of BV/TV due to the strong negative correlations observed in tables 2.5 to 2.7. The observed patterns in trabecular thickness and BV/TV are not completely the same, but follow the same trend in many VOIs. Tb.Sp indeed appears as a mirror image of the BV/TV pattern throughout the 17 VOIs. The only exception is the dorsal MT1 base which contains lower Tb.Sp than would be predicted if Tb.Sp exactly mirrored BV/TV (see Figure 2.6). This low Tb.Sp appears to be a result of relatively high Conn.D, which is the highest of all 17 VOIs. The patterns observed in DA show little resemblance to the patterns observed for any other property, as would be expected based on the low coefficients of determination between DA and the other properties. Patterns in Conn.D equally showed little resemblance to the patterns observed in other properties, but most closely resembles a mirror image of Tb.Th. This would be expected from the significant negative correlations between Tb.Th and Conn.D, suggesting that when trabeculae thicken, they may merge together reducing the number of connections per unit volume. It is

interesting to note that while VOIs often obtain high BV/TV by thickening trabeculae (R^2=.71), other VOIs appear to do so through increased Conn.D. Significant differences are observed in BV/TV in the first metatarsal, despite relatively constant trabecular thickness throughout the four VOIs. In the first metatarsal BV/TV is driven by an increase in the relative number of trabeculae. The mechanisms that underlie how BV/TV is increased are not understood at present, and may be a consequence of loading conditions, growth and development, metabolic factors, bone morphology (presence/absence of cortical shaft), or genetics.

Variation in BV/TV and DA between VOIs generally conforms to predictions based on the biomechanical literature with more strenuously loaded locations within individual bones containing higher BV/TV ratios, and unidirectionally loaded regions containing anisotropic trabecular structures. In the calcaneus, trabecular thickness is higher and Conn.D lower compared to the talus and the MT1. Most VOIs were quite anisotropic with values between 0.7 and 0.8. The following chapters will examine variation within and between human populations, in the context of variation in body mass, sex, age, and habitual activity.

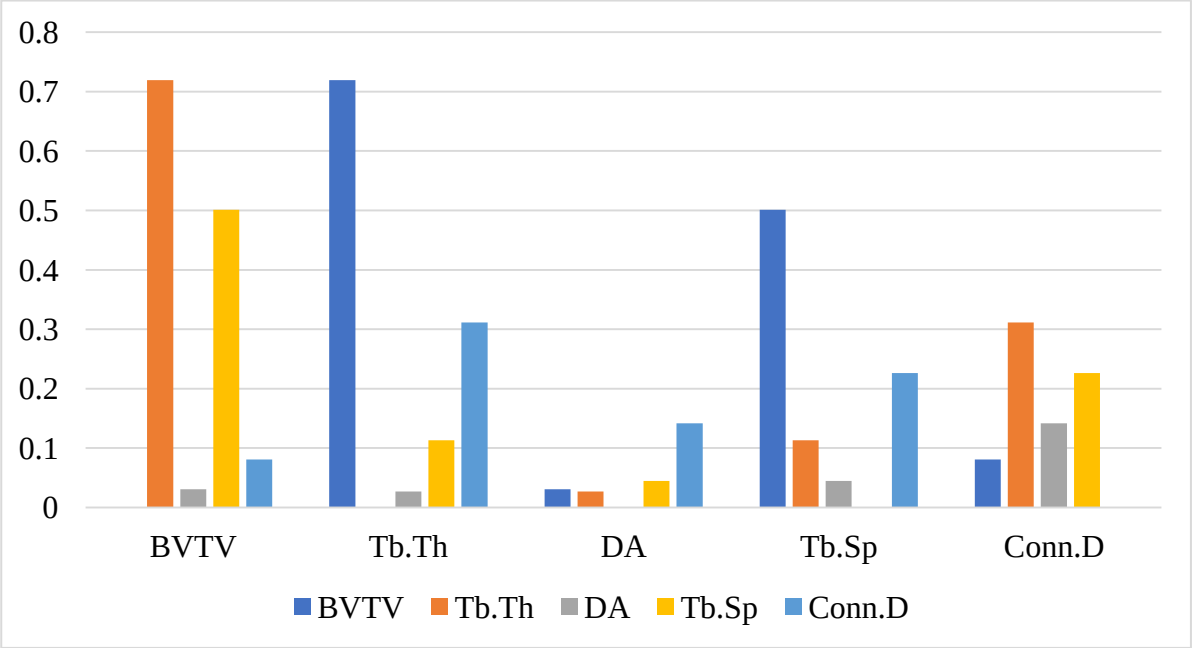

Figure 2.7. Mean coefficients of determination (R^2) between trabecular bone properties. Calculated as the mean of R^2 of all individual volumes of interest.

Chapter 3 - Body mass, bone dimensions, and trabecular bone properties

Introduction

Significant allometric scaling between body mass and trabecular architecture has been reported (Doube et al., 2011; Fajardo et al., 2013; Barak et al., 2013; Ryan and Shaw, 2013; Christen et al., 2015). The way forces travel through a bone will depend to some extent on its size and shape. Thus, it is expected that bone dimensions may affect the underlying trabecular structure. Before trabecular structure can be interpreted in the context of habitual behaviour, sex, age, or diet, the effects of body mass and bone dimensions need to be understood and accounted for if necessary. It is currently unknown if trabecular bone structure correlates more strongly with bone dimensions rather than body mass.

This chapter will explore correlations between trabecular structural properties and body mass, and linear bone dimensions. The objective is to determine which of these aspects of individual variation has a significant effect on underlying trabecular structure. If a significant relationship between body mass and/or bone dimensions is demonstrated, the variable can be corrected for in subsequent analyses to obtain a clearer image of other potential sources of variation such as habitual behaviour, sex, and age.

Materials and methods

This chapter uses coefficients of determination (R^2) to examine the variance in trabecular properties explained by body mass and linear bone dimensions (Figure 3.1 and Appendix 3.1). Coefficients of determination between body mass and bone dimensions, and trabecular properties are calculated pairwise in a pooled sex and population sample, as well as for separate populations (sample size in Table 3.1). Correlations are calculated using the linear bone dimensions and body mass estimates provided in Appendix 3.2, and in volumes of interest defined in Chapter 2. For regressions between body mass and trabecular properties, see Chapter 4. Body mass was estimated based on femoral head dimensions using equations taken from the Ruff (1997). Femoral head superoinferior height was measured to the nearest hundredth of a millimetre using digital callipers.

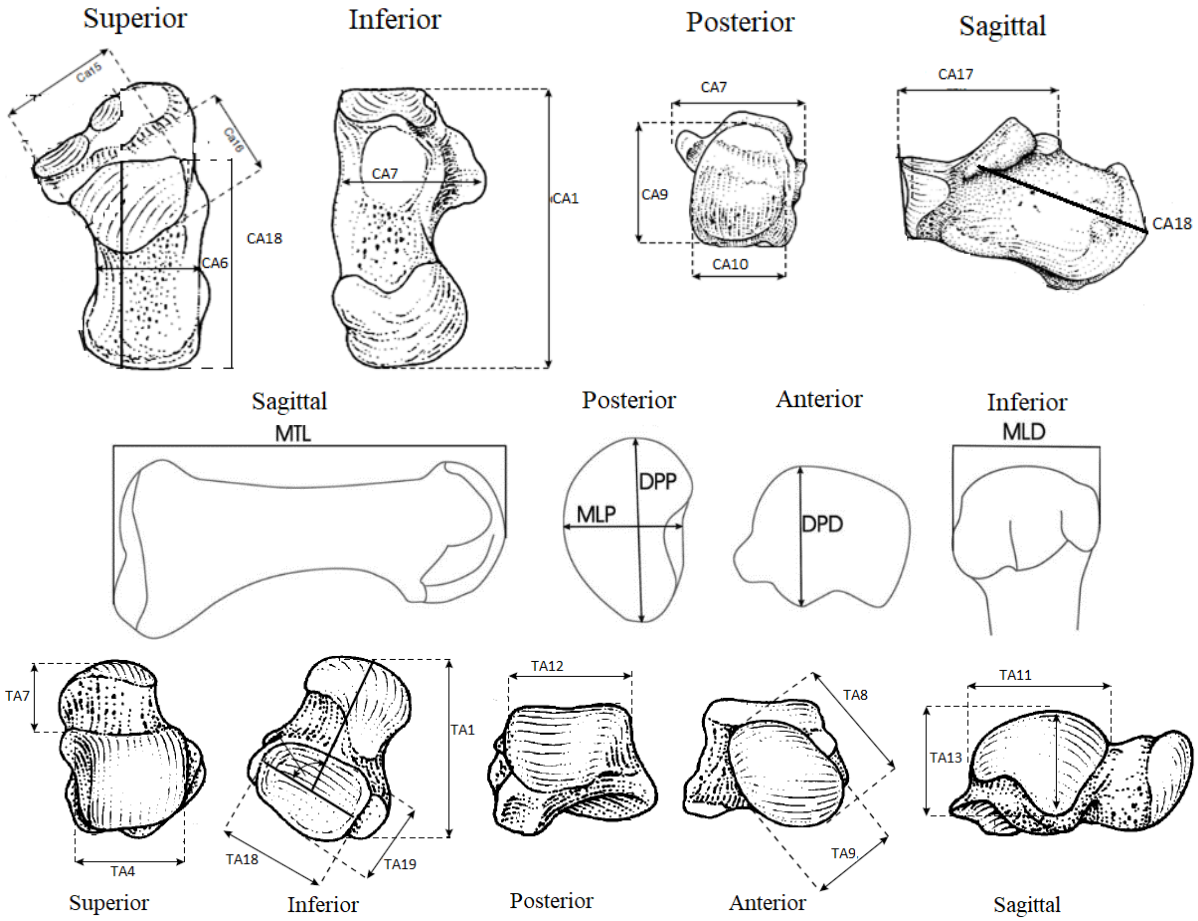

Figure 3.1. Linear bone dimensions used in this chapter in the calcaneus (top), first metatarsal (middle), and talus (bottom).

Table 3.1. Sample size used in this chapter for each population and sex per VOI. Achilles tendon (AT), calcaneal tuber (CT), plantar ligaments (PL), posterior talar facet (PP: posterior, PC: central, PA: anterior), calcaneocuboid (CC), dorsal base (BD), plantar base (BP), dorsal head (HD), plantar head (HP), talar head (TH), anterior calcaneal facet (ACF), posterior calcaneal facet (PCF), trochlea (lateral: TL, central: TC, medial: TM).

		Black Earth		**Jebel Moya**			**Kerma**		**St Johns**		**Total**
		Sex		**Sex**			**Sex**		**Sex**		
		M	**F**	**M**	**F**	**I**	**M**	**F**	**M**	**F**	
Calcaneus	AT	7	10	8	2	5	9	7	9	11	69
	CC	7	6	9	2	5	12	7	8	9	66
	CT	7	9	10	2	5	12	7	8	10	71
	PA	7	6	8	2	4	12	7	9	11	67
	PC	6	7	8	2	4	12	6	9	11	66
	PP	7	8	9	1	4	12	5	9	11	67
	PL	6	6	5	1	5	11	7	8	10	60
MT1	BD	7	8	5	2	2	9	5	9	9	56
	BP	6	7	2	2	1	9	4	9	9	49
	HD	8	9	5	3	3	9	4	9	9	59
	HP	7	7	4	2	2	9	4	9	9	53
Talus	ACF	5	8	5	2	3	13	7	8	11	62
	PCF	5	7	7	4	4	12	6	6	11	62
	TH	5	6	10	4	5	12	7	8	11	68
	TL	7	8	10	4	5	10	5	7	11	67
	TC	6	8	9	4	3	12	5	7	11	65
	TM	7	8	9	3	3	10	5	7	11	63

Hypotheses

There are significant correlations between all bone dimensions and body mass, except for the shape indices (Figure 3.2). Thus, a significant part of the explained variance between bone dimensions and trabecular properties is shared with body mass. Regardless, it is predicted that body mass will have the largest effect as it directly influences the magnitude of loading on the foot and is strongly correlated to bone size. Ryan and Shaw (2013) found strong correlations between femoral head height and Tb.Th, Tb.Sp, and Conn.D (R^2>.5), intermediate strength correlations with BV/TV (R^2=.36) and weak correlations with DA (R^2=.17) in the femoral head of 34 primate species. Thus, as body mass and linear bone dimensions are highly correlated, the strongest correlations are predicted to be found with Tb.Th, Tb.Sp, and Conn.D while weaker correlations are predicted to be found for BV/TV and DA.

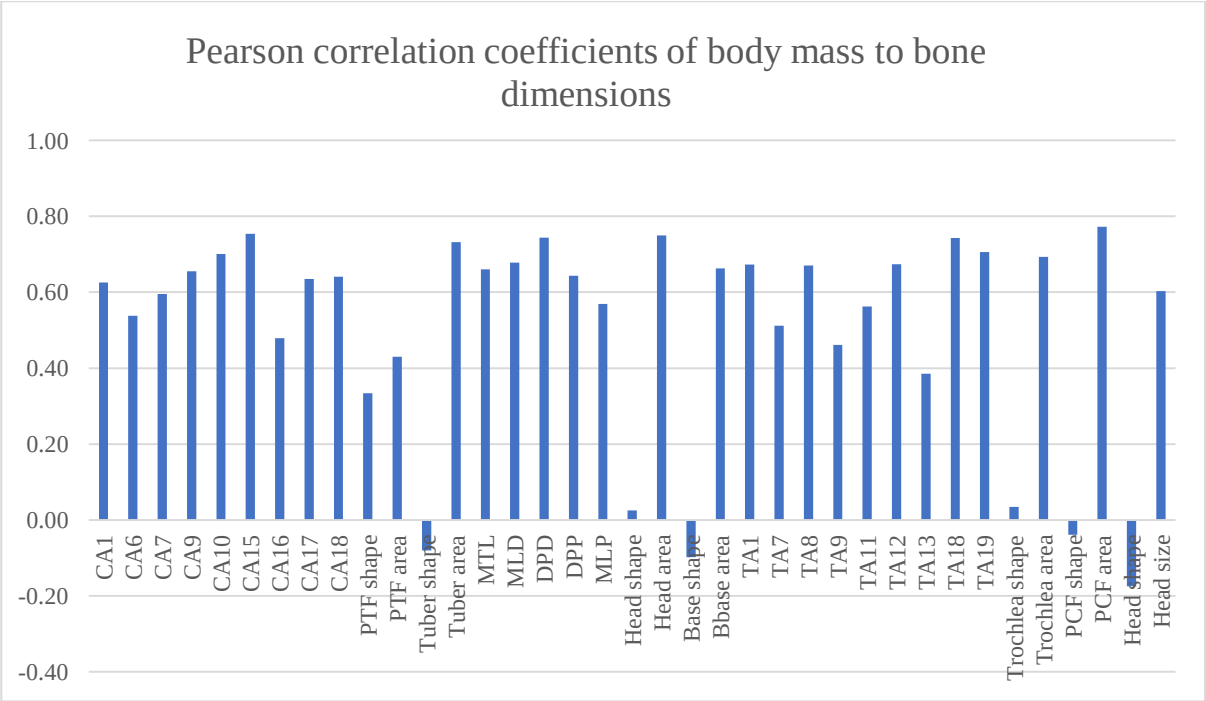

Figure 3.2. Pearson correlation coefficients between body mass and bone dimensions. For definitions of linear bone measurements see Figure 3.1.

Results

Differences in body mass and linear bone dimensions between populations are discussed in Appendix 3.2. No significant differences were found between populations in pooled sex body mass. The Black Earth males had lower mean body mass and the Jebel Moya females had significantly lower body mass compared to other populations. Significant differences are found between populations in external bone measurements in males, females, and pooled sex samples. No sex differences are found in the relationships between body mass, linear measurements, and trabecular properties, thus, pooled sex populations are for the rest of this chapter. Boxplots of the mean and standard deviation of body mass and linear bone dimensions used in this thesis are provided in Figure 3.3.

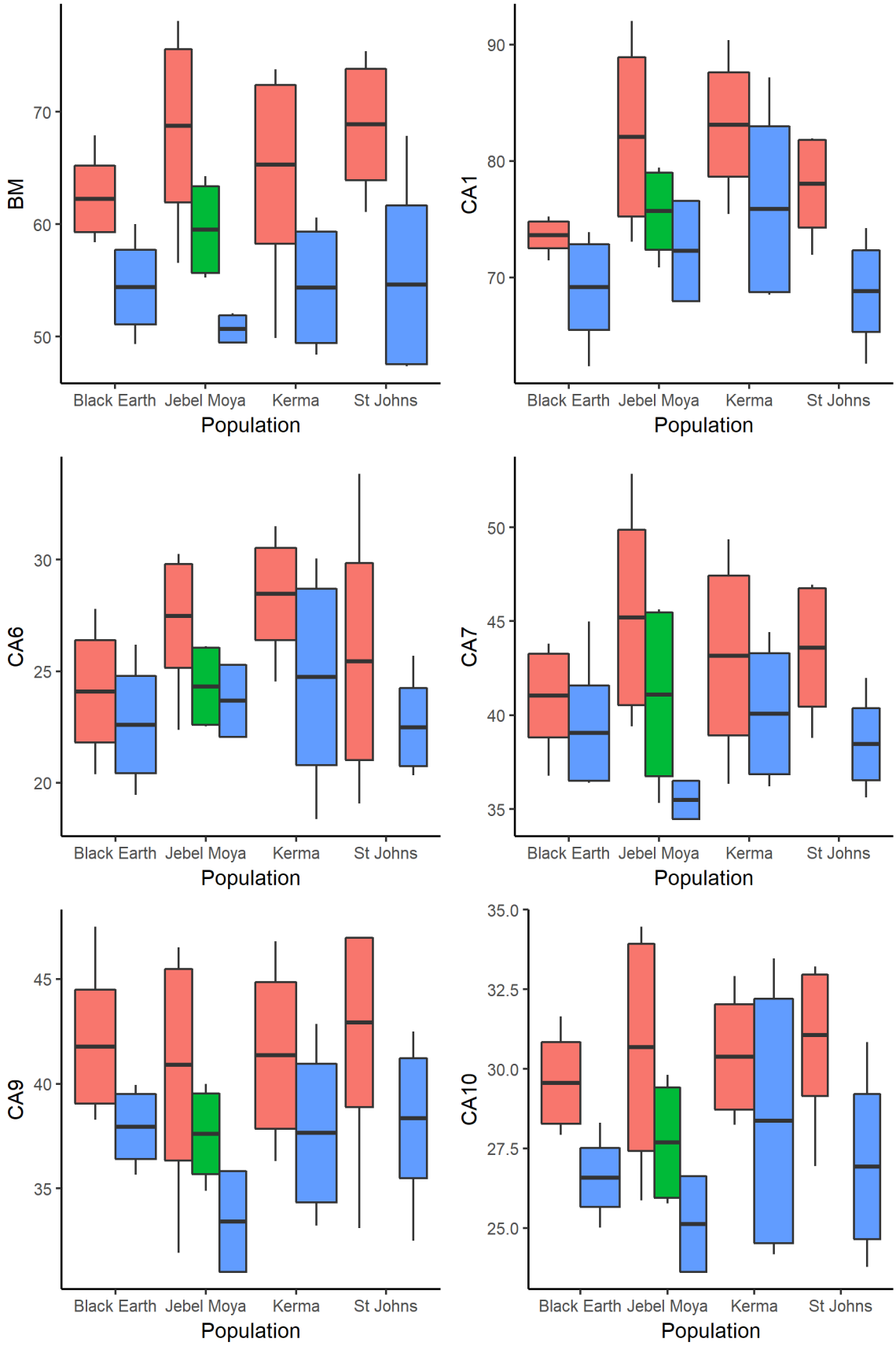
BM
70
60
50
Black Earth
Jebel Moya
Kerma
St Johns
Population
CA1
90
80
70
Black Earth
Jebel Moya
Kerma
St Johns
Population
CA6
30
25
20
Black Earth
Jebel Moya
Kerma
St Johns
Population
CA7
50
45
40
35
Black Earth
Jebel Moya
Kerma
St Johns
Population
CA9
45
40
35
Black Earth
Jebel Moya
Kerma
St Johns
Population
CA10
35.0
32.5
30.0
27.5
25.0
Black Earth
Jebel Moya
Kerma
St Johns
Population

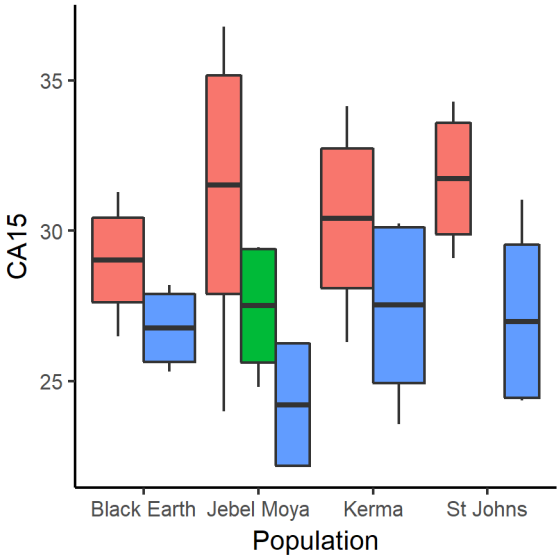
CA15
35
30
25
Black Earth
Jebel Moya
Kerma
St Johns
Population

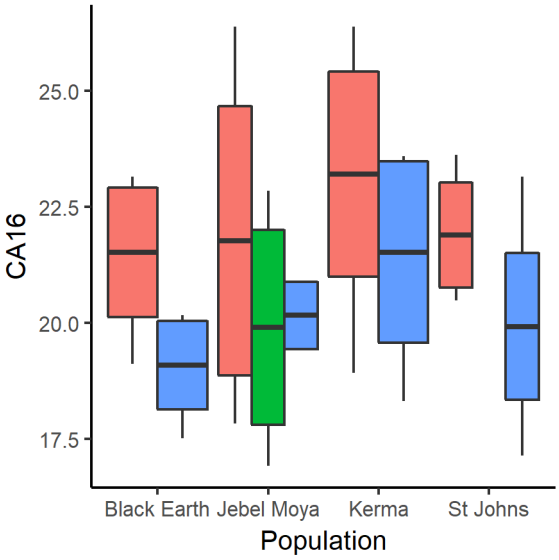
CA16
25.0
22.5
20.0
17.5
Black Earth
Jebel Moya
Kerma
St Johns
Population

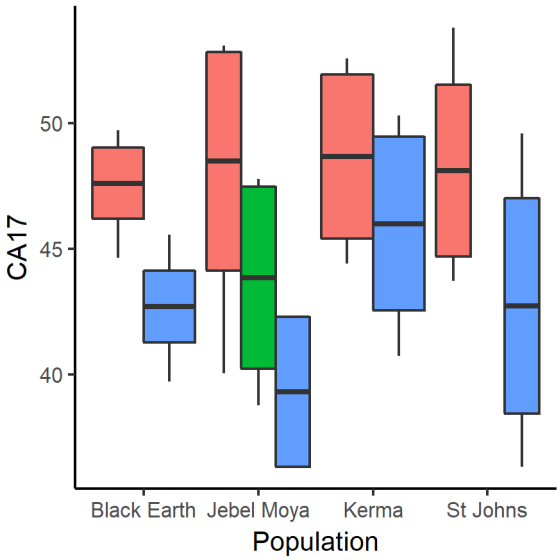
CA17
50
45
40
Black Earth
Jebel Moya
Kerma
St Johns
Population

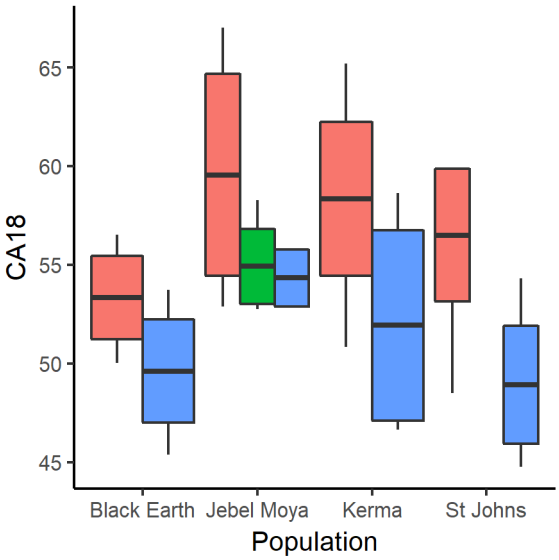
CA18
65
60
55
50
45
Black Earth
Jebel Moya
Kerma
St Johns
Population

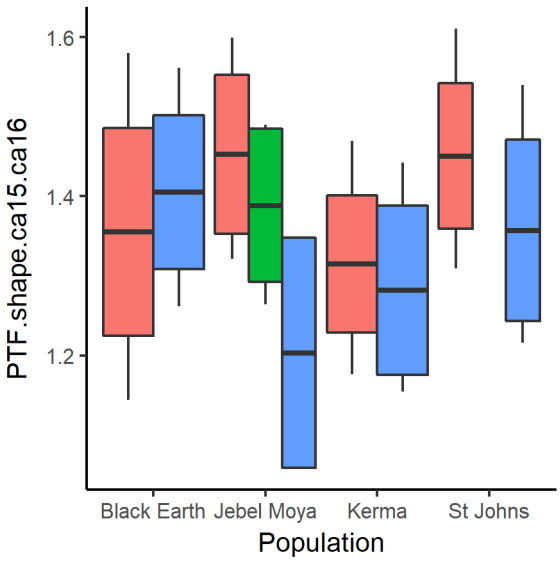
PTF.shape.ca15.ca16
1.6
1.4
1.2
Black Earth
Jebel Moya
Kerma
St Johns
Population

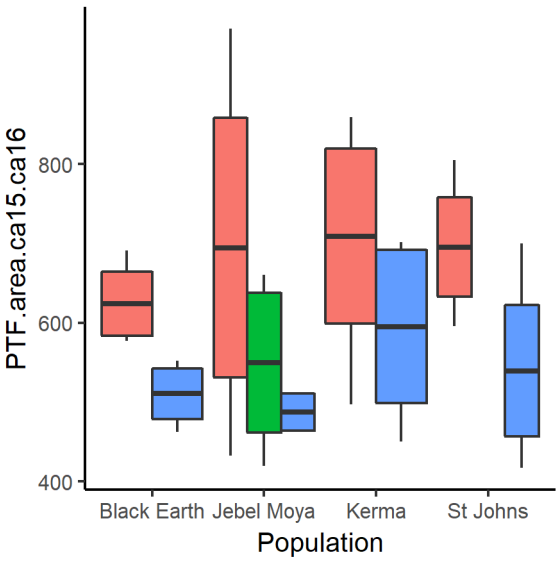
PTF.area.ca15.ca16
800
600
400
Black Earth
Jebel Moya
Kerma
St Johns
Population

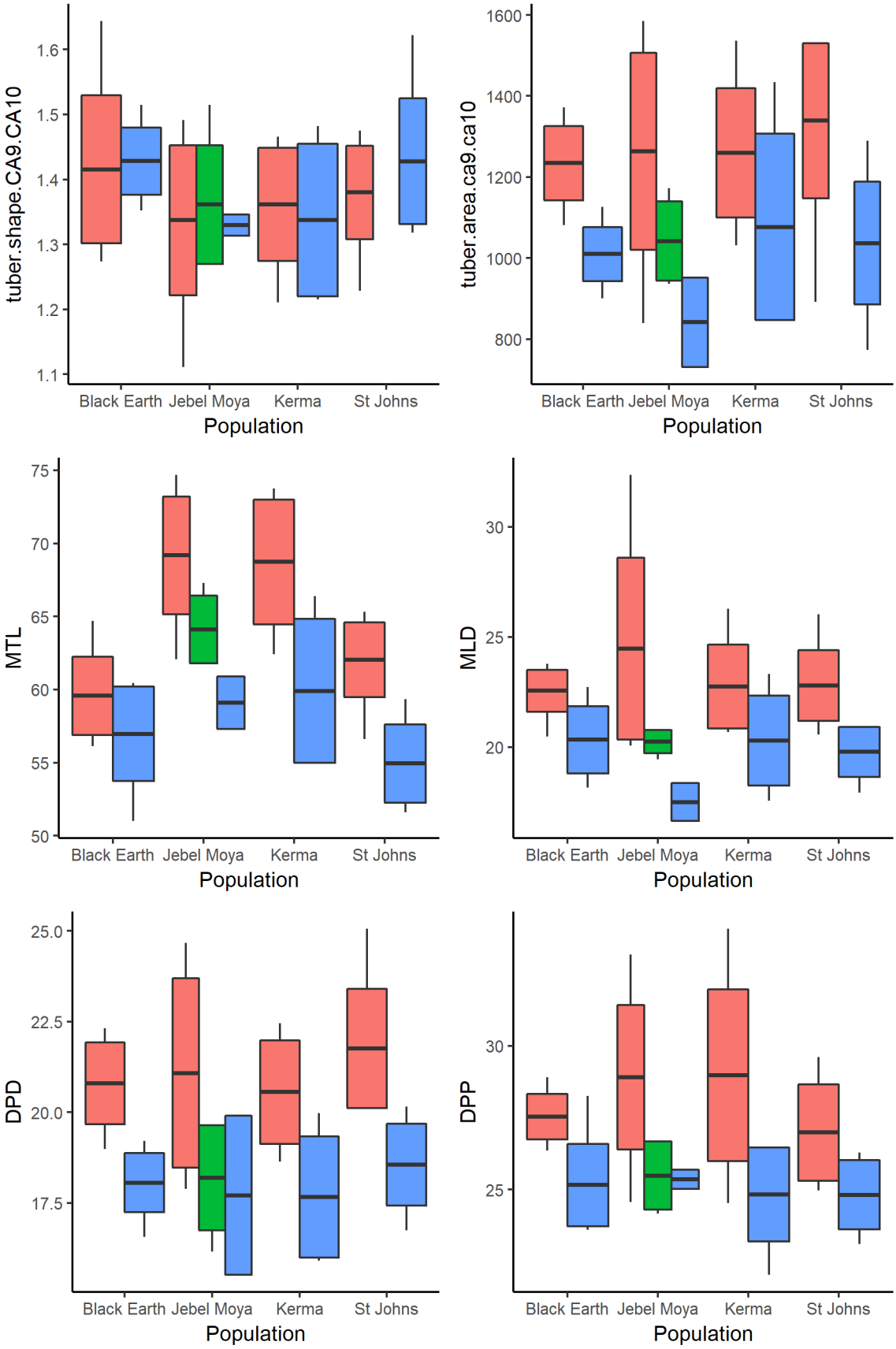
tuber.shape.CA9.CA10
1.6
1.5
1.4
1.3
1.2
1.1
Black Earth
Jebel Moya
Kerma
St Johns
Population
tuber.area.ca9.ca10
1600
1400
1200
1000
800
Black Earth
Jebel Moya
Kerma
St Johns
Population
MTL
75
70
65
60
55
50
Black Earth
Jebel Moya
Kerma
St Johns
Population
MLD
30
25
20
Black Earth
Jebel Moya
Kerma
St Johns
Population
DPD
25.0
22.5
20.0
17.5
Black Earth
Jebel Moya
Kerma
St Johns
Population
DPP
30
25
Black Earth
Jebel Moya
Kerma
St Johns
Population

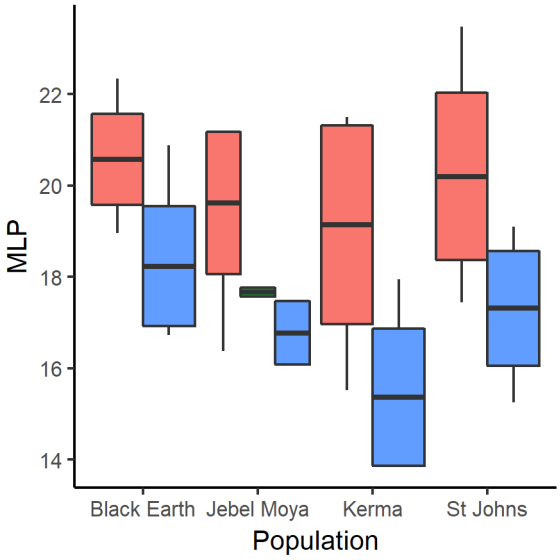
MLP
22
20
18
16
14
Black Earth
Jebel Moya
Kerma
St Johns
Population

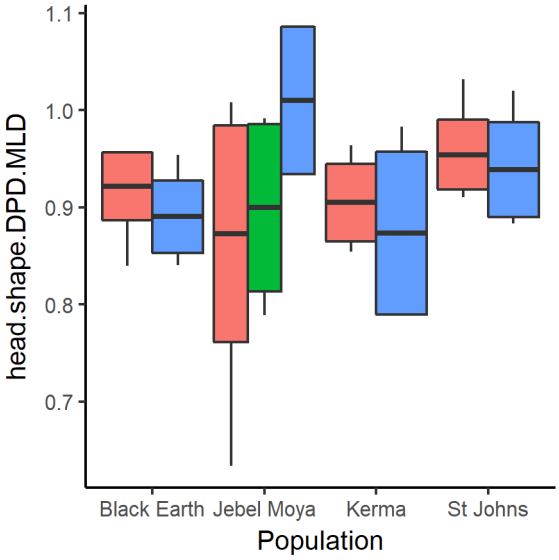
head.shape.DPD.MLD
1.1
1.0
0.9
0.8
0.7
Black Earth
Jebel Moya
Kerma
St Johns
Population

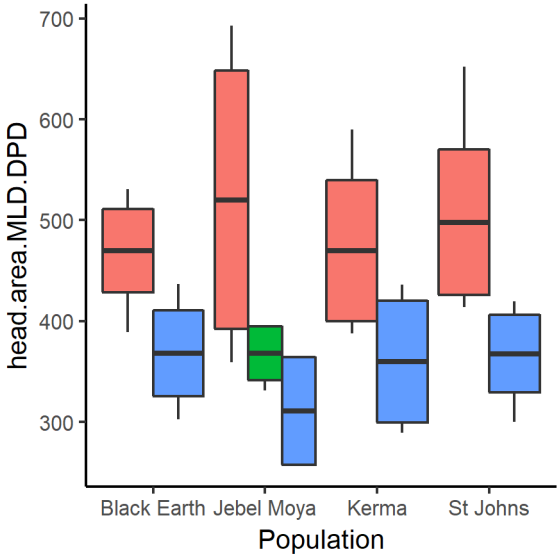
head.area.MLD.DPD
700
600
500
400
300
Black Earth
Jebel Moya
Kerma
St Johns
Population

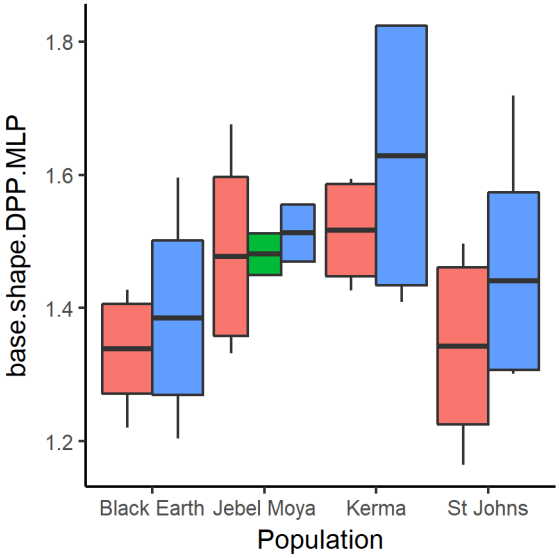
base.shape.DPP.MLP
1.8
1.6
1.4
1.2
Black Earth
Jebel Moya
Kerma
St Johns
Population

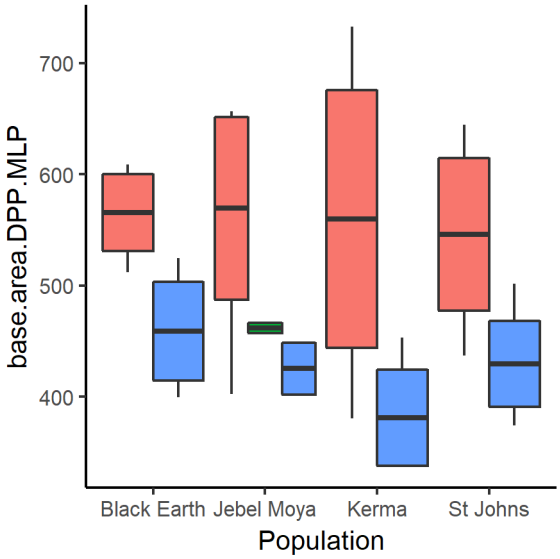
base.area.DPP.MLP
700
600
500
400
Black Earth
Jebel Moya
Kerma
St Johns
Population

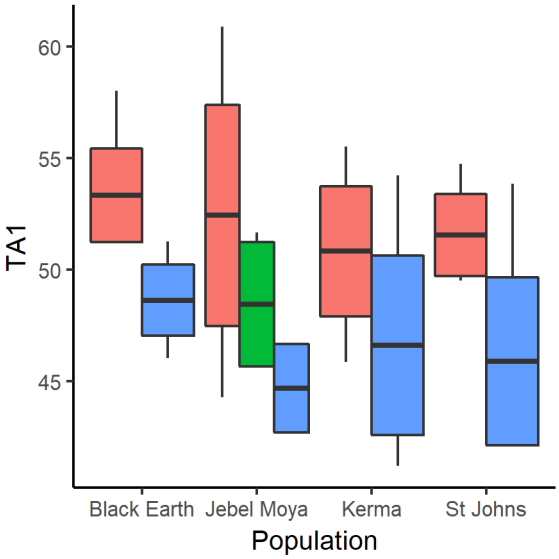
TA1
60
55
50
45
Black Earth
Jebel Moya
Kerma
St Johns
Population

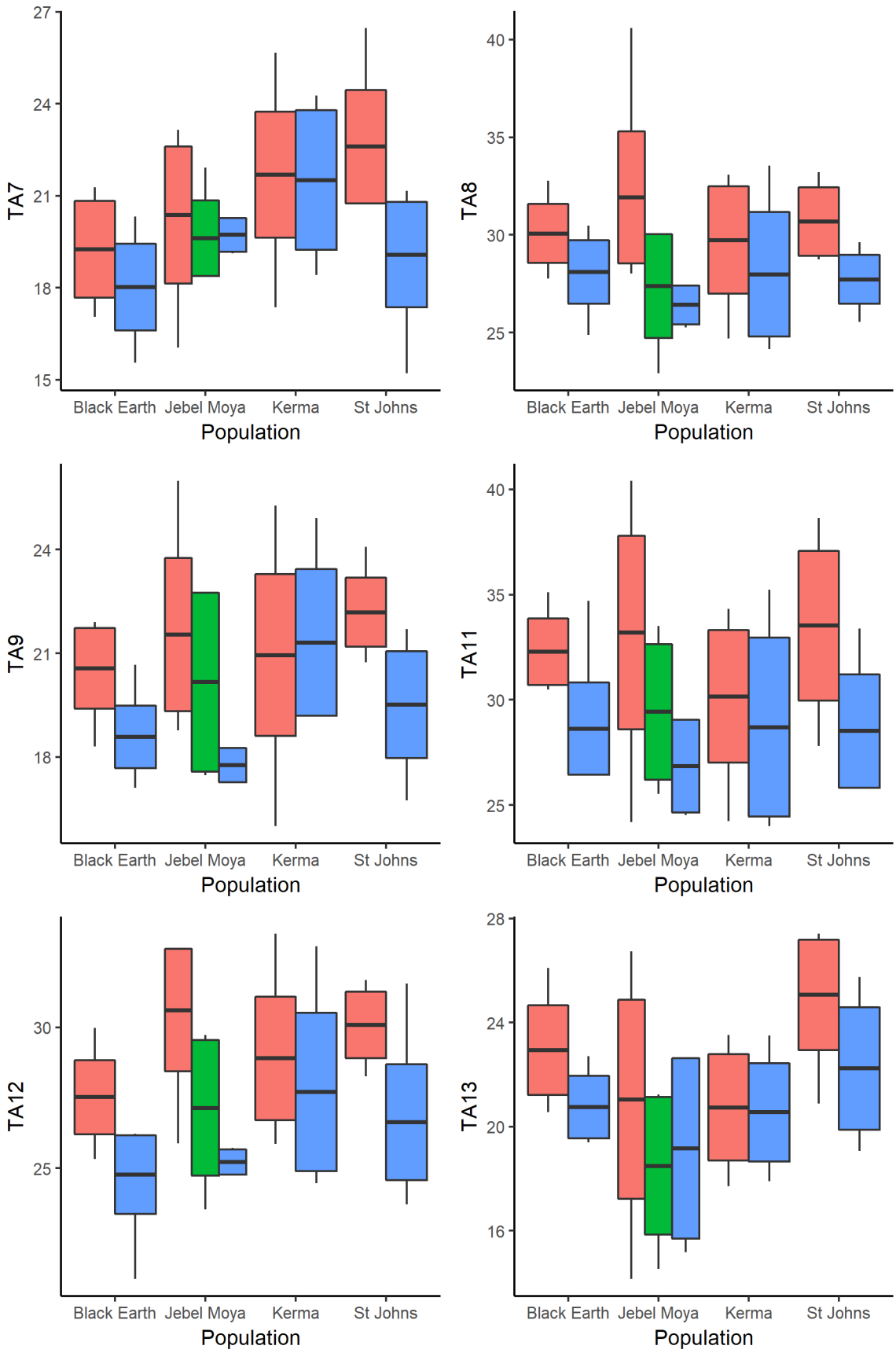
TA7
27
24
21
18
15
Black Earth
Jebel Moya
Kerma
St Johns
Population
TA8
40
35
30
25
Black Earth
Jebel Moya
Kerma
St Johns
Population
TA9
24
21
18
Black Earth
Jebel Moya
Kerma
St Johns
Population
TA11
40
35
30
25
Black Earth
Jebel Moya
Kerma
St Johns
Population
TA12
30
25
Black Earth
Jebel Moya
Kerma
St Johns
Population
TA13
28
24
20
16
Black Earth
Jebel Moya
Kerma
St Johns
Population

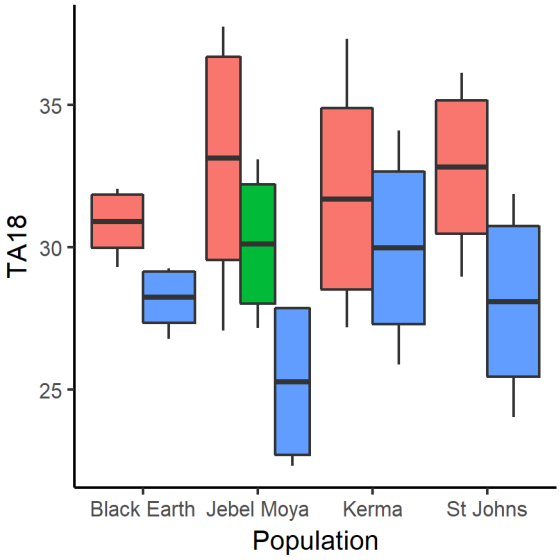
TA18
35
30
25
Black Earth
Jebel Moya
Kerma
St Johns
Population

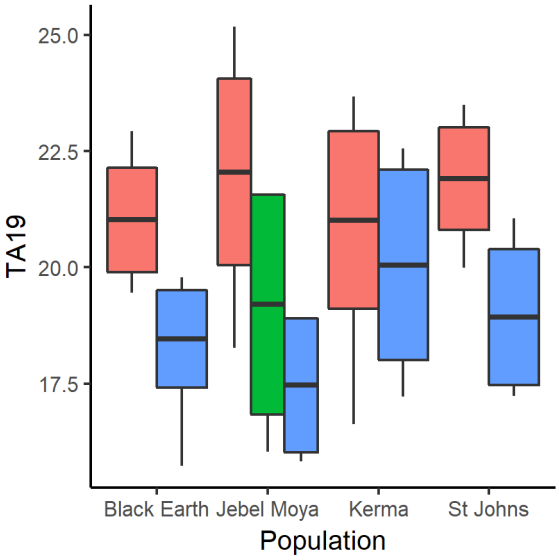
TA19
25.0
22.5
20.0
17.5
Black Earth
Jebel Moya
Kerma
St Johns
Population

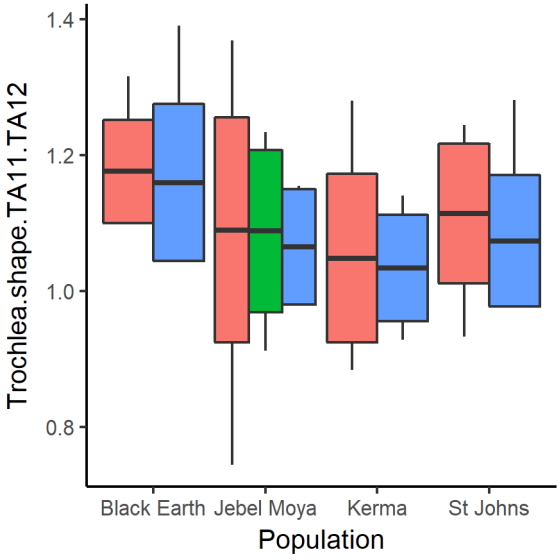
Trochlea.shape.TA11.TA12
1.4
1.2
1.0
0.8
Black Earth
Jebel Moya
Kerma
St Johns
Population

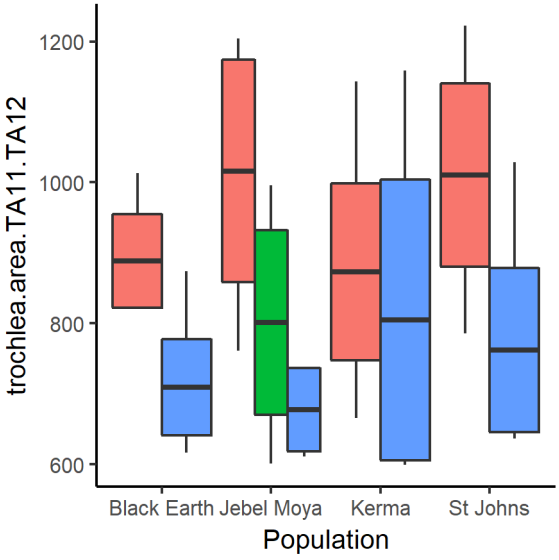
trochlea.area.TA11.TA12
1200
1000
800
600
Black Earth
Jebel Moya
Kerma
St Johns
Population

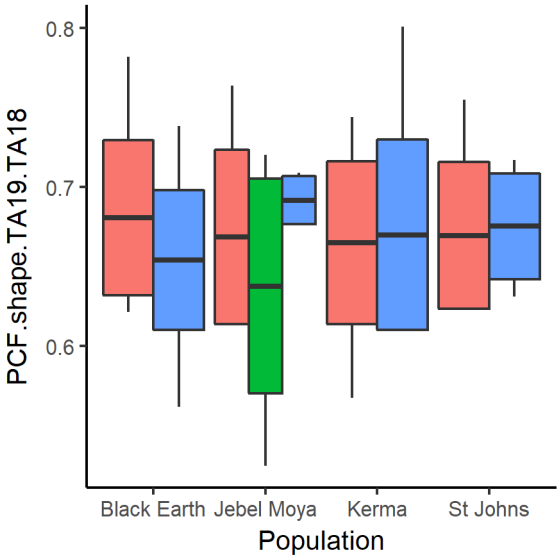
PCF.shape.TA19.TA18
0.8
0.7
0.6
Black Earth
Jebel Moya
Kerma
St Johns
Population

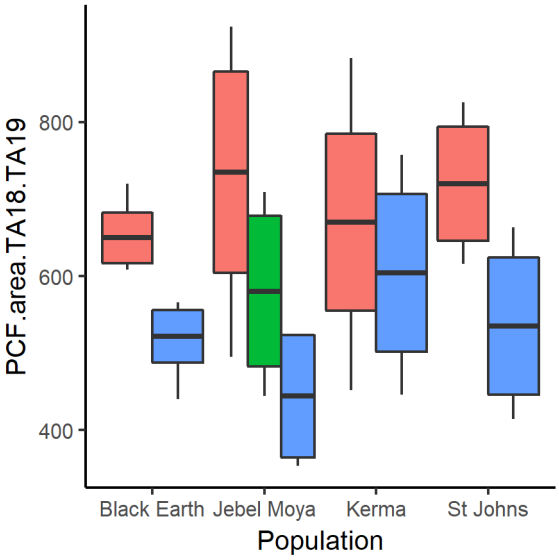
PCF.area.TA18.TA19
800
600
400
Black Earth
Jebel Moya
Kerma
St Johns
Population

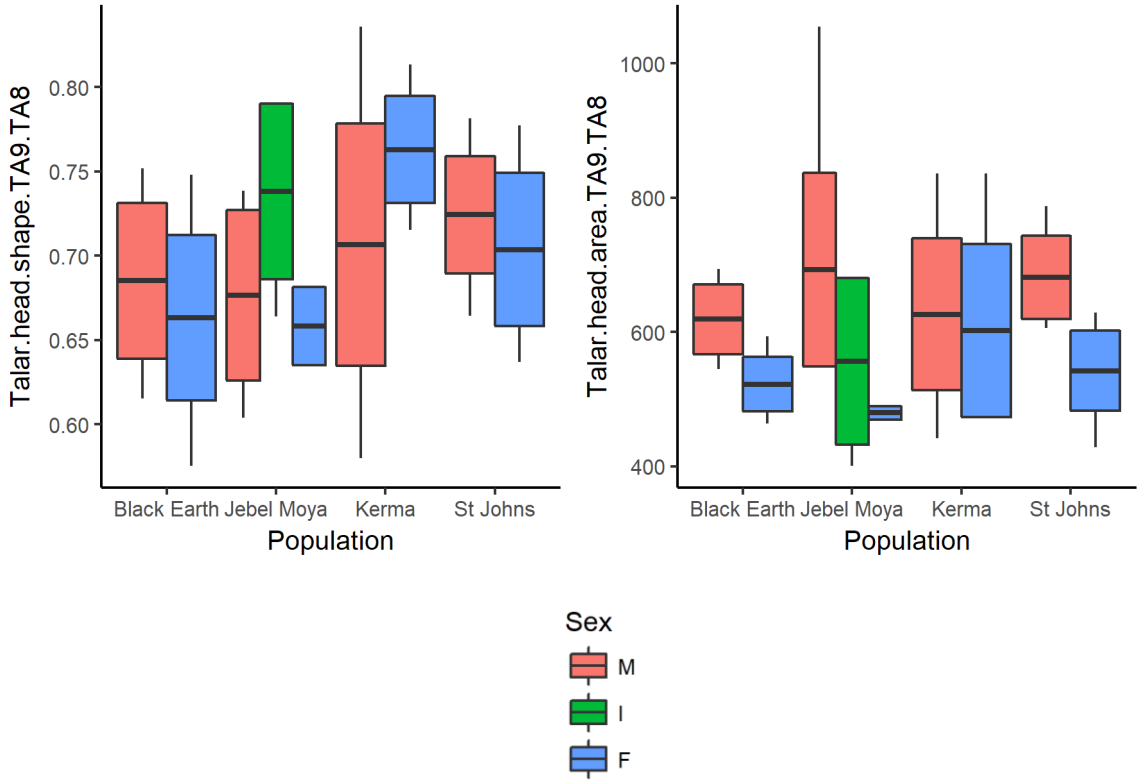

Figure 3.3. Boxplots of body mass, bone size and shape indices. Diamonds indicate pooled sex means. M=male, F=female, I=indeterminate. BM =body mass.

The coefficients of determination between trabecular properties of pooled sex and population samples, and bone dimensions and body mass are presented in figures 3.4 to 3.6. The data is presented in each figure as the mean R^2 of all trabecular properties per VOI to illustrate differences in correlations between VOIs, and as the mean R^2 of all VOIs per trabecular property to illustrate differences in correlations between different trabecular properties. Mean and standard deviations of coefficients of determination are provided for each population per bone in Appendix 3.3.

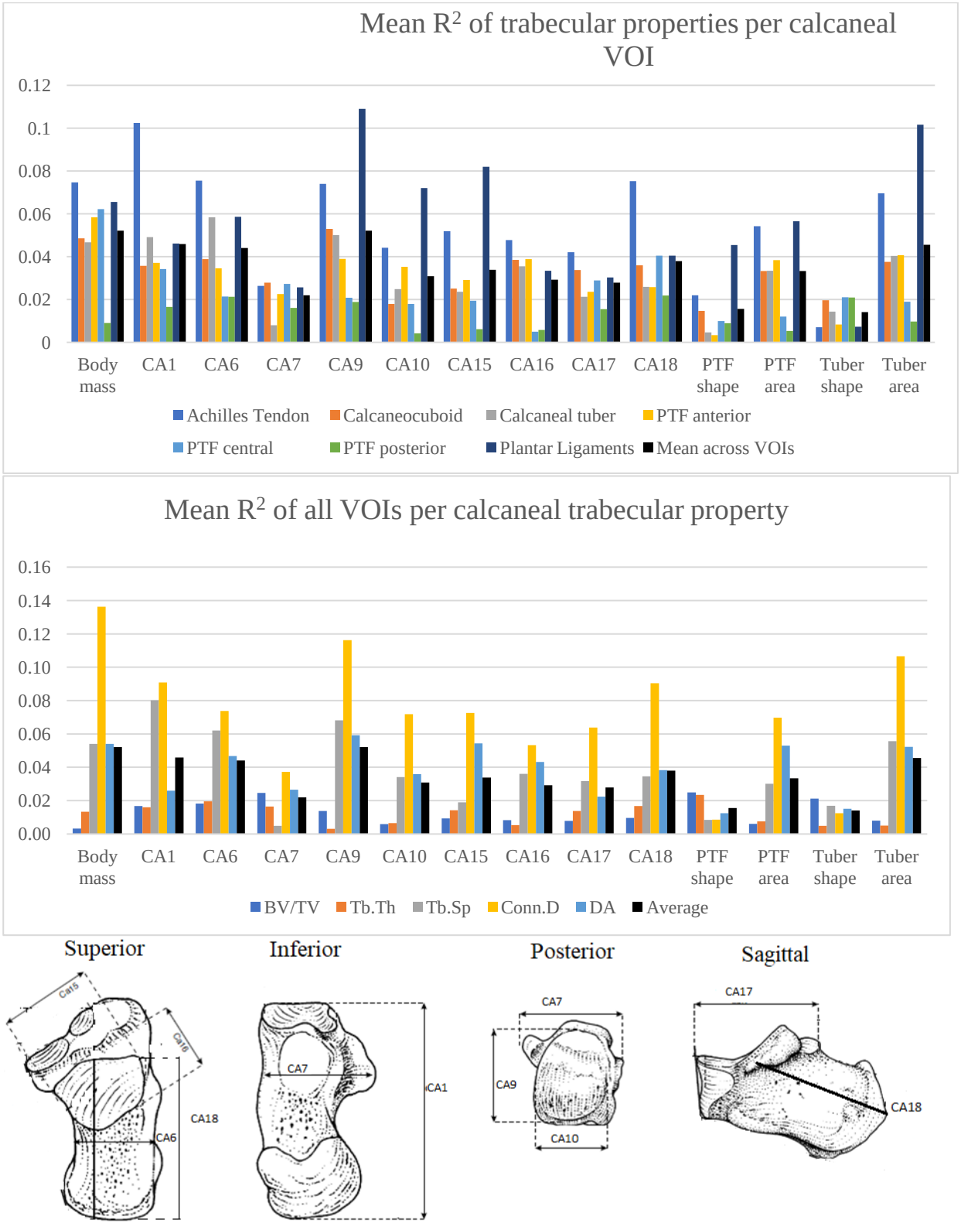

Figure 3.4. Mean coefficients of determination between calcaneal trabecular properties, body mass, and bone dimensions.

The highest mean coefficients of determination with trabecular properties in the calcaneus are found with body mass, tuber height (CA9), and tuber area (Figure 3.4). Both shape indices show lower correlations with trabecular properties than the linear bone dimensions. The trabecular properties in the central and posterior VOIs of the posterior talar facet correlate poorly with all bone dimensions,

and trabecular structure in the posterior PTF correlates poorly with body mass. Of all trabecular properties Conn.D has the largest coefficient of determination with all but the two shape indices. Tb.Sp also correlates strongly with calcaneal bone dimensions.

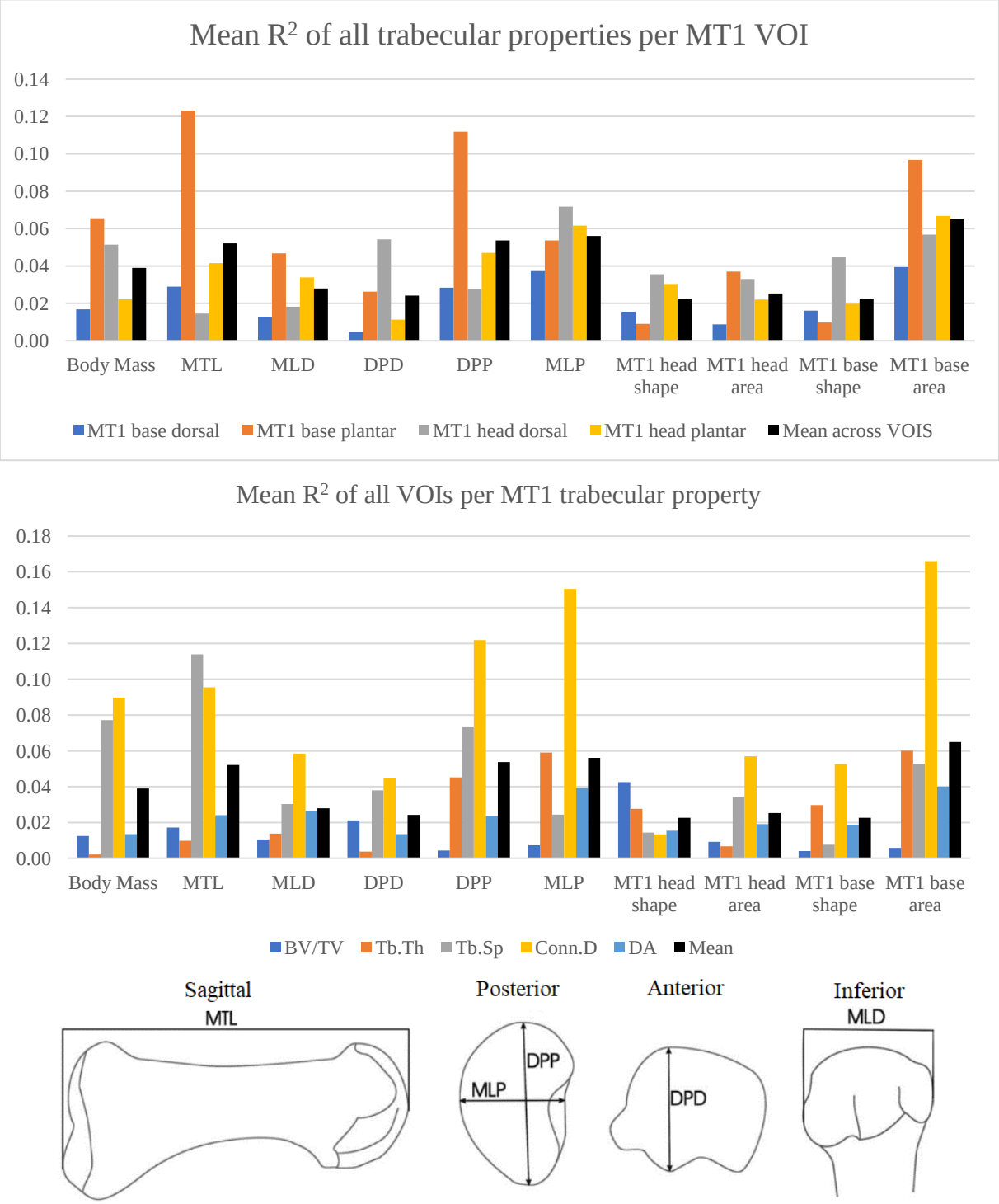

Figure 3.5. Coefficients of determination between MT1 trabecular properties, body mass, and bone dimensions.

The greatest R^2 value is found in the MT1 base area, closely followed by base height (DPP) base breadth (MLP), and metatarsal length (MTL) (Figure 3.5). Similarly to the calcaneus, the highest R^2

values are found between bone dimensions and Conn.D, followed by Tb.Sp and Tb.Th. Both shape indices and the head dimensions show the lowest correlations with bone dimensions.

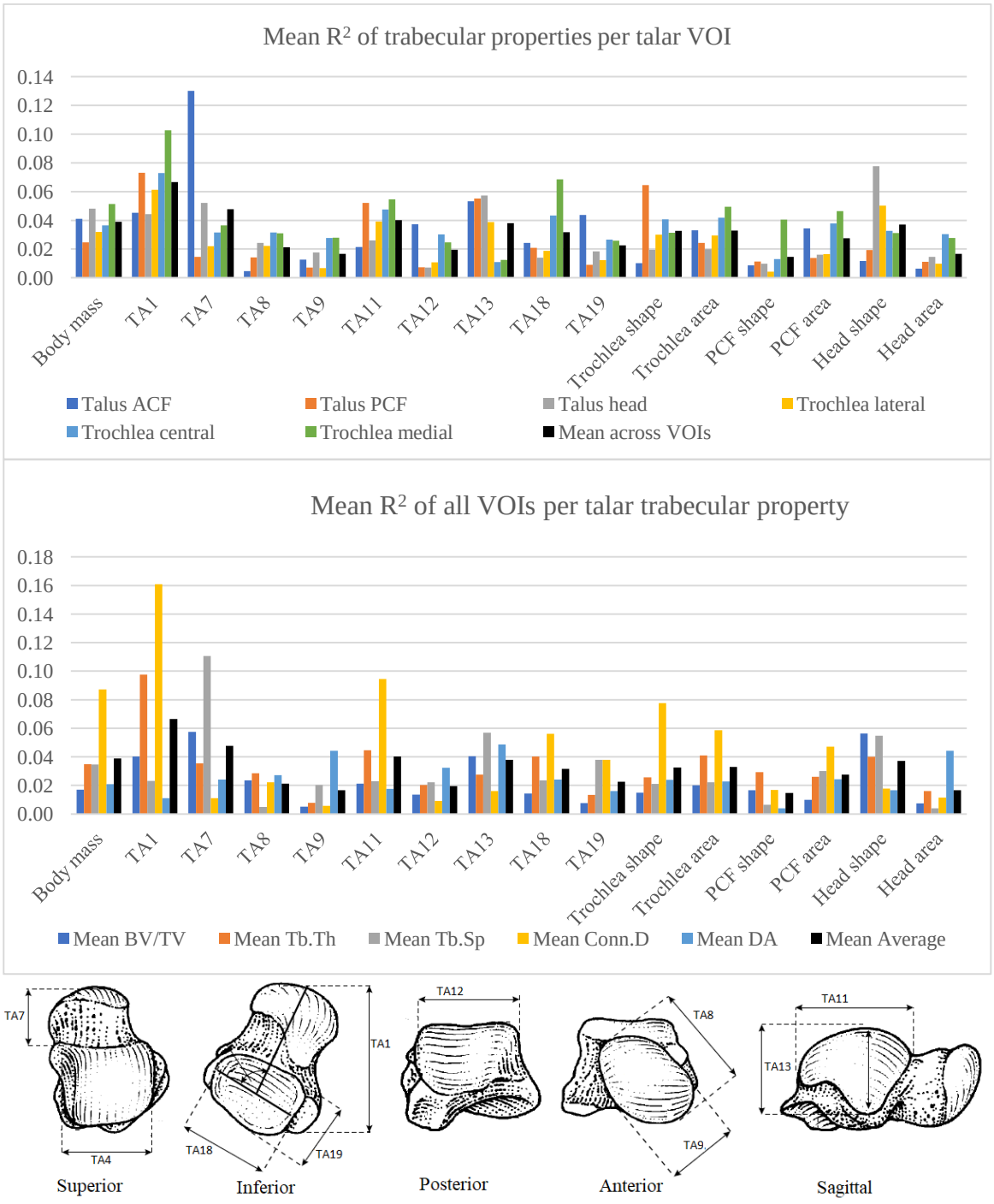

Figure 3.6. Mean coefficients of determination between talar trabecular properties, body mass, and bone dimensions.

The greatest mean R^2 was found for talar length (TA1) resulting from large contributions of Conn.D and Tb.Th (Figure 3.6). While in the calcaneus and MT1 Conn.D was strongly correlated to body mass and bone dimensions, in the talus only body mass, talar length (TA1), trochlear length (TA11), and trochlea shape show strong correlations with Conn.D. Other trabecular properties correlate less strongly with body mass and bone dimensions.

The results presented above suggest that body mass is not always account for the greatest variance in trabecular properties. However, data presented in Appendix 3.2 demonstrated that there is greater variation in bone dimensions between populations than in body size. Thus, it is likely that differences in trabecular structure between populations lead to higher correlations with bone dimensions when significant between population differences in bone dimensions are present. Below, R^2 values are presented that were calculated as the average of mean R^2 values of individual populations. These R^2 values are plotted per trabecular bone property against body mass and bone size and shape variables, and are calculated from the mean of all volumes of interest. Calculating these as the average of R^2 of each population eliminates error caused by differences between populations in bone size, body mass, and trabecular structure, and increases overall strength of the correlations.

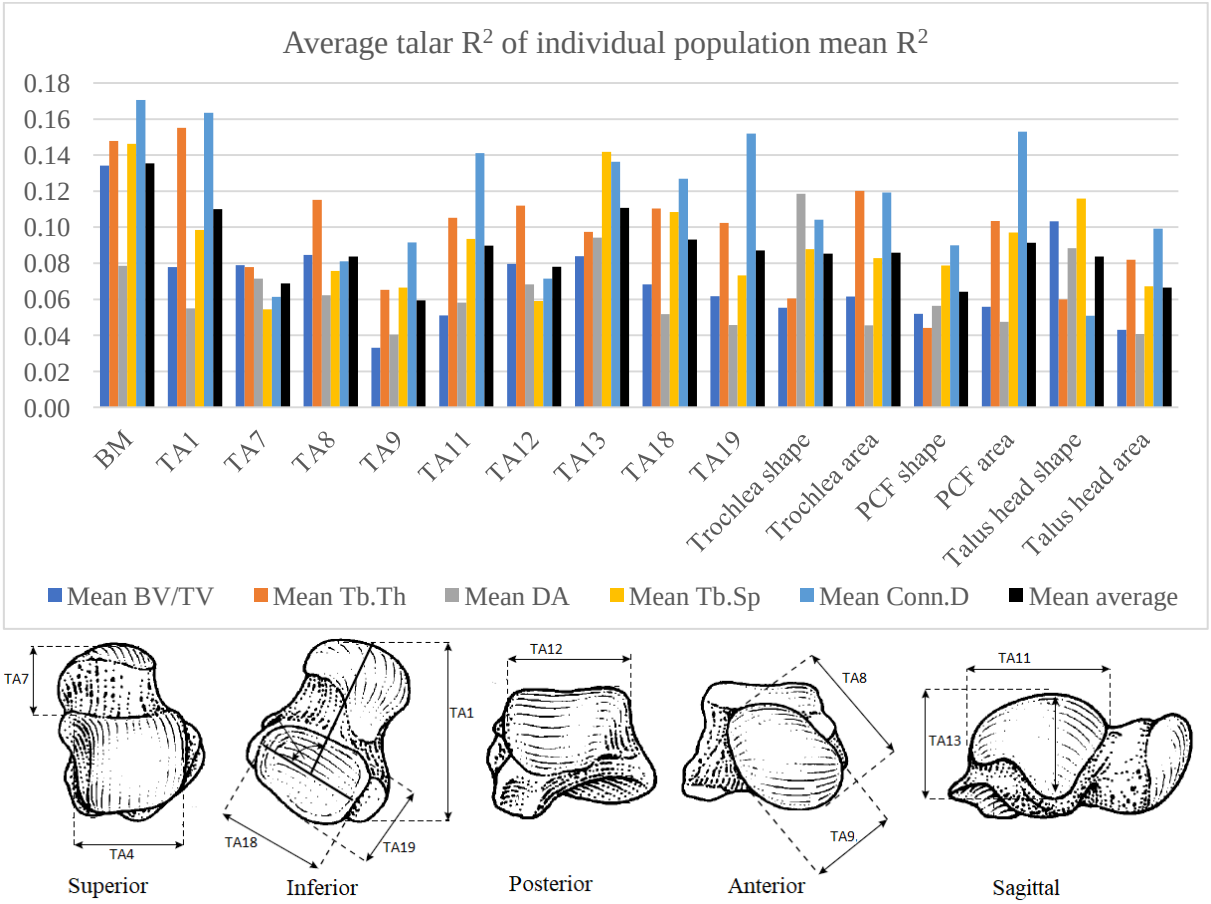

Figure 3.7. Mean R^2 values per trabecular property calculated from the means of individual populations in the talus. BM is body mass.

Figure 3.7 represents the coefficients of determination between talar trabecular properties and body mass and bone dimensions, calculated by taking the mean of R^2 values of all talar VOIs calculated for individual populations. Calculating R^2 as the average of population mean coefficients of determination increases R^2 substantially compared to the method used before which used the mean R^2 of pooled populations. This indicates that population differences in behaviour and morphology between populations were obscuring relationships between body mass, bone dimensions, and trabecular properties.

These results indicate that for the talus, body mass accounts for the greatest amount of variance in trabecular properties. This is a different result than was shown by Figure 3.6, where body mass showed a particularly weak correlation with trabecular properties. Conn.D is most affected by body mass and bone dimensions, evidenced by its consistently high R^2 values. Body mass is strongly correlated with all properties except for DA, which has a consistently low R^2 for most bone dimensions.

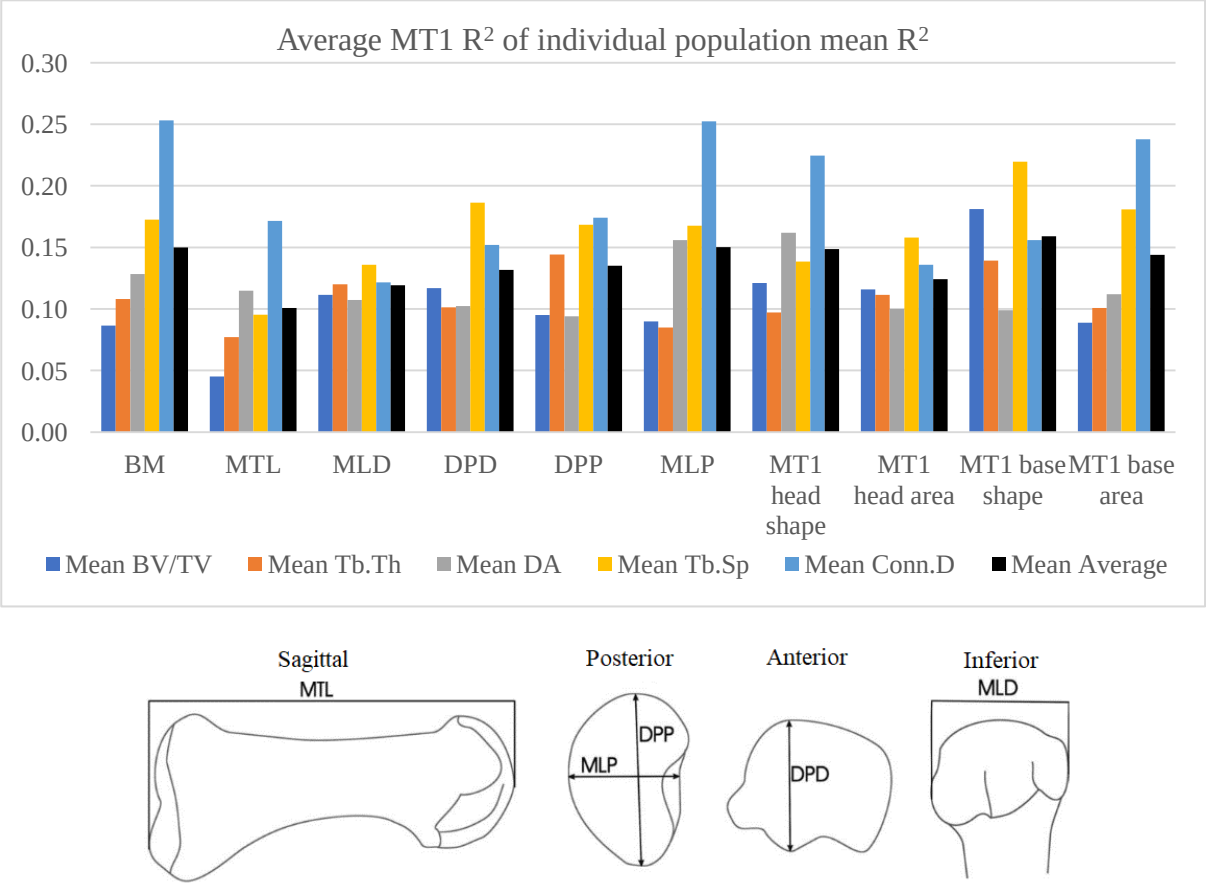

Figure 3.8. Mean R^2 values per trabecular property calculated from the means of individual populations in the first metatarsal. BM is body mass.

The coefficients of determination presented in Figure 3.8 indicate that Conn.D and Tb.Sp are most strongly correlated with body mass and bone dimensions. The variables that account for the greatest amount of variance in trabecular properties are body mass, base breadth, head shape, base shape, or base area. Similar to the talus, calculating R^2 as the average of population means substantially increases the amount of variance accounted for by body mass and bone dimensions.

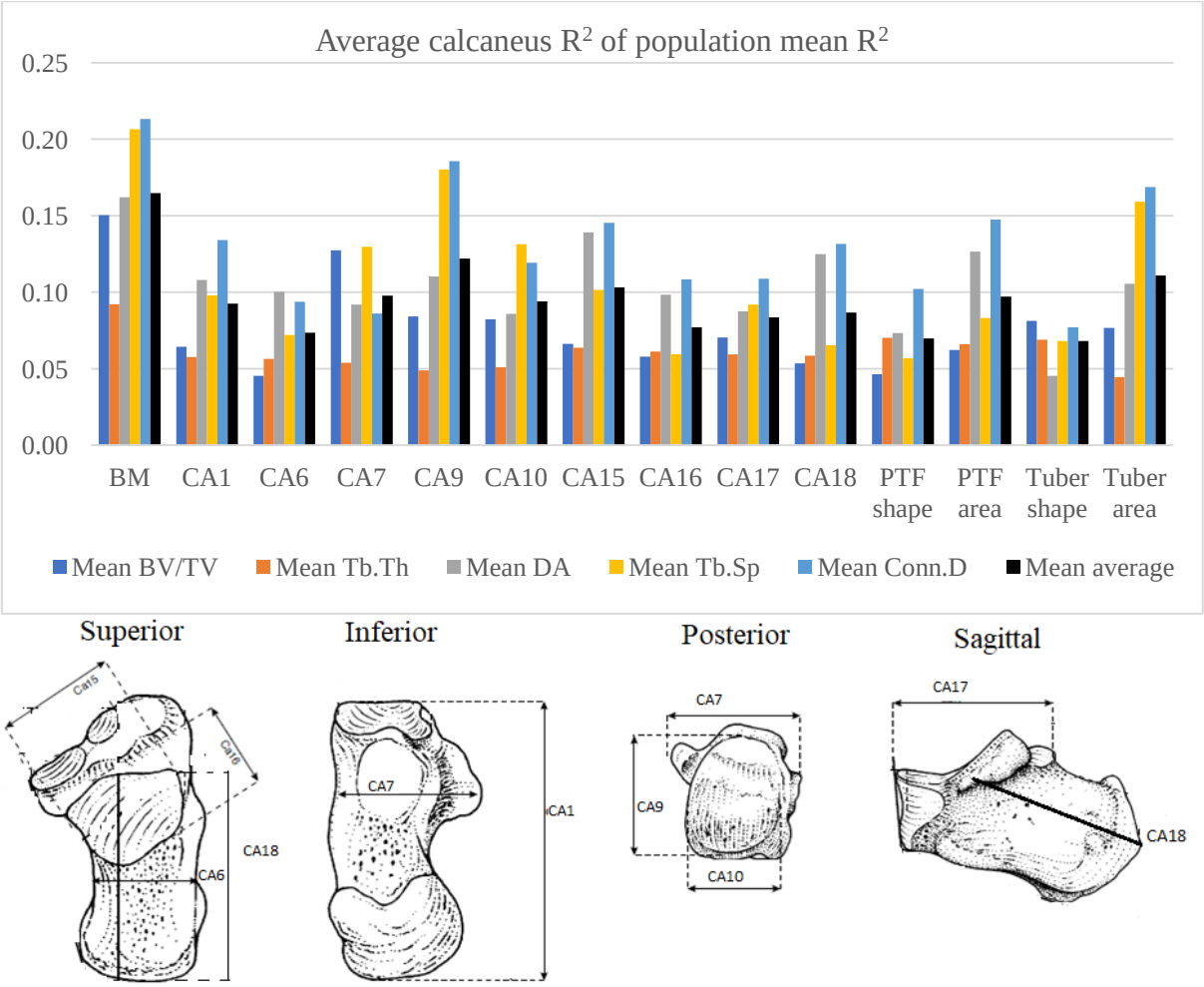

Figure 3.9. Mean R^2 values per trabecular property calculated from the means of individual populations in the calcaneus. BM is body mass.

The coefficients of determination presented in Figure 3.9 indicate that Conn.D and Tb.Sp are most strongly correlated to body mass and bone dimensions. Body mass accounts for a larger amount of variance compared to bone dimensions in the calcaneus.

Pearson correlation coefficients (R) between trabecular properties and body mass and bone dimensions are calculated to assess potential differences in the directionality of correlations between VOIs. Correlation coefficients were calculated pairwise from a pooled population sample for each VOI and presented in Figure 3.10 and Table 3.2. Conn.D correlates negatively, and Tb.Sp correlates positively with body mass in all VOIs. BV/TV and Tb.Th do not correlate significantly with body mass. DA correlates positively with body mass the PL and PA but does not correlate significantly with any other VOI. Thus, in the current sample significant correlations are always negative for Conn.D, and always positive for Tb.Sp and DA.

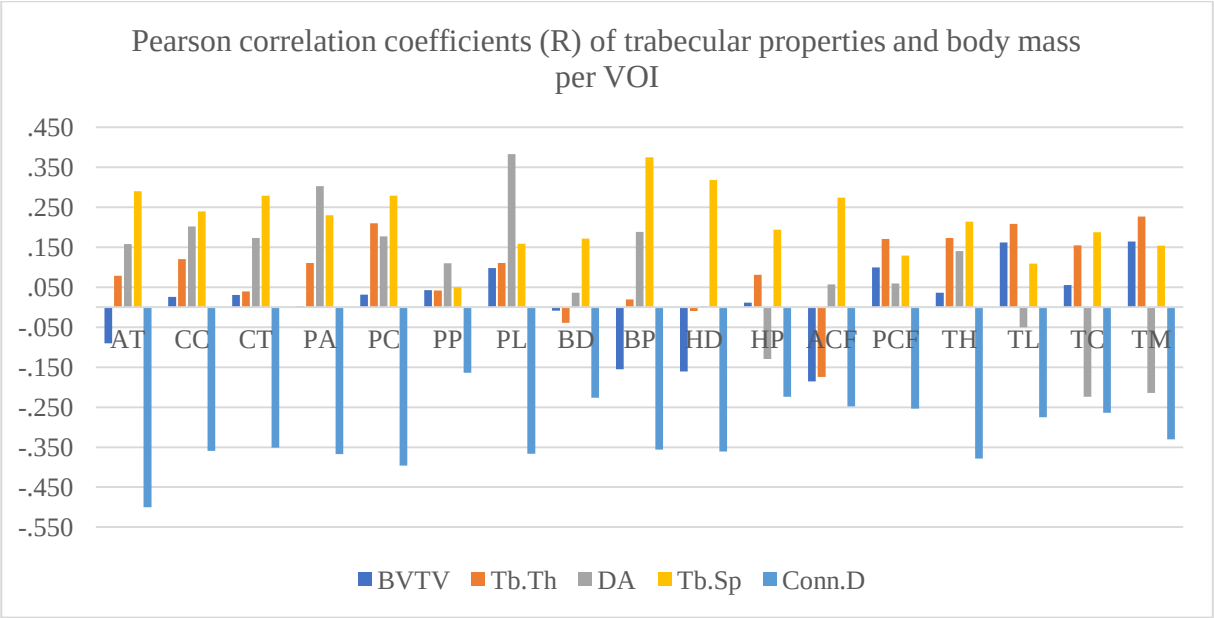

Figure 3.10. Pearson correlation coefficients of trabecular properties with body mass per VOI in a pooled population sample. Volumes of interest: Achilles tendon (AT), calcaneal tuber (CT), plantar ligaments (PL), posterior talar facet (PP: posterior, PC: central, PA: anterior), calcaneocuboid (CC), dorsal base (BD), plantar base (BP), dorsal head (HD), plantar head (HP), talar head (TH), anterior calcaneal facet (ACF), posterior calcaneal facet (PCF), trochlea (lateral: TL, central: TC, medial: TM).

Table 3.2. Pearson correlation coefficients between body mass and trabecular properties in a pooled population, pooled sex sample. Volumes of interest: Achilles tendon (AT), calcaneal tuber (CT), plantar ligaments (PL), posterior talar facet (PP: posterior, PC: central, PA: anterior), calcaneocuboid (CC), dorsal base (BD), plantar base (BP), dorsal head (HD), plantar head (HP), talar head (TH), anterior calcaneal facet (ACF), posterior calcaneal facet (PCF), trochlea (lateral: TL, central: TC, medial: TM).

VOI		N	BVTV	Tb.Th	DA	Tb.Sp	Conn.D
AT	**R**	**69**	-.090	.079	.158	**.290**	**-.500**
	p		.468	.525	.201	**.017**	**.000**
CC	**R**	**66**	.026	.121	.202	.240	**-.359**
	p		.840	.342	.109	.056	**.004**
CT	**R**	**71**	.031	.039	.173	**.279**	**-.351**
	p		.804	.749	.158	**.021**	**.003**
PA	**R**	**66**	.002	.111	**.303**	.230	**-.367**
	p		.988	.378	**.015**	.067	**.003**
PC	**R**	**66**	.031	.210	.177	**.279**	**-.396**
	p		.806	.095	.162	**.026**	**.001**
PP	**R**	**66**	.042	.042	.110	.050	-.164
	p		.739	.744	.388	.693	.195
PL	**R**	**59**	.098	.111	**.383**	.158	**-.366**
	p		.461	.402	**.003**	.231	**.004**
BD	**R**	**56**	-.008	-.039	.036	.172	-.227
	p		.951	.782	.796	.214	.099
BP	**R**	**49**	-.155	.019	.189	**.375**	**-.356**
	p		.293	.897	.199	**.009**	**.013**
HD	**R**	**57**	-.161	-.010	.002	**.318**	**-.361**
	p		.232	.943	.989	**.016**	**.006**
HP	**R**	**53**	.012	.082	-.129	.194	-.224
	p		.934	.562	.357	.165	.107
ACF	**R**	**62**	-.186	-.175	.057	**.274**	-.248
	p		.152	.179	.663	**.033**	.054
PCF	**R**	**62**	.100	.171	.060	.129	-.253
	p		.448	.192	.650	.327	.051
TH	**R**	**68**	.036	.174	.141	.214	**-.379**
	p		.775	.167	.264	.087	**.002**
TL	**R**	**66**	.162	.209	-.050	.109	**-.275**
	p		.201	.100	.692	.396	**.028**
TC	**R**	**65**	.056	.155	-.224	.188	**-.264**
	p		.666	.230	.080	.144	**.038**
TM	**R**	**63**	.164	.227	-.214	.154	**-.330**
	p		.206	.079	.097	.240	**.009**

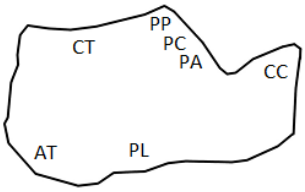

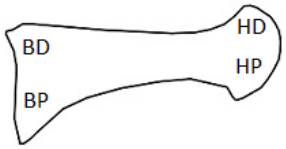

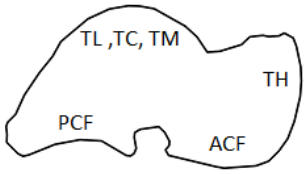

Discussion

No differences are found in the strength of coefficients of determinations between males and females. As such, pooled sex samples were examined in this chapter. When populations are pooled, external bone dimensions can account for similar or greater variance in trabecular properties than body mass. When the correlations are examined within individual populations the effects of body mass are stronger than those of external bone dimensions. This indicates that the large coefficients of determination of external bone dimensions in the pooled sample are high because they reflect significant between-population differences in bone dimensions and trabecular properties (see Appendix 3.2). Body mass does not differ significantly between populations and is thus less biased than linear bone dimensions. Partial correlations between external dimensions and trabecular properties, after removing the variance associated with body mass, are not significant, except for a small number of isolated random significant results (not reported here). This indicates that the significant correlations between trabecular structure and linear bone dimensions reported in this chapter largely resulted from the shared variance between body mass and bone dimensions. Mean R^2 between trabecular properties and body mass are roughly equal in different bones (calcaneus=.165, MT1=.153, talus=.136). Because body mass is not a bone specific measurement, does not significantly differ between pooled sex populations, and accounts for the largest amount of variance, it is the most suitable variable to be used to standardize trabecular properties in subsequent analyses that examine the influence of behavioural variation on trabecular structure. The remaining variance which is not shared with body mass may be attributed to variation in genetics, age, sex, diet, and behaviour. The Pearson correlation coefficients reported in Table 3.2 demonstrate that while some variation between VOIs is found, all significant correlations scale in the same directions: negative for Conn.D and positive for Tb.Sp and DA.

Conclusions

The results from this chapter suggest that trabecular properties are significantly correlated to body mass in volumes of interest throughout the foot. While bone dimensions potentially influence trabecular structure when the variance associated with body mass is accounted for, the effects are not significant within individual populations. In Chapter 4 the relationship between trabecular structure and body mass is examined further and body mass controlled variables will be generated using linear regression.

Chapter 4 - Regressions of body mass and trabecular structure

Introduction

Significant correlations were found between body mass and trabecular structure in Chapter 3. To clearly identify the effects of behavioural variation on trabecular structure, the effects of body mass need to be understood and statistically accounted for. There is a substantial literature on allometric scaling of trabecular bone in primates (Fajardo et al., 2013; Ryan and Shaw, 2013), mammals and birds (Swartz et al., 1998; Doube et al., 2011; M.M; Barak et al., 2013; Christen et al., 2015). Larger animals generally have (absolutely) thicker and more widely separated struts. However, relative to body mass they are thinner and closer together. BV/TV scales with weak positive allometry indicating that larger animals possess slightly denser trabecular structure relative to smaller animals. No relationship was found between DA and body mass across different species (Doube et al., 2011; Barak et al., 2013; Ryan and Shaw, 2013). This is most likely a consequence of the fact that DA is more strongly influenced by joint morphology, posture, and behaviour (Ryan and Krovitz, 2006; Fajardo et al., 2013; Saers et al., 2016). Previous work has focused on allometry in different species of greatly varying body mass, but within species variation has not been widely investigated. It is not implausible that within species a relationship may be found between DA and body mass which has previously been obscured by interspecific variation.

Several constraining metabolic and biomechanical factors have been proposed to underlie the observed scaling patterns between body mass and trabecular structure. Osteocyte function places constraints on the minimum and maximum dimensions of individual trabeculae (Mullender and Huiskes, 1995; Mullender et al., 1996; Christen et al., 2015). Trabeculae must be larger than 30-60μm, as this is the size of the lacunae created by osteoblasts (Barak et al., 2013). Osteocyte function determines maximum thickness as osteocytes can only function at a distance of 0.230mm away from the bone surface (Lozupone and Favia, 1990). This constrains the maximum diameter of trabeculae to twice this size: 0.460mm. Differences between small and large bodied animals may be driven partly by the requirement to maintain adequate surface area for calcium deposition and release (Swartz et al., 1998; Kerschnitzki et al., 2013).

It remains important to consider that trabecular bone is just one part of the skeletal system and that bone strength is in large part determined by cortical bone morphology. Due to the metabolic factors described above, the increased loads associated with larger body mass may be compensated for with a change in cortical rather than trabecular bone mass/distribution. Additionally, large animals adopt different limb postures to compensate for increased loading (Biewener, 1989; Schmitt, 1999; Polk, 2002), reducing strain on trabeculae.

Methods

Following the protocol from Ryan and Shaw (2013, 2015), regressions were performed between body mass and trabecular properties for each VOI. If a regression is significant, the unstandardized residuals will be used in future analyses as body mass standardized variables. To standardize for body mass, a pooled-sex population sample is required. Although the Black Earth have a relatively low body mass, no significant differences were found in body mass between pooled-sex populations. Thus, populations can be pooled without differences between populations biasing the regression slope as a consequence of differences in body mass. Chapter 2 showed there are significant sex-specific differences in body mass between populations with the Black Earth males and Jebel Moya females having relatively low body mass compared to males or females from other populations. Regressions of body mass and trabecular properties will be briefly discussed for males and females.

Ordinary least-squares (OLS) regression analyses are performed for each trabecular bone variable against body mass in a pooled population sample. Following recommendations in Smith (2009) OLS was used instead of RMA because these equations will be used to correct for the effects of body mass on trabecular properties. If the assumptions of OLS regression are violated a robust regression technique is employed (iteratively re-weighted regression using Hubert weights (Wilcox, 2005)). This technique down-weighs outliers according to how far they are from the best-fit line, and iteratively re-fits the model until convergence is achieved. All variables were normally distributed except for Conn.D, which required a log10 transformation in every VOI to meet the linearity assumption of linear regression models. All regressions were performed in R version 3.2.

Body mass was estimated based on femoral head dimensions using equations taken from the Ruff (1997). Femoral head superoinferior height was measured to the nearest hundredth of a millimetre using digital callipers.

Due to the preservation of the archaeological specimens, trabecular properties could not be calculated in all 17 VOIs for many individuals. Only 25 individuals have all 17 VOIs present (Jebel Moya: 2, Kerma: 8, St. Johns: 10, Black Earth: 5). Regressions were run pairwise to maintain maximum sample size for each VOI (Table 4.1). While this reduces the utility of comparisons of regressions between VOIs, it guarantees maximum statistical power to the relationships found in each VOI.

Table 4.1. Sample size used in this chapter for each population and sex per VOI. Achilles tendon (AT), calcaneal tuber (CT), plantar ligaments (PL), posterior talar facet (PP: posterior, PC: central, PA: anterior), calcaneocuboid (CC), dorsal base (BD), plantar base (BP), dorsal head (HD), plantar head (HP), talar head (TH), anterior calcaneal facet (ACF), posterior calcaneal facet (PCF), trochlea (lateral: TL, central: TC, medial: TM).

		Black Earth		**Jebel Moya**			**Kerma**		**St Johns**		**Total**
		Sex		**Sex**			**Sex**		**Sex**		
		M	**F**	**M**	**F**	**I**	**M**	**F**	**M**	**F**	
Calcaneus	AT	7	10	8	2	5	9	7	9	11	69
	CC	7	6	9	2	5	12	7	8	9	66
	CT	7	9	10	2	5	12	7	8	10	71
	PA	7	6	8	2	4	12	7	9	11	67
	PC	6	7	8	2	4	12	6	9	11	66
	PP	7	8	9	1	4	12	5	9	11	67
	PL	6	6	5	1	5	11	7	8	10	60
MT1	BD	7	8	5	2	2	9	5	9	9	56
	BP	6	7	2	2	1	9	4	9	9	49
	HD	8	9	5	3	3	9	4	9	9	59
	HP	7	7	4	2	2	9	4	9	9	53
Talus	ACF	5	8	5	2	3	13	7	8	11	62
	PCF	5	7	7	4	4	12	6	6	11	62
	TH	5	6	10	4	5	12	7	8	11	68
	TL	7	8	10	4	5	10	5	7	11	67
	TC	6	8	9	4	3	12	5	7	11	65
	TM	7	8	9	3	3	10	5	7	11	63

Hypotheses

Based on interspecific allometric studies BV/TV, Tb.Th, and Tb.Sp are predicted to increase with body mass, and Conn.D is predicted to decrease with body mass. DA is predicted to be unaffected by body mass (Doube et al., 2011; Fajardo et al., 2013; Barak et al., 2013; Ryan and Shaw, 2013).

Results

Mean body mass of pooled sex populations is presented in Figure 4.1. The results of the regressions between body mass and trabecular properties of pooled sex and pooled populations are presented in tables 4.2 to 4.4 and plots are presented in Appendix 4.1 and 4.2. Regression tables for males and females are presented in Appendix 4.3 and plotted in Appendix 4.4. Substantial variation was found between VOIs in the strength of relationships between body mass and trabecular properties.

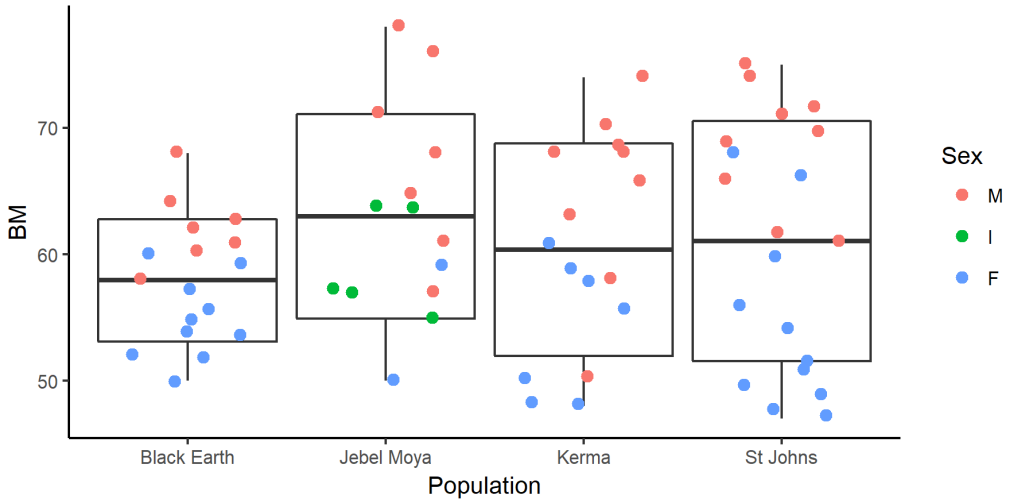

Figure 4.1. Mean body mass ±1 standard deviation of body mass for each population, whiskers correspond to maximum and minimum. Individual points represent individuals with colour denoting sex.

Table 4.2. First metatarsal regressions between body mass and trabecular properties in a pooled population, pooled sex sample. Significant results are shown in bold. CL- is the lower confidence interval and CL+ represents the upper confidence interval.

First metatarsal pooled sex and populations								
VOI	**Variable**	**Method**	**intercept**	**slope**	**CL-**	**CL+**	**R^2**	***p***
Head dorsal (HD)	BV/TV	OLS	0.513	-0.001	-0.004	0.001	0.026	0.232
	Tb.Th	Robust	0.249	0.000			0.000	0.818
	Tb.Sp	**OLS**	**0.295**	**0.002**	**0.000**	**0.004**	**0.101**	**0.016**
	log10 Conn.D	**OLS**	**1.144**	**-0.005**	**-0.010**	**-0.001**	**0.097**	**0.019**
N=57	DA	OLS	0.736	0.000	-0.002	0.002	0.000	0.989
Head plantar (HP)	BV/TV	OLS	0.318	0.000	-0.002	0.002	0.000	0.934
	Tb.Th	Robust	0.227	0.001			0.007	0.458
	Tb.Sp	OLS	0.464	0.002	-0.001	0.005	0.038	0.165
N=53	log10 Conn.D	OLS	0.910	-0.003	-0.008	0.001	0.050	0.106
	DA	OLS	0.675	-0.001	-0.003	0.001	0.017	0.357
Base dorsal (BD)	BV/TV	OLS	0.409	0.000	-0.004	0.002	0.000	0.952
	Tb.Th	Robust	0.264	-0.001			0.002	0.841
	Tb.Sp	OLS	0.347	0.001	-0.001	0.003	0.030	0.214
N=56	log10 Conn.D	Robust	1.014	-0.003			0.038	0.222
	DA	OLS	0.745	0.000	-0.002	0.002	0.001	0.796
Base plantar (BP)	BV/TV	OLS	0.351	-0.001	-0.003	0.001	0.024	0.293
	Tb.Th	OLS	0.234	0.000	-0.001	0.001	0.000	0.897
	Tb.Sp	**OLS**	**0.327**	**0.004**	**0.001**	**0.007**	**0.141**	**0.009**
N=49	**log10 Conn.D**	**OLS**	**1.186**	**-0.007**	**-0.012**	**-0.002**	**0.139**	**0.009**
	DA	OLS	0.483	0.002	-0.001	0.004	0.036	0.199

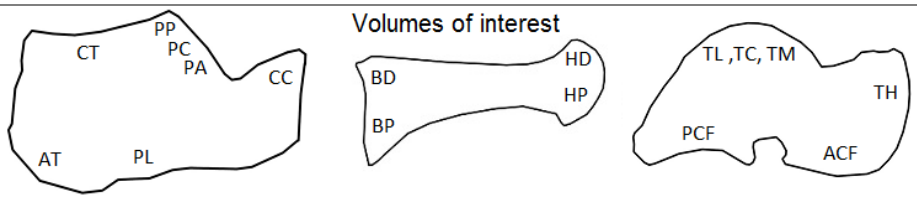

Significant regressions were found between body mass and Conn.D (negative) and Tb.Sp (positive) in the dorsal head and plantar base VOIs (Table 4.2). No significant relationships were found in the plantar head and dorsal base.

Similar significant relationships are found in all bones and VOIs. An example of these scaling relationships is presented in Figure 4.2 for the Achilles tendon VOI. Plots of all other VOIs are presented in Appendix 4.1 and 4.2.

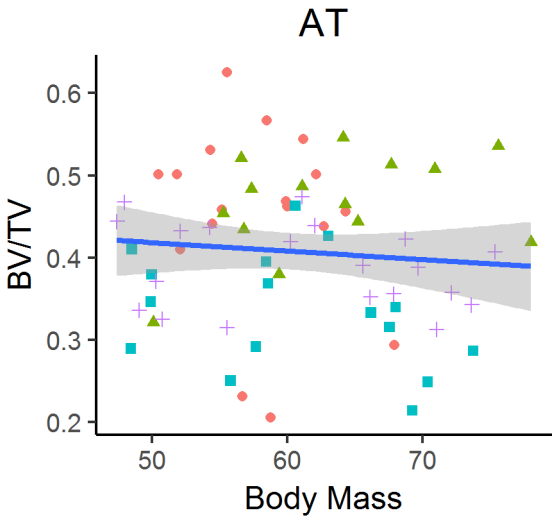
AT
BV/TV
0.6
0.5
0.4
0.3
0.2
50
60
70
Body Mass

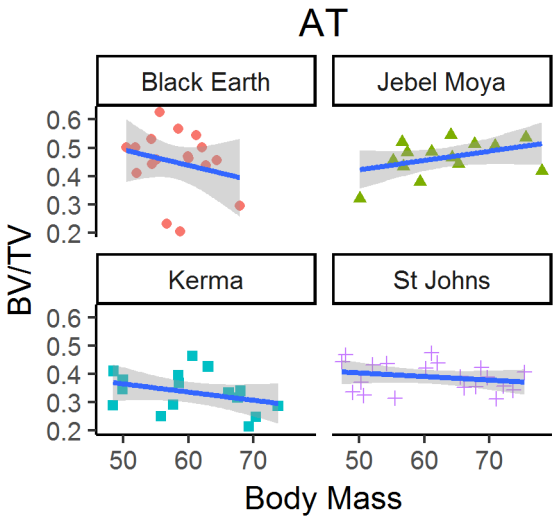
AT
Black Earth
Jebel Moya
Kerma
St Johns
BV/TV
0.6
0.5
0.4
0.3
0.2
50
60
70
Body Mass

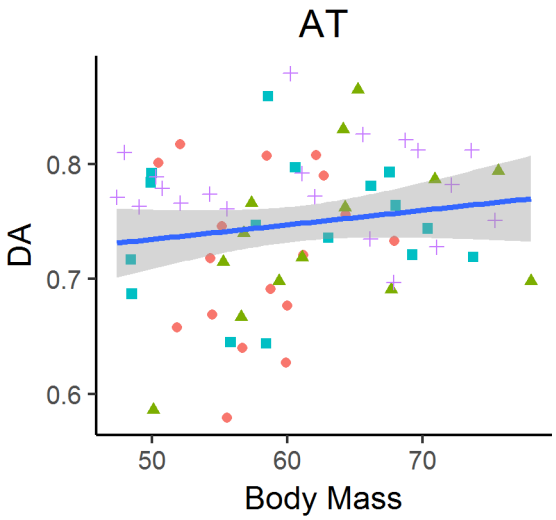
AT
DA
0.8
0.7
0.6
50
60
70
Body Mass

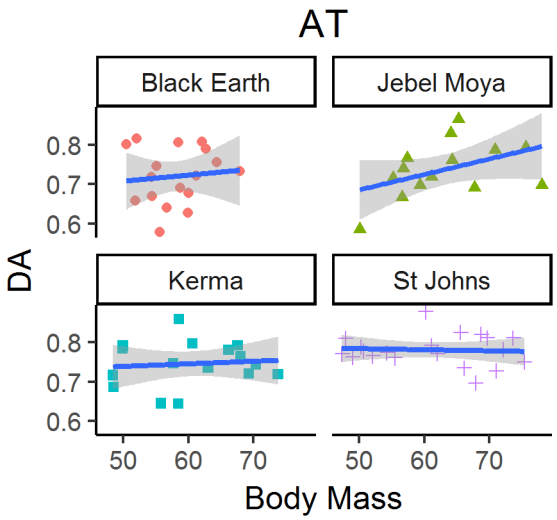
AT
Black Earth
Jebel Moya
Kerma
St Johns
DA
0.8
0.7
0.6
50
60
70
Body Mass

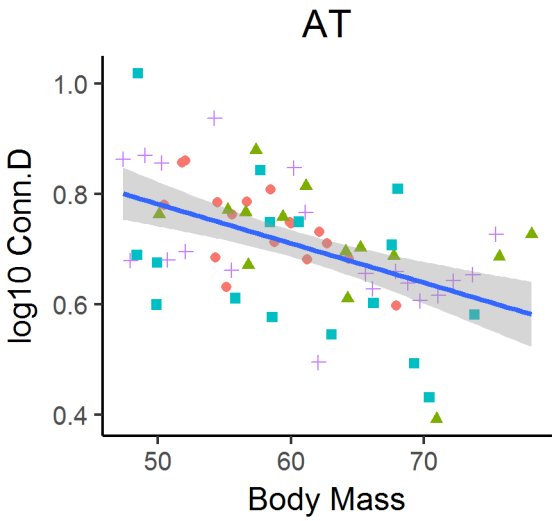
AT
log10 Conn.D
1.0
0.8
0.6
0.4
50
60
70
Body Mass

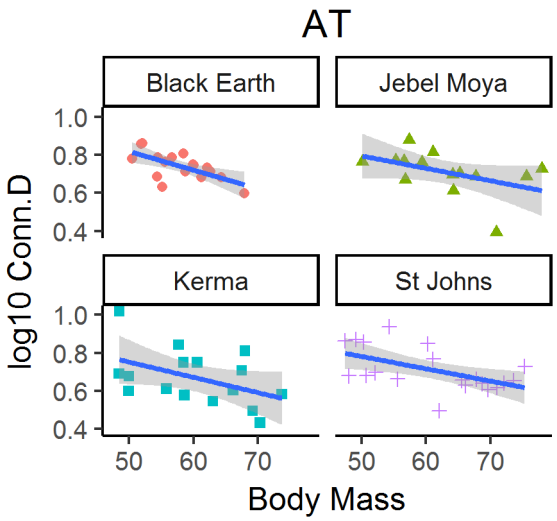
AT
Black Earth
Jebel Moya
Kerma
St Johns
log10 Conn.D
1.0
0.8
0.6
0.4
50
60
70
Body Mass

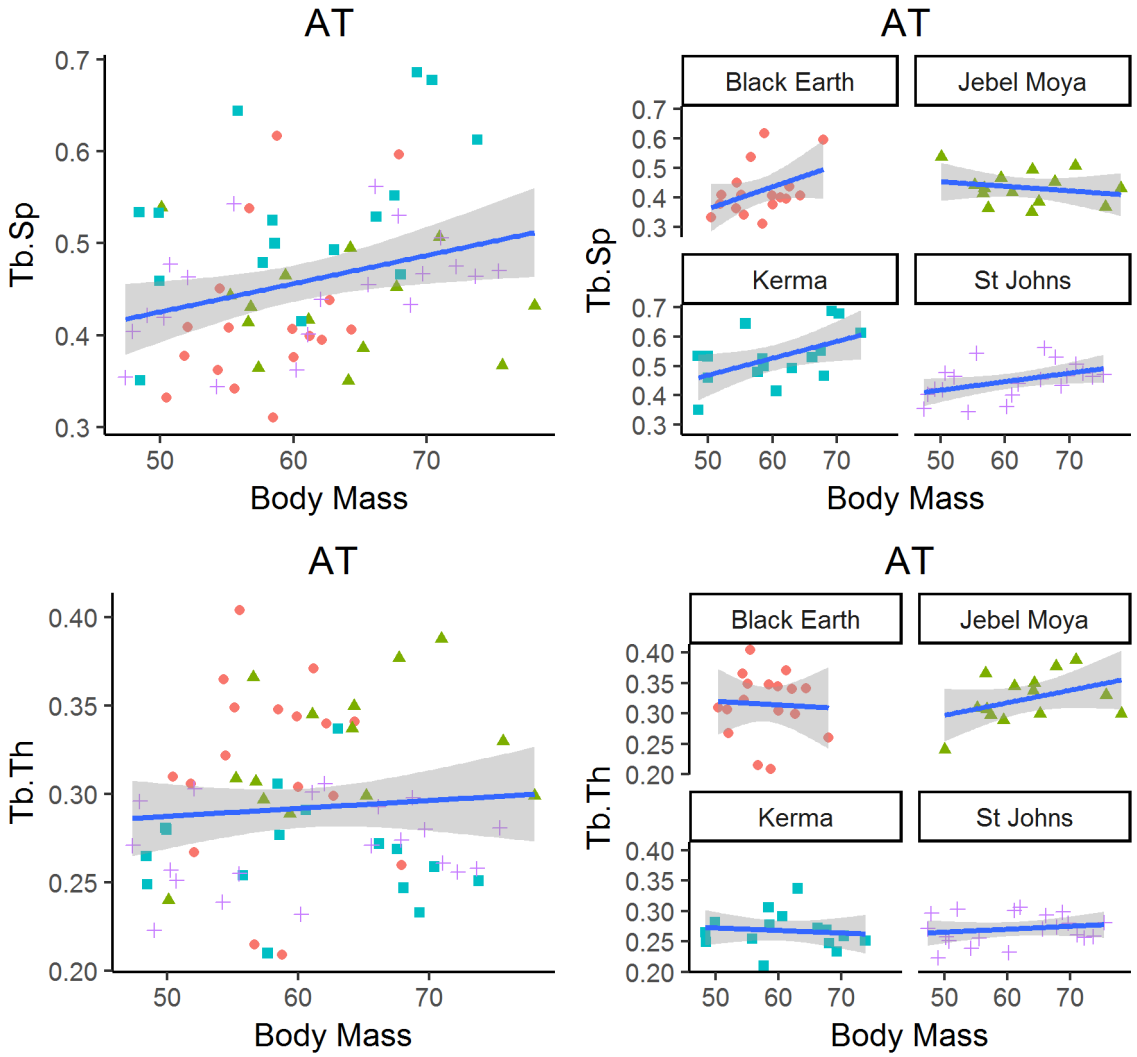

Figure 4.2. Examples of OLS regressions between body mass and trabecular properties in pooled and individual populations in the Achilles tendon VOI.

Table 4.3. Regressions between body mass and trabecular properties in a pooled population, pooled sex sample in the calcaneus. Significant results are shown in bold. CL- is the lower confidence interval and CL+ represents the upper confidence interval.

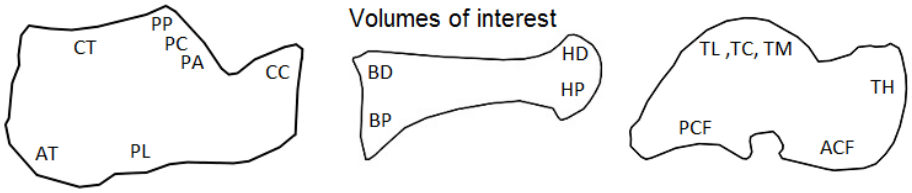

Calcaneus pooled sex and populations								
VOI	**Variable**	**Method**	**intercept**	**slope**	**CL-**	**CL+**	**R^2**	***p***
Achilles Tendon (AT)	BV/TV	OLS	0.470	-0.001	-0.004	0.002	0.008	0.469
	Tb.Th	Robust	0.266	0.000			0.006	0.575
	Tb.Sp	**Robust**	**0.281**	**0.003**			**0.084**	**0.030**
N=69	DA	OLS	0.672	0.001	-0.001	0.003	0.025	0.201
	log10	**OLS**	**1.139**	**-0.007**	**-0.010**	**-0.004**	**0.249**	**0.000**

	Conn.D							
Calcaneo-cuboid (CC)	BV/TV	OLS	0.393	0.000	-0.003	0.003	0.001	0.840
	Tb.Th	OLS	0.280	0.001	-0.001	0.003	0.015	0.342
	Tb.Sp	**Robust**	**0.327**	**0.003**			**0.058**	**0.045**
N=66	DA	OLS	0.633	0.001	-0.000	0.003	0.041	0.109
	log10 Conn.D	**OLS**	**0.994**	**-0.007**	**-0.011**	**-0.002**	**0.139**	**0.003**
Plantar Ligament (PL)	BV/TV	OLS	0.236	0.001	-0.002	0.004	0.010	0.461
	Tb.Th	**Robust**	0.250	0.001			0.012	0.353
	Tb.Sp	OLS	0.568	0.003	-0.002	0.007	0.025	0.231
N=60	**DA**	**OLS**	**0.518**	**0.003**	**0.001**	**0.005**	**0.147**	**0.003**
	log10 Conn.D	**OLS**	**0.820**	**-0.008**	**-0.013**	**-0.003**	**0.135**	**0.004**
PTF Anterior (PA)	BV/TV	OLS	0.468	0.000	-0.003	0.003	0.000	0.988
	Tb.Th	OLS	0.335	0.001	-0.001	0.003	0.012	0.378
	Tb.Sp	OLS	0.357	0.003	-0.000	0.006	0.053	0.067
N=66	**DA**	**Robust**	**0.417**	**0.005**			**0.092**	**0.001**
	log10 Conn.D	**Robust**	**0.876**	**-0.006**			**0.112**	**0.014**
PTF Central (PC)	BV/TV	OLS	0.515	0.000	-0.003	0.004	0.001	0.806
	Tb.Th	OLS	0.292	0.002	0.000	0.004	0.044	0.095
	Tb.Sp	**OLS**	**0.292**	**0.003**	**0.000**	**0.005**	**0.078**	**0.026**
N=66	DA	Robust	0.480	0.002			0.032	0.206
	log10 Conn.D	**Robust**	**0.940**	**-0.006**			**0.132**	**0.008**
PTF Posterior (PP)	BV/TV	OLS	0.448	0.001	-0.002	0.003	0.002	0.739
	Tb.Th	OLS	0.357	0.000	-0.002	0.002	0.002	0.744
	Tb.Sp	OLS	0.493	0.001	-0.002	0.003	0.003	0.693
N=66	DA	OLS	0.665	0.001	-0.001	0.003	0.012	0.388
	log10 Conn.D	OLS	0.656	-0.002	-0.006	0.002	0.015	0.341
Calcaneal Tuber (CT)	BV/TV	OLS	0.329	0.000	-0.002	0.002	0.001	0.804
	Tb.Th	OLS	0.314	0.000	-0.001	0.002	0.002	0.749
	Tb.Sp	**OLS**	**0.413**	**0.004**	**0.001**	**0.008**	**0.078**	**0.021**
N=71	DA	OLS	0.744	0.001	0.000	0.002	0.030	0.159
	log10 Conn.D	**OLS**	**0.740**	**-0.007**	**-0.011**	**-0.003**	**0.130**	**0.003**

In the calcaneus, significant negative relationships between body mass and Conn.D were found in the AT, CC, PL, PA, PC, and CT VOIs (Table 4.3). Significant positive relationships were found between body mass and Tb.Sp in the AT, CC, PC, and CT VOIs. Finally, a significant positive relationship was found between body mass and DA in the PL and PA VOIs.

Table 4.4. Regressions between body mass and trabecular properties in the talus. Significant results are shown in bold. CL- is the lower confidence interval and CL+ represents the upper confidence interval.

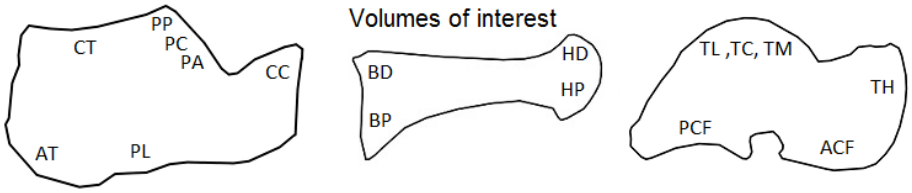

Talus pooled sex and populations								
VOI	**Variable**	**Method**	**intercept**	**slope**	**CL-**	**CL+**	**R^2**	***p***
Anterior Calcaneal Facet (ACF)	BV/TV	OLS	0.419	-0.002	-0.004	0.001	0.035	0.152
	Tb.Th	OLS	0.324	-0.001	-0.002	0.000	0.031	0.179
	Tb.Sp	**OLS**	**0.429**	**0.003**	**0.000**	**0.007**	**0.075**	**0.033**
	DA	Robust	0.635	0.001			0.000	0.429
N=62	log10 Conn.D	Robust	0.819	-0.003			0.063	0.150
Talar head (TH)	BV/TV	OLS	0.456	0.000	-0.003	0.003	0.001	0.775
	Tb.Th	OLS	0.244	0.001	-0.000	0.003	0.030	0.167
N=68	Tb.Sp	OLS	0.322	0.002	-0.000	0.004	0.046	0.087
	DA	OLS	0.765	0.001	-0.002	0.002	0.020	0.264
	log10 Conn.D	**OLS**	**1.084**	**-0.007**	**-0.011**	**-0.003**	**0.149**	**0.002**
Posterior Calcaneal Facet (PCF)	BV/TV	OLS	0.356	0.001	-0.002	0.004	0.010	0.448
	Tb.Th	OLS	0.229	0.001	-0.001	0.003	0.029	0.192
	Tb.Sp	OLS	0.429	0.001	-0.001	0.003	0.017	0.327
	DA	OLS	0.740	0.000	-0.001	0.002	0.004	0.065
N=62	log10 Conn.D	OLS	0.962	-0.004	-0.009	0.000	0.061	0.056
Trochlea Central (TC)	BV/TV	OLS	0.374	0.001	-0.002	0.003	0.003	0.666
	Tb.Th	OLS	0.230	0.001	-0.001	0.003	0.024	0.230
	Tb.Sp	OLS	0.374	0.002	-0.001	0.004	0.035	0.144
N=65	DA	OLS	0.797	-0.002	-0.004	0.000	0.050	0.080
	log10 Conn.D	**OLS**	**1.014**	**-0.004**	**-0.007**	**0.000**	**0.068**	**0.041**
Trochlea Lateral (TL)	BV/TV	OLS	0.340	0.002	-0.001	0.005	0.022	0.244
	Tb.Th	OLS	0.207	0.002	-0.000	0.003	0.041	0.107
	Tb.Sp	OLS	0.369	0.001	-0.001	0.003	0.012	0.396
N=66	DA	OLS	0.790	-0.000	-0.002	0.001	0.003	0.649
	log10 Conn.D	**OLS**	**1.045**	**-0.005**	**-0.010**	**-0.001**	**0.078**	**0.025**
Trochlea Medial (TM)	BV/TV	OLS	0.340	0.001	-0.001	0.004	0.027	0.206
	Tb.Th	OLS	0.206	0.001	-0.000	0.002	0.051	0.079
	Tb.Sp	OLS	0.382	0.001	-0.001	0.003	0.024	0.240
N=63	DA	OLS	0.763	-0.002	-0.004	0.000	0.046	0.097
	log10 Conn.D	**OLS**	**1.116**	**-0.005**	**-0.008**	**-0.001**	**0.106**	**0.010**

In the talus, significant negative relationships between body mass and Conn.D were found in the TH, PCF, TC, TL, and TM VOIs (Table 4.4). A significant positive relationship was found between body mass and Tb.Sp in the ACF.

Regressions for pooled population male and female samples are provided in Appendix 4.3. For the males one regression table is provided with all males from all populations, and one where the Black Earth males were excluded from the male sample because they had a significantly lower body mass. The low body mass combined with a "robust" trabecular structure (comprised of high BV/TV and Tb.Th, low Tb.Sp and Conn.D, most likely resulting from high levels of physical activity (see Chapter 7) significantly influenced the regressions. Fewer significant regressions were found in the separated male and female analyses compared to the pooled sex regression, most likely due to the lower sample sizes. In the male sample the only significant results were positive regressions with Tb.Sp in the dorsal MT1 head, and the central posterior talar facet of the calcaneus. In the males excluding Black Earth, the only significant negative regressions were found in Conn.D in the dorsal MT1 head and in the talar head. The females also showed a significant negative relationship with Conn.D in the dorsal MT1 head, Achilles tendon and talar head. A significant positive relationship was found between female Tb.Sp and body mass in the calcaneocuboid and posterior calcaneal facet. Finally, a significant positive relationship was found with female DA in the anterior and central posterior talar facet of the calcaneus.

These results confirm the findings from the pooled sample that the strongest effects of body mass are found in Conn.D and Tb.Sp, and to a lesser extent in DA. The significant relationships all follow the same direction (positive for Tb.Sp and negative for Conn.D) in the pooled and sex-specific analyses. This eliminates any concern that the trends found in the pooled sex sample are the result of sexual dimorphism that is unrelated to body mass. Thus, it is justified to use unstandardized residuals from significant regressions as body mass controlled variables when examining differences between groups. Sex differences in regression slopes are found in cortical bone cross-sectional properties (Ruff, 2000; Davies, 2012). However, the small sample sizes in this study prevent this possibility to be investigated for trabecular bone.

Discussion

There is some variation in the scaling relationship between body mass and trabecular properties in the 17 VOIs in the foot. However, all significant results scale in similar direction (positive for Tb.Sp and DA, and negative for Conn.D). The differences in slope may be related to differences in sample size and composition per VOI, measurement error, and variation in loading conditions per VOI. All significant regressions with body mass and Conn.D followed a negative slope. This shows that in these VOIs the average number of interconnected struts per unit volume decreases as body mass increases. The opposite is found for trabecular spacing which increases with body mass. Finally, a significant positive relationship was found between body mass and anisotropy in the plantar ligament and anterior

PTF VOIs of the calcaneus. BV/TV, Tb.Th, and Tb.Sp were predicted to increase with body mass, and Conn.D is predicted to decrease with body mass. Predicted significant increases in BV/TV and Tb.Th were not found.

A very weak positive allometric relationship between BV/TV and body mass has previously been reported, suggesting that total trabecular bone volume in the proximal humerus and femur scales with very slight positive allometry with body size (Doube et al., 2011; Ryan and Shaw, 2013). This weak scaling relationship is consistent with observations that total joint volume and trabecular volume scale isometrically with body mass (Rafferty, 1996; MacLatchy and Muller, 2002). This suggests that in the current sample BV/TV approximates isometry, or no change in ratio with a change in size. Perhaps the range in body mass was is too small and errors due to differences in genetics, environment and behaviour too large, obscuring the slight positive allometry that was found in previous work (Doube et al., 2011; Ryan and Shaw, 2013). Given this scaling relationship, there are theoretically several ways trabecular structure can vary in response to changes in body size. Ryan and Shaw (2013) found strong negative allometric relationship between body mass and trabecular thickness in a large sample of primates, indicating that trabecular thickness increases more slowly in proportion to body mass than would be expected. Large individuals thus have relatively thin trabeculae compared with smaller individuals. No significant scaling was found between body mass and trabecular thickness. However, trabeculae become significantly less interconnected and more widely spaced with increasing body mass. How can BV/TV scale isometrically when there are fewer and more widely spaced trabeculae with increased body mass, without an increase in trabecular thickness? A potential explanation is a change in structure from rods to plate-like trabeculae which would not necessarily result in an increase in trabecular thickness. A change from rods to plates with increasing body mass would also explain the decrease in connectivity density as multiple rods may fuse into a single plate. Unfortunately, rod-to-plate ratios were not calculated in this study. Recent work has demonstrated that the widely used structure model index does not reflect plate-rod geometry (Salmon et al., 2015). It was not feasible to calculate the recently proposed ellipsoid factor (Doube, 2015) for the current sample size due to time constraints, as this would take roughly 1500 hours to calculate. A final explanation for the observations is that the range in body mass in the current sample was is too small and errors due to differences in genetics and behaviour too large, thereby obscuring the increase in Tb.Th and BV/TV with body mass observed in interspecific studies.

Tb.Sp and Conn.D scale with negative allometry within humans, primates and mammals (Doube et al., 2011; Ryan and Shaw, 2013). Conn.D is a volumetric quantity (number connections per mm^3) which one would expect to scale isometrically with body mass. In the current study trabeculae became more widely separated and less interconnected with increasing body mass. Strong correlations were observed between Conn.D and Tb.Sp, and body mass. Currey (2002) states that when bone density is controlled for, Conn.D and Tb.Sp do not significantly contribute to bone strength or stiffness. However, Conn.D is an important factor in clinical studies of age-related bone loss (see Chapter 6).

Two significant positive relationships were unexpectedly found between body mass and degree of anisotropy. A very weak but statistically significant negative relationship between body mass and DA has been found in primate humeral and femoral heads (Ryan and Shaw, 2013). Inspection of pooled and individual regressions shows that in the anterior VOI of the posterior talar facet of the calcaneus a positive regression is found in the Black Earth, Kerma, and St. Johns populations (Figure 4.3, significant in Kerma with $p<.001$, $R^2=.55$). In the plantar ligaments, a positive relationship is found in all four individual populations that was significant in Black Earth ($p=.034$, $R^2=.38$) and Jebel Moya ($p=.014$, $R^2=.51$). It is thus unlikely that these findings are caused by an anomaly in a single population. These unexpected findings may be related to specific loading conditions of the regions in which these VOIs are located. Previous studies of allometry use large VOIs from mobile, multidirectionally loaded ball-and-socket joints (proximal humerus and femur), which are not representative of the effects of a strong unidirectional load on the functional adaptation of DA. Both VOIs are subjected to stress from a single primary direction, thus, increasing anisotropy would be a suitable strategy to cope with increased loads associated with increased body mass. However, if this explanation is true, a positive relationship would be expected in more than just two VOIs because numerous other VOIs were also predicted to be subjected to strong unidirectional loads (see Chapter 2). Findings in the literature may have been obscured by pooling of multiple species with different behaviours and joint morphologies (Doube et al., 2011; Fajardo et al., 2013; Ryan and Shaw, 2013), or combinations of different bones (Barak et al., 2013). However, it is also possible that the two significant regressions with DA are false positives due to the large number of regressions performed in this chapter. The relationship of body mass with trabecular structure within humans during ontogeny will be further investigated in Chapter 8 where the ontogeny of the human calcaneus is examined in relation to gait development and body growth.

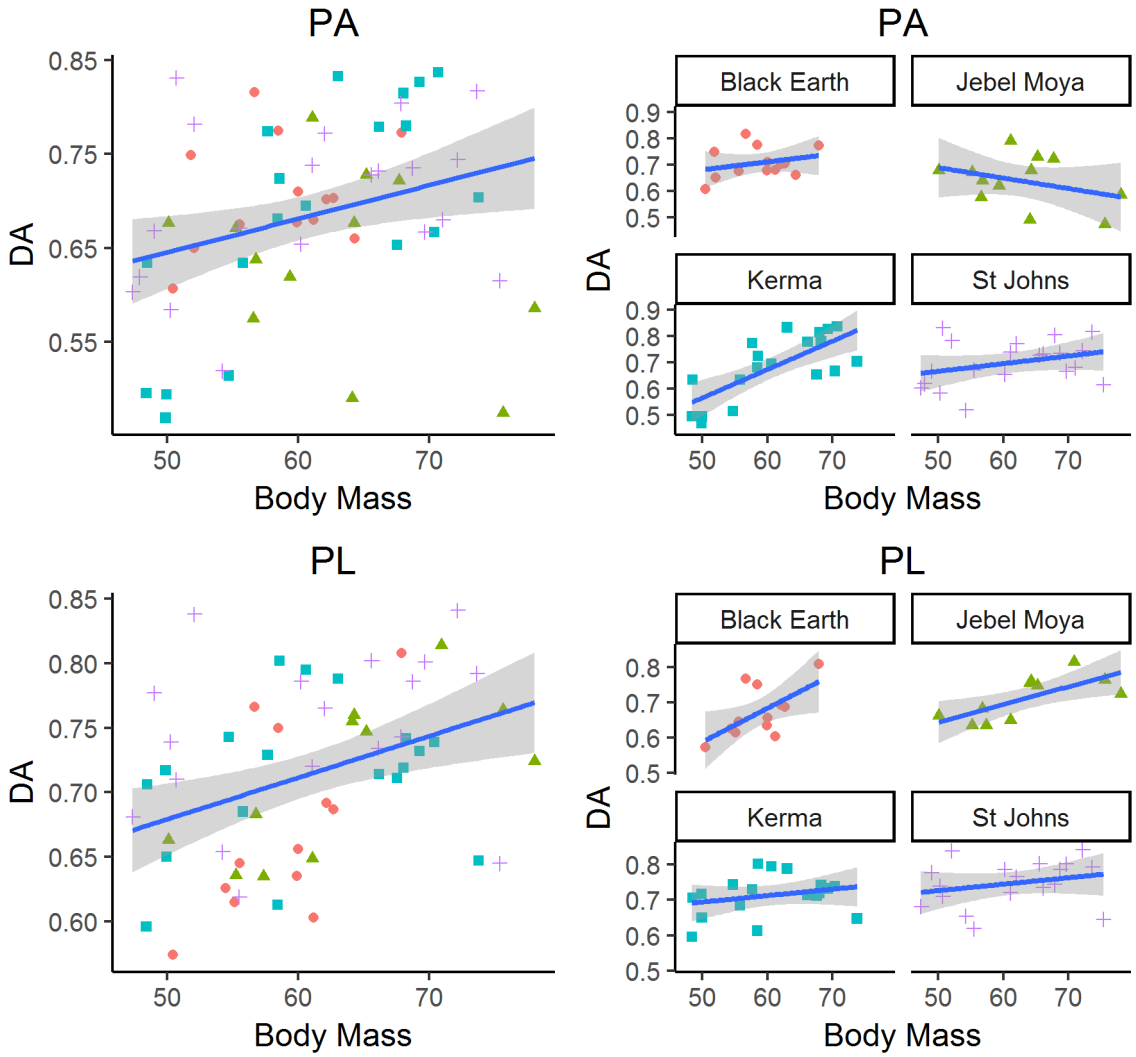

Figure 4.3. Significant OLS regressions of DA to body mass in pooled populations broken down into individual populations. PA: anterior posterior talar facet, PL: plantar ligaments.

The effects of variation in external bone shape rather than size on trabecular architecture are important to understand for the study of human evolution, as fossil hominins present a range of different morphologies. Using whole bone methods of analysing trabecular structure (Tsegai et al., 2013; Gross et al., 2014; Kivell, 2016) could contribute to understanding the effects of external bone morphology on internal structure, particularly on anisotropy and directionality of trabeculae. The best way to investigate the relationship between shape and trabecular organization is to study animals where factors such as body mass, diet, activity, and environment can be controlled. Computer modelling and finite element analysis may also be a rewarding approach by allowing researchers to artificially manipulate shape and observe changes in the flow of stress throughout a bone.

Conclusion

Significant relationships were found between body mass and trabecular properties in the human foot. With increasing body mass trabeculae become significantly more widely spaced and less interconnected. Predicted increases in BV/TV and Tb.Th with body mass were not found, presumably because the slope is too shallow to detect in the small range of body masses in the current sample. Similar significant scaling relationships were found in female, male, and pooled sex samples. However, less significant results were found due to the lower sample size of single sex samples. Differences in slopes of significant regressions could not be found between males and females due to low sample size and large confidence intervals. Residuals from the significant regressions will be used as body mass standardized variables in the following chapters.

Chapter 5 - Sexual dimorphism in trabecular structure

Introduction

Sexual dimorphism is found in human body mass, size, shape, physiology, and behaviour, but little is known about sexual dimorphism in human trabecular structure. There are significant differences in bone mass between men and women with ageing (Duan et al., 2001; Seeman, 2001). Eckstein et al. (2007) found that sex differences in BV/TV were region specific throughout the skeleton in elderly people. However, elderly individuals do not represent the average human population. Khosla et al. (2006) found significantly greater BV/TV (26%) in the distal radius of young adult males compared to females. Thus far, no significant sexual dimorphism has been observed in primates (Dr. Tim Ryan, personal communication). Saers et al. (2016) and a recent study by Chirchir et al. (2017) found no sexual dimorphism in bone volume fraction in the upper and lower limbs in various archaeological samples. This chapter investigates sexual dimorphism in trabecular architecture in the feet of four different human archaeological populations.

Differences between men and women in diaphyseal bone modeling affect their response to mechanical loading as well as the regions where bone is deposited (Callewaert et al., 2010). The opposing action of sex steroids in males and females partially underlie the sexual dimorphism observed in human cortical bone structure. Due to different regulatory effects of sex hormones, periosteal expansion is inhibited in favour of endocortical apposition in females during cortical bone growth (Callewaert et al., 2010). This results in males having larger total diaphyseal cross-sectional areas resulting in greater resistance to compression and bending loads in long bones. In female trabecular bone regulation, oestrogen receptor activation is required for normal bone growth. In males, these are also required during cortical bone growth, while for trabecular growth androgen receptor activation is exclusively responsible. Aside from sex hormones, insulin-like growth factor 1 (IGF1) is more abundant in male mice during puberty. IGF1 has a strong effect on bone formation in mice and humans, although extrapolation of mice data on humans should be treated with care (Callewaert et al., 2010; Jepsen et al., 2015). Sexual dimorphism is not only determined by androgen action in males and oestrogen action in females, but also by complex sex- and time-specific interactions between sex hormones, IGF1, and mechanical loading, particularly during growth (Del Giudice et al., 2009; Callewaert et al., 2010). These complex and incompletely understood sex differences in bone growth and maintenance complicate interpretations of sexual dimorphism in the context of behavioural variation between males and females.

After correcting for the effects of body mass, the observed sexual dimorphism in limb bone diaphyseal midshaft rigidity and shape is interpreted as reflecting differences in behaviour in past populations (Ruff, 1987; Carlson et al., 2007). This assumption is based on the observation that after correcting for the effects of body mass, differences between males and females are low in modern humans compared to prehistoric populations (Ruff, 1987, 2008). Sexual dimorphism in lower limb robusticity and shape

has been reducing since the Palaeolithic (Ruff, 1987). Among hunter gatherers, males tend to have significantly more robust, and more anteroposteriorly strengthened lower limb diaphyses than females. This is interpreted as the result of greater terrestrial mobility in males (Ruff, 2008). This sexual dimorphism is reduced in agriculturalists and even further in modern industrial populations (Ruff, 2008). This has been interpreted as a reduction in the differences in mobility between men and women with men becoming increasingly less mobile. However, recent research has demonstrated that after correcting for body mass and bone length, modern industrial white and black males have significantly more robust femora than white and black females (Jepsen et al., 2015). While lower limb bone diaphyseal strength shows significant sexual dimorphism in past and present populations, little is known about trabecular bone. In this chapter, sexual dimorphism in trabecular structure is investigated within the talus, calcaneus and first metatarsal of four different human populations.

Sexual dimorphism in lower limb diaphyseal rigidity in study populations

Previous work has examined the cross-sectional geometry of the Black Earth (Shaw et al., 2014), Jebel Moya, and Kerma populations (Nikita et al., 2011; Stock et al., 2011). Cross-sectional properties of the femoral and tibial midshaft taken from Nikita et al. (2011) are summarised in Table 5.1. TA/BM is the total area of a bone cross-section divided by body mass. This represents a measure of a bone's compressive strength, and is strongly correlated to torsional rigidity (J). I_x/I_y represents anteroposterior divided by mediolateral bending rigidity. I_{max}/I_{min} is the ratio of maximum divided by minimum bending rigidity. The femoral and tibial properties were averaged between left and right sides as very little bilateral asymmetry was present. In the femur and tibia of the Kerma and Jebel Moya, sexual dimorphism in TA was significant ($p<.001$ in the femur and $p<.05$ in the tibia). No significant sexual dimorphism was found in shape indices (Nikita et al., 2011). In both populations, the males have significantly higher TA than females, even after correcting for the effects of body mass. This is interpreted as a reflection of greater male mobility relative to females (Nikita et al., 2011; Stock et al., 2011).

Table 5.1. Summary statistics of cross-sectional properties published in Nikita et al. (2011). TA/BM is total area divided by body mass. Data are reported for the right limb.

	Males (n=18)			**Females (n=24)**		
	TA/BM	**I_x/I_y**	**I_{max}/I_{min}**	**TA/BM**	**I_x/I_y**	**I_{max}/I_{min}**
Femur						
Kerma	870.7±19.4	1.29 ±0.05	1.37±0.04	773.0±12.0	1.14±0.04	1.29±0.02
Jebel Moya	962.3±10.7	1.32±0.05	1.52±0.04	828.1±18.1	1.28±0.05	1.39±0.05
Tibia						
Kerma	760.1±21.8	1.88±0.08	1.99±0.08	627.6±13.1	2.24±0.13	2.27±0.13
Jebel Moya	850.1±17.9	1.89±0.09	1.93±0.09	760.1±21.0	1.97±0.13	1.98±0.13

Cross-sectional properties of the Black Earth femoral midshaft provided by Dr. Tim Ryan are summarized in Table 5.2. No significant sexual dimorphism was found in the Black Earth in I_{max}/I_{min}, nor in body mass standardized indices of torsional rigidity (J), section modulus (Zp), or compressive

strength (CSA). This suggests that male and female Black Earth individuals had equally rigid femoral diaphyses after correcting for the effects of body mass, suggesting that they were likely equally mobile. The tibia is often regarded as a better proxy of mobility in archaeological populations (Stock, 2006), but no data exists on tibial cross-sectional rigidity in the Black Earth.

Midshaft cross-sectional properties of thirteen femora matching the Kerma individuals used in this study were calculated and presented in Table 5.2. Body mass corrected J and Zp were significantly larger in males compared to females. This indicates that males have greater femoral torsional rigidity and strength, presumably due to higher levels of terrestrial mobility. The values in Table 5.1 and 5.2 are slightly different because the values in Table 5.1 are taken from Nikita et al. (2011), while Table 5.2 is calculated based on data provided by Dr. Tim Ryan and Dr. Colin Shaw. The values are slightly different for Kerma in the two tables due to different sample sizes.

Table 5.2. Summary statistics and t-tests of body mass standardized cross-sectional properties of the femoral midshaft of Black Earth and Kerma males and females.

Cross-sectional properties							**Levene's Test**		**T-test**		
	Property	**Sex**	**N**	**Mean**	**S.D.**	**S.E.**	**F**	***p***	**t**	**df**	***p***
Black Earth	I_{max}/I_{min}	M	11	1.33	0.16	0.05	.784	.387	.519	18	.610
		F	9	1.29	0.22	0.07					
	J	M	11	33111	7503	2262	.112	.742	.226	18	.824
		F	9	32175	10993	3664					
	Zp	M	11	965	170	51	.065	.802	-.027	18	.979
		F	9	968	236	79					
	CSA	M	11	668	74	22	.471	.501	.152	18	.881
		F	9	662	112	37					
Kerma	I_{max}/I_{min}	M	8	1.36	0.15	0.05	.713	.416	1.912	11	.082
		F	5	1.21	0.09	0.04					
	J	M	7	18885	3441	1300	5.179	.049	3.669	6.889	**.008**
		F	4	13929	727	363					
	Zp	M	7	954	95	36	2.756	.131	2.731	9	**.023**
		F	4	816	38	18					
	CSA	M	8	585	117	41	1.098	.317	.747	11	.471
		F	*5*	*544*	*46*	*20*					

Methods

Sexual dimorphism in trabecular structure is examined in pooled and individual populations (Table 5.3).

Table 5.3. Sample size used in this chapter for each population and sex per VOI. Achilles tendon (AT), calcaneal tuber (CT), plantar ligaments (PL), posterior talar facet (PP: posterior, PC: central, PA: anterior), calcaneocuboid (CC), dorsal base (BD), plantar base (BP), dorsal head (HD), plantar head (HP), talar head (TH), anterior calcaneal facet (ACF), posterior calcaneal facet (PCF), trochlea (lateral: TL, central: TC, medial: TM).

		Black Earth		**Jebel Moya**			**Kerma**		**St Johns**		**Total**
		Sex		**Sex**			**Sex**		**Sex**		
		M	**F**	**M**	**F**	**I**	**M**	**F**	**M**	**F**	
Calcaneus	AT	7	10	8	2	5	9	7	9	11	69
	CC	7	6	9	2	5	12	7	8	9	66
	CT	7	9	10	2	5	12	7	8	10	71
	PA	7	6	8	2	4	12	7	9	11	67
	PC	6	7	8	2	4	12	6	9	11	66
	PP	7	8	9	1	4	12	5	9	11	67
	PL	6	6	5	1	5	11	7	8	10	60
MT1	BD	7	8	5	2	2	9	5	9	9	56
	BP	6	7	2	2	1	9	4	9	9	49
	HD	8	9	5	3	3	9	4	9	9	59
	HP	7	7	4	2	2	9	4	9	9	53
Talus	ACF	5	8	5	2	3	13	7	8	11	62
	PCF	5	7	7	4	4	12	6	6	11	62
	TH	5	6	10	4	5	12	7	8	11	68
	TL	7	8	10	4	5	10	5	7	11	67
	TC	6	8	9	4	3	12	5	7	11	65
	TM	7	8	9	3	3	10	5	7	11	63

The Jebel Moya population was excluded from the pooled population due to its unequal sex ratio with very few females. The relative robusticity of this population would artificially increase male robusticity relative to females if included in the pooled sample. Independent t-tests are used to assess sexual dimorphism in trabecular structure in a pooled population sample as well as within individual populations, in every VOI. Mann-Whitney U tests were used when groups were not normally distributed. A Bonferroni correction for multiple comparisons was calculated, reducing α from .05 to .003 (=.05/17 VOIs). Strong correlations reported previously between trabecular properties in different

VOIs suggest that the variables under consideration are highly interconnected, in which case Armstrong (2014) argues that it is not advisable to perform a Bonferroni correction. Following recommendations by Armstrong (2014), the results will be discussed both with and without corrected α levels. Based on the strong correlations between trabecular properties across VOIs (mean R of pairwise comparisons between the 17 VOIs throughout the foot: BV/TV=.72, Tb.Th=.73, DA=.20, residual Tb.Sp=.62, residual Conn.D=.52) it is expected that sexual dimorphism should be evident in multiple VOIs. Thus, isolated significant results in BV/TV, Tb.Th, residual Conn.D, and residual Tb.Sp will be regarded as false positives. However, this does not apply to DA due to the low and nonsignificant correlations between DA in different VOIs. Trabecular properties are plotted using boxplots with the median and interquartile range to illustrate the distribution of the data for males and females.

Ryan and Shaw (2012) argued that using suites of trabecular variables may be the most appropriate method for assessing intergroup variation in these complex structures. Thus, multivariate principal components analysis is used to assess sexual dimorphism. One-way ANOVA will be performed on the individual principal components to see if combinations of related variables better discriminate between populations or volumes of interest. The ratio of sample size to number of variables is important in PCA. When the 5 variables are used in a combination of all 7 calcaneal VOIs there is n N:p ratio of 48 individuals to 35 variables. A ratio of 5:1 is often cited as a minimum rule of thumb to produce accurate results. However, experimental validation of this rule of thumb is minimal (Osborne and Costello, 2004). A PCA will be run with all combined variables, but PCA's will also be run for each individual VOI to ensure a suitable N:p ratio. PCA's are performed for individual as well as pooled population samples. MANOVA will be run on the first three principal components to assess sexual dimorphism in correlated suites of trabecular properties.

The degree of sexual dimorphism was calculated within populations. In a review of methods of quantifying sexual dimorphism, Smith (1999) demonstrated that a ratio of male/female mean sufficiently represents sexual dimorphism. Due to the large standard deviations for residual property means, the ratios of the means are not representative and thus discarded.

Hypotheses

More rigid (robust) trabecular architectures are associated with higher BV/TV, thicker and less widely separated trabeculae, with fewer connections between trabeculae (Hodgskinson and Currey, 1990; Goulet et al., 1994; Odgaard et al., 1997; Kabel et al., 1999; Ulrich et al., 1999; Rubin et al., 2002; Mittra et al., 2005; Rincón-Kohli and Zysset, 2009; Barak et al., 2011; Karim and Vashishth, 2011; Ryan and Shaw, 2015). An increase in DA results in an increase in bone stiffness in the primary direction of anisotropy but a decrease in stiffness if the structure is loaded from different directions. DA was shown to be responsive to changes in direction of loading (Barak et al., 2011). Lack of significant correlations between BV/TV and DA (Chapter 3) suggests that DA is more likely a

reflection of loading directionality than magnitude. Potential differences in DA are thus hypothesized to reflect differences loading directions between males and females.

Sexual dimorphism in lower limb cortical bone rigidity and shape indices has decreased with time (Ruff, 1987, 2008; Macintosh et al., 2014; Ruff et al., 2015). Hunter-gatherers exhibit the greatest sexual dimorphism, followed by agriculturalists, and it is lowest in modern populations after correcting for differences in body mass. In the current study, no sexual dimorphism was found in the limb bone diaphyses of the Black Earth hunter-gatherers, but significant sexual dimorphism was found in the Kerma and Jebel Moya. Unfortunately, no CT-scans are available to assess sexual dimorphism in diaphyseal cross-sectional properties in the St. Johns population. The Kerma and Jebel Moya males have significantly stronger femoral and tibial diaphyses compared to females (Nikita et al., 2011; Stock et al., 2011). This is interpreted as the result of differences in mobility between males and females with men being more mobile. This would suggest that significant sexual dimorphism will be present in trabecular architecture between males and females with males being more robust in Kerma and Jebel Moya (see below for a description of what constitutes trabecular robusticity). It is predicted that the St. Johns will be less sexually dimorphic compared to the Kerma and Jebel Moya, but with males still possessing significantly more robust trabecular structures than females, based on trend of significant decline in lower limb rigidity through time (Ruff, 2008). No sexual dimorphism is predicted to be found in the Black Earth population based on the lack of sexual dimorphism in femoral cross-sectional geometry.

The above predictions rely on the premise that trabecular bone follows similar adaptive patterns as cortical bone. However, Shaw and Ryan (2012) found that trabecular and cortical bone do not necessarily covary. Using discriminant function analysis, Ryan and Shaw (2012) did manage to find significant relationship between trabecular architecture and locomotor mode. They suggest that considering suites of variation in trabecular properties using multivariate statistical methods may be a more suitable approach for studying trabecular bone functional adaptation (Ryan and Shaw, 2012). Here sexual dimorphism is examined using univariate t-tests and Mann-Whitney U tests as well as multivariate principal components analysis. PCA was chosen over DFA because it makes no prior assumptions of group membership, and the strong correlations between trabecular properties are no issue in PCA.

Results

A table summarizing significant differences in trabecular structure between pooled males and pooled females is given in Table 5.4. Sexual dimorphism in the pooled population excluding Jebel Moya are given in Figure 5.1.

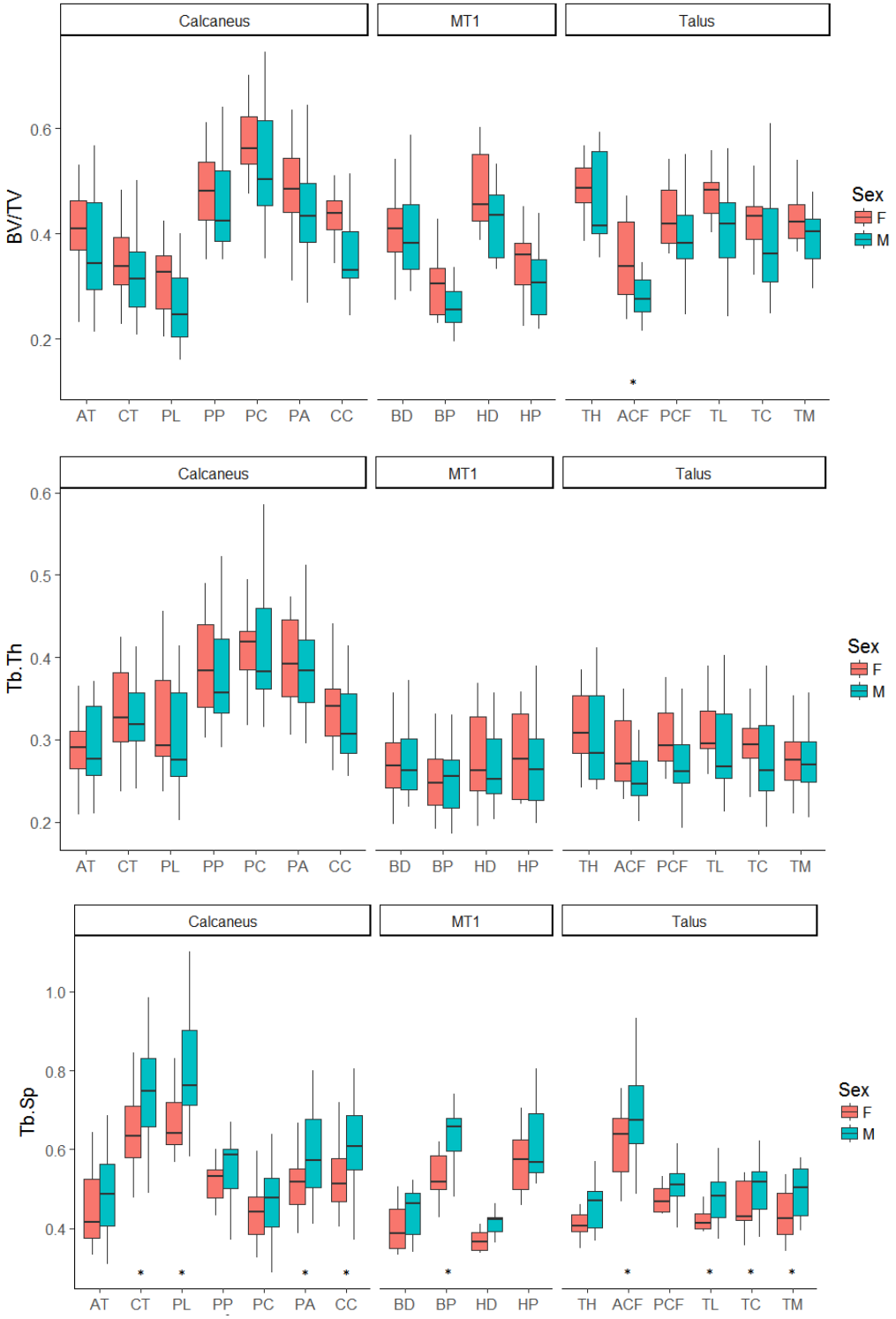
Calcaneus
MT1
Talus
BV/TV
0.6
0.4
0.2
AT CT PL PP PC PA CC
BD BP HD HP
TH ACF PCF TL TC TM
Sex
F
M
Tb.Th
0.6
0.5
0.4
0.3
0.2
Tb.Sp
1.0
0.8
0.6
0.4

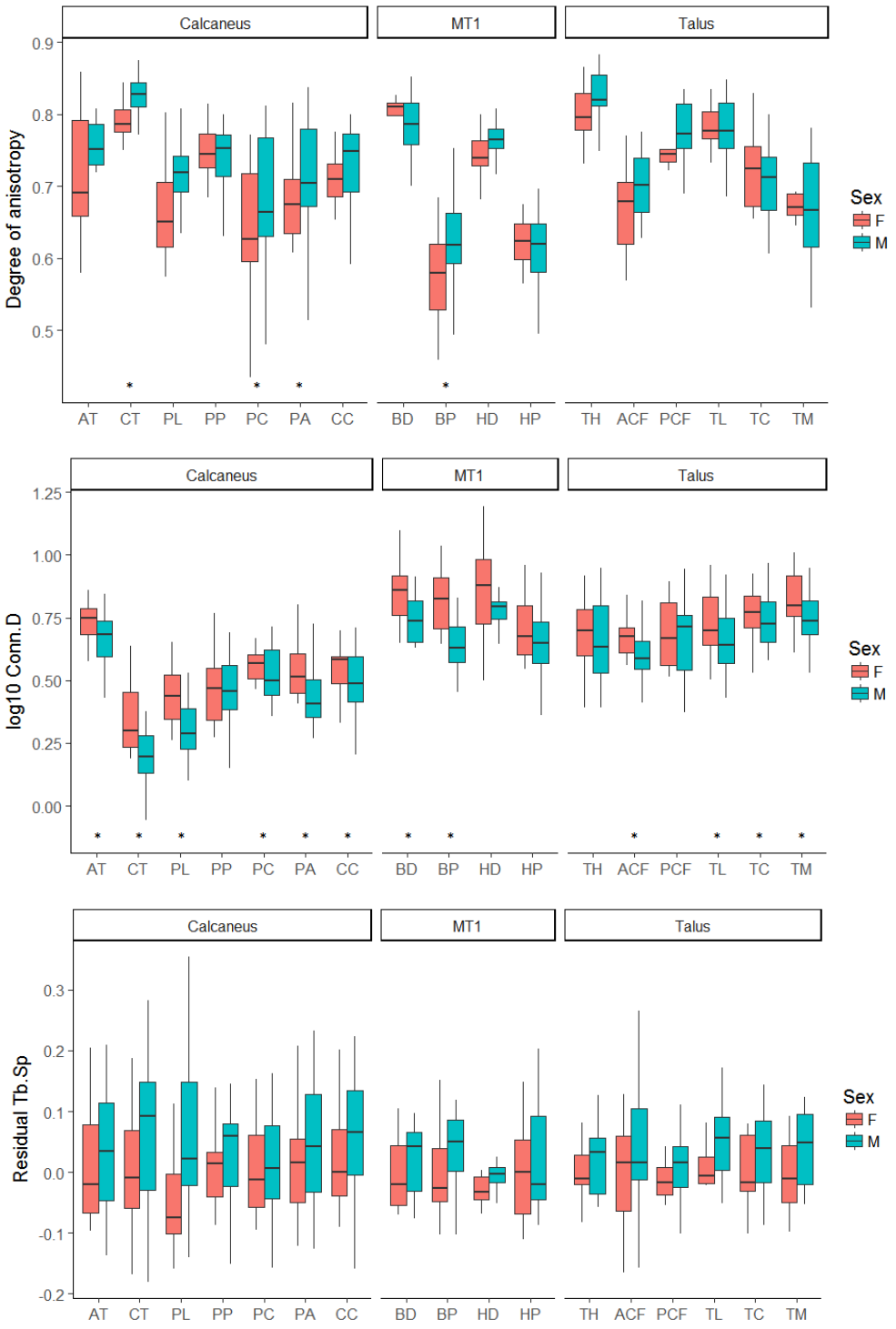
Calcaneus
MT1
Talus
Degree of anisotropy
0.9
0.8
0.7
0.6
0.5
AT CT PL PP PC PA CC
BD BP HD HP
TH ACF PCF TL TC TM
Sex
F
M
log10 Conn.D
1.25
1.00
0.75
0.50
0.25
0.00
Residual Tb.Sp
0.3
0.2
0.1
0.0
-0.1
-0.2

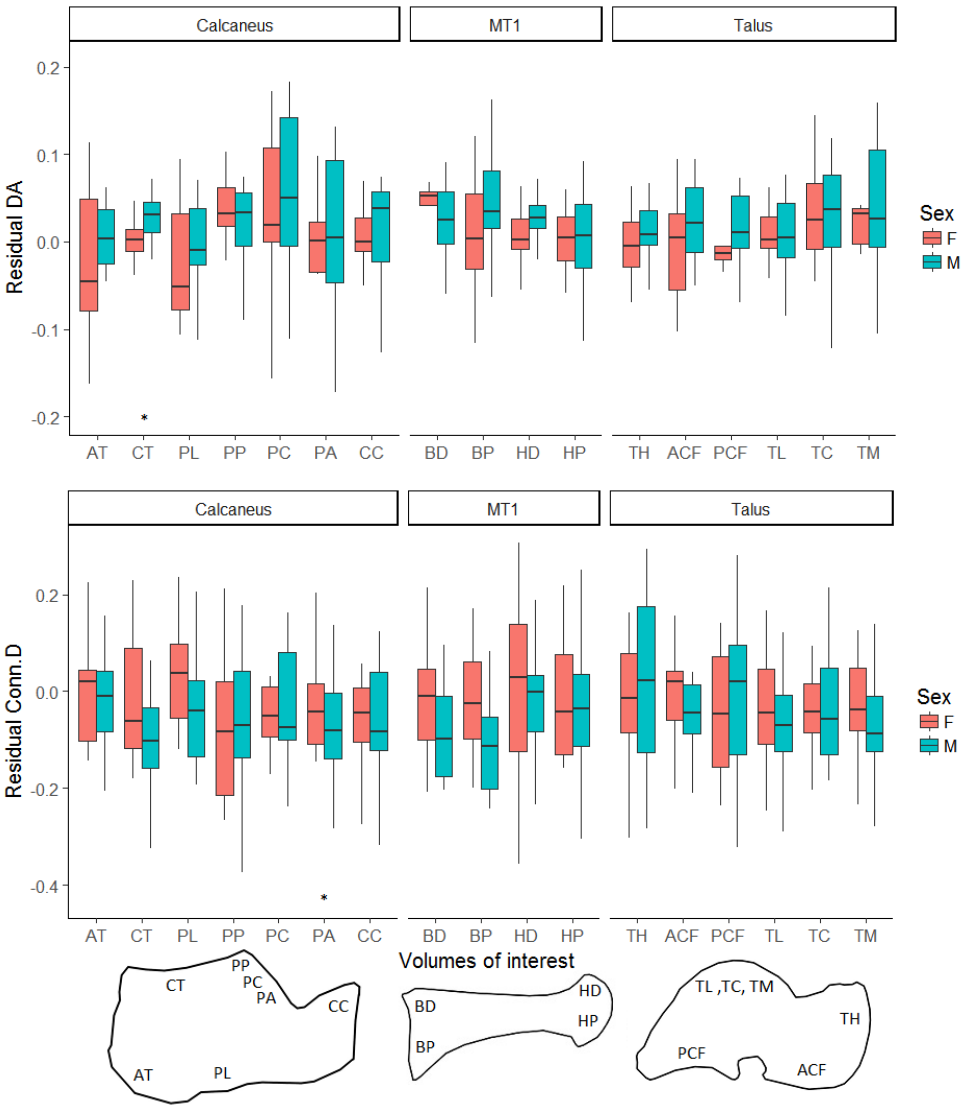

*Figure 5.1. Boxplots of pooled population sexual dimorphism excluding Jebel Moya. Volumes of interest: Achilles tendon (AT), calcaneal tuber (CT), plantar ligaments (PL), posterior talar facet (PP: posterior, PC: central, PA: anterior), calcaneocuboid (CC), dorsal base (BD), plantar base (BP), dorsal head (HD), plantar head (HP), talar head (TH), anterior calcaneal facet (ACF), posterior calcaneal facet (PCF), trochlea (lateral: TL, central: TC, medial: TM). *indicates a significant difference (p<.05).*

Table 5.4. Summary table of significant sexual dimorphism of a pooled sample excluding Jebel Moya. Volumes of interest: Achilles tendon (AT), calcaneal tuber (CT), plantar ligaments (PL), posterior talar facet (PP: posterior, PC: central, PA: anterior), calcaneocuboid (CC), dorsal base (BD), plantar base (BP), dorsal head (HD), plantar head (HP), talar head (TH), anterior calcaneal facet (ACF), posterior calcaneal facet (PCF), trochlea (lateral: TL, central: TC, medial: TM).

Pooled		**BV/TV**	**Tb.Th**	**DA**	**Tb.Sp**	**Conn.D**	**Res. Tb.Sp**	**Res. Conn.D**	**Res.Da**
Calcaneus	AT					F>M			
	CC				M>F	F>M			
	CT			M>F	M>F	F>M			M>F
	PA			M>F	M>F	F>M		F>M	
	PC			M>F		F>M			
	PP								
	PL				M>F	F>M			
MT1	BD					F>M			
	BP			M>F	M>F	F>M			
	HD								
	HP								
Talus	ACF	F>M			M>F	F>M			
	PCF								
	TH								
	TL				M>F	F>M			
	TC				M>F	F>M			
	TM				M>F	F>M			

A few clear trends can be observed in Table 5.4 where in 11 out of 17 VOIs females have more interconnected struts than males and in 9 out of 17 VOIs males have significantly more widely separated struts. However, when correcting for differences in body size there is only one significant difference in the PA where females have higher Conn.D than males. BV/TV is significantly higher in females in the ACF VOI. Males have significantly more anisotropic trabeculae in the calcaneal tuber, posterior and central PTF, and the plantar base of the first metatarsal. After correcting for body mass the males have more anisotropic structures in the calcaneal tuber.

After Bonferroni correction (α=.003) only Conn.D remained significant in the PA, PC, and TM VOIs. The fact that the significant results are highly consistent in different VOIs, particularly in DA, Tb.Sp, and Conn.D suggests that there is indeed a pattern of differences between males and females. The lack of significant differences after the Bonferroni correction most likely results from an inflated type II error rate. The isolated significant result in residual Conn.D is interpreted as a false positive.

Sexual dimorphism in individual populations

Sexual dimorphism in the Black Earth population is plotted in Figure 5.2.


Calcaneus
MT1
Talus
BV/TV
Tb.Th
DA
Residual DA
Sex
F
M
AT CT PL PP PC PA CC
BD BP HD HP
TH ACF PCF TL TC TM

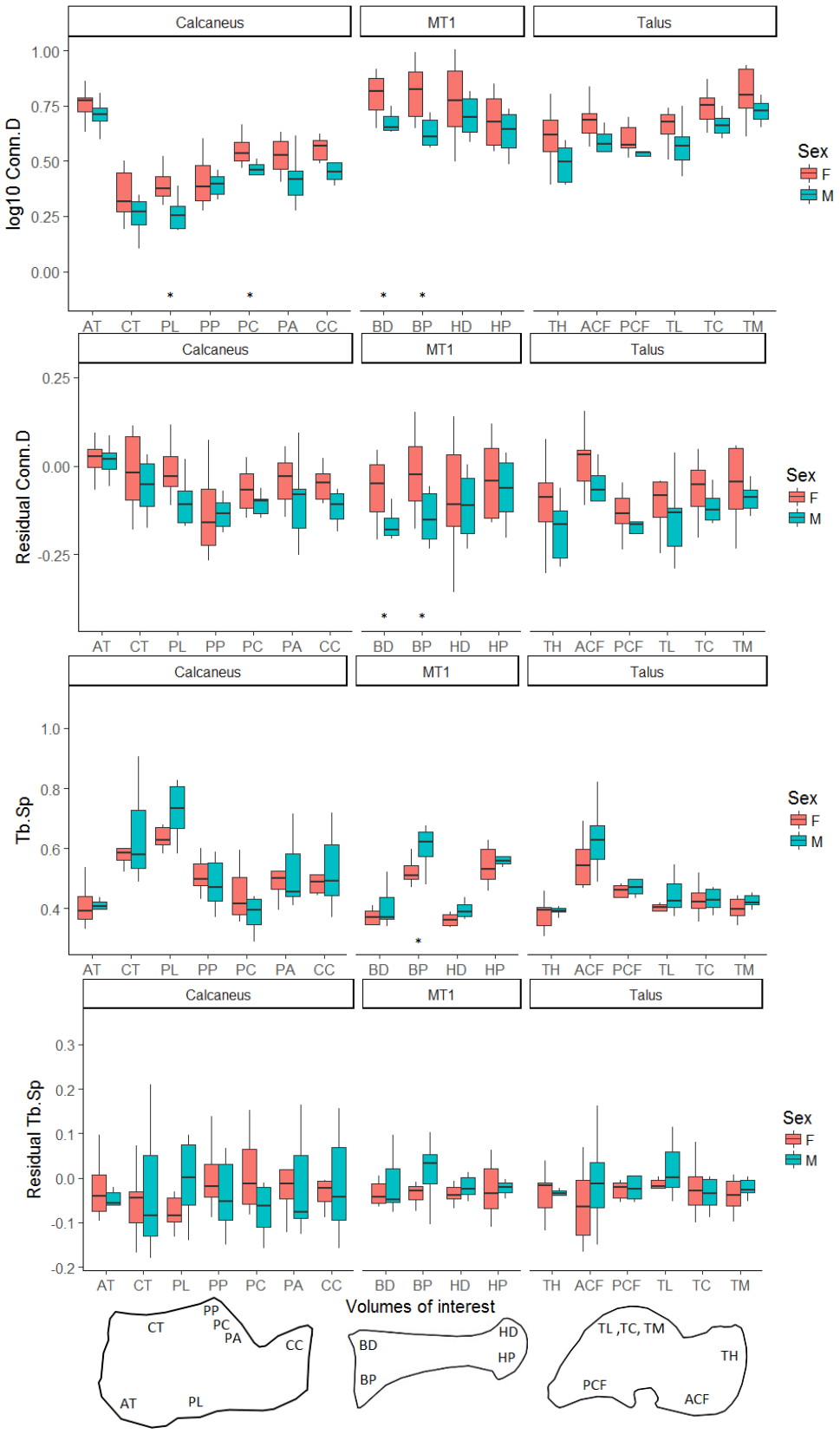

Figure 5.2. Boxplots of the median and interquartile range of male and female Black Earth trabecular properties. Volumes of interest: Achilles tendon (AT), calcaneal tuber (CT), plantar ligaments (PL), posterior talar facet (PP: posterior, PC: central, PA: anterior), calcaneocuboid (CC), dorsal base (BD), plantar base (BP), dorsal head (HD), plantar head (HP), talar head (TH), anterior calcaneal facet (ACF), posterior calcaneal facet (PCF), trochlea (lateral: TL, central: TC, medial: TM).

Table 5.5. Summary table of significant sexual dimorphism in Black Earth. Volumes of interest: Achilles tendon (AT), calcaneal tuber (CT), plantar ligaments (PL), posterior talar facet (PP: posterior, PC: central, PA: anterior), calcaneocuboid (CC), dorsal base (BD), plantar base (BP), dorsal head (HD), plantar head (HP), talar head (TH), anterior calcaneal facet (ACF), posterior calcaneal facet (PCF), trochlea (lateral: TL, central: TC, medial: TM).

Black Earth		BV/TV	Tb.Th	DA	Tb.Sp	Conn.D	Res. Tb.Sp	Res. Conn.D	Res.Da
Calcaneus	AT								
	CC								
	CT								
	PA								
	PC					F>M			
	PP								
	PL					F>M			
MT1	BD					F>M		F>M	
	BP				M>F	F>M		F>M	
	HD								
	HP								
Talus	ACF								
	PCF								
	TH								
	TL								
	TC								
	TM								

Few significant differences were found between males and females in the Black Earth population (Table 5.5). Mean BV/TV and Tb.Th were higher in males in most VOIs but not significantly, and no differences were found in anisotropy. Males do have significantly more widely separated struts in the plantar base of the first metatarsal. Females display significantly greater Conn.D in both MT1 base VOIs, the central PTF, and the plantar ligaments. After removing variation associated with body mass the differences in dorsal and plantar MT1 base remain significant. No significant differences were found after applying a Bonferroni correction.

Trabecular properties in males and females from Jebel Moya are plotted in Figure 5.3.

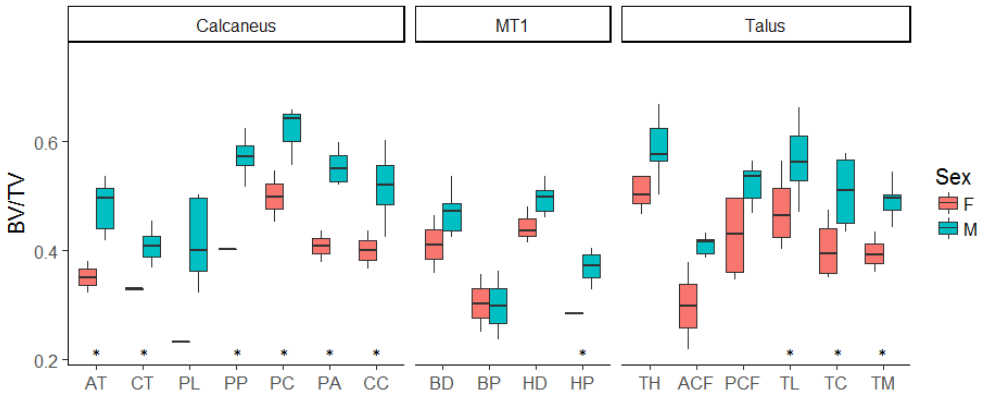

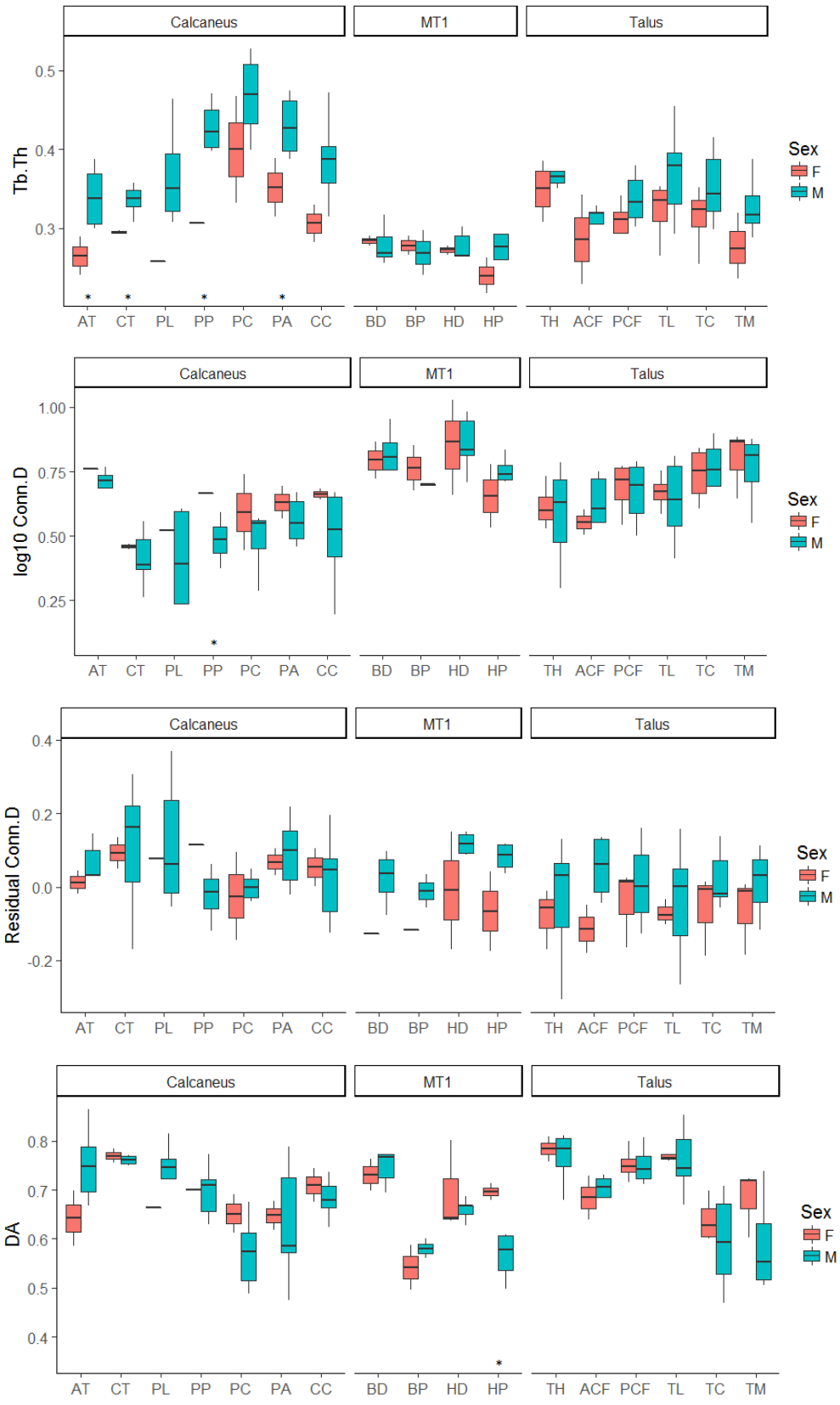
Calcaneus
MT1
Talus
Tb.Th
log10 Conn.D
Residual Conn.D
DA
Sex
F
M
AT CT PL PP PC PA CC
BD BP HD HP
TH ACF PCF TL TC TM

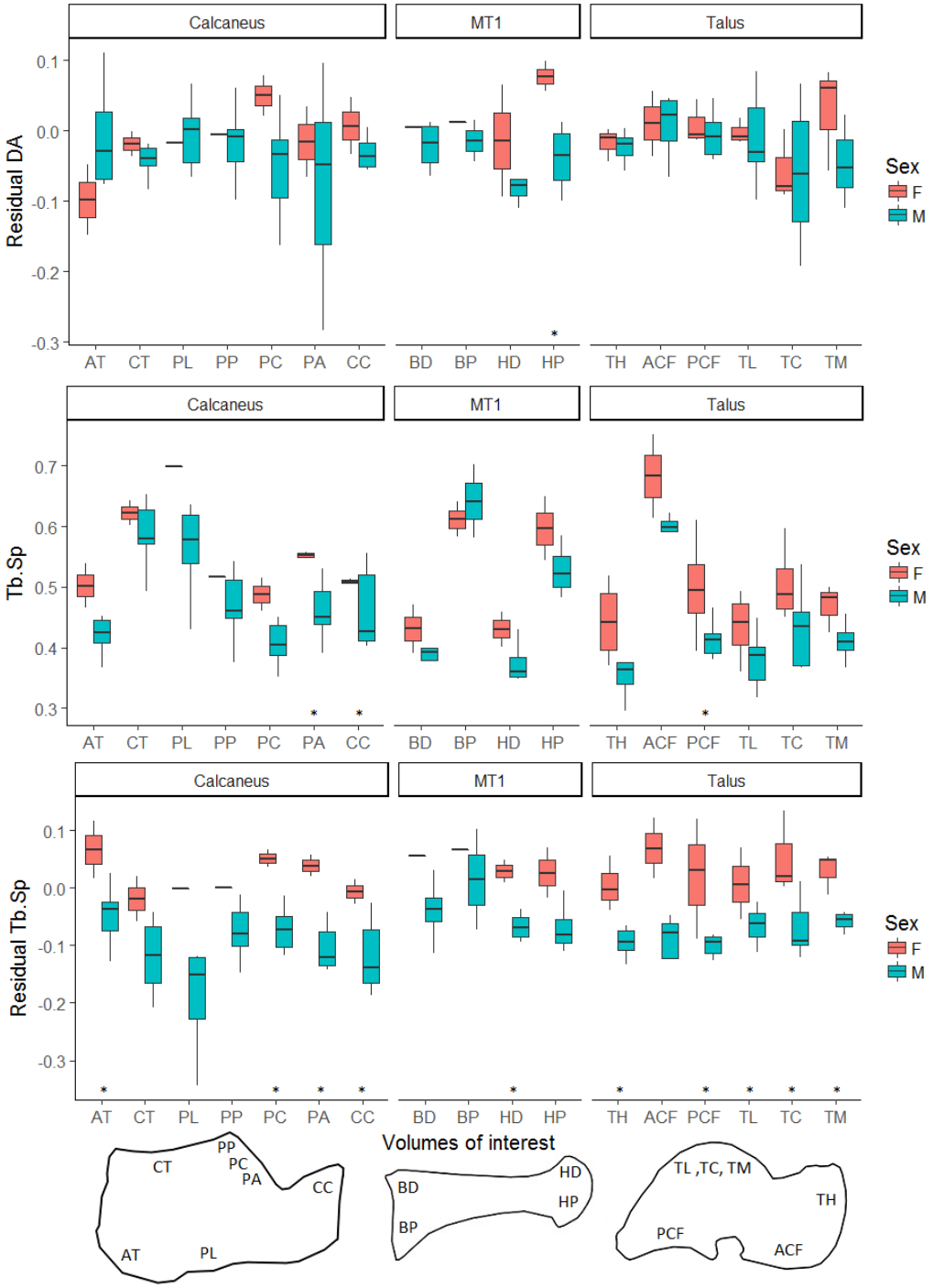

Figure 5.3. Boxplots of the median and interquartile range of male and female trabecular properties in Jebel Moya. Volumes of interest: Achilles tendon (AT), calcaneal tuber (CT), plantar ligaments (PL), posterior talar facet (PP: posterior, PC: central, PA: anterior), calcaneocuboid (CC), dorsal base (BD), plantar base (BP), dorsal head (HD), plantar head (HP), talar head (TH), anterior calcaneal facet (ACF), posterior calcaneal facet (PCF), trochlea (lateral: TL, central: TC, medial: TM).

Table 5.6. Summary table of significant sexual dimorphism in Jebel Moya. Volumes of interest: Achilles tendon (AT), calcaneal tuber (CT), plantar ligaments (PL), posterior talar facet (PP: posterior, PC: central, PA: anterior), calcaneocuboid (CC), dorsal base (BD), plantar base (BP), dorsal head (HD), plantar head (HP), talar head (TH), anterior calcaneal facet (ACF), posterior calcaneal facet (PCF), trochlea (lateral: TL, central: TC, medial: TM).

Jebel Moya		BV/TV	Tb.Th	DA	Tb.Sp	Conn.D	Res. Tb.Sp	Res. Conn.D	Res. Da
Calcaneus	AT	M>F	M>F				F>M		
	CC	M>F			F>M		F>M		
	CT	M>F	M>F						
	PA	M>F	M>F		F>M		F>M		
	PC	M>F					F>M		
	PP	M>F	M>F			F>M			
	PL								
MT1	BD								
	BP								
	HD						F>M		
	HP	M>F		F>M					F>M
Talus	ACF								
	PCF				F>M		F>M		
	TH						F>M		
	TL	M>F					F>M		
	TC	M>F					F>M		
	TM	M>F					F>M		

The Jebel Moya are difficult to interpret due to the small number of females relative to males (Table 5.6). Only in the talar VOIs and the HD VOI was there more than two female to compare to the males. It is quite likely that some of the individuals of indeterminate sex are females, and since they are all more similar to males than the females, it is likely that sexual dimorphism is lower than Figure 5.3 suggests. Significant differences in BV/TV and Tb.Th were only found in calcaneal VOIs where there are only two females. Males have significantly higher BV/TV in the medial trochlea and all calcaneal VOIs except the plantar ligaments. Males also have significantly thicker trabeculae at the Achilles tendon, the three PTF VOIs, and the medial trochlea of the talus. Males have significantly higher DA in at the Achilles tendon both before and after correcting for body mass. Females possess greater Conn.D in the PP and BP VOIs, but not after correcting for body mass. After correcting for body mass, females have significantly higher Tb.Sp in more VOIs than prior to body mass corrections, particularly in the talus and calcaneus.

After Bonferroni correction (α=.003) only BV/TV and Tb.Th remain significant in the PP VOI. The consistency of significant results between different VOIs suggests that there is indeed a pattern of differences between males and females. The lack of significant differences after the Bonferroni correction most likely results from an inflated type II error rate (Armstrong, 2014).

Trabecular properties for the Kerma males and females are plotted in Figure 5.4.

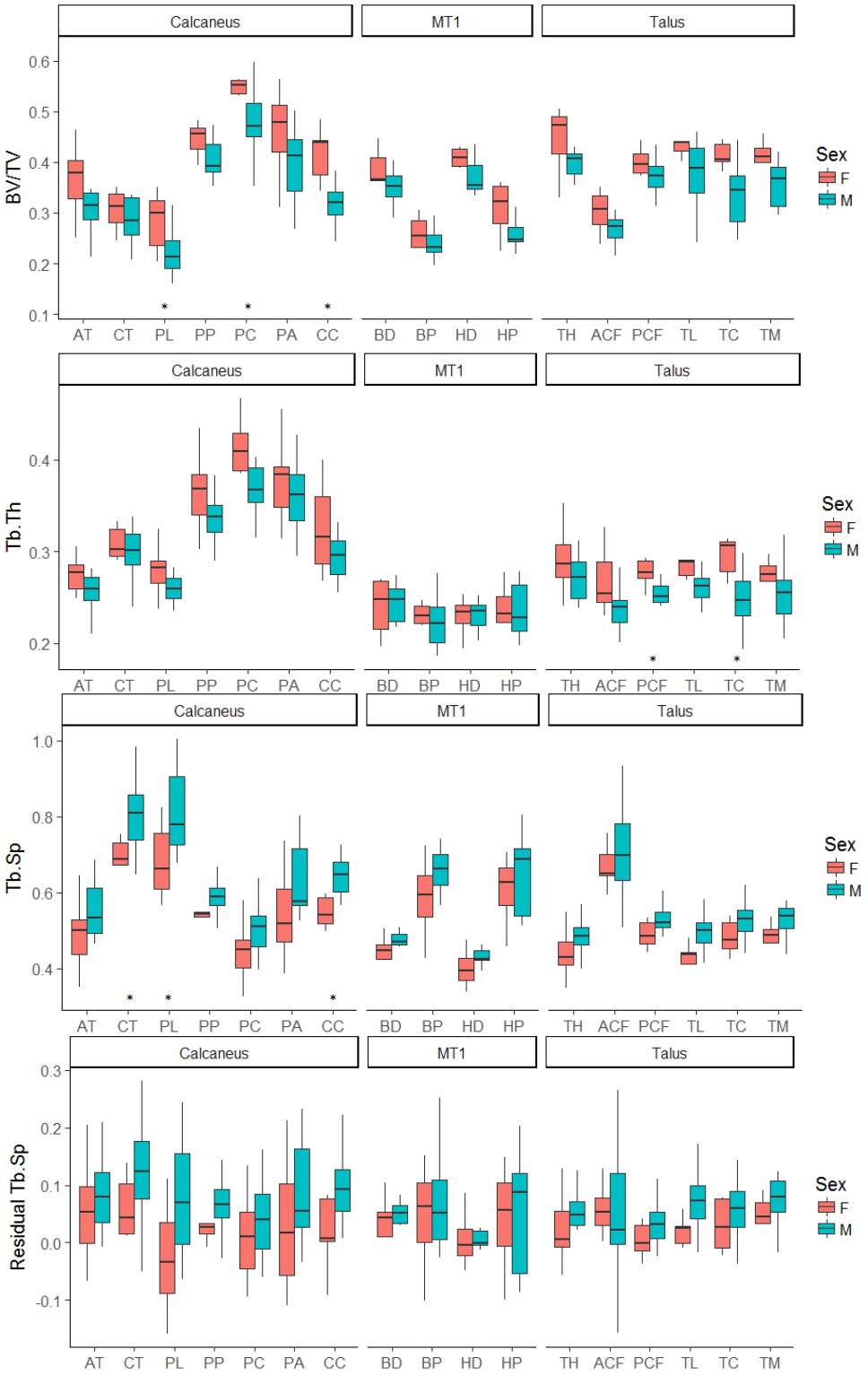
Calcaneus
MT1
Talus
BV/TV
Tb.Th
Tb.Sp
Residual Tb.Sp
AT CT PL PP PC PA CC
BD BP HD HP
TH ACF PCF TL TC TM
Sex
F
M

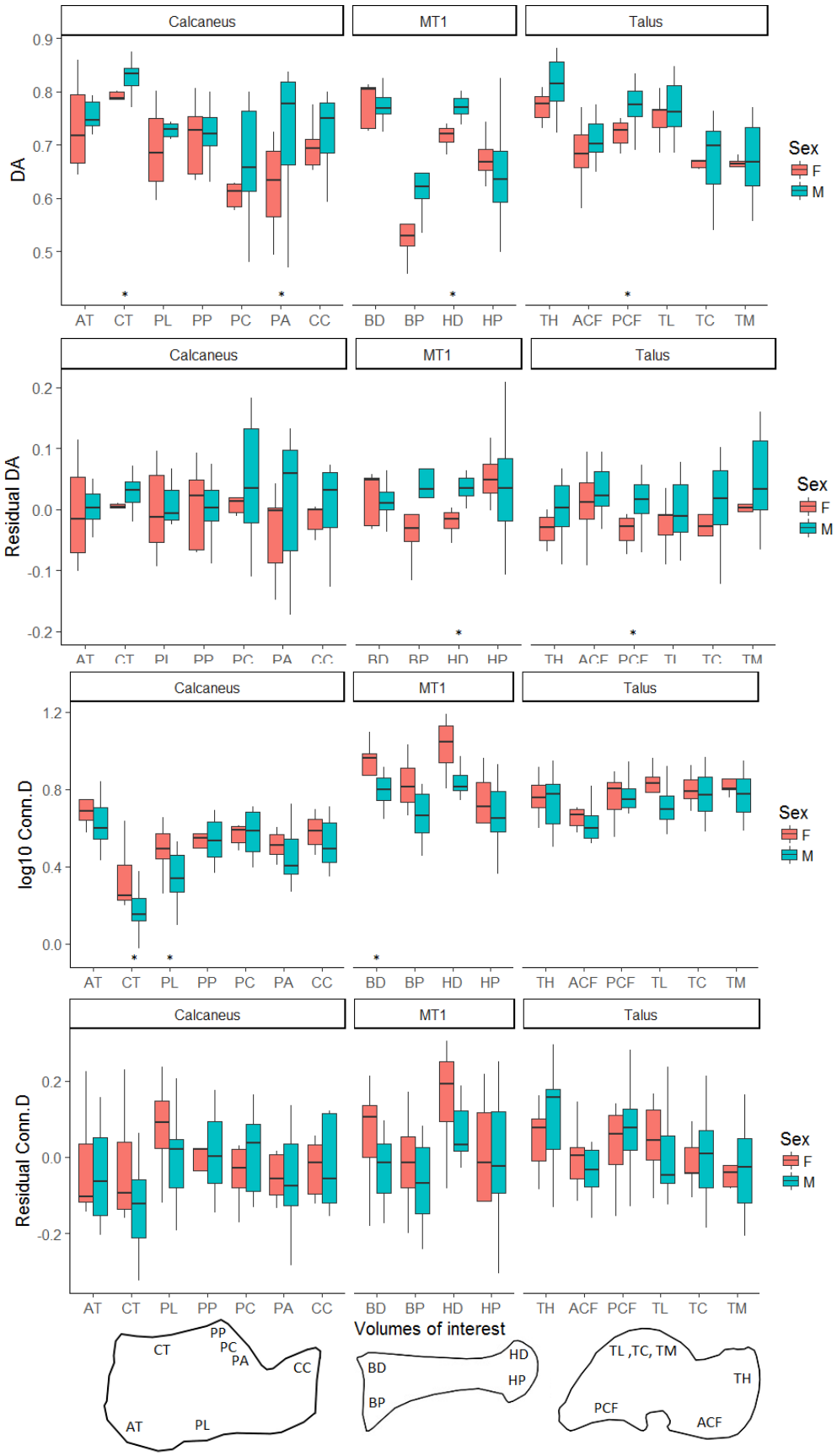

Figure 5.4. Boxplots of the median and interquartile range of male and female trabecular properties in Kerma. Volumes of interest: Achilles tendon (AT), calcaneal tuber (CT), plantar ligaments (PL), posterior talar facet (PP: posterior, PC: central, PA: anterior), calcaneocuboid (CC), dorsal base (BD), plantar base (BP), dorsal head (HD), plantar head (HP), talar head (TH), anterior calcaneal facet (ACF), posterior calcaneal facet (PCF), trochlea (lateral: TL, central: TC, medial: TM).

Table 5.7. Summary table of significant sexual dimorphism in Kerma. Volumes of interest: Achilles tendon (AT), calcaneal tuber (CT), plantar ligaments (PL), posterior talar facet (PP: posterior, PC: central, PA: anterior), calcaneocuboid (CC), dorsal base (BD), plantar base (BP), dorsal head (HD), plantar head (HP), talar head (TH), anterior calcaneal facet (ACF), posterior calcaneal facet (PCF), trochlea (lateral: TL, central: TC, medial: TM).

Kerma		BV/TV	Tb.Th	DA	Tb.Sp	Conn.D	Res. Tb.Sp	Res. Conn.D	Res.Da
Calcaneus	AT								
	CC	F>M			M>F				
	CT			M>F	M>F	F>M			
	PA			M>F					
	PC	F>M							
	PP								
	PL	F>M			M>F	F>M			
MT1	BD					F>M			
	BP								
	HD			M>F					M>F
	HP								
Talus	ACF								
	PCF		F>M	M>F					M>F
	TH								
	TL				M>F				
	TC	F>M	F>M						
	TM								

The Kerma females have higher BV/TV and thicker trabeculae in all VOIs compared to the males (Table 5.7). Females have significantly greater BV/TV in the CC, PC, PL, and TC VOIs, and significantly thicker trabeculae compared to males in the PCF and TC VOIs. The males have significantly more anisotropic structures in the CT, PA, PL, and TL VOIs. After correcting for body mass DA remained significantly higher in males in the HD and PCF VOIs. Males have more widely separated trabecular struts in the PL and TL VOIs, as well as the CC, and CT VOIs although not after controlling for variance associated with body mass. Females have more interconnected structures in all VOIs, and significantly so in the BD VOIs, as well as the CT and PL VOIs, although not after body mass corrections. No significant differences were found after applying a Bonferroni correction.

Trabecular properties for the St. Johns males and females are plotted in Figure 5.5.

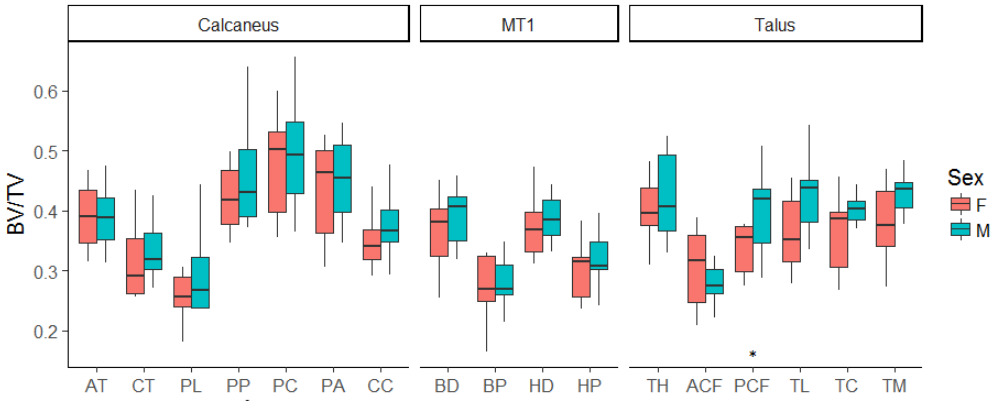

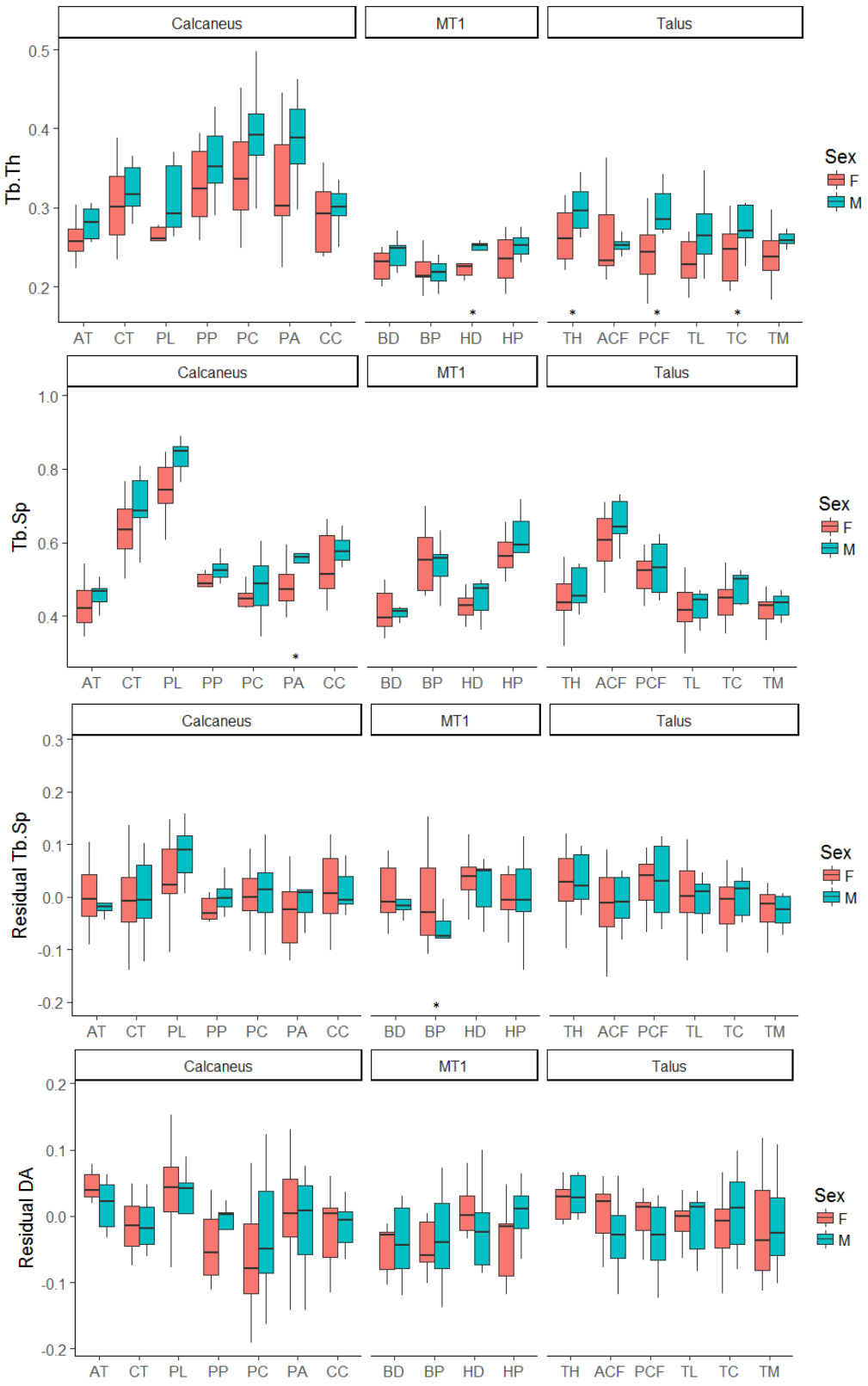
Calcaneus
MT1
Talus
Tb.Th
Tb.Sp
Residual Tb.Sp
Residual DA
Sex
F
M
AT CT PL PP PC PA CC
BD BP HD HP
TH ACF PCF TL TC TM

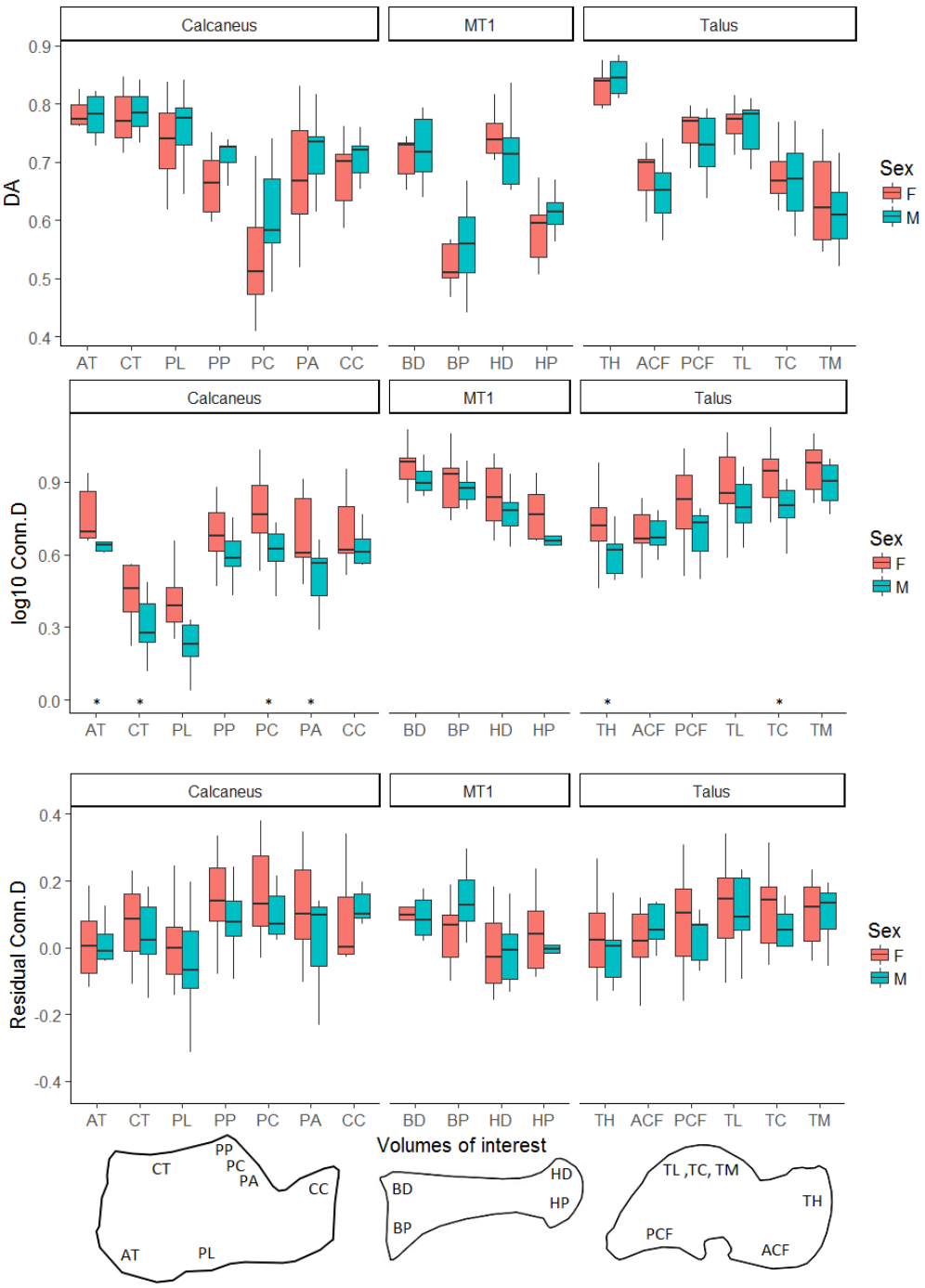

Figure 5.5. Boxplots of the median and interquartile range of male and female trabecular properties in St. Johns. Volumes of interest: Achilles tendon (AT), calcaneal tuber (CT), plantar ligaments (PL), posterior talar facet (PP: posterior, PC: central, PA: anterior), calcaneocuboid (CC), dorsal base (BD), plantar base (BP), dorsal head (HD), plantar head (HP), talar head (TH), anterior calcaneal facet (ACF), posterior calcaneal facet (PCF), trochlea (lateral: TL, central: TC, medial: TM).

Table 5.8. Summary table of significant sexual dimorphism in St. Johns. Volumes of interest: Achilles tendon (AT), calcaneal tuber (CT), plantar ligaments (PL), posterior talar facet (PP: posterior, PC: central, PA: anterior), calcaneocuboid (CC), dorsal base (BD), plantar base (BP), dorsal head (HD), plantar head (HP), talar head (TH), anterior calcaneal facet (ACF), posterior calcaneal facet (PCF), trochlea (lateral: TL, central: TC, medial: TM).

St. Johns		BV/TV	Tb.Th	DA	Tb.Sp	Conn.D	Res. Tb.Sp	Res. Conn.D	Res.Da
Calcaneus	AT					F>M			
	CC								
	CT					F>M			
	PA				M>F	F>M			
	PC					F>M			
	PP								
	PL								
MT1	BD								
	BP						F>M		
	HD		M>F						
	HP								
Talus	ACF								
	PCF	M>F	M>F						
	TH		M>F			F>M			
	TL								
	TC		M>F			F>M			
	TM								

The St. Johns males have greater mean BV/TV in the talus but only significantly greater in the PCF (Table 5.8). The males tend to have thicker trabeculae, and significantly so in the HD, PCF, TH, and TC VOIs. Males have significantly more widely spaced trabeculae in the PA VOI. Females have more interconnected struts in the AT, CT, PA, PC, TH, and TC VOIs, although no significant differences were found when differences in body mass were corrected for. Finally, females have significantly more widely separated struts in the plantar MT1 base when body mass differences were corrected. No significant differences were found after applying a Bonferroni correction.

Principal components analysis

A Principal components analysis was run on a pooled population sample. Volumes of interest were combined per bone. A biplot of the first two principal components for the calcaneus is provided in Figure 5.6. Summary tables and t-test on principal components are provided in Appendix 5.1.

PC1 receives the biggest contribution from BV/TV and Tb.Th, but no significant differences are found between males and females. Females score significantly higher on PC2 which is strongly influenced by Conn.D, Tb.Sp, and DA. After removing the variance in trabecular properties associated with BV/TV on PC1, females possess greater residual Conn.D and more isotropic structures in general than the males in a pooled population sample.

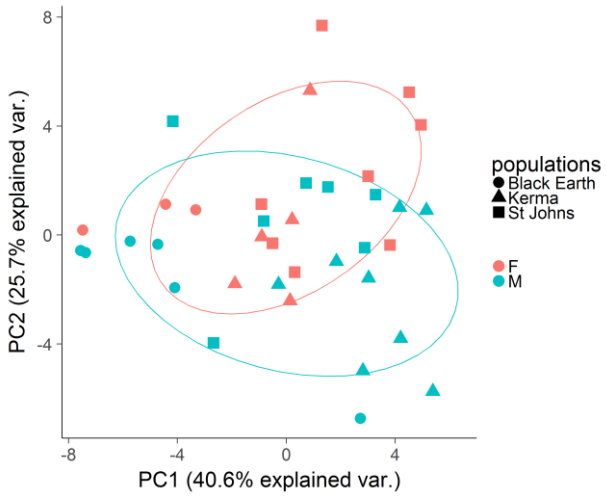

Figure 5.6. Biplot of the first two principal components of a PCA of the seven calcaneal VOIs in a pooled population sample.

The results for the first metatarsal are presented in Figure 5.7. No significant sexual dimorphism was found in any of the principal components.

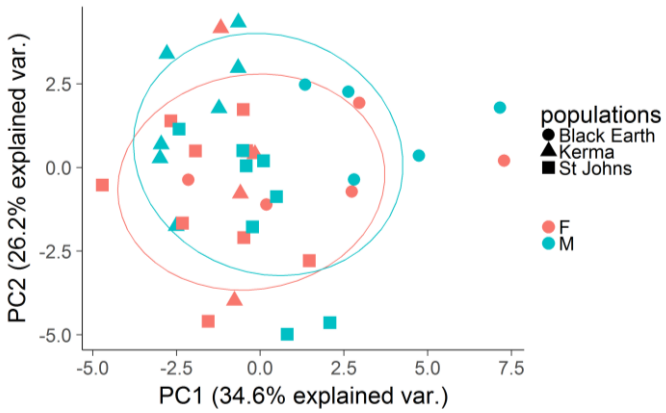

Figure 5.7. Biplot of the first two principal components of a PCA of four first metatarsal VOIs in a pooled population sample.

The results for the talus are presented in Figure 5.8. No sexual dimorphism was found in any of the first five principal components.

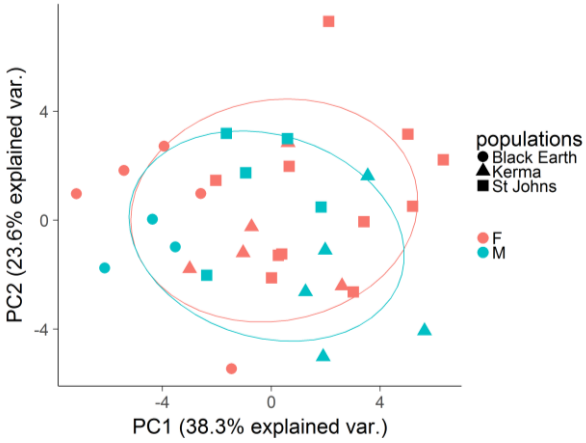

Figure 5.8. Biplot of the first two principal components of a PCA of pooled talar VOIs in a pooled population sample.

PCA's are discussed below for each bone in all four populations (figures 5.9 to 5.12), and results of MANOVA's of principal components are provided in Appendix 5.2. PCAs for individual VOIs per population are provided in Appendix 5.3 along with MANOVA's between principal components.

Biplots of the first two principal components of the Black Earth are provided in Figure 5.9. The Black Earth females fall marginally but significantly higher on PC2 of the calcaneus compared to the males (p=.045, df=1,7). PC2 is correlated negatively with DA indicating that females have somewhat lower calcaneal DA compared to males. The only significant difference in individual VOIs is found in the calcaneal tuber where males fall lower on PC3, which is associated with greater anisotropy.

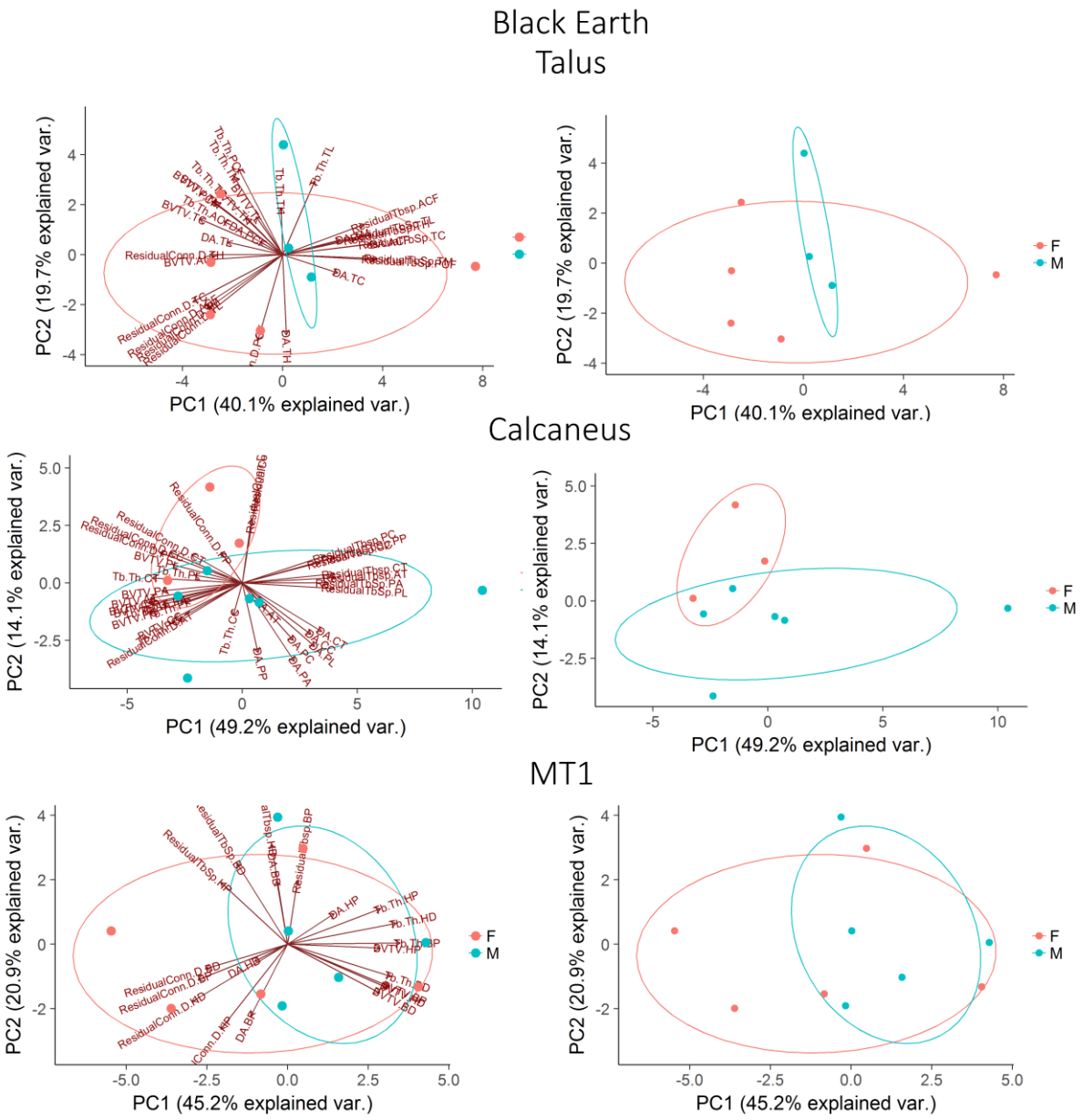

Figure 5.9. Biplot of PC1 and PC2 and corresponding vectors for trabecular properties in Black Earth.

Biplots of the first two principal components of the Kerma are provided in Figure 5.10. MANOVA results indicate that there is significant sexual dimorphism in the calcaneus in a combination of the

first three principal components (p=.008, df=3,9). The females fall significantly higher on PC1 in the calcaneus (p=.005, df=1,11) and the talus (p=.02, df=1,8) indicating that they have greater BV/TV, Tb.Th, and lower residual Tb.Sp compared to the males. In the MT1 the females fall lower on PC2 which is negatively correlated with BV/TV and Tb.Th, although it is not significant (p=.07, df=1,9).

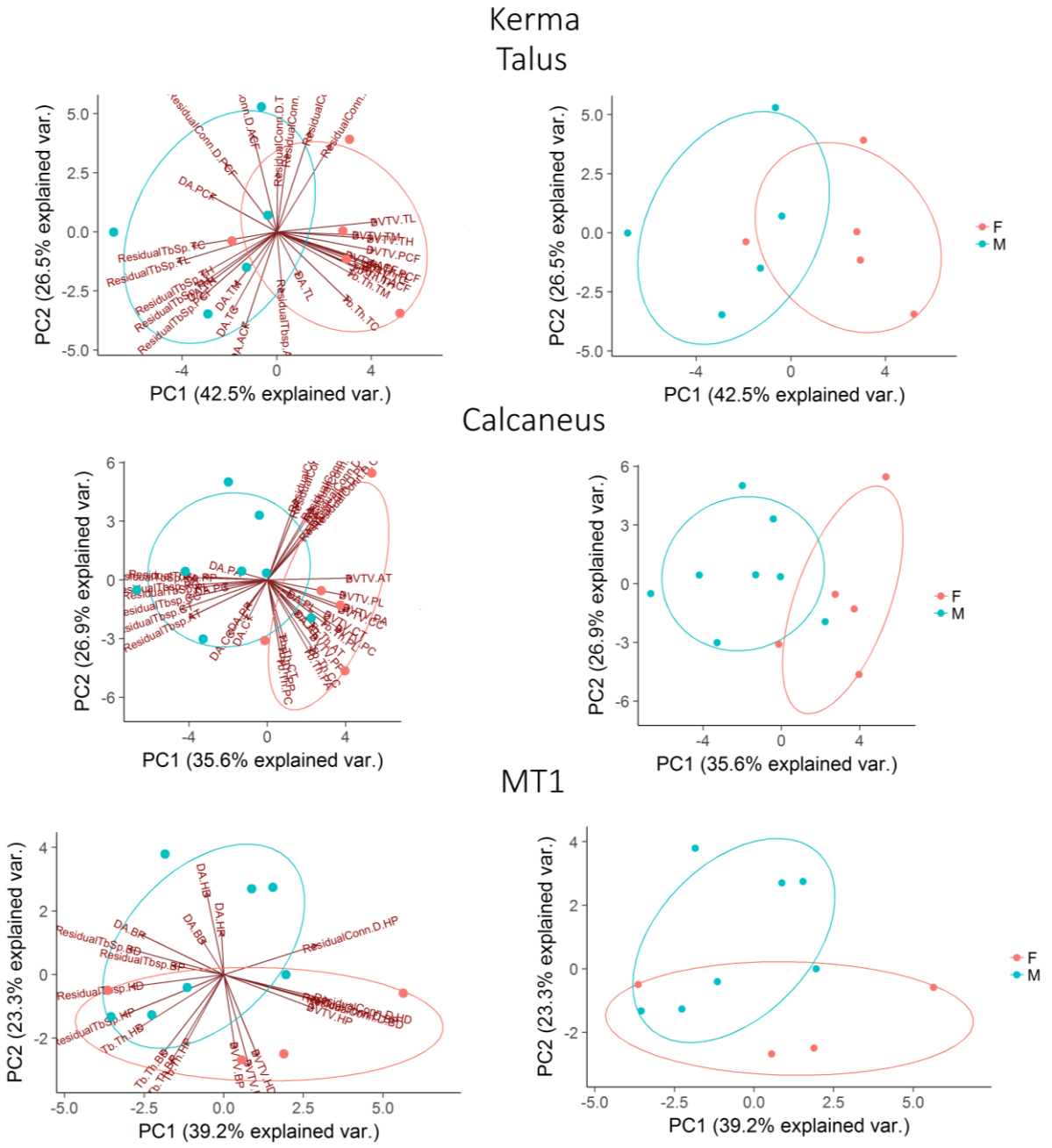

Figure 5.10. Biplot of PC1 and PC2 and corresponding vectors for trabecular properties in Kerma.

Biplots of the first two principal components of the Jebel Moya are provided in Figure 5.11. In both the talus and calcaneus the males fall lower on PC1 which is strongly correlated with BV/TV and Tb.Th and negatively correlated with residual Tb.Sp. A MANOVA could only be performed on the calcaneus due to low sample size in the talus. The MANOVA is significant overall (p=.010, df=3,1), and for PC1 (p=.024, df=1,3).

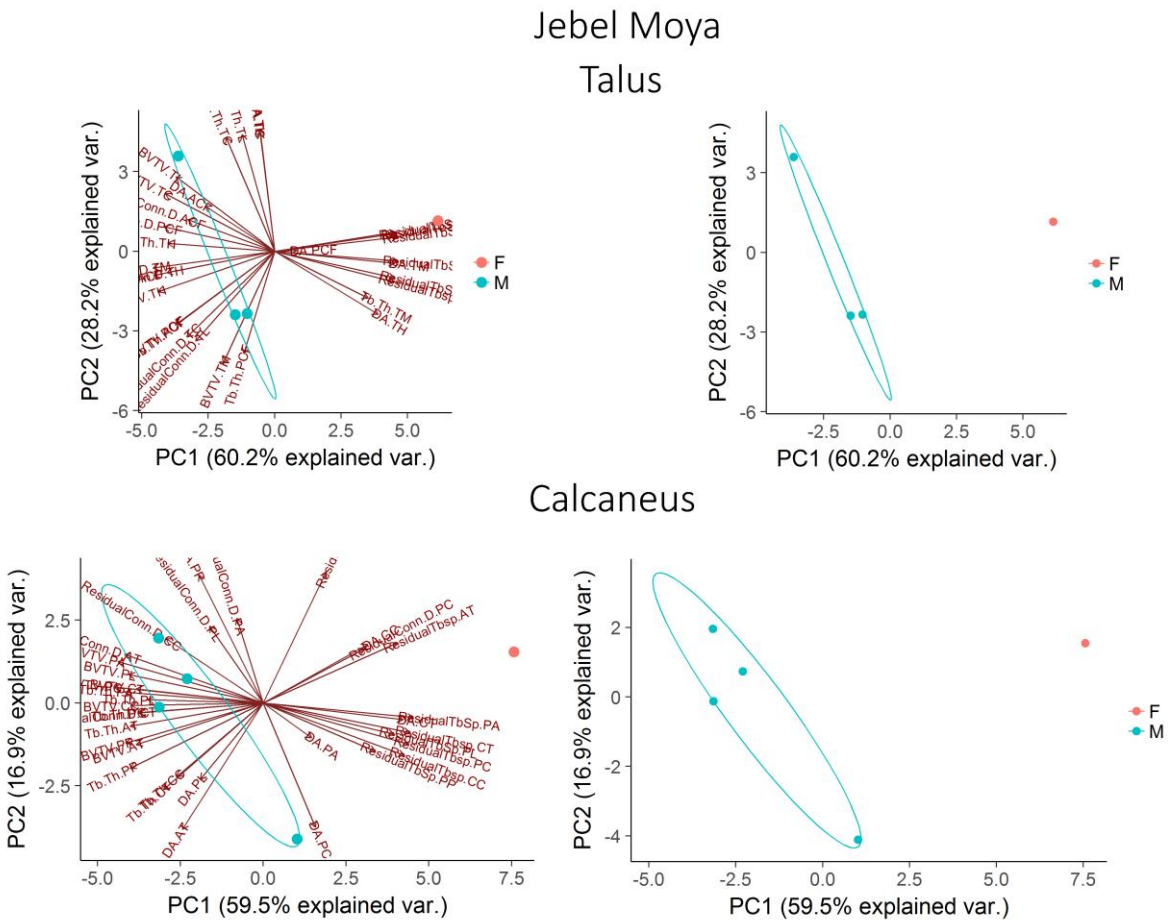

Figure 5.11. Biplot of PC1 and PC2 and corresponding vectors for trabecular properties in Jebel Moya.

Biplots of the first two principal components of the St. Johns are provided in Figure 5.12. On average, the males fall higher on principal components associated with BV/TV, but no significant sexual dimorphism is found in the first three principal components.

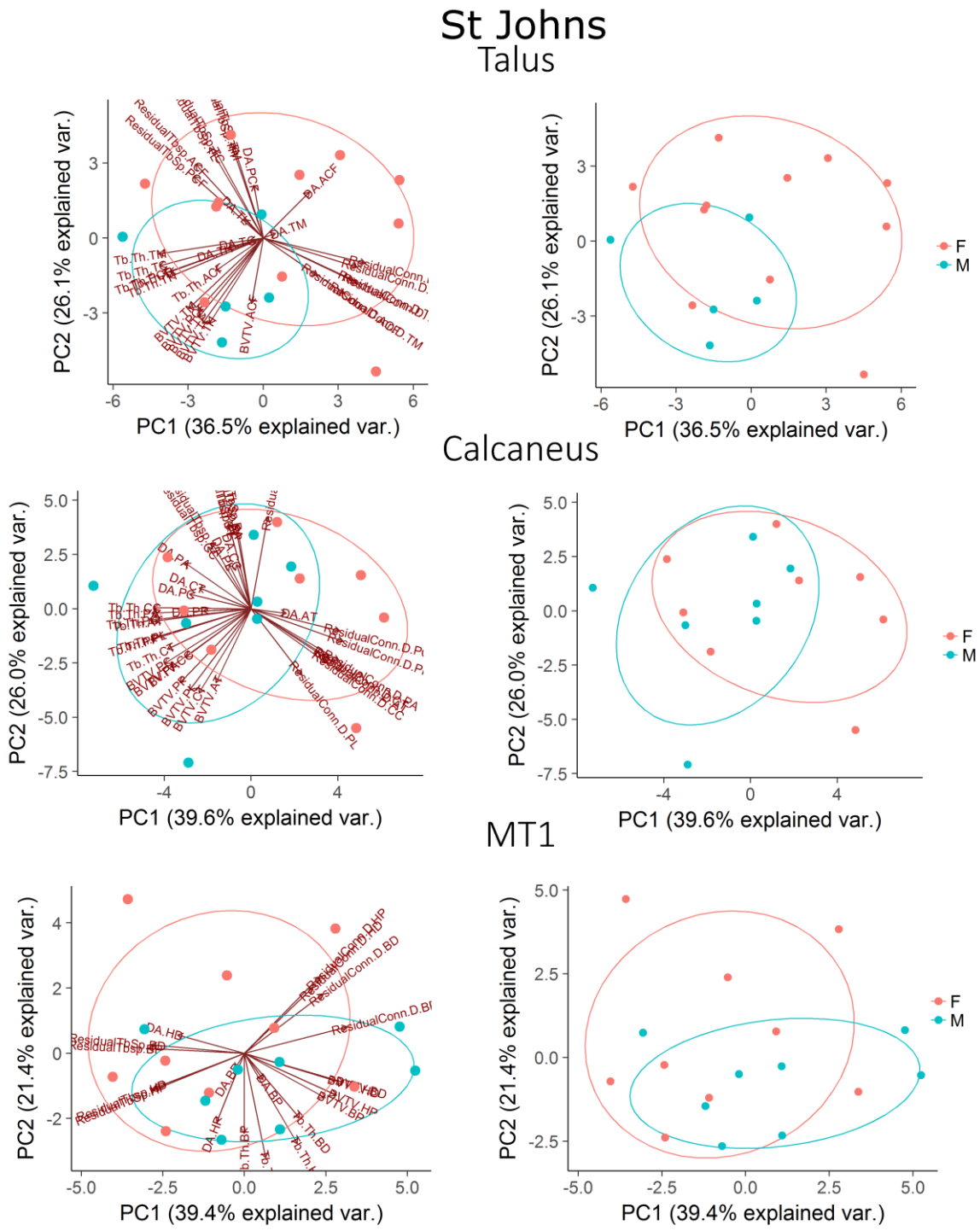

Figure 5.12. Biplot of PC1 and PC2 and corresponding vectors for trabecular properties in St. Johns.

Discussion

Little significant sexual dimorphism was found in the pooled population sample after body mass corrections in univariate analyses. Within populations, the patterns of significant sexual dimorphism vary substantially. The results generally do not correspond with predictions based on archaeological data and lower limb cross-sectional geometric analysis.

No significant sexual dimorphism was found in the cross-sectional properties of the femur in the Black Earth. From this it was predicted that no differences would be found between males and females after accounting for body size. Virtually no sexual dimorphism was found in the trabecular properties of the Black Earth. Only in the first metatarsal base did females possess significantly greater residual Conn.D compared to males. Using suites of trabecular properties in a principal components analysis showed significant sexual dimorphism in the calcaneus where males were associated with more anisotropic trabecular structure.

Based on sexual dimorphism in lower limb diaphyseal rigidity, the Jebel Moya males were predicted to possess greater BV/TV and associated Tb.Th, and lower associated Tb.Sp and Conn.D. The predictions were correct as higher male BV/TV and Tb.Th, and lower Tb.Sp were indeed found in many VOIs. However, these results are unreliable due to the small sample size, particularly of females. All but one VOI where significant differences were found were located in the calcaneus, where there was only one Jebel Moya female. It is quite likely that some of the individuals of indeterminate sex were females, and as all indeterminate individuals are more male-like than the females, it is likely that sexual dimorphism is lower than these results suggest. Thus, the significant sexual dimorphism found in the Jebel Moya is unlikely to be a true representation of the actual dimorphism of population. It is worth reporting these data, but these results are considered unreliable and will not be discussed further in this thesis.

Kerma males were predicted to possess greater BV/TV and associated Tb.Th, and lower associated Tb.Sp and Conn.D because males have significantly more robust absolute and body mass corrected lower limb diaphyses. Instead it was found that females have higher mean BV/TV and thicker mean trabeculae in all VOIs. Females display significantly greater BV/TV in the CC, PC, PL, and TC VOIs. Females also possess thicker trabeculae compared to males in the PCF and TC VOIs. After correcting for body mass no differences were found in Tb.Sp and Conn.D. The males have significantly more anisotropic structures in the CT, PA, PL, and TL VOIs, and in the HD and PCF after body mass corrections. Significant sexual dimorphism was also found using combined suites of trabeculae in PCA's in the talus and calcaneus while sexual dimorphism was just not significant in the first metatarsal. Thus, counter to predictions, the females have thicker trabeculae and greater BV/TV compared to males, and significantly so in a number of VOIs.

It was predicted the St. Johns males would have stiffer trabecular structures than females, but that sexual dimorphism would be lower compared to the Kerma and Jebel Moya. These predictions were

based on long term trends in long bone robusticity and observations of sexual dimorphism in modern industrial populations (Ruff, 2008; Jepsen et al., 2015), not actual biomechanical comparisons of the skeletal material. Mean BV/TV, Tb.Th, and Tb.Sp were higher and Conn.D lower in males compared to females. Significance was reached for BV/TV only in the PCF and for Tb.Th in HD, PCF, TH, and TC. After removing the variation associated with body mass the females had significantly higher Tb.Sp than males in the BP. In suites of properties analysed using PCA no significant sexual dimorphism was found, although on average males did fall higher on principal components associated with BV/TV.

Most significant sex differences were found in Tb.Sp and Conn.D, but not after correcting for variance associated with body mass. It is possible that this variance is related to sex differences independent of body mass that are being corrected for due to the inherent difference in male and female body mass. Regressions were run between body mass and trabecular properties in males and females in Chapter 4 to test for this possibility. Similar relationships between body mass and trabecular properties were found in both sexes and the pooled sex sample, indicating that the driving factor behind sex differences in Tb.Sp and Conn.D is indeed body mass.

Experiments on animals (Jee et al., 1983; Pontzer et al., 2006; Sugiyama et al., 2010; Barak et al., 2011) and studies of human athletes (Chang et al., 2008; Modlesky et al., 2008; Shaw and Stock, 2009a, 2009b; Harrison et al., 2011) clearly demonstrate that both limb cross-sections as well as trabecular architecture are responsive to mechanical loading. Previous work in humans has demonstrated that BV/TV follows the same decrease through time as diaphyseal rigidity, and follows predictions that more active populations have higher BV/TV than less active ones (Chirchir et al., 2015; Ryan and Shaw, 2015; Saers et al., 2016; Scherf et al., 2016). Due to the responsiveness of trabecular bone to mechanical loading evident from experimental studies it was predicted that significant sexual dimorphism would be present in the archaeological populations as a result of sexual divisions of labour where males were predicted to be more mobile than females based on archaeological and biomechanical data. The observed sexual dimorphism was much less pronounced than was expected based on dimorphism in lower limb diaphyseal rigidity and shape. In the Kerma sample, findings were the opposite of what was predicted based on lower limb cross-sectional geometry. The results show that sexual dimorphism in cross-sectional diaphyseal properties and trabecular bone structure do not necessarily covary.

The underlying mechanisms behind sexual dimorphism in skeletal growth and maintenance are complex and not well understood (Seeman, 2001; Callewaert et al., 2010; Jepsen et al., 2015). In males, cortical periosteal and medullary size increase during growth whereas in females periosteal bone formation is partially inhibited hormonally (Callewaert et al., 2010). Thus, it is possible that male and female diaphyseal cross-sectional geometry drifts apart in more active populations due to sex differences in the norms of reaction to loading. If this is true, then when both males and females are equally active, the osteogenic response to equal loading may be greater in males relative to females,

and this difference will only become greater with increased activity. This would explain the decreasing sexual dimorphism over time with reducing activity levels that is generally observed in the archaeological record. However, this hypothesis does not correspond to the findings in the Black Earth where males and females are equally robust in femoral trabecular and cortical structure, despite being a highly mobile population. A small number of experimental studies indicate that, in mice, there is sexual dimorphism in sensitivity of diaphyseal cortical bone to mechanical loading. The lower limbs of male mice show greater sensitivity to swimming than female mice (Gordon et al., 1993). Wallace et al. (2007) reported that male wild-type mice were significantly more responsive to exercise than females after 3 weeks of treadmill running, resulting in a greater increase in cross-sectional properties of the tibial diaphysis. However, in this study female mice started with more robust bones relative to body mass and may therefore have been strained less and may not have required additional bone formation (Wallace et al., 2007). Lynch et al. (2010) found no sex differences in the responsiveness of trabecular bone to loading in C57Bl/6 mice. Both male and female mice showed a similar increase in BV/TV and Tb.Th and a decrease in Tb.Sp. In rats, males also showed a stronger response to loading compared to females. However, male rats grow faster than females, and when correcting for increased growth rates no differences were found between male and female rats (Mosley and Lanyon, 2002). The different findings between rats and mice further emphasize that findings in animal models need not necessarily be applicable to other species.

Little experimental work has been performed to assess sex differences in the response to loading in humans. Ryan et al. (2004) found no significant sex differences in bone mineral density after a 6-month regimen of resistive training in young (25±1) and old (69±1) men and women. However, this study examined only adults who no longer grow and are less responsive to loading than adolescents. Ballard et al. (2005) found that after 6 months of training, males had significantly greater concentrations of NTx (N-telopeptide). This marker is usually found in similar concentrations in both sexes and is indicative of bone turnover. Unfortunately, they did not measure the bone directly and this remains indirect evidence of increased metabolic activity in the males. Two papers examining humeral (Jones et al., 1977), and radial (Ducher et al., 2005) bilateral asymmetry in tennis players found greater mean asymmetry in male tennis players relative to females. However, these studies were not longitudinal, contained low sample sizes, and contained variation in starting age and estimated hours trained between individuals. The females in Ducher et al. (2005) used mostly two-handed backhands whereas the males preferred the one-handed technique. Based on the little work that has been performed it is currently unknown if there are significant sex differences in the norms of reaction to loading in humans.

Regardless of whether there are sex differences in the response of cortical bone to loading, the poor correspondence between cortical and trabecular architecture has been observed in a number of studies (Carlson and Judex, 2007; Carlson et al., 2008; Lazenby et al., 2008; Shaw and Ryan, 2012). Lazenby et al. (2008) found significant bilateral asymmetry in both trabecular and diaphyseal structure in the

human metacarpals, but reduced asymmetry in articular dimensions. This supports the articular constraint model which proposes that articular surfaces cannot afford to be as plastic as diaphyses or trabecular bone as this may lead to harmful asymmetry and thus impede joint function. Ryan and Shaw (2012) found significant correspondence between humeral diaphyseal rigidity and trabecular structure in the humeral head in a pooled group of anthropoid primates, but no correspondence between femoral diaphyseal and femoral head trabecular bone properties. Correlations between femoral diaphyseal and trabecular properties for the Black Earth, Kerma, and Norris Farms samples (see Saers et al. 2016) are reported in Appendix 5.4. In a sample of pooled populations and sexes strong significant correlations were found between femoral head BV/TV, Tb.Th and Conn.D, and diaphyseal cross-sectional properties, while correlations were less strong in the distal femur. Trabecular structure in the Black Earth correlated significantly with the diaphyseal cross-sectional properties in the distal femur but not the femoral head. Significant correlations were found between diaphyseal and trabecular structure in the femoral head and the distal femur in the Norris Farms. In the Kerma no significant correlations were found except between I_{max}/I_{min} and BV/TV in the femoral head. These population differences in correlations between cortical and trabecular structure certainly merit further experimental investigation. As cortical and trabecular architecture are demonstrably informative of habitual loading, they should ideally be considered alongside one another when inferring habitual loading from skeletal variation. However, considerably more experimental work is required to understand what can (and cannot) be from inferred both tissues.

A potential source for the complex correlations between cortical and trabecular bone properties in different populations is that both tissues may be responsive to different types of loading. There has been considerable discussion on whether trabecular structure adapts to more frequent but low-magnitude loading, or rare but high-magnitude loading (Gross and Srinivasan, 2006; Garman et al., 2007; Judex and Carlson, 2009; Judex et al., 2009; Robling, 2009; Kivell, 2016). It is commonly proposed that mechanical stimuli must be large enough to exceed a certain strain threshold to start bone modelling (Frost, 2003). During locomotion roughly 2.000-3.000 microstrain are induced which signals damaged tissue to be remodeled (Rubin et al., 2001). However, Rubin et al. (2001; 2002) argue that very small strains (eg. those induced during standing) are strong determinants of trabecular bone strength. They demonstrate experimentally that in sheep 5 microstrain at 30Hz (0.1% of strain that causes yield failure in bone) can have a substantial effect on trabecular bone mass and structure, but has no effect on cortical bone. After one year of treatment with 5 microstrain for 20 minutes five times per week, experimental sheep had 32% greater trabecular bone volume, 45% greater trabecular number and 36% reduced trabecular spacing, but no differences were found in cortical bone properties (Rubin et al., 2001). No differences between groups were found in the forelimb which was not subjected to treatment. This suggests that the treatment only affects the region of the skeleton that is strained. It also shows that very weak strains can potentially encourage a significant modelling response in trabecular but not in cortical bone. Rubin and Mcleod (1996) argue that the same

osteogenic effects are produced by a strain of .001 at 1Hz for 100 seconds and a strain of .0002 at 60Hz for 10 minutes (Rubin and McLeod, 1996). Whole body vibrations (rather that vibrations targeting one limb as in Rubin et al. 2001) causing extremely low-magnitude, high-frequency strains significantly increased cortical as well as trabecular bone structures in mice (Xie et al., 2008). In a small clinical trial, 10 minutes of whole body vibration (30Hz, 0.3g) also resulted in significant cortical and trabecular bone increases in human females (Gilsanz et al., 2006). These results show that low magnitude, high frequency strains can result in a significant osteogenic response of the skeleton (Mosley and Lanyon, 1998; Currey, 2002). Other studies have clearly demonstrated that when strain rate is kept constant, increasing strain magnitude increases the osteogenic response of bone tissue (Rubin and Lanyon, 1985; Mosley et al., 1997). Strain needs to be dynamic (strain rate larger than 0) rather than static (strain rate 0). Static strain at a magnitude that normally stimulates bone formation produces a remodeling response similar to disuse resulting in bone loss (Lanyon and Rubin, 1984; Judex et al., 2009).

In vivo experiments show that trabecular bone mass and orientation is responsive to peak strains (Pontzer et al., 2006; Barak et al., 2011). Running on a treadmill for 15 minutes per day for one month increased sheep trabecular bone mass and orientation significantly (Barak et al., 2011). Somewhat contrasting previous experimental findings (Rubin et al., 2001; Pontzer et al., 2006; Barak et al., 2011), Carlson and Judex (2007) found significant differences in cortical bone shape adaptation to different types of loading in mice (turning versus linear movement, housed in cages with curved or straight tubes), but Carlson et al. (2008) did not find a trabecular response in DA in the distal femoral metaphysis of the same mice. However, the metaphysis of the distal femur would not be expected to be subjected to multidirectional loading due to its location above a hinge joint. Overall, trabecular bone located in joints is not subjected to the same loads as long bone diaphyses and should not necessarily be expected to respond in a similar fashion. These studies demonstrate potential differences in sensitivity cortical and trabecular bone to strain magnitude and frequency, indicating that trabecular and cortical bone may be informative on different types of loading. More work is required to investigate the stimuli to which trabecular and cortical bone respond. One hypothetical scenario may be that trabecular bone increases mass preferentially in response to high frequency loading, regardless of magnitude, and cortical bone requires a certain strain magnitude threshold to be overcome in order to start modelling. In this scenario populations where males experience greater high-magnitude loading whereas they both experience similar levels of low magnitude high frequency loading (eg. from standing) would result in little sexual dimorphism in trabecular bone but significant dimorphism in cortical structure.

Trabecular bone is not an isolated structure but one component of the musculoskeletal system including the cortical shell, cartilage, and soft tissues. It is possible that the increased cortical bone of males reduces the strain in trabeculae and thus the need for trabeculae to respond. This would explain why there is such little dimorphism in the Black Earth who have similar diaphyseal cross-sectional

properties, and the findings in the Kerma where males have more robust cortical diaphyses and the females have greater trabecular BV/TV. While increased diaphyseal bone mass was found in the Kerma and Jebel Moya males, the foot bones considered here would not benefit from increased long bone cortical strength. It is possible that the males also have thicker cortical shells in the calcaneus, talus, and first metatarsal compared to the females in these populations. Unfortunately, cortical shell thickness is not recorded in the current study. The interaction between the cortical shell and underlying trabecular structure would be a very interesting topic for experimental studies, particularly using finite element analysis (eg. Cotter et al. (2011)).

The results presented in this chapter may also be a consequence of different metabolic functions and constraints in trabecular versus cortical bone. Seeman et al. (2001) proposed an untested hypothesis that oestrogen influenced endocortical bone packing in females may be a reserve for foetal skeletogenesis without compromising the mother's own bone strength. Endocortical bone provides a lower mechanical advantage compared to periosteal bone. A similar argument can be proposed for trabecular bone, as its large surface area makes it an important source of calcium ions (Kerschnitzki et al., 2013). Women lose significant amount of trabecular bone during pregnancy and lactation but regain the bone post-menses (Drinkwater and Chesnut, 1991; Ritchie et al., 1998; Kovacs, 2005). Birds are known to possess mechanically virtually useless medullary trabeculae (Currey, 2002) which acts solely as a calcium reservoir for creating eggshell and are destroyed at the beginning of the egg-laying period (Dacke et al., 1993). Young Female mice possess more bone than they require mechanically (Wallace et al., 2007) which may also function as a reserve for pregnancy. The hypothesis that females possess increased trabecular bone as a buffer for pregnancy remains to be tested in humans.

The previous discussions focused on sexual dimorphism in the amount of trabecular bone (BV/TV) but has not discussed the difference found in anisotropy. Differences in DA are were hypothesized to reflect differences in the nature of activities between males and females. The anisotropy of a trabecular structure is hypothesized to reflect the variation in directionality of loading beneath a joint. Saers et al. (2016) found significantly more anisotropic trabeculae in the human tibia compared to the more multidirectionally loaded femoral head and condyles. For all significant differences, the males had more anisotropic structures than the females. Results from Chapter 4 showed a significant effect of body mass on DA in the PA and PL VOIs, but this effect was difficult to explain. After correcting for the effects of body mass, males have more anisotropic structures compared to females in a small number of VOIs in the Kerma and pooled population sample while females have more anisotropic structures in the plantar MT1 head in the Jebel Moya. In the pooled population sample (excluding Jebel Moya) significant sexual dimorphism in DA was found in the CT, PA, PC, and BP VOIs. OLS regressions were run between body mass and DA to assess whether differences in body mass can account for the sexual dimorphism (Table 5.9).

Table 5.9. OLS regressions between DA and body mass in VOIs where significant sexual dimorphism was found.

		Pooled		Male		Female	
	VOI	**R^2**	***p***	**R^2**	***p***	**R^2**	***p***
Pooled excl. Jebel Moya	CT	**.105**	**.004**	.000	.873	.140	.059
	PA	**.246**	**.000**	**.167**	**.031**	**.230**	**.018**
	PC	**.110**	**.016**	.001	.870	**.250**	**.013**
	BP	.042	.183	.006	.727	.037	.420
Jebel Moya	AT	.198	.111	.056	.609	NA*	NA*
Kerma	CT	**.316**	**.012**	.111	.289	.120	.448
	PA	**.547**	**.000**	**.415**	**.024**	**.668**	**.025**
	HD	**.501**	**.007**	.183	.250	.045	.789
	PCF	.129	.144	.011	.740	.059	.664

*1 individual

All significant regressions between body mass and DA were positive. In the PA VOI in the Kerma and the pooled population group there were significant positive relationships between DA and body mass in males, females, and pooled sex. Here the significant relationship appears to be influenced by body mass rather than sex. The relationship is less clear in the other populations. In pooled population PC the pooled sex and females correlate significantly positively with body mass, but the males do not. In other VOIs only the pooled populations or no subgroups as all correlate with body mass. Thus, for all VOIs except PA there is no clear link between body mass and sexual dimorphism in DA. However, it should be kept in mind that sex-specific sample sizes in individual populations were quite small which significantly reduces statistical power.

It is unlikely that the findings reported in this chapter are due to inconsistent VOI placement, as it is consistently the males that have higher DA. There are three main interpretations possible for the greater anisotropy in males: 1) it is an adaptation to sex differences in loading directionality, 2) the underlying cause is genetic/related to differences in bone growth, 3) it is a by-product of changes in other trabecular properties. The first explanation results from differences in habitual loading while the last two explanations result from genetic/ontogenetic processes. Experimental work has provided strong indications that trabecular bone directionality adapts to loading directionality in different animals (Pontzer et al., 2006; Barak et al., 2011). These studies varied the angle at which joints were placed on the ground resulting in adaptation of the orientation of trabecular structure within joints. However, Barak et al. (2011) found no differences in fabric anisotropy between exercised and control groups. In studies on mice which manipulated the directionality of lower limb loading between groups (running through straight or curving tube), clear differences were found in diaphyseal cross-sectional shape but no differences were found in trabecular anisotropy (Carlson and Judex, 2007; Carlson et al., 2008; Wallace et al., 2013). So, while reduced loading directionality in males may be a plausible explanation of the observed sexual dimorphism, supporting experimental evidence is lacking.

Genetic mechanisms underlying bone modeling may also affect sex differences in the degree of anisotropy. Males have a longer growth period which may provide additional time for trabeculae to structurally optimise during an age when bone is most responsive to loading. The effects of genetic factors are clear from experiments with inbred mouse strains which allow the effects of genetics to be isolated from environmental factors (Judex et al., 2004, 2009). A study that used two strains of mice that show the greatest difference in response to unloading (BALB and C3H) tested for sex differences within these strains. Males from the two strains showed similar bone loss responses to unloading, but female BALB mice lost twice as much bone as males, while C3H females lost only half as much as C3H males. This shows that in similarly inbred strains, responses to loading conditions can vary substantially between males and females (Judex et al., 2004, 2009).

Finally, sexual dimorphism in DA may be a by-product of differences in connectivity density. Strong negative regressions are found between Conn.D and DA in a pooled sex, pooled population sample, as well as in male and female specific samples. The negative regressions are also significant in most VOIs between DA and residual Conn.D in pooled sex as well as male and female samples, suggesting that differences in body mass do not explain this phenomenon. Thus, the greater anisotropy observed in males may be a by-product of their lower Conn.D compared to females.

Conclusion

Less sexual dimorphism was observed in the archaeological populations than was predicted. The most striking finding was that females had greater BV/TV in the Kerma while males possessed greater lower limb diaphyseal rigidity. Another interesting finding was that in all populations males tended to have more anisotropic trabecular structures than females. Finally, the lack of strong correlations between cortical and trabecular bone properties was somewhat unexpected. The discussion of these results of this chapter is somewhat speculative due to the lack of understanding of the mechanisms which underlie the responsiveness of bone to loading and potential trade-offs between metabolic and mechanical functions of bone in males and females. More experimental research will be required to investigate the mechanisms underlying sexual dimorphism in cortical and trabecular bone. Ideally, longitudinal studies on growing athletes practicing a range of sports should be done where both cortical and trabecular bone is quantified and differences in exercise history, diet, and genetics can be considered. The best alternative is to carefully design experiments with animal models where the factors underlying bone formation can be controlled and manipulated.

The results in this chapter demonstrated the value of using suites of correlated trabecular bone properties in a principal components analysis for investigating group differences. Both multivariate and univariate methods provided complementary information on trabecular structure. Univariate ANOVA clearly showed differences in morphological properties, while the multivariate PCA combined strongly correlated variables into single factors, generating a simple picture of variation between groups. However, sample size was a problem in this chapter, particularly when multiple VOIs

were combined in the PCA's. Future research investigating sexual dimorphism should endeavour to obtain larger samples.

Chapter 6 - Trabecular structure and age

Introduction

Osteoporosis is an age-related condition characterized by a reduction in bone mass and deterioration of skeletal structure that significantly increases an individual's susceptibility to fractures. Post-menopausal women are particularly at risk of osteoporotic fracture (Riggs et al., 2004; Borer, 2005). Increased life expectancy and relatively low levels of physical activity are thought to be the primary cause behind the significantly increased prevalence of osteoporosis in the industrialized world (Greendale et al., 1995; Schlecht et al., 2012). This chapter will begin with a review of the recent literature on age-related bone loss, after which the effects of age-related bone loss in the archaeological populations used in the current study are examined.

Trabecular bone is continuously remodelled by Basic Multicellular Units (BMU) throughout life. Within each BMU more bone is resorbed than formed, resulting in an accumulating net loss of bone which is the basis of age-related bone loss (Seeman, 2001; Currey, 2002). Women have a greater risk of fractures than men, but the amount of trabecular bone lost during ageing is overall similar in men and women (Kalender et al., 1989; Mosekilde, 1990; see Figure 6.1). This discrepancy partly results from qualitative rather than quantitative differences between men and women in the way bone is lost (Duan et al., 2001; Seeman, 2001). Aaron et al. (1987) found that bone mass in the male ilium was lost through trabecular thinning whereas females mostly lost connections between trabeculae. In women, trabecular bone loss accelerates at menopause due to increased remodeling as a result of oestrogen deficiency (Seeman, 2001). In males, there is no increased bone loss during mid-life, but bone keeps reducing steadily due to reduced bone formation and trabecular thinning. Aaron et al. (1987) argue that greater maintenance of connectivity in males maintains a greater trabecular surface area that is available for remodeling, so that bone loss continues longer in males. Female trabeculae are perforated and lose connectivity which decreases the structural integrity, whereas in males the struts become thinner but remain connected (Aaron et al., 1987; Duan et al., 2001, see Figure 6.1). Khosla et al. (2006) found that in the distal radius men have higher BV/TV and thicker trabeculae following puberty but lose bone at the same rate as women. These differences explain why rates of distal radial fractures are rare in men but common in women (Khosla et al., 2006).

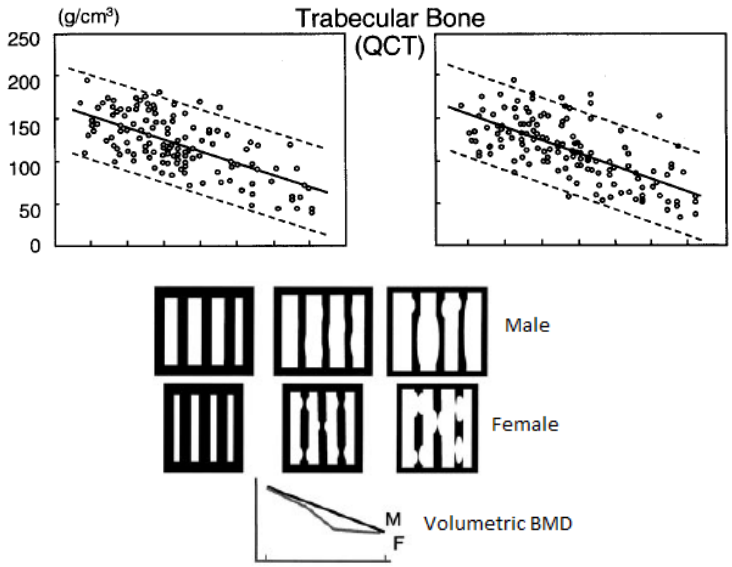

Figure 6.1. Schematic representation of quantitative (top, left is male, right is female) and qualitative (bottom) differences in male and female vertebral trabecular and cortical bone loss. From Seeman (2001).

Trabecular bone is heterogeneous in structure throughout the skeleton as well as within individual bones (Amling et al., 1996; Hildebrand et al., 1999; Saers et al., 2016). Differences in the rates of bone loss have been found in skeletal sites between men and women, suggesting that age related bone loss is both region and sex specific (Lundeen et al., 2000; Judex et al., 2004; Rupprecht et al., 2006; Eckstein et al., 2007; Lochmüller et al., 2008; Djuric et al., 2010). Lochmüller et al. (2008) reported significant sex differences in patterns of age-related bone loss in the lateral and medial femoral neck, femoral trochanter, T10 and L2 vertebrae, distal radius, calcaneus, and the iliac crest of age-matched males and females. They used µCT scanning to image bones from a German cadaveric sample of 75 males and 75 females aged between 52–99 years. Males showed no age-related bone loss in any anatomical site. In females, there was a significant age-related decrease in BV/TV at most sites. Bone loss was greatest in the iliac crest and lowest at the distal radius. At most sites, they report that the reduction in BV/TV was associated with a decrease in trabecular number and an increase in trabecular separation. Reduction in BV/TV was associated with a significant decrease in trabecular thickness in the female calcaneus. Djuric et al. (2010) explored the variation of trabecular structure with age and sex in the inferior and superior femoral neck and the intertrochanteric region in a Serbian population of 26 males and 26 females aged between 26–96 years. They found significant reductions in BV/TV and Conn.D in all three regions in females. In males, BV/TV was reduced significantly in the lateral neck and intertrochanteric region, and Conn.D was reduced significantly in all three regions. No significant loss in Tb.Th was found in either sex in any region. Bone loss was greatest in the intertrochanteric regions in females and in the lateral neck in males. This finding agrees with epidemiological data of greater rates of cervical fractures in males and trochanteric fractures in females (Kannus et al., 1996; Löfman et al., 2002). Rupprecht et al. (2006) examined regional variation in age related bone loss in males and females in the posterior, anterior and superior regions

of the calcaneus using 60 age matched German individuals aged between 20 and 80 years old. They found no significant sex differences in bone loss, although they did find a trend that might be significant with a higher sample size. Like the findings in Chapter 2, the greatest BV/TV was found in the superior calcaneus, under the posterior talar facet. The greatest bone loss was also found in the superior part of the calcaneus which was likely caused by a perforation of plates into rod-like structures (Rupprecht et al., 2006).

The effects of genetics and early life conditions on adult bone mass are complex and not well understood. Adult trabecular bone mass (mg/cm^3) can be accurately predicted in boys and girls from birth (Loro et al., 2000; Seeman, 2001). Longitudinal studies have demonstrated that an individual's volumetric BMD maintains the same position within a normal population distribution at 18 years old as at 2 years of age (Seeman, 2001). This is the same pattern as can be seen in the literature on human growth for height, weight, and other anthropometric variables (Bogin, 1999). This observation underlines the importance of genetic factors and early life conditions on adult bone structure. Lundeen et al. (2000) reported no significant differences in rates of bone loss between the superior and inferior femoral neck of Caucasian women. However, they found a significant increase in variance with age. They argued that preferential bone loss was not characteristic for the whole population and more plausibly resulted from unknown predisposing factors in a few individuals. Truong et al. (2006) found significant differences in gene expression and trabecular structural changes in a sample of osteoarthritic patients versus controls. In an experiment with three inbred strains of mice, Judex et al. (2004) found that genetic factors significantly influence bone mass and morphology in a region-specific way within and between bones.

Age related bone loss in the past

Biological anthropologists have long been interested in patterns of age-related bone loss in past populations (Agarwal, 2007). Increased sedentism, reduced activity levels, and a longer lifespan are the main factors thought to underlie the increased prevalence of osteoporosis in the industrialized world (Agarwal, 2007; Karasik, 2008). Fragility fractures are uncommon in active modern forager populations (Aspray et al., 1996). However, foragers do experience age-related reductions in bone quantity and quality (Madimenos et al., 2011). Spinal fractures are the most common osteoporotic fracture in humans. Interestingly, they do not occur in apes, even in cases of severe osteopenia (Cotter et al., 2011). Finite element analysis showed that after correcting for body mass humans have weaker vertebrae compared to all other primates resulting from a thinner cortical shell and lower BV/TV (Cotter et al., 2011). They argue that the less dense but relatively broader vertebral bodies of modern humans are an adaptation to bipedal locomotion with osteoporotic spine fractures as a by-product (Cotter et al., 2011).

Greater rates of bone loss have been observed in modern North American Inuit populations relative to age-matched white U.S. populations (Mazess and Mather, 1975; Harper et al., 1984). This discrepancy

is attributed to the acidotic effect of the high-protein Inuit diet. The effects of protein intake on bone are dose-dependent, and related to calcium and vitamin D intake (Agarwal, 2007). Archaeological Inuit populations possess thicker cortices with lower BMC and increased intracortical porosity compared to white U.S. population (Thompson et al., 1981, 1983; Agarwal, 2007). Significant age-related bone loss in both sexes was also reported in an archaeological population of Inuit foragers (Wallace et al., 2014). The effects on bone mass of changes in diet and activity associated with the transition to agriculture have been investigated in archaeological populations (Pfeiffer and Lazenby, 1994; Agarwal, 2007). Cultivated grains are estimated to contain about a quarter of the calcium present in uncultivated plants (Eaton et al., 1988; Eaton and Nelson, 1991). This has been suggested as one of the causes behind observed reductions in bone mass with the adoption of agriculture (see Agarwal, 2007). However, the clinical literature regarding the relationship between calcium intake and bone fragility is inconclusive. Calcium supplementation has been demonstrated to be ineffective in preventing bone loss in older women (Elders et al., 1994), and in preventing fractures (Feskanich et al., 1994), and may even promote fractures (Abelow et al., 1992). Kneissel et al. (1994) found a dramatic loss of trabecular bone mass and quality in the fourth lumbar vertebra of a bronze age Austrian skeletal sample. They show that this archaeological population followed similar age and sex related patterns of bone loss to modern European populations. Kneissel et al. (1997) found large plate-like trabeculae in young adults from a medieval Nubian population, but found osteopenic states with thin rod-like trabeculae in both sexes in individuals over 50. Ethnohistoric data suggested that these individuals were physically active and unlikely to suffer from deficiencies in Vitamin D or calcium intake. This finding is particularly interesting in that African ancestry, a physically active lifestyle, and high levels of osteoarthritis present in the population are all thought to be "protective" against age-related bone loss (Kneissel et al., 1997; Agarwal, 2007). Brickley (1997) found that patterns of bone loss in two populations from London, dated between 1700 and 1850, mirrored those seen in the present day British population. In a medieval British population, Agarwal et al. (2004) found a significant decrease in trabecular connectivity between young and middle adults, but no statistical differences between the middle and old adults in either sex. The same population showed relatively few fragility fractures (McEwan et al., 2004). The authors cautiously argue that perhaps high levels of physical activity prevented bone-loss related fractures in this population (Agarwal et al., 2004; McEwan et al., 2004).

The osteological paradox challenges bioarchaeologists to consider the effects of demographic non-stationarity, heterogeneous frailty, and selective mortality on health and demographic inferences in past populations (Wood et al., 1992; Wright and Yoder, 2003; DeWitte and Stojanowski, 2015). The effects of hidden heterogeneity in frailty and selective mortality may affect patterns of age-related changes in trabecular structure within and between population samples. This thesis is not designed to address any of the concerns raised by the osteological paradox, but it is important to consider its implications to understand the limits of what can be inferred from the data discussed in this chapter.

Bioarchaeological research has demonstrated that differences in frailty and selective mortality patterns with age are found between past populations (Wood et al., 1992; DeWitte and Stojanowski, 2015). Differences in frailty and selective mortality are expected occur in populations from different environments with different subsistence patterns and levels of technology. Individuals with severe movement impairing pathologies such as osteoarthritis were excluded in this thesis. Thus, this decision may have excluded the most physically active individuals from the analysis. Another potential issue is that of demographic non-stationarity. Cemeteries may have been used for different lengths of time, thus being an aggregate of different time periods where there may have been different stresses on the population (war, natural disaster, famine) as well as immigration and emigration. Hidden heterogeneity in frailty is difficult to assess in skeletal samples. The individuals who die at a certain age do not necessarily represent the living population of individuals of that age, as the individuals with the highest frailty are most likely to die at a given age. Sex and social status may be different sources of hidden heterogeneity in frailty in different populations. The implications of the osteological paradox are substantial for studies examining age-related changes in trabecular structure with age. However, the current study makes no attempt to specifically understand age related bone loss in past populations. Rather, the objective of the chapter is to see whether there are effects of age in the samples that should be considered in interpretations of trabecular structure.

In summary, rates of bone loss in modern human populations are site and sex specific and partially under the control of predisposing genetic factors. Studies of highly active past populations show that while bone is lost with age, fragility related fractures are rare, indicating sufficient buffering against age-related bone loss to prevent osteoporotic fractures. The individuals examined in this thesis were selected to be pathology free young to mature adults to reduce potential effects of age related bone loss. However, a small number of old adults were included in the study when no younger individuals were available. This chapter examines the effects of age on trabecular structure within the populations used in this study. This study was not designed to examine the effects of age in archaeological populations in general and does not attempt to do this.

Materials and methods

The Jebel Moya could not be reliably aged due to the fragmentary and incomplete nature of the collection. Broad age categories were used for the remaining three populations: young adult (18-25 years), mature adult (26-45 years), old adult (>46 years) (Brothwell, 1981; Brooks and Suchey, 1990; Buikstra and Ubelaker, 1994). For St. Johns and Kerma, age was determined using the morphology of the pubic symphysis (Brooks and Suchey, 1990) and molar wear (Brothwell, 1981). Age-at-death for the Black Earth individuals was estimated using the multifactorial method described in Lovejoy et al. (1985). These ages were obtained from a database at the Center for Archaeological Investigations, University of Southern Illinois, and converted into the three categories used for the other populations. Sex was determined by dimorphic characteristics of the pelvis and skull (Buikstra and Ubelaker,

1994). Determination of age was possible for 10 Kerma, 19 Black Earth and 17 St. Johns individuals (Table 6.1.).

Table 6.1. Frequency table of the number of males (M), females (F), and pooled sex (P) individuals used in this chapter. Achilles tendon (AT), calcaneal tuber (CT), plantar ligaments (PL), posterior talar facet (PP: posterior, PC: central, PA: anterior), calcaneocuboid (CC), dorsal base (BD), plantar base (BP), dorsal head (HD), plantar head (HP), talar head (TH), anterior calcaneal facet (ACF), posterior calcaneal facet (PCF), trochlea (lateral: TL, central: TC, medial: TM).

			Black Earth			Kerma			St Johns			Pooled		
			M	F	P	M	F	P	M	F	P	M	F	P
Calcaneus	AT	Young	1	2	3	0	2	2	1	3	4	2	7	9
		Mature	6	5	11	3	1	4	6	6	12	15	12	27
		Old	0	3	3	0	1	1	1	0	1	1	4	5
	CC	Young	1	1	2	0	2	2	1	2	3	2	5	7
		Mature	6	3	9	5	1	6	6	5	11	17	9	26
		Old	0	2	2	0	1	1	1	0	1	1	3	4
	CT	Young	1	2	3	0	2	2	1	2	3	2	6	8
		Mature	6	5	11	5	1	6	5	6	11	16	12	28
		Old	0	2	2	0	1	1	1	0	1	1	3	4
	PA	Young	1	2	3	0	2	2	1	3	4	2	7	9
		Mature	6	2	8	5	1	6	6	6	12	17	9	26
		Old	0	2	2	0	1	1	1	0	1	1	3	4
	PC	Young	1	2	3	0	2	2	1	3	4	2	7	9
		Mature	5	2	7	5	1	6	6	6	12	16	9	25
		Old	0	3	3	0	1	1	1	0	1	1	4	5
	PP	Young	1	2	3	0	2	2	1	3	4	2	7	9
		Mature	6	3	9	5	0	5	6	6	12	17	9	26
		Old	0	3	3	0	1	1	1	0	1	1	4	5
	PL	Young	1	1	2	0	2	2	1	2	3	2	5	7
		Mature	5	4	9	4	1	5	5	6	11	14	11	25
		Old	0	1	1	0	1	1	1	0	1	1	2	3
MT1	BD	Young	1	2	3	0	2	2	1	3	4	2	7	9
		Mature	6	3	9	4	1	5	6	4	10	16	8	24
		Old	0	3	3	0	0	0	1	0	1	1	3	4
	BP	Young	1	2	3	0	2	2	1	3	4	2	7	9
		Mature	5	3	8	4	1	5	6	4	10	15	8	23
		Old	0	2	2	0	0	0	1	0	1	1	2	3
	HD	Young	1	2	3	0	2	2	1	3	4	2	7	9
		Mature	7	4	11	4	1	5	6	4	10	17	9	26
		Old	0	3	3	0	0	0	1	0	1	1	3	4

	HP	Young	1	2	3	0	2	2	1	3	4	2	7	9
		Mature	6	3	9	4	1	5	6	4	10	16	8	24
		Old	0	2	2	0	0	0	1	0	1	1	2	3
Talus	ACF	Young	0	1	1	0	2	2	1	3	4	1	6	7
		Mature	5	3	8	6	1	7	5	6	11	16	10	26
		Old	0	4	4	0	1	1	1	0	1	1	5	6
	PCF	Young	1	2	3	0	2	2	1	3	4	2	7	9
		Mature	4	2	6	6	1	7	3	6	9	13	9	22
		Old	0	3	3	0	1	1	1	0	1	1	4	5
	TH	Young	1	2	3	0	2	2	1	3	4	2	7	9
		Mature	4	2	6	5	1	6	5	6	11	14	9	23
		Old	0	2	2	0	1	1	1	0	1	1	3	4
	TL	Young	1	2	3	0	2	2	1	3	4	2	7	9
		Mature	6	3	9	3	1	4	5	6	11	14	10	24
		Old	0	3	3	0	1	1	0	0	0	0	4	4
	TC	Young	1	1	2	0	2	2	1	3	4	2	6	8
		Mature	5	3	8	5	1	6	5	6	11	15	10	25
		Old	0	4	4	0	1	1	0	0	0	0	5	5
	TM	Young	1	2	3	0	2	2	1	3	4	2	7	9
		Mature	6	3	9	5	1	6	5	6	11	16	10	26
		Old	0	3	3	0	1	1	0	0	0	0	4	4

Research questions, hypotheses, and statistical analysis

Age related bone loss in modern industrial populations is well documented. However, the effects of age on the three-dimensional microstructure of more active past populations are not well studied. The current study is not designed to specifically examine age related bone loss in archaeological populations. Due to the low sample sizes per population and the fact that most individuals belonged to the broad mature adult category, it is not possible to assess potential differences in the rates of bone loss between these populations or sexes. The objective of this chapter is to ascertain whether age is a factor that will require consideration when interpreting variation between the populations examined in this study.

From the clinical literature a general pattern of trabecular bone loss with age can be predicted (Seeman, 2001). With increasing age BV/TV and Conn.D are reduced while Tb.Sp increases. Tb.Th does not always change with age but when it does it decreases, particularly in males (Seeman, 2001). DA is also often found to increase as connections between trabeculae are severed. Thus, it is hypothesized that overall BV/TV and Conn.D decrease while Tb.Sp increases with age. As the

strongest associations between age and trabecular microstructure have been found with Tb.Sp and Conn.D (Djuric et al., 2010), it is expected that Tb.Th will also be reduced with age. As trabeculae are thickest in their primary direction of loading, it is predicted that trabecular structure will become more anisotropic with age as thinner trabeculae are lost more quickly. Specific questions explored in this chapter are discussed below.

How are age categories distributed across sex and populations?

Age distribution in pooled and individual populations are assessed with tables and bar charts. Chi-square tests are used to assess differences in sample distributions of age categories. Due to limited sample sizes males and females are pooled in all subsequent analyses.

Is there a significant effect of age in the pooled and individual populations?

To assess statistically significant differences between age categories, one-way ANOVA of trabecular properties between age categories are performed per VOI in a pooled sample. Hochberg's GT-2 and Games-Howell post-hoc tests are used for pairwise comparisons. Both post-hoc tests are suitable for comparing groups of unequal size (Field, 2013). Conn.D was log10 transformed to satisfy the normality assumption. Partial Spearman correlations are used to quantify the strength of the correlations between age categories and trabecular structure while accounting for variation in body mass. Correlations are performed for every VOI in a pooled population sample and individual populations. Unfortunately, it is not possible to run a repeated measures ANOVA to test for differences in age related bone loss between VOIs due to the low number of individuals where all VOIs were present. Armstrong (2014) advises against using Bonferroni corrections when comparing highly related variables. Due to the strong correlations between trabecular properties in different VOIs, significant results are considered likely to be true if they occur in multiple VOIs. Isolated significant findings are regarded as probable false positives.

Should age be considered when examining the effects of habitual activity on trabecular structure?

Populations are examined in the context of differences in terrestrial mobility levels in Chapter 7. Differences in sample demography might have a significant effect on population average trabecular properties and it is important to take these into account. The results from this chapter will be used to inform how data will be interpreted in the context of variation in habitual behaviour.

Results

Table 6.2 summarizes the distribution of individuals per age category and sex in the Black Earth, St. Johns, Kerma, and pooled populations. Frequency and percentages of individuals in each age category per population are presented in Figure 6.2. Most individuals fall into the broad mature adult category with a roughly even distribution of individuals in the young and old adult categories. Seven out of nine young adults and five out of six old adults are female. Thus, there is a difference in the distributions of males and females with males concentrated in the mature adult category and females distributed more

widely across age categories. The Kerma females are distributed roughly equally across all age categories while all six males are concentrated in the mature adult category. A Chi-square test shows that ages are distributed similarly in all three populations (X^2=2.036, df=4, *p*=.729). The distribution of age categories is not equally distributed across sexes in a pooled population (X^2=6.951, df=2, *p*=.031). In individual populations age categories are equally distributed per sex in the Black Earth and St. Johns samples, but not in Kerma (X^2=6.429, df=2, *p*=.040).

Table 6.2. Frequencies of individuals per age category, sex, and population.

Populations	**Young adult (18-25)**		**Mature adult (26-45)**		**Old adult (46+)**		**Total**
	M	F	M	F	M	F	
Black Earth	1	2	7	5	0	4	19
Kerma	0	2	6	1	0	1	10
St. Johns	1	3	6	6	1	0	17
Pooled	2	7	19	12	1	5	46

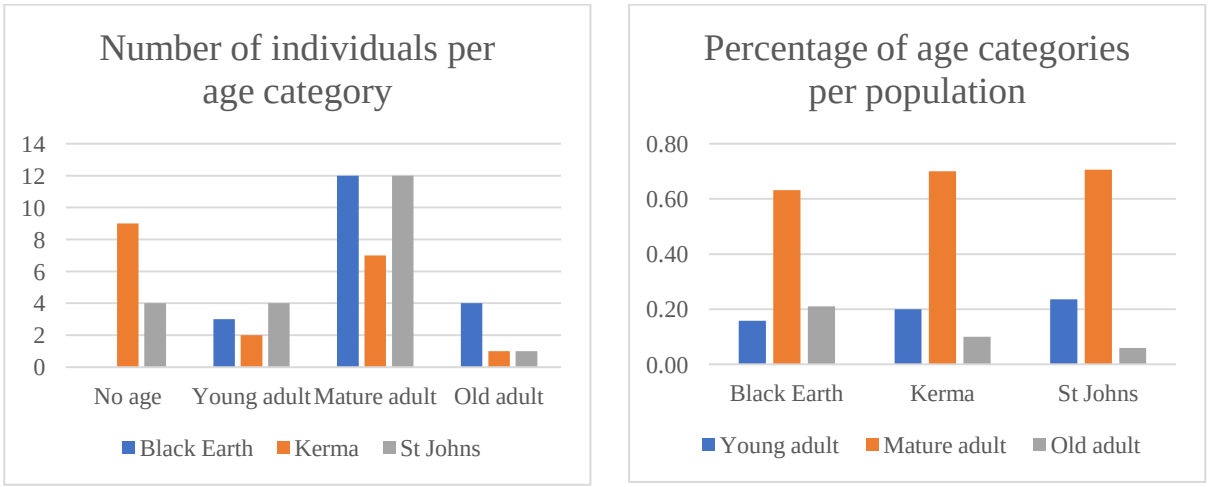

Figure 6.2. Frequency and percentages of individuals per population and age category.

Trabecular structure with age in a pooled population sample

Boxplots of trabecular properties in the three age categories for a pooled sex and pooled population sample are presented in Figure 6.3. Results from pairwise comparisons of one-way ANOVA of trabecular properties between age categories in a pooled sex, pooled population sample are provided in Appendix 6.1.

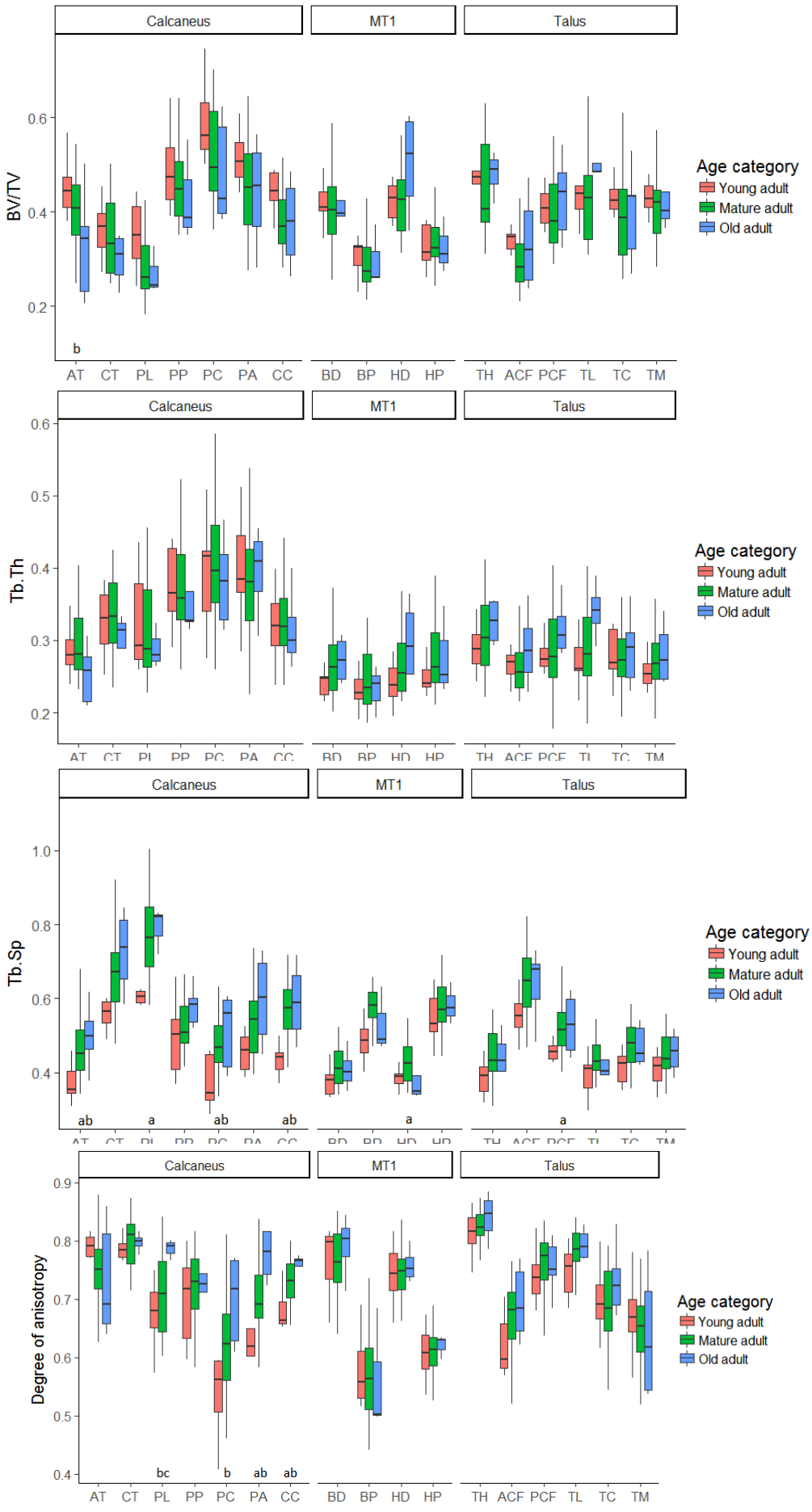
Calcaneus
MT1
Talus
BV/TV
Tb.Th
Tb.Sp
Degree of anisotropy
Age category
Young adult
Mature adult
Old adult
AT CT PL PP PC PA CC
BD BP HD HP
TH ACF PCF TL TC TM
b
ab a ab ab
a
a
bc b ab ab

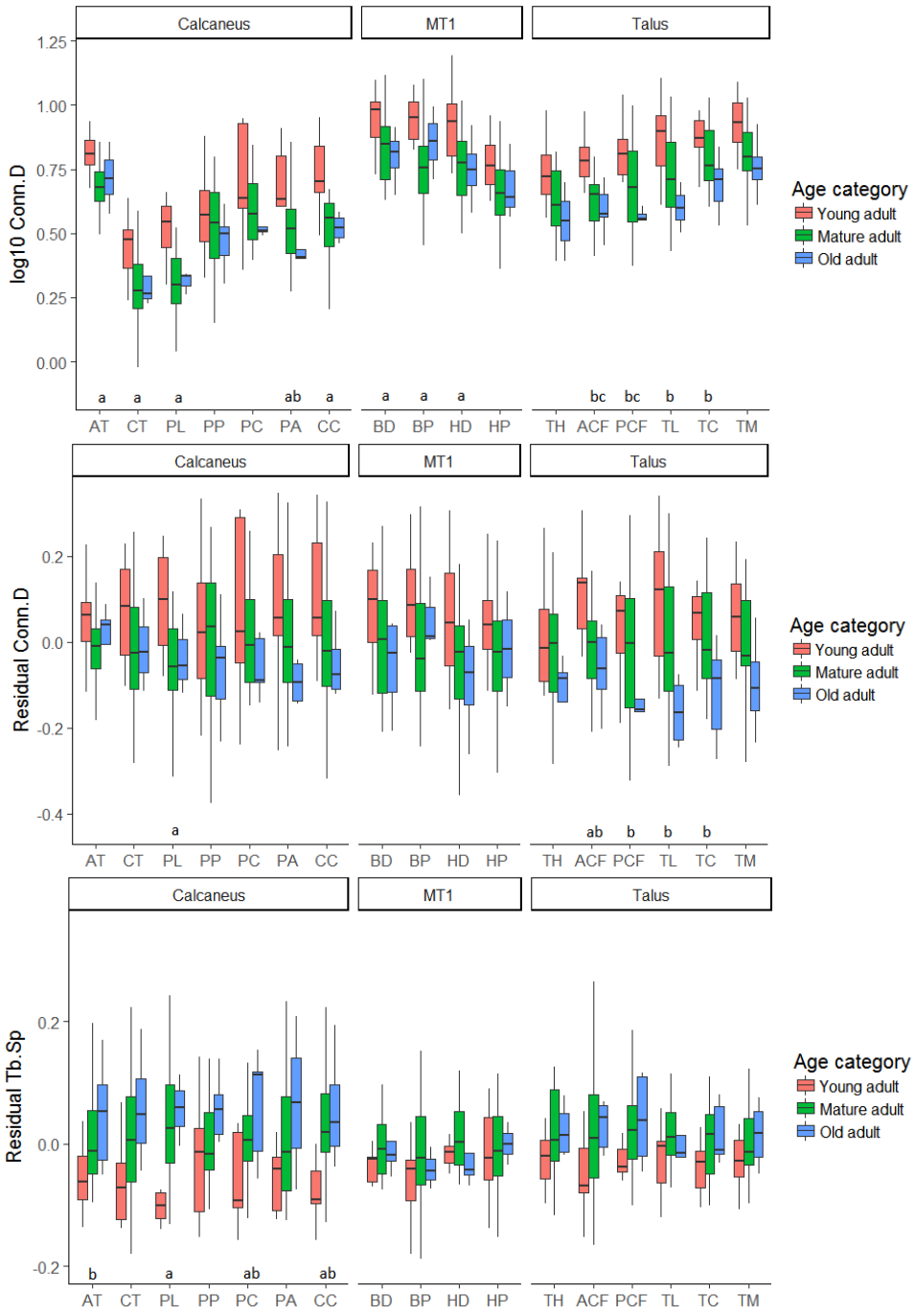
Calcaneus
MT1
Talus
log10 Conn.D
1.25
1.00
0.75
0.50
0.25
0.00
a a a ab a a a a bc bc b b
AT CT PL PP PC PA CC BD BP HD HP TH ACF PCF TL TC TM
Age category
Young adult
Mature adult
Old adult
Residual Conn.D
0.2
0.0
-0.2
-0.4
a ab b b b
Residual Tb.Sp
b a ab ab

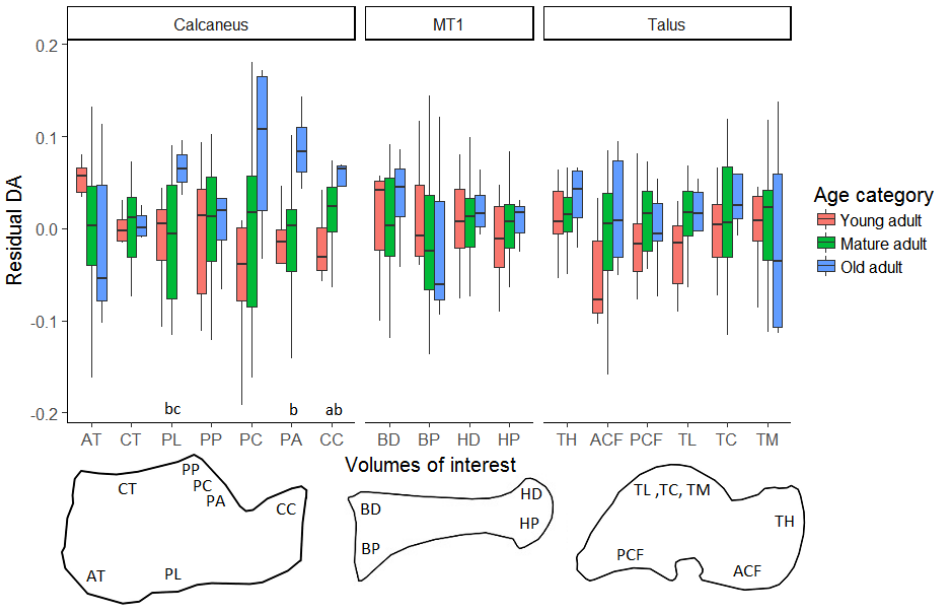

Figure 6.3. Boxplots of the median and interquartile range of trabecular properties in three age categories in a pooled sex pooled population sample. Letters indicate significant ($p<.05$) differences between: young and mature adults (a), young and old adults (b), mature and old adults (c). Achilles tendon (AT), calcaneal tuber (CT), plantar ligaments (PL), posterior talar facet (PP: posterior, PC: central, PA: anterior), calcaneocuboid (CC), dorsal base (BD), plantar base (BP), dorsal head (HD), plantar head (HP), talar head (TH), anterior calcaneal facet (ACF), posterior calcaneal facet (PCF), trochlea (lateral: TL, central: TC, medial: TM).

Distinct patterns of change in trabecular structure appear with increasing age throughout the three bones. In the calcaneus, a decrease in mean BV/TV is found but this is only significant in the Achilles tendon. There is no significant decrease in Tb.Th in any VOI. Mean Tb.Sp increases with age in most VOIs, but after correcting for body mass the only significant results are found in the calcaneus. In all VOIs mean connectivity density reduces with age. The same pattern remains after correcting for body mass but significance of the differences was generally lost except in the talus due to increased standard deviations. Whenever DA significantly differs between age categories there is always an increase in anisotropy with age. Significant results for DA are only found in the calcaneus both before and after body mass corrections.

In the calcaneus, there was a trend of decreasing BV/TV with age, however this trend only reached significance in the Achilles tendon. A significant decrease in mean Conn.D and an increase in mean Tb.Sp with age were found in most VOIs. Finally, a trend of increasing DA with age was found in all but the AT and PP VOIs. After correcting for body mass, residual Tb.Sp significantly increases with age four VOIs. After correcting for body mass, residual DA significantly increases with age in three VOIs. Young adults have lower residual DA compared to mature and old adults. After correcting for body mass, residual Conn.D is significantly lower compared to mature adults in the PL.

Fewer significant differences between age categories were observed in the first metatarsal than in the calcaneus. This may result from differences in sample demography as one old adult did not have a MT1. No significant differences were observed between age categories for DA, BV/TV, or Tb.Th. Conn.D significantly decreases with age in all but the plantar head VOI. In the dorsal head a

significant increase in Tb.Sp is observed between young and mature adults. After correcting for the effects of body mass no differences were found in DA, Tb.Sp, and Conn.D.

Fewer significant results were also obtained in the talus compared to the calcaneus, possibly due to a smaller number of mature adults. No significant differences were found between age categories for BV/TV, Tb.Th or DA in any talar VOI. A trend of decreasing Conn.D with age is found in all talar VOIs and reaches significance in all but the talar head and medial trochlea both before and after correcting for body mass. A trend of increased Tb.Sp with age is found in all VOIs but only reached significance in the PCF. After correcting for body mass no significant differences between age categories were found in Tb.Sp.

Partial Spearman correlations correcting for variation in body mass between age categories and trabecular properties in a pooled sex, pooled population sample are presented in Appendix 6.2. A significant negative correlation between Conn.D and age was found in all VOIs across all three bones. Significant positive correlations between age and Tb.Sp were only found in the calcaneus, where all VOIs were either significant or close to significance. Significant positive correlations were found between anisotropy and age in the CC, PA, and PC VOIs, while a negative correlation fell just short of significance in the AT. Counter to predictions, significant positive correlations between Tb.Th and age were found in the dorsal MT1 head. No significant were found between age and BV/TV.

Trabecular structure with age in individual populations

Patterns of trabecular structure per volume of interest are presented graphically in Figure 6.4 for the calcaneus, Figure 6.5 for the first metatarsal, and Figure 6.6 for the talus. Pearson correlations per population are presented in Appendix 6.2. Kerma and St. Johns both have only one old adult and two to three young adults with the remaining individuals falling in the mature adult category. The Kerma sample contains no old adult first metatarsals. The Black Earth sample consist of 3 young adults, 4 old adults and 12 mature adults. Due to the low number of individuals in the young and old adult categories, these patterns cannot provide information on broader trends within the populations.

Overall, BV/TV shows very similar patterns in all VOIs in Kerma and St. Johns. In St. Johns BV/TV decreases with age in most VOIs. Kerma BV/TV reduces from young to mature adults in most VOIs and increases from mature to old adult in all VOIs of the talus and calcaneus. The patterns of BV/TV in Black Earth differ somewhat for each bone. There is a clear reduction in BV/TV in the calcaneus. In the talus, BV/TV does not change with age, and in the MT1 BV/TV slightly increases from young adults to mature and old adults.

There is a clear trend of reduction in Conn.D from young to mature adults in all populations. In the Kerma and St. Johns populations Conn.D decreases from mature to old adults, while in Black Earth there is a slight increase in mean Conn.D in the first metatarsal.

The degree of anisotropy tends to increase with age, but there is more local variation in DA with age between volumes of interest. In St. Johns DA increases with age in the calcaneus, does not change with age in the MT1, and decreases with age in the central and medial trochlea while increasing in the other talar VOIs. in the Kerma DA increases from young to mature adults in most VOIs. In the calcaneus, DA either increased or levelled out from mature to old adults while in the talus DA decreased. There is little change with age in DA in the talus or MT1 in Black Earth. In the calcaneus, DA does not change with age in the CT and PP VOIs, reduces from young to old adults in the AT, and increases from mature to old adults in the other VOIs.

In St. Johns, mean Tb.Sp increases with age in all VOIs. In Black Earth Tb.Sp increases in all calcaneal and talar VOIs but stays roughly level in the MT1. Tb.Sp consistently increases from young to mature adults in the Kerma sample but then decreases from mature to old adults in the calcaneus and talus.

Tb.Th shows very similar patterns between VOIs in each population. However, the patterns per population are quite different. In the Black Earth Tb.Th increases from young to mature adult and then decreases from mature to old adults. Tb.Th increases from young to mature adults in the calcaneus and MT1 in Kerma while it decreases in the talus. Tb.Th then increases from mature to old adults in the calcaneus and talus. In the pooled population sample the predicted drop in Tb.Th was not found. Examination of Figures 7.4 to 7.6 shows that the Kerma and St. Johns have old adults with unusually thick trabeculae. Because the Black Earth have thicker trabeculae in general compared to the other populations, trabecular thickness in old adult Black Earth individuals in equal to trabecular thickness in mature adults from St. Johns and Kerma.

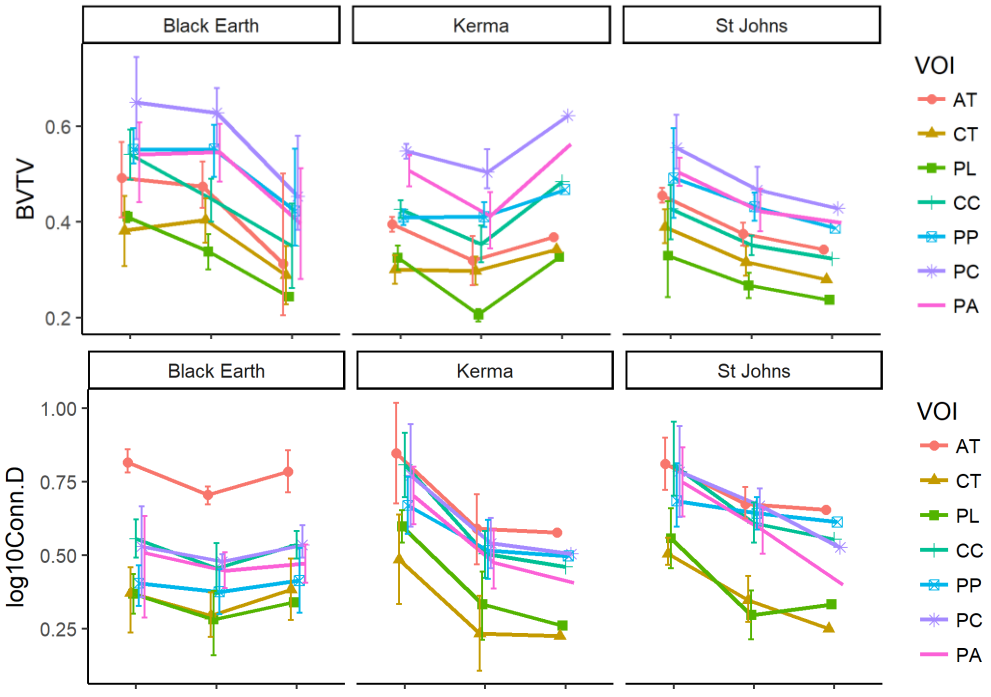

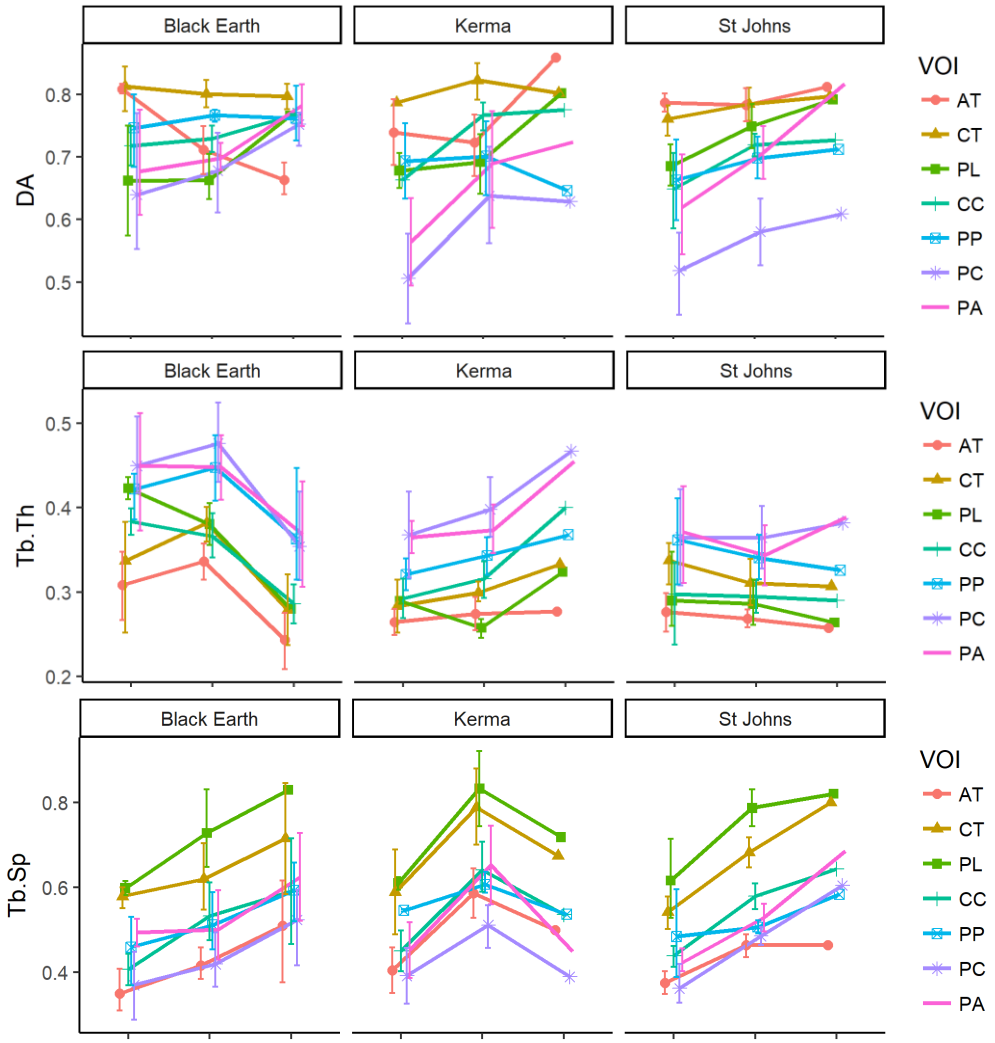
Black Earth
Kerma
St Johns
DA
0.8
0.7
0.6
0.5
VOI
AT
CT
PL
CC
PP
PC
PA
Black Earth
Kerma
St Johns
Tb.Th
0.5
0.4
0.3
0.2
VOI
AT
CT
PL
CC
PP
PC
PA
Black Earth
Kerma
St Johns
Tb.Sp
0.8
0.6
0.4
VOI
AT
CT
PL
CC
PP
PC
PA

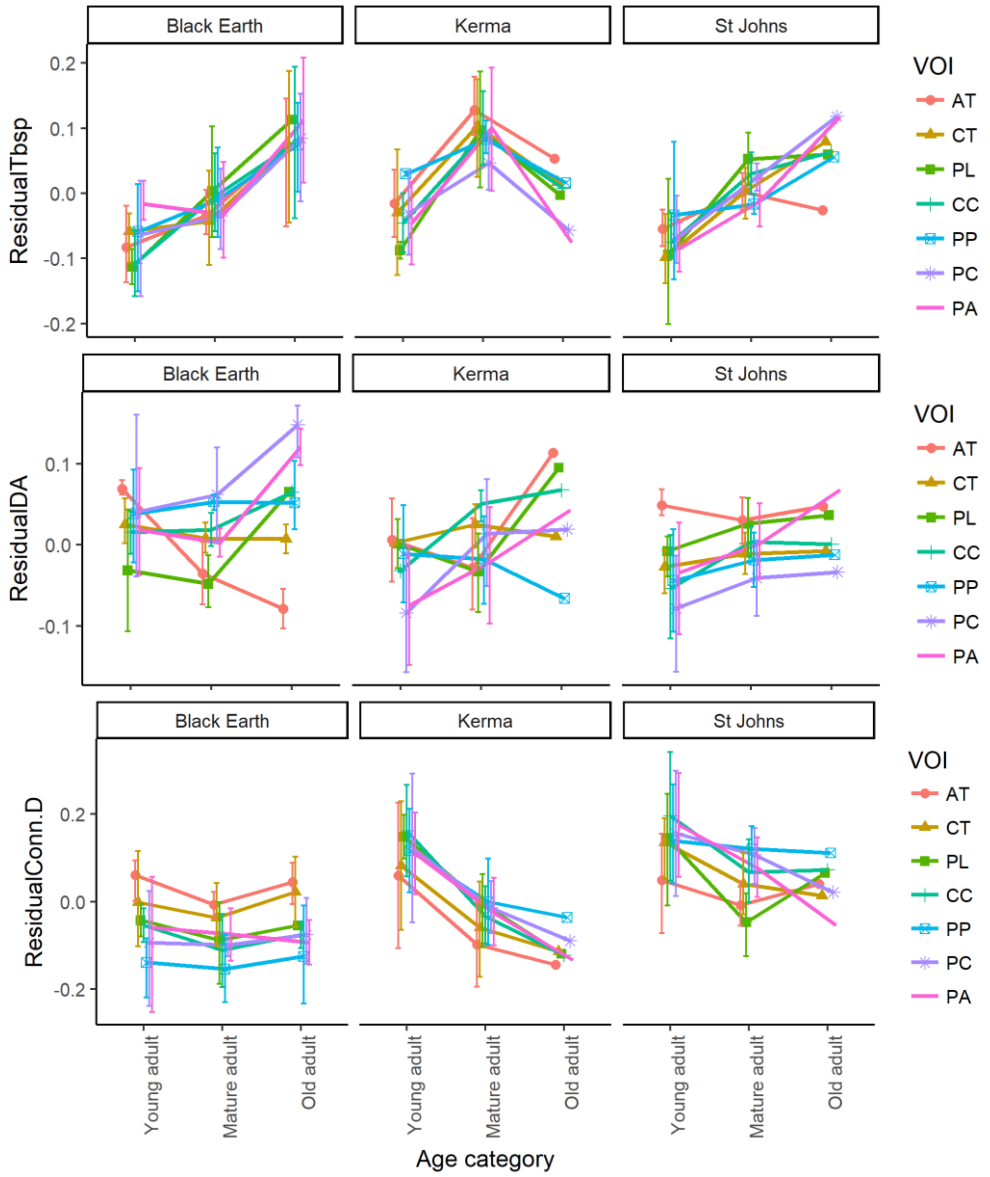

Figure 6.4. Calcaneal trabecular structure with age in three populations. Individual data points are plotted with the lines representing the mean and standard deviation of each volume of interest. Volumes of interest: Achilles tendon (AT), calcaneal tuber (CT), plantar ligaments (PL), posterior talar facet (PP: posterior, PC: central, PA: anterior), calcaneocuboid (CC).

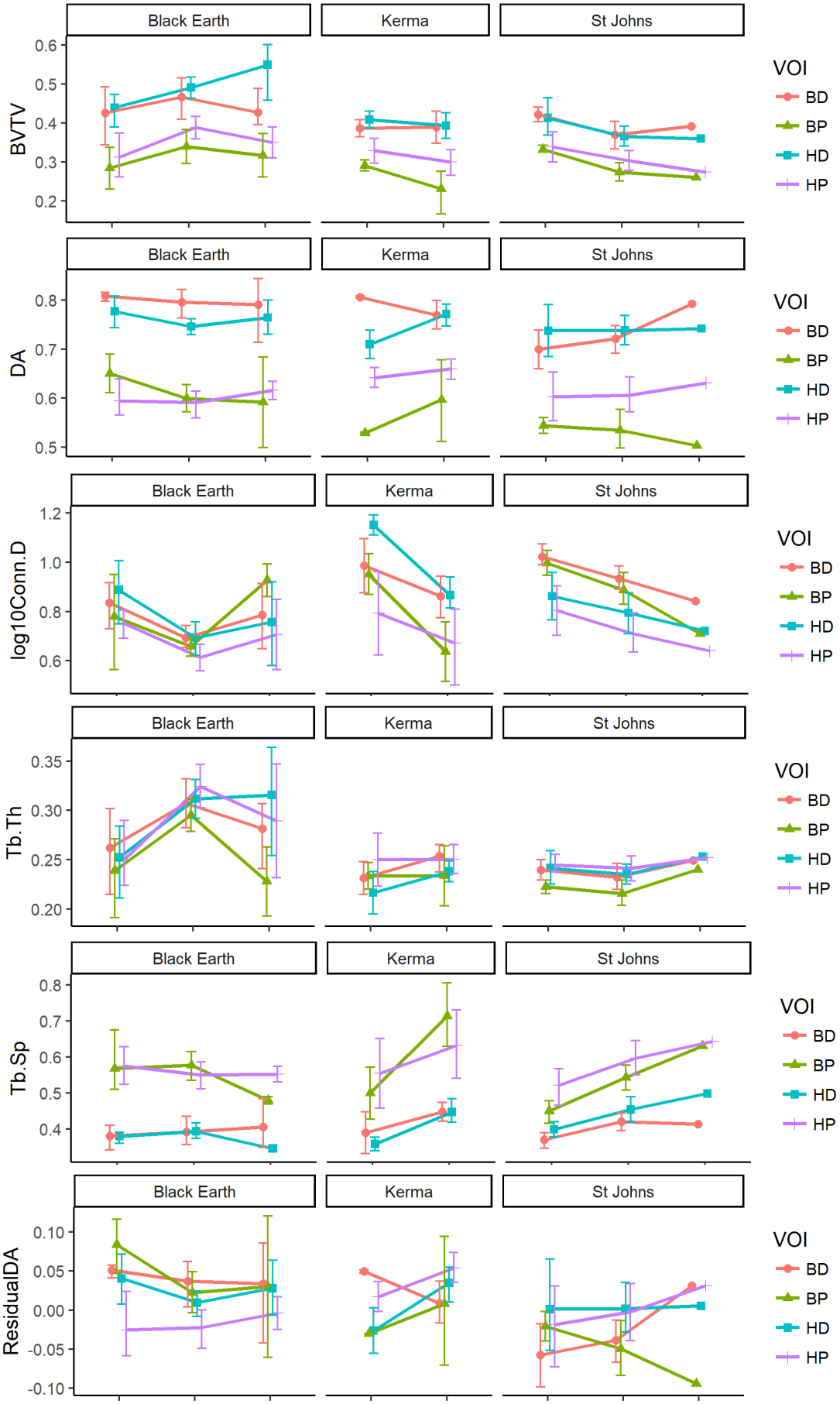
Black Earth
Kerma
St Johns
BVTV
DA
log10Conn.D
Tb.Th
Tb.Sp
ResidualDA
VOI
BD
BP
HD
HP

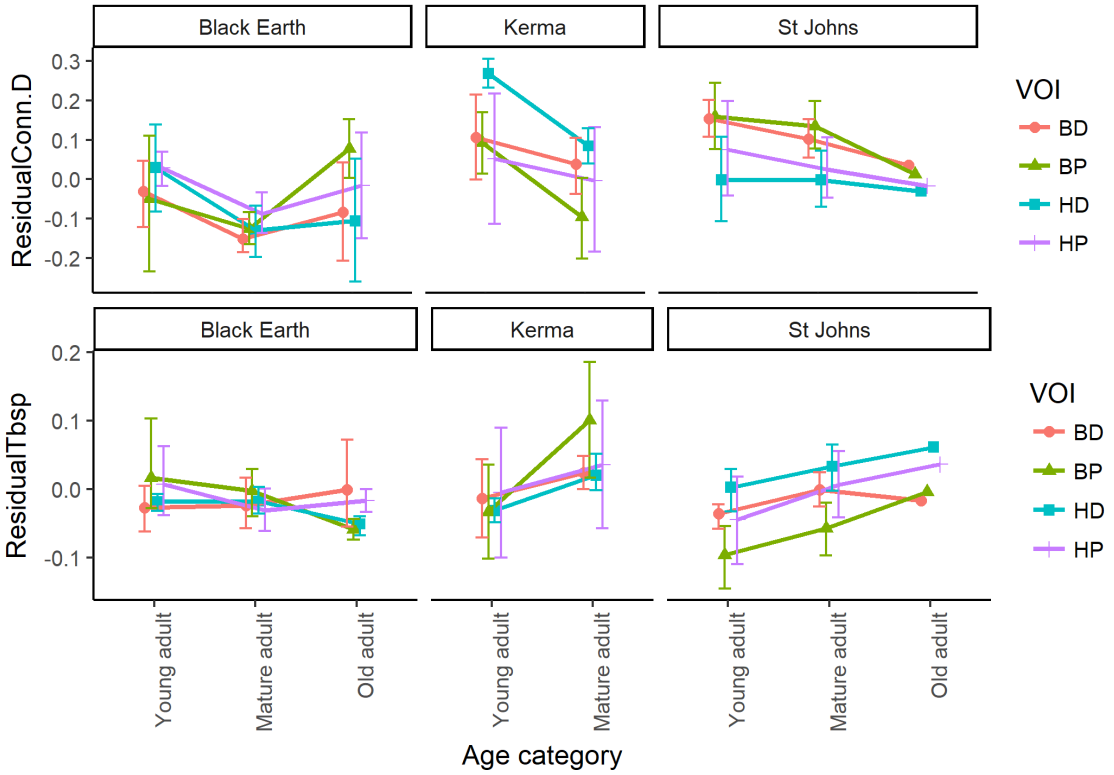

Figure 6.5. MT1 trabecular structure with age in three populations. Individual data points are plotted with the lines representing the mean and standard deviation of each volume of interest. Volumes of interest: dorsal base (BD), plantar base (BP), dorsal head (HD), plantar head (HP).

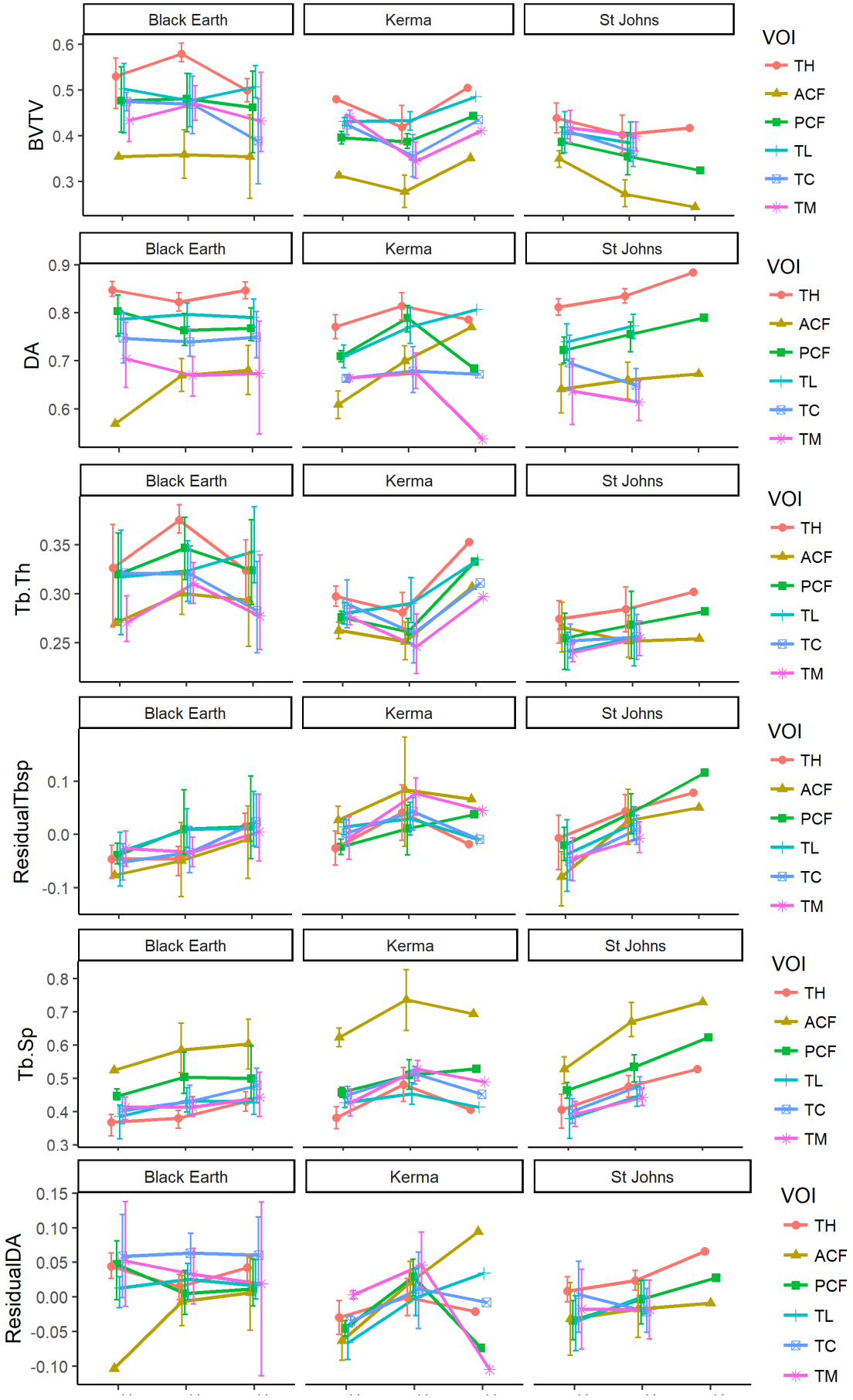
Black Earth
Kerma
St Johns
BVTV
DA
Tb.Th
ResidualTbsp
Tb.Sp
ResidualDA
VOI
TH
ACF
PCF
TL
TC
TM

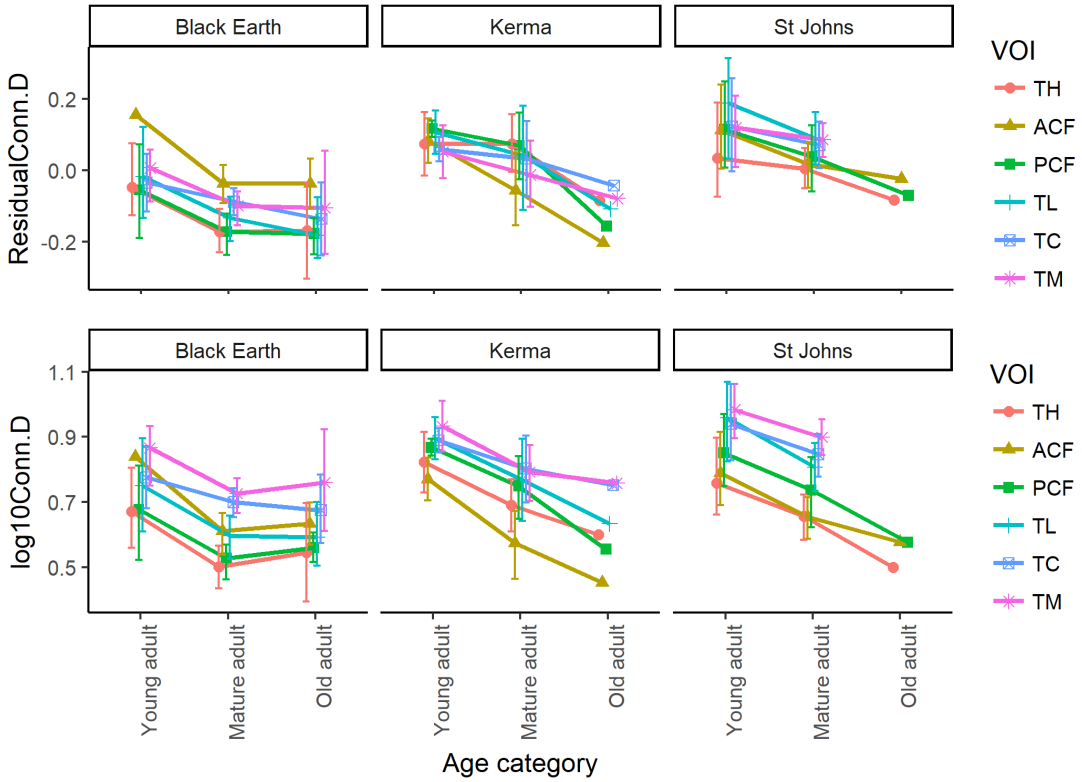

Figure 6.6. Talar trabecular structure with age in three populations. Individual data points are plotted with the lines representing the mean and standard deviation of each volume of interest. Volumes of interest: talar head (TH), anterior calcaneal facet (ACF), posterior calcaneal facet (PCF), trochlea (lateral: TL, central: TC, medial: TM).

Partial Spearman correlations, correcting for variation in body mass, between age category and trabecular properties in a pooled sex sample for individual populations are presented in Appendix 6.2. Varying patterns of significant Spearman correlations were found between the populations.

Few significant partial correlations were found with age and trabecular structure in the Black Earth sample, despite having the most equal distribution of age categories of the three populations. While the pooled population sample showed significant negative correlations between age and Conn.D, no significant correlations were observed in Black Earth. A significant negative correlation was found between DA and age in the Achilles tendon. Trabecular thickness showed a nonsignificant trend of reduction with age in the calcaneus and talus, but an increase in the MT1. A significant negative correlation is found between age and BV/TV in the plantar ligaments. A significant positive correlation is found between age and BV/TV in the dorsal MT1 head.

Strong partial correlations ($\rho > .7$) were found between age and trabecular structure in the Kerma sample. However, due to the small sample size these correlations were often not significant. Correlations between age and Conn.D fell just short of significance. No significant relationship was found between Tb.Sp and age. A significant positive correlation was found between DA and age categories in the anterior calcaneal facet of the talus, and a perfect positive correlation was found in the plantar MT1 head. Strong positive correlations were found between age and Tb.Th in the CC, PP, and BD. No significant correlations were found between BV/TV and age.

The greatest number of significant partial correlations between trabecular structure and age were found in the St. Johns population. Significant negative correlations with Conn.D were found in the BD, and BP. Positive correlations between age and Tb.Sp were found in all three bones, particularly in the calcaneus. A strong negative correlation between age and DA was found in the plantar base of the first metatarsal. There was a trend of reduction in Tb.Th with age but not significantly. Significant negative correlations were found between BV/TV and age in all VOIs except for the talar head.

Discussion

Age categories used in this study were very broad aside from the young adults. Mature adults cover the range of ages between 26 and 45 while old adults contained all age estimates over 46. During sample selection, individuals showing signs of pathology were excluded. The chance of procuring injuries, diseases, and degenerative conditions such as osteoarthritis increase with age. Because of this, it is more likely that old adults fall closer to 46 than older ages. Of the individuals for whom age could be determined, 20% were young adults, 67% were mature adults, 13% were old adults. The low number of young and old adults relative to the mature adult category lowers the statistical power of the models discussed in this chapter. Four out of six old adults are from Black Earth, and only one old adult was male. Skeletal ageing methods tend to overestimate age in young adults while underestimating age in older individuals (Martrille et al., 2007). Thus, despite the large age categories it is possible that some individuals in the mature adult group were misclassified. The Black Earth population is significantly more robust than Kerma or St. Johns (higher BV/TV and Tb.Th, lower Conn.D and Tb.Sp, see Chapter 7). Because Black Earth is such a robust population, and because most old adults are Black Earth, average BV/TV and Tb.Th are increased while Tb.Sp is reduced in the pooled population old adults relative to the younger age categories which receive more equal contributions from each population. This lowers the average differences between old and mature adults, and explains why expected reductions in Tb.Th and BV/TV were not often observed in the pooled population sample. Males were largely concentrated in the mature adult category while females were more spread out, accounting for 78% of the young adults and 83% of old adults in pooled populations. Little sexual dimorphism was found in Chapter 5 after correcting for variation in body mass in the pooled populations sample. Partial Spearman correlations were used to account for variation in body mass and to reduce sexual dimorphism resulting from body mass differences. However, the clinical literature often, though not always, reports significant differences in bone loss between men and women (Duan et al., 2001; Seeman, 2001; Eckstein et al., 2007; Lochmüller et al., 2008; Djuric et al., 2010). Small sample size, demography, and between-population variation unfortunately prevents the investigation of sex specific variation in age-related bone loss in this study.

Predictions based on results from the clinical literature were generally supported in the pooled population sample. As predicted, increased anisotropy of the trabecular structure often accompanies reductions in connectivity. Significant negative partial Pearson correlations, controlling for differences in body mass, between Conn.D and DA were found in all but three VOIs in the pooled population

sample. No variables besides Conn.D were consistently found to correlate with DA, whereas Conn.D was often found to significantly correlate with Tb.Sp, Tb.Th, and occasionally BV/TV. It was demonstrated in chapters 3 and 4 that body mass significantly correlates with Conn.D. By accounting for variation in body mass this leaves either age or between population variation as the most likely factor behind the strong correlations between DA and Conn.D. Negative correlations between DA and Conn.D are reported in Chapter 5 for both a pooled sex sample as well as in males and females separately, suggesting that sex differences do not explain this phenomenon. Trabeculae are thickest in the main direction of loading. This is illustrated using the calcaneocuboid VOI in Figure 6.7, which is primarily loaded from the anterior direction. The degree of anisotropy presumably increases with age while connectivity is lost because the thinner trabeculae in the non-primary loading directions are removed faster.

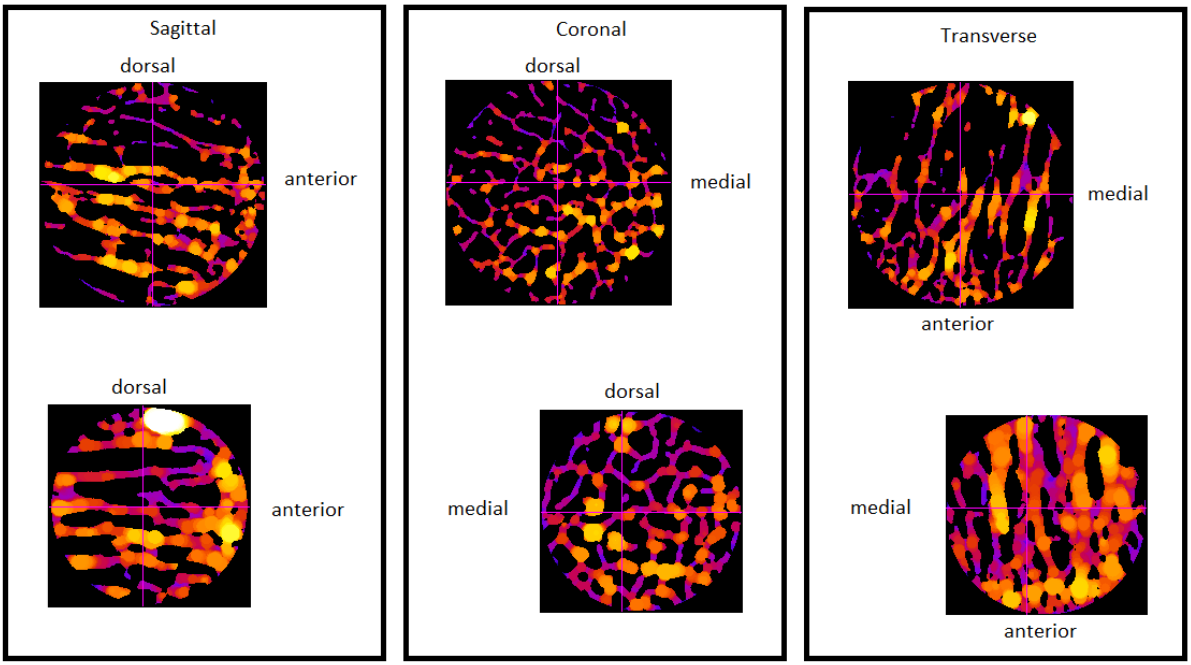

Figure 6.7. Trabecular thickness mapped in the calcaneocuboid VOI in an old adult (top) and a mature adult (bottom) from the St. Johns population. Brightness increases with thickness. The VOI is loaded in compression from the anterior direction.

While Conn.D showed the strongest relationship with age in the pooled sample, this relationship was much less clear in the individual populations. After correcting for body mass using residual Conn.D, fewer significant differences were found between age categories in pooled population sample. No significant correlations were found between age categories and Conn.D in Black Earth. A possible cause is that all old adults from Black earth were female, who were shown in Chapter 5 to have greater mean Conn.D compared to males, although the difference is reduced after body mass corrections. Significant positive correlations were often found between Tb.Sp and age in the pooled population sample. However, in Black Earth and Kerma the correlations were often not strong enough to reach significance. It was predicted that a higher rate of bone loss would be found in the populations with relatively high Conn.D and low Tb.Th and thus a high surface-area-to-volume ratio (Kerma, St.

Johns). While stronger correlations were found between age and Conn.D in Kerma and St. Johns, the sample composition precludes any general conclusions. Throughout previous chapters Conn.D was found to correlate significantly with bone dimensions, body mass, sex, and age. Additionally, Saers et al. (2016) found a relationship between Conn.D and terrestrial mobility where Conn.D decreased with increasing mobility (Chapter 7). Taken together, this suggests that care should be taken when interpreting variation in Conn.D as it is clearly a complex variable.

In general, BV/TV showed a negative correlation with age in most VOIs and populations. The strongest negative correlations between BV/TV and age were found in St. Johns where all but the talar head VOIs showed a significant negative correlation with age. It was predicted that trabeculae would become thinner with age. Instead significant increase in thickness was observed in the Kerma population. In the pooled population there was a single significant positive correlation between Tb.Th and age. Thus, the observed reductions in BV/TV were associated with a reduction in connectivity, but not thickness.

Considerable differences were found in the patterns of trabecular structure with age between the three populations. It is interesting that the St. Johns population as the most recent and sedentary of the three groups also shows the strongest reduction in BV/TV with age. The Black Earth population shows no significant reduction in Conn.D. One explanation is that the Black Earth sample has relatively thicker and less interconnected trabeculae compared to Kerma and St. Johns. The thicker trabeculae may prevent connectivity from being lost for a longer time compared to the other populations, as trabeculae take longer to sever through remodeling. Another explanation is that in the old adults from Black Earth are all female who have higher mean Conn.D and residual Conn.D compared to males (see Chapter 5). Regardless, these findings are limited in power due to the large age categories, small sample sizes, low numbers of young and old adults, and substantial genetic, dietary, and environmental differences between populations. Thus, these findings are not informative about variation in age related bone loss between these archaeological populations.

Rupprecht et al. (2006) reported a greater regional rate of bone loss with age in the calcaneus in the region beneath the posterior talar facet, compared to other regions of the calcaneus. This finding was not replicated in the pooled population sample nor in individual populations in this study. However, the composition of the sample precludes an accurate assessment of the patterns of bone loss in the archaeological populations.

One of the goals of this chapter was to determine how the inclusion of old adults affects population average values of trabecular properties. Z-scores were calculated to determine where the six old adults fall within their specific population's distribution for each trabecular variable (mean z-scores: Table 6.2, Figure 6.8). Large standard deviations in Table 6.2 indicate that there is significant variation between VOIs in the location of individuals around the population mean. The results show that BE01, BE106, and F394 often stay within one standard deviation of the population mean. BE106 and K47

fall above their population mean BV/TV and Tb.Th, and below the population mean in Tb.Sp which is the opposite of what would be expected from old adults. BE04 and BE187 show relatively large z-scores, falling two standard deviations above or below the mean for BV/TV, Tb.Th, and Tb.Sp. This indicates that on average these individuals fall near the edges of the population's normal distribution. Overall these z-scores demonstrate that while some of the old adults fall near the tails of the normal distribution, they are not substantial outliers within their respective populations.

Table 6.3. Population specific mean individual z-scores of the six old adults (mean±SD).

Z-score	BE01	BE04	BE106	BE187	F394	K47
BV/TV	-0.33±0.62	-1.78±0.25	1.01±0.37	-1.00±1.08	-0.56±0.35	1.31±0.39
Tb.Th	-0.71±0.68	-1.82±0.22	0.85±0.58	-0.81±1.11	0.18±0.52	1.62±0.70
DA	0.36±0.84	-0.29±0.58	-0.95±0.86	0.76±0.97	0.66±0.64	0.15±1.12
Tb.Sp	-0.37±0.42	1.38±0.58	-0.58±0.37	1.20±0.81	1.10±0.64	-0.69±0.50
Conn.D	1.07±0.72	0.33±0.78	-0.19±0.58	-0.61±0.58	-0.81±0.34	-0.74±0.41

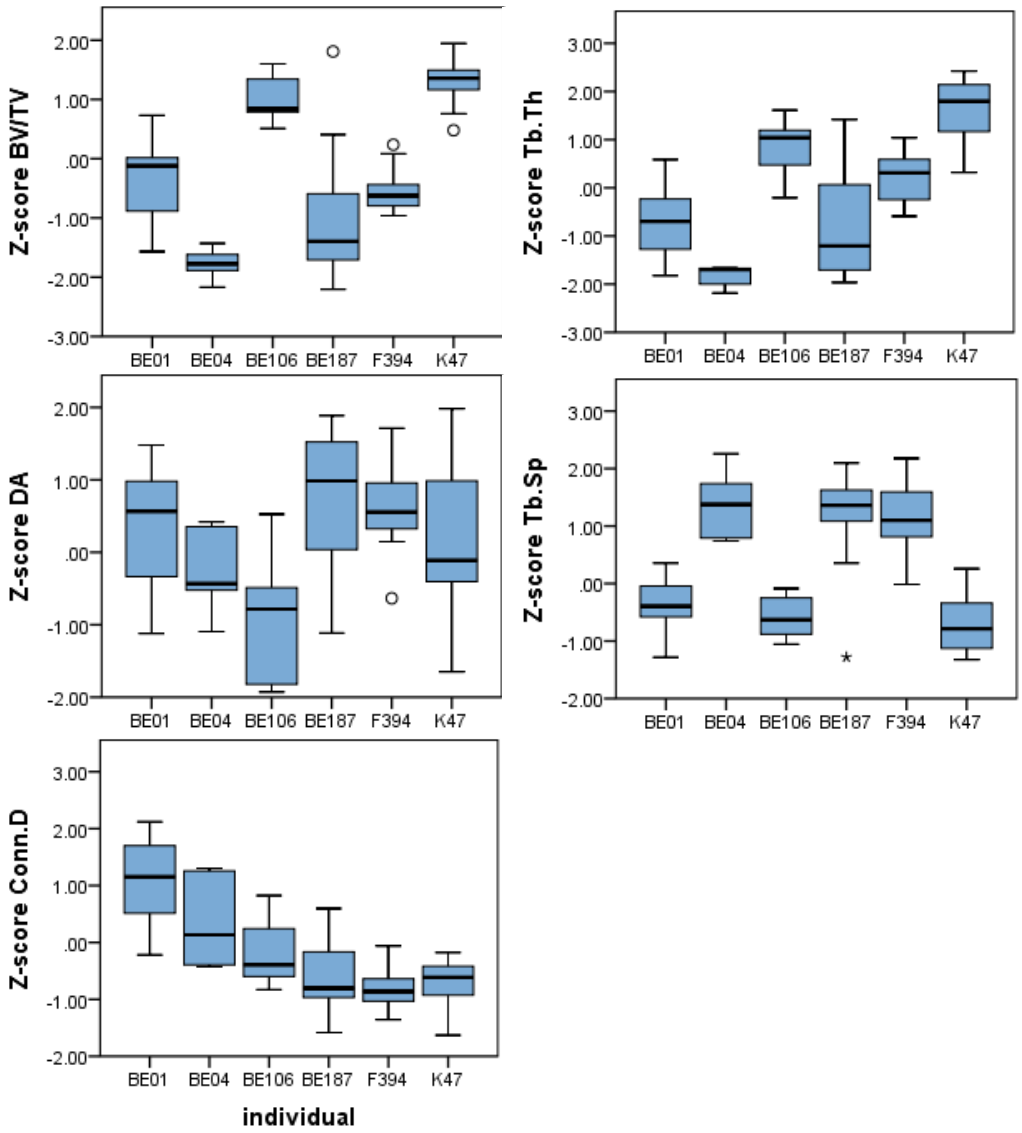

Figure 6.8. Population specific z-scores for the six old adults.

Conclusion

The main aim of this chapter was to determine whether age is an important variable to factor into interpretations of trabecular structure in this thesis. There are significant effects of age on trabecular properties in all populations used in this study. These effects should be considered in the subsequent analyses where variation in trabecular properties between populations is interpreted in the context of variation in inferred terrestrial mobility. The distribution of individuals across age categories did not significantly differ between populations (Table 6.1, Figure 6.2). There were differences in the relationships between age and trabecular properties between populations. However, these differences are most likely consequences of small sample size and unequal distribution of individuals across age groups.

Age-at-death is an important variable that should be considered when examining the effects of other factors on trabecular structure. BV/TV and Tb.Th are not strongly affected by age in the pooled populations sample, but do show a significant decline with age in Black Earth. DA tends to increase with age but not often significantly. Tb.Sp and Conn.D are most strongly affected by age in the pooled and individual populations, but these variables are least informative about loading (Maquer et al., 2015; Saers et al., 2016). A good approach for future analyses might be to use an ANCOVA that accounts for the effects of body mass and age, or using residuals from multiple regression (see Appendix 7.5). This approach does require that mean body mass and age are similar across all studied populations, and therefore this approach would not be possible for interspecific analyses without prior corrections. Applying this approach to the current study would exclude all Jebel Moya and half of the Kerma because they could not be aged due to their fragmentary and incomplete state. Instead, age will not be included as a covariate in the statistical models, but will be considered when interpreting results. Z-scores of old adults indicate that most old adults are not substantial outliers within populations. Taken together, the results of this chapter show that no population will be particularly more strongly affected by age-related bone changes than others.

The relationship between age and trabecular structure in archaeological populations certainly merits further investigation. Unfortunately, the current study was not designed to specifically study the relationship between age and trabecular structure in archaeological populations. Bone loss has been reported to be region and sex specific (Eckstein et al., 2007; Lochmüller et al., 2008; Djuric et al., 2010), and the large spread of z-scores in old adult individuals provides some support for these claims. Future work on age-related bone loss in the past should include significantly larger sample sizes of both men and women and a more equal distribution of age categories. Multiple anatomical locations should ideally be studied from multiple archaeological populations. Such a study should be able to provide insight on human trabecular bone loss through time and space.

Chapter 7 - Terrestrial mobility and variation in trabecular structure

Introduction

Trabecular bone may be a useful proxy to infer behaviour from hominin fossil morphology. However, a better understanding the effects of habitual behaviour on within species variation in trabecular morphology is needed first. A review of the literature on the relationship between trabecular bone structure and mechanical loading is provided in Chapter 1. In this chapter, variation in trabecular morphology in the calcaneus, talus, and first metatarsal is examined and interpreted in the context of behavioural and environmental differences between populations.

Hypotheses

Experimental work has demonstrated that trabecular bone is responsive to habitual loading (Pontzer et al., 2006; Sugiyama et al., 2010; Barak et al., 2011); thus, trabecular structure is predicted to vary between populations based on relative levels of terrestrial mobility. Mobility is defined here as the total sum of all locomotor activities using the lower limb (Pearson et al., 2014). Because the biomechanics of bipedal locomotion are expected to be very similar between all populations, trabecular morphology is expected to follow similar distribution throughout the foot in the four populations. Variation between populations is predicted to be the result of differences in loading magnitude and frequency (Rubin et al., 2001; Barak et al., 2011). However, previous chapters have demonstrated significant effects of age, sex, and body mass on trabecular structure which need to be considered when interpreting between-population variation. Other factors may also influence trabecular structure such as genetics (Turner et al., 2000; Judex et al., 2004, 2009; Wallace et al., 2012, 2017) and climate (Devlin et al., 2016). Three hypotheses are generated which would be expected in the case that either terrestrial mobility, genetic distance, or climatic effects dominate the variation in trabecular structure between human populations.

The first set of predictions should be followed if differences in terrestrial mobility levels underlie the variation in trabecular structure between populations. Trabecular bone structure is highly correlated with the elastic properties of bone. High BV/TV, Tb.Th, and low Conn.D and Tb.Sp are associated with high levels of mechanical strain (Hodgskinson and Currey, 1990; Goulet et al., 1994; Odgaard et al., 1997; Ulrich et al., 1999; Kabel et al., 1999; Rubin et al., 2001; Rubin et al., 2002; Mittra et al., 2005; Pontzer et al., 2006; Polk et al., 2008; Rincón-Kohli and Zysset, 2009; Barak et al., 2011; Karim and Vashishth, 2011; Ryan and Shaw, 2015; Saers et al., 2016). A combination of BV/TV and DA can predict 97% of variance in finite element predicted bone stiffness (Maquer et al., 2015). Populations who experience greater levels of mechanical loading through greater terrestrial mobility should have stronger trabecular structures to accommodate the increased loads. With increasing levels of terrestrial mobility, and thus high levels of loading, it is predicted that BV/TV and Tb.Th will increase while

Tb.Sp and Conn.D are predicted to decrease. As gait is expected to have been largely similar between populations, no differences in fabric anisotropy are predicted between populations. The Black Earth foragers and the Jebel Moya pastoralists are predicted to be more mobile than the Kerma agriculturalists and the medieval urban St. Johns population. Biomechanical analyses suggest that both Jebel Moya and Black Earth have more robust tibial and femoral midshaft diaphyses than the Kerma. Unfortunately, no lower limb cross-sectional data is currently available for St. Johns. The transition from foraging to agriculture and urban life has resulted in a significant reduction in terrestrial mobility, culminating in extremely sedentary lifestyles in modern industrial populations (Ruff, 2008; Ruff et al., 2015). Based on the historical trend of reduced cortical bone rigidity, the St. Johns population is predicted to be less mobile than the pastoralists and foragers (Ruff, 2008; Macintosh et al., 2014). The archaeological, behavioural, and biomechanical data available for these populations is described in detail in Appendix 1.1. It is not possible to infer a ranking of terrestrial mobility per population from the archaeological data. Therefore, the four populations will be broadly divided into two categories. The mobile category consists of the Black Earth foragers and the Jebel Moya pastoralists. The sedentary category consists of the St. Johns and the Kerma populations. Therefore, Black Earth and Jebel Moya are predicted to have greater BV/TV and Tb.Th, and lower Tb.Sp and Conn.D compared to the sedentary Kerma and St. Johns in all VOIs throughout the foot.

Genetic differences between populations could lead to differences in the norms of reaction to mechanical loading and thus mimic behavioural signals (Turner et al., 2000; Judex et al., 2004; Wallace et al., 2012, 2017). Over eighty percent of genetic diversity in humans in found within populations (Li et al., 2008), and there is little evidence that alleles affecting bone mechanoresponsiveness are unequally distributed between populations (Styrkarsdottir et al., 2010). Thus, there is little reason to believe that analyses that test differences in bone structure between populations should be biased by genetic factors (Wallace et al., 2017). However, recent research using outbred mice suggests that differences in bone mechanoresponsiveness may arise in separate populations (Wallace et al., 2015). If the effects of genetic variation dominate variation in trabecular structure, more closely related populations would be expected to show less between group variation than more distantly related groups in a simple isolation by distance model (Relethford, 2004). If geographic distance between archaeological sites is taken as a proxy for genetic distance (Relethford, 1994; Ramachandran et al., 2005; Li et al., 2008; Betti et al., 2009), the Jebel Moya and Kerma would be expected to show the greatest similarities in trabecular structure, followed by St. Johns, and finally Black Earth.

Recent work suggests there may be a significant effect of temperature on trabecular bone mass and strut thickness (Devlin et al., 2016). The relationship between temperature and bone during growth and development are not well understood, but cold dwelling humans are also known to possess lower cortical thickness than those from warmer environments (Wallace et al., 2014). Devlin et al. (2016) investigated the relationship between temperature and trabecular bone structure in groups mice with ad

libitum access to food and water. They found mice housed at 66-72 °F had 43-66% lower BV/TV and 35-46% lower Tb.Th than mice held at 78 °F. Thus, these results indicate that temperature has a significant effect on bone structure, despite unrestricted access to energy and water. The mobile Jebel Moya and sedentary Kerma hail from the warm and arid environment of north Africa (annual mean actual temperature in Khartoum: 29.9°C, monthly mean range 23.3 – 34.5°C). The sedentary St. Johns and mobile Black Earth are from more temperate northern latitudes (annual mean temperature Cambridge: mean 10.3°C, monthly mean range 4 – 18°C; Illinois: mean 10.7°C, monthly mean range -3.1 – 24.1°C). Following the results of Devlin et al. (2016) two clusters should be formed: one by the North African populations and one by the temperate northern latitude populations. In this case BV/TV and Tb.Th should be higher in the North African samples compared to the St. Johns and Black Earth samples.

Materials and methods

Trabecular structure is compared between the four populations in all 17 VOIs throughout the foot. All populations will be analysed in pooled sex, and sex-specific samples (Table 7.1).

Table 7.1. Sample size used in this chapter for each population and sex per VOI. Achilles tendon (AT), calcaneal tuber (CT), plantar ligaments (PL), posterior talar facet (PP: posterior, PC: central, PA: anterior), calcaneocuboid (CC), dorsal base (BD), plantar base (BP), dorsal head (HD), plantar head (HP), talar head (TH), anterior calcaneal facet (ACF), posterior calcaneal facet (PCF), trochlea (lateral: TL, central: TC, medial: TM).

		Black Earth		Jebel Moya			Kerma		St Johns		Total
		Sex		**Sex**			**Sex**		**Sex**		
		M	**F**	**M**	**F**	**I**	**M**	**F**	**M**	**F**	
Calcaneus	AT	7	10	8	2	5	9	7	9	11	69
	CC	7	6	9	2	5	12	7	8	9	66
	CT	7	9	10	2	5	12	7	8	10	71
	PA	7	6	8	2	4	12	7	9	11	67
	PC	6	7	8	2	4	12	6	9	11	66
	PP	7	8	9	1	4	12	5	9	11	67
	PL	6	6	5	1	5	11	7	8	10	60
MT1	BD	7	8	5	2	2	9	5	9	9	56
	BP	6	7	2	2	1	9	4	9	9	49
	HD	8	9	5	3	3	9	4	9	9	59
	HP	7	7	4	2	2	9	4	9	9	53
Talus	ACF	5	8	5	2	3	13	7	8	11	62
	PCF	5	7	7	4	4	12	6	6	11	62
	TH	5	6	10	4	5	12	7	8	11	68
	TL	7	8	10	4	5	10	5	7	11	67
	TC	6	8	9	4	3	12	5	7	11	65
	TM	7	8	9	3	3	10	5	7	11	63

Statistical analysis

Due to taphonomic damage, many individuals miss some volumes of interest. This leaves the choice to maximise sample size per VOI or to only use individuals who possess all VOIs per bone. Listwise one-way ANOVA will be used to assess significant population differences in trabecular properties per VOI. Running the analysis listwise will ensure that only individuals who have all VOIs present per bone are included in the analysis, and that the patterns throughout the bones are unaffected by different sample compositions. After the initial ANOVA, a post-hoc analysis will be run with Hochberg's GT2 if Levene's test is nonsignificant and Games-Howell if there is unequal variance. The same analysis will be run pairwise to maximise sample size and statistical power per VOI, and the differences between the two methods are compared at the end of the results section.

Conn.D was log10 transformed in all VOIs to comply with the normality assumption of ANOVA. Significant regressions were found between body mass and Tb.Sp, Conn.D and DA Tb.Th (Chapter 4). The residuals created from regressions between trabecular properties and body mass are used as body mass corrected variables following the methods described in Ryan and Shaw (2012). Body mass standardised residuals are examined in addition to raw values for log10Conn.D, Tb.Sp, and DA. The method of ANOVA with body mass corrected residuals was chosen over ANCOVA with body mass as a covariate because ANOVA has fewer assumptions and because robust regression was used in a subset of the analyses in Chapter 4. Some of the non-Gaussian distributions and outliers are corrected for using robust regressions and this may in some cases be more accurate than using ANCOVA. While p-values differ slightly between multivariate ANCOVA and ANOVA using residuals, the same general patterns of significant differences are observed when results from the two methods are compared. The differences between methodologies can be partly related to the fact that residuals are based on a larger dataset while ANCOVA uses a smaller listwise dataset where individuals with missing VOIs are cut from the entire analysis. Finally, an advantage of using the body mass standardised residuals is that they can also be used as body mass standardized variables in principal components analysis.

Ryan and Shaw (2012) argue that using suites of trabecular variables may be the most appropriate method for assessing intergroup variation in these complex trabecular structures. Multivariate principal components analysis (PCA) is used to assess group differences in combined suites of variables. One-way ANOVA will be performed on the individual principal components to test whether combined suites of related variables better discriminate between populations than single variables. The ratio of sample size to number of variables is important in PCA as reliability increases with larger ratios. Thus, when the 5 variables are used in a combination of all 7 calcaneal VOIs there is an N:p ratio of 48 individuals to 35 variables. A ratio of 5:1 is often cited as a minimum rule of thumb to produce accurate results. However, experimental validation of this rule of thumb is minimal (Osborne and Costello, 2004). Running PCA's with all combined variables and VOIs is therefore problematic due to the high N:p ratio. However, the strong correlations between trabecular properties across VOIs likely mitigate the effects of the large ratio of variables to subjects. Running a PCA on correlated variables from multiple VOIs has little effect on the eigenvectors but likely increases the eigenvalues of each component. In other words, this will increase the variance explained by the first few principal components but it will not affect where individuals fall on each component. Regardless, PCA's will also be run for each individual VOI to ensure a suitable N:p ratio. The main determinants of bone strength are BV/TV and DA (Currey, 2002; Maquer et al., 2015). Conn.D, Tb.Th and Tb.Sp are strongly correlated to BV/TV and are mechanically less informative (Maquer et al., 2015). Thus, to inform about the mechanically relevant properties of bone, combinations of just DA and BV/TV can be run for all VOIs with a more appropriate N:p ratio of 48 individuals to 14 variables in the calcaneus.

Trabecular properties are plotted using boxplots with the median and interquartile range to illustrate the distribution of the data for males and females.

Results

Variation in calcaneal trabecular structure between populations

Boxplots of trabecular properties per VOI are presented in Figure 7.1 for each pooled-sex population. Listwise one-way ANOVA tables are presented in Appendix 7.1. A summary of significant differences between populations is provided in Table 7.2.

Table 7.2. Significant pairwise comparisons of calcaneal trabecular properties between populations. Populations are colour coded to aid interpretation: Black Earth (B), Jebel Moya (J), Kerma (K), St. Johns (S). Achilles tendon (AT), calcaneal tuber (CT), plantar ligaments (PL), posterior talar facet (PP: posterior, PC: central, PA: anterior), calcaneocuboid (CC).

Calcaneus – ANOVA significant pairwise comparisons							
	AT	CC	CT	PA	PC	PP	PL
BV/TV	B>K,S J>K	B>K,S J>K,S	B>K,S J>K,S	B>K,S J>K	B>K,S J>K,S	B>K,S J>K,S	B>K J>K,S
Tb.Th	B>K,S J>K,S	B>K,S J>K,S	B>K,S J>K,S	B>K,S J>K,S	B>K,S J>K,S	B>K,S J>K,S	B>K,S J>K,S
Tb.Sp	K>B,J,S	K>B,J S>J	K>B,J	K>B		K>S	S>J
Res. Tb.Sp	K>B,J,S	K>B,J S>J	K>B,J,S	K>B,J		K>J	K>J S>J
Conn.D		S>B	J>K		S>B,J	S>B	
Res. Conn.D		S>B	J>K S>K	S>B	S>B,J	S>B,J,K K>B	J>B
DA							S>B
Res. DA					B>S	B>S	S>B

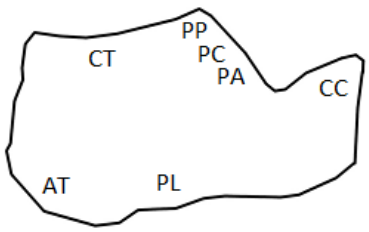

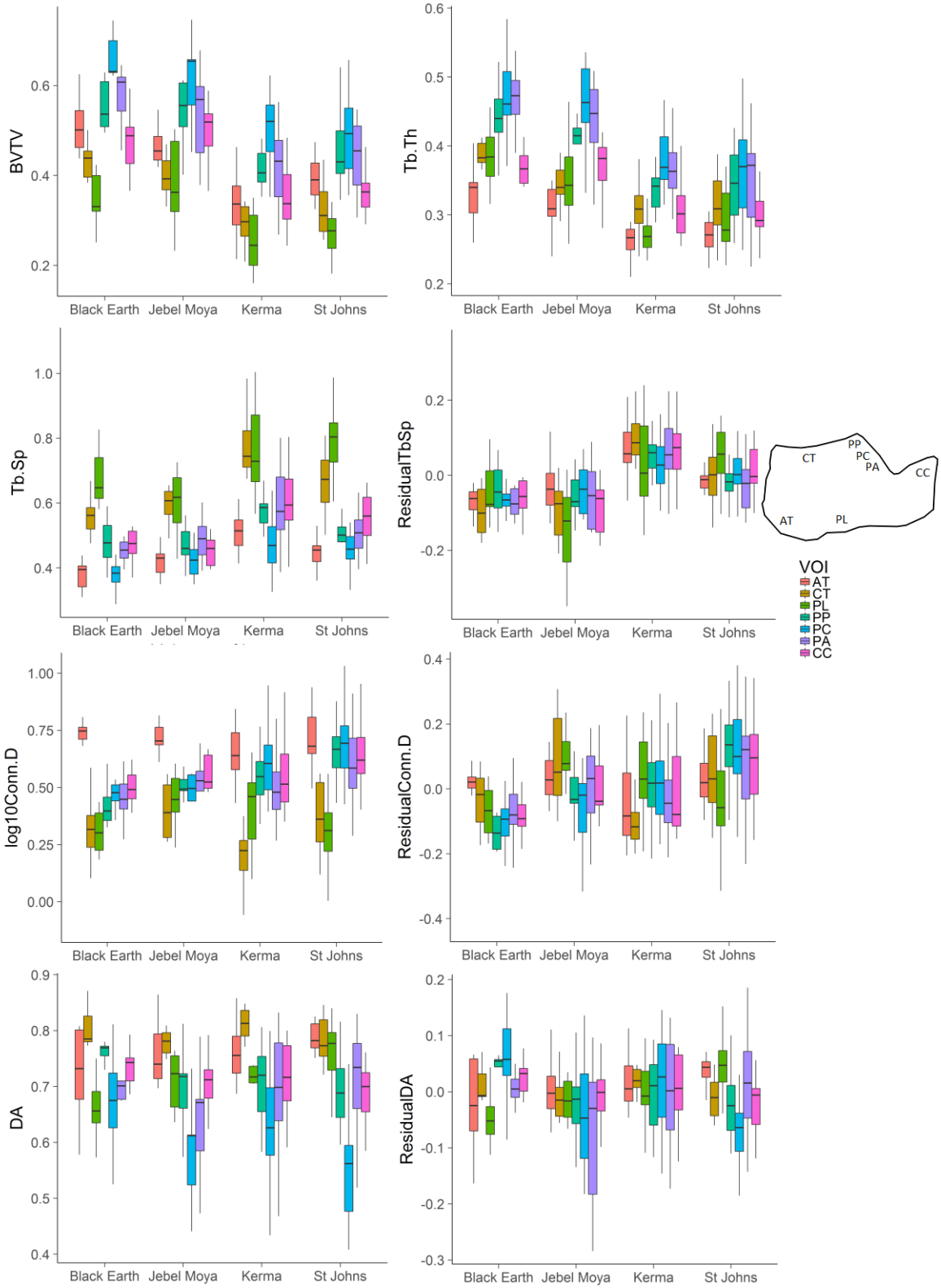

Figure 7.1. Median and interquartile range of trabecular properties per VOI for each pooled-sex population. Individuals with missing cases were deleted from all plots. Volumes of interest: Achilles tendon (AT), calcaneal tuber (CT), plantar ligaments (PL), posterior talar facet (PP: posterior, PC: central, PA: anterior), calcaneocuboid (CC).

The mobile Black Earth population is characterised by dense trabecular structures consisting of thick, closely-packed, and relatively few interconnected trabeculae. The Black Earth have significantly greater BV/TV and thicker trabeculae than Kerma and St. Johns in most VOIs. The Black Earth

sample has significantly lower DA than St. Johns in the PL and PP VOI. After correcting for the effects of body mass, residual DA was significantly greater than the St. Johns in the PC, PP, and PL. Significantly lower Tb.Sp and residual Tb.Sp was found in Black Earth compared to Kerma in the AT, CC, CT, and PA VOIs. The Black Earth sample has significantly less interconnected trabecular structures compared to St. Johns in the CC, PC, and PP VOIs. After correcting for the effects of body mass, residual Conn.D was significantly lower than St. Johns in the CC, PA, PC, PP, significantly lower than Kerma in the PP, and lower compared to Jebel Moya in the PL.

The mobile Jebel Moya have similar trabecular structure as the Black Earth. Overall, they are characterised by dense trabecular structures with thick, closely packed, but highly interconnected trabeculae. They have significantly greater BV/TV than Kerma in all VOIs and greater than St. Johns in most VOIs. Jebel Moya have thicker trabeculae compared to Kerma and St. Johns in all but the calcaneal tuber, and more closely packed structures than the Kerma in four VOIs. After correcting for body mass Jebel Moya has lower residual Tb.Sp than Kerma in all but the PP VOI. Relative to St. Johns the Jebel Moya have lower Tb.Sp and residual Tb.Sp in the CC and PL.

The sedentary Kerma have relatively gracile trabecular structures with low mean BV/TV, and thin, widely spaced, and relatively well interconnected struts. BV/TV is significantly lower in the Kerma compared to the mobile Jebel Moya and Black Earth in all calcaneal VOIs. No significant differences are found in DA or residual DA between Kerma and the other populations. The Kerma individuals have significantly thinner trabeculae than Black Earth in all VOIs, and compared to Jebel Moya in all but the calcaneal tuber. The Kerma have significantly more widely separated trabeculae in general compared to the other populations before and after correcting for body mass.

The sedentary St. Johns have relatively gracile trabecular structures with relatively low trabecular volume and thin, highly separated, and most highly interconnected struts of all populations. St. Johns has significantly lower BV/TV and Tb.Th than the Black Earth and Jebel Moya. After correcting for body mass, the St. Johns sample has significantly lower residual DA in the PC and PP and significantly higher in the PL compared to Black Earth. Trabeculae are significantly more widely spaced compared to Jebel Moya in the CC and PL both before and after correcting for body mass. However, they have significantly lower Tb.Sp compared to Kerma in the AT.

Are the patterns of variation in trabecular properties throughout the calcaneus similar in every population?

The patterns of variation in trabecular properties throughout the calcaneus were described in a pooled sex, pooled population sample in Chapter 2. Here it is examined whether all populations follow this same general pattern of variation or whether there are unique patterns in different populations (Figure 7.2). Lines are added between points representing the population mean in to aid visualization of the patterns throughout the bone. The same pattern as found in the pooled populations in Chapter 2 is found for BV/TV in each individual population. Populations generally follow the same distribution of

Tb.Th, Tb.Sp, and Conn.D throughout the calcaneus, although St. Johns deviates somewhat from the other groups in Conn.D. The greatest variation between populations is found in the distribution of anisotropy throughout the calcaneus. In all populations, the lowest DA is found in the PC, but St. Johns has exceptionally low DA relative to other VOIs. The Black Earth sample has relatively high DA in the PC and relatively low DA in the AT and PL compared to other VOIs.

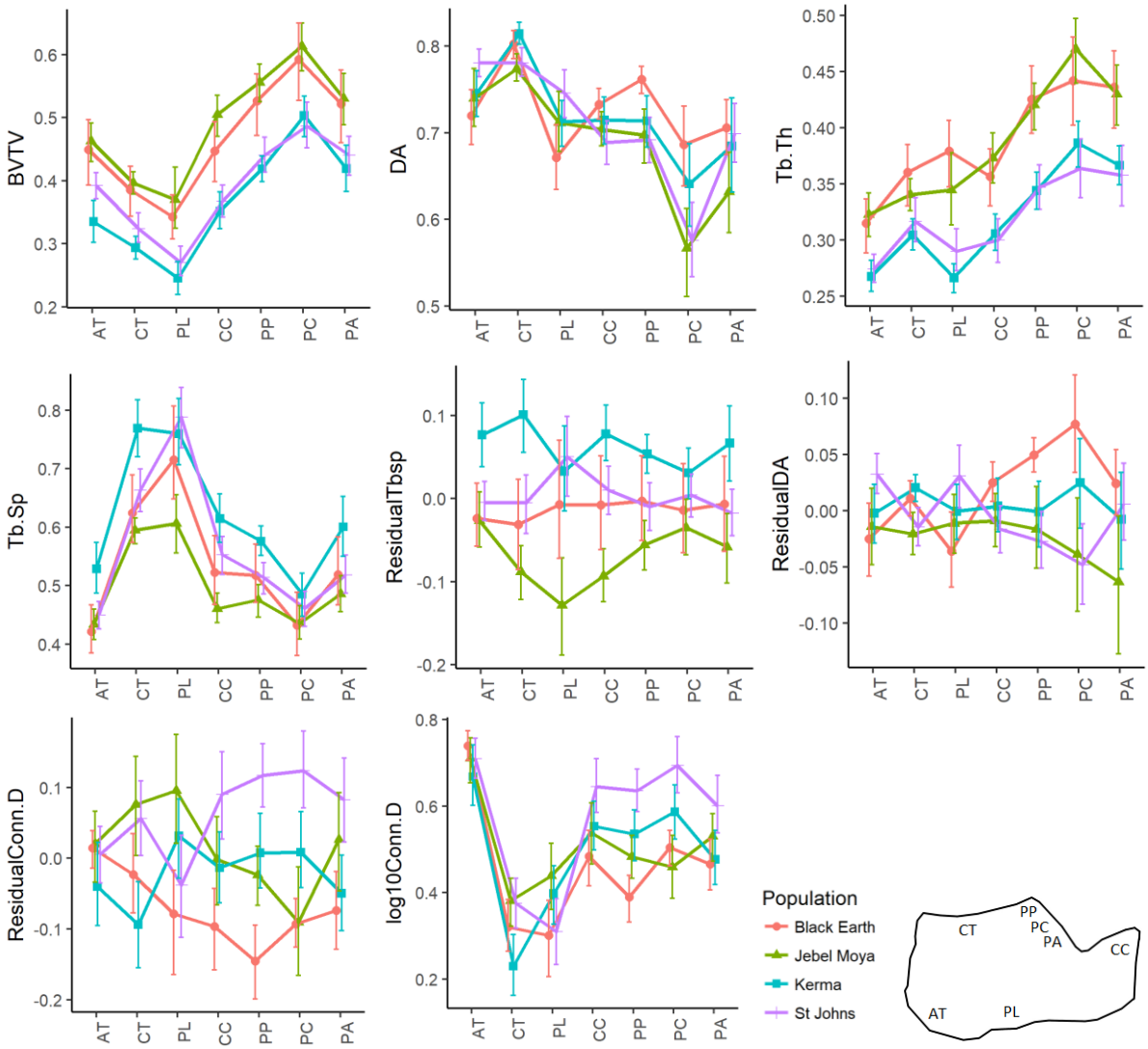

Figure 7.2. Mean and standard deviation of calcaneal trabecular properties for every population. Volumes of interest: Achilles tendon (AT), calcaneal tuber (CT), plantar ligaments (PL), posterior talar facet (PP: posterior, PC: central, PA: anterior), calcaneocuboid (CC).

Principal Components Analysis

A principal components analysis was run including BV/TV, Tb.Th, DA, residual Tb.Sp, and residual Conn.D from all calcaneal volumes of interest. The first three principal components are presented in Figure 7.3 and tables are presented in Appendix 7.1. The first five principal components account for 80% of the total variance with the first two components accounting for 66%. None of the first five principal components correlated significantly with body mass or age category.

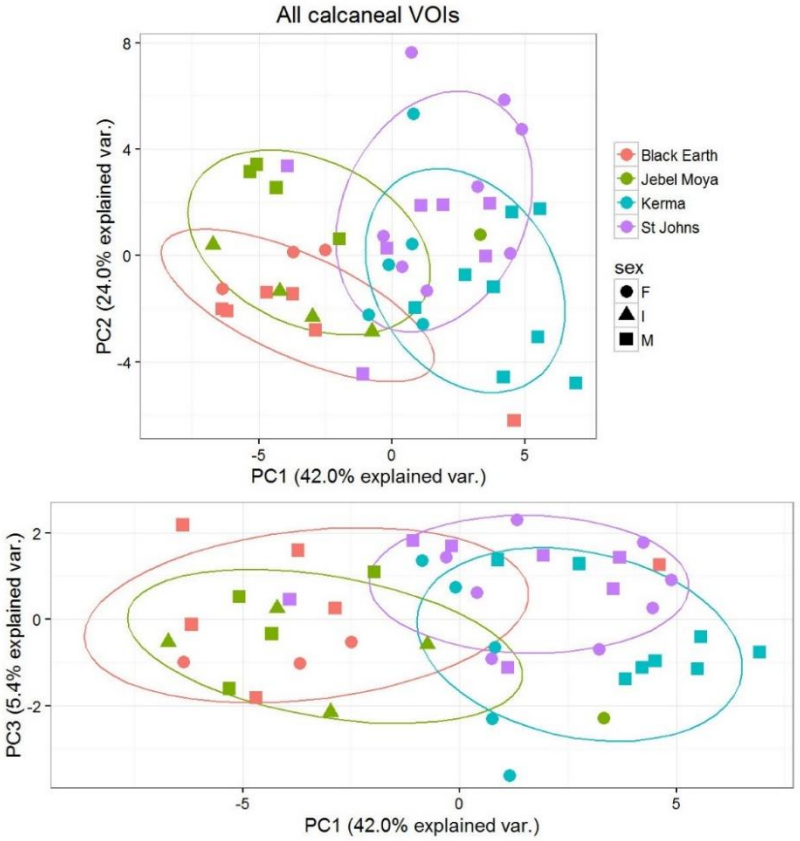

Figure 7.3. Biplot of PC1, PC2, and PC3 of seven calcaneal VOIs.

The greatest contributions to PC1 come from BV/TV, Tb.Th and residual Tb.Sp with similarly strong contributions from these variables in each VOI. BV/TV and Tb.Th correlate negatively with PC1 while residual Tb.Sp correlates positively. Black Earth and Jebel Moya cluster on the negative side of PC1 indicating they tend to have higher BV/TV and Tb.Th and lower Tb.Sp compared to Kerma and St. Johns. Pairwise post-hoc comparisons indicate that indeed Jebel Moya and Black Earth are significantly different from Kerma and Black Earth. All VOIs correlate with similar strength to PC1 indicating that no VOI disproportionally contributes to PC1.

PC2 accounts for 24% of total variance and correlates strongly with residual Conn.D that is uncorrelated to BV/TV, with smaller correlations with Tb.Sp, DA and Tb.Th depending on VOI. Residual Conn.D correlates positively with PC2 while Tb.Th, Tb.Sp, and DA correlate negatively. St. Johns and Jebel Moya cluster high on PC2 while Black Earth and Kerma cluster on the lower end. The

Black Earth individuals fall significantly lower on PC2 than St. Johns. PC3 accounts for 5% of total variance and correlates positively with DA and negatively with Conn.D. St. Johns falls significantly higher on PC3 compared to Kerma while falling just short of significance with Jebel Moya. No significant population differences are found in PC4 and PC5.

PC1 separates populations based on trabecular variables that are most strongly related to loading magnitude (high BV/TV, Tb.Th and low Tb.Sp), resulting in two clusters based on inferred mobility levels with the mobile Black Earth and Jebel Moya significantly different from Kerma and St. Johns. PC2 and PC3 relate to structural variation that is uncorrelated to BV/TV.

Finally, a PCA was performed using combinations of DA and BV/TV from all calcaneal VOIs, resulting in a total of 14 variables and 48 individuals (Figure 7.4). These variables were chosen because they are the two mechanically most relevant variables (Maquer et al., 2015), and reduces the N:p ratio. PC1 correlates negatively with BV/TV in all VOIs and PC2 correlates positively with DA in most VOIs. The St. Johns and Kerma have significantly greater PC1 scores compared to Black Earth and Jebel Moya. St. Johns fall significantly lower than the Black Earth on PC2. No significant differences are found in PC3 to PC5.

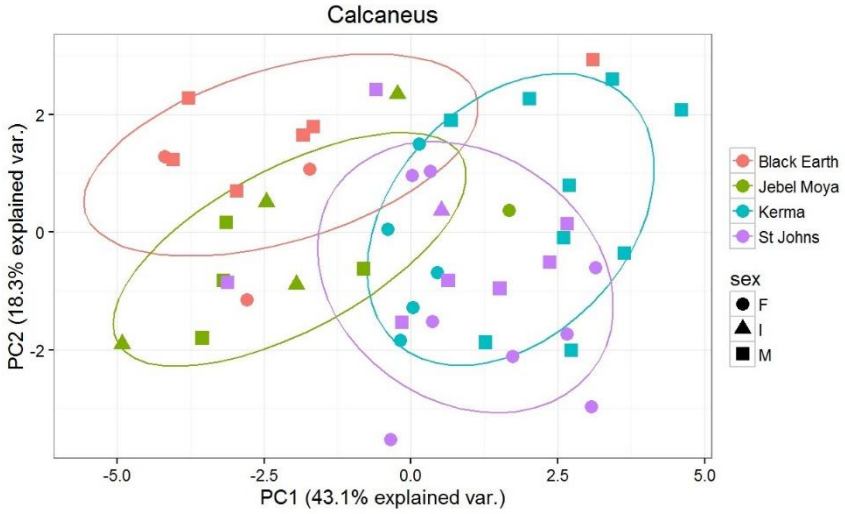

Figure 7.4. PCA combining BV/TV and DA from seven calcaneal VOIs.

Variation in first metatarsal trabecular structure between populations

Boxplots of first metatarsal trabecular properties per VOI are presented in Figure 7.5 for each pooled-sex population. Listwise one-way ANOVA tables are provided in Appendix 7.1. Due to the listwise analysis sample sizes are limited, particularly in the Jebel Moya which has been reduced to four individuals. The Black Earth are reduced to 10, the Kerma to 13, and the St. Johns to 18 individuals. Significant results are presented in Table 7.3.

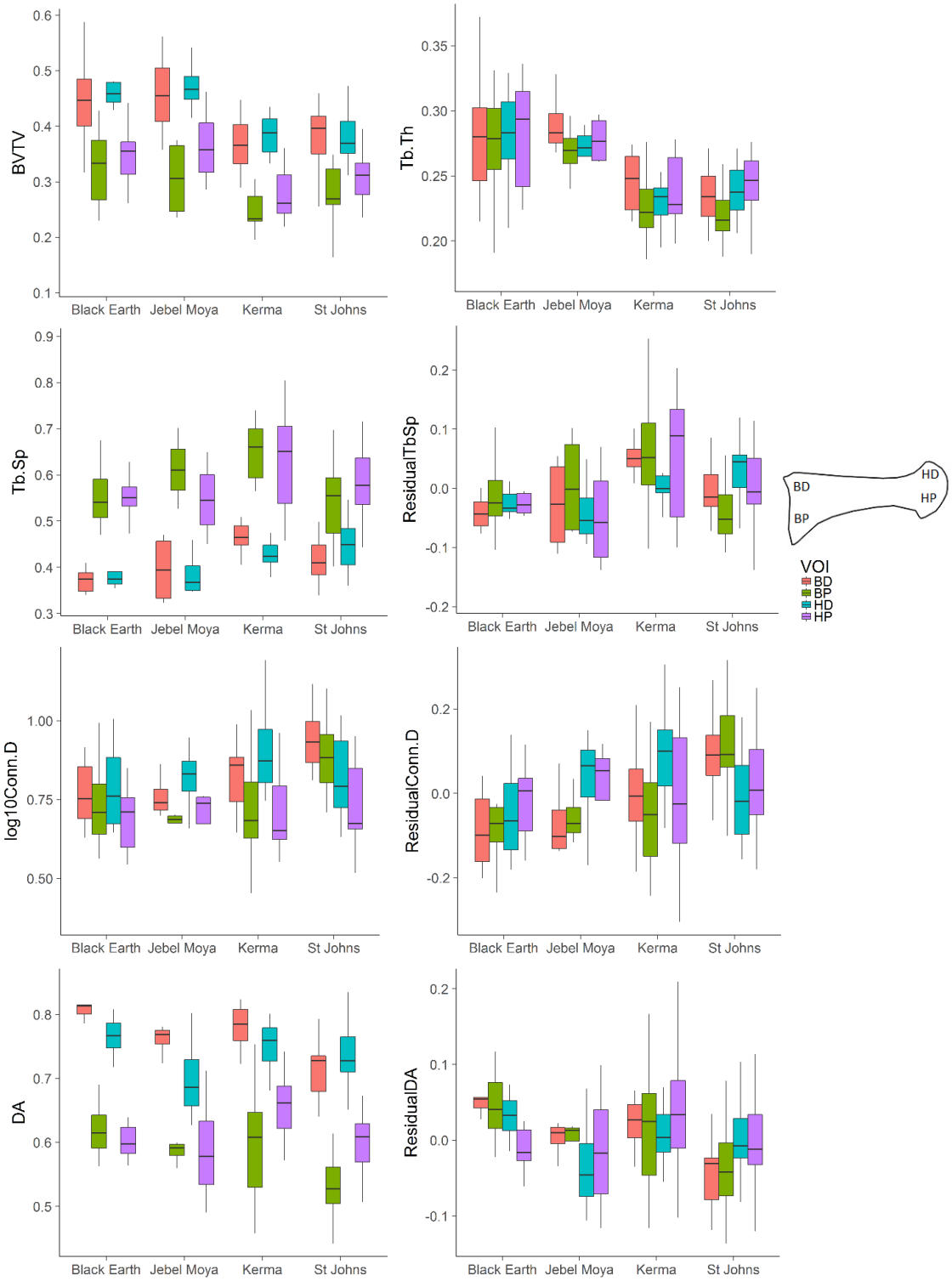

Figure 7.5. Median and interquartile range of first metatarsal trabecular properties per VOI for each pooled-sex population. Volumes of interest: dorsal base (BD), plantar base (BP), dorsal head (HD), plantar head (HP).

Table 7.3. Significant pairwise comparisons of first metatarsal trabecular properties between populations. Populations are colour coded to aid interpretation: Black Earth (B), Jebel Moya (J), Kerma (K), St. Johns (S). Dorsal base (BD), plantar base (BP), dorsal head (HD), plantar head (HP).

First Metatarsal – ANOVA significant pairwise comparisons				
	BD	BP	HD	HP
BV/TV	B>K	B>K	B>K,S J>K,S	B>K J>K
Tb.Th	B>S	B>S J>S	B>K,S J>K	B>K J>K
Tb.Sp	K>B	K>S	S>B	
Res. Tb.Sp	K>B	K>S		
Conn.D	S>B,J	S>B,J,K		
Res. Conn.D	S>B,J	S>B,K	K>B	
DA	B>S K>S	B>S J>S		
Res. DA	B>S K>S	B>S		

Overall, the mobile Black Earth have a dense trabecular structure consisting of thick, close-packed, relatively anisotropic and poorly interconnected trabeculae, as well as the greatest mean BV/TV in all VOIs. BV/TV is significantly greater compared to Kerma in all VOIs, and greater than St. Johns in the dorsal head. The Black Earth individuals have the thickest trabeculae on average in all VOIs. The differences are significant between St. Johns in all but the plantar head, and with Kerma in both head VOIs. Black Earth have significantly higher DA and residual DA than St. Johns in both MT1 head VOIs. Black Earth have significantly less interconnected trabeculae than St. Johns in the base. After correcting for the effects of body mass the Black Earth sample has significantly less interconnected structures than St. Johns in the base and in the dorsal head compared to Kerma.

The mobile Jebel Moya have a dense trabecular structure consisting of thick trabeculae. They have significantly higher BV/TV than Kerma in the head and compared to St. Johns in the dorsal head. Jebel Moya have significantly thicker trabeculae than Kerma in the head. They also have thicker trabecular compared to St. Johns but this just misses significance in all but the plantar base. The Jebel Moya have significantly greater DA than St. Johns in the in the plantar base, but not after correcting for the effects of body mass. Compared to St. Johns, the Jebel Moya sample has significantly less interconnected structures in the base before and after correcting for the effects of body mass. The low number of significant differences between Jebel Moya and other populations is likely a result of low sample size.

The sedentary Kerma have the most widely spaced trabeculae with low BV/TV and thin trabeculae compared to the mobile populations. They have significantly lower BV/TV than the Black Earth in all VOIs and compared to Jebel Moya in the base. The Kerma have significantly thinner trabeculae than

Black Earth and Jebel Moya in the head; more anisotropic structures in the dorsal base compared to St. Johns and more widely spaced trabeculae compared to Black Earth in the dorsal base. Compared to St. Johns the Kerma have more widely spaced and less interconnected trabeculae in the plantar base. After correcting for body mass, they have significantly more interconnected trabeculae in the dorsal head compared to the Black Earth.

The sedentary St. Johns have low BV/TV with relatively thin, isotropic, and well-connected trabeculae. The St. Johns have significantly lower BV/TV compared to Black Earth and Jebel Moya in the dorsal head; and significantly thinner trabeculae than Black Earth in the base and dorsal head, and compared to Jebel Moya in the plantar base. They have more isotropic structures compared to Black Earth and Kerma in the dorsal base and compared to Black Earth and Jebel Moya in the plantar base. Finally, the St. Johns have more interconnected structures in the dorsal base compared to Black Earth and Jebel Moya, and compared to Black Earth, Jebel Moya and Kerma in the plantar base.

Are the patterns throughout the first metatarsal similar in between populations?

In Chapter 2 the patterns of variation in trabecular properties throughout the first metatarsal were described in a pooled sex, pooled population sample. Here it is examined whether all populations follow this same general pattern of variation or whether there are unique patterns in different populations (Figure 7.6).

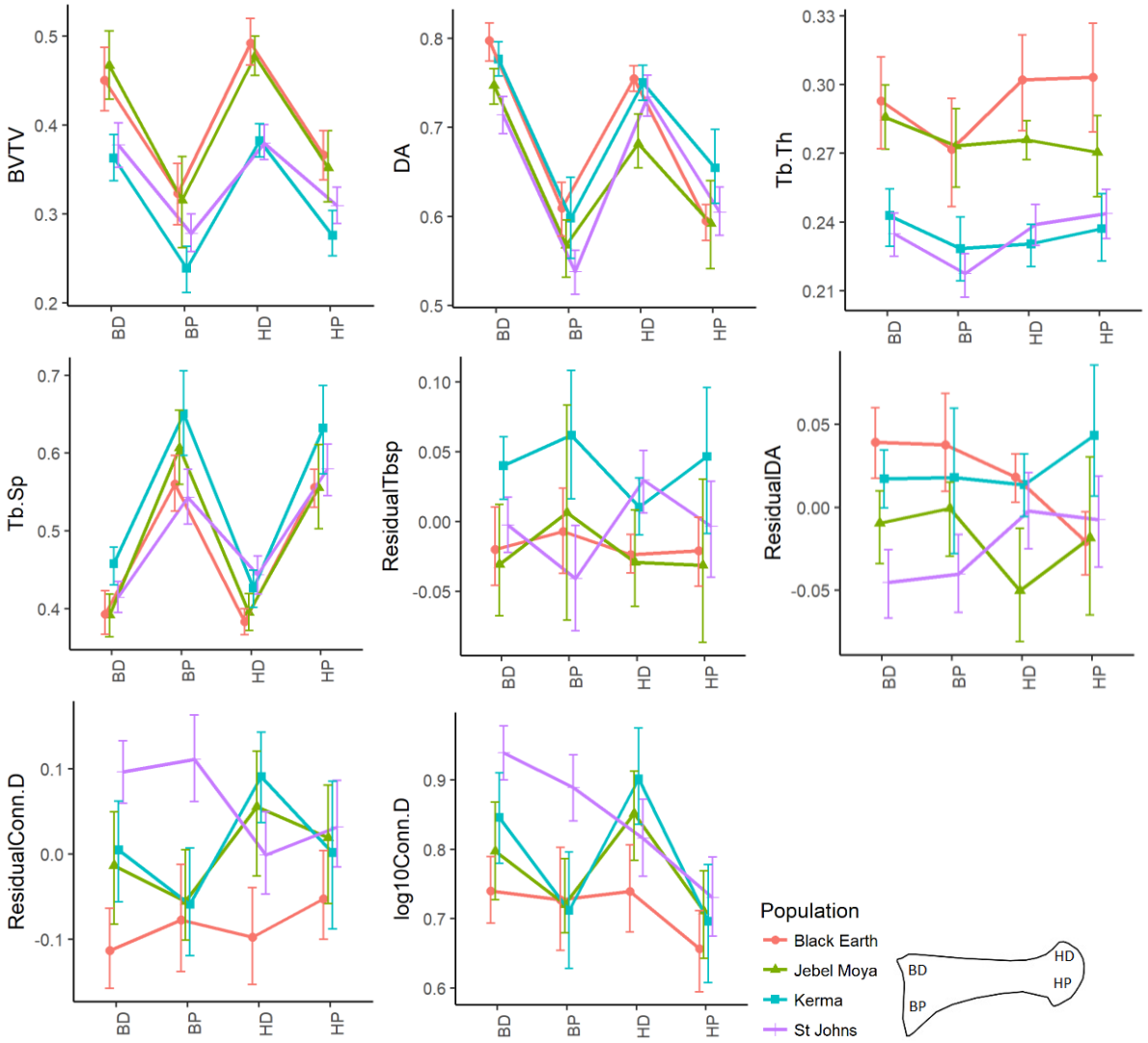

Figure 7.6. Mean and standard deviation of trabecular properties per population throughout the first metatarsal. Volumes of interest: dorsal base (BD), plantar base (BP), dorsal head (HD), plantar head (HP).

Very similar patterns in BV/TV throughout the first metatarsal are found in all populations. All populations have substantially greater BV/TV in the dorsal regions compared to the plantar regions. Similar general patterns are also observed in trabecular thickness and anisotropy, with greater anisotropy in the dorsal VOIs. All populations Tb.Sp mirrors BV/TV with the highest spacing in the plantar VOIs. The patterns in log10 Conn.D are similar in Jebel Moya and Kerma with the highest Conn.D in the dorsal VOIs. Black Earth follow the same pattern although the differences between dorsal and plantar are less pronounced. The pattern in St. Johns is different in that the base has a more interconnected structure than the head.

Principal components analysis

Principal Components Analysis (PCA) was run on a suite of five trabecular bone properties in four VOIs of the first metatarsal resulting in 20 variables compared between 44 individuals. Biplots of PC1, PC2 and PC3 are presented in Figure 7.7 and tables are presented in Appendix 7.2. The first five principal components account for 83% of the total variance with the first two components accounting for 62%. None of the first five principal components correlated significantly with body mass or age categories. Very little overlap is found between sedentary and mobile populations in Figure 7.7.

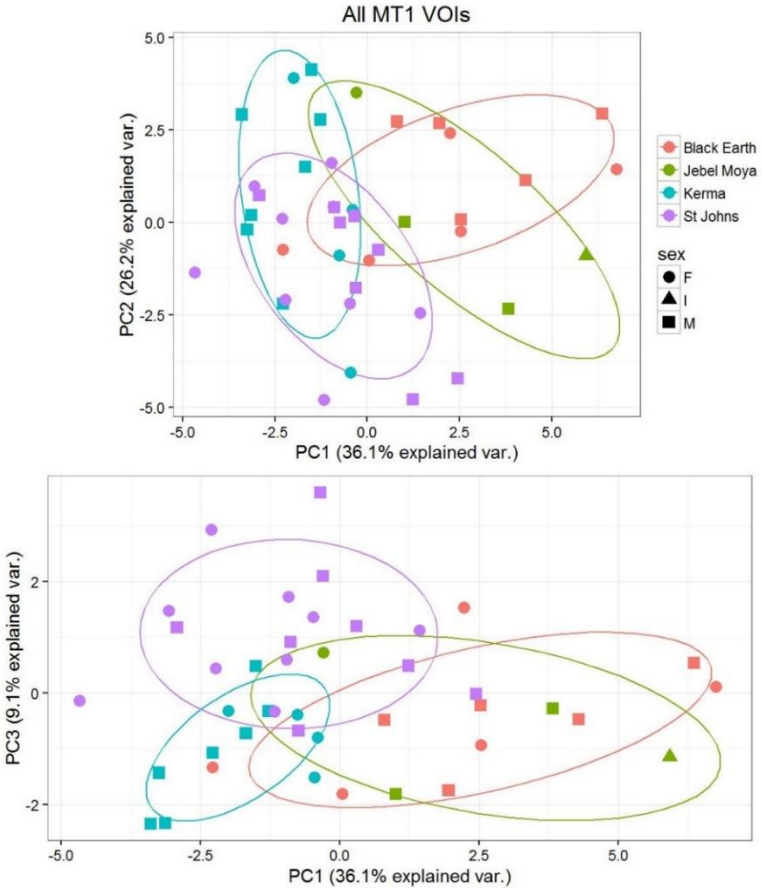

Figure 7.7. Biplots of PC1, PC2 and PC3 for a pooled sample of four first metatarsal VOIs.

PC1 correlates positively with BV/TV and Tb.Th with similarly strong contributions from these variables in each VOI. To a lesser extent PC1 also correlates negatively with residual Tb.Sp. Black Earth and Jebel Moya cluster significantly more positively on PC1 compared to Kerma and St. Johns. Black Earth and Jebel Moya show a larger spread on PC1 indicating more intra-population variation in these populations. All VOIs contribute roughly equally to PC1, with the exception that residual Tb.Sp correlates particularly strongly in the dorsal base.

PC2 accounts for 26.2% of total variance and correlates strongly negatively with residual Conn.D, while smaller positive correlations occur with residual Tb.Sp, DA and Tb.Th depending on VOI. While the general ANOVA is significant, subsequent pairwise post-hoc tests did not yield significant

differences. The difference between St. Johns and Black Earth just fails to reach significance with St. Johns falling lower on PC2 (p=.054).

PC3 accounts for 9.1% of total variance and correlates negatively with DA in the base. In the head PC3 correlates negatively with residual Conn.D and positively with residual Tb.Sp. The St. Johns fall significantly higher on PC3 than all other populations. No significant population differences are found in PC4 an PC5.

The results from the first metatarsal resemble those found in the calcaneus. PC1 was found to clearly separate populations based on trabecular variables that are most strongly related to loading magnitude (high BV/TV associated with greater Tb.Th and lower Tb.Sp). This resulted in two clusters based on inferred mobility levels with the mobile Black Earth and Jebel Moya significantly different from Kerma and St. Johns. PC2 and PC3 are related to morphological variation but the properties correlated to PC2 and PC3 do not indicate an increase in structural rigidity because BV/TV was not strongly correlated.

PCA was performed using combinations of DA and BV/TV from all MT1 VOIs, resulting in a total of 8 variables and 48 individuals (Figure 7.8). These variables were chosen because they are the two mechanically most relevant variables (Maquer et al., 2015), and reduces the N:p ratio. PC1 correlates positively with BV/TV and PC2 correlates negatively with DA in all VOIs. Black Earth and Jebel Moya differ significantly from Kerma and St. Johns on PC1. St. Johns falls significantly higher on PC2 compared to Black Earth and Kerma. No significant differences are found on PC3 to PC5.

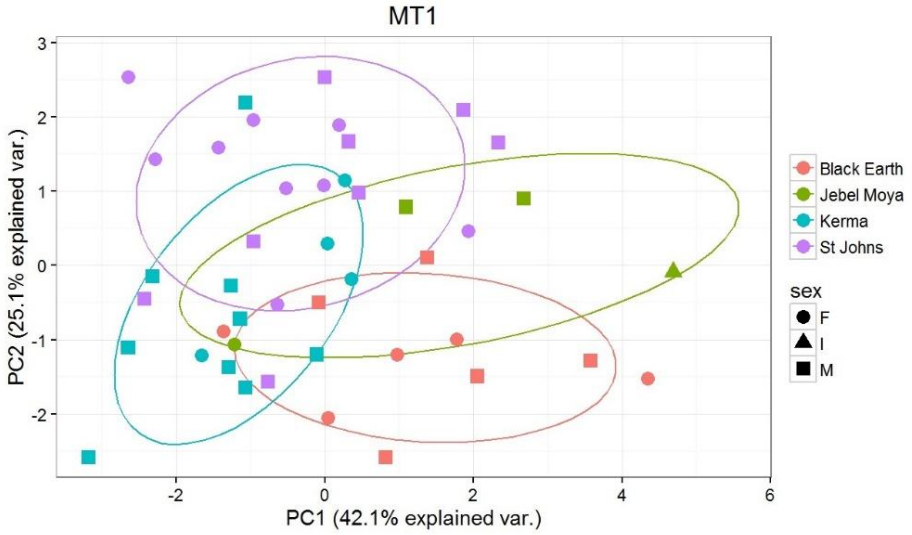

Figure 7.8. Biplot of PC1 and PC2 of combinations of DA and BV/TV in all MT1 VOIs.

Variation in talar trabecular structure between populations

Boxplots of talar trabecular properties per VOI are presented in Figure 7.9 for each pooled-sex population. Listwise one-way ANOVA tables are presented in Appendix 7.1. Sample size is 8 individuals for Black Earth and Jebel Moya, 12 for Kerma, and 16 for St. Johns. Table 7.4 summarizes significant pairwise comparisons between populations.

Table 7.4. Significant pairwise comparisons of talar trabecular properties between populations. Populations are abbreviated and colour coded to aid interpretation: Black Earth (B), Jebel Moya (J), Kerma (K), St. Johns (S). Talar head (TH), anterior calcaneal facet (ACF), posterior calcaneal facet (PCF), trochlea (lateral: TL, central: TC, medial: TM).

Talus – ANOVA significant pairwise comparisons						
	ACF	PCF	TH	TL	TC	TM
BV/TV	J>K,S	B>K,S J>K,S	B>K,S J>K,S	B>K,S J>K,S	B>K,S J>K,S	J>K
Tb.Th	J>K,S	B>K,S J>K,S	B>K,S J>K,S	B>S J>K,S	B>S J>K,S	J>K,S
Tb.Sp		S>J		K>J	K>B,S	K>B,J,S
Res. Tb.Sp	K>B,J	K>J S>J	K>J	K>J	K>B,S	K>B,J,S
Conn.D		K>B S>B	K>B S>B	S>B,J	S>B,J,K	S>B,J,K
Res. Conn.D		K>B S>B	K>B S>B	K>B S>B	S>B,K	S>B,K
DA			B>J S>J		B>J,S	B>J
Res. DA			B>J S>J		B>J	

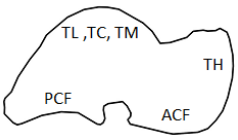

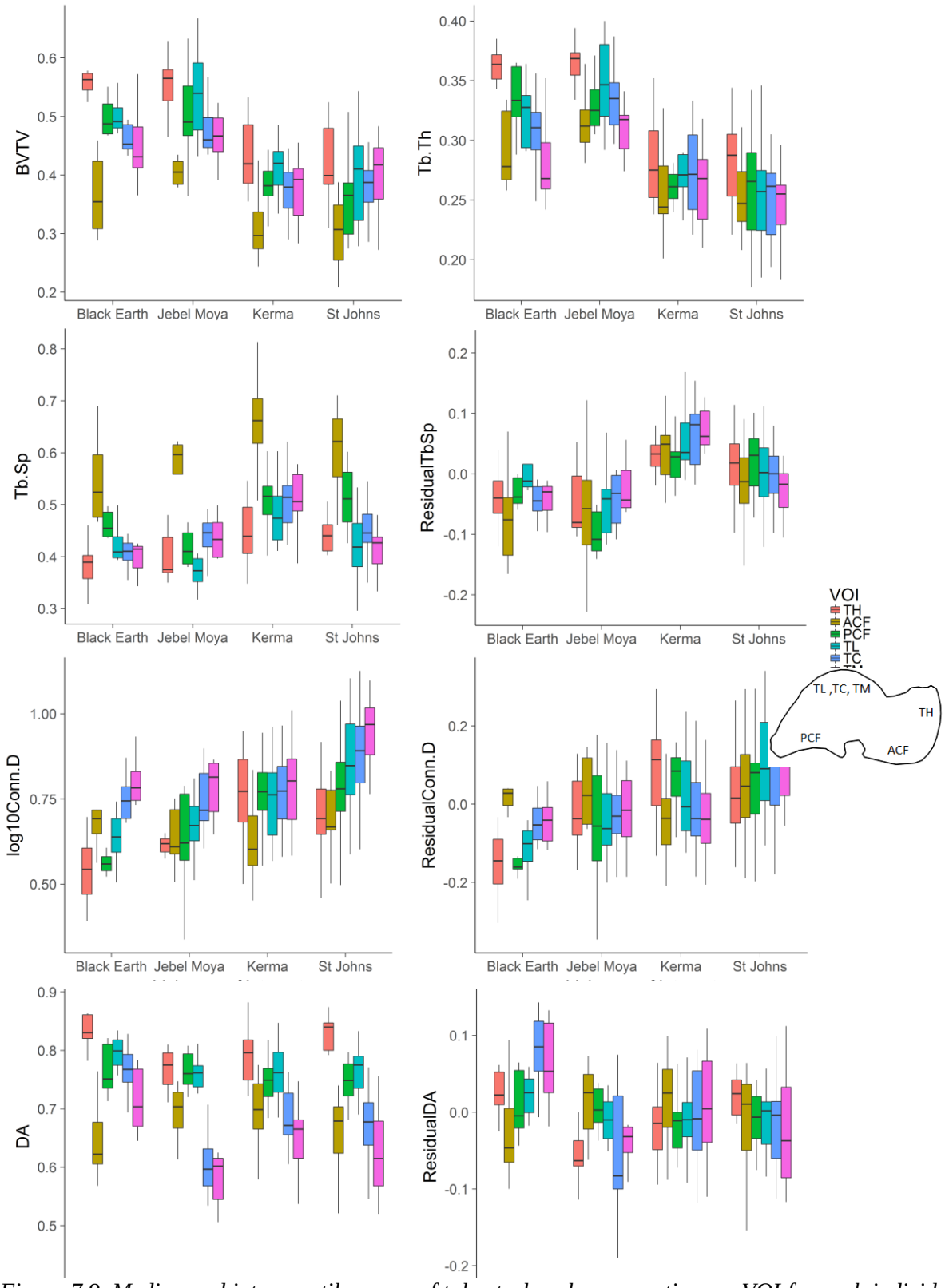

Figure 7.9. Median and interquartile range of talus trabecular properties per VOI for each individual pooled-sex population. Volumes of interest: talar head (TH), anterior calcaneal facet (ACF), posterior calcaneal facet (PCF), trochlea (lateral: TL, central: TC, medial: TM).

Overall, the mobile Black Earth have a dense trabecular structure consisting of thick, close-packed and poorly interconnected trabeculae. Black Earth has significantly greater BV/TV and thicker trabeculae Kerma and St. Johns in most VOIs. They have significantly more close-packed trabeculae in the trochlea compared to the Kerma. Compared to St. Johns, Black Earth have significantly less

interconnected structures in all but the ACF, and have significantly more anisotropic structures in the central and medial trochlea compared to St. Johns and Jebel Moya.

The Jebel Moya have a dense trabecular structure with thick and relatively poorly interconnected struts. They have significantly greater BV/TV and thicker trabeculae compared to Kerma and St. Johns, and more isotropic trabeculae relative to Black Earth. After removing the effects of body mass the Jebel Moya sample has more tightly packed structures relative to Kerma in the all VOIs except the central trochlea. The Jebel Moya have less interconnected trabeculae than St. Johns in the trochlea, but no longer after accounting for differences in body mass.

The sedentary Kerma have relatively low bone volume fraction, with thin, widely spaced and highly interconnected struts. They have significantly lower BV/TV and Tb.Th than Jebel Moya and Black Earth, and more widely spaced trabeculae in the trochlea. Before and after correcting for body mass Kerma have significantly more interconnected structures than Black Earth, but significantly less interconnected than St. Johns. No significant differences in anisotropy are found between Kerma and the other populations.

Overall, the St. Johns sample has a relatively gracile trabecular structure with low bone volume fraction and thin and relatively widely spaced and highly interconnected struts. They have significantly less BV/TV and lower Tb.Th than Jebel Moya and Black Earth. Trabecular spacing is significantly lower than Kerma in the trochlea. Trabeculae are significantly more anisotropic compared to Jebel Moya in the talar head, but more isotropic compared to Black Earth in central trochlea. The St. Johns have more interconnected trabeculae compared to the other populations, particularly Black Earth.

Are the patterns throughout the talus similar in between populations?

In Chapter 2 the patterns of variation in trabecular properties throughout the talus were described in a pooled sex, pooled population sample. Here it is examined whether all populations follow this same general pattern of variation or whether there are unique patterns in different populations (Figure 7.10).

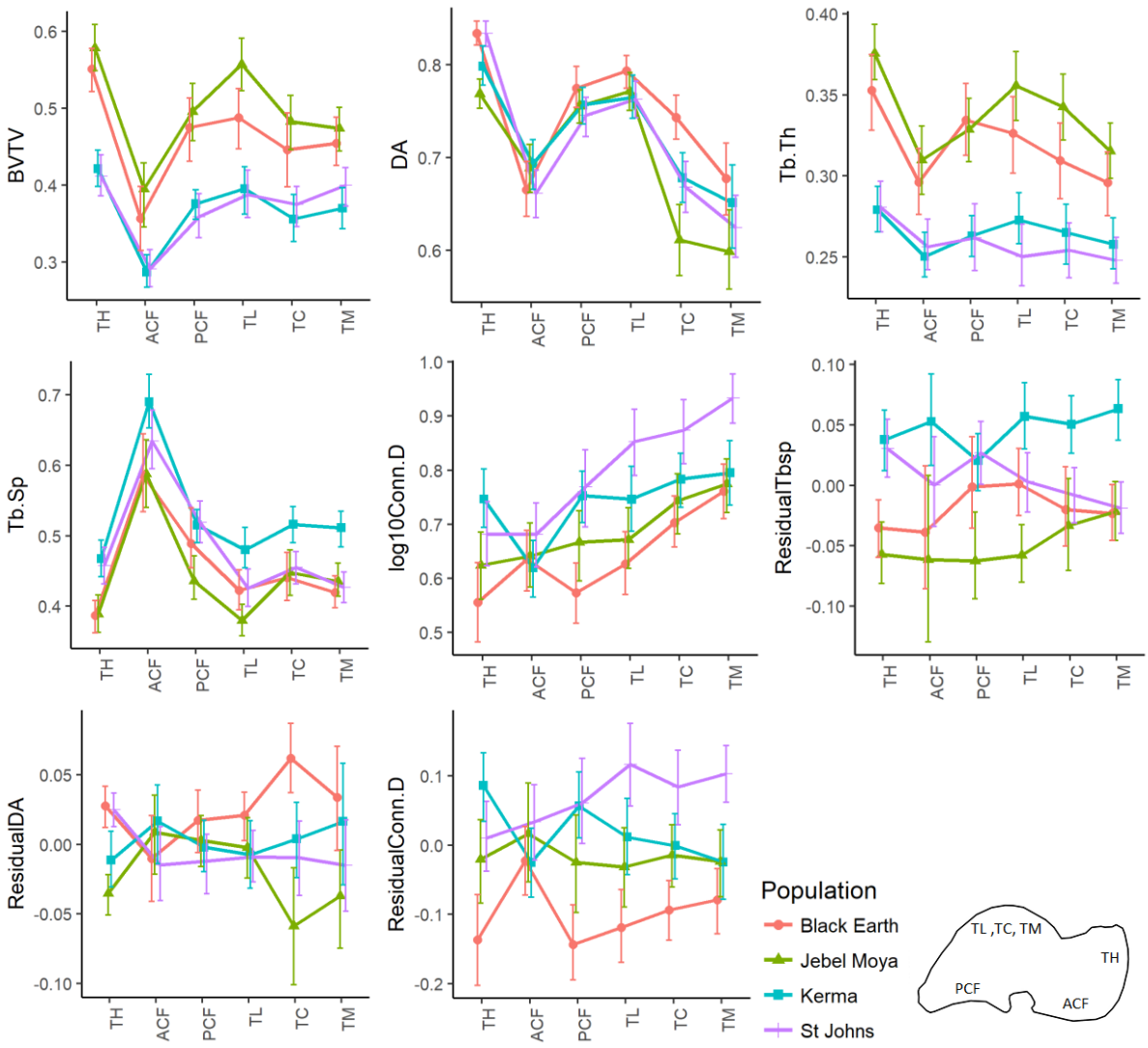

Figure 7.10. Mean and standard deviation of trabecular properties per population throughout the talus. Volumes of interest: talar head (TH), anterior calcaneal facet (ACF), posterior calcaneal facet (PCF), trochlea (lateral: TL, central: TC, medial: TM).

Very similar patterns in BV/TV, Tb.Th, Tb.Sp and DA are found in VOIs throughout the talus in all populations. The talar head has the highest BV/TV with the thickest struts and the most anisotropic structure in all populations. Upon these similar patterns of variation throughout the talus a signal of mobility is superimposed with mobile populations showing greater BV/TV and Tb.Th throughout the talus. There is little variation between populations in patterns of DA throughout the talus. Exceptions are Jebel Moya who have relatively low DA in the central and medial trochlea whereas Black Earth has relatively high trochlear DA compared to the other populations. The highest DA tends to be found in the talar head while the medial trochlea contains the lowest DA. Trabecular separation follows similar patterns throughout the talus in all populations. Conn.D increases from the lateral to the medial trochlea. Interestingly, there is very little inter-population variation in Conn.D in the ACF.

Principal Components Analysis – talus

Principal Components Analysis (PCA) was run on a suite of five trabecular bone properties in six VOIs of the talus resulting in 30 variables compared between 40 individuals. Biplots of PC1, PC2 and PC3 are presented in Figure 7.11 and tables are provided in Appendix 7.1. The first five principal components account for 80% of the total variance with the first two components accounting for 63%. None of the first five principal components correlated significantly with body mass or age categories.

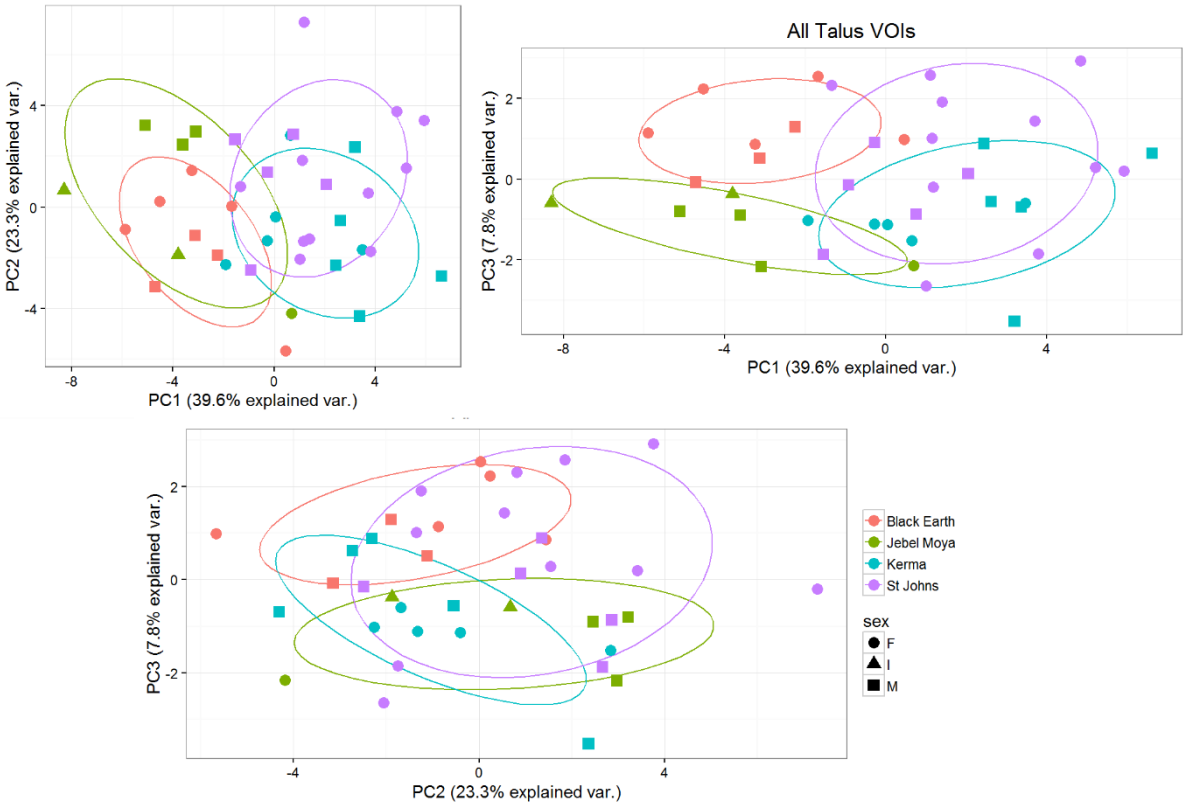

Figure 7.11. Biplots of PC1, PC2 and PC3 for a pooled sample of six talar VOIs.

PC1 correlates negatively with BV/TV and Tb.Th and to a lesser extent positively with residual Tb.Sp. Black Earth and Jebel Moya cluster on the negative side of PC1 indicating they have significantly higher BV/TV and Tb.Th and lower Tb.Sp in all VOIs compared to Kerma and St. Johns who cluster on the positive side. PC2 correlates negatively with residual Tb.Sp and positively with residual Conn.D but no significant group differences were found in PC2. PC3 correlates positively with DA in all but the ACF VOI. The mobile Black Earth cluster significantly higher on PC3 compared to Kerma and Jebel Moya. No significant pairwise comparisons were found between populations in PC4 and PC5.

The results from the talus resemble those found in the calcaneus and the first metatarsal. PC1 separates populations based on trabecular variables that are most strongly related to loading magnitude (high BV/TV with associated high Tb.Th and low Tb.Sp). This results in two clusters based on inferred mobility levels with the mobile Black Earth and Jebel Moya significantly different from Kerma and St. Johns. PC2 and PC3 are related more to morphological variation but do not indicate an increase in

structural rigidity as they are uncorrelated to BV/TV. While PC2 accounted for 23.3% of total variance, no significant population differences were found. PC3 separates Black Earth from the other populations based on their overall more anisotropic trabecular structure. Based on PC1 and PC3 the populations can be very successfully separated, with the more robust and mobile populations clustering on the negative end of PC1 and subsequently separating the mobile populations based on more anisotropic structures in the Black Earth sample on PC3.

PCA was performed using combinations of DA and BV/TV from all talar VOIs (Figure 7.12). These variables were chosen because they are the two mechanically most relevant variables (Maquer et al., 2015), and reduces the N:p ratio. PC1 correlates negatively with BV/TV while PC2 correlates positively with DA. Jebel Moya and Black Earth cluster significantly lower on PC1 compared to St. Johns and Kerma while the Black Earth fall significantly higher on PC2 than all other populations. These results show that the mobile Black Earth and Jebel Moya have significantly more robust trabecular structures, and that the Black Earth samle has more anisotropic trabecular structures throughout the talus.

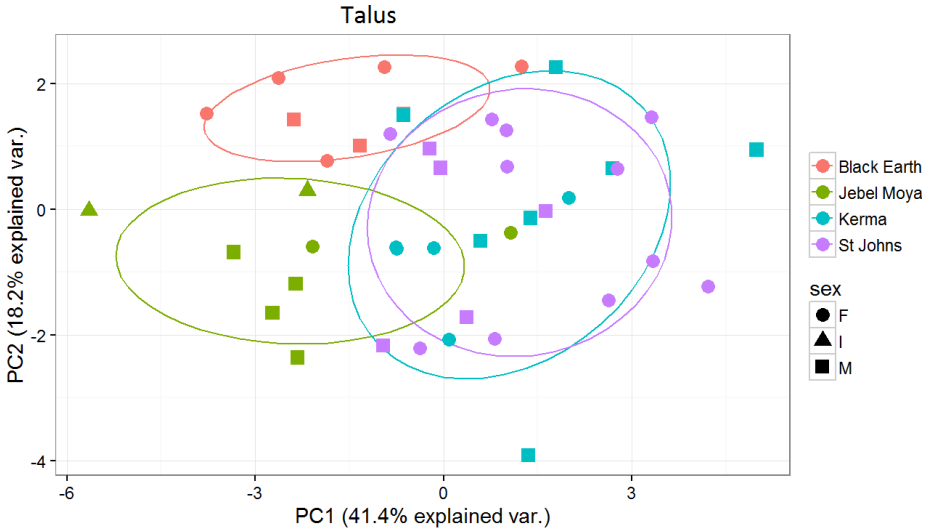

Figure 7.12. PCA of combinations of DA and BV/TV in six talar VOIs.

Principal components analysis of individual VOIs

Principal components analysis was run for each individual VOI. This results in larger ratio of variables (5 for each VOI) to individuals (maximum N=67 in CT, and minimum N=47 in HP). The first two principal components are plotted for every VOI in figures 7.13 to 7.15. One-way ANOVAs and post-hoc tests of PC1 to PC5 are summarised in tables 7.5 and 7.6, and Appendix 7.3. Principal component scores per variable are listed in Appendix 7.3. Similar results are found across most VOIs. Principal components 1 to 3 account for over 94-98% of total variance in all VOIs. The PCA's performed on individual VOIs produce similar results to the combined VOI PCA's performed earlier.

In all VOIs PC1 accounts for roughly 50% of total variance and correlates most strongly with BV/TV, Tb.Th, and to a lesser extent Tb.Sp. The only exception is BP where PC1 correlates strongly with

Tb.Sp and Conn.D while PC2 correlates with BV/TV and Tb.Th. In all but BP the populations cluster significantly on PC1 where the mobile populations associated with greater BV/TV and Tb.Th, and lower Tb.Sp. Significant differences between both the mobile Jebel Moya and Black Earth, and both the sedentary Kerma and St. Johns are found in 11 out of 17 VOIs. In the remaining VOIs significant differences were found but not between all mobile and sedentary populations.

PC2 accounts for roughly 30-38% of total variance and significant differences are found between populations in all but the AT, ACF, and PCF VOIs. PC2 correlates with consistently strong with Conn.D, and receives contributions from DA, Tb.Sp, and Tb.Th depending on the VOI. No clustering is found in PC2 based on mobility levels. Instead clusters form in 10 out of 17 VOIs with Kerma and Black Earth on one side and Jebel Moya and St. Johns on the other. These clusters form because of relatively high DA and low Conn.D in Kerma and Black Earth compared to St. Johns and Jebel Moya after the variance that is related to BV/TV is removed by PC1.

PC3 accounts for roughly 10-20% of total variance and significant differences are found in AT, PL, HD, TC. In the majority of VOIs DA correlates most strongly with PC3. Black Earth falls significantly lower compared to St. Johns in the AT as a result of their more isotropic structure. In PL Black Earth falls significantly lower on PC3 than all other populations, indicating they have significantly more isotropic trabeculae. In the TC the Black Earth sample falls significantly higher on PC3 compared to Jebel Moya and Kerma, and St. Johns fall significantly higher than Jebel Moya, indicating their trabeculae are more anisotropic.

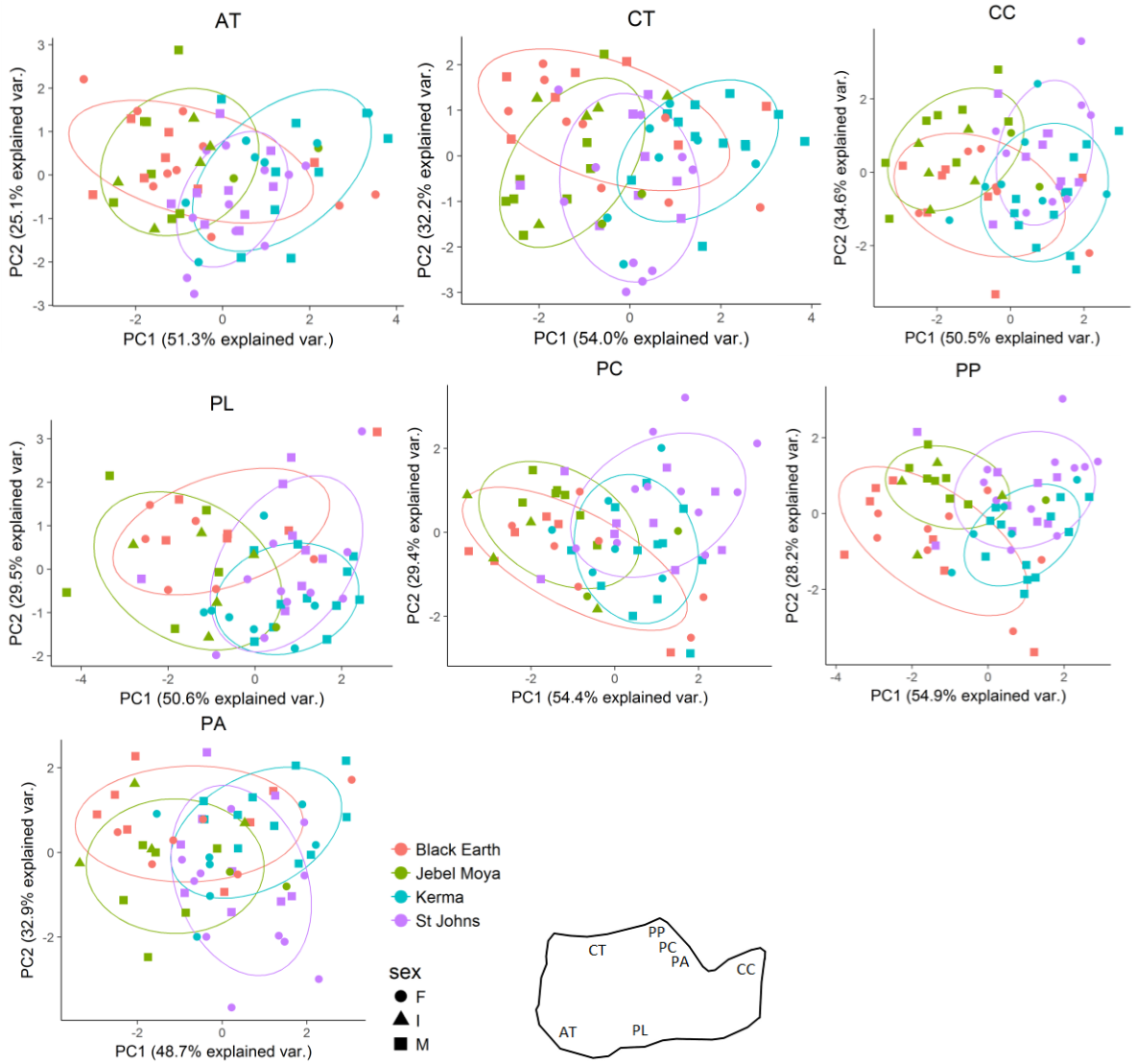

Figure 7.13. Biplot of principal components 1 and 2 of the calcaneal VOIs. Achilles tendon (AT), calcaneal tuber (CT), plantar ligaments (PL), posterior talar facet (PP: posterior, PC: central, PA: anterior), calcaneocuboid (CC).

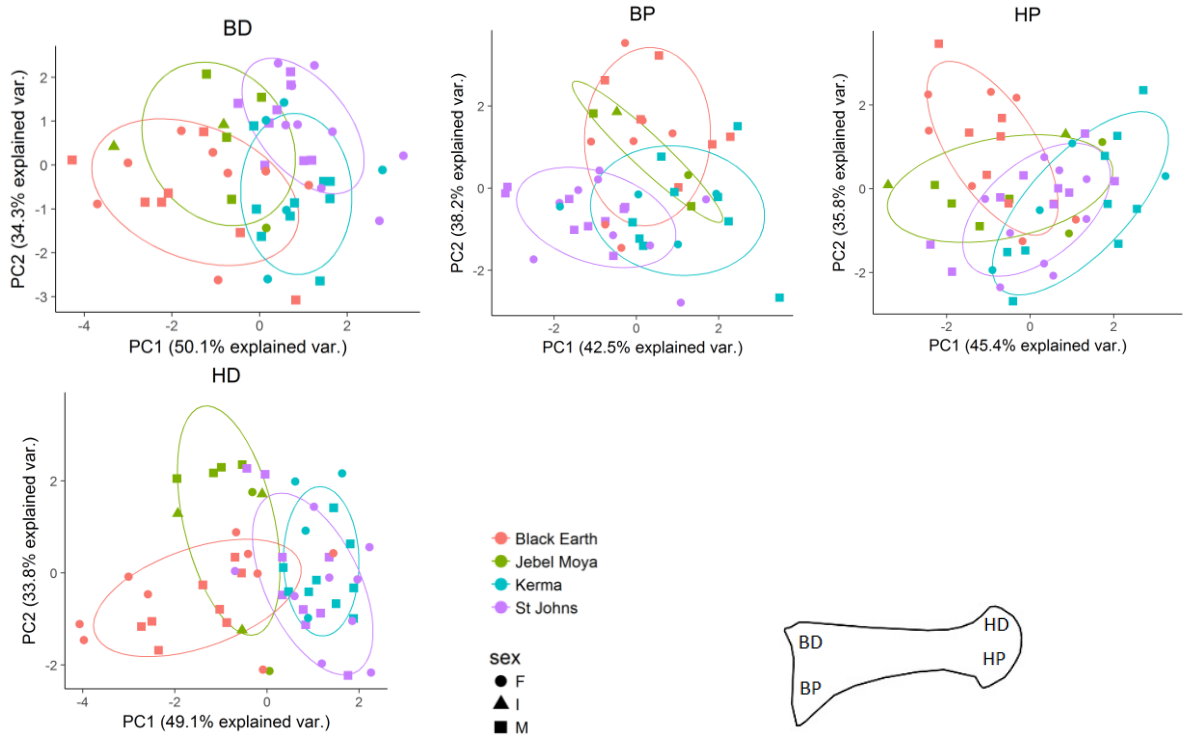

Figure 7.14. Biplot of principal components 1 and 2 of the MT1 VOIs. Dorsal base (BD), plantar base (BP), dorsal head (HD), plantar head (HP), talar head (TH).

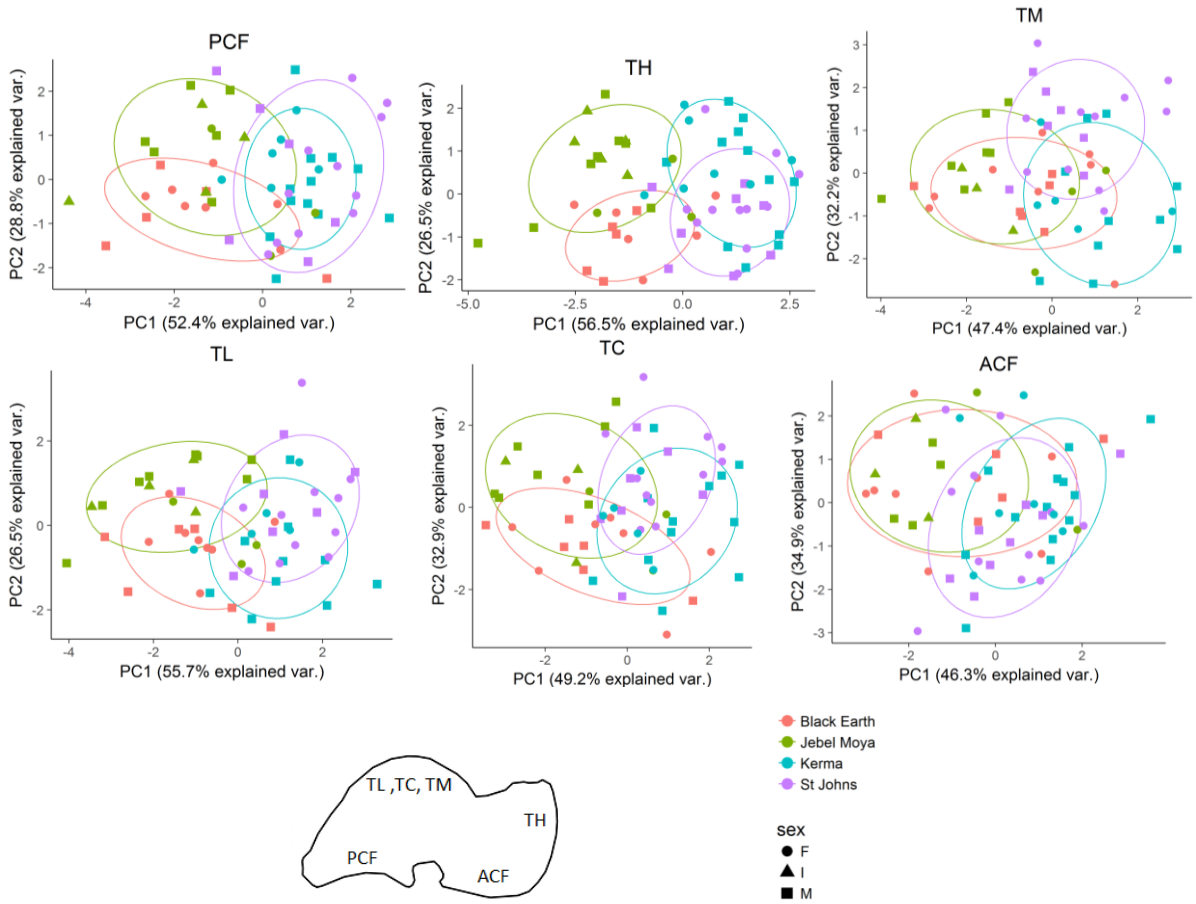

Figure 7.15. Biplot of principal components 1 and 2 of the talar VOIs. Talar head (TH), anterior calcaneal facet (ACF), posterior calcaneal facet (PCF), trochlea (lateral: TL, central: TC, medial: TM).

Table 7.5. ANOVA and significant pairwise post-hoc comparisons between populations in PC1. Populations are abbreviated, and colour coded to aid interpretation: Black Earth (BE), Jebel Moya (JM), Kerma (K), St. Johns (SJ). Achilles tendon (AT), calcaneal tuber (CT), plantar ligaments (PL), posterior talar facet (PP: posterior, PC: central, PA: anterior), calcaneocuboid (CC), dorsal base (BD), plantar base (BP), dorsal head (HD), plantar head (HP), talar head (TH), anterior calcaneal facet (ACF), posterior calcaneal facet (PCF), trochlea (lateral: TL, central: TC, medial: TM).

PC1					
	ANOVA				
VOI	**Levene P**	**F**	**df**	**p**	**Sig. Post-hoc**
AT	.133	9.63	3, 63	**.000**	K > BE, JM
CC	.417	17.169	3, 60	**.000**	BE, JM < SJ, K
CT	.030	13.105	3, 64	**.000**	K > BE, JM, SJ & SJ> JM
PA	.226	7.089	3, 56	**.000**	BE < K & JM < K, SJ
PC	.246	11.105	3, 60	**.000**	BE, JM < K, SJ
PP	.304	13.723	3, 55	**.000**	BE, JM < K, SJ
PL	3.99	9.674	3, 53	**.000**	BE, JM < K, SJ
BD	.044	16.061	3, 46	**.000**	BE, JM < K, SJ
BP	.786	6.713	3, 44	**.001**	SJ > BE, K
HD	.001	25.944	3, 53	**.000**	BE, JM < K, SJ
HP	.110	5.867	3, 46	**.002**	K < BE, JM
ACF	.163	6.591	3, 50	**.001**	K > BE, JM
PCF	.601	13.335	3, 48	**.000**	BE, JM < K, SJ
TH	.942	32.183	3, 54	**.000**	BE, JM > K, SJ
TL	.176	16.655	3, 51	**.000**	BE, JM < K, SJ
TC	.736	10.545	3, 51	**.000**	BE, JM < K, SJ
TM	.721	9.822	3, 49	**.000**	K<BE,JM & SJ<JM

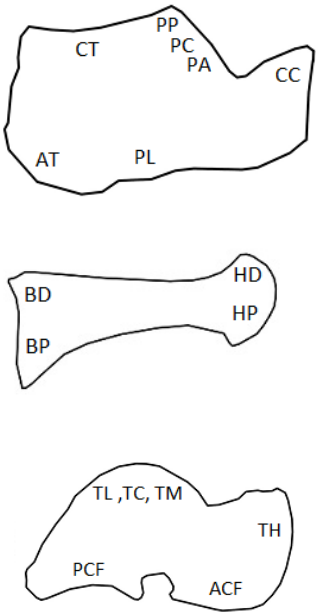

Table 7.6. ANOVA and significant post-hoc comparisons between populations for PC2 and PC3. Populations are abbreviated and colour coded to aid interpretation: Black Earth (BE), Jebel Moya (JM), Kerma (K), St. Johns (SJ). Achilles tendon (AT), calcaneal tuber (CT), plantar ligaments (PL), posterior talar facet (PP: posterior, PC: central, PA: anterior), calcaneocuboid (CC), dorsal base (BD), plantar base (BP), dorsal head (HD), plantar head (HP), talar head (TH), anterior calcaneal facet (ACF), posterior calcaneal facet (PCF), trochlea (lateral: TL, central: TC, medial: TM).

PC2						**PC3**				
	ANOVA					**ANOVA**				
VOI	**Levene P**	**F**	**df**	**p**	**Sig. Post-hoc**	**Levene P**	**F**	**df**	**p**	**Sig. Post-hoc**
AT	.434	2.665	3, 63	.055		.075	2.733	3, 63	.051	BE < SJ
CC	.873	4.917	3, 60	**.004**	JM > BE, K SJ > K	.596	.390	3, 60	.761	
CT	.342	4.705	3, 64	**.005**	BE > SJ	.216	.092	3, 64	.964	
PA	.312	4.099	3, 56	**.011**	BE > SJ	.007	3.338	3, 56	**.026**	
PC	.956	4.446	3, 60	**.007**	SJ > BE, K	.431	1.461	3, 60	.234	
PP	.415	7.616	3, 55	**.000**	BE > JM, SJ JM < BE, K SJ < K	.249	.345	3, 55	.793	
PL	.293	4.838	3, 53	**.005**	BE > K	.966	6.760	3, 53	**.001**	BE < JM, K, SJ
BD	.981	7.040	3, 46	**.001**	SJ < BE, K	.222	.941	3, 46	.429	
BP	.545	10.140	3, 44	**.000**	BE < K, SJ	.201	.303	3, 44	.823	
HD	.280	4.277	3, 53	**.009**	JM > BE, SJ	.408	3.261	3, 53	**.028**	
HP	.152	3.952	3, 46	**.014**	BE < SJ	.035	.189	3, 46	.903	
ACF	.655	1.777	3, 50	.164		.155	.514	3, 50	.674	
PCF	.018	2.042	3, 48	.120		.282	.931	3, 48	.433	
TH	.559	7.769	3, 54	**.000**	BE > JM, K SJ > JM	.973	1.410	3, 54	.250	
TL	.925	5.649	3, 51	**.002**	JM < BE, K SJ < BE, K	.469	.884	3, 51	.456	
TC	.806	4.668	3, 51	**.006**	BE < JM, SJ	.414	7.188	3, 51	**.000**	BE > JM, K SJ > JM
TM	.909	8.056	3, 49	**.000**	SJ > BE, K	.828	2.378	3, 49	.081	

Comparisons between listwise and pairwise ANOVA

The pairwise ANOVA does not exclude individuals when values are missing, resulting in greater sample sizes. The pairwise ANOVA tables and figures are provided in Appendix 7.2. A summary of significant results in pairwise and listwise ANOVA's is provided in Table 7.7.

Significant outcomes of pairwise and listwise ANOVA's are identical in 52% of cases and only marginally different in most others. Marginal differences between the two approaches are often

because a result is just significant in one and just not significant in the other. Overall, pairwise comparisons yield greater numbers of statistically significant differences between populations. Similar patterns of significant differences are also found between VOIs indicating that this is likely a reflection of true trends of differences between populations. The greater number of statistically significant differences in the pairwise comparisons are therefore unlikely to be due to differences in sample composition and most likely a result of greater sample sizes for each VOI. Using pairwise and listwise ANOVA produces similar significant outcomes and would lead to the same interpretation of results. Therefore, using either method does not bias the interpretations of the data.

Table 7.7. Comparison between significant ANOVA results from listwise and pairwise analyses. Identical results are shown in grey.

	BV/TV		Tb.Th		Tb.Sp		Res. Tb.Sp		Conn.D		Res. Conn.D		DA		Res. DA	
	Listwise	Pairwise	Listwise	Pairwise	Listwise	Pairwise	Listwise	Pairwise	Listwise	Pairwise	Listwise	Pairwise	Listwise	Pairwise	Listwise	Pairwise
AT	B>K,S J>K	B>K J> K,S	B>K,S J>K,S	B>K,S J>K,S	K>B,J,S	K>B,J,S	K>B,J,S	K>B,J,S						S>B		S>B
CC	B>K,S J>K,S	B>K,S J>K,S	B>K,S J>K,S	B>K,S J>K,S	K>B,J S>J	K>B,J S>J	K>B,J S>J	K>B,J S>J B>J	S>B	S>B	S>B	S>B				
CT	B>K,S J>K,S	B>K J> K,S	B>K,S J>K,S	B>K,S	K>B,J	K>B,J,S	K>B,J,S	K>B,J,S	J>K	J>K S>K	J>K S>K			K>J,S		K>J,S
PA	B>K,S J>K	B>K J> K,S	B>K,S J>K,S	B>K,S J>K,S	K>B	K>J,S	K>B,J	K>J,S		S>K	S>B	S>B,K				
PC	B>K,S J>K,S	B>K,S J>K,S	B>K,S J>K,S	B>K J>K,S					S>B,J	S>B,J	S>B,J	S>B,J,K		B>J,S	B>S	B>J,S
PP	B>K,S J>K,S	B>K,S J>K,S	B>K,S J>K,S	B>K,S J>K,S	K>S	K>J	K>J	K>J	S>B	S>B,J,K K>B	S>B,J,K K>B	S>B,J,K K>B		B>J,S	B>S	B>J,S
PL	B>K J>K,S	B>K,S J>K,S	B>K,S J>K,S	B>K,S J>K,S	S>J	K>J S>J	K>J S>J	K>J S>J			J>B	J>B	S>B	S>B	S>B	S>B
BD	B>K	B>K,S J>K,S	B>S	B>K,S J>K,S	K>B	K>B,J	K>B	K>B,J	S>B,J	S>B	S>B,J		B>S K>S	B>S K>S	B>S K>S	
BP	B>K	B>K	B>S J>S	B> K,S J>S	K>S	K>S	K>S	K>S	S>B,J,K	S>B,J,K	S>B,K	S>B,K	B>S J>S	B>S	B>S	B>S
HD	B>K,S J>K,S	B>K,S J>K,S	B>K,S J>K	B>K,S J>K,S	S>B	S>B,J		S>B,J		K>B	K>B	J>B K>B		B>J K>J		B>J K>J
HP	B>K J>K	B>K,S J>K	B>K J>K	B>K,S												
ACF	J>K,S	B>K,S J>K,S	J>K,S	B>K,S J>K,S		K>B	K>B,J	K>B,J								
PCF	B>K,S J>K,S	B>K,S J>K,S	B>K,S J>K,S	B>K,S J>K,S	S>J	K>J,S S>J	K>J S>J	K>J S>J	K>B S>B	K>B S>B	K>B S>B	K>B S>B				
TH	B>K,S J>K,S	B>K,S J>K,S	B>K,S J>K,S	B>K,S J>K,S		K>B,J S>B,J	K>J	K>B,J S>B,J	K>B S>B	K>B	K>B S>B	K>B S>B	B>J S>J	B>J S>J,K	B>J S>J	B>J,K S>J,K
TL	B>K,S J>K,S	B>K,S J>K,S	B>S J>K,S	B>K,S J>K,S	K>J	K>B,J,S S>J	K>J	B>J K>J,S S>J	S>B,J	S>B,J	K>B S>B	K>B S>B,J				
TC	B>K,S J>K,S	B>K J>K,S	B>S J>K,S	B>K,S J>K,S	K>B,S	K>B,J,S	K>B,S	K>B,J,S	S>B,J,K	S>B,J	S>B,K	S>B	B>J,S	B>J,K,S K>J	B>J	B>J,S
TM	J>K	B>K J>K,S	J>K,S	B>S J> K,S	K>B,J,S	K>B,J,S	K>B,J,S	K>B,J,S	S>B,J,K	S>B,J,K	S>B,K	S>B,J,K	B>J			

Patterns of variation in males and females

Plots of mean trabecular properties in VOIs throughout the foot in males and females are presented in Appendix 7.4. Among males, Kerma have the lowest mean BV/TV and Tb.Th, and the highest Tb.Sp, while Black Earth and Jebel Moya show the opposite pattern. After correcting for body mass, Kerma have the highest residual Tb.Sp, Jebel Moya have the lowest mean residual Tb.Sp, and Black Earth and St. Johns fall in between. Conn.D is highly variable throughout the foot but in general Black Earth have the lowest mean Conn.D and residual Conn.D. Anisotropy varies between VOIs, but Jebel Moya tend to have low average DA and Black Earth tend to have high DA and residual DA.

Patterns throughout the foot in the females are similar to the males, but the relationships between populations differ. The Black Earth females have the highest mean BV/TV and the thickest trabeculae. Jebel Moya have low BV/TV in the calcaneus, medium BV/TV in the first metatarsal, and high BV/TV in the talus. This disparity between bones in Jebel Moya results from the small female sample size and missing VOIs. The Kerma females have medium to high BV/TV and the lowest BV/TV is found in the St. Johns females. Similar between population relationships are found in Tb.Th. In contrast to the males, the female Jebel Moya show a medium level of DA. The Black Earth individuals have the lowest Tb.Sp before and after correcting for body mass. The Black Earth have the lowest Conn.D overall and Jebel Moya has low Conn.D in the first metatarsal and talus. St. Johns and Kerma have relatively high Conn.D.

Discussion

Significant between-population variation in trabecular properties was found using univariate ANOVA and multivariate PCA. The mobile Jebel Moya and Black Earth have greater BV/TV the sedentary Kerma and St. Johns. This greater BV/TV is associated with thicker, less widely spaced, and less interconnected trabecular structures than the sedentary Kerma and St. Johns populations. Trabecular bone stiffness is largely determined by BV/TV (Rincón-Kohli and Zysset, 2009; Maquer et al., 2015). Jebel Moya and Black Earth tend to have significantly less interconnected trabecular structures, particularly in the first metatarsal and the talus. The mobile Jebel Moya and Black Earth also show significantly more close-packed structures than the sedentary populations, indicated by lower Tb.Sp before and after body mass corrections. There were no consistent between-group differences in the degree of anisotropy. However, DA was significantly higher in Black Earth in several VOIs throughout the three bones, while Jebel Moya tended to have somewhat lower average DA. In all principal components analysis the largest variance was accounted for by BV/TV and variables correlated to BV/TV, most notably Tb.Th and Tb.Sp. Most PCAs resulted in significant clustering of the mobile populations on the side of PC1 associated with greater BV/TV. Thus, the largest variance in this sample of four human populations corresponds to variation which clusters groups based on levels of mobility. These findings support the predictions based upon the assumption that variation in mechanical loading, and thus terrestrial mobility, is the main factor underlying between-population variation in trabecular bone structure.

Saers et al. (2016) studied three human groups classified as mobile, intermediate, and sedentary. They found significant differences in BV/TV between the three populations throughout the lower limb. This result suggested that trabecular bone might reflect subtle differences in mobility levels in archaeological populations. Based on archaeological data, the populations used in the current analysis could not be classified into more specific categories than relatively mobile or sedentary. The results fit the predictions in that the mobile populations have significantly higher BV/TV compared to the two sedentary populations. However, any subtle differences in mobility that could not be predicted based on the archaeological evidence, but most likely would have existed, were not found.

BV/TV can be increased by increasing trabecular thickness, number, fusing rods into plates, or a combination of the three. The number of trabeculae is represented by Conn.D which measures the number of connections per unit area. Fusing rods into plates would reduce the number of trabeculae and thus Conn.D, but keep trabecular thickness level because Tb.Th is calculated by fitting a sphere inside the bone until air is reached (Dougherty and Kunzelmann, 2007). Increasing BV/TV by thickening trabeculae is shown to be mechanically the optimal of reducing strain (Ding et al., 2002; Mittra et al., 2005; Cotter et al., 2011; Ryan and Shaw, 2013), as finite element models show lower strains in thicker struts (Doube et al., 2011). Trabeculae thicken in response to loading during ontogeny with larger animals developing thicker trabeculae (Ruimerman et al., 2005; Ryan and Krovitz, 2006; Gosman and Ketcham, 2009; Ryan and Shaw, 2013). However, a negative allometric relationship was found in interspecific analyses between body mass and trabecular thickness, indicating that as body mass increases, trabeculae increase only thicken slightly (Doube et al., 2011; Ryan and Shaw, 2013). This may result from the limited depth at which osteocytes are able to function (Lozupone and Favia, 1990; Mullender and Huiskes, 1995). Thus, the negative allometric relationship may be a compromise between mechanical and metabolic pressures. Changes in Conn.D or plate-rod geometry may be preferred in some cases, however, the factors determining the way in which BV/TV is increased are not understood.

Significant differences are found in Conn.D between different populations. Previous work has shown that with all other variables remaining equal, a change in Conn.D has no effect on bone stiffness (Maquer et al., 2015). However, Conn.D tends to be significantly lower in mobile groups compared to the sedentary groups, particularly the St. Johns, although this result is not found in all VOIs. Presumably the reduction in Conn.D is a side effect of the increased BV/TV in the mobile groups. The thicker rods in the mobile groups may fuse into plates, thereby reducing connectivity per unit volume. The hypothesis is not tested here because recent work has shown that current methods of quantifying rodness and plateness are not suitable for trabecular structures (Salmon et al., 2015). A recently proposed method of quantifying plate-rod geometry called the ellipsoid factor (Doube, 2015) was not used as calculation time for this variable was too high for the large sample used in this study. However, locations throughout the skeleton that exhibit the largest levels of mechanical loading also tend to have plate-like trabecular structures (see qualitative descriptions of trabecular structure in

Chapter 2). The formation of plates may be a consequence of the maximum thickness of trabeculae. The significant differences in trabecular spacing between mobile and sedentary groups are also presumably a side-effect of the increase in trabecular thickness which reduces the average space between trabeculae. Relationships were found in this thesis between Conn.D and bone dimensions, body mass, sex, age, and terrestrial mobility. Thus, Conn.D is a complex variable that should be interpreted with care.

Result reported in Chapter 6 show there are significant differences in trabecular structure between individuals belonging to different age categories. Because of the large number of individuals who could not be aged, it was not feasible to include age category as a covariate in the models used in this chapter. However, age category could be inferred for most of the individuals from the mobile Black Earth and sedentary St. Johns samples. Differences were assessed between Black Earth and St. Johns while controlling for both body mass and age category and reported in Appendix 7.5. After correcting for the effects of age and body mass the mobile Black Earth still show more robust trabecular structures consisting of significantly greater BV/TV and Tb.Th, and relatively low Conn.D. Age category was found not to significantly affect the analysis when included as a covariate. This finding provides greater confidence in the results obtained from the analyses in this current chapter where age category was not included as a covariate.

Using multivariate principal components analysis, groups were separated on PC1 with two clusters based on variables strongly correlated to mechanical loading. In all PCAs, PC1 correlated strongly with BV/TV, Tb.Th, and Tb.Sp, and sometimes with Conn.D. PC1 is interpreted as the variation related to bone stiffness (BV/TV), and the contributions of other variables to BV/TV. PC2 to 5 do not separate populations based on inferred terrestrial mobility levels and thus may be regarded as reflecting variance in trabecular structure unrelated to BV/TV and thus unrelated to loading. If the variance explained by PC2 to 5 is unrelated to levels of terrestrial mobility, how should significant population differences in these components be interpreted? In most VOIs as well as in the pooled VOI PCA's, PC2 correlated with the variance in Tb.Sp, Conn.D and DA that was not correlated to BV/TV. Clusters form in 10 out of 17 individual VOIs and in the pooled PCA's with Kerma and Black Earth on one side and Jebel Moya and St. Johns on the other. Thus, these clusters are formed by combinations of mobile and sedentary populations as well as populations from different environments. Neither differences in climate, activity, or genetic distance explain the clusters on PC2. The clustering is driven by high DA and low Conn.D, which in Chapter 6 was shown to be associated with old age. Regressions between age category and PC2 are significant in 11 out of 17 VOIs, but not when VOIs were pooled for each bone (Table 7.8). When regressions were significant Black Earth and Kerma clustered on one side while Jebel Moya and St. Johns clustered on the other side. Table 7.8. suggests that between 0 and 30% of PC2 can be explained by age in different VOIs. The number of individuals with known age categories differed per VOI, and differences in sample composition and size likely

underlie variation in significance and size of coefficients of determination between VOIs presented in Table 7.8.

Table 7.8. Regressions between age and PC2 in different PCAs. + indicates a significant positive slope, - indicates a significant negative slope. Achilles tendon (AT), calcaneal tuber (CT), plantar ligaments (PL), posterior talar facet (PP: posterior, PC: central, PA: anterior), calcaneocuboid (CC), dorsal base (BD), plantar base (BP), dorsal head (HD), plantar head (HP), talar head (TH), anterior calcaneal facet (ACF), posterior calcaneal facet (PCF), trochlea (lateral: TL, central: TC, medial: TM).

Bone	**VOI**	**N**	**R^2**	***P***	**slope**
Calcaneus	pooled	**27**	**.15**	**.048**	**-**
	AT	41	.04	.240	
	CC	**37**	**.30**	**<.001**	**-**
	CT	40	.00	.795	
	PA	**36**	**.18**	**.009**	**+**
	PC	**39**	**.31**	**<.001**	**-**
	PP	**37**	**.12**	**.032**	**+**
	PL	34	.04	.233	
MT1	pooled	29	.05	.243	
	BD	**33**	**.12**	**.045**	**+**
	BP	35	.00	.922	
	HD	39	.08	.080	-
	HP	33	.06	.174	
Talus	pooled	**25**	**.30**	**.004**	**-**
	ACF	35	.11	.056	+
	PCF	**32**	**.20**	**.011**	**-**
	TH	**33**	**.18**	**.013**	**+**
	TC	**35**	**.12**	**.040**	**-**
	TM	34	.11	.057	-
	TL	**33**	**.24**	**.003**	**+**

In most VOIs PC3 correlates strongly to DA as well as Tb.Sp and Conn.D. The contributions of these variables differ between VOIs and thus reflect local rather than systemic variation. Kerma and Jebel Moya tend to cluster on PC3 in individual and well as pooled PCA's, although the differences are usually not significant. This clustering results largely from between-population variation in DA with lower DA in the North African populations. However, a causative mechanism behind the observed clustering on PC3 is not obvious. The clustering of North African populations on PC3 indicates a potential genetic or environmental effect. However, a larger and more diverse sample of human populations would be required to test this hypothesis.

In the univariate analyses BV/TV and Tb.Th show very similar patterns across VOIs in all populations, with a signal of terrestrial mobility superimposed upon it. The regions that were predicted to receive the greatest levels of mechanical loading during gait were found to contain highest BV/TV. Tb.Sp also shows very consistent patterns throughout the foot, but the differences between populations are less strong. Conn.D, and DA also show similar patterns throughout the foot between populations, but there was greater local variation between VOIs and populations. As predicted, Conn.D and Tb.Sp were in general lower in the more mobile populations. However, the between population differences were less strong in these variables than in BV/TV and Tb.Th.

Local variation in DA in certain VOIs merits some closer inspection. It was predicted that greater terrestrial mobility should not necessarily lead to predictable group differences in anisotropy. Significantly greater DA was found in the Black Earth population in the calcaneus, talus, and first metatarsal. The fact that this is observed in VOIs throughout the different foot bones indicates that it is unlikely that this is a result of VOI placement errors. Significant sexual dimorphism was found in DA in the previous chapter with males having greater DA in all significant cases. However, fewer significant differences were found after accounting for body mass. The effects of body mass can be excluded because the Black Earth have significantly greater residual DA as well as raw DA, despite having low body mass. Saers et al. (2016) did not find exceptionally high DA in the lower limbs of the Black Earth population relative to Kerma or Norris Farms, indicating that this may be a phenomenon specific to the foot. Experimental work where mobility levels were manipulated have not shown adaptation in the degree of fabric anisotropy to differential levels of loading (Barak et al., 2011). Potential factors which may underlie this significant variation in trabecular structure are differences in terrain, subsistence behaviour, footwear, genetics, or external bone morphology affecting internal structure.

Variation in anisotropy is usually interpreted as resulting from variation in loading direction with high anisotropy indicating less variation in loading direction (Barak et al., 2013; Saers et al., 2016). If the observed variation in DA between populations is related to loading directionality, then St. Johns and Jebel Moya should be subjected to greater variation in loading of the foot. Recent research has demonstrated significant differences in gait biomechanics between habitually shod and unshod individuals, most notably during running (Lieberman et al., 2010; Hatala et al., 2013). In an analysis comparing the gait of habitually shod versus unshod endurance runners, Lieberman et al. (2010) found that shod runners most frequently use rear foot strikes, whereas habitually unshod runners often use a forefoot strike or midfoot strike when running. The reason that shod individuals use heel strikes is that they have shoes that are designed to make heel strikes more comfortable. They report that rear-foot strike causes a large transient force in shod runners and even larger in the unshod runners. Forefoot strike on the other hand produces no transient, resulting in a smoother application of force. They found that at similar speeds, the magnitudes of peak vertical force during the impact period are three times lower in the barefoot forefoot strikers than the shod rear-foot strikers. These significant differences between shod and unshod locomotion may result in significantly different stress distributions throughout the foot during gait, and in turn affect trabecular architecture. In a study comparing the trabecular architecture of the first and second metatarsal heads between chimpanzees and humans Griffin and colleagues (2010 b) used a human sample consisting of both shod and unshod individuals. The authors tested for differences between the groups but found no significant differences in BV/TV and DA. However, sample sizes were small (n shod = 3, n unshod = 10). The presence or type of footwear used by populations included in this study are not known. However, Willems et al. (2017) demonstrate that walking using traditional South Indian Kolhapuri footwear only subtly alters foot

biomechanics compared to unshod individuals. They note that the footwear offers protection from the substrate but walking resembles barefoot gait. Therefore, the presence of traditional footwear may not be very different from unshod gait. However, one might still expect larger differences in gait between different types of footwear. Kolhapuri footwear is a type of sandal and gait might be more different in populations habitually using slippers instead. An investigation of archaeological populations with known footwear would be an interesting avenue of research. High resolution pQCT analysis comparing shod and barefoot runners would be an ideal test of the influence of footwear on trabecular bone structure.

Terrain and substrate affect foot placement, loading, gait, and energetics of locomotion (Voloshina and Ferris, 2013). Populations inhabiting rougher terrain tend to have more robust lower limbs relative to populations inhabiting flatter regions (Ruff, 1999; Pearson et al., 2008; Sparacello and Marchi, 2008; Higgins, 2014). Movement across sloped terrain increases anteroposterior stress on the lower limb while irregular terrain increases mediolateral bending throughout the lower limb (Higgins, 2014). In an analysis of flat, mountain, and mixed terrain species, Higgins (2014) found significantly increased cross-sectional strength in the tibiae of non-flat terrain species. Uneven terrain affects foot posture during gait and presumably affects unshod individuals to greater extent than shod individuals. Thus, populations inhabiting uneven terrain would be expected to experience greater variation in loading direction due to differences in foot posture, with this effect being greater in unshod versus shod populations. Greater variation in loading directions would be expected to result in more isotropic structures. Similar variation may be expected as a result of terrain moisture and texture (e.g. sandy versus rocky desert). Differences in subsistence behaviour may affect placement of the feet in similar ways as terrain would. Little variation in terrain ruggedness is present in populations included in this study. Examining trabecular structure in the lower limb and foot of animals or human populations inhabiting different terrain would be an interesting avenue for future research.

Genetics may affect the anisotropy of a trabecular structure through variation in growth plate function or placement (Lovejoy et al., 2003). Another possibility might be that variation in external bone shape affects the way in which forces are distributed through a bone. Currently there is no literature on this topic. Partial Pearson correlations correcting for body mass show no significant correlations between DA and measures of bone shape (PTF shape, tuber shape, MT1 head and base shape, trochlea shape, PCF shape, talar head shape). However, these are very crude ratios of limited aspects of variation in bone shape. Finite element analysis could be performed in the future to model stress distributions throughout differently shaped bones to assess the effects of external shape on internal trabecular morphology. It may also be worth combining geometric morphometrics of external bone shape with the analysis of trabecular structure to further elucidate the integration of external morphology and internal trabecular architecture.

The dietary shift towards cultivated grains in agriculturalists is associated with reduced calcium intake in some populations (Eaton and Nelson, 1991; Heaney, 2003). Stable isotope, archaeobotanical, and

zoological data point towards a broad diet consumed by the inhabitants of Kerma, including sheep, goats, cattle, aquatic resources, legumes, and cereals (Bonnet, 1986; Thompson et al., 2008). The Black Earth foragers subsisted on a diverse diet of large and small mammals, birds, fish, and seasonally available plant resources (Jefferies and Lynch, 1983). Hutton-Macdonald (1999) reports that 5 out of 2411 Jebel Moya teeth had caries (0.2%). She showed that the Jebel Moya sample did not exhibit the high levels of dental disease which are commonly known from peoples who cultivate grains. This is interpreted as likely being indicative of a non-cultivating, non-high carbohydrate consuming population (Hutton Macdonald, 1999). Calculus was recorded in almost all dentitions of individuals from St. Johns, suggesting a diet rich in carbohydrates, presumably cereals, combined with poor oral hygiene (Cessford, 2015). In addition to the mobility differences, these dietary factors could have contributed to a reduction in bone mass in the agriculturalists compared to foragers and pastoralists. The relative contributions of the mechanical, environmental, dietary, and genetic factors to trabecular bone ontogeny are poorly understood and require further investigation (Judex et al., 2004; Wallace et al., 2012). Despite the potential effects of confounding variables, past work suggests habitual activity plays a significant role in determining adult bone stiffness (Ruff et al., 1984; Bridges, 1989; Stock and Pfeiffer, 2001; Shaw and Stock, 2009b, 2013; Ryan and Shaw, 2015; Chirchir et al., 2017; Stieglitz et al., 2017).

Conclusion

A strong relationship is reported between categories of terrestrial mobility and trabecular bone morphology in the calcaneus, talus, and first metatarsal of human populations. Patterns of variation in trabecular properties throughout the 17 volumes of interest of the foot are similar between populations, with a morphological signature of mobility superimposed upon them. Mobile populations have higher bone volume fraction with thicker, more closely packed, and less interconnected trabecular structures throughout the foot. DA shows no relationship with relative mobility level, but it is suggested that variation in DA may relate to differences in subsistence activities, terrain, footwear, or genetics. Trabecular structure does not discriminate these four populations based on genetic distance or differences in environment. The results from this chapter provides support for recent work suggesting that trabecular bone structure may be used to infer habitual behaviour in past populations (Ryan and Shaw, 2015; Saers et al., 2016; Scherf et al., 2016; Chirchir et al., 2017).

A greater understanding of intraspecific variation and adaptive constraints on trabecular bone are needed to provide a context in which to interpret fossil hominin morphology. The results from this chapter provide an initial step in this direction by providing data on trabecular bone variation in the human foot in multiple populations. Comparisons of structural variation throughout the foot should be performed with a more diverse sample of human populations and nonhuman primates, to tease out potential effects of climate, terrain, diet, and genetic distance. By carefully selecting samples, a better understanding of the range of variation among human populations and the environmental and behavioural conditions under which trabecular bone structure varies can be obtained.

Chapter 8 - Ontogeny of trabecular bone in the human calcaneus

Introduction

Fossil bones are both useful for making functional and phylogenetic inferences and challenging to interpret. Bones have various mechanical and metabolic functions and can be highly canalized as well as responsive to mechanical loading and environmental factors (Lieberman, 1997; Carter and Beaupré, 2001; Currey, 2002). Comparisons of adult bone structure can therefore be misleading when the growth and development of its features is not understood. Adult bone morphology is influenced by a combination of genetic and epigenetic factors throughout ontogeny (Carter and Beaupré, 2001). Mechanical loading is essential for normal skeletal growth, starting with prenatal muscle contractions and continuing throughout life (Carter and Beaupré, 2001; Pitsillides, 2006; Rot et al., 2014). The ability of trabecular bone to reflect habitual loading patterns has been demonstrated experimentally (Barak et al., 2011), but human trabecular bone ontogeny is not thoroughly studied (Ryan and Krovitz, 2006; Cunningham and Black, 2009; Reissis and Abel, 2012; Raichlen et al., 2015; Ryan et al., 2017). Adult trabecular bone structures are the product of structures that are established during ontogeny and modified by biological and mechanical factors during growth (Carter and Beaupré, 2001; Ryan and Krovitz, 2006; Gosman and Ketcham, 2009). The development of bipedal gait represents a natural experiment with which to test hypotheses about locomotor influences on bone development. Data on the interaction between trabecular bone growth and neuromuscular development in humans may enable assessments of hominin life history through study of juvenile fossils (Raichlen et al., 2015). In this chapter, calcaneal trabecular bone structure is quantified in a range of juveniles and interpreted in the context of gait maturation and growth.

Bone growth

The calcaneus commences ossification prenatally and is one of the few osseous foot bones at birth but one of the last bones to complete fusion at its secondary ossification centre, between 18 and 20 years of age (Scheuer and Black, 2004; Schaefer et al., 2009). This means there is a long period of morphological change in the calcaneus alongside behavioural changes in gait. Ossification occurs through a precise sequence of perichondral and endochondral ossification (Schaefer et al., 2009). At birth, the calcaneus is recognisable as a nodule with a flattened area just distal to the centre of the dorsal surface. Afterwards the bone elongates rapidly, assuming its distinctive shape (Schaefer et al., 2009). The calcaneal epiphysis at the end of the tuber appears between 9 and 12 years of age, but fusion is not completed until the end of puberty (Scheuer and Black, 2004).

Bone growth occurs via the transformation of growth plate cartilage into bone through a series of cell and matrix changes (Byers et al., 2000; Parfitt et al., 2000; Burr and Organ, 2017). The transformation from growth plate cartilage to trabecular bone is similar amongst mammals, indicating a highly regulated process (Frost and Jee, 1994 a; Byers et al., 2000). This process sets up a basic trabecular structure which is later modified through metabolic and mechanical factors. Byers and colleagues

(2000) report that BV/TV and Tb.Th increased with age while the number of trabeculae decreased from birth to adulthood in human ribs. The authors noted that trabecular structure changed most rapidly during the first year of life. Frost and Jee (1994 b) argue that the effects of mechanical usage during this period of rapid bone growth explain many of the features observed during the ossification process. They propose a model which states that mechanical strain is the controlling mechanism for endochondral ossification, in which the underloaded elements of the dense bone structure during the first years of life are removed and bone is added in strained areas, resulting in a mechanically adapted state (Frost and Jee, 1994 b). This model correctly predicts observations of bone loss at early stages of ontogeny, and explains it as the result of the removal of redundant material based on lack of mechanical strain. Most work on trabecular bone ontogeny has been performed on a range of non-human mammal species (Nafei et al., 2000; Tanck et al., 2001; Wolschrijn and Weijs, 2004; Gorissen et al., 2016). In a study of pig vertebrae and tibiae, Tanck and colleagues (2001) found that BV/TV and anisotropy increase with age and body mass, with a time-lag between increases in bone mass and anisotropy. They argue that bone mass is added first, and subsequently refined into an efficiently oriented structure. This process was also found in two studies of human trabecular ontogeny in the tibia and femur (Ryan and Krovitz, 2006; Gosman and Ketcham, 2009). At birth, trabecular architecture in the long bone epiphyses is dense and constructed of numerous small anisotropic trabeculae. During the first year of life, BV/TV, anisotropy, and trabecular number decrease. Trabecular bone is subsequently reorganized into fewer, thicker, and more complexly organized systems of trabeculae (Ryan and Krovitz, 2006; Gosman and Ketcham, 2009). The results from studies on humans and other animals suggest a similarity in the developmental process of trabecular bone across species and anatomical sites. Primary trabecular bone is deposited in a uniform way: dense and uniformly oriented. However, these initial morphologies then appear to remodel rapidly under the influence of mechanical loading.

Ryan et al. (2015) found largely similar patterns of trabecular development in the humerus, femur and tibia until the age of 4 with significant divergence in BV/TV between the proximal humerus and the proximal femur after this age. The proximal femur obtained significantly greater BV/TV compared to the other anatomical regions. This work demonstrates that all VOIs started with high BV/TV which was lost throughout the first year of life, followed by an increase in BV/TV. Trabecular thickness and separation increase from birth until adulthood in all VOIs. Conn.D starts out very high at birth, rapidly decreases within the first year of life, and steadily decreases throughout life from 1-2 years of age (Ryan et al., 2015). Gosman (2007) found changes in relative BV/TV in the posterior tibial condyles corresponding to the development of the femoral bicondylar angle. Similarities are found between the development of trabecular and cortical bone in humans, with a rapid increase in femoral relative to humeral trabecular and cortical bone rigidity as bipedal locomotion begins to develop (Ruff, 2003; Ryan et al., 2017). This pattern contrasts with the patterns of growth found in quadrupedal baboons where the humerus and femur are relatively equal throughout development (Ruff, 2003).

While few studies of prenatal development of trabecular structure exist, they can show how bones develop in the absence of gravitational loading. An increase in BV/TV was reported between weeks 16 and 24 in human foetal vertebrae (Nuzzo et al., 2003), and in weeks 16 to 41 in the proximal femur (Salle et al., 2002). However, Reissis and Abel (2012) found no increase in BV/TV throughout foetal development in the proximal femur and humerus. The three studies on foetal trabecular development have found a steady increase in trabecular thickness during prenatal growth. McColl et al. (2006) reported that the oldest bone in foetuses contained thicker struts than more recently formed bone. No sexual dimorphism has been found in foetal trabecular bone (McColl et al., 2006; Reissis and Abel, 2012). This small set of studies suggest very similar development of trabecular structures throughout the human foetal skeleton (Reissis and Abel, 2012). Trabeculae are laid down in thin and numerous struts, and are modelled into structures consisting of thicker and less numerous trabeculae. No differences in trabecular structure are found between the humeral and femoral metaphysis in pre-ambulatory infants (Reissis and Abel, 2012; Ryan et al., 2017). The trabecular structure of the femur and humerus only diverge after the femur becomes weight-bearing during the acquisition of gait (Ryan et al., 2017).

Development of gait in human children

The gait of children differs substantially from that of adults (Levine et al., 2012). Children have a wider walking base, smaller stride lengths and lower walking speeds. The gait of young children does not include a heel strike or toe-off, and they contact the ground with a flat foot and an extended knee (Figure 8.1).

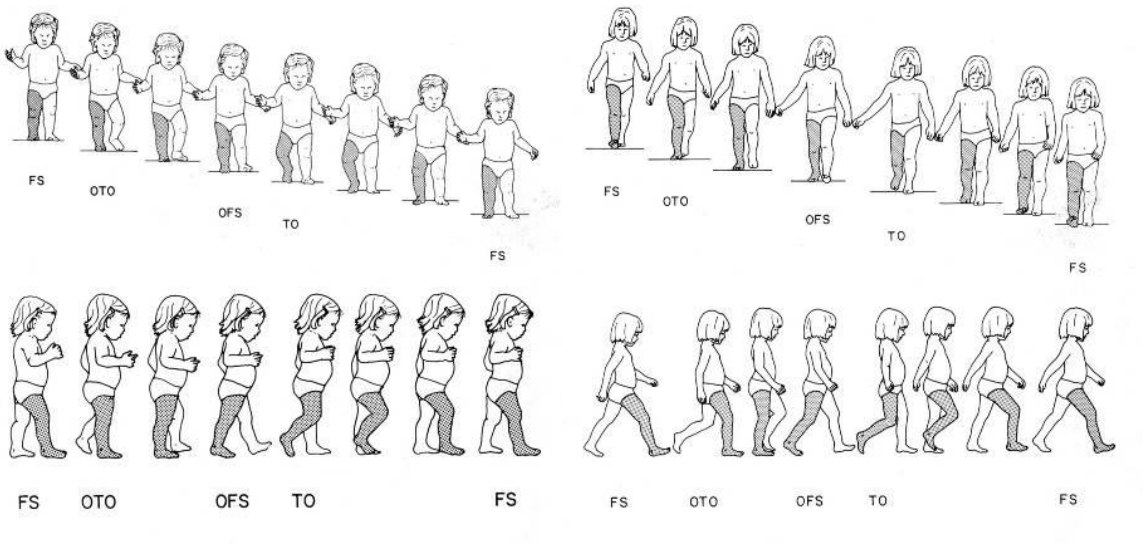

Figure 8.1. Gait in a child of 1 (left) and 4 (right) years old (from: Sutherland et al., 1988).

Independent walking starts roughly between 10 and 17 months, and at this point an infant is able to propel itself forward unassisted (Zeininger, 2013). At one year of age the tibialis anterior is too weak to dorsiflex the foot during swing, resulting in a plantigrade foot at touchdown (Rose and Gamble, 2006). One year olds are also unable to create enough torque at the ankle to propel themselves forward

into swing (Hallemans et al., 2005, 2006). Instead of a propulsive toe-off, the plantigrade foot is lifted at the end of stance. Plantigrady increases the base of support for the foot and may be an important feature in young children for balance control (Hallemans et al., 2006). The lateral-to-medial transfer of the centre of pressure characteristic of adult gait develops around 18 months of age (Bertsch et al., 2004). A true heel strike does not occur until 18-24 months on average (Zeininger, 2013). Zeininger (2013) found a significant increase in ground reaction force underneath the calcaneus in children using a heel strike compared to those who did not. By around two years of age the muscles associated with plantarflexion are sufficiently strengthened to propel the foot in a distinctive toe-off phase and most children have adopted the adult pattern of knee flexion and extension (Zeininger, 2013). The longitudinal arch begins to form as soon as walking starts, but the arch does not fully develop until the age of four to six (Bertsch et al., 2004). With increasing longitudinal arch height, peak plantar pressures on the fore- and hindfoot increase while pressure is reduced in the midfoot to adult levels between age five and six (Bertsch et al., 2004; Zeininger, 2013). By age four central nervous maturation approaches adult levels, after which gait differences between adults and juveniles come down largely to allometry (Sutherland, 1997). However, patterns of muscle activation do not fully resemble those of adults until the child reaches roughly 15 years of age (Sutherland et al., 1980; Sutherland, 1997). The walking base is about 70% of hip width at the age of one, it reaches about 45% at age three to four, and reaches adult proportions of around 30% around age seven (Levine et al., 2012).

Linking the development of gait to trabecular structure

Some authors have argued that trabecular morphology is highly canalized throughout ontogeny based on the placement of mesenchymal cells (Lovejoy et al., 2003; Cunningham and Black, 2009; Gorissen et al., 2016). Some support for this claim is provided by Skedros and colleagues (Skedros et al., 2004, 2007) who found adult tensile bands present in utero in the calcaneal tuber of mule deer. However, prenatal muscle contractions are essential for healthy bone development (Carter and Beaupré, 2001; Pitsillides, 2006; Rot et al., 2014). As deer's muscles must also be strong enough for locomotion at birth, therefore, muscle contractions in utero may be a plausible alternative explanation for the adult morphology in foetal deer. Strong canalization of adult trabecular morphology does not hold up against the body of literature demonstrating trabecular bone's adaptability to mechanical loading, at least in the appendicular skeleton (Tardieu, 1999; Pontzer et al., 2006; Tardieu et al., 2006, 2015; Chang et al., 2008; Barak et al., 2011; Mitchell et al., 2015; Ryan et al., 2017).

Human adult calcaneal trabecular structure consists of three distinctive systems with a triangular zone of low-density in the centre (Chapter 2). Compressive trajectories extend posteriorly and anteriorly along the superior half of the calcaneus and tensile trajectories extend along the inferior half (Giddings et al., 2000). In this chapter, trabecular bone ontogeny will be examined by sampling the three main trabecular systems in relation to maturation of gait and body mass. All muscles and ligaments have formed in utero (Carter and Beaupré 2001), but the prenatally ossified part of the calcaneus is

surrounded by relatively thick cartilage during early growth. The presence of cartilage presumably reduces stress on the ossified parts of the calcaneus by spreading out the mechanical stresses before they reach the bone. VOI locations for this study are constrained by the fact that their respective locations must be ossified by the time bipedal walking starts to test hypotheses on the effects of gait maturation.

VOI placement

Trabecular bone properties are calculated in three VOIs located under the posterior talar facet (PTF), the calcaneocuboid facet (CC), and superior to the plantar Ligaments (PL) (Figure 8.2). These volumes of interest are chosen because these regions of the calcaneus ossify within the first year of life and can thus represent bone growth from the moment that gait develops. VOIs were standardized as 17% of maximum anteroposterior length of the ossified parts of the calcaneus in individuals below 6 years of age, and 13% of maximum calcaneal length in older individuals. Calcaneal length is chosen to standardize VOIs because it correlates strongly femoral head breadth throughout ontogeny in great apes (R^2 = 0.96, Dunsworth, 2006), and therefore correlates with bone size as well as body mass. The chosen VOI sizes guarantee that more than three trabecular lengths are present within each VOI, fulfilling the continuum assumption (Harrigan et al., 1988). These volumes are approximately anatomically homologous across all individuals in this study, and provide insight into trabecular bone structure at different stages of development.

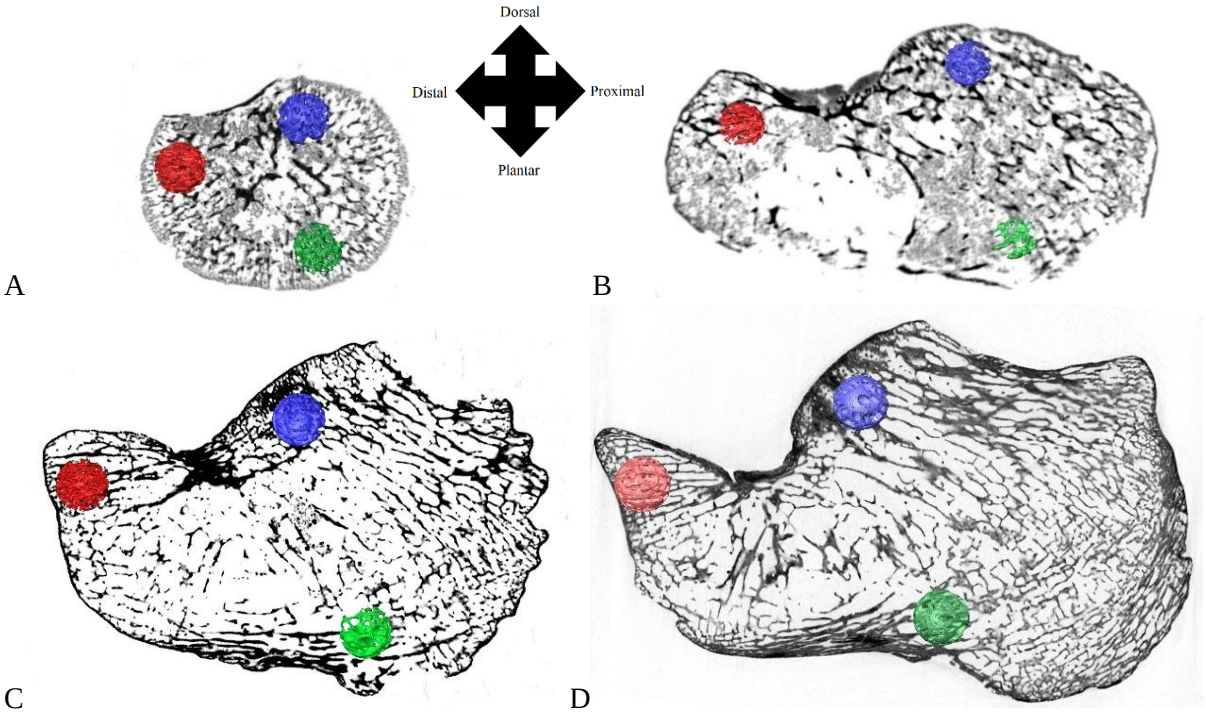

Figure 8.2. VOI locations in calcanei of individuals at different stages of development. 1±1 months (A), 12±4 months (B), 10 years (C), adult (D). VOIs: Plantar ligaments (PL, green), Calcaneocuboid (CC, red), Posterior talar facet (PTF, blue).

Hypotheses

Previous work on trabecular bone ontogeny has suggested that changes in mechanical loading influences trabecular structure during growth (Ryan and Krovitz, 2006; Gosman and Ketcham, 2009; Zeininger, 2013; Raichlen et al., 2015; Milovanovic et al., 2017; Ryan et al., 2017). The complex developmental sequence of gait acquisition in humans allows the correspondence between changes in mechanical loading and trabecular development to be examined. The following predictions should be followed if trabecular bone development is shaped to a significant extent by mechanical loading associated with the acquisition of adult human gait and increases in body mass.

Neonate: (0-1 years). Bone is laid down in similar ways across mammalian species. Newly ossified trabecular bone is characterized by a dense and anisotropic structure consisting of many thin struts, radiating from an ossification centre inside the cartilage (high BV/TV, DA, Conn.D, and low Tb.Th) (Wolschrijn and Weijs, 2004; Ryan et al., 2017). Trabecular structure in the ossified calcaneal sphere should be isotropic as a whole, but with trabeculae radiating anisotropically from the ossification centre. The trabecular bone is predicted to be resorbed in the first year of life due to lack of mechanical loading, resulting in a decline BV/TV and Conn.D, and an increase in Tb.Sp. Average trabecular thickness increases prenatally in the absence of mechanical loading and is therefore expected to increase at the same rate in the first year after birth. As the child starts crawling/standing bone will be deposited in strained areas. This is expected to affect the compressive calcaneocuboid (CC) and posterior talar facet (PTF) more than the plantar ligament VOI (PL) as tension in this region is not as expected to be very high until toe-off starts. Thus, if BV/TV starts increasing at the end of the first year of life, it is predicted to increase more on the compressive PTF and CC VOIs than in the tensile PL VOI.

Young infant (1-2 years). Children start to walk between 10 and 17 months of age. This new mechanical stimulation combined with increases in body size is predicted to initiate reorganization of the trabecular architecture. Redundant trabeculae are expected to be removed, further lowering Conn.D, and highly strained areas are expected to demonstrate an increase in BV/TV through thickening of existing trabecular struts. Trabeculae are predicted to start adapting to the complex loading patterns associated with bipedal walking and are thus expected to vary regionally in volume fraction and directionality. Finite element models predict higher compressive loading in adults during standing in the PTF compared to the CC and PL VOIs (Giddings et al., 2000; Gefen and Seliktar, 2004). Thus, it is predicted that the PTF VOI will experience a greater increase in BV/TV than the CC and PL VOI after the child starts walking. Heel strike develops at roughly 18-24 months of age (Zeininger, 2013). Heel strike is expected to be difficult to detect in trabecular structure because the part of the heel that strikes the ground is made of cartilage at the point the heel strike phase of gait develops. The transient force produced by heel strike may increase BV/TV under the posterior talar facet. Before 2 years of age infants still lack a toe-off phase, it is thus expected that the tensile bands

measured by the VOI will see a lesser increase in BV/TV and Tb.Th compared to the CC and PTF VOIs.

Infant (2-7 years). The development of the toe-off phase around 2 years of age increases tension on the plantar side of the calcaneus and compression on the calcaneocuboid joint and posterior talar facet. Force for toe-off is provided largely by the triceps surae muscles attached to the Achilles tendon. The Achilles tendon is attached posteriorly to the calcaneal tuber near the secondary ossification centre which does not fuse until the end of puberty (Scheuer and Black, 2004). However, toe-off also increases tension in the plantar fascia and plantar ligaments of the calcaneus (Giddings et al., 2000; Gefen and Seliktar, 2004). The presence of increased tensile strain associated with the addition of the toe-off phase can be tested by examining the appearance of this tensile band of trabeculae. Toe-off is the most strenuous phase of gait and all VOIs are predicted to experience greater loading than before. Trabecular structure is predicted to remodel in response to these increased loads resulting in increased DA, BV/TV, and Tb.Th and a reduction in Conn.D. Neuromuscular control of the lower limbs approaches adult levels at the age of 4. Gait gradually matures between the ages of 2 and 7 through a reduction of step width, and increased body size and motor control, resulting in more stereotypical loading from increasingly more predictable directions. This should increase DA in all VOIs along with increases in BV/TV, Tb.Sp and Tb.Th, and reductions in Conn.D related to increased body mass (Raichlen et al., 2015).

Child (7-12 years). Changes in trabecular morphology after age 7 are predicted to be the product of changes in body size and proportions. Thus, changes in trabecular structure after the age of 7 years should be primarily predictable from allometry. In Chapter 4 a significant positive regression was found between body mass and DA in both sexes and all four populations in the plantar ligaments. Thus, DA is predicted to increase with body mass and age in the plantar ligament VOI but not in the CC or PTF. A slight increase in BV/TV and Tb.Th, and a decrease in Conn.D and Tb.Sp would be predicted based on allometric relationships previously noted in the literature (Doube et al., 2011; Fajardo et al., 2013; Ryan and Shaw, 2013).

Adolescent (12-20 years). Body mass and bone deposition increase rapidly during the pubertal growth spurt and individuals would be expected to start participation in adult activities. Trabecular properties are predicted to follow allometric scaling patterns as gait does not differ from adults. As BV/TV scales with slight positive allometry (Ryan and Shaw, 2013), this is expected to lead to slightly increased BV/TV. Tb.Th and Tb.Sp are predicted to increase while Conn.D decreases. DA is not predicted to change as gait patterns no longer change in the calcaneocuboid and posterior talar facet VOIs. However, DA is predicted to increase in the plantar ligaments following findings from Chapter 4 where a positive relationship was found between body mass and DA.

Materials and Methods

Two skeletal populations are examined: Norris Farms (1300 AD, USA, n=14, aged 0 to 5 years) and St. Johns (1200-1500AD, UK, n=8, aged 8 to 20 years). The Norris Farms were scanned using an ONMI-X HD600 High-Resolution X-ray computed tomography (HRCT) scanner at the Center for Quantitative Imaging (CQI), Pennsylvania State University (Ryan and Krovitz, 2006). The St. Johns were scanned using an identical protocol with a Nikon XTH 225 ST HRCT laboratory scanning system at the Cambridge Biotomography Centre, University of Cambridge. The St. Johns were scanned using optimised energy settings (125 kV, 135 µA, 1080 views), and the Norris Farms and Black Earth scans were made using source energy settings 180 kV, 110 µA, and between 2800 and 4800 views.

Individuals younger than 5 and older than 8 belong to separate populations, scanned with different scanners, at different resolutions. The St. Johns population showed strong similarities in trabecular architecture to the Kerma population in Chapter 7. Saers et al. (2016) compared the Norris Farms population to the Kerma and found that Norris Farms have significantly higher BV/TV and Tb.Th in the lower limb than the sedentary Kerma population. It is therefore expected that the Norris Farms population would have significantly greater calcaneal BV/TV and Tb.Th, and lower Tb.Sp and Conn.D compared to St. Johns. It is not known when these differences in trabecular properties appear during ontogeny. However, based on these findings it would be expected that either juvenile St. Johns individuals would have greater Tb.Sp and Conn.D, and lower BV/TV and Tb.Th than Norris Farms individuals of similar age. The gap between individuals aged 5 and 8 makes it unclear how the growth curves of the two populations fit together. Therefore, while presented in the same figures, the curves generated in this chapter will be interpreted as two separate entities.

Table 8.1. The sample used in this chapter.

Individual	Population	Age estimate (years)	Age range (years)	Body mass (kg)
NF-821218	Norris Farms	0.17	0-0.35	
NF-821029	Norris Farms	0.17	0-0.35	
NF-821019	Norris Farms	0.5	0.25-0.75	
NF-821051	Norris Farms	0.75	0.5-1	
NF-820614	Norris Farms	1	0.67-1.33	6.99
NF-821100	Norris Farms	1	0.67-1.33	6.63
NF-821014	Norris Farms	1.5	1-2	8.11
NF-821026	Norris Farms	2	1.33-2.67	8.36
NF-821207	Norris Farms	2	1.33-2.67	8.63
NF-821113	Norris Farms	2.5	2-3	10.89
NF-821214	Norris Farms	3	2-4	9.28
NF-820683	Norris Farms	3	2-4	12.34
NF-819938	Norris Farms	3.25	2.5-4	10.86
NF-821012	Norris Farms	5	4-6	9.73
JDS10-F525-2768---5077	St. Johns	8	7-9	26.19
JDS10-F354-3171---2201	St. Johns	10	9-11	28.23
JDS10-F379-3248---2752	St. Johns	10	9-11	30.58
JDS10-F890-1547---284	St. Johns	10	8-10	35.80
JDS10-F741-1327---2808	St. Johns	11	10-12	42.14
JDS10-F944-3393---2354	St. Johns	11.5	10-13	37.89
JDS10-F390-3267---2292	St. Johns	12	11-13	41.53
JDS10-F359-3199---2273	St. Johns	17	15-19	64.33
JDS10-F889-1544---2845	St. Johns	17	14-20	56.42

Age and body mass estimation

Growth varies within and between populations based on sex, nutrition, disease, season, and numerous other factors (Bogin, 1999). This introduces an amount of uncertainty in the estimation of age-at-death (Scheuer and Black, 2004). Age was estimated by dental eruption and skeletal epiphyseal fusion using fusion times presented in Scheuer and Black (2004). Body mass was estimated using age-specific femoral head diameter equations presented in Ruff (2007). Body mass should therefore be considered rough estimates due to the uncertainty associated with age estimations. Age-at-death and body mass estimates for the Norris Farms juveniles were determined by Milner and Smith (1990). Age-at-death estimations often result in a range of ages. When plotting trabecular properties against age the mean of

the age range is chosen. It should thus be kept in mind that these age in fact reflect the mean value of a potential age range.

Statistics

All variables except for Tb.Th have a nonlinear relationship with age and body mass, so no linear models can be fitted to this data. Instead spearman correlations are used whenever data is monotonic. Only DA in the PTF and CC violates the monotony assumption. In this case, no correlations are performed. Locally weighted polynomial regressions (LOESS) with a smoothing parameter of 0.8 were used to plot the trabecular bone properties to age and body mass estimates using R 3.3.1.

Resolution dependency

The three youngest Norris Farms juveniles are scanned at a resolution of 12µm and the other Norris Farms juveniles are scanned at 26µm. All St. Johns individuals were scanned using a different scanner at a resolution of 47µm. Following the method used by Ryan and Shaw (2012) resolutions were artificially reduced in Avizo 6.3 using the resample module with a Lanczos filter. VOIs were downsampled to lower resolutions from 12 to 19, 26, 33, 40, and 47µm. Least squares linear regression analysis was run for each variable to test for significant influences of resolution on trabecular properties. Statistically significant results were not found in the juveniles that were scanned at resolutions of 26µm. In the three individuals that were scanned at 12µm a significant relationship was found between voxel dimensions and Tb.Th (ANOVA: df=1,16, F=75.426, p<.001) and Conn.D (ANOVA: df=1,4, F=72.925, p=.001) (Figure 8.3).

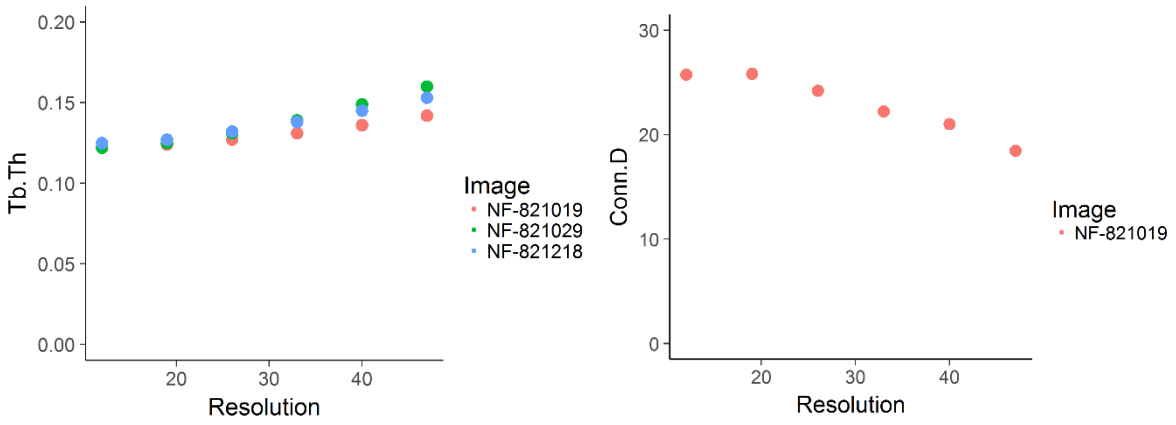

Figure 8.3. Relationships between voxel dimensions (µm) and Tb.Th (mm) and Conn.D (mm^{-3}) in Norris Farms juveniles.

Small trabeculae are blurred out at higher resolutions, resulting in a decrease in Conn.D and an increase in Tb.Th. However, the differences between scans at 12 and 26µm are slight and are not significant in a one-way ANOVA. Thus, all Norris Farms juveniles are comparable to each other without requiring corrections for resolution dependency. The thicker and less interconnected trabeculae found in older individuals are unlikely to result from resolution effects, and most likely reflect reality. However, these results do show that higher resolutions cannot accurately pick up small

trabeculae. It is possible that Conn.D is underestimated and Tb.Th overestimated in the lower resolution scans if very thin trabeculae are present. Visual examination of lower resolution VOIs does not indicate that small trabeculae are missed. It is therefore deemed unnecessary to correct for possible effects of scan resolution in this chapter.

Results

Qualitative description of calcaneal trabecular ontogeny

The central part of the calcaneus has commenced ossification at birth, but the calcaneal tuber and the dorsal and anterior articular surfaces still consist of cartilage. The cartilage ossifies in all directions from the spherical ossification centre except anterodorsally where the cortex is already reached at birth. For each age category sagittal cross-sections through juvenile calcanei will be presented in each figure as a two-dimensional orthoslices and a cross-section through a three-dimensional volume rendering.

In individuals aged between 0-2 months (n=2) trabecular bone structure is highly isotropic with trabeculae radiating anisotropically from a central area (Figure 8.4). The centre consists of thicker, more widely spaced and fewer trabeculae than the peripheral areas, suggesting that the older trabeculae in the centre have modelled into thicker, more widely spaced structures relative to the younger peripheral bone (Reissis and Abel, 2012; Ryan et al., 2017). Thick trabeculae are also found dorsally in the calcaneus near the depression just anterior to the posterior talar facet. No evidence is found for the organization into the three distinctive bands of trabeculae that are found in adults.

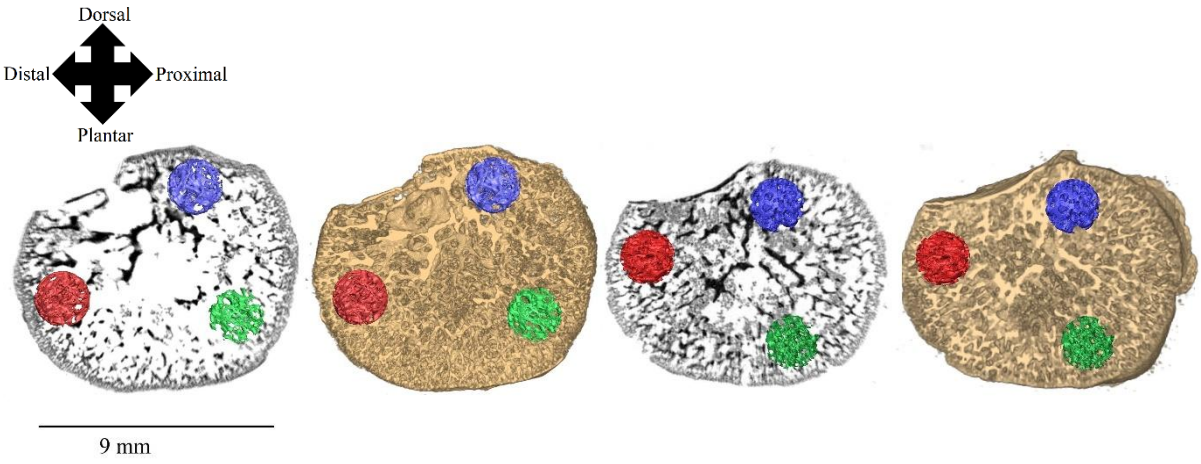

Figure 8.4. Sagittal cross-section of calcanei of two 0-2 months old. VOIs: Plantar ligaments (PL, green), Calcaneocuboid (CC, red), Posterior talar facet (PTF, blue).

In an individual aged between 3-9 months (n=1) the calcaneus is elongated anteriorly and no longer resembles a sphere in sagittal cross section (Figure 8.5). Trabeculae no longer radiate from a single centre but are organized less regularly. A central low-density zone is present and denser regions are found in the calcaneocuboid and posterior talar facet. The plantar side of the calcaneus is very low in trabecular bone on the lateral side but denser on the medial side. There are signs of the compressive

bands being formed being formed at the calcaneocuboid and posterior talar facet. Some trabeculae are also organized in the direction of tensile stress from the plantar ligaments. The trabeculae are longest and thickest around the low-density centre and appear more isotropic in the anterior and posterior portions. The bone is still expanding anteriorly and posteriorly.

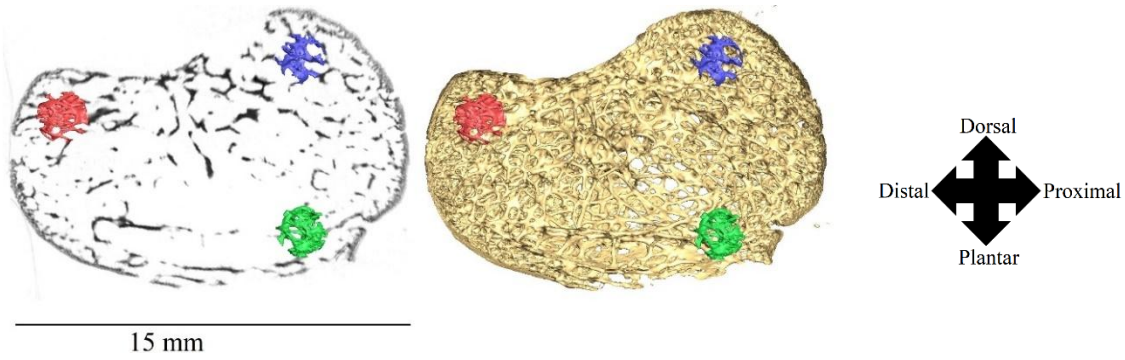

Figure 8.5. Sagittal cross-section of a 3-9 months old individual. VOIs: Plantar ligaments (PL, green), Calcaneocuboid (CC, red), Posterior talar facet (PTF, blue).

In one individual aged 6-12 months (n=1) the calcaneus is elongated posteriorly (Figure 8.6). Compressive bands are visible running from the posterior talar facet to the inferior posterior portion. Compressive bands are also visible on the dorsal portion of the calcaneocuboid joint. The thickest bands are found around to the low-density zone. A small tensile band of trabeculae near the plantar ligaments is found posterior to the low-density zone.

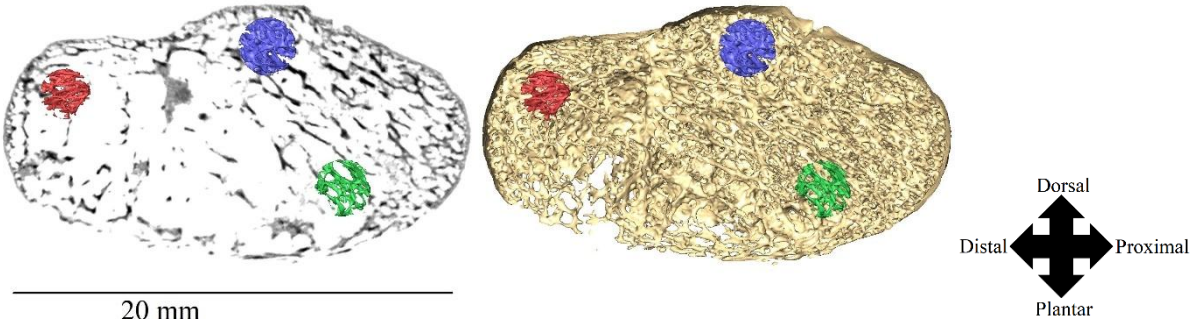

Figure 8.6. Sagittal cross-section of a 6-12 months old individual. VOIs: Plantar ligaments (PL, green), Calcaneocuboid (CC, red), Posterior talar facet (PTF, blue).

In individuals aged 8-16 months (n=2) the plantar tensile band is expanding (Figure 8.7). Trabeculae in the cuboid and posterior talar facet regions are oriented in the directions from which they are loaded.

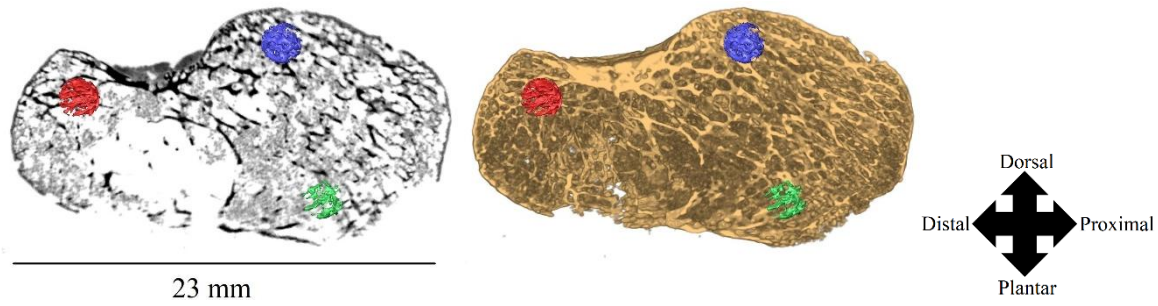

Figure 8.7. Sagittal cross-section of an 8-16 months old individual. VOIs: Plantar ligaments (PL, green), Calcaneocuboid (CC, red), Posterior talar facet (PTF, blue).

At the age of 12-24 months (n=1) the calcaneus increasingly resembles the adult form externally and internally (Figure 8.8). Compressive bands are present dorsally and on the plantar side tensile bands have clearly formed. The tensile bands start from about ¾ anteriorly on the medial side of the plantar surface at the plantar ligament insertion.

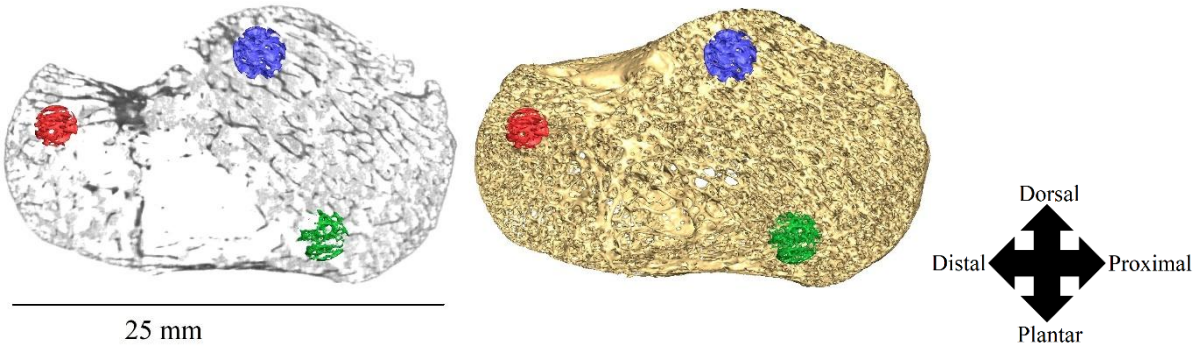

Figure 8.8. Sagittal cross-section of a 12-24 months old individual. VOIs: Plantar ligaments (PL, green), Calcaneocuboid (CC, red), Posterior talar facet (PTF, blue).

In two individuals aged 16-32 months (n=2) similar patterns are observed as in the 12-24-month-old individual (Figure 8.9). Tensile bands found but not as strongly present as in older individuals. Plate-like trabeculae are appearing in the posterior talar facet.

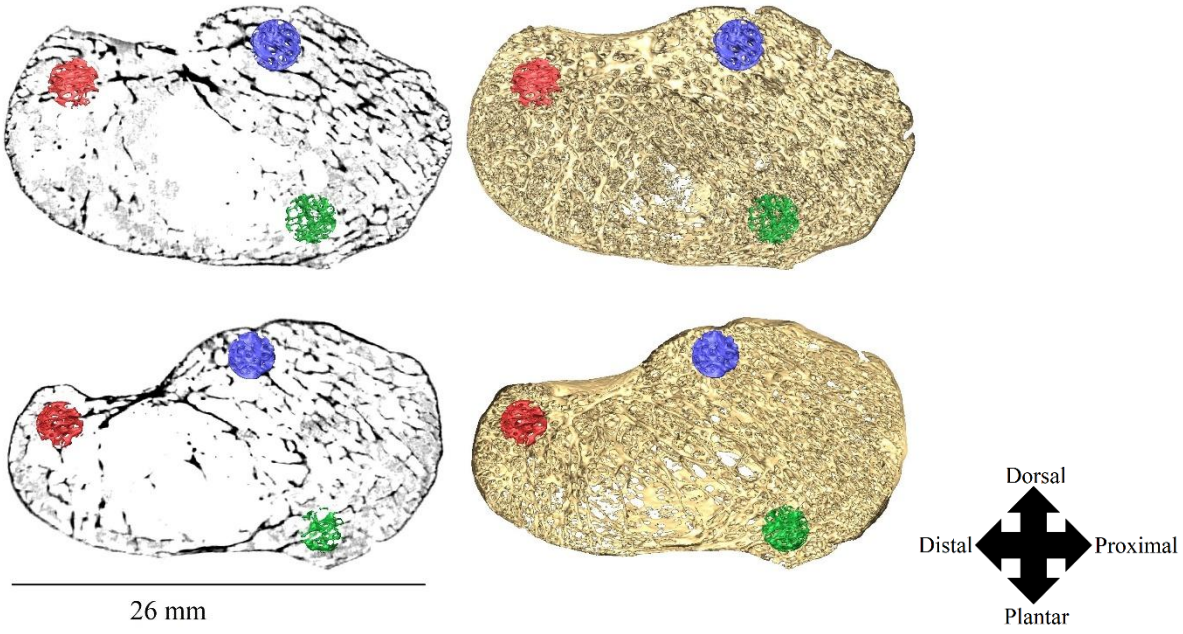

Figure 8.9. Sagittal cross-sections in two 16-32 months old individuals. VOIs: Plantar ligaments (PL, green), Calcaneocuboid (CC, red), Posterior talar facet (PTF, blue).

In one individual aged 24-36 months more trabeculae are found compared to younger individuals (Figure 8.10). The tensile trabecular system near the plantar ligaments is located on the medial side, most likely due to eversion of the foot at toe-off.

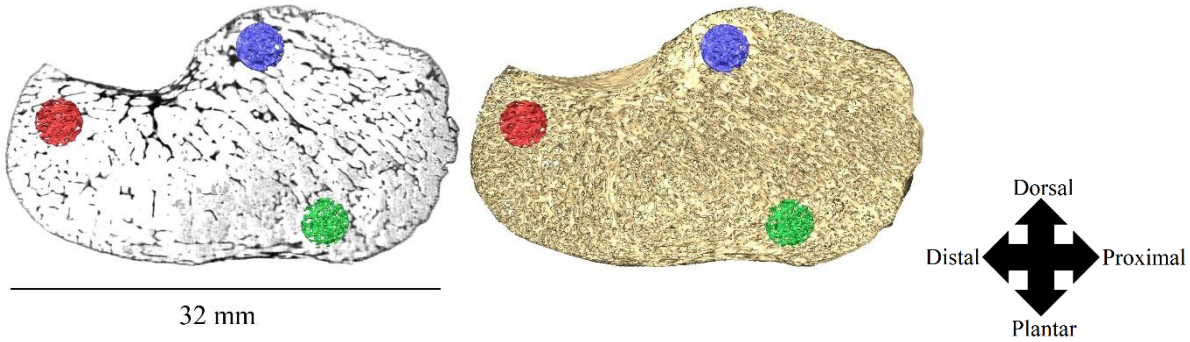

Figure 8.10. Sagittal cross-section of a 24-36 months old individual. VOIs: Plantar ligaments (PL, green), Calcaneocuboid (CC, red), Posterior talar facet (PTF, blue).

The calcaneal tuber continues to expand posteriorly in three individuals aged 24-48 months (n=3). Plate-like trabeculae begin to appear near the posterior talar facet and the insertion of the plantar ligaments (Figure 8.11).

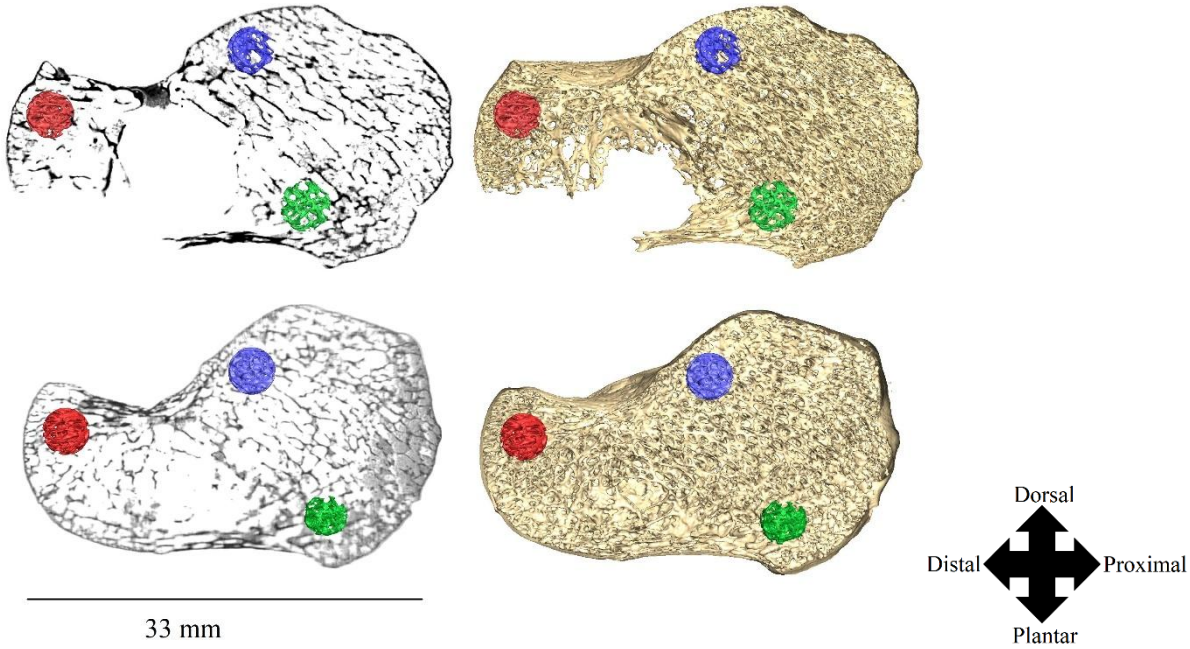

Figure 8.11. Sagittal cross-sections in two 24-48 months old individuals. VOIs: Plantar ligaments (PL, green), Calcaneocuboid (CC, red), Posterior talar facet (PTF, blue).

Plates are formed near the posterior talar facet, calcaneocuboid and plantar ligaments in the individual aged 48-72 months (Figure 8.12). The secondary ossification centre appears around the age of 5, but is not found for this individual (Christman, 2003; Scheuer and Black, 2004). The posterior talar facet and cuboid joint are still not fully ossified. The trabeculae at the plantar ligament insertion continue to thicken in response to the maturation of gait and increases in body mass.

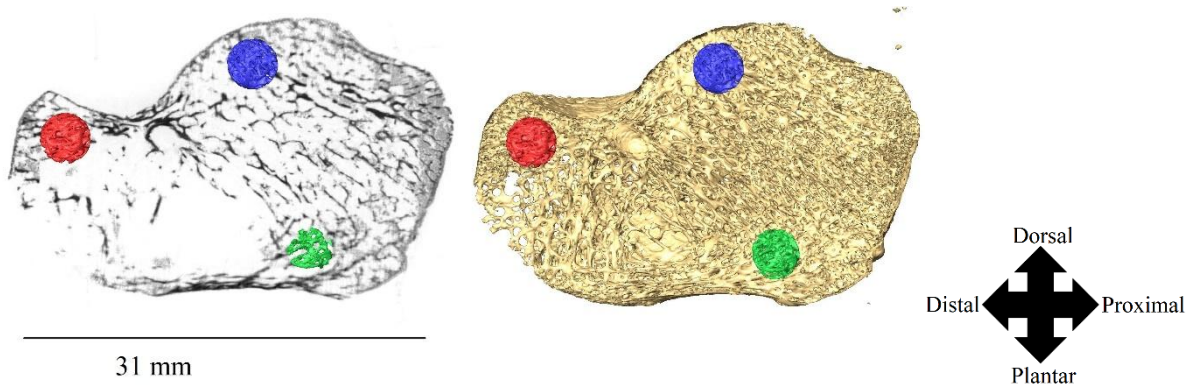

Figure 8.12. Sagittal cross-section of a 48-72 months old individual. VOIs: Plantar ligaments (PL, green), Calcaneocuboid (CC, red), Posterior talar facet (PTF, blue).

At 8 years old (n=1) the calcaneocuboid and talar articulations are fully ossified, but the posterior part of the tuber is still ossifying (Figure 8.13). The calcaneus has increased in size significantly and trabeculae have become thick and plate-like at the plantar ligament insertion and posterior talar facet.

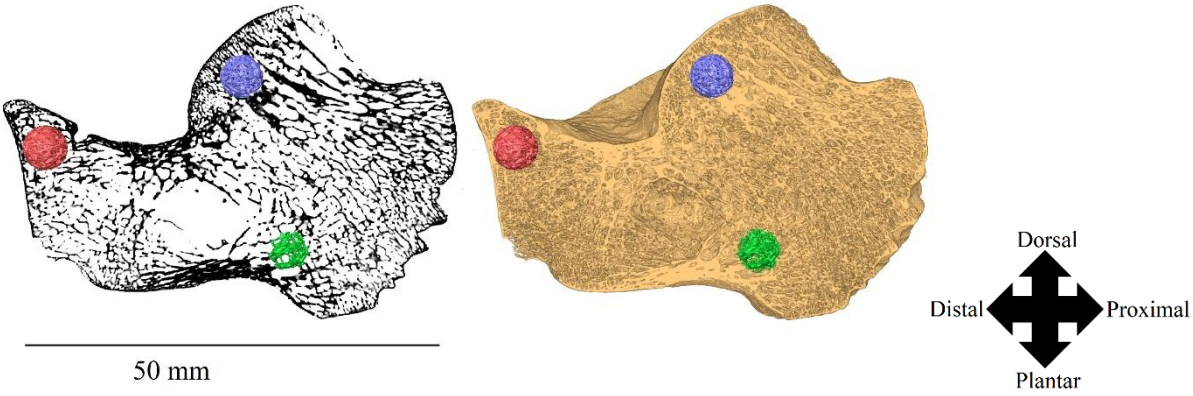

Figure 8.13. Sagittal cross-section of an 8-year-old individual. VOIs: Plantar ligaments (PL, green), Calcaneocuboid (CC, red), Posterior talar facet (PTF, blue).

Juveniles aged 10-12 years old (n=6) show similar external and internal morphology to the 8-year-old (Figure 8.14 and 8.15). The calcaneal tuber has not fused with the secondary ossification centre.

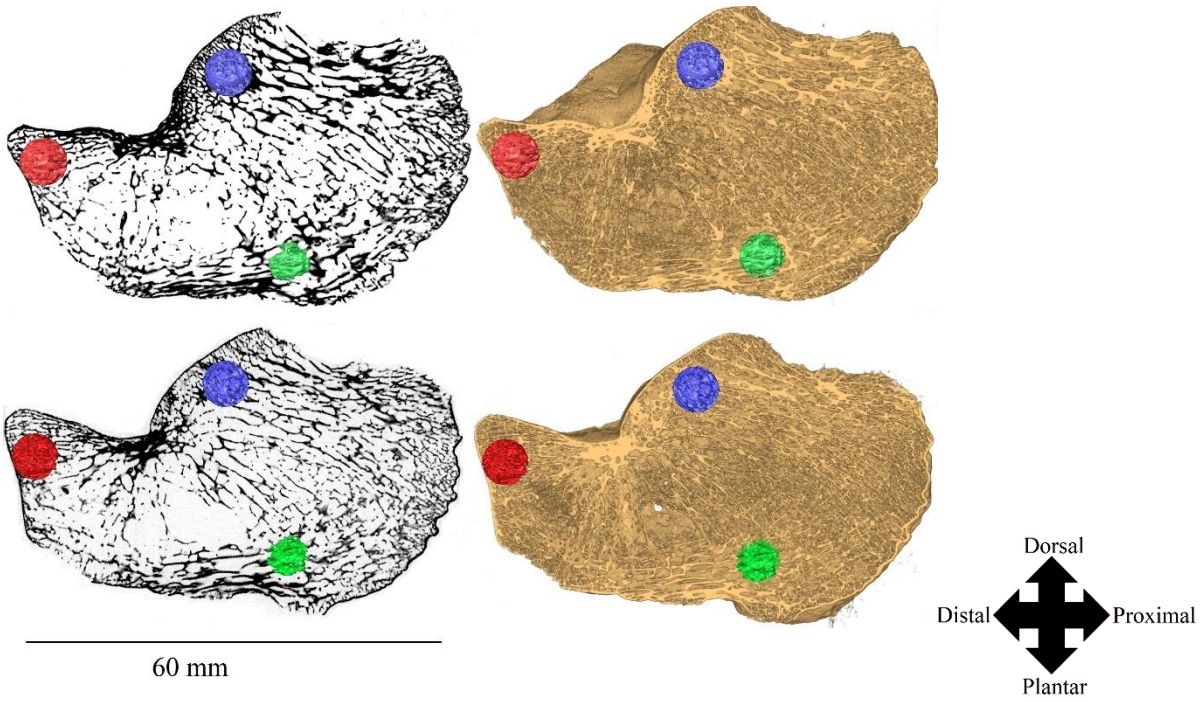

Figure 8.14. Sagittal cross-sections of two 10-year-old individuals. VOIs: Plantar ligaments (PL, green), Calcaneocuboid (CC, red), Posterior talar facet (PTF, blue).

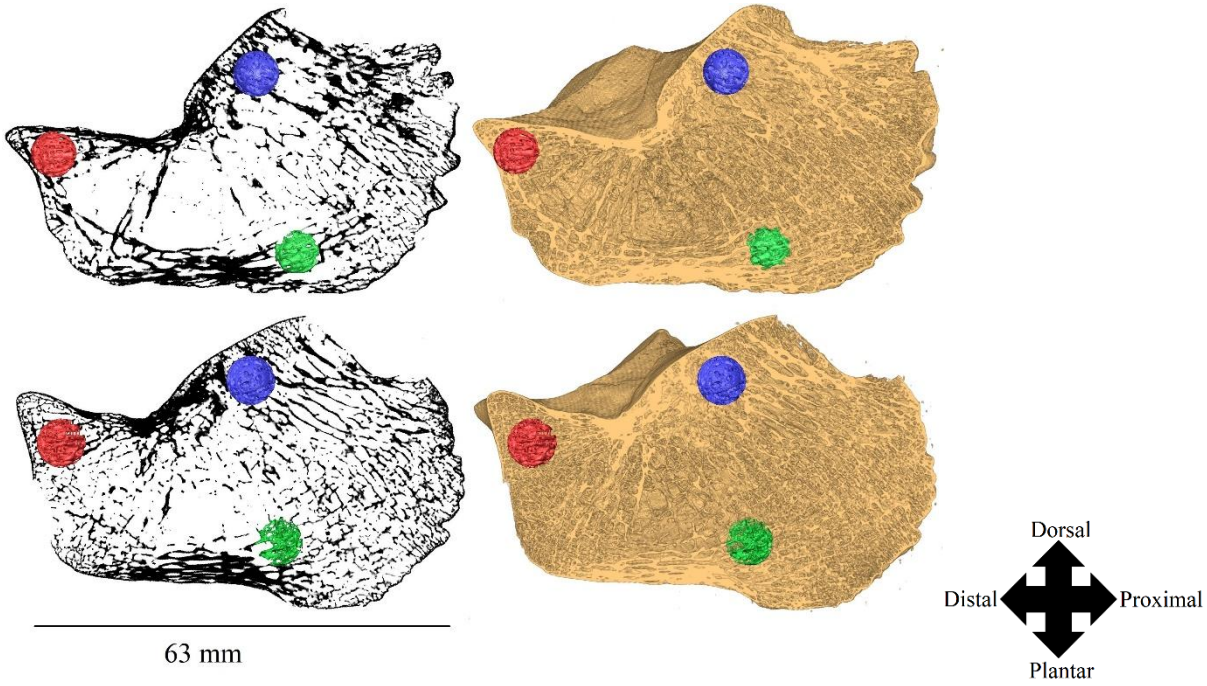

Figure 8.15. Sagittal cross-sections of two 12-year-old individuals. VOIs: Plantar ligaments (PL, green), Calcaneocuboid (CC, red), Posterior talar facet (PTF, blue).

Adult morphology is reached and the secondary ossification centre at the posterior tuber is almost fully fused in the two individuals aged 17 years old. The tensile band between the plantar fascia and the Achilles tendon has formed (Figure 8.16). This band was not present in previous categories because the secondary ossification centre is not fused.

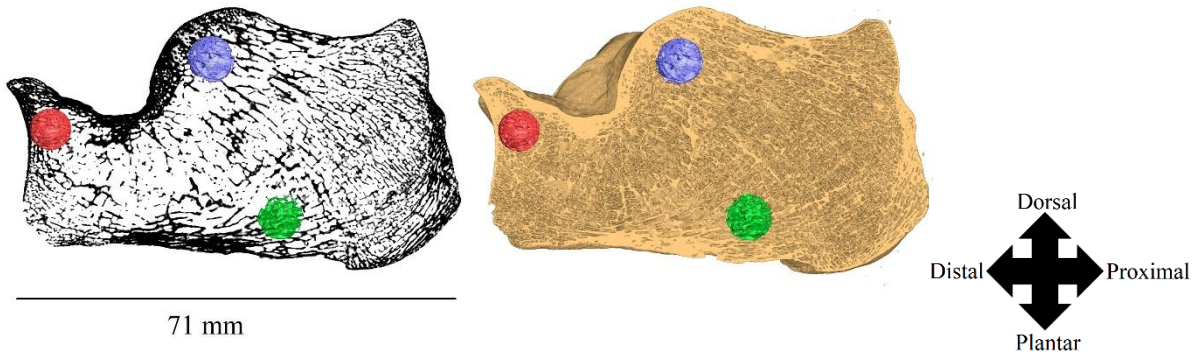

Figure 8.16. Sagittal cross-section of a 17-year-old individual. VOIs: Plantar ligaments (PL, green), Calcaneocuboid (CC, red), Posterior talar facet (PTF, blue).

Quantitative description of calcaneal trabecular growth

Trabecular structure is quantified throughout ontogeny in three volumes of interest (see figures 8.4-8.16). Trabecular properties are plotted against age (Figure 8.17) and body mass (Figure 8.19).

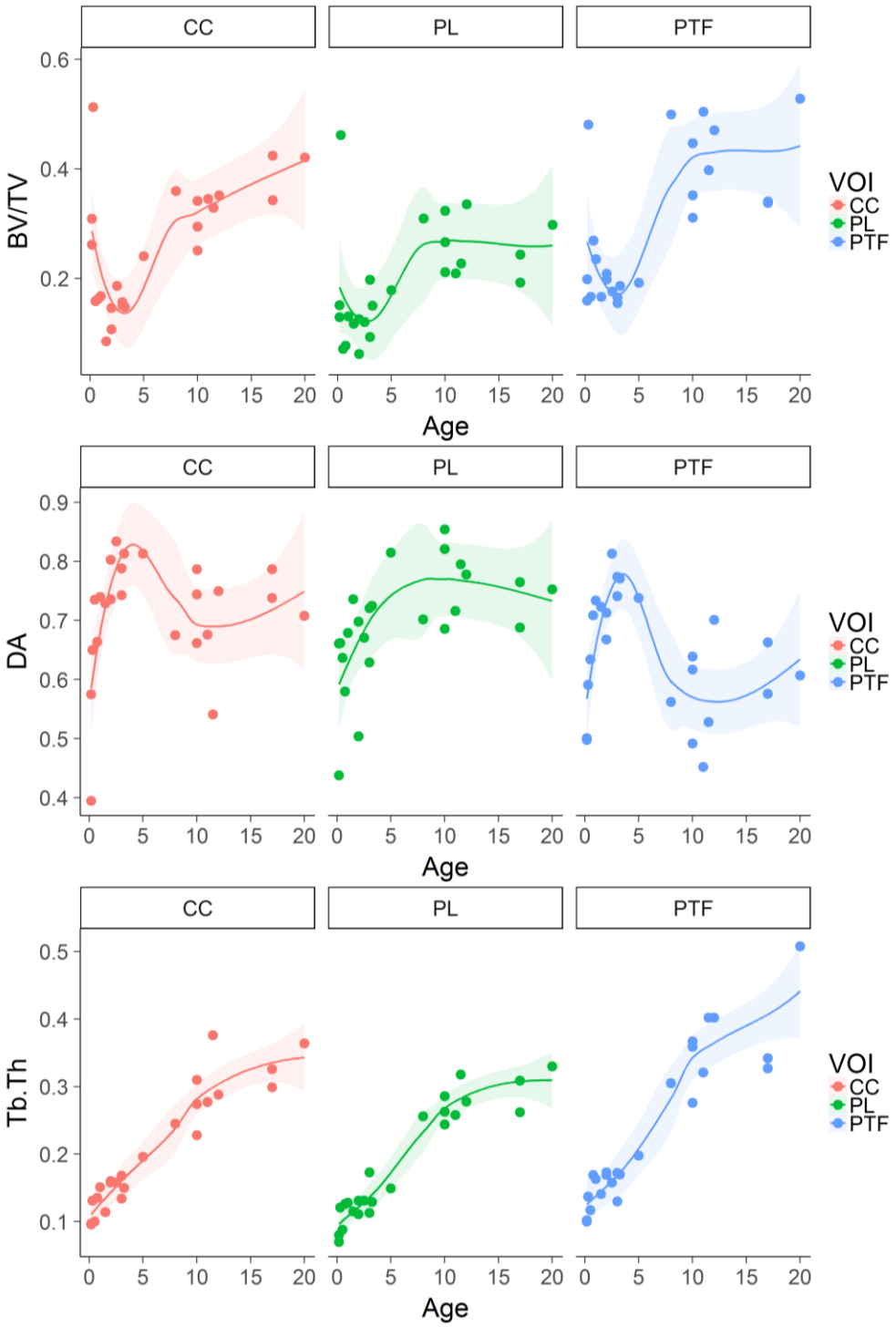

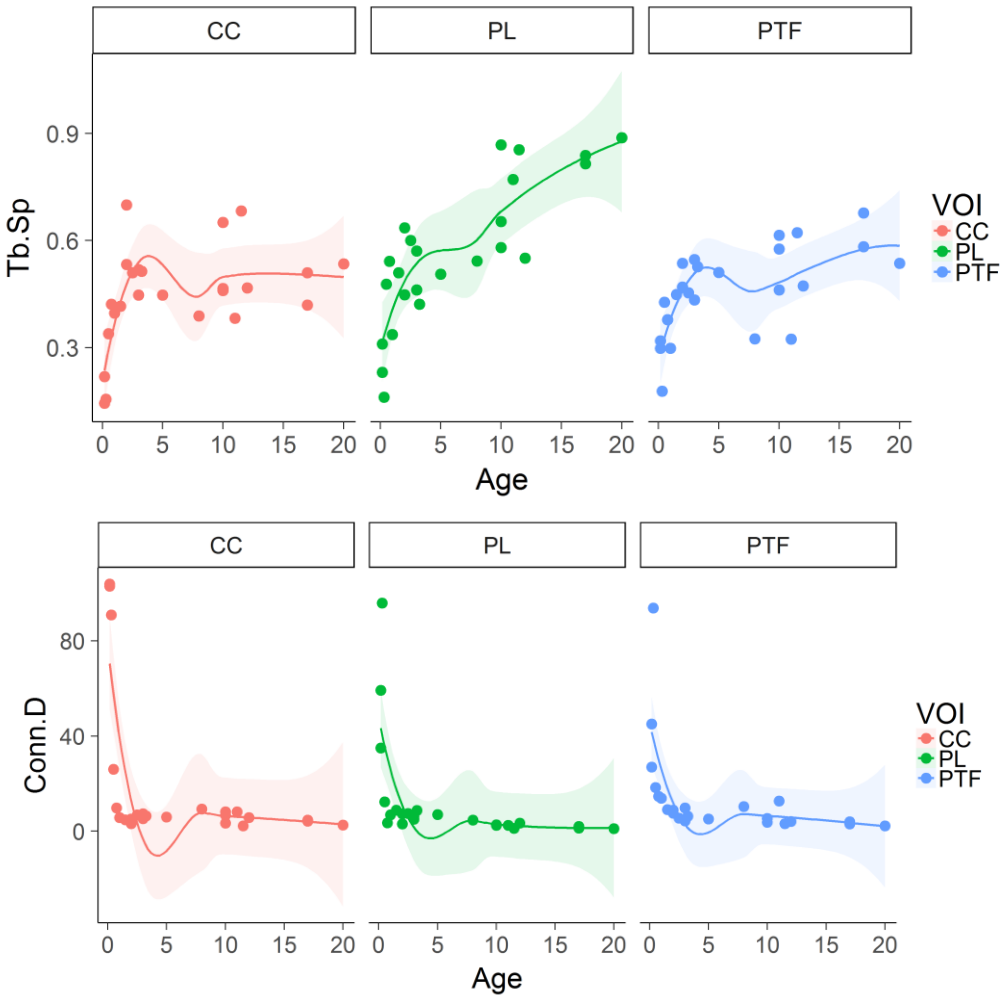

Figure 8.17. Trabecular bone properties plotted against age in the calcaneocuboid (CC), plantar ligaments (PL), and posterior talar facet (PTF) VOIs.

Trabecular structure in the calcaneocuboid (CC) VOI is very dense but relatively isotropic at birth. Bone volume fraction is reduced in the second half of the first year of life, while Tb.Sp, Tb.Th, and DA increase and Conn.D is sharply reduced. BV/TV remains low until about 4 years of age, and increases after the age of 5, continuing to rise until adulthood. Anisotropy increases steadily until the age of 5, but has decreased and remains constant from the age of 8 onwards where it varies around a mean of 0.7. Trabecular thickness increases constantly from birth until adulthood. Trabecular spacing increases from birth until about 3 years of age and varies around a mean of 0.55 until adulthood.

Trabecular structure in the posterior talar facet (PTF) starts out very dense, strongly interconnected, and isotropic with low trabecular spacing and very thin struts. During the first year of life BV/TV is reduced and remains around .25 until the age of 4. Between the age of 5 and 8 years BV/TV has increased and remains around .45 from the age of 8 onward. Trabecular thicken gradually throughout ontogeny until adulthood. Connectivity density decreases quickly after birth and then continues in a gentle decline until adulthood. Trabecular spacing increases substantially from birth until the age of 5 after which it levels off with individuals varying around a mean value of 0.6.

At birth, trabecular structure in the plantar ligaments (PL) starts out very dense, strongly interconnected, and isotropic with low trabecular separation and very thin struts. In the first year of life BV/TV drops further compared to the other VOIs reaching values as low as .06 between ages 1 and 2. After the age of 2 years BV/TV increases to about .18 until 5 years of age, and remains around .27 from the age of 8 until adulthood. The increase in trabecular thickness levels off around the age of 12. The Degree of anisotropy steadily increases from .38 at birth to around .7 to .8 after the age of 5.

Body mass was not estimated for individuals younger than 1 years of age. While body mass and age are highly correlated (Pearson r=.965, p=<.001), the different rates of growth in body mass with age (Figure 8.18) may lead to different patterns with trabecular properties. However, the relationships found between body mass and trabecular properties are identical to the relationships between age and trabecular properties.

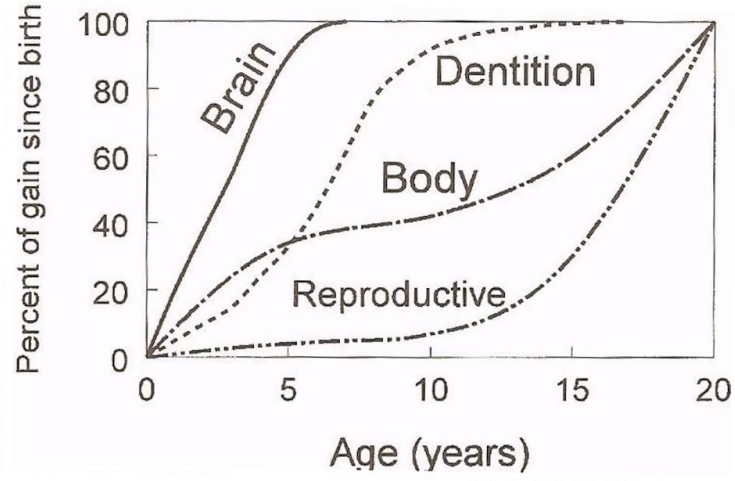

Figure 8.18. Growth curves for different body tissues (From Bogin (1999) , p. 73). "Body" indicates growth in total body mass.

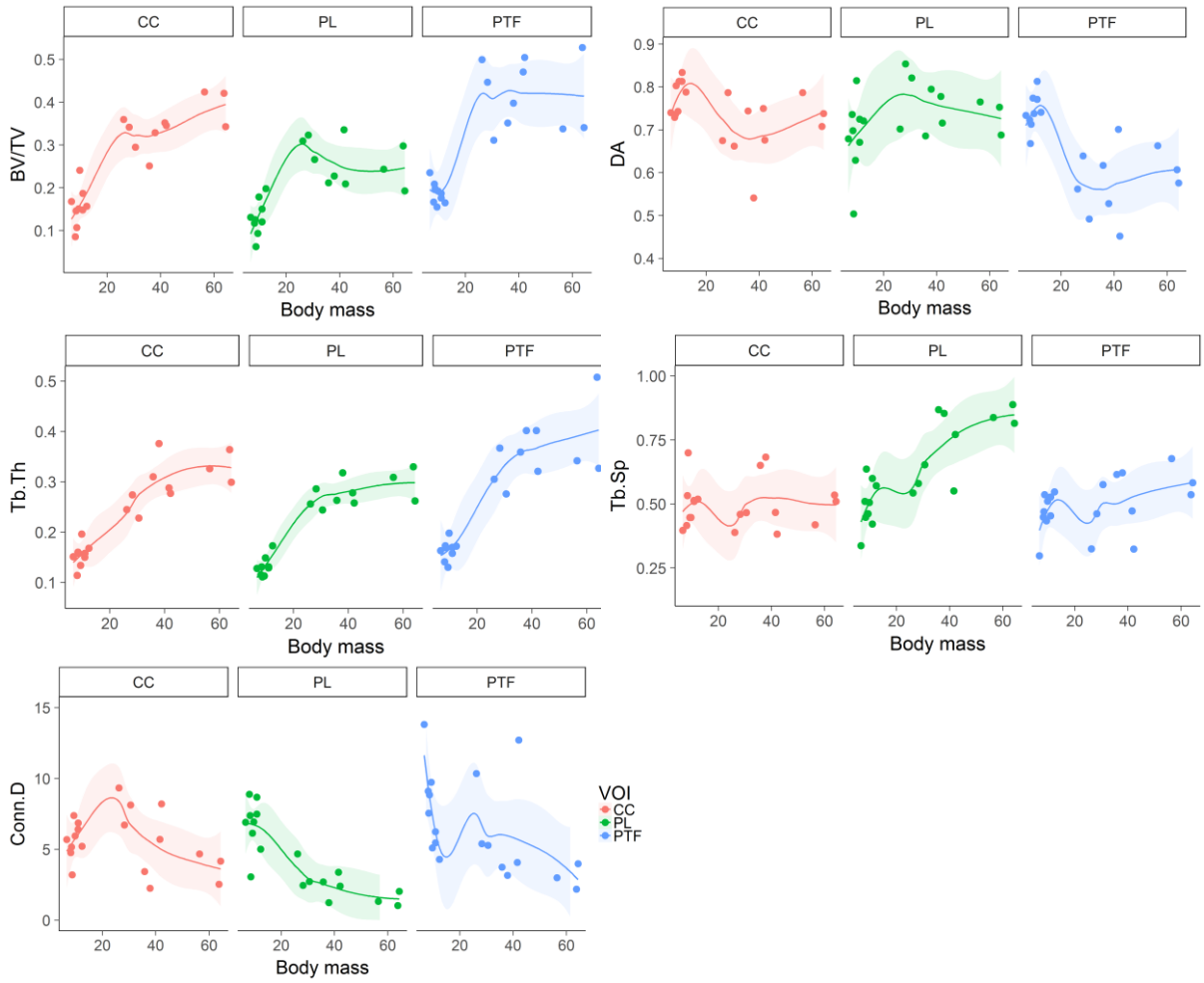

Figure 8.19. Trabecular bone properties plotted against body mass in the calcaneocuboid (CC), plantar ligaments (PL), and posterior talar facet (PTF) VOIs.

Differences between VOIs:

The differences between VOIs can be more easily spotted when variables are plotted in the same figure (Figure 8.20).

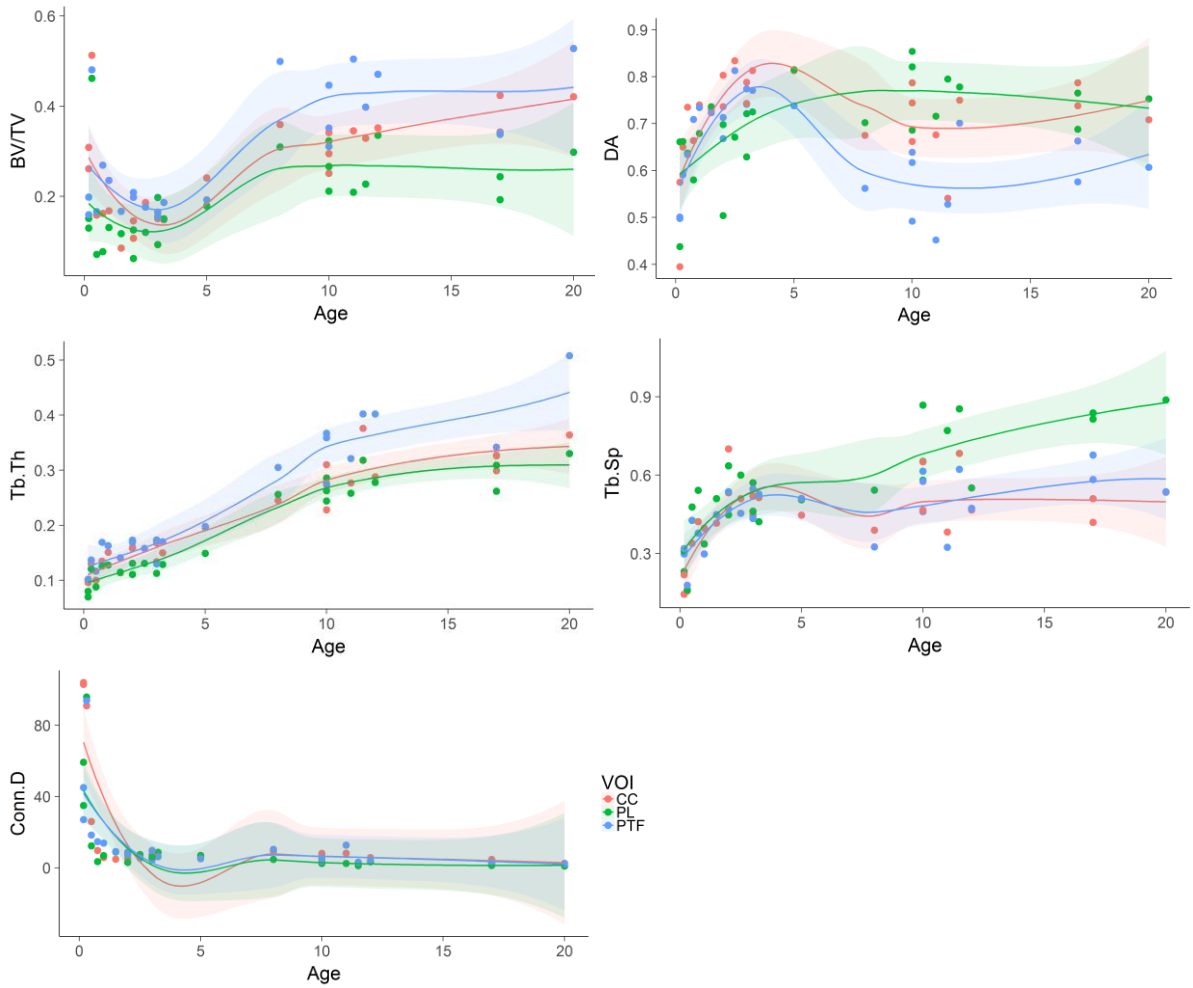

Figure 8.20. Trabecular properties plotted against age in the calcaneocuboid (CC), plantar ligaments (PL), and posterior talar facet (PTF) VOIs.

From birth, BV/TV is consistently lower in the plantar ligament VOI compared to both compressive VOIs. Between the ages of 2 and 5 BV/TV starts to increase again in all VOIs. From the age of 8 onwards a pattern similar to adults has emerged with PTF having the highest BV/TV, followed by CC, and PL having the lowest BV/TV. Thus, somewhere between 5 and 8 years of age the VOIs start to diverge. Unfortunately, no individuals of this age are present in the sample. Trabecular thickness increases steadily from birth until the age of 12 in all VOIs. The degree of anisotropy increases rapidly in all VOIs from birth to the age of 5, but the plantar ligaments lag behind the other VOIs. However, from the age of 8 onwards anisotropy is highest in the plantar ligaments, lower in the calcaneocuboid, and lowest in the PTF. Trabecular spacing increases rapidly from birth until the age of 4 in all VOIs. Only in the plantar ligaments does Tb.Sp continue to increase until adulthood. Trabecular structure starts out highly interconnected at birth, but connectivity density drops rapidly in the first year of life in all VOIs and decreases gently until adulthood.

How do trabecular properties correlate with age, body mass, and other trabecular properties? Do correlations differ between VOIs?

Listwise and pairwise correlations between age, body mass, and trabecular properties are presented in Appendix 8.1. Scatterplots of all trabecular properties are provided in Appendix 8.2. Pairwise analysis uses the maximum sample size per combination of variables, while listwise analysis uses the same sample size for each comparison. Because individuals younger than 1 year old do not have an associated body mass, and because two individuals could not be aged, the listwise analysis excludes seven individuals. Spearman correlations can be used whenever data is monotonic. DA violates the monotonicity assumption in the CC and PTF VOIs when plotted against body mass and age and thus no correlations can be performed here.

The same patterns are found in pairwise and listwise correlations. In all VOIs significant positive correlations are found between age and all properties except for Conn.D which correlates negatively. Similar correlations are found between trabecular properties and body mass, except that in the PL no significant result is found between body mass and DA, and in the PTF no significant correlations are found for Tb.Sp or Conn.D. When correlations are significant they all correlate in the same directions in all VOIs (negatively with Conn.D and positively for all the others). Particularly interesting are the correlations between BV/TV and DA. In the PTF there is a significant negative correlation while in PL there is a strong positive correlation, and in CC there is no correlation. Thus, with age trabecular structure becomes significantly more anisotropic and denser in the PL, but significantly denser and more isotropic in the PTF.

Discussion

It was predicted that bone would start out very dense and anisotropic at birth and that BV/TV would reduce in the first year of life in the absence of substantial strain. Loading associated with unassisted bipedal walking should initiate remodeling from the age of 1 year onwards. Bone morphology was hypothesized to change rapidly between the age of 1 and 5 with the addition of heel strike, toe-off and increasing neuromuscular control. Finally, it was predicted that after obtaining adult gait patterns around 7 years if age, trabecular structure would follow allometric scaling due to increases in body mass without changes in gait.

These predictions were followed closely by BV/TV which starts out high at birth, reduces during the first year of life, but only increases substantially from the age of 3 to 5. Between the age of 5 and 8 BV/TV is substantially increased and changes little after the age of 8. The increase in body mass during the adolescent growth spurt does not appear to affect BV/TV. This follows the prediction that trabecular properties follow allometric scaling rules after the adoption of adult gait patterns. Analyses in Chapter 4 showed no significant relationship between body mass and BV/TV, although Ryan and Shaw (2013) found a slight positive allometry in primates with a large range of body masses.

It was predicted that trabecular structures would be dense and highly interconnected with small thin struts at birth. It was predicted that some of these struts would be removed while others were thickened in correspondence to loading. This pattern was largely followed in the sense that Conn.D reduces with age while Tb.Th and DA increase. However, neither Conn.D nor Tb.Th were affected in by the adoption of adult gait patterns. Instead Conn.D reduced sharply after ossification and declines steadily after that with increasing body mass. Tb.Th shows a strong positive correlation to body mass in all VOIs and increases steadily with increasing age.

DA increases rapidly from birth until 5 years of age in all VOIs. This follows the prediction that the generalised trabecular structures laid out during ossification are remodelled into more directionally organized trabeculae under the influence of habitual loading. From the age of 8 onwards, trabeculae in the compressive CC and PTF VOIs become more isotropic while the structure in the PL remains highly anisotropic. This does not conform to predictions based on allometric scaling or the adoption of adult gait patterns. Instead this may reflect the increase in BV/TV through more plate-like rather than rod-like trabeculae. Current methods of quantifying plate-rod geometry in are unsuitable for use on trabecular structure (Salmon et al., 2015). However, visual inspection of individuals aged over 8 years old does suggest a substantial increase in plate-like trabeculae. Plate-like geometry reduces the degree of anisotropy and may therefore explain why the CC and PTF become more isotropic after the age of 5. Previous studies on human trabecular bone ontogeny in the tibia and femur found that trabeculae are laid out anisotropically, become more isotropic during the first year of life, and more anisotropically again as gait develops (Ryan and Krovitz, 2006; Gosman and Ketcham, 2009). However, the opposite pattern was found in the current study for the calcaneus. This different pattern can be explained as a result of differences in the growth of the long bones relative to the calcaneus. The calcaneus ossifies radially from a central node whereas the long bones ossify in a single direction. Close inspection of the cross-sections throughout growing bones (Figure 8.4) shows that trabeculae form orthogonal to the growth plate. Thus, differences in ossification between long bone epiphyses and the more irregularly shaped calcaneus likely explain the differences in initial isotropy of the calcaneus.

Overall, the results suggest that trabecular structure remodels under the effects of mechanical loading during gait maturation as suggested by previous studies (Wolschrijn and Weijs, 2004; Ryan and Krovitz, 2006; Gosman and Ketcham, 2009; Raichlen et al., 2015; Ryan et al., 2017). It is interesting that after the ages of 5 to 8 BV/TV and DA level off. This indicates that the largest changes in microstructure occur while gait develops. After the gait of children has matured to closely resemble the adult state, changes in trabecular structure follow allometric predictions.

Appearance of adult morphology

BV/TV and DA reach adult levels somewhere between the ages of 5 and 8. In case of BV/TV this may be interpreted as obtaining adult morphology. Allometric studies show that BV/TV scales isometrically, or with slight positive allometry (Doube et al., 2011; Barak et al., 2013; Fajardo et al.,

2013; Ryan and Shaw, 2013, Chapter 4). Because BV/TV is a shape variable, isometry constitutes no change in shape with a change in size. As body size increases bone size and mass also increase, but not BV/TV. Thus, adult BV/TV is reached when gait has obtained its adult characteristics. DA also reaches adult levels in all VOIs between the ages of 5 and 8. Because gait at this age closely resembles that of adults, there are no further changes in the directionality of loading to which trabecular bone needs to adapt through changes in DA. It is however clear that DA is not only affected by loading directionality (see discussion in the previous paragraph).

In the plantar ligaments, trabecular separation increases until adulthood. In the compressive calcaneocuboid and posterior talar facet VOIs trabecular spacing does not increase after the age of 3. The lack of increase in Tb.Sp in the CC and PTF are surprising given the significant positive regressions found in Chapter 4 between body mass and Tb.Sp. Conn.D decreases rapidly during the first year of life and continues to decrease slowly from then on until death in all VOIs, matching negative relationships found in chapters 4 and 6 between Conn.D and age/body mass. Tb.Th continues to increase with age until adulthood in all VOIs. This would be predicted from the literature on interspecific trabecular bone allometry (Doube et al., 2011; Barak et al., 2013; Ryan and Shaw, 2013). Thus, the prediction that only allometric scaling should affect trabecular structure after gait maturation is confirmed for all variables except for Tb.Sp in the CC and PTF VOIs.

Does trabecular structure reflect the development of gait?

A dense and generalized trabecular structure is set up during endochondral ossification similarly to other animals and anatomical locations (Carter and Beaupré, 2001; Ryan and Krovitz, 2006; Reissis and Abel, 2012; Ryan et al., 2015). Trabecular bone subsequently reorganizes into fewer, thicker, and directionally organized systems of trabeculae. It was predicted that excessive bone laid out during endochondral ossification would be resorbed during the first year of life due to lack of sufficient strain. In the first year of life bone is rapidly remodelled from about 100 to 5-20 connections per unit volume. Anisotropy rapidly increases with the decreasing Conn.D indicating that trabeculae oriented in certain directions are favoured while others are removed. The space between trabeculae rapidly increases as trabeculae are removed and the remaining trabeculae gradually thicken. The increased anisotropy suggests that specifically oriented trabeculae are favoured. However, BV/TV continues to decrease which is consistent with a trabecular structure that is not being strained enough to maintain. This suggests either genetic canalization, or some effects of loading prior to the adoption of unassisted bipedal walking in the first year of life. It is unknown whether muscle contractions in the first year of life produce enough strain for certain trabeculae not to be removed. Controlled experiments are required to test whether mechanical loading, genetic factors, or a combination of both underlie this selective loss of trabecular bone mass during the first year of life.

It was predicted that the increased loading with the development of bipedal gait from 1 year onwards begins to reshape the 3 regions from a generalized structure into adult morphology. At around 1 year

of age compressive bands start forming at the posterior talar facet and the calcaneocuboid joint, and tensile bands form at the plantar ligaments. At 1.5 years of age these three trabecular bands have clearly formed. As the bone grows in external dimensions, trabeculae become less numerous, thicker, further separated and more directionally oriented. Trabecular orientation varies per VOI, corresponding to the primary compressive and tensile loading directions placed upon the calcaneus during gait. The posterior talar facet VOI experiences the highest mechanical loading during adult gait, followed by calcaneocuboid and finally the plantar ligament VOIs (see Figure 2.2). The posterior talar facet consistently has the highest BV/TV with the most plate-like and thickest trabeculae, followed by the calcaneocuboid joint and the plantar ligaments. This indicates that adaptations to loading magnitude are expressed from the first year of life onwards. Conn.D sharply reduces within the first six months after birth and almost flattens out in the second half of the first year of life. Thus, this occurs before the development of unassisted bipedal walking in children at the age of 1. A plausible explanation is that the sudden increase in habitual loading associated with crawling and standing, and a reduction in surface area, stops the rapid resorption of trabeculae between 6 and 12 months of age. The thickening of trabeculae in older children may merge struts together, further reducing Conn.D.

It was predicted that the compressive VOIs should increase in BV/TV more quickly than the plantar ligament VOI between the ages of 1 and 2. This prediction was made because the plantar ligaments were not expected to produce much tensile stress without a fully developed longitudinal arch and an absence of propulsive toe-off. It was predicted that after 2 years of age the rate of increase in BV/TV should increase in all VOIs after the addition of a toe-off phase, as toe-off is the most strenuous part of gait. Indeed, BV/TV does not change after the initial dip in the first year of life (see figures in Appendix 8.3). When toe-off phase develops at the age of 2, BV/TV increases in the CC and PL, but not in the PTF. However, the PTF already has higher BV/TV and thus may not require additional bone mass to be added. However, BV/TV does not increase as rapidly as was expected with the addition of toe-off.

When toe-off develops after 2 years of age, anisotropy no longer increases in the PTF and CC. There is substantially more variation in DA with increasing age in the PL, whereas DA in the CC and PTF increases steadily. Visual inspection of outliers with low DA in the PL (individual NF821207 - 2 years old, and NF821051 – 8 months old) shows that in these individuals the PL VOI captures both the tensile bands from the plantar ligaments as well as the compressive bands coming from the PTF which are orthogonal and therefore reduce DA. When these two outliers are removed the increase in DA is very similar in all three VOIs until the age of 3, after which DA continues to increase until the age of 5 in the plantar ligaments. This may be a consequence of the fact that the plantar ligament region ossifies later than the other two regions. The longitudinal arch begins developing at 1 years of age but does not finish developing until 4-6 years. Presumably, increased longitudinal arch height will increase tensile stress on the plantar ligaments. Increases in arch height until roughly 5 years of age

may explain why DA in the PL continues to increase until this age, and levels off when maximum arch height is obtained.

A significant problem in interpreting the patterns of trabecular properties with age is that the forces on the foot during gait are not well studied in children. Zeininger (2013) found a significant increase in ground reaction force between 16-month olds (0.89 body weights) compared to 34-month olds (0.95 body weights). This indicates that forces on the calcaneus increase even when correcting for increases in body mass between 16- and 34-month-old children. So why does BV/TV not increase when children start walking independently, but only between the age of 5 and 8? One potential explanation is the incomplete ossification of the calcaneus and the cuboid in young children. The calcaneocuboid facet and the posterior talar facet do not ossify until after age 5 (see figures 8.12 and 8.13). The cartilaginous portions of the CC and PTF VOIs may provide a buffer to the forces of gait. It is possible that when these joints have ossified between 5-8 years of age, the forces placed upon these regions significantly increases with the lack of cartilage buffering. Support for this hypothesis is given by the fact that BV/TV increases with proximity to the subchondral bone plate. Until about 5 years of age the softer foot structure and lower ratio of foot area to body mass result in considerably reduced peak pressures in the infants compared to adults (Hennig and Rosenbaum, 1991). Peak pressures on the heel during gait in 2-year-old children were about one third of those found in adults (Hennig and Rosenbaum, 1991).

The adolescent growth spurt coincides with the onset of puberty and entails significant hormonal changes and an increase in body mass in boys and girls (Bogin, 1999; Lewis, 2007). Females increase in the velocity of growth around 10 years, while the male growth spurt commences around 12 years of age (Lewis, 2007). Unfortunately, there are no individuals between the ages of 12 and 17 in the sample. However, the differences between individuals aged 12 and adults can provide an indication of the amount of change in trabecular structure that takes place during the adolescent growth spurt. Regression lines of the trabecular properties with age of individuals between the ages of 8 and 20 years are plotted in Appendix 8.4. No change in BV/TV occurs in the PL and PTF VOIs, but a significant positive regression is found in the CC between BV/TV and age ($p=.0322$, $R^2=.456$). While strong correlations are found between body mass and Tb.Th in all VOIs, the regressions are not significant. A strong positive correlation is found between age and Tb.Sp in the plantar ligaments, but this also fails to reach significance ($p=.061$, $R^2=.373$). No change in DA is found with age in any of the VOIs. Conn.D shows a strong negative correlation with age in all VOIs, but only reaches significance in the plantar ligaments ($R^2=.519$, $p=.019$). A very similar pattern appears when body mass is plotted with trabecular properties rather than age. While most regressions are not significant, the similarities with regressions reported in Chapter 4 suggest that significant results would likely be found with an increased sample size.

The results from this study confirm previous accounts of trabecular bone ontogeny in which a dense and generalized structure is laid out during endochondral ossification, and later refined to resemble

adult morphology. Experimental work in growing sheep indicates that trabecular bone responds to alterations in loading direction within weeks when a certain strain threshold is crossed (Barak et al., 2011). This demonstrates the significant role that mechanical loading plays in shaping trabecular bone morphology. A similar conclusion can be drawn from the observations in the current study, where trabecular bone was found to adapt gradually to loading associated with the maturation of gait. However, this does not exclude potential effects of genetics through, for example, the placement of mesenchymal cells as suggested by Lovejoy et al. (2003). The results from this work adds to a growing body of evidence supporting the substantial role of mechanical loading in forming both the cortical and trabecular components of the human skeleton (Tardieu, 1999; Ryan and Krovitz, 2006; Tardieu et al., 2006; Gosman and Ketcham, 2009; Barak et al., 2011; Raichlen et al., 2015; Ryan et al., 2017).

Methodological limitations

Individuals younger than 5 and older than 8 belong to separate populations, scanned with different scanners, at different resolutions. The St. Johns population showed strong similarities in trabecular architecture to the Kerma population in Chapter 7. Saers et al. (2016) compared the Norris Farms population to the Kerma and found that Norris Farms have significantly higher BV/TV and Tb.Th in the lower limb than the sedentary Kerma population. It is therefore expected that the Norris Farms population would have significantly greater calcaneal BV/TV compared to St. Johns. Cultural differences in the development of bipedal gait likely exist as well, mainly through the amount of time a baby is carried or allowed to crawl or walk (Tracer et al., 2000; Tracer, 2002). While these practices are unknowable for most archaeological populations, it is not expected that such cultural variation would have a very strong effect on the timing of locomotor development, particularly later in childhood. The gap between individuals aged 5 and 8 makes it unclear how the growth curves of the two populations fit together.

One drawback of using a volume of interest based approach is that the location and size of VOIs are likely not completely homologous. The VOI locations here were chosen because they roughly develop within the first six months of life. However, the articular facets of the calcaneocuboid and posterior talar facet have not fully ossified in the Norris Farms juveniles. Future studies should consider recently developed methods that quantify trabecular structure throughout whole bones, eliminating the need of using VOIs (Tsegai et al., 2013).

Previous chapters have shown that there is substantial variation in trabecular properties within populations. This variation can be detected from the first year of life onwards (Loro et al., 2000; Seeman, 2001). Due to the considerable within population variation, inaccuracies in age estimation, and the combination of two distinct populations, only broad inferences can be made from this study. These issues are common within many anthropological analyses. The similarities found between results reported in this chapter and in the literature on animals and human populations suggests that the

trends reported here are common to mammalian species (Wolschrijn and Weijs, 2004; Ryan and Krovitz, 2006; Gosman and Ketcham, 2009; Gorissen et al., 2016; Ryan et al., 2017). This is the only study of calcaneal trabecular bone development from birth until adulthood, and thus provides valuable insight into the ontogeny of human calcaneal trabecular bone.

Anthropological implications

Understanding ontogeny of trabecular bone structure is relevant to understanding a range of questions in biological anthropology. It relates to bone functional adaptation and behavioural inferences from morphology, the evolution of hominin life-history, potential factors influencing skeletal growth in bioarchaeology, and age-related bone loss in past and present populations (Ryan et al., 2017). Studies of ontogeny of cortical and trabecular structures can provide insights into the mechanical and non-mechanical influences on adult morphology (Ruff, 2005; Ryan et al., 2017). The results of this chapter confirm findings from previous work suggesting that changes in mechanical loading related to the development of bipedal gait result in distinctive trabecular structures (Wolschrijn and Weijs, 2004; Ryan and Krovitz, 2006; Gosman and Ketcham, 2009; Gosman et al., 2010; Acquaah et al., 2015; Gorissen et al., 2016; Ryan et al., 2017). These findings can aid reconstructions of hominin locomotor behaviour and evolutionary changes in life-history. However, a greater understanding is needed first regarding changes in trabecular and cortical bone throughout the postcranium of humans and primates. Growth curves for body mass, age, and trabecular properties in humans and primates would be a valuable dataset for comparisons with hominin fossils. Work on dental and skeletal indicators of growth suggest that australopiths followed a growth trajectory similar to that of chimpanzees, and that early *Homo* from Dmanisi and Turkana grew in stature slightly faster relative to modern humans (Dean, 2016). If patterns of australopith and early *Homo* gait maturation can be determined from trabecular bone, this will be informative about the evolution of their respective life histories if matched to accurate age estimates. However, experimental work is first required to determine whether growth curves of trabecular development are regular and well enough defined to be informative on maturation of gait in humans and great apes.

The study of trabecular bone ontogeny may be of interest to bioarchaeologists. Bone development through time and space has the potential to produce insight into skeletal development and health across variety of cultural and environmental contexts. This will address important questions on the role of habitual behaviour, environment, culture, diet, and genetics on modern age-related bone loss. Ethnographic evidence indicates that the nature of childhood is exceptionally heterogeneous, resulting from factors such as gender, age, birth order and ethnicity. Substantial variation can be found in childhood within and between cultures. Children as young as two to five years old may contribute to household economies, and children as young as five work producing goods for sale and adult profit. Children are estimated to have made up between 40 and 65 percent of past populations (Lillehammer, 2010). Past cultures can therefore not truly be understood without considering children. Because of this, researchers increasingly argue for integrating research on children and childhood into all of

archaeology. Future work should assess whether trabecular bone analysis has the potential to contribute to the field of childhood archaeology by mapping out cultural variation in the habitual activities of children in the past.

Conclusion

This study demonstrates that three regions of the calcaneus develop into distinct adult morphologies through varying developmental trajectories. Changes in trabecular structure were found in the first five years of life that were consistent with predictions based on the development of gait. During the first year of life trabeculae are resorbed leading to a less dense structure with more anisotropic and fewer, but on average thicker trabeculae. After the adoption of unassisted walking, new bone is formed as a response to increased loading. Trabeculae are thickened in the direction of loading resulting in a denser and more anisotropic structure in all three VOIs. Trabecular bone follows predictions based on allometry after gait has matured. The greatest changes in trabecular structure therefore occur while gait develops prior to 8 years of age. These findings support the idea that the calcaneus may be used to track gait maturation in humans. Through comparisons with primate samples this may be a developed into a method of tracking neuromuscular development in hominins, especially when combined with data from the rest of the postcranium (Ryan and Krovitz, 2006; Gosman, 2007; Ryan et al., 2007, 2015, 2017; Gosman and Ketcham, 2009; Raichlen et al., 2015). Future work should consider the ontogeny of trabecular bone in several human populations and primate species.

The extent to which trabecular morphology is genetically canalized throughout growth remains to be determined. Experimental work has demonstrated significant plasticity throughout ontogeny (Barak et al., 2011; Tardieu et al., 2015), but work on precocial animals has been used to suggest that adult morphology emerges prenatally (Skedros et al., 2004, 2007; Gorissen et al., 2016). Comparing trabecular bone development in different types of animals from prenatal to adulthood should provide interesting new data regarding the amount of genetic canalization of trabecular bone structure.

Chapter 9 - Conclusions

Synthesis of findings from the thesis

This thesis focused on the functional adaptation and ontogeny of trabecular bone in the human foot. The aim was to tease apart the factors underlying variation in human trabecular microstructure to determine whether trabecular structure may serve as a useful proxy for inferring behaviour in the past. This is the first study to investigate the three-dimensional trabecular structure in multiple human foot bones, both qualitatively and quantitatively. This work uniquely combines a broad sample of behaviourally and environmentally variable human populations and assessed trabecular variation in these populations from the perspective of various factors including, habitual activity, age, sex, body mass, as well as growth and development. The sample is the largest intraspecies sample used in a study of three-dimensional trabecular structure in both number of individuals and number of populations. To date, this the most thorough study of human trabecular bone variation.

Chapter 2 showed that trabecular bone structure in the talus, calcaneus, and first metatarsal conforms to predictions based on biomechanical models. Regions of the bone subjected to the greatest stress during gait contained the greatest bone volume fraction (BV/TV) and directionally more uniformly loaded regions had more anisotropic structures. Chapter 3 showed that body mass can explain a significant portion of variation in trabecular structure, and that linear bone dimensions do not affect the underlying trabecular structure when variance associated with body mass is controlled. Regressions were performed between body mass and trabecular properties in Chapter 4. Trabeculae become significantly more widely spaced and less interconnected with an increase in body mass. Residuals from significant regressions were used in subsequent chapters as body mass corrected variables. In Chapter 5, significant sexual dimorphism in trabecular structure was predicted based on previous analyses of limb bone cross-sectional geometry. However, little sexual dimorphism was found in trabecular properties after controlling for the effects of body mass. Significant differences in trabecular structure were found between three age categories in Chapter 6. Unfortunately, age could not be inferred for many individuals and therefore could not be statistically controlled for in subsequent analyses. It was concluded that future work should control for age whenever possible. Inferred levels of terrestrial mobility were found to strongly correlate with trabecular properties in Chapter 7. The four human populations showed similar patterns of trabecular properties throughout the foot with a signal of mobility category superimposed upon it. More mobile populations possessed greater bone volume fraction with thicker, fewer, and more closely packed trabeculae. Results from Chapter 8 demonstrate that trabecular bone in the foot develops similarly to trabecular bone in other mammals and anatomical locations, indicating a highly conserved process. Trabecular bone was shown to be deposited in a uniform way and is subsequently reorganized through mechanical loading associated with the maturation of gait.

Chapters 7 and 8 demonstrate that both the forces incurred through terrestrial mobility and during the development of gait shape the trabecular structures observed in the adult foot. Recently published work on foot binding provides additional evidence for the plasticity of trabecular structure and the role of mechanical loading in shaping the internal trabecular structure of the human foot (Reznikov et al., 2017). The results from Chapters 4 to 6 indicate that significant portions of noise in the data can be attributed to variation in age, sex, and body mass. This work has demonstrated that trabecular bone may serve as a useful proxy of habitual behaviour in hominin fossils and past populations when all contributing factors are carefully considered and ideally statistically controlled for.

Implications for the study of human evolution

Habitual bipedalism is one of the defining attributes of the human species, yet its first appearance in the hominin fossil record, and the nature of foot function in fossil hominins are debated (Stern and Susman, 1983; Langdon et al., 1991; Stern, 2000; Senut et al., 2001; Ward, 2002; Harcourt-Smith and Aiello, 2004; Richmond and Jungers, 2008; DeSilva, 2009; Lovejoy et al., 2009; Haile-Selassie et al., 2012; Almécija et al., 2013; Harcourt-Smith et al., 2015). The fossil record provides a complex image of the evolution of the foot, with roughly contemporary species showing substantial variation in foot morphology and inferred function. External bone morphology can arguably contain unused retentions of ancestral traits that are no longer functional and provide a false indication of habitual behaviour (Gould and Lewontin, 1979; Ward, 2002). Results presented in this dissertation have shown that trabecular bone structure is not as strictly bound by a genetic *bauplan* as external features. Results presented in this dissertation indicate that trabecular bone adapts to both intensity and directionality of loading during life, supporting the idea that trabecular bone may be effective at distinguishing locomotor correlates from phylogenetic baggage. The analysis of trabecular structure in fossil hominins can therefore be used to complement functional analyses based on external morphology and provide new insights into the evolution of human bipedalism.

The results from Chapter 7 and recently published work point towards a strong relationship between terrestrial mobility and trabecular structure in the foot and lower limbs (Saers et al., 2016; Chirchir et al., 2017; Reznikov et al., 2017; Stieglitz et al., 2017). The emergence of *Homo erectus* was accompanied by an increase in brain size (McHenry and Coffing, 2000), variation in body mass (Will and Stock, 2015), increasingly efficient bipedal locomotion (Pontzer, 2007), and increased levels of terrestrial mobility (Braun et al., 2009). The high levels of terrestrial mobility throughout the evolution of the genus *Homo* indicates that the human skeleton evolved in a context of substantial and persistent mechanical loading during life (Bramble and Lieberman, 2004; Raichlen et al., 2012; Shaw and Stock, 2013). Trends over the past 10.000 years in trabecular bone (Chirchir et al., 2015, 2017; Ryan and Shaw, 2015) and cortical bone (Holt, 2003; Shaw and Stock, 2013; Macintosh et al., 2014; Ruff et al., 2015) point to a significant decrease in skeletal robusticity in human populations after the adoption of agriculture. These trends culminate in the increasing prevalence of osteoporosis in industrialised societies and have been associated with increasingly sedentary lifestyles (Borer, 2005). To interpret

these important trends in robusticity throughout human evolution, a more detailed understanding of the factors underlying variation in trabecular bone microstructure is required. The results presented in this dissertation have provided a first step by demonstrating that trabecular bone in the human foot can serve as a proxy for terrestrial mobility in bioarchaeological studies. However, trabecular bone was also shown to be a complex structure, influenced by numerous non-behavioural variables. The next step should be to increase sample sizes and the numbers of populations and anatomical locations examined in bioarchaeological analyses of trabecular bone. Future work should attempt to correct for the influence of age and body mass, and explore potential effects of diet and climate on trabecular structure. Only by taking an integrated approach can we hope to confidently interpret the patterns of trabecular bone variation in the past.

Methodological considerations

Using seventeen volumes of interest throughout this dissertation presented both advantages and disadvantages. Collecting and analysing all VOIs was a time-consuming process. The considerable number of variables result in inflated type I error rates, although this was mitigated by the strong correlations between properties across VOIs. Using seventeen VOIs resulted in missing values due to poor preservation of some of the archaeological material. A choice had to be made for each analysis whether it was most appropriate to run analyses listwise or pairwise. Fortunately, the differences between listwise or pairwise approaches were slight and appeared to result from differences in sample size rather than sample composition.

The merits of using multiple VOIs per bone depend on the question that is asked. Results from Chapters 2 and 7 showed that patterns of trabecular properties throughout the human foot were very similar between populations, with a signature of mobility superimposed upon them. Scaling relationships with body mass were also similar throughout all VOIs. These results suggest that questions relating to the effects of loading intensity, allometry, and age may be answerable using a single VOI per bone. Time saved through this procedure could be spent collecting larger samples. However, data not published in this thesis clearly show clear species-specific patterns of talar BV/TV and anisotropy in humans and great apes. Using numerous VOIs per bone is therefore a productive approach to examine interspecies variation in trabecular structure.

Using VOIs to study calcaneal ontogeny in Chapter 8 showed interesting patterns with age. It was challenging to find homologous VOI locations and sizes, although similarities in the patterns between VOIs suggest that this was not a substantial issue. An advantage of using VOIs is that statistical tests can be performed. However, visual inspection of 3D models was found to be highly informative in interpreting quantitative results from the VOIs. A better approach to studying trabecular bone ontogeny would be to use whole bone quantifications of trabecular structure (see Gross et al. 2014).

Chapters 3 to 6 showed that numerous factors underlie variation in trabecular structure, including inferred terrestrial mobility, age, sex, body mass, and potentially bone shape. Because age could not be

inferred for many individuals it was not possible to include it as a covariate in statistical models. Future work should endeavour to statistically account for the effects of age and body mass when attempting to infer behavioural differences between human populations.

Areas for further study

The current study examined trabecular structure in foot bones with similar biomechanical functions. It is expected that the strong similarities found in the patterns throughout the foot are a consequence of this relatively constrained loading environment. It is still an open question whether skeletal elements that are more variably loaded such as the upper limb will exhibit similar conservation of patterns of variation between populations. Results from Chapter 2 showed that BV/TV in the foot is proportional to loading magnitude during gait, with the greatest BV/TV occurring in the regions subjected to the greatest loading. In a study on trabecular structure throughout the lower limb, Saers et al. (2016) report that BV/TV is lowest in the distal tibia despite this region being subjected to the highest loading. This discrepancy may be due to canalization in the distal tibia or differences in form/function of tarsals and long bones. Future work should endeavour to map trabecular structure in skeletal elements with different biomechanical functions throughout the postcranium in various human populations. Such a study would be able to assess how much variation is systemic and how much is plastic in response to joint loading.

Experimental work has demonstrated that trabecular bone adapts to mechanical loading and this thesis has provided evidence that this can be observed in past human populations with substantially different inferred mobility levels. However, controlled experimental studies are needed to assess whether trabecular bone can be used to detect more subtle signals of habitual activity in past populations. This question is best addressed through experiments that alter the frequency, duration, and intensity of loading in groups of animals. This study design also allows investigation of potential differences in mechanoresponsiveness of cortical and trabecular bone. Inbred mouse strains can be used to eliminate noise caused by genetic variation within populations. The experiments can be repeated with outbred mice to test whether subtle differences in loading can be detected in genetically variable populations (cf. Wallace et al. 2015).

Fossils and archaeological samples are often damaged and incomplete, but their trabecular structures may still provide a wealth of information. Body mass has no significant effects on adult human BV/TV and DA, and very minor effects on large interspecific samples. This, indicates that fragmentary fossils may still provide data on joint loading directionality and magnitude. Similar patterns of variation in BV/TV were observed in VOIs throughout the human foot between human populations. Correlations of BV/TV between VOIs are highly significant with correlation coefficients greater than .80 within bones and .70 between foot bones. This indicates that BV/TV in one VOI can potentially be predicted from other VOIs. Disarticulated and broken archaeological bones may therefore still be useful in assessments of population mobility level in the past. However, such

methods are likely only suitable to anatomical locations with constrained biomechanical functions such as the human foot that are loaded predictably during life.

Correlations between lower limb cortical and trabecular bone parameters reported in Appendix 5.4 were weak and differed per population. Both tissues are influenced by their loading environment, but the weak correlations show that other factors also underlie their adult morphologies. There are numerous possible explanations for this finding and many questions for future research regarding the dynamics of both tissues. Cortical and trabecular bone may be affected differently by mechanical loading, respond differently at different ages, and between sexes. Only when they are considered in conjunction can we obtain insight into what both tissues can tell about behaviour in the past.

It remains unclear how variation in external shape and cortical shell thickness within and across species affects the underlying trabecular morphology. These are crucial methodological issues that need to be addressed before confident inferences of hominin behaviour can be made from fossil trabecular morphology. Both methodological issues can be tackled through a combination of a large dataset of skeletal elements varying in size and shape, with hypotheses generated through finite element analysis. Finite element analysis can be used on models of bones with varying external shapes to assess potential variation in stress distribution associated with different morphologies. These stress distributions can then be compared to trabecular and cortical structures across a large sample of modern humans and apes. Cortical shell thickness and its potential covariance with underlying trabecular structure can be examined using currently available methods.

Much anthropological work has focused on correlating locomotor mode to trabecular bone structure in various primate species. Numerous studies have examined interspecific variation in single volumes of interest. It is shown in Chapters 2 and 7 that all human populations show similar patterns of trabecular properties distributed throughout the foot. Unpublished work comparing the talus of humans to great apes shows each species has a distinctive pattern of trabecular properties throughout the talus. This result indicates that interspecies locomotor correlates are best assessed using multiple volumes of interest to investigate variation in patterns of trabecular bone structure. Using this approach, trabecular structure can be used to infer both habitual activity levels as well as locomotor mode in fossil hominins.

The combination of a large and diverse sample, combined with the focus on numerous potential variables affecting trabecular bone variation has resulted in the most thorough study of intra-species trabecular structure and its underlying mechanisms to date. This dissertation has demonstrated that there is substantial intraspecies variation in trabecular structure that can be correlated to various behavioural and non-behavioural factors. Trabecular bone in the calcaneus changes in predictably to changes in gait in growing children, suggesting trabecular structure reflects the loading environment during life. These results contribute to a growing body of evidence indicating that analysis of

trabecular structure has tremendous potential for bioarchaeologists and paleoanthropologists to paint an ever more detailed picture of life in the past.

References

Aaron, J.E., Makins, N.B., Sagreiya, K., 1987. The microanatomy of trabecular bone loss in normal aging men and women. Clin. Orthop. Relat. Res. 215, 260–271.

Abelow, B.J., Holford, T.R., Insogna, K.L., 1992. Cross-cultural association between dietary animal protein and hip fracture: a hypothesis. Calcif. Tissue Int. 50, 14–8.

Acquaah, F., Robson Brown, K.A., Ahmed, F., Jeffery, N., Abel, R.L., 2015. Early trabecular development in human vertebrae: Overproduction, constructive regression, and refinement. Front. Endocrinol. (Lausanne). 6.

Addison, F., 1949. Jebel Moya. Oxford University Press, London.

Agarwal, S.C., 2007. Light and Broken Bones: Examining and Interpreting Bone Loss and Osteoporosis in Past Populations. Biol. Anthropol. Hum. Skelet. Second Ed. 387–410.

Agarwal, S.C., Dumitriu, M., Tomlinson, G.A., Grynpas, M.D., 2004. Medieval trabecular bone architecture: the influence of age, sex, and lifestyle. Am. J. Phys. Anthropol. 124, 33–44.

Akhter, M.P., Cullen, D.M., Pedersen, E.A., Kimmel, D.B., Recker, R.R., 1998. Bone response to in vivo mechanical loading in two breeds of mice. Calcif. Tissue Int. 63, 442–449.

Allen, J.A., 1877. The Influence of Physical Conditions of the Genesis of Species. Radic. Rev. 1, 108–140.

Almécija, S., Tallman, M., Alba, D.M., Pina, M., Moyà-Solà, S., Jungers, W.L., 2013. The femur of Orrorin tugenensis exhibits morphometric affinities with both Miocene apes and later hominins. Nat. Commun. 4, 2888.

Amling, M., Herden, S., Posl, M., Hahn, M., Ritzel, H., Delling, G., 1996. Heterogeneity of the skeleton: comparison of the trabecular microarchitecture of the spine, the iliac crest, the femur, and the calcaneus. J. Bone Miner. Res. 11, 36–45.

Armstrong, R.A., 2014. When to use the Bonferroni correction. Ophthalmic Physiol. Opt. J. Br. Coll. Ophthalmic Opt. 34, 502–508.

Aspray, T.J., Prentice, A., Cole, T.J., Sawo, Y., Reeve, J., Francis, R.M., 1996. Low bone mineral content is common but osteoporotic fractures are rare in elderly rural Gambian women. J. bone Miner. Res. 11, 1019–25.

Athavale, S.A., Joshi, S.D., Joshi, S.S., 2008. Internal architecture of the talus. Foot Ankle Int. 29, 82–6.

Badyaev, A., Martin, T., 2000. Individual variation in growth trajectories: phenotypic and genetic correlations in ontogeny of the house finch (Carpodacus mexicanus). J. Evol. Biol. 13, 290–301.

Ballard, T.L.P., Clapper, J.A., Specker, B.L., Binkley, T.L., Vukovich, M.D., 2005. Effect of protein supplementation during a 6-mo strength and conditioning program on insulin-like growth factor I and markers of bone turnover in young adults. Am. J. Clin. Nutr. 81, 1442–1448.

Barak, M.M., Lieberman, D.E., Hublin, J.-J., 2011. A Wolff in sheep's clothing: trabecular bone adaptation in response to changes in joint loading orientation. Bone. 49, 1141–51.

Barak, M.M., Lieberman, D.E., Hublin, J.J., 2013. Of mice, rats and men: Trabecular bone architecture in mammals scales to body mass with negative allometry. J. Struct. Biol. 183, 123–131.

Barak, M.M., Lieberman, D.E., Raichlen, D., Pontzer, H., Warrener, A.G., Hublin, J.-J., 2013. Trabecular evidence for a human-Like gait in Australopithecus africanus. PLoS One. 8, e77687.

Bergmann, C., 1847. Ueber die Verhältnisse der Wärmeökonomie der Thiere zu ihrer Grösse (Concerning the relationship of heat conservation of animals to their size). Gottinger Stud. 3,

595–708.

Bertsch, C., Unger, H., Winkelmann, W., Rosenbaum, D., 2004. Evaluation of early walking patterns from plantar pressure distribution measurements. First year results of 42 children. Gait Posture. 19, 235–242.

Betti, L., Balloux, F., Amos, W., Hanihara, T., Manica, A., 2009. Distance from Africa, not climate, explains within-population phenotypic diversity in humans. Proc. R. Soc. B Biol. Sci. 276, 809–814.

Biewener, A., 1989. Scaling body support in mammals: limb posture and muscle mechanics. Science (80-.). 245, 45–48.

Birmingham, R., Eisenberg, L.E., 2000. Indian Mounds of Wisconsin. University of Wisconsin Press, Madison.

Bogin, B., 1999. Patterns of Human Growth, Second edi. ed. Cambridge University Press, Cambridge.

Bonnet, C., 1986. Les fouilles archeologique de Kerma (Soudan). In: Bonnet, C., Privati, B., Simon, C., Chaix, L., de Paepe, P. (Eds.), Kerma. Musee d'art et d'histoire, Geneva, pp. 1–41.

Borer, K.T., 2005. Physical activity in the prevention and amelioration of osteoporosis in women : interaction of mechanical, hormonal and dietary factors. Sports Med. 35, 779–830.

Bramble, D.M., Lieberman, D.E., 2004. Endurance running and the evolution of Homo. Nature. 432, 345–52.

Brass, M., 2014. The southern frontier of the Meroitic state: the view from Jebel Moya. African Archaeol. Rev. 425–445.

Brass, M., 2015a. Results from the re-investigation of Hencry Wellcome's 1911-14 excavations at Jebel Moya. Sudan and Nubia. 19, 170–180.

Brass, M., 2015b. Interactions and pastoralism along the southern and southeastern frontiers of the Meroitic State, Sudan. J. World Prehistory. 3, 4–37.

Brass, M., Schwenniger, J.-L., 2013. Jebel Moya (Sudan): New dates from a mortuary complex at the southern Meroitic frontier. Azania Archaeol. Res. Africa. 48, 455–472.

Braun, D.R., Harris, J.W.K., Maina, D.N., 2009. Oldowan raw material procurement and use: evidence from the Koobi Fora formation. Archaeometry. 51, 26–42.

Brickley, M., 1997. Age-Related Bone Loss And Osteoporosis In Archaeological Bone: A Study Of Two London Collections, Redcross Way and Farringdon Street. University College London.

Bridges, P.S., 1989. with the Changes in Activities in the Shift to Agriculture United States1 Southeastern. Curr. Anthropol. 30, 385–394.

Brooks, A.S., Suchey, J.M., 1990. Skeletal age determination based on the os pubis: a comparison of the Acsádi-Nemeskéri and Suchey-Brooks methods. Hum. Evol. 5, 227–238.

Brothwell, D.R., 1981. Digging up bones: the excavation, treatment, and study of human skeletal remains. Cornell University Press, New York.

Buikstra, J., Ubelaker, D.H., 1994. Standards for data collection from human remains. In: Arkansas Archaeological Survey. Report Number 44.

Buikstra, J.E., Milner, G.R., 1991. Isotopic and archaeological interpretations of diet in the central mississippi valley. J. Archaeol. Sci. 18, 319–329.

Burger, E.H., Klein-Nulend, J., 1999. Mechanotransduction in bone: role of the lacuno-canalicular network. FASEB J. 13 Suppl, S101-12.

Burr, D.B., Organ, J.M., 2017. Postcranial Skeletal Development and Its Evolutionary Implications.

In: Percival, C.J., Richtsmeier, J.T. (Eds.), Building Bones Bone Formation and Development in Anthropology. Cambridge University Press, Cambridge, pp. 148–174.

Byers, S., Moore, A., Byard, R., Fazzalari, N., 2000. Quantitative histomorphometric analysis of the human growth plate from birth to adolescence. Bone. 27, 495–501.

Calhoun, J.H., Li, F., Ledbetter, B.R., Viegas, S.F., 1994. A comprehensive study of pressure distribution in the ankle joint with inversion and eversion. Foot Ankle Int. 15, 125–133.

Callewaert, F., Sinnesael, M., Gielen, E., Boonen, S., Vanderschueren, D., 2010. Skeletal sexual dimorphism: Relative contribution of sex steroids, GH-IGF1, and mechanical loading. J. Endocrinol. 207, 127–134.

Carlson, K.J., Grine, F.E., Pearson, O.M., 2007. Robusticity and sexual dimorphism in the postcranium of modern hunter-gatherers from Australia. Am. J. Phys. Anthropol. 134, 9–23.

Carlson, K.J., Judex, S., 2007. Increased non-linear locomotion alters diaphyseal bone shape. J. Exp. Biol. 210, 3117–3125.

Carlson, K.J., Lublinsky, Ã.S., Judex, S., 2008. Do different locomotor modes during growth modulate trabecular architecture in the murine hind limb ? Integr. Comp. Biol. 48, 385–393.

Carter, D.R., Beaupré, G.S., 2001. Skeletal function and form: mechanobiology of skeletal development, aging and regeneration. Cambridge University Press, New York.

Cessford, C., 2012. The Old Divinity School, Cambridge. An archaeological excavation. Cambridge.

Cessford, C., 2015. The St. John's Hospital Cemetery and Environs, Cambridge: Contextualizing the Medieval Urban Dead. Archaeol. J. 172, 52–120.

Chang, G., Pakin, S.K., Schweitzer, M.E., Saha, P.K., Regatte, R.R., 2008. Adaptations in trabecular bone microarchitecture in Olympic athletes determined by 7T MRI. J. Magn. Reson. Imaging. 27, 1089–95.

Chirchir, H., Kivell, T.L., Ruff, C.B., Hublin, J., Carlson, K.J., Zipfel, B., 2015. Recent origin of low trabecular bone density in modern humans. Proc. Natl. Acad. Sci. 112, 366–371.

Chirchir, H., Ruff, C.B., Junno, J.-A., Potts, R., 2017. Low trabecular bone density in recent sedentary modern humans. Am. J. Phys. Anthropol. e23138.

Christen, P., Ito, K., Ellouz, R., Boutroy, S., Sornay-Rendu, E., Chapurlat, R.D., van Rietbergen, B., 2014. Bone remodelling in humans is load-driven but not lazy. Nat. Commun. 5, 4855.

Christen, P., Ito, K., van Rietbergen, B., 2015. A potential mechanism for allometric trabecular bone scaling in terrestrial mammals. J. Anat. n/a-n/a.

Christman, R.A., 2003. Foot and ankle radiology. Churchill Livingston Elsevier, Philadelphia.

Churchill, S.E., 1994. Human upper body evolution in the Eurasian later Pleistocene. University of New Mexico.

Cotter, M.M., Loomis, D. a, Simpson, S.W., Latimer, B., Hernandez, C.J., 2011. Human evolution and osteoporosis-related spinal fractures. PLoS One. 6, e26658.

Cowgill, L.W., 2010. The ontogeny of Holocene and Late Pleistocene human postcranial strength. Am. J. Phys. Anthropol. 141, 16–37.

Cunningham, C.A., Black, S.M., 2009. Anticipating bipedalism: trabecular organization in the newborn ilium. J. Anat. 214, 817–29.

Currey, J.., 1984. The mechanical adaptations of bone. Princeton University Press.

Currey, J.., 2003. The many adaptations of bone. J. Biomech. 36, 1487–1495.

Currey, J.D., 2002. Bones: structure and mechanics. Princeton University Press, Princeton.

Dacke, C.G., Arkle, S., Cook, D.J., Wormstone, I.M., Jones, S., Zaidi, M., Bascal, Z. a., 1993. Medullary Bone and Avian Calcium Regulation. J. Exp. Biol. 88, 63–88.

Davies, T.G., 2012. Cross-sectional variation in the human femur and tibia: the influence of physique and habitual mobility on diaphiseal morphology. University of Cambridge.

Dawe, E.J.C., Davis, J., 2011. Anatomy and biomechanics of the foot and ankle. Orthop. Trauma. 25, 279–286.

De Groote, I., Humphrey, L.T., 2011. Body mass and stature estimation based on the first metatarsal in humans. Am. J. Phys. Anthropol. 144, 625–632.

Dean, M., 2016. Measures of maturation in early fossil hominins: Events at the first transition from australopiths to early Homo. Philos. Trans. R. Soc. London Biol. Sci. 371, 1–12.

Del Giudice, M., Angeleri, R., Manera, V., 2009. The juvenile transition: A developmental switch point in human life history. Dev. Rev. 29, 1–31.

DeSilva, J.M., 2009. Functional morphology of the ankle and the likelihood of climbing in early hominins. Proc. Natl. Acad. Sci. U. S. A. 106, 6567–6572.

DeSilva, J.M., Devlin, M.J., 2012. A comparative study of the trabecular bony architecture of the talus in humans, non-human primates, and Australopithecus. J. Hum. Evol. 63, 536–51.

Devlin, M.J., Robbins, A., Shipp, L., Alajbegovic, K., 2016. Cold exposure decreases trabecular bone mass in young mice: implications for human bone acquisition. In: The 85th Annual Meeting of the American Association of Physical Anthropologists.

DeWitte, S.N., Stojanowski, C.M., 2015. The Osteological Paradox 20 Years Later: Past Perspectives, Future Directions. J. Archaeol. Res. 23, 397–450.

Ding, M., Odgaard, A., Linde, F., Hvid, I., 2002. Age-related variations in the microstructure of human tibial cancellous bone. J. Orthop. Res. 20, 615–21.

Djuric, M., Djonic, D., Milovanovic, P., Nikolic, S., Marshall, R., Marinkovic, J., Hahn, M., 2010. Region-specific sex-dependent pattern of age-related changes of proximal femoral cancellous bone and its implications on differential bone fragility. Calcif. Tissue Int. 86, 192–201.

Doube, M., 2010. BoneJ: free and extensible bone image analysis in Image J. Bone. 47, 1076–1079.

Doube, M., 2015. The ellipsoid factor for quantification of rods, plates, and intermediate forms in 3D geometries. Front. Endocrinol. (Lausanne). 6, 1–5.

Doube, M., Klosowski, M.M., Wiktorowicz-Conroy, A.M., Hutchinson, J.R., Shefelbine, S.J., 2011. Trabecular bone scales allometrically in mammals and birds. Proc. Biol. Sci. 278, 3067–73.

Dougherty, R., Kunzelmann, K.-H., 2007. Computing local thickness of 3D structures with ImageJ. Microsc. Microanal. 13, 1678–1679.

Drinkwater, B.L., Chesnut, C.H., 1991. Bone density changes during pregnancy and lactation in active women: a longitudinal study. Bone Miner. 14, 153–160.

Duan, Y., Turner, C.H., Kim, B.T., Seeman, E., 2001. Sexual dimorphism in vertebral fragility is more the result of gender differences in age-related bone gain than bone loss. J. Bone Miner. Res. 16, 2267–2275.

Dubois, L., Girard, M., Girard, A., Tremblay, R., Boivin, M., Perusse, D., others, 2007. Genetic and environmental influences on body size in early childhood: a twin birth-cohort study. Twin Res. Hum. Genet. 10, 479–485.

Ducher, G., Courteix, D., Même, S., Magni, C., Viala, J.F., Benhamou, C.L., 2005. Bone geometry in response to long-term tennis playing and its relationship with muscle volume: A quantitative magnetic resonance imaging study in tennis players. Bone. 37, 457–466.

Dunsworth, H.M., 2006. Proconsul heseloni feet from Rusinga Island, Kenya. The Pennsylvania State University.

Eaton, B.., Nelson, D.., 1991. Calcium in evolutionary perspective. Am. J. Clin. Nutr. 281–287.

Eaton, S.B., Konner, M., Shostak, M., 1988. Stone Aagers in the fast lane: chronic degenerative diseases in evolutionary perspective. Am. J. Med. 84, 739–749.

Eckstein, F., Matsuura, M., Kuhn, V., Priemel, M., Müller, R., Link, T.M., Lochmüller, E.-M., 2007. Sex differences of human trabecular bone microstructure in aging are site-dependent. J. Bone Miner. Res. 22, 817–824.

Elders, P.J., Lips, P., Netelenbos, J.C., van Ginkel, F.C., Khoe, E., van der Vijgh, W.J., van der Stelt, P.F., 1994. Long-term effect of calcium supplementation on bone loss in perimenopausal women. J. Bone Miner. Res. 9, 963–70.

Elftman, H., 1960. The transverse tarsal joint and its control. Clin. Orthop. 17, 41–46.

Erdemir, A., Hamel, A.J., Fauth, A.R., Piazza, S.J., Sharkey, N.A., 2004. Dynamic loading of the plantar aponeurosis in walking. J. Bone Joint Surg. Am. 86–A, 546–52.

Eriksen, E.F., 1986. Normal and pathological remodeling of human trabecular bone: three dimensional reconstruction of the remodeling sequence in normals and in metabolic bone disease. Endocr. Rev. 7, 379–408.

Fajardo, R.J., Desilva, J.M., Manoharan, R.K., Schmitz, J.E., Maclatchy, L.M., Bouxsein, M.L., 2013. Lumbar vertebral body bone microstructural scaling in small to medium-sized strepsirhines. Anat. Rec. 296, 210–226.

Fajardo, R.J., Müller, R., 2001. Three-dimensional analysis of nonhuman primate trabecular architecture using micro-computed. Am. J. Phys. Anthropol. 336, 327–336.

Fajardo, R.J., Müller, R., Ketcham, R.A., Colbert, M., 2007. Nonhuman anthropoid primate femoral neck trabecular architecture and its relationship to locomotor mode. Anat. Rec. 290, 422–436.

Feskanich, D., Colditz, G., Stampfer, M., Willett, W., 1994. Dietary calcium and bone-fractures in middle-aged women. J. Epidemiol. 139, 55–55.

Field, A., 2013. Discovering Statistics Using R, Statistics.

Forwood, M.R.., Burr, D.B., 1993. Physical activity and bone mass: exercises in futility? Bone Miner. 21, 89–112.

Frankel, V.H., Nording, M., 2012. Biomechanics of Bone. In: Nording, M., Frankel, V.H. (Eds.), In: Frankel, V.H., Nordin, M. (Eds.) Basic Biomechanics of the Musculoskeletal System. Wolters Kluwer, Baltimore, USA, pp. 24–59.

Frost, H.M., 2003. Bone's mechanostat: a 2003 update. Anat. Rec. A. Discov. Mol. Cell. Evol. Biol. 275, 1081–101.

Frost, H.M., Jee, W.S., 1994a. Perspectives: applications of a biomechanical model of the endochondral ossification mechanism. Anat. Rec. 240, 447–55.

Frost, H.M., Jee, W.S., 1994b. Perspectives: a vital biomechanical model of the endochondral ossification mechanism. Anat. Rec. 240, 435–46.

Garman, R., Gaudette, G., Donahue, L., Rubin, C., Judex, S., 2007. Low-level accelerations applied in the absence of weight bearing can enhance trabecular bone formation. J. Orthop. Res. 25, 732–740.

Gefen, A., 2002. Stress analysis of the standing foot following surgical plantar fascia release. J. Biomech. 35, 629–637.

Gefen, A., Megido-Ravid, M., Itzchak, Y., Arcan, M., 2000. Biomechanical analysis of the three-

dimensional foot structure during gait: a basic tool for clinical applications. J. Biomech. Eng. 122, 630–639.

Gefen, A., Seliktar, R., 2004. Comparison of the trabecular architecture and the isostatic stress flow in the human calcaneus. Med. Eng. Phys. 26, 119–29.

Giddings, V.L., Beaupré, G.S., Whalen, R.T., Carter, D.R., 2000. Calcaneal loading during walking and running. Med. Sci. Sport. excercise. 32, 627–634.

Gilsanz, V., Wren, T. AL, Sanchez, M., Dorey, F., Judex, S., Rubin, C., 2006. Low-Level, High-Frequency Mechanical Signals Enhance Musculoskeletal Development of Young Women With Low BMD. J. Bone Miner. Res. 21, 1464–1474.

Glasoe, W.M., Yack, H.J., Saltzman, C.L., 1999. Anatomy and biomechanics of the first ray. Phys. Ther. 79, 854–859.

Gordon, K., Levy, C., Perl, M., Weeks, O., 1993. Experimental perturbation of the development of sexual size dimorphism in the mouse skeleton. Growth, Dev. aging GDA. 58, 95–104.

Gorissen, B.M.C., Wolschrijn, C.F., van Vilsteren, A.A.M., van Rietbergen, B., van Weeren, P.R., 2016. Trabecular bone of precocials at birth; Are they prepared to run for the wolf(f)? J. Morphol. 277, 948–956.

Gosman, J., 2007. Patterns in Ontogeny of Human Trabecular bone from Sunwatch Village in the Prehistoric Ohio valley. Ohio State University.

Gosman, J.H., Ketcham, R.A., 2009. Patterns in ontogeny of human trabecular bone from SunWatch Village in the Prehistoric Ohio Valley: general features of microarchitectural change. Am. J. Phys. Anthropol. 138, 318–32.

Gosman, J.H., Ryan, T.M., Raichlen, D.A., 2010. Trabecular bone ontogeny and locomotor development in humans and non-human primates.

Gould, S.J., Lewontin, R.C., 1979. The Spandrels of San Marco and the Panglossian Paradigm: A Critique of the Adaptationist Programme. Proc. R. Soc. B Biol. Sci. 205, 581–598.

Goulet, R.W., Goldstein, S.A., Ciarelli, M.J., Kuhn, J.L., Brown, M.B., Feldkamp, L.A., 1994. The relationship between the structural and orthogonal compressive properties of trabecular bone. J. Biomech. 27, 375–89.

Greendale, G., Barrett-Connor, E., Edelstein, S., Ingles, S., Haile, R., 1995. Lifetime leisure exercise and osteoporosis. Clin. J. Sport Med. 141, 951–959.

Griffin, N.L., D'Août, K., Richmond, B., Gordon, A., Aerts, P., 2010a. Comparative in vivo forefoot kinematics of Homo sapiens and Pan paniscus. J. Hum. Evol. 59, 608–19.

Griffin, N.L., D'Août, K., Ryan, T.M., Richmond, B.G., Ketcham, R.A., Postnov, A., 2010b. Comparative forefoot trabecular bone architecture in extant hominids. J. Hum. Evol. 59, 202–13.

Grine, F.E., Jungers, W.L., Tobias, P. V, Pearson, O.M., 1995. Fossil Homo femur from Berg Aukas, northern Namibia. Am. J. Phys. Anthropol. 97, 151–85.

Gross, T., Kivell, T.L., Skinner, M.M., Nguyen, N.H., Pahr, D.H., 2014. A CT-image-based framework for the holistic analysis of cortical and trabecular bone morphology. Palaeontol. Electron. 17, 1–13.

Gross, T.S., Srinivasan, S., 2006. Building bone mass through exercise: could less be more? Br. J. Sports Med. 40, 2–3.

Grundy, M., Tosh, P.A., McLeish, R.D., Smidt, L., 1975. An investigation of the centres of pressure under the foot while walking. J. Bone Joint Surg. Br. 57, 98–103.

Haapasalo, H., Kontulainen, S., Sievänen, H., Kannus, P., Järvinen, M., Vuori, I., 2000. Exercise-induced bone gain is due to enlargement in bone size without a change in volumetric bone

density: a peripheral quantitative computed tomography study of the upper arms of male tennis players. Bone. 27, 351–7.

Hagins, M., Pappas, E., 2012. Biomechanics of the Foot and Ankle. In: Nording, M., Frankel, V.H. (Eds.), Basic Biomechanics of the Musculoskeletal System. Wolters Kluwer, Baltimore, USA, pp. 224–253.

Haile-Selassie, Y., Saylor, B.Z., Deino, A., Levin, N.E., Alene, M., Latimer, B.M., 2012. A new hominin foot from Ethiopia shows multiple Pliocene bipedal adaptations. Nature. 483, 565–9.

Hallemans, A., De Clercq, D., Otten, B., Aerts, P., 2005. 3D joint dynamics of walking in toddlers A cross-sectional study spanning the first rapid development phase of walking. Gait Posture. 22, 107–18.

Hallemans, A., De Clercq, D., Van Dongen, S., Aerts, P., 2006. Changes in foot-function parameters during the first 5 months after the onset of independent walking: a longitudinal follow-up study. Gait Posture. 23, 142–8.

Harcourt-Smith, W.E.H., Aiello, L.C., 2004. Fossils, feet and the evolution of human bipedal locomotion. J. Anat. 204, 403–16.

Harcourt-Smith, W.E.H., Throckmorton, Z., Congdon, K.A., Zipfel, B., Deane, A.S., Drapeau, M.S.M., Churchill, S.E., Berger, L.R., DeSilva, J.M., 2015. The foot of Homo naledi. Nat. Commun. 6, 8432.

Harper, A.B., Laughlin, W.S., Mazess, R.B., 1984. Bone Mineral Content in St . Lawrence Island Eskimos. Hum. Biol. 56, 63–78.

Harrigan, T., Jasty, M., Mann, R., Harris, W., 1988. Limitations of the Continuum Assumption in Cancellous Bone. J. Biomech. 21, 269–275.

Harrison, L.C. V, Nikander, R., Sikiö, M., Luukkaala, T., Helminen, M.T., Ryymin, P., Soimakallio, S., Eskola, H.J., Dastidar, P., Sievänen, H., 2011. MRI texture analysis of femoral neck: Detection of exercise load-associated differences in trabecular bone. J. Magn. Reson. Imaging. 34, 1359–66.

Hatala, K.G., Dingwall, H.L., Wunderlich, R.E., Richmond, B.G., 2013. Variation in foot strike patterns during running among habitually barefoot populations. PLoS One. 8, e52548.

Heaney, R.P., 2003. How does bone support calcium homeostasis? Bone. 33, 264–268.

Hennig, E.M., Rosenbaum, D., 1991. Pressure distribution patterns under the feet of children in comparision with adults. Foot Ankle Int. 15, 35–40.

Higgins, R.W., 2014. The effects of terrain on long bone robusticity and cross-sectional shape in lower limb bones of bovids, Neandertals, and Upper Paleolithic modern humans. In: Carlson, K., Marchi, D. (Eds.), Reconstructing Mobility. Springer, pp. 227–252.

Hildebrand, T., Laib, A., Müller, R., Dequeker, J., Rüegsegger, P., 1999. Direct three-dimensional morphometric analysis of human cancellous bone: microstructural data from spine, femur, iliac crest, and calcaneus. J. Bone Miner. Res. 14, 1167–1174.

Hildebrand, T., Ruegsegger, P., 1997. A new method for the model-independent assessment of thickness in three-dimensional images. J. Microsc. 185, 67–75.

Hodgskinson, R., Currey, J.D., 1990. The Effect of Variation in Structure on the Young's Modulus of Cancellous Bone: A Comparison of Human and Non-Human Material. Proc. Inst. Mech. Eng. Part H J. Eng. Med. 204, 115–121.

Holliday, T.W., 1997. Postcranial evidence of cold adaptation in European Neandertals. Am. J. Phys. Anthropol. 104, 245–58.

Holt, B.M., 2003. Mobility in Upper Paleolithic and Mesolithic Europe: evidence from the lower limb.

Am. J. Phys. Anthropol. 122, 200–15.

Homminga, J., Mccreadie, B.R., Weinans, H., Huiskes, R., 2003. The dependence of the elastic properties of osteoporotic cancellous bone on volume fraction and fabric. J. Biomech. 36, 1461–1467.

Huiskes, R., Ruimerman, R., van Lenthe, G.H., Janssen, J.D., 2000. Effects of mechanical forces on maintenance and adaptation of form in trabecular bone. Nature. 405, 704–6.

Hutton Macdonald, R., 1999. In the teeth of the problem: Dental anthropology and the reconstruction of African dietary regimes. University College London.

Inaoka, T., Lean, J., Besscho, T., Chow, J., Mackay, A., Kokubo, T., Chambers, T., 1995. Squential Analysis of Gene Expression After an Osteogenic Stimulus: C-FOS Expression is Induced in Osteocytes. Biochem. Biophys. Res. Commun. 217, 264–270.

Irish, J.D., Konigsberg, L., 2007. The ancient inhabitants of Jebel Moya Redux: Measures of Population Affinity based on dental morphology. Int. J. Osteoarchaeol. 17, 138–156.

Ito, M., 2011. Recent progress in bone imaging for osteoporosis research. J. Bone Miner. Metab. 29, 131–40.

Jacob, H.A.C., 2001. Forces acting in the forefoot during normal gait - An estimate. Clin. Biomech. 16, 783–792.

Jatkar, A., Kurland, I.J., Judex, S., 2016. Diets High in Fat or Fructose Differentially Modulate Bone Health and Lipid Metabolism. Calcif. Tissue Int. 100, 1–9.

Jee, W.S.S., Wronski, T.J., Morey, E.R., Kimmel, D.B., 1983. Effects of spaceflight on trabecular bone in rats. Am. J. Physiol. 244, R310–R314.

Jefferies, R.W., 1990. A technological and functional analysis of middle Archaic hafted endscrapers from the Black Earth site, Saline County, Illinois. Midcont. J. Archaeol. 15, 3–36.

Jefferies, R.W., 2013. The Archaeology of Carrier Mills: 10,000 Years in the Saline Valley of Illinois. Carbondale, IL.

Jefferies, R.W., Avery, G.E., 1982. The Carrier Mills Archaeological Project: Human Adaptation in the Saline Valley. Carbondale, IL.

Jefferies, R.W., Lynch, B.M., 1983. Dimensions of Middle Archaic Cultural Adaptation at the Black Earth Site, Saline County, Illinois. Archaic Hunters Gatherers Am. Midwest. 299–322.

Jepsen, K.J., Bigelow, E.M.R., Schlecht, S.H., 2015. Women Build Long Bones With Less Cortical Mass Relative to Body Size and Bone Size Compared With Men. Clin. Orthop. Relat. Res. 473, 2530–2539.

Jones, H., Priest, J., Hayes, W., Tichenor, C., Nagel, D., 1977. Humeral hypertrophy in response to exercise. J. Bone Jt. Surg. 59, 204–208.

Judex, S., Carlson, K.J., 2009. Is Bone's Response to Mechanical Signals Dominated by Gravitational Loading? Med. Sci. Sport. Exerc. 41, 2037–2043.

Judex, S., Garman, R., Squire, M., Donahue, L.-R., Rubin, C., 2004. Genetically based influences on the site-specific regulation of trabecular and cortical bone morphology. J. Bone Miner. Res. 19, 600–6.

Judex, S., Gupta, S., Rubin, C., 2009. Regulation of mechanical signals in bone. Orthod. Craniofacial Res. 12, 94–104.

Jung, G.-U., Lee, U.-Y., Kim, D.-H., Kwak, D.-S., Ahn, Y.-W., Kim, Y.-S., 2014. The body mass estimation from human talus: inductive approach and 3D morphometric study (919.1). FASEB J. 28, 919.1.

Kabel, J., Odgaard, a, van Rietbergen, B., Huiskes, R., 1999. Connectivity and the elastic properties of cancellous bone. Bone. 24, 115–20.

Kalender, W.A., Felsenberg, D., Louis, O., Lopez, P., Klotz, E., Osteaux, M., Fraga, J., 1989. Reference values for trabecular and cortical vertebral bone density in single and dual-energy quantitative computed tomography. Eur. J. Radiol. 9, 75–80.

Kannus, P., Parkkari, J., Sievänen, H., Heinonen, a, Vuori, I., Järvinen, M., 1996. Epidemiology of hip fractures. Bone. 18, 57S–63S.

Karasik, D., 2008. Osteoporosis: an evolutionary perspective. Hum. Genet. 124, 349–56.

Karim, L., Vashishth, D., 2011. Role of trabecular microarchitecture in the formation, accumulation, and morphology of microdamage in human cancellous bone. J. Orthop. Res. 29, 1739–1744.

Keaveny, T.M., Morgan, E.F., Niebur, G.L., Yeh, O.C., 2001. Biomechanics of trabecular bone. Annu. Rev. Biomed. Eng. 3, 307–333.

Kerschnitzki, M., Kollmannsberger, P., Burghammer, M., Duda, G.N., Weinkamer, R., Wagermaier, W., Fratzl, P., 2013. Architecture of the osteocyte network correlates with bone material quality. J. Bone Miner. Res. 28, 1837–1845.

Kesavan, C., Mohan, S., Oberholtzer, S., Wergedal, J.E., Baylink, D.J., 2005. Mechanical loading-induced gene expression and BMD changes are different in two inbred mouse strains. J. Appl. Physiol. 99, 1951–7.

Kesavan, C., Mohan, S., Srivastava, A.K., Kapoor, S., Wergedal, J.E., Yu, H., Baylink, D.J., 2006. Identification of genetic loci that regulate bone adaptive response to mechanical loading in C57BL/6J and C3H/HeJ mice intercross. Bone. 39, 634–643.

Khosla, S., Riggs, B.L., Atkinson, E.J., Oberg, A.L., McDaniel, L.J., Holets, M., Peterson, J.M., Melton, L.J., 2006. Effects of Sex and Age on Bone Microstructure at the Ultradistal Radius: A Population-Based Noninvasive In Vivo Assessment. J. Bone Miner. Res. 21, 124–131.

Kimizuka, M., Kurosawa, H., Fukubayashi, T., 1980. Load-bearing pattern of the ankle: joint contact area and pressure distribution. Arch. Orthop. Trauma. Surg. 96, 45–49.

Kivell, T.L., 2016. A review of trabecular bone functional adaptation: what have we learned from trabecular analyses in extant hominoids and what can we apply to fossils? J. Anat. 228, 569–594.

Kivell, T.L., Skinner, M.M., Lazenby, R., Hublin, J.-J., 2011. Methodological considerations for analyzing trabecular architecture: an example from the primate hand. J. Anat. 218, 209–25.

Kneissel, M., Roschger, P., Steiner, W., Schamall, D., Kalchhauser, G., Boyde, A., Teschler-Nicola, M., 1997. Cancellous bone structure in the growing and aging lumbar spine in a historic nubian population. Calcif. Tissue Int. 61, 95–100.

Knothe Tate, M.L., 2003. "Whither flows the fluid in bone?" An osteocyte's perspective. J. Biomech. 36, 1409–1424.

Kopperdahl, D.L., Pearlman, J.L., Keaveny, T.M., 2000. Biomechanical consequences of an isolated overload on the human vertebral body. J. Orthop. Res. 18, 685–90.

Kovacs, C.S., 2005. Calcium and bone metabolism during pregnancy and lactation. J. Mammary Gland Biol. Neoplasia. 10, 105–118.

Kreighbaum, E., Barthels, K.M., 1996. Biomechanics: a qualitative approach for studying human movement., Fourth edi. ed. Allyn and Bacon, Needham Heights.

Kurki, H.K., Ginter, J.K., Stock, J.T., Pfeiffer, S., 2008. Adult proportionality in small-bodied foragers: a test of ecogeographic expectations. Am. J. Phys. Anthropol. 136, 28–38.

Langdon, J.H., Bruckner, J., Baker, H.H., 1991. Pedal mechanics and bipedalism in early hominids. In: Coppens, Y., Senut, B. (Eds.), Origine(s) de La Bipédie Chez Les Hominidés. Paris, pp. 159–

167.

Lanyon, L.E., Rubin, C.T., 1984. Static vs dynamic loads as an influence on bone remodelling. J. Biomech. 17, 897–905.

Latimer, B., Lovejoy, C.O., 1989. The calcaneus of Australopithecus afarensis and its implications for the evolution of bipedality. Am. J. Phys. Anthropol. 78, 369–86.

Lawrence, E., 1995. Henderson's Dictionary of Biological Terms, Eleventh E. ed. Singapore Publishers, Singapore.

Lazenby, R.A., Cooper, D.M.L., Angus, S., Hallgrímsson, B., 2008. Articular constraint, handedness, and directional asymmetry in the human second metacarpal. J. Hum. Evol. 54, 875–85.

Lazenby, R.A., Skinner, M.M., Hublin, J.J., Boesch, C., 2011a. Metacarpal trabecular architecture variation in the chimpanzee (Pan troglodytes): Evidence for locomotion and tool-use? Am. J. Phys. Anthropol. 144, 215–225.

Lazenby, R.A., Skinner, M.M., Kivell, T.L., Hublin, J.-J., 2011b. Scaling VOI size in 3D μCT studies of trabecular bone: a test of the over-sampling hypothesis. Am. J. Phys. Anthropol. 144, 196–203.

Lean, J.M., Jagger, C.J., Chambers, T., Chow, J., 1995. Increased insulin-like growth factor I mRNA expression in rat osteocytes in response to mechanical stimulation. Am. J. Physiol. 268, 318–327.

Levine, D., Richards, J., Whittle, M.W., 2012. Whittle's Gait Analysis, Fifth edit. ed. Churchill Livingston Elsevier.

Lewis, M.E., 2007. The Bioarchaeology of Children, first. ed. Cambridge University Press, Cambridge.

Li, J.Z., Absher, D.M., Tang, H., Southwick, A.M., Casto, A.M., Ramachandran, S., Cann, H.M., Barsh, G.S., Feldman, M., Cavalli-Sforza, L.L., Myers, R.M., 2008. Worldwide human relationships inferred from genome-wide patterns of variation. Science. 319, 1100–4.

Lieberman, D.E., 1997. Making Behavioral and Phylogenetic Inferences from Hominid Fossils: Considering the Developmental Influence of Mechanical Forces. Annu. Rev. Anthropol. 26, 185–210.

Lieberman, D.E., Polk, J.D., Demes, B., 2004. Predicting long bone loading from cross-sectional geometry. Am. J. Phys. Anthropol. 123, 156–171.

Lieberman, D.E., Venkadesan, M., Werbel, W.A., Daoud, A.I., D'Andrea, S., Davis, I.S., Mang'eni, R.O., Pitsiladis, Y., 2010. Foot strike patterns and collision forces in habitually barefoot versus shod runners. Nature. 463, 531–5.

Lillehammer, G., 2010. Archaeology of Children. Complutum. 21, 15–45.

Lochmüller, E.-M., Matsuura, M., Bauer, J., Hitzl, W., Link, T.M., Müller, R., Eckstein, F., 2008. Site-Specific Deterioration of Trabecular Bone Architecture in Men and Women With Advancing Age. J Bone Min. Res. 23, 1964–1973.

Löfman, O., Berglund, K., Larsson, L., Toss, G., 2002. Changes in hip fracture epidemiology: Redistribution between ages, genders and fracture types. Osteoporos. Int. 13, 18–25.

Logan, A.L., 1995. The foot and ankle: Clinical applications.

Loro, M.L., Sayre, J., Roe, T.F., Goran, M.I., Kaufman, F.R., Gilsanz, V., 2000. Early identification of children predisposed to low peak bone mass and osteoporosis later in life. J. Clin. Endocrinol. Metab. 85, 3908–3918.

Lovejoy, C., Collum, M., Reno, P., Rosenman, B., 2003. Developmental Biology and Human Evolution. Annu. Rev. Anthropol. 32, 85–109.

Lovejoy, C.O., Meindl, R.S., Mensforth, R.P., Barton, T.J., 1985. Multifactorial determination of skeletal age at death: a method and blind tests of its accuracy. Am. J. Phys. Anthropol. 68, 1–14.

Lovejoy, C.O., Suwa, G., Simpson, S.W., Matternes, J.H., White, T.D., 2009. The Great Divides: Ardipithecus ramidus Reveals the Postcrania of Our Last Common Ancestors with African Apes. Science (80-.). 326, 73–73, 100–106.

Lozupone, E., Favia, A., 1990. The Structure of the Trabeculae of Cancellous Bone. 2. Long Bones and Mastoid. Calcif. Tissue Int. 46, 367–372.

Lundeen, G.A., Vajda, E.G., Bloebaum, R.D., 2000. Age-related cancellous bone loss in the proximal femur of Caucasian females. Osteoporos. Int. 11, 505–511.

Lynch, M.E., Main, R.P., Xu, Q., Walsh, D.J., Schaffler, M.B., Wright, T.M., van der Meulen, M.C.H., 2010. Cancellous bone adaptation to tibial compression is not sex dependent in growing mice. J. Appl. Physiol. 109, 685–691.

Maat, G.J.R., 2005. Two millennia of male stature development and population health and wealth in the Low Countries. Int. J. Osteoarchaeol. 15, 276–290.

Macchiarelli, R., Bondioli, L., Galichon, V., Tobias, P. V, 1999. Hip bone trabecular architecture shows uniquely distinctive locomotor behaviour in South African australopithecines. J. Hum. Evol. 36, 211–32.

Macintosh, A.A., Davies, T.G., Ryan, T.M., Shaw, C.N., Stock, J.T., 2013. Periosteal versus true cross-sectional geometry: a comparison along humeral, femoral, and tibial diaphyses. Am. J. Phys. Anthropol. 150, 442–52.

Macintosh, A.A., Pinhasi, R., Stock, J.T., 2014. Lower limb skeletal biomechanics track long-term decline in mobility across ~6150 years of agriculture in Central Europe. J. Archaeol. Sci. 52, 376–390.

MacLatchy, L., Muller, R., 2002. A comparison of the femoral head and neck trabecular architecture of Galago and Perodicticus using micro-computed tomography (microCT). J. Hum. Evol. 43, 89–105.

Madimenos, F.C., Snodgrass, J.J., Blackwell, A.D., Liebert, M.A., Cepon, T.J., Sugiyama, L.S., 2011. Normative calcaneal quantitative ultrasound data for the indigenous Shuar and non-Shuar Colonos of the Ecuadorian Amazon. Arch. Osteoporos. 6, 39–49.

Maga, M., Kappelman, J., Ryan, T.M., Ketcham, R.A., 2006. Preliminary observations on the calcaneal trabecular microarchitecture of extant large-bodied hominoids. Am. J. Phys. Anthropol. 129, 410–7.

Maquer, G., Musy, S.N., Wandel, J., Gross, T., Zysset, P.K., 2015. Bone volume fraction and fabric anisotropy are better determinants of trabecular bone stiffness than other morphological variables. J. Bone Miner. Res. 30, 1000–1008.

Marchi, D., Sparacello, V.S., Holt, B.M., Formicola, V., 2006. Biomechanical Approach to the Reconstruction of Activity Patterns in Neolithic Western Liguria , Italy. Am. J. Phys. Anthropol. 131, 447–455.

Martrille, L., Ubelaker, D.H., Cattaneo, C., Seguret, F., Tremblay, M., Baccino, E., 2007. Comparison of four skeletal methods for the estimation of age at death on white and black adults. J. Forensic Sci. 52, 302–307.

Mazess, R.B., Mather, W.E., 1975. Bone Mineral Content in Canadian Eskimos. Hum. Biol. 47, 45–63.

McColl, D.J., Abel, R.L., Spears, I.M., Macho, G.A., 2006. Automated method to measure trabecular thickness from microcomputed tomographic scans and its application. Anat. Rec. 288, 982–988.

McEwan, J.M., Mays, S., Blake, G.M., 2004. Measurements of Bone Mineral Density of the Radius in

a Medieval Population. Calcif. Tissue Int. 74, 157–161.

McHenry, H.M., 1992. Body Size and Proportions in Early Hominids. Am. J. Phys. Anthropol. 87, 407–431.

McHenry, H.M., Coffing, K., 2000. Australopithecus to Homo: Transformations in body and mind. Annu. Rev. Anthropol. 29, 125–146.

Menkes, A., Mazel, S., Redmond, R.A., Libanati, C.R., Gundberg, C.M., Hagberg, J.M., Hurley, B.E.N.F., Mazel, S., Koffler, K., Zizic, T.M., Pratley, R.E., 1993. Strength training increases regional bone mineral density and bone remodeling in middle-aged and older men. J. Appl. Physiol. 74, 2478–2484.

Milner, G.R., Anderson, E., Smith, V.G., 1991. Warfare in late prehistoric west-central Illinois. Am. Antiq. 56, 581–603.

Milner, G.R., Smith, V.G., 1990. Oneata human skeletal remains. In: Santure, S., Harn, A., Esarey, D. (Eds.), Archaeological Investigations at the Morton Village and Norris Farms 36 Cemetery. Illinois State Museum, Springfield, pp. 111–148.

Milovanovic, P., Djonic, D., Hahn, M., 2017. Region-dependent patterns of trabecular bone growth in the human proximal femur : A study of 3D bone microarchitecture from early postnatal to late childhood period. Am. J. Phys. Anthropol. 1–11.

Mitchell, D.M., Tuck, P., Ackerman, K.E., Cano Sokoloff, N., Woolley, R., Slattery, M., Lee, H., Bouxsein, M.L., Misra, M., 2015. Altered trabecular bone morphology in adolescent and young adult athletes with menstrual dysfunction. Bone. 81, 24–30.

Mittra, E., Rubin, C., Qin, Y.X., 2005. Interrelationship of trabecular mechanical and microstructural properties in sheep trabecular bone. J. Biomech. 38, 1229–1237.

Modlesky, C.M., Majumdar, S., Dudley, G.A., 2008. Trabecular bone microarchitecture in female collegiate gymnasts. Osteoporos. Int. 19, 1011–8.

Morris, D.H., Jones, M.E., Schoemaker, M.J., Ashworth, A., Swerdlow, A.J., 2012. Familial concordance for height and its components: Analyses from the breakthrough generations study. Am. J. Hum. Biol. 24, 22–27.

Mosekilde, L., 1990. Sex differences in age-related changes in vertebral body size, density and biomechanical competence in normal individuals. Bone. 11, 67–73.

Mosley, J.R., Lanyon, L.E., 1998. Strain rate as a controlling influence on adaptive modeling in response to dynamic loading of the ulna in growing male rats. Bone. 23, 313–318.

Mosley, J.R., Lanyon, L.E., 2002. Growth rate rather than gender determines the size of the adaptive response of the growing skeleton to mechanical strain. Bone. 30, 314–319.

Mosley, J.R., March, B.M., Lynch, J., Lanyon, L.E., 1997. Strain magnitude related changes in whole bone architecture in growing rats. Bone. 20, 191–198.

Muehleman, C., Bareither, D., Manion, B.L., 1999. A densitometric analysis of the human first metatarsal bone. J. Anat. 195 (Pt 2, 191–197.

Mukherjee, R., Trevor, J., Rao, C., 1955. The ancient inhabitants of Jebel Moya. Cambridge University Press, Cambridge.

Mullender, M.G., Huiskes, R., 1995. Proposal for the Regulatory Mechanism of Wolff â€™ s Law. J. Orthop. Res. 13, 503–512.

Mullender, M.G., Huiskes, R., Versleyen, H., Buma, P., 1996. Osteocyte density and histomorphometric parameters in cancellous bone of the proximal femur in five mammalian species. J. Orthop. Res. 14, 972–979.

Nafei, A., Danielsen, C., Linde, F., Hvid, I., 2000. Properties of growing trabecular ovine bone: Part I.

J. Bone Jt. Surg. 82, 910–920.

Nikita, E., Siew, Y.Y., Stock, J., Mattingly, D., Lahr, M.M., 2011. Activity patterns in the Sahara Desert: an interpretation based on cross-sectional geometric properties. Am. J. Phys. Anthropol. 146, 423–34.

Nuzzo, S., Meneghini, C., Braillon, P., Bouvier, R., Mobilio, S., Peyrin, F., 2003. Microarchitectural and physical changes during fetal growth in human vertebral bone. J. Bone Miner. Res. 18, 760–768.

Odgaard, A., 1997. Three-Dimensional Methods for Quantification of Cancellous Bone Architecture. Bone. 20, 315–328.

Odgaard, A., Kabel, J., van Rietbergen, B., Dalstra, M., Huiskes, R., 1997. Fabric and elastic principal directions of calcellous bone are closely related. J. Biomech. 30, 487–495.

Odgaard, a, Gundersen, H.J., 1993. Quantification of connectivity in cancellous bone, with special emphasis on 3-D reconstructions. Bone. 14, 173–82.

Orne, N., Webster, M., 1995. The English medieval hospital 1070-1570. Yale University Press, London.

Osborne, J., Costello, A., 2004. Sample size and subject to item ratio in principal components analysis. Pract. Assessment, Res. Eval. 9.

Pal, G.P., Routal, R. V, 1998. Architecture of the cancellous bone of the human talus. Anat. Rec. 252, 185–93.

Parfitt, A.M., 2002. Misconceptions (2): Turnover is always higher in cancellous than in cortical bone. Bone. 30, 807–809.

Parfitt, A.M., Travers, R., Rauch, F., Glorieux, F.H., 2000. Structural and cellular changes during bone growth in healthy children. Bone. 27, 487–494.

Parr, W.C.H., Chamoli, U., Jones, a., Walsh, W.R., Wroe, S., 2013. Finite element micro-modelling of a human ankle bone reveals the importance of the trabecular network to mechanical performance: New methods for the generation and comparison of 3D models. J. Biomech. 46, 200–205.

Pearson, O.M., 1997. Postcranial Morphology and the Origin of Modern Humans. Vasa. Stony Brook.

Pearson, O.M., 2000. Activity, climate , and postcranial robusticity human origins and scenarios. Curr. Anthropol. 41, 569–607.

Pearson, O.M., Cordero, R.M., Busby, A.M., 2008. How different were Neanderthal's habitual activities? A comparative analysis with diverse groups of recent humans. In: Harvati, K., Harrison, T. (Eds.), Neanderthals Revisited: New Approaches and Perspectives. Springer, Dordrecht, pp. 135–152.

Pearson, O.M., Lieberman, D.E., 2004. The aging of Wolff's "law": ontogeny and responses to mechanical loading in cortical bone. Am. J. Phys. Anthropol. Suppl 39, 63–99.

Pearson, O.M., Petersen, T., Sparacello, V.S., Daneshvari, S., Grine, F.E., 2014. Activity, "body shape", and cross-sectional geometry of the femur and tibia. In: Carlson, KJ, and Marchi, D (eds) Reconstructing mobility: environmental, behavioral, and morphological determinants. Springer, New York.

Pfeiffer, S.., Lazenby, R., 1994. Low bone mass in past and present aboriginal populations. In: Draper, H.H. (Ed.), Advances in Nutritional Research. Plenum Press, New York, pp. 35–51.

Pitsillides, A.A., 2006. Early effects of embryonic movement: "A shot out of the dark." J. Anat. 208, 417–431.

Polk, J.D., 2002. Adaptive and phylogenetic influences on musculoskeletal design in cercopithecine

primates. J. Exp. Biol. 205, 3399–3412.

Polk, J.D., Blumenfeld, J., Ahluwalia, D., 2008. Knee posture predicted from subchondral apparent density in the distal femur: An experimental validation. Anat. Rec. 291, 293–302.

Pomeroy, E., Stock, J.T., 2012. Estimation of stature and body mass from the skeleton among coastal and mid-altitude Andean populations. Am. J. Phys. Anthropol. 147, 264–79.

Pomeroy, E., Zakrzewski, S.R., 2009. Sexual Dimorphism in Diaphyseal Cross-sectional Shape in the Medieval Muslim Population of Ecija, Spain, and Anglo-Saxon Great Chesterford , UK. Int. J. Osteoarchaeol. 19, 50–65.

Pontzer, H., 2007. Effective limb length and the scaling of locomotor cost in terrestrial animals. J. Exp. Biol. 210, 1752–1761.

Pontzer, H., Lieberman, D.E., Momin, E., Devlin, M.J., Polk, J.D., Hallgrímsson, B., Cooper, D.M.L., 2006. Trabecular bone in the bird knee responds with high sensitivity to changes in load orientation. J. Exp. Biol. 209, 57–65.

Price, M., 2013. How Did the Social Changes of the Fourteenth Century Affect the Everyday Lives of English People? A Case Study from St. John's Divinity School. University of Cambridge.

Rafferty, K.L., 1996. Joint design in primates: external and subarticular properties in relation to body size and locomotor behavior. Johns Hopkins Universty.

Raichlen, D.A., Armstrong, H., Lieberman, D.E., 2011. Calcaneus length determines running economy: implications for endurance running performance in modern humans and Neandertals. J. Hum. Evol. 60, 299–308.

Raichlen, D.A., Foster, A.D., Gerdeman, G.L., Seillier, A., Giuffrida, A., 2012. Wired to run: exercise-induced endocannabinoid signaling in humans and cursorial mammals with implications for the "runner"s high'. J. Exp. Biol. 215, 1331–1336.

Raichlen, D.A., Gordon, A.D., Foster, A.D., Webber, J.T., Sukhdeo, S.M., Scott, R.S., Gosman, J.H., Ryan, T.M., 2015. An ontogenetic framework linking locomotion and trabecular bone architecture with applications for reconstructing hominin life history. J. Hum. Evol. 81, 1–12.

Ramachandran, S., Deshpande, O., Roseman, C.C., Rosenberg, N.A., Feldman, M.W., Cavalli-Sforza, L.L., 2005. Support from the relationship of genetic and geographic distance in human populations for a serial founder effect originating in Africa. Proc. Natl. Acad. Sci. U. S. A. 102, 15942–15947.

Reissis, D., Abel, R.L., 2012. Development of fetal trabecular micro-architecture in the humerus and femur. J. Anat. 220, 496–503.

Relethford, J.H., 1994. Craniometric variation among modern human populations. Am. J. Phys. Anthropol. 95, 53–62.

Relethford, J.H., 2004. Global Patterns of Isolation by Distance Based on Genetic and Morphological Data. Hum. Biol. 76, 499–513.

Reznikov, N., Chase, H., Ben, Y., Tarle, V., Singer, M., Brumfeld, V., Shahar, R., Weiner, S., 2016. Acta Biomaterialia Inter-trabecular angle : A parameter of trabecular bone architecture in the human proximal femur that reveals underlying topological motifs. Acta Biomater. 44, 65–72.

Reznikov, N., Phillips, C., Cooke, M., Garbout, A., Ahmed, F., Stevens, M.M., 2017. Functional Adaptation of the Calcaneus in Historical Foot Binding. J. Bone Miner. Res.

Richmond, B.G., Jungers, W.L., 2008. Orrorin tugenensis femoral morphology and the evolution of hominin bipedalism. Science. 319, 1662–5.

Riggs, B.L., Melton Iii, L.J., Robb, R.A., Camp, J.J., Atkinson, E.J., Peterson, J.M., Rouleau, P.A., McCollough, C.H., Bouxsein, M.L., Khosla, S., 2004. Population-based study of age and sex

differences in bone volumetric density, size, geometry, and structure at different skeletal sites. J. Bone Miner. Res. 19, 1945–1954.

Rincón-Kohli, L., Zysset, P.K., 2009. Multi-axial mechanical properties of human trabecular bone. Biomech. Model. Mechanobiol. 8, 195–208.

Ritchie, L.D., Fung, E.B., Halloran, B.P., Turnlund, J.R., Van Loan, M.D., Cann, C.E., King, J.C., 1998. A longitudinal study of calcium homeostasis during human pregnancy and lactation and after resumption of menses. Am. J. Clin. Nutr. 67, 693–701.

Robling, A.G., 2009. Is bone's response to mechanical signals dominated by muscle forces? Med. Sci. Sports Exerc. 41, 2044–2049.

Robling, A.G., Li, J., Shultz, K.L., Beamer, W.G., Turner, C.H., 2003. Evidence for a skeletal mechanosensitivity gene on mouse Chromosome 4. FASEB J. 17, 324–326.

Robling, A.G., Turner, C.H., 2002. Mechanotransduction in bone: Genetic effects on mechanosensitivity in mice. Bone. 31, 562–569.

Robling, A.G., Warden, S.J., Shultz, K.L., Beamer, W.G., Turner, C.H., 2007. Genetic effects on bone mechanotransduction in congenic mice harboring bone size and strength quantitative trait loci. J. Bone Miner. Res. 22, 984–991.

Rose, J., Gamble, J.G., 2006. Human Walking, Third Edit. ed. Lippincott Williams & Wilkins, Philadelphia.

Rot, I., Mardesic-Brakus, S., Costain, W.J., Saraga-Babic, M., Kablar, B., 2014. Role of skeletal muscle in mandible development. Histol. Histopathol.

Rubin, C., Turner, A., Mallinckrodt, C., Jerome, C., Mcleod, K., Bain, S., 2002. Mechanical strain, induced noninvasively in the high-frequency domain, is anabolic to cancellous bone, but not cortical bone. Bone. 30, 445–452.

Rubin, C., Turner, A.S., Müller, R., Mittra, E., McLeod, K., Lin, W., Qin, Y.-X., 2002. Quantity and quality of trabecular bone in the femur are enhanced by a strongly anabolic, noninvasive mechanical intervention. J. Bone Miner. Res. 17, 349–357.

Rubin, C., Turner, S., Bain, S., Mallinckrod, C., McLeod, K., 2001. Low mechanical signals strengthen long bones. Nature. 412, 603–604.

Rubin, C.T., Lanyon, L.E., 1985. Regulation of bone mass by mechanical strain magnitude. Calcif Tissue Int. 37, 411–417.

Rubin, C.T., McLeod, K.J., 1996. Inhibition of osteopenia by biophysical intervention. In: Marcus, R., Feldman, D., Kelsey, J. (Eds.), Osteoporosis. Academic Press, San Diego, pp. 351–371.

Ruff, C.B., 1987. Sexual dimorphism in human lower limb bone structure: relationship to subsistence strategy and sexual division of labor. J. Hum. Evol. 16, 391–416.

Ruff, C.B., 1994. Morphological adaptation to climate in modern and fossil hominids. Am. J. Phys. Anthropol. 37, 65–107.

Ruff, C.B., 1999. Skeletal structure and behavioral patterns of prehistoric Great Basin populations. In: Hemphill, B., Larsen, C. (Eds.), Understanding Prehistoric Lifeways in the Great Basin Wetlands: Bioarchaeological Reconstruction and Interpretation. University of Utah Press, Salt Lake City, pp. 290–320.

Ruff, C.B., 2000. Body size, body shape, and long bone strength in modern humans. J. Hum. Evol. 38, 269–90.

Ruff, C.B., 2003. Ontogenetic adaptation to bipedalism: age changes in femoral to humeral length and strength proportions in humans, with a comparison to baboons. J. Hum. Evol. 45, 317–349.

Ruff, C.B., 2005. Mechanical determinants of bone form: insights from skeletal remains. J.

Musculoskelet. Neuronal Interact. 5, 202–12.

Ruff, C.B., 2007. Body size prediction from juvenile skeletal remains. Am. J. Phys. Anthropol. 188, 698–716.

Ruff, C.B., 2008. Biomechanical Analyses of Archaeological Human Skeletons. In: Katzenberg, M.A., Saunders, S.R. (Ed.), Biological Anthropology of the Human Skeleton. Wiley - Blackwell, Chichester, pp. 183–206.

Ruff, C.B., Hayes, W.C., 1983. Cross-sectional geometry of Pecos Pueblo femora and tibiae--a biomechanical investigation: I. Method and general patterns of variation. Am. J. Phys. Anthropol. 60, 359–81.

Ruff, C.B., Holt, B., Niskanen, M., Sladek, V., Berner, M., Garofalo, E., Garvin, H.M., Hora, M., Junno, J., Schuplerova, E., Vilkama, R., Whittey, E., 2015. Gradual decline in mobility with the adoption of food production in Europe. Proc. Natl. Acad. Sci. 112, 7147–7152.

Ruff, C.B., Larsen, C.S., Hayes, W.C., 1984. Structural changes in the femur with the transition to agriculture on the Georgia coast. Am. J. Phys. Anthropol. 64, 125–36.

Ruff, C.B., Scott, W.W., Liu, a Y., 1991. Articular and diaphyseal remodeling of the proximal femur with changes in body mass in adults. Am. J. Phys. Anthropol. 86, 397–413.

Ruimerman, R., Hilbers, P., van Rietbergen, B., Huiskes, R., 2005. A theoretical framework for strain-related trabecular bone maintenance and adaptation. J. Biomech. 38, 931–941.

Rupprecht, M., Pogoda, P., Mumme, M., Rueger, J.M., Püschel, K., Amling, M., 2006. Bone microarchitecture of the calcaneus and its changes in aging: A histomorphometric analysis of 60 human specimens. J. Orthop. Res. 24, 664–674.

Ryan, A.S., Ivey, F.M., Hurlbut, D.E., Martel, G.F., Lemmer, J.T., Sorkin, J.D., Metter, E.J., Fleg, J.L., Hurley, B.F., 2004. Regional bone mineral density after resistive training in young and older men and women. Scand. J. Med. Sci. Sports. 14, 16–23.

Ryan, T., Sukhdeo, S., Perchalski, B., Hubbel, Z., Raichlen, D., Gosman, J., 2015. Ontogenetic development of trabecular bone in the human postcranial skeleton. In: The 84th Annual Meeting of the American Association of Physical Anthropologists.

Ryan, T.M., Krovitz, G.E., 2006. Trabecular bone ontogeny in the human proximal femur. J. Hum. Evol. 51, 591–602.

Ryan, T.M., Raichlen, D.A., Gosman, J.H., 2017. Structural and Mechanical Changes in Trabecular Bone during Early Development in the Human Femur and Humerus. In: Percival, C.J., Richtsmeier, J.T. (Eds.), Building Bones: Bone Formation and Development in Anthropology. Cambridge University Press, Cambridge, pp. 281–302.

Ryan, T.M., Shaw, C.N., 2012. Unique suites of trabecular bone features characterize locomotor behavior in human and non-human anthropoid primates. PLoS One. 7, e41037.

Ryan, T.M., Shaw, C.N., 2013. Trabecular bone microstructure scales allometrically in the primate humerus and femur. Proc. Biol. Sci. 280, 20130172.

Ryan, T.M., Shaw, C.N., 2015. Gracility of the modern Homo sapiens skeleton is the result of decreased biomechanical loading. Proc. Natl. Acad. Sci. 112, 372–377.

Ryan, T.M., van Rietbergen, B., Krovitz, G.E., 2007. Mechanical Adaptation of the Trabecular Bone in the Growing Human Femur and Humerus. Am. J. Phys. Anthropol. Suppl. 44, 203.

Ryan, T.M., Walker, A., 2010. Trabecular bone structure in the humeral and femoral heads of anthropoid primates. Anat. Rec. 293, 719–29.

Saers, J.P.P., Cazorla-Bak, Y., Shaw, C.N., Stock, J.T., Ryan, T.M., 2016. Trabecular bone structural variation throughout the human lower limb. J. Hum. Evol. 97, 97–108.

Salle, B.L., Rauch, F., Travers, R., Bouvier, R., Glorieux, F.H., 2002. Human fetal bone development: histomorphometric evaluation of the proximal femoral metaphysis. Bone. 30, 823–828.

Salmon, P.L., Ohlsson, C., Shefelbine, S.J., Doube, M., 2015. Structure Model Index Does Not Measure Rods and Plates in Trabecular Bone. Front. Endocrinol. (Lausanne). 6, 1–10.

Saparin, P., Scherf, H., Hublin, J.-J., Fratzl, P., Weinkamer, R., 2011. Structural adaptation of trabecular bone revealed by position resolved analysis of proximal femora of different primates. Anat. Rec. (Hoboken). 294, 55–67.

Sarrafian, S.K., Kelikian, A.S., 2011a. Osteology. In: Kelikian, A.S. (Ed.), Sarrafian's Anatomy of the Foot and Ankle. Wolters-Kluwer, Philadelphia, pp. 40–119.

Sarrafian, S.K., Kelikian, A.S., 2011b. Functional Anatomy of the Foot and Ankle. In: Kelikian, A.S.. (Ed.), Sarrafian's Anatomy of the Foot and Ankle. Wolters-Kluwer, Philadelphia, pp. 507–644.

Schaefer, M., Black, S., Scheuer, L., 2009. Juvenile osteology: a laboratory and field manual. Elsevier Academic Press, London.

Scherf, H., Harvati, K., Hublin, J.-J., 2013. A comparison of proximal humeral cancellous bone of great apes and humans. J. Hum. Evol. 65, 29–38.

Scherf, H., Wahl, J., Hublin, J.J., Harvati, K., 2016. Patterns of activity adaptation in humeral trabecular bone in Neolithic humans and present-day people. Am. J. Phys. Anthropol. 159, 106–115.

Scheuer, L., Black, S.M., 2004. The Juvenile Skeleton. London.

Schlecht, S.H., Pinto, D.C., Agnew, A.M., Stout, S.D., 2012. Brief communication: The effects of disuse on the mechanical properties of bone: What unloading tells us about the adaptive nature of skeletal tissue. Am. J. Phys. Anthropol. 149, 599–605.

Schmitt, D., 1999. Compliant walking in primates. J. Zool. 248, 149–160.

Seeman, E., 2001. Clinical review 137: Sexual dimorphism in skeletal size, density, and strength. J. Clin. Endocrinol. Metab. 86, 4576–4584.

Senut, B., Pickford, M., Gommery, D., Mein, P., Cheboi, K., 2001. First hominid from the Miocene (Lukeino Formation , Kenya). C. R. Acad. Sci. Paris, Sci. la Terre des planètes / Earth Planet. Sci. 332. 332, 137–144.

Shaw, C.N., Ryan, T.M., 2012. Does skeletal anatomy reflect adaptation to locomotor patterns? Cortical and trabecular architecture in human and nonhuman anthropoids. Am. J. Phys. Anthropol. 147, 187–200.

Shaw, C.N., Stock, J.T., 2009a. Habitual throwing and swimming correspond with upper limb diaphyseal strength and shape in modern human athletes. Am. J. Phys. Anthropol. 140, 160–72.

Shaw, C.N., Stock, J.T., 2009b. Intensity, repetitiveness, and directionality of habitual adolescent mobility patterns influence the tibial diaphysis morphology of athletes. Am. J. Phys. Anthropol. 140, 149–59.

Shaw, C.N., Stock, J.T., 2013. Extreme mobility in the Late Pleistocene? Comparing limb biomechanics among fossil Homo, varsity athletes and Holocene foragers. J. Hum. Evol. 64, 242–9.

Shaw, C.N., Stock, J.T., Davies, T.G., Ryan, T.M., 2014. Does the Distribution and Variation in Cortical Bone Along Lower Limb Diaphyses Refl ect Selection for Locomotor Economy? In: Carlson, K andJ Marchi, D. (eds). In: Reconstructing Mobility. pp. 49–66.

Skedros, J.G., Baucom, S.L., 2007. Mathematical analysis of trabecular "trajectories" in apparent trajectorial structures: the unfortunate historical emphasis on the human proximal femur. J. Theor. Biol. 244, 15–45.

Skedros, J.G., Hunt, K.J., Bloebaum, R.D., 2004. Relationships of Loading History and Structural and Material Characteristics of Bone: Development of the Mule Deer Calcaneus. J. Morphol. 259, 281–307.

Skedros, J.G., Sorenson, S.M., Hunt, K.J., Holyoak, J.D., 2007. Ontogenetic structural and material variations in ovine calcanei: A model for interpreting bone adaptation. Anat. Rec. 290, 284–300.

Skinner, M.M., Stephens, N.B., Tsegai, Z.J., Foote, A.C., Nguyen, N.H., Gross, T., Pahr, D.H., Hublin, J., Kivell, T.L., 2015. Human-like hand use in Australopithecus africanus. Science (80-.). 347, 395–400.

Smith, R.J., 1999. Statistics of sexual size dimorphism. J. Hum. Evol. 36, 423–458.

Smith, R.J., 2009. Use and misuse of the reduced major axis for line-fitting. Am. J. Phys. Anthropol. 140, 476–486.

Sparacello, V., Marchi, D., 2008. Mobility and subsistence economy: a diachronic comparison between two groups settled in the same geographical area (Liguria, Italy). Am. J. Phys. Anthropol. 136, 485–95.

Sparacello, V.S., Pearson, O.M., Coppa, A., Marchi, D., 2011. Changes in skeletal robusticity in an iron age agropastoral group: the Samnites from the Alfedena necropolis (Abruzzo, Central Italy). Am. J. Phys. Anthropol. 144, 119–30.

Starling, A.P., Stock, J.T., 2007. Dental Indicators of Health and Stress in Early Egyptian and Nubian Agriculturalists : A Difficult Transition and Gradual Recovery. Am. J. Phys. Anthropol. 134, 520–528.

Stern, J.T., 2000. Climbing to the top: A personal memoir of Australopithecus afarensis. Evol. Anthropol. Issues, News, Rev. 9, 113–133.

Stern, J.T., Susman, R.L., 1983. The locomotor anatomy of Australopithecus afarensis. Am. J. Phys. Anthropol. 60, 279–317.

Stieglitz, J., Trumble, B.C., Kaplan, H., Gurven, M., 2017. Horticultural activity predicts later localized limb status in a contemporary pre-industrial population. Am. J. Phys. Anthropol.

Stock, J., Pfeiffer, S., 2001. Linking structural variability in long bone diaphyses to habitual behaviors: foragers from the southern African Later Stone Age and the Andaman Islands. Am. J. Phys. Anthropol. 115, 337–48.

Stock, J.T., 2006. Hunter-gatherer postcranial robusticity relative to patterns of mobility, climatic adaptation, and selection for tissue economy. Am. J. Phys. Anthropol. 131, 194–204.

Stock, J.T., 2009. Ecogeographic variation in the ontogeny of hunter-gatherer physique and skeletal robusticity. Am. J. Phys. Anthropol. Suppl.

Stock, J.T., O'Neill, M.C., Ruff, C.B., Zabecki, M., Shackelford, L.L., Rose, J.C., 2011. Body size, Skeletal Biomechanics, Mobility and Habitual Activity from the Late Palaeolithic o the Mid-Dynastic Nile Valley. In: In: Stock, J.T., Pinhasi, R. (Eds) The Bioarchaeology of the Transition to Agriculture. Wiley - Blackwell, Chichester, pp. 347–367.

Styrkarsdottir, U., Halldorsson, B. V., Gudbjartsson, D.F., Tang, N.L.S., Koh, J.M., Xiao, S.M., Kwok, T.C.Y., Kim, G.S., Chan, J.C.N., Cherny, S., Lee, S.H., Kwok, A., Ho, S., Gretarsdottir, S., Kostic, J.P., Palsson, S.T., Sigurdsson, G., Sham, P.C., Kim, B.J., Kung, A.W.C., Kim, S.Y., Woo, J., Leung, P.C., Kong, A., Thorsteinsdottir, U., Stefansson, K., 2010. European bone mineral density loci are also associated with BMD in East-Asian populations. PLoS One. 5.

Su, A., Carlson, K.J., 2017. Comparative analysis of trabecular bone structure and orientation in South African hominin tali. J. Hum. Evol. 106, 1–18.

Su, A., Wallace, I.J., Nakatsukasa, M., 2013. Trabecular bone anisotropy and orientation in an Early Pleistocene hominin talus from East Turkana, Kenya. J. Hum. Evol. 64, 667–77.

Sugiyama, T., Price, J.S., Lanyon, L.E., 2010. Functional adaptation to mechanical loading in both cortical and cancellous bone is controlled locally and is confined to the loaded bones. Bone. 46, 314–321.

Sutherland, D., 1997. The development of mature gait. Gait Posture. 6, 163–170.

Sutherland, D., Olshen, R., Biden, E., Wyatt, M., 1988. The development of mature walking. Mac Keith Press, Philadelphia.

Sutherland, D.H., Olshen, R., Cooper, L., Woo, S.L., 1980. The Development of Mature Gait. J. Bone Jt. Surg. 62, 336–353.

Swartz, S.M., Parker, A., Huo, C., 1998. Theoretical and empirical scaling patterns and topological homology in bone trabeculae. J. Exp. Biol. 201, 573–90.

Tanck, E., Homminga, J., van Lenthe, G.., Huiskes, R., 2001. Increase in bone volume fraction precedes architectural adaptation in growing bone. Bone. 28, 650–654.

Tardieu, C., 1999. Ontogeny and phylogeny of femoro-tibial characters in humans and hominid fossils: Functional influence and genetic determinism. Am. J. Phys. Anthropol. 110, 365–377.

Tardieu, C., Bonneau, N., Akbal, E., Ozgozen, L., Bicer, O., Demirhan, O., Herrel, A., 2015. Quadrupedal subjects in a family (Adana, Turkey): comparison between two adult brothers' skeletons, one bipedal, one quadrupedal. Are they similar or different? In: 5th Annual Meeting of the European Society for the Study of Human Evolution. London, p. 218.

Tardieu, C., Glard, Y., Garron, E., Boulay, C., Jouve, J.L., Dutour, O., Boetsch, G., Bollini, G., 2006. Relationship between formation of the femoral bicondylar angle and trochlear shape: Independence of diaphyseal and epiphyseal growth. Am. J. Phys. Anthropol. 130, 491–500.

Thompson, A.H., Chaix, L., Richards, M.P., 2008. Stable isotopes and diet at Ancient Kerma, Upper Nubia (Sudan). J. Archaeol. Sci. 35, 376–387.

Thompson, D.D., Posner, A.S., Laughlin, W.. S.., Blumenthal, N.C., 1983. Comparison of bone apatite in osteoporotic and normal Eskimos. Calcif. Tissue Int. 392–393.

Thompson, D.D., Salter, E.M., Laughlin, W.S., 1981. Bone Core Analysis of Baffin Island Skeletons. Arctic Anthropol. 18, 87–96.

Tracer, D., 2002. Did the australopithecines crawl? Am. J. Phys. Antrhopology. 34, 156–157.

Tracer, D., Wyckhoff, S., Wimmer, M., Gardner, S., 2000. Prone to crawl: cultural contingency and early life locomotor development. Am. J. Hum. Biol. 12, 278.

Trinkaus, E., Churchill, S.E., Ruff, C.B., 1994. Postcranial robusticity in Homo. II: Humeral bilateral asymmetry and bone plasticity. Am. J. Phys. Anthropol. 93, 1–34.

Trinkaus, E., Ruff, C.B., 2012. Femoral and Tibial Diaphyseal Cross-Sectional Geometry in Pleistocene. PaleoAnthropology. 13–62.

Truong, L.-H., Kuliwaba, J.S., Tsangari, H., Fazzalari, N.L., 2006. Differential gene expression of bone anabolic factors and trabecular bone architectural changes in the proximal femoral shaft of primary hip osteoarthritis patients. Arthritis Res. Ther. 8, R188.

Tsegai, Z.J., Kivell, T.L., Gross, T., Nguyen, N.H., Pahr, D.H., Smaers, J.B., Skinner, M.M., 2013. Trabecular bone structure correlates with hand posture and use in hominoids. PLoS One. 8, e78781.

Turner, C.H., Hsieh, Y., Muller, R., Bouxsein, M.L., Baylink, D.J., Rosen, C.J., Grynpas, M.D., Donahue, L.R.A.E., Beamer, W.G., 2000. Genetic regulation of cortical and trabecular bone strength and microstructure in inbred strains of mice. J. Bone Miner. Res. 15, 1126–1131.

Ulrich, D., van Rietbergen, B., Laib, A., Rüegsegger, P., 1999. The ability of three-dimensional structural indices to reflect mechanical aspects of trabecular bone. Bone. 25, 55–60.

Villotte, S., Churchill, S.E., Dutour, O.J., Henry-Gambier, D., 2010. Subsistence activities and the sexual division of labor in the European Upper Paleolithic and Mesolithic: evidence from upper limb enthesopathies. J. Hum. Evol. 59, 35–43.

Voloshina, A.S., Ferris, D.P., 2013. Biomechanics and energetics of running on uneven terrain. J. Exp. Biol. 216, 711–719.

von Meyer, G., 1867. Die architektur der spongiosa. Arch. für Pathol. Anat. und Physiol. und für Klin. Medizin. 34, 615–628.

Wallace, I.J., Demes, B., Judex, S., 2017. Ontogenetic and Genetic Influences on Bone's Responsiveness to Mechanical Signals. In: Percival, C.J., Richtsmeier, J.T. (Eds.), Building Bones: Bone Formation and Development in Anthropology. Cambridge University Press, Camb, pp. 205–232.

Wallace, I.J., Demes, B., Mongle, C., Pearson, O.M., Polk, J.D., Lieberman, D.E., 2014. Exercise-induced bone formation is poorly linked to local strain magnitude in the sheep tibia. PLoS One. 9, e99108.

Wallace, I.J., Judex, S., Demes, B., 2015. Effects of load-bearing exercise on skeletal structure and mechanics differ between outbred populations of mice. Bone. 72, 1–8.

Wallace, I.J., Kwaczala, A.T., Judex, S., Demes, B., Carlson, K.J., 2013. Physical activity engendering loads from diverse directions augments the growing skeleton. J. Musculoskelet. Neuronal Interact. 13, 283–8.

Wallace, I.J., Nesbitt, A., Mongle, C., Gould, E.S., Grine, F.E., 2014. Age-related variation in limb bone diaphyseal structure among Inuit foragers from Point Hope, northern Alaska. Arch. Osteoporos. 9.

Wallace, I.J., Tommasini, S.M., Judex, S., Garland, T., Demes, B., 2012. Genetic variations and physical activity as determinants of limb bone morphology: an experimental approach using a mouse model. Am. J. Phys. Anthropol. 148, 24–35.

Wallace, I.J., Winchester, J.M., Su, A., Boyer, D.M., Konow, N., 2017. Physical activity alters limb bone structure but not entheseal morphology. J. Hum. Evol. 107, 14–18.

Wallace, J.M., Rajachar, R.M., Allen, M.R., Bloomfield, S.A., Robey, P.G., Young, M.F., Kohn, D.H., 2007. Exercise-induced changes in the cortical bone of growing mice are bone- and gender-specific. Bone. 40, 1120–1127.

Ward, C. V., 2002. Interpreting the posture and locomotion of Australopithecus afarensis: Where do we stand? Am. J. Phys. Anthropol. 119, 185–215.

Warden, S.J., Mantila Roosa, S.M., Kersh, M.E., Hurd, A.L., Fleisig, G.S., Pandy, M.G., Fuchs, R.K., 2014. Physical activity when young provides lifelong benefits to cortical bone size and strength in men. Proc. Natl. Acad. Sci. U. S. A. 111, 5337–42.

Wells, J.C.K., Stock, J.T., 2007. The biology of the colonizing ape. Yearb. Phys. Anthropol. 50, 191–222.

Wells, J.C.K., Stock, J.T., 2011. Re-examining heritability: genetics, life history and plasticity. Trends Endocrinol. Metab. 22, 421–8.

Wilcox, R., 2005. Introduction to robust estimation and hypothesis testing, Second edi. ed. Elsevier, San Francisco.

Will, M., Stock, J.T., 2015. Spatial and temporal variation of body size among early Homo. J. Hum. Evol. 2015.

Willems, C., Stassijns, G., Cornelis, W., D'Août, K., 2017. Biomechanical implications of walking with indigenous footwear. Am. J. Phys. Anthropol. 162, 782–793.

Wolff, J., 1867. Ueber die innere Architectur der Knochen und ihre Bedeutung für die Frage vom Knochenwachsthum. Arch. für Pathol. Anat. und Physiol. und für Klin. Med. 50, 389–450.

Wolschrijn, C.F., Weijs, W. a, 2004. Development of the trabecular structure within the ulnar medial coronoid process of young dogs. Anat. Rec. A. Discov. Mol. Cell. Evol. Biol. 278, 514–519.

Wood, J.W., Milner, G.R., Harpending, H.C., Weiss, K.M., Cohen, M.N., Eisenberg, L.E., Hutchinson, D.L., Jankauskas, R., Cesnys, G., Katzenberg, M.A., Lukacs, J.R., McGrath, J.W., Roth, E.A., Ubelaker, D.H., Wilkinson, R.G., 1992. The Osteological Paradox: Problems of Inferring Prehistoric Health from Skeletal Samples [and Comments and Reply]. Curr. Anthropol. 33, 343–370.

Wright, L.E., Yoder, C.J., 2003. Recent progress in bioarchaeology: Approaches to the Osteological Paradox. J. Archaeol. Res. 11, 43–70.

Xie, L., Rubin, C., Judex, S., 2008. Enhancement of the adolescent murine musculoskeletal system using low-level mechanical vibrations. J. Appl. Physiol. 104, 1056–62.

Zeininger, A., Patel, B.A., Zipfel, B., Carlson, K.J., 2016. Trabecular architecture in the StW 352 fossil hominin calcaneus. J. Hum. Evol. 97, 145–158.

Zeininger, A.D., 2013. Ontogeny of Bipedalism : Pedal Mechanics and Trabecular Bone Morphology. University of Texas Austin.

Zysset, P.K., Curnier, A., 1996. A 3D damage model for trabecular bone based on fabric tensors. J. Biomech. 29, 1549–58.

Zysset, P.K., Guo, X.E., Hoffler, E., Goldstein, S.A., 1999. Elastic modulus and hardness of cortical and trabecular bone lamellae measured by nanoindentation in the human femur. J. Biomech. 32, 1005–1012.

Appendix 1.

Appendix 1.1 Archaeological samples

Jebel Moya

This skeletal collection hails from Jebel Moya site 100 which is situated on the Jebel Moya massif in the southern Gezira Pain in modern Sudan. It is the largest mortuary complex of a pastoral society in sub-Saharan Africa (Brass, 2015a). The site was excavated by the Wellcome expedition between 1911 and 1914, but only published in 1949 (Addison, 1949). Unfortunately, the skeletal collection was poorly housed and moved repeatedly in the 40-year hiatus between excavation (Irish and Konigsberg, 2007), thus, of the over 3137 skeletons originally excavated, 98 crania and a handful of post-cranial elements survived to allow study. The skeletal material is housed at the Duckworth Laboratory, Cambridge. There was no depositional bias in favour of either sex at Jebel Moya, however, many of the surviving postcranial remains included in the current study could not be sexed.

Jebel Moya is situated about 250km south-south-east of Khartoum, south of the confluence of the Blue and White Niles. The site has been dated by OSL dating of pottery sherds between roughly 2000BC and AD 1000, and is divided into three phases based on pottery. The only ceramics definitely associated with graves all come from assemblage 3, dated by OSL to 100BC to AD 1000 (Brass and Schwenniger, 2013). The first conclusive evidence for burial activity is dated to the first century BC. This primary burial phase is interpreted as the mortuary complex of a mobile pastoral population engaged in trade with the ancient city of Meroe. The Jebel Moya people passed Sub-Saharan resources northwards via trading stations along the Nile in exchange for manufactured goods and non-local raw materials like iron and copper (Brass and Schwenniger, 2013). The burials at Jebel Moya are relatively poor in terms of grave goods compared to others in the region. They consist of shallow graves and lacked signs of hierarchical leadership except for one cluster of 27 richer burials (Brass, 2014, 2015b).

A study of population affiliation was performed by Irish and Konigsberg (2007) using dental characteristics of the extant teeth. They compared Jebel Moya to 18 north and sub-Saharan African populations. Cranially the Jebel Moya are akin to sub-Saharan populations whereas dentally they most closely resemble North African groups, namely Nubian A and Ethiopians, followed by the Badari and Kerma (Irish and Konigsberg, 2007). This means that either the Jebel Moya are an admixed group comprised of genetic elements from populations surrounding central Sudan; and/or a heterogeneous population consisting of individuals from a large surrounding region (Irish and Konigsberg, 2007). Irish and Konigsberg (2007) showed that the Jebel Moya do not show larger levels of dental variation than their comparative populations, indicating that the Jebel Sahaba were a homogeneous population. They argue that Jebel Moya dental morphology represents a population that, although unique, was relatively uniform and stable in its composition over a span of some 3000 years. The Jebel Moya are thus dentally North African, cranially sub-Saharan, and culturally they are a mix of both regions their own distinct style included. From this data it appears that the Jebel Moya likely started out as a diverse

group and came to be a population that exhibited its own distinctive biocultural identity (Irish and Konigsberg, 2007).

Jebel Moya was a pastoralist society that focused on zebu cattle, which were introduced in the mid first millennium BC and which can travel greater distances with less food and water (Brass, 2015b). Hutton-Macdonald (1999) reports that 5 out of 2.411 Jebel Moya teeth had caries (0.2%). She showed that the Jebel Moya sample did not exhibit the high levels of dental disease which are commonly known from peoples who cultivate grains. This is interpreted as likely being indicative of a non-cultivating, non-high carbohydrate consuming population (Hutton Macdonald, 1999). No artefacts such as sickles or hoes that might indicate harvesting have been found at Jebel Moya, and only one grindstone was found in the burial assemblages. 55 of the burials are associated with cattle bones, either parts of the animal or as a separate cattle inhumation. Several small clay cattle figurines were also found, though none were part of the burial assemblages (Brass and Schwenniger, 2013; Brass, 2015a, 2015b).

Biomechanical properties of the lower limbs of the Jebel Moya are reported in Nikita et al. (2011) (Table 1.1.1). There is significant sexual dimorphism in the Jebel Moya in lower limb total subperiosteal area (TA) with males have 14.9% higher body mass standardized TA compared to the females in the femur and 9.75% in the tibia (Nikita et al., 2011). This is interpreted as indicative of a sexual division of labour and that the males were more mobile compared to the females. Nikita et al. (2011) found that both Jebel Moya males and females had more robust lower limb diaphyseal cross-sections compared to the agricultural Kerma population which is also studied in this thesis. This suggests that the pastoralist subsistence mode of the Jebel Moya included greater levels of terrestrial mobility compared to the agricultural Kerma population.

Table 1.1.1. Lower limb cross-sectional geometric properties for males and females from the Kerma and Jebel Moya populations. Taken from Nikita et al. (2011).

	Males			**Females**		
	TA	**I_x/I_y**	**I_{max}/I_{min}**	**TA**	**I_x/I_y**	**I_{max}/I_{min}**
Femur Kerma	870.7 ± 19.4	1.29 ± 0.05	1.37 ± 0.04	773.0 ± 12.0	1.14 ± 0.04	1.29 ± 0.02
Femur Jebel Moya	962.3 ± 10.7	1.32 ± 0.05	1.52 ± 0.04	828.1 ± 18.1	1.28 ± 0.05	1.39 ± 0.05
Tibia Kerma	760.1 ± 21.8	1.88 ± 0.08	1.99 ± 0.08	627.6 ± 13.1	2.24 ± 0.13	2.27 ± 0.13
Tibia Jebel Moya	850.1 ± 17.9	1.89 ± 0.09	1.93 ± 0.09	760.1 ± 21.0	1.97 ± 0.13	1.98 ± 0.13

Kerma

The Kerma population was excavated from a cemetery associated with the city of Kerma in Nubia, near the third Cataract of the Nile River. Kerma was the capital of the Upper Nubian kingdom of Kush. Kerma culture is divided into three main phases, Ancient Kerma (2500 to 2050 BC), Middle

Kerma (2050 to 1750BC), and Classic Kerma (1750 to 1500 BC) (Thompson et al., 2008). Kerma was one of the first urban centres that arose in Africa, with a highly stratified society evidenced by large variation in the size of tombs and grave goods (Thompson et al., 2008). Kerma was located on a strategic position on one of the widest floodplains of the Upper Nile, enabling productive agriculture in the otherwise inhospitable environment. Agriculture was well developed, and herding was also a significant economic activity. Other economic activities included crafting and trading goods such as faience, copper items, and fine ceramics (Thompson et al., 2008).

The Kerma skeletons examined in this study were excavated from the ‘‘Eastern Cemetery’’ at Kerma by between 1913 and 1916, and belong to the Middle and Classic Kerma periods (Nikita et al., 2011). Significant sexual dimorphism has been noted in the Kerma sample (Nikita et al., 2011; Stock et al., 2011). Men were over two standard deviations taller than the women and possessed significantly greater polar second moments of area in the femur and the tibia (Stock et al., 2011), and total subperiosteal area (Nikita et al., 2011). Compared the Kerma females, the males have 11.65% larger femoral TA and 18% tibial TA. Very little sexual dimorphism is found in contemporary humans after correcting for differences in body size, indicating that these large differences in sexual dimorphism indicate that males were likely more mobile compared to the females.

Comparisons of Kerma to other regional samples (Starling and Stock, 2007) indicate that they were in comparatively good health. Starling and Stock investigated the prevalence of enamel hypoplasia in North African populations before, during, and after the adoption of agriculture in the region. They report an increase in enamel hypoplasia during the early adoption of agriculture and note subsequent improvements, culminating in the Kerma population which had the lowest number of enamel hypoplasia. Increased stature was also observed in the Kerma population relative to earlier samples (Stock et al., 2011). Nikita et al. (2011) compared the cross-sectional properties of Kerma to the Jebel Moya. The femoral midshafts of the Kerma populations were significantly more gracile which is interpreted by as indicative of reduced mobility associated with an agricultural subsistence strategy (Stock et al., 2011). Stable isotope, archaeobotanical, and zoological data point towards a broad diet consumed by the inhabitants of Kerma. The faunal dietary component consisted of a mix of sheep, goat, cattle, and aquatic resources. Cereals were excavated from bakeries that housed rows of ovens capable of producing large quantities of bread (Bonnet, 1988). The cemetery also yielded grains of barley (*Hordeum vulgare*), cucurbits (Curcurbitaceae), and legumes (Leguminosae) (Thompson et al., 2008).

Cross-sectional properties were also calculated for 17 individuals for which femoral trabecular bone structure was studied and published in Saers et al. (2016) (Figure 1.1.2). This sample was smaller than the one studied by Nikita et al. (2011) but include individuals that were included in the current study (both lower limbs and foot bones). Sexual dimorphism was observed most strongly in J and Zp, but failed to reach significance in all variables. However, it is expected that significant sexual dimorphism would be found if a larger sample size was included. Additionally, the effects of terrestrial mobility

are often more strongly reflected in the tibia compared to the femur (Stock, 2006; Davies, 2012). From these results and the results presented in Nikita et al. (2011) and Stock et al. (2011) it can be concluded that males were more robust relative to body mass, and thus likely more mobile compared to females.

Table 1.1.2. Cross-sectional properties and sexual dimorphism of the femoral midshaft of the Kerma population.

Kerma						**Levene's Test**		**T-test**		
	Sex	**N**	**Mean**	**S.D.**	**S.E.**	**F**	***p***	**t**	**df**	***p***
I_{max}/I_{min}	M	11	1.33	0.16	0.05	2.18	.16	1.50	15	.16
	F	6	1.23	0.08	0.03					
J	M	9	19402.74	4403.47	1467.82	2.24	.16	1.94	12	.08
	F	5	15147.08	2794.38	1249.69					
Zp	M	9	992.25	149.14	49.71	1.07	.32	2.12	12	.06
	F	5	841.47	66.64	29.80					
CA	M	10	597.78	113.16	35.79	.98	.34	.82	14	.43
	F	6	557.26	52.32	21.36					

Black Earth

Black Earth are a population of Middle Archaic hunter gatherers from southern Illinois, USA, dated to 3000 B.C. Based on the variety of tools, the number and diversity of features, the numerous burials, and the seasonal availability of the botanical and faunal species represented, it appears that Middle Archaic groups occupied the Black Earth site on a long-term, perhaps year-round basis (Jefferies and Lynch, 1983; Jefferies, 1990). Individuals from the Black Earth site subsisted mainly on white-tailed deer, other large and small mammals, birds, fish, and seasonally available nuts, and seeds (Lopinot and Lynch, 1979, Brietburg, 1980). These floral and faunal remains from the Black Earth site indicate a highly mobile population with a large and diverse home-range, used for both seasonal and year-round foraging activities. No sexual dimorphism was found in body mass corrected cross-sectional properties (Table 1.1.3).

Table 1.1.3. Cross-sectional properties and sexual dimorphism of the femoral midshaft of the Black Earth population.

Black Earth						**Levene's Test**		**T-test**		
	Sex	**N**	**Mean**	**S.D.**	**S.E.**	**F**	***p***	**t**	**df**	***p***
I_{max}/I_{min}	M	11	1.33	0.16	0.05	.784	.387	.519	18	.610
	F	9	1.29	0.22	0.07					
J	M	11	33111.43	7503.37	2262.35	.112	.742	.226	18	.824
	F	9	32175.06	10993.33	3664.44					
Zp	M	11	965.45	170.35	51.36	.065	.802	-.027	18	.979
	F	9	967.90	236.17	78.72					
CA	M	11	668.45	73.62	22.20	.471	.501	.152	18	.881
	F	9	662.14	111.96	37.32					

Norris Farms

Norris Farms #36 is a late prehistoric cemetery from the central Illinois River Valley, associated with the Oneota culture. The skeletal collection is housed at Pennsylvania State University, USA, and dated to approximately 1300 A.D., the people from Norris Farms #36 practised a form of village agriculture supplemented with foraging. Their diet included deer, bison, fish, nuts, wild rice, corn, beans, and squash (Buikstra and Milner, 1991; Birmingham and Eisenberg, 2000). The Oneota population was likely habitually unshod (Milner and Smith, 1990). At least a third of the individuals showed clear osteological signs that they died of violent trauma including scalping and decapitation. Individuals as well as single sex groups were likely attacked while foraging, indicated by several interments which included only males and females. The observed violence at Norris Farms was part of a regional phenomenon that is found in other local sites. Deaths are likely all from small scale attacks, and no evidence is found of massacres. It is expected that the violence was a result of competition for hunting grounds by local groups (Milner et al., 1991).

The Norris Farms skeletal assemblage consists of over a hundred juvenile skeletons. 18 juvenile calcanei from individuals below the age of 6 were examined in this thesis. The cross-sectional geometric properties of the femoral midshaft of the Norris Farms adults are given in Table 1.1.4.

Table 1.1.4. Cross-sectional properties and sexual dimorphism of the femoral midshaft of the Norris Farms population.

Norris Farms						**Levene's Test**		**T-test**		
	Sex	**N**	**Mean**	**S.D.**	**S.E.**	**F**	***p***	**t**	**df**	***p***
I_{max}/I_{min}	M	10	1.36	0.16	0.05	0.01	0.91	1.546	18	0.139
	F	10	1.25	0.15	0.05					
J	M	10	31342	5798	1833	0.79	0.39	1.686	18	0.109
	F	10	27616	3900	1233					
Zp	M	10	944.86	149.24	47.19	2.80	0.11	1.951	18	0.067
	F	10	837.77	88.64	28.03					
CA	M	10	607.23	83.98	26.56	1.62	0.22	1.927	18	0.070
	F	10	547.40	50.87	16.09					

St. Johns

The St. Johns - Old Divinity School site is a medieval cemetery that was excavated from Cambridge, UK, between 2010 and 2012 (Cessford, 2012). The excavation focused only on part of the cemetery in advance of re-development of the Divinity School (Cessford, 2012). The cemetery was associated with the nearby Hospital of St. John the Evangelist. The cemetery was established around AD 1230 and went out of use when the hospital was converted into a part of St. Johns College in 1511 (Cessford, 2012). Over 400 individuals were excavated out of an estimated 1000-1500 burials. The cemetery presumably contains burials from members of the hospital, the sick, servants, poor scholars, and minor benefactors (Cessford, 2012). Rules of the hospital specifically excluded pregnant women, lepers, cripples, the wounded, and the insane. Burials consisted of individuals of all ages except that no children under 5 were present. While medieval hospitals had many functions, their primary role was as religious institutions while secondary functions included charity to the poor, sick and travellers as well as centres of education (Cessford, 2012). Thus, despite being called a hospital, institutions such as this largely excluded the sick and saw themselves as retirement homes, places of hospitality and were not involved in difficult health care (Orne and Webster, 1995). However, the hospital was strongly affected by the Black Death in 1349, when most of the brethren died in a short period (Cessford, 2012).

The osteological report from the excavation states that the mean stature of individuals from the cemetery was low for the period, indicating low standards of living. Presence of pathologies was relatively low compared to other sites from the period (Cessford, 2012). Calculus was recorded in almost all the dentitions, suggesting a diet rich in carbohydrates, presumably cereals, combined with poor oral hygiene (Cessford, 2015). Stable isotope analysis on 106 individuals indicates minimal marine resource consumption. No changes in diet were found over time and no differences in stable isotope ratios were found between sexes (Price, 2013).

Appendix 2.

Appendix 2.1 Biomechanics of the foot

The primary tasks of the human foot and ankle complex is to provide a stable, adaptable, and efficient interface between the rest of the body and the ground during stance. The foot has to be relatively pliable when first contacting the ground to absorb the shock of impact, and has to function as a rigid lever when propelling the body forward at the end of stance (Hagins and Pappas, 2012). The foot is generally divided into three units. The rearfoot consists of the talus and the calcaneus. The midfoot is comprised of the tarsal bones (cuboid, navicular, and three cuneiform bones). The forefoot consists of the metatarsals and the phalanges. The foot is further described as consisting of three arches: the medial and lateral longitudinal arch and the transversal arch. The medial longitudinal arch is prominently involved in the absorption of most of the shock of impact during gait. The medial longitudinal arch consists of the calcaneus, the talus, the navicular, the three cuneiforms, and the first, second, and third metatarsals. The shape of the arch combined with the plantar fascia on the plantar side creates a spring mechanism that is essential for modern human bipedal locomotion. The lateral arch is composed of the calcaneus, the cuboid, and the fourth and fifth metatarsals. The transversal arch runs across the midfoot and provides support and flexibility to the foot.

The human gait cycle

To find the most suitable places to look for function related variation in trabecular bone architecture, it is important to understand the human gait cycle. Gait cycle is defined as "*the time between two successive occurrences of one of the repetitive events of* walking" (Levine et al., 2012). It is standard procedure to consider the first initial ground contact of the heel as the beginning of a gait cycle (Levine et al., 2012). The human gait can be broken down into two phases: the stance phase, where the foot is touching the ground, and the swing phase, when the foot is in the air (Logan, 1995). The stance phase starts when the heel touches the ground (heel strike), and it ends when the foot of the same leg touches off (toe-off). Levine and colleagues (2012) identify seven major events during the gait cycle, breaking it down into seven periods (Figure 2.1.1).

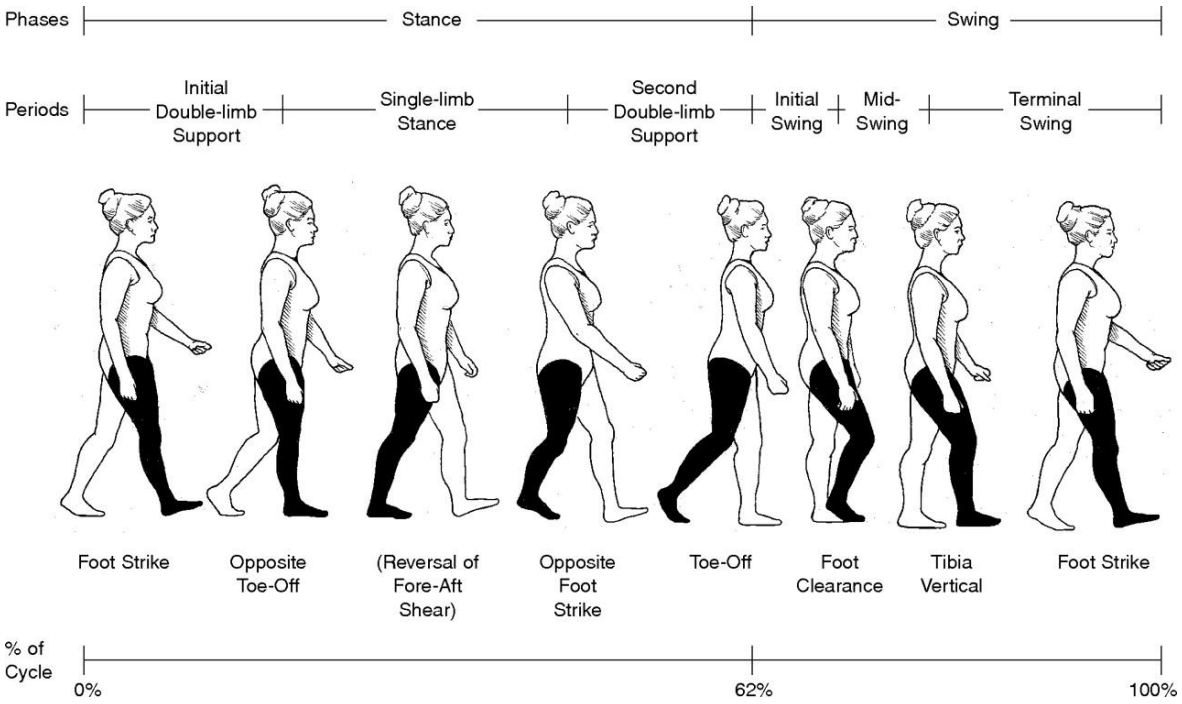

Figure 2.1.1. Positions of the lower limb during a single gait cycle.

The stance phase of a walking gait cycle of the knee and ankle will be briefly described here. The gait cycle starts when the foot makes first contact with the ground. The loading response period of the stance phase starts, and lasts roughly the first 10% of the gait cycle (Levine et al., 2012). When walking, first contact is normally made with the heel (heel strike). The ground reaction force changes direction from upwards during the heel strike transient, to upwards and posterior, increasing rapidly in magnitude. The knee is fully extended at the time of initial ground contact, and flexes slightly during loading response. The ankle is generally close to neutral position and slightly supinated. The posteriorly orientated ground reaction force produces an external plantarflexor moment at the ankle, which is resisted in a controlled manner by the tibialis anterior muscle, in order to prevent a 'foot slap' (Rose and Gamble, 2006; Levine et al., 2012). The loading response is a phase of double support between initial contact and toe-off of the opposite foot. The plantarflexion movement is accompanied by pronation of the foot and internal rotation of the tibia. These movements are coupled due to the morphology of the ankle and subtalar joint, and thus always occur together.

The mid-stance phase begins with opposite toe-off and lasts until roughly 30% of the cycle. Opposite toe-off ends the double support phase. The forefoot makes contact with the ground while the opposite foot lifts off. The knee continues to flex and eventually reaches its peak flexion angle of the stance phase in early mid-stance, after which the knee starts extending again. In the ankle, the 'mid-stance rocker' occurs and continues into terminal stance. The rocker is characterized by the forward rotation of the tibia about the ankle joint whilst the foot remains flat on the ground. Thus, the ankle changes from plantarflexion to dorsiflexion with the triceps surae contracting posteriorly. The supination movement of the foot peaks in midstance and then reverses (Levine et al., 2012). The ground reaction

force moves forward beneath the foot from the time the foot is placed flat on the ground, and moves anteriorly (Grundy et al., 1975; Zeininger, 2013).

The transition from mid-stance to terminal stance is marked by the rising of the heel from the ground. The peak of knee-extension is close to the moment of heel rise, after which the knee starts flexing slightly. The peak of ankle dorsiflexion is reached after heel rise. The triceps surae maintains the angle initially as the knee begins to flex, and moves to plantarflexion late in terminal stance (Levine et al., 2012). The knee rotates externally which causes the foot to become increasingly supinated while the toes remain flat on the ground (Levine et al., 2012). Pronation and supination of the subtalar joint creates flexibility and rigidity, respectively, in the transverse tarsal joint (Hagins and Pappas, 2012). Elftman (1960) demonstrated that the major axes of the oblique talonavicular joint and the longitudinal calcaneocuboid joint are parallel when the subtalar joint is everted. This allows motion in the transverse tarsal joint in a "loose packed" position. When the subtalar joint inverts the axes of these joints become convergent, locking the transverse tarsal joint in a "close-packed" position (Hagins and Pappas, 2012). This provides rigidity to the midfoot, and is a highly significant function during gait. It allows the foot to become a rigid lever during mid-stance to toe-off providing a significant mechanical advantage for push off. After heel rise the centre of pressure (COP) moves forward along the lateral mid-foot, it then rolls over from the lateral to medial side of the foot, moving the COP under the metatarsal heads (Zeininger, 2013). The direction and magnitude of a typical ground reaction force vector during walking gait is shown in Figure 2.1.2.

Initial contact of the contralateral limb occurs at 50% of the gait cycle, when the opposite foot reaches the ground, marking the end of single support and the beginning of the pre-swing phase. The leg is rotating anteriorly about the forefoot rather than the ankle joint (Levine et al., 2012). In the ankle, the ground reaction force vector is well in front of the ankle joint, producing a high dorsiflexor moment. This moment is opposed by correspondingly high contraction of the triceps surae which plantarflexes the foot, whilst extension of the metatarsophalangeal joint causes a tightening of the plantar fascia. The foot reaches maximal supination with hind-foot inversion, coupled with external tibial rotation this results in a tightly locked mid-foot high stability. This locking mechanism turns the foot into a rigid lever, aiding push-off (Elftman, 1960; Rose and Gamble, 2006; Hagins and Pappas, 2012; Levine et al., 2012). The power produced by the triceps surae before toe-off is the highest power in the gait cycle and serves to accelerate the limb into the swing phase (Levine et al., 2012). Toe-off occurs roughly around 60% of the gait cycle, prior to which the internal plantarflexor moment generated by the triceps surae declines rapidly as ground reaction forces reduce (Levine et al., 2012).

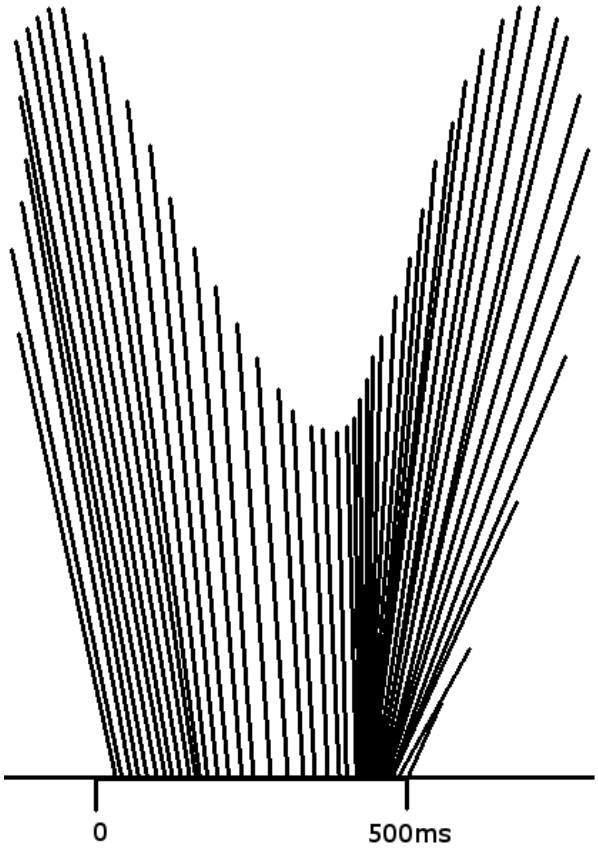

Figure 2.1.2. A 'butterfly diagram' of the ground reaction force vector at 10ms intervals of one step from heel strike to toe-off. Maximum magnitude is roughly 1.2 body weights. Adapted from (Levine et al., 2012).

During walking, the forces on the lower limbs are highest during heel strike, when the body needs to absorb the shock of touching the ground by braking, and at the end of midstance, before toe-off when the body needs to be pushed upwards and forwards (Lieberman et al., 2010). It is expected that trabecular structures in the ankle, heel, and forefoot will be adapted to the forces associated with these two periods of stance.

In running the pattern described above is altered by the addition of a non-support phase (instead of a double support phase) between the swing and stance phase, and by an increase in the range of motion of the movements of the articulations of the lower limb. The increased range of motion is required to facilitate increased force absorption during weight bearing and greater propulsion during push-off (Kreighbaum and Barthels, 1996). During running, the foot-ground angle, the angle of ankle flexion, and the location of the COP vary considerably compared to walking (Giddings et al., 2000). During running the maximum vertical force on the supporting foot is roughly 3 times an individual's body weight compared to 1.2 during walking (Kreighbaum and Barthels, 1996; Giddings et al., 2000).

The gait of children differs from that of adults in the following ways (Levine et al., 2012):

- Children have a wider walking base
- Stride length and speed are lower in children
- Young children do not have a heel strike or toe-off during stance and make contact with a flat foot
- The knee is mostly extended during stance in children

Independent walking starts roughly between 10 and 17 months, and at this point an infant is able to propel itself forward unassisted (Zeininger 2013). At one year of age the tibialis anterior is too weak to dorsiflex the foot during swing, resulting in a plantigrade foot at touchdown (Rose and Gamble, 2006). One year old are also unable to create enough torque at the ankle to propel themselves forward into swing (Hallemans et al., 2005, 2006). Instead of a propulsive toe-off, the plantigrade foot is lifted at the end of stance. A true heel strike does not occur until 18-24 months on average (Zeininger 2013). By around two years of age the muscles associated with plantarflexion are sufficiently strengthened to propel the foot in a distinctive toe-off phase (Zeininger 2013). At around two years of age most children have adopted the adult pattern of knee flexion and extension during stance. By age four the relative durations of the swing and stance phases have reached adult proportions. The walking base is about 70% of hip width at the age of 1, it reaches about 45% at age 3.5, and reaches adult proportions of around 30% at age 7 (Levine et al., 2012).

The above described gait patterns were established by studying modern individuals from industrialized areas of the world, who have grown up wearing modern shoes. Thus, these gait patterns may not be reflective of the gaits of past human populations. Recent research has demonstrated significant differences in gait patterns between habitually shod and unshod individuals, most notably during running (Lieberman et al., 2010; Hatala et al., 2013). In an analysis comparing the gaits of habitually shod versus unshod endurance runners, Lieberman and colleagues (2010) found that shod runners solely use rear foot strikes, whereas habitually unshod runners reported that using rear foot strikes without shoes gets painful (also depending on speed and substrate) and therefore often use a forefoot strike or midfoot strike when running. The reason that shod individuals use heel strikes is that they have shoes that are designed to make heel strikes more comfortable. In their kinematic analysis, it was found that rear-foot strike causes a large transient force in shod runners and even larger in the unshod runners. Forefoot strike on the other hand produces no transient, resulting in a smoother application of force. They found that at similar speeds, the magnitudes of peak vertical force during the impact period are three times lower in the barefoot forefoot strikers than the shod rear-foot strikers.

Appendix 2.2 Protocols for volume of interest placement

Instructions for taking measurements in AVIZO

1 - Open dataset (for example C:\CT Data\Jaap Saers\Jebel Moya) in Avizo. Open DICOM images if they are there. That means I have already reoriented the scans. Otherwise open the TIFF images.

2 – when opening tiff files, input the **voxel dimensions** (x, y, z) found in the text document accompanying the image data. This sets the resolution of the image. This is very important, because this tells the computer how large each pixel is, and thus the size of the specimen.

3- Attach an orthoslice and an isosurface (threshold depends on population / scanning settings). Downsample the isosurface by 4 to prevent the computer from slowing down too much.

4 - Explore if the bone is oriented correctly. The correct orientations of the calcaneus, talus and first metatarsal can be found below.

3. Bones can be oriented incorrectly and sometimes must be re-oriented. Here are examples of CORRECT orientation:

First, Make sure to set the viewer to Orthographic.

Instructions for orienting the calcaneus

- The calcaneus should be placed in anatomical position
- The medial and lateral plantar processes should be horizontal, as if touching the ground
- The calcaneocuboid joint should be vertical

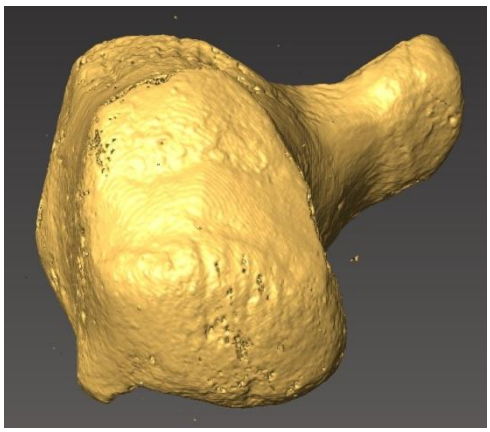

XY view.

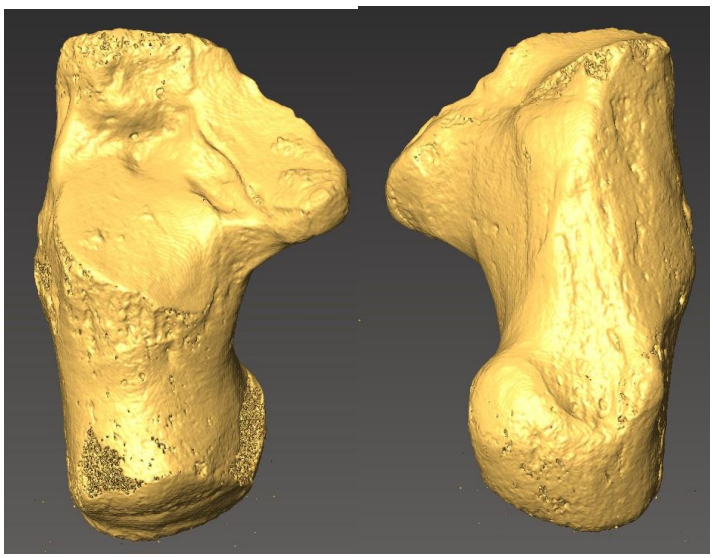

XZ view.

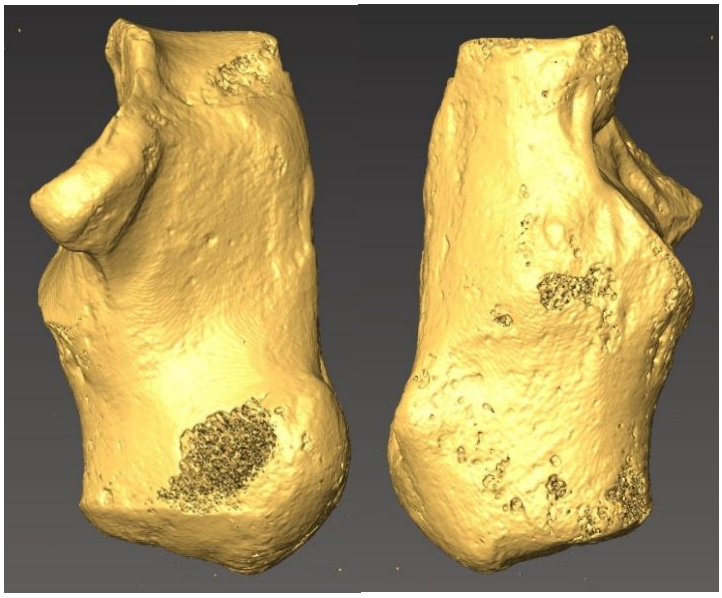

YZ view. Place the calcaneus in anatomical position. The cuboid articular facet should be roughly vertical. The plantar processes should be horizontal. Touching the hypothetical ground

Instructions for orienting the first metatarsal

- The dorsal aspect of the shaft should be straight along the xz plane
- the slice in the sagittal plane should go along thelong-axis of the bone
- the ridges next to the grooves for the sesamoid bones should be horizontal

YZ. The dorsal aspect of the shaft should be straight along the xz orthoslice

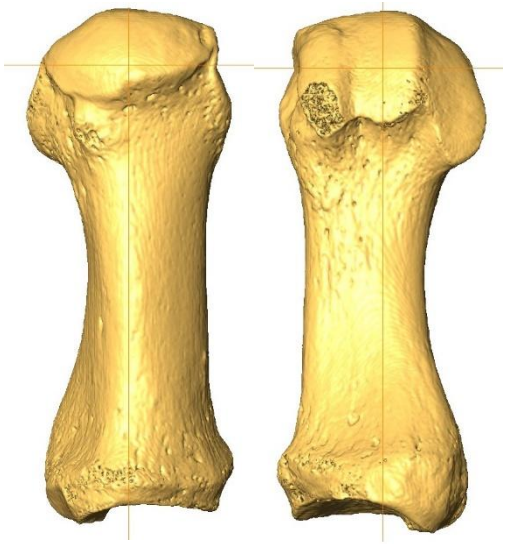

XZ. The YZ orthoslice should run through the long axis of the first metatarsal.

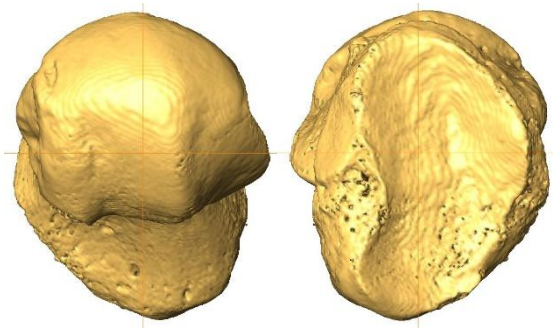

XY. The ridges next to the grooves for the sesamoid bones should be horizontal (as if resting on the XZ orthoslice.

Instructions for orienting the talus

- Trochlea should be flat and the talar head should be below the trochlea when viewed from the front.
- The Trochlea should be pointing forward, running parallel to the sagittal plane.
- The talar head should be below the trochlea. The tip of the lateral malleolus should be at the same height as the tip of the medial malleolus.

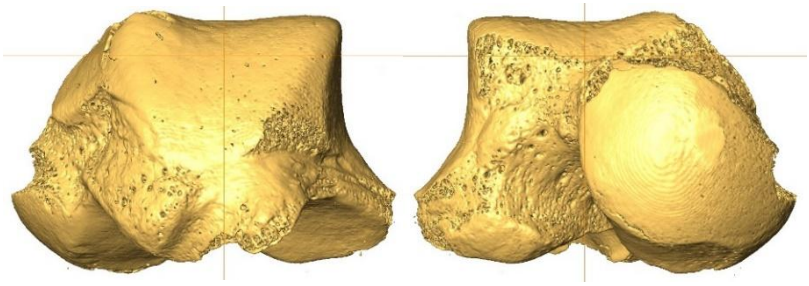

XY view. The trochlea should be flat and the talar head should be below the trochlea when viewed from the front.

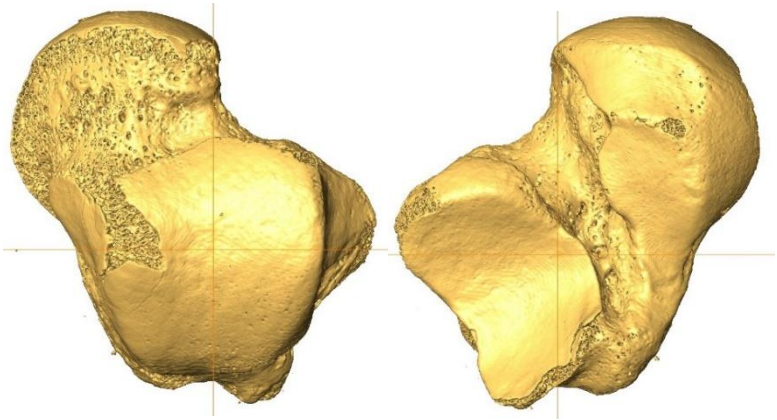

XZ view. The Trochlea should be pointing forward, running parallel to the sagittal plane.

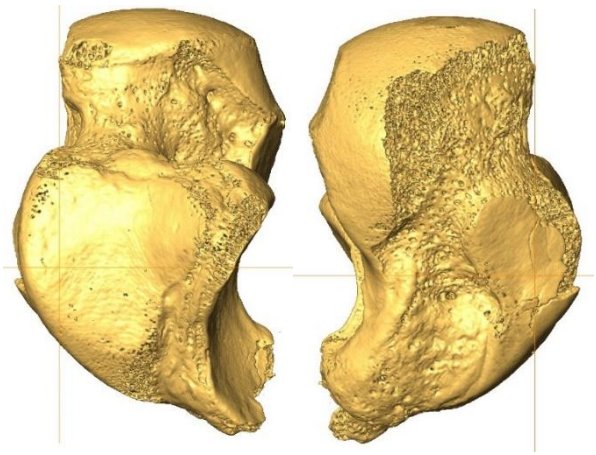

YZ view. The talar head should be below the trochlea. The tip of the lateral malleolus should be at the same height as the tip of the medial malleolus.

4. To correct misaligned bones, Press the anatomical plane button on the top of the screen.

5. Go to Transform Editor by clicking on the data set, and then going to the Properties Window and selecting the button that looks like a cube with green nodes.

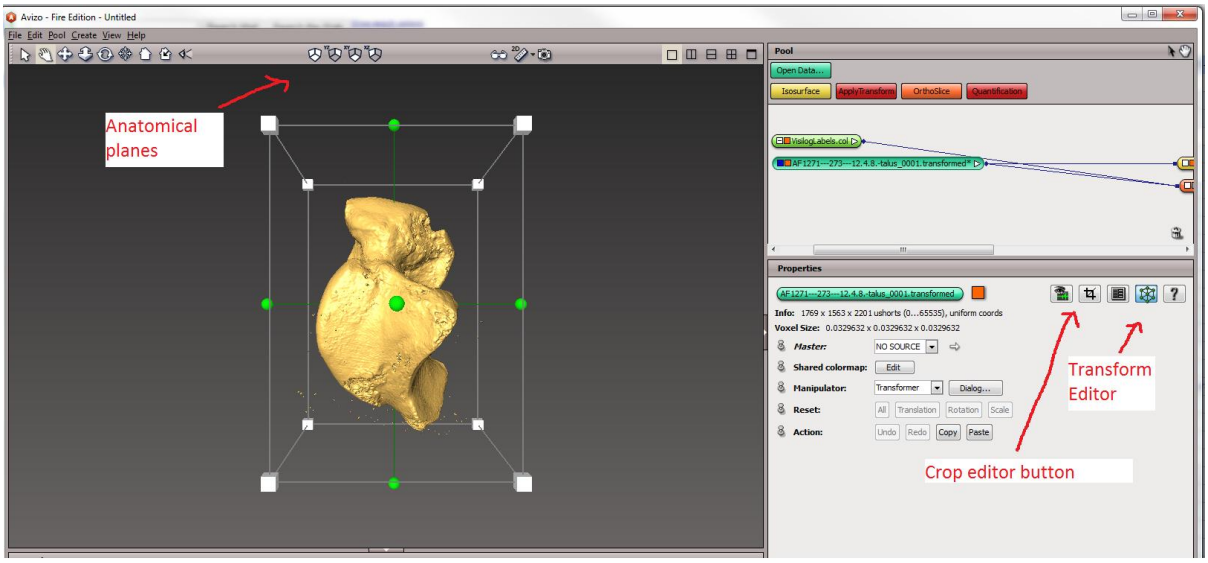

6. On your screen, there should appear a box, and two perpendicular axes with green spheres on each end. You will need to go to the arrow key (in the top left corner of the viewer window) and click and drag one of the green spheres. This rotates the data set in just one plane, which is what you want. **Align the bone in the XY XZ and YZ planes so that they correspond with the pictures in this document.**

7. When you're done, and you can click on the Transform Editor button again to get rid of the box and spheres.

8. Right-click on the data set and go to Compute>Apply Transform. Click on "extended," "Voxel Size" and leave the padding value at 0. Click Apply. You may receive a message warning you that the dataset will be very large - click CONTINUE to this. Wait for the sampling to be completed and a new dataset to appear in the Pool.

9. Click on the **newly transformed** data set and go to the crop editor button (crop symbol with line running through it) in properties. **Ensure the minimum coordinates are set at 0,0,0. Hit okay**.

10. If you are using a dataset from the **Norris Farms** population there is one extra step to take.

Click on the new dataset, then on the crop button in Properties, if the three voxel size values are not exactly the same you need to transform the data by following these steps:

- Right click on the new dataset, then Compute>Resample

- Filter= Lanczos

- Click on Voxel Size and for x, y and z type in the largest value that you see above for 'Input voxel size:' (i.e. if the Input voxel size = 0.054, 0.054, 0.056, you input 0.056, 0.056, 0.056)

- Click Apply - and a new 'resampled' dataset will appear.

11. **Save the dataset**. Create a new folder called DICOM inside the folder where your data is from. Then save the new dataset by right clicking on the newly transformed dataset in avizo and clicking "save as". Then save the dataset as DICOM files.

12. Now that the dataset is transformed and in its correct anatomical position you can start taking the external measurements listed at the start of this document. Add them to the excel file in the folder (D:\Jaap\external measurements).

13. Measurements can be taken with the ruler icon on the top of the screen. A 3d measurement takes a measurement between two specific parts of the bone. A 2d measurement can be taken anywhere. The measurements at the start of this document will tell you whether you need to use a 2d or 3d measurement. **Make sure to set the viewer to Orthographic. Otherwise the 2D measurements are represented in pixels rather than millimetres. In the picture below the viewer is not yet set to orthographic.**

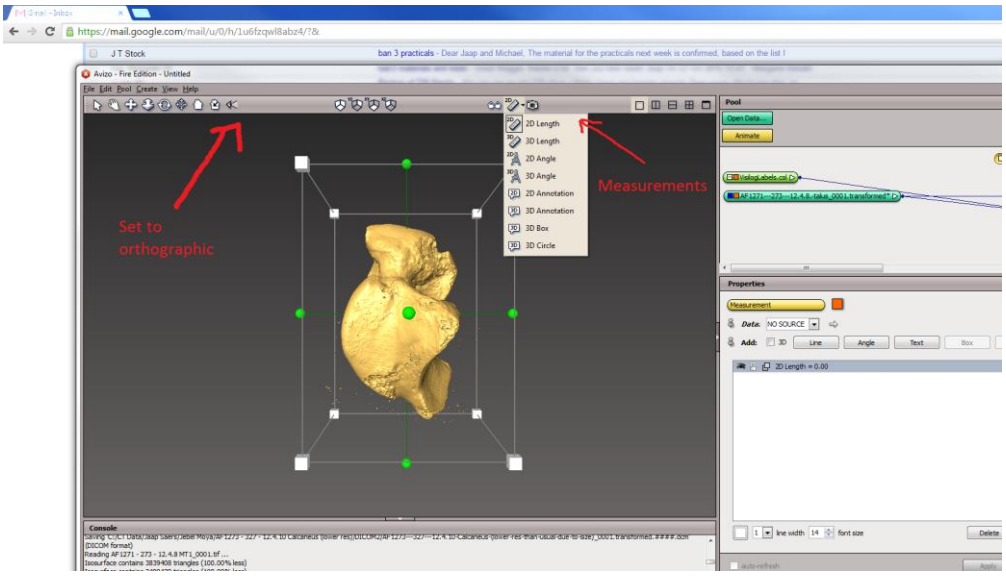

Protocols for placing spherical volumes of interest

Use the AutoVOI script to automatically place spherical VOIs in the correct locations within the bounding box. Variation in external morphology of the bones may require the position of the spheres to be manually adjusted. The following guide describes the process of placing the 17 VOIs throughout the calcaneus, talus, and first metatarsal.

How to create a spherical VOI in Avizo

Create a cube using *extract subvolume* or the cubing script. Then when a cubic VOI is taken, add *Volume Edit* to it. In volume edit, click *tool*->change draw to transformer->then change box to ellipsoid. Then, Cut the outside. This results in a spherical voi

To be able to calculate Tb.Sp two spheres need to be created-> one with a black background and one with a "white" background. To create the one with the 'white' background use *volume edit* and before cutting the 'outside' set *padding value* to 1 value above the minimum value of "window" in the "data info" of the dataset.

Calcaneus

The following protocols are established to ensure that all cubes are placed in homologous locations. VOI diameters are all standardized by calcaneus length which shows a strong correlation with body mass of all linear calcaneal dimensions.

Region of interest determination

A bounding box should be placed around the calcaneus which should tightly contain the maximum width and length of the calcaneus. The height of the bounding box should be between the most plantar aspect of the tuber and the most dorsal aspect of the posterior talar facet.

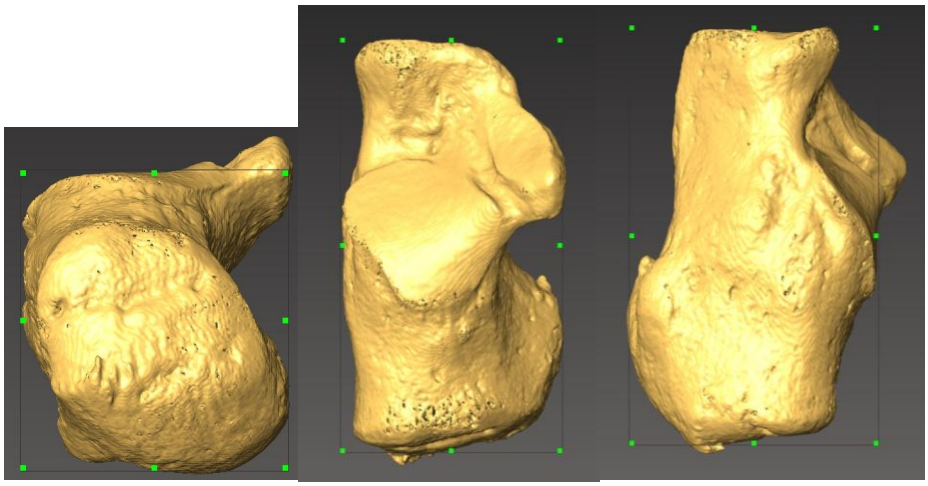

XY view *XZ View* *YZ view*

Calcaneocuboid VOI (CC)

The diameter of the CC VOI is 12% of calcaneus length as defined by the bounding box length. This VOi should be placed on the lateral side of the calcaneocuboid joint, just beneath the joint surface.

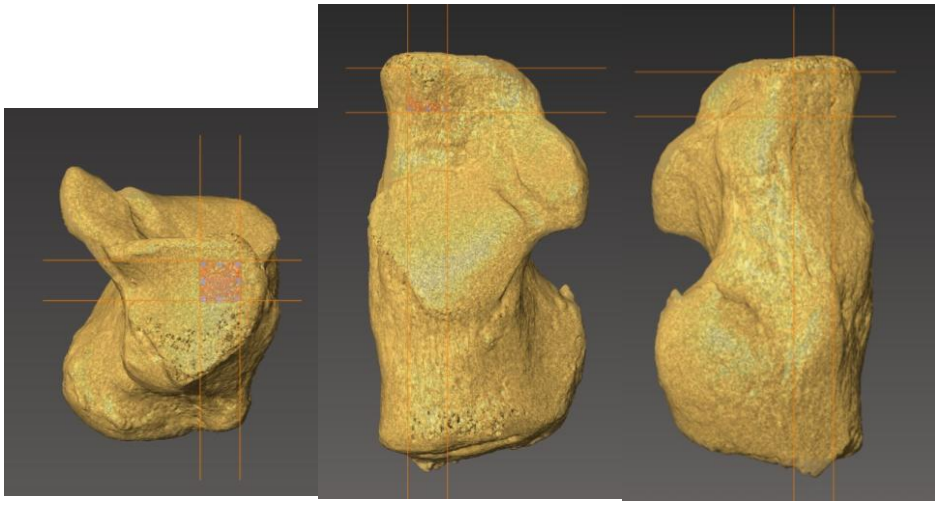

XY *XZ* *XZ*

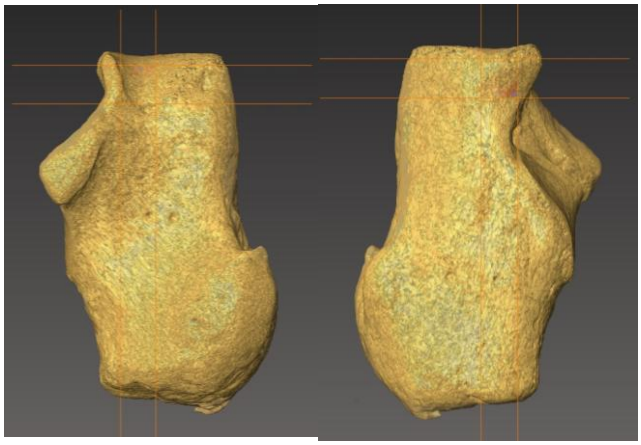

YZ

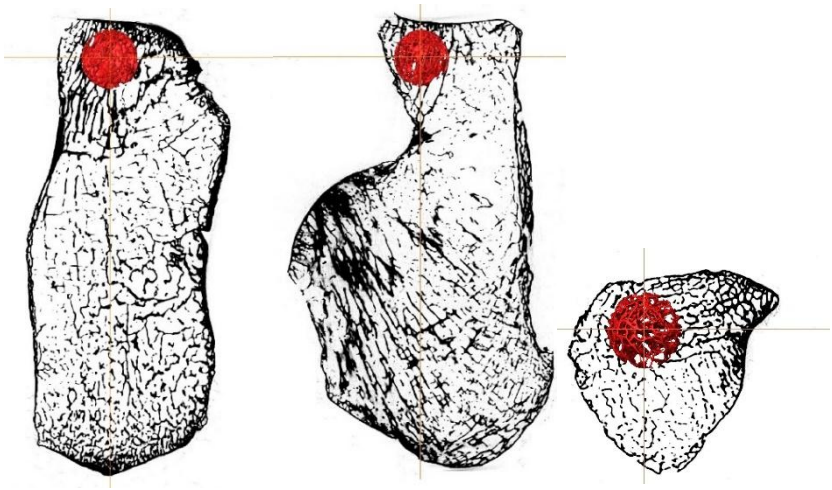

XZ *YZ* *XY*

Plantar ligaments VOI (PL)

The plantar ligament VOI is 10% of total calcaneal length as defined by the maximum length of the ROI. It is located on the medial side of the calcaneus, below the plantar ligament insertions and anterior to the plantar fascia insertion.

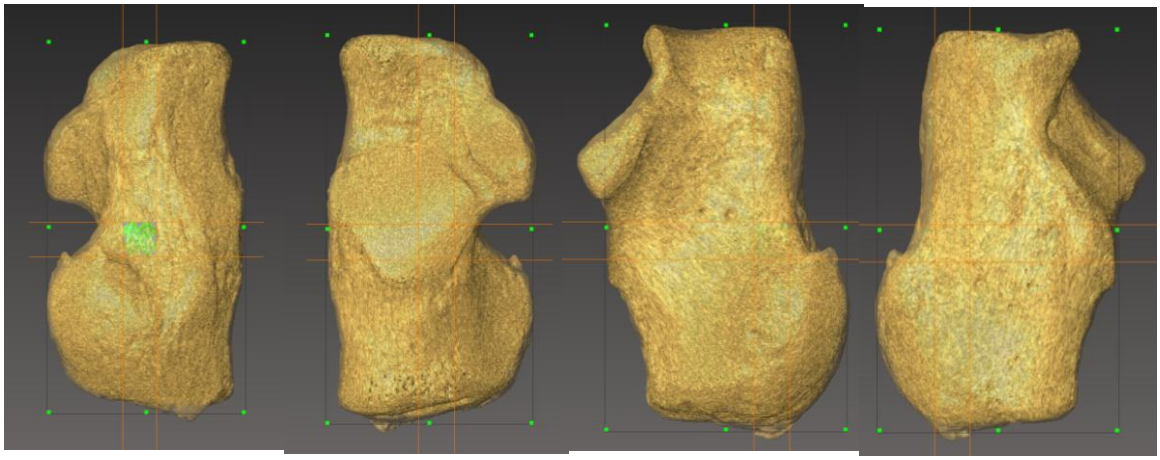

XZ *YZ*

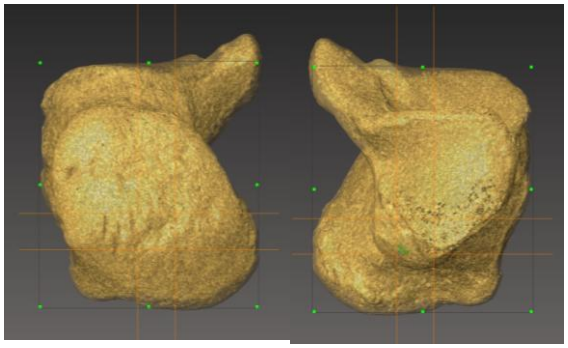

XY

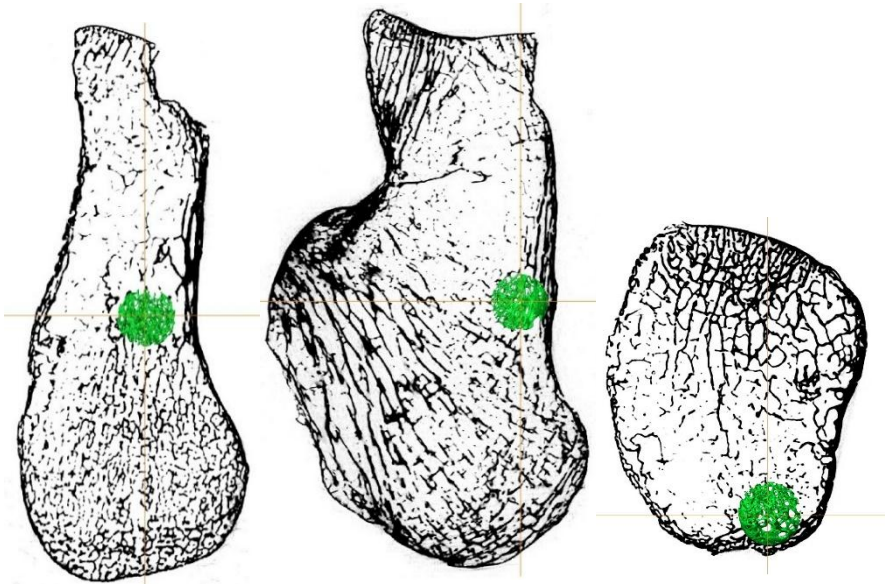

XZ *YZ* *XY*

Posterior talar facet (PTF)

PTF VOI length is 10% of calcaneal length measured by the ROI length. The VOIs should be placed just beneath the posterior talar articular facet. One VOI is placed on the centrally on the posterior end of the PTF, one is placed centrally on the anterior side of the PTF, and one centrally in the centre of the PTF.

Posterior VOI (PP)

XY

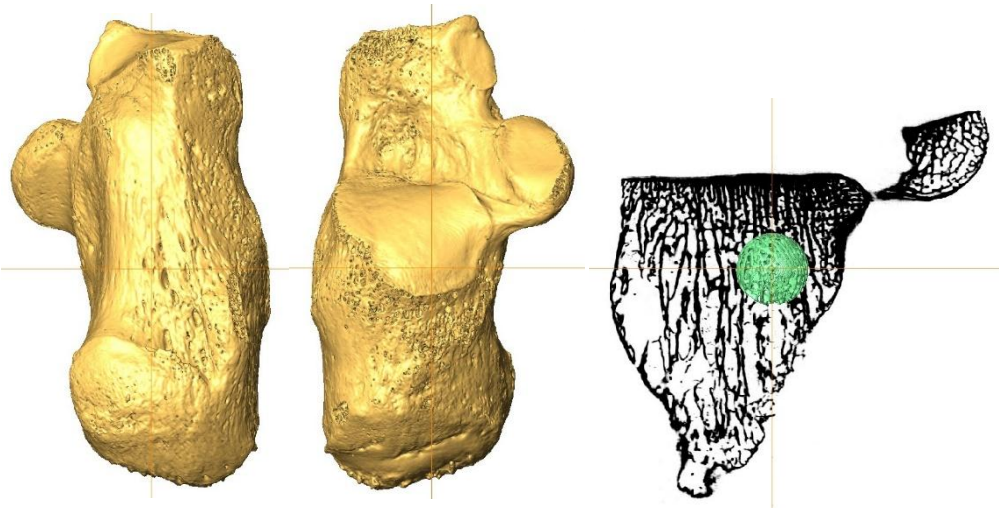

XZ

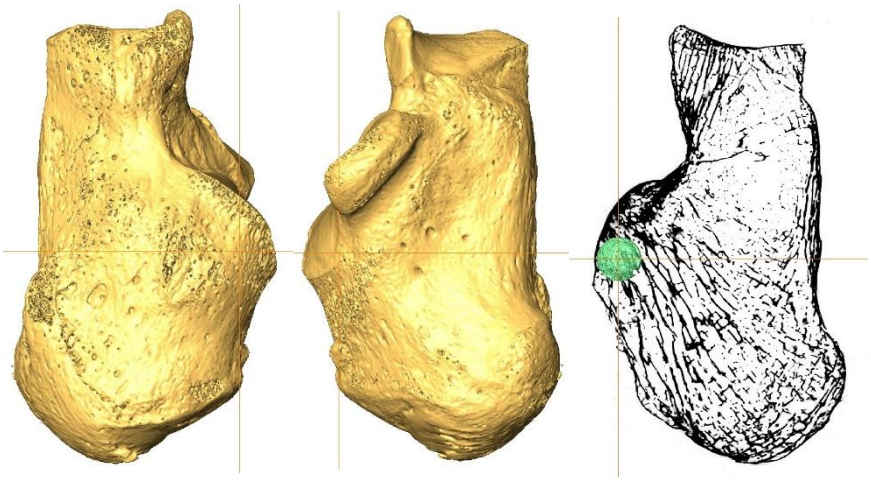

YZ

Central VOI (PC)

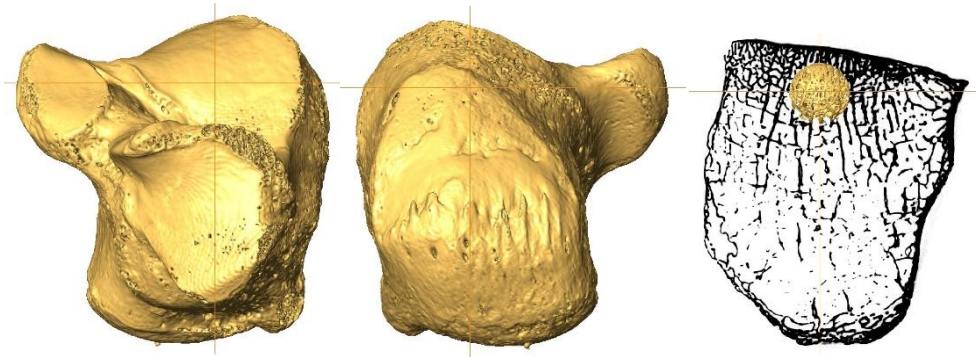

XY

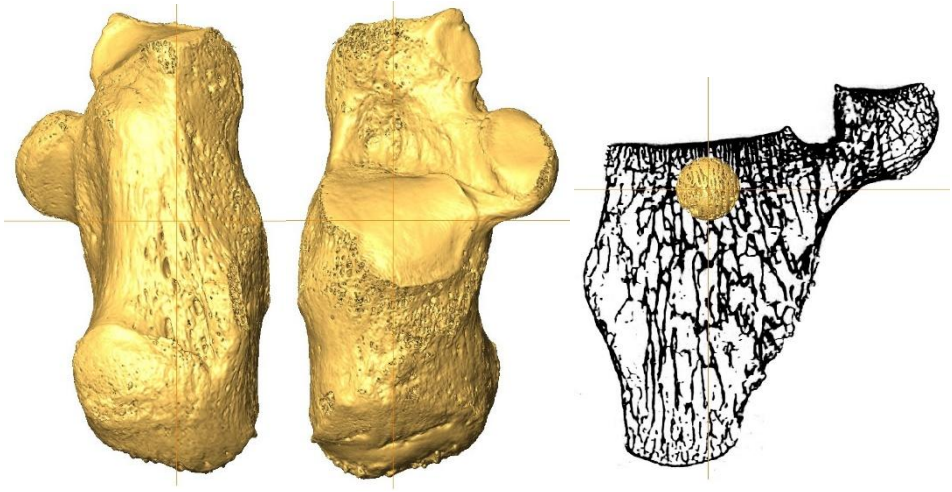

XZ

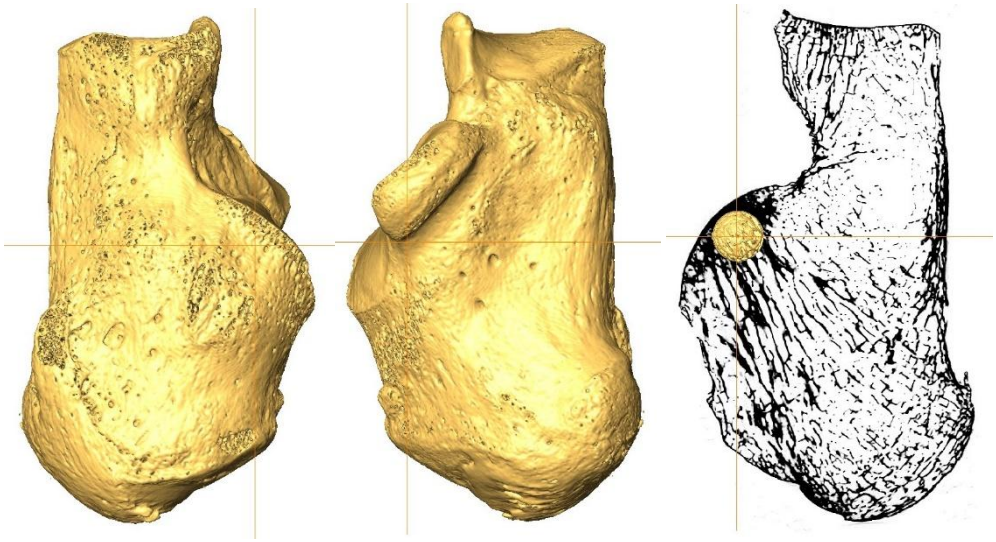

YZ

Anterior VOI (PA)

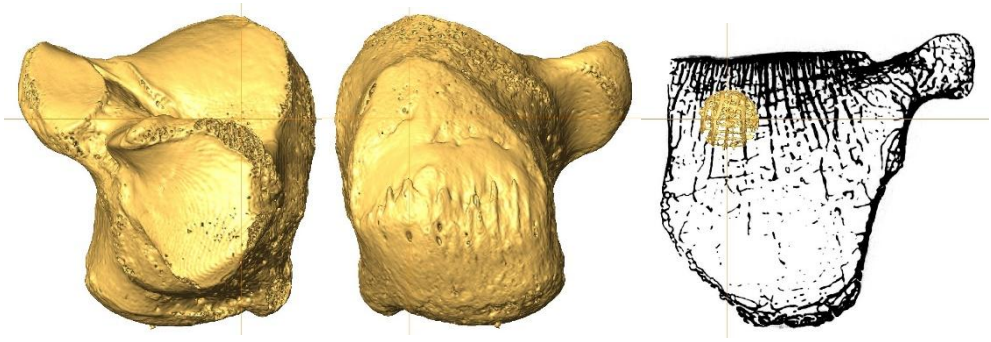

XY

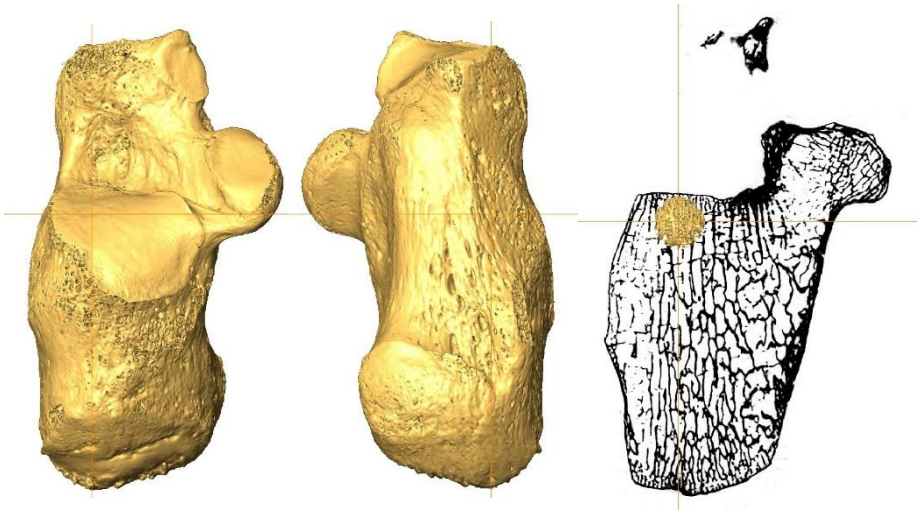

XZ

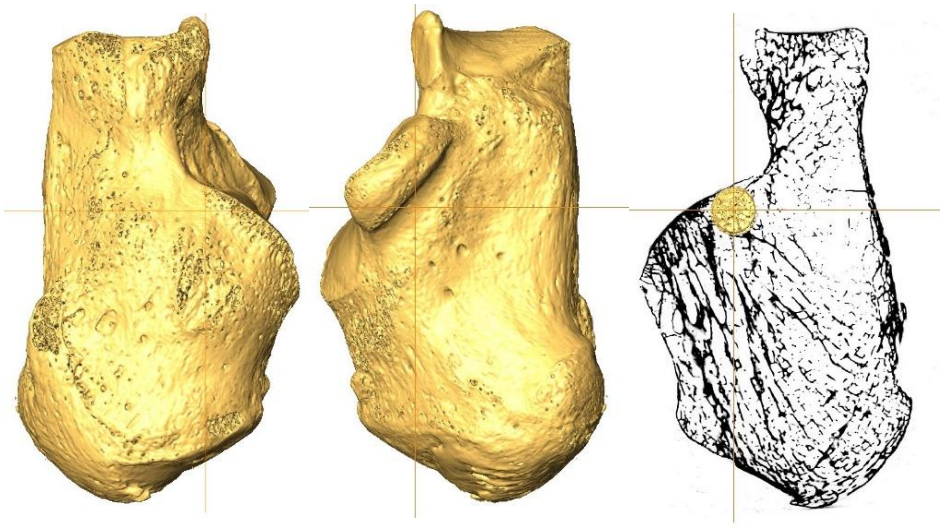

YZ

Calcaneal tuber

Placed in centrally inside the ROI and dorsally and slightly medially in the calcaneal tuber halfway between the posterior calcaneal facet and the most dorsal/proximal end of the calcaneal tuber. The diameter is 20% of the calcaneal (ROI) length.

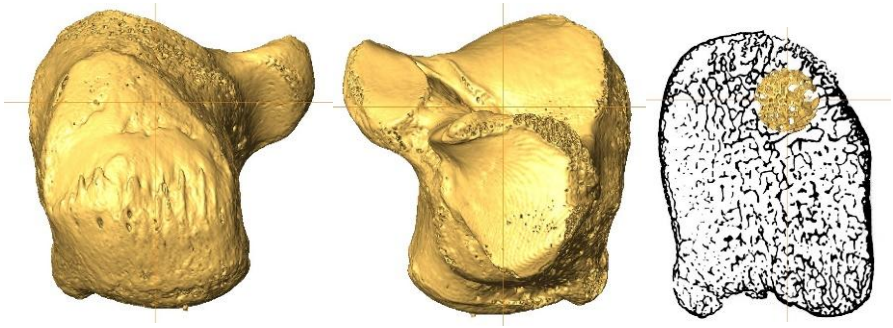

XY

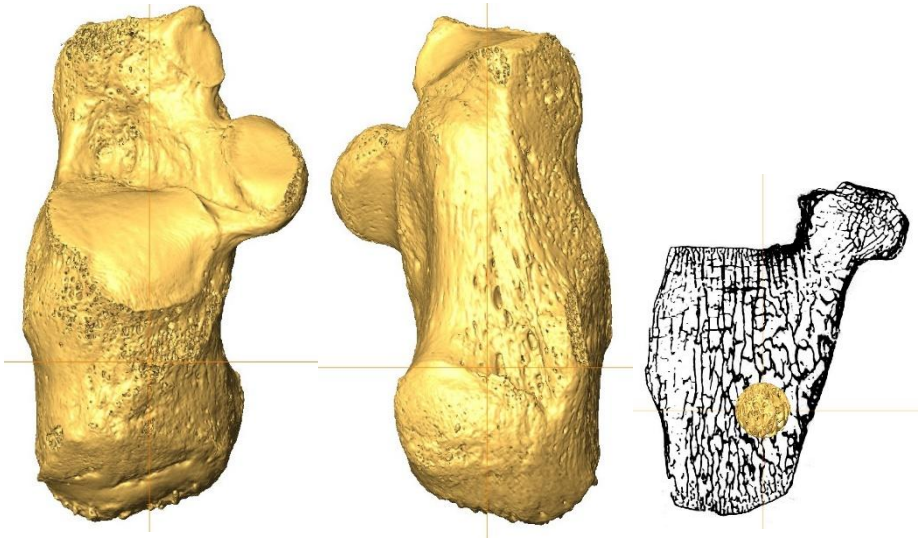

XZ

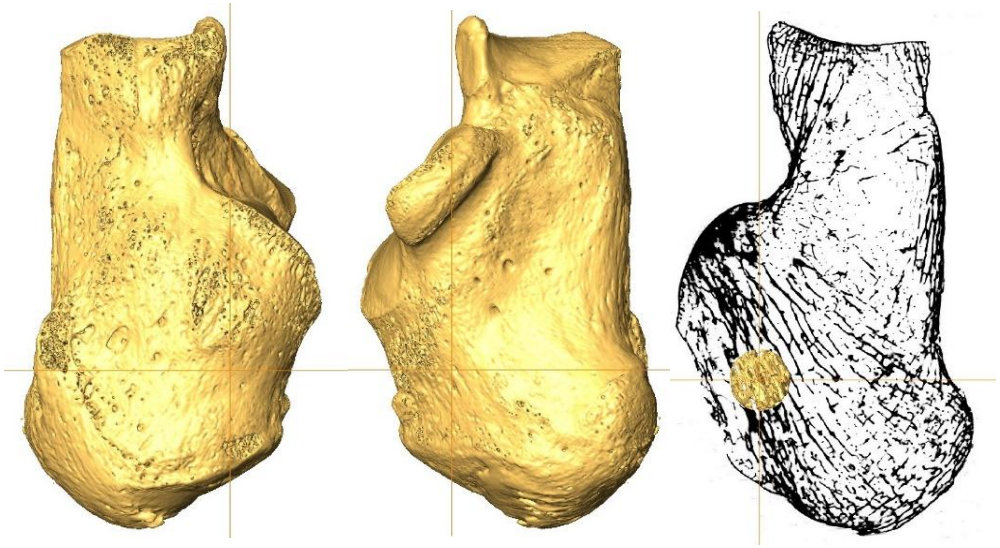

YZ

Achilles tendon.

The VOI is 8% length of calcaneal length. It is placed between the Achilles tendon insertion and the plantar fascia insertion, just inside the cortex and two thirds on the way to the Achilles tendon insertion, from the plantar fascia insertion.

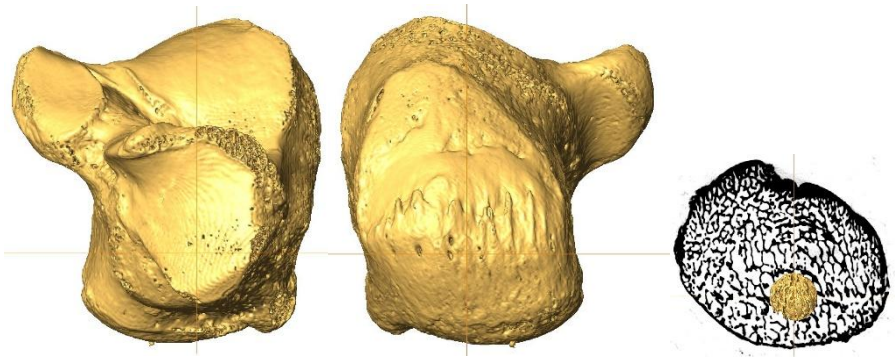

XY

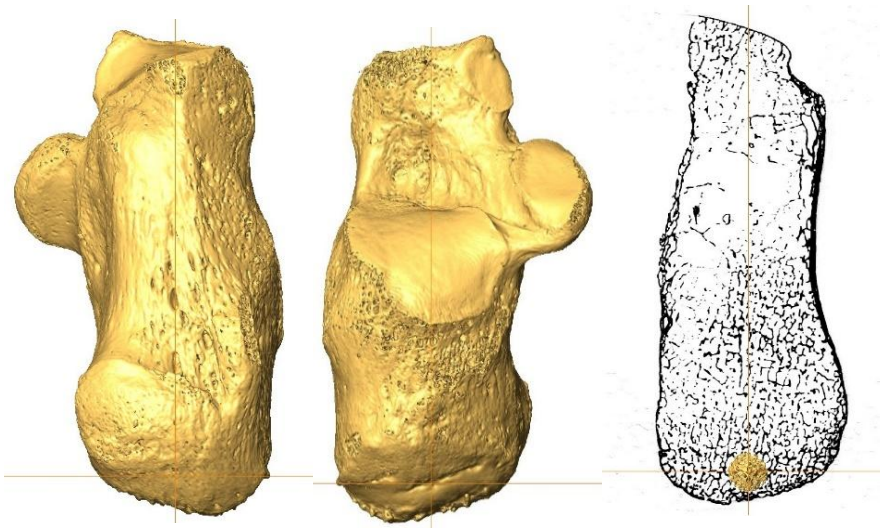

XZ

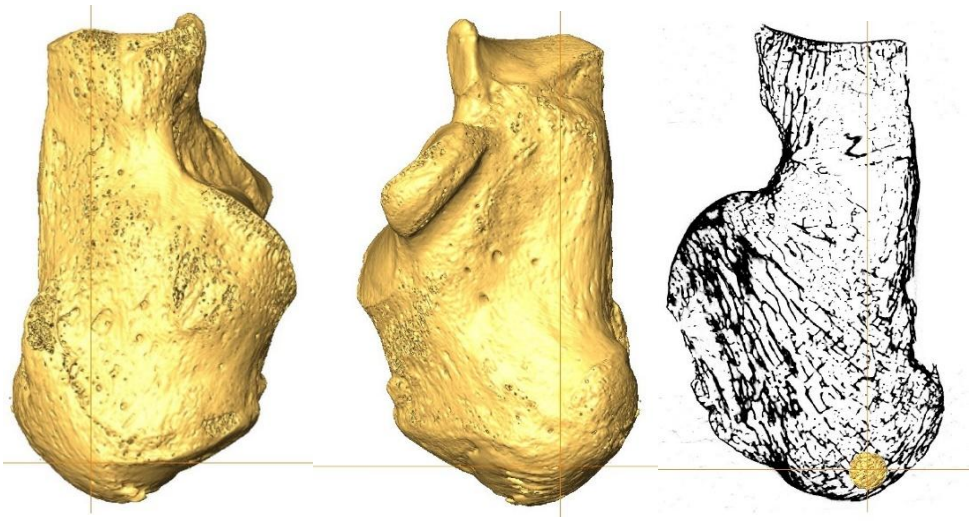

YZ

Talus

Talar length is highly correlated with body mass and talar size, and is thus used to standardize the VOIs. Two different ROIs are used to place VOIs; one for the trochlea and one for the other three VOIs.

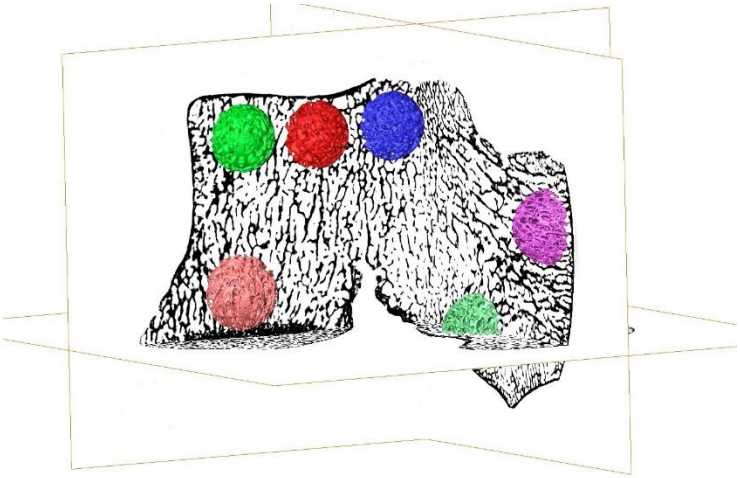

VOIs: trochlea (lateral=green, central=red, medial=blue), anterior calcaneal facet (light green), posterior calcaneal facet (salmon), talar head (purple).

Trochlea VOIs: lateral central and medial

A bounding box is placed along the maximum length of the talus and the maximum superior breadth of the trochlea, not taking into account the breadth of the medial or lateral malleolus. VOI diameter is calculated as 26% of bounding box breadth. This breadth corresponds to trochlear breadth (measurement T12) and is highly correlated to body mass in all populations. VOIs are placed equally spaced apart at 25, 50, and 75% of bounding box breadth. VOIs should be placed just below the articular surface at the most dorsal point of the trochlea

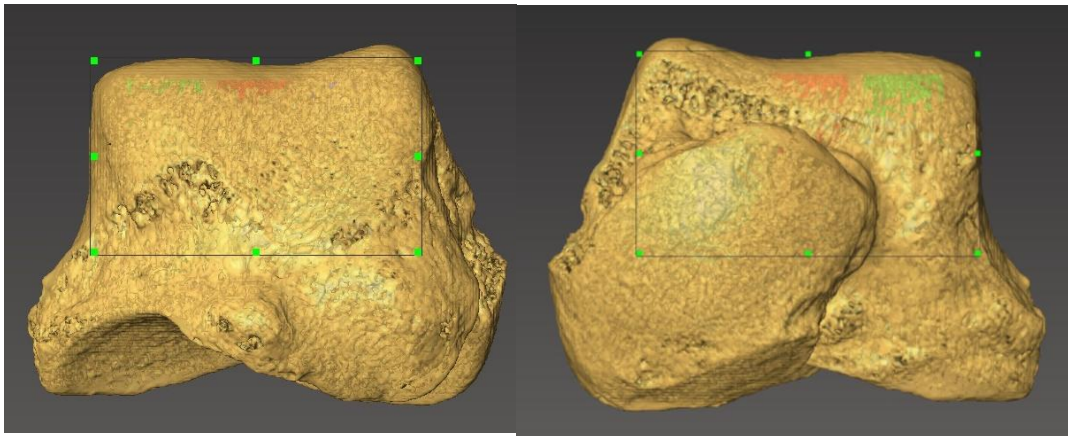

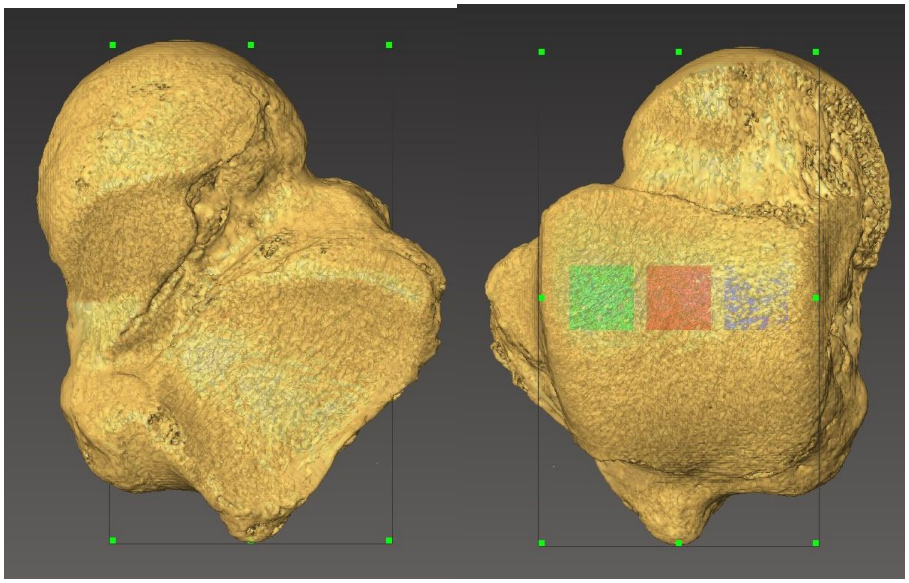

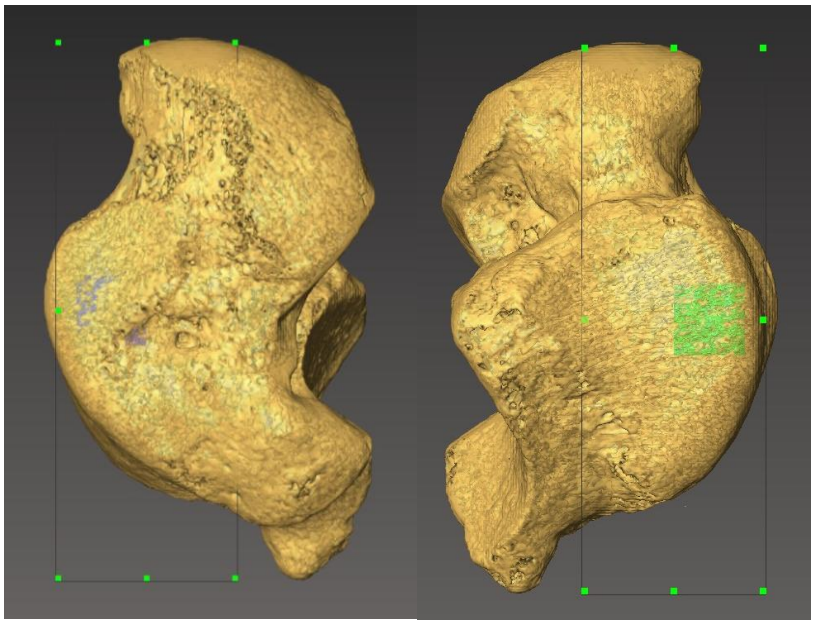

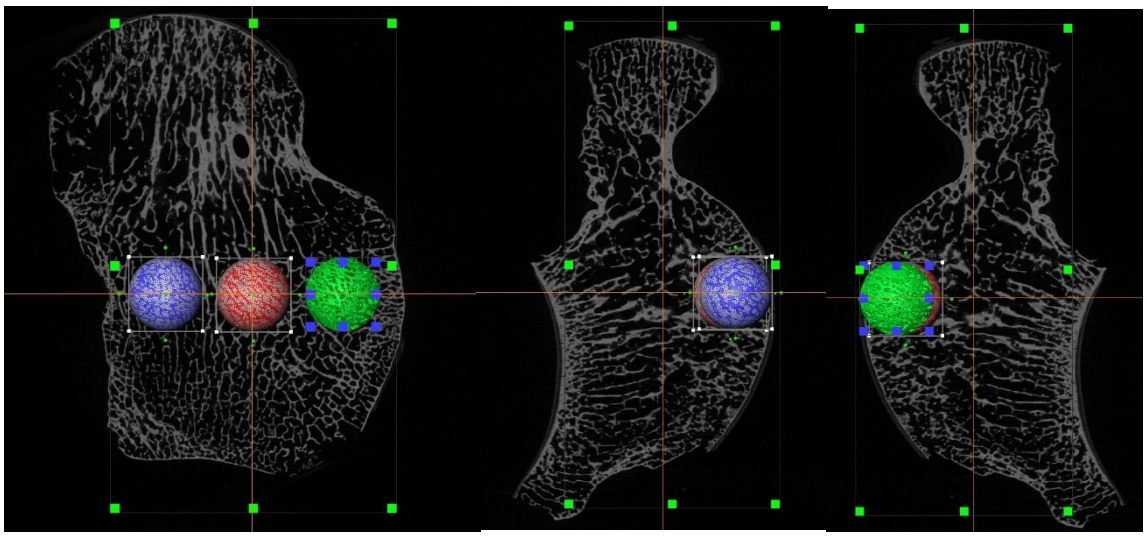

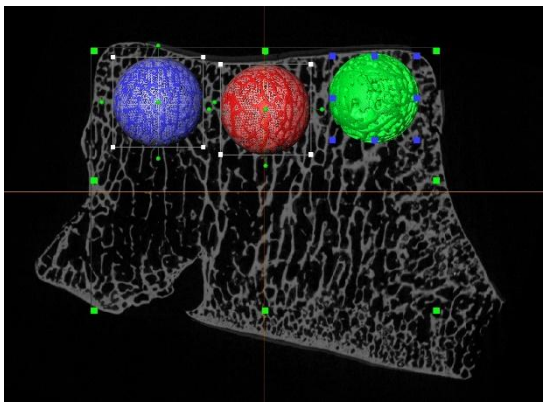

Talar Head (TH)

The ROI remains along the maximum length of the talus and the maximum width of the talar head and dorsoplantar height of the talus. The sphere's diameter is scaled to 15% of talar length and is placed at the maximum mediolateral curvature of the talar head. Talar length (measurement TA1) is strongly correlated to body mass in all populations used in this thesis.

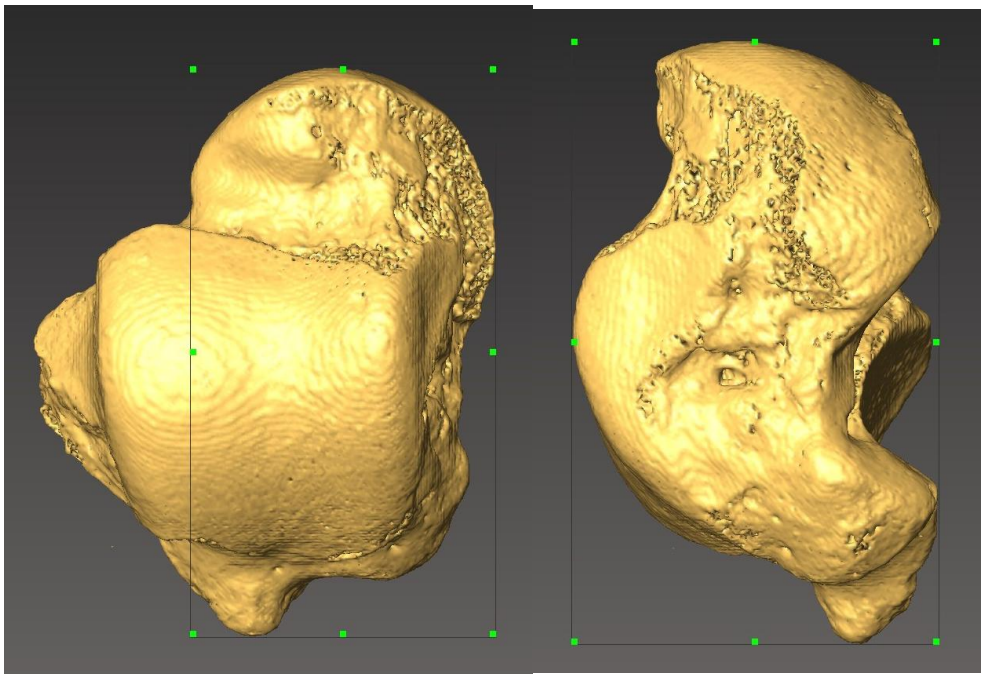

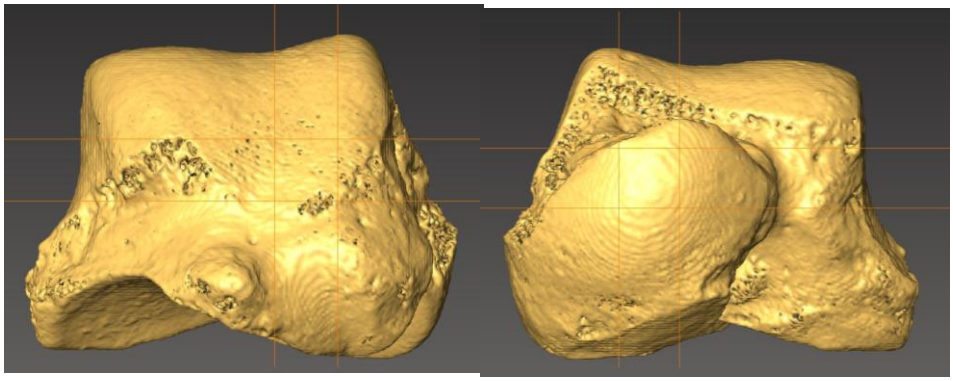

XY

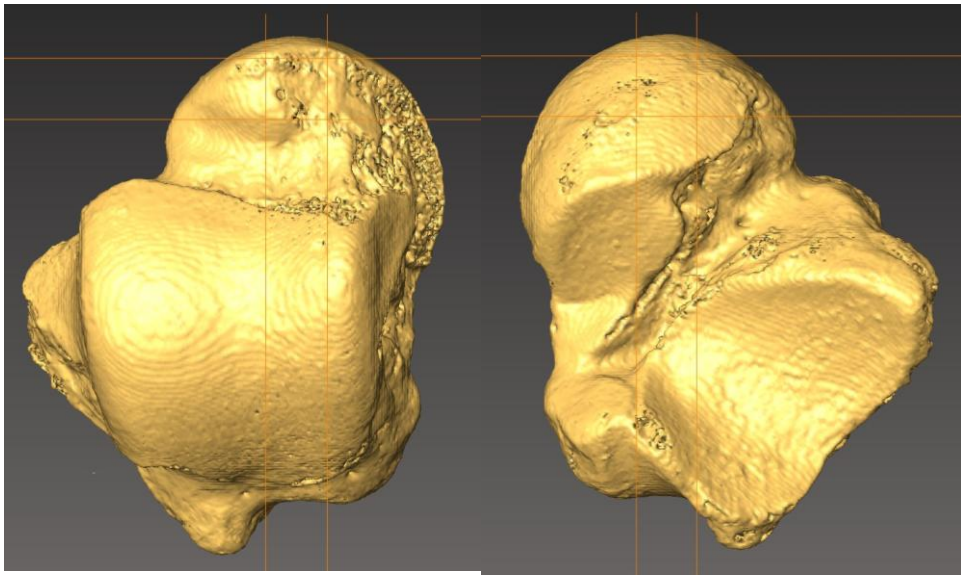

XZ

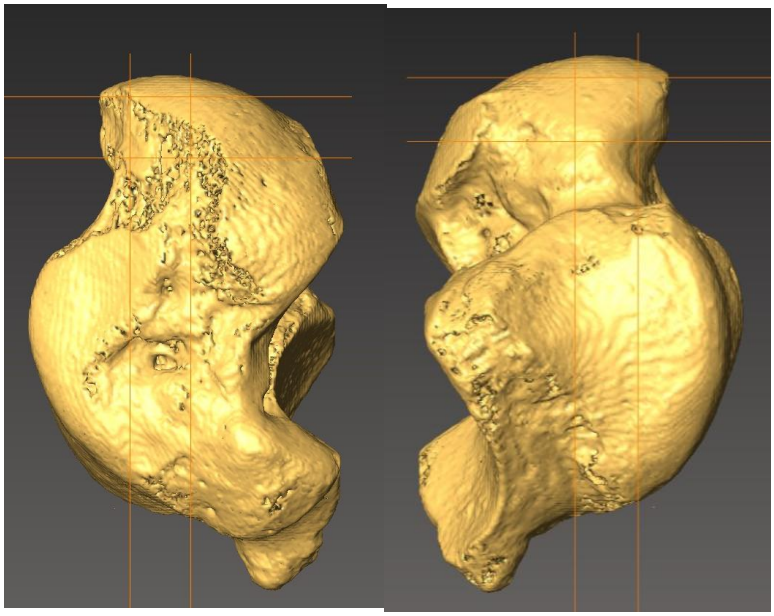

YZ

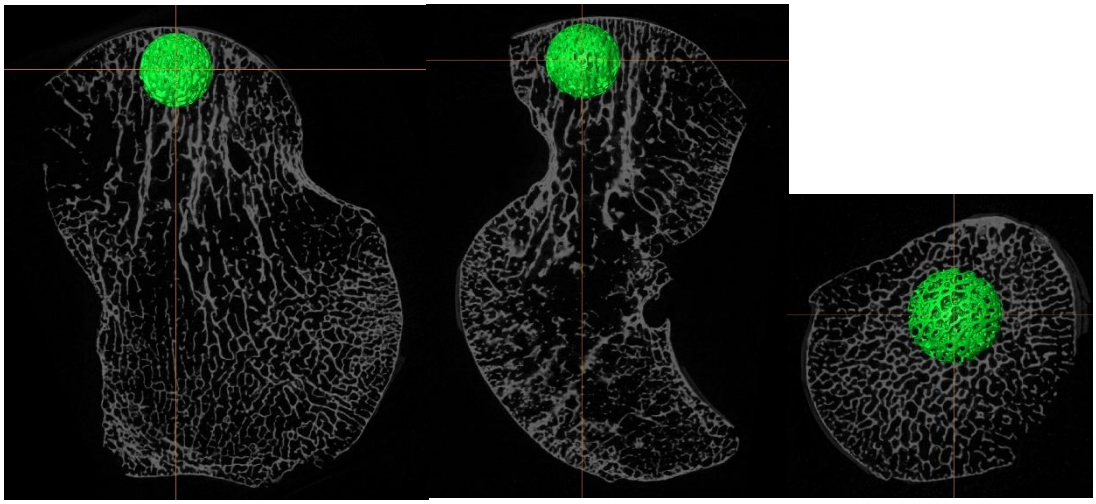

XZ *YZ* *XY*

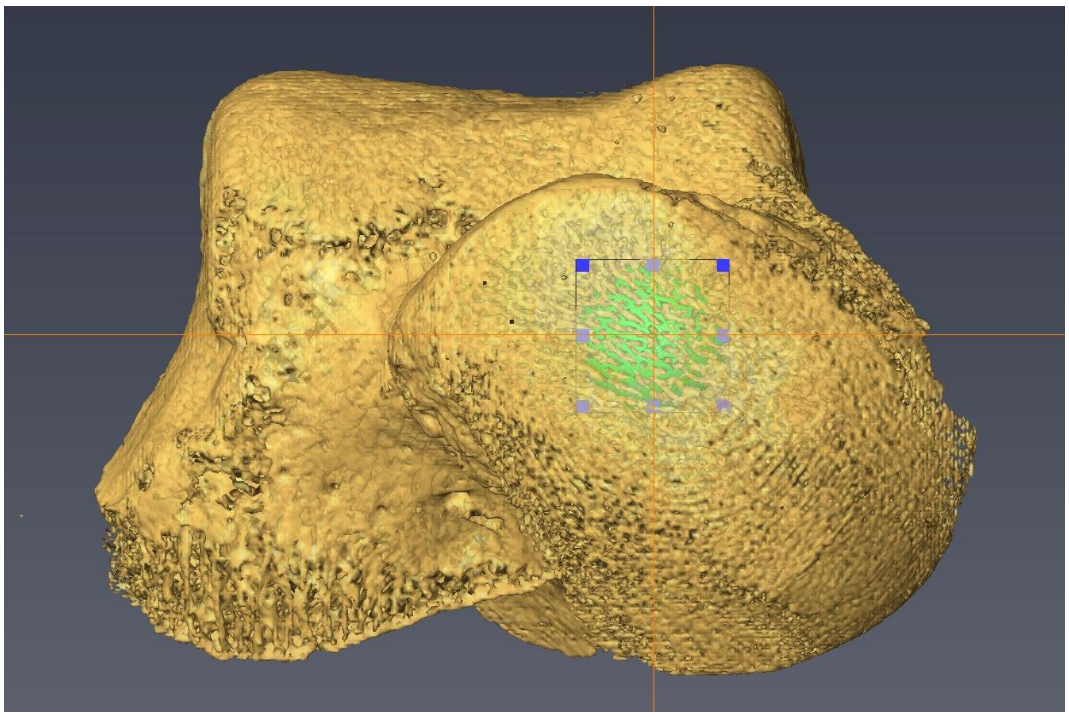

XY

Anterior calcaneal facet (ACF)

The bounding box is identical to the one used for the talar head (TH). VOI is scaled to 15% of maximum talar length and is placed just deep to the anterior calcaneal facet.

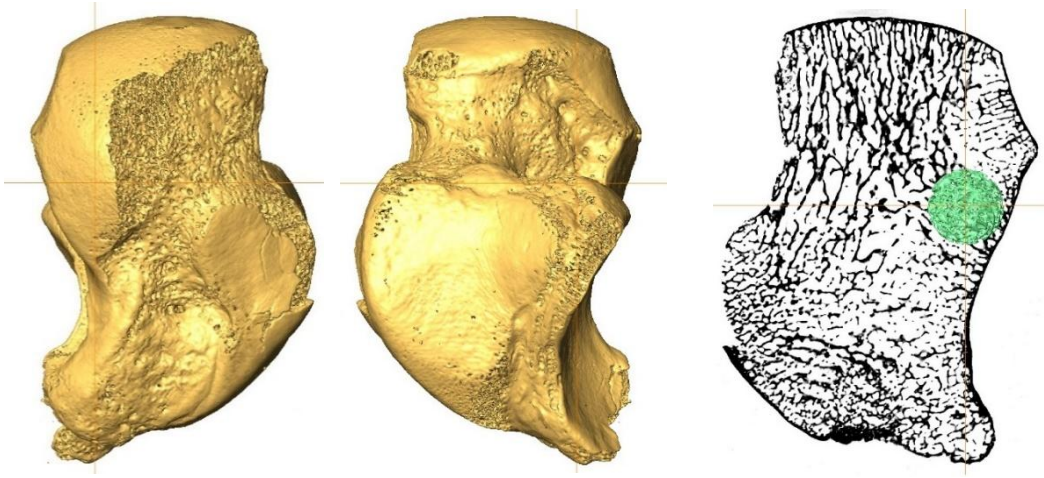

YZ

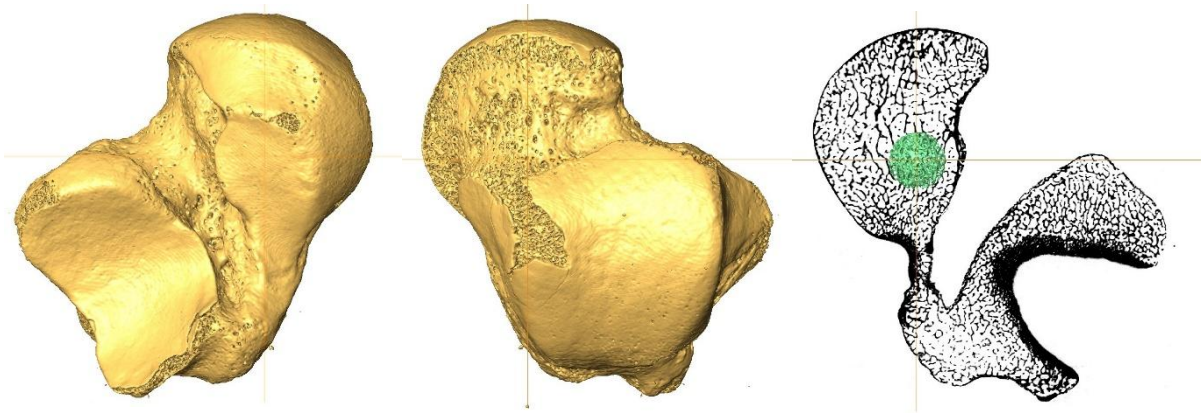

XZ

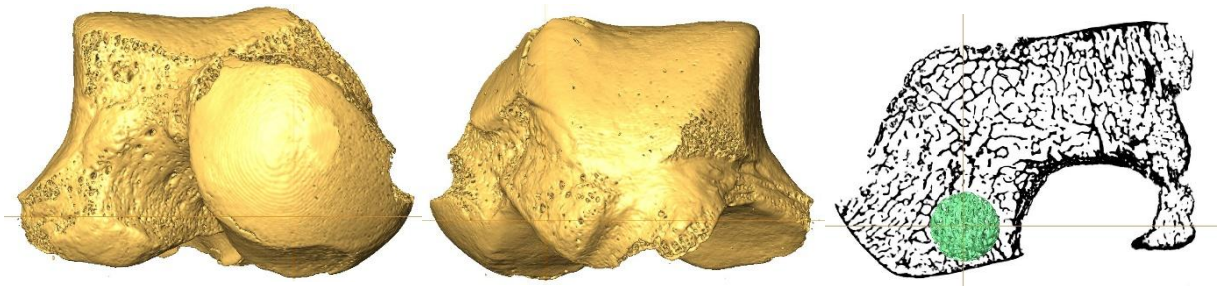

XY

Posterior calcaneal facet

The bounding box is identical to the one used for the talar head (TH). The VOI is 15% of maximum talar length and is placed just under the posterior calcaneal facet just below the articular surface.

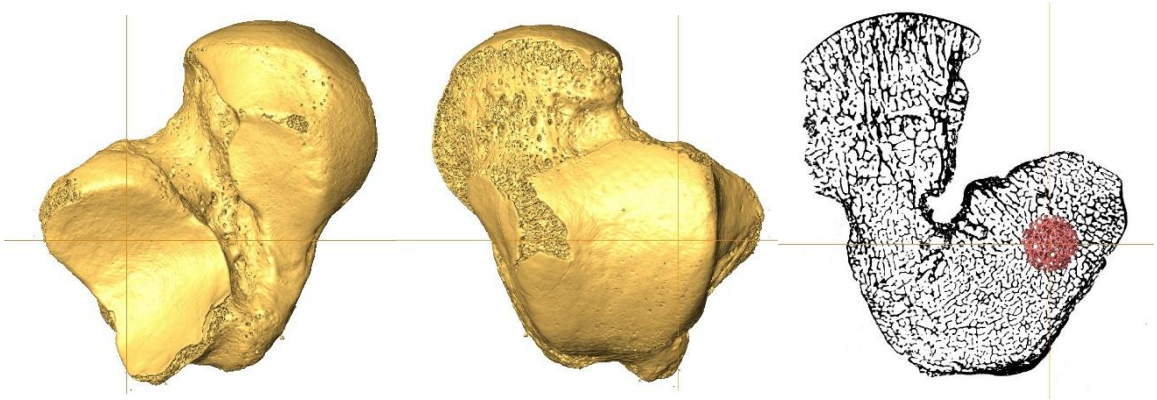

XZ

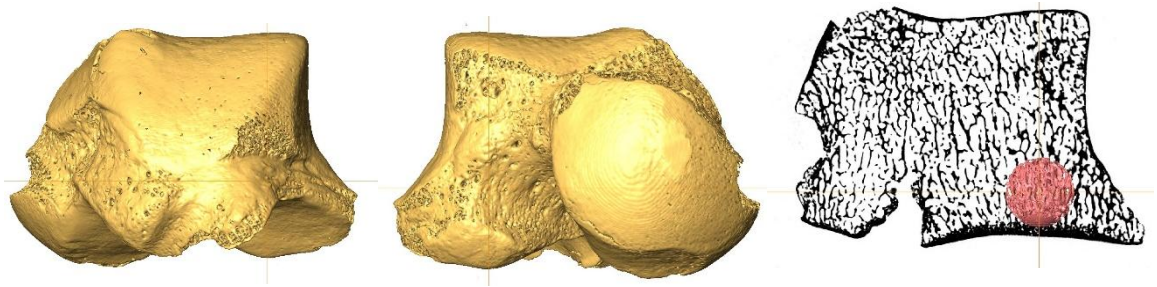

XY

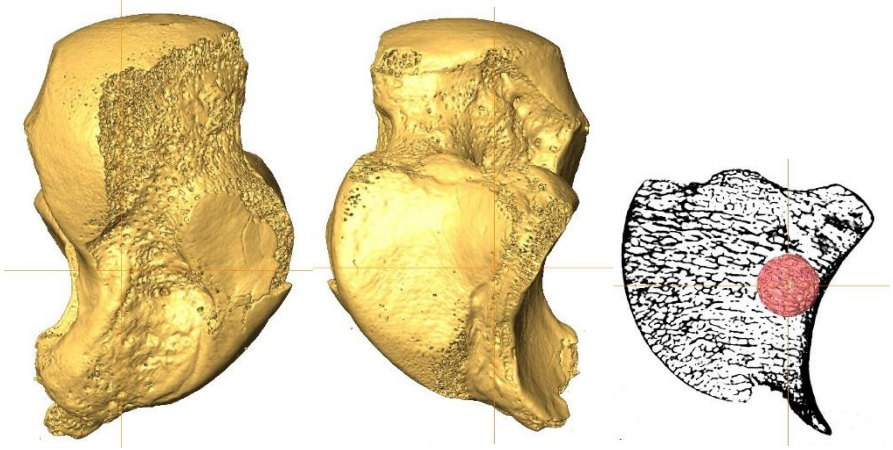

YZ

First Metatarsal

First metatarsal head

Open the MT1 cubing script and place a bounding box around the mt1 head as shown in the pictures below.

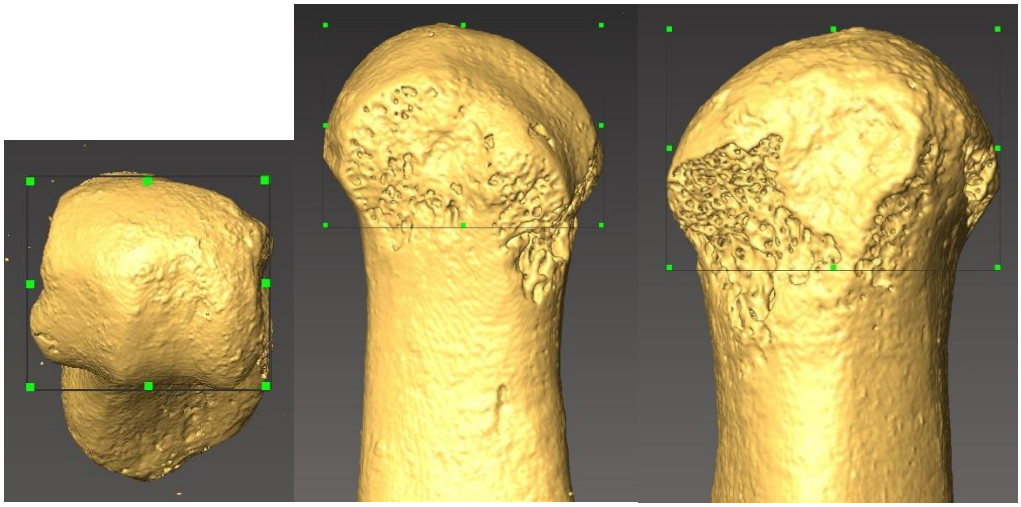

XY *YZ* *YZ*

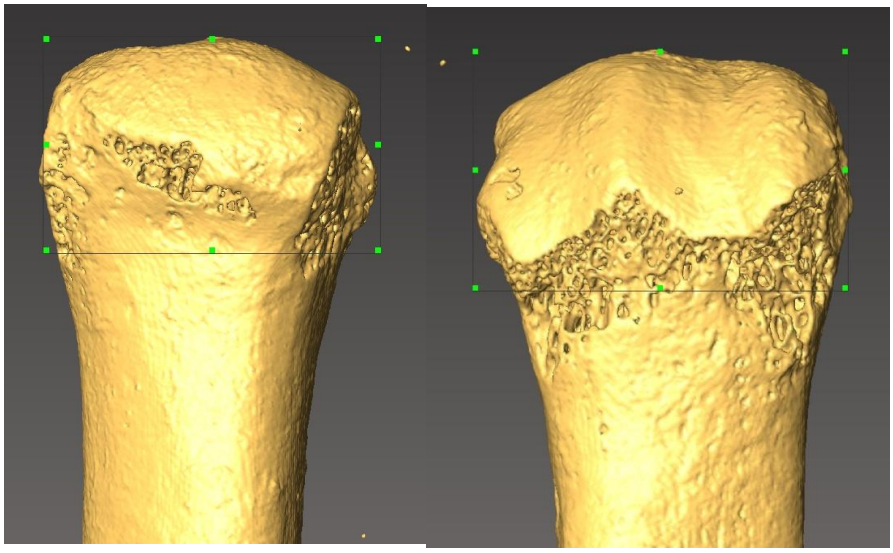

XZ *XZ*

Two spheres are placed in the MT1 head: one dorsal and one plantar on top of each other. The spheres scaled to a diameter of 35% of the height of the first metatarsal head, measured by the bounding box. This corresponds to dorsoplantar height of the first metatarsal head (measurement DPD) and is strongly correlated to body mass in all populations. Spheres are placed just beneath the articular surface.

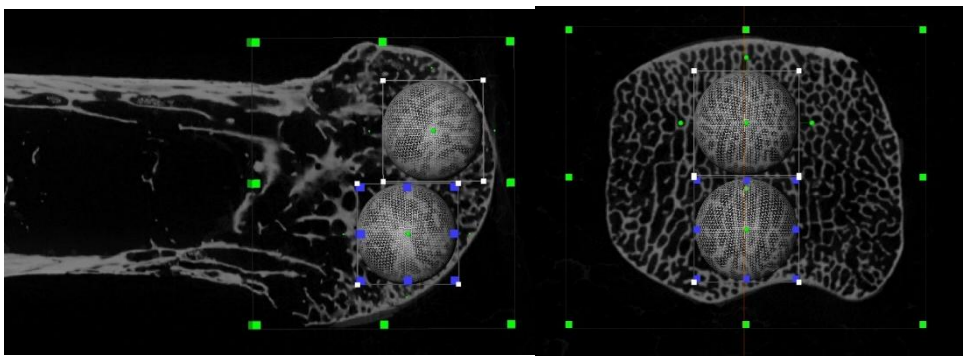

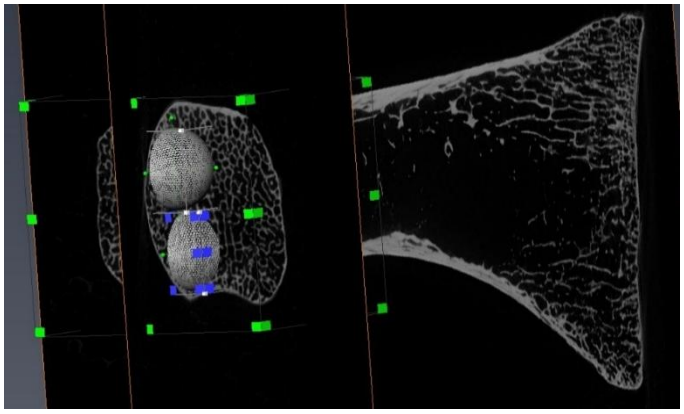

First metatarsal base

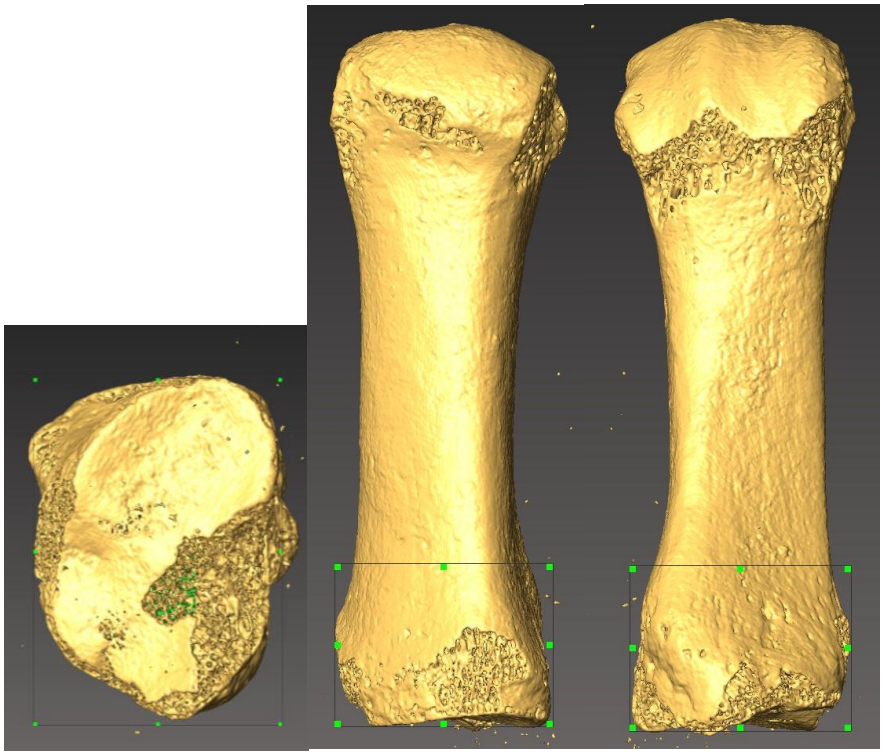

XY *XZ* *XZ*

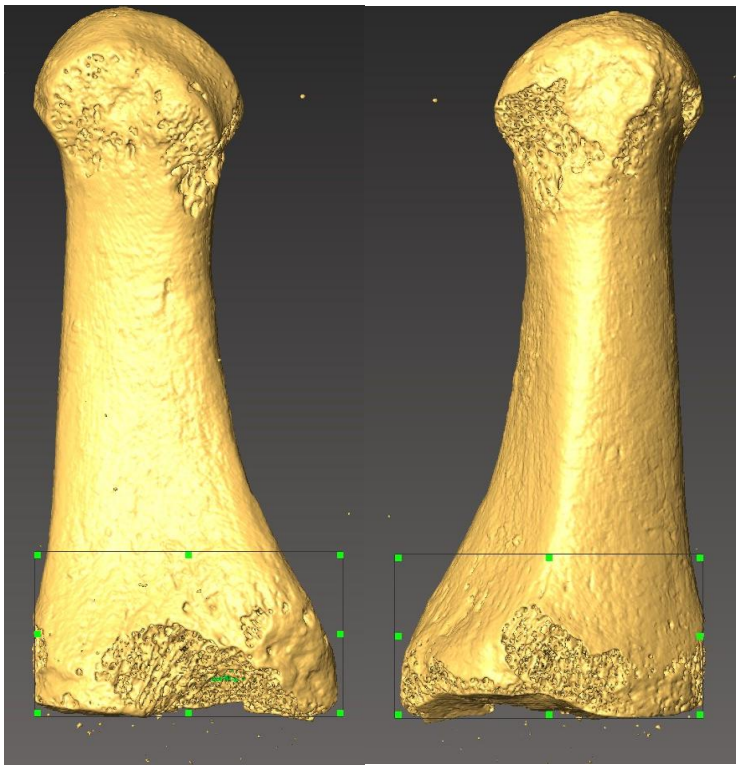

YZ *YZ*

Two spheres are placed in the MT1 base: one dorsal and one plantar. Spheres are scaled to 25% of the greatest bounding box dimension, which for the MT1 base is the height of the first metatarsal base. Dorsoplantar height of the first metatarsal bsae (measurement DPP) is strongly correlated to body mass in all populations. The spheres are then automatically placed in the correct location inside the bounding box using the autoVOI script.

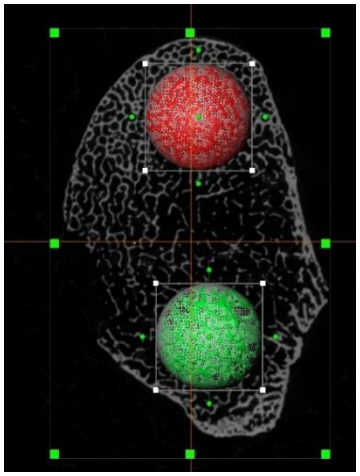

XY

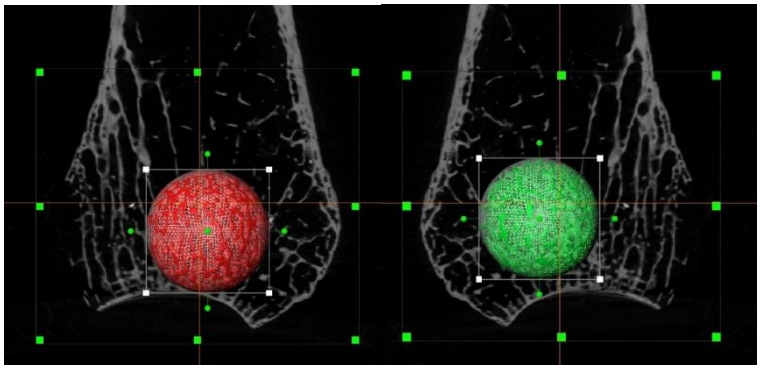

XZ

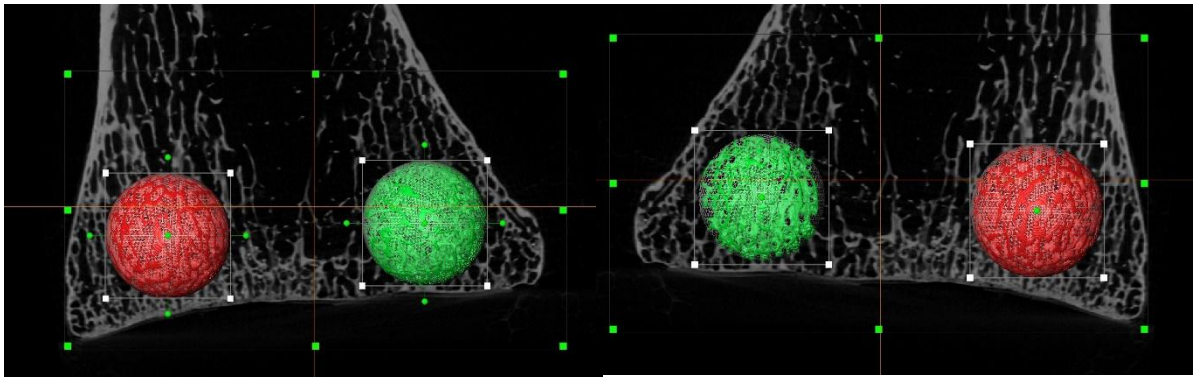

YZ

Trabecular Analysis Using Bone J

1. Open a trabecular cube (that has already been cropped for the ROI from the bone)
    i. RAW: File>Import>Raw>(select one of the slices in the file of interest)>(insert width & height of the images, as well as number of images, offset to first image=0)
    OR
    ii. DICOM: File>Import>Image Sequence>>(select one of the slices in the file of interest)>OK

IF Trabecular cube will not threshold properly (all black background once macro is run): re-open image, Adjust >Brightness/Contrast > Auto – then move the minimum so that the indicator line contacts the left-most side of the data on the histogram.

Then: Image>Type>8-bit…then run Trab Plug in.

2. To Run Bone J Macro (Bone_J_Auto)
    a. Plug-ins > Macros > Trab
        i. (see note at bottom of document re. having macros start up immediately)

OR

3. Plugins > Bone J > Optimise Threshold
    a. Check both 'Threshold Only' and 'Apply Threshold'
    b. Your trabecular data should now be binary – not all black, nor all white.
4. All in Bone J (Plugins > Bone J)
        i. Volume Fraction
            1. Algorithm: Voxel
        ii. Thickness
            1. Check Thickness and Spacing, (don't check Graphic Result – unless you desire an image output of thickness values for each trabeculae)
        iii. Structure Model index
            1. SMI Method: Hildebrand & Ruegsegger
        iv. Anisotropy
            1. Use all defaults
        v. Purify
            1. Labelling Algorithm: Multithreaded
        vi. Connectivity

    1. Use all defaults
5. Run these processes (or the macro compiled which runs all of these automatically, see instructions below) for each bone, at each resolution.
6. Copy the results into an excel spreadsheet.

To write a new Macro: Plug-ins > Macros > Record

Plug-ins>Macros>Start-Up Macros – at the bottom of this text file paste in the macro that you have built – encapsulate the whole macro – at start and end with the proper brackets – as seen in earlier text.

Appendix 2.3 Summary statistics of trabecular properties

Table 2.3.1. Summary table of trabecular properties in males (M), females (F), and pooled sex (P) samples. S.E. indicates the standard error and S.D. indicates the standard deviation.

VOI			Black Earth			Jebel Moya				Kerma			St. Johns				Pooled			
			M	F	P	M	F	I	P	M	F	P	M	F	I	P	M	F	I	P
Achilles tendon	BV/TV	Mean	0.47	0.44	0.45	0.48	0.35	0.48	0.46	0.31	0.37	0.33	0.39	0.39	0.46	0.39	0.41	0.40	0.47	0.41
		S.E.	0.03	0.04	0.03	0.02	0.03	0.02	0.02	0.02	0.03	0.02	0.02	0.02		0.01	0.02	0.02	0.02	0.01
		S.D.	0.09	0.13	0.11	0.04	0.04	0.04	0.06	0.06	0.07	0.07	0.05	0.05		0.05	0.09	0.09	0.04	0.09
		N	7	10	17	8	2	5	15	9	7	16	9	11	1	21	33	30	6	69
	Tb.Th	Mean	0.33	0.31	0.31	0.34	0.26	0.32	0.32	0.26	0.27	0.27	0.28	0.26	0.35	0.27	0.30	0.28	0.33	0.29
		S.E.	0.01	0.02	0.01	0.01	0.02	0.01	0.01	0.01	0.01	0.01	0.01	0.01		0.01	0.01	0.01	0.01	0.01
		S.D.	0.04	0.06	0.05	0.04	0.03	0.02	0.04	0.04	0.02	0.03	0.02	0.03		0.03	0.04	0.04	0.02	0.04
		N	7	10	17	8	2	5	15	9	7	16	9	11	1	21	33	30	6	69
	DA	Mean	0.75	0.70	0.72	0.75	0.64	0.76	0.74	0.75	0.73	0.75	0.78	0.78	0.78	0.78	0.76	0.73	0.76	0.75
		S.E.	0.02	0.02	0.02	0.02	0.06	0.02	0.02	0.01	0.03	0.01	0.01	0.01		0.01	0.01	0.01	0.02	0.01
		S.D.	0.06	0.07	0.07	0.07	0.08	0.04	0.07	0.03	0.08	0.06	0.03	0.05		0.04	0.05	0.08	0.04	0.06
		N	7	10	17	8	2	5	15	9	7	16	9	11	1	21	33	30	6	69
	Tb.Sp	Mean	0.42	0.42	0.42	0.43	0.50	0.42	0.43	0.56	0.49	0.53	0.47	0.43	0.45	0.45	0.47	0.45	0.42	0.46
		S.E.	0.03	0.03	0.02	0.02	0.04	0.03	0.01	0.03	0.04	0.02	0.02	0.02		0.01	0.01	0.02	0.02	0.01
		S.D.	0.09	0.09	0.09	0.04	0.05	0.06	0.05	0.08	0.09	0.09	0.05	0.07		0.06	0.08	0.08	0.06	0.08
		N	7	10	17	8	2	5	15	9	7	16	9	11	1	21	33	30	6	69
	Conn.D	Mean	5.17	5.84	5.56	5.04	5.77	5.45	5.27	4.41	5.60	4.93	4.45	5.99	5.09	5.28	4.73	5.83	5.39	5.27
		S.E.	0.29	0.30	0.22	0.42	0.03	0.61	0.29	0.49	0.85	0.47	0.26	0.46		0.31	0.19	0.27	0.50	0.17
		S.D.	0.77	0.94	0.91	1.18	0.04	1.36	1.14	1.47	2.25	1.88	0.77	1.53		1.42	1.11	1.47	1.23	1.37
		N	7	10	17	8	2	5	15	9	7	16	9	11	1	21	33	30	6	69
Calcaneo-cuboid	BV/TV	Mean	0.46	0.43	0.45	0.52	0.40	0.53	0.50	0.32	0.40	0.35	0.37	0.36	0.39	0.37	0.41	0.39	0.50	0.41
		S.E.	0.04	0.04	0.03	0.02	0.04	0.02	0.02	0.01	0.03	0.02	0.02	0.02		0.01	0.02	0.02	0.03	0.01
		S.D.	0.10	0.09	0.09	0.06	0.05	0.04	0.06	0.04	0.08	0.07	0.06	0.06		0.05	0.10	0.07	0.07	0.09

		N	7	6	13	9	2	5	16	12	7	19	8	9	1	18	36	24	6	66
	Tb.Th	Mean	0.37	0.34	0.36	0.38	0.31	0.38	0.37	0.29	0.33	0.31	0.31	0.29	0.37	0.30	0.33	0.31	0.38	0.33
		S.E.	0.02	0.02	0.01	0.02	0.02	0.01	0.01	0.01	0.02	0.01	0.01	0.01		0.01	0.01	0.01	0.01	0.01
		S.D.	0.04	0.06	0.05	0.05	0.03	0.03	0.05	0.03	0.05	0.04	0.03	0.04		0.04	0.05	0.05	0.03	0.05
		N	7	6	13	9	2	5	16	12	7	19	8	9	1	18	36	24	6	66
	DA	Mean	0.74	0.73	0.73	0.68	0.71	0.74	0.70	0.73	0.70	0.71	0.71	0.68	0.58	0.69	0.71	0.70	0.71	0.71
		S.E.	0.01	0.01	0.01	0.01	0.03	0.01	0.01	0.02	0.02	0.01	0.01	0.02		0.01	0.01	0.01	0.03	0.01
		S.D.	0.04	0.03	0.04	0.03	0.05	0.03	0.04	0.07	0.04	0.06	0.04	0.06		0.06	0.05	0.05	0.07	0.05
		N	7	6	13	9	2	5	16	12	7	19	8	9	1	18	36	24	6	66
	Tb.Sp	Mean	0.53	0.52	0.52	0.46	0.51	0.45	0.46	0.65	0.55	0.61	0.57	0.53	0.60	0.55	0.56	0.53	0.47	0.54
		S.E.	0.05	0.04	0.03	0.02	0.01	0.02	0.01	0.02	0.04	0.02	0.02	0.03		0.02	0.02	0.02	0.03	0.01
		S.D.	0.13	0.10	0.12	0.06	0.01	0.04	0.05	0.07	0.10	0.09	0.06	0.09		0.07	0.11	0.09	0.07	0.10
		N	7	6	13	9	2	5	16	12	7	19	8	9	1	18	36	24	6	66
	Conn.D	Mean	2.90	3.46	3.16	3.35	4.60	3.69	3.62	3.42	4.35	3.76	4.14	5.24	3.44	4.65	3.46	4.48	3.65	3.85
		S.E.	0.32	0.30	0.23	0.37	0.22	0.51	0.27	0.27	0.70	0.32	0.34	0.69		0.39	0.17	0.35	0.42	0.17
		S.D.	0.84	0.75	0.82	1.11	0.31	1.13	1.09	0.94	1.85	1.38	0.96	2.06		1.66	1.02	1.73	1.02	1.39
		N	7	6	13	9	2	5	16	12	7	19	8	9	1	18	36	24	6	66
Calcaneal tuber	BV/TV	Mean	0.40	0.38	0.39	0.41	0.33	0.40	0.40	0.29	0.31	0.29	0.33	0.32	0.35	0.32	0.35	0.33	0.39	0.35
		S.E.	0.03	0.03	0.02	0.01	0.00	0.02	0.01	0.01	0.01	0.01	0.02	0.02		0.01	0.01	0.01	0.02	0.01
		S.D.	0.09	0.08	0.08	0.03	0.00	0.05	0.04	0.04	0.04	0.04	0.05	0.06		0.06	0.07	0.07	0.05	0.07
		N	7	9	16	10	2	5	17	12	7	19	8	10	1	19	37	28	6	71
	Tb.Th	Mean	0.37	0.35	0.36	0.34	0.29	0.36	0.34	0.30	0.31	0.30	0.32	0.30	0.39	0.32	0.33	0.32	0.36	0.33
		S.E.	0.01	0.02	0.01	0.01	0.00	0.01	0.01	0.01	0.02	0.01	0.01	0.02		0.01	0.01	0.01	0.01	0.01
		S.D.	0.04	0.07	0.06	0.02	0.00	0.03	0.03	0.03	0.04	0.03	0.03	0.05		0.04	0.04	0.05	0.03	0.05
		N	7	9	16	10	2	5	17	12	7	19	8	10	1	19	37	28	6	71
	DA	Mean	0.82	0.79	0.80	0.76	0.77	0.79	0.77	0.83	0.79	0.81	0.79	0.77	0.80	0.78	0.80	0.78	0.80	0.79
		S.E.	0.01	0.01	0.01	0.01	0.01	0.02	0.01	0.01	0.01	0.01	0.01	0.01		0.01	0.01	0.01	0.02	0.00
		S.D.	0.03	0.03	0.03	0.03	0.02	0.05	0.03	0.03	0.03	0.03	0.04	0.05		0.04	0.04	0.03	0.04	0.04
		N	7	9	16	10	2	5	17	12	7	19	8	10	1	19	37	28	6	71
	Tb.Sp	Mean	0.64	0.61	0.62	0.59	0.62	0.60	0.59	0.81	0.70	0.77	0.70	0.63	0.66	0.66	0.69	0.64	0.61	0.67

		S.E.	0.06	0.04	0.03	0.02	0.02	0.02	0.01	0.03	0.05	0.03	0.03	0.03		0.02	0.02	0.02	0.02	0.01
		S.D.	0.15	0.11	0.13	0.05	0.03	0.05	0.05	0.10	0.12	0.12	0.09	0.08		0.09	0.13	0.10	0.05	0.12
		N	7	9	16	10	2	5	17	12	7	19	8	10	1	19	37	28	6	71
	Conn.D	Mean	2.06	2.28	2.18	2.54	2.88	2.24	2.49	1.53	2.33	1.82	2.08	2.85	2.11	2.48	2.02	2.54	2.22	2.24
		S.E.	0.32	0.20	0.18	0.22	0.07	0.28	0.16	0.13	0.39	0.18	0.20	0.24		0.17	0.12	0.15	0.23	0.09
		S.D.	0.85	0.60	0.70	0.71	0.10	0.62	0.65	0.45	1.02	0.79	0.58	0.77		0.76	0.73	0.78	0.56	0.77
		N	7	9	16	10	2	5	17	12	7	19	8	10	1	19	37	28	6	71
Calc PTF anterior	BV/TV	Mean	0.54	0.50	0.52	0.54	0.41	0.57	0.53	0.40	0.46	0.42	0.46	0.43	0.41	0.44	0.47	0.45	0.53	0.47
		S.E.	0.04	0.05	0.03	0.02	0.03	0.05	0.02	0.02	0.03	0.02	0.02	0.02		0.02	0.02	0.02	0.05	0.01
		S.D.	0.10	0.12	0.11	0.05	0.04	0.11	0.08	0.08	0.09	0.09	0.07	0.08		0.07	0.10	0.09	0.12	0.10
		N	7	6	13	8	2	4	14	12	7	19	9	11	1	21	36	26	5	67
	Tb.Th	Mean	0.45	0.42	0.44	0.43	0.35	0.47	0.43	0.36	0.38	0.37	0.38	0.33	0.42	0.36	0.40	0.37	0.46	0.39
		S.E.	0.03	0.03	0.02	0.01	0.04	0.02	0.01	0.01	0.02	0.01	0.02	0.02		0.01	0.01	0.01	0.02	0.01
		S.D.	0.07	0.06	0.07	0.04	0.05	0.05	0.05	0.04	0.05	0.04	0.05	0.07		0.06	0.06	0.07	0.05	0.07
		N	7	6	13	8	2	4	14	12	7	19	9	11	1	21	36	26	5	67
	DA	Mean	0.71	0.70	0.71	0.64	0.65	0.62	0.63	0.72	0.62	0.68	0.72	0.68	0.71	0.70	0.70	0.67	0.64	0.68
		S.E.	0.02	0.03	0.02	0.04	0.03	0.04	0.03	0.04	0.04	0.03	0.02	0.03		0.02	0.02	0.02	0.04	0.01
		S.D.	0.05	0.07	0.06	0.11	0.04	0.09	0.09	0.12	0.09	0.12	0.06	0.10		0.08	0.10	0.09	0.09	0.10
		N	7	6	13	7	2	4	13	12	7	19	9	11	1	21	35	26	5	66
	Tb.Sp	Mean	0.52	0.52	0.52	0.46	0.55	0.50	0.49	0.64	0.54	0.60	0.56	0.48	0.59	0.52	0.55	0.51	0.52	0.53
		S.E.	0.05	0.05	0.03	0.02	0.01	0.04	0.02	0.03	0.05	0.03	0.03	0.02		0.02	0.02	0.02	0.04	0.01
		S.D.	0.12	0.11	0.11	0.04	0.01	0.09	0.06	0.10	0.12	0.11	0.08	0.06		0.08	0.11	0.09	0.09	0.10
		N	7	6	13	8	2	4	14	11	7	18	9	11	1	21	35	26	5	66
	Conn.D	Mean	2.69	3.40	3.02	3.68	4.31	2.71	3.49	2.89	3.63	3.16	3.34	5.18	2.70	4.27	3.14	4.29	2.71	3.55
		S.E.	0.28	0.28	0.22	0.25	0.62	0.33	0.23	0.29	0.49	0.26	0.28	0.55		0.37	0.15	0.31	0.25	0.16
		S.D.	0.75	0.68	0.78	0.71	0.88	0.66	0.86	1.00	1.28	1.14	0.84	1.82		1.71	0.90	1.58	0.57	1.33
		N	7	6	13	8	2	4	14	12	7	19	9	11	1	21	36	26	5	67
Calc PTF central	BV/TV	Mean	0.63	0.56	0.59	0.62	0.50	0.65	0.61	0.48	0.55	0.50	0.50	0.47	0.51	0.49	0.54	0.52	0.62	0.54
		S.E.	0.05	0.05	0.03	0.01	0.05	0.05	0.02	0.02	0.02	0.02	0.03	0.03		0.02	0.02	0.02	0.05	0.01
		S.D.	0.11	0.12	0.12	0.04	0.07	0.10	0.08	0.07	0.05	0.07	0.10	0.08		0.09	0.11	0.09	0.11	0.10

		N	6	7	13	8	2	4	14	12	6	18	9	11	1	21	35	26	5	66
	Tb.Th	Mean	0.48	0.41	0.44	0.47	0.40	0.51	0.47	0.38	0.40	0.39	0.39	0.34	0.42	0.36	0.42	0.38	0.49	0.41
		S.E.	0.03	0.02	0.02	0.02	0.07	0.02	0.02	0.01	0.02	0.01	0.02	0.02		0.01	0.01	0.01	0.02	0.01
		S.D.	0.07	0.07	0.08	0.05	0.10	0.03	0.06	0.04	0.05	0.05	0.06	0.07		0.07	0.07	0.07	0.05	0.07
		N	6	7	13	8	2	4	14	12	6	18	9	11	1	21	35	26	5	66
	DA	Mean	0.69	0.68	0.69	0.55	0.65	0.55	0.57	0.66	0.60	0.64	0.60	0.54	0.74	0.58	0.63	0.60	0.59	0.61
		S.E.	0.04	0.03	0.02	0.03	0.04	0.06	0.03	0.03	0.04	0.02	0.03	0.03		0.02	0.02	0.02	0.06	0.01
		S.D.	0.10	0.09	0.09	0.10	0.05	0.13	0.10	0.10	0.09	0.10	0.09	0.09		0.10	0.11	0.10	0.14	0.11
		N	6	7	13	8	2	4	14	12	6	18	9	11	1	21	35	26	5	66
	Tb.Sp	Mean	0.41	0.45	0.43	0.42	0.49	0.44	0.43	0.51	0.45	0.49	0.48	0.44	0.53	0.46	0.46	0.45	0.46	0.46
		S.E.	0.05	0.04	0.03	0.02	0.03	0.03	0.02	0.02	0.04	0.02	0.03	0.02		0.02	0.01	0.01	0.03	0.01
		S.D.	0.12	0.09	0.10	0.06	0.04	0.06	0.06	0.07	0.09	0.08	0.08	0.06		0.07	0.09	0.07	0.07	0.08
		N	6	7	13	8	2	4	14	12	6	18	9	11	1	21	35	26	5	66
	Conn.D	Mean	2.85	3.58	3.24	3.15	4.14	2.27	3.04	3.84	4.50	4.06	4.19	6.33	3.15	5.26	3.60	5.00	2.45	4.06
		S.E.	0.14	0.22	0.17	0.26	1.35	0.36	0.28	0.29	0.89	0.34	0.29	0.67		0.45	0.16	0.42	0.33	0.21
		S.D.	0.34	0.59	0.61	0.74	1.91	0.73	1.04	1.01	2.17	1.46	0.88	2.23		2.04	0.95	2.15	0.74	1.72
		N	6	7	13	8	2	4	14	12	6	18	9	11	1	21	35	26	5	66
Calc PTF posterior	BV/TV	Mean	0.55	0.50	0.53	0.57	0.40	0.55	0.56	0.41	0.45	0.42	0.46	0.42	0.48	0.44	0.49	0.45	0.54	0.48
		S.E.	0.04	0.03	0.03	0.01		0.03	0.02	0.01	0.02	0.01	0.03	0.02		0.01	0.02	0.01	0.03	0.01
		S.D.	0.10	0.10	0.10	0.03		0.06	0.06	0.04	0.04	0.04	0.08	0.06		0.07	0.10	0.07	0.06	0.09
		N	7	8	15	9	1	4	14	12	5	17	9	11	1	21	37	25	5	67
	Tb.Th	Mean	0.45	0.40	0.43	0.43	0.31	0.43	0.42	0.34	0.37	0.34	0.36	0.33	0.43	0.35	0.39	0.36	0.43	0.38
		S.E.	0.02	0.02	0.02	0.01		0.01	0.01	0.01	0.02	0.01	0.01	0.01		0.01	0.01	0.01	0.01	0.01
		S.D.	0.06	0.07	0.06	0.03		0.03	0.04	0.03	0.05	0.04	0.04	0.05		0.05	0.06	0.06	0.02	0.06
		N	7	8	15.00	9	1	4	14.00	12	5	17.00	9	11	1	21.00	37	25	5	67
	DA	Mean	0.77	0.75	0.76	0.70	0.70	0.70	0.70	0.71	0.71	0.71	0.71	0.67	0.79	0.69	0.72	0.70	0.72	0.71
		S.E.	0.00	0.01	0.01	0.02		0.05	0.02	0.02	0.03	0.02	0.02	0.02		0.01	0.01	0.01	0.04	0.01
		S.D.	0.01	0.04	0.03	0.05		0.10	0.06	0.06	0.07	0.06	0.06	0.06		0.06	0.05	0.06	0.10	0.06
		N	7	8	15	9	1	4	14	12	5	17	9	11	1	21	37	25	5	67
	Tb.Sp	Mean	0.51	0.52	0.52	0.47	0.52	0.49	0.48	0.59	0.55	0.58	0.51	0.51	0.54	0.51	0.53	0.52	0.50	0.52

		S.E.	0.05	0.03	0.03	0.02		0.03	0.01	0.02	0.01	0.01	0.02	0.02		0.01	0.01	0.01	0.03	0.01
		S.D.	0.14	0.07	0.11	0.06		0.06	0.06	0.06	0.03	0.05	0.06	0.07		0.06	0.09	0.06	0.06	0.08
		N	7	8	15	9	1	4	14	12	5	17	9	11	1	21	37	25	5	67
	Conn.D	Mean	2.38	2.65	2.52	3.02	4.65	2.94	3.11	3.50	3.69	3.56	4.01	5.04	2.66	4.48	3.30	3.99	2.88	3.52
		S.E.	0.19	0.26	0.16	0.21		0.18	0.18	0.26	0.60	0.24	0.29	0.41		0.28	0.15	0.31	0.15	0.15
		S.D.	0.49	0.74	0.63	0.63		0.35	0.69	0.90	1.34	1.01	0.86	1.36		1.29	0.93	1.54	0.33	1.22
		N	7	8	15	9	1	4	14	12	5	17	9	11	1	21	37	25	5	67
Plantar ligament	BV/TV	Mean	0.33	0.36	0.34	0.42	0.23	0.35	0.37	0.22	0.28	0.25	0.29	0.26	0.22	0.27	0.29	0.29	0.33	0.30
		S.E.	0.03	0.03	0.02	0.04		0.03	0.03	0.01	0.02	0.01	0.03	0.01		0.01	0.02	0.01	0.03	0.01
		S.D.	0.06	0.07	0.06	0.08		0.08	0.09	0.05	0.06	0.06	0.07	0.04		0.06	0.09	0.07	0.08	0.08
		N	6	6	12	5	1	5	11	11	7	18	8	10	1	19	30	24	6	60
	Tb.Th	Mean	0.38	0.38	0.38	0.37	0.26	0.34	0.34	0.26	0.28	0.27	0.31	0.27	0.34	0.29	0.31	0.30	0.34	0.31
		S.E.	0.01	0.03	0.01	0.03		0.02	0.02	0.01	0.01	0.01	0.02	0.01		0.01	0.01	0.01	0.01	0.01
		S.D.	0.03	0.07	0.05	0.06		0.04	0.06	0.03	0.03	0.03	0.05	0.04		0.04	0.06	0.06	0.03	0.06
		N	6	6	12	5	1	5	11	11	7	18	8	10	1	19	30	24	6	60
	DA	Mean	0.70	0.65	0.67	0.74	0.66	0.69	0.71	0.73	0.69	0.71	0.76	0.73	0.74	0.75	0.73	0.70	0.70	0.71
		S.E.	0.03	0.03	0.02	0.03		0.03	0.02	0.01	0.03	0.01	0.02	0.02		0.01	0.01	0.02	0.02	0.01
		S.D.	0.07	0.06	0.07	0.06		0.06	0.06	0.03	0.08	0.06	0.06	0.07		0.06	0.06	0.08	0.06	0.07
		N	6	6	12	5	1	5	11	11	7	18	8	10	1	19	30	24	6	60
	Tb.Sp	Mean	0.77	0.66	0.72	0.56	0.70	0.63	0.61	0.81	0.68	0.76	0.80	0.76	0.96	0.79	0.76	0.71	0.69	0.73
		S.E.	0.07	0.04	0.04	0.04		0.04	0.03	0.03	0.04	0.03	0.04	0.03		0.03	0.03	0.02	0.06	0.02
		S.D.	0.18	0.09	0.15	0.08		0.09	0.09	0.11	0.10	0.12	0.12	0.11		0.12	0.15	0.10	0.15	0.13
		N	6	6	12	5	1	5	11	11	7	18	8	10	1	19	30	24	6	60
	Conn.D	Mean	1.72	2.51	2.11	2.78	3.33	2.89	2.88	2.27	3.21	2.64	1.90	2.56	1.18	2.21	2.15	2.77	2.60	2.44
		S.E.	0.23	0.20	0.19	0.51		0.33	0.26	0.20	0.34	0.21	0.27	0.30		0.21	0.15	0.17	0.39	0.11
		S.D.	0.57	0.49	0.65	1.15		0.74	0.88	0.67	0.89	0.88	0.77	0.95		0.92	0.82	0.85	0.96	0.88
		N	6	6	12	5	1	5	11	11	7	18	8	10	1	19	30	24	6	60
MT1 base dorsal	BV/TV	Mean	0.46	0.45	0.45	0.47	0.41	0.51	0.47	0.36	0.37	0.36	0.39	0.36		0.38	0.41	0.40	0.51	0.41
		S.E.	0.03	0.02	0.02	0.02	0.05	0.05	0.02	0.01	0.03	0.01	0.02	0.02		0.01	0.01	0.02	0.05	0.01
		S.D.	0.08	0.07	0.07	0.04	0.08	0.07	0.06	0.04	0.06	0.05	0.05	0.07		0.06	0.07	0.07	0.07	0.07

		N	7	8	15	5	2	2	9	9	5	14	9	9	0	18	30	24	2	56
	Tb.Th	Mean	0.30	0.28	0.29	0.28	0.28	0.31	0.29	0.24	0.24	0.24	0.24	0.23		0.23	0.26	0.25	0.31	0.26
		S.E.	0.01	0.02	0.01	0.01	0.01	0.02	0.01	0.01	0.01	0.01	0.01	0.01		0.00	0.01	0.01	0.02	0.01
		S.D.	0.04	0.05	0.04	0.02	0.01	0.03	0.02	0.02	0.03	0.02	0.02	0.02		0.02	0.04	0.04	0.03	0.04
		N	7	8	15	5	2	2	9	9	5	14	9	9	0	18	30	24	2	56
	DA	Mean	0.79	0.80	0.80	0.75	0.73	0.77	0.75	0.78	0.78	0.78	0.72	0.71		0.71	0.76	0.76	0.77	0.76
		S.E.	0.02	0.01	0.01	0.02	0.03	0.02	0.01	0.01	0.02	0.01	0.02	0.01		0.01	0.01	0.01	0.02	0.01
		S.D.	0.05	0.04	0.04	0.04	0.05	0.02	0.03	0.03	0.04	0.04	0.06	0.04		0.05	0.05	0.06	0.02	0.05
		N	7	8	15	5	2	2	9	9	5	14	8	9	0	17	29	24	2	55
	Tb.Sp	Mean	0.41	0.38	0.39	0.39	0.43	0.36	0.39	0.47	0.44	0.46	0.41	0.42		0.41	0.42	0.41	0.36	0.42
		S.E.	0.03	0.02	0.01	0.02	0.04	0.02	0.02	0.01	0.03	0.01	0.01	0.02		0.01	0.01	0.01	0.02	0.01
		S.D.	0.07	0.05	0.06	0.05	0.06	0.03	0.05	0.03	0.07	0.05	0.02	0.06		0.04	0.05	0.06	0.03	0.05
		N	7	8	15	5	2	2	9	9	5	14	9	9	0	18	30	24	2	56
	Conn.D	Mean	4.74	6.44	5.65	6.45	6.32	6.70	6.48	6.45	8.79	7.29	8.24	9.51		8.87	6.59	8.07	6.70	7.23
		S.E.	0.20	0.53	0.36	0.86	1.04	1.70	0.56	0.41	1.23	0.58	0.40	0.76		0.44	0.32	0.50	1.70	0.29
		S.D.	0.53	1.49	1.41	1.92	1.47	2.41	1.69	1.24	2.76	2.15	1.19	2.27		1.87	1.75	2.45	2.41	2.18
		N	7	8	15	5	2	2	9	9	5	14	9	9	0	18	30	24	2	56
MT1 base plantar	BV/TV	Mean	0.32	0.32	0.32	0.30	0.30	0.37	0.32	0.23	0.26	0.24	0.28	0.27		0.28	0.27	0.29	0.37	0.28
		S.E.	0.03	0.03	0.02	0.06	0.05		0.03	0.02	0.02	0.01	0.01	0.02		0.01	0.01	0.01		0.01
		S.D.	0.07	0.07	0.06	0.09	0.07		0.07	0.05	0.04	0.05	0.04	0.06		0.05	0.06	0.06		0.06
		N	6	7	13	2	2	1	5	9	4	13	9	9	0	18	26	22	1	49
	Tb.Th	Mean	0.29	0.26	0.27	0.27	0.28	0.27	0.27	0.23	0.23	0.23	0.22	0.22		0.22	0.24	0.24	0.27	0.24
		S.E.	0.01	0.02	0.01	0.03	0.01		0.01	0.01	0.01	0.01	0.01	0.01		0.01	0.01	0.01		0.01
		S.D.	0.03	0.05	0.04	0.04	0.02		0.02	0.03	0.01	0.03	0.02	0.03		0.02	0.04	0.04		0.04
		N	6	7	13	2	2	1	5	9	4	13	9	9	0	18	26	22	1	49
	DA	Mean	0.62	0.60	0.61	0.58	0.54	0.60	0.57	0.63	0.53	0.60	0.56	0.52		0.54	0.60	0.55	0.60	0.58
		S.E.	0.02	0.02	0.02	0.02	0.05		0.02	0.03	0.03	0.02	0.02	0.01		0.01	0.01	0.01		0.01
		S.D.	0.05	0.06	0.06	0.03	0.07		0.04	0.08	0.07	0.09	0.07	0.03		0.06	0.07	0.06		0.07
		N	6	7	13	2	2	1	5	9	4	13	9	9	0	18	26	22	1	49
	Tb.Sp	Mean	0.60	0.52	0.56	0.64	0.61	0.53	0.61	0.68	0.59	0.65	0.53	0.55		0.54	0.61	0.55	0.53	0.58

		S.E.	0.03	0.02	0.02	0.06	0.03		0.03	0.03	0.06	0.03	0.03	0.03		0.02	0.02	0.02		0.01
		S.D.	0.07	0.04	0.07	0.09	0.04		0.07	0.10	0.12	0.11	0.08	0.09		0.08	0.10	0.08		0.09
		N	6	7	13	2	2	1	5	9	4	13	9	9	0	18	26	22	1	49
	Conn.D	Mean	4.30	6.76	5.62	5.01	5.93	4.73	5.32	4.74	7.14	5.48	7.77	8.24		8.00	5.70	7.36	4.73	6.43
		S.E.	0.29	0.78	0.55	0.03	1.19		0.45	0.46	1.35	0.58	0.67	0.77		0.50	0.41	0.48		0.33
		S.D.	0.72	2.07	1.99	0.04	1.68		1.01	1.39	2.70	2.11	2.01	2.32		2.12	2.10	2.26		2.29
		N	6	7	13	2	2	1	5	9	4	13	9	9	0	18	26	22	1	49
MT1 head dorsal	BV/TV	Mean	0.48	0.50	0.49	0.50	0.44	0.48	0.48	0.37	0.41	0.38	0.39	0.37		0.38	0.43	0.43	0.48	0.43
		S.E.	0.01	0.03	0.01	0.01	0.02	0.03	0.01	0.01	0.01	0.01	0.01	0.02		0.01	0.01	0.02	0.03	0.01
		S.D.	0.04	0.08	0.06	0.03	0.03	0.05	0.04	0.04	0.02	0.04	0.04	0.05		0.05	0.06	0.08	0.05	0.07
		N	8	9	17	5	3	3	11	9	4	13	9	9	0	18	31	25	3	59
	Tb.Th	Mean	0.31	0.30	0.30	0.28	0.27	0.28	0.28	0.23	0.23	0.23	0.25	0.23		0.24	0.26	0.26	0.28	0.26
		S.E.	0.01	0.02	0.01	0.01	0.00	0.01	0.00	0.01	0.01	0.01	0.01	0.01		0.00	0.01	0.01	0.01	0.01
		S.D.	0.03	0.05	0.04	0.02	0.01	0.02	0.02	0.02	0.02	0.02	0.02	0.02		0.02	0.04	0.05	0.02	0.04
		N	8	9	17	5	3	3	11	9	4	13	9	9	0	18	31	25	3	59
	DA	Mean	0.76	0.75	0.75	0.66	0.69	0.71	0.68	0.77	0.72	0.75	0.72	0.75		0.73	0.73	0.74	0.71	0.73
		S.E.	0.01	0.01	0.01	0.01	0.05	0.03	0.02	0.01	0.01	0.01	0.02	0.01		0.01	0.01	0.01	0.03	0.01
		S.D.	0.03	0.03	0.03	0.02	0.09	0.04	0.05	0.03	0.03	0.04	0.06	0.04		0.05	0.05	0.05	0.04	0.05
		N	8	9	17	5	3	3	11	9	4	13	9	9	0	18	31	25	3	59
	Tb.Sp	Mean	0.40	0.37	0.38	0.37	0.43	0.39	0.40	0.44	0.40	0.43	0.45	0.44		0.44	0.42	0.41	0.39	0.41
		S.E.	0.01	0.01	0.01	0.02	0.02	0.03	0.01	0.01	0.03	0.01	0.02	0.02		0.01	0.01	0.01	0.03	0.01
		S.D.	0.03	0.04	0.04	0.03	0.03	0.06	0.04	0.03	0.06	0.04	0.05	0.05		0.05	0.05	0.05	0.06	0.05
		N	8	9	17	5	3	3	11	9	4	13	9	9	0	18	31	25	3	59
	Conn.D	Mean	5.15	6.31	5.76	7.38	7.52	7.12	7.35	7.16	11.11	8.37	6.22	7.43		6.82	6.40	7.63	7.12	6.96
		S.E.	0.39	0.78	0.46	0.82	1.77	1.00	0.59	0.45	1.99	0.82	0.60	0.72		0.48	0.30	0.59	1.00	0.31
		S.D.	1.11	2.34	1.91	1.83	3.07	1.73	1.96	1.36	3.98	2.96	1.79	2.17		2.03	1.69	2.97	1.73	2.36
		N	8	9	17	5	3	3	11	9	4	13	9	9	0	18	31	25	3	59
MT1 head plantar	BV/TV	Mean	0.36	0.37	0.37	0.37	0.28	0.39	0.35	0.26	0.31	0.28	0.32	0.30		0.31	0.32	0.32	0.39	0.32
		S.E.	0.02	0.03	0.01	0.02	0.00	0.08	0.02	0.01	0.03	0.01	0.02	0.02		0.01	0.01	0.01	0.08	0.01
		S.D.	0.05	0.07	0.06	0.03	0.00	0.11	0.06	0.04	0.06	0.05	0.05	0.05		0.05	0.06	0.06	0.11	0.06

		N	7	7	14	4	2	2	8	9	4	13	9	9	0	18	29	22	2	53
	Tb.Th	Mean	0.30	0.30	0.30	0.28	0.24	0.29	0.27	0.24	0.24	0.24	0.25	0.23		0.24	0.26	0.26	0.29	0.26
		S.E.	0.02	0.02	0.01	0.01	0.02	0.01	0.01	0.01	0.01	0.01	0.00	0.01		0.01	0.01	0.01	0.01	0.01
		S.D.	0.05	0.05	0.05	0.02	0.03	0.01	0.03	0.03	0.03	0.03	0.01	0.03		0.02	0.04	0.05	0.01	0.04
		N	7	7	14	4	2	2	8	9	4	13	9	9	0	18	29	22	2	53
	DA	Mean	0.59	0.60	0.60	0.57	0.70	0.54	0.59	0.65	0.68	0.65	0.61	0.60		0.60	0.61	0.62	0.54	0.61
		S.E.	0.02	0.01	0.01	0.03	0.02	0.05	0.03	0.03	0.03	0.02	0.01	0.02		0.01	0.01	0.01	0.05	0.01
		S.D.	0.05	0.03	0.04	0.05	0.02	0.07	0.08	0.09	0.05	0.08	0.04	0.07		0.06	0.07	0.06	0.07	0.07
		N	7	7	14	4	2	2	8	9	4	13	9	9	0	18	29	22	2	53
	Tb.Sp	Mean	0.57	0.54	0.56	0.53	0.60	0.57	0.56	0.64	0.60	0.63	0.59	0.57		0.58	0.59	0.57	0.57	0.58
		S.E.	0.01	0.03	0.01	0.02	0.05	0.12	0.03	0.04	0.05	0.03	0.03	0.02		0.02	0.02	0.01	0.12	0.01
		S.D.	0.03	0.07	0.05	0.04	0.07	0.17	0.08	0.11	0.11	0.11	0.10	0.05		0.08	0.09	0.07	0.17	0.08
		N	7	7	14	4	2	2	8	9	4	13	9	9	0	18	29	22	2	53
	Conn.D	Mean	4.36	5.00	4.68	5.73	4.71	4.85	5.26	5.01	5.95	5.30	5.12	6.07		5.60	4.99	5.58	4.85	5.23
		S.E.	0.35	0.54	0.32	0.38	1.31	0.91	0.39	0.63	1.16	0.55	0.60	0.51		0.40	0.29	0.35	0.91	0.22
		S.D.	0.94	1.44	1.21	0.76	1.86	1.29	1.11	1.89	2.33	1.98	1.80	1.54		1.70	1.54	1.66	1.29	1.59
		N	7	7	14	4	2	2	8	9	4	13	9	9	0	18	29	22	2	53
Talus ACF	BV/TV	Mean	0.33	0.37	0.36	0.41	0.30	0.44	0.40	0.27	0.31	0.29	0.28	0.30		0.29	0.31	0.33	0.44	0.32
		S.E.	0.04	0.03	0.02	0.01	0.08	0.03	0.02	0.01	0.02	0.01	0.01	0.02		0.01	0.01	0.01	0.03	0.01
		S.D.	0.08	0.08	0.08	0.02	0.11	0.05	0.07	0.04	0.06	0.05	0.03	0.07		0.06	0.07	0.08	0.05	0.08
		N	5	8	13	5	2	3	10	13	7	20	8	11	0	19	31	28	3	62
	Tb.Th	Mean	0.29	0.30	0.30	0.31	0.29	0.32	0.31	0.24	0.27	0.25	0.25	0.26		0.26	0.26	0.27	0.32	0.27
		S.E.	0.02	0.02	0.01	0.01	0.06	0.02	0.01	0.01	0.01	0.01	0.00	0.01		0.01	0.01	0.01	0.02	0.01
		S.D.	0.04	0.04	0.04	0.02	0.08	0.04	0.04	0.03	0.04	0.03	0.01	0.05		0.04	0.04	0.05	0.04	0.04
		N	5	8	13	5	2	3	10	13	7	20	8	11	0	19	31	28	3	62
	DA	Mean	0.69	0.65	0.67	0.69	0.68	0.69	0.69	0.70	0.68	0.69	0.65	0.67		0.66	0.68	0.67	0.69	0.68
		S.E.	0.02	0.02	0.02	0.02	0.04	0.03	0.01	0.02	0.02	0.01	0.02	0.02		0.01	0.01	0.01	0.03	0.01
		S.D.	0.05	0.07	0.06	0.05	0.06	0.06	0.05	0.07	0.06	0.06	0.06	0.06		0.06	0.06	0.06	0.06	0.06
		N	5	8	13	5	2	3	10	13	7	20	8	11	0	19	31	28	3	62
	Tb.Sp	Mean	0.64	0.55	0.59	0.58	0.68	0.54	0.59	0.70	0.67	0.69	0.68	0.60		0.63	0.66	0.61	0.54	0.63

		S.E.	0.06	0.03	0.03	0.03	0.07	0.05	0.03	0.03	0.02	0.02	0.04	0.02		0.02	0.02	0.02	0.05	0.01
		S.D.	0.13	0.09	0.11	0.06	0.10	0.09	0.09	0.11	0.05	0.09	0.11	0.08		0.10	0.11	0.09	0.09	0.10
		N	5	8	13	5	2	3	10	13	7	20	8	11	0	19	31	28	3	62
	Conn.D	Mean	3.75	4.86	4.43	4.41	3.60	5.16	4.47	4.14	4.65	4.32	4.73	5.22		5.01	4.27	4.86	5.16	4.58
		S.E.	0.36	0.36	0.30	0.44	0.40	0.59	0.32	0.33	0.47	0.27	0.39	0.55		0.35	0.19	0.27	0.59	0.16
		S.D.	0.80	1.02	1.06	0.98	0.56	1.02	1.01	1.18	1.23	1.19	1.11	1.83		1.55	1.08	1.43	1.02	1.27
		N	5	8	13	5	2	3	10	13	7	20	8	11	0	19	31	28	3	62
Talus PCF	BV/TV	Mean	0.49	0.47	0.48	0.52	0.43	0.52	0.50	0.36	0.40	0.38	0.40	0.34		0.36	0.43	0.40	0.52	0.42
		S.E.	0.05	0.02	0.02	0.01	0.04	0.04	0.02	0.01	0.01	0.01	0.03	0.01		0.02	0.02	0.01	0.04	0.01
		S.D.	0.11	0.06	0.08	0.04	0.08	0.08	0.07	0.05	0.03	0.05	0.08	0.04		0.06	0.09	0.07	0.08	0.09
		N	5	7	12	7	4	4	15	12	6	18	6	11	0	17	30	28	4	62
	Tb.Th	Mean	0.35	0.32	0.33	0.34	0.30	0.34	0.33	0.25	0.28	0.26	0.30	0.24		0.26	0.30	0.28	0.34	0.29
		S.E.	0.02	0.01	0.01	0.01	0.02	0.02	0.01	0.01	0.01	0.01	0.01	0.01		0.01	0.01	0.01	0.02	0.01
		S.D.	0.05	0.04	0.04	0.03	0.04	0.05	0.04	0.02	0.03	0.03	0.03	0.04		0.05	0.05	0.05	0.05	0.05
		N	5	7	12	7	4	4	15	12	6	18	6	11	0	17	30	28	4	62
	DA	Mean	0.77	0.78	0.77	0.75	0.75	0.77	0.76	0.77	0.72	0.76	0.73	0.76		0.75	0.76	0.75	0.77	0.76
		S.E.	0.02	0.02	0.01	0.01	0.02	0.02	0.01	0.01	0.01	0.01	0.02	0.01		0.01	0.01	0.01	0.02	0.01
		S.D.	0.05	0.04	0.04	0.03	0.04	0.04	0.04	0.04	0.03	0.04	0.06	0.04		0.05	0.05	0.04	0.04	0.04
		N	5	7	12	7	4	4	15	12	6	18	6	11	0	17	30	28	4	62
	Tb.Sp	Mean	0.51	0.48	0.49	0.41	0.50	0.41	0.44	0.53	0.49	0.52	0.53	0.51		0.52	0.50	0.50	0.41	0.49
		S.E.	0.05	0.02	0.02	0.01	0.04	0.01	0.02	0.02	0.01	0.01	0.03	0.02		0.02	0.01	0.01	0.01	0.01
		S.D.	0.10	0.06	0.08	0.03	0.09	0.02	0.06	0.06	0.04	0.05	0.08	0.06		0.06	0.08	0.06	0.02	0.07
		N	5	7	12	7	4	4	15	12	6	18	6	11	0	17	30	28	4	62
	Conn.D	Mean	3.29	4.25	3.85	4.83	4.97	4.73	4.84	5.74	5.97	5.81	4.96	6.96		6.25	4.96	5.78	4.73	5.32
		S.E.	0.25	0.42	0.30	0.45	0.56	0.97	0.34	0.38	0.64	0.32	0.50	0.74		0.55	0.26	0.40	0.97	0.23
		S.D.	0.56	1.12	1.02	1.19	1.12	1.94	1.30	1.32	1.58	1.37	1.22	2.46		2.29	1.41	2.10	1.94	1.81
		N	5	7	12	7	4	4	15	12	6	18	6	11	0	17	30	28	4	62
Talus head	BV/TV	Mean	0.57	0.53	0.55	0.60	0.52	0.59	0.58	0.41	0.45	0.42	0.42	0.40		0.41	0.49	0.46	0.59	0.48
		S.E.	0.01	0.03	0.01	0.02	0.03	0.02	0.02	0.01	0.02	0.01	0.03	0.02		0.01	0.02	0.02	0.02	0.01
		S.D.	0.01	0.06	0.05	0.08	0.06	0.04	0.07	0.05	0.06	0.06	0.07	0.05		0.06	0.11	0.08	0.04	0.10

		N	5	6	11	10	4	5	19	12	7	19	8	11	0	19	35	28	5	68
	Tb.Th	Mean	0.37	0.33	0.35	0.38	0.35	0.39	0.38	0.27	0.29	0.28	0.30	0.27		0.28	0.32	0.30	0.39	0.32
		S.E.	0.01	0.02	0.01	0.01	0.02	0.01	0.01	0.01	0.01	0.01	0.01	0.01		0.01	0.01	0.01	0.01	0.01
		S.D.	0.02	0.05	0.04	0.05	0.03	0.03	0.04	0.03	0.04	0.03	0.03	0.03		0.04	0.06	0.05	0.03	0.06
		N	5	6	11	10	4	5	19	12	7	19	8	11	0	19	35	28	5	68
	DA	Mean	0.83	0.83	0.83	0.77	0.78	0.76	0.77	0.81	0.77	0.80	0.85	0.83		0.83	0.81	0.81	0.76	0.81
		S.E.	0.01	0.01	0.01	0.01	0.01	0.01	0.01	0.01	0.01	0.01	0.01	0.01		0.01	0.01	0.01	0.01	0.01
		S.D.	0.02	0.03	0.03	0.05	0.02	0.02	0.04	0.05	0.03	0.05	0.03	0.03		0.03	0.05	0.04	0.02	0.05
		N	5	6	11	10	4	5	19	12	7	19	8	11	0	19	35	28	5	68
	Tb.Sp	Mean	0.39	0.38	0.39	0.37	0.44	0.38	0.39	0.48	0.44	0.47	0.47	0.45		0.46	0.44	0.43	0.38	0.43
		S.E.	0.01	0.02	0.01	0.02	0.03	0.02	0.01	0.02	0.02	0.01	0.02	0.02		0.01	0.01	0.01	0.02	0.01
		S.D.	0.01	0.06	0.04	0.06	0.07	0.04	0.06	0.06	0.07	0.06	0.06	0.06		0.06	0.07	0.07	0.04	0.07
		N	5	6	11	10	4	5	19	12	7	19	8	11	0	19	35	28	5	68
	Conn.D	Mean	3.14	4.26	3.75	4.11	4.18	5.24	4.42	5.73	5.93	5.80	4.10	5.72		5.04	4.53	5.24	5.24	4.87
		S.E.	0.29	0.55	0.36	0.46	0.44	0.54	0.31	0.51	0.55	0.37	0.31	0.56		0.39	0.28	0.31	0.54	0.20
		S.D.	0.65	1.35	1.19	1.47	0.87	1.20	1.33	1.77	1.46	1.62	0.88	1.86		1.70	1.64	1.66	1.20	1.64
		N	5	6	11	10	4	5	19	12	7	19	8	11	0	19	35	28	5	68
Trochlea lateral	BV/TV	Mean	0.48	0.50	0.49	0.57	0.47	0.61	0.56	0.37	0.44	0.40	0.43	0.36		0.39	0.46	0.43	0.61	0.46
		S.E.	0.04	0.02	0.02	0.02	0.04	0.03	0.02	0.02	0.01	0.02	0.03	0.02		0.02	0.02	0.01	0.03	0.01
		S.D.	0.11	0.05	0.08	0.07	0.07	0.07	0.08	0.07	0.03	0.07	0.07	0.06		0.07	0.11	0.08	0.07	0.10
		N	7	8	15	10	4	5	19	10	5	15	7	11	0	18	34	28	5	67
	Tb.Th	Mean	0.33	0.32	0.33	0.37	0.32	0.36	0.36	0.26	0.29	0.27	0.27	0.24		0.25	0.31	0.28	0.36	0.30
		S.E.	0.02	0.01	0.01	0.02	0.02	0.02	0.01	0.01	0.01	0.01	0.02	0.01		0.01	0.01	0.01	0.02	0.01
		S.D.	0.06	0.04	0.05	0.05	0.04	0.04	0.05	0.03	0.03	0.03	0.05	0.04		0.05	0.06	0.05	0.04	0.06
		N	7	8	15	10	4	4	18	10	5	15	7	11	0	18	34	28	4	66
	DA	Mean	0.79	0.80	0.79	0.76	0.77	0.79	0.77	0.77	0.75	0.76	0.76	0.77		0.76	0.77	0.77	0.79	0.77
		S.E.	0.02	0.01	0.01	0.02	0.01	0.01	0.01	0.02	0.02	0.01	0.02	0.01		0.01	0.01	0.01	0.01	0.01
		S.D.	0.05	0.02	0.04	0.06	0.02	0.03	0.04	0.05	0.05	0.05	0.05	0.04		0.04	0.05	0.04	0.03	0.04
		N	7	8	15	10	4	5	19	10	5	15	7	11	0	18	34	28	5	67
	Tb.Sp	Mean	0.44	0.41	0.42	0.38	0.43	0.34	0.38	0.50	0.44	0.48	0.43	0.43		0.43	0.44	0.42	0.34	0.42

		S.E.	0.03	0.02	0.02	0.01	0.03	0.02	0.01	0.02	0.01	0.02	0.02	0.02		0.01	0.01	0.01	0.02	0.01
		S.D.	0.06	0.05	0.06	0.04	0.06	0.03	0.05	0.06	0.03	0.06	0.05	0.07		0.06	0.07	0.05	0.03	0.07
		N	6	8	14	10	4	5	19	10	5	15	7	11	0	18	33	28	5	66
	Conn.D	Mean	3.80	4.91	4.39	4.56	4.72	5.69	4.89	5.29	6.74	5.77	6.56	8.05		7.47	5.03	6.44	5.69	5.67
		S.E.	0.36	0.50	0.34	0.44	0.37	0.82	0.33	0.44	0.79	0.42	0.66	0.78		0.56	0.28	0.45	0.82	0.25
		S.D.	0.96	1.41	1.31	1.40	0.75	1.84	1.44	1.39	1.77	1.62	1.74	2.59		2.36	1.64	2.39	1.84	2.09
		N	7	8	15	10	4	5	19	10	5	15	7	11	0	18	34	28	5	67
Trochlea central	BV/TV	Mean	0.46	0.43	0.45	0.51	0.40	0.52	0.48	0.33	0.41	0.36	0.39	0.36		0.37	0.41	0.40	0.52	0.41
		S.E.	0.04	0.04	0.03	0.02	0.03	0.04	0.02	0.02	0.01	0.02	0.02	0.02		0.01	0.02	0.01	0.04	0.01
		S.D.	0.10	0.10	0.10	0.06	0.06	0.07	0.07	0.06	0.03	0.06	0.05	0.06		0.06	0.10	0.08	0.07	0.09
		N	6	8	14	9	4	3	16	12	5	17	7	11	0	18	34	28	3	65
	Tb.Th	Mean	0.32	0.30	0.31	0.35	0.31	0.35	0.34	0.25	0.30	0.27	0.28	0.24		0.25	0.30	0.28	0.35	0.29
		S.E.	0.02	0.02	0.01	0.01	0.02	0.01	0.01	0.01	0.01	0.01	0.01	0.01		0.01	0.01	0.01	0.01	0.01
		S.D.	0.05	0.05	0.05	0.04	0.04	0.01	0.04	0.04	0.02	0.04	0.03	0.04		0.04	0.06	0.05	0.01	0.05
		N	6	8	14	9	4	3	16	12	5	17	7	11	0	18	34	28	3	65
	DA	Mean	0.74	0.75	0.74	0.60	0.64	0.62	0.61	0.68	0.68	0.68	0.67	0.67		0.67	0.67	0.69	0.62	0.67
		S.E.	0.02	0.02	0.01	0.03	0.02	0.06	0.02	0.02	0.01	0.01	0.03	0.02		0.01	0.01	0.01	0.06	0.01
		S.D.	0.06	0.04	0.05	0.09	0.05	0.11	0.08	0.07	0.03	0.06	0.07	0.06		0.06	0.08	0.06	0.11	0.08
		N	6	8	14	9	4	3	16	12	5	17	7	11	0	18	34	28	3	65
	Tb.Sp	Mean	0.45	0.43	0.44	0.43	0.51	0.43	0.45	0.53	0.48	0.52	0.48	0.44		0.46	0.48	0.46	0.43	0.47
		S.E.	0.03	0.02	0.02	0.02	0.03	0.03	0.02	0.02	0.02	0.01	0.02	0.02		0.01	0.01	0.01	0.03	0.01
		S.D.	0.07	0.07	0.07	0.06	0.07	0.05	0.07	0.05	0.05	0.06	0.04	0.06		0.05	0.07	0.06	0.05	0.07
		N	6	8	14	9	4	3	16	12	5	17	7	11	0	18	34	28	3	65
	Conn.D	Mean	4.66	5.54	5.16	5.80	5.60	5.55	5.70	6.17	6.45	6.25	6.36	8.69		7.78	5.84	6.95	5.55	6.31
		S.E.	0.24	0.47	0.30	0.53	0.70	0.47	0.34	0.48	0.61	0.37	0.53	0.70		0.54	0.26	0.43	0.47	0.24
		S.D.	0.60	1.32	1.13	1.58	1.39	0.82	1.35	1.66	1.37	1.55	1.40	2.33		2.29	1.51	2.26	0.82	1.92
		N	6	8	14	9	4	3	16	12	5	17	7	11	0	18	34	28	3	65
Trochlea medial	BV/TV	Mean	0.46	0.45	0.45	0.50	0.40	0.48	0.47	0.36	0.40	0.37	0.43	0.38		0.40	0.43	0.41	0.48	0.42
		S.E.	0.02	0.03	0.02	0.02	0.02	0.02	0.02	0.01	0.03	0.01	0.01	0.02		0.01	0.01	0.01	0.02	0.01
		S.D.	0.05	0.08	0.06	0.05	0.04	0.04	0.06	0.04	0.07	0.05	0.04	0.06		0.06	0.07	0.07	0.04	0.07

	N	7	8	15	9	3	3	15	10	5	15	7	11	0	18	33	27	3	63
Tb.Th	Mean	0.31	0.29	0.30	0.32	0.28	0.33	0.32	0.25	0.27	0.26	0.26	0.24		0.25	0.29	0.26	0.33	0.28
	S.E.	0.01	0.02	0.01	0.01	0.02	0.01	0.01	0.01	0.02	0.01	0.01	0.01		0.01	0.01	0.01	0.01	0.01
	S.D.	0.04	0.04	0.04	0.03	0.04	0.01	0.03	0.03	0.03	0.03	0.02	0.03		0.03	0.04	0.04	0.01	0.04
	N	7	8	15	9	3	3	15	10	5	15	7	11	0	18	33	27	3	63
DA	Mean	0.67	0.69	0.68	0.58	0.68	0.56	0.60	0.66	0.64	0.65	0.61	0.63		0.62	0.63	0.66	0.56	0.64
	S.E.	0.03	0.03	0.02	0.03	0.04	0.05	0.02	0.03	0.03	0.02	0.03	0.02		0.02	0.02	0.01	0.05	0.01
	S.D.	0.08	0.07	0.07	0.08	0.07	0.09	0.09	0.11	0.06	0.09	0.07	0.08		0.07	0.09	0.07	0.09	0.08
	N	7	8	15	9	3	3	15	10	5	15	7	11	0	18	33	27	3	63
Tb.Sp	Mean	0.43	0.41	0.42	0.42	0.47	0.44	0.44	0.53	0.48	0.51	0.43	0.43		0.43	0.46	0.44	0.44	0.45
	S.E.	0.01	0.02	0.01	0.02	0.02	0.02	0.01	0.01	0.03	0.01	0.01	0.02		0.01	0.01	0.01	0.02	0.01
	S.D.	0.04	0.05	0.05	0.05	0.04	0.04	0.05	0.04	0.06	0.05	0.04	0.06		0.05	0.06	0.06	0.04	0.06
	N	6	8	14	9	3	3	15	10	5	15	7	11	0	18	32	27	3	62
Conn.D	Mean	5.19	6.60	5.94	6.06	6.47	5.86	6.10	6.12	7.15	6.46	7.97	9.33		8.80	6.30	7.80	5.86	6.92
	S.E.	0.37	0.58	0.39	0.47	1.02	0.35	0.34	0.56	0.81	0.46	0.61	0.65		0.48	0.30	0.43	0.35	0.26
	S.D.	0.98	1.64	1.51	1.42	1.77	0.61	1.30	1.76	1.80	1.78	1.62	2.17		2.04	1.72	2.24	0.61	2.06
	N	7	8	15	9	3	3	15	10	5	15	7	11	0	18	33	27	3	63

Appendix 3.

Appendix 3.1 List of external bone measurements

The reference numbers of each talar and calcaneal measurement come from Jay Stock's Osteometric Data Collection System v2.3, except for CA18 which comes from Raichlen et al. (2011). The measurements of the first metatarsal come from de Groote & Humphrey (2011).

Calcaneus

- CA1 Maximum calcaneus length. anterior-most point to posterior-most point along the long axis of the calcaneus.
- CA6 minimum breadth of calcaneal body - the smallest transverse diameter across the body of the calcaneus, usually located midway between the talar articular surface and the most dorsal extent of the tuber calcanei (Pearson,1997).
- CA7-sustentaculum tali breadth - maximum medio-lateral breadth of the calcaneus at the location of the maximum medial extent of the sustentaculum tali.
- CA9 - tuberosity height (Br7,M7) - maximum supero-inferior height of the calcaneal tuberosity.
- CA10 - tuberosity breadth (Br8,M8) - maximum mediolateral breadth of the calcaneal tuberosity (js).
- CA15 - posterior talar length (Br9,M9) - maximum length of the posterior talar
- CA16 - posterior talar breadth (Br10,M10) - maximum breadth of the posterior talar articular surface of the calcaneus, taken perpendicular to Posterior Talar Facet Length.
- CA17 - load arm length - the projected distance from the most posterior point of the posterior articular surface for the talus, to the most anterior/superior point on the cuboidal facet.
- CA18 - Raichlen(2011) – Calcaneal Tuber Length: the maximum distance between the posterior edge of the calcaneal tuberosity and the anterior edge of the posterior talocalcaneal surface.
- PTF shape - CA15/CA16. This divides posterior talar facet length by posterior talar facet breadth. A value below 1 indicates a broad PTF and a value above 1 indicates a long PTF.
- PTF area - CA15*CA16. This roughly quantifies the size of the PTF.
- Tuber shape - CA9/CA10. This measure divides tuber height by tuber breadth. A value >1 indicates high tuber whereas a value <1 indicates a broad tuber.
- Tuber area -CA9*CA10. This roughly quantifies the area and thus the robustness of the tuber.

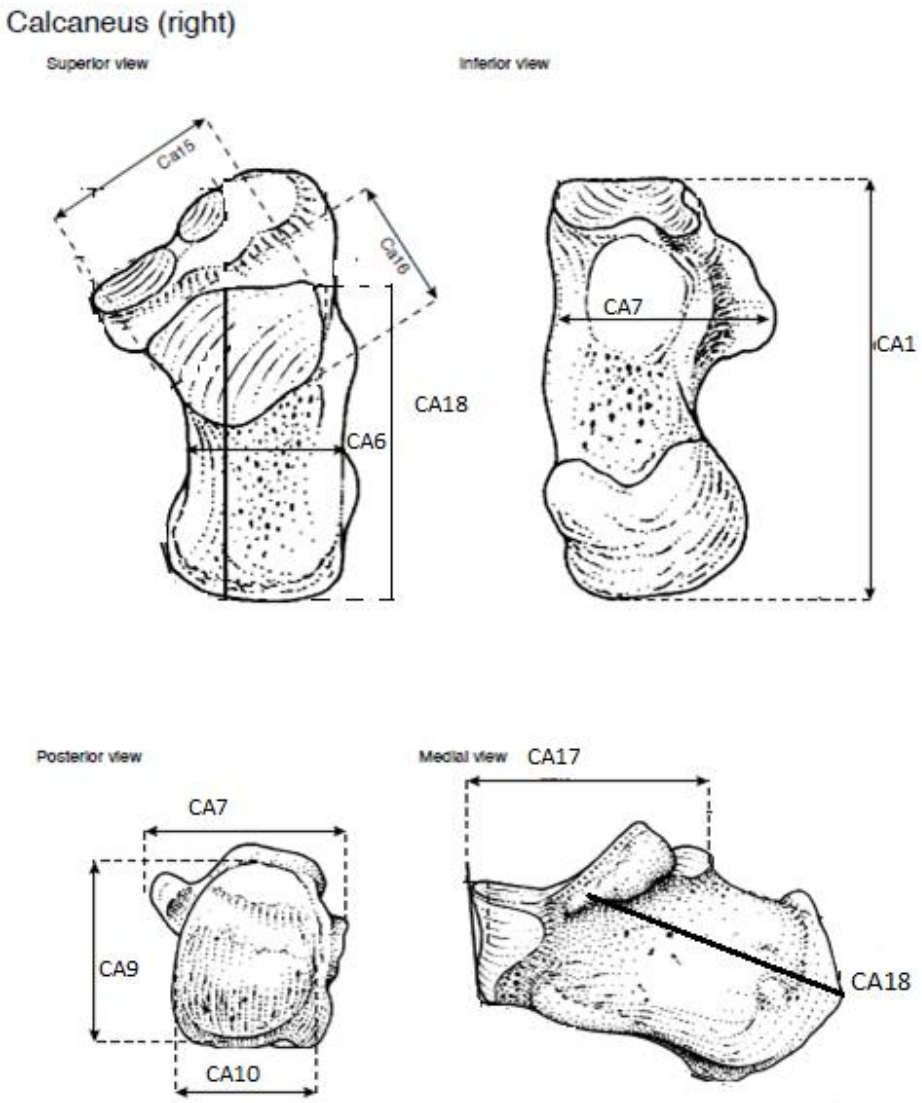

Figure 3.1.1. External measurements of the calcaneus.

First Metatarsal

Measurements from Groote & Humphrey (2011):

- **MTL** - metatarsal length.
- **MLD** - mediolateral diameter of the distal articulation.
- **DPD** - dorsoplantar diameter of the distal articulation.
- **DPP** - dorsoplantar diameter of the proximal articulation.
- **MLP** - mediolateral diameter of the proximal articulation.
- **Head shape** DPD/MLD. Head height is divided by head breadth. Values >1 indicate a high MT1 head, values <1 indicate a broad MT1 head.
- **Head area** MLD*DPD. This measure roughly indicates the size of the MT1 head.
- **Base shape** DPP/MLP. Base height is divided by base breadth. Values >1 indicate a MT1 base, values <1 indicate a broad base.
- **Base area** DPP*MLP. This measure roughly indicates the size of the MT1 base.

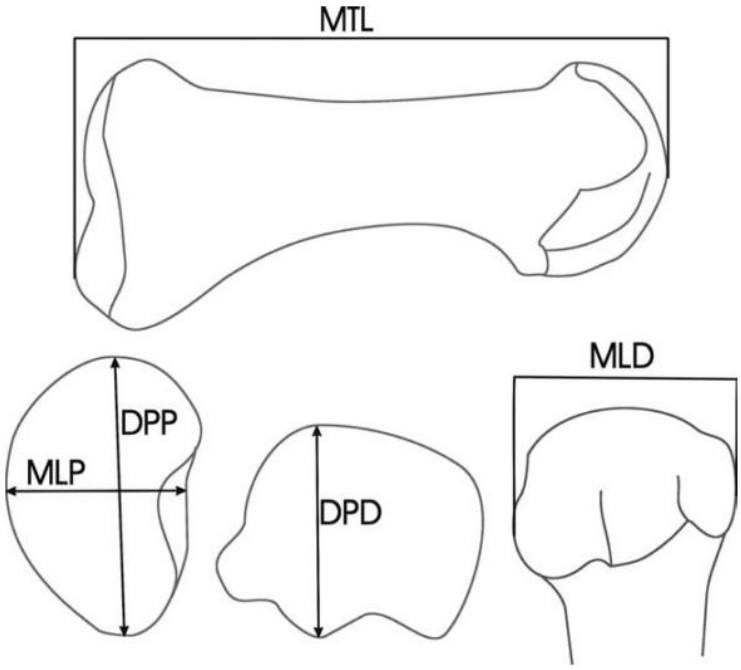

Figure 3.1.2. External measurements of the first metatarsal.

Talus

- **TA1** - talar length - the distance from the flexor hallucis longus groove to the most anterior point of the head, measured parallel to the long axis of the trochlea (M1; Pearson, 1997).
- **TA4**- physiological (articular) breadth - the widest breadth of the trochlea, measured perpendicular to the long axis (M2b; Pearson 1997).
- **TA7-** length of head plus neck - the distance from the anterior median edge of the trochlea to the most distal point of the head, measured parallel to the long axis of the head and neck (M8; Pearson 1997).
- **TA8**- head length - maximum length of the navicular articular surface
- **TA9**- head breadth - maximum breadth of the navicular articular surface, measured perpendicular to head length
- **TA11**- trochlear length - maximum length measured among the medial margin
- **TA12**- trochlear breadth - measured at the superior margin
- **TA13**- trochlear height - maximum height of lateral margin, measured against vertical plane
- **TA18**- posterior calcaneal length - maximum length of the talo-calcaneal articular surface
- **TA19**- posterior calcaneal breadth - maximum breadth of the talocalcaneal articular surface
- **Trochlea shape** TA11/TA12. Trochlear length is divided by trochlear breadth. A value <1 indicates a broader trochlea while values >1 indicate a long trochlea.
- **Trochlea area** TA11*TA12. This is a rough measure of trochlear size.
- **PCF shape** TA19/TA18. PCF breadth is divided by PCF length. Values <1 indicate a broader PCF while values >1 indicate a longer PCF.
- **PCF area** TA18*TA19. This value roughly quantifies PCF size.
- **Talar head shape** TA9/TA8. Talar head breadth is divided by head height. A value <1 indicates a wider talar head and a value >1 a higher talar head.
- **Talar head area** TA9*TA8. This is a rough measure of talar head size.

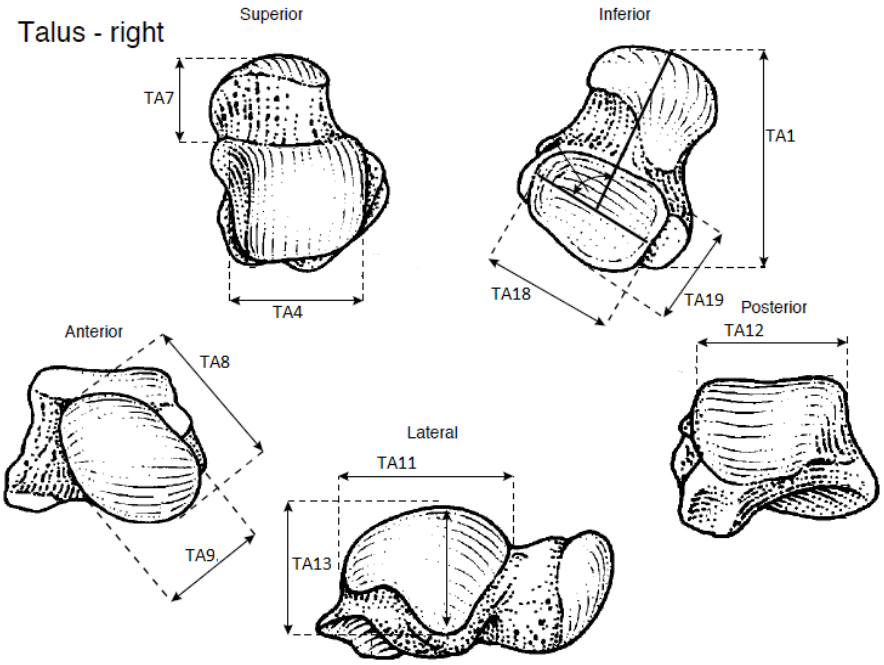

Figure 3.1.3. External measurements of the talus.

Appendix 3.2 Osteometric variation between populations

Introduction

The bulk of this thesis will consider variation in trabecular bone architecture of the foot in four human populations. Variation in body mass and bone dimensions is explored between populations and sexes so that these may be considered in subsequent analyses of trabecular microstructure.

Materials and methods

External dimensions of the talus, calcaneus, and first metatarsal of the Kerma, St. Johns, Jebel Moya, and Black Earth populations were measured. Additionally, the geometric mean of the linear measurements was calculated per bone. Body mass and linear bone dimensions are compared using one-way ANOVA with Games-Howell or Hochberg GT2 post hoc tests depending on Levene's test for homogeneity of variance.

Results

No significant differences were found between populations in pooled sex body mass (Figure 3.2.1, Table 3.2.1). The Black Earth males have a lower mean body mass compared to the other males, although this difference avoids statistical significance. In the females, the Jebel Moya have a significantly lower body mass compared to the Black Earth, although the Jebel Moya sample consists of only 3 females. It is plausible that some of the indeterminate individuals were female, which would have raised the average female body mass (Figure 3.2.1).

Summary statistics of linear bone measurements per population and sex are provided in Table 3.2.2. Calcaneal, first metatarsal, and talar bone size and shape indices of males and females from four populations are presented graphically as boxplots in Figure 3.2.2 with the median, interquartile range, minimum, and maximum values. The results of one-way pairwise ANOVA between populations in pooled sex, males, and females are presented in Table 3.2.3.

The results presented in Table 3.2.3 show that there are significant differences in absolute bone dimensions between populations. Whenever significant differences are found in bone dimensions the African populations tend to have larger values compared to the Black Earth and St. Johns, and in general, the Black Earth possess the smallest bone dimensions. Interestingly, the significant differences in males and females tend to arise in different bone dimensions.

Conclusion

No significant differences were found between populations in pooled sex body mass, but significant differences were found between populations in both males and females. Significant differences are found between populations in external bone measurements in males, females, and pooled sex samples. The Black Earth males had significantly lower mean body mass and the Jebel Moya females had

significantly lower body mass. The significant differences in bone dimensions and body mass should be considered in future analyses.

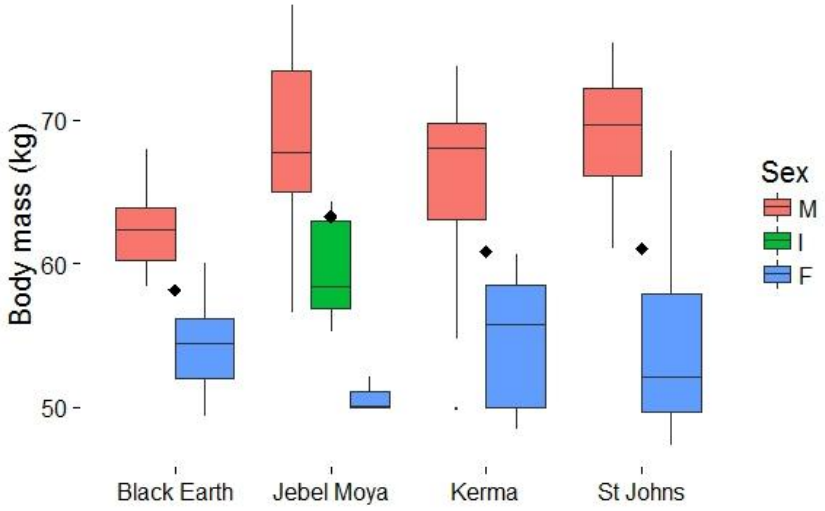

Figure 3.2.1. Body mass in males and females of the four human populations. Diamonds indicate pooled sex means. M=male, F=female, I=indeterminate.

Table 3.2.1. Summary statistics of body mass.

		N	Mean (SD)	Std. Error	Levene *p*	ANOVA *p*	Post-hoc
Black Earth	pooled	21	58.147 (5.045)	1.101	.010	.246	
	male	10	62.238 (2.962)	0.936	.084	.045	
	female	11	54.427 (3.323)	1.001	.020	.692	>JM, p=.049
Jebel Moya	pooled	20	63.276 (8.681)	1.941	.010	.246	
	male	11	68.752 (6.826)	2.058	.084	.045	
	female	3	50.698 (1.203)	0.695	.020	.692	<BE, p=.049
Kerma	pooled	22	60.847(8.250)	1.759	.010	.246	
	male	13	65.324 (7.051)	1.955	.084	.045	
	female	9	54.378 (4.943)	1.647	.020	.692	
St. Johns	pooled	20	61.038 (9.459)	2.115	.010	.246	
	male	9	68.879 (4.954)	1.651	.084	.045	
	female	11	54.621 (7.053)	2.126	.020	.692	
Total	pooled	83	60.795 (8.071)	0.886			
	male	43	66.227 (6.251)	0.953			
	female	34	54.148 (5.062)	0.868			

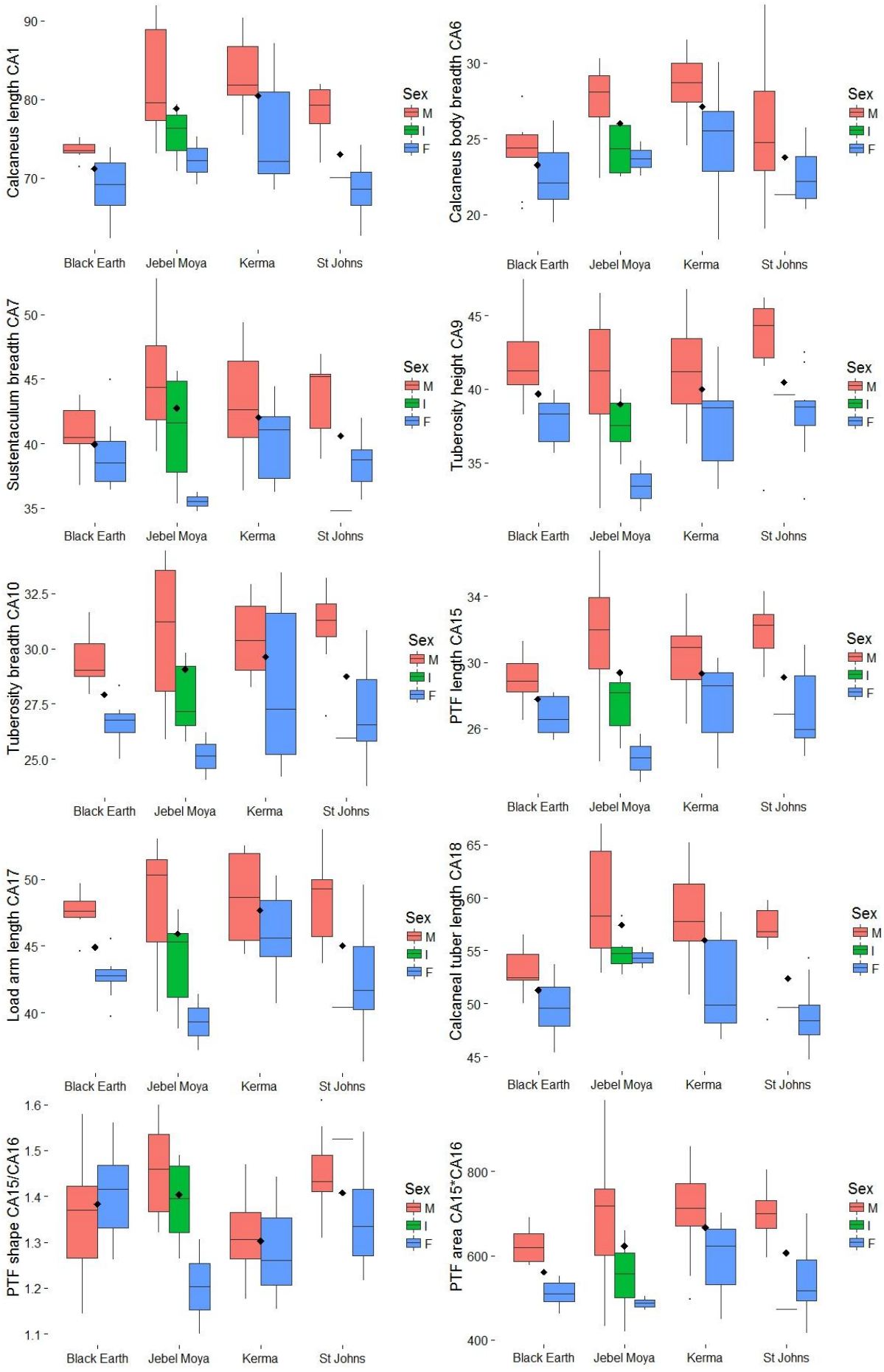
Calcaneus length CA1
Calcaneus body breadth CA6
Sustentaculum breadth CA7
Tuberosity height CA9
Tuberosity breadth CA10
PTF length CA15
Load arm length CA17
Calcaneal tuber length CA18
PTF shape CA15/CA16
PTF area CA15*CA16
Black Earth
Jebel Moya
Kerma
St Johns
Sex
M
I
F

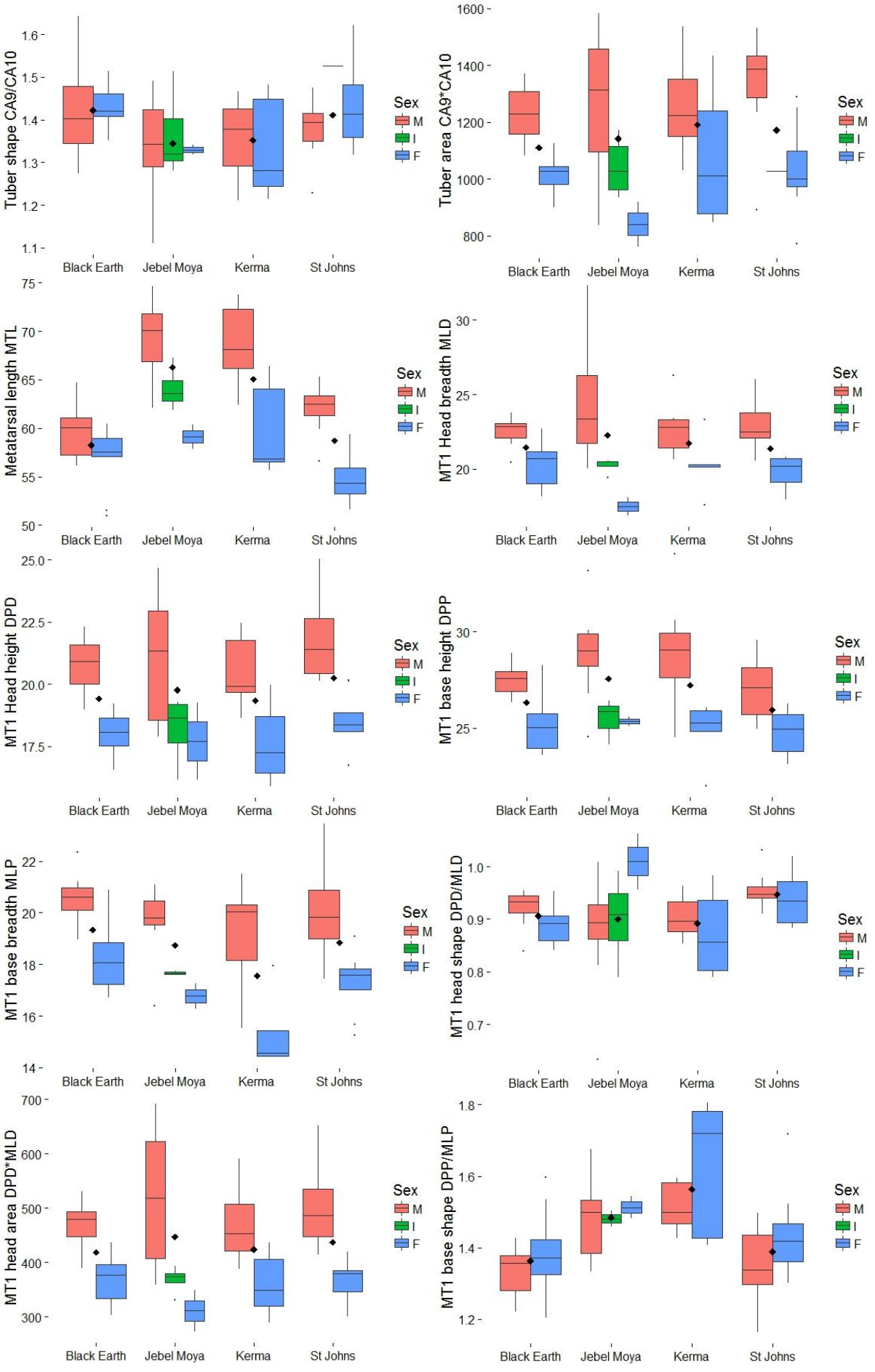
Tuber shape CA9/CA10
Tuber area CA9*CA10
Metatarsal length MTL
MT1 Head breadth MLD
MT1 Head height DPD
MT1 base height DPP
MT1 base breadth MLP
MT1 head shape DPD/MLD
MT1 head area DPD*MLD
MT1 base shape DPP/MLP
Black Earth
Jebel Moya
Kerma
St Johns
Sex
M
I
F

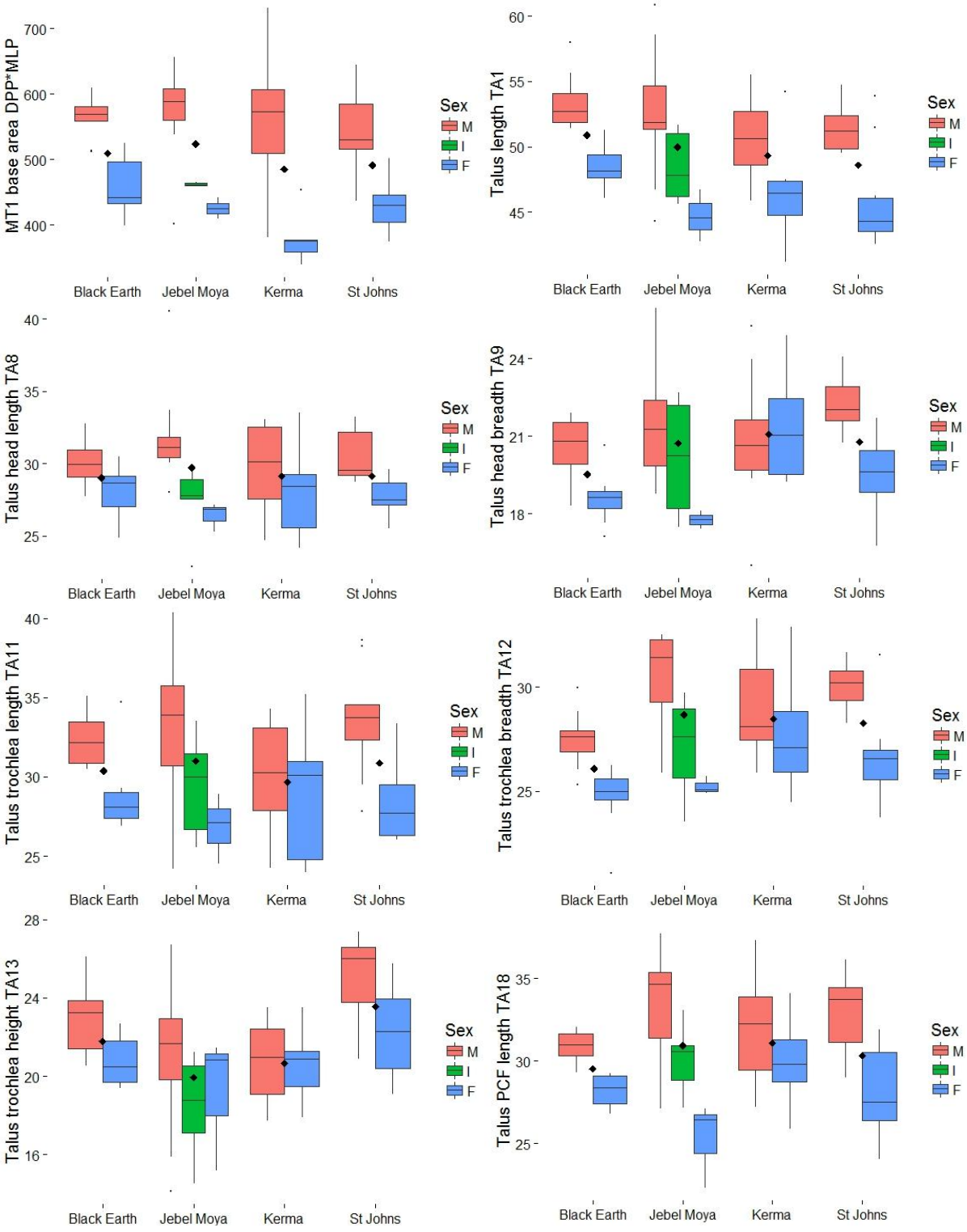
MT1 base area DPP*MLP
700
600
500
400
Black Earth
Jebel Moya
Kerma
St Johns
Sex
M
I
F
Talus length TA1
60
55
50
45
Talus head length TA8
40
35
30
25
Talus head breadth TA9
24
21
18
Talus trochlea length TA11
Talus trochlea breadth TA12
30
25
Talus trochlea height TA13
28
24
20
16
Talus PCF length TA18
35
30
25

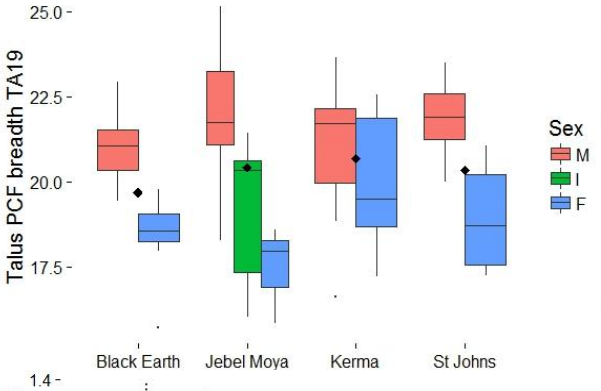
Talus PCF breadth TA19
25.0
22.5
20.0
17.5
Black Earth
Jebel Moya
Kerma
St Johns
Sex
M
I
F

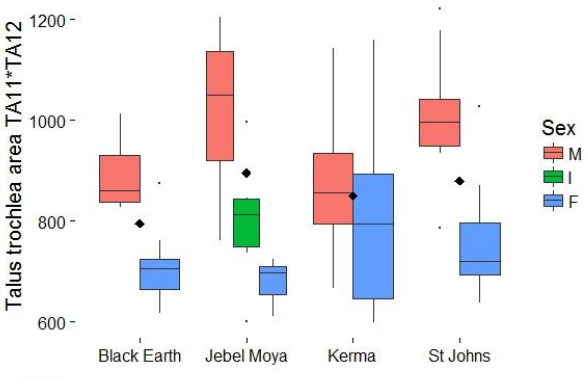
Talus trochlea area TA11*TA12
1200
1000
800
600
Black Earth
Jebel Moya
Kerma
St Johns
Sex
M
I
F

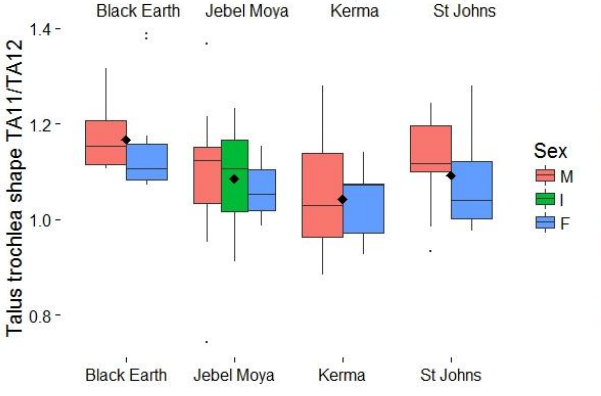
Talus trochlea shape TA11/TA12
1.4
1.2
1.0
0.8
Black Earth
Jebel Moya
Kerma
St Johns
Sex
M
I
F

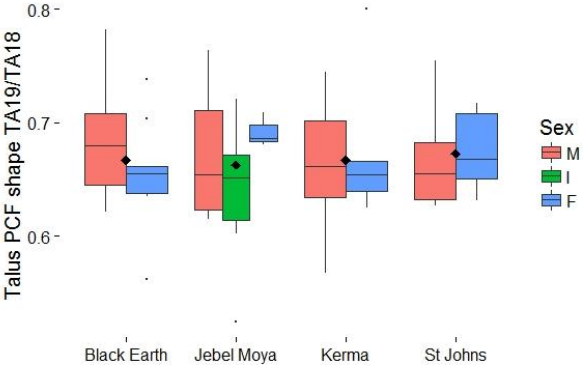
Talus PCF shape TA19/TA18
0.8
0.7
0.6
Black Earth
Jebel Moya
Kerma
St Johns
Sex
M
I
F

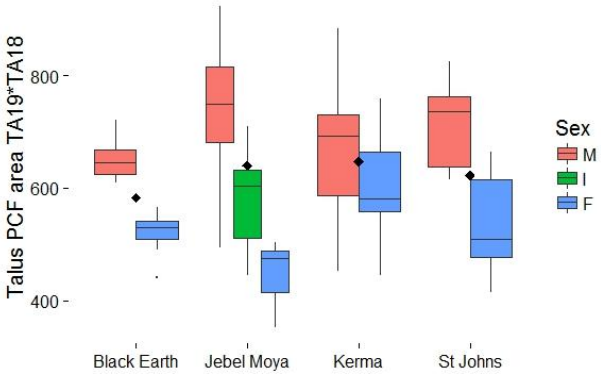
Talus PCF area TA19*TA18
800
600
400
Black Earth
Jebel Moya
Kerma
St Johns
Sex
M
I
F

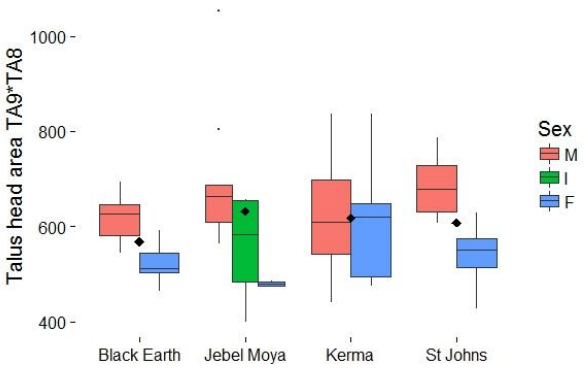
Talus head area TA9*TA8
1000
800
600
400
Black Earth
Jebel Moya
Kerma
St Johns
Sex
M
I
F

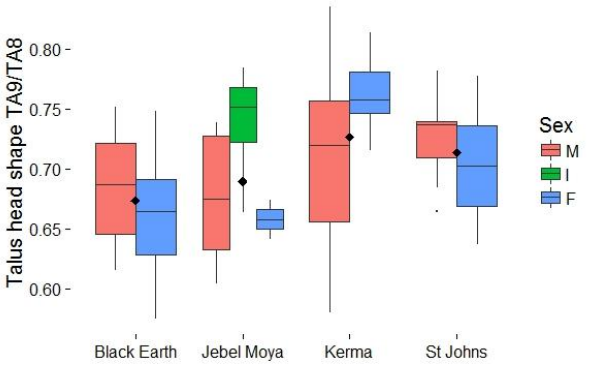
Talus head shape TA9/TA8
0.80
0.75
0.70
0.65
0.60
Black Earth
Jebel Moya
Kerma
St Johns
Sex
M
I
F

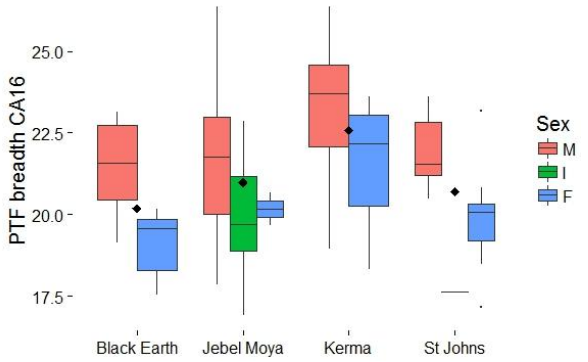
PTF breadth CA16
25.0
22.5
20.0
17.5
Black Earth
Jebel Moya
Kerma
St Johns
Sex
M
I
F

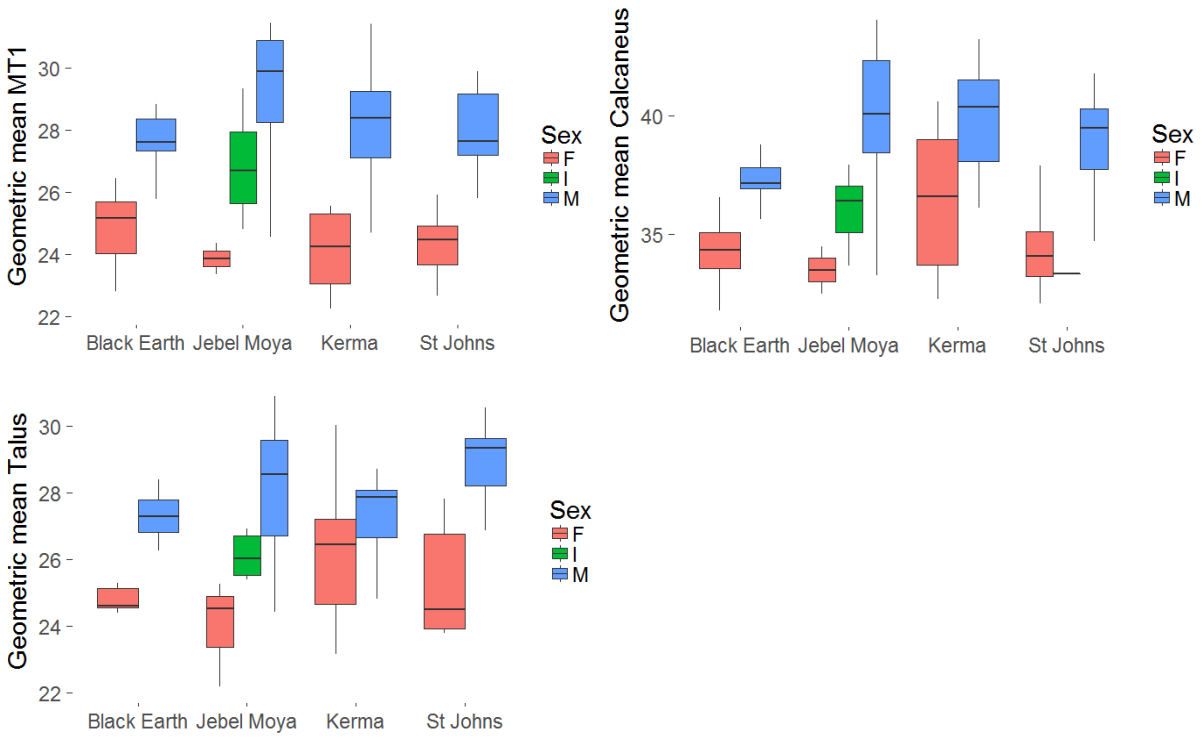

Figure 3.2.2. Boxplots of bone size and shape indices. Diamonds indicate pooled sex means. M=male, F=female, I=indeterminate.

Table 3.2.2. Summary statistics of osteometrics for individual and pooled populations. M=male, F=female, I=indeterminate, P=pooled.

		Populations																
		Black Earth			**Jebel Moya**				**Kerma**			**St. Johns**				**Pooled**		
		Sex			**Sex**				**Sex**			**Sex**				**Sex**		
		M	**F**	**P**	**M**	**F**	**I**	**P**	**M**	**F**	**P**	**M**	**F**	**I**	**P**	**M**	**F**	**I**	**P**
CA1	Mean	73.65	69.17	71.19	82.07	72.28	75.71	78.86	83.13	75.87	80.45	78.06	68.81	70.05	73.04	79.59	70.82	74.90	75.75
	S.E.	.38	1.11	.80	2.16	3.04	1.35	1.56	1.29	2.70	1.49	1.26	1.11		1.30	.92	.97	1.40	.78
	S.D.	1.14	3.68	3.59	6.84	4.30	3.31	6.62	4.49	7.13	6.49	3.77	3.50		5.80	5.81	5.32	3.70	6.83
	N	9	11	20	10	2	6	18	12	7	19	9	10	1	20	40	30	7	77
CA6	Mean	24.10	22.60	23.28	27.48	23.68	24.32	26.00	28.47	24.74	27.10	25.43	22.49	21.30	23.76	26.55	23.14	23.89	24.98
	S.E.	.77	.66	.52	.74	1.15	.71	.62	.60	1.50	.77	1.47	.55		.78	.51	.48	.74	.38
	S.D.	2.30	2.18	2.31	2.33	1.62	1.73	2.61	2.07	3.96	3.36	4.42	1.75		3.49	3.25	2.61	1.95	3.33
	N	9	11	20	10	2	6	18	12	7	19	9	10	1	20	40	30	7	77
CA7	Mean	41.05	39.05	39.95	45.21	35.49	41.11	42.76	43.17	40.08	42.03	43.60	38.47	34.78	40.59	43.30	38.86	40.20	41.29
	S.E.	.74	.77	.57	1.48	.72	1.78	1.24	1.23	1.21	.94	1.05	.61		.85	.62	.47	1.75	.47
	S.D.	2.22	2.54	2.55	4.67	1.02	4.35	5.28	4.25	3.21	4.10	3.16	1.92		3.79	3.91	2.60	4.64	4.09
	N	9	11	20	10	2	6	18	12	7	19	9	10	1	20	40	30	7	77
CA9	Mean	41.77	37.95	39.67	40.91	33.42	37.60	38.97	41.35	37.65	39.99	42.92	38.36	39.63	40.47	41.69	37.71	37.89	39.79
	S.E.	.91	.47	.64	1.45	1.70	.78	1.03	1.01	1.25	.87	1.35	.90		.89	.59	.49	.72	.43
	S.D.	2.72	1.55	2.86	4.57	2.40	1.92	4.36	3.49	3.31	3.81	4.05	2.86		4.00	3.70	2.69	1.91	3.74
	N	9	11	20	10	2	6	18	12	7	19	9	10	1	20	40	30	7	77
CA10	Mean	29.56	26.58	27.92	30.68	25.13	27.69	29.06	30.38	28.36	29.64	31.06	26.93	25.96	28.74	30.42	27.02	27.44	28.82
	S.E.	.43	.28	.42	1.03	1.07	.71	.77	.48	1.45	.63	.64	.72		.66	.34	.44	.65	.31
	S.D.	1.29	.93	1.86	3.25	1.51	1.73	3.26	1.65	3.84	2.75	1.91	2.28		2.94	2.14	2.41	1.71	2.76
	N	9	11	20	10	2	6	18	12	7	19	9	10	1	20	40	30	7	77
CA15	Mean	29.02	26.76	27.78	31.52	24.21	27.51	29.37	30.40	27.53	29.34	31.72	26.98	26.86	29.11	30.67	26.84	27.41	28.88
	S.E.	.47	.34	.38	1.15	1.44	.77	.92	.67	.98	.63	.62	.81		.72	.41	.39	.66	.34
	S.D.	1.41	1.13	1.69	3.63	2.04	1.89	3.92	2.32	2.59	2.75	1.86	2.55		3.23	2.60	2.14	1.74	3.00
	N	9	11	20	10	2	6	18	12	7	19	9	10	1	20	40	30	7	77

CA16	Mean	21.52	19.09	20.18	21.78	20.17	19.90	20.97	23.21	21.53	22.59	21.90	19.92	17.61	20.70	22.18	20.01	19.57	21.09
	S.E.	.46	.29	.38	.92	.52	.86	.61	.64	.74	.51	.38	.50		.40	.33	.30	.79	.25
	S.D.	1.39	.95	1.69	2.90	.73	2.10	2.58	2.21	1.95	2.22	1.13	1.58		1.80	2.11	1.67	2.10	2.23
	N	9	11	20	10	2	6	18	12	7	19	9	10	1	20	40	30	7	77
CA17	Mean	47.60	42.70	44.90	48.48	39.30	43.84	45.92	48.67	46.00	47.69	48.10	42.72	40.42	45.03	48.26	43.25	43.35	45.86
	S.E.	.47	.43	.64	1.37	2.11	1.48	1.18	.94	1.31	.80	1.14	1.35		1.05	.51	.64	1.35	.47
	S.D.	1.42	1.43	2.86	4.35	2.98	3.63	4.99	3.27	3.46	3.50	3.42	4.28		4.69	3.22	3.51	3.56	4.16
	N	9	11	20	10	2	6	18	12	7	19	9	10	1	20	40	30	7	77
CA18	Mean	53.33	49.61	51.28	59.55	54.34	54.92	57.43	58.33	51.93	55.97	56.50	48.92	49.65	52.37	57.10	50.24	54.16	54.16
	S.E.	.70	.79	.67	1.62	1.02	.78	1.08	1.13	1.82	1.19	1.12	.95		1.09	.69	.65	1.00	.58
	S.D.	2.11	2.61	3.02	5.12	1.44	1.91	4.59	3.90	4.82	5.21	3.37	3.00		4.88	4.35	3.55	2.65	5.07
	N	9	11	20	10	2	6	18	12	7	19	9	10	1	20	40	30	7	77
MTL	Mean	59.58	56.97	58.27	69.18	59.10	64.11	66.29	68.73	59.90	65.05	62.05	54.94		58.70	64.37	57.08	64.11	61.46
	S.E.	.84	1.02	.71	1.42	1.27	1.16	1.33	1.62	2.20	1.81	.85	.95		1.08	.91	.74	1.16	.73
	S.D.	2.67	3.22	3.18	4.02	1.79	2.32	4.98	4.28	4.93	6.28	2.55	2.68		4.44	5.32	3.70	2.32	5.79
	N	10	10	20	8	2	4	14	7	5	12	9	8	0	17	34	25	4	63
MLD	Mean	22.56	20.33	21.45	24.47	17.51	20.25	22.27	22.75	20.30	21.73	22.80	19.78		21.38	23.11	19.92	20.25	21.66
	S.E.	.30	.48	.38	1.46	.61	.27	1.10	.72	.91	.65	.53	.40		.50	.41	.32	.27	.32
	S.D.	.95	1.53	1.69	4.12	.86	.53	4.12	1.90	2.03	2.25	1.60	1.14		2.06	2.39	1.60	.53	2.56
	N	10	10	20	8	2	4	14	7	5	12	9	8	0	17	34	25	4	63
DPD	Mean	20.79	18.06	19.43	21.08	17.71	18.19	19.77	20.56	17.66	19.35	21.75	18.55		20.25	21.06	18.11	18.19	19.71
	S.E.	.36	.26	.38	.92	1.55	.73	.71	.54	.75	.60	.55	.40		.52	.30	.24	.73	.27
	S.D.	1.13	.82	1.70	2.61	2.19	1.45	2.65	1.43	1.67	2.08	1.64	1.12		2.15	1.74	1.18	1.45	2.11
	N	10	10	20	8	2	4	14	7	5	12	9	8	0	17	34	25	4	63
DPP	Mean	27.53	25.16	26.34	28.90	25.36	25.48	27.57	28.97	24.83	27.25	26.98	24.81		25.96	28.00	25.00	25.48	26.67
	S.E.	.25	.45	.37	.89	.23	.69	.73	1.13	.73	.93	.56	.43		.44	.37	.26	.69	.29
	S.D.	.79	1.44	1.66	2.51	.33	1.19	2.65	2.99	1.64	3.23	1.68	1.20		1.81	2.14	1.30	1.19	2.32
	N	10	10	20	8	2	3	13	7	5	12	9	8	0	17	34	25	3	62
MLP	Mean	20.57	18.23	19.34	19.61	16.77	17.66	18.74	19.14	15.36	17.57	20.20	17.31		18.84	19.94	17.24	17.66	18.72
	S.E.	.33	.41	.38	.59	.49	.07	.53	.82	.67	.77	.61	.44		.52	.30	.33	.07	.27

	S.D.	1.00	1.31	1.65	1.56	.69	.10	1.75	2.17	1.50	2.68	1.83	1.26		2.14	1.67	1.63	.10	2.10
	N	9	10	19	7	2	2	11	7	5	12	9	8	0	17	32	25	2	59
TA1	Mean	53.35	48.64	50.88	52.45	44.70	48.46	49.96	50.83	46.61	49.36	51.56	45.90		48.58	51.97	46.91	48.46	49.72
	S.E.	.66	.48	.66	1.57	1.14	1.14	1.12	.81	1.52	.86	.61	1.19		.95	.50	.58	1.14	.45
	S.D.	2.10	1.59	3.01	4.96	1.98	2.78	4.87	2.92	4.02	3.84	1.83	3.77		4.13	3.24	3.25	2.78	4.01
	N	10	11	21	10	3	6	19	13	7	20	9	10	0	19	42	31	6	79
TA7	Mean	19.25	18.02	18.61	20.38	19.72	19.62	20.03	21.68	21.51	21.62	22.60	19.08		20.75	20.99	19.32	19.62	20.23
	S.E.	.50	.42	.35	.71	.32	.51	.40	.57	.86	.46	.62	.54		.57	.35	.38	.51	.25
	S.D.	1.58	1.41	1.58	2.23	.55	1.24	1.76	2.05	2.28	2.08	1.85	1.72		2.50	2.26	2.09	1.24	2.26
	N	10	11	21	10	3	6	19	13	7	20	9	10	0	19	42	31	6	79
TA8	Mean	30.07	28.10	29.04	31.92	26.42	27.38	29.74	29.74	27.98	29.12	30.68	27.73		29.13	30.54	27.79	27.38	29.24
	S.E.	.48	.49	.40	1.07	.58	1.18	.89	.76	1.20	.66	.59	.40		.48	.39	.34	1.18	.31
	S.D.	1.51	1.62	1.83	3.37	1.00	2.65	3.76	2.74	3.18	2.95	1.76	1.26		2.11	2.55	1.92	2.65	2.69
	N	10	11	21	10	3	5	18	13	7	20	9	10	0	19	42	31	5	78
TA9	Mean	20.56	18.58	19.52	21.54	17.76	20.17	20.72	20.95	21.31	21.08	22.19	19.51		20.78	21.26	19.47	20.17	20.50
	S.E.	.37	.27	.31	.70	.35	1.30	.61	.65	.80	.50	.33	.49		.43	.29	.33	1.30	.24
	S.D.	1.17	.90	1.43	2.22	.49	2.59	2.45	2.34	2.12	2.21	1.00	1.54		1.87	1.88	1.81	2.59	2.05
	N	10	11	21	10	2	4	16	13	7	20	9	10	0	19	42	30	4	76
TA11	Mean	32.29	28.63	30.37	33.20	26.85	29.43	31.01	30.16	28.70	29.65	33.52	28.52		30.89	32.11	28.44	29.43	30.47
	S.E.	.50	.66	.58	1.46	1.27	1.32	1.04	.87	1.60	.79	1.18	.85		.91	.55	.51	1.32	.41
	S.D.	1.58	2.19	2.65	4.60	2.20	3.23	4.52	3.15	4.25	3.53	3.55	2.70		3.98	3.53	2.83	3.23	3.67
	N	10	11	21	10	3	6	19	13	7	20	9	10	0	19	42	31	6	79
TA12	Mean	27.52	24.78	26.08	30.61	25.22	27.14	28.66	28.89	27.71	28.48	30.09	26.63		28.27	29.23	26.08	27.14	27.83
	S.E.	.42	.42	.42	.69	.25	.98	.68	.61	1.06	.54	.39	.65		.56	.33	.40	.98	.30
	S.D.	1.32	1.40	1.93	2.17	.44	2.41	2.97	2.18	2.81	2.42	1.18	2.05		2.42	2.11	2.22	2.41	2.63
	N	10	11	21	10	3	6	19	13	7	20	9	10	0	19	42	31	6	79
TA13	Mean	22.93	20.75	21.79	21.05	19.15	18.49	19.94	20.73	20.54	20.67	25.06	22.23		23.57	22.26	21.03	18.49	21.49
	S.E.	.54	.36	.40	1.21	2.00	1.08	.80	.57	.71	.43	.71	.74		.60	.46	.38	1.08	.32
	S.D.	1.72	1.20	1.82	3.83	3.46	2.64	3.47	2.04	1.89	1.94	2.12	2.35		2.62	2.98	2.14	2.64	2.82
	N	10	11	21	10	3	6	19	13	7	20	9	10	0	19	42	31	6	79

TA18	Mean	30.92	28.25	29.52	33.13	25.28	30.12	30.94	31.70	29.99	31.10	32.82	28.09		30.33	32.10	28.30	30.12	30.46
	S.E.	.30	.27	.36	1.13	1.49	.86	.94	.88	1.01	.68	.78	.84		.79	.43	.43	.86	.35
	S.D.	.95	.91	1.64	3.58	2.58	2.10	4.08	3.19	2.68	3.06	2.34	2.65		3.44	2.79	2.42	2.10	3.15
	N	10	11	21	10	3	6	19	13	7	20	9	10	0	19	42	31	6	79
TA19	Mean	21.02	18.46	19.68	22.05	17.46	19.20	20.43	21.02	20.05	20.68	21.91	18.93		20.34	21.45	18.88	19.20	20.27
	S.E.	.35	.32	.37	.64	.83	.96	.62	.53	.77	.44	.37	.46		.45	.25	.29	.96	.24
	S.D.	1.12	1.05	1.68	2.01	1.45	2.36	2.69	1.91	2.05	1.96	1.10	1.46		1.98	1.65	1.60	2.36	2.09
	N	10	11	21	10	3	6	19	13	7	20	9	10	0	19	42	31	6	79
Calc PTF shape	Mean	1.36	1.41	1.38	1.45	1.20	1.39	1.40	1.31	1.28	1.30	1.45	1.36	1.53	1.41	1.39	1.35	1.41	1.37
	S.E.	.04	.03	.03	.03	.10	.04	.03	.02	.04	.02	.03	.04		.03	.02	.02	.04	.01
	S.D.	.13	.10	.11	.10	.14	.10	.12	.09	.11	.09	.09	.11		.11	.12	.12	.10	.12
	N	9	11	20	10	2	6	18	12	7	19	9	10	1	20	40	30	7	77
Calc PTF area	Mean	623.9	510.7	561.6	631.4	325.0	549.9	561.0	654.4	520.8	603.5	695.4	539.5	473.0	606.3	650.6	504.8	538.9	583.4
	S.E.	13.3	9.6	15.1	78.6	162.8	35.9	53.8	61.9	80.8	50.0	20.9	26.2		24.4	28.0	26.7	32.3	19.7
	S.D.	40.0	31.7	67.4	260.7	281.9	88.0	240.6	223.1	228.5	229.3	62.8	82.7		109.3	181.4	151.1	85.4	176.9
	N	9	11	20	11	3	6	20	13	8	21	9	10	1	20	42	32	7	81
Calc tuber shape	Mean	1.42	1.43	1.42	1.34	1.33	1.36	1.34	1.36	1.34	1.35	1.38	1.43	1.53	1.41	1.37	1.40	1.38	1.38
	S.E.	.04	.02	.02	.04	.01	.04	.02	.03	.04	.02	.02	.03		.02	.02	.02	.04	.01
	S.D.	.11	.05	.08	.12	.02	.09	.10	.09	.12	.10	.07	.10		.09	.10	.09	.10	.10
	N	9	11	20	10	2	6	18	12	7	19	9	10	1	20	40	30	7	77
Calc tuber area	Mean	1234.4	1009.6	1110.8	1263.9	841.5	1041.9	1143.0	1259.6	1076.4	1192.1	1339.1	1037.0	1028.8	1172.5	1272.9	1023.1	1040.0	1154.4
	S.E.	30.6	20.1	30.9	76.9	78.3	39.8	56.6	46.2	87.0	46.8	63.8	47.8		50.1	28.1	27.7	33.7	23.1
	S.D.	91.9	66.6	138.0	243.1	110.7	97.5	240.2	160.1	230.2	203.9	191.5	151.0		223.9	177.6	151.9	89.2	202.5
	N	9	11	20	10	2	6	18	12	7	19	9	10	1	20	40	30	7	77
MT1 head shape	Mean	.92	.89	.91	.87	1.01	.90	.90	.91	.87	.89	.95	.94		.95	.92	.91	.90	.91
	S.E.	.01	.01	.01	.04	.05	.04	.03	.02	.04	.02	.01	.02		.01	.01	.01	.04	.01
	S.D.	.04	.04	.04	.11	.08	.09	.11	.04	.08	.06	.04	.05		.04	.07	.06	.09	.07
	N	10	10	20	8	2	4	14	7	5	12	9	8	0	17	34	25	4	63
MT1 head area	Mean	469.7	368.2	419.0	520.2	311.0	368.1	446.9	469.6	359.9	423.9	498.0	367.7		436.7	489.1	361.8	368.1	430.9
	S.E.	13.1	13.5	14.8	45.2	37.8	13.2	35.1	26.4	27.1	24.5	24.1	13.5		21.3	13.9	9.1	13.2	11.5

	S.D.	41.4	42.7	66.3	127.9	53.5	26.5	131.3	69.8	60.5	84.7	72.2	38.2		87.9	80.8	45.7	26.5	91.4
	N	10	10	20	8	2	4	14	7	5	12	9	8	0	17	34	25	4	63
MT1 base shape	Mean	1.34	1.39	1.36	1.48	1.51	1.48	1.48	1.52	1.63	1.56	1.34	1.44		1.39	1.41	1.46	1.48	1.43
	S.E.	.02	.04	.02	.05	.03	.02	.03	.03	.09	.04	.04	.05		.03	.02	.03	.02	.02
	S.D.	.07	.12	.10	.12	.04	.03	.09	.07	.19	.14	.12	.13		.13	.12	.16	.03	.14
	N	9	10	19	7	2	2	11	7	5	12	9	8	0	17	32	25	2	59
MT1 base area	Mean	565.3	458.8	509.3	569.4	425.3	461.8	523.7	559.7	381.1	485.3	545.9	429.5		491.1	559.5	431.2	461.8	501.8
	S.E.	11.5	14.1	15.4	31.0	16.4	3.3	27.4	43.7	19.3	37.0	22.8	13.6		19.7	13.1	9.7	3.3	11.6
	S.D.	34.6	44.4	67.1	82.1	23.1	4.7	90.9	115.7	43.2	128.2	68.3	38.6		81.1	74.1	48.5	4.7	89.2
	N	9	10	19	7	2	2	11	7	5	12	9	8	0	17	32	25	2	59
Tochlea shape	Mean	1.18	1.16	1.17	1.09	1.06	1.09	1.09	1.05	1.03	1.04	1.11	1.07		1.09	1.10	1.09	1.09	1.10
	S.E.	.02	.03	.02	.05	.05	.05	.03	.03	.03	.02	.03	.03		.02	.02	.02	.05	.01
	S.D.	.08	.12	.10	.17	.08	.12	.14	.12	.08	.11	.10	.10		.10	.13	.11	.12	.12
	N	10	11	21	10	3	6	19	13	7	20	9	10	0	19	42	31	6	79
Trochlea area	Mean	888.9	709.3	794.8	1016.2	677.3	801.2	894.8	872.9	804.5	848.9	1010.3	761.9		879.6	940.3	744.6	801.2	852.9
	S.E.	21.0	20.5	24.6	49.9	34.2	53.6	43.9	34.9	75.3	34.4	43.4	36.8		40.1	21.2	22.4	53.6	18.2
	S.D.	66.4	68.0	112.9	157.8	59.2	131.3	191.4	125.7	199.2	153.7	130.2	116.3		174.8	137.6	125.0	131.3	161.4
	N	10	11	21	10	3	6	19	13	7	20	9	10	0	19	42	31	6	79
PCF shape	Mean	.68	.65	.67	.67	.69	.64	.66	.67	.67	.67	.67	.68		.67	.67	.67	.64	.67
	S.E.	.02	.01	.01	.02	.01	.03	.01	.01	.02	.01	.02	.01		.01	.01	.01	.03	.01
	S.D.	.05	.04	.05	.05	.02	.07	.06	.05	.06	.05	.05	.03		.04	.05	.04	.07	.05
	N	10	11	21	10	3	6	19	13	7	20	9	10	0	19	42	31	6	79
PCF area	Mean	649.6	521.5	582.5	735.1	443.9	580.4	640.3	670.1	604.2	647.0	720.0	534.8		622.6	691.4	537.0	580.4	622.4
	S.E.	10.5	10.3	16.0	41.5	46.0	40.1	36.0	31.9	38.8	25.2	24.8	28.2		28.5	15.6	15.4	40.1	13.5
	S.D.	33.2	34.1	73.3	131.1	79.7	98.3	156.8	115.0	102.6	112.7	74.3	89.2		124.3	100.9	85.5	98.3	119.9
	N	10	11	21	10	3	6	19	13	7	20	9	10	0	19	42	31	6	79
Talar head shape	Mean	.69	.66	.67	.68	.66	.74	.69	.71	.76	.73	.72	.70		.71	.70	.70	.74	.70
	S.E.	.01	.01	.01	.02	.02	.03	.01	.02	.01	.01	.01	.01		.01	.01	.01	.03	.01
	S.D.	.05	.05	.05	.05	.02	.05	.05	.07	.03	.07	.03	.05		.04	.06	.06	.05	.06
	N	10	11	21	10	2	4	16	13	7	20	9	10	0	19	42	30	4	76

Talar head size	Mean	618.7	522.1	568.1	692.7	479.3	556.2	631.9	626.2	601.8	617.7	681.5	542.1		608.2	652.1	544.5	556.2	604.6
	S.E.	16.4	12.1	14.6	45.6	7.0	62.0	37.6	31.4	48.7	25.9	20.7	18.8		21.3	16.0	14.6	62.0	12.5
	S.D.	51.9	40.3	66.8	144.3	9.8	124.0	150.6	113.2	128.8	116.0	62.0	59.6		92.7	103.6	79.8	124.0	108.5
	N	10	11	21	10	2	4	16	13	7	20	9	10	0	19	42	30	4	76
Geomean Calcaneus	Mean	37.34	34.33	35.69	39.79	33.49	36.04	37.84	39.87	36.40	38.59	39.12	34.46	33.32	36.50	39.11	34.80	35.65	37.12
	S.E.	.31	.42	.43	1.05	1.00	.65	.83	.65	1.23	.71	.76	.64		.71	.39	.41	.68	.36
	S.D.	.93	1.38	1.93	3.31	1.42	1.60	3.50	2.26	3.25	3.09	2.27	2.04		3.18	2.49	2.25	1.79	3.13
	N	10	11	21	11	3	6	20	13	9	22	9	11	1	21	44	36	7	111
Geomean MT1	Mean	27.74	24.89	26.32	29.17	23.88	26.89	27.76	28.18	24.09	26.48	27.83	24.39		26.21	28.19	24.49	26.89	26.64
	S.E.	.39	.38	.42	.85	.50	.99	.75	.84	.64	.81	.49	.38		.53	.32	.23	.99	.30
	S.D.	1.22	1.19	1.87	2.40	.71	1.97	2.80	2.21	1.42	2.80	1.46	1.09		2.17	1.84	1.17	1.97	2.39
	N	10	11	21	11	3	6	20	13	9	22	9	11	1	21	44	36	7	111
Geomean Talus	Mean	27.27	24.74	25.94	28.15	24.00	25.59	26.69	27.19	26.19	26.84	28.94	25.27		27.01	27.81	25.17	25.59	26.61
	S.E.	.22	.21	.32	.65	.93	.70	.56	.52	.88	.46	.37	.51		.53	.26	.29	.70	.23
	S.D.	.69	.69	1.46	2.05	1.60	1.71	2.45	1.87	2.32	2.04	1.12	1.61		2.32	1.67	1.62	1.71	2.09
	N	10	11	21	11	3	6	20	13	9	22	9	11	1	21	44	36	7	111

Table 3.2.3. ANOVA and pairwise post-hoc comparisons between populations of linear measurements, and articular size and shape.

Variable	Pooled			Male			Female		
	Levene P	ANOVA F	Post Hoc	Levene p	ANOVA F	Post Hoc	Levene p	ANOVA F	Post Hoc
CA1	.155	11.802	BE<JM,K SJ<JM,K	.000	8.603	BE<JM,K,SJ SJ<K	.011	3.848	
CA6	.672	7.177	BE<JM,K SJ<K	.095	4.823	BE<JM,K	.149	1.301	
CA7	.031	1.971		.124	1.940		.201	1.891	
CA9	.248	.523		.407	.497		.261	2.139	
CA10	.025	1.332		.007	.790		.000	1.305	
CA15	.007	1.267		.095	2.305		.030	1.304	
CA16	.248	4.781	K>BE,SJ	.095	1.458		.175	4.026	BE<K
CA17	.098	1.909		.002	.202		.041	2.936	
CA18	.060	8.013	BE<JM,K SJ<JM	.042	4.745	BE<JM,K	.021	2.241	
PTF area	.010	.401		.038	.275		.002	1.745	
PTF shape	.621	3.691	K<JM,SJ	.489	4.855	K<JM,SJ	.882	3.159	
Tuber area	.043	.592		.077	.570		.005	1.342	
Tuber shape	.513	3.624		.416	1.077		.007	2.391	BE>JM
MTL	.031	12.659	BE<JM,K SJ<JM,K	.245	17.571	BE<JM,K SJ<JM,K	.123	2.425	
DPD	.418	.367		.009	1.152		.105	2.095	
DPP	.024	.598		.182	.732		.572	.666	
MLD	.020	1.605		.006	1.965		.784	.166	
MLP		1.855		.244	1.123		.847	5.447	BE>K
MT1 head shape	.017	2.305	BE<SJ	.067	2.491		.057	4.104	JM>K
MT1 head area	.025	.292		.005	.740		.526	.931	
MT1 base shape	.264	8.771	BE<JM,K SJ<K	.297	7.048	BE<JM,K SJ<K	.118	3.625	BE<K
MT1 base area	.007	.470		.155	.148		.555	3.925	BE>K
TA1	.108	1.189		.094	1.286		.290	2.032	
TA7	.537	8.305	BE<K,SJ	.934	5.543	BE<K,SJ	.068	6.114	K>BE,SJ
TA8	.087	.266		.380	1.594		.036	.610	
TA9	.225	2.412		.152	1.422		.054	5.854	K>BE,JM
TA11	.140	.543		.089	2.325		.053	.332	
TA12	.107	4.964	BE<JM,K,SJ	.091	5.657	BE<JM,SJ	.191	3.630	BE<K
TA13	.025	7.492	SJ>JM,K	.116	6.233	SJ>JM,K	.094	2.254	
TA18	.002	1.058		.007	1.375		.084	3.375	K>JM
TA19	.254	.846		.160	1.222		.033	2.660	
Talus head area	.174	1.246		.165	1.413		.013	2.172	SJ>JM
Talus head shape	.278	3.969	BE<K	.074	1.507		.454	8.127	K>BE,JM
Talus PCF area	.014	1.205		.031	1.720		.034	3.413	
Talus PCF shape	.739	.136		.902	.194		.667	.773	
Trochlea area	.051	1.542		.247	4.027		.036	1.206	
Trochlea shape	.569	4.488	BE>K	.291	2.122		.876	2.668	
Geomean calcaneus	.050	3.748	BE<K	.060	2.344		.026	1.785	
Geomean MT1	.079	1.379		.263	1.085		.631	.766	
Geomean talus	.149	1.033		.065	2.771		.016	1.853	

Appendix 3.3 Mean coefficients of determination per bone

Table 3.3.1. Mean coefficients of determination between body mass, bone dimensions, and trabecular properties in the calcaneus.

Black Earth	**BVTV**		**Tb.Th**		**Tb.Sp**		**DA**		**Conn.D**	
	Mean	**SD**	**Mean**	**SD**	**Mean**	**SD**	**Mean**	**SD**	**Mean**	**SD**
BM	.088	.141	.026	.057	.196	.151	.154	.133	.268	.183
CA1	.030	.029	.040	.056	.065	.062	.083	.078	.177	.100
CA6	.063	.087	.092	.071	.023	.037	.095	.049	.078	.091
CA7	.043	.086	.037	.077	.037	.044	.089	.085	.092	.103
CA9	.109	.102	.041	.046	.213	.147	.167	.171	.174	.202
CA10	.022	.026	.047	.063	.028	.039	.098	.072	.163	.136
CA15	.021	.021	.023	.019	.065	.087	.127	.147	.207	.166
CA16	.073	.054	.098	.084	.018	.012	.101	.064	.203	.192
CA17	.026	.041	.070	.078	.023	.030	.052	.056	.175	.162
CA18	.027	.049	.021	.020	.047	.064	.167	.164	.165	.115
CA PTF shape	.059	.088	.053	.041	.043	.059	.069	.085	.089	.089
CA PTF area	.051	.036	.078	.071	.023	.041	.141	.086	.257	.156
CA tuber shape	.141	.093	.149	.118	.074	.044	.021	.028	.106	.109
CA tuber area	.030	.031	.019	.012	.098	.083	.147	.131	.185	.126

Jebel Moya	**BVTV**		**Tb.Th**		**Tb.Sp**		**DA**		**Conn.D**	
	Mean	**SD**	**Mean**	**SD**	**Mean**	**SD**	**Mean**	**SD**	**Mean**	**SD**
BM	.346	.211	.263	.202	.173	.181	.167	.158	.112	.100
CA1	.161	.146	.136	.121	.090	.202	.179	.167	.085	.079
CA6	.051	.063	.069	.098	.036	.056	.109	.081	.059	.060
CA7	.411	.141	.132	.080	.358	.219	.128	.110	.080	.079
CA9	.143	.133	.129	.142	.104	.137	.062	.089	.053	.058
CA10	.247	.157	.108	.164	.253	.198	.074	.079	.007	.005
CA15	.188	.188	.153	.149	.130	.222	.136	.071	.058	.034
CA16	.125	.112	.099	.109	.121	.142	.055	.047	.039	.049
CA17	.216	.177	.115	.125	.161	.226	.128	.117	.031	.031
CA18	.106	.098	.140	.131	.055	.089	.151	.147	.115	.133
CA PTF shape	.074	.061	.088	.059	.036	.036	.100	.090	.187	.159
CA PTF area	.156	.152	.126	.127	.133	.198	.085	.048	.037	.018
CA tuber shape	.044	.035	.040	.050	.110	.097	.063	.072	.073	.061
CA tuber area	.216	.167	.127	.171	.190	.179	.070	.066	.025	.027

Kerma	**BVTV**		**Tb.Th**		**Tb.Sp**		**DA**		**Conn.D**	
	Mean	**SD**	**Mean**	**SD**	**Mean**	**SD**	**Mean**	**SD**	**Mean**	**SD**
BM	.146	.056	.030	.027	.290	.093	.222	.181	.249	.095
CA1	.048	.041	.032	.046	.087	.089	.078	.051	.097	.131
CA6	.032	.036	.059	.102	.083	.087	.084	.061	.122	.155
CA7	.036	.035	.029	.046	.061	.078	.053	.056	.047	.071
CA9	.024	.032	.020	.014	.123	.106	.112	.081	.274	.182
CA10	.037	.048	.030	.039	.099	.105	.068	.058	.154	.205
CA15	.037	.034	.029	.031	.057	.036	.169	.153	.110	.099

CA16	.005	.005	.031	.041	.051	.046	.084	.063	.107	.073
CA17	.022	.026	.039	.042	.058	.088	.092	.073	.130	.185
CA18	.055	.045	.039	.048	.072	.071	.092	.097	.071	.103
CA PTF shape	.042	.066	.070	.111	.034	.051	.052	.051	.012	.013
CA PTF area	.019	.014	.026	.022	.056	.044	.134	.117	.122	.097
CA tuber shape	.027	.039	.062	.046	.025	.025	.058	.086	.102	.119
CA tuber area	.029	.045	.020	.021	.125	.114	.097	.071	.250	.204

St. Johns	**BVTV**		**Tb.Th**		**Tb.Sp**		**DA**		**Conn.D**	
	Mean	**SD**	**Mean**	**SD**	**Mean**	**SD**	**Mean**	**SD**	**Mean**	**SD**
BM	.021	.019	.049	.029	.167	.112	.106	.055	.224	.102
CA1	.020	.030	.022	.027	.150	.091	.092	.098	.178	.093
CA6	.036	.022	.006	.008	.145	.118	.114	.134	.116	.104
CA7	.019	.020	.018	.023	.063	.052	.098	.095	.125	.079
CA9	.061	.060	.005	.006	.282	.083	.101	.070	.243	.111
CA10	.023	.031	.019	.022	.146	.081	.103	.082	.154	.083
CA15	.018	.018	.050	.029	.154	.112	.125	.098	.207	.051
CA16	.029	.028	.018	.021	.048	.052	.154	.154	.084	.043
CA17	.017	.022	.014	.014	.125	.112	.079	.071	.099	.046
CA18	.027	.018	.035	.020	.088	.080	.089	.075	.176	.098
CA PTF shape	.010	.011	.069	.050	.114	.083	.072	.104	.121	.068
CA PTF area	.023	.024	.033	.029	.121	.094	.147	.129	.174	.056
CA tuber shape	.114	.101	.025	.033	.064	.028	.040	.058	.027	.033
CA tuber area	.033	.050	.012	.013	.225	.091	.108	.061	.216	.102

Pooled	**BVTV**		**Tb.Th**		**Tb.Sp**		**DA**		**Conn.D**	
	Mean	**SD**	**Mean**	**SD**	**Mean**	**SD**	**Mean**	**SD**	**Mean**	**SD**
BM	.150	.107	.092	.079	.206	.134	.162	.132	.213	.120
CA1	.064	.061	.058	.063	.098	.111	.108	.098	.134	.101
CA6	.045	.052	.057	.070	.072	.075	.100	.081	.094	.103
CA7	.127	.071	.054	.056	.130	.098	.092	.087	.086	.083
CA9	.084	.082	.049	.052	.180	.118	.110	.103	.186	.138
CA10	.082	.066	.051	.072	.131	.106	.086	.073	.119	.107
CA15	.066	.065	.064	.057	.101	.114	.139	.117	.145	.088
CA16	.058	.050	.061	.064	.060	.063	.098	.082	.109	.089
CA17	.070	.066	.059	.065	.092	.114	.088	.079	.109	.106
CA18	.054	.053	.058	.055	.065	.076	.125	.121	.132	.113
CA PTF shape	.046	.057	.070	.066	.057	.057	.073	.083	.102	.082
CA PTF area	.062	.057	.066	.062	.083	.094	.127	.095	.147	.082
CA tuber shape	.081	.067	.069	.062	.068	.049	.045	.061	.077	.081
CA tuber area	.077	.073	.044	.054	.159	.117	.105	.082	.169	.115

Table 3.3.2. Mean coefficients of determination between body mass, bone dimensions, and trabecular properties in the first metatarsal.

Black Earth	**BV/TV**		**Tb.Th**		**Tb.Sp**		**DA**		**Conn.D**	
	Mean	**SD**	**Mean**	**SD**	**Mean**	**SD**	**Mean**	**SD**	**Mean**	**SD**
BM	.023	.014	.082	.064	.283	.131	.013	.008	.398	.120
MTL	.084	.084	.006	.004	.143	.169	.178	.140	.143	.105
MLD	.187	.074	.019	.017	.316	.047	.035	.039	.106	.059
DPD	.104	.050	.010	.013	.172	.141	.053	.063	.153	.150
DPP	.048	.049	.015	.026	.288	.156	.041	.032	.233	.112
MLP	.033	.027	.072	.050	.183	.220	.033	.025	.312	.135
MT1 head shape	.065	.072	.056	.061	.135	.138	.044	.029	.085	.063
MT1 head area	.147	.055	.012	.010	.243	.113	.041	.052	.136	.113
MT1 base shape	.053	.060	.060	.064	.116	.065	.083	.076	.068	.061
MT1 base area	.029	.023	.049	.029	.242	.220	.018	.026	.346	.147

Jebel Moya	**BV/TV**		**Tb.Th**		**Tb.Sp**		**DA**		**Conn.D**	
	Mean	**SD**	**Mean**	**SD**	**Mean**	**SD**	**Mean**	**SD**	**Mean**	**SD**
BM	.229	.136	.276	.253	.127	.067	.241	.299	.216	.298
MTL	.059	.080	.155	.193	.025	.022	.077	.043	.195	.142
MLD	.133	.128	.205	.140	.044	.055	.110	.114	.106	.127
DPD	.179	.167	.240	.207	.246	.111	.052	.036	.025	.016
DPP	.241	.149	.185	.170	.126	.044	.051	.045	.121	.086
MLP	.128	.100	.117	.130	.094	.108	.360	.241	.203	.236
MT1 head shape	.159	.172	.238	.126	.074	.085	.329	.350	.317	.391
MT1 head area	.158	.117	.233	.163	.116	.077	.062	.103	.045	.051
MT1 base shape	.279	.298	.302	.409	.415	.374	.124	.120	.067	.055
MT1 base area	.196	.182	.140	.192	.109	.100	.165	.108	.130	.153

Kerma	**BV/TV**		**Tb.Th**		**Tb.Sp**		**DA**		**Conn.D**	
	Mean	**SD**	**Mean**	**SD**	**Mean**	**SD**	**Mean**	**SD**	**Mean**	**SD**
BM	.085	.073	.011	.014	.223	.184	.195	.211	.269	.207
MTL	.028	.051	.043	.046	.073	.096	.148	.126	.127	.128
MLD	.114	.122	.093	.019	.069	.101	.177	.092	.047	.053
DPD	.178	.238	.031	.033	.205	.093	.225	.122	.249	.197
DPP	.081	.092	.103	.116	.134	.153	.167	.129	.088	.108
MLP	.141	.121	.132	.115	.198	.022	.167	.118	.302	.177
MT1 head shape	.247	.225	.078	.102	.295	.126	.200	.210	.485	.291
MT1 head area	.149	.204	.052	.039	.150	.116	.208	.037	.151	.146
MT1 base shape	.242	.311	.101	.092	.240	.204	.171	.178	.460	.316
MT1 base area	.116	.103	.129	.125	.178	.077	.164	.110	.214	.150

St. Johns	**BV/TV**		**Tb.Th**		**Tb.Sp**		**DA**		**Conn.D**	
	Mean	**SD**	**Mean**	**SD**	**Mean**	**SD**	**Mean**	**SD**	**Mean**	**SD**
BM	.008	.014	.063	.070	.058	.062	.065	.064	.130	.080
MTL	.009	.007	.104	.053	.140	.136	.056	.051	.220	.061
MLD	.012	.015	.164	.121	.114	.083	.107	.089	.228	.052
DPD	.006	.006	.124	.076	.123	.076	.080	.038	.182	.030
DPP	.010	.007	.273	.143	.125	.090	.116	.057	.254	.040

MLP	.057	.022	.018	.016	.195	.051	.064	.066	.192	.035
MT1 head shape	.013	.010	.018	.025	.050	.054	.074	.031	.012	.009
MT1 head area	.009	.010	.147	.097	.123	.083	.090	.060	.211	.033
MT1 base shape	.150	.042	.094	.057	.108	.086	.018	.027	.030	.022
MT1 base area	.015	.010	.086	.072	.195	.081	.099	.082	.260	.044

Pooled	**BV/TV**		**Tb.Th**		**Tb.Sp**		**DA**		**Conn.D**	
	Mean	**SD**	**Mean**	**SD**	**Mean**	**SD**	**Mean**	**SD**	**Mean**	**SD**
BM	.087	.059	.108	.100	.173	.111	.128	.145	.253	.176
MTL	.045	.056	.077	.074	.095	.106	.115	.090	.171	.109
MLD	.111	.085	.120	.074	.136	.071	.107	.084	.121	.072
DPD	.117	.115	.101	.082	.186	.105	.102	.065	.152	.098
DPP	.095	.074	.144	.114	.168	.111	.094	.065	.174	.087
MLP	.090	.068	.085	.078	.168	.100	.156	.113	.252	.146
MT1 head shape	.121	.119	.097	.078	.139	.101	.162	.155	.224	.188
MT1 head area	.116	.097	.111	.077	.158	.097	.100	.063	.136	.086
MT1 base shape	.181	.178	.139	.155	.220	.182	.099	.100	.156	.113
MT1 base area	.089	.080	.101	.105	.181	.120	.112	.081	.238	.124

Table 3.3.3. Mean coefficients of determination between body mass, bone dimensions, and trabecular properties in the talus.

Black Earth	**BV/TV**		**Tb.Th**		**Tb.Sp**		**DA**		**Conn.D**	
	Mean	**SD**	**Mean**	**SD**	**Mean**	**SD**	**Mean**	**SD**	**Mean**	**SD**
BM	.147	.158	.129	.201	.214	.122	.046	.074	.308	.117
TA1	.097	.137	.091	.123	.083	.071	.007	.009	.126	.059
TA7	.142	.182	.135	.187	.065	.049	.117	.166	.077	.071
TA8	.099	.101	.109	.104	.068	.106	.061	.048	.114	.160
TA9	.052	.041	.069	.079	.014	.011	.017	.016	.123	.066
TA11	.035	.054	.034	.051	.056	.066	.043	.049	.008	.010
TA12	.053	.063	.038	.048	.020	.015	.040	.052	.004	.003
TA13	.192	.121	.126	.098	.330	.188	.121	.085	.232	.133
TA18	.100	.111	.076	.081	.138	.109	.042	.040	.156	.096
TA19	.033	.043	.051	.065	.138	.092	.055	.097	.297	.123
Trochlea shape	.022	.019	.023	.025	.043	.037	.142	.149	.009	.012
Trochlea area	.052	.081	.043	.066	.042	.050	.012	.025	.007	.005
PCF shape	.011	.008	.047	.022	.071	.068	.101	.100	.235	.135
PCF area	.059	.071	.060	.080	.154	.100	.040	.077	.267	.116
Talus head shape	.094	.144	.107	.153	.042	.053	.080	.086	.039	.030
Talus head area	.054	.084	.073	.133	.033	.039	.009	.008	.151	.114

Jebel Moya	**BV/TV**		**Tb.Th**		**Tb.Sp**		**DA**		**Conn.D**	
	Mean	**SD**	**Mean**	**SD**	**Mean**	**SD**	**Mean**	**SD**	**Mean**	**SD**
BM	.150	.130	.181	.093	.079	.071	.085	.107	.090	.061
TA1	.050	.063	.108	.092	.017	.021	.070	.083	.041	.048
TA7	.036	.055	.051	.029	.010	.010	.043	.045	.023	.027

TA8	.058	.053	.062	.073	.110	.048	.070	.040	.017	.023
TA9	.027	.031	.106	.170	.017	.029	.055	.083	.046	.070
TA11	.067	.076	.118	.093	.006	.011	.047	.063	.184	.066
TA12	.064	.069	.076	.056	.023	.035	.098	.095	.016	.023
TA13	.041	.061	.058	.093	.050	.069	.042	.034	.039	.065
TA18	.095	.104	.115	.090	.035	.032	.069	.052	.037	.033
TA19	.038	.046	.080	.071	.013	.016	.031	.040	.038	.027
Trochlea shape	.030	.022	.033	.034	.037	.070	.106	.108	.217	.100
Trochlea area	.078	.087	.133	.105	.001	.000	.049	.070	.101	.059
PCF shape	.055	.039	.055	.059	.028	.025	.053	.067	.036	.051
PCF area	.063	.069	.094	.064	.026	.029	.052	.055	.033	.029
Talus head shape	.127	.131	.043	.067	.229	.090	.079	.097	.066	.057
Talus head area	.026	.028	.077	.115	.047	.061	.069	.071	.042	.085

Kerma	**BV/TV**		**Tb.Th**		**Tb.Sp**		**DA**		**Conn.D**	
	Mean	**SD**	**Mean**	**SD**	**Mean**	**SD**	**Mean**	**SD**	**Mean**	**SD**
BM	.139	.048	.096	.079	.155	.084	.099	.126	.098	.074
TA1	.019	.029	.023	.031	.046	.063	.067	.049	.069	.052
TA7	.036	.030	.016	.031	.052	.073	.052	.041	.044	.049
TA8	.029	.058	.035	.061	.019	.023	.069	.118	.013	.013
TA9	.027	.031	.009	.012	.059	.045	.078	.083	.026	.034
TA11	.026	.022	.016	.009	.009	.006	.025	.029	.007	.005
TA12	.052	.061	.052	.069	.058	.063	.051	.060	.022	.024
TA13	.022	.013	.012	.019	.060	.047	.107	.128	.073	.031
TA18	.013	.014	.029	.035	.006	.003	.038	.033	.023	.050
TA19	.033	.038	.021	.018	.026	.037	.042	.043	.050	.070
Trochlea shape	.137	.109	.113	.097	.080	.078	.051	.044	.041	.048
Trochlea area	.007	.007	.006	.009	.017	.019	.031	.052	.003	.003
PCF shape	.086	.090	.067	.101	.064	.091	.037	.046	.031	.025
PCF area	.007	.007	.016	.022	.004	.004	.040	.045	.034	.063
Talus head shape	.055	.075	.046	.097	.076	.110	.151	.177	.069	.074
Talus head area	.029	.033	.022	.030	.039	.030	.063	.124	.011	.017

St. Johns	**BV/TV**		**Tb.Th**		**Tb.Sp**		**DA**		**Conn.D**	
	Mean	**SD**	**Mean**	**SD**	**Mean**	**SD**	**Mean**	**SD**	**Mean**	**SD**
BM	.101	.082	.186	.102	.137	.111	.084	.087	.186	.070
TA1	.145	.121	.400	.179	.248	.146	.076	.073	.417	.096
TA7	.102	.085	.110	.063	.091	.149	.074	.074	.102	.076
TA8	.152	.103	.255	.130	.106	.129	.049	.052	.181	.032
TA9	.026	.030	.077	.055	.175	.075	.011	.016	.171	.055
TA11	.076	.086	.253	.150	.303	.190	.117	.164	.366	.052
TA12	.149	.095	.282	.145	.135	.092	.084	.064	.243	.085
TA13	.080	.078	.194	.107	.127	.068	.106	.120	.201	.122
TA18	.065	.055	.221	.131	.255	.137	.059	.088	.292	.065
TA19	.143	.109	.257	.140	.116	.103	.055	.071	.224	.045
Trochlea shape	.033	.048	.073	.067	.191	.224	.176	.193	.149	.071
Trochlea area	.109	.098	.298	.164	.271	.143	.090	.135	.366	.074

PCF shape	.056	.023	.008	.005	.151	.047	.035	.022	.058	.052
PCF area	.094	.076	.244	.138	.204	.131	.057	.083	.278	.051
Talus head shape	.138	.071	.044	.043	.117	.120	.044	.026	.030	.042
Talus head area	.064	.039	.156	.090	.150	.101	.022	.023	.193	.029

Pooled	**BV/TV**		**Tb.Th**		**Tb.Sp**		**DA**		**Conn.D**	
	Mean	**SD**	**Mean**	**SD**	**Mean**	**SD**	**Mean**	**SD**	**Mean**	**SD**
BM	.134	.105	.148	.119	.146	.097	.079	.099	.171	.081
TA1	.078	.088	.155	.106	.098	.075	.055	.054	.164	.064
TA7	.079	.088	.078	.078	.054	.070	.072	.082	.061	.055
TA8	.085	.079	.115	.092	.076	.077	.062	.064	.081	.057
TA9	.033	.033	.065	.079	.067	.040	.040	.049	.092	.056
TA11	.051	.059	.105	.076	.094	.068	.058	.076	.141	.034
TA12	.080	.072	.112	.080	.059	.051	.068	.068	.071	.034
TA13	.084	.068	.097	.079	.142	.093	.094	.092	.136	.088
TA18	.068	.071	.110	.084	.108	.070	.052	.053	.127	.061
TA19	.062	.059	.102	.074	.073	.062	.046	.063	.152	.067
Trochlea shape	.055	.050	.060	.056	.088	.102	.119	.124	.104	.058
Trochlea area	.062	.068	.120	.086	.083	.053	.046	.071	.119	.035
PCF shape	.052	.040	.044	.047	.079	.058	.056	.059	.090	.066
PCF area	.056	.056	.103	.076	.097	.066	.047	.065	.153	.065
Talus head shape	.103	.105	.060	.090	.116	.093	.088	.096	.051	.051
Talus head area	.043	.046	.082	.092	.067	.058	.041	.057	.099	.061

Appendix 4.

Appendix 4.1 Plots of OLS regressions

Calcaneus

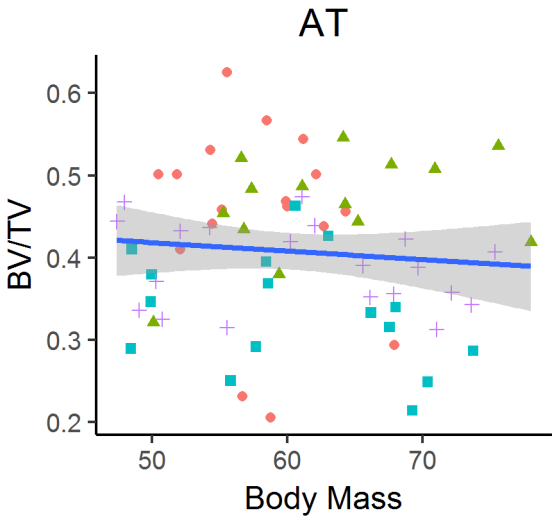

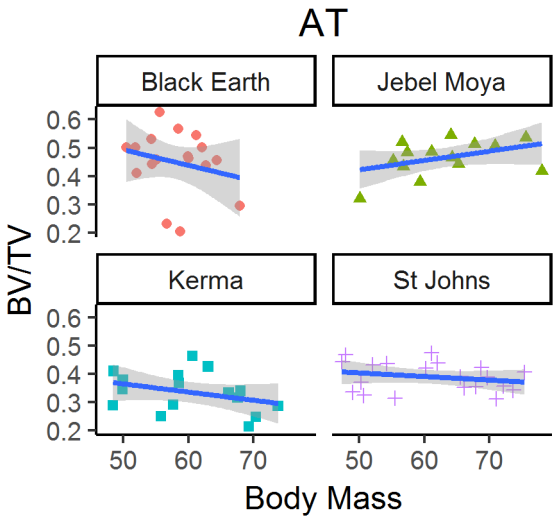

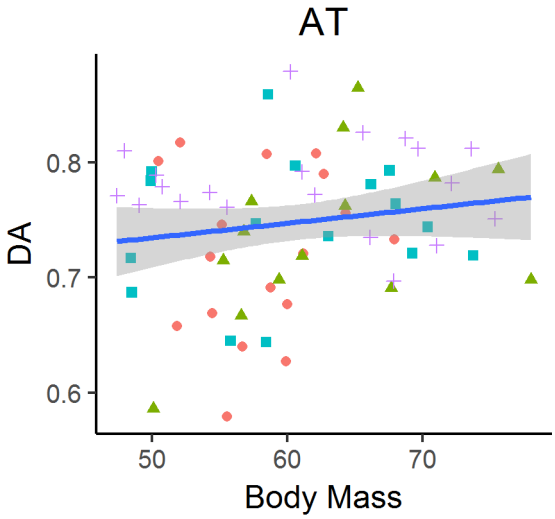

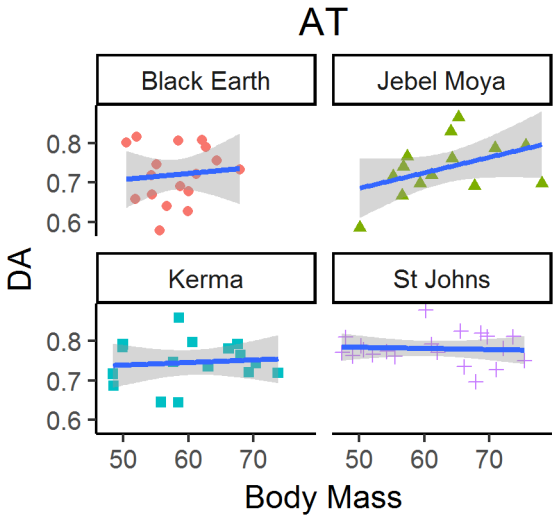

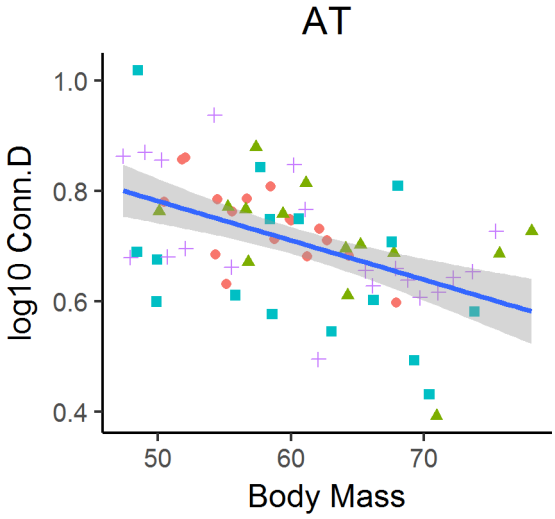

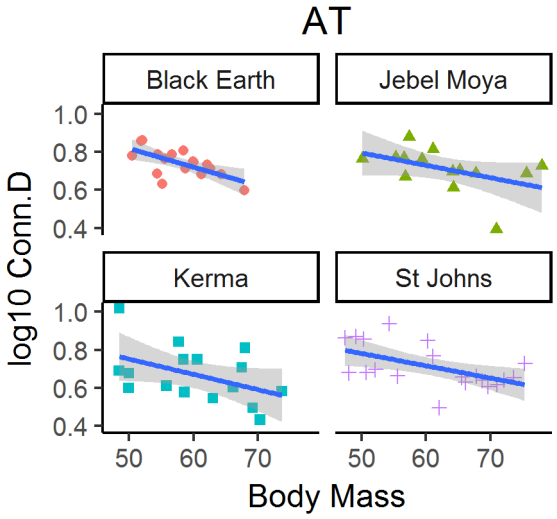

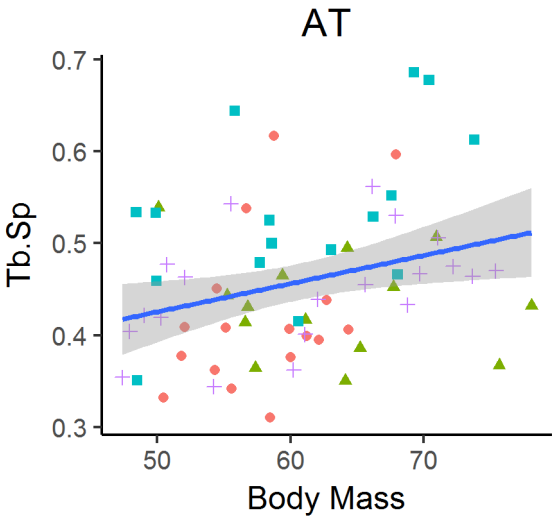
AT
Tb.Sp
Body Mass
0.7
0.6
0.5
0.4
0.3
50
60
70

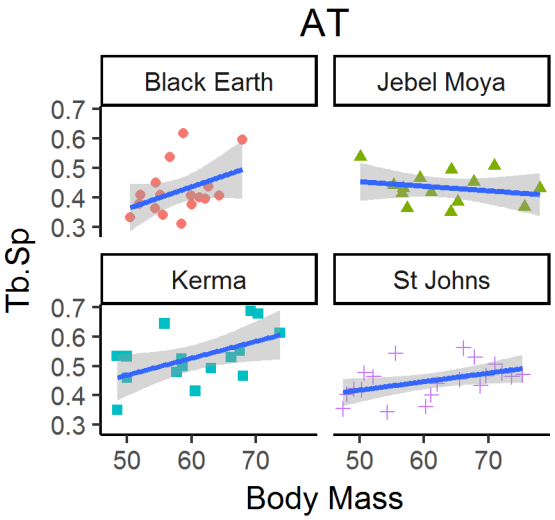
AT
Black Earth
Jebel Moya
Kerma
St Johns
Tb.Sp
Body Mass
0.7
0.6
0.5
0.4
0.3
50
60
70

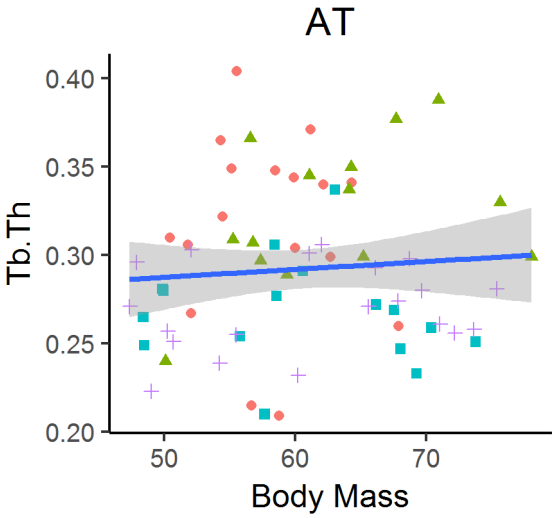
AT
Tb.Th
Body Mass
0.40
0.35
0.30
0.25
0.20
50
60
70

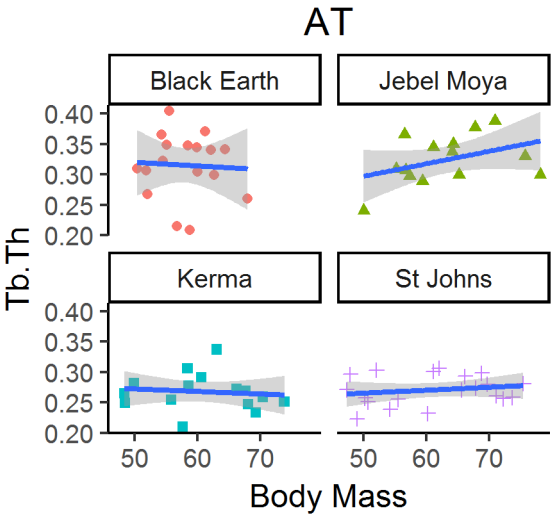
AT
Black Earth
Jebel Moya
Kerma
St Johns
Tb.Th
Body Mass
0.40
0.35
0.30
0.25
0.20
50
60
70

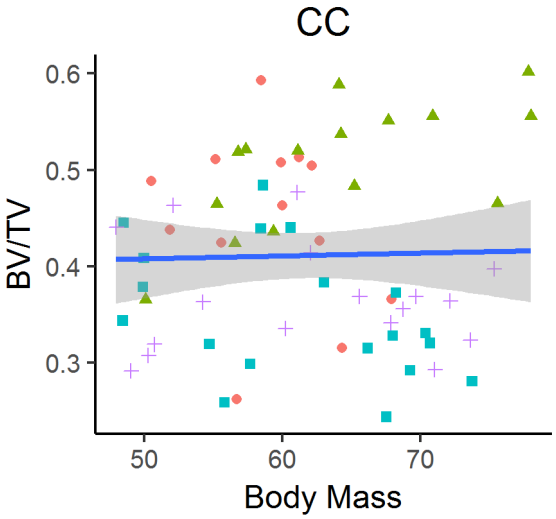
CC
BV/TV
Body Mass
0.6
0.5
0.4
0.3
50
60
70

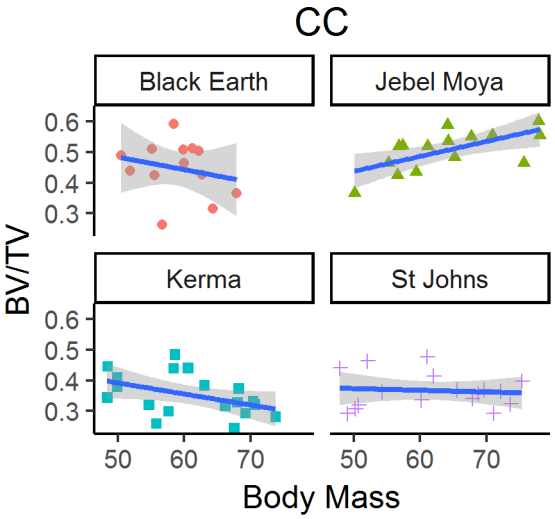
CC
Black Earth
Jebel Moya
Kerma
St Johns
BV/TV
Body Mass
0.6
0.5
0.4
0.3
50
60
70

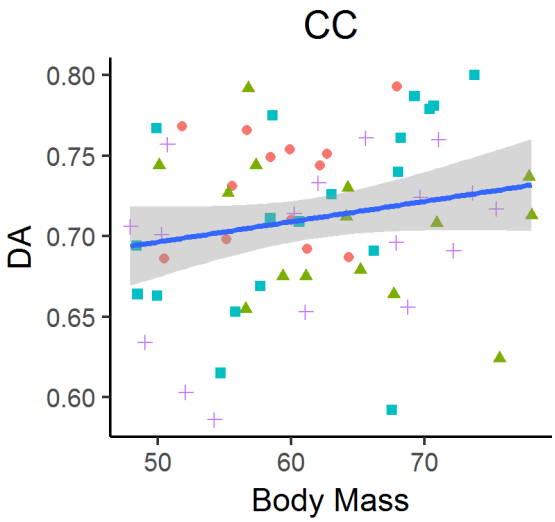
CC
DA
0.80
0.75
0.70
0.65
0.60
50
60
70
Body Mass

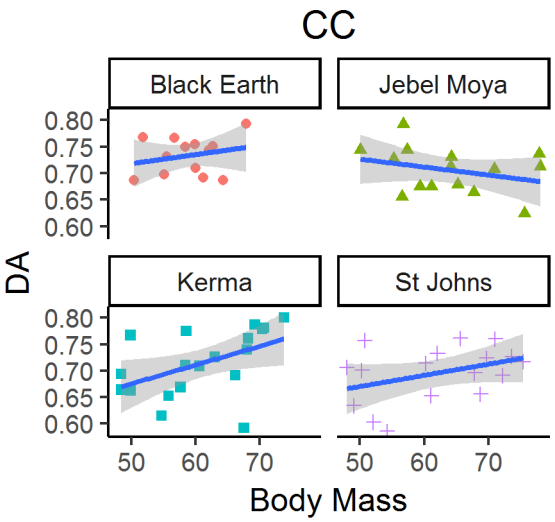
CC
Black Earth
Jebel Moya
Kerma
St Johns
DA
0.80
0.75
0.70
0.65
0.60
50
60
70
Body Mass

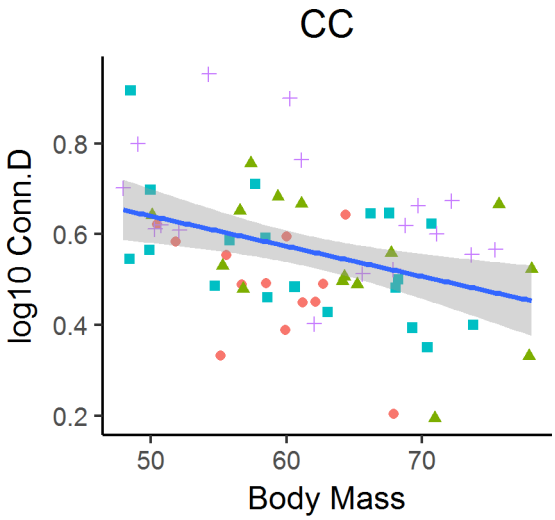
CC
log10 Conn.D
0.8
0.6
0.4
0.2
50
60
70
Body Mass

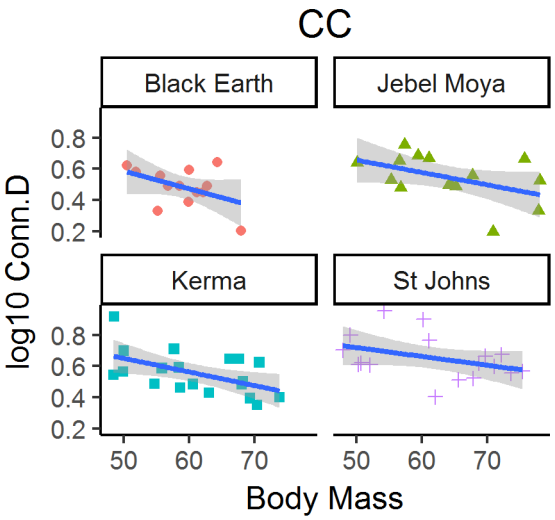
CC
Black Earth
Jebel Moya
Kerma
St Johns
log10 Conn.D
0.8
0.6
0.4
0.2
50
60
70
Body Mass

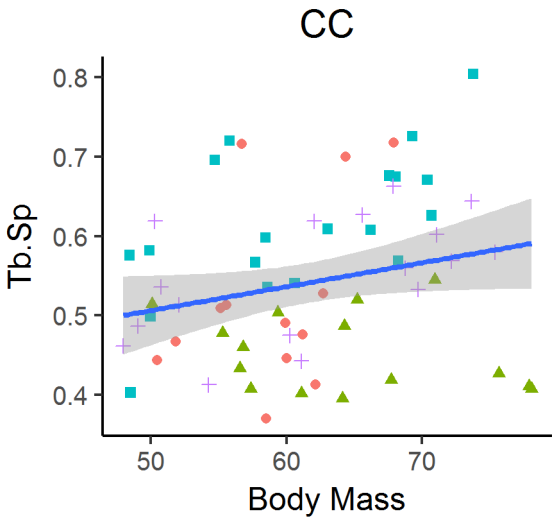
CC
Tb.Sp
0.8
0.7
0.6
0.5
0.4
50
60
70
Body Mass

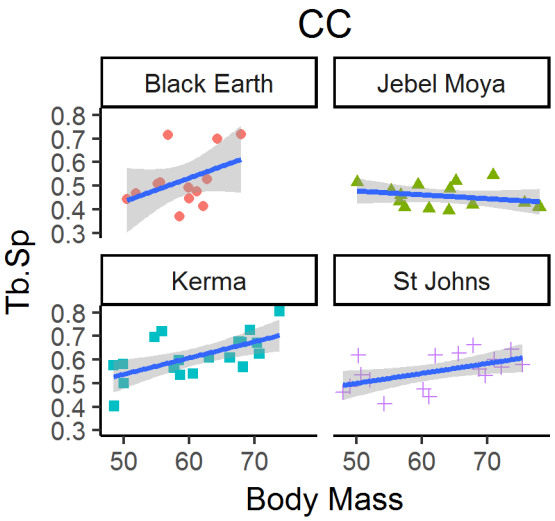
CC
Black Earth
Jebel Moya
Kerma
St Johns
Tb.Sp
0.8
0.7
0.6
0.5
0.4
0.3
50
60
70
Body Mass

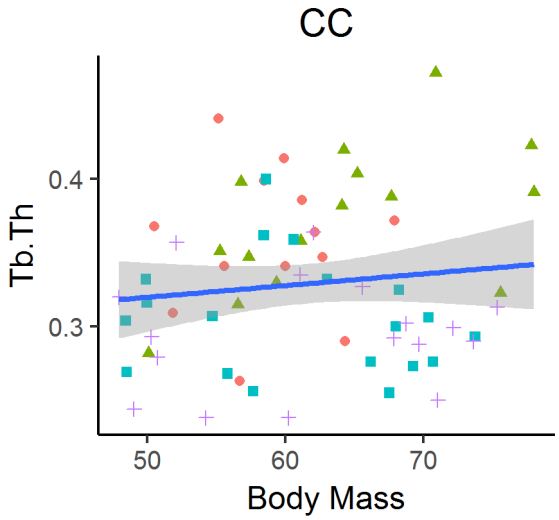
CC
Tb.Th
0.4
0.3
50
60
70
Body Mass

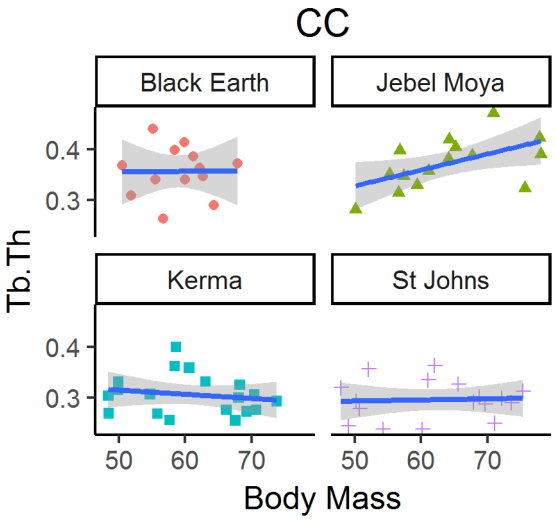
CC
Black Earth
Jebel Moya
Kerma
St Johns
Tb.Th
0.4
0.3
50
60
70
Body Mass

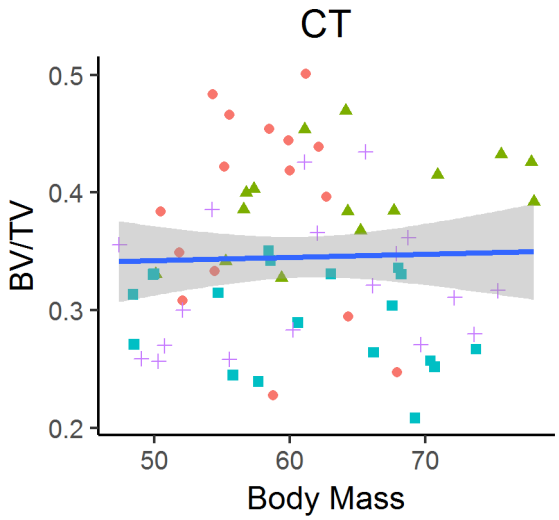
CT
BV/TV
0.5
0.4
0.3
0.2
50
60
70
Body Mass

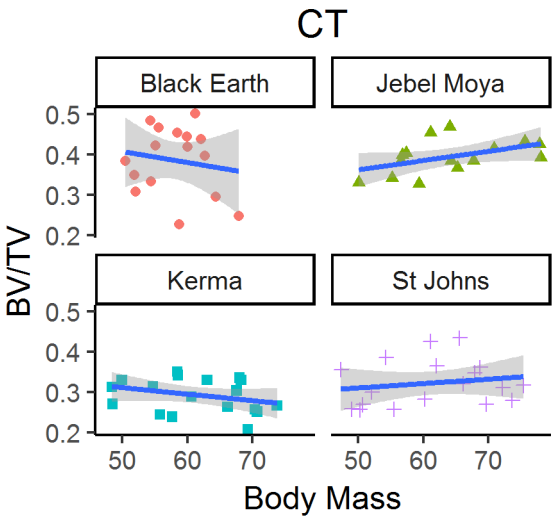
CT
Black Earth
Jebel Moya
Kerma
St Johns
BV/TV
0.5
0.4
0.3
0.2
50
60
70
Body Mass

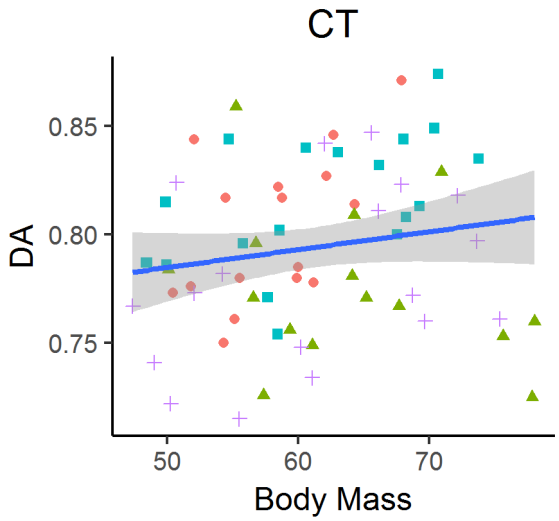
CT
DA
0.85
0.80
0.75
50
60
70
Body Mass

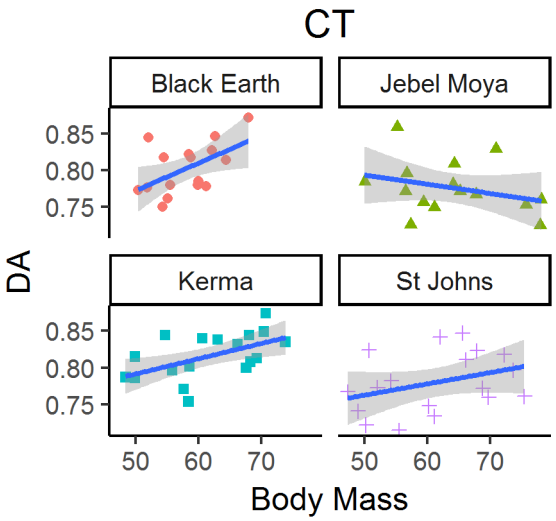
CT
Black Earth
Jebel Moya
Kerma
St Johns
DA
0.85
0.80
0.75
50
60
70
Body Mass

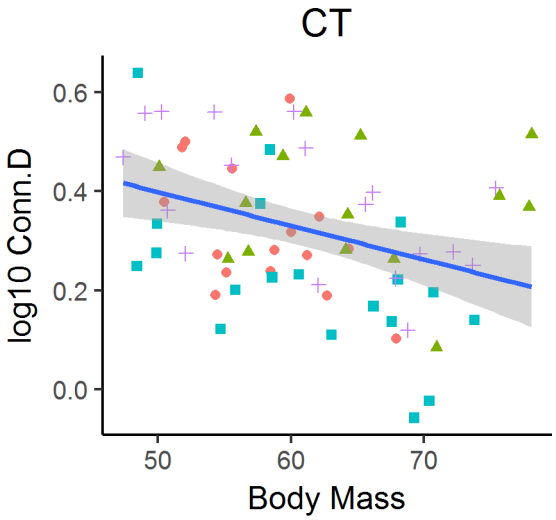
CT
log10 Conn.D
0.6
0.4
0.2
0.0
50
60
70
Body Mass

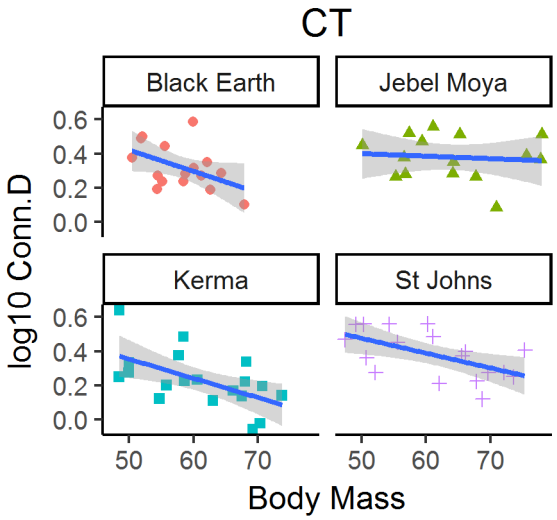
CT
Black Earth
Jebel Moya
Kerma
St Johns
log10 Conn.D
0.6
0.4
0.2
0.0
50
60
70
Body Mass

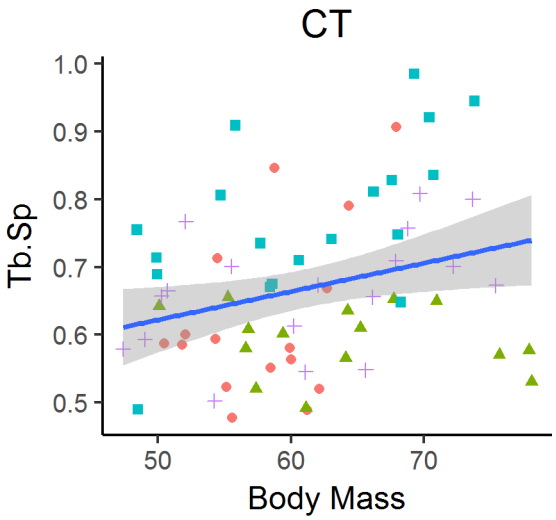
CT
Tb.Sp
1.0
0.9
0.8
0.7
0.6
0.5
50
60
70
Body Mass

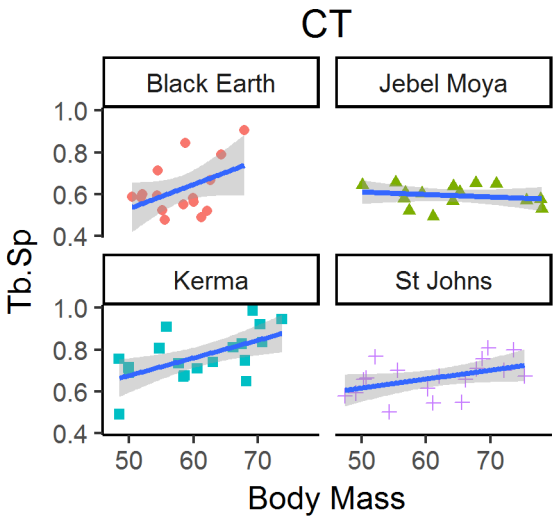
CT
Black Earth
Jebel Moya
Kerma
St Johns
Tb.Sp
1.0
0.8
0.6
0.4
50
60
70
Body Mass

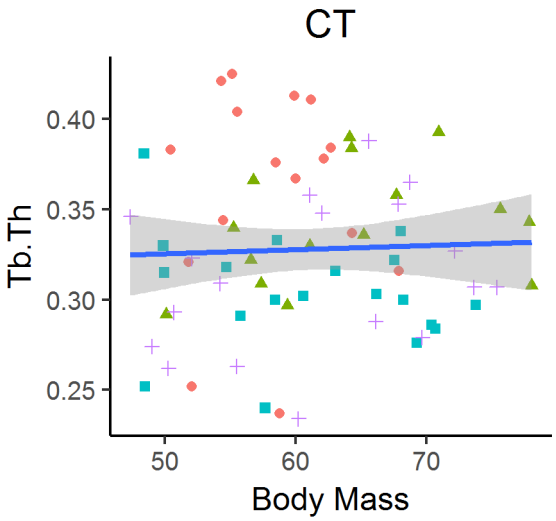
CT
Tb.Th
0.40
0.35
0.30
0.25
50
60
70
Body Mass

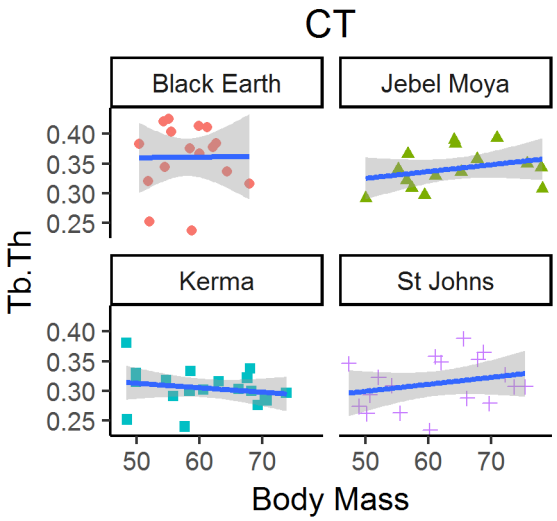
CT
Black Earth
Jebel Moya
Kerma
St Johns
Tb.Th
0.40
0.35
0.30
0.25
50
60
70
Body Mass

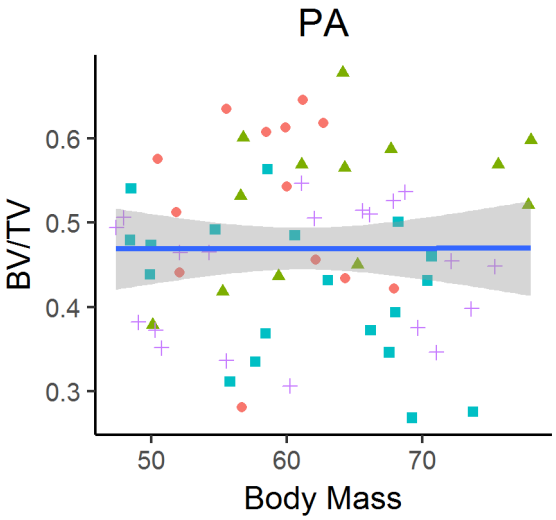
PA
BV/TV
0.6
0.5
0.4
0.3
50
60
70
Body Mass

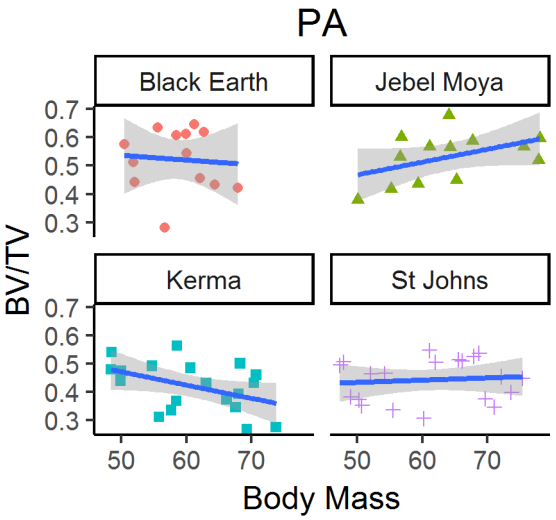
PA
Black Earth
Jebel Moya
Kerma
St Johns
BV/TV
0.7
0.6
0.5
0.4
0.3
50
60
70
Body Mass

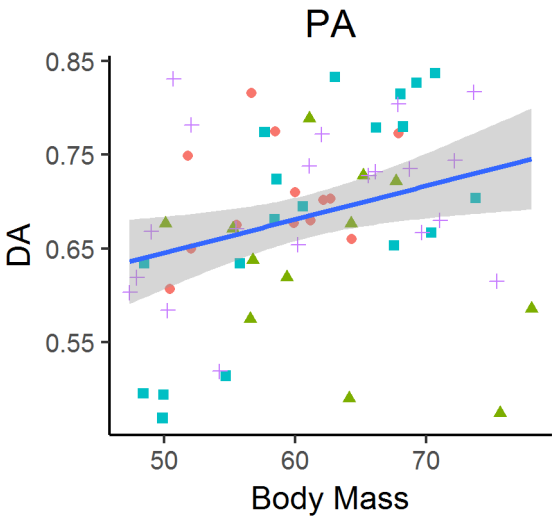
PA
DA
0.85
0.75
0.65
0.55
50
60
70
Body Mass

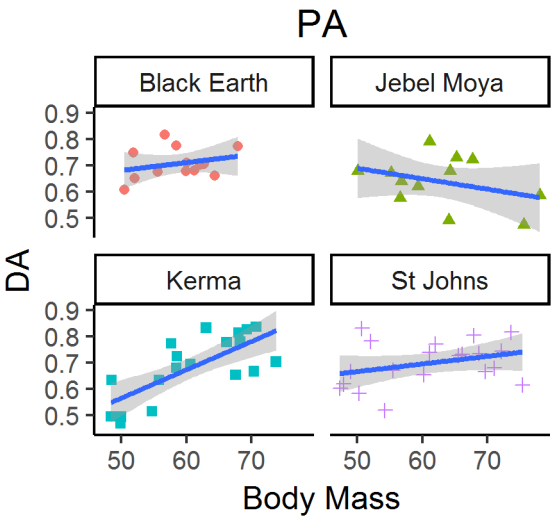
PA
Black Earth
Jebel Moya
Kerma
St Johns
DA
0.9
0.8
0.7
0.6
0.5
50
60
70
Body Mass

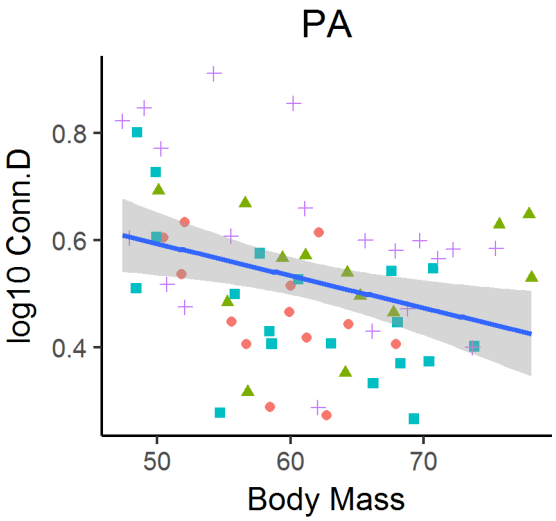
PA
log10 Conn.D
0.8
0.6
0.4
50
60
70
Body Mass

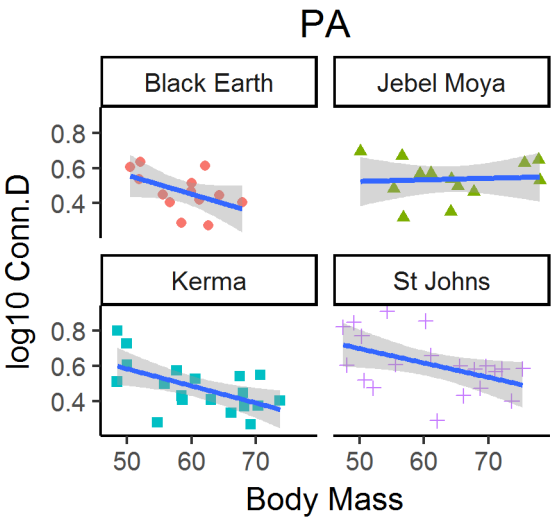
PA
Black Earth
Jebel Moya
Kerma
St Johns
log10 Conn.D
0.8
0.6
0.4
50
60
70
Body Mass

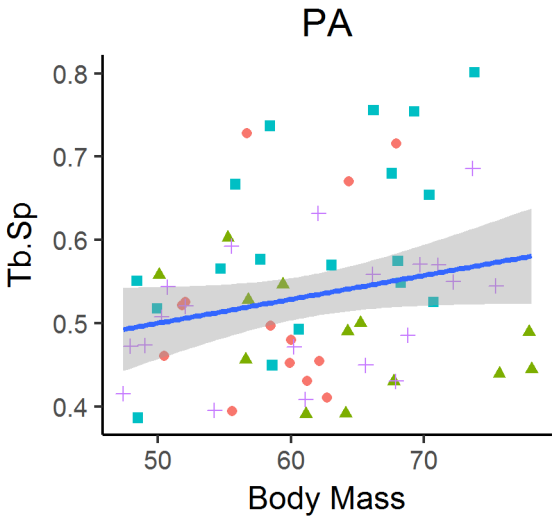
PA
Tb.Sp
0.8
0.7
0.6
0.5
0.4
50
60
70
Body Mass

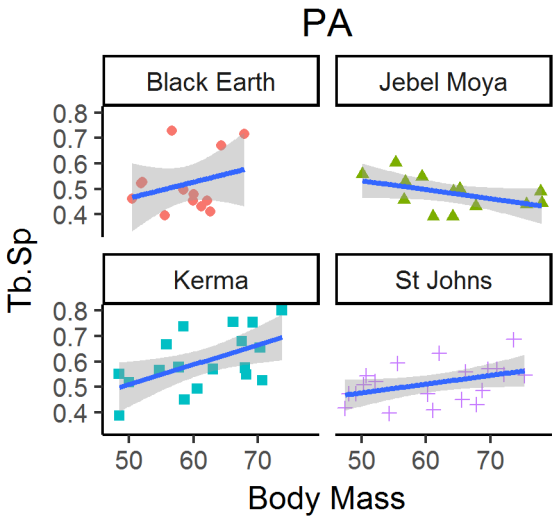
PA
Black Earth
Jebel Moya
Kerma
St Johns
Tb.Sp
0.8
0.7
0.6
0.5
0.4
50
60
70
Body Mass

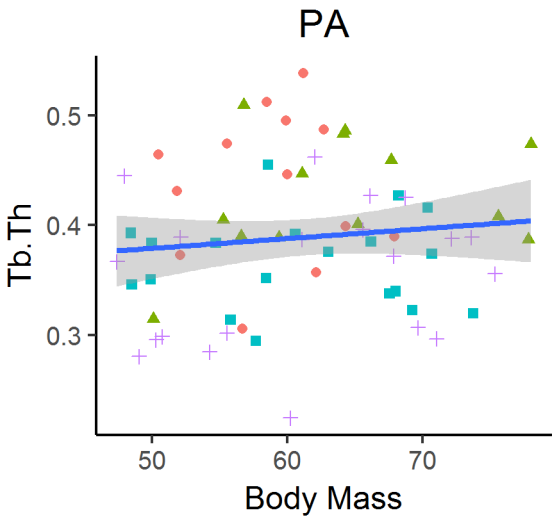
PA
Tb.Th
0.5
0.4
0.3
50
60
70
Body Mass

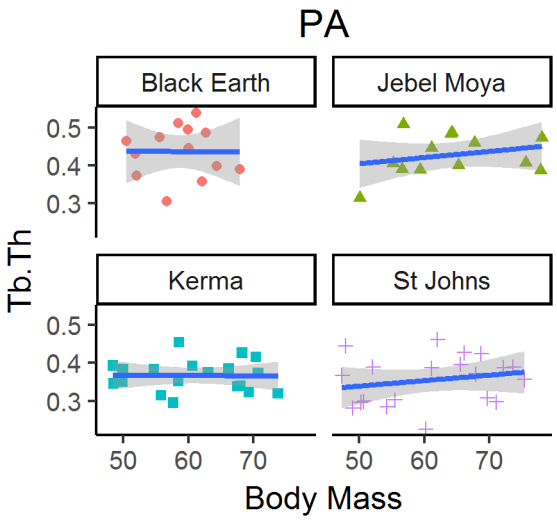
PA
Black Earth
Jebel Moya
Kerma
St Johns
Tb.Th
0.5
0.4
0.3
50
60
70
Body Mass

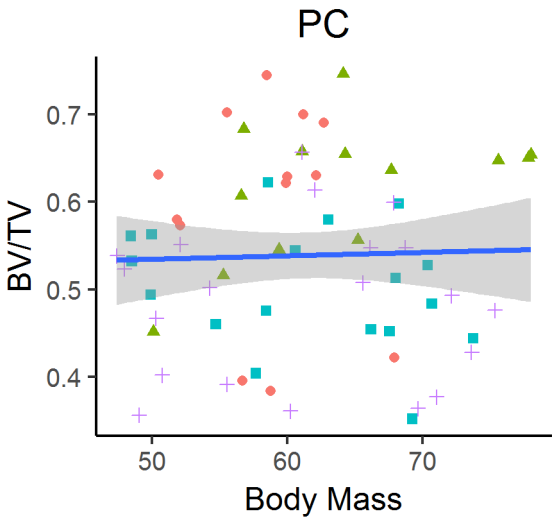
PC
BV/TV
0.7
0.6
0.5
0.4
50
60
70
Body Mass

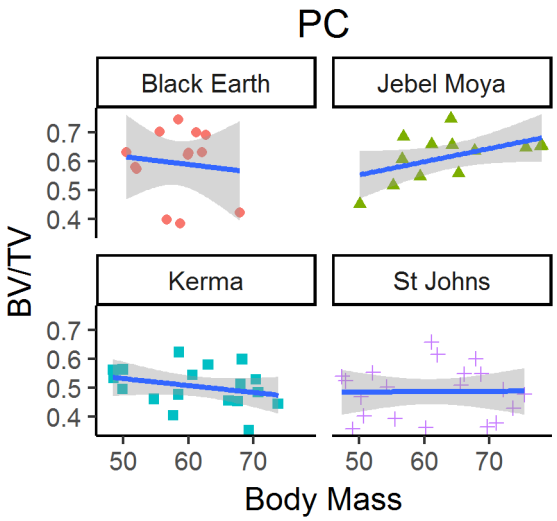
PC
Black Earth
Jebel Moya
Kerma
St Johns
BV/TV
0.7
0.6
0.5
0.4
50
60
70
Body Mass

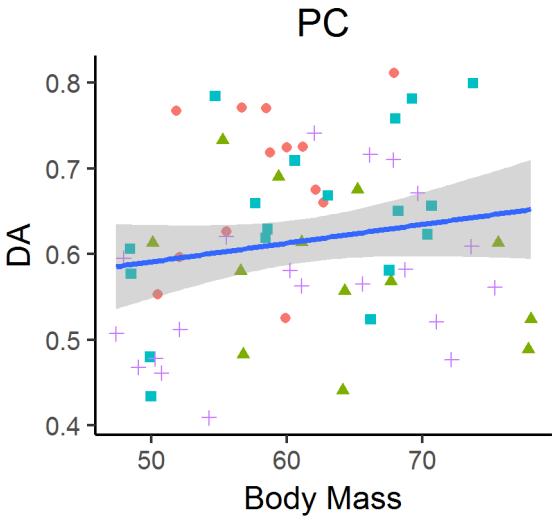
PC
DA
0.8
0.7
0.6
0.5
0.4
50
60
70
Body Mass

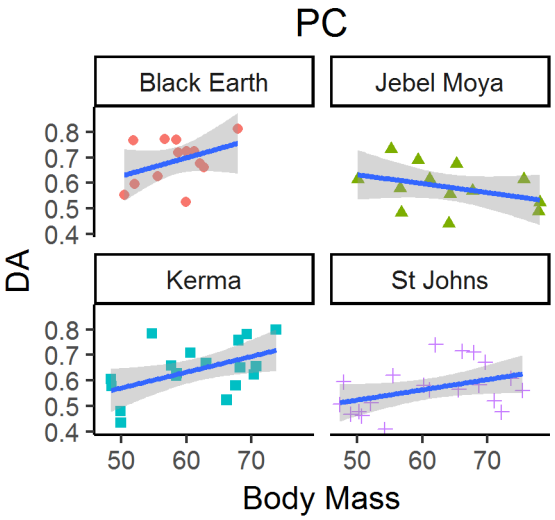
PC
Black Earth
Jebel Moya
Kerma
St Johns
DA
0.8
0.7
0.6
0.5
0.4
50
60
70
Body Mass

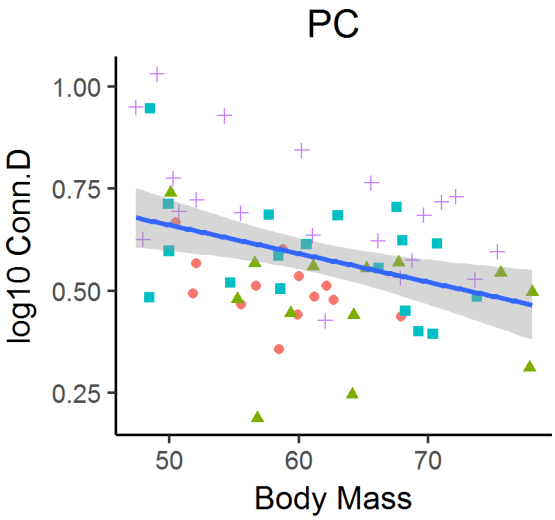
PC
log10 Conn.D
1.00
0.75
0.50
0.25
50
60
70
Body Mass

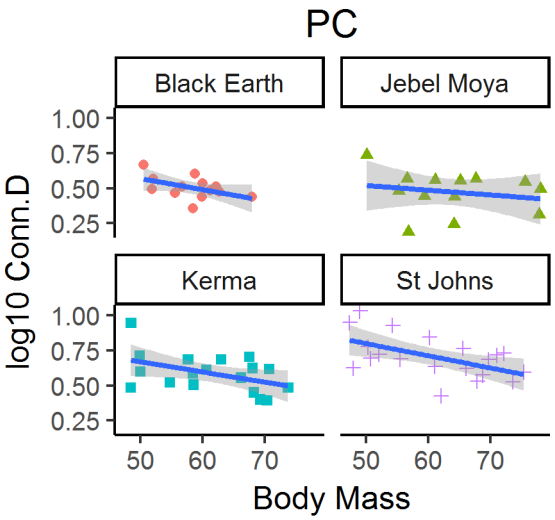
PC
Black Earth
Jebel Moya
Kerma
St Johns
log10 Conn.D
1.00
0.75
0.50
0.25
50
60
70
Body Mass

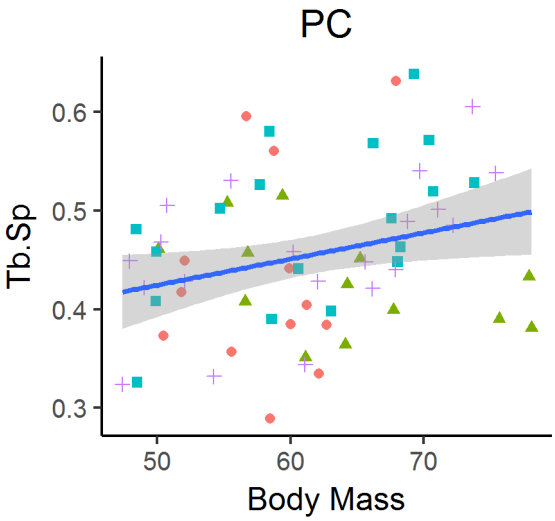
PC
Tb.Sp
0.6
0.5
0.4
0.3
50
60
70
Body Mass

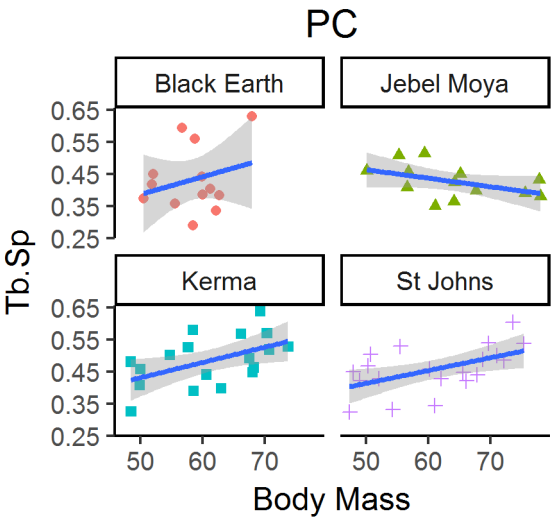
PC
Black Earth
Jebel Moya
Kerma
St Johns
Tb.Sp
0.65
0.55
0.45
0.35
0.25
50
60
70
Body Mass

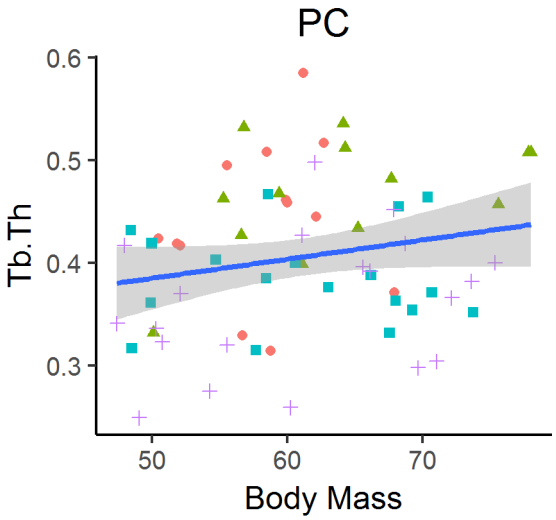
PC
Tb.Th
0.6
0.5
0.4
0.3
50
60
70
Body Mass

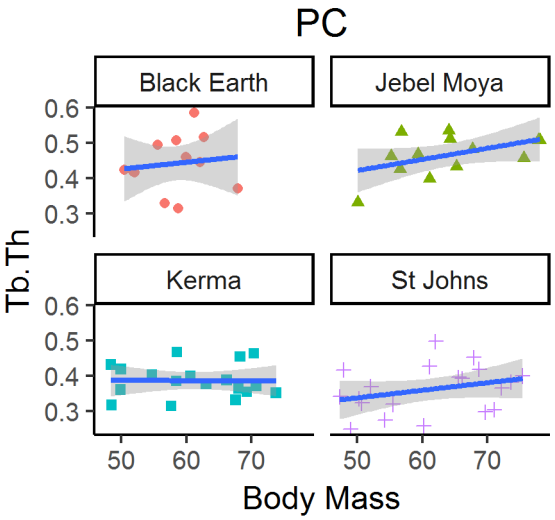
PC
Black Earth
Jebel Moya
Kerma
St Johns
Tb.Th
0.6
0.5
0.4
0.3
50
60
70
Body Mass

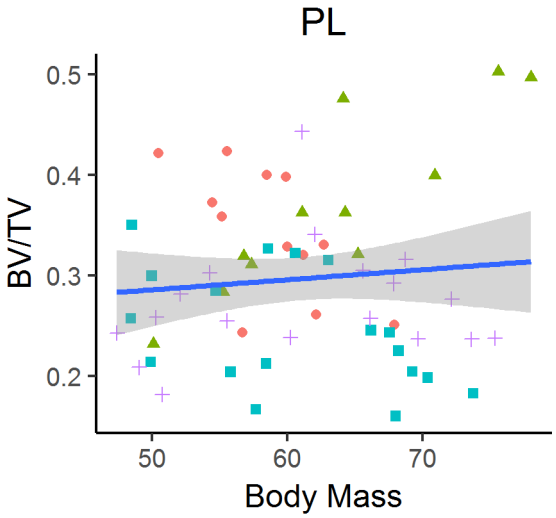
PL
BV/TV
0.5
0.4
0.3
0.2
50
60
70
Body Mass

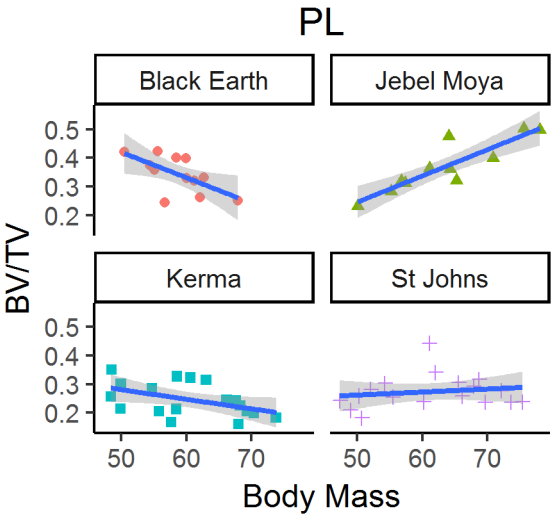
PL
Black Earth
Jebel Moya
Kerma
St Johns
BV/TV
0.5
0.4
0.3
0.2
50
60
70
Body Mass

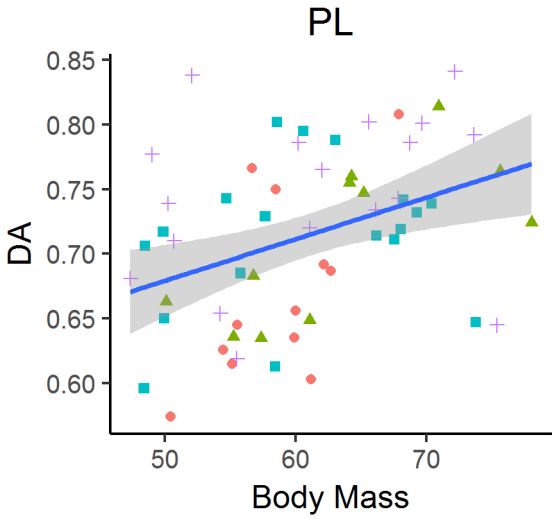
PL
DA
0.85
0.80
0.75
0.70
0.65
0.60
50
60
70
Body Mass

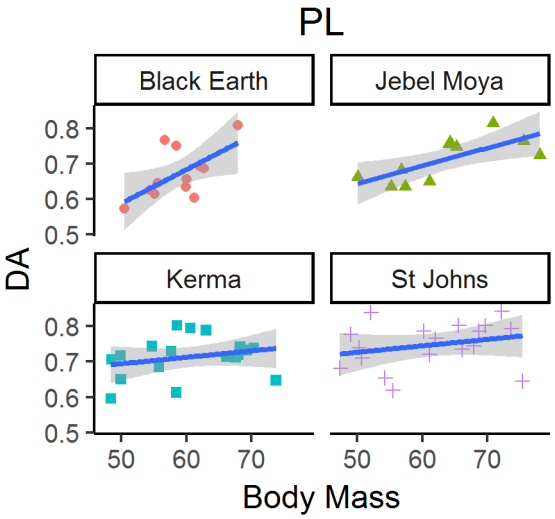
PL
Black Earth
Jebel Moya
Kerma
St Johns
DA
0.8
0.7
0.6
0.5
50
60
70
Body Mass

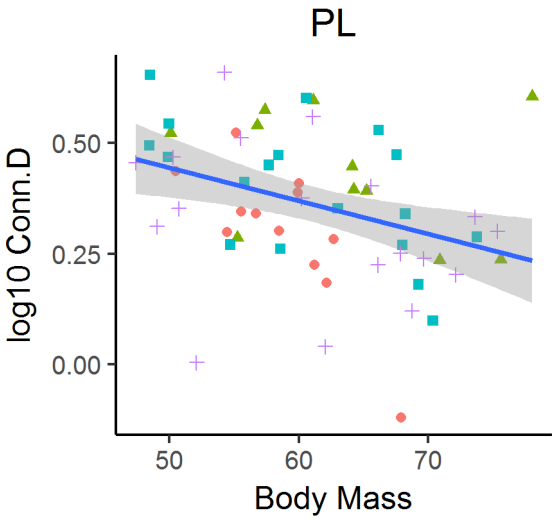
PL
log10 Conn.D
0.50
0.25
0.00
50
60
70
Body Mass

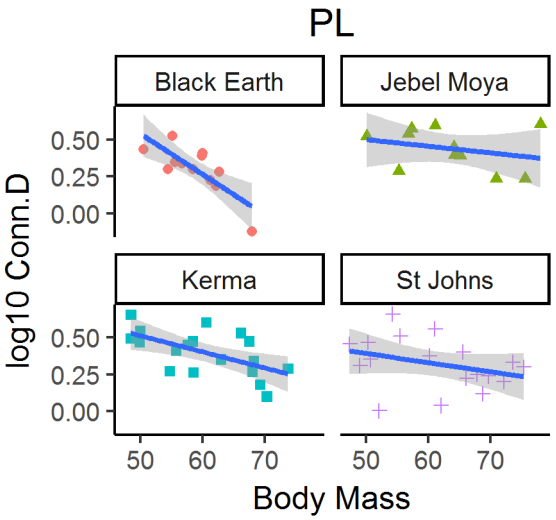
PL
Black Earth
Jebel Moya
Kerma
St Johns
log10 Conn.D
0.50
0.25
0.00
50
60
70
Body Mass

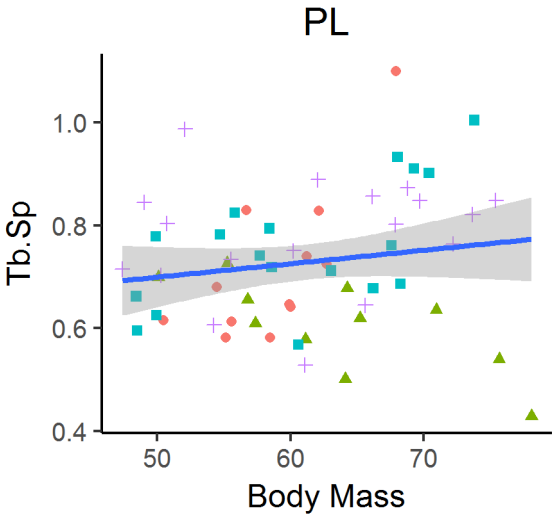
PL
Tb.Sp
1.0
0.8
0.6
0.4
50
60
70
Body Mass

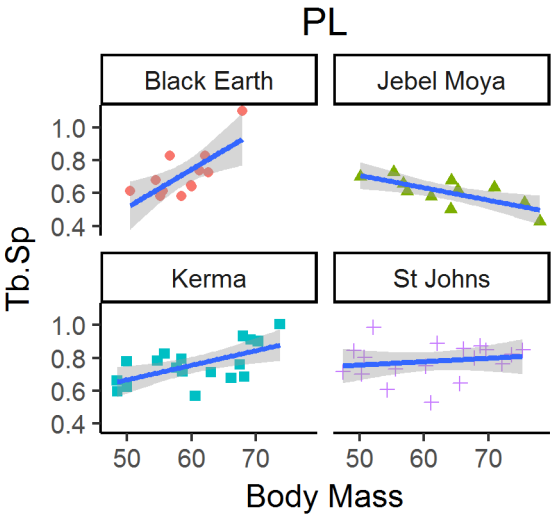
PL
Black Earth
Jebel Moya
Kerma
St Johns
Tb.Sp
1.0
0.8
0.6
0.4
50
60
70
Body Mass

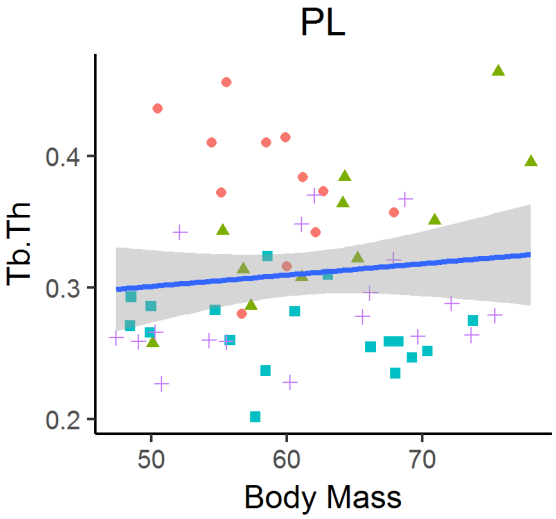
PL
Tb.Th
0.4
0.3
0.2
50
60
70
Body Mass

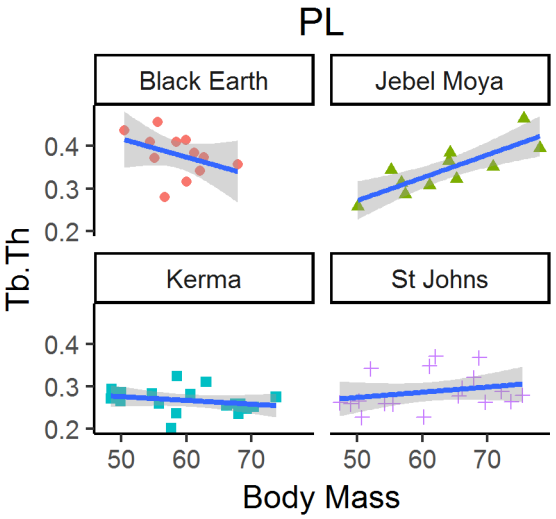
PL
Black Earth
Jebel Moya
Kerma
St Johns
Tb.Th
0.4
0.3
0.2
50
60
70
Body Mass

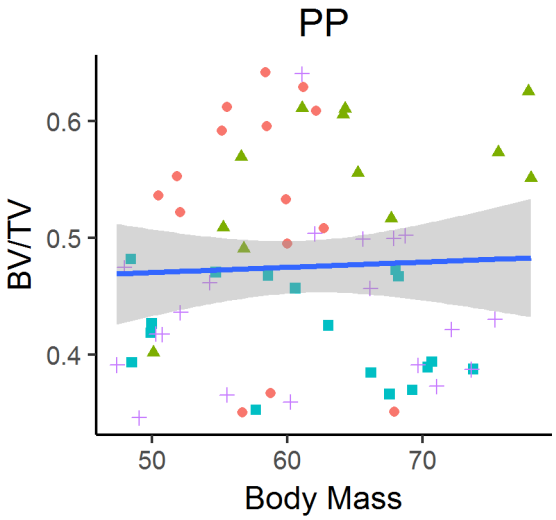
PP
BV/TV
0.6
0.5
0.4
50
60
70
Body Mass

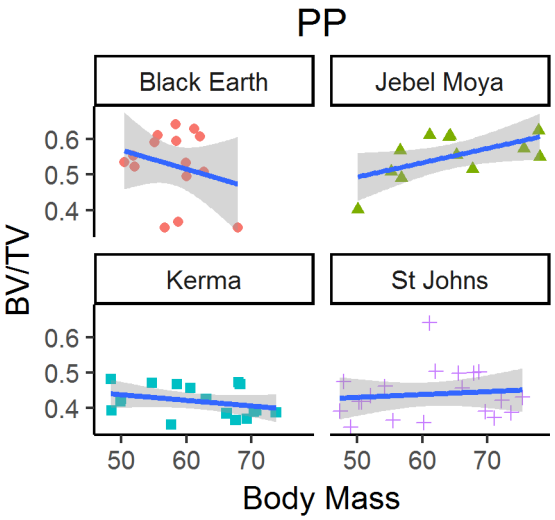
PP
Black Earth
Jebel Moya
Kerma
St Johns
BV/TV
0.6
0.5
0.4
50
60
70
Body Mass

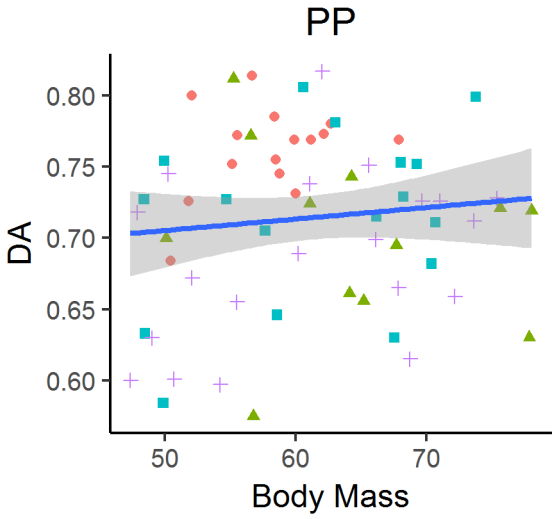
PP
DA
0.80
0.75
0.70
0.65
0.60
50
60
70
Body Mass

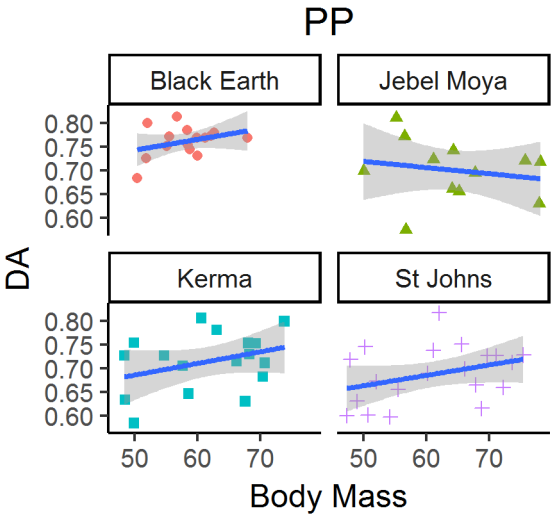
PP
Black Earth
Jebel Moya
Kerma
St Johns
DA
0.80
0.75
0.70
0.65
0.60
50
60
70
Body Mass

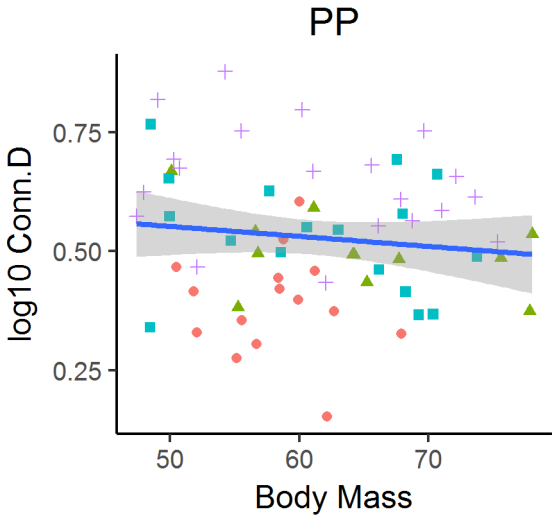
PP
log10 Conn.D
0.75
0.50
0.25
50
60
70
Body Mass

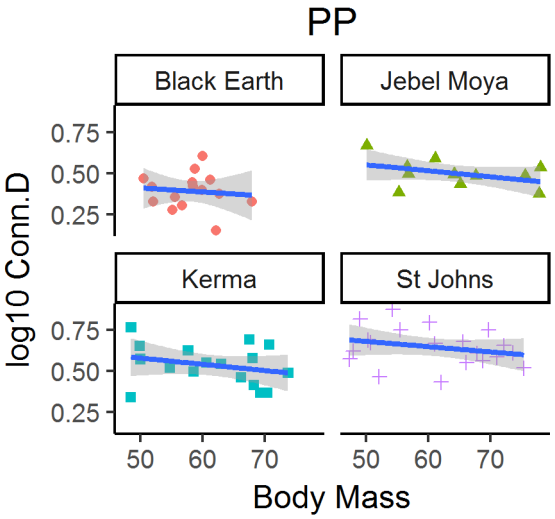
PP
Black Earth
Jebel Moya
Kerma
St Johns
log10 Conn.D
0.75
0.50
0.25
50
60
70
Body Mass

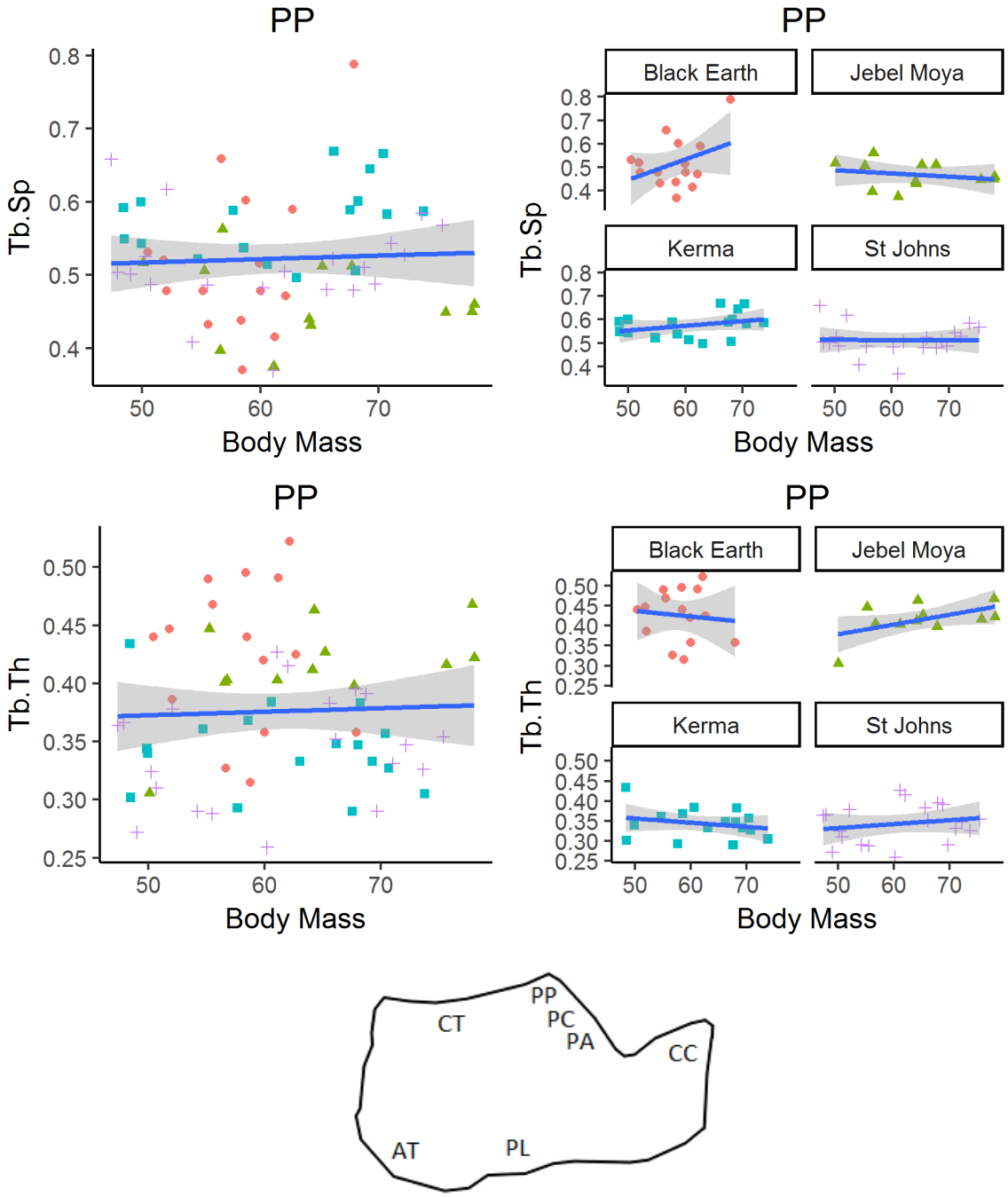

Figure 4.1.1. Plots of OLS regressions between body mass and trabecular properties in pooled and individual populations in the calcaneus.

Talus

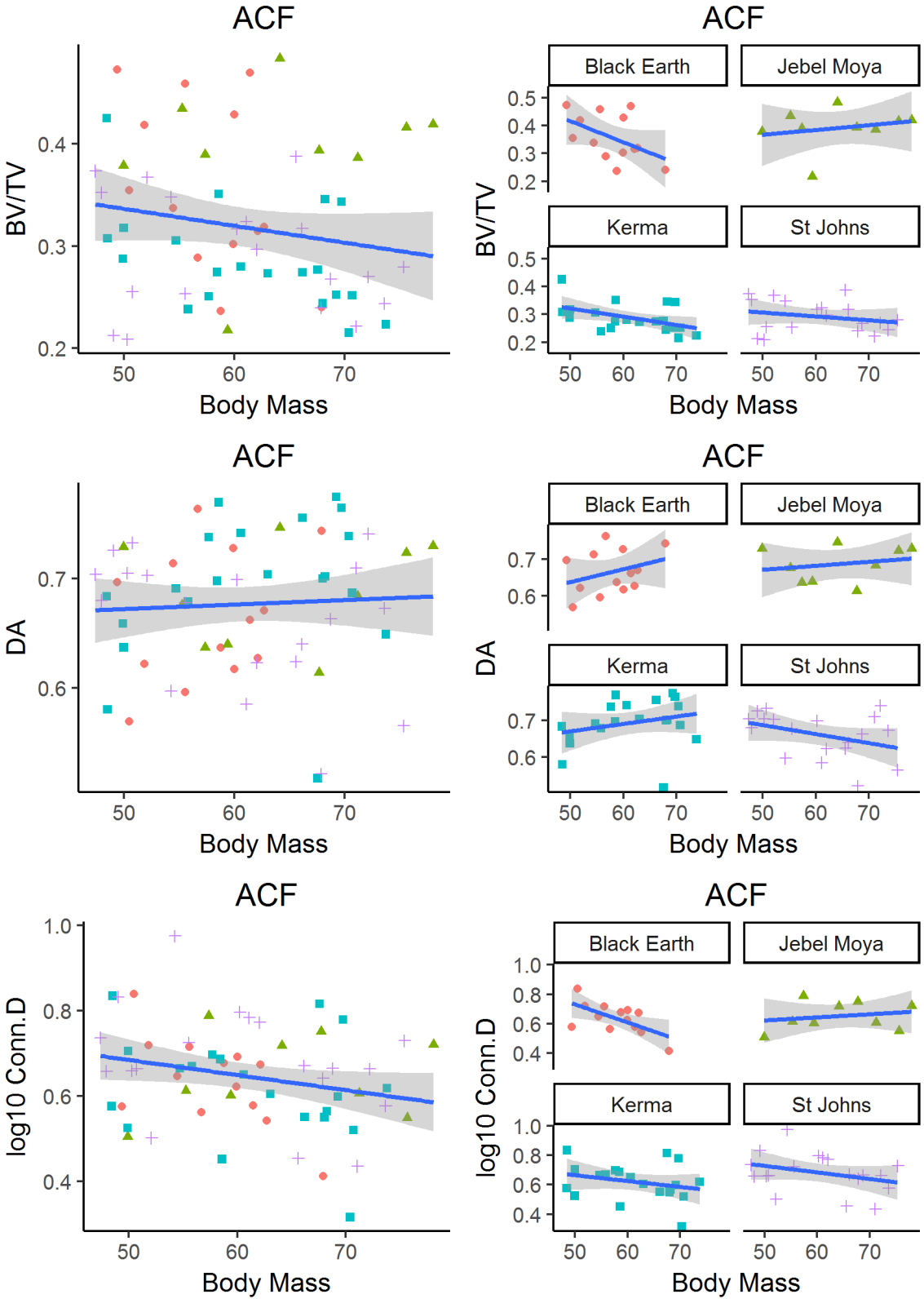
ACF
BV/TV
Body Mass
Black Earth
Jebel Moya
Kerma
St Johns
ACF
DA
Body Mass
ACF
log10 Conn.D
Body Mass

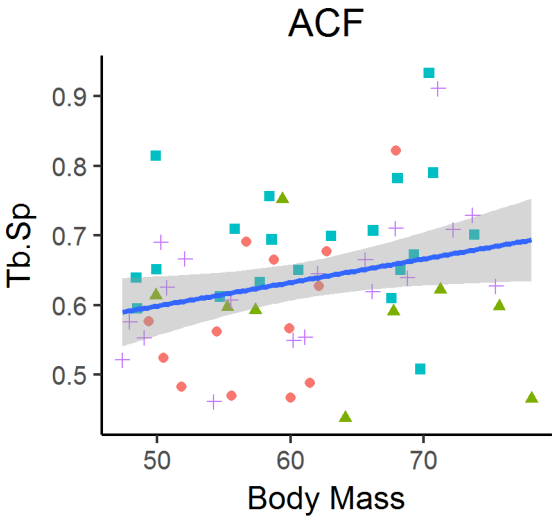
ACF
Tb.Sp
0.9
0.8
0.7
0.6
0.5
50
60
70
Body Mass

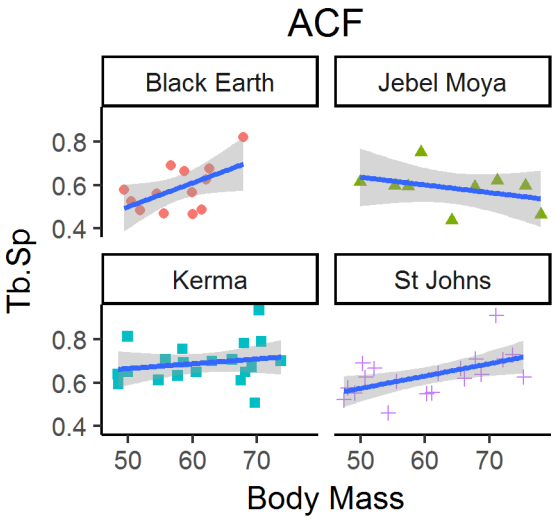
ACF
Black Earth
Jebel Moya
Kerma
St Johns
Tb.Sp
0.8
0.6
0.4
50
60
70
Body Mass

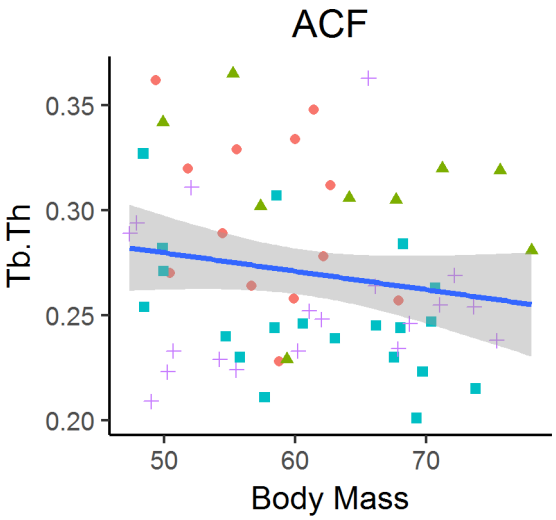
ACF
Tb.Th
0.35
0.30
0.25
0.20
50
60
70
Body Mass

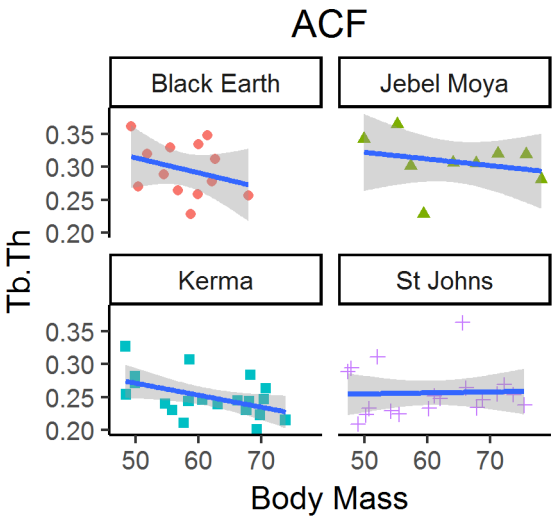
ACF
Black Earth
Jebel Moya
Kerma
St Johns
Tb.Th
0.35
0.30
0.25
0.20
50
60
70
Body Mass

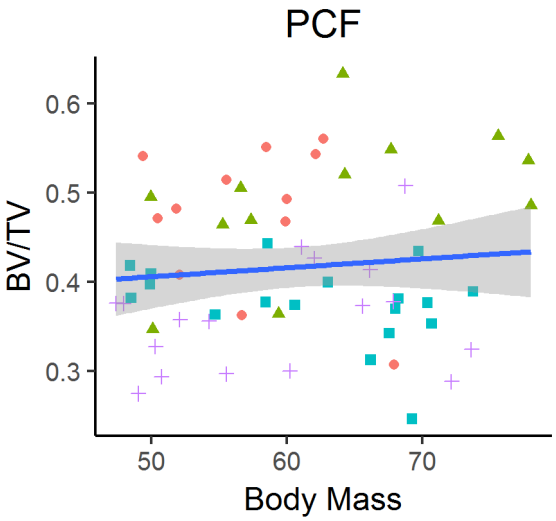
PCF
BV/TV
0.6
0.5
0.4
0.3
50
60
70
Body Mass

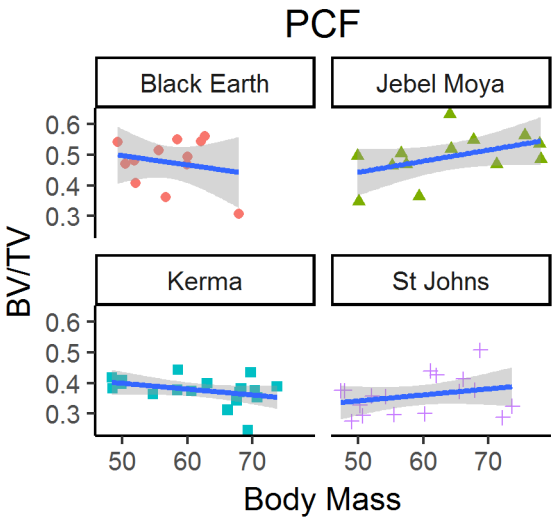
PCF
Black Earth
Jebel Moya
Kerma
St Johns
BV/TV
0.6
0.5
0.4
0.3
50
60
70
Body Mass

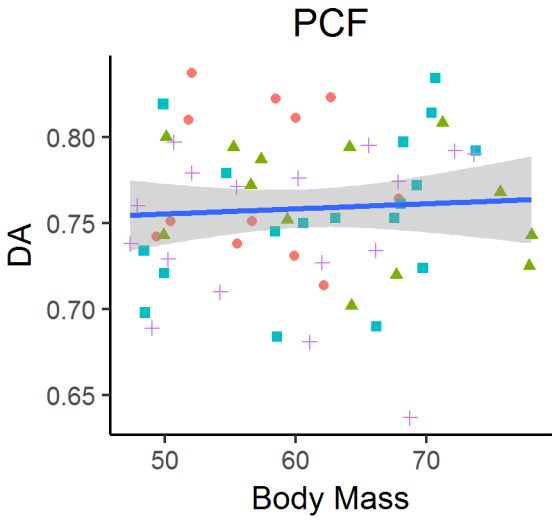
PCF
DA
0.80
0.75
0.70
0.65
50
60
70
Body Mass

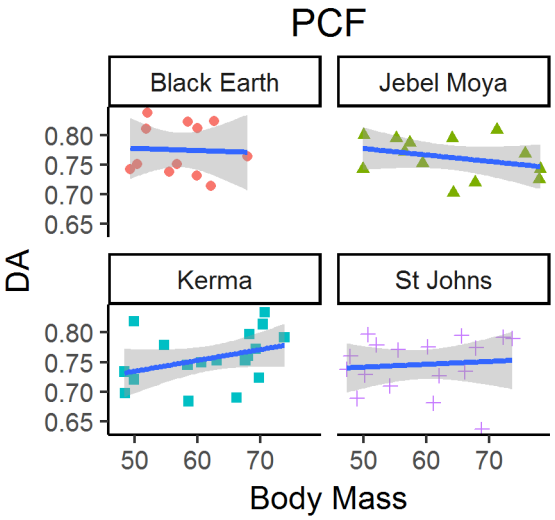
PCF
Black Earth
Jebel Moya
Kerma
St Johns
DA
0.80
0.75
0.70
0.65
50
60
70
Body Mass

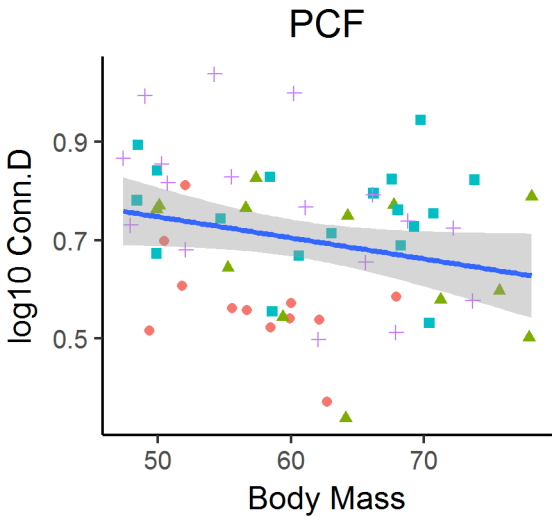
PCF
log10 Conn.D
0.9
0.7
0.5
50
60
70
Body Mass

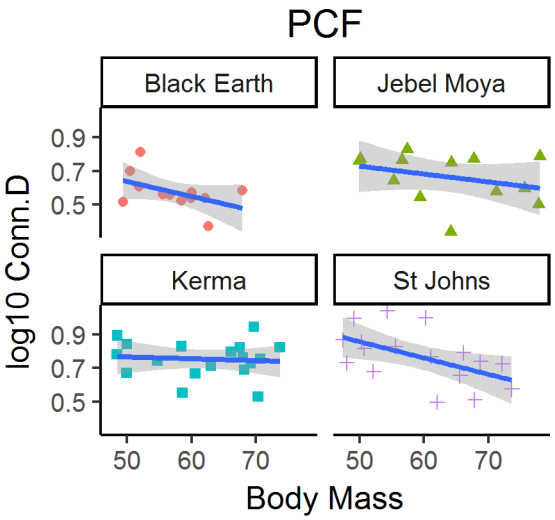
PCF
Black Earth
Jebel Moya
Kerma
St Johns
log10 Conn.D
0.9
0.7
0.5
50
60
70
Body Mass

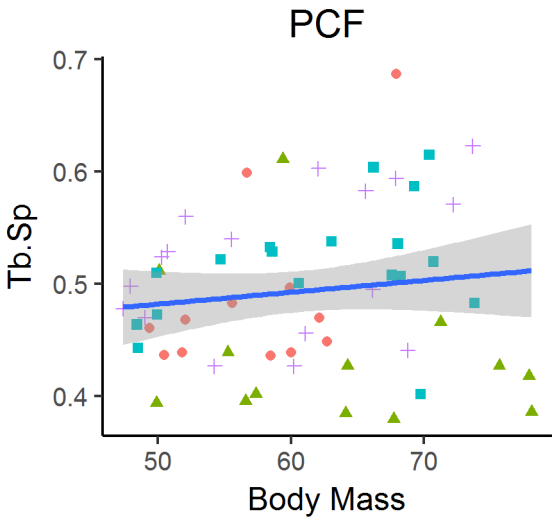
PCF
Tb.Sp
0.7
0.6
0.5
0.4
50
60
70
Body Mass

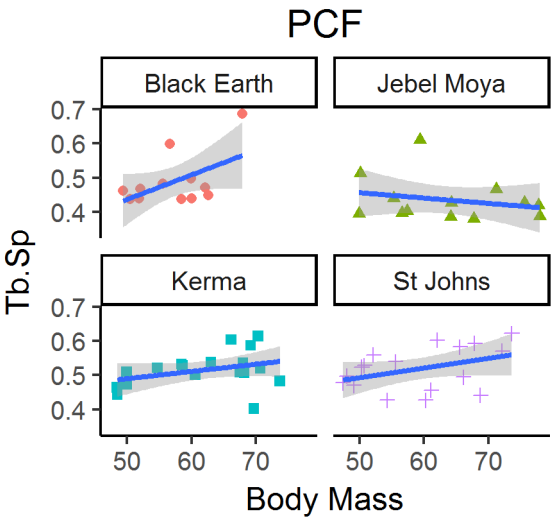
PCF
Black Earth
Jebel Moya
Kerma
St Johns
Tb.Sp
0.7
0.6
0.5
0.4
50
60
70
Body Mass

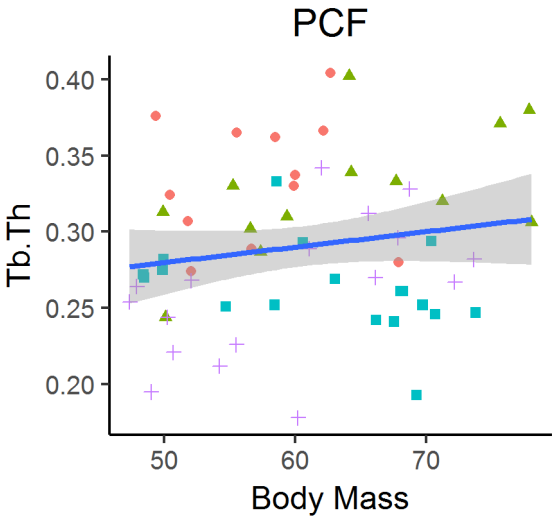
PCF
Tb.Th
0.40
0.35
0.30
0.25
0.20
50
60
70
Body Mass

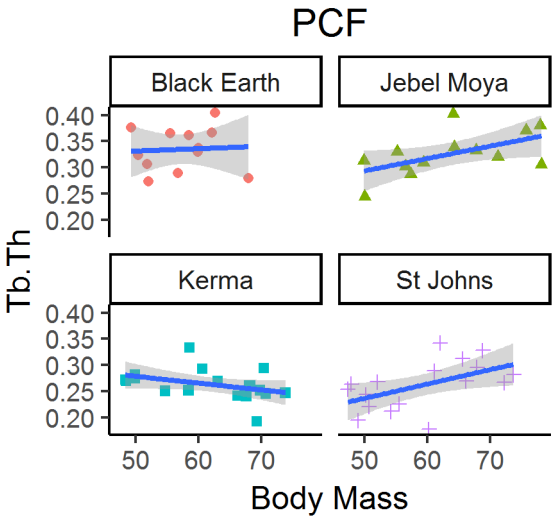
PCF
Black Earth
Jebel Moya
Kerma
St Johns
Tb.Th
0.40
0.35
0.30
0.25
0.20
50
60
70
Body Mass

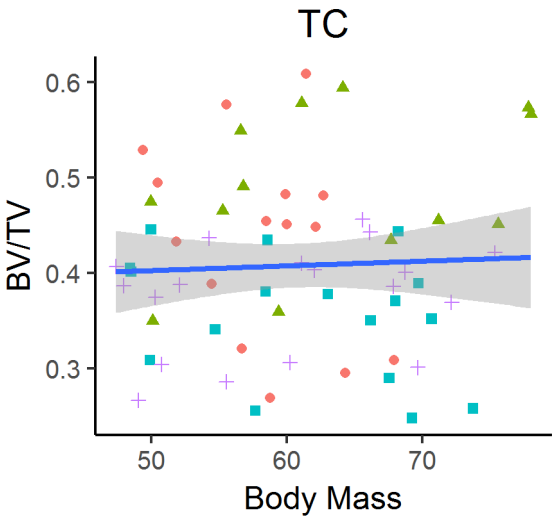
TC
BV/TV
0.6
0.5
0.4
0.3
50
60
70
Body Mass

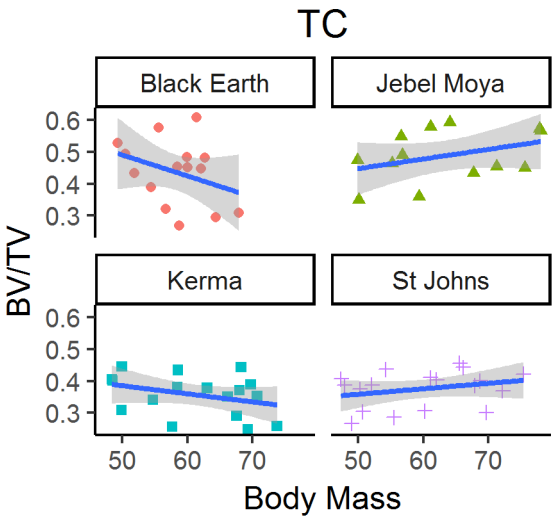
TC
Black Earth
Jebel Moya
Kerma
St Johns
BV/TV
0.6
0.5
0.4
0.3
50
60
70
Body Mass

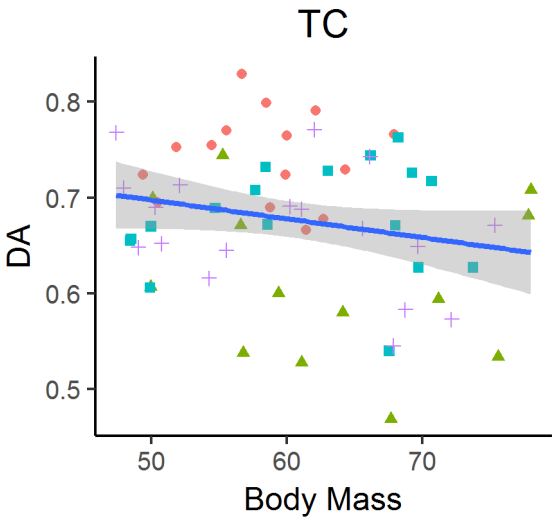
TC
DA
0.8
0.7
0.6
0.5
50
60
70
Body Mass

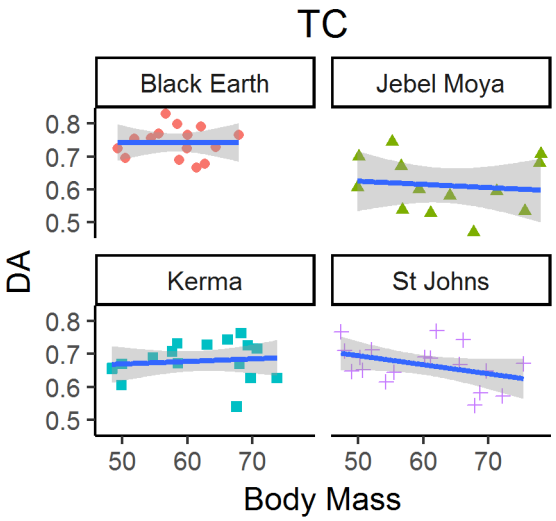
TC
Black Earth
Jebel Moya
Kerma
St Johns
DA
0.8
0.7
0.6
0.5
50
60
70
Body Mass

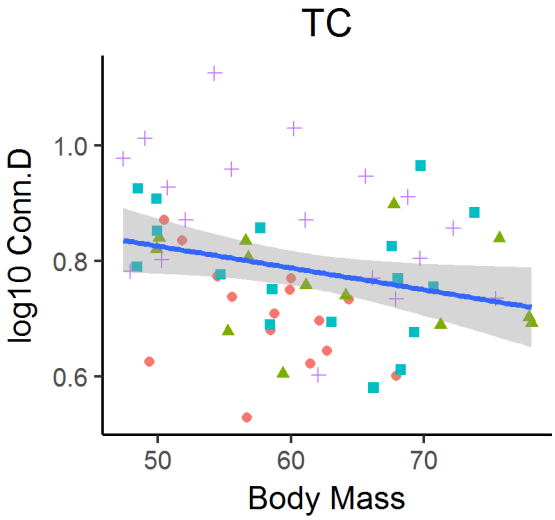
TC
log10 Conn.D
1.0
0.8
0.6
50
60
70
Body Mass

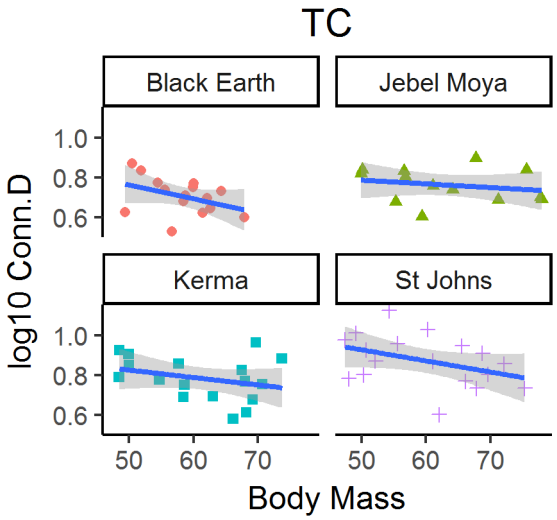
TC
Black Earth
Jebel Moya
Kerma
St Johns
log10 Conn.D
1.0
0.8
0.6
50
60
70
Body Mass

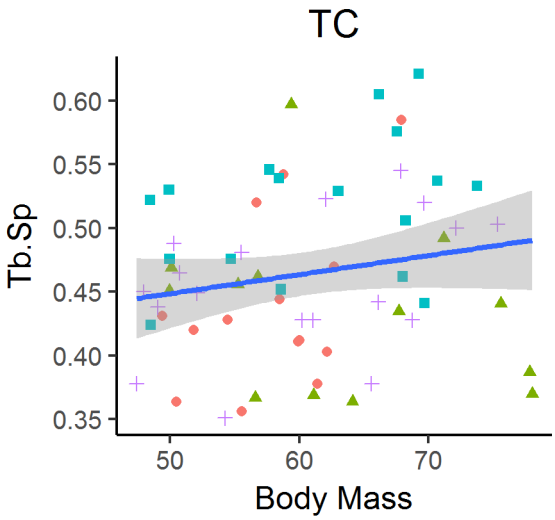
TC
Tb.Sp
0.60
0.55
0.50
0.45
0.40
0.35
50
60
70
Body Mass

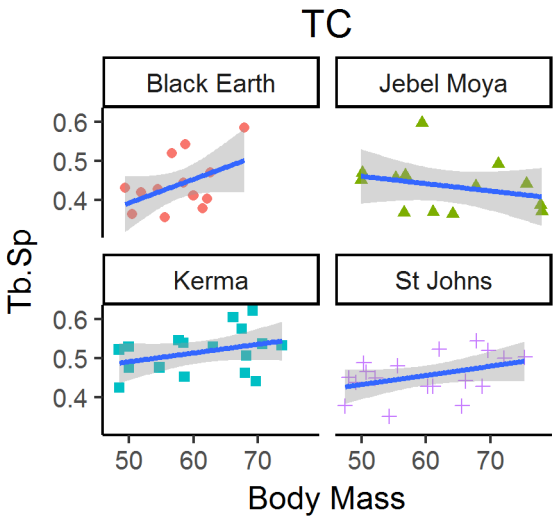
TC
Black Earth
Jebel Moya
Kerma
St Johns
Tb.Sp
0.6
0.5
0.4
50
60
70
Body Mass

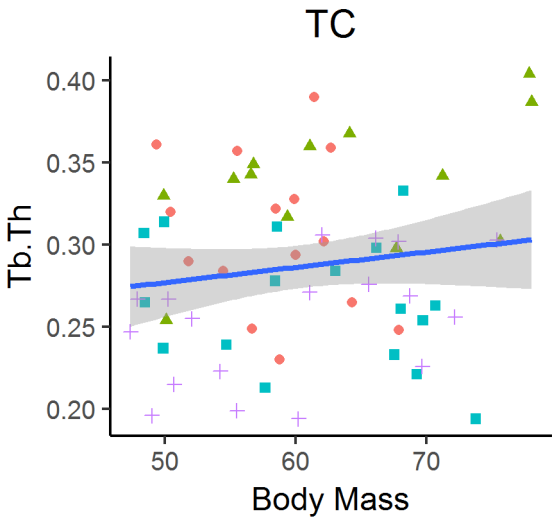
TC
Tb.Th
0.40
0.35
0.30
0.25
0.20
50
60
70
Body Mass

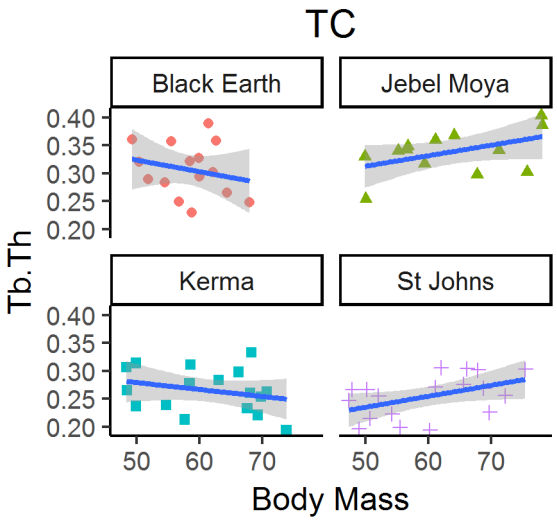
TC
Black Earth
Jebel Moya
Kerma
St Johns
Tb.Th
0.40
0.35
0.30
0.25
0.20
50
60
70
Body Mass

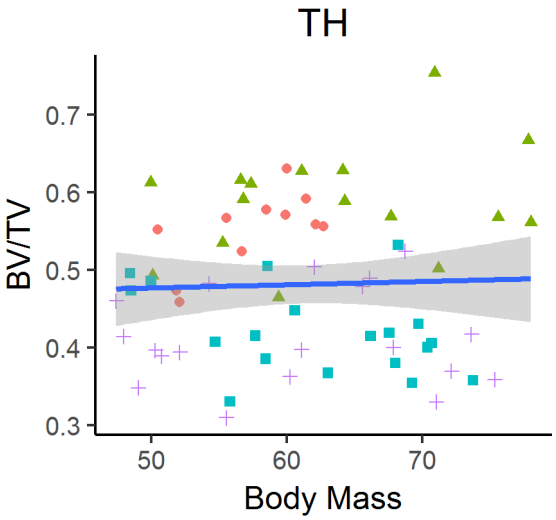
TH
BV/TV
0.7
0.6
0.5
0.4
0.3
50
60
70
Body Mass

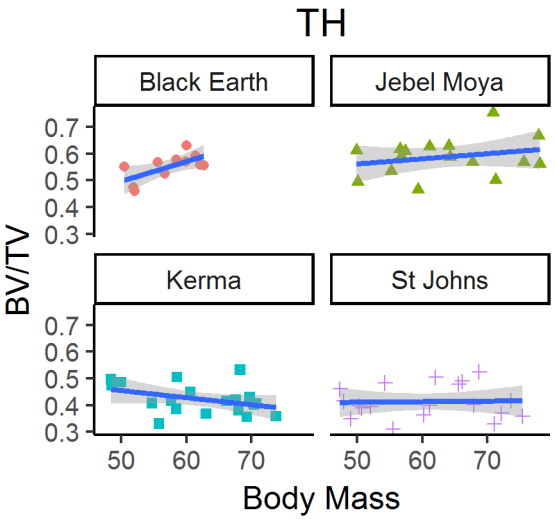
TH
Black Earth
Jebel Moya
Kerma
St Johns
BV/TV
0.7
0.6
0.5
0.4
0.3
50
60
70
Body Mass

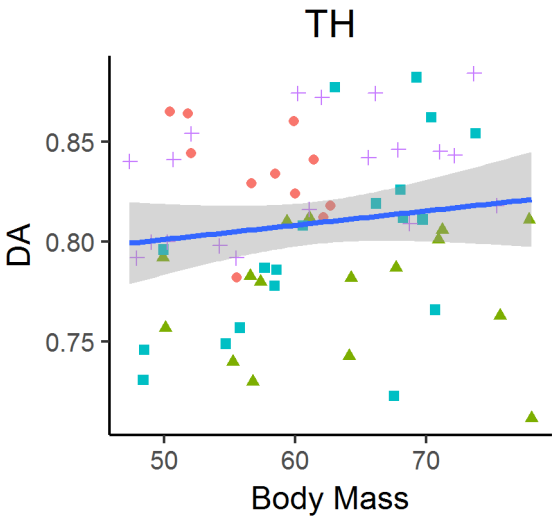
TH
DA
0.85
0.80
0.75
50
60
70
Body Mass

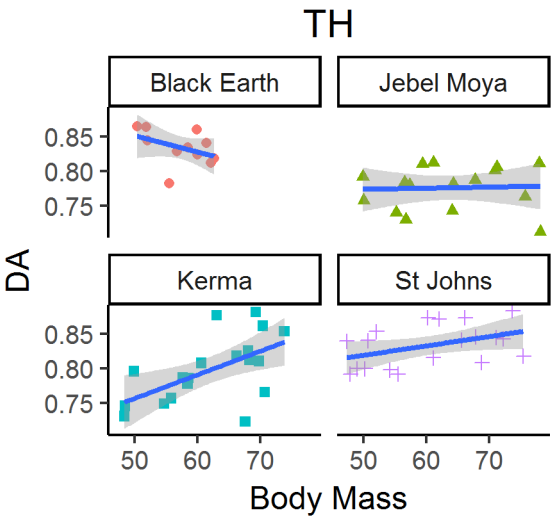
TH
Black Earth
Jebel Moya
Kerma
St Johns
DA
0.85
0.80
0.75
50
60
70
Body Mass

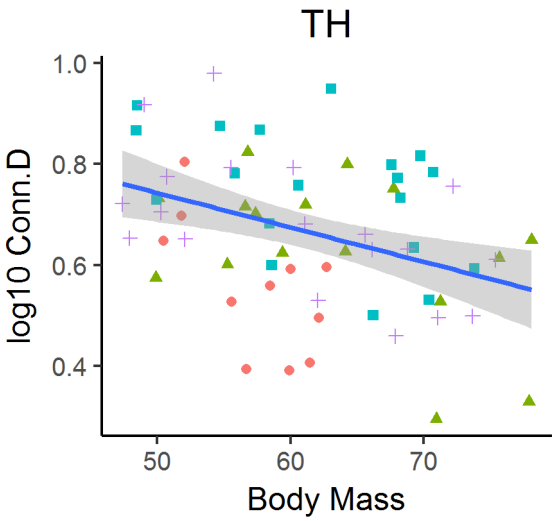
TH
log10 Conn.D
1.0
0.8
0.6
0.4
50
60
70
Body Mass

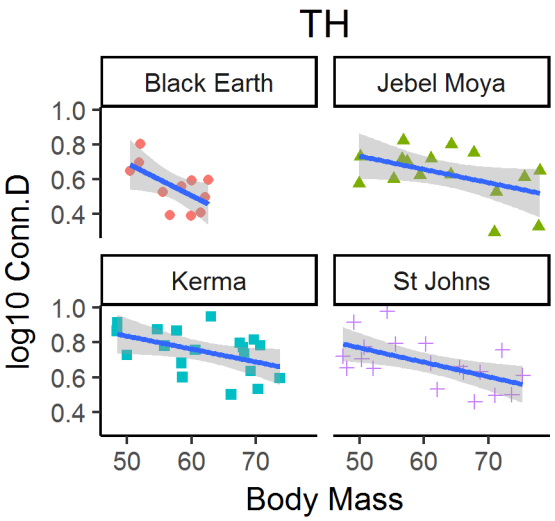
TH
Black Earth
Jebel Moya
Kerma
St Johns
log10 Conn.D
1.0
0.8
0.6
0.4
50
60
70
Body Mass

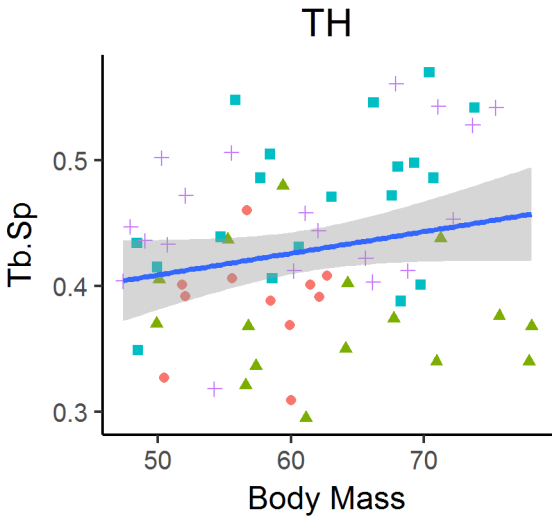
TH
Tb.Sp
0.5
0.4
0.3
50
60
70
Body Mass

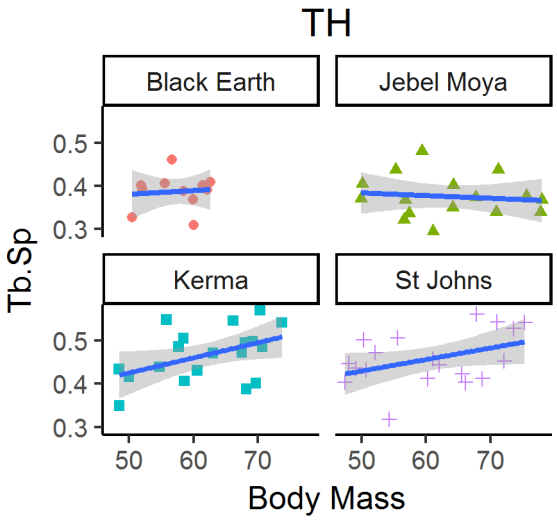
TH
Black Earth
Jebel Moya
Kerma
St Johns
Tb.Sp
0.5
0.4
0.3
50
60
70
Body Mass

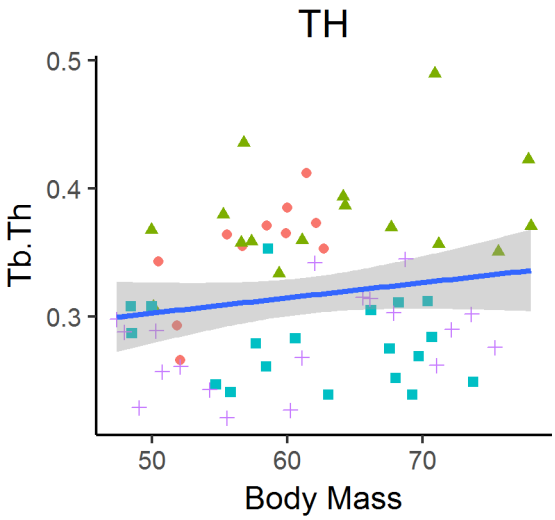
TH
Tb.Th
0.5
0.4
0.3
50
60
70
Body Mass

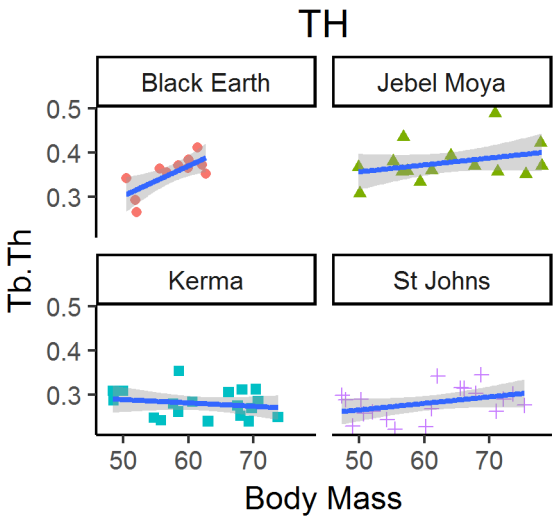
TH
Black Earth
Jebel Moya
Kerma
St Johns
Tb.Th
0.5
0.4
0.3
50
60
70
Body Mass

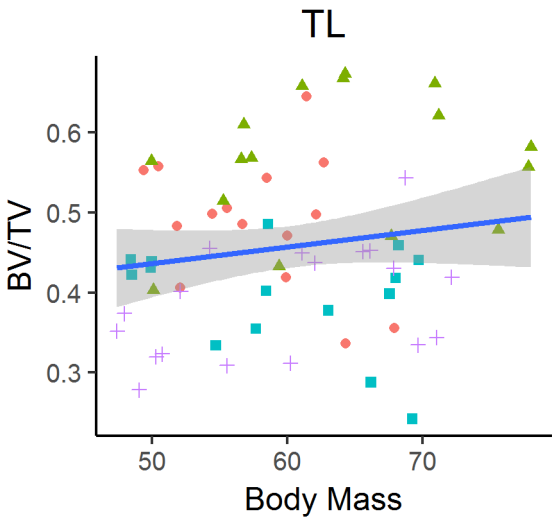
TL
BV/TV
0.6
0.5
0.4
0.3
50
60
70
Body Mass

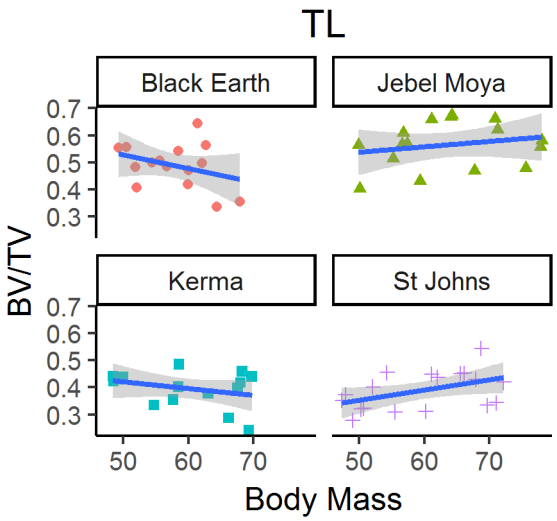
TL
Black Earth
Jebel Moya
Kerma
St Johns
BV/TV
0.7
0.6
0.5
0.4
0.3
50
60
70
Body Mass

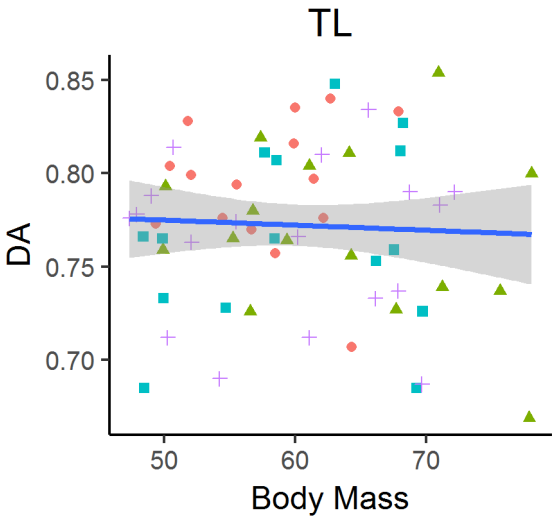
TL
DA
0.85
0.80
0.75
0.70
50
60
70
Body Mass

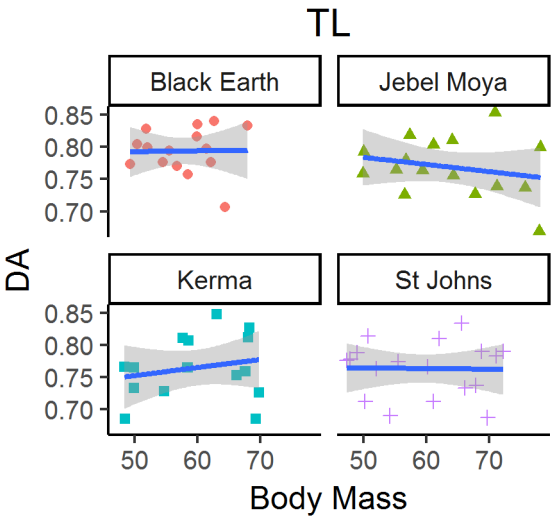
TL
Black Earth
Jebel Moya
Kerma
St Johns
DA
0.85
0.80
0.75
0.70
50
60
70
Body Mass

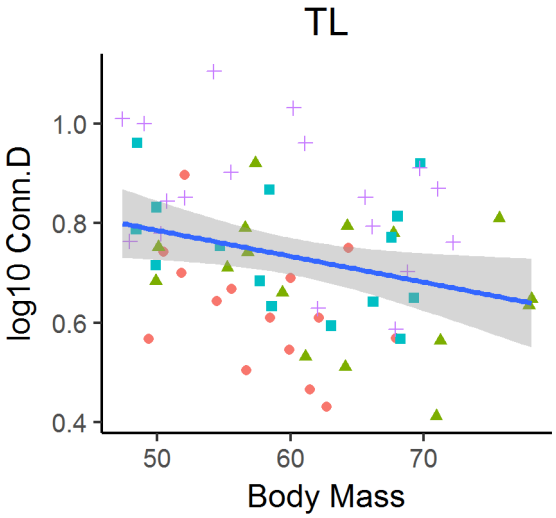
TL
log10 Conn.D
1.0
0.8
0.6
0.4
50
60
70
Body Mass

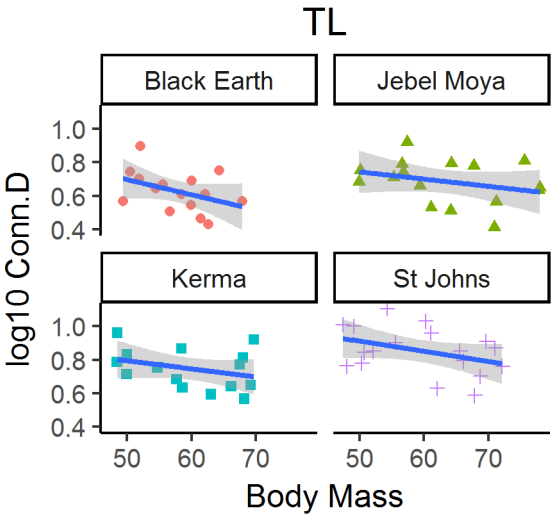
TL
Black Earth
Jebel Moya
Kerma
St Johns
log10 Conn.D
1.0
0.8
0.6
0.4
50
60
70
Body Mass

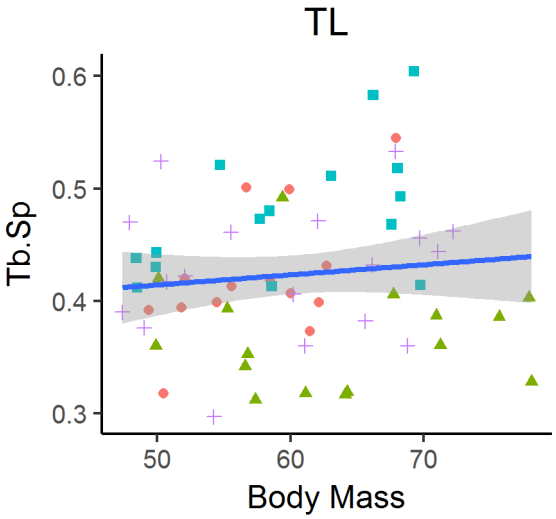
TL
Tb.Sp
0.6
0.5
0.4
0.3
50
60
70
Body Mass

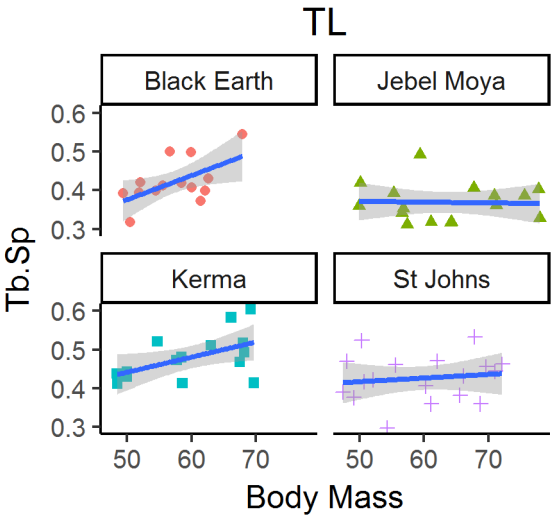
TL
Black Earth
Jebel Moya
Kerma
St Johns
Tb.Sp
0.6
0.5
0.4
0.3
50
60
70
Body Mass

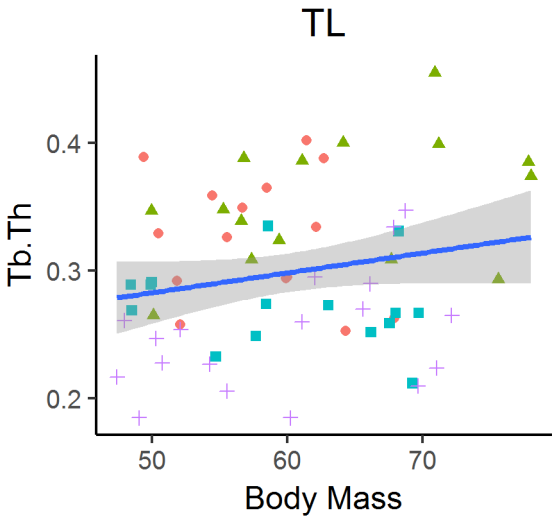
TL
Tb.Th
0.4
0.3
0.2
50
60
70
Body Mass

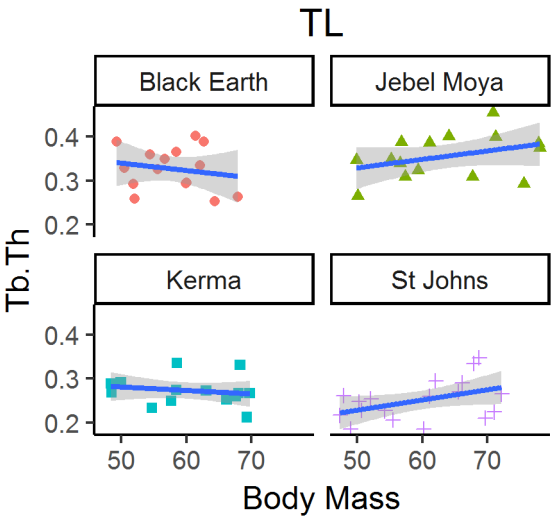
TL
Black Earth
Jebel Moya
Kerma
St Johns
Tb.Th
0.4
0.3
0.2
50
60
70
Body Mass

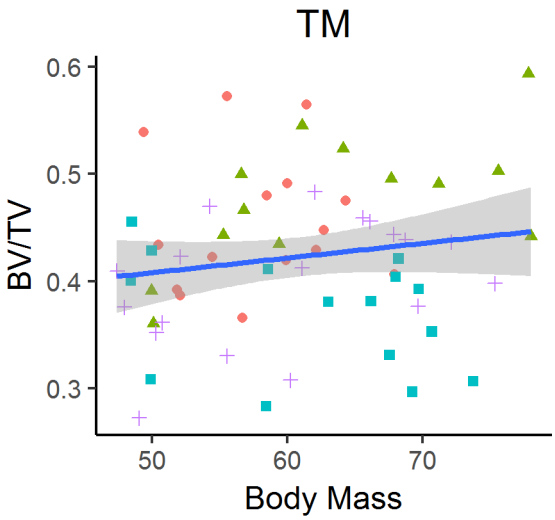
TM
BV/TV
0.6
0.5
0.4
0.3
50
60
70
Body Mass

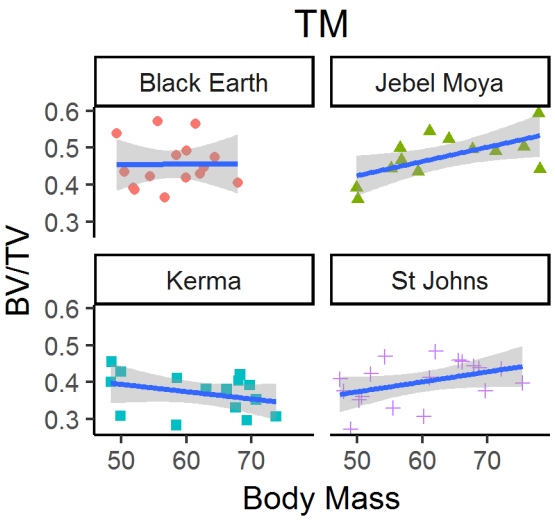
TM
Black Earth
Jebel Moya
Kerma
St Johns
BV/TV
0.6
0.5
0.4
0.3
50
60
70
Body Mass

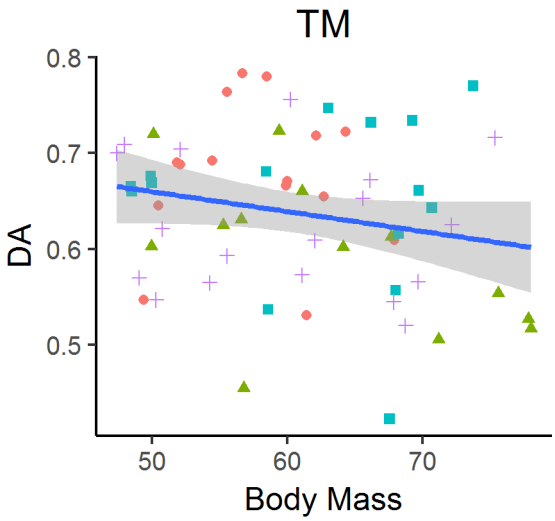
TM
DA
0.8
0.7
0.6
0.5
50
60
70
Body Mass

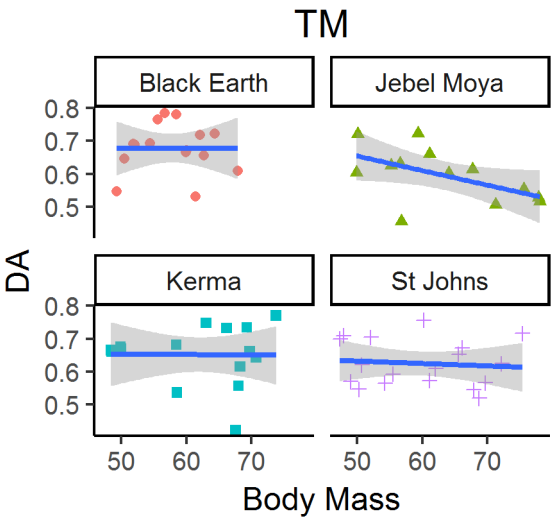
TM
Black Earth
Jebel Moya
Kerma
St Johns
DA
0.8
0.7
0.6
0.5
50
60
70
Body Mass

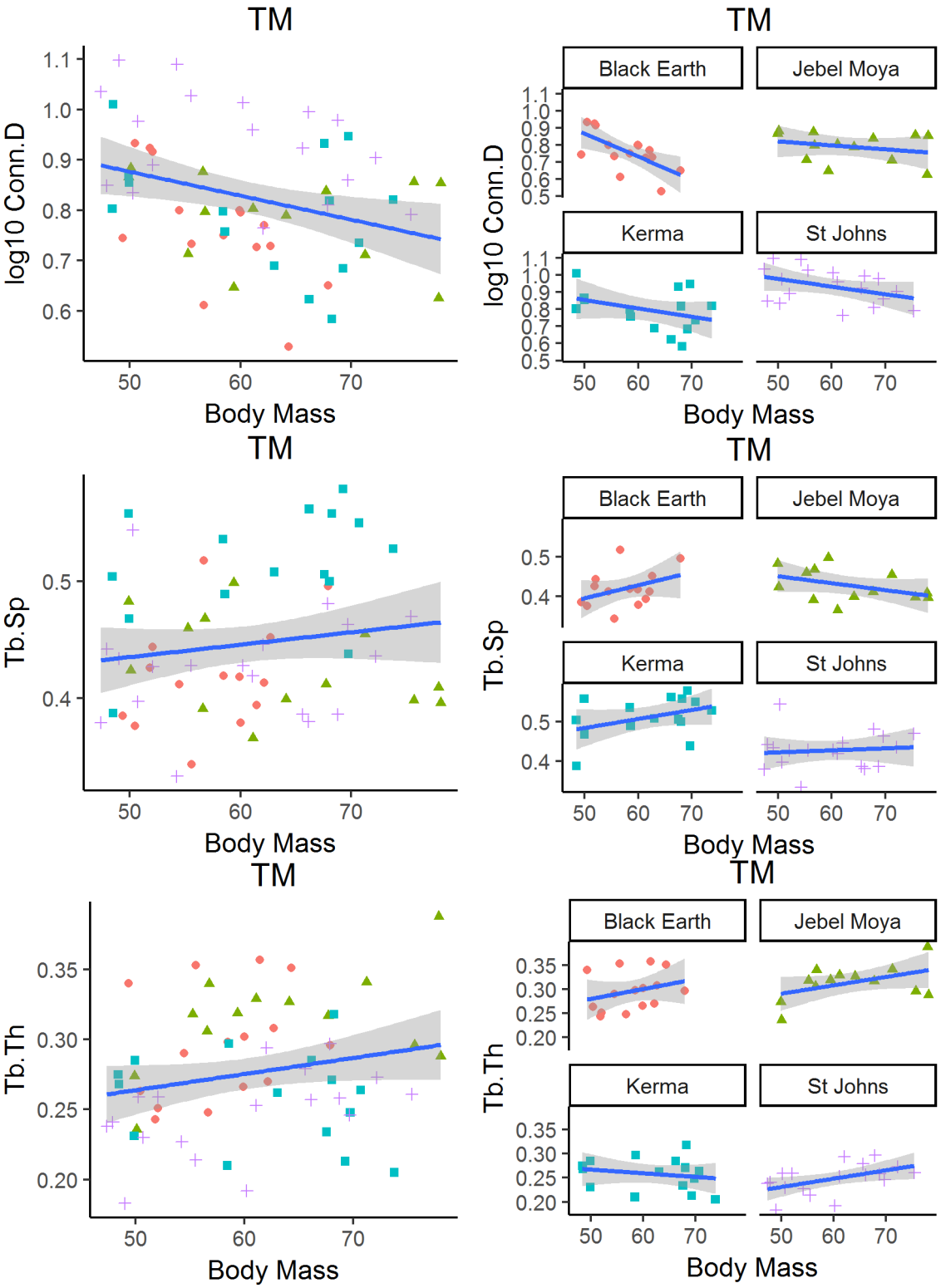

Figure 4.1.2. Plots of OLS regressions between body mass and trabecular properties in pooled and individual populations in the talus.

First metatarsal

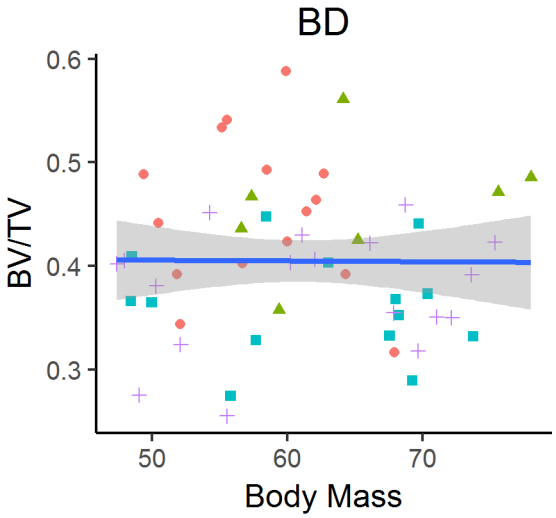

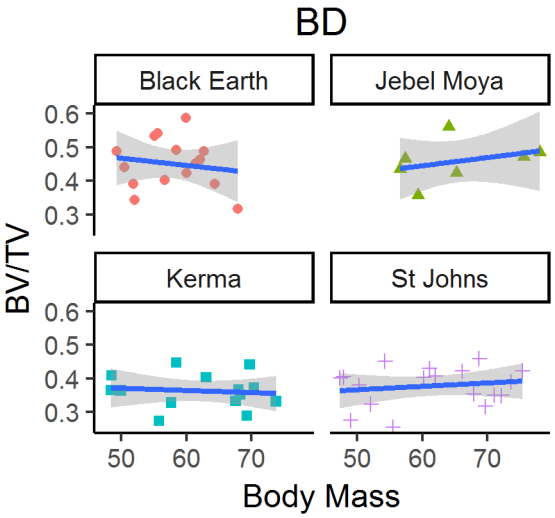

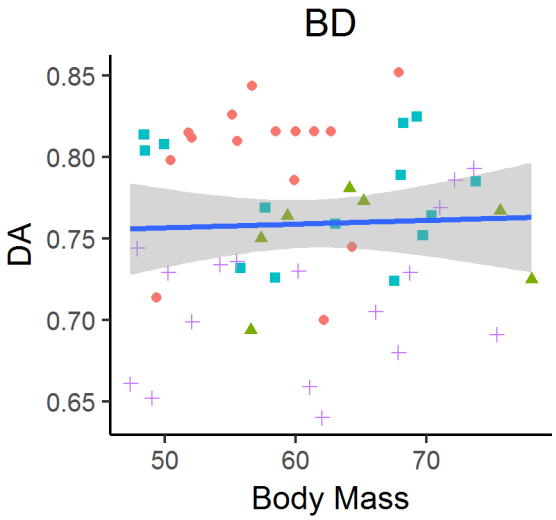

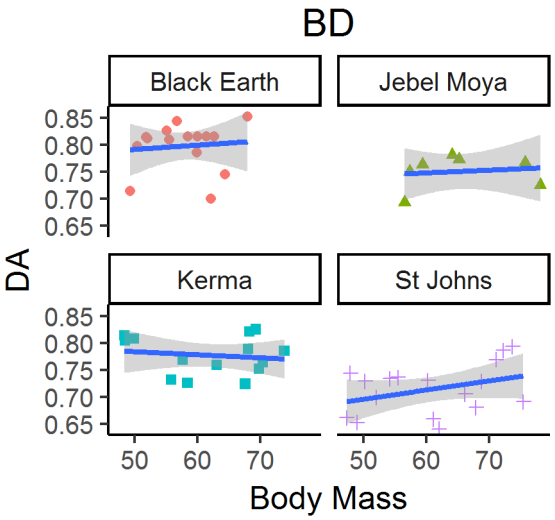

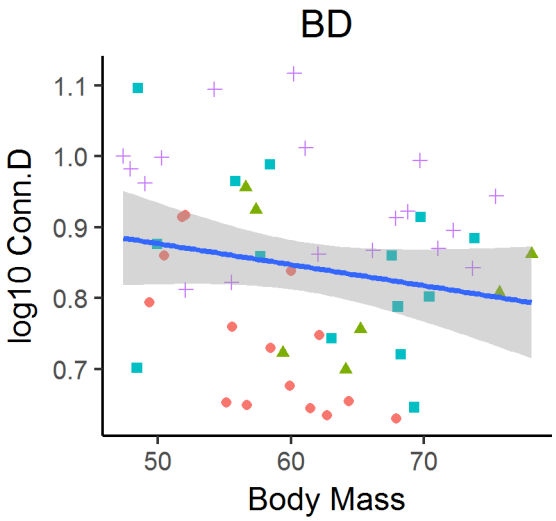

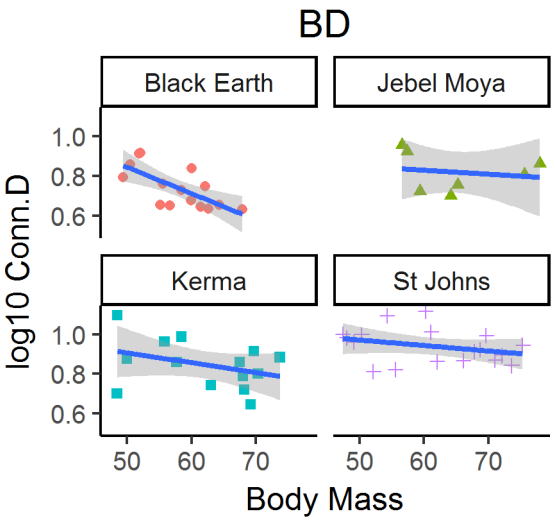

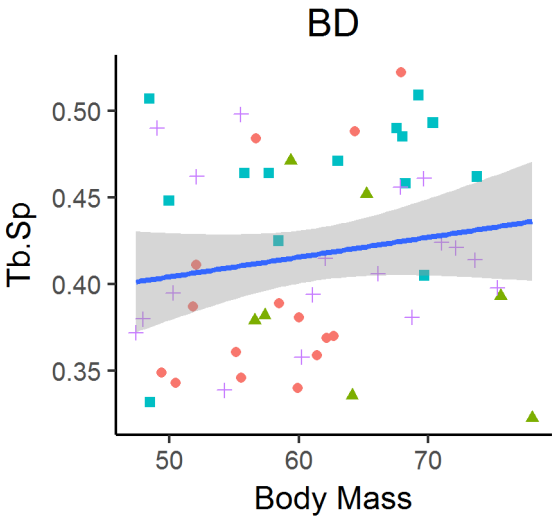
BD
Tb.Sp
0.50
0.45
0.40
0.35
50
60
70
Body Mass

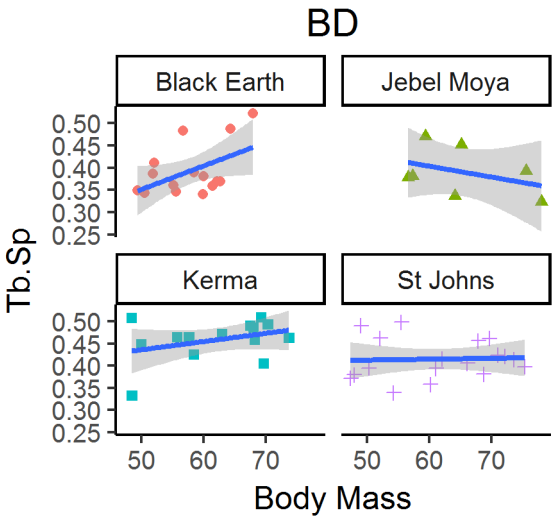
BD
Black Earth
Jebel Moya
Kerma
St Johns
Tb.Sp
0.50
0.45
0.40
0.35
0.30
0.25
50
60
70
Body Mass

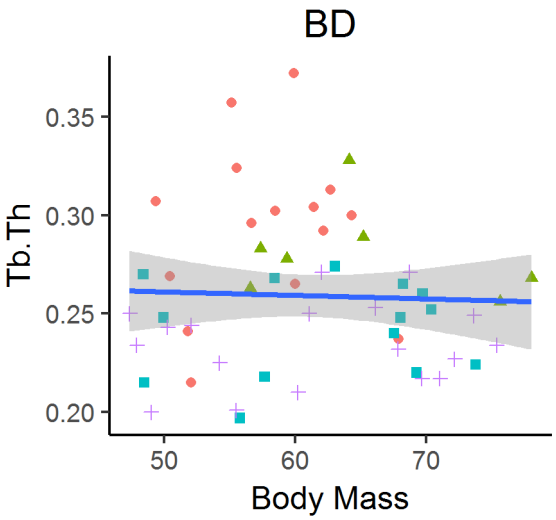
BD
Tb.Th
0.35
0.30
0.25
0.20
50
60
70
Body Mass

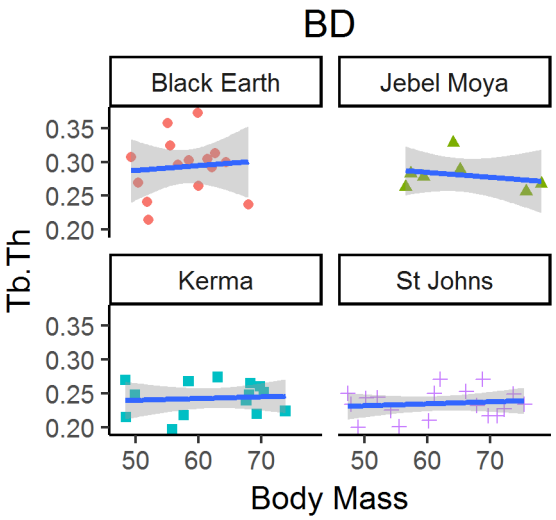
BD
Black Earth
Jebel Moya
Kerma
St Johns
Tb.Th
0.35
0.30
0.25
0.20
50
60
70
Body Mass

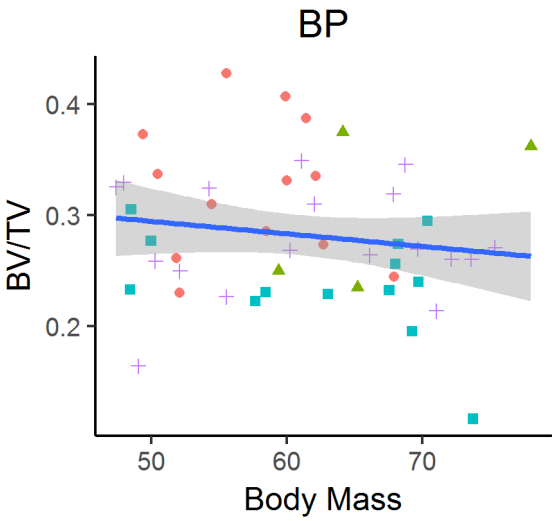
BP
BV/TV
0.4
0.3
0.2
50
60
70
Body Mass

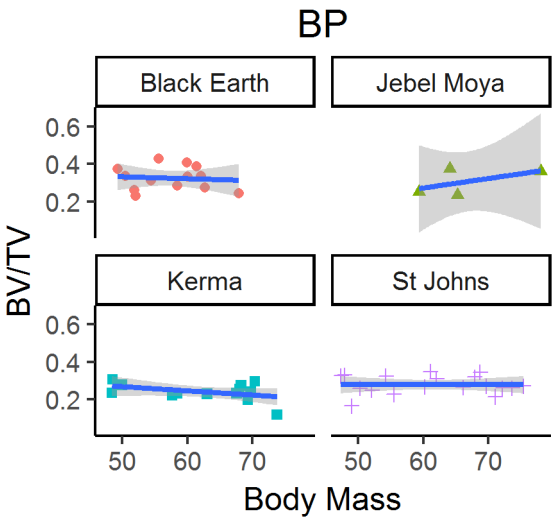
BP
Black Earth
Jebel Moya
Kerma
St Johns
BV/TV
0.6
0.4
0.2
50
60
70
Body Mass

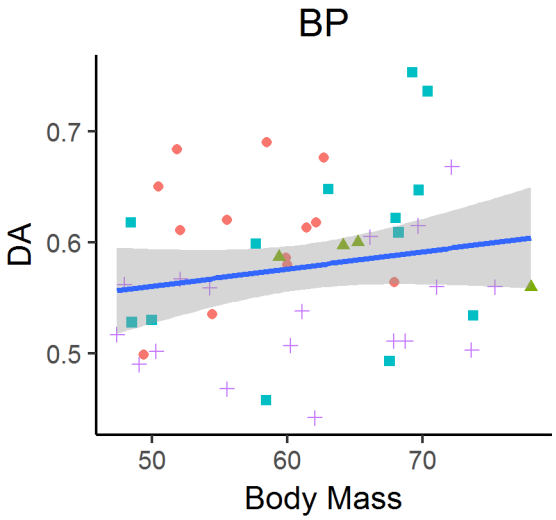
BP
DA
0.7
0.6
0.5
50
60
70
Body Mass

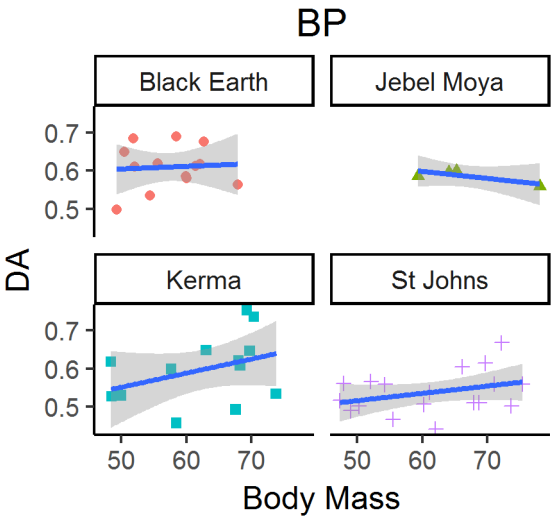
BP
Black Earth
Jebel Moya
Kerma
St Johns
DA
0.7
0.6
0.5
50
60
70
Body Mass

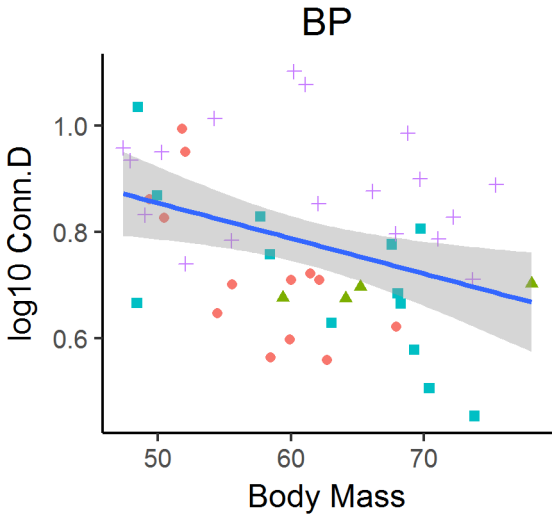
BP
log10 Conn.D
1.0
0.8
0.6
50
60
70
Body Mass

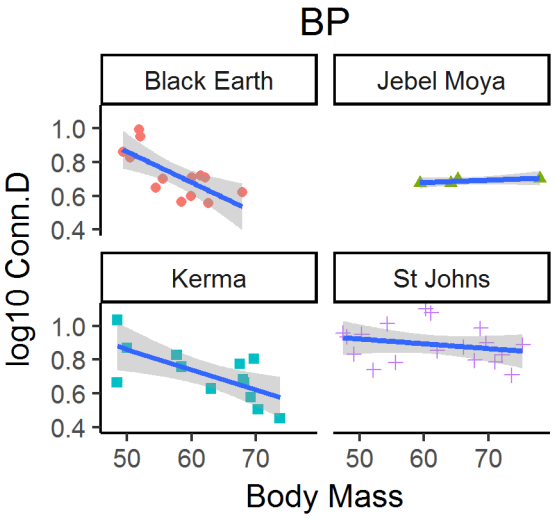
BP
Black Earth
Jebel Moya
Kerma
St Johns
log10 Conn.D
1.0
0.8
0.6
0.4
50
60
70
Body Mass

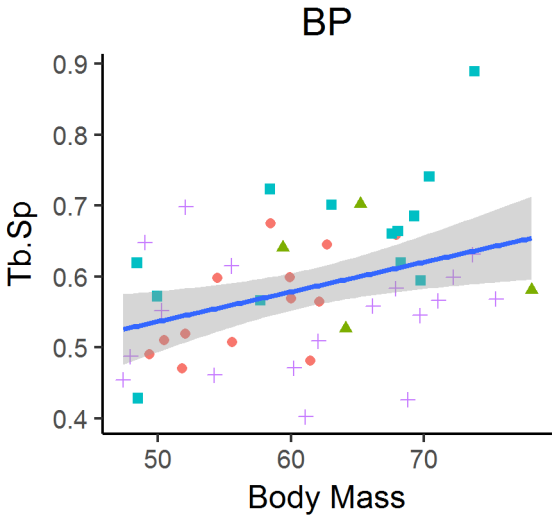
BP
Tb.Sp
0.9
0.8
0.7
0.6
0.5
0.4
50
60
70
Body Mass

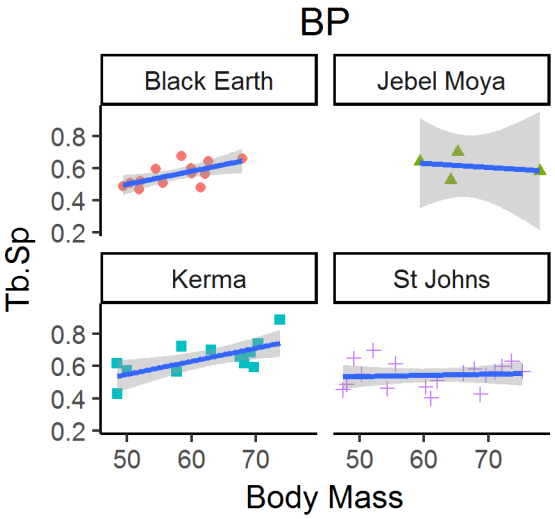
BP
Black Earth
Jebel Moya
Kerma
St Johns
Tb.Sp
0.8
0.6
0.4
0.2
50
60
70
Body Mass

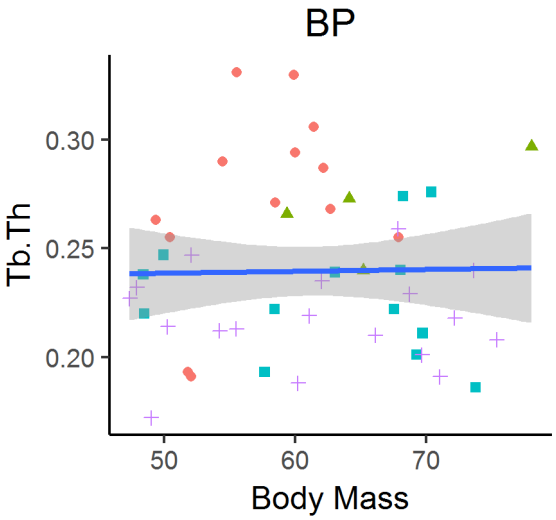
BP
Tb.Th
0.30
0.25
0.20
50
60
70
Body Mass

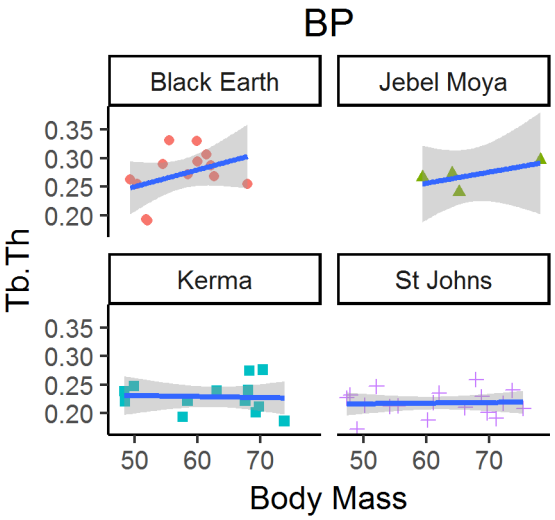
BP
Black Earth
Jebel Moya
Kerma
St Johns
Tb.Th
0.35
0.30
0.25
0.20
50
60
70
Body Mass

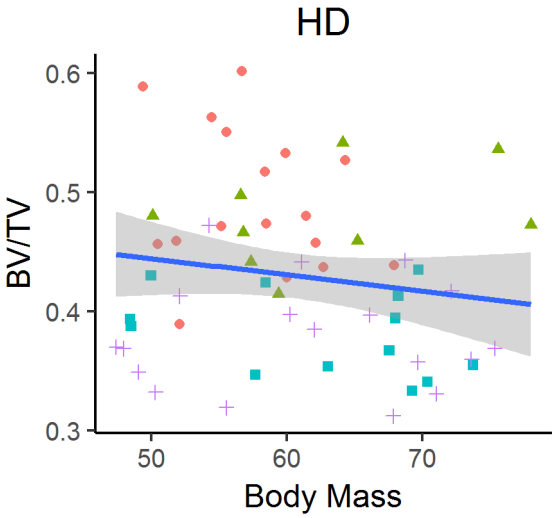
HD
BV/TV
0.6
0.5
0.4
0.3
50
60
70
Body Mass

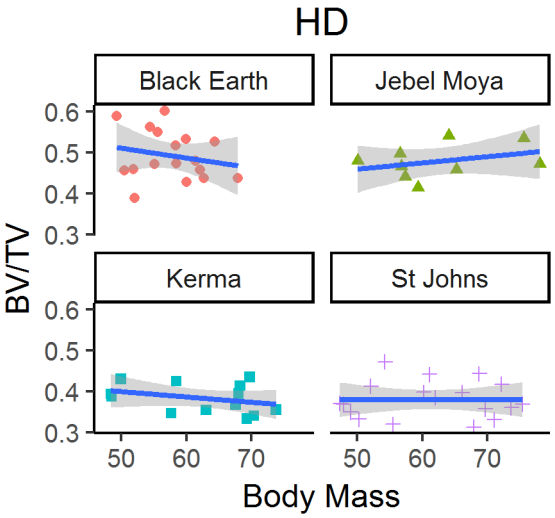
HD
Black Earth
Jebel Moya
Kerma
St Johns
BV/TV
0.6
0.5
0.4
0.3
50
60
70
Body Mass

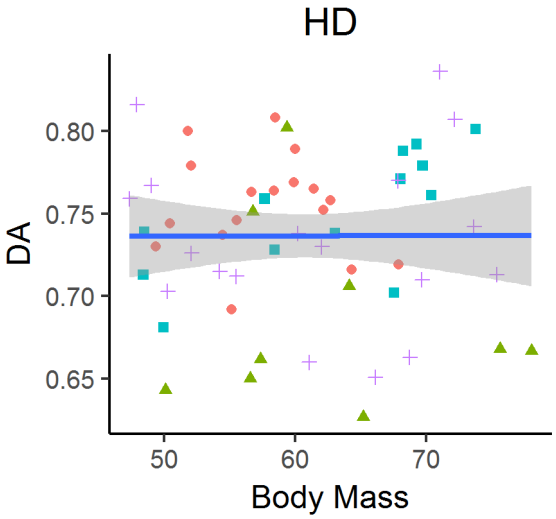
HD
DA
0.80
0.75
0.70
0.65
50
60
70
Body Mass

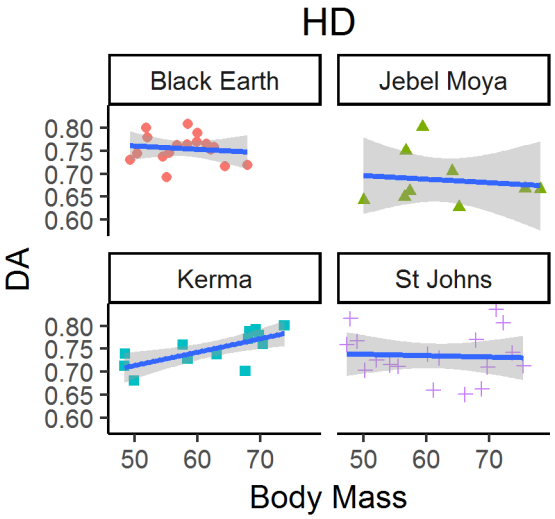
HD
Black Earth
Jebel Moya
Kerma
St Johns
DA
0.80
0.75
0.70
0.65
0.60
50
60
70
Body Mass

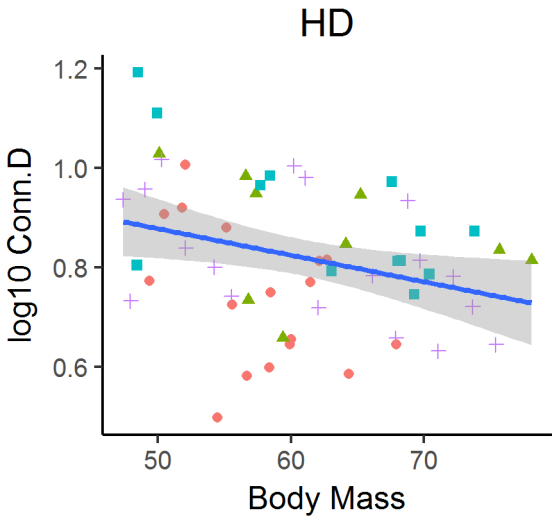
HD
log10 Conn.D
1.2
1.0
0.8
0.6
50
60
70
Body Mass

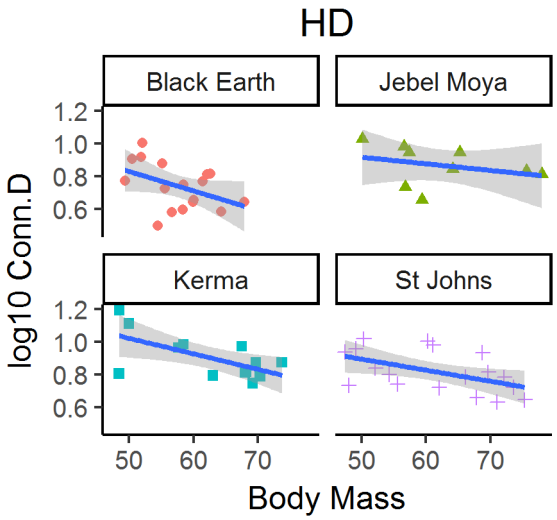
HD
Black Earth
Jebel Moya
Kerma
St Johns
log10 Conn.D
1.2
1.0
0.8
0.6
50
60
70
Body Mass

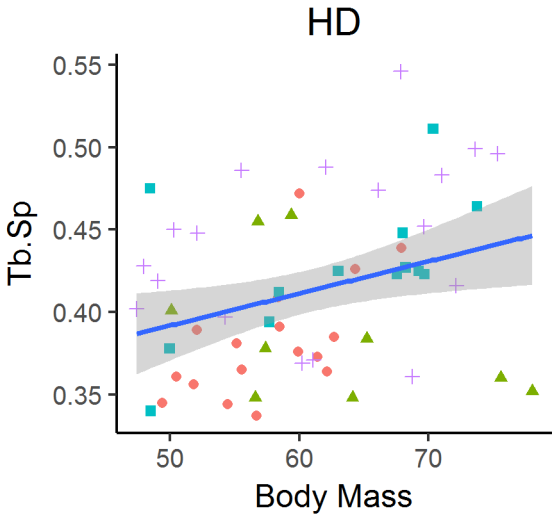
HD
Tb.Sp
0.55
0.50
0.45
0.40
0.35
50
60
70
Body Mass

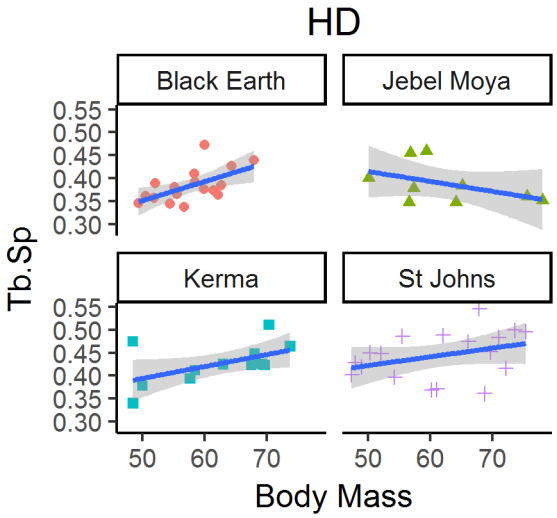
HD
Black Earth
Jebel Moya
Kerma
St Johns
Tb.Sp
0.55
0.50
0.45
0.40
0.35
0.30
50
60
70
Body Mass

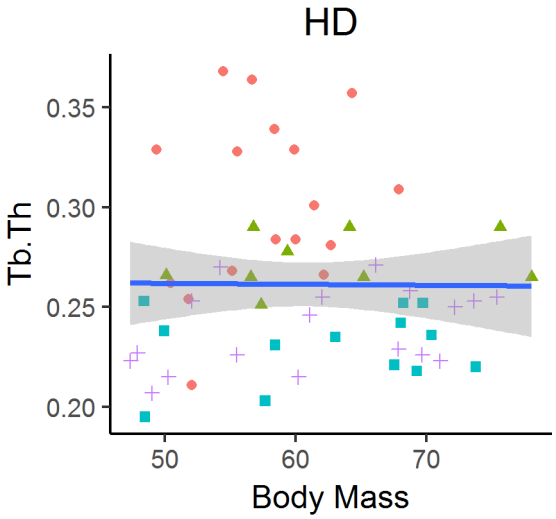
HD
Tb.Th
0.35
0.30
0.25
0.20
50
60
70
Body Mass

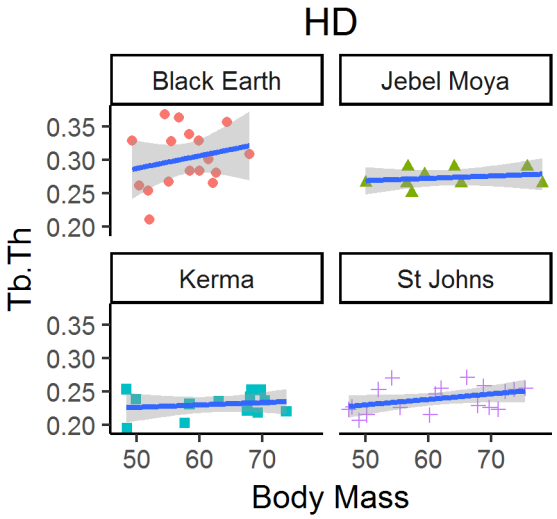
HD
Black Earth
Jebel Moya
Kerma
St Johns
Tb.Th
0.35
0.30
0.25
0.20
50
60
70
Body Mass

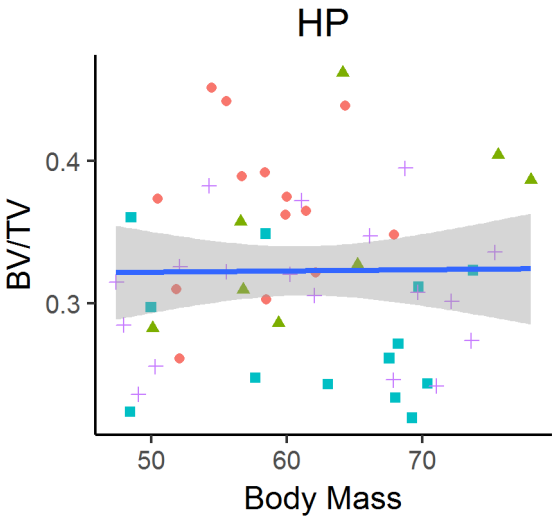
HP
BV/TV
0.4
0.3
50
60
70
Body Mass

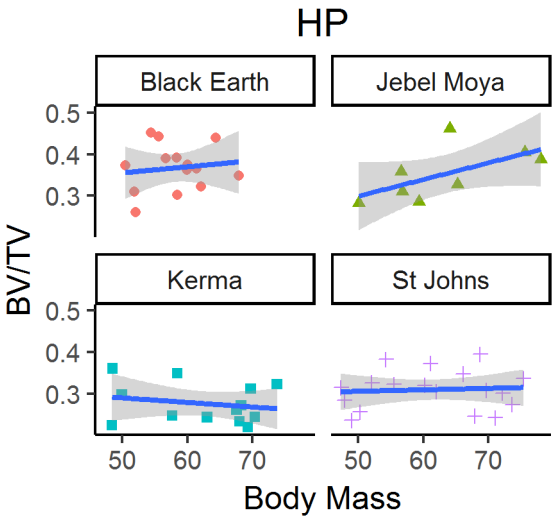
HP
Black Earth
Jebel Moya
Kerma
St Johns
BV/TV
0.5
0.4
0.3
50
60
70
Body Mass

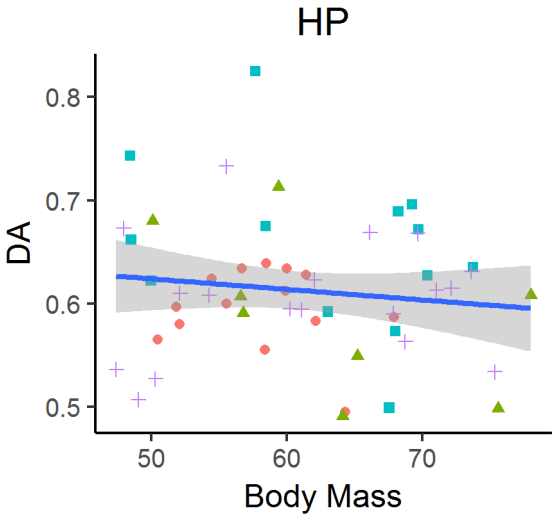
HP
DA
0.8
0.7
0.6
0.5
50
60
70
Body Mass

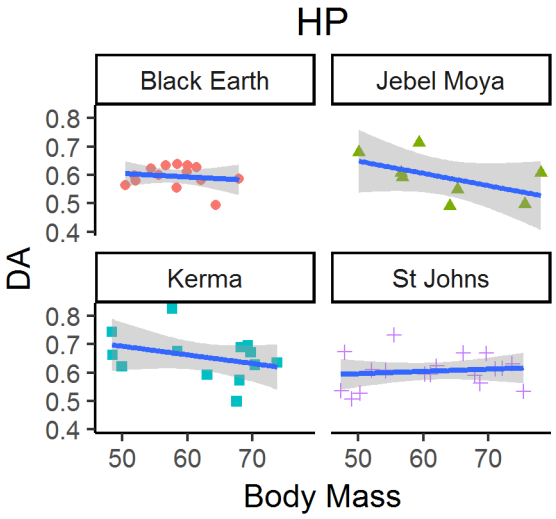
HP
Black Earth
Jebel Moya
Kerma
St Johns
DA
0.8
0.7
0.6
0.5
0.4
50
60
70
Body Mass

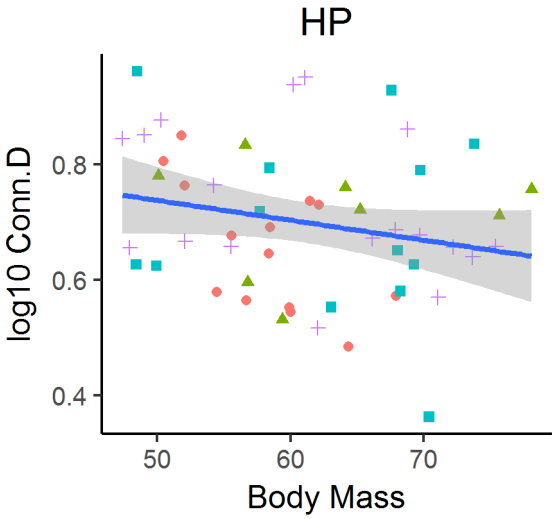
HP
log10 Conn.D
0.8
0.6
0.4
50
60
70
Body Mass

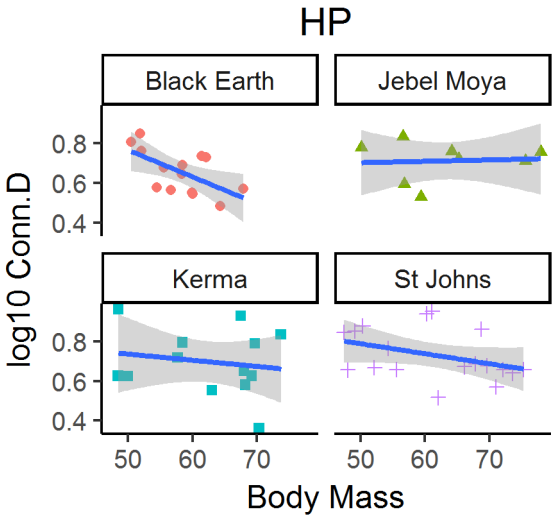
HP
Black Earth
Jebel Moya
Kerma
St Johns
log10 Conn.D
0.8
0.6
0.4
50
60
70
Body Mass

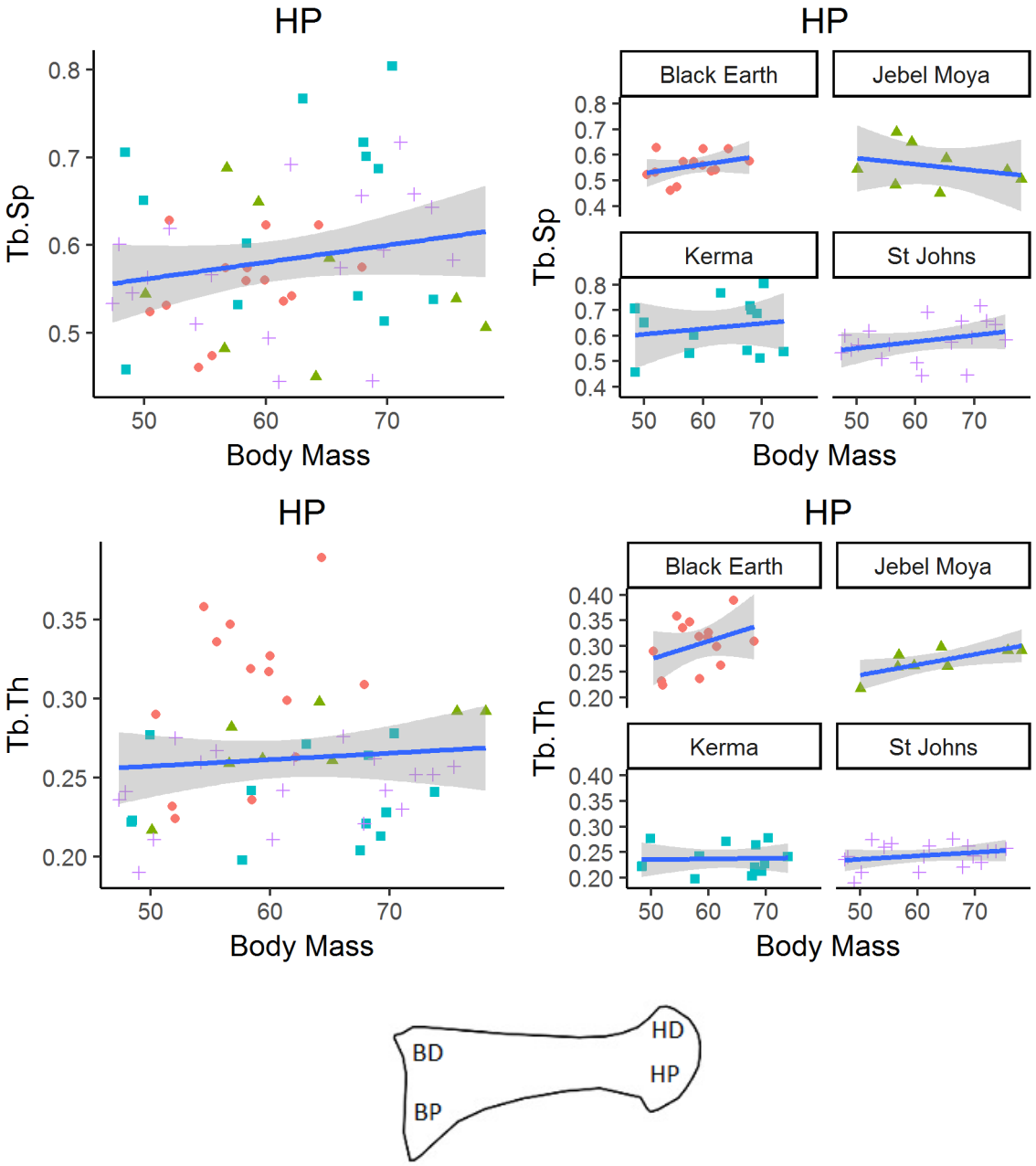

Figure 4.1.3. Plots of OLS regressions between body mass and trabecular properties in pooled and individual populations in the first metatarsal.

Appendix 4.2 Plots of robust regressions

Calcaneus

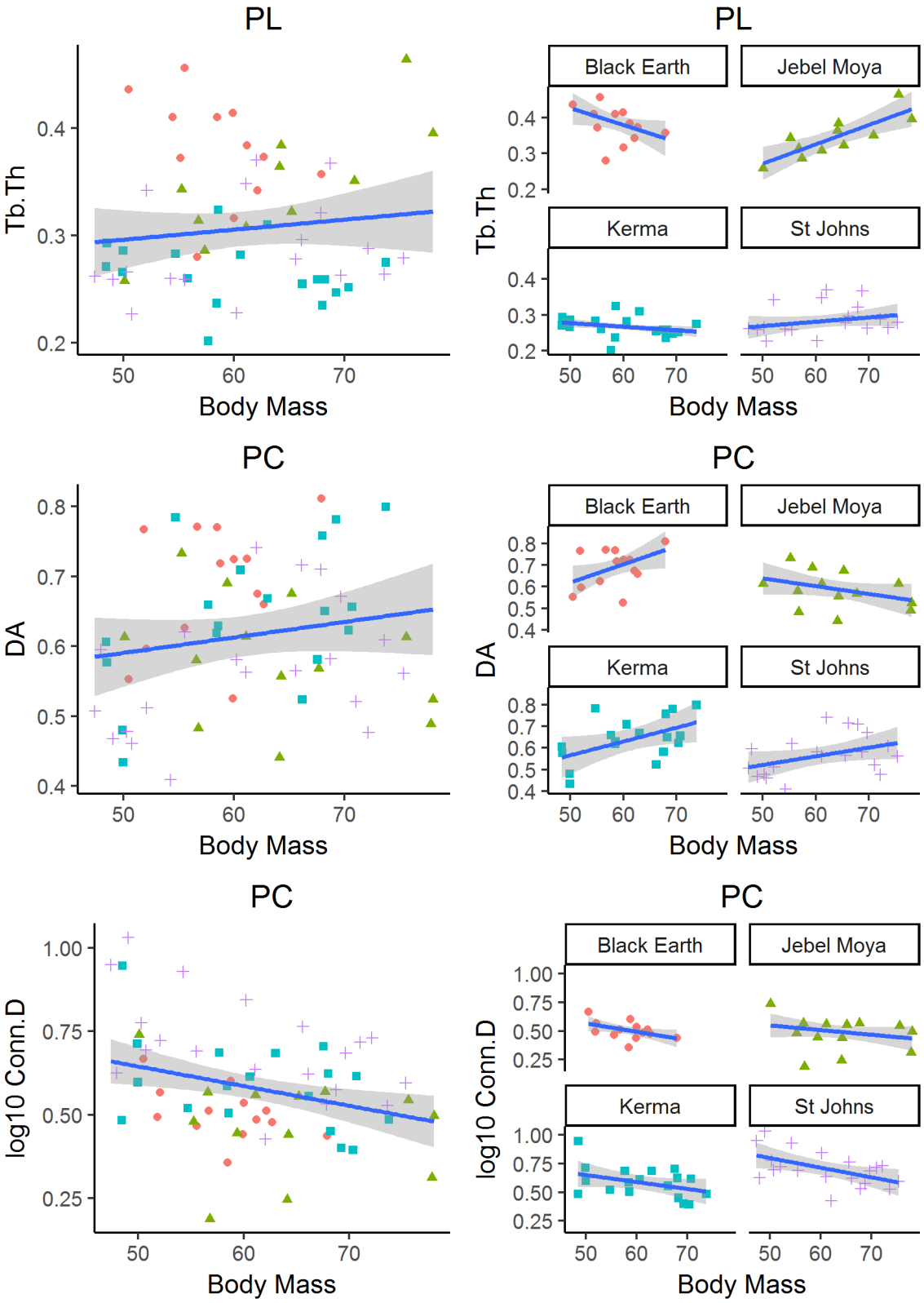

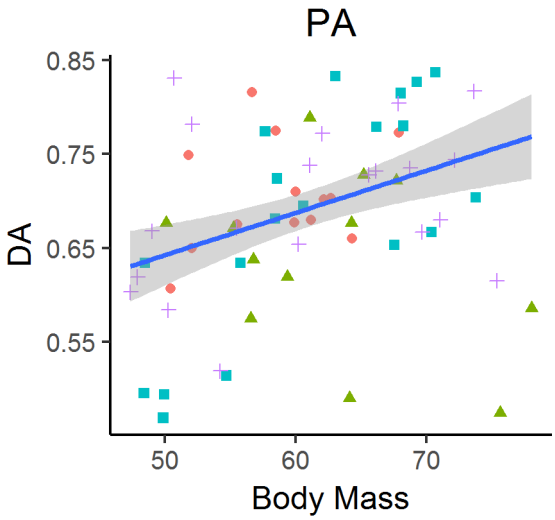
PA
DA
0.85
0.75
0.65
0.55
50
60
70
Body Mass

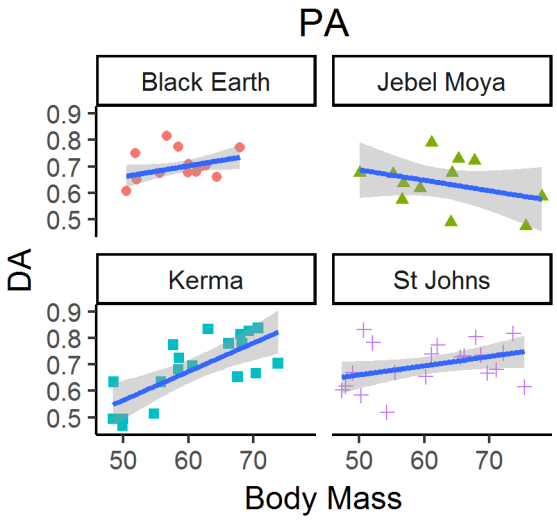
PA
Black Earth
Jebel Moya
Kerma
St Johns
DA
0.9
0.8
0.7
0.6
0.5
50
60
70
Body Mass

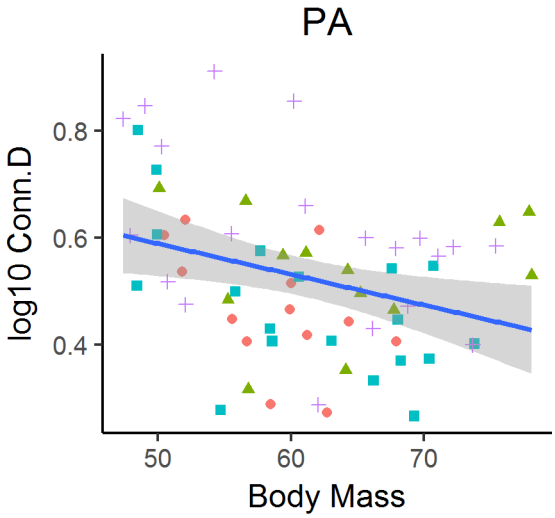
PA
log10 Conn.D
0.8
0.6
0.4
50
60
70
Body Mass

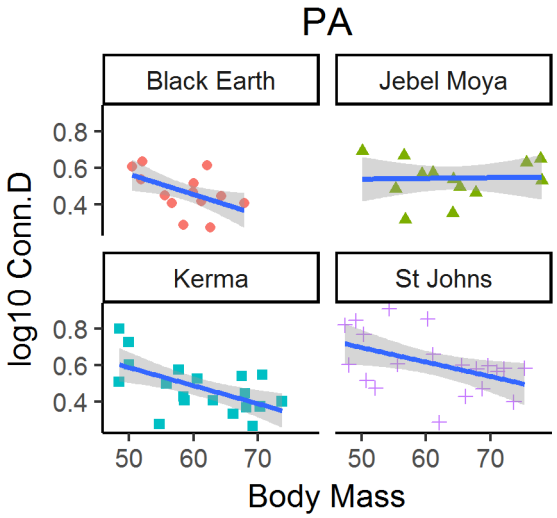
PA
Black Earth
Jebel Moya
Kerma
St Johns
log10 Conn.D
0.8
0.6
0.4
50
60
70
Body Mass

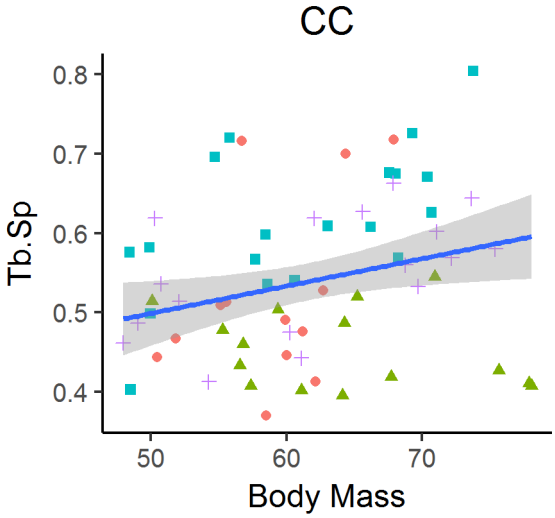
CC
Tb.Sp
0.8
0.7
0.6
0.5
0.4
50
60
70
Body Mass

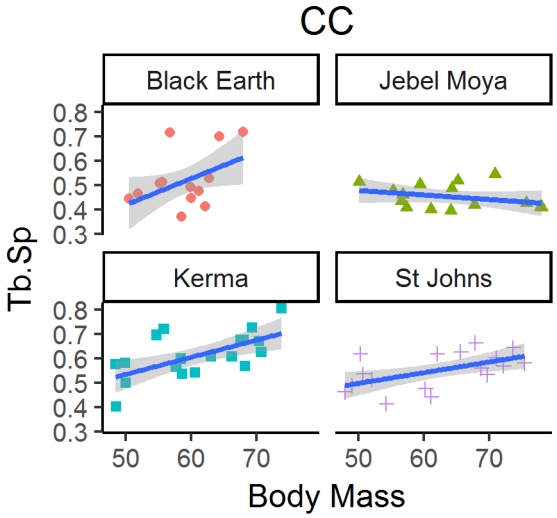
CC
Black Earth
Jebel Moya
Kerma
St Johns
Tb.Sp
0.8
0.7
0.6
0.5
0.4
0.3
50
60
70
Body Mass

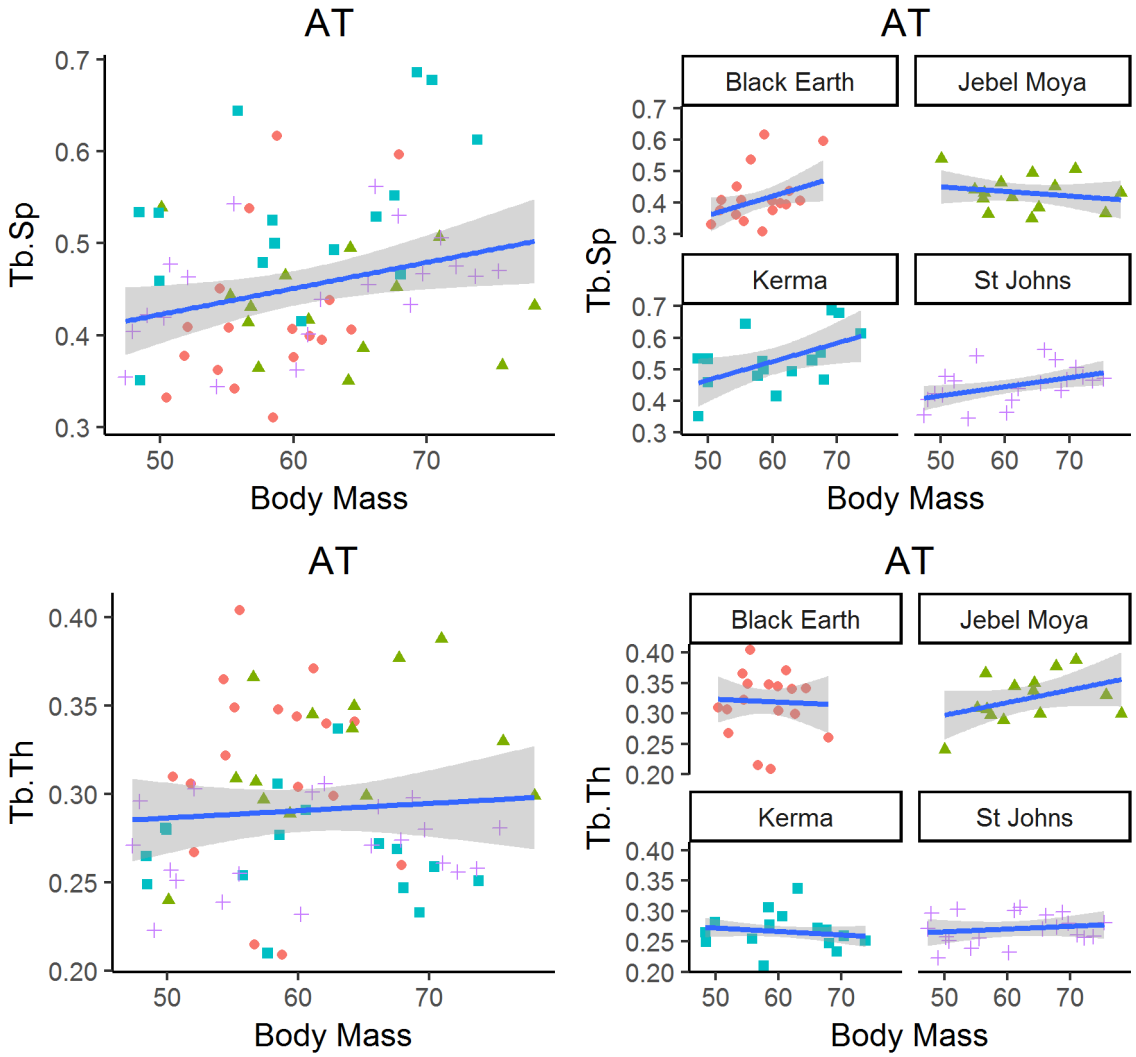

Figure 4.2.1. Plots of robust regressions with Huber weights between body mass and trabecular properties in pooled and individual populations in the calcaneus.

Talus

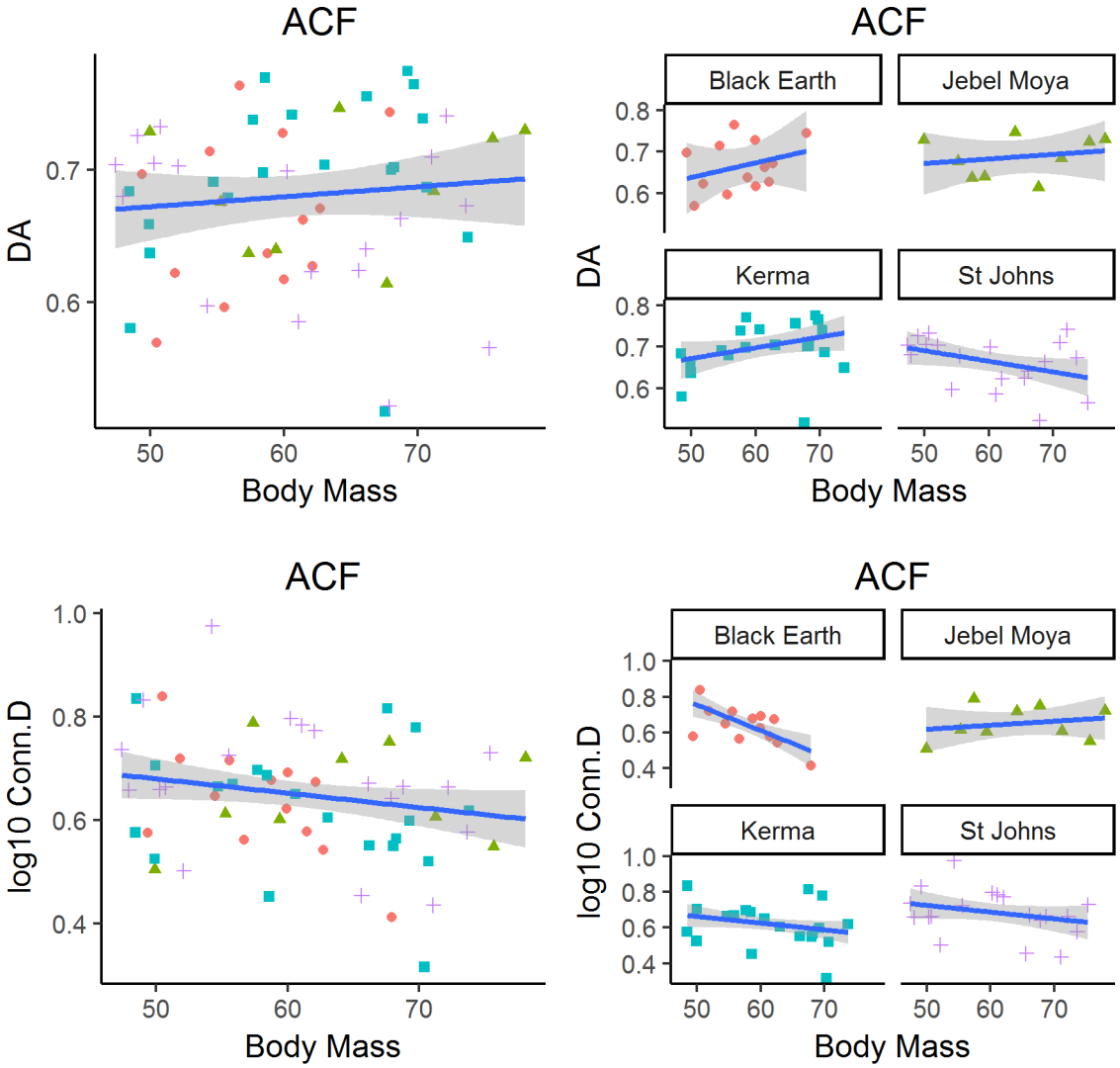

Figure 4.2.2. Plots of robust regressions with Huber weights between body mass and trabecular properties in pooled and individual populations in the talus.

First metatarsal

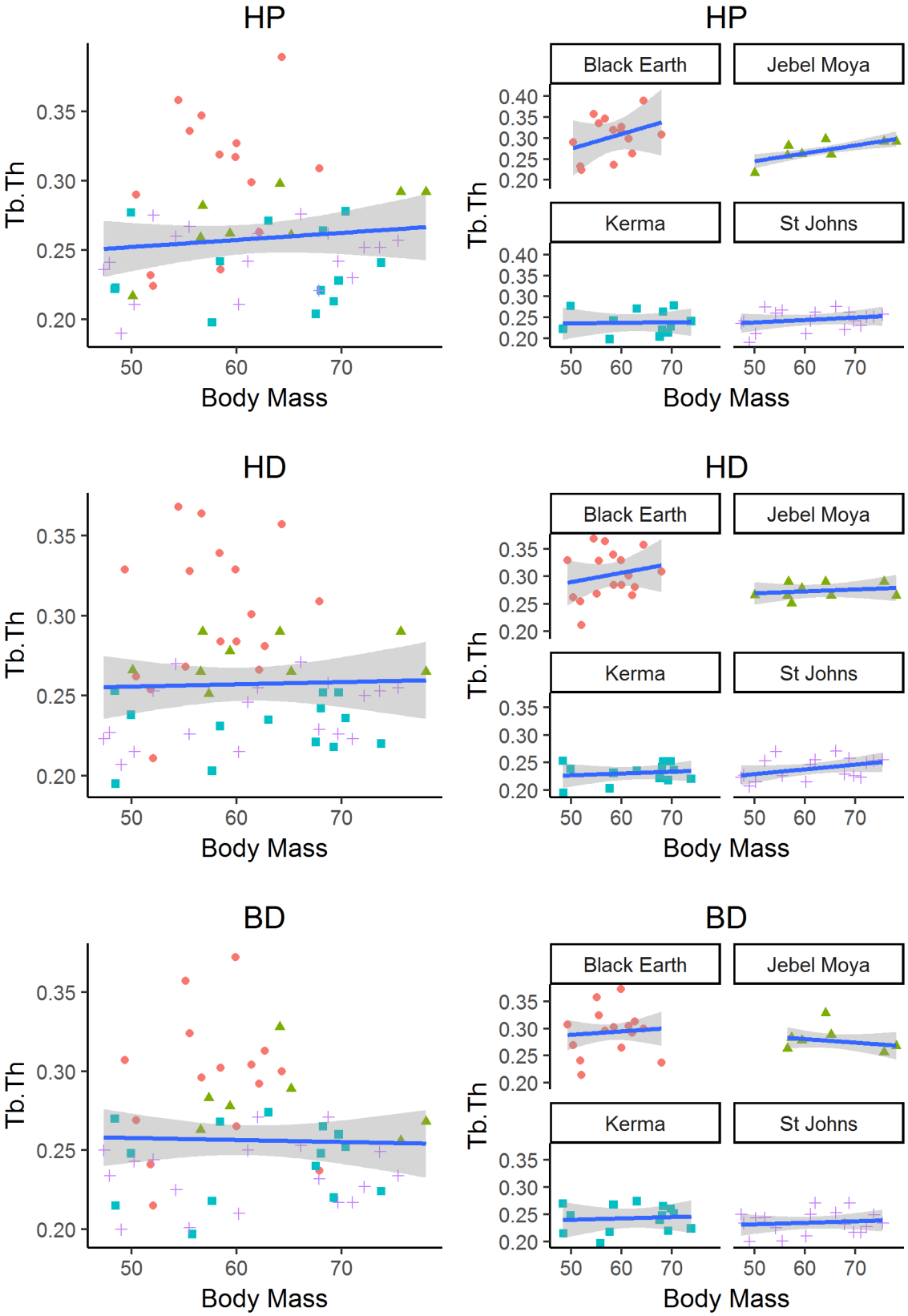

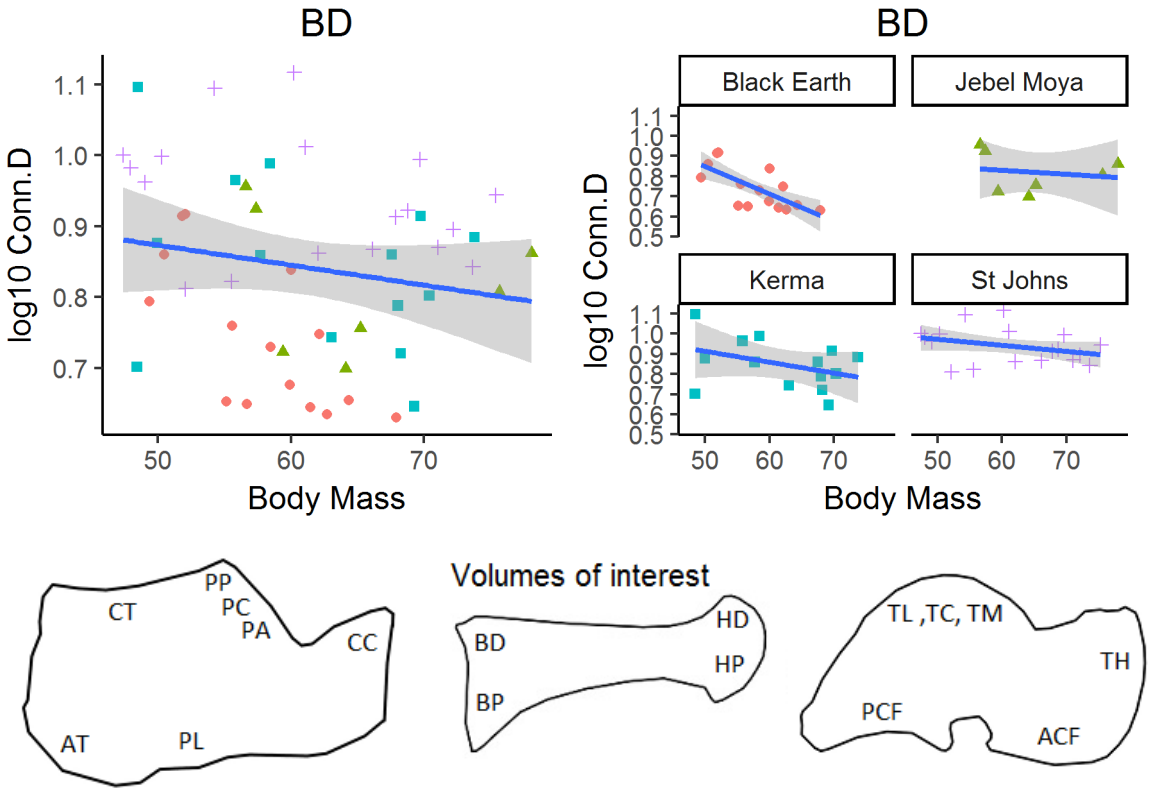

Figure 4.2.3. Plots of robust regressions with Huber weights between body mass and trabecular properties in pooled and individual populations in the first metatarsal. Achilles tendon (AT), calcaneal tuber (CT), plantar ligaments (PL), posterior talar facet (PP: posterior, PC: central, PA: anterior), calcaneocuboid (CC), dorsal base (BD), plantar base (BP), dorsal head (HD), plantar head (HP), talar head (TH), anterior calcaneal facet (ACF), posterior calcaneal facet (PCF), trochlea (lateral: TL, central: TC, medial: TM).

Appendix 4.3 Regressions for males and females

Table 4.3.1. Regressions of body mass and trabecular properties in males. Volumes of interest: Achilles tendon (AT), calcaneal tuber (CT), plantar ligaments (PL), posterior talar facet (PP: posterior, PC: central, PA: anterior), calcaneocuboid (CC), dorsal base (BD), plantar base (BP), dorsal head (HD), plantar head (HP), talar head (TH), anterior calcaneal facet (ACF), posterior calcaneal facet (PCF), trochlea (lateral: TL, central: TC, medial: TM).

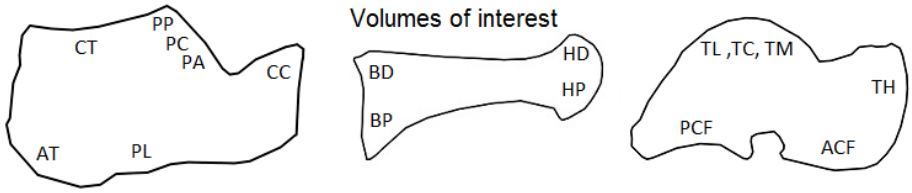

Regressions between body mass and trabecular structure in males								
VOI	**Variable**	**Method**	**intercept**	**slope**	**CL-**	**CL+**	**R^2**	***p***
HD	BV/TV	OLS	.657	-.004	-.008	.000	.103	.083
	Tb.Th	OLS	.386	-.002	-.004	.000	.087	.114
	Tb.Sp	OLS	.213	.003	.000	.006	.141	**.041**
	log10Conn.D	OLS	.921	-.002	-.009	.006	.009	.613
	DA	OLS	.739	.000	-.004	.004	.000	.980
HP	BV/TV	OLS	.367	-.001	-.005	.003	.005	.706
	Tb.Th	OLS	.303	-.001	-.003	.002	.008	.650
	Tb.Sp	OLS	.416	.003	-.003	.009	.029	.373
	log10Conn.D	OLS	.734	-.001	-.010	.008	.001	.848
	DA	OLS	.752	-.002	-.007	.002	.034	.336
BD	BV/TV	OLS	.613	-.003	-.008	.001	.068	.170
	Tb.Th	OLS	.459	-.003	-.005	-.001	.230	**.008**
	Tb.Sp	OLS	.360	.001	-.003	.005	.011	.587
	log10Conn.D	OLS	.497	.005	-.003	.012	.057	.213
	DA	OLS	.697	.001	-.003	.005	.011	.602
BP	BV/TV	OLS	.509	-.003	-.008	.001	.089	.139
	Tb.Th	OLS	.374	-.002	-.005	.001	.077	.169
	Tb.Sp	OLS	.303	.005	-.003	.012	.060	.227
	log10Conn.D	OLS	.772	-.001	-.012	.011	.001	.913
	DA	OLS	.700	-.002	-.007	.004	.013	.586
AT	BV/TV	OLS	.668	-.004	-.009	.001	.072	.139
	Tb.Th	OLS	.426	-.002	-.004	.001	.069	.146
	Tb.Sp	OLS	.236	.004	-.001	.009	.069	.145
	log10Conn.D	OLS	.996	-.005	-.011	.001	.085	.105
	DA	OLS	.721	.001	-.002	.003	.005	.696
CC	BV/TV	OLS	.426	.000	-.006	.005	.000	.913
	Tb.Th	OLS	.354	.000	-.003	.003	.002	.817
	Tb.Sp	OLS	.443	.002	-.004	.008	.011	.541
	log10Conn.D	OLS	.715	-.003	-.010	.004	.142	.415
	DA	OLS	.627	.001	-.001	.004	.028	.339
PL	BV/TV	OLS	.234	.001	-.004	.006	.004	.730
	Tb.Th	OLS	.297	.000	-.003	.004	.001	.887
	Tb.Sp	OLS	.629	.002	-.007	.011	.007	.653

	log10Conn.D	OLS	.589	-.004	-.014	.005	.030	.361
	DA	OLS	.599	.002	-.001	.005	.053	.223
PA	BV/TV	OLS	.662	-.003	-.008	.002	.038	.262
	Tb.Th	OLS	.492	-.001	-.005	.002	.025	.368
	Tb.Sp	OLS	.279	.004	-.002	.010	.052	.197
	log10Conn.D	OLS	.415	.001	-.006	.008	.003	.772
	DA	OLS	.562	.002	-.003	.008	.021	.414
PC	BV/TV	OLS	.739	-.003	-.009	.003	.035	.292
	Tb.Th	OLS	.442	.000	-.004	.003	.002	.826
	Tb.Sp	OLS	.157	.005	.000	.009	.130	**.036**
	log10Conn.D	OLS	.694	-.002	-.008	.004	.018	.452
	DA	OLS	.792	-.002	-.007	.003	.026	.359
PP	BV/TV	OLS	.695	-.003	-.008	.002	.052	.186
	Tb.Th	OLS	.495	-.002	-.005	.001	.038	.259
	Tb.Sp	OLS	.336	.003	-.002	.008	.044	.225
	log10Conn.D	OLS	.495	.000	-.006	.007	.000	.957
	DA	OLS	.797	-.001	-.004	.002	.020	.423
CT	BV/TV	OLS	.486	-.002	-.006	.002	.035	.280
	Tb.Th	OLS	.411	-.001	-.003	.001	.042	.236
	Tb.Sp	OLS	.444	.004	-.003	.011	.037	.268
	log10Conn.D	OLS	.407	-.002	-.010	.006	.008	.619
	DA	OLS	.858	-.001	-.003	.001	.020	.416
ACF	BV/TV	OLS	.294	.000	-.004	.004	.000	.960
	Tb.Th	OLS	.263	.000	-.002	.002	.000	.978
	Tb.Sp	OLS	.637	.000	-.006	.007	.001	.894
	log10Conn.D	OLS	.705	-.001	-.008	.006	.005	.708
	DA	OLS	.612	.001	-.003	.005	.012	.564
TH	BV/TV	OLS	.605	-.002	-.008	.004	.011	.564
	Tb.Th	OLS	.299	.000	-.003	.004	.001	.847
	Tb.Sp	OLS	.261	.003	-.002	.007	.051	.208
	log10Conn.D	OLS	1.066	-.007	-.015	.002	.066	.147
	DA	OLS	.842	.000	-.003	.002	.003	.768
PCF	BV/TV	OLS	.488	-.001	-.006	.004	.005	.711
	Tb.Th	OLS	.304	.000	-.003	.003	.000	.927
	Tb.Sp	OLS	.518	.000	-.005	.004	.000	.911
	log10Conn.D	OLS	.556	.002	-.006	.009	.009	.629
	DA	OLS	.787	.000	-.003	.002	.003	.761
TC	BV/TV	OLS	.348	.001	-.004	.006	.004	.736
	Tb.Th	OLS	.232	.001	-.002	.004	.012	.536
	Tb.Sp	OLS	.447	.000	-.003	.004	.002	.814
	log10Conn.D	OLS	.797	-.001	-.006	.005	.001	.831
	DA	OLS	.836	-.002	-.007	.002	.042	.255
TL	BV/TV	OLS	.357	.002	-.005	.008	.008	.620
	Tb.Th	OLS	.234	.001	-.003	.005	.013	.542
	Tb.Sp	OLS	.500	-.001	-.005	.003	.007	.649
	log10Conn.D	OLS	.565	.002	-.006	.010	.007	.664
	DA	OLS	.833	-.001	-.004	.002	.016	.493
TM	BV/TV	OLS	.415	.000	-.004	.005	.000	.912

	Tb.Th	OLS	.266	.000	-.002	.003	.002	.831
	Tb.Sp	OLS	.447	.000	-.004	.004	.000	.939
	log10Conn.D	OLS	.839	-.001	-.008	.006	.002	.832
	DA	OLS	.902	-.004	-.009	.001	.088	.104

Table 4.3.2. Regressions of body mass and trabecular properties in males, excluding the Black Earth population. Volumes of interest: Achilles tendon (AT), calcaneal tuber (CT), plantar ligaments (PL), posterior talar facet (PP: posterior, PC: central, PA: anterior), calcaneocuboid (CC), dorsal base (BD), plantar base (BP), dorsal head (HD), plantar head (HP), talar head (TH), anterior calcaneal facet (ACF), posterior calcaneal facet (PCF), trochlea (lateral: TL, central: TC, medial: TM).

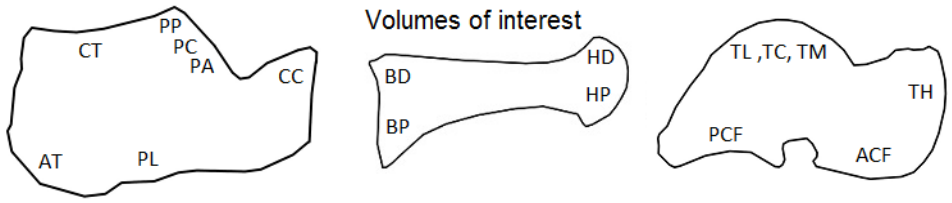

Regressions between body mass and trabecular structure in males excluding Black Earth								
VOI	**Variable**	**Method**	**intercept**	**slope**	**CL-**	**CL+**	**R^2**	***p***
HD	BV/TV	OLS	0.40	0.000	-0.005	0.005	0.00	0.98
	Tb.Th	OLS	0.19	0.001	-0.001	0.002	0.04	0.37
	Tb.Sp	OLS	0.28	0.002	-0.002	0.006	0.06	0.28
	log10Conn.D	OLS	1.47	-0.009	-0.017	-0.002	0.27	**0.01**
	DA	OLS	0.57	0.002	-0.003	0.007	0.05	0.33
HP	BV/TV	OLS	0.20	0.002	-0.003	0.006	0.02	0.48
	Tb.Th	OLS	0.15	0.001	-0.001	0.003	0.09	0.17
	Tb.Sp	OLS	0.49	0.002	-0.007	0.010	0.00	0.68
	log10Conn.D	OLS	0.91	-0.003	-0.015	0.008	0.02	0.56
	DA	OLS	0.90	-0.004	-0.010	0.001	0.11	0.14
BD	BV/TV	OLS	0.33	0.001	-0.004	0.005	0.01	0.69
	Tb.Th	OLS	0.29	-0.001	-0.002	0.001	0.03	0.42
	Tb.Sp	Robust	0.51	-0.001			0.03	0.41
	log10Conn.D	OLS	0.94	-0.001	-0.009	0.006	0.01	0.71
	DA	OLS	0.55	0.003	-0.001	0.007	0.12	0.13
BP	BV/TV	OLS	0.28	-0.000	-0.006	0.005	0.00	0.93
	Tb.Th	OLS	0.14	0.001	-0.002	0.004	0.04	0.39
	Tb.Sp	OLS	0.19	0.006	-0.004	0.016	0.08	0.23
	log10Conn.D	OLS	1.41	-0.010	-0.024	0.005	0.10	0.19
	DA	OLS	0.54	0.001	-0.007	0.009	0.00	0.83
AT	BV/TV	OLS	0.47	-0.001	-0.007	0.005	0.01	0.65
	Tb.Th	OLS	0.34	-0.001	-0.004	0.002	0.01	0.58
	Tb.Sp	OLS	0.41	0.001	-0.004	0.007	0.01	0.66
	log10Conn.D	OLS	0.87	-0.003	-0.011	0.004	0.04	0.37
	DA	OLS	0.74	0.000	-0.003	0.003	0.00	0.82
CC	BV/TV	OLS	0.24	0.002	-0.003	0.008	0.03	0.41
	Tb.Th	OLS	0.27	0.001	-0.002	0.004	0.01	0.57
	Tb.Sp	OLS	0.60	-0.001	-0.007	0.006	0.00	0.88
	log10Conn.D	OLS	0.85	-0.005	-0.012	0.003	0.06	0.21

	DA	OLS	0.57	0.002	-0.001	0.005	0.07	0.19
PL	BV/TV	OLS	0.10	0.003	-0.003	0.009	0.04	0.36
	Tb.Th	OLS	0.14	0.002	-0.001	0.006	0.08	0.19
	Tb.Sp	OLS	0.76	-0.000	-0.010	0.009	0.00	0.99
	log10Conn.D	OLS	0.67	-0.005	-0.015	0.005	0.05	0.29
	DA	OLS	0.69	0.001	-0.003	0.004	0.01	0.65
PA	BV/TV	OLS	0.48	-0.000	-0.006	0.005	0.00	0.87
	Tb.Th	OLS	0.35	0.001	-0.002	0.003	0.00	0.74
	Tb.Sp	OLS	0.43	0.002	-0.005	0.009	0.01	0.57
	log10Conn.D	OLS	0.54	-0.000	-0.008	0.007	0.00	0.84
	DA	Robust	0.57	0.002			0.03	0.49
PC	BV/TV	OLS	0.52	0.000	-0.006	0.006	0.00	0.99
	Tb.Th	OLS	0.29	0.002	-0.002	0.005	0.04	0.31
	Tb.Sp	OLS	0.28	0.003	-0.001	0.007	0.07	0.18
	log10Conn.D	OLS	0.90	-0.005	-0.011	0.001	0.10	0.10
	DA	OLS	0.75	-0.002	-0.007	0.004	0.02	0.48
PP	BV/TV	OLS	0.49	-0.000	-0.005	0.005	0.00	0.87
	Tb.Th	OLS	0.33	0.001	-0.002	0.003	0.01	0.69
	Tb.Sp	OLS	0.46	0.001	-0.004	0.006	0.01	0.63
	log10Conn.D	OLS	0.77	-0.003	-0.009	0.003	0.05	0.25
	DA	OLS	0.70	0.000	-0.003	0.003	0.00	0.93
CT	BV/TV	OLS	0.33	0.000	-0.004	0.004	0.00	0.99
	Tb.Th	OLS	0.31	0.000	-0.002	0.002	0.00	0.88
	Tb.Sp	OLS	0.64	0.001	-0.006	0.008	0.00	0.76
	log10Conn.D	OLS	0.31	-0.001	-0.010	0.009	0.00	0.88
	DA	OLS	0.85	-0.001	-0.003	0.001	0.02	0.46
ACF	BV/TV	OLS	0.21	0.001	-0.003	0.005	0.02	0.49
	Tb.Th	OLS	0.20	0.001	-0.001	0.003	0.03	0.41
	Tb.Sp	OLS	0.77	-0.002	-0.009	0.006	0.01	0.67
	log10Conn.D	OLS	0.74	-0.002	-0.009	0.006	0.01	0.65
	DA	OLS	0.61	0.001	-0.003	0.005	0.01	0.61
TH	BV/TV	OLS	0.41	0.001	-0.006	0.008	0.00	0.79
	Tb.Th	Robust	0.18	0.002			0.06	0.26
	Tb.Sp	OLS	0.34	0.002	-0.003	0.007	0.02	0.52
	log10Conn.D	OLS	1.54	-0.013	-0.022	-0.004	0.26	**0.01**
	DA	OLS	0.80	0.000	-0.003	0.003	0.00	0.90
PCF	BV/TV	OLS	0.31	0.001	-0.004	0.007	0.01	0.58
	Tb.Th	OLS	0.19	0.002	-0.001	0.004	0.05	0.28
	Tb.Sp	OLS	0.59	-0.001	-0.006	0.004	0.01	0.58
	log10Conn.D	OLS	0.86	-0.002	-0.009	0.005	0.02	0.54
	DA	OLS	0.77	-0.000	-0.003	0.003	0.00	0.94
TC	BV/TV	OLS	0.20	0.003	-0.003	0.008	0.05	0.29
	Tb.Th	OLS	0.14	0.002	-0.001	0.005	0.08	0.17
	Tb.Sp	OLS	0.54	-0.001	-0.005	0.003	0.01	0.66
	log10Conn.D	OLS	0.94	-0.002	-0.008	0.004	0.03	0.42
	DA	OLS	0.73	-0.001	-0.006	0.004	0.01	0.61
TL	BV/TV	OLS	0.23	0.003	-0.003	0.010	0.04	0.32
	Tb.Th	OLS	0.14	0.002	-0.002	0.006	0.07	0.22

	Tb.Sp	OLS	0.53	-0.001	-0.001	0.003	0.02	0.53
	log10Conn.D	OLS	0.79	-0.001	-0.009	0.007	0.00	0.79
	DA	OLS	0.81	-0.001	-0.004	0.002	0.01	0.64
TM	BV/TV	OLS	0.31	0.002	-0.003	0.007	0.02	0.49
	Tb.Th	OLS	0.20	0.001	-0.002	0.004	0.03	0.43
	Tb.Sp	OLS	0.54	-0.001	-0.006	0.003	0.01	0.59
	log10Conn.D	OLS	1.01	-0.003	-0.011	0.005	0.03	0.43
	DA	OLS	0.82	-0.003	-0.009	0.003	0.05	0.29

Table 4.3.3. Regressions of body mass and trabecular properties in females. Volumes of interest: Achilles tendon (AT), calcaneal tuber (CT), plantar ligaments (PL), posterior talar facet (PP: posterior, PC: central, PA: anterior), calcaneocuboid (CC), dorsal base (BD), plantar base (BP), dorsal head (HD), plantar head (HP), talar head (TH), anterior calcaneal facet (ACF), posterior calcaneal facet (PCF), trochlea (lateral: TL, central: TC, medial: TM).

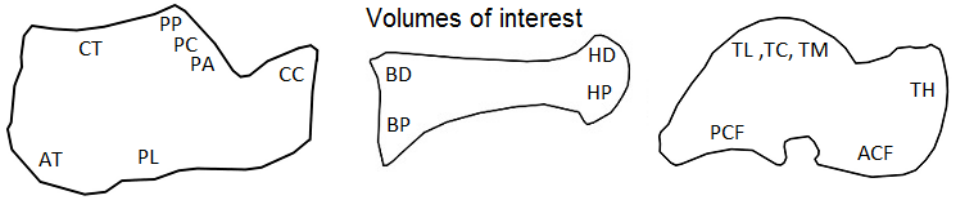

Regressions between body mass and trabecular structure in females								
VOI	**Variable**	**Method**	**intercept**	**slope**	**CL-**	**CL+**	**R^2**	***p***
HD	BV/TV	OLS	0.45	-0.000	-0.008	0.007	0.00	0.91
	Tb.Th	OLS	0.18	0.001	-0.003	0.006	0.02	0.50
	Tb.Sp	OLS	0.19	0.004	-0.001	0.009	0.13	0.09
	log10Conn.D	OLS	1.64	-0.015	-0.029	-0.000	0.18	**0.04**
	DA	OLS	0.68	0.001	-0.002	0.005	0.02	0.51
HP	BV/TV	Robust	0.17	0.003			0.04	0.28
	Tb.Th	Robust	0.15	0.002			0.05	0.42
	Tb.Sp	OLS	0.49	0.002	-0.005	0.008	0.01	0.63
	log10Conn.D	OLS	1.05	-0.006	0.017	0.005	0.06	0.28
	DA		0.59	0.001	-0.005	0.006	0.00	0.87
BD	BV/TV	OLS	0.37	0.001	-0.006	0.007	0.00	0.88
	Tb.Th	OLS	0.24	0.000	-0.004	0.004	0.00	0.93
	Tb.Sp	OLS	0.34	0.001	-0.004	0.007	0.01	0.60
	log10Conn.D	OLS	0.96	-0.001	-0.014	0.011	0.00	0.85
	DA	OLS	0.78	-0.000	-0.006	0.005	0.00	0.89
BP	BV/TV	OLS	0.22	0.001	-0.005	0.007	0.01	0.66
	Tb.Th	OLS	0.14	0.002	-0.002	0.005	0.05	0.32
	Tb.Sp	OLS	0.35	0.004	-0.004	0.011	0.06	0.32
	log10Conn.D	OLS	1.12	-0.005	-0.017	0.007	0.04	0.41
	DA	OLS	0.67	-0.002	-0.008	0.004	0.04	0.42
AT	BV/TV	OLS	0.47	-0.001	-0.008	0.006	0.01	0.71
	Tb.Th	Robust	0.26	0.000			0.00	0.87
	Tb.Sp	OLS	0.22	0.004	-0.002	0.010	0.07	0.18
	log10Conn.D	OLS	1.15	-0.007	-0.015	0.000	0.14	**0.05**
	DA	OLS	0.73	0.000	-0.006	0.006	0.00	0.98

CC	BV/TV	OLS	0.40	-0.000	-0.006	0.006	0.00	0.94
	Tb.Th	OLS	0.23	0.002	-0.003	0.006	0.03	0.45
	Tb.Sp	OLS	0.17	0.007	0.000	0.013	0.18	**0.04**
	log10Conn.D	OLS	1.14	-0.009	-0.021	0.002	0.12	0.10
	DA	OLS	0.56	0.003	-0.001	0.007	0.08	0.20
PL	BV/TV	OLS	0.21	0.001	-0.004	0.007	0.01	0.59
	Tb.Th	Robust	0.23	0.001			0.00	0.60
	Tb.Sp	OLS	0.70	0.000	-0.008	0.009	0.00	0.95
	log10Conn.D	Robust	0.80	0.007			0.04	0.16
	DA	OLS	0.44	0.005	-0.001	0.011	0.11	0.11
PA	BV/TV	OLS	0.42	0.001	-0.007	0.008	0.00	0.85
	Tb.Th	OLS	0.34	0.000	-0.005	0.006	0.00	0.86
	Tb.Sp	Robust	0.57	-0.001			0.00	0.66
	log10Conn.D	Robust	1.07	-0.009			0.09	0.12
	DA	OLS	0.25	0.008	0.002	0.014	0.22	**0.02**
PC	BV/TV	OLS	0.47	0.001	-0.006	0.008	0.00	0.82
	Tb.Th	OLS	0.23	0.003	-0.003	0.008	0.05	0.30
	Tb.Sp	OLS	0.28	0.003	-0.003	0.008	0.05	0.28
	log10Conn.D	OLS	1.17	-0.009	-0.021	0.003	0.10	0.13
	DA	OLS	0.12	0.009	0.002	0.016	0.24	**0.01**
PP	BV/TV	OLS	0.35	0.002	-0.004	0.008	0.02	0.49
	Tb.Th	OLS	0.32	0.001	-0.004	0.006	0.00	0.77
	Tb.Sp	OLS	0.70	-0.003	-0.008	0.001	0.08	0.16
	log10Conn.D	OLS	0.53	0.001	-0.013	0.014	0.00	0.92
	DA	OLS	0.55	0.003	-0.002	0.008	0.06	0.23
CT	BV/TV	OLS	0.18	0.003	-0.002	0.008	0.05	0.27
	Tb.Th	OLS	0.24	0.001	-0.003	0.006	0.02	0.51
	Tb.Sp	OLS	0.51	0.002	-0.006	0.011	0.01	0.54
	log10Conn.D	OLS	0.89	-0.009	-0.019	0.001	0.13	0.06
	DA	OLS	0.65	0.003	-0.000	0.005	0.14	0.06
ACF	BV/TV	OLS	0.46	-0.002	-0.008	0.003	0.03	0.38
	Tb.Th	OLS	0.31	-0.001	-0.004	0.003	0.01	0.70
	Tb.Sp	OLS	0.36	0.005	-0.001	0.011	0.09	0.13
	log10Conn.D	OLS	0.95	-0.005	-0.014	0.004	0.05	0.25
	DA	OLS	0.81	-0.003	-0.007	0.002	0.05	0.27
TH	BV/TV	OLS	0.50	-0.001	-0.007	0.006	0.00	0.81
	Tb.Th	OLS	0.25	0.001	-0.003	0.004	0.01	0.67
	Tb.Sp	OLS	0.25	0.003	-0.002	0.008	0.08	0.17
	log10Conn.D	OLS	1.26	-0.010	-0.020	-0.001	0.17	**0.04**
	DA	OLS	0.70	0.002	-0.001	0.005	0.08	0.16
PCF	BV/TV	OLS	0.43	-0.001	-0.006	0.005	0.00	0.79
	Tb.Th	OLS	0.20	0.001	0.002	0.005	0.02	0.46
	Tb.Sp	OLS	0.24	0.005	0.001	0.008	0.22	**0.02**
	log10Conn.D	OLS	1.30	-0.010	-0.021	0.000	0.14	0.06
	DA	OLS	0.66	0.002	-0.001	0.005	0.06	0.23
TC	BV/TV	OLS	0.45	-0.001	-0.007	0.005	0.00	0.75
	Tb.Th	OLS	0.29	-0.000	-0.004	0.003	0.00	0.86
	Tb.Sp	OLS	0.35	0.002	-0.002	0.006	0.03	0.39

	log10Conn.D	OLS	1.04	-0.004	-0.014	0.001	0.02	0.44
	DA	OLS	0.78	-0.002	-0.006	0.003	0.02	0.50
TL	BV/TV	OLS	0.37	0.001	-0.005	0.007	0.01	0.71
	Tb.Th	OLS	0.21	0.001	-0.003	0.006	0.02	0.53
	Tb.Sp	OLS	0.29	0.002	-0.002	0.007	0.06	0.24
	log10Conn.D	OLS	1.10	-0.006	-0.017	0.006	0.04	0.32
	DA	OLS	0.70	0.001	-0.002	0.004	0.04	0.33
TM	BV/TV	OLS	0.34	0.001	-0.004	0.007	0.01	0.62
	Tb.Th	OLS	0.20	0.001	-0.002	0.004	0.02	0.49
	Tb.Sp	OLS	0.40	0.001	-0.004	0.005	0.00	0.75
	log10Conn.D	OLS	1.15	-0.005	-0.014	0.004	0.05	0.26
	DA	OLS	0.68	-0.001	-0.006	0.005	0.00	0.83

Appendix 4.4 Plots of regressions in males and females

Calcaneus

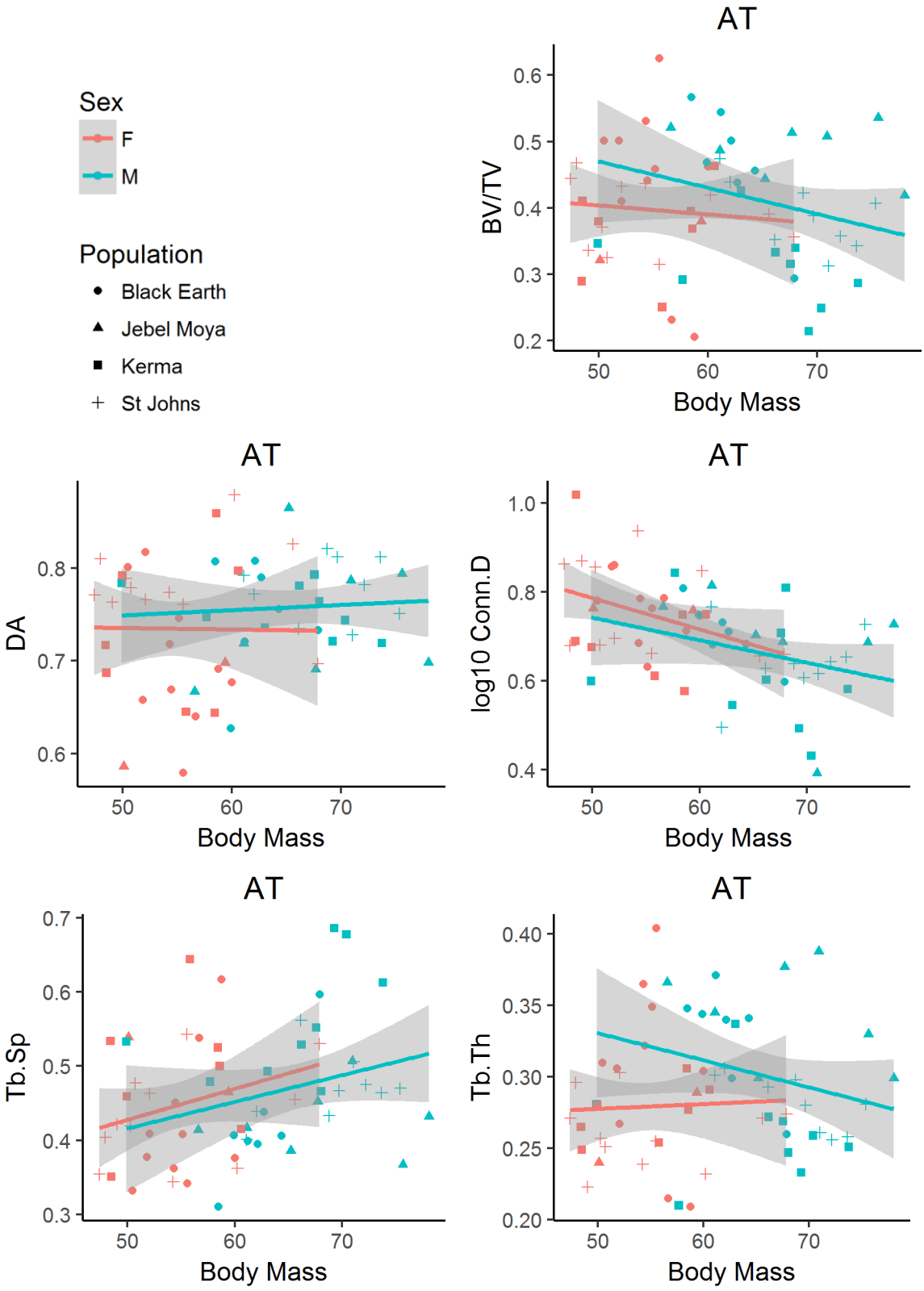

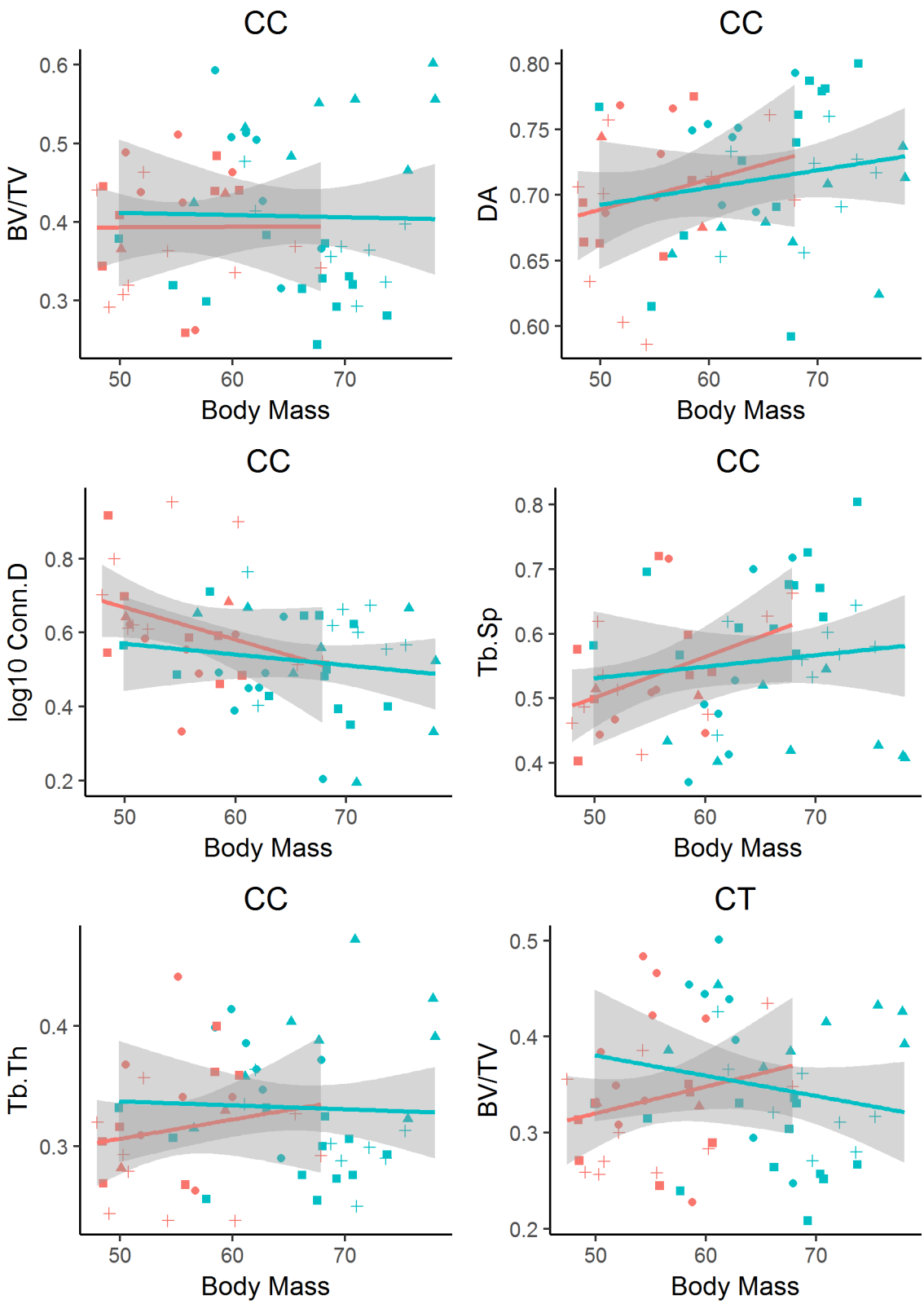
CC
BV/TV
0.6
0.5
0.4
0.3
50
60
70
Body Mass
CC
DA
0.80
0.75
0.70
0.65
0.60
50
60
70
Body Mass
CC
log10 Conn.D
0.8
0.6
0.4
0.2
50
60
70
Body Mass
CC
Tb.Sp
0.8
0.7
0.6
0.5
0.4
50
60
70
Body Mass
CC
Tb.Th
0.4
0.3
50
60
70
Body Mass
CT
BV/TV
0.5
0.4
0.3
0.2
50
60
70
Body Mass

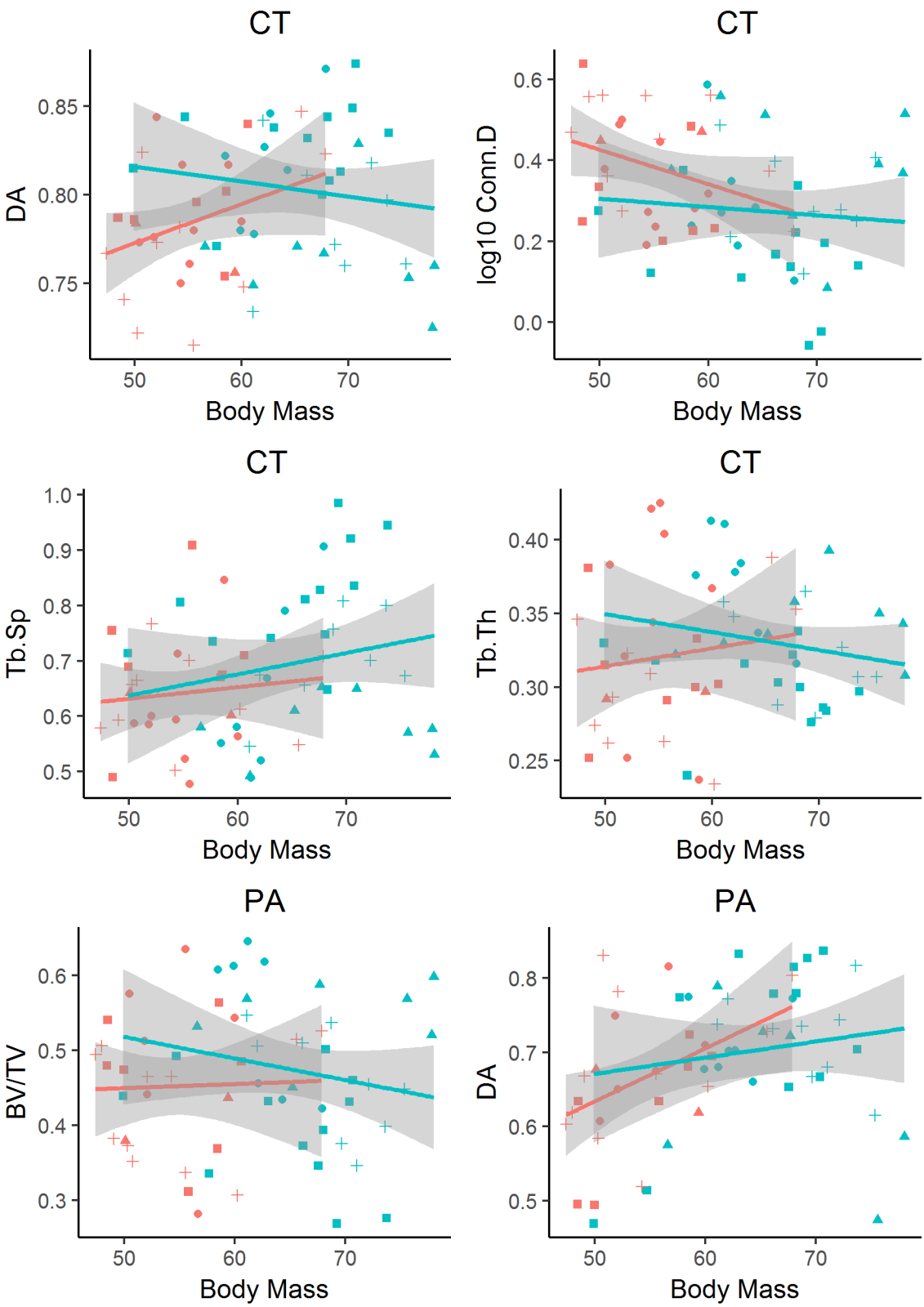
CT
DA
0.85
0.80
0.75
50
60
70
Body Mass
CT
log10 Conn.D
0.6
0.4
0.2
0.0
50
60
70
Body Mass
CT
Tb.Sp
1.0
0.9
0.8
0.7
0.6
0.5
50
60
70
Body Mass
CT
Tb.Th
0.40
0.35
0.30
0.25
50
60
70
Body Mass
PA
BV/TV
0.6
0.5
0.4
0.3
50
60
70
Body Mass
PA
DA
0.8
0.7
0.6
0.5
50
60
70
Body Mass

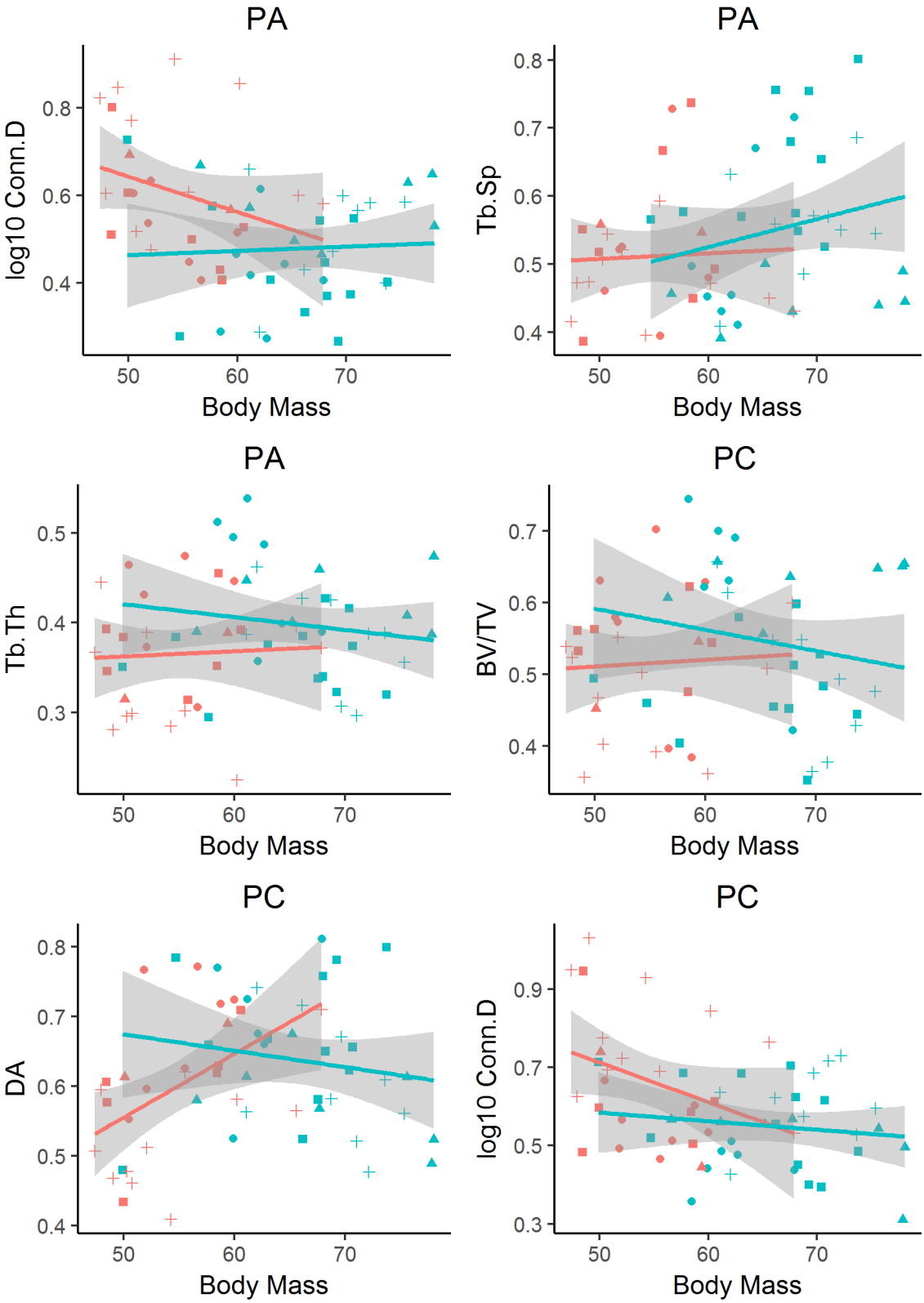
PA
log10 Conn.D
0.8
0.6
0.4
50
60
70
Body Mass
PA
Tb.Sp
0.8
0.7
0.6
0.5
0.4
50
60
70
Body Mass
PA
Tb.Th
0.5
0.4
0.3
50
60
70
Body Mass
PC
BV/TV
0.7
0.6
0.5
0.4
50
60
70
Body Mass
PC
DA
0.8
0.7
0.6
0.5
0.4
50
60
70
Body Mass
PC
log10 Conn.D
0.9
0.7
0.5
0.3
50
60
70
Body Mass

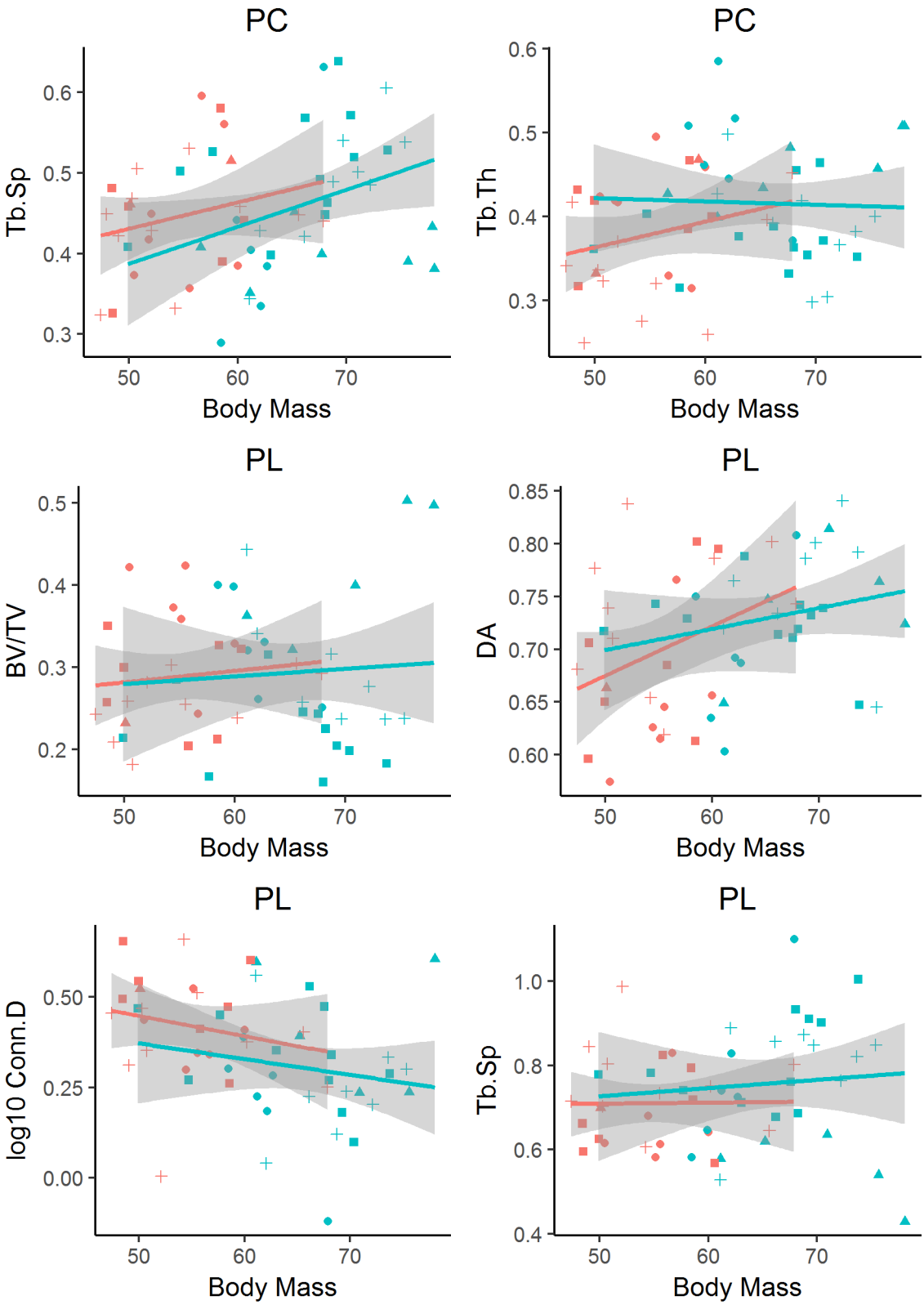
PC
Tb.Sp
0.6
0.5
0.4
0.3
50
60
70
Body Mass
PC
Tb.Th
0.6
0.5
0.4
0.3
50
60
70
Body Mass
PL
BV/TV
0.5
0.4
0.3
0.2
50
60
70
Body Mass
PL
DA
0.85
0.80
0.75
0.70
0.65
0.60
50
60
70
Body Mass
PL
log10 Conn.D
0.50
0.25
0.00
50
60
70
Body Mass
PL
Tb.Sp
1.0
0.8
0.6
0.4
50
60
70
Body Mass

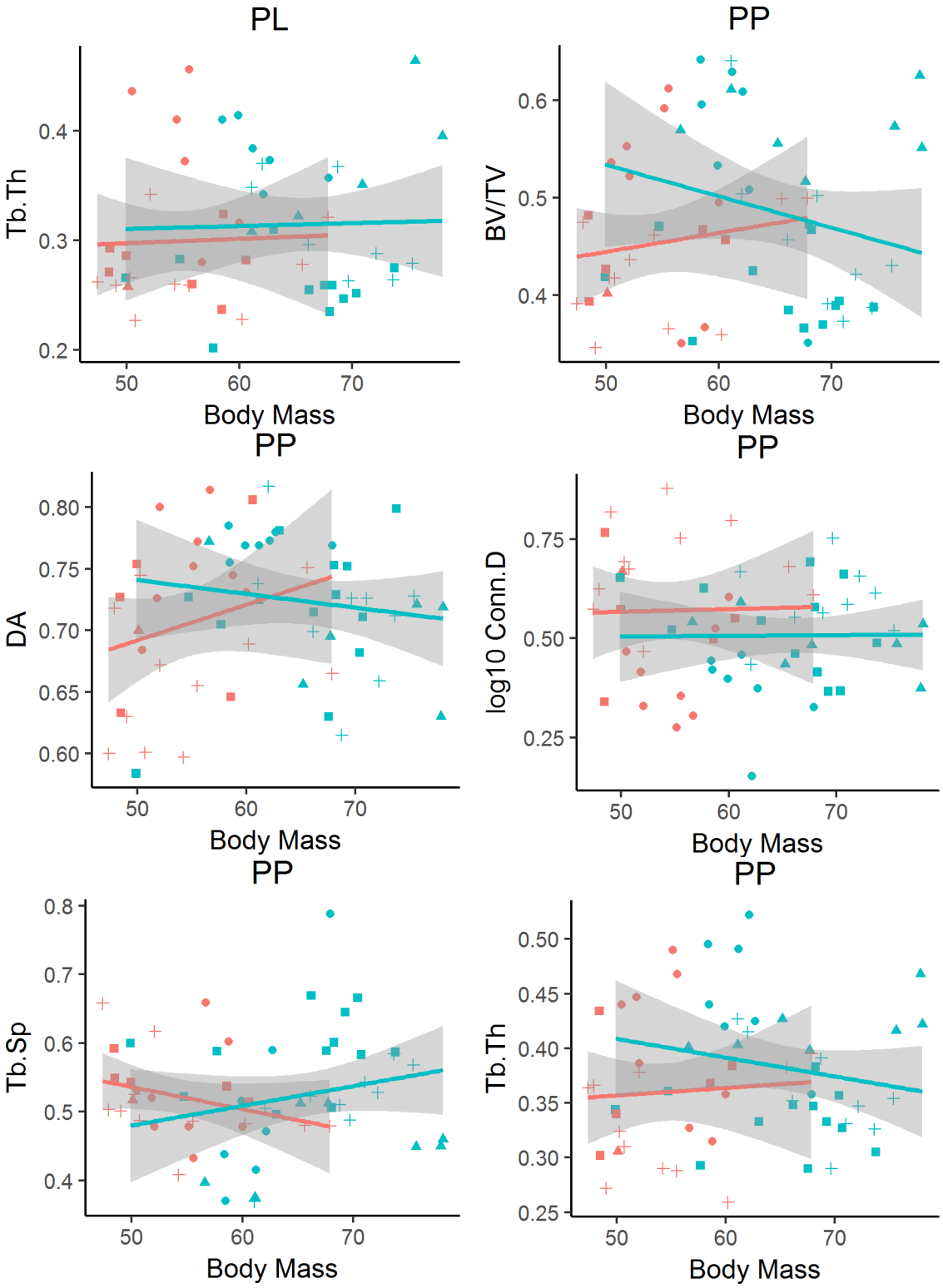

Figure 4.4.1. Plots of regressions of body mass and trabecular properties in males and females in the calcaneus.

Talus

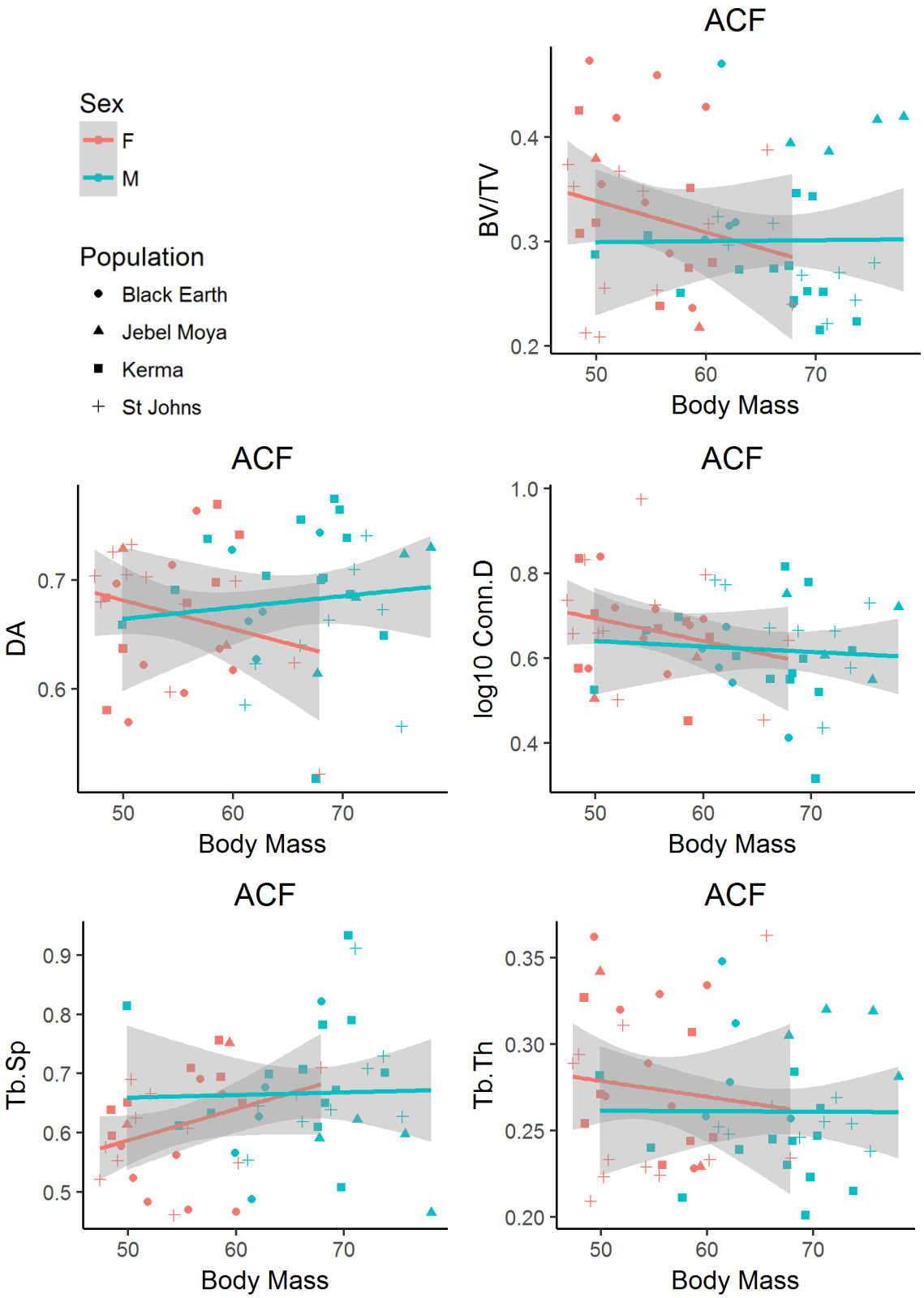
Sex
F
M
Population
Black Earth
Jebel Moya
Kerma
St Johns
ACF
BV/TV
Body Mass
DA
log10 Conn.D
Tb.Sp
Tb.Th
50
60
70

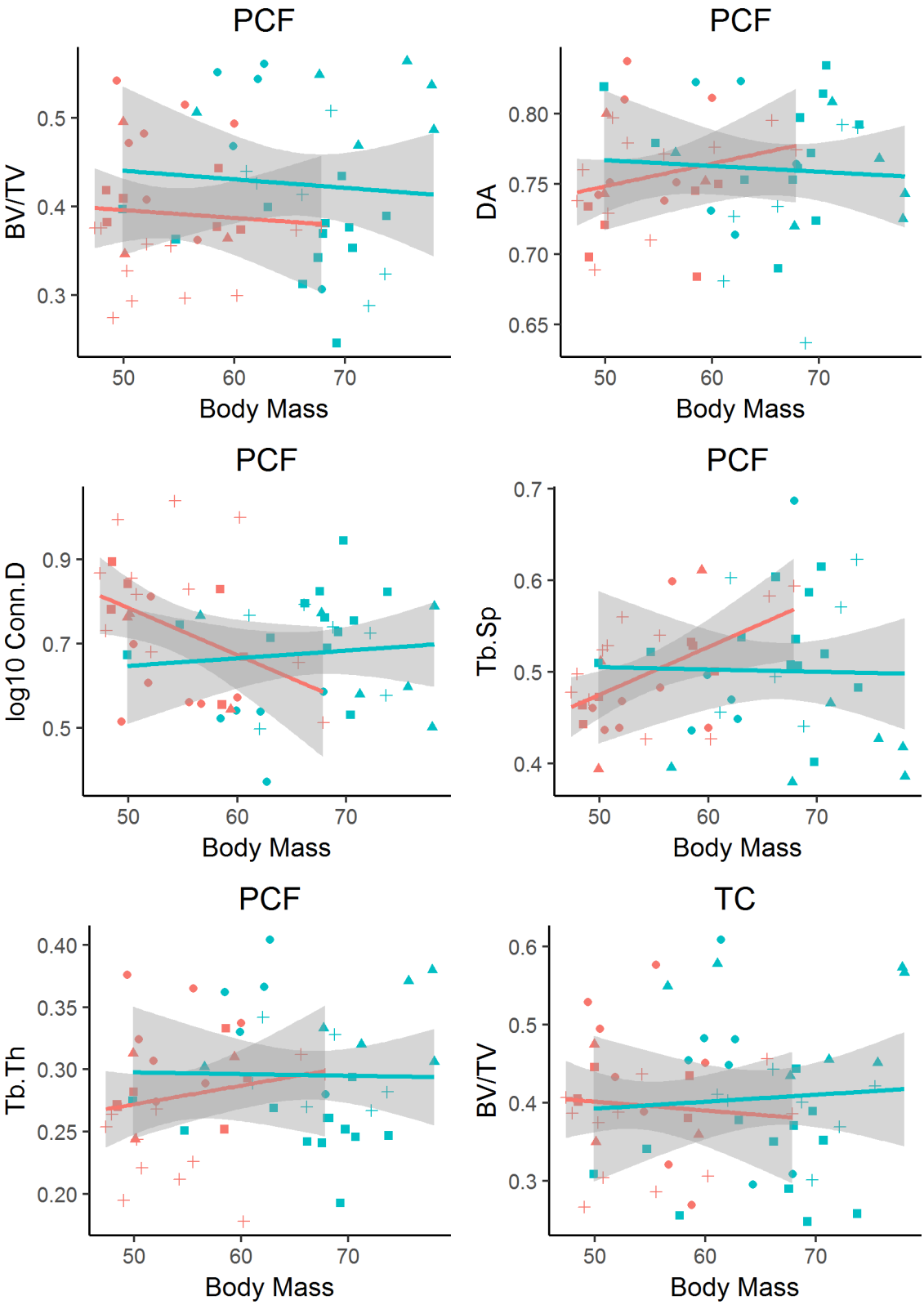
PCF
BV/TV
0.5
0.4
0.3
50
60
70
Body Mass
PCF
DA
0.80
0.75
0.70
0.65
50
60
70
Body Mass
PCF
log10 Conn.D
0.9
0.7
0.5
50
60
70
Body Mass
PCF
Tb.Sp
0.7
0.6
0.5
0.4
50
60
70
Body Mass
PCF
Tb.Th
0.40
0.35
0.30
0.25
0.20
50
60
70
Body Mass
TC
BV/TV
0.6
0.5
0.4
0.3
50
60
70
Body Mass

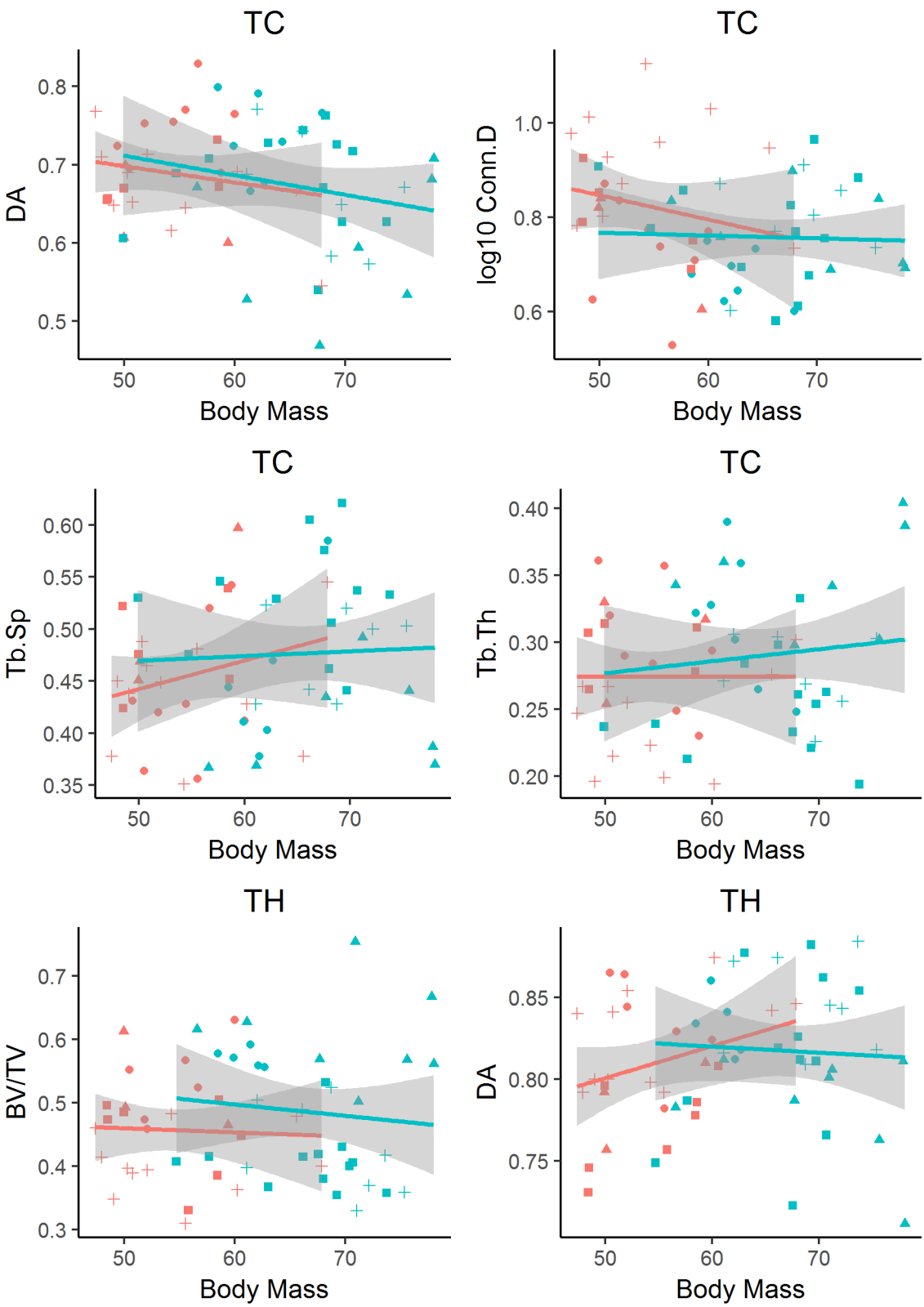
TC
DA
0.8
0.7
0.6
0.5
50
60
70
Body Mass
TC
log10 Conn.D
1.0
0.8
0.6
50
60
70
Body Mass
TC
Tb.Sp
0.60
0.55
0.50
0.45
0.40
0.35
50
60
70
Body Mass
TC
Tb.Th
0.40
0.35
0.30
0.25
0.20
50
60
70
Body Mass
TH
BV/TV
0.7
0.6
0.5
0.4
0.3
50
60
70
Body Mass
TH
DA
0.85
0.80
0.75
50
60
70
Body Mass

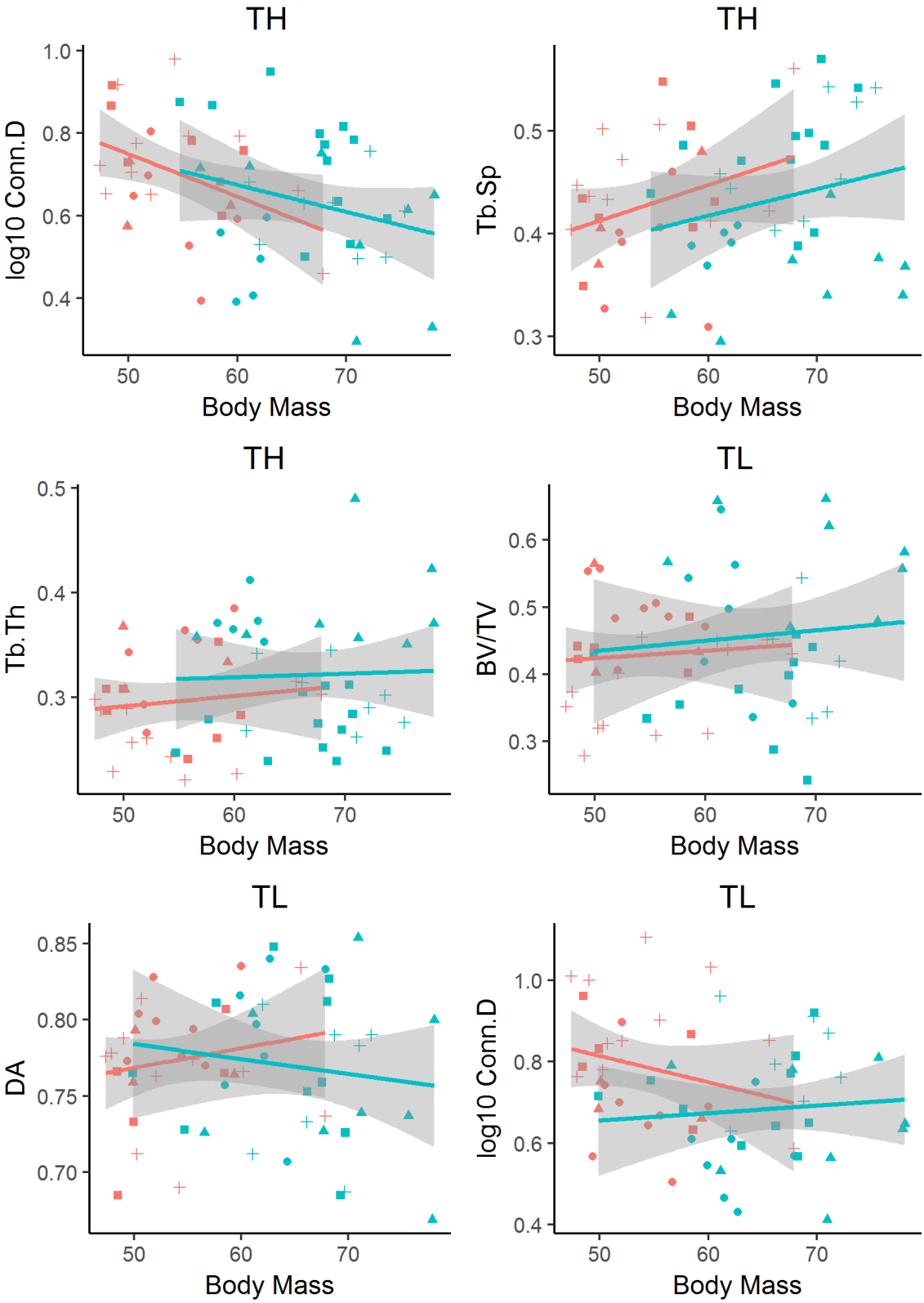
TH
log10 Conn.D
1.0
0.8
0.6
0.4
50
60
70
Body Mass
TH
Tb.Sp
0.5
0.4
0.3
50
60
70
Body Mass
TH
Tb.Th
0.5
0.4
0.3
50
60
70
Body Mass
TL
BV/TV
0.6
0.5
0.4
0.3
50
60
70
Body Mass
TL
DA
0.85
0.80
0.75
0.70
50
60
70
Body Mass
TL
log10 Conn.D
1.0
0.8
0.6
0.4
50
60
70
Body Mass

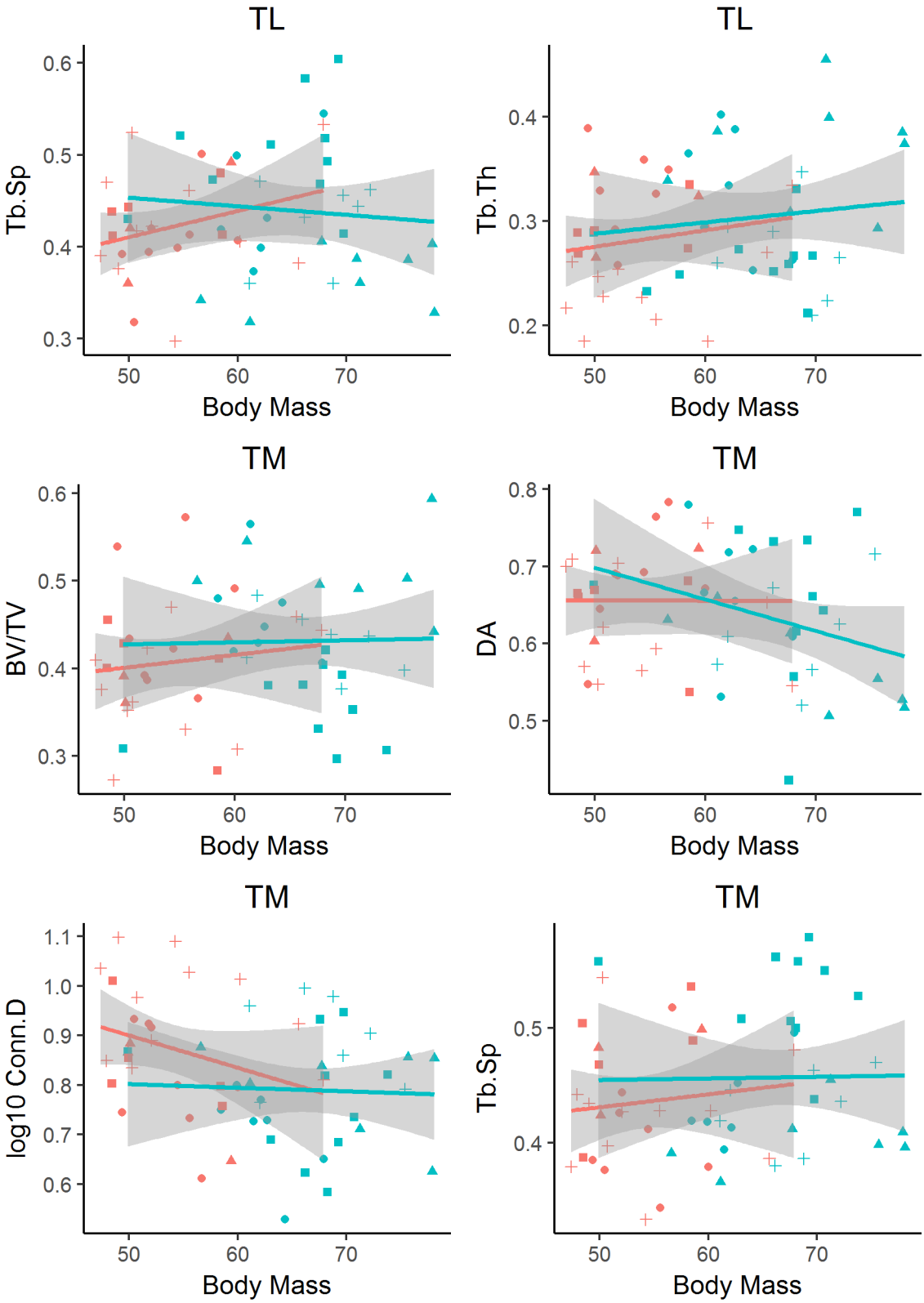
TL
Tb.Sp
0.6
0.5
0.4
0.3
50
60
70
Body Mass
TL
Tb.Th
0.4
0.3
0.2
50
60
70
Body Mass
TM
BV/TV
0.6
0.5
0.4
0.3
50
60
70
Body Mass
TM
DA
0.8
0.7
0.6
0.5
50
60
70
Body Mass
TM
log10 Conn.D
1.1
1.0
0.9
0.8
0.7
0.6
50
60
70
Body Mass
TM
Tb.Sp
0.5
0.4
50
60
70
Body Mass

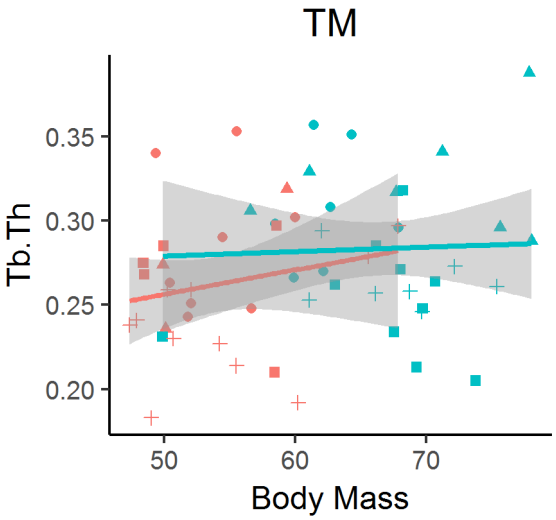

Figure 4.4.2. Plots of regressions of body mass and trabecular properties in males and females in the talus.

First metatarsal

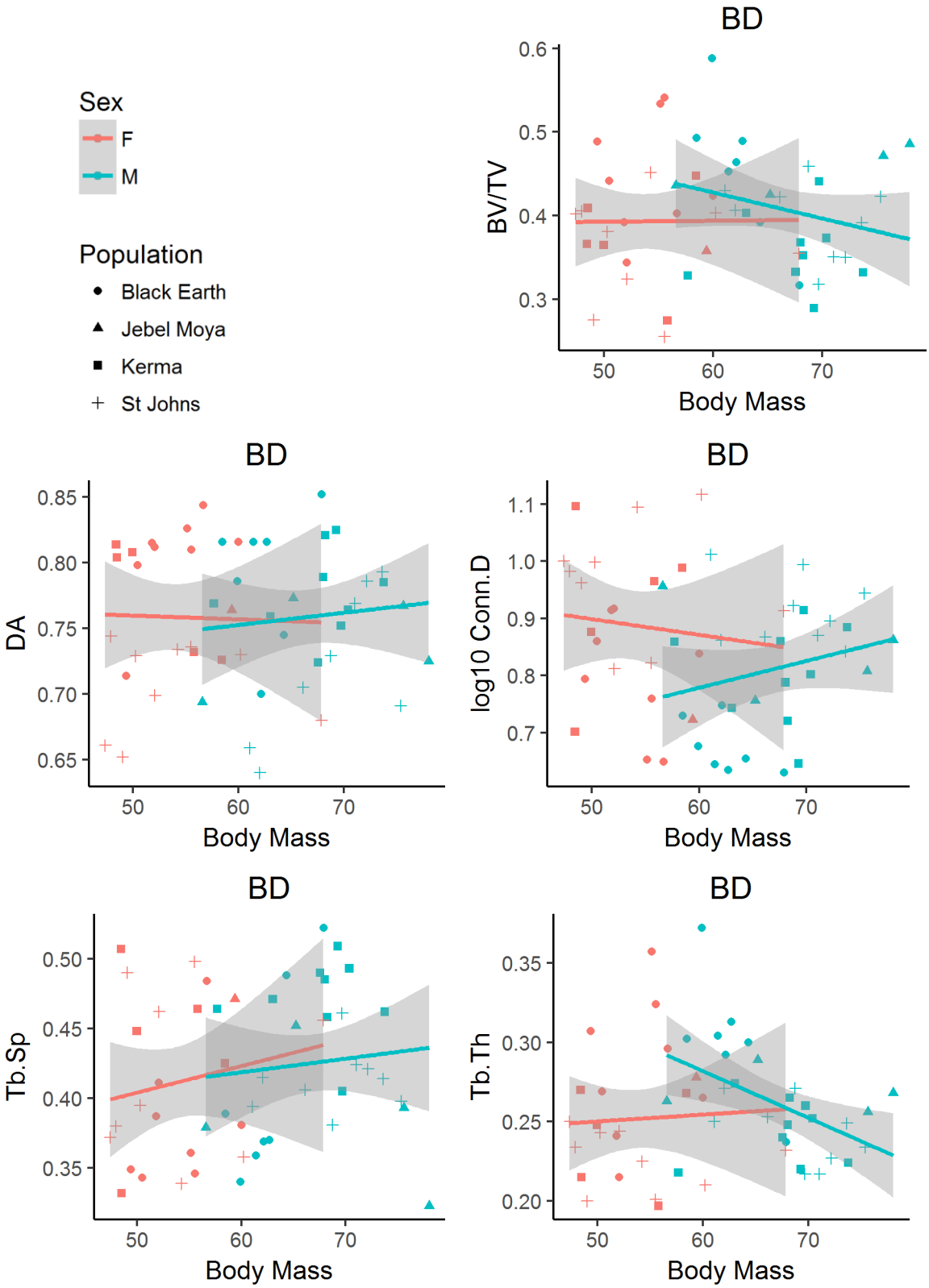

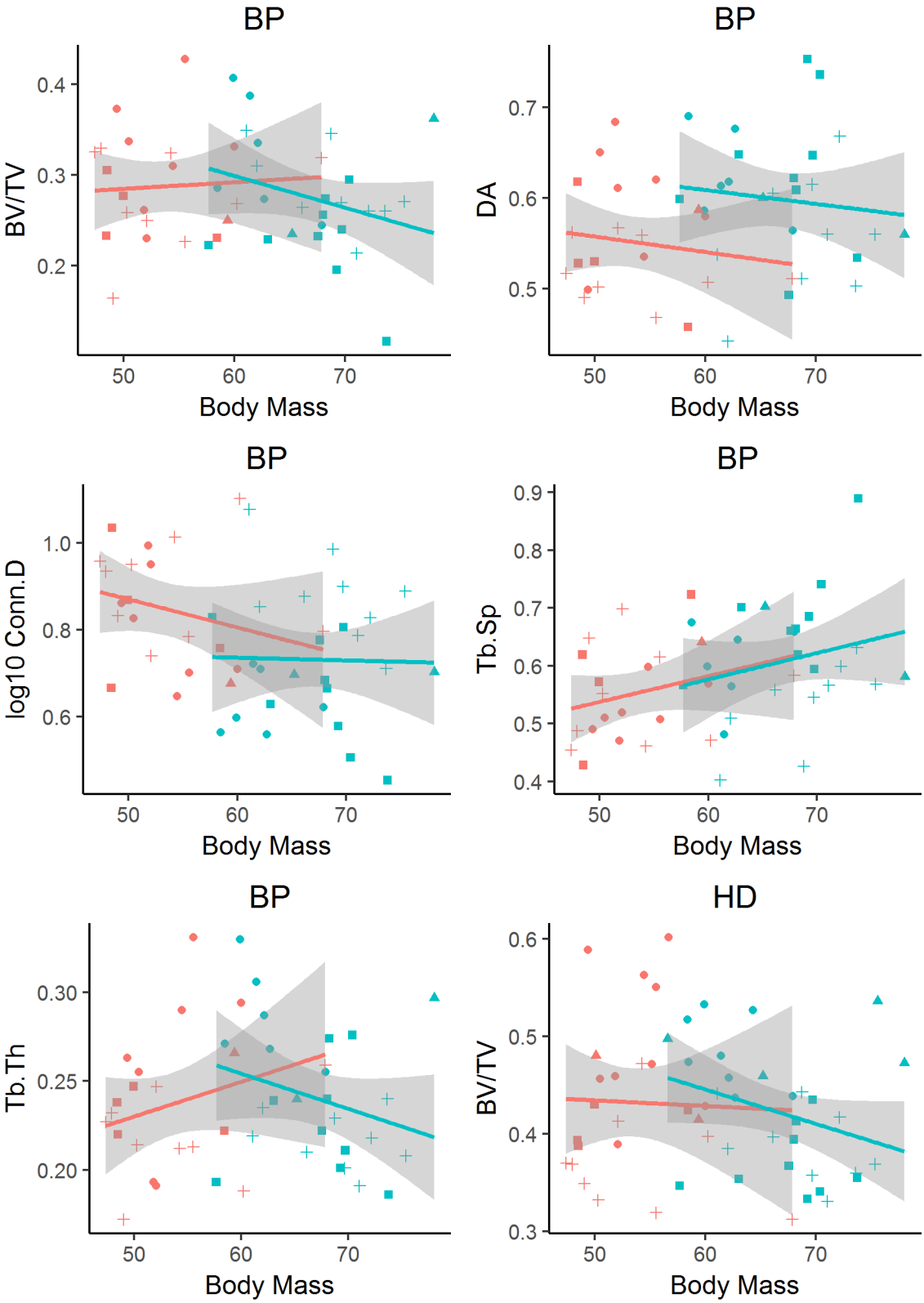
BP
BV/TV
0.4
0.3
0.2
50
60
70
Body Mass
BP
DA
0.7
0.6
0.5
50
60
70
Body Mass
BP
log10 Conn.D
1.0
0.8
0.6
50
60
70
Body Mass
BP
Tb.Sp
0.9
0.8
0.7
0.6
0.5
0.4
50
60
70
Body Mass
BP
Tb.Th
0.30
0.25
0.20
50
60
70
Body Mass
HD
BV/TV
0.6
0.5
0.4
0.3
50
60
70
Body Mass

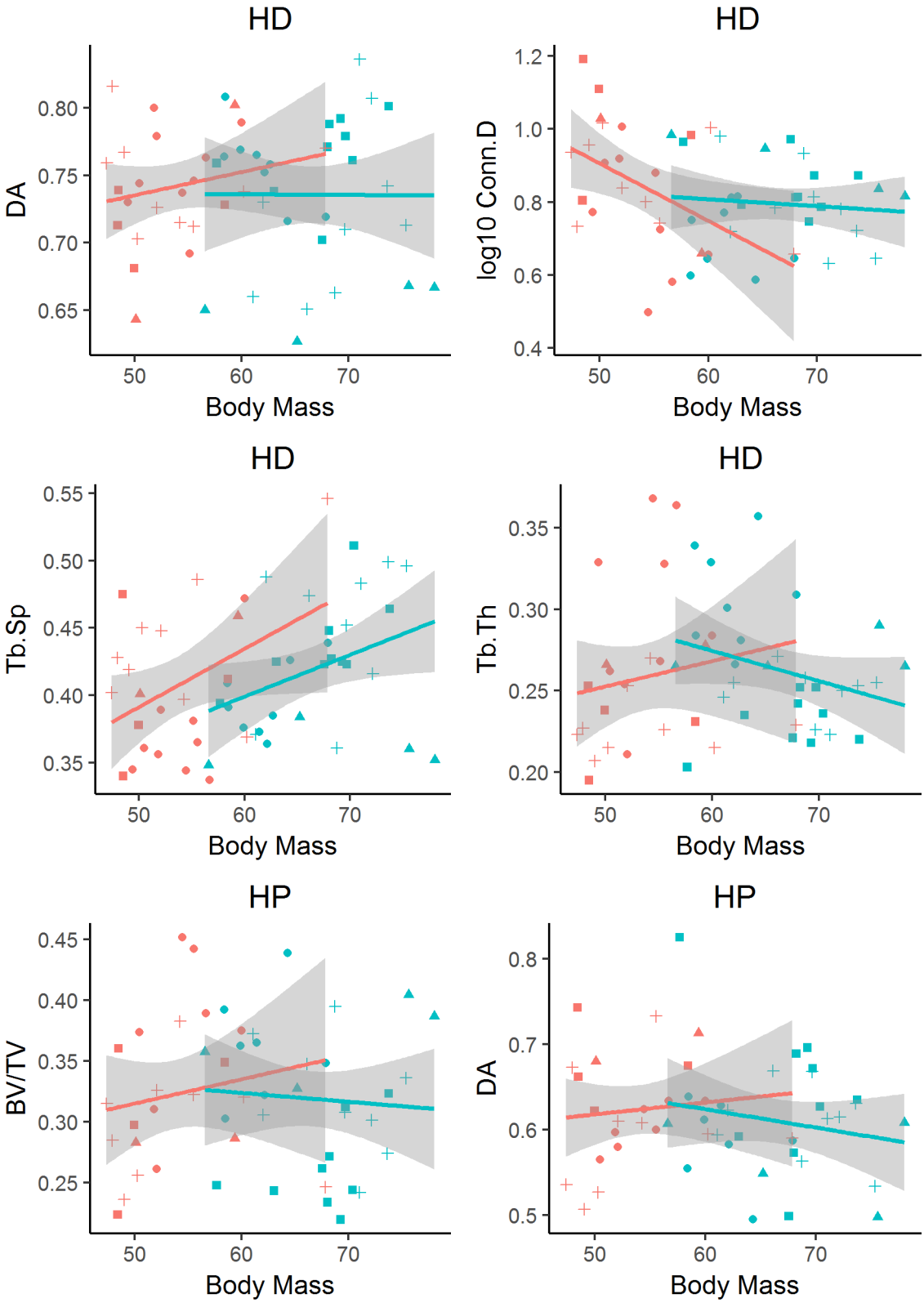
HD
DA
0.80
0.75
0.70
0.65
50
60
70
Body Mass
HD
log10 Conn.D
1.2
1.0
0.8
0.6
0.4
50
60
70
Body Mass
HD
Tb.Sp
0.55
0.50
0.45
0.40
0.35
50
60
70
Body Mass
HD
Tb.Th
0.35
0.30
0.25
0.20
50
60
70
Body Mass
HP
BV/TV
0.45
0.40
0.35
0.30
0.25
50
60
70
Body Mass
HP
DA
0.8
0.7
0.6
0.5
50
60
70
Body Mass

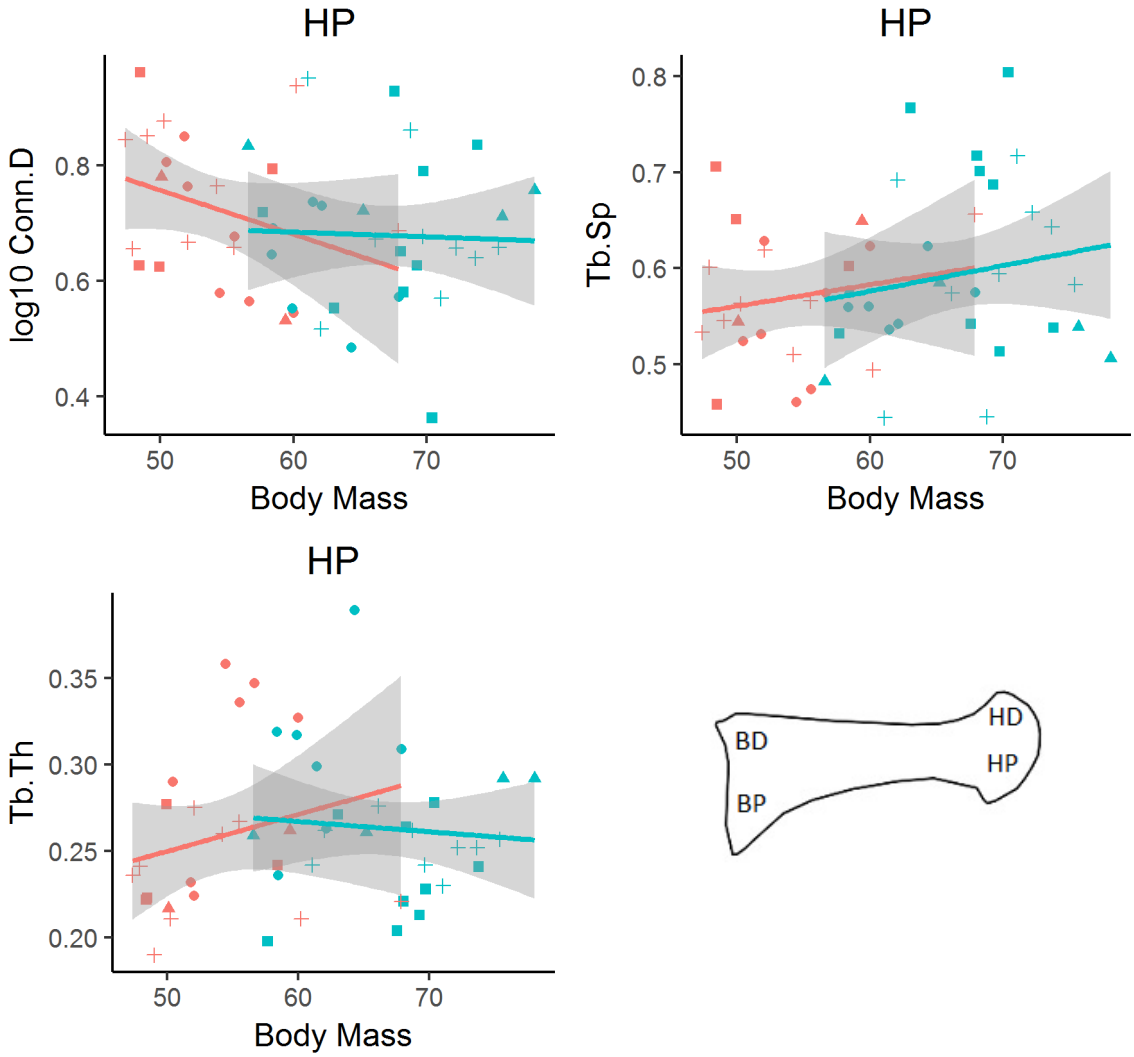

Figure 4.4.3. Regressions of body mass and trabecular properties in males and females in the first metatarsal. Achilles tendon (AT), calcaneal tuber (CT), plantar ligaments (PL), posterior talar facet (PP: posterior, PC: central, PA: anterior), calcaneocuboid (CC), dorsal base (BD), plantar base (BP), dorsal head (HD), plantar head (HP), talar head (TH), anterior calcaneal facet (ACF), posterior calcaneal facet (PCF), trochlea (lateral: TL, central: TC, medial: TM).

Appendix 5.

Appendix 5.1 PCA in a pooled population sample

Table 5.1.1. Variance explained by each principal component and importance of variables to principal components in the calcaneus. Variables larger than 1.9 are in bold.

Calcaneus		**PC1**	**PC2**	**PC3**	**PC4**	**PC5**
Standard deviation		3.77	2.97	1.46	1.24	1.15
Proportion of Variance		0.41	0.25	0.06	0.04	0.04
Cumulative Proportion		0.41	0.66	0.72	0.76	0.80
	Variables	**PC1**	**PC2**	**PC3**	**PC4**	**PC5**
Achilles tendon (AT)	BV/TV	**-0.225**	0.126	0.080	-0.085	0.078
	Tb.Th	**-0.235**	-0.039	-0.015	0.019	0.097
	Res. DA	0.058	0.086	**0.324**	0.155	**-0.309**
	Res. Tb.Sp	0.152	**-0.233**	-0.111	0.158	-0.046
	Res. Conn.D	0.004	**0.254**	-0.077	**-0.289**	0.141
Calcaneocuboid (CC)	BV/TV	**-0.231**	0.029	0.146	-0.022	-0.007
	Tb.Th	**-0.214**	-0.130	0.122	-0.002	0.034
	Res. DA	-0.035	**-0.209**	0.015	**-0.388**	-0.032
	Res. Tb.Sp	0.148	**-0.211**	-0.128	-0.036	0.014
	Res. Conn.D	0.094	**0.287**	-0.023	0.104	-0.066
Calcaneal tuber (CT)	BV/TV	**-0.241**	0.070	-0.043	-0.004	0.017
	Tb.Th	**-0.226**	-0.052	-0.095	0.141	0.046
	Res. DA	-0.023	**-0.205**	0.103	-0.141	**-0.339**
	Res. Tb.Sp	0.173	**-0.222**	-0.031	0.138	-0.052
	Res. Conn.D	-0.021	**0.274**	-0.066	-0.196	**0.265**
PTF anterior (PA)	BV/TV	**-0.241**	0.038	0.014	0.168	-0.011
	Tb.Th	**-0.223**	-0.116	-0.019	0.187	-0.072
	Res. DA	-0.006	-0.101	**0.446**	**-0.208**	-0.113
	Res. Tb.Sp	0.158	**-0.209**	-0.098	-0.018	-0.069
	Res. Conn.D	0.094	**0.275**	-0.042	-0.043	0.198
PTF central (PC)	BV/TV	**-0.250**	-0.015	-0.018	0.076	-0.114
	Tb.Th	**-0.220**	-0.137	-0.083	0.106	-0.068
	Res. DA	-0.065	**-0.190**	0.052	**-0.454**	-0.010
	Res. Tb.Sp	0.189	-0.161	-0.118	0.106	0.117
	Res. Conn.D	0.140	**0.246**	0.127	0.000	0.050
PTF posterior (PP)	BV/TV	**-0.245**	0.034	-0.029	-0.017	0.009
	Tb.Th	**-0.231**	-0.088	-0.038	0.056	0.080
	Res. DA	-0.113	-0.140	-0.132	**-0.425**	-0.034
	Res. Tb.Sp	0.138	**-0.205**	-0.073	0.172	0.103
	Res. Conn.D	0.130	**0.246**	0.081	-0.008	-0.121
Plantar ligaments (PL)	BV/TV	**-0.218**	0.081	0.018	0.123	-0.102
	Tb.Th	**-0.231**	-0.043	0.053	0.111	**0.212**
	Res. DA	0.080	0.021	**0.574**	0.042	-0.107
	Res. Tb.Sp	0.122	-0.180	**0.194**	0.000	**0.493**
	Res. Conn.D	0.025	**0.190**	**-0.371**	-0.113	**-0.481**

Table 5.1.2. Summary statistics and t-tests between sexes for PCA of combined calcaneus VOIs.

Calcaneus						**Levene's Test**		**t-test**		
	Sex	**N**	**Mean**	**S.D**	**S.E.**	**F**	***p***	**t**	**df**	***p***
PC1	M	21	-.0296	4.1574	.9072	2.60	.116	-.054	35	.957
	F	16	.0388	3.3306	.8327					
PC2	M	21	-.9392	2.7953	.6100	0.00	.970	-2.339	35	**.025**
	F	16	1.2327	2.8018	.7005					
PC3	M	21	-.1047	1.3118	.2863	0.70	.407	-.494	35	.625
	F	16	.1374	1.6739	.4185					
PC4	M	21	-.0927	1.3085	.2855	0.00	.966	-.516	35	.609
	F	16	.1216	1.1716	.2929					
PC5	M	21	.0669	1.1387	.2485	0.01	.908	.401	35	.691
	F	16	-.0878	1.1948	.2987					

Table 5.1.3. Variance explained by each principal component and importance of variables to principal components in the first metatarsal. Variables larger than 1.9 are in bold

MT1		**PC1**	**PC2**	**PC3**	**PC4**	**PC5**
Standard deviation		2.63	2.29	1.39	1.17	1.03
Proportion of Variance		0.35	0.26	0.10	0.07	0.05
Cumulative Proportion		0.35	0.61	0.71	0.77	0.83
	Variable	**PC1**	**PC2**	**PC3**	**PC4**	**PC5**
Base Dorsal (BD)	BV/TV	**0.327**	-0.094	0.012	-0.102	0.180
	Tb.Th	**0.325**	0.092	0.026	0.117	**0.259**
	Res. DA	0.100	**0.191**	**-0.464**	-0.061	**-0.274**
	Res. Tb.Sp	**-0.240**	**0.248**	0.023	**0.328**	-0.064
	Res. Conn.D	-0.143	**-0.336**	0.118	**-0.194**	0.008
Base Plantar (BP)	BV/TV	**0.320**	-0.101	0.158	**-0.192**	0.037
	Tb.Th	**0.318**	0.151	0.099	0.061	0.136
	Res. DA	0.094	**0.206**	**-0.398**	**-0.287**	0.030
	Res. Tb.Sp	-0.123	**0.291**	-0.104	**0.392**	**0.218**
	Res. Conn.D	-0.062	**-0.374**	0.121	**-0.258**	-0.169
Head Dorsal (HD)	BV/TV	**0.338**	-0.062	-0.175	0.109	0.017
	Tb.Th	**0.340**	0.096	0.083	0.102	-0.074
	Res. DA	-0.024	0.182	**-0.249**	**-0.513**	**0.230**
	Res. Tb.Sp	-0.165	**0.208**	**0.486**	-0.060	-0.049
	Res. Conn.D	-0.144	**-0.253**	**-0.314**	**0.263**	0.088
Head Plantar (HP)	BV/TV	**0.278**	**-0.197**	0.038	0.173	**-0.269**
	Tb.Th	**0.304**	0.110	0.165	0.122	-0.214
	Res. DA	-0.037	0.171	-0.103	-0.073	**-0.705**
	Res. Tb.Sp	-0.114	**0.331**	0.145	**-0.210**	0.152
	Res. Conn.D	-0.077	**-0.357**	**-0.237**	0.177	0.130

Table 5.1.4. Summary statistics and t-tests between sexes for PCA of combined MT1 VOIs.

MT1						Levene's Test		t-test		
Sex		**N**	**Mean**	**S.D**	**S.E.**	**F**	***p***	**t**	**df**	***p***
PC1	M	22	.224	2.672	.598	.166	.686	.547	36	.588
	F	18	-.249	2.641	.622					
PC2	M	22	.400	2.397	.536	.081	.777	1.139	36	.262
	F	18	-.444	2.146	.506					
PC3	M	22	-.104	1.461	.327	.015	.904	-.482	36	.633
	F	18	.116	1.346	.317					.
PC4	M	22	.035	1.162	.260	.623	.435	.192	36	.849
	F	18	-.039	1.213	.286					
PC5	M	22	-.017	1.042	.233	.054	.817	-.108	36	.915
	F	18	.019	1.056	.249					

Table 5.1.5. Summary statistics and t-tests between sexes for PCA of combined talus VOIs.

Talus						Levene's Test		t-test		
Sex		**N**	**Mean**	**S.D**	**S.E.**	**F**	***p***	**t**	**df**	***p***
PC1	M	13	-.202	3.341	.927	.003	.959	-.269	32	.790
	F	21	.125	3.499	.764					
PC2	M	13	-.597	2.570	.713	.000	.987	-1.029	32	.311
	F	21	.369	2.714	.592					
PC3	M	13	.443	1.526	.423	.634	.432	1.256	32	.218
	F	21	-.274	1.672	.365					
PC4	M	13	-.386	1.406	.390	1.386	.248	-1.388	32	.175
	F	21	.239	1.189	.259					
PC5	M	13	.450	.939	.260	1.483	.232	1.874	32	.070
	F	21	-.279	1.190	.260					

Table 5.1.6. Variance explained by each principal component and importance of variables to principal components in the talus. Variables larger than 1.9 are in bold.

		PC1	PC2	PC3	PC4	PC5
Standard deviation		3.39	2.66	1.63	1.29	1.14
Proportion of Variance		0.38	0.24	0.09	0.06	0.04
Cumulative Proportion		0.38	0.62	0.71	0.76	0.81
	Variables	**PC1**	**PC2**	**PC3**	**PC4**	**PC5**
Anterior calcaneal facet (ACF)	BV/TV	-0.190	0.111	**-0.221**	0.109	**-0.412**
	Tb.Th	**-0.218**	0.018	-0.164	**0.338**	**-0.311**
	DA	0.087	**-0.195**	**-0.253**	0.010	-0.015
	Tb.Sp	0.075	**-0.263**	0.187	**0.229**	-0.024
	Conn.D	0.073	**0.250**	0.108	**-0.358**	0.169
Posterior calcaneal facet (PCF)	BV/TV	**-0.266**	0.054	0.085	-0.065	0.092
	Tb.Th	**-0.278**	-0.031	0.100	0.054	0.138
	DA	-0.019	-0.061	**-0.295**	**0.402**	0.177
	Tb.Sp	0.072	**-0.277**	-0.022	0.136	-0.027
	Conn.D	**0.236**	0.159	0.022	-0.101	**-0.205**
Trochlea central (TC)	BV/TV	**-0.264**	0.055	0.012	-0.170	-0.004
	Tb.Th	**-0.264**	-0.047	0.068	-0.126	0.050
	DA	-0.012	-0.042	**-0.408**	-0.091	**0.405**
	Tb.Sp	0.156	**-0.240**	0.114	0.128	-0.101
	Conn.D	0.172	0.168	0.071	**0.224**	-0.078
Trochlea lateral (TL)	BV/TV	**-0.248**	0.091	0.154	0.062	0.110
	Tb.Th	**-0.246**	-0.085	**0.219**	0.013	0.158
	DA	-0.133	-0.042	**-0.195**	**0.372**	**0.367**
	Tb.Sp	0.086	**-0.321**	0.035	-0.073	-0.058
	Conn.D	0.180	**0.250**	-0.049	0.043	**-0.244**
Trochlea medial (TM)	BV/TV	**-0.258**	0.090	0.008	0.004	-0.159
	Tb.Th	**-0.254**	-0.087	0.129	-0.019	-0.090
	DA	-0.113	-0.154	**-0.345**	**-0.348**	-0.046
	Tb.Sp	0.133	**-0.275**	0.168	-0.030	-0.022
	Conn.D	0.118	**0.315**	-0.048	**0.190**	0.000
Talar head (TH)	BV/TV	**-0.230**	0.103	0.047	0.033	-0.158
	Tb.Th	**-0.235**	-0.073	0.151	0.115	-0.184
	DA	-0.066	-0.121	**-0.441**	**-0.201**	**-0.246**
	Tb.Sp	0.115	**-0.301**	0.139	-0.027	-0.080
	Conn.D	0.117	**0.311**	0.018	0.113	0.152

Appendix 5.2 PCA using combined VOIs per bone

Black Earth

Table 5.2.1. Variance explained by each principal component and importance of variables to principal components in the calcaneus – Black Earth.

Calcaneus		**PC1**	**PC2**	**PC3**	**PC4**	**PC5**
Standard deviation		4.1490	2.2183	1.85175	1.76516	1.47134
Proportion of Variance		0.4918	0.1406	0.09797	0.08902	0.06185
Cumulative Proportion		0.4918	0.6324	0.73040	0.81942	0.88128
	Variable	**PC1**	**PC2**	**PC3**	**PC4**	**PC5**
Achilles tendon (AT)	BV/TV	-0.22	-0.07	0.02	0.07	0.04
	Tb.Th	-0.19	-0.10	-0.07	0.25	0.07
	DA	0.04	-0.09	0.34	-0.19	-0.06
	Residual Tb.Sp	0.22	0.02	-0.11	0.11	0.12
	Residual Conn.D	-0.15	-0.17	0.11	-0.14	-0.31
Calcaneo cuboid (CC)	BV/TV	-0.16	-0.16	0.13	-0.10	-0.30
	Tb.Th	-0.02	-0.15	-0.16	0.08	-0.40
	DA	0.16	-0.23	-0.10	0.12	-0.18
	Residual Tb.Sp	0.19	0.09	-0.27	0.11	0.17
	Residual Conn.D	-0.17	0.14	0.17	-0.23	0.13
Calcaneal tuber (CT)	BV/TV	-0.22	-0.09	0.03	0.09	0.08
	Tb.Th	-0.22	0.02	-0.11	0.17	0.05
	DA	0.19	-0.22	0.09	-0.02	0.04
	Residual Tb.Sp	0.22	0.04	-0.12	-0.11	-0.07
	Residual Conn.D	-0.12	0.13	-0.12	0.30	-0.29
PTF anterior (PA)	BV/TV	-0.19	-0.03	-0.27	-0.08	0.15
	Tb.Th	-0.15	-0.08	-0.32	-0.18	0.12
	DA	0.12	-0.35	0.01	-0.13	-0.05
	Residual Tb.Sp	0.21	0.00	-0.04	-0.10	-0.20
	Residual Conn.D	0.02	0.29	0.29	0.23	-0.15
PTF central (PC)	BV/TV	-0.22	-0.13	0.03	-0.09	0.10
	Tb.Th	-0.17	-0.18	-0.07	-0.03	0.35
	DA	0.12	-0.26	0.11	-0.19	0.20
	Residual Tb.Sp	0.20	0.12	-0.23	0.08	0.03
	Residual Conn.D	0.03	0.39	0.22	-0.01	0.15
PTF posterior (PP)	BV/TV	-0.22	-0.10	0.13	0.15	0.06
	Tb.Th	-0.14	-0.09	0.21	0.33	0.08
	DA	0.04	-0.31	-0.09	0.29	0.20
	Residual Tb.Sp	0.22	0.11	-0.10	0.02	0.02
	Residual Conn.D	-0.05	0.14	-0.19	-0.42	0.09
Plantar ligaments (PL)	BV/TV	-0.17	0.08	-0.26	-0.10	-0.21
	Tb.Th	-0.11	0.03	-0.29	0.12	-0.14
	DA	0.17	-0.28	0.02	-0.06	-0.10
	Residual Tb.Sp	0.22	-0.02	0.06	0.17	0.11
	Residual Conn.D	-0.20	0.14	-0.03	-0.15	-0.11

Table 5.2.2. Variance explained by each principal component and importance of variables to principal components in the first metatarsal – Black Earth.

MT1		**PC1**	**PC2**	**PC3**	**PC4**	**PC5**
Standard deviation		3.0063	2.0426	1.6107	1.26643	1.1279
Proportion of Variance		0.4519	0.2086	0.1297	0.08019	0.0636
Cumulative Proportion		0.4519	0.6605	0.7902	0.87040	0.9340
	Variables	**PC1**	**PC2**	**PC3**	**PC4**	**PC5**
Base Dorsal (BD)	BV/TV	0.26	-0.21	-0.23	0.03	-0.12
	Tb.Th	0.30	-0.14	-0.17	-0.05	-0.12
	DA	-0.03	0.27	0.03	0.05	0.66
	Residual Tb.Sp	-0.15	0.34	0.18	-0.33	0.15
	Residual Conn.D	-0.24	-0.10	-0.05	0.39	-0.04
Base Plantar (BP)	BV/TV	0.29	-0.18	0.04	0.22	-0.06
	Tb.Th	0.32	0.00	-0.02	0.06	-0.13
	DA	-0.11	-0.30	-0.29	-0.17	0.35
	Residual Tb.Sp	0.03	0.27	-0.29	-0.44	-0.16
	Residual Conn.D	-0.26	-0.15	0.20	0.29	0.10
Head Dorsal (HD)	BV/TV	0.29	-0.18	-0.02	-0.09	0.19
	Tb.Th	0.31	0.09	0.06	-0.11	0.19
	DA	-0.09	-0.07	-0.54	0.22	0.15
	Residual Tb.Sp	-0.05	0.42	-0.07	0.33	0.00
	Residual Conn.D	-0.28	-0.24	0.07	-0.01	-0.07
Head Plantar (HP)	BV/TV	0.27	-0.02	0.24	0.23	0.21
	Tb.Th	0.27	0.15	0.24	0.25	0.02
	DA	0.13	0.13	-0.43	0.16	0.27
	Residual Tb.Sp	-0.19	0.26	-0.24	0.22	-0.28
	Residual Conn.D	-0.19	-0.36	0.08	-0.12	0.19

Table 5.2.3. Variance explained by each principal component and importance of variables to principal components in the talus – Black Earth.

Talus		**PC1**	**PC2**	**PC3**	**PC4**	**PC5**
Standard deviation		3.47	2.43	2.15	1.65	1.55
Proportion of Variance		0.40	0.20	0.15	0.09	0.08
Cumulative Proportion		0.40	0.60	0.75	0.84	0.92
	Variables	**PC1**	**PC2**	**PC3**	**PC4**	**PC5**
Anterior calcaneal facet (ACF)	BV/TV	-0.20	-0.02	-0.15	0.37	-0.11
	Tb.Th	-0.16	0.13	-0.01	0.41	-0.20
	DA	0.26	0.04	0.04	-0.12	-0.23
	Residual Tb.Sp	0.23	0.12	0.16	-0.14	0.21
	Residual Conn.D	-0.22	-0.20	-0.11	-0.04	0.22
Posterior calcaneal facet (PCF)	BV/TV	-0.20	0.21	0.10	-0.06	0.06
	Tb.Th	-0.12	0.34	0.08	-0.11	0.07
	DA	-0.06	0.05	0.30	0.30	-0.28
	Residual Tb.Sp	0.26	-0.02	-0.17	0.03	0.04
	Residual Conn.D	-0.07	-0.34	-0.19	-0.04	0.13
Talar head (TH)	BV/TV	-0.10	0.15	-0.18	-0.27	-0.26
	Tb.Th	0.00	0.19	-0.25	-0.31	-0.14
	DA	0.01	-0.32	0.25	-0.16	-0.06
	Residual Tb.Sp	0.20	0.06	0.00	0.28	0.21
	Residual Conn.D	-0.20	0.00	0.25	0.23	0.04
Trochlea lateral (TL)	BV/TV	-0.07	0.15	0.19	0.10	0.43
	Tb.Th	0.09	0.29	0.15	-0.01	0.31
	DA	-0.15	0.05	0.28	0.04	-0.36
	Residual Tb.Sp	0.22	0.08	-0.07	-0.05	-0.32
	Residual Conn.D	-0.20	-0.23	-0.17	0.09	0.05
Trochlea central (TC)	BV/TV	-0.23	0.14	-0.09	-0.09	0.07
	Tb.Th	-0.17	0.25	0.05	-0.15	0.07
	DA	0.15	-0.07	-0.30	0.22	-0.02
	Residual Tb.Sp	0.25	0.04	0.18	0.13	-0.11
	Residual Conn.D	-0.25	-0.19	0.05	-0.07	-0.02
Trochlea medial (TM)	BV/TV	-0.19	0.21	-0.24	0.07	-0.04
	Tb.Th	-0.14	0.31	-0.18	0.07	-0.05
	DA	0.16	0.06	-0.30	0.27	0.12
	Residual Tb.Sp	0.26	-0.02	0.18	0.06	-0.01
	Residual Conn.D	-0.21	-0.22	0.17	-0.09	0.02

Table 5.2.4. Significant MANOVA's – Black Earth.

Calcaneus	**Black Earth**	**Df**	**Pillai**	**approx F**	**num Df**	**den Df**	***p***
All PCs	Sex	1	0.54123	1.9662	3	5	0.2375
	Residuals	7					
		Df	**Sum Sq**	**Mean Sq**	**F value**	***p***	
PC1	Sex	1	11.446	11.446	0.6345	0.4519	
	Residuals	7	126.269	18.038			
PC2	Sex	1	18.031	18.0307	5.916	**0.04527**	
	Residuals	7	21.334	3.0478			
PC3	Sex	1	0.0021	0.0021	5.00E-04	0.9822	
	Residuals	7	27.4298	3.9185			
MT1	**Black Earth**	**Df**	**Pillai**	**approx F**	**num Df**	**den Df**	***p***
All PCs	Sex	1	0.19689	0.49032	3	6	0.7017
	Residuals	8					
		Df	**Sum Sq**	**Mean Sq**	**F value**	***p***	
PC1	Sex	1	11.665	11.665	1.3394	0.2805	
	Residuals	8	69.675	8.7094			
PC2	Sex	1	0.865	0.8651	0.1887	0.6755	
	Residuals	8	36.685	4.5856			
PC3	Sex	1	0.7108	0.71077	0.2512	0.6297	
	Residuals	8	22.6376	2.8297			
Talus	**Black Earth**	**Df**	**Pillai**	**approx F**	**num Df**	**den Df**	***p***
All PCs	Sex	1	0.28172	0.52296	3	4	0.6894
	Residuals	6					
		Df	**Sum Sq**	**Mean Sq**	**F value**	***p***	
PC1	Sex	1	1.073	1.0732	0.0774	0.7902	
	Residuals	6	83.188	13.8646			
PC2	Sex	1	7.571	7.5711	1.3441	0.2904	
	Residuals	6	33.797	5.6328			
PC3	Sex	1	2.7917	2.7917	0.5643	0.4809	
	Residuals	6	29.6824	4.9471			

Kerma

Table 5.2.5. Variance explained by each principal component and importance of variables to principal components in the calcaneus – Kerma.

Calcaneus		**PC1**	**PC2**	**PC3**	**PC4**	**PC5**
Standard deviation		3.5302	3.0663	1.9395	1.53259	1.3950
Proportion of Variance		0.3561	0.2686	0.1075	0.06711	0.0556
Cumulative Proportion		0.3561	0.6247	0.7322	0.79928	0.8549
	Variable	**PC1**	**PC2**	**PC3**	**PC4**	**PC5**
Achilles tendon (AT)	BV/TV	0.25	0.01	-0.15	0.02	0.20
	Tb.Th	0.14	-0.16	-0.09	0.03	0.43
	DA	0.10	-0.12	0.00	-0.16	0.16
	Residual Tb.Sp	-0.23	-0.13	0.13	-0.09	-0.02
	Residual Conn.D	0.09	0.26	-0.11	0.16	-0.16
Calcaneo cuboid (CC)	BV/TV	0.23	-0.11	-0.03	-0.16	-0.17
	Tb.Th	0.14	-0.25	-0.13	-0.08	-0.06
	DA	-0.11	-0.19	-0.23	-0.10	-0.27
	Residual Tb.Sp	-0.24	-0.06	-0.12	0.21	0.08
	Residual Conn.D	0.09	0.28	0.15	-0.05	0.06
Calcaneal tuber (CT)	BV/TV	0.19	-0.13	-0.04	0.27	0.06
	Tb.Th	0.05	-0.21	0.09	0.39	0.10
	DA	-0.06	-0.14	-0.30	0.00	0.19
	Residual Tb.Sp	-0.26	-0.10	0.04	0.03	0.13
	Residual Conn.D	0.17	0.22	0.01	0.07	-0.21
PTF anterior (PA)	BV/TV	0.25	-0.10	0.11	-0.08	-0.18
	Tb.Th	0.13	-0.26	0.12	-0.17	0.01
	DA	-0.09	0.03	-0.39	-0.23	0.07
	Residual Tb.Sp	-0.25	0.01	0.05	0.06	0.29
	Residual Conn.D	0.15	0.23	0.04	0.11	-0.13
PTF central (PC)	BV/TV	0.22	-0.17	0.02	0.07	-0.07
	Tb.Th	0.04	-0.29	0.15	-0.09	-0.07
	DA	-0.13	-0.02	-0.38	0.10	-0.19
	Residual Tb.Sp	-0.24	-0.02	0.19	-0.07	0.08
	Residual Conn.D	0.13	0.25	-0.17	-0.01	0.10
PTF posterior (PP)	BV/TV	0.15	-0.21	-0.05	0.30	-0.15
	Tb.Th	0.05	-0.25	0.14	0.16	-0.08
	DA	-0.06	-0.09	-0.23	0.28	0.20
	Residual Tb.Sp	-0.19	0.01	0.29	-0.23	0.03
	Residual Conn.D	0.14	0.25	-0.13	-0.02	0.06
Plantar ligaments (PL)	BV/TV	0.24	-0.05	0.06	-0.15	0.15
	Tb.Th	0.18	-0.15	-0.04	-0.06	0.10
	DA	0.07	-0.05	-0.31	-0.43	0.08
	Residual Tb.Sp	-0.21	-0.03	-0.17	0.11	-0.25
	Residual Conn.D	0.13	0.18	0.08	0.12	0.36

Table 5.2.6. Variance explained by each principal component and importance of variables to principal components in the first metatarsal – Kerma.

MT1		**PC1**	**PC2**	**PC3**	**PC4**	**PC5**
Standard deviation		2.7992	2.1598	1.6103	1.2513	1.1164
Proportion of Variance		0.3918	0.2332	0.1296	0.0783	0.0623
Cumulative Proportion		0.3918	0.6250	0.7547	0.8329	0.8953
	Variables	**PC1**	**PC2**	**PC3**	**PC4**	**PC5**
Base Dorsal (BD)	BV/TV	0.08	-0.37	0.10	0.20	0.14
	Tb.Th	-0.19	-0.33	0.17	-0.14	0.06
	DA	-0.07	0.14	-0.31	0.14	0.47
	Residual Tb.Sp	-0.30	0.11	0.04	-0.36	-0.07
	Residual Conn.D	0.31	-0.11	0.14	0.25	-0.09
Base Plantar (BP)	BV/TV	0.03	-0.30	-0.43	0.07	-0.13
	Tb.Th	-0.17	-0.35	-0.18	0.11	-0.21
	DA	-0.26	0.16	-0.27	0.26	-0.14
	Residual Tb.Sp	-0.16	0.04	0.53	0.13	0.03
	Residual Conn.D	0.29	-0.10	-0.28	-0.19	-0.08
Head Dorsal (HD)	BV/TV	0.11	-0.33	0.05	-0.22	0.41
	Tb.Th	-0.27	-0.22	0.14	-0.20	0.14
	DA	-0.05	0.33	0.11	0.42	-0.06
	Residual Tb.Sp	-0.29	-0.05	0.15	0.02	0.07
	Residual Conn.D	0.33	-0.10	-0.03	0.04	-0.06
Head Plantar (HP)	BV/TV	0.28	-0.14	0.21	0.26	0.19
	Tb.Th	-0.12	-0.29	0.08	0.43	-0.03
	DA	-0.01	0.17	-0.16	0.09	0.63
	Residual Tb.Sp	-0.32	-0.17	-0.11	0.09	-0.02
	Residual Conn.D	0.29	0.12	0.20	-0.22	-0.08

Table 5.2.7. Variance explained by each principal component and importance of variables to principal components in the talus– Kerma.

Talus		**PC1**	**PC2**	**PC3**	**PC4**	**PC5**
Standard deviation		3.5718	2.8174	1.62505	1.41412	1.27814
Proportion of Variance		0.4253	0.2646	0.08803	0.06666	0.05445
Cumulative Proportion		0.4253	0.6898	0.77787	0.84453	0.89899
	Variables	**PC1**	**PC2**	**PC3**	**PC4**	**PC5**
Anterior calcaneal facet (ACF)	BV/TV	0.20	-0.08	-0.21	-0.15	-0.03
	Tb.Th	0.23	-0.13	-0.10	-0.13	0.06
	DA	-0.08	-0.31	0.03	0.04	-0.07
	Residual Tb.Sp	0.01	-0.20	0.34	0.07	0.44
	Residual Conn.D	-0.06	0.32	-0.05	0.08	0.09
Posterior calcaneal facet (PCF)	BV/TV	0.25	-0.06	0.20	-0.07	0.07
	Tb.Th	0.25	-0.11	0.12	-0.04	-0.03
	DA	-0.17	0.12	0.29	-0.22	-0.03
	Residual Tb.Sp	-0.20	-0.22	-0.05	-0.04	-0.01
	Residual Conn.D	-0.13	0.22	-0.05	0.19	0.32
Talar head (TH)	BV/TV	0.25	-0.02	-0.27	0.01	0.00
	Tb.Th	0.21	-0.12	-0.32	-0.07	0.04
	DA	-0.17	-0.16	0.23	0.20	-0.29
	Residual Tb.Sp	-0.19	-0.14	0.01	-0.16	0.35
	Residual Conn.D	0.00	0.19	0.37	-0.03	-0.28
Trochlea lateral (TL)	BV/TV	0.26	0.03	0.17	-0.13	0.12
	Tb.Th	0.25	-0.11	0.09	-0.14	0.06
	DA	0.06	-0.14	0.42	-0.31	-0.05
	Residual Tb.Sp	-0.26	-0.10	-0.04	0.10	-0.05
	Residual Conn.D	0.03	0.26	0.05	0.18	0.46
Trochlea central (TC)	BV/TV	0.24	-0.12	0.11	0.18	0.18
	Tb.Th	0.19	-0.23	-0.03	0.08	0.17
	DA	-0.11	-0.26	0.10	0.33	0.10
	Residual Tb.Sp	-0.22	-0.05	-0.26	-0.22	0.01
	Residual Conn.D	0.14	0.29	0.05	0.05	-0.13
Trochlea medial (TM)	BV/TV	0.21	-0.01	0.01	0.35	-0.20
	Tb.Th	0.20	-0.14	-0.04	0.17	-0.17
	DA	-0.11	-0.18	0.00	0.42	0.00
	Residual Tb.Sp	-0.20	-0.18	-0.09	-0.29	0.10
	Residual Conn.D	0.09	0.33	0.04	-0.01	0.07

Table 5.2.8. Significant MANOVA's - Kerma.

Calcaneus	**Kerma**	**Df**	**Pillai**	**approx F**	**num Df**	**den Df**	***p***
all	Sex	1	0.71826	7.6482	3	9	**0.007586**
	Residuals	11					
		Df	**Sum Sq**	**Mean Sq**	**F value**	***p***	
PC1	Sex	1	79.781	79.781	12.579	**0.004578**	
	Residuals	11	69.765	6.342			
PC2	Sex	1	5.492	5.4916	0.5628	0.4689	
	Residuals	11	107.335	9.7577			
PC3	Sex	1	6.143	6.1434	1.733	0.2148	
	Residuals	11	38.995	3.545			

MT1	**Kerma**	**Df**	**Pillai**	**approx F**	**num Df**	**den Df**	***p***
all	Sex	1	0.44022	1.835	3	7	0.2288
	Residuals	9					
		Df	**Sum Sq**	**Mean Sq**	**F value**	***p***	
PC1	Sex	1	7.744	7.7443	0.9871	0.3464	
	Residuals	9	70.609	7.8454			
PC2	Sex	1	15.303	15.3027	4.3939	0.06552	
	Residuals	9	31.344	3.4827			
PC3	Sex	1	0.3455	0.34555	0.1216	0.7354	
	Residuals	9	25.5841	2.84268			

Talus	**Kerma**	**Df**	**Pillai**	**approx F**	**num Df**	**den Df**	***p***
all	Sex	1	0.55131	2.4574	3	6	0.1606
	Residuals	8					
		Df	**Sum Sq**	**Mean Sq**	**F value**	***p***	
PC1	Sex	1	58.69	58.69	8.3651	**0.02013**	
	Residuals	8	56.129	7.016			
PC2	Sex	1	0.415	0.4149	0.0467	0.8343	
	Residuals	8	71.025	8.8782			
PC3	Sex	1	0.8164	0.81639	0.2846	0.6082	
	Residuals	8	22.9507	2.86884			

St. Johns

Table 5.2.9. Variance explained by each principal component and importance of variables to principal components in the calcaneus – St. Johns.

Calcaneus		**PC1**	**PC2**	**PC3**	**PC4**	**PC5**
Standard deviation		3.7233	3.0175	1.6807	1.55608	1.3069
Proportion of Variance		0.3961	0.2601	0.0807	0.06918	0.0488
Cumulative Proportion		0.3961	0.6562	0.7369	0.80612	0.8549
	Variable	**PC1**	**PC2**	**PC3**	**PC4**	**PC5**
Achilles tendon (AT)	BV/TV	-0.09	-0.23	0.27	-0.24	0.02
	Tb.Th	-0.24	-0.04	0.14	-0.13	0.06
	DA	0.09	-0.01	0.03	-0.43	-0.42
	Residual Tb.Sp	-0.10	0.20	-0.10	0.32	0.13
	Residual Conn.D	0.20	-0.16	0.03	0.02	0.18
Calcaneo cuboid (CC)	BV/TV	-0.16	-0.15	0.25	-0.13	0.04
	Tb.Th	-0.24	0.00	0.06	-0.13	0.08
	DA	-0.04	0.14	-0.44	-0.28	-0.06
	Residual Tb.Sp	-0.11	0.19	-0.28	0.05	0.18
	Residual Conn.D	0.19	-0.17	0.15	-0.02	-0.18
Calcaneal tuber (CT)	BV/TV	-0.13	-0.26	-0.13	0.03	-0.15
	Tb.Th	-0.21	-0.12	-0.12	0.17	-0.18
	DA	-0.13	0.06	-0.31	0.16	-0.29
	Residual Tb.Sp	-0.06	0.26	0.24	0.00	-0.01
	Residual Conn.D	0.19	-0.15	-0.09	-0.16	0.23
PTF anterior (PA)	BV/TV	-0.20	-0.18	-0.01	0.18	-0.03
	Tb.Th	-0.25	-0.01	-0.02	0.01	-0.09
	DA	-0.17	0.14	-0.10	0.10	-0.28
	Residual Tb.Sp	-0.04	0.26	0.04	-0.21	0.05
	Residual Conn.D	0.22	-0.16	-0.01	0.04	0.06
PTF central (PC)	BV/TV	-0.22	-0.17	0.02	0.10	0.10
	Tb.Th	-0.25	-0.03	-0.12	-0.03	0.10
	DA	-0.15	0.05	-0.11	-0.24	-0.04
	Residual Tb.Sp	0.04	0.28	-0.09	-0.15	0.03
	Residual Conn.D	0.22	-0.07	0.08	0.12	-0.14
PTF posterior (PP)	BV/TV	-0.18	-0.23	-0.07	0.03	0.02
	Tb.Th	-0.25	-0.10	-0.04	0.03	0.05
	DA	-0.12	-0.01	-0.14	-0.47	0.19
	Residual Tb.Sp	-0.04	0.25	0.17	-0.02	0.13
	Residual Conn.D	0.23	-0.10	-0.11	0.05	-0.18
Plantar ligaments (PL)	BV/TV	-0.15	-0.25	0.06	-0.08	-0.05
	Tb.Th	-0.23	-0.08	0.20	0.04	0.00
	DA	-0.05	0.14	0.14	-0.08	-0.50
	Residual Tb.Sp	-0.05	0.26	0.29	0.09	0.04
	Residual Conn.D	0.13	-0.20	-0.29	-0.08	0.09

Table 5.2.10. Variance explained by each principal component and importance of variables to principal components in the first metatarsal– St. Johns.

MT1		**PC1**	**PC2**	**PC3**	**PC4**	**PC5**
Standard deviation		2.8065	2.0700	1.4735	1.37927	1.00775
Proportion of Variance		0.3938	0.2142	0.1086	0.09512	0.05078
Cumulative Proportion		0.3938	0.6081	0.7166	0.81175	0.86253
	Variables	**PC1**	**PC2**	**PC3**	**PC4**	**PC5**
Base Dorsal (BD)	BV/TV	0.30	-0.12	-0.07	0.26	-0.04
	Tb.Th	0.17	-0.27	0.26	0.24	-0.30
	DA	-0.03	-0.06	-0.51	-0.12	0.06
	Residual Tb.Sp	-0.28	0.04	0.26	-0.25	-0.01
	Residual Conn.D	0.24	0.25	-0.21	0.18	0.13
Base Plantar (BP)	BV/TV	0.25	-0.18	0.08	0.33	0.09
	Tb.Th	0.00	-0.33	0.18	0.27	-0.15
	DA	0.06	-0.11	-0.45	-0.19	-0.46
	Residual Tb.Sp	-0.29	0.02	0.10	-0.24	-0.27
	Residual Conn.D	0.31	0.11	-0.12	0.09	0.20
Head Dorsal (HD)	BV/TV	0.28	-0.11	-0.08	-0.24	-0.23
	Tb.Th	0.16	-0.37	-0.03	-0.16	-0.14
	DA	-0.20	0.08	-0.40	0.27	-0.14
	Residual Tb.Sp	-0.28	-0.15	0.14	0.21	0.13
	Residual Conn.D	0.21	0.27	0.17	-0.18	-0.23
Head Plantar (HP)	BV/TV	0.28	-0.17	0.08	-0.28	0.14
	Tb.Th	0.07	-0.43	0.01	-0.25	0.06
	DA	-0.08	-0.29	-0.16	-0.20	0.56
	Residual Tb.Sp	-0.28	-0.15	-0.16	0.24	-0.17
	Residual Conn.D	0.23	0.32	0.12	-0.09	-0.04

Table 5.2.11. Variance explained by each principal component and importance of variables to principal components in the talus– St. Johns.

Talus		**PC1**	**PC2**	**PC3**	**PC4**	**PC5**
Standard deviation		3.309	2.798	1.9877	1.36767	1.20658
Proportion of Variance		0.365	0.261	0.1317	0.06235	0.04853
Cumulative Proportion		0.365	0.626	0.7577	0.82001	0.86854
	Variables	**PC1**	**PC2**	**PC3**	**PC4**	**PC5**
Anterior calcaneal facet (ACF)	BV/TV	-0.03	-0.21	-0.36	0.12	-0.17
	Tb.Th	-0.13	-0.10	-0.37	-0.15	-0.05
	DA	0.12	0.15	-0.19	-0.08	0.45
	Residual Tb.Sp	-0.18	0.23	-0.02	-0.22	0.05
	Residual Conn.D	0.15	-0.12	0.27	0.19	-0.08
Posterior calcaneal facet (PCF)	BV/TV	-0.18	-0.23	0.12	0.16	0.18
	Tb.Th	-0.27	-0.11	0.04	-0.09	0.13
	DA	-0.02	0.17	-0.32	-0.22	-0.36
	Residual Tb.Sp	-0.19	0.20	-0.13	-0.19	-0.13
	Residual Conn.D	0.28	-0.08	0.05	0.04	0.01
Talar head (TH)	BV/TV	-0.14	-0.27	0.00	0.07	0.20
	Tb.Th	-0.25	-0.12	0.03	-0.02	0.26
	DA	-0.10	-0.03	-0.23	0.07	-0.04
	Residual Tb.Sp	-0.09	0.30	0.08	0.05	-0.12
	Residual Conn.D	0.25	-0.09	0.05	-0.23	-0.05
Trochlea lateral (TL)	BV/TV	-0.16	-0.27	0.10	-0.15	-0.03
	Tb.Th	-0.25	-0.11	0.17	-0.14	0.03
	DA	-0.05	0.06	-0.24	-0.34	0.48
	Residual Tb.Sp	-0.14	0.29	0.02	0.11	-0.10
	Residual Conn.D	0.25	-0.14	-0.10	0.04	-0.16
Trochlea central (TC)	BV/TV	-0.17	-0.25	-0.06	0.08	-0.21
	Tb.Th	-0.28	-0.09	0.05	0.10	-0.07
	DA	-0.04	-0.01	-0.27	0.53	0.20
	Residual Tb.Sp	-0.13	0.28	0.15	0.03	-0.01
	Residual Conn.D	0.24	-0.13	-0.03	-0.27	-0.08
Trochlea medial (TM)	BV/TV	-0.20	-0.22	-0.01	-0.09	-0.21
	Tb.Th	-0.28	-0.05	0.03	-0.13	-0.17
	DA	0.03	0.01	-0.44	0.21	-0.02
	Residual Tb.Sp	-0.08	0.29	0.12	0.18	-0.03
	Residual Conn.D	0.22	-0.18	0.04	-0.19	0.05

Table 5.2.12. Significant MANOVA's – St. Johns.

Calcaneus	**St. Johns**	**Df**	**Pillai**	**approx F**	**num Df**	**den Df**	***p***
all	Sex	1	0.16767	0.73861	3	11	0.5507
	Residuals	13					
		Df	**Sum Sq**	**Mean Sq**	**F value**	***p***	
PC1	Sex	1	30.335	30.335	2.4083	0.1447	
	Residuals	13	163.747	12.596			
PC2	Sex	1	0.574	0.5739	0.0588	0.8122	
	Residuals	13	126.897	9.7613			
PC3	Sex	1	0.271	0.27143	0.0898	0.7691	
	Residuals	13	39.273	3.02103			

MT1	**St. Johns**	**Df**	**Pillai**	**approx F**	**num Df**	**den Df**	***p***
all	Sex	1	0.24548	1.4098	3	13	0.2845
	Residuals	15					
		Df	**Sum Sq**	**Mean Sq**	**F value**	***p***	
PC1	Sex	1	11.54	11.5401	1.512	0.2378	
	Residuals	15	114.48	7.6323			
PC2	Sex	1	8.982	8.982	2.2615	0.1534	
	Residuals	15	59.575	3.9717			
PC3	Sex	1	0.795	0.79521	0.3514	0.5622	
	Residuals	15	33.946	2.26308			

Talus	**St. Johns**	**Df**	**Pillai**	**approx F**	**num Df**	**den Df**	***p***
all	Sex	1	0.38178	2.4702	3	12	0.1119
	Residuals	14					
		Df	**Sum Sq**	**Mean Sq**	**F value**	***p***	
PC1	Sex	1	21.513	21.513	2.11	0.1684	
	Residuals	14	142.739	10.196			
PC2	Sex	1	20.001	20.0008	2.8739	0.1121	
	Residuals	14	97.432	6.9594			
PC3	Sex	1	4.77	4.7698	1.2255	0.287	
	Residuals	14	54.492	3.8923			

Jebel Moya

Table 5.2.13. Variance explained by each principal component and importance of variables to principal components in the calcaneus – Jebel Moya.

Calcaneus		**PC1**	**PC2**	**PC3**	**PC4**
Standard deviation		4.5649	2.4329	2.2168	1.8245
Proportion of Variance		0.5954	0.1691	0.1404	0.09511
Cumulative Proportion		0.5954	0.7645	0.9049	1
	Variable	**PC1**	**PC2**	**PC3**	**PC4**
Achilles tendon (AT)	BV/TV	-0.18	-0.11	0.15	0.18
	Tb.Th	-0.19	-0.06	0.01	0.24
	DA	-0.12	-0.34	0.05	-0.02
	Residual Tb.Sp	0.19	0.16	-0.09	0.07
	Residual Conn.D	-0.20	0.13	-0.10	-0.04
Calcaneo cuboid (CC)	BV/TV	-0.19	-0.01	-0.21	-0.08
	Tb.Th	-0.13	-0.20	-0.26	-0.17
	DA	0.15	0.16	-0.24	-0.16
	Residual Tb.Sp	0.20	-0.14	-0.02	0.05
	Residual Conn.D	-0.14	0.18	0.26	0.15
Calcaneal tuber (CT)	BV/TV	-0.18	0.04	0.03	0.29
	Tb.Th	-0.14	-0.24	0.17	0.16
	DA	0.20	-0.05	-0.02	-0.20
	Residual Tb.Sp	0.21	-0.08	0.06	0.02
	Residual Conn.D	-0.18	-0.03	-0.23	-0.14
PTF anterior (PA)	BV/TV	-0.21	0.11	-0.01	0.00
	Tb.Th	-0.20	0.03	-0.18	-0.05
	DA	0.07	-0.09	-0.35	0.27
	Residual Tb.Sp	0.22	-0.04	0.01	-0.04
	Residual Conn.D	-0.04	0.23	0.36	-0.07
PTF central (PC)	BV/TV	-0.22	0.04	-0.02	0.05
	Tb.Th	-0.18	-0.03	-0.01	-0.30
	DA	0.08	-0.34	0.07	0.24
	Residual Tb.Sp	0.21	-0.11	0.01	-0.02
	Residual Conn.D	0.15	0.15	0.27	-0.13
PTF posterior (PP)	BV/TV	-0.20	-0.11	-0.07	0.15
	Tb.Th	-0.19	-0.18	-0.05	-0.08
	DA	-0.09	0.35	0.09	0.14
	Residual Tb.Sp	0.16	-0.13	0.07	-0.31
	Residual Conn.D	0.09	0.36	-0.05	0.13
Plantar ligaments (PL)	BV/TV	-0.19	0.08	0.13	-0.17
	Tb.Th	-0.17	0.01	0.25	-0.17
	DA	-0.09	-0.21	0.23	-0.31
	Residual Tb.Sp	0.19	-0.08	0.02	0.25
	Residual Conn.D	-0.08	0.21	-0.34	-0.13

Table 5.2.14. Variance explained by each principal component and importance of variables to principal components in the first metatarsal – Jebel Moya

MT1		**PC1**	**PC2**	**PC3**
Standard deviation		3.8235	2.3197	5.17E-15
Proportion of Variance		0.7309	0.2691	0.00E+00
Cumulative Proportion		0.7309	1	1.00E+00
	Variables	**PC1**	**PC2**	**PC3**
Base Dorsal (BD)	BV/TV	-0.26	0.09	-0.30
	Tb.Th	0.17	0.33	-0.39
	DA	0.23	0.21	-0.29
	Residual Tb.Sp	0.26	0.09	0.04
	Residual Conn.D	-0.26	-0.04	-0.02
Base Plantar (BP)	BV/TV	-0.23	-0.19	-0.09
	Tb.Th	-0.18	-0.32	0.11
	DA	0.20	0.28	0.46
	Residual Tb.Sp	0.22	0.22	0.06
	Residual Conn.D	-0.26	0.03	-0.05
Head Dorsal (HD)	BV/TV	-0.23	0.20	-0.15
	Tb.Th	0.20	-0.28	-0.58
	DA	0.16	-0.34	0.11
	Residual Tb.Sp	0.25	-0.13	0.01
	Residual Conn.D	-0.16	0.33	-0.01
Head Plantar (HP)	BV/TV	-0.26	0.03	-0.13
	Tb.Th	-0.24	-0.16	0.22
	DA	0.13	-0.38	-0.11
	Residual Tb.Sp	0.26	-0.04	0.04
	Residual Conn.D	-0.24	0.18	-0.01

Table 5.2.15. Variance explained by each principal component and importance of variables to principal components in the talus – Jebel Moya.

Talus		**PC1**	**PC2**	**PC3**	**PC4**
Standard deviation		4.2488	2.9066	1.8708	3.86E-15
Proportion of Variance		0.6017	0.2816	0.1167	0.00E+00
Cumulative Proportion		0.6017	0.8833	1	1.00E+00
	Variables	**PC1**	**PC2**	**PC3**	**PC4**
Anterior calcaneal facet (ACF)	BV/TV	-0.23	-0.07	0.03	0.06
	Tb.Th	-0.19	-0.20	0.06	0.04
	DA	-0.13	0.13	0.40	0.14
	Residual Tb.Sp	0.23	-0.09	-0.01	0.03
	Residual Conn.D	-0.17	0.09	-0.36	-0.09
Posterior calcaneal facet (PCF)	BV/TV	-0.19	-0.20	0.02	0.04
	Tb.Th	-0.06	-0.29	0.27	0.24
	DA	0.04	0.00	0.53	-0.66
	Residual Tb.Sp	0.23	0.05	0.08	0.06
	Residual Conn.D	-0.21	0.07	-0.21	-0.10
Talar head (TH)	BV/TV	-0.22	-0.11	-0.03	-0.11
	Tb.Th	-0.20	0.02	-0.27	-0.31
	DA	0.20	-0.18	-0.11	-0.17
	Residual Tb.Sp	0.23	0.04	-0.03	0.02
	Residual Conn.D	-0.21	-0.06	-0.25	-0.07
Trochlea lateral (TL)	BV/TV	-0.19	0.21	0.01	0.01
	Tb.Th	-0.06	0.32	-0.11	0.03
	DA	-0.03	0.34	0.07	0.47
	Residual Tb.Sp	0.23	-0.07	-0.06	0.03
	Residual Conn.D	-0.15	-0.25	0.14	0.01
Trochlea central (TC)	BV/TV	-0.21	0.16	0.02	-0.05
	Tb.Th	-0.09	0.32	0.01	-0.12
	DA	-0.03	0.33	0.14	-0.14
	Residual Tb.Sp	0.23	-0.03	0.01	0.02
	Residual Conn.D	-0.17	-0.24	-0.06	-0.02
Trochlea medial (TM)	BV/TV	-0.10	-0.31	0.03	0.15
	Tb.Th	0.18	-0.13	-0.29	-0.06
	DA	0.23	-0.03	-0.12	-0.16
	Residual Tb.Sp	0.23	0.05	-0.05	-0.01
	Residual Conn.D	-0.23	-0.05	0.06	0.00

Table 5.2.16. Significant MANOVA's – Jebel Moya.

Calcaneus	**Jebel Moya**	**Df**	**Pillai**	**approx F**	**num Df**	**den Df**	***p***
all	Sex	1	0.99994	5919.1	3	1	**0.009554**
	Residuals	3					
		Df	**Sum Sq**	**Mean Sq**	**F value**	***p***	
PC1	Sex	1	71.528	71.528	18.145	**0.02373**	
	Residuals	3	11.826	3.942			
PC2	Sex	1	2.9832	2.9832	0.4325	0.5577	
	Residuals	3	20.692	6.8973			
PC3	Sex	1	0.3108	0.3108	0.0482	0.8403	
	Residuals	3	19.3452	6.4484			

Appendix 5.3 PCA in individual VOIs

Black Earth

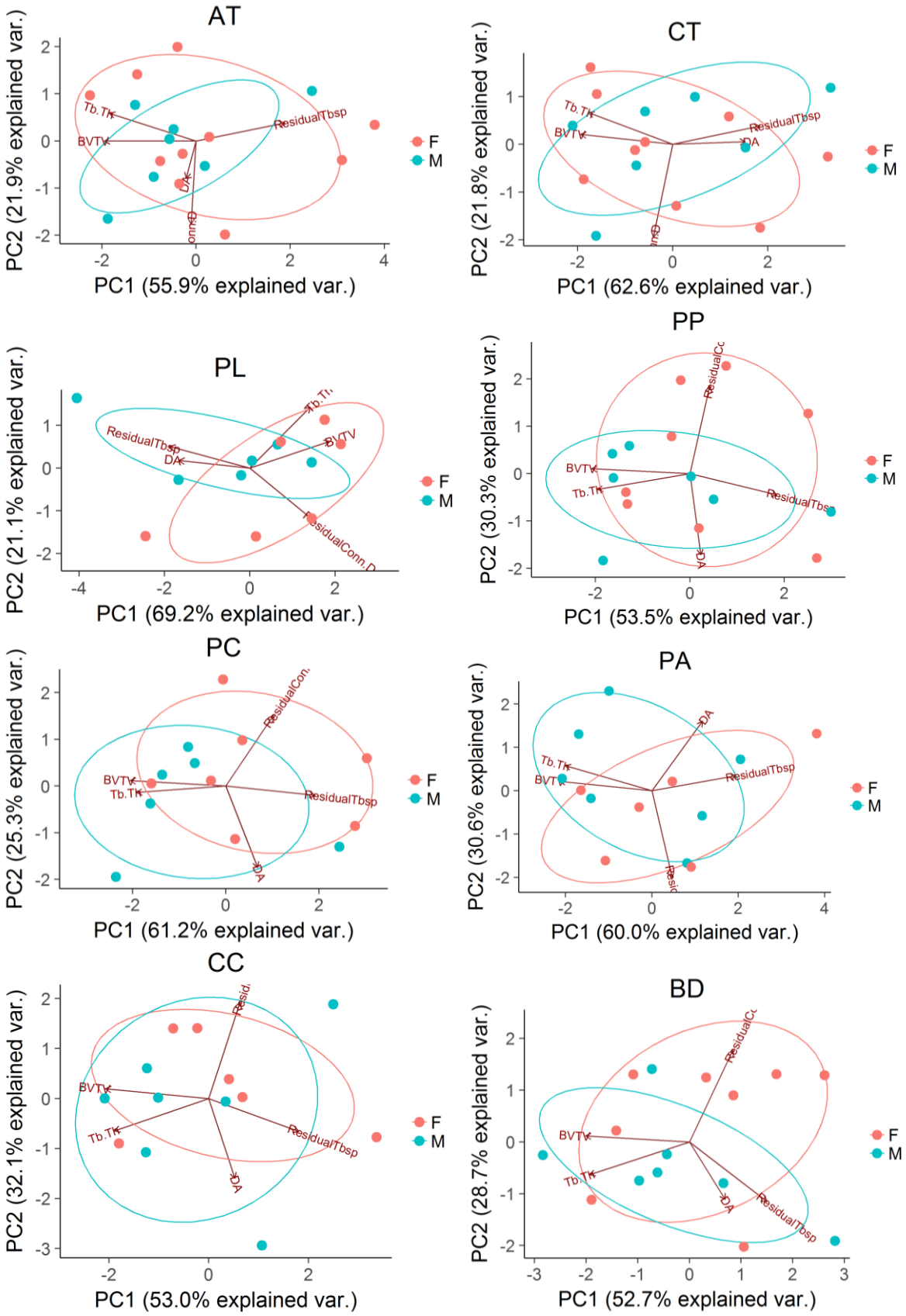

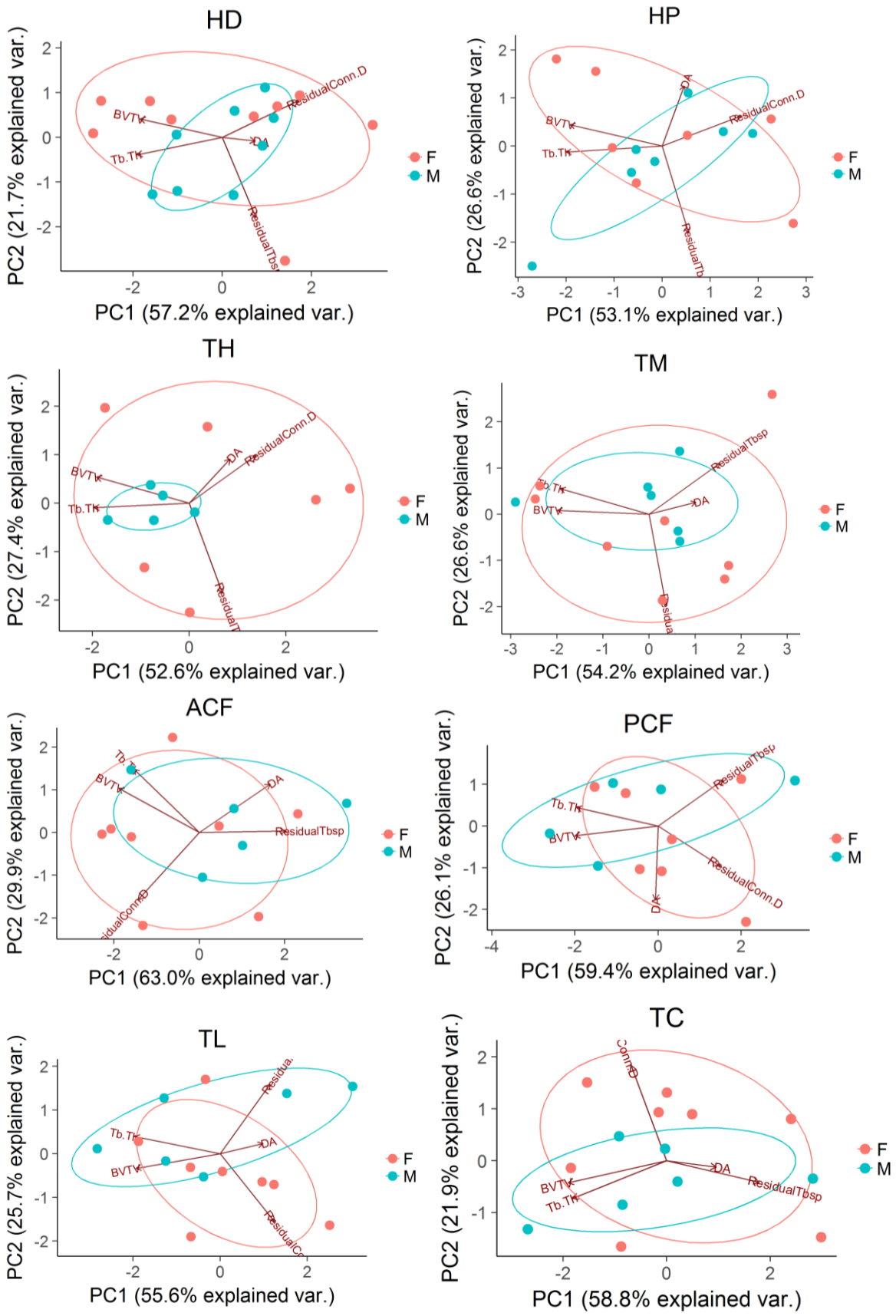

Figure 5.3.1. Biplots of the first two principal components per VOI in Black Earth. Achilles tendon (AT), calcaneal tuber (CT), plantar ligaments (PL), posterior talar facet (PP: posterior, PC: central, PA: anterior), calcaneocuboid (CC), dorsal base (BD), plantar base (BP), dorsal head (HD), plantar head (HP), talar head (TH), anterior calcaneal facet (ACF), posterior calcaneal facet (PCF), trochlea (lateral: TL, central: TC, medial: TM).

Table 5.3.1. PCA rotations of VOIs that have significant MANOVAs – Black Earth.

Black Earth						
PL		**PC1**	**PC2**	**PC3**	**PC4**	**PC5**
	Standard deviation	1.769	1.043	0.730	0.457	0.196
	Proportion of Variance	0.626	0.218	0.107	0.042	0.008
	Cumulative Proportion	0.626	0.844	0.951	0.992	1.000
	BV/TV	-0.543	0.100	-0.275	0.101	0.781
	Tb.Th	-0.496	0.316	-0.097	-0.734	-0.325
	DA	0.427	0.026	-0.889	-0.160	0.002
	Residual Tb.Sp	0.513	0.182	0.352	-0.548	0.528
	Residual Conn.D	-0.115	-0.925	-0.019	-0.352	0.077
TL		**PC1**	**PC2**	**PC3**	**PC4**	**PC5**
	Standard deviation	1.668	1.133	0.933	0.182	0.180
	Proportion of Variance	0.556	0.257	0.174	0.007	0.007
	Cumulative Proportion	0.556	0.813	0.987	0.993	1.000
	BV/TV	-0.572	-0.147	0.221	-0.130	0.765
	Tb.Th	-0.582	0.170	-0.003	-0.613	-0.506
	DA	0.291	0.101	0.928	-0.198	-0.065
	Residual Tb.Sp	0.338	0.694	-0.250	-0.443	0.382
	Residual Conn.D	0.368	-0.677	-0.165	-0.609	0.089

Table 5.3.2. Significant MANOVA's – Black Earth.

Black Earth MANOVA							
	CT	**Df**	**Pillai**	**approx F**	**num Df**	**den Df**	***p***
all	Sex	1	0.39742	2.6382	3	12	0.09735
	Residuals	14					
		Df	**Sum Sq**	**Mean Sq**	**F value**	***p***	
PC1	Sex	1	0.014	0.014	0.0042	0.9495	
	Residuals	14	46.947	3.3534			
PC2	Sex	1	0.1804	0.18042	0.1564	0.6985	
	Residuals	14	16.1506	1.15362			
PC3	Sex	1	3.0881	3.08813	8.8042	0.01019	*
	Residuals	14	4.9106	0.35076			
	TL	**Df**	**Pillai**	**approx F**	**num Df**	**den Df**	***p***
all	Sex	1	0.25561	1.1446	3	10	0.3779
	Residuals	12					
		Df	**Sum Sq**	**Mean Sq**	**F value**	***p***	
PC1	Sex	1	0.406	0.40582	0.1362	0.7185	
	Residuals	12	35.744	2.97865			
PC2	Sex	1	3.8152	3.8152	3.5599	0.08362	.
	Residuals	12	12.8606	1.0717			
PC3	Sex	1	0.1766	0.17657	0.1902	0.6705	
	Residuals	12	11.1425	0.92854			

Kerma

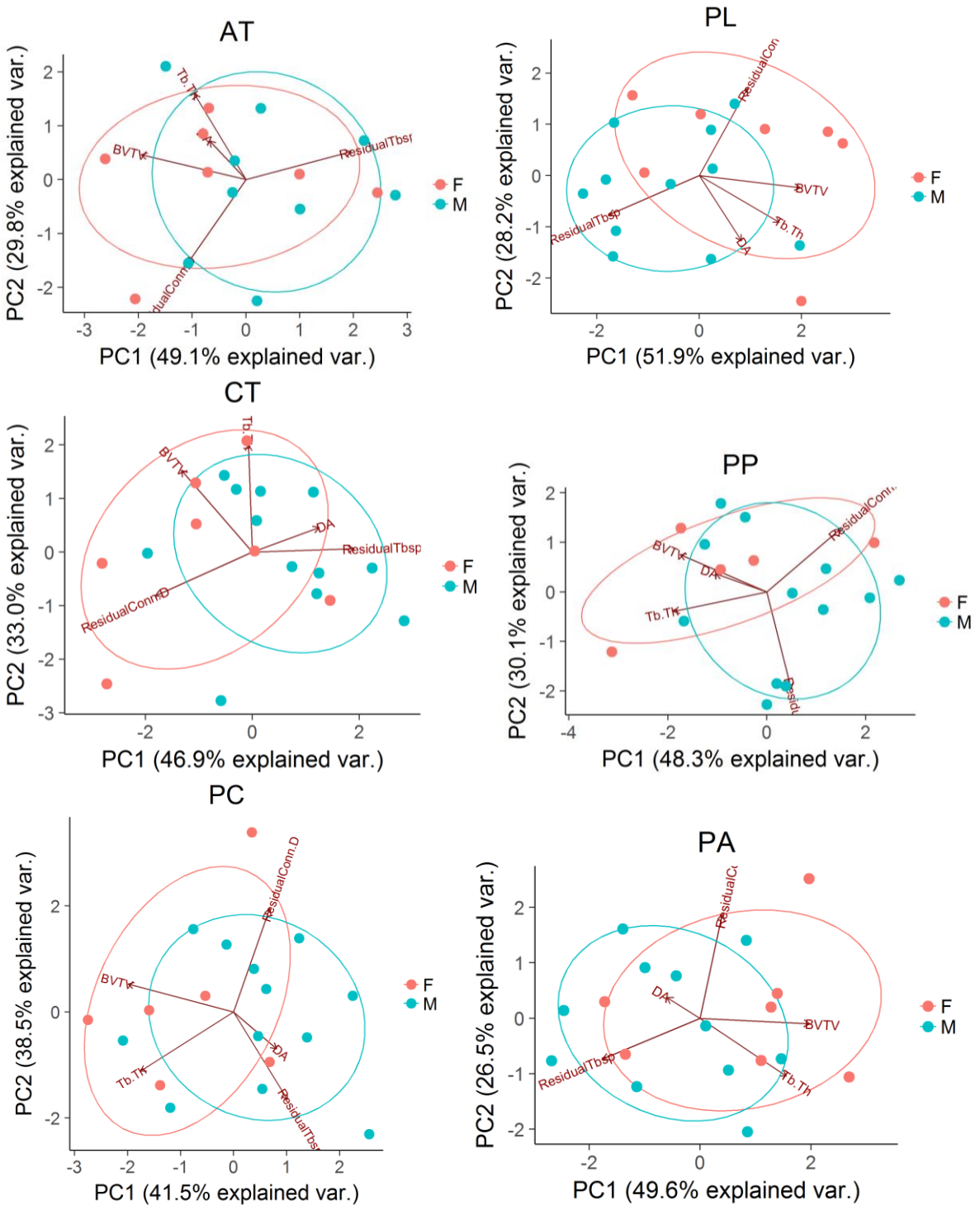
AT
PC2 (29.8% explained var.)
PC1 (49.1% explained var.)
BVTV
DA
F
M
PL
PC2 (28.2% explained var.)
PC1 (51.9% explained var.)
BVTV
Tb.Th
DA
F
M
CT
PC2 (33.0% explained var.)
PC1 (46.9% explained var.)
BVTV
DA
ResidualTbsp
F
M
PP
PC2 (30.1% explained var.)
PC1 (48.3% explained var.)
BVTV
DA
Tb.Th
F
M
PC
PC2 (38.5% explained var.)
PC1 (41.5% explained var.)
BVTV
Tb.Th
DA
F
M
PA
PC2 (26.5% explained var.)
PC1 (49.6% explained var.)
DA
BVTV
Tb.Th
F
M

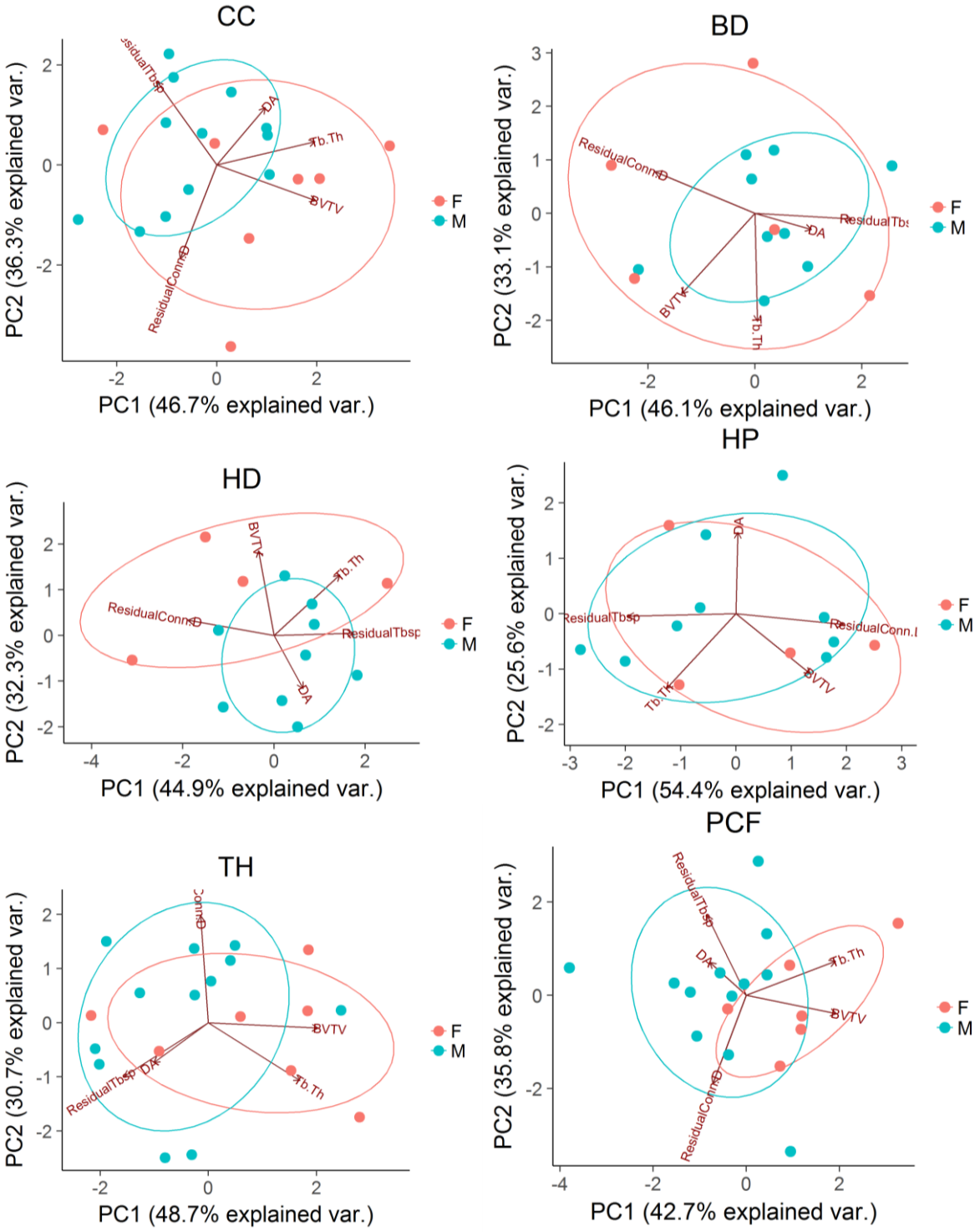
CC
PC2 (36.3% explained var.)
PC1 (46.7% explained var.)
DA
Tb.Th
BVTV
ResidualConnD
F
M
BD
PC2 (33.1% explained var.)
PC1 (46.1% explained var.)
ResidualConnD
DA
BVTV
Tb.Th
F
M
HD
PC2 (32.3% explained var.)
PC1 (44.9% explained var.)
BVTV
Tb.Th
ResidualConnD
ResidualTbsp
DA
F
M
HP
PC2 (25.6% explained var.)
PC1 (54.4% explained var.)
DA
ResidualTbsp
BVTV
Tb.Th
F
M
TH
PC2 (30.7% explained var.)
PC1 (48.7% explained var.)
BVTV
ResidualTbsp
DA
Tb.Th
F
M
PCF
PC2 (35.8% explained var.)
PC1 (42.7% explained var.)
ResidualTbsp
DA
Tb.Th
BVTV
ResidualConnD
F
M

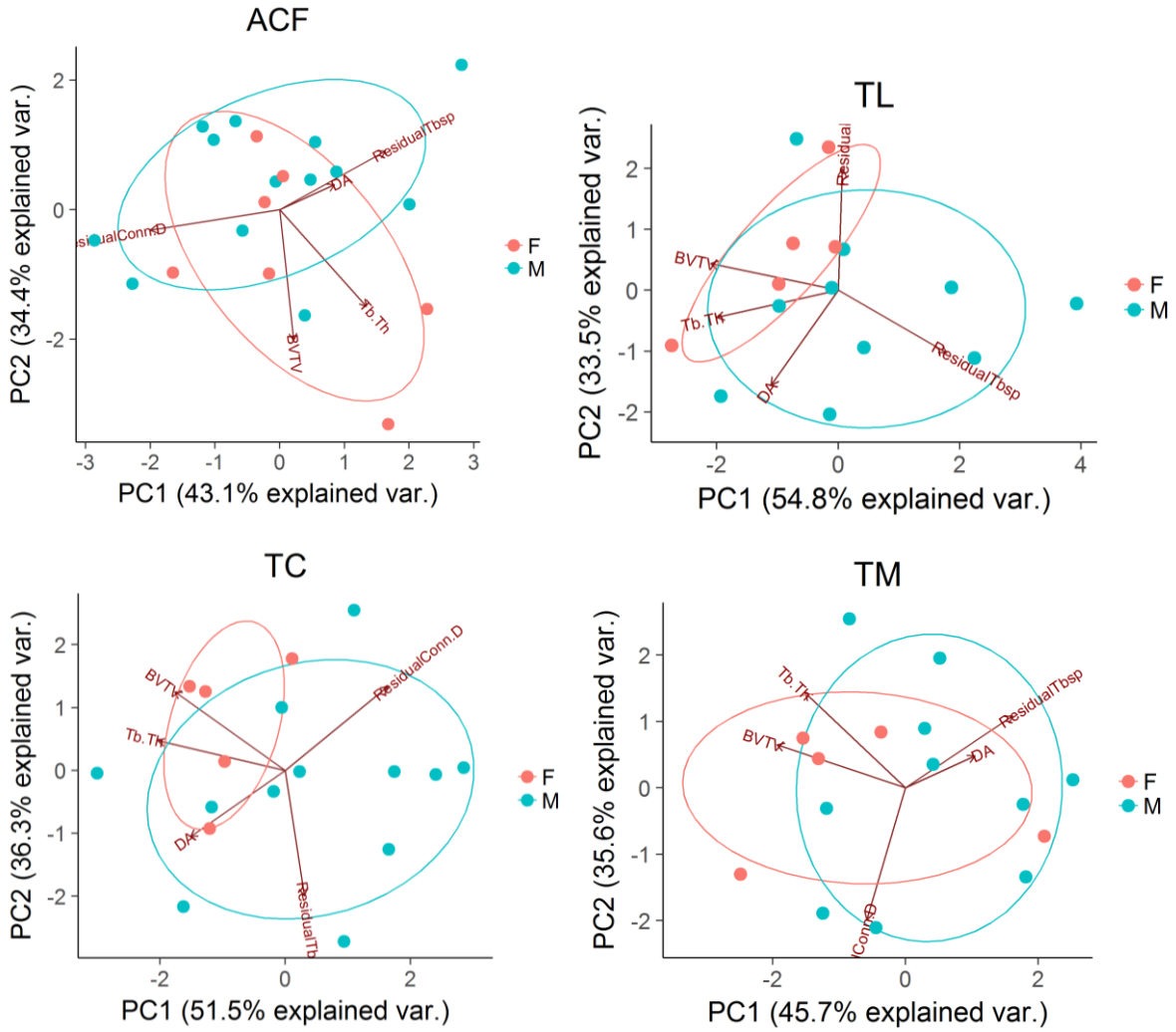

Figure 5.3.2. Biplots of the first two principal components per VOI in Kerma. Achilles tendon (AT), calcaneal tuber (CT), plantar ligaments (PL), posterior talar facet (PP: posterior, PC: central, PA: anterior), calcaneocuboid (CC), dorsal base (BD), plantar base (BP), dorsal head (HD), plantar head (HP), talar head (TH), anterior calcaneal facet (ACF), posterior calcaneal facet (PCF), trochlea (lateral: TL, central: TC, medial: TM).

Table 5.3.3. PCA rotations of VOIs that have significant MANOVAs - Kerma. Achilles tendon (AT), calcaneal tuber (CT), plantar ligaments (PL), posterior talar facet (PP: posterior, PC: central, PA: anterior), calcaneocuboid (CC), dorsal base (BD), plantar base (BP), dorsal head (HD), plantar head (HP), talar head (TH), anterior calcaneal facet (ACF), posterior calcaneal facet (PCF), trochlea (lateral: TL, central: TC, medial: TM).

Kerma						
CT		**PC1**	**PC2**	**PC3**	**PC4**	**PC5**
	Standard deviation	1.532	1.286	0.868	0.384	0.315
	Proportion of Variance	0.469	0.331	0.151	0.030	0.020
	Cumulative Proportion	0.469	0.800	0.951	0.980	1.000
	BV/TV	-0.415	0.567	-0.062	0.465	-0.534
	Tb.Th	-0.023	0.745	0.177	-0.573	0.290
	DA	0.390	0.171	-0.884	-0.133	-0.135
	Residual Tb.Sp	0.594	0.022	0.399	-0.208	-0.666
	Residual Conn.D	-0.567	-0.304	-0.152	-0.628	-0.411
PL		**PC1**	**PC2**	**PC3**	**PC4**	**PC5**
	Standard deviation	1.611	1.188	0.854	0.465	0.221
	Proportion of Variance	0.519	0.282	0.146	0.043	0.010
	Cumulative Proportion	0.519	0.801	0.947	0.990	1.000
	BV/TV	0.595	-0.098	0.220	-0.149	-0.752
	Tb.Th	0.471	-0.372	0.506	0.372	0.495
	DA	0.249	-0.521	-0.780	0.241	-0.012
	Residual Tb.Sp	-0.531	-0.313	0.236	0.615	-0.432
	Residual Conn.D	0.283	0.695	-0.177	0.635	-0.044
PA		**PC1**	**PC2**	**PC3**	**PC4**	**PC5**
	Standard deviation	1.575	1.151	0.980	0.454	0.173
	Proportion of Variance	0.496	0.265	0.192	0.041	0.006
	Cumulative Proportion	0.496	0.761	0.953	0.994	1.000
	BV/TV	0.628	-0.043	-0.009	0.102	-0.770
	Tb.Th	0.493	-0.453	-0.209	-0.622	0.347
	DA	-0.189	0.162	-0.955	-0.035	-0.157
	Residual Tb.Sp	-0.558	-0.319	0.160	-0.549	-0.511
	Residual Conn.D	0.127	0.816	0.136	-0.548	-0.017
CC		**PC1**	**PC2**	**PC3**	**PC4**	**PC5**
	Standard deviation	1.527	1.348	0.824	0.356	0.214
	Proportion of Variance	0.467	0.363	0.136	0.025	0.009
	Cumulative Proportion	0.467	0.830	0.966	0.991	1.000
	BV/TV	0.605	-0.247	-0.107	0.153	-0.734
	Tb.Th	0.601	0.161	-0.326	0.417	0.576
	DA	0.297	0.398	0.864	0.088	0.004
	Residual Tb.Sp	-0.366	0.578	-0.202	0.614	-0.339
	Residual Conn.D	-0.224	-0.649	0.309	0.647	0.123
HD		**PC1**	**PC2**	**PC3**	**PC4**	**PC5**
	Standard deviation	1.499	1.270	0.923	0.482	0.239
	Proportion of Variance	0.449	0.323	0.170	0.047	0.011
	Cumulative Proportion	0.449	0.772	0.942	0.989	1.000

	BV/TV	-0.112	0.718	-0.369	0.168	0.554
	Tb.Th	0.475	0.514	-0.209	-0.128	-0.671
	DA	0.209	-0.450	-0.804	0.328	-0.009
	Residual Tb.Sp	0.574	0.019	0.417	0.686	0.161
	Residual Conn.D	-0.623	0.130	0.021	0.614	-0.466
PCF		**PC1**	**PC2**	**PC3**	**PC4**	**PC5**
	Standard deviation	1.461	1.338	0.946	0.357	0.233
	Proportion of Variance	0.427	0.358	0.179	0.025	0.011
	Cumulative Proportion	0.427	0.785	0.964	0.989	1.000
	BV/TV	0.636	-0.140	0.252	-0.480	0.531
	Tb.Th	0.629	0.264	-0.038	-0.067	-0.727
	DA	-0.259	0.255	0.908	-0.126	-0.167
	Residual Tb.Sp	-0.278	0.617	-0.332	-0.654	0.062
	Residual Conn.D	-0.236	-0.681	-0.028	-0.567	-0.397
TC		**PC1**	**PC2**	**PC3**	**PC4**	**PC5**
	Standard deviation	1.605	1.347	0.706	0.317	0.105
	Proportion of Variance	0.515	0.363	0.100	0.020	0.002
	Cumulative Proportion	0.515	0.878	0.978	0.998	1.000
	BV/TV	-0.502	0.426	-0.161	0.150	-0.720
	Tb.Th	-0.580	0.161	-0.386	0.272	0.644
	DA	-0.430	-0.358	0.746	0.361	-0.003
	Residual Tb.Sp	0.087	-0.677	-0.502	0.468	-0.251
	Residual Conn.D	0.467	0.454	0.128	0.745	0.069
TH		**PC1**	**PC2**	**PC3**	**PC4**	**PC5**
	Standard deviation	1.560	1.240	0.895	0.430	0.211
	Proportion of Variance	0.487	0.307	0.160	0.037	0.009
	Cumulative Proportion	0.487	0.794	0.954	0.991	1.000
	BV/TV	0.627	-0.038	0.136	-0.081	-0.762
	Tb.Th	0.524	-0.417	-0.015	-0.543	0.507
	DA	-0.312	-0.287	0.888	-0.166	-0.066
	Residual Tb.Sp	-0.484	-0.386	-0.423	-0.529	-0.397
	Residual Conn.D	-0.044	0.770	0.117	-0.625	0.012
ACF		**PC1**	**PC2**	**PC3**	**PC4**	**PC5**
	Standard deviation	1.468	1.311	1.010	0.272	0.179
	Proportion of Variance	0.431	0.344	0.204	0.015	0.006
	Cumulative Proportion	0.431	0.775	0.979	0.994	1.000
	BV/TV	0.070	-0.743	0.157	-0.231	0.604
	Tb.Th	0.441	-0.551	-0.207	-0.007	-0.677
	DA	0.278	0.142	0.880	-0.296	-0.200
	Residual Tb.Sp	0.537	0.333	-0.391	-0.636	0.206
	Residual Conn.D	-0.659	-0.116	-0.069	-0.674	-0.306

Table 5.3.4. Significant MANOVA's - Kerma. Achilles tendon (AT), calcaneal tuber (CT), plantar ligaments (PL), posterior talar facet (PP: posterior, PC: central, PA: anterior), calcaneocuboid (CC), dorsal base (BD), plantar base (BP), dorsal head (HD), plantar head (HP), talar head (TH), anterior calcaneal facet (ACF), posterior calcaneal facet (PCF), trochlea (lateral: TL, central: TC, medial: TM).

Kerma

CT		**Df**	**Pillai**	**approx F**	**num Df**	**den Df**	***p***
all	Sex	1	0.3418	2.5965	3	15	0.09086
	Residuals	17					
		Df	**Sum Sq**	**Mean Sq**	**F value**	***p***	
PC1	Sex	1	8.871	8.8705	4.5182	0.04849	
	Residuals	17	33.375	1.9633			
PC2	Sex	1	0.0278	0.02781	0.0159	0.9011	
	Residuals	17	29.7165	1.74803			
PC3	Sex	1	1.7747	1.77475	2.5603	0.128	
	Residuals	17	11.7842	0.69319			

PL		**Df**	**Pillai**	**approx F**	**num Df**	**den Df**	***p***
all	Sex	1	0.45867	3.954	3	14	0.03101
	Residuals	16					
		Df	**Sum Sq**	**Mean Sq**	**F value**	***p***	
PC1	Sex	1	9.093	9.0932	4.1554	0.05838	
	Residuals	16	35.013	2.1883			
PC2	Sex	1	1.7996	1.7996	1.298	0.2713	
	Residuals	16	22.183	1.3864			
PC3	Sex	1	2.2011	2.20111	3.452	0.08167	
	Residuals	16	10.2021	0.63763			

PA		**Df**	**Pillai**	**approx F**	**num Df**	**den Df**	***p***
all	Sex	1	0.39399	3.0339	3	14	0.06449
	Residuals	16					
		Df	**Sum Sq**	**Mean Sq**	**F value**	***p***	
PC1	Sex	1	6.689	6.6889	3.0164	0.1016	
	Residuals	16	35.48	2.2175			
PC2	Sex	1	0.232	0.23199	0.1666	0.6885	
	Residuals	16	22.277	1.39231			
PC3	Sex	1	3.6713	3.6713	4.6467	0.04668	
	Residuals	16	12.6414	0.7901			

CC		**Df**	**Pillai**	**approx F**	**num Df**	**den Df**	***p***
all	Sex	1	0.42283	3.663	3	15	0.03674
	Residuals	17					
		Df	**Sum Sq**	**Mean Sq**	**F value**	***p***	
PC1	Sex	1	7.424	7.4236	3.6509	0.07305	
	Residuals	17	34.567	2.0334			
PC2	Sex	1	3.8399	3.8399	2.2629	0.1509	
	Residuals	17	28.847	1.6969			
PC3	Sex	1	1.5702	1.57025	2.5082	0.1317	
	Residuals	17	10.6429	0.62606			

HD		**Df**	**Pillai**	**approx F**	**num Df**	**den Df**	***p***
all	Sex	1	0.52294	3.2885	3	9	0.07214
	Residuals	11					
		Df	**Sum Sq**	**Mean Sq**	**F value**	***p***	
PC1	Sex	1	2.8716	2.8716	1.3118	0.2764	
	Residuals	11	24.08	2.1891			
PC2	Sex	1	5.6201	5.6201	4.5012	0.05741	
	Residuals	11	13.7344	1.2486			
PC3	Sex	1	1.2873 1	0.2873	1.586	0.234	
	Residuals	11	8.9284 0	0.81167			

PCF		**Df**	**Pillai**	**approx F**	**num Df**	**den Df**	***p***
all	Sex	1	0.47211	4.1735	3	14	0.0263
	Residuals	16					
		Df	**Sum Sq**	**Mean Sq**	**F value**	***p***	
PC1	Sex	1	11.777	11.7771	7.6855	0.0136	
	Residuals	16	24.518	1.5324			
PC2	Sex	1	0.1519	0.15188	0.0803	0.7805	
	Residuals	16	30.2675	1.89172			
PC3	Sex	1	2.168	2.168	2.6618	0.1223	
	Residuals	16	13.032	0.8145			

PC		Df	Pillai	approx F	num Df	den Df	*p*
	Sex	1	0.22717	1.3717	3	14	0.2921
	Residuals	16					
		Df	**Sum Sq**	**Mean Sq**	**F value**	***p***	
PC1	Sex	1	6.8718	6.8718	3.8655	0.06689	
	Residuals	16	28.4438	1.7777			
PC2	Sex	1	0.391	0.39096	0.1935	0.6659	
	Residuals	16	32.33	2.02066			
PC3	Sex	1	0.3108	0.31083	0.3371	0.5696	
	Residuals	16	14.7523	0.92202			

TH		Df	Pillai	approx F	num Df	den Df	*p*
all	Sex	1	0.28564	1.9993	3	15	0.1574
	Residuals	17					
		Df	**Sum Sq**	**Mean Sq**	**F value**	***p***	
PC1	Sex	1	6.865	6.8655	3.1611	0.0933	
	Residuals	17	36.921	2.1718			
PC2	Sex	1	0.4038	0.40377	0.2519	0.6222	
	Residuals	17	27.2532	1.60313			
PC3	Sex	1	1.6483	1.6483	2.1927	0.157	
	Residuals	17	12.7789	0.7517			

ACF		Df	Pillai	approx F	num Df	den Df	*p*
all	Sex	1	0.2036	1.3635	3	16	0.2896
	Residuals	18					
		Df	**Sum Sq**	**Mean Sq**	**F value**	***p***	
PC1	Sex	1	0.556	0.55566	0.2478	0.6247	
	Residuals	18	40.368	2.24269			
PC2	Sex	1	5.5559	5.5559	3.6884	0.07078	
	Residuals	18	27.1133	1.5063			
PC3	Sex	1	0.3872	0.38718	0.3666	0.5524	
	Residuals	18	19.0113	1.05619			

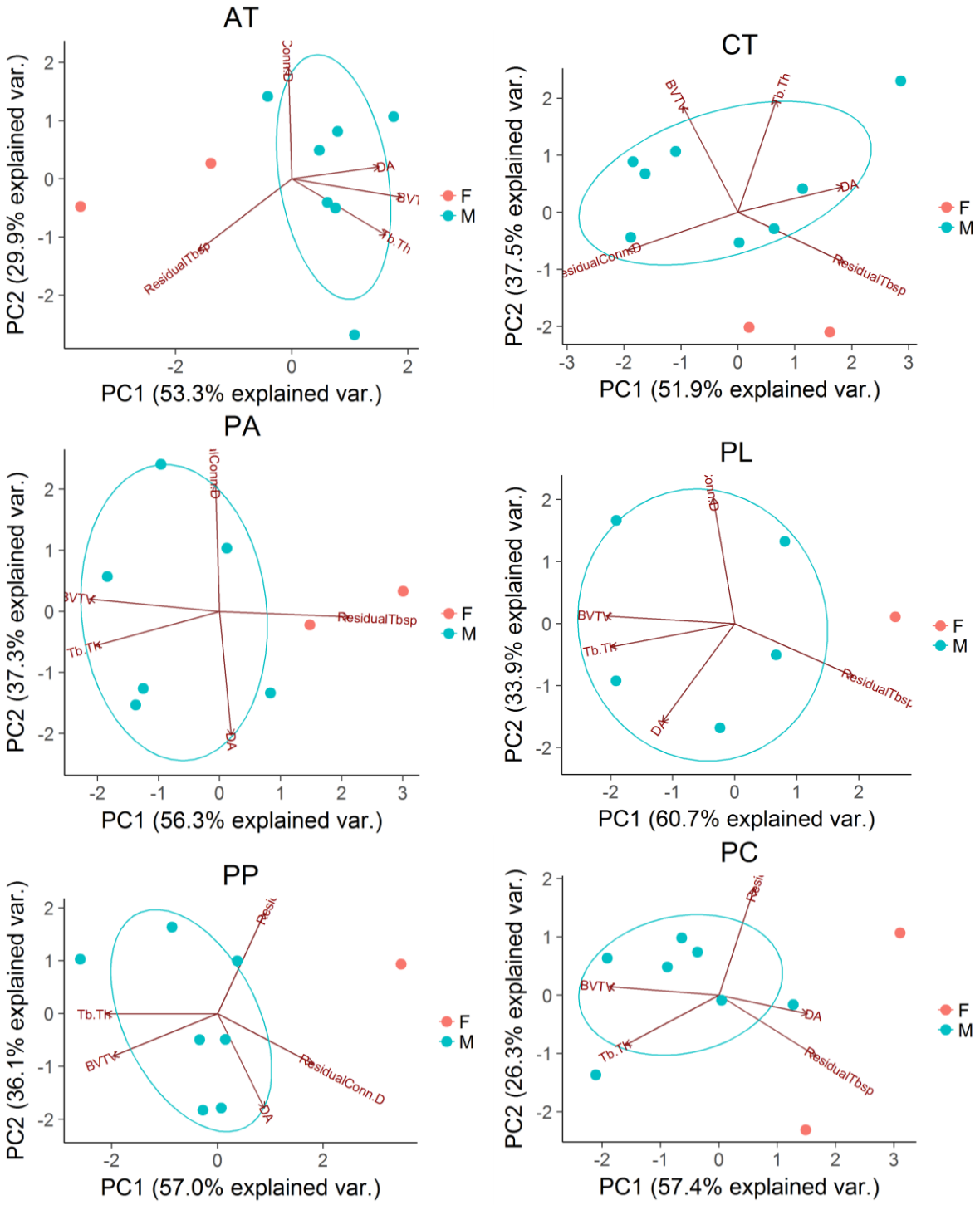
AT
PC2 (29.9% explained var.)
PC1 (53.3% explained var.)
DA
ResidualTbsp
Tb.Th
F
M
CT
PC2 (37.5% explained var.)
PC1 (51.9% explained var.)
BVTV
Tb.Th
DA
ResidualTbsp
F
M
PA
PC2 (37.3% explained var.)
PC1 (56.3% explained var.)
BVTV
Tb.Th
ResidualTbsp
DA
F
M
PL
PC2 (33.9% explained var.)
PC1 (60.7% explained var.)
BVTV
Tb.Th
DA
F
M
PP
PC2 (36.1% explained var.)
PC1 (57.0% explained var.)
Tb.Th
BVTV
ResidualConn.D
DA
F
M
PC
PC2 (26.3% explained var.)
PC1 (57.4% explained var.)
BVTV
DA
Tb.Th
ResidualTbsp
F
M

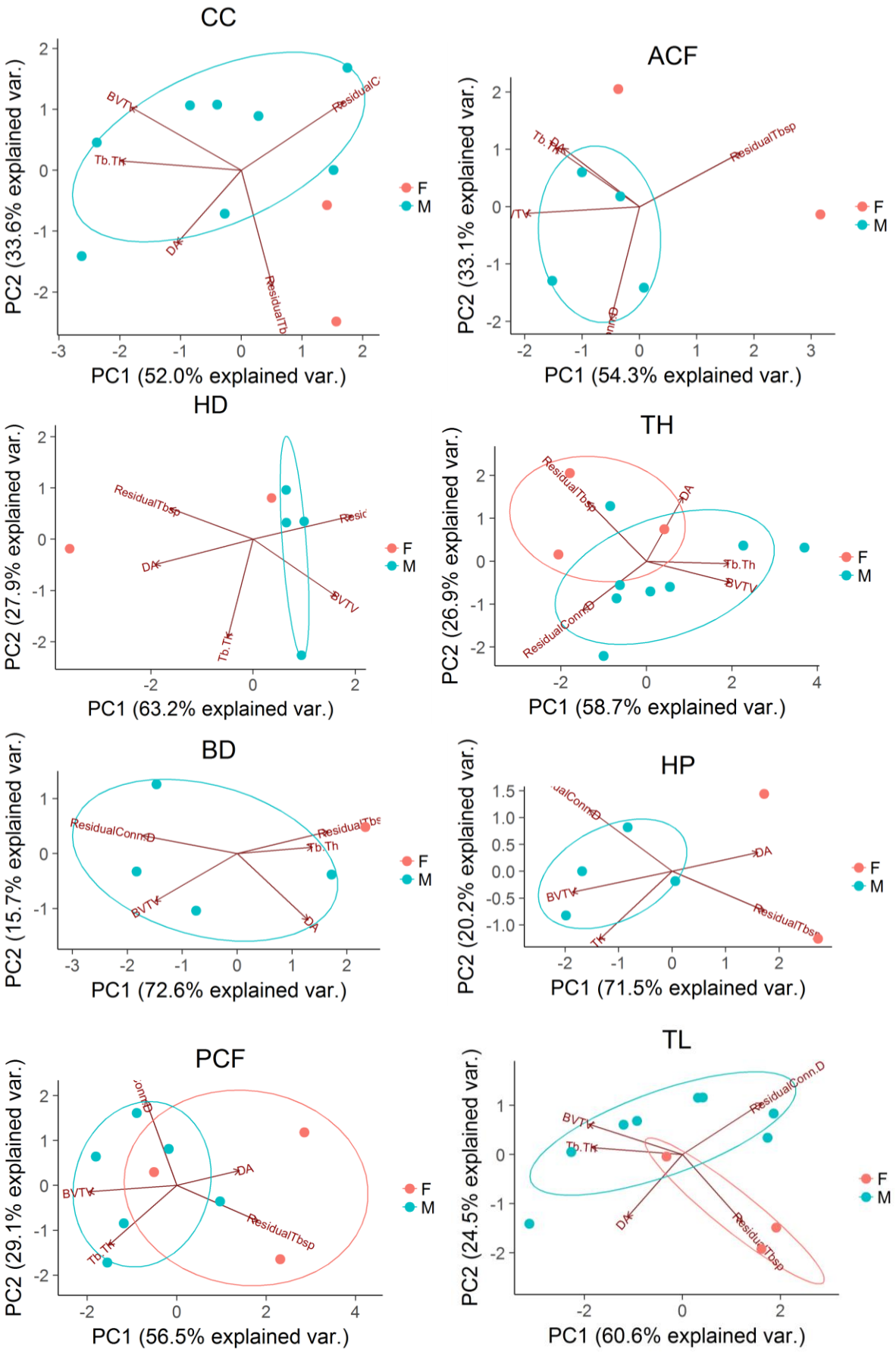
CC
PC2 (33.6% explained var.)
PC1 (52.0% explained var.)
BVTV
Tb.Th
DA
F
M
ACF
PC2 (33.1% explained var.)
PC1 (54.3% explained var.)
ResidualTbsp
HD
PC2 (27.9% explained var.)
PC1 (63.2% explained var.)
ResidualTbsp
DA
BVTV
Tb.Th
TH
PC2 (26.9% explained var.)
PC1 (58.7% explained var.)
ResidualTbsp
DA
Tb.Th
BVTV
BD
PC2 (15.7% explained var.)
PC1 (72.6% explained var.)
Tb.Th
BVTV
DA
HP
PC2 (20.2% explained var.)
PC1 (71.5% explained var.)
DA
BVTV
ResidualTbsp
PCF
PC2 (29.1% explained var.)
PC1 (56.5% explained var.)
DA
BVTV
Tb.Th
ResidualTbsp
TL
PC2 (24.5% explained var.)
PC1 (60.6% explained var.)
BVTV
Tb.Th
DA
ResidualConn.D
ResidualTbsp

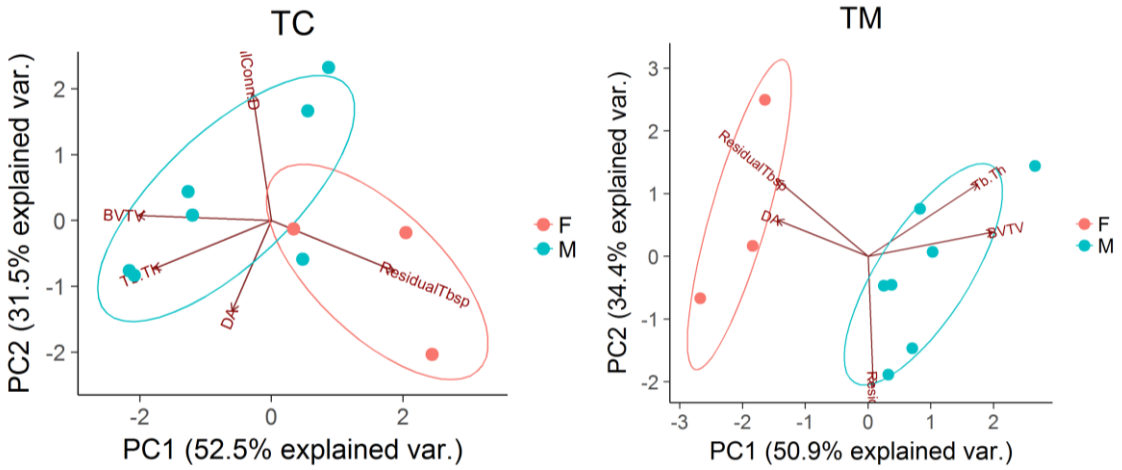

Figure 5.3.3. Biplots of the first two principal components per VOI in Jebel Moya. Achilles tendon (AT), calcaneal tuber (CT), plantar ligaments (PL), posterior talar facet (PP: posterior, PC: central, PA: anterior), calcaneocuboid (CC), dorsal base (BD), plantar base (BP), dorsal head (HD), plantar head (HP), talar head (TH), anterior calcaneal facet (ACF), posterior calcaneal facet (PCF), trochlea (lateral: TL, central: TC, medial: TM).

Table 5.3.5. PCA rotations of VOIs that have significant MANOVAs – Jebel Moya. Achilles tendon (AT), calcaneal tuber (CT), plantar ligaments (PL), posterior talar facet (PP: posterior, PC: central, PA: anterior), calcaneocuboid (CC), dorsal base (BD), plantar base (BP), dorsal head (HD), plantar head (HP), talar head (TH), anterior calcaneal facet (ACF), posterior calcaneal facet (PCF), trochlea (lateral: TL, central: TC, medial: TM).

Jebel Moya						
AT		**PC1**	**PC2**	**PC3**	**PC4**	**PC5**
	Standard deviation	1.632	1.222	0.875	0.234	0.148
	Proportion of Variance	0.533	0.299	0.153	0.011	0.004
	Cumulative Proportion	0.533	0.832	0.985	0.996	1.000
	BV/TV	0.573	-0.127	0.327	-0.493	-0.553
	Tb.Th	0.485	-0.388	0.406	0.602	0.296
	DA	0.452	0.082	-0.755	0.350	-0.310
	Residual Tb.Sp	0.481	-0.493	0.075	0.334	-0.638
	Residual Conn.D	0.018	0.764	0.390	0.401	-0.321
CT		**PC1**	**PC2**	**PC3**	**PC4**	**PC5**
	Standard deviation	1.610	1.370	0.576	0.359	0.264
	Proportion of Variance	0.519	0.376	0.066	0.026	0.014
	Cumulative Proportion	0.519	0.894	0.960	0.986	1.000
	BV/TV	-0.279	0.629	-0.044	0.546	-0.475
	Tb.Th	0.193	0.664	-0.189	-0.696	-0.017
	DA	0.530	0.152	0.824	0.071	-0.104
	Residual Tb.Sp	0.539	-0.297	-0.378	-0.014	-0.691
	Residual Conn.D	-0.559	-0.226	0.374	-0.460	-0.534
PP		**PC1**	**PC2**	**PC3**	**PC4**	**PC5**
	Standard deviation	1.689	1.343	0.510	0.269	0.110
	Proportion of Variance	0.570	0.361	0.052	0.015	0.002
	Cumulative Proportion	0.570	0.931	0.983	0.998	1.000
	BV/TV	-0.545	-0.279	0.149	-0.046	-0.775
	Tb.Th	-0.580	-0.002	-0.158	-0.681	0.418
	DA	0.243	-0.618	-0.738	-0.085	-0.085
	Residual Tb.Sp	0.244	0.657	-0.371	-0.404	-0.456
	Residual Conn.D	0.498	-0.329	0.520	-0.603	-0.096
PC		**PC1**	**PC2**	**PC3**	**PC4**	**PC5**
	Standard deviation	1.694	1.148	0.728	0.520	0.123
	Proportion of Variance	0.574	0.264	0.106	0.054	0.003
	Cumulative Proportion	0.574	0.837	0.943	0.997	1.000
	BV/TV	-0.554	0.063	-0.388	0.319	0.661
	Tb.Th	-0.472	-0.372	-0.181	-0.773	-0.092
	DA	0.446	-0.137	-0.874	0.014	-0.133
	Residual Tb.Sp	0.490	-0.452	0.213	-0.213	0.682
	Residual Conn.D	0.178	0.796	-0.083	-0.505	0.268
CC		**PC1**	**PC2**	**PC3**	**PC4**	**PC5**
	Standard deviation	1.612	1.296	0.796	0.274	0.112
	Proportion of Variance	0.520	0.336	0.127	0.015	0.003
	Cumulative Proportion	0.520	0.856	0.982	0.997	1.000

	BV/TV	-0.535	0.380	-0.018	0.282	0.699
	Tb.Th	-0.588	0.057	0.359	0.370	-0.621
	DA	-0.312	-0.439	-0.814	0.194	-0.100
	Residual Tb.Sp	0.151	-0.700	0.397	0.483	0.311
	Residual Conn.D	0.498	0.412	-0.226	0.716	-0.138
TC		**PC1**	**PC2**	**PC3**	**PC4**	**PC5**
	Standard deviation	1.621	1.255	0.846	0.254	0.137
	Proportion of Variance	0.525	0.315	0.143	0.013	0.004
	Cumulative Proportion	0.525	0.840	0.983	0.996	1.000
	BV/TV	-0.604	0.030	-0.169	0.399	0.668
	Tb.Th	-0.534	-0.283	-0.362	-0.694	-0.147
	DA	-0.179	-0.529	0.814	-0.098	0.126
	Residual Tb.Sp	0.557	-0.295	-0.213	-0.338	0.665
	Residual Conn.D	-0.086	0.743	0.364	-0.484	0.271
TM		**PC1**	**PC2**	**PC3**	**PC4**	**PC5**
	Standard deviation	1.595	1.312	0.813	0.251	0.110
	Proportion of Variance	0.509	0.344	0.132	0.013	0.002
	Cumulative Proportion	0.509	0.853	0.985	0.998	1.000
	BV/TV	0.594	0.140	-0.275	-0.466	-0.578
	Tb.Th	0.521	0.417	0.041	-0.140	0.730
	DA	-0.431	0.209	-0.824	-0.236	0.190
	Residual Tb.Sp	-0.434	0.443	0.493	-0.604	-0.087
	Residual Conn.D	0.024	-0.753	0.033	-0.585	0.299

Table 5.3.6. Significant MANOVA's – Jebel Moya. Achilles tendon (AT), calcaneal tuber (CT), plantar ligaments (PL), posterior talar facet (PP: posterior, PC: central, PA: anterior), calcaneocuboid (CC), dorsal base (BD), plantar base (BP), dorsal head (HD), plantar head (HP), talar head (TH), anterior calcaneal facet (ACF), posterior calcaneal facet (PCF), trochlea (lateral: TL, central: TC, medial: TM).

Jebel Moya

AT		**Df**	**Pillai**	**approx F**	**num Df**	**den Df**	***p***
all	Sex	1	0.78129	5.9539	3	5	0.04184
	Residuals	7					
		Df	**Sum Sq**	**Mean Sq**	**F value**	***p***	
PC1	Sex	1	16.2395	16.2395	22.423	**0.002119**	
	Residuals	7	5.0696	0.7242			
PC2	Sex	1	0.0277	0.02767	0.0162	0.9022	
	Residuals	7	11.9227	1.70324			
PC3	Sex	1	0.1035 0	0.10346	0.1202	0.739	
	Residuals	7	6.0232 0	0.86045			

CT		Df	Pillai	approx F	num Df	den Df	*p*
all	Sex	1	0.71481	5.0129	3	6	0.04496
	Residuals	8					
		Df	**Sum Sq**	**Mean Sq**	**F value**	***p***	
PC1	Sex	1	2.0473	2.0473	0.7694	0.406	
	Residuals	8	21.2864	2.6608			
PC2	Sex	1	10.5556	10.5556	13.318	0.0065	
	Residuals	8	6.3405	0.7926			
PC3	Sex	1	0.00698	0.00698	0.0187	0.8946	
	Residuals	8	2.98139	0.37267			

PP		Df	Pillai	approx F	num Df	den Df	*p*
all	Sex	1	0.87566	9.3901	3	4	0.02776
	Residuals	6					
		Df	**Sum Sq**	**Mean Sq**	**F value**	***p***	
PC1	Sex	1	13.8336	13.8336	13.555	0.01031	
	Residuals	6	6.1231	1.0205			
PC2	Sex	1	0.9971	0.99709	0.5142	0.5003	
	Residuals	6	11.6355	1.93925			
PC3	Sex	1	0.18822	0.18822	0.6931	0.437	
	Residuals	6	1.62945	0.27158			

PC		Df	Pillai	approx F	num Df	den Df	*p*
all	Sex	1	0.7376	4.6851	3	5	0.06473
	Residuals	7					
		Df	**Sum Sq**	**Mean Sq**	**F value**	***p***	
PC1	Sex	1	13.5841	13.584	10.16	0.01533	
	Residuals	7	9.3593	1.337			
PC2	Sex	1	0.9888	0.98879	0.7248 0	0.4227	
	Residuals	7	9.5493	1.36419			
PC3	Sex	1	0.219	0.21901	0.3817 0	0.5563	
	Residuals	7	4.0168	0.57383			

CC		Df	Pillai	approx F	num Df	den Df	*p*
all	Sex	1	0.70531	4.7868	3	6	0.04938
	Residuals	8					
		Df	**Sum Sq**	**Mean Sq**	**F value**	***p***	
PC1	Sex	1	5.5279	5.5279	2.4775	0.1541	
	Residuals	8	17.8502	2.2313			
PC2	Sex	1	5.8337	5.8337	5.0242	0.0553	
	Residuals	8	9.2889	1.1611			
PC3	Sex	1	0.4743	0.47427	0.725	0.4193	
	Residuals	8	5.2335	0.65419			

TC		Df	Pillai	approx F	num Df	den Df	*p*
all	Sex	1	0.69197	4.4929	3	6	0.05602
	Residuals	8					
		Df	**Sum Sq**	**Mean Sq**	**F value**	***p***	
PC1	Sex	1	11.09	11.0896	7.0701	0.02885	
	Residuals	8	12.548	1.5685			
PC2	Sex	1	2.6104	2.6104	1.8058	0.2159	
	Residuals	8	11.5642	1.4455			
PC3	Sex	1	0.2489	0.24893	0.3218	0.5861	
	Residuals	8	6.1894	0.77367			

TM		Df	Pillai	approx F	num Df	den Df	*p*
all	Sex	1	0.9158	21.754	3	6	0.001264
	Residuals	8					
		Df	**Sum Sq**	**Mean Sq**	**F value**	***p***	
PC1	Sex	1	18.0838	18.0838	30.137	0.0005807	
	Residuals	8	4.8004	0.6001			
PC2	Sex	1	1.8993	1.8993	1.1175	0.3213	
	Residuals	8	13.5966	1.6996			
PC3	Sex	1	0.0178	0.01784	0.0241	0.8805	
	Residuals	8	5.9262	0.74078			

St. Johns

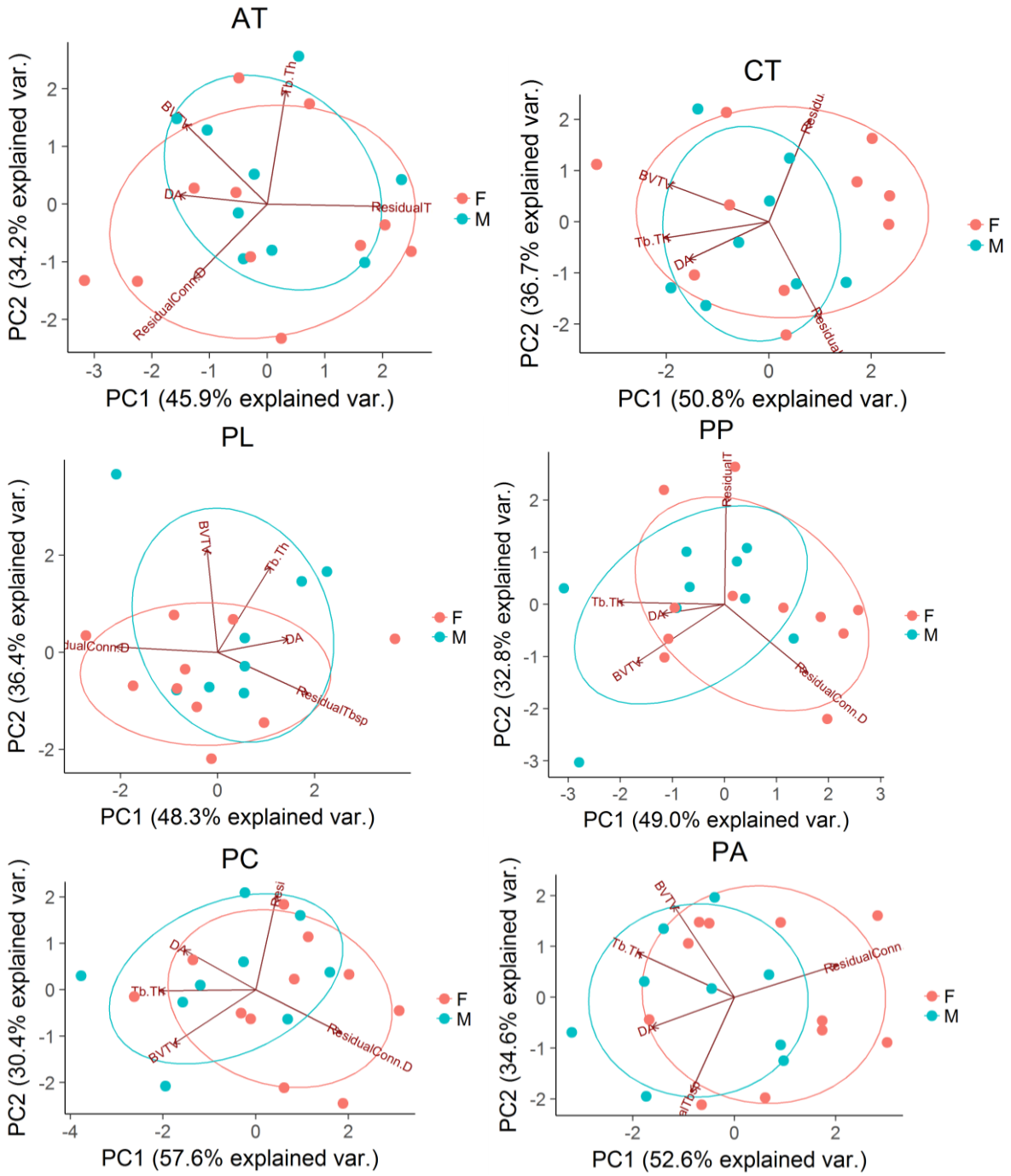
AT
PC2 (34.2% explained var.)
PC1 (45.9% explained var.)
Tb.Th
BVTV
DA
ResidualT
ResidualConn.D
F
M
CT
PC2 (36.7% explained var.)
PC1 (50.8% explained var.)
BVTV
Tb.Th
DA
F
M
PL
PC2 (36.4% explained var.)
PC1 (48.3% explained var.)
BVTV
Tb.Th
DA
ResidualTbsp
F
M
PP
PC2 (32.8% explained var.)
PC1 (49.0% explained var.)
ResidualT
Tb.Th
DA
BVTV
ResidualConn.D
F
M
PC
PC2 (30.4% explained var.)
PC1 (57.6% explained var.)
DA
Tb.Th
BVTV
ResidualConn.D
F
M
PA
PC2 (34.6% explained var.)
PC1 (52.6% explained var.)
BVTV
Tb.Th
DA
ResidualConn
F
M

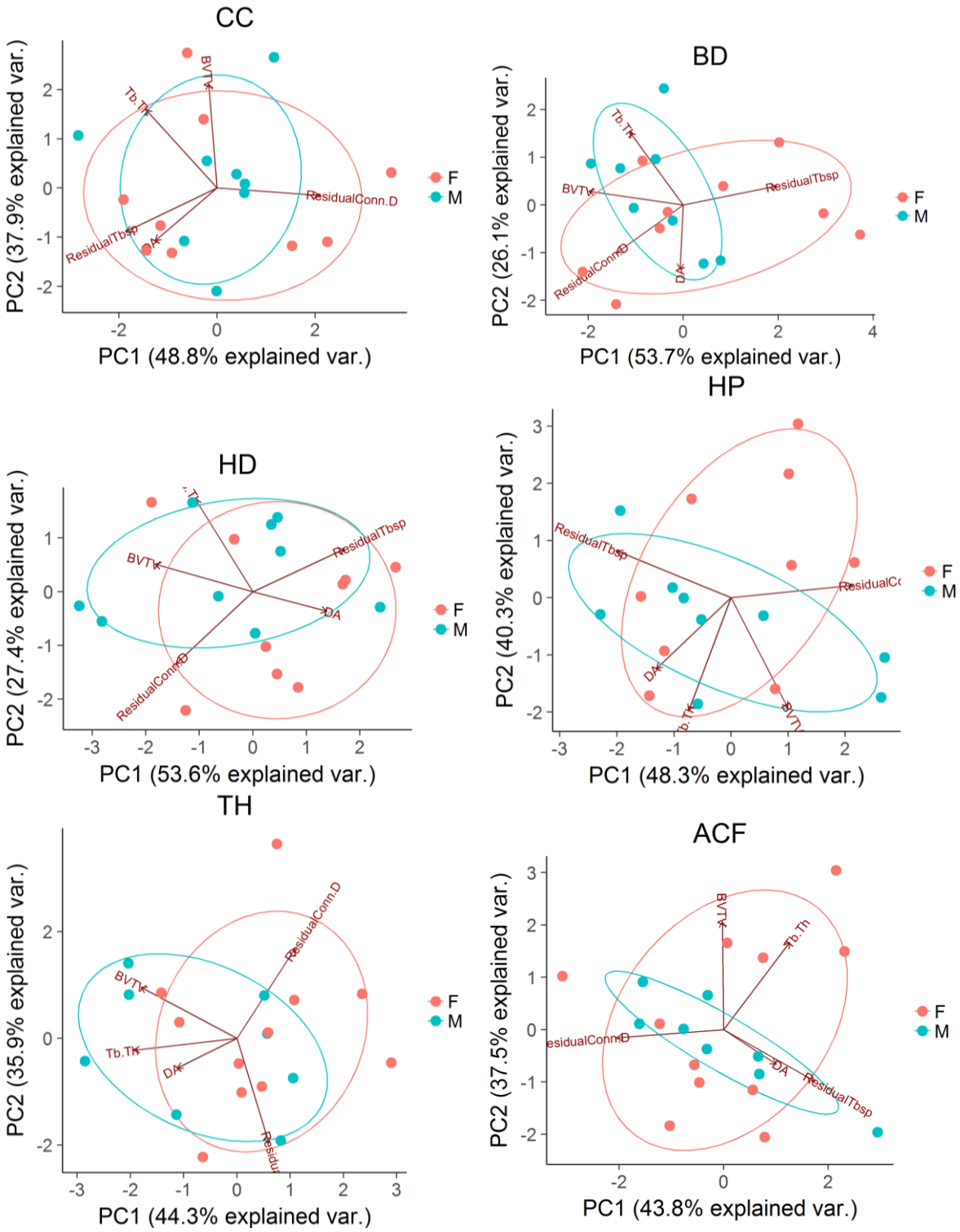
CC
PC2 (37.9% explained var.)
PC1 (48.8% explained var.)
BVTv
Tb.Th
ResidualConn.D
ResidualTbsp
DA
F
M
BD
PC2 (26.1% explained var.)
PC1 (53.7% explained var.)
HD
PC2 (27.4% explained var.)
PC1 (53.6% explained var.)
HP
PC2 (40.3% explained var.)
PC1 (48.3% explained var.)
TH
PC2 (35.9% explained var.)
PC1 (44.3% explained var.)
ACF
PC2 (37.5% explained var.)
PC1 (43.8% explained var.)

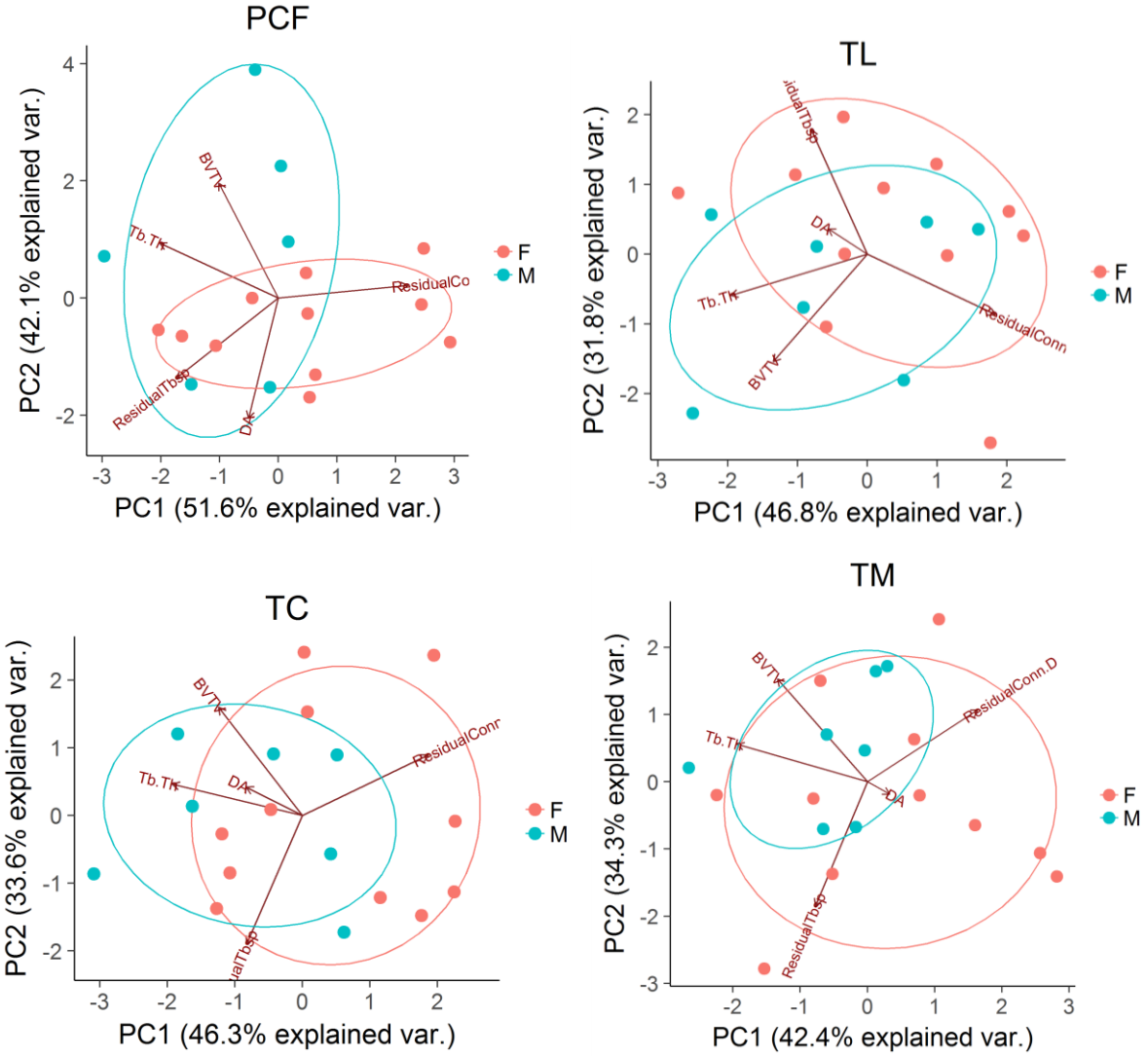

Figure 5.3.4. Biplots of the first two principal components per VOI in St. Johns. Achilles tendon (AT), calcaneal tuber (CT), plantar ligaments (PL), posterior talar facet (PP: posterior, PC: central, PA: anterior), calcaneocuboid (CC), dorsal base (BD), plantar base (BP), dorsal head (HD), plantar head (HP), talar head (TH), anterior calcaneal facet (ACF), posterior calcaneal facet (PCF), trochlea (lateral: TL, central: TC, medial: TM).

Table 5.3.7. PCA rotations of VOIs that have significant MANOVAs – St. Johns.

St. Johns						
PP		**PC1**	**PC2**	**PC3**	**PC4**	**PC5**
	Standard deviation	1.566	1.281	0.891	0.296	0.161
	Proportion of Variance	0.490	0.328	0.159	0.017	0.005
	Cumulative Proportion	0.490	0.819	0.977	0.995	1.000
	BV/TV	-0.510	-0.413	0.289	-0.173	0.675
	Tb.Th	-0.615	0.016	0.253	-0.358	-0.655
	DA	-0.361	-0.066	-0.921	-0.124	0.049
	Residual Tb.Sp	0.010	0.768	0.032	-0.551	0.324
	Residual Conn.D	0.481	-0.484	-0.061	-0.723	-0.091
PA		**PC1**	**PC2**	**PC3**	**PC4**	**PC5**

	Standard deviation	1.622	1.316	0.740	0.258	0.146
	Proportion of Variance	0.527	0.346	0.110	0.013	0.004
	Cumulative Proportion	0.527	0.873	0.982	0.996	1.000
	BV/TV	-0.339	0.629	-0.073	-0.024	0.696
	Tb.Th	-0.538	0.305	-0.327	-0.409	-0.586
	DA	-0.458	-0.205	0.823	-0.265	0.040
	Residual Tb.Sp	-0.240	-0.648	-0.443	-0.399	0.408
	Residual Conn.D	0.574	0.223	0.122	-0.776	0.063
BD		**PC1**	**PC2**	**PC3**	**PC4**	**PC5**
	Standard deviation	1.638	1.142	0.969	0.226	0.151
	Proportion of Variance	0.537	0.261	0.188	0.010	0.005
	Cumulative Proportion	0.537	0.798	0.985	0.995	1.000
	BV/TV	-0.598	0.124	-0.059	0.379	0.693
	Tb.Th	-0.338	0.657	-0.349	-0.561	-0.132
	DA	-0.020	-0.580	-0.771	-0.222	0.142
	Residual Tb.Sp	0.591	0.172	0.089	-0.372	0.689
	Residual Conn.D	-0.424	-0.432	0.523	-0.595	0.082
TC		**PC1**	**PC2**	**PC3**	**PC4**	**PC5**
	Standard deviation	1.522	1.296	0.975	0.180	0.145
	Proportion of Variance	0.463	0.336	0.190	0.006	0.004
	Cumulative Proportion	0.463	0.799	0.989	0.996	1.000
	BV/TV	-0.390	0.590	-0.224	-0.651	0.158
	Tb.Th	-0.606	0.171	-0.300	0.496	-0.516
	DA	-0.262	0.155	0.916	-0.078	-0.248
	Residual Tb.Sp	-0.259	-0.700	-0.105	-0.536	-0.382
	Residual Conn.D	0.586	0.330	-0.096	-0.192	-0.708
PCF		**PC1**	**PC2**	**PC3**	**PC4**	**PC5**
	Standard deviation	1.606	1.451	0.475	0.268	0.140
	Proportion of Variance	0.516	0.421	0.045	0.014	0.004
	Cumulative Proportion	0.516	0.937	0.982	0.996	1.000
	BV/TV	-0.278	0.596	-0.449	0.155	-0.585
	Tb.Th	-0.555	0.285	-0.066	-0.647	0.433
	DA	-0.139	-0.623	-0.766	-0.078	-0.001
	Residual Tb.Sp	-0.476	-0.414	0.447	-0.218	-0.596
	Residual Conn.D	0.607	0.066	-0.091	-0.710	-0.339

Table 5.3.8. Significant MANOVA's – St. Johns. Achilles tendon (AT), calcaneal tuber (CT), plantar ligaments (PL), posterior talar facet (PP: posterior, PC: central, PA: anterior), calcaneocuboid (CC), dorsal base (BD), plantar base (BP), dorsal head (HD), plantar head (HP), talar head (TH), anterior calcaneal facet (ACF), posterior calcaneal facet (PCF), trochlea (lateral: TL, central: TC, medial: TM).

St. Johns

PP		**Df**	**Pillai**	**approx F**	**num Df**	**den Df**	***p***
all	Sex	1	0.20328	1.3608	3	16	0.2904
	Residuals	18					
		Df	**Sum Sq**	**Mean Sq**	**F value**	***p***	
PC1	Sex	1	6.811	6.8107	3.0829	0.09612	
	Residuals	18	39.766	2.2092			
PC2	Sex	1	0.0016	0.00164	9.00E-04	0.9758	
	Residuals	18	31.1965	1.73314			
PC3	Sex	1	0.8591	0.85912	1.088	0.3107	
	Residuals	18	14.2129	0.78961			

PA		**Df**	**Pillai**	**approx F**	**num Df**	**den Df**	***p***
all	Sex	1	0.17903	1.163	3	16	0.3546
	Residuals	18					
		Df	**Sum Sq**	**Mean Sq**	**F value**	***p***	
PC1	Sex	1	8.247	8.2472	3.5543	0.07564	
	Residuals	18	41.766	2.3203			
PC2	Sex	1	0.065	0.06458	0.0354	0.8529	
	Residuals	18	32.834	1.8241			
PC3	Sex	1	0.126	7 0.12669	0.2216	0.6434	
	Residuals	18	10.288	8 0.57160			

BD		**Df**	**Pillai**	**approx F**	**num Df**	**den Df**	***p***
all	Sex	1	0.33761	2.2087	3	13	0.1358
	Residuals	15					
		Df	**Sum Sq**	**Mean Sq**	**F value**	***p***	
PC1	Sex	1	4.4	4.4001	1.7128	0.2103	
	Residuals	15	38.534	2.5689			
PC2	Sex	1	1.2135	1.2135	0.926	0.3512	
	Residuals	15	19.6564	1.3104			
PC3	Sex	1	2.6572	2.65721	3.2256	0.09266	
	Residuals	15	12.3566	0.82378			

PCF		Df	Pillai	approx F	num Df	den Df	*p*
all	Sex	1	0.32528	2.0891	3	13	0.1512
	Residuals	15					
		Df	**Sum Sq**	**Mean Sq**	**F value**	***p***	
PC1	Sex	1	5.881	5.8814	2.4936	0.1352	
	Residuals	15	35.38	2.3587			
PC2	Sex	1	6.0315	6.0315	3.2735	0.09049	
	Residuals	15	27.638	1.8425			
PC3	Sex	1	0.013	0.012987	0.0542	0.819	
	Residuals	15	3.5917	0.239444			

TC		Df	Pillai	approx F	num Df	den Df	*p*
all	Sex	1	0.21141	1.251	3	14	0.3289
	Residuals	16					
		Df	**Sum Sq**	**Mean Sq**	**F value**	***p***	
PC1	Sex	1	6.946	6.9461	3.4266	0.0827	
	Residuals	16	32.434	2.0271			
PC2	Sex	1	0	0.00001	0	0.9983	
	Residuals	16	28.542	1.78385			
PC3	Sex	1	0.5663	0.56629	0.5807	0.4571	
	Residuals	16	15.6042	0.97526			

Appendix 5.4 Correlations between femoral cortical and trabecular properties

Pearson correlations between trabecular and cortical bone properties are reported in this appendix for individual and pooled population samples.

Table 5.4.1. Correlations between body mass standardized femoral midshaft cross-sectional properties and femoral trabecular bone properties in a pooled sex, pooled population sample of Black Earth, Kerma, and Norris Farms.

Pooled		**Proximal femur**				**Distal femur**			
		I_{max}/I_{min}	J	Zp	CSA	I_{max}/I_{min}	J	Zp	CSA
BV/TV	R	-.05	**.54**	**.29**	**.50**	-.09	**.33**	.01	.18
	p	.73	**<.005**	**.04**	**<.005**	.53	**.02**	.94	.22
	N	51	**51**	**51**	**51**	50	**50**	50	50
Tb.Th	R	-.07	**.59**	**.30**	**.44**	.004	**.41**	0	.1
	p	.65	**<.005**	**.03**	**<.005**	.79	**<.005**	.98	.47
	N	51	**51**	**51**	**51**	50	**50**	50	50
Tb.Sp	R	.11	-.03	-.05	-.19	.14	.14	.03	-.14
	p	.46	.83	.73	.19	.33	.34	.84	.34
	N	51	51	51	51	50	50	50	50
DA	R	-.11	**.41**	.12	.06	.01	.25	-.04	-.09
	p	.46	**<.005**	.40	.68	.92	.07	.81	.53
	N	51	**51**	51	51	50	50	50	50
Conn.D	R	-.06	**-.64**	-.24	**-.28**	-.06	**-.38**	-.04	0
	p	.69	**<.005**	.10	**.05**	.66	**.01**	.78	.99
	N	51	**51**	51	**51**	50	**50**	50	50

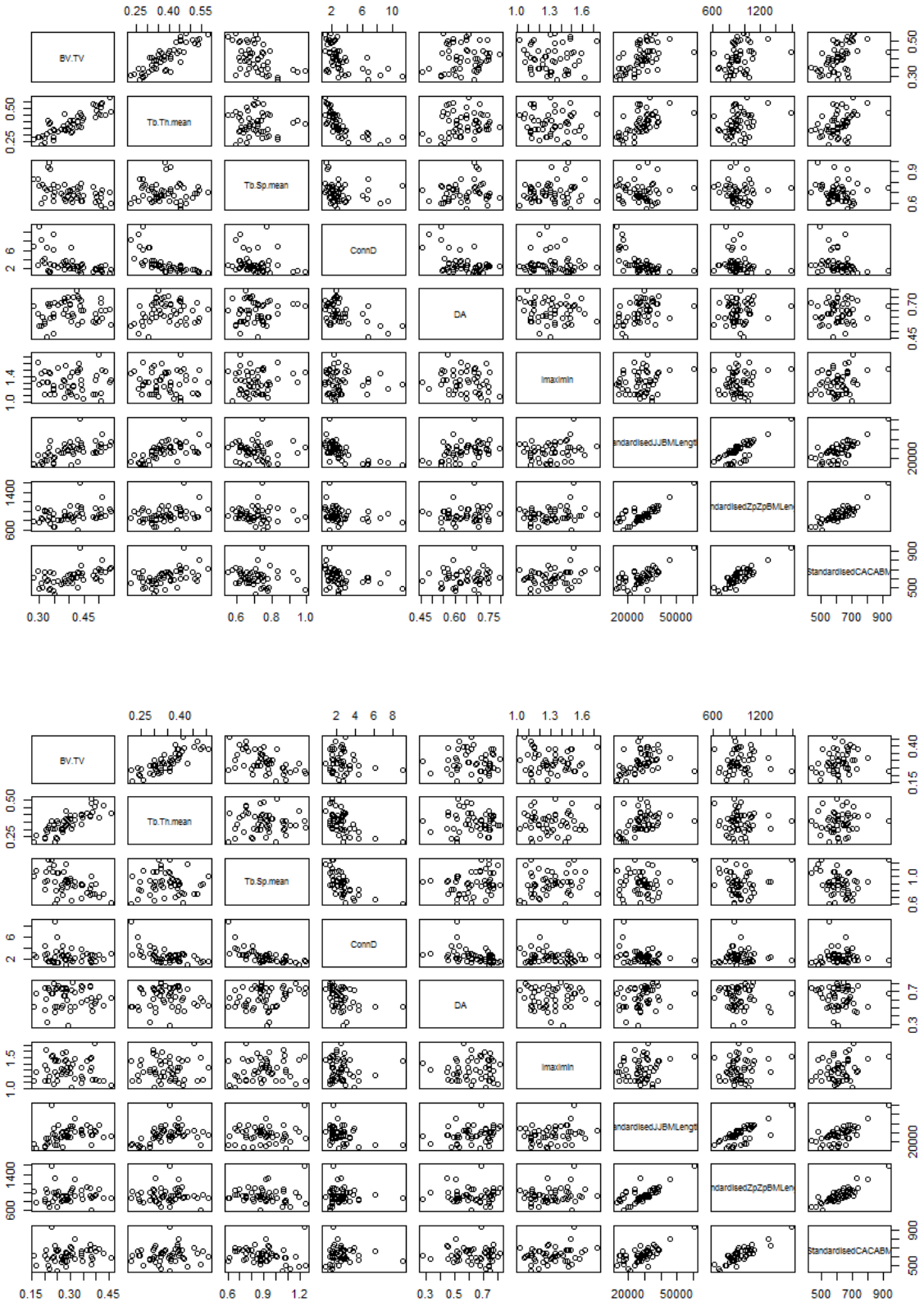

Figure 5.4.1. Correlation matrices between trabecular properties of the proximal (top) and distal (bottom) femur and diaphyseal cross-sectional properties.

Table 5.4.2. Correlations between body mass standardized femoral diaphyseal cross-sectional properties and femoral trabecular bone properties in Black Earth.

Black Earth		**Proximal femur**				**Distal femur**			
		I_{max}/I_{min}	J	Zp	CA	I_{max}/I_{min}	J	Zp	CA
BV/TV	R	-.052	.057	.127	.214	-.311	**-.510**	-.438	-.439
	p	.829	.811	.592	.364	.194	**.026**	.061	.060
	N	20	20	20	20	19	**19**	19	19
Tb.Th	R	-.007	.050	.182	.182	.149	-.401	-.343	-.310
	p	.975	.835	.442	.443	.542	.089	.151	.197
	N	20	20	20	20	19	19	19	19
Tb.Sp	R	.140	-.025	-.038	-.143	**.462**	.417	.385	.354
	p	.556	.917	.875	.547	**.046**	.075	.104	.138
	N	20	20	20	20	**19**	19	19	19
DA	R	-.319	.286	.311	.178	-.038	.225	.164	.168
	p	.170	.221	.183	.452	.878	.354	.501	.492
	N	20	20	20	20	19	19	19	19
Conn.D	R	-.175	-.115	-.173	-.097	-.408	-.071	-.041	-.056
	p	.460	.630	.466	.683	.083	.772	.866	.821
	N	20	20	20	20	19	19	19	19

Table 5.4.3. Correlations between femoral cross-sectional properties and femoral trabecular bone properties in Norris Farms.

Norris Farms		**Proximal femur**				**Distal femur**			
		I_{max}/I_{min}	J	Zp	CA	I_{max}/I_{min}	J	Zp	CA
BV/TV	R	.177	**.566**	**.686**	**.857**	.049	**.596**	**.689**	**.655**
	p	.454	**.009**	**.001**	**.000**	.836	**.006**	**.001**	**.002**
	N	20	**20**	**20**	**20**	20	**20**	**20**	**20**
Tb.Th	R	-.184	**.601**	**.598**	**.536**	-.131	.320	.359	.169
	p	.439	**.005**	**.005**	**.015**	.583	.168	.120	.476
	N	20	**20**	**20**	**20**	20	20	20	20
Tb.Sp	R	-.033	.080	-.038	-.254	-.225	-.406	**-.503**	**-.588**
	p	.890	.737	.873	.279	.341	.075	**.024**	**.006**
	N	20	20	20	20	20	20	**20**	**20**
DA	R	-.088	.412	.385	**.494**	-.154	.300	.262	.051
	p	.713	.071	.093	**.027**	.517	.198	.264	.831
	N	20	20	20	**20**	20	20	20	20
Conn.D	R	.078	**-.465**	-.400	-.337	.165	.002	.038	.199
	p	.745	**.039**	.080	.146	.488	.995	.873	.399
	N	20	**20**	20	20	20	20	20	20

Table 5.4.4. Correlations between femoral cross-sectional properties and femoral trabecular bone properties in Kerma.

Kerma		**Proximal Femur**				**Distal Femur**			
		$I_{max}/_{Imin}$	J	Zp	CA	I_{max}/I_{min}	J	Zp	CA
BV/TV	R	**-.599**	-.292	-.043	.432	.041	.237	.177	.522
	p	**.031**	.383	.901	.140	.891	.482	.602	.067
	n	**13**	11	11	13	14	11	11	13
Tb.Th	R	-.483	-.305	-.066	-.083	.145	.476	.484	.298
	p	.094	.362	.848	.787	.621	.139	.132	.323
	n	13	11	11	13	14	11	11	13
Tb.Sp	R	.334	.074	-.018	-.437	.190	.202	.205	-.360
	p	.264	.830	.959	.135	.515	.551	.544	.226
	n	13	11	11	13	14	11	11	13
Conn.D	R	-.197	-.593	-.567	.073	-.032	-.287	-.288	.069
	p	.518	.054	.069	.813	.914	.391	.391	.823
	n	13	11	11	13	14	11	11	13
DA	R	.228	-.070	-.290	-.219	.316	-.079	-.367	-.305
	p	.453	.837	.386	.472	.270	.817	.267	.310
	n	13	11	11	13	14	11	11	13

Appendix 6.

Appendix 6.1 ANOVA between age categories

Table 6.1.1. ANOVA of trabecular properties between age categories in a pooled population sample. Volumes of interest: Achilles tendon (AT), calcaneal tuber (CT), plantar ligaments (PL), posterior talar facet (PP: posterior, PC: central, PA: anterior), calcaneocuboid (CC), dorsal base (BD), plantar base (BP), dorsal head (HD), plantar head (HP), talar head (TH), anterior calcaneal facet (ACF), posterior calcaneal facet (PCF), trochlea (lateral: TL, central: TC, medial: TM).

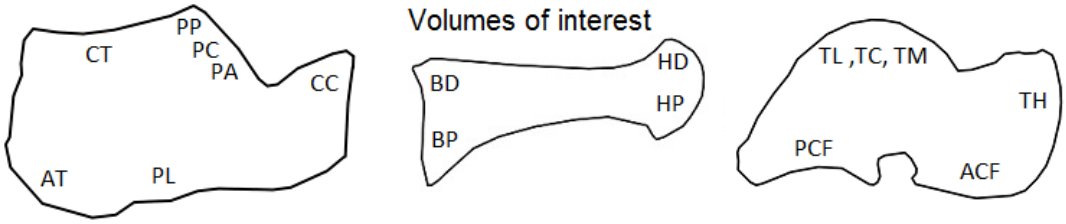

VOI	Summary statistics						Pairwise comparisons			
		Age	N	Mean	S.D.	S.E.	Post-hoc	comparison		*P*
AT	BV/TV	Young	9	0.45	0.06	0.02	Hochberg	Young	Mature	0.40
		Mature	27	0.41	0.09	0.02			Old	**0.04**
		Old	5	0.33	0.12	0.05		Mature	Old	0.19
		Total	41	0.41	0.09	0.01				
	Tb.Th	Young	9	0.28	0.03	0.01	Hochberg	Young	Mature	0.82
		Mature	27	0.30	0.04	0.01			Old	0.45
		Old	5	0.25	0.04	0.02		Mature	Old	0.11
		Total	41	0.29	0.04	0.01				
	DA	Young	9	0.78	0.04	0.01	Games-Howell	Young	Mature	0.11
		Mature	27	0.74	0.07	0.01			Old	0.54
		Old	5	0.73	0.10	0.04		Mature	Old	0.96
		Total	41	0.75	0.07	0.01				
	Tb.Sp	Young	9	0.37	0.05	0.02	Hochberg	Young	Mature	**0.01**
		Mature	27	0.46	0.08	0.02			Old	**0.02**
		Old	5	0.50	0.09	0.04		Mature	Old	0.71
		Total	41	0.45	0.09	0.01				
	log10 Conn.D	Young	9	0.82	0.11	0.04	Hochberg	Young	Mature	**0.00**
		Mature	27	0.67	0.09	0.02			Old	0.20
		Old	5	0.72	0.11	0.05		Mature	Old	0.76
		Total	41	0.71	0.11	0.02				
	Res. Tb.Sp	Young	9	-.055	.05	.017	Hochberg	Young	Mature	.103
		Mature	27	.005	.076	.015			Old	**.044**
		Old	5	.048	.090	.040		Mature	Old	.553
		Total	41	-.002	.078	.012				
	Res. Conn.D	Young	9	.055	.116	.039	Hochberg	Young	Mature	.121
		Mature	27	-.020	.086	.017			Old	.723
		Old	5	.006	.090	.040		Mature	Old	.916
		Total	41	-.001	.096	.015				
	Res. DA	Young	9	0.05	0.04	0.01	Games-Howell	Young	Mature	.130
		Mature	27	-0.01	0.07	0.01			Old	.260
		Old	5	-0.02	0.09	0.04		Mature	Old	.984

		Total	41	0.00	0.07	0.01				
CC	BV/TV	Young	7	0.46	0.07	0.03	Hochberg	Young	Mature	.071
		Mature	26	0.39	0.07	0.01			Old	.228
		Old	4	0.38	0.10	0.05		Mature	Old	.995
		Total	37	0.40	0.08	0.01				
	Tb.Th	Young	7	0.32	0.05	0.02	Hochberg	Young	Mature	.997
		Mature	26	0.32	0.05	0.01			Old	.998
		Old	4	0.32	0.06	0.03		Mature	Old	.983
		Total	37	0.32	0.05	0.01				
	DA	Young	7	0.67	0.05	0.02	Hochberg	Young	Mature	**.002**
		Mature	26	0.73	0.04	0.01			Old	**.003**
		Old	4	0.76	0.02	0.01		Mature	Old	.530
		Total	37	0.72	0.05	0.01				
	Tb.Sp	Young	7	0.43	0.04	0.02	Hochberg	Young	Mature	**.001**
		Mature	26	0.58	0.09	0.02			Old	**.017**
		Old	4	0.59	0.11	0.06		Mature	Old	.989
		Total	37	0.55	0.10	0.02				
	log10 Conn.D	Young	7	0.74	0.16	0.06	Hochberg	Young	Mature	**.004**
		Mature	26	0.53	0.14	0.03			Old	.055
		Old	4	0.52	0.06	0.03		Mature	Old	.999
		Total	37	0.57	0.16	0.03				
	Res. Tb.Sp	Young	7	-.076	.052	.020	Hochberg	Young	Mature	**.009**
		Mature	26	.032	.082	.016			Old	**.035**
		Old	4	.057	.101	.050		Mature	Old	.917
		Total	37	.014	.089	.015				
	Res. Conn.D	Young	7	.115	.157	.059	Hochberg	Young	Mature	.102
		Mature	26	-.018	.144	.028			Old	.199
		Old	4	-.050	.088	.044		Mature	Old	.962
		Total	37	.004	.149	.024				
	Res. DA	Young	7	-0.03	0.05	0.02	Hochberg	Young	Mature	**.022**
		Mature	26	0.02	0.04	0.01			Old	**.010**
		Old	4	0.05	0.03	0.02		Mature	Old	.412
		Total	37	0.01	0.04	0.01				
CT	BV/TV	Young	8	0.36	0.06	0.02	Hochberg	Young	Mature	.910
		Mature	28	0.35	0.08	0.01			Old	.405
		Old	4	0.30	0.06	0.03		Mature	Old	.557
		Total	40	0.35	0.07	0.01				
	Tb.Th	Young	8	0.32	0.05	0.02	Hochberg	Young	Mature	.911
		Mature	28	0.34	0.05	0.01			Old	.831
		Old	4	0.30	0.04	0.02		Mature	Old	.475
		Total	40	0.33	0.05	0.01				
	DA	Young	8	0.79	0.03	0.01	Games-Howell	Young	Mature	.679
		Mature	28	0.80	0.04	0.01			Old	.733
		Old	4	0.80	0.02	0.01		Mature	Old	.995
		Total	40	0.80	0.04	0.01				
	Tb.Sp	Young	8	0.57	0.06	0.02	Hochberg	Young	Mature	.058

		Mature	28	0.68	0.13	0.02			Old	.090
		Old	4	0.73	0.12	0.06		Mature	Old	.843
		Total	40	0.66	0.12	0.02				
	log10 Conn.D	Young	8	0.45	0.13	0.05	Hochberg	Young	Mature	**.038**
		Mature	28	0.30	0.15	0.03			Old	.306
		Old	4	0.31	0.12	0.06		Mature	Old	.999
		Total	40	0.33	0.15	0.02				
	Res. Tb.Sp	Young	8	-0.07	0.07	0.02	Hochberg	Young	Mature	.251
		Mature	28	0.01	0.11	0.02			Old	.165
		Old	4	0.06	0.10	0.05		Mature	Old	.725
		Total	40	0.00	0.11	0.02				
	Res. Conn.D	Young	8	0.07	0.12	0.04	Hochberg	Young	Mature	.310
		Mature	28	-0.01	0.13	0.03			Old	.632
		Old	4	-0.01	0.09	0.05		Mature	Old	1.000
		Total	40	0.00	0.13	0.02				
	Res. DA	Young	8	0.00	0.03	0.01	Hochberg	Young	Mature	.989
		Mature	28	0.00	0.04	0.01			Old	.996
		Old	4	0.00	0.02	0.01		Mature	Old	1.000
		Total	40	0.00	0.04	0.01				
PA	BV/TV	Young	9	0.52	0.05	0.02	Hochberg	Young	Mature	.352
		Mature	25	0.46	0.10	0.02			Old	.465
		Old	4	0.44	0.13	0.06		Mature	Old	.972
		Total	38	0.47	0.10	0.02				
	Tb.Th	Young	9	0.40	0.07	0.02	Hochberg	Young	Mature	.965
		Mature	25	0.38	0.08	0.02			Old	1.000
		Old	4	0.40	0.07	0.03		Mature	Old	.988
		Total	38	0.39	0.07	0.01				
	DA	Young	9	0.63	0.09	0.03	Hochberg	Young	Mature	**.012**
		Mature	25	0.71	0.06	0.01			Old	**.003**
		Old	4	0.78	0.05	0.02		Mature	Old	.217
		Total	38	0.70	0.08	0.01				
	Tb.Sp	Young	9	0.45	0.05	0.02	Hochberg	Young	Mature	.071
		Mature	25	0.55	0.11	0.02			Old	.068
		Old	4	0.60	0.13	0.07		Mature	Old	.718
		Total	38	0.53	0.11	0.02				
	log10 Conn.D	Young	9	0.66	0.18	0.06	Hochberg	Young	Mature	**.031**
		Mature	25	0.51	0.13	0.03			Old	**.040**
		Old	4	0.44	0.07	0.03		Mature	Old	.723
		Total	38	0.54	0.16	0.03				
	Res. Conn.D	Young	9	0.08	0.17	0.06	Hochberg	Young	Mature	.411
		Mature	26	0.01	0.13	0.03			Old	.116
		Old	4	-0.09	0.05	0.03		Mature	Old	.453
		Total	39	0.01	0.14	0.02				
	Res. DA	Young	9	-0.03	0.08	0.03	Hochberg	Young	Mature	.814
		Mature	26	0.00	0.07	0.01			Old	**.038**
		Old	4	0.09	0.04	0.02		Mature	Old	.069
		Total	39	0.00	0.08	0.01				
	Res. Tb.Sp	Young	9	-0.05	0.06	0.02	Hochberg	Young	Mature	.351

		Mature	26	0.00	0.10	0.02			Old	.131
		Old	4	0.07	0.12	0.06		Mature	Old	.548
		Total	39	0.00	0.10	0.02				
PC	BV/TV	Young	9	0.58	0.08	0.03	Hochberg	Young	Mature	.300
		Mature	25	0.52	0.11	0.02			Old	.214
		Old	5	0.48	0.11	0.05		Mature	Old	.822
		Total	39	0.53	0.10	0.02				
	Tb.Th	Young	9	0.39	0.07	0.02	Hochberg	Young	Mature	.982
		Mature	25	0.40	0.08	0.02			Old	.989
		Old	5	0.38	0.06	0.03		Mature	Old	.914
		Total	39	0.40	0.07	0.01				
	DA	Young	9	0.56	0.11	0.04	Hochberg	Young	Mature	.253
		Mature	25	0.62	0.10	0.02			Old	**.039**
		Old	5	0.70	0.08	0.03		Mature	Old	.308
		Total	39	0.62	0.10	0.02				
	Tb.Sp	Young	9	0.37	0.06	0.02	Hochberg	Young	Mature	**.004**
		Mature	25	0.47	0.07	0.01			Old	**.005**
		Old	5	0.51	0.10	0.05		Mature	Old	.626
		Total	39	0.46	0.09	0.01				
	log10 Conn.D	Young	9	0.70	0.20	0.07	Games-Howell	Young	Mature	.313
		Mature	25	0.59	0.13	0.03			Old	.091
		Old	5	0.53	0.04	0.02		Mature	Old	.205
		Total	39	0.60	0.15	0.02				
	Res. Tb.Sp	Young	9	-0.06	0.07	0.02	Hochberg	Young	Mature	**.041**
		Mature	25	0.01	0.07	0.01			Old	**.013**
		Old	5	0.06	0.09	0.04		Mature	Old	.408
		Total	39	0.00	0.08	0.01				
	Res. Conn.D	Young	9	0.07	0.19	0.06	Hochberg	Young	Mature	.791
		Mature	25	0.02	0.13	0.03			Old	.312
		Old	5	-0.06	0.07	0.03		Mature	Old	.579
		Total	39	0.02	0.14	0.02				
	Res. DA	Young	9	-0.04	0.10	0.03	Hochberg	Young	Mature	.621
		Mature	25	0.00	0.09	0.02			Old	.070
		Old	5	0.09	0.09	0.04		Mature	Old	.214
		Total	39	0.00	0.10	0.02				
PP	BV/TV	Young	9	0.49	0.09	0.03	Hochberg	Young	Mature	.862
		Mature	26	0.47	0.09	0.02			Old	.433
		Old	5	0.42	0.08	0.04		Mature	Old	.668
		Total	40	0.47	0.09	0.01				
	Tb.Th	Young	9	0.37	0.06	0.02	Hochberg	Young	Mature	.996
		Mature	26	0.38	0.07	0.01			Old	.961
		Old	5	0.36	0.05	0.02		Mature	Old	.879
		Total	40	0.37	0.06	0.01				
	DA	Young	9	0.70	0.07	0.02	Hochberg	Young	Mature	.690
		Mature	26	0.72	0.06	0.01			Old	.773
		Old	5	0.73	0.06	0.03		Mature	Old	.996
		Total	40	0.72	0.06	0.01				
	Tb.Sp	Young	9	0.49	0.10	0.03	Hochberg	Young	Mature	.546
		Mature	26	0.53	0.08	0.02			Old	.150

		Old	5	0.58	0.06	0.02		Mature	Old	.470
		Total	40	0.53	0.08	0.01				
	log10 Conn.D	Young	9	0.59	0.17	0.06	Hochberg	Young	Mature	.692
		Mature	26	0.53	0.17	0.03			Old	.488
		Old	5	0.47	0.12	0.05		Mature	Old	.864
		Total	40	0.53	0.16	0.03				
	Res. Tb.Sp	Young	9	-0.03	0.10	0.03	Hochberg	Young	Mature	.657
		Mature	26	0.00	0.08	0.02			Old	.173
		Old	5	0.06	0.05	0.02		Mature	Old	.441
		Total	40	0.00	0.08	0.01				
	Res. DA	Young	9	-0.01	0.07	0.02	Hochberg	Young	Mature	.891
		Mature	26	0.01	0.06	0.01			Old	.865
		Old	5	0.02	0.06	0.03		Mature	Old	.988
		Total	40	0.00	0.06	0.01				
	Res. Conn.D	Young	9	0.04	0.17	0.06	Hochberg	Young	Mature	.900
		Mature	26	0.00	0.17	0.03			Old	.609
		Old	5	-0.06	0.13	0.06		Mature	Old	.819
		Total	40	0.00	0.16	0.03				
PL	BV/TV	Young	7	0.35	0.07	0.03	Hochberg	Young	Mature	.056
		Mature	25	0.28	0.07	0.01			Old	.230
		Old	3	0.27	0.05	0.03		Mature	Old	.989
		Total	35	0.29	0.07	0.01				
	Tb.Th	Young	7	0.33	0.07	0.03	Hochberg	Young	Mature	.948
		Mature	25	0.31	0.07	0.01			Old	.774
		Old	3	0.29	0.03	0.02		Mature	Old	.894
		Total	35	0.31	0.06	0.01				
	DA	Young	7	0.68	0.06	0.02	Games-Howell	Young	Mature	.506
		Mature	25	0.71	0.07	0.01			Old	**.005**
		Old	3	0.79	0.02	0.01		Mature	Old	**.002**
		Total	35	0.71	0.07	0.01				
	Tb.Sp	Young	7	0.61	0.06	0.02	Hochberg	Young	Mature	**.004**
		Mature	25	0.78	0.12	0.02			Old	.066
		Old	3	0.79	0.06	0.04		Mature	Old	.995
		Total	35	0.74	0.13	0.02				
	log10 Conn.D	Young	7	0.52	0.13	0.05	Hochberg	Young	Mature	**.004**
		Mature	25	0.30	0.15	0.03			Old	.141
		Old	3	0.31	0.04	0.03		Mature	Old	.999
		Total	35	0.34	0.17	0.03				
	Res. Conn.D	Young	7	0.09	0.13	0.05	Hochberg	Young	Mature	**.036**
		Mature	25	-0.05	0.13	0.03			Old	.396
		Old	3	-0.04	0.09	0.05		Mature	Old	.994
		Total	35	-0.02	0.14	0.02				
	Res. DA	Young	7	-0.01	0.05	0.02	Games-Howell	Young	Mature	1.000
		Mature	25	-0.01	0.07	0.01			Old	**.047**
		Old	3	0.07	0.03	0.02		Mature	Old	**.032**
		Total	35	-0.01	0.07	0.01				
	Res. Tb.Sp	Young	7	-0.10	0.07	0.03	Hochberg	Young	Mature	**.009**
		Mature	25	0.04	0.11	0.02			Old	.108

		Old	3	0.06	0.06	0.03		Mature	Old	.996
		Total	35	0.02	0.12	0.02				
BD	BV/TV	Young	9	0.42	0.05	0.02	Hochberg	Young	Mature	1.000
		Mature	23	0.41	0.08	0.02			Old	1.000
		Old	4	0.42	0.05	0.02		Mature	Old	.999
		Total	36	0.42	0.07	0.01				
	Tb.Th	Young	9	0.25	0.03	0.01	Hochberg	Young	Mature	.455
		Mature	23	0.27	0.05	0.01			Old	.591
		Old	4	0.27	0.03	0.02		Mature	Old	.988
		Total	36	0.26	0.04	0.01				
	DA	Young	9	0.76	0.06	0.02	Hochberg	Young	Mature	1.000
		Mature	23	0.76	0.05	0.01			Old	.726
		Old	4	0.79	0.06	0.03		Mature	Old	.692
		Total	36	0.76	0.06	0.01				
	Tb.Sp	Young	9	0.38	0.04	0.01	Hochberg	Young	Mature	.223
		Mature	23	0.41	0.05	0.01			Old	.694
		Old	4	0.41	0.06	0.03		Mature	Old	.996
		Total	36	0.40	0.05	0.01				
	log10 Conn.D	Young	9	0.95	0.12	0.04	Hochberg	Young	Mature	**.044**
		Mature	23	0.82	0.14	0.03			Old	.165
		Old	4	0.80	0.11	0.06		Mature	Old	.986
		Total	36	0.85	0.14	0.02				
	Res. Tb.Sp	Young	9	-0.03	0.04	0.01	Hochberg	Young	Mature	.509
		Mature	23	0.00	0.05	0.01			Old	.803
		Old	4	0.00	0.05	0.03		Mature	Old	1.000
		Total	36	-0.01	0.05	0.01				
	Res. DA	Young	9	0.00	0.06	0.02	Hochberg	Young	Mature	1.000
		Mature	23	0.00	0.05	0.01			Old	.750
		Old	4	0.03	0.06	0.03		Mature	Old	.662
		Total	36	0.01	0.06	0.01				
	Res. Conn.D	Young	9	0.08	0.12	0.04	Hochberg	Young	Mature	.271
		Mature	23	-0.01	0.14	0.03			Old	.269
		Old	4	-0.05	0.12	0.06		Mature	Old	.882
		Total	36	0.01	0.14	0.02				
BP	BV/TV	Young	9	0.31	0.04	0.01	Hochberg	Young	Mature	.809
		Mature	23	0.29	0.07	0.01			Old	.995
		Old	3	0.30	0.06	0.04		Mature	Old	.990
		Total	35	0.29	0.06	0.01				
	Tb.Th	Young	9	0.23	0.02	0.01	Games-Howell	Young	Mature	.379
		Mature	23	0.25	0.05	0.01			Old	.997
		Old	3	0.23	0.04	0.02		Mature	Old	.795
		Total	35	0.24	0.04	0.01				
	DA	Young	9	0.58	0.06	0.02	Hochberg	Young	Mature	.996
		Mature	23	0.57	0.07	0.02			Old	.988
		Old	3	0.56	0.11	0.06		Mature	Old	.997
		Total	35	0.57	0.07	0.01				
	Tb.Sp	Young	9	0.50	0.08	0.03	Hochberg	Young	Mature	.054

		Mature	23	0.59	0.10	0.02			Old	.952
		Old	3	0.53	0.09	0.05		Mature	Old	.635
		Total	35	0.56	0.10	0.02				
	log10 Conn.D	Young	9	0.91	0.15	0.05	Hochberg	Young	Mature	**.036**
		Mature	23	0.75	0.16	0.03			Old	.917
		Old	3	0.85	0.14	0.08		Mature	Old	.635
		Total	35	0.80	0.17	0.03				
	Res. Tb.Sp	Young	9	-0.04	0.08	0.03	Hochberg	Young	Mature	.569
		Mature	23	0.00	0.09	0.02			Old	1.000
		Old	3	-0.04	0.03	0.02		Mature	Old	.874
		Total	35	-0.02	0.09	0.01				
	Res. DA	Young	9	0.01	0.06	0.02	Hochberg	Young	Mature	.775
		Mature	23	-0.01	0.07	0.01			Old	.947
		Old	3	-0.01	0.12	0.07		Mature	Old	1.000
		Total	35	-0.01	0.07	0.01				
	Res. Conn.D	Young	9	0.07	0.15	0.05	Hochberg	Young	Mature	.453
		Mature	23	-0.01	0.16	0.03			Old	.997
		Old	3	0.06	0.08	0.05		Mature	Old	.879
		Total	35	0.02	0.15	0.03				
HD	BV/TV	Young	9	0.42	0.04	0.01	Hochberg	Young	Mature	.999
		Mature	26	0.42	0.07	0.01			Old	.194
		Old	4	0.50	0.11	0.06		Mature	Old	.149
		Total	39	0.43	0.07	0.01				
	Tb.Th	Young	9	0.24	0.03	0.01	Hochberg	Young	Mature	.260
		Mature	26	0.27	0.05	0.01			Old	.077
		Old	4	0.30	0.06	0.03		Mature	Old	.446
		Total	39	0.26	0.05	0.01				
	DA	Young	9	0.74	0.05	0.02	Hochberg	Young	Mature	.996
		Mature	26	0.75	0.04	0.01			Old	.924
		Old	4	0.76	0.03	0.02		Mature	Old	.951
		Total	39	0.75	0.04	0.01				
	Tb.Sp	Young	9	0.38	0.03	0.01	Games-Howell	Young	Mature	**.009**
		Mature	26	0.43	0.05	0.01			Old	1.000
		Old	4	0.38	0.08	0.04		Mature	Old	.576
		Total	39	0.41	0.05	0.01				
	log10 Conn.D	Young	9	0.93	0.16	0.05	Hochberg	Young	Mature	**.011**
		Mature	26	0.77	0.14	0.03			Old	.100
		Old	4	0.75	0.14	0.07		Mature	Old	.994
		Total	39	0.80	0.16	0.02				
	Res. Tb.Sp	Young	9	-0.01	0.03	0.01	Hochberg	Young	Mature	.568
		Mature	26	0.01	0.05	0.01			Old	.973
		Old	4	-0.02	0.06	0.03		Mature	Old	.501
		Total	39	0.00	0.05	0.01				
	Res. DA	Young	9	0.01	0.05	0.02	Hochberg	Young	Mature	.996
		Mature	26	0.01	0.04	0.01			Old	.925
		Old	4	0.02	0.03	0.02		Mature	Old	.950
		Total	39	0.01	0.04	0.01				
	Res. Conn.D	Young	9	0.07	0.15	0.05	Hochberg	Young	Mature	.153

		Mature	26	-0.04	0.14	0.03			Old	.202
		Old	4	-0.09	0.13	0.07		Mature	Old	.894
		Total	39	-0.02	0.15	0.02				
HP	BV/TV	Young	9	0.33	0.04	0.01	Hochberg	Young	Mature	.986
		Mature	24	0.33	0.06	0.01			Old	1.000
		Old	3	0.32	0.06	0.03		Mature	Old	.988
		Total	36	0.33	0.06	0.01				
	Tb.Th	Young	9	0.25	0.02	0.01	Hochberg	Young	Mature	.335
		Mature	24	0.27	0.05	0.01			Old	.684
		Old	3	0.28	0.06	0.04		Mature	Old	1.000
		Total	36	0.27	0.04	0.01				
	DA	Young	9	0.61	0.05	0.02	Hochberg	Young	Mature	.999
		Mature	24	0.61	0.05	0.01			Old	.979
		Old	3	0.62	0.02	0.01		Mature	Old	.988
		Total	36	0.61	0.05	0.01				
	Tb.Sp	Young	9	0.55	0.07	0.02	Hochberg	Young	Mature	.527
		Mature	24	0.59	0.09	0.02			Old	.884
		Old	3	0.58	0.06	0.03		Mature	Old	1.000
		Total	36	0.58	0.08	0.01				
	log10 Conn.D	Young	9	0.78	0.12	0.04	Hochberg	Young	Mature	.087
		Mature	24	0.67	0.14	0.03			Old	.608
		Old	3	0.68	0.15	0.09		Mature	Old	.994
		Total	36	0.70	0.14	0.02				
	Res. Tb.Sp	Young	9	-0.02	0.08	0.03	Hochberg	Young	Mature	.930
		Mature	24	0.00	0.08	0.02			Old	.977
		Old	3	0.00	0.03	0.02		Mature	Old	1.000
		Total	36	-0.01	0.08	0.01				
	Res. DA	Young	9	-0.01	0.05	0.02	Hochberg	Young	Mature	.843
		Mature	24	0.00	0.05	0.01			Old	.908
		Old	3	0.01	0.03	0.02		Mature	Old	.997
		Total	36	0.00	0.05	0.01				
	Res. Conn	Young	9	0.05	0.12	0.04	Hochberg	Young	Mature	.368
		Mature	24	-0.02	0.14	0.03			Old	.812
		Old	3	-0.02	0.13	0.08		Mature	Old	1.000
		Total	36	0.00	0.13	0.02				
ACF	BV/TV	Young	9	0.33	0.04	0.01	Hochberg	Young	Mature	.478
		Mature	24	0.33	0.06	0.01			Old	.999
		Old	3	0.32	0.06	0.03		Mature	Old	.623
		Total	36	0.33	0.06	0.01				
	Tb.Th	Young	9	0.25	0.02	0.01	Hochberg	Young	Mature	1.000
		Mature	24	0.27	0.05	0.01			Old	.642
		Old	3	0.28	0.06	0.04		Mature	Old	.514
		Total	36	0.27	0.04	0.01				
	DA	Young	9	0.61	0.05	0.02	Hochberg	Young	Mature	.124
		Mature	24	0.61	0.05	0.01			Old	.096

		Old	3	0.62	0.02	0.01		Mature	Old	.835
		Total	36	0.61	0.05	0.01				
	Tb.Sp	Young	9	0.55	0.07	0.02	Hochberg	Young	Mature	.087
		Mature	24	0.59	0.09	0.02			Old	.440
		Old	3	0.58	0.06	0.03		Mature	Old	.962
		Total	36	0.58	0.08	0.01				
	log10 Conn.D	Young	9	0.78	0.12	0.04	Games-Howell	Young	Mature	**.009**
		Mature	24	0.67	0.14	0.03			Old	**.012**
		Old	3	0.68	0.15	0.09		Mature	Old	.842
		Total	36	0.70	0.14	0.02				
	Res. DA	Young	9	-0.05	0.05	0.02	Hochberg	Young	Mature	.188
		Mature	24	0.00	0.06	0.01			Old	.118
		Old	3	0.02	0.06	0.03		Mature	Old	.793
		Total	36	-0.01	0.06	0.01				
	Res. Conn.D	Young	9	0.11	0.11	0.04	Hochberg	Young	Mature	**.031**
		Mature	24	-0.02	0.12	0.02			Old	**.027**
		Old	3	-0.06	0.09	0.04		Mature	Old	.777
		Total	36	0.00	0.12	0.02				
	Res. Tb.Sp	Young	7	-0.05	0.07	0.03	Hochberg	Young	Mature	.375
		Mature	26	0.02	0.12	0.02			Old	.649
		Old	6	0.01	0.07	0.03		Mature	Old	1.000
		Total	39	0.01	0.11	0.02				
PCF	BV/TV	Young	9	0.42	0.06	0.02	Hochberg	Young	Mature	.902
		Mature	22	0.40	0.08	0.02			Old	.990
		Old	5	0.43	0.09	0.04		Mature	Old	.814
		Total	36	0.41	0.08	0.01				
	Tb.Th	Young	9	0.28	0.04	0.01	Hochberg	Young	Mature	.986
		Mature	22	0.29	0.06	0.01			Old	.499
		Old	5	0.32	0.04	0.02		Mature	Old	.556
		Total	36	0.29	0.05	0.01				
	DA	Young	9	0.75	0.05	0.02	Hochberg	Young	Mature	.591
		Mature	22	0.77	0.05	0.01			Old	.982
		Old	5	0.76	0.05	0.02		Mature	Old	.930
		Total	36	0.76	0.05	0.01				
	Tb.Sp	Young	9	0.46	0.02	0.01	Games-Howell	Young	Mature	**.003**
		Mature	22	0.52	0.07	0.01			Old	.229
		Old	5	0.53	0.08	0.04		Mature	Old	.953
		Total	36	0.50	0.07	0.01				
	log10 Conn.D	Young	9	0.80	0.14	0.05	Games-Howell	Young	Mature	.165
		Mature	22	0.68	0.16	0.03			Old	**.003**
		Old	5	0.56	0.03	0.02		Mature	Old	**.009**
		Total	36	0.69	0.16	0.03				
	Res. Tb.Sp	Young	9	-0.03	0.03	0.01	Hochberg	Young	Mature	.143
		Mature	22	0.02	0.07	0.01			Old	.176
		Old	5	0.04	0.07	0.03		Mature	Old	.929
		Total	36	0.01	0.07	0.01				

	Res. DA	Young	9	-0.01	0.05	0.02	Hochberg	Young	Mature	.699
		Mature	22	0.01	0.05	0.01			Old	.990
		Old	5	0.00	0.05	0.02		Mature	Old	.949
		Total	36	0.00	0.05	0.01				
	Res. Conn.D	Young	9	0.06	0.14	0.05	Games-Howell	Young	Mature	.580
		Mature	22	-0.01	0.16	0.03			Old	**.046**
		Old	5	-0.15	0.06	0.03		Mature	Old	.169
		Total	36	-0.01	0.16	0.03				
TH	BV/TV	Young	9	0.48	0.06	0.02	Hochberg	Young	Mature	.828
		Mature	23	0.45	0.10	0.02			Old	1.000
		Old	4	0.48	0.05	0.02		Mature	Old	.909
		Total	36	0.46	0.08	0.01				
	Tb.Th	Young	9	0.30	0.04	0.01	Hochberg	Young	Mature	.928
		Mature	23	0.31	0.05	0.01			Old	.685
		Old	4	0.33	0.03	0.02		Mature	Old	.855
		Total	36	0.31	0.05	0.01				
	DA	Young	9	0.81	0.04	0.01	Hochberg	Young	Mature	.752
		Mature	23	0.83	0.03	0.01			Old	.472
		Old	4	0.84	0.04	0.02		Mature	Old	.800
		Total	36	0.82	0.03	0.01				
	Tb.Sp	Young	9	0.39	0.05	0.02	Hochberg	Young	Mature	.051
		Mature	23	0.45	0.07	0.01			Old	.341
		Old	4	0.45	0.06	0.03		Mature	Old	.999
		Total	36	0.44	0.07	0.01				
	log10 Conn.D	Young	9	0.74	0.13	0.04	Games-Howell	Young	Mature	.093
		Mature	23	0.62	0.13	0.03			Old	.105
		Old	4	0.55	0.13	0.07		Mature	Old	.569
		Total	36	0.65	0.14	0.02				
	Res. Conn.D	Young	9	0.02	0.13	0.04	Hochberg	Young	Mature	.843
		Mature	23	-0.02	0.14	0.03			Old	.233
		Old	4	-0.13	0.12	0.06		Mature	Old	.408
		Total	36	-0.02	0.14	0.02				
	Res. Tb.Sp	Young	9	-0.02	0.05	0.02	Hochberg	Young	Mature	.220
		Mature	23	0.02	0.07	0.01			Old	.513
		Old	4	0.02	0.05	0.02		Mature	Old	1.000
		Total	36	0.01	0.06	0.01				
	Res. DA	Young	9	0.01	0.04	0.01	Hochberg	Young	Mature	.992
		Mature	23	0.02	0.03	0.01			Old	.647
		Old	4	0.03	0.04	0.02		Mature	Old	.691
		Total	36	0.02	0.03	0.01				
TL	BV/TV	Young	9	0.44	0.07	0.02	Hochberg	Young	Mature	.964
		Mature	23	0.43	0.09	0.02			Old	.554
		Old	4	0.50	0.03	0.02		Mature	Old	.294
		Total	36	0.44	0.08	0.01				
	Tb.Th	Young	9	0.28	0.05	0.02	Hochberg	Young	Mature	.899
		Mature	23	0.29	0.06	0.01			Old	.141
		Old	4	0.34	0.04	0.02		Mature	Old	.218
		Total	36	0.29	0.06	0.01				

	DA	Young	9	0.75	0.05	0.02	Hochberg	Young	Mature	.088
		Mature	23	0.78	0.04	0.01			Old	.191
		Old	4	0.79	0.03	0.01		Mature	Old	.959
		Total	36	0.78	0.04	0.01				
	Tb.Sp	Young	9	0.39	0.06	0.02	Hochberg	Young	Mature	.055
		Mature	23	0.44	0.05	0.01			Old	.663
		Old	4	0.43	0.05	0.03		Mature	Old	.889
		Total	36	0.43	0.06	0.01				
	log10 Conn.D	Young	9	0.88	0.15	0.05	Games-Howell	Young	Mature	.055
		Mature	23	0.72	0.16	0.03			Old	**.005**
		Old	4	0.60	0.08	0.04		Mature	Old	.134
		Total	36	0.75	0.17	0.03				
	Res. Tb.Sp	Young	9	-0.02	0.06	0.02	Hochberg	Young	Mature	.139
		Mature	23	0.02	0.05	0.01			Old	.700
		Old	4	0.01	0.05	0.02		Mature	Old	.970
		Total	36	0.01	0.05	0.01				
	Res. DA	Young	9	-0.03	0.04	0.01	Hochberg	Young	Mature	.107
		Mature	23	0.01	0.04	0.01			Old	.205
		Old	4	0.02	0.03	0.01		Mature	Old	.950
		Total	36	0.00	0.04	0.01				
	Res. Conn.D	Young	9	0.10	0.15	0.05	Hochberg	Young	Mature	.248
		Mature	23	0.00	0.16	0.03			Old	**.020**
		Old	4	-0.16	0.08	0.04		Mature	Old	.167
		Total	36	0.01	0.17	0.03				
TC	BV/TV	Young	8	0.43	0.04	0.01	Hochberg	Young	Mature	.665
		Mature	25	0.40	0.09	0.02			Old	.864
		Old	5	0.40	0.10	0.05		Mature	Old	1.000
		Total	38	0.40	0.08	0.01				
	Tb.Th	Young	8	0.28	0.04	0.01	Hochberg	Young	Mature	1.000
		Mature	25	0.28	0.05	0.01			Old	.981
		Old	5	0.29	0.05	0.02		Mature	Old	.958
		Total	38	0.28	0.05	0.01				
	DA	Young	8	0.70	0.06	0.02	Hochberg	Young	Mature	.919
		Mature	25	0.69	0.07	0.01			Old	.764
		Old	5	0.73	0.06	0.03		Mature	Old	.368
		Total	38	0.69	0.07	0.01				
	Tb.Sp	Young	8	0.41	0.04	0.02	Hochberg	Young	Mature	.060
		Mature	25	0.47	0.06	0.01			Old	.231
		Old	5	0.47	0.05	0.02		Mature	Old	1.000
		Total	38	0.46	0.06	0.01				
	log10 Conn.D	Young	8	0.89	0.13	0.05	Games-Howell	Young	Mature	.205
		Mature	25	0.79	0.13	0.03			Old	**.049**
		Old	5	0.69	0.12	0.05		Mature	Old	.285
		Total	38	0.80	0.14	0.02				
	Res. Tb.Sp	Young	8	-0.04	0.04	0.02	Hochberg	Young	Mature	.215
		Mature	25	0.00	0.06	0.01			Old	.260
		Old	5	0.02	0.05	0.02		Mature	Old	.949

		Total	38	0.00	0.06	0.01				
	Res. DA	Young	8	0.01	0.06	0.02	Hochberg	Young	Mature	.994
		Mature	25	0.01	0.07	0.01			Old	.656
		Old	5	0.05	0.06	0.03		Mature	Old	.667
		Total	38	0.02	0.06	0.01				
	Res. Conn.D	Young	8	0.07	0.13	0.05	Hochberg	Young	Mature	.612
		Mature	25	0.01	0.13	0.03			Old	**.043**
		Old	5	-0.12	0.12	0.05		Mature	Old	.129
		Total	38	0.01	0.13	0.02				
TM	BV/TV	Young	9	0.43	0.04	0.01	Hochberg	Young	Mature	.837
		Mature	25	0.41	0.07	0.01			Old	1.000
		Old	4	0.43	0.08	0.04		Mature	Old	.940
		Total	38	0.41	0.07	0.01				
	Tb.Th	Young	9	0.26	0.02	0.01	Hochberg	Young	Mature	.864
		Mature	25	0.27	0.04	0.01			Old	.678
		Old	4	0.28	0.05	0.02		Mature	Old	.897
		Total	38	0.27	0.04	0.01				
	DA	Young	9	0.67	0.07	0.02	Hochberg	Young	Mature	.848
		Mature	25	0.64	0.07	0.01			Old	.915
		Old	4	0.64	0.12	0.06		Mature	Old	.999
		Total	38	0.65	0.07	0.01				
	Tb.Sp	Young	9	0.41	0.04	0.01	Hochberg	Young	Mature	.141
		Mature	25	0.45	0.06	0.01			Old	.461
		Old	4	0.45	0.06	0.03		Mature	Old	1.000
		Total	38	0.44	0.06	0.01				
	log10 Conn.D	Young	9	0.93	0.11	0.04	Games-Howell	Young	Mature	.051
		Mature	25	0.83	0.11	0.02			Old	.133
		Old	4	0.76	0.13	0.06		Mature	Old	.626
		Total	38	0.84	0.12	0.02				
	Res. Conn.D	Young	9	0.07	0.10	0.03	Hochberg	Young	Mature	.371
		Mature	25	0.00	0.12	0.02			Old	.073
		Old	4	-0.10	0.12	0.06		Mature	Old	.340
		Total	38	0.00	0.12	0.02				
	Res. Tb.Sp	Young	9	-0.03	0.04	0.01	Hochberg	Young	Mature	.336
		Mature	25	0.00	0.06	0.01			Old	.486
		Old	4	0.01	0.06	0.03		Mature	Old	.983
		Total	38	0.00	0.06	0.01				
	Res. DA	Young	9	0.01	0.07	0.02	Hochberg	Young	Mature	.999
		Mature	25	0.01	0.07	0.01			Old	.947
		Old	4	-0.01	0.12	0.06		Mature	Old	.890
		Total	38	0.01	0.07	0.01				

Appendix 6.2 Partial Spearman correlations

Table 6.2.1. Partial spearman correlations between trabecular properties and age categories in a pooled population sample. Volumes of interest: Achilles tendon (AT), calcaneal tuber (CT), plantar ligaments (PL), posterior talar facet (PP: posterior, PC: central, PA: anterior), calcaneocuboid (CC), dorsal base (BD), plantar base (BP), dorsal head (HD), plantar head (HP), talar head (TH), anterior calcaneal facet (ACF), posterior calcaneal facet (PCF), trochlea (lateral: TL, central: TC, medial: TM).

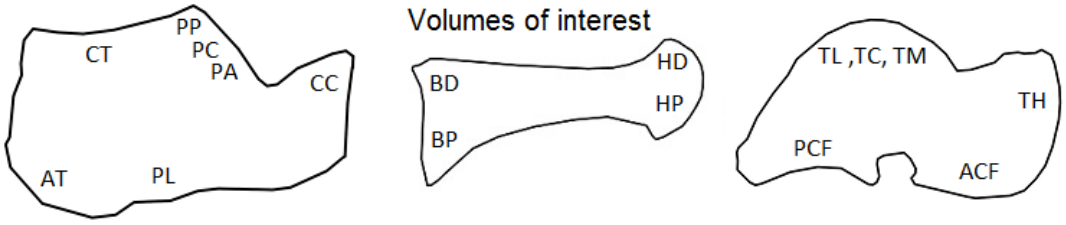

Populations	partial Spearman correlation accounting for body mass (2-tailed)							
	VOI	**N**		**BV/TV**	**Tb.Th**	**DA**	**Tb.Sp**	**Conn.D**
Pooled	AT	42	Rho	-.303	-.097	-.308	**.409**	-.187
			p	.057	.554	.053	**.009**	.247
	CC	37	Rho	-.249	-.015	**.486**	**.449**	**-.411**
			p	.143	.932	**.003**	**.006**	**.013**
	CT	40	Rho	-.188	-.046	-.078	.291	-.167
			p	.251	.782	.638	.072	.310
	PA	38	Rho	-.204	-.008	**.367**	.284	**-.372**
			p	.219	.963	**.023**	.089	**.021**
	PC	39	Rho	-.277	-.055	**.334**	**.407**	-.212
			p	.093	.744	**.041**	**.011**	.201
	PP	40	Rho	-.217	-.041	.047	.280	-.193
			p	.185	.804	.779	.084	.238
	PL	35	Rho	-.285	-.092	.201	**.442**	-.312
			p	.103	.604	.256	**.009**	.072
	BD	36	Rho	.000	.266	.095	.158	**-.356**
			p	.998	.117	.587	.357	**.033**
	BP	35	Rho	-.094	.130	-.222	.140	-.175
			p	.598	.464	.207	.429	.321
	HD	39	Rho	.242	**.355**	-.003	-.120	**-.322**
			p	.143	**.029**	.988	.474	**.049**
	HP	36	Rho	.106	.242	.071	.040	-.233
			p	.545	.161	.685	.818	.178
	ACF	39	Rho	-.054	.152	.308	.206	**-.415**
			p	.750	.363	.060	.215	**.010**
	PCF	36	Rho	.015	.233	.053	.315	**-.393**
			p	.930	.177	.763	.065	**.020**
	TH	36	Rho	.037	.192	.059	.199	-.276
			p	.833	.270	.735	.251	.108
	TL	36	Rho	.151	.325	.294	.119	**-.449**
			p	.381	.053	.082	.495	**.006**
	TC	38	Rho	-.152	.037	.118	.262	**-.346**

			p	.369	.827	.487	.117	**.036**
	TM	38	Rho	-.106	.132	-.098	.192	**-.367**
			p	.528	.429	.559	.255	**.023**
Black Earth	AT	17	Rho	-.306	-.294	**-.674**	.447	-.070
			p	.249	.269	**.004**	.082	.797
	CC	13	Rho	-.534	-.557	.524	.519	-.153
			p	.074	.060	.080	.083	.635
	CT	16	Rho	-.185	-.132	-.310	.130	.035
			p	.509	.639	.260	.645	.902
	PA	13	Rho	-.206	-.292	.475	.146	-.108
			p	.521	.357	.119	.651	.737
	PC	13	Rho	-.552	-.444	.377	.479	.159
			p	.063	.148	.227	.115	.621
	PP	15	Rho	-.278	-.211	-.028	.436	-.043
			p	.335	.469	.924	.119	.885
	PL	12	Rho	**-.668**	-.551	.219	.576	-.020
			p	**.025**	.079	.518	.063	.954
	BD	15	Rho	-.062	.146	.054	.087	-.310
			p	.835	.618	.855	.767	.281
	BP	13	Rho	.174	.128	-.309	-.479	.242
			p	.589	.691	.328	.116	.448
	HD	17	Rho	**.502**	.407	-.146	**-.499**	-.294
			p	**.048**	.118	.590	**.049**	.269
	HP	14	Rho	.303	.373	.172	-.252	-.244
			p	.315	.210	.574	.406	.421
	ACF	13	Rho	-.258	-.057	.430	.404	-.384
			p	.418	.861	.163	.193	.218
	PCF	12	Rho	-.062	.150	-.337	.424	-.319
			p	.857	.660	.310	.194	.339
	TH	11	Rho	-.231	-.049	-.127	.528	-.328
			p	.521	.893	.727	.117	.354
	TL	14	Rho	-.072	.138	-.039	.042	-.411
			p	.807	.639	.895	.891	.145
	TC	14	Rho	-.424	-.304	-.072	.474	-.382
			p	.149	.312	.816	.102	.197
	TM	14	Rho	-.093	.004	.000	.201	-.477
			p	.753	.990	.999	.510	.085
Kerma	AT	7	Rho	-.352	.443	.267	.348	-.573
			p	.494	.379	.609	.499	.235
	CC	9	Rho	.182	**.756**	.478	.219	-.602
			p	.666	**.030**	.230	.602	.114
	CT	9	Rho	.305	.681	.071	-.001	-.274
			p	.463	.063	.867	.998	.511
	PA	8	Rho	.180	.522	.316	.088	-.407
			p	.670	.185	.446	.850	.318
	PC	9	Rho	.206	.614	.407	-.044	-.350
			p	.625	.105	.317	.917	.396

	PP	8	Rho	.525	**.767**	-.277	.002	-.375
			p	.227	**.044**	.547	.997	.408
	PL	8	Rho	-.044	.127	.403	.364	-.692
			p	.926	.785	.370	.423	.085
	BD	7	Rho	.054	**.936**	-.677	.588	-.286
			p	.919	**.006**	.139	.220	.583
	BP	7	Rho	-.762	.107	.216	.629	-.585
			p	.079	.840	.681	.181	.223
	HD	7	Rho	.041	.465	.073	.728	-.778
			p	.939	.353	.891	.101	.068
	HP	7	Rho	-.474	.017	**1.000**	.349	-.322
			p	.342	.974	**0.000**	.497	.534
	ACF	10	Rho	.442	.434	**.775**	.221	-.637
			p	.234	.243	**.014**	.567	.065
	PCF	10	Rho	.338	.323	-.091	.505	-.636
			p	.374	.396	.817	.166	.066
	TH	9	Rho	.176	.289	-.068	.103	-.312
			p	.676	.487	.873	.808	.452
	TL	7	Rho	.780	.748	.803	-.282	-.506
			p	.067	.087	.054	.589	.306
	TC	9	Rho	-.138	.046	.082	.162	-.309
			p	.744	.914	.846	.702	.456
	TM	9	Rho	-.396	.116	-.341	.316	-.490
			p	.332	.784	.408	.445	.217
St. Johns	AT	17	Rho	**-.718**	-.388	.163	.420	-.249
			p	**.002**	.138	.547	.105	.352
	CC	15	Rho	**-.692**	-.246	.441	**.645**	-.503
			p	**.006**	.396	.114	**.013**	.067
	CT	15	Rho	**-.766**	-.512	.071	**.604**	-.270
			p	**.001**	.061	.811	**.022**	.351
	PA	17	Rho	**-.571**	-.142	.410	**.621**	-.453
			p	**.021**	.600	.115	**.010**	.078
	PC	17	Rho	**-.567**	-.259	.130	**.584**	-.057
			p	**.022**	.332	.631	**.017**	.833
	PP	17	Rho	**-.521**	-.419	.030	.287	.099
			p	**.039**	.106	.911	.281	.715
	PL	15	Rho	**-.571**	-.263	.374	**.539**	-.410
			p	**.033**	.363	.188	**.047**	.145
	BD	14	Rho	**-.662**	-.230	.202	**.595**	**-.572**
			p	**.010**	.429	.508	**.025**	**.033**
	BP	15	Rho	**-.862**	.075	**-.735**	**.801**	**-.589**
			p	**.000**	.798	**.003**	**.001**	**.027**
	HD	15	Rho	**-.557**	-.424	.067	.378	.116
			p	**.039**	.131	.819	.183	.693
	HP	15	Rho	**-.541**	-.118	.010	.223	-.129
			p	**.046**	.689	.974	.443	.660
	ACF	16	Rho	**-.660**	-.345	.490	**.581**	-.391

		p	**.007**	.208	.064	**.023**	.150
PCF	14	Rho	**-.679**	-.306	.519	.536	-.138
		p	**.011**	.309	.069	.059	.653
TH	16	Rho	-.298	-.014	.415	.289	.021
		p	.281	.962	.124	.295	.941
TL	15	Rho	**-.697**	-.147	.373	.390	-.342
		p	**.006**	.615	.189	.168	.231
TC	15	Rho	**-.695**	-.246	-.125	.470	-.046
		p	**.006**	.396	.670	.090	.876
TM	15	Rho	-.497	.055	-.048	.406	-.218
		p	.071	.851	.870	.150	.454

Appendix 7.

Appendix 7.1 Listwise ANOVA

Calcaneus

Table 7.1.1. ANOVA of BV/TV between pooled sex populations. Achilles tendon (AT), calcaneal tuber (CT), plantar ligaments (PL), posterior talar facet (PP: posterior, PC: central, PA: anterior), calcaneocuboid (CC), dorsal base (BD), plantar base (BP), dorsal head (HD), plantar head (HP), talar head (TH), anterior calcaneal facet (ACF), posterior calcaneal facet (PCF), trochlea (lateral: TL, central: TC, medial: TM).

ANOVA – pooled sex calcaneus BV/TV							**Test of Homogeneity of Variances**			
		Sum of Squares	**df**	**Mean Square**	**F**	***p***	**Levene Statistic**	**df1**	**df2**	***p***
AT	Between Groups	.153	3	.051	11.294	**.000**	.244	3	44	.865
	Within Groups	.199	44	.005						
	Total	.352	47							
CC	Between Groups	.183	3	.061	15.556	**.000**	.789	3	44	.507
	Within Groups	.173	44	.004						
	Total	.356	47							
CT	Between Groups	.116	3	.039	12.801	**.000**	.691	3	44	.563
	Within Groups	.133	44	.003						
	Total	.248	47							
PA	Between Groups	.178	3	.059	8.333	**.000**	.440	3	44	.725
	Within Groups	.313	44	.007						
	Total	.491	47							
PC	Between Groups	.206	3	.069	9.053	**.000**	.225	3	44	.879
	Within Groups	.333	44	.008						
	Total	.539	47							
PP	Between Groups	.147	3	.049	10.839	**.000**	.906	3	44	.446
	Within Groups	.199	44	.005						
	Total	.346	47							
PL	Between Groups	.116	3	.039	7.668	**.000**	1.503	3	44	.227
	Within Groups	.222	44	.005						
	Total	.338	47							

Table 7.1.2. Pairwise post-hoc comparisons of BV/TV between pooled sex populations. Achilles tendon (AT), calcaneal tuber (CT), plantar ligaments (PL), posterior talar facet (PP: posterior, PC: central, PA: anterior), calcaneocuboid (CC), dorsal base (BD), plantar base (BP), dorsal head (HD), plantar head (HP), talar head (TH), anterior calcaneal facet (ACF), posterior calcaneal facet (PCF), trochlea (lateral: TL, central: TC, medial: TM).

Pooled sex calcaneus BV/TV pairwise post hoc comparisons									
Summary statistics						**Post Hoc**			
VOI	**Population**	**N**	**Mean**	**S.D**	**S.E.**	**type**	**pairwise comparison**		***p***
AT	Black Earth	9	0.49	0.09	0.03	Hochberg	Black Earth	Jebel Moya	.880
	Jebel Moya	9	0.46	0.07	0.02			Kerma	**.000**
	Kerma	14	0.34	0.07	0.02			St. Johns	**.012**
	St. Johns	16	0.40	0.05	0.01		Jebel Moya	Kerma	**.001**
	Total	48	0.41	0.09	0.01			St. Johns	.214

							Kerma	St. Johns	.101
CC	Black Earth	9	0.48	0.07	0.02	Hochberg	Black Earth	Jebel Moya	.961
	Jebel Moya	9	0.50	0.07	0.02			Kerma	**.000**
	Kerma	14	0.36	0.07	0.02			St. Johns	**.001**
	St. Johns	16	0.37	0.05	0.01		Jebel Moya	Kerma	**.000**
	Total	48	0.41	0.09	0.01			St. Johns	**.000**
							Kerma	St. Johns	.995
CT	Black Earth	9	0.42	0.07	0.02	Hochberg	Black Earth	Jebel Moya	.969
	Jebel Moya	9	0.40	0.05	0.02			Kerma	**.000**
	Kerma	14	0.29	0.04	0.01			St. Johns	**.002**
	St. Johns	16	0.33	0.06	0.01		Jebel Moya	Kerma	**.000**
	Total	48	0.35	0.07	0.01			St. Johns	**.020**
							Kerma	St. Johns	.430
PA	Black Earth	9	0.57	0.08	0.03	Hochberg	Black Earth	Jebel Moya	.960
	Jebel Moya	9	0.54	0.10	0.03			Kerma	**.001**
	Kerma	14	0.42	0.09	0.02			St. Johns	**.005**
	St. Johns	16	0.44	0.07	0.02		Jebel Moya	Kerma	**.011**
	Total	48	0.48	0.10	0.01			St. Johns	.055
							Kerma	St. Johns	.964
PC	Black Earth	9	0.64	0.09	0.03	Hochberg	Black Earth	Jebel Moya	.994
	Jebel Moya	9	0.62	0.09	0.03			Kerma	**.003**
	Kerma	14	0.50	0.07	0.02			St. Johns	**.001**
	St. Johns	16	0.49	0.09	0.02		Jebel Moya	Kerma	**.019**
	Total	48	0.55	0.11	0.02			St. Johns	**.005**
							Kerma	St. Johns	.999
PP	Black Earth	9	0.54	0.09	0.03	Hochberg	Black Earth	Jebel Moya	1.000
	Jebel Moya	9	0.55	0.07	0.02			Kerma	**.000**
	Kerma	14	0.41	0.04	0.01			St. Johns	**.012**
	St. Johns	16	0.45	0.07	0.02		Jebel Moya	Kerma	**.000**
	Total	48	0.47	0.09	0.01			St. Johns	**.008**
							Kerma	St. Johns	.622
PL	Black Earth	9	0.35	0.07	0.02	Hochberg	Black Earth	Jebel Moya	.973
	Jebel Moya	9	0.37	0.10	0.03			Kerma	**.013**
	Kerma	14	0.25	0.06	0.02			St. Johns	.089
	St. Johns	16	0.27	0.06	0.02		Jebel Moya	Kerma	**.001**
	Total	48	0.30	0.08	0.01			St. Johns	**.010**
							Kerma	St. Johns	.914

Table 7.1.3. ANOVA of DA between pooled sex populations. Achilles tendon (AT), calcaneal tuber (CT), plantar ligaments (PL), posterior talar facet (PP: posterior, PC: central, PA: anterior), calcaneocuboid (CC), dorsal base (BD), plantar base (BP), dorsal head (HD), plantar head (HP), talar head (TH), anterior calcaneal facet (ACF), posterior calcaneal facet (PCF), trochlea (lateral: TL, central: TC, medial: TM).

ANOVA - pooled sex calcaneus DA							**Test of Homogeneity of Variances**			
		Sum of Squares	**df**	**Mean Square**	**F**	***p***	**Levene Statistic**	**df1**	**df2**	***p***
AT	Between Groups	.023	3	.008	2.147	.108	3.275	3	44	**.030**
	Within Groups	.160	44	.004						
	Total	.184	47							
CC	Between Groups	.018	3	.006	2.077	.117	1.657	3	44	.190
	Within Groups	.125	44	.003						
	Total	.142	47							
CT	Between Groups	.009	3	.003	2.647	.061	1.209	3	44	.318
	Within Groups	.050	44	.001						
	Total	.059	47							
PA	Between Groups	.033	3	.011	1.155	.338	2.227	3	44	.098
	Within Groups	.424	44	.010						
	Total	.457	47							
PC	Between Groups	.075	3	.025	2.421	.079	.095	3	44	.962
	Within Groups	.454	44	.010						
	Total	.528	47							
PP	Between Groups	.023	3	.008	1.995	.129	2.159	3	44	.106
	Within Groups	.168	44	.004						
	Total	.191	47							
PL	Between Groups	.045	3	.015	4.287	.010	.335	3	44	.800
	Within Groups	.155	44	.004						
	Total	.201	47							

Table 7.1.4. Pairwise post-hoc comparisons of DA between pooled sex populations. Achilles tendon (AT), calcaneal tuber (CT), plantar ligaments (PL), posterior talar facet (PP: posterior, PC: central, PA: anterior), calcaneocuboid (CC), dorsal base (BD), plantar base (BP), dorsal head (HD), plantar head (HP), talar head (TH), anterior calcaneal facet (ACF), posterior calcaneal facet (PCF), trochlea (lateral: TL, central: TC, medial: TM).

Pooled sex calcaneus DA pairwise post hoc comparisons									
Summary statistics						**Post Hoc**			
VOI	**Population**	**N**	**Mean**	**S.D**	**S.E.**	**type**	**pairwise comparison**		***p***
AT	Black Earth	9	.73	.08	.03	Games-Howell	Black Earth	Jebel Moya	.966
	Jebel Moya	9	.74	.08	.03			Kerma	.709
	Kerma	14	.76	.04	.01			St. Johns	.247
	St. Johns	16	.79	.04	.01		Jebel Moya	Kerma	.959
	Total	48	.76	.06	.01			St. Johns	.505
							Kerma	St. Johns	.321
CC	Black Earth	9	.73	.03	.01	Hochberg	Black Earth	Jebel Moya	.915
	Jebel Moya	9	.71	.05	.02			Kerma	.978

	Kerma	14	.72	.06	.02			St. Johns	.141
	St. Johns	16	.68	.06	.01		Jebel Moya	Kerma	1.000
	Total	48	.71	.06	.01			St. Johns	.769
							Kerma	St. Johns	.378
CT	Black Earth	9	.81	.04	.01	Hochberg	Black Earth	Jebel Moya	.669
	Jebel Moya	9	.78	.03	.01			Kerma	.997
	Kerma	14	.81	.03	.01			St. Johns	.482
	St. Johns	16	.78	.04	.01		Jebel Moya	Kerma	.256
	Total	48	.80	.04	.01			St. Johns	1.000
							Kerma	St. Johns	.103
PA	Black Earth	9	.70	.05	.02	Hochberg	Black Earth	Jebel Moya	.674
	Jebel Moya	9	.64	.10	.03			Kerma	.999
	Kerma	14	.68	.12	.03			St. Johns	1.000
	St. Johns	16	.71	.09	.02		Jebel Moya	Kerma	.846
	Total	48	.69	.10	.01			St. Johns	.376
							Kerma	St. Johns	.968
PC	Black Earth	9	.67	.10	.03	Hochberg	Black Earth	Jebel Moya	.318
	Jebel Moya	9	.58	.09	.03			Kerma	.891
	Kerma	14	.63	.11	.03			St. Johns	.100
	St. Johns	16	.57	.10	.03		Jebel Moya	Kerma	.853
	Total	48	.61	.11	.02			St. Johns	1.000
							Kerma	St. Johns	.496
PP	Black Earth	9	.76	.03	.01	Hochberg	Black Earth	Jebel Moya	.326
	Jebel Moya	9	.70	.07	.02			Kerma	.466
	Kerma	14	.71	.07	.02			St. Johns	.129
	St. Johns	16	.70	.07	.02		Jebel Moya	Kerma	.999
	Total	48	.71	.06	.01			St. Johns	1.000
							Kerma	St. Johns	.975
PL	Black Earth	9	.67	.07	.02	Hochberg	Black Earth	Jebel Moya	.710
	Jebel Moya	9	.71	.05	.02			Kerma	.396
	Kerma	14	.72	.06	.02			St. Johns	**.007**
	St. Johns	16	.76	.06	.01		Jebel Moya	Kerma	1.000
	Total	48	.72	.07	.01			St. Johns	.269
							Kerma	St. Johns	.318

Table 7.1.5. ANOVA of residual DA between pooled sex populations. Achilles tendon (AT), calcaneal tuber (CT), plantar ligaments (PL), posterior talar facet (PP: posterior, PC: central, PA: anterior), calcaneocuboid (CC), dorsal base (BD), plantar base (BP), dorsal head (HD), plantar head (HP), talar head (TH), anterior calcaneal facet (ACF), posterior calcaneal facet (PCF), trochlea (lateral: TL, central: TC, medial: TM).

ANOVA - pooled sex calcaneus residual DA							**Test of Homogeneity of Variances**			
		Sum of Squares	**df**	**Mean Square**	**F**	***p***	**Levene Statistic**	**df1**	**df2**	***p***
AT	Between Groups	.022	3	.007	2.020	.125	2.919	3	43	**.045**
	Within Groups	.157	43	.004						
	Total	.179	46							
CC	Between Groups	.014	3	.005	1.771	.167	1.084	3	43	.366
	Within Groups	.110	43	.003						
	Total	.123	46							
CT	Between Groups	.011	3	.004	3.313	.029	2.141	3	43	.109
	Within Groups	.047	43	.001						
	Total	.058	46							
PA	Between Groups	.041	3	.014	1.491	.230	4.003	3	43	**.013**
	Within Groups	.397	43	.009						
	Total	.438	46							
PC	Between Groups	.102	3	.034	4.124	.012	.348	3	43	.791
	Within Groups	.355	43	.008						
	Total	.458	46							
PP	Between Groups	.029	3	.010	2.813	.051	2.134	3	43	.110
	Within Groups	.148	43	.003						
	Total	.177	46							
PL	Between Groups	.040	3	.013	4.091	.012	.388	3	43	.762
	Within Groups	.141	43	.003						
	Total	.181	46							

Table 7.1.6. Pairwise post-hoc comparisons of residual DA between pooled sex populations. Achilles tendon (AT), calcaneal tuber (CT), plantar ligaments (PL), posterior talar facet (PP: posterior, PC: central, PA: anterior), calcaneocuboid (CC), dorsal base (BD), plantar base (BP), dorsal head (HD), plantar head (HP), talar head (TH), anterior calcaneal facet (ACF), posterior calcaneal facet (PCF), trochlea (lateral: TL, central: TC, medial: TM).

Pooled sex calcaneus residual DA pairwise post hoc comparisons									
Summary statistics						**Post Hoc**			
VOI	**Population**	**N**	**Mean**	**S.D**	**S.E.**	**type**	**pairwise comparison**		***p***
AT	Black Earth	9	-.020	.084	.028	Games-Howell	Black Earth	Jebel Moya	.983
	Jebel Moya	9	-.006	.078	.026			Kerma	.735
	Kerma	14	.012	.046	.012			St. Johns	.277
	St. Johns	15	.038	.042	.011		Jebel Moya	Kerma	.922
	Total	47	.011	.062	.009			St. Johns	.431
							Kerma	St. Johns	.397
CC	Black Earth	9	.026	.031	.010	Hochberg	Black Earth	Jebel Moya	.829
	Jebel Moya	9	-.001	.053	.018			Kerma	.963

	Kerma	14	.008	.058	.016			St. Johns	.183
	St. Johns	15	-.021	.051	.013		Jebel Moya	Kerma	.998
	Total	47	.000	.052	.008			St. Johns	.925
							Kerma	St. Johns	.530
CT	Black Earth	9	.015	.032	.011	Hochberg	Black Earth	Jebel Moya	.469
	Jebel Moya	9	-.011	.040	.013			Kerma	.998
	Kerma	14	.021	.020	.005			St. Johns	.308
	St. Johns	15	-.012	.038	.010		Jebel Moya	Kerma	.157
	Total	47	.003	.035	.005			St. Johns	1.000
							Kerma	St. Johns	.061
PA	Black Earth	9	.014	.039	.013	Games-Howell	Black Earth	Jebel Moya	.345
	Jebel Moya	9	-.066	.130	.043			Kerma	.884
	Kerma	14	-.008	.101	.027			St. Johns	1.000
	St. Johns	15	.013	.092	.024		Jebel Moya	Kerma	.674
	Total	47	-.008	.098	.014			St. Johns	.407
							Kerma	St. Johns	.932
PC	Black Earth	9	.064	.086	.029	Hochberg	Black Earth	Jebel Moya	.121
	Jebel Moya	9	-.038	.102	.034			Kerma	.783
	Kerma	14	.017	.094	.025			St. Johns	**.015**
	St. Johns	15	-.059	.084	.022		Jebel Moya	Kerma	.643
	Total	47	-.009	.100	.015			St. Johns	.995
							Kerma	St. Johns	.163
PP	Black Earth	9	.043	.027	.009	Hochberg	Black Earth	Jebel Moya	.196
	Jebel Moya	9	-.016	.066	.022			Kerma	.373
	Kerma	14	-.002	.065	.017			St. Johns	**.042**
	St. Johns	15	-.026	.061	.016		Jebel Moya	Kerma	.993
	Total	47	-.004	.062	.009			St. Johns	.999
							Kerma	St. Johns	.839
PL	Black Earth	9	-.039	.062	.021	Hochberg	Black Earth	Jebel Moya	.920
	Jebel Moya	9	-.013	.038	.013			Kerma	.431
	Kerma	14	.003	.058	.015			St. Johns	**.011**
	St. Johns	15	.041	.063	.016		Jebel Moya	Kerma	.982
	Total	47	.004	.063	.009			St. Johns	.153
							Kerma	St. Johns	.381

Table 7.1.7. ANOVA of Tb.Th between pooled sex populations. Achilles tendon (AT), calcaneal tuber (CT), plantar ligaments (PL), posterior talar facet (PP: posterior, PC: central, PA: anterior), calcaneocuboid (CC), dorsal base (BD), plantar base (BP), dorsal head (HD), plantar head (HP), talar head (TH), anterior calcaneal facet (ACF), posterior calcaneal facet (PCF), trochlea (lateral: TL, central: TC, medial: TM).

ANOVA - pooled sex calcaneus Tb.Th							**Test of Homogeneity of Variances**			
		Sum of Squares	**df**	**Mean Square**	**F**	***p***	**Levene Statistic**	**df1**	**df2**	***p***
AT	Between Groups	.032	3	.011	9.187	.000	.699	3	44	.558
	Within Groups	.051	44	.001						
	Total	.083	47							
CC	Between Groups	.049	3	.016	10.293	.000	.721	3	44	.545
	Within Groups	.069	44	.002						
	Total	.118	47							
CT	Between Groups	.035	3	.012	8.024	.000	1.250	3	44	.303
	Within Groups	.063	44	.001						
	Total	.098	47							
PA	Between Groups	.095	3	.032	9.758	.000	1.064	3	44	.374
	Within Groups	.142	44	.003						
	Total	.237	47							
PC	Between Groups	.105	3	.035	8.745	.000	.609	3	44	.613
	Within Groups	.175	44	.004						
	Total	.280	47							
PP	Between Groups	.072	3	.024	9.966	.000	1.486	3	44	.231
	Within Groups	.105	44	.002						
	Total	.177	47							
PL	Between Groups	.097	3	.032	15.604	.000	1.934	3	44	.138
	Within Groups	.091	44	.002						
	Total	.187	47							

Table 7.1.8. Pairwise post-hoc comparisons of Tb.Th between pooled sex populations. Achilles tendon (AT), calcaneal tuber (CT), plantar ligaments (PL), posterior talar facet (PP: posterior, PC: central, PA: anterior), calcaneocuboid (CC), dorsal base (BD), plantar base (BP), dorsal head (HD), plantar head (HP), talar head (TH), anterior calcaneal facet (ACF), posterior calcaneal facet (PCF), trochlea (lateral: TL, central: TC, medial: TM).

Pooled sex calcaneus Tb.Th pairwise post hoc comparisons									
Summary statistics						**Post Hoc**			
VOI	**Population**	**N**	**Mean**	**S.D**	**S.E.**	**type**	**pairwise comparison**		***p***
AT	Black Earth	9	.331	.043	.014	Hochberg	Black Earth	Jebel Moya	.832
	Jebel Moya	9	.313	.034	.011			Kerma	**.000**
	Kerma	14	.266	.030	.008			St. Johns	**.001**
	St. Johns	16	.274	.033	.008		Jebel Moya	Kerma	**.014**
	Total	48	.289	.042	.006			St. Johns	**.050**
							Kerma	St. Johns	.989
CC	Black Earth	9	.370	.026	.009	Hochberg	Black Earth	Jebel Moya	1.000

	Jebel Moya	9	.367	.044	.015			Kerma	**.002**
	Kerma	14	.305	.041	.011			St. Johns	**.001**
	St. Johns	16	.301	.042	.011		Jebel Moya	Kerma	**.004**
	Total	48	.328	.050	.007			St. Johns	**.001**
							Kerma	St. Johns	1.000
CT	Black Earth	9	.381	.029	.010	Hochberg	Black Earth	Jebel Moya	.226
	Jebel Moya	9	.344	.033	.011			Kerma	**.000**
	Kerma	14	.306	.036	.010			St. Johns	**.002**
	St. Johns	16	.320	.045	.011		Jebel Moya	Kerma	.138
	Total	48	.332	.046	.007			St. Johns	.563
							Kerma	St. Johns	.909
PA	Black Earth	9	.462	.058	.019	Hochberg	Black Earth	Jebel Moya	.905
	Jebel Moya	9	.436	.060	.020			Kerma	**.001**
	Kerma	14	.365	.043	.011			St. Johns	**.000**
	St. Johns	16	.354	.065	.016		Jebel Moya	Kerma	**.032**
	Total	48	.393	.071	.010			St. Johns	**.007**
							Kerma	St. Johns	.996
PC	Black Earth	9	.474	.061	.020	Hochberg	Black Earth	Jebel Moya	1.000
	Jebel Moya	9	.464	.068	.023			Kerma	**.008**
	Kerma	14	.381	.050	.013			St. Johns	**.001**
	St. Johns	16	.366	.072	.018		Jebel Moya	Kerma	**.022**
	Total	48	.409	.077	.011			St. Johns	**.004**
							Kerma	St. Johns	.987
PP	Black Earth	9	.435	.055	.018	Hochberg	Black Earth	Jebel Moya	.858
	Jebel Moya	9	.410	.044	.015			Kerma	**.000**
	Kerma	14	.341	.039	.010			St. Johns	**.001**
	St. Johns	16	.349	.055	.014		Jebel Moya	Kerma	**.010**
	Total	48	.374	.061	.009			St. Johns	**.024**
							Kerma	St. Johns	.998
PL	Black Earth	9	.387	.046	.015	Hochberg	Black Earth	Jebel Moya	.417
	Jebel Moya	9	.350	.060	.020			Kerma	**.000**
	Kerma	14	.268	.031	.008			St. Johns	**.000**
	St. Johns	16	.293	.047	.012		Jebel Moya	Kerma	**.001**
	Total	48	.314	.063	.009			St. Johns	**.026**
							Kerma	St. Johns	.570

Table 7.1.9. ANOVA of Tb.Sp between pooled sex populations. Achilles tendon (AT), calcaneal tuber (CT), plantar ligaments (PL), posterior talar facet (PP: posterior, PC: central, PA: anterior), calcaneocuboid (CC), dorsal base (BD), plantar base (BP), dorsal head (HD), plantar head (HP), talar head (TH), anterior calcaneal facet (ACF), posterior calcaneal facet (PCF), trochlea (lateral: TL, central: TC, medial: TM).

ANOVA - pooled sex calcaneus Tb.Sp							**Test of Homogeneity of Variances**			
		Sum of Squares	**df**	**Mean Square**	**F**	***p***	**Levene Statistic**	**df1**	**df2**	***p***
AT	Between Groups	.090	3	.030	5.656	.002	1.672	3	43	.187
	Within Groups	.229	43	.005						
	Total	.320	46							
CC	Between Groups	.151	3	.050	6.964	.001	1.012	3	43	.397
	Within Groups	.311	43	.007						
	Total	.462	46							
CT	Between Groups	.245	3	.082	7.166	.001	1.127	3	43	.349
	Within Groups	.489	43	.011						
	Total	.734	46							
PA	Between Groups	.105	3	.035	3.771	.017	1.626	3	43	.197
	Within Groups	.399	43	.009						
	Total	.504	46							
PC	Between Groups	.047	3	.016	2.625	.063	.409	3	43	.747
	Within Groups	.259	43	.006						
	Total	.306	46							
PP	Between Groups	.065	3	.022	3.818	.016	1.738	3	43	.173
	Within Groups	.244	43	.006						
	Total	.309	46							
PL	Between Groups	.216	3	.072	4.110	.012	.414	3	43	.744
	Within Groups	.752	43	.017						
	Total	.968	46							

Table 7.1.10. Pairwise post-hoc comparisons of Tb.Sp between pooled sex populations. Achilles tendon (AT), calcaneal tuber (CT), plantar ligaments (PL), posterior talar facet (PP: posterior, PC: central, PA: anterior), calcaneocuboid (CC), dorsal base (BD), plantar base (BP), dorsal head (HD), plantar head (HP), talar head (TH), anterior calcaneal facet (ACF), posterior calcaneal facet (PCF), trochlea (lateral: TL, central: TC, medial: TM).

Pooled sex calcaneus Tb.Sp pairwise post hoc comparisons									
Summary statistics						**Post Hoc**			
VOI	**Population**	**N**	**Mean**	**S.D**	**S.E.**	**type**	**pairwise comparison**		***p***
AT	Black Earth	9	.399	.084	.028	Hochberg	Black Earth	Jebel Moya	.949
	Jebel Moya	9	.429	.060	.020			Kerma	**.003**
	Kerma	13	.519	.097	.027			St. Johns	.663
	St. Johns	16	.442	.046	.011		Jebel Moya	Kerma	**.037**
	Total	47	.452	.083	.012			St. Johns	.999
							Kerma	St. Johns	**.039**
CC	Black Earth	9	.488	.099	.033	Hochberg	Black Earth	Jebel Moya	.948

	Jebel Moya	9	.454	.048	.016			Kerma	**.015**
	Kerma	13	.607	.105	.029			St. Johns	.334
	St. Johns	16	.555	.074	.019		Jebel Moya	Kerma	**.001**
	Total	47	.537	.100	.015			St. Johns	**.040**
							Kerma	St. Johns	.487
CT	Black Earth	9	.593	.131	.044	Hochberg	Black Earth	Jebel Moya	1.000
	Jebel Moya	9	.590	.055	.018			Kerma	**.002**
	Kerma	13	.771	.131	.036			St. Johns	.476
	St. Johns	16	.666	.091	.023		Jebel Moya	Kerma	**.002**
	Total	47	.667	.126	.018			St. Johns	.423
							Kerma	St. Johns	.067
PA	Black Earth	9	.477	.095	.032	Hochberg	Black Earth	Jebel Moya	1.000
	Jebel Moya	9	.483	.073	.024			Kerma	**.037**
	Kerma	13	.597	.125	.035			St. Johns	.907
	St. Johns	16	.516	.080	.020		Jebel Moya	Kerma	.053
	Total	47	.525	.105	.015			St. Johns	.953
							Kerma	St. Johns	.163
PC	Black Earth	9	.400	.097	.032	Hochberg	Black Earth	Jebel Moya	.993
	Jebel Moya	9	.421	.053	.018			Kerma	.107
	Kerma	13	.482	.085	.024			St. Johns	.247
	St. Johns	16	.466	.071	.018		Jebel Moya	Kerma	.369
	Total	47	.449	.082	.012			St. Johns	.661
							Kerma	St. Johns	.994
PP	Black Earth	9	.510	.123	.041	Hochberg	Black Earth	Jebel Moya	.870
	Jebel Moya	9	.472	.057	.019			Kerma	.264
	Kerma	13	.575	.058	.016			St. Johns	1.000
	St. Johns	16	.504	.061	.015		Jebel Moya	Kerma	**.018**
	Total	47	.519	.082	.012			St. Johns	.890
							Kerma	St. Johns	.086
PL	Black Earth	9	.721	.162	.054	Hochberg	Black Earth	Jebel Moya	.320
	Jebel Moya	9	.602	.099	.033			Kerma	.992
	Kerma	13	.754	.140	.039			St. Johns	.734
	St. Johns	16	.792	.123	.031		Jebel Moya	Kerma	.064
	Total	47	.731	.145	.021			St. Johns	**.008**
							Kerma	St. Johns	.971

Table 7.1.11. ANOVA of residual Tb.Sp between pooled sex populations. Achilles tendon (AT), calcaneal tuber (CT), plantar ligaments (PL), posterior talar facet (PP: posterior, PC: central, PA: anterior), calcaneocuboid (CC), dorsal base (BD), plantar base (BP), dorsal head (HD), plantar head (HP), talar head (TH), anterior calcaneal facet (ACF), posterior calcaneal facet (PCF), trochlea (lateral: TL, central: TC, medial: TM).

ANOVA - pooled sex calcaneus residual Tb.Sp							**Test of Homogeneity of Variances**			
		Sum of Squares	**df**	**Mean Square**	**F**	***p***	**Levene Statistic**	**df1**	**df2**	***p***
AT	Between Groups	.089	3	.030	6.277	.001	1.432	3	42	.247
	Within Groups	.198	42	.005						
	Total	.286	45							
CC	Between Groups	.152	3	.051	8.702	.000	.065	3	42	.978
	Within Groups	.245	42	.006						
	Total	.397	45							
CT	Between Groups	.245	3	.082	8.580	.000	.179	3	42	.910
	Within Groups	.400	42	.010						
	Total	.645	45							
PA	Between Groups	.107	3	.036	4.394	.009	.617	3	42	.608
	Within Groups	.340	42	.008						
	Total	.447	45							
PC	Between Groups	.043	3	.014	2.721	.056	.319	3	42	.812
	Within Groups	.222	42	.005						
	Total	.265	45							
PP	Between Groups	.067	3	.022	3.913	.015	1.740	3	42	.173
	Within Groups	.238	42	.006						
	Total	.305	45							
PL	Between Groups	.202	3	.067	4.160	.011	.090	3	42	.965
	Within Groups	.678	42	.016						
	Total	.880	45							

Table 7.1.12. Pairwise post-hoc comparisons of residual Tb.Sp between pooled sex populations. Achilles tendon (AT), calcaneal tuber (CT), plantar ligaments (PL), posterior talar facet (PP: posterior, PC: central, PA: anterior), calcaneocuboid (CC), dorsal base (BD), plantar base (BP), dorsal head (HD), plantar head (HP), talar head (TH), anterior calcaneal facet (ACF), posterior calcaneal facet (PCF), trochlea (lateral: TL, central: TC, medial: TM).

Pooled sex calcaneus residual Tb.Sp pairwise post hoc comparisons									
Summary statistics						**Post Hoc**			
VOI	**Population**	**N**	**Mean**	**S.D**	**S.E.**	**type**	**pairwise comparison**		***p***
AT	Black Earth	9	-.051	.074	.025	Hochberg	Black Earth	Jebel Moya	.991
	Jebel Moya	9	-.032	.077	.026			Kerma	**.002**
	Kerma	13	.064	.082	.023			St. Johns	.780
	St. Johns	15	-.016	.043	.011		Jebel Moya	Kerma	**.015**
	Total	46	-.003	.080	.012			St. Johns	.994
							Kerma	St. Johns	**.022**
CC	Black Earth	9	-.044	.090	.030	Hochberg	Black Earth	Jebel Moya	.731

	Jebel Moya	9	-.091	.070	.023			Kerma	**.009**
	Kerma	13	.068	.080	.022			St. Johns	.433
	St. Johns	15	.011	.067	.017		Jebel Moya	Kerma	**.000**
	Total	46	-.004	.094	.014			St. Johns	**.017**
							Kerma	St. Johns	.289
CT	Black Earth	9	-.070	.120	.040	Hochberg	Black Earth	Jebel Moya	.999
	Jebel Moya	9	-.088	.082	.027			Kerma	**.001**
	Kerma	13	.101	.104	.029			St. Johns	.544
	St. Johns	15	-.006	.085	.022		Jebel Moya	Kerma	**.000**
	Total	46	-.004	.120	.018			St. Johns	.263
							Kerma	St. Johns	**.037**
PA	Black Earth	9	-.052	.086	.029	Hochberg	Black Earth	Jebel Moya	1.000
	Jebel Moya	9	-.058	.095	.032			Kerma	**.034**
	Kerma	13	.062	.104	.029			St. Johns	.982
	St. Johns	15	-.026	.075	.019		Jebel Moya	Kerma	**.022**
	Total	46	-.013	.100	.015			St. Johns	.947
							Kerma	St. Johns	.079
PC	Black Earth	9	-.051	.089	.030	Hochberg	Black Earth	Jebel Moya	1.000
	Jebel Moya	9	-.039	.070	.023			Kerma	.105
	Kerma	13	.027	.074	.021			St. Johns	.364
	St. Johns	15	.005	.061	.016		Jebel Moya	Kerma	.228
	Total	46	-.008	.077	.011			St. Johns	.622
							Kerma	St. Johns	.967
PP	Black Earth	9	-.012	.122	.041	Hochberg	Black Earth	Jebel Moya	.844
	Jebel Moya	9	-.051	.059	.020			Kerma	.280
	Kerma	13	.053	.057	.016			St. Johns	1.000
	St. Johns	15	-.021	.061	.016		Jebel Moya	Kerma	**.017**
	Total	46	-.004	.082	.012			St. Johns	.921
							Kerma	St. Johns	.075
PL	Black Earth	9	-.004	.151	.050	Hochberg	Black Earth	Jebel Moya	.200
	Jebel Moya	9	-.132	.121	.040			Kerma	.996
	Kerma	13	.025	.122	.034			St. Johns	.899
	St. Johns	15	.050	.120	.031		Jebel Moya	Kerma	**.040**
	Total	46	-.003	.140	.021			St. Johns	**.009**
							Kerma	St. Johns	.996

Table 7.1.13. ANOVA of log10 Conn.D between pooled sex populations. Achilles tendon (AT), calcaneal tuber (CT), plantar ligaments (PL), posterior talar facet (PP: posterior, PC: central, PA: anterior), calcaneocuboid (CC), dorsal base (BD), plantar base (BP), dorsal head (HD), plantar head (HP), talar head (TH), anterior calcaneal facet (ACF), posterior calcaneal facet (PCF), trochlea (lateral: TL, central: TC, medial: TM).

ANOVA - pooled sex calcaneus log10Conn.D							**Test of Homogeneity of Variances**			
		Sum of Squares	**df**	**Mean Square**	**F**	***p***	**Levene Statistic**	**df1**	**df2**	***p***
AT	Between Groups	.029	3	.010	0.764	.520	3.155	3	44	**.034**
	Within Groups	.566	44	.013						
	Total	.595	47							
CC	Between Groups	.181	3	.060	3.261	.030	1.032	3	44	.388
	Within Groups	.814	44	.019						
	Total	.995	47							
CT	Between Groups	.239	3	.080	3.663	.019	.162	3	44	.921
	Within Groups	.957	44	.022						
	Total	1.196	47							
PA	Between Groups	.153	3	.051	2.300	.090	.627	3	44	.602
	Within Groups	.979	44	.022						
	Total	1.132	47							
PC	Between Groups	.366	3	.122	5.612	.002	1.206	3	44	.319
	Within Groups	.958	44	.022						
	Total	1.324	47							
PP	Between Groups	.360	3	.120	8.065	.000	.864	3	44	.467
	Within Groups	.655	44	.015						
	Total	1.015	47							
PL	Between Groups	.231	3	.077	2.786	.052	.351	3	44	.789
	Within Groups	1.218	44	.028						
	Total	1.449	47							

Table 7.1.14. Pairwise post-hoc comparisons of log10 Conn.D between pooled sex populations.

Pooled sex calcaneus log10Conn.D pairwise post hoc comparisons									
Summary statistics						**Post Hoc**			
VOI	**Population**	**N**	**Mean**	**S.D**	**S.E.**	**type**	**pairwise comparison**		***p***
AT	Black Earth	9	.730	.062	.021	Games-Howell	Black Earth	Jebel Moya	.963
	Jebel Moya	9	.716	.061	.020			Kerma	.523
	Kerma	14	.666	.154	.041			St. Johns	.974
	St. Johns	16	.715	.115	.029		Jebel Moya	Kerma	.700
	Total	48	.704	.113	.016			St. Johns	1.000
							Kerma	St. Johns	.764
CC	Black Earth	9	.472	.125	.042	Hochberg	Black Earth	Jebel Moya	.718
	Jebel Moya	9	.556	.079	.026			Kerma	.672
	Kerma	14	.552	.157	.042			St. Johns	**.023**
	St. Johns	16	.644	.146	.037		Jebel Moya	Kerma	1.000
	Total	48	.569	.146	.021			St. Johns	.541

							Kerma	St. Johns	.344
CT	Black Earth	9	.319	.143	.048	Hochberg	Black Earth	Jebel Moya	.815
	Jebel Moya	9	.400	.113	.038			Kerma	.484
	Kerma	14	.216	.171	.046			St. Johns	.977
	St. Johns	16	.364	.144	.036		Jebel Moya	Kerma	**.032**
	Total	48	.319	.160	.023			St. Johns	.992
							Kerma	St. Johns	.052
PA	Black Earth	9	.448	.120	.040	Hochberg	Black Earth	Jebel Moya	.928
	Jebel Moya	9	.513	.120	.040			Kerma	.975
	Kerma	14	.495	.149	.040			St. Johns	.111
	St. Johns	16	.599	.175	.044		Jebel Moya	Kerma	1.000
	Total	48	.524	.155	.022			St. Johns	.667
							Kerma	St. Johns	.320
PC	Black Earth	9	.486	.085	.028	Hochberg	Black Earth	Jebel Moya	1.000
	Jebel Moya	9	.472	.168	.056			Kerma	.380
	Kerma	14	.600	.147	.039			St. Johns	**.013**
	St. Johns	16	.685	.162	.041		Jebel Moya	Kerma	.255
	Total	48	.583	.168	.024			St. Johns	**.007**
							Kerma	St. Johns	.518
PP	Black Earth	9	.395	.122	.041	Hochberg	Black Earth	Jebel Moya	.276
	Jebel Moya	9	.509	.083	.028			Kerma	.055
	Kerma	14	.536	.126	.034			St. Johns	**.000**
	St. Johns	16	.640	.135	.034		Jebel Moya	Kerma	.995
	Total	48	.539	.147	.021			St. Johns	.073
							Kerma	St. Johns	.132
PL	Black Earth	9	.273	.169	.056	Hochberg	Black Earth	Jebel Moya	.171
	Jebel Moya	9	.447	.131	.044			Kerma	.343
	Kerma	14	.405	.165	.044			St. Johns	1.000
	St. Johns	16	.293	.182	.046		Jebel Moya	Kerma	.991
	Total	48	.351	.176	.025			St. Johns	.173
							Kerma	St. Johns	.360

Table 7.1.15. ANOVA of residual log10 Conn.D in between pooled sex populations.

ANOVA - pooled sex calcaneus residual log10Conn.D							**Test of Homogeneity of Variances**			
		Sum of Squares	**df**	**Mean Square**	**F**	***p***	**Levene Statistic**	**df1**	**df2**	***p***
AT	Between Groups	.037	3	.012	1.224	.313	4.616	3	43	**.007**
	Within Groups	.435	43	.010						
	Total	.472	46							
CC	Between Groups	.225	3	.075	5.050	.004	.980	3	43	.411
	Within Groups	.640	43	.015						
	Total	.865	46							
CT	Between Groups	.282	3	.094	5.428	.003	.529	3	43	.665
	Within Groups	.745	43	.017						
	Total	1.027	46							
PA	Between Groups	.201	3	.067	3.717	.018	.584	3	43	.629
	Within Groups	.774	43	.018						
	Total	.975	46							
PC	Between Groups	.406	3	.135	7.721	.000	1.943	3	43	.137
	Within Groups	.754	43	.018						
	Total	1.160	46							
PP	Between Groups	.407	3	.136	10.281	.000	.457	3	43	.714
	Within Groups	.567	43	.013						
	Total	.974	46							
PL	Between Groups	.236	3	.079	3.468	.024	.347	3	43	.792
	Within Groups	.976	43	.023						
	Total	1.213	46							

Table 7.1.16. Pairwise post-hoc comparisons of residual log10Conn.D between pooled sex populations.

Pooled sex calcaneus residual log10Conn.D pairwise post hoc comparisons									
Summary statistics						**Post Hoc**			
VOI	**Population**	**N**	**Mean**	**S.D**	**S.E.**	**type**	**pairwise comparison**		***p***
AT	Black Earth	9	.018	.040	.013	Games-Howell	Black Earth	Jebel Moya	.975
	Jebel Moya	9	.029	.074	.025			Kerma	.482
	Kerma	14	-.039	.136	.036			St. Johns	1.000
	St. Johns	15	.020	.099	.026		Jebel Moya	Kerma	.426
	Total	47	.004	.101	.015			St. Johns	.994
							Kerma	St. Johns	.553
CC	Black Earth	9	-.103	.100	.033	Hochberg	Black Earth	Jebel Moya	.334
	Jebel Moya	9	.005	.099	.033			Kerma	.466
	Kerma	14	-.016	.128	.034			St. Johns	**.003**
	St. Johns	15	.092	.138	.036		Jebel Moya	Kerma	.999
	Total	47	.006	.137	.020			St. Johns	.442
							Kerma	St. Johns	.118
CT	Black Earth	9	-.012	.128	.043	Hochberg	Black Earth	Jebel Moya	.450
	Jebel Moya	9	.093	.145	.048			Kerma	.434

	Kerma	14	-.109	.132	.035			St. Johns	.827
	St. Johns	15	.051	.125	.032		Jebel Moya	Kerma	**.005**
	Total	47	-.001	.149	.022			St. Johns	.971
							Kerma	St. Johns	**.013**
PA	Black Earth	9	-.085	.113	.038	Hochberg	Black Earth	Jebel Moya	.697
	Jebel Moya	9	.000	.134	.045			Kerma	.927
	Kerma	14	-.032	.115	.031			St. Johns	**.020**
	St. Johns	15	.090	.160	.041		Jebel Moya	Kerma	.993
	Total	47	.003	.146	.021			St. Johns	.516
							Kerma	St. Johns	.102
PC	Black Earth	9	-.101	.073	.024	Hochberg	Black Earth	Jebel Moya	1.000
	Jebel Moya	9	-.094	.173	.058			Kerma	.215
	Kerma	14	.018	.129	.034			St. Johns	**.001**
	St. Johns	15	.125	.135	.035		Jebel Moya	Kerma	.272
	Total	47	.008	.159	.023			St. Johns	**.002**
							Kerma	St. Johns	.194
PP	Black Earth	9	-.139	.119	.040	Hochberg	Black Earth	Jebel Moya	.171
	Jebel Moya	9	-.019	.082	.027			Kerma	**.033**
	Kerma	14	.004	.122	.033			St. Johns	**.000**
	St. Johns	15	.125	.122	.031		Jebel Moya	Kerma	.998
	Total	47	.011	.146	.021			St. Johns	**.028**
							Kerma	St. Johns	**.040**
PL	Black Earth	9	-.099	.142	.047	Hochberg	Black Earth	Jebel Moya	**.041**
	Jebel Moya	9	.102	.141	.047			Kerma	.190
	Kerma	14	.041	.131	.035			St. Johns	.952
	St. Johns	15	-.046	.176	.045		Jebel Moya	Kerma	.916
	Total	47	-.002	.162	.024			St. Johns	.137
							Kerma	St. Johns	.550

Table 7.1.17. PCA scores - calcaneus. Variables contributing >.15 are in bold.

	PC1	PC2	PC3	PC4	PC5
Standard deviation	3.83	2.90	1.38	1.33	1.10
Proportion of Variance	0.42	0.24	0.05	0.05	0.03
Cumulative Proportion	0.42	0.66	0.71	0.76	0.80

PC scores

VOI	Properties	PC1	PC2	PC3	PC4	PC5
AT	BV/TV	**-0.23**	0.06	0.14	-0.08	0.11
	Tb.Th	**-0.22**	-0.09	0.05	-0.06	0.13
	DA	0.02	0.06	**0.39**	**0.37**	**-0.16**
	Res. Tb.Sp	**0.18**	**-0.18**	**-0.19**	0.06	0.00
	Res. Conn.D	-0.04	**0.26**	0.01	-0.28	-0.04
CC	BV/TV	**-0.23**	-0.02	0.04	0.07	-0.13
	Tb.Th	**-0.20**	-0.16	0.07	0.08	-0.12
	DA	0.01	**-0.23**	-0.02	**-0.15**	**-0.39**
	Res. Tb.Sp	**0.19**	-0.16	-0.03	-0.07	0.06
	Res. Conn.D	0.04	**0.31**	0.02	0.04	0.02
CT	BV/TV	**-0.24**	0.01	0.01	-0.07	0.03
	Tb.Th	**-0.20**	-0.12	-0.01	0.02	**0.16**
	DA	0.04	**-0.24**	0.12	-0.09	**-0.25**
	Res. Tb.Sp	**0.20**	**-0.17**	-0.05	0.13	0.05
	Res. Conn.D	-0.08	**0.26**	-0.04	**-0.18**	-0.02
PA	BV/TV	**-0.24**	-0.01	-0.03	0.14	0.01
	Tb.Th	**-0.21**	-0.16	-0.05	0.14	-0.07
	DA	0.07	-0.13	**0.38**	**-0.19**	**-0.22**
	Res. Tb.Sp	**0.19**	**-0.17**	-0.12	-0.02	-0.02
	Res. Conn.D	0.05	**0.29**	0.03	-0.13	**0.16**
PC	BV/TV	**-0.24**	-0.06	-0.03	0.07	-0.03
	Tb.Th	**-0.20**	**-0.17**	-0.08	0.10	-0.07
	DA	0.02	**-0.20**	**0.21**	**-0.44**	-0.08
	Res. Tb.Sp	**0.20**	-0.12	**-0.14**	0.08	0.05
	Res. Conn.D	0.12	**0.25**	**0.19**	-0.12	0.13
PP	BV/TV	**-0.24**	-0.02	0.04	-0.07	0.03
	Tb.Th	**-0.21**	-0.14	0.01	-0.05	0.13
	DA	-0.04	-0.16	0.04	**-0.47**	-0.03
	Res. Tb.Sp	**0.17**	-0.16	-0.14	**0.17**	0.11
	Res. Conn.D	0.09	**0.27**	0.08	0.04	-0.17
PL	BV/TV	**-0.23**	0.05	-0.02	0.11	-0.02
	Tb.Th	**-0.22**	-0.07	0.07	0.01	**0.27**
	DA	0.07	0.01	**0.54**	**0.27**	**-0.18**
	Res. Tb.Sp	**0.17**	-0.15	**0.21**	-0.06	**0.36**
	Res. Conn.D	-0.05	**0.19**	**-0.36**	-0.04	**-0.50**

Table 7.1.18. ANOVA of PC scores between pooled sex populations.

ANOVA - Calcaneus pooled VOIs							**Levene's Test**			
		Sum of Squares	**df**	**Mean Square**	**F**	***p***	**Levene Statistic**	**df1**	**df2**	***p***
PC1	Between Groups	337.59	3	112.531	14.61	**.000**	.065	3	42	.978
	Within Groups	323.46	42	7.701						
	Total	661.05	45							
PC2	Between Groups	86.44	3	28.812	4.16	**.011**	.749	3	42	.529
	Within Groups	290.82	42	6.924						
	Total	377.25	45							
PC3	Between Groups	17.80	3	5.935	3.70	**.019**	.411	3	42	.746
	Within Groups	67.30	42	1.602						
	Total	85.11	45							
PC4	Between Groups	7.81	3	2.603	1.53	.220	2.600	3	42	.065
	Within Groups	71.31	42	1.698						
	Total	79.12	45							
PC5	Between Groups	9.52	3	3.174	2.96	**.043**	.375	3	42	.771
	Within Groups	45.07	42	1.073						
	Total	54.59	45							

Table 7.1.19. Pairwise post-hoc comparisons of PC scores between pooled sex populations.

Calcaneus	Populations	N	Mean	S.D.	S.E.	Hochberg's GT2		*p*
PC1	Black Earth	9	-3.54	3.40	1.13	Black Earth	Jebel Moya	1.000
	Jebel Moya	9	-3.12	3.02	1.01		Kerma	**.000**
	Kerma	13	2.76	2.49	0.69		St. Johns	**.000**
	St. Johns	15	1.60	2.45	0.63	Jebel Moya	Kerma	**.000**
	Total	46	0.00	3.83	0.57		St. Johns	**.001**
						Kerma	St. Johns	.843
PC2	Black Earth	9	-1.87	1.90	0.63	Black Earth	Jebel Moya	.316
	Jebel Moya	9	0.49	2.30	0.77		Kerma	.958
	Kerma	13	-0.95	2.79	0.77		St. Johns	**.016**
	St. Johns	15	1.65	3.00	0.77	Jebel Moya	Kerma	.751
	Total	46	0.00	2.90	0.43		St. Johns	.873
						Kerma	St. Johns	.071
PC3	Black Earth	9	0.10	1.34	0.45	Black Earth	Jebel Moya	.788
	Jebel Moya	9	-0.62	1.18	0.39		Kerma	.772
	Kerma	13	-0.58	1.48	0.41		St. Johns	.696
	St. Johns	15	0.81	1.05	0.27	Jebel Moya	Kerma	1.000
	Total	46	0.00	1.38	0.20		St. Johns	.059
						Kerma	St. Johns	**.035**
PC4	Black Earth	9	-0.81	0.90	0.30	Black Earth	Jebel Moya	.393
	Jebel Moya	9	0.28	1.78	0.59		Kerma	.556
	Kerma	13	0.06	1.52	0.42		St. Johns	.277
	St. Johns	15	0.27	0.92	0.24	Jebel Moya	Kerma	.999
	Total	46	0.00	1.33	0.20		St. Johns	1.000
						Kerma	St. Johns	.998
PC5	Black Earth	9	0.60	1.08	0.36	Black Earth	Jebel Moya	.166
	Jebel Moya	9	-0.49	1.02	0.34		Kerma	.137
	Kerma	13	-0.44	0.87	0.24		St. Johns	.987
	St. Johns	15	0.32	1.14	0.29	Jebel Moya	Kerma	1.000
	Total	46	0.00	1.10	0.16		St. Johns	.343
						Kerma	St. Johns	.294

MT1

Table 7.1.20. ANOVA of BV/TV between pooled sex populations.

ANOVA - pooled sex MT1 BV/TV							**Test of Homogeneity of Variances**			
		Sum of Squares	**df**	**Mean Square**	**F**	***p***	**Levene Statistic**	**df1**	**df2**	***p***
BD	Between Groups	.054	3	.018	4.478	**.008**	1.389	3	41	.260
	Within Groups	.166	41	.004						
	Total	.220	44							
BP	Between Groups	.044	3	.015	4.768	**.006**	1.650	3	41	.193
	Within Groups	.127	41	.003						
	Total	.172	44							
HD	Between Groups	.074	3	.025	12.898	**.000**	.140	3	41	.936
	Within Groups	.078	41	.002						
	Total	.152	44							
HP	Between Groups	.040	3	.013	5.221	**.004**	.716	3	41	.548
	Within Groups	.105	41	.003						
	Total	.146	44							

Table 7.1.21. Pairwise post-hoc comparisons of BV/TV between pooled sex populations.

Pooled sex MT1 BV/TV pairwise post hoc comparisons									
Summary statistics						**Post Hoc**			
VOI	**Population**	**N**	**Mean**	**S.D**	**S.E.**	**type**	**pairwise comparison**		***p***
BD	Black Earth	10	.446	.083	.026	Hochberg	Black Earth	Jebel Moya	1.000
	Jebel Moya	4	.457	.087	.043			Kerma	**.041**
	Kerma	13	.370	.046	.013			St. Johns	.058
	St. Johns	18	.378	.057	.014		Jebel Moya	Kerma	.114
	Total	45	.398	.071	.011			St. Johns	.158
							Kerma	St. Johns	1.000
BP	Black Earth	10	.325	.069	.022	Hochberg	Black Earth	Jebel Moya	.992
	Jebel Moya	4	.305	.073	.036			Kerma	**.004**
	Kerma	13	.239	.048	.013			St. Johns	.214
	St. Johns	18	.278	.049	.012		Jebel Moya	Kerma	.228
	Total	45	.280	.062	.009			St. Johns	.939
							Kerma	St. Johns	.302
HD	Black Earth	10	.467	.047	.015	Hochberg	Black Earth	Jebel Moya	1.000
	Jebel Moya	4	.472	.052	.026			Kerma	**.000**
	Kerma	13	.383	.036	.010			St. Johns	**.000**
	St. Johns	18	.380	.045	.011		Jebel Moya	Kerma	**.005**
	Total	45	.408	.059	.009			St. Johns	**.003**
							Kerma	St. Johns	1.000
HP	Black Earth	10	.346	.050	.016	Hochberg	Black Earth	Jebel Moya	.986
	Jebel Moya	4	.366	.077	.038			Kerma	**.012**
	Kerma	13	.276	.048	.013			St. Johns	.356
	St. Johns	18	.309	.047	.011		Jebel Moya	Kerma	**.021**
	Total	45	.313	.058	.009			St. Johns	.263
							Kerma	St. Johns	.367

Table 7.1.22. ANOVA of DA between pooled sex populations.

ANOVA - pooled sex MT1 DA							**Test of Homogeneity of Variances**		
		Sum of Squares	**df**	**Mean Square**	**F**	***p***	**Levene Statistic**	**df1**	**df2**	***p***
BD	Between Groups	.059	3	.020	12.296	**.000**	1.269	3	40	.298
	Within Groups	.064	40	.002						
	Total	.123	43							
BP	Between Groups	.058	3	.019	4.921	**.005**	3.251	3	40	.032
	Within Groups	.156	40	.004						
	Total	.213	43							
HD	Between Groups	.015	3	.005	2.276	.094	1.805	3	40	.162
	Within Groups	.086	40	.002						
	Total	.100	43							
HP	Between Groups	.028	3	.009	2.256	.097	2.225	3	40	.100
	Within Groups	.163	40	.004						
	Total	.191	43							

Table 7.1.23. Pairwise post-hoc comparisons of DA between pooled sex populations.

Pooled sex MT1 DA pairwise post hoc comparisons									
Summary statistics						**Post Hoc**			
VOI	**Population**	**N**	**Mean**	**S.D**	**S.E.**	**type**	**pairwise comparison**		***p***
BD	Black Earth	10	.802	.039	.012	Hochberg	Black Earth	Jebel Moya	.417
	Jebel Moya	4	.761	.025	.013			Kerma	.719
	Kerma	13	.780	.034	.009			St. Johns	**.000**
	St. Johns	17	.713	.046	.011		Jebel Moya	Kerma	.952
	Total	44	.757	.053	.008			St. Johns	.212
							Kerma	St. Johns	**.000**
BP	Black Earth	10	.621	.042	.013	Games-Howell	Black Earth	Jebel Moya	.180
	Jebel Moya	4	.586	.018	.009			Kerma	.837
	Kerma	13	.598	.088	.024			St. Johns	**.001**
	St. Johns	17	.533	.053	.013		Jebel Moya	Kerma	.965
	Total	44	.577	.070	.011			St. Johns	**.021**
							Kerma	St. Johns	.128
HD	Black Earth	10	.767	.028	.009	Hochberg	Black Earth	Jebel Moya	.109
	Jebel Moya	4	.700	.075	.037			Kerma	.939
	Kerma	13	.750	.037	.010			St. Johns	.433
	St. Johns	17	.735	.053	.013		Jebel Moya	Kerma	.337
	Total	44	.744	.048	.007			St. Johns	.684
							Kerma	St. Johns	.947
HP	Black Earth	10	.602	.025	.008	Hochberg	Black Earth	Jebel Moya	1.000
	Jebel Moya	4	.590	.095	.047			Kerma	.296
	Kerma	13	.654	.080	.022			St. Johns	1.000
	St. Johns	17	.601	.058	.014		Jebel Moya	Kerma	.399
	Total	44	.616	.067	.010			St. Johns	1.000
							Kerma	St. Johns	.157

Table 7.1.24. ANOVA of residual DA between pooled sex populations.

ANOVA - pooled sex MT1 residual DA							**Test of Homogeneity of Variances**			
		Sum of Squares	**df**	**Mean Square**	**F**	***p***	**Levene Statistic**	**df1**	**df2**	***p***
BD	Between Groups	.057	3	.019	11.786	**.000**	1.246	3	38	.307
	Within Groups	.061	38	.002						
	Total	.119	41							
BP	Between Groups	.057	3	.019	4.863	**.006**	3.714	3	38	.019
	Within Groups	.148	38	.004						
	Total	.205	41							
HD	Between Groups	.013	3	.004	2.024	.127	1.679	3	38	.188
	Within Groups	.083	38	.002						
	Total	.097	41							
HP	Between Groups	.021	3	.007	1.660	.192	2.085	3	38	.118
	Within Groups	.160	38	.004						
	Total	.181	41							

Table 7.1.25. Pairwise post-hoc comparisons of residual DA between pooled sex populations.

Pooled sex MT1 residual DA pairwise post hoc comparisons									
Summary statistics						**Post Hoc**			
VOI	**Population**	**N**	**Mean**	**S.D**	**S.E.**	**type**	**pairwise comparison**		***p***
BD	Black Earth	10	.043	.039	.012	Hochberg	Black Earth	Jebel Moya	.431
	Jebel Moya	4	.002	.025	.013			Kerma	.715
	Kerma	11	.020	.034	.010			St. Johns	**.000**
	St. Johns	17	-.045	.046	.011		Jebel Moya	Kerma	.969
	Total	42	-.002	.054	.008			St. Johns	.217
							Kerma	St. Johns	**.001**
BP	Black Earth	10	.047	.046	.015	Games-Howell	Black Earth	Jebel Moya	.156
	Jebel Moya	4	.002	.026	.013			Kerma	.730
	Kerma	11	.015	.092	.028			St. Johns	**.001**
	St. Johns	17	-.043	.051	.012		Jebel Moya	Kerma	.974
	Total	42	-.002	.071	.011			St. Johns	.115
							Kerma	St. Johns	.264
HD	Black Earth	10	.032	.028	.009	Hochberg	Black Earth	Jebel Moya	.134
	Jebel Moya	4	-.032	.074	.037			Kerma	.844
	Kerma	11	.010	.039	.012			St. Johns	.468
	St. Johns	17	.001	.053	.013		Jebel Moya	Kerma	.550
	Total	42	.008	.049	.007			St. Johns	.725
							Kerma	St. Johns	.998
HP	Black Earth	10	-.013	.029	.009	Hochberg	Black Earth	Jebel Moya	1.000
	Jebel Moya	4	-.013	.093	.047			Kerma	.352
	Kerma	11	.040	.082	.025			St. Johns	1.000
	St. Johns	17	-.010	.060	.015		Jebel Moya	Kerma	.666
	Total	42	.002	.066	.010			St. Johns	1.000
							Kerma	St. Johns	.286

Table 7.1.26. ANOVA of Tb.Th between pooled sex populations.

ANOVA - MT1 pooled Tb.Th							**Test of Homogeneity of Variances**			
		Sum of Squares	**df**	**Mean Square**	**F**	***p***	**Levene Statistic**	**df1**	**df2**	***p***
BD	Between Groups	.020	3	.007	8.055	**.000**	3.738	3	41	.018
	Within Groups	.035	41	.001						
	Total	.055	44							
BP	Between Groups	.024	3	.008	7.906	**.000**	3.085	3	41	.038
	Within Groups	.041	41	.001						
	Total	.065	44							
HD	Between Groups	.020	3	.007	11.892	**.000**	2.766	3	41	.054
	Within Groups	.023	41	.001						
	Total	.043	44							
HP	Between Groups	.017	3	.006	6.325	**.001**	3.264	3	41	.031
	Within Groups	.036	41	.001						
	Total	.052	44							

Table 7.1.27. Pairwise post-hoc comparisons of Tb.Th between pooled sex populations.

Pooled sex MT1 Tb.Th pairwise post hoc comparisons									
Summary statistics						**Post Hoc**			
VOI	**Population**	**N**	**Mean**	**S.D**	**S.E.**	**type**	**pairwise comparison**		***p***
BD	Black Earth	10	.282	.047	.015	Games-Howell	Black Earth	Jebel Moya	.968
	Jebel Moya	4	.291	.026	.013			Kerma	.173
	Kerma	13	.246	.021	.006			St. Johns	**.050**
	St. Johns	18	.235	.021	.005		Jebel Moya	Kerma	.110
	Total	45	.253	.035	.005			St. Johns	.057
							Kerma	St. Johns	.452
BP	Black Earth	10	.271	.049	.016	Games-Howell	Black Earth	Jebel Moya	.999
	Jebel Moya	4	.269	.023	.012			Kerma	.113
	Kerma	13	.228	.028	.008			St. Johns	**.032**
	St. Johns	18	.217	.022	.005		Jebel Moya	Kerma	.094
	Total	45	.237	.038	.006			St. Johns	**.044**
							Kerma	St. Johns	.646
HD	Black Earth	10	.282	.037	.012	Hochberg	Black Earth	Jebel Moya	.992
	Jebel Moya	4	.274	.012	.006			Kerma	**.000**
	Kerma	13	.230	.018	.005			St. Johns	**.000**
	St. Johns	18	.239	.020	.005		Jebel Moya	Kerma	**.014**
	Total	45	.249	.031	.005			St. Johns	.059
							Kerma	St. Johns	.888
HP	Black Earth	10	.283	.042	.013	Games-Howell	Black Earth	Jebel Moya	.988
	Jebel Moya	4	.278	.019	.009			Kerma	**.038**
	Kerma	13	.237	.028	.008			St. Johns	.070
	St. Johns	18	.243	.024	.006		Jebel Moya	Kerma	**.044**
	Total	45	.253	.034	.005			St. Johns	.083
							Kerma	St. Johns	.899

Table 7.1.28. ANOVA of Tb.Sp between pooled sex populations.

ANOVA - pooled sex MT1 Tb.Sp							**Test of Homogeneity of Variances**			
		Sum of Squares	**df**	**Mean Square**	**F**	***p***	**Levene Statistic**	**df1**	**df2**	***p***
BD	Between Groups	.034	3	.011	4.411	**.009**	1.262	3	41	.300
	Within Groups	.105	41	.003						
	Total	.138	44							
BP	Between Groups	.100	3	.033	4.292	**.010**	.345	3	41	.793
	Within Groups	.317	41	.008						
	Total	.417	44							
HD	Between Groups	.025	3	.008	3.829	**.017**	.899	3	41	.450
	Within Groups	.089	41	.002						
	Total	.115	44							
HP	Between Groups	.043	3	.014	2.059	.121	3.655	3	41	.020
	Within Groups	.285	41	.007						
	Total	.328	44							

Table 7.1.29. Pairwise post-hoc comparisons of Tb.Sp between pooled sex populations.

Pooled sex MT1 Tb.Sp pairwise post hoc comparisons									
Summary statistics						**Post Hoc**			
VOI	**Population**	**N**	**Mean**	**S.D**	**S.E.**	**type**	**pairwise comparison**		***p***
BD	Black Earth	10	.384	.054	.017	Hochberg	Black Earth	Jebel Moya	.999
	Jebel Moya	4	.395	.076	.038			Kerma	**.008**
	Kerma	13	.457	.048	.013			St. Johns	.576
	St. Johns	18	.414	.044	.010		Jebel Moya	Kerma	.199
	Total	45	.418	.056	.008			St. Johns	.982
							Kerma	St. Johns	.135
BP	Black Earth	10	.555	.071	.023	Hochberg	Black Earth	Jebel Moya	.844
	Jebel Moya	4	.612	.075	.038			Kerma	.077
	Kerma	13	.650	.109	.030			St. Johns	.999
	St. Johns	18	.542	.081	.019		Jebel Moya	Kerma	.971
	Total	45	.583	.097	.015			St. Johns	.630
							Kerma	St. Johns	**.010**
HD	Black Earth	10	.388	.038	.012	Hochberg	Black Earth	Jebel Moya	1.000
	Jebel Moya	4	.385	.052	.026			Kerma	.304
	Kerma	13	.426	.043	.012			St. Johns	**.028**
	St. Johns	18	.443	.052	.012		Jebel Moya	Kerma	.565
	Total	45	.421	.051	.008			St. Johns	.165
							Kerma	St. Johns	.892
HP	Black Earth	10	.556	.046	.015	Games-Howell	Black Earth	Jebel Moya	.997
	Jebel Moya	4	.547	.087	.044			Kerma	.147
	Kerma	13	.632	.108	.030			St. Johns	.764
	St. Johns	18	.579	.077	.018		Jebel Moya	Kerma	.444
	Total	45	.587	.086	.013			St. Johns	.901
							Kerma	St. Johns	.457

Table 7.1.30. ANOVA of residual Tb.Sp between pooled sex populations.

ANOVA - pooled sex MT1 residual Tb.Sp							**Test of Homogeneity of Variances**			
		Sum of Squares	**df**	**Mean Square**	**F**	***p***	**Levene Statistic**	**df1**	**df2**	***p***
BD	Between Groups	.034	3	.011	4.449	**.009**	1.775	3	39	.168
	Within Groups	.099	39	.003						
	Total	.133	42							
BP	Between Groups	.094	3	.031	4.585	**.008**	.473	3	39	.703
	Within Groups	.267	39	.007						
	Total	.362	42							
HD	Between Groups	.025	3	.008	4.082	**.013**	.854	3	39	.473
	Within Groups	.078	39	.002						
	Total	.103	42							
HP	Between Groups	.044	3	.015	2.242	.099	3.924	3	39	.015
	Within Groups	.254	39	.007						
	Total	.297	42							

Table 7.1.31. Pairwise post-hoc comparisons of residual Tb.Sp between pooled sex populations.

Pooled sex MT1 residual Tb.Sp pairwise post hoc comparisons									
Summary statistics						**Post Hoc**			
VOI	**Population**	**N**	**Mean**	**S.D**	**S.E.**	**type**	**pairwise comparison**		***p***
BD	Black Earth	10	-.030	.051	.016	Hochberg	Black Earth	Jebel Moya	1.000
	Jebel Moya	4	-.027	.082	.041			Kerma	**.010**
	Kerma	11	.044	.046	.014			St. Johns	.688
	St. Johns	18	-.003	.045	.011		Jebel Moya	Kerma	.108
	Total	43	.000	.056	.009			St. Johns	.943
							Kerma	St. Johns	.101
BP	Black Earth	10	-.015	.060	.019	Hochberg	Black Earth	Jebel Moya	.998
	Jebel Moya	4	.006	.090	.045			Kerma	.100
	Kerma	11	.075	.090	.027			St. Johns	.959
	St. Johns	18	-.041	.087	.021		Jebel Moya	Kerma	.643
	Total	43	-.001	.093	.014			St. Johns	.878
							Kerma	St. Johns	**.004**
HD	Black Earth	10	-.019	.034	.011	Hochberg	Black Earth	Jebel Moya	.972
	Jebel Moya	4	-.039	.063	.031			Kerma	.501
	Kerma	11	.013	.040	.012			St. Johns	.052
	St. Johns	18	.030	.049	.011		Jebel Moya	Kerma	.285
	Total	43	.008	.049	.008			St. Johns	.051
							Kerma	St. Johns	.903
HP	Black Earth	10	-.020	.046	.015	Games-Howell	Black Earth	Jebel Moya	.949
	Jebel Moya	4	-.046	.096	.048			Kerma	.210
	Kerma	11	.054	.107	.032			St. Johns	.888
	St. Johns	18	-.004	.074	.017		Jebel Moya	Kerma	.390
	Total	43	.003	.084	.013			St. Johns	.838
							Kerma	St. Johns	.429

Table 7.1.32. ANOVA of log10 Conn.D between pooled sex populations.

ANOVA - pooled sex MT1 log10Conn.D							**Test of Homogeneity of Variances**			
		Sum of Squares	**df**	**Mean Square**	**F**	***p***	**Levene Statistic**	**df1**	**df2**	***p***
BD	Between Groups	.238	3	.079	7.565	**.000**	.872	3	41	.463
	Within Groups	.430	41	.010						
	Total	.668	44							
BP	Between Groups	.326	3	.109	6.434	**.001**	2.443	3	41	.078
	Within Groups	.692	41	.017						
	Total	1.017	44							
HD	Between Groups	.092	3	.031	1.853	.153	.203	3	41	.894
	Within Groups	.678	41	.017						
	Total	.770	44							
HP	Between Groups	.014	3	.005	.263	.851	1.015	3	41	.396
	Within Groups	.734	41	.018						
	Total	.748	44							

Table 7.1.33. Pairwise post-hoc comparisons of log10 Conn.D between pooled sex populations.

Pooled sex MT1 log10Conn.D pairwise post hoc comparisons									
Summary statistics						**Post Hoc**			
VOI	**Population**	**N**	**Mean**	**S.D**	**S.E.**	**type**	**pairwise comparison**		***p***
BD	Black Earth	10	.772	.106	.034	Hochberg	Black Earth	Jebel Moya	1.000
	Jebel Moya	4	.760	.072	.036			Kerma	.573
	Kerma	13	.837	.123	.034			St. Johns	**.001**
	St. Johns	18	.939	.088	.021		Jebel Moya	Kerma	.716
	Total	45	.857	.123	.018			St. Johns	**.017**
							Kerma	St. Johns	.051
BP	Black Earth	10	.739	.143	.045	Hochberg	Black Earth	Jebel Moya	.983
	Jebel Moya	4	.687	.014	.007			Kerma	.996
	Kerma	13	.712	.157	.044			St. Johns	**.032**
	St. Johns	18	.889	.111	.026		Jebel Moya	Kerma	1.000
	Total	45	.787	.152	.023			St. Johns	**.043**
							Kerma	St. Johns	**.003**
HD	Black Earth	10	.784	.126	.040	Hochberg	Black Earth	Jebel Moya	.998
	Jebel Moya	4	.817	.119	.060			Kerma	.186
	Kerma	13	.902	.135	.038			St. Johns	.986
	St. Johns	18	.816	.127	.030		Jebel Moya	Kerma	.816
	Total	45	.834	.132	.020			St. Johns	1.000
							Kerma	St. Johns	.363
HP	Black Earth	10	.692	.106	.034	Hochberg	Black Earth	Jebel Moya	1.000
	Jebel Moya	4	.692	.109	.054			Kerma	1.000
	Kerma	13	.696	.164	.046			St. Johns	.976
	St. Johns	18	.730	.127	.030		Jebel Moya	Kerma	1.000
	Total	45	.709	.130	.019			St. Johns	.996
							Kerma	St. Johns	.980

Table 7.1.34. ANOVA of residual log10 Conn.D in between pooled sex populations.

ANOVA - pooled sex MT1 residual log10Conn.D							**Test of Homogeneity of Variances**			
		Sum of Squares	**df**	**Mean Square**	**F**	***p***	**Levene Statistic**	**df1**	**df2**	***p***
BD	Between Groups	.244	3	.081	8.609	**.000**	.473	3	39	.703
	Within Groups	.368	39	.009						
	Total	.612	42							
BP	Between Groups	.325	3	.108	8.036	**.000**	.815	3	39	.494
	Within Groups	.525	39	.013						
	Total	.850	42							
HD	Between Groups	.121	3	.040	3.082	**.038**	.121	3	39	.947
	Within Groups	.508	39	.013						
	Total	.629	42							
HP	Between Groups	.018	3	.006	.352	.788	1.265	3	39	.300
	Within Groups	.657	39	.017						
	Total	.675	42							

Table 7.1.35. Pairwise post-hoc comparisons of residual log10Conn.D between pooled sex populations.

Pooled sex MT1 residual log10Conn.D pairwise post hoc comparisons									
Summary statistics						**Post Hoc**			
VOI	**Population**	**N**	**Mean**	**S.D**	**S.E.**	**type**	**pairwise comparison**		***p***
BD	Black Earth	10	-.084	.092	.029	Hochberg	Black Earth	Jebel Moya	1.000
	Jebel Moya	4	-.068	.096	.048			Kerma	.331
	Kerma	11	-.005	.120	.036			St. Johns	**.000**
	St. Johns	18	.095	.084	.020		Jebel Moya	Kerma	.841
	Total	43	.012	.121	.018			St. Johns	**.026**
							Kerma	St. Johns	.064
BP	Black Earth	10	-.062	.120	.038	Hochberg	Black Earth	Jebel Moya	1.000
	Jebel Moya	4	-.056	.065	.033			Kerma	1.000
	Kerma	11	-.071	.128	.039			St. Johns	**.003**
	St. Johns	18	.111	.114	.027		Jebel Moya	Kerma	1.000
	Total	43	.009	.142	.022			St. Johns	.075
							Kerma	St. Johns	**.001**
HD	Black Earth	10	-.052	.105	.033	Hochberg	Black Earth	Jebel Moya	.802
	Jebel Moya	4	.028	.138	.069			Kerma	**.032**
	Kerma	11	.095	.121	.036			St. Johns	.832
	St. Johns	18	-.001	.110	.026		Jebel Moya	Kerma	.891
	Total	43	.014	.122	.019			St. Johns	.998
							Kerma	St. Johns	.180
HP	Black Earth	10	-.019	.094	.030	Hochberg	Black Earth	Jebel Moya	.999
	Jebel Moya	4	.012	.129	.065			Kerma	1.000
	Kerma	11	-.001	.171	.052			St. Johns	.903
	St. Johns	18	.031	.118	.028		Jebel Moya	Kerma	1.000
	Total	43	.009	.127	.019			St. Johns	1.000
							Kerma	St. Johns	.987

Table 7.1.36. PCA scores – first metatarsal. Variables contributing >.15 are in bold.

Principal components MT1						
		PC1	**PC2**	**PC3**	**PC4**	**PC5**
Standard deviation		2.686	2.2888	1.35061	1.1975	0.97208
Proportion of Variance		0.3607	0.2619	0.09121	0.0717	0.04725
Cumulative Proportion		0.3607	0.6227	0.71386	0.7856	0.83281
PC scores						
VOI	**Properties**	**PC1**	**PC2**	**PC3**	**PC4**	**PC5**
BD	BV/TV	**0.33**	-0.05	0.02	-0.05	**0.19**
	Tb.Th	**0.31**	0.14	-0.01	0.16	**0.21**
	DA	0.07	**0.21**	**-0.44**	**-0.26**	**-0.24**
	Res. Tb.Sp	**-0.27**	**0.21**	-0.07	**0.29**	-0.11
	Res. Conn.D	-0.11	**-0.35**	0.17	-0.15	0.03
BP	BV/TV	**0.32**	-0.06	0.22	-0.16	0.07
	Tb.Th	**0.29**	**0.19**	0.10	0.08	0.08
	DA	0.06	**0.22**	**-0.34**	**-0.36**	0.17
	Res. Tb.Sp	**-0.15**	**0.26**	**-0.22**	**0.39**	0.09
	Res. Conn.D	-0.03	**-0.37**	**0.20**	**-0.23**	-0.09
HD	BV/TV	**0.34**	-0.01	-0.17	0.03	-0.02
	Tb.Th	**0.31**	0.16	0.08	0.08	-0.09
	DA	-0.08	**0.18**	-0.03	**-0.54**	**0.28**
	Res. Tb.Sp	**-0.21**	**0.18**	**0.45**	0.08	-0.02
	Res. Conn.D	-0.08	**-0.29**	**-0.40**	0.18	0.02
HP	BV/TV	**0.31**	-0.14	0.01	0.10	**-0.28**
	Tb.Th	**0.29**	0.15	0.14	0.11	-0.23
	DA	-0.09	0.16	-0.01	**-0.25**	**-0.72**
	Res. Tb.Sp	**-0.18**	**0.30**	0.15	-0.07	0.21
	Res. Conn.D	-0.01	**-0.37**	**-0.27**	0.08	0.07

Table 7.1.37. ANOVA of PC scores between pooled sex populations.

ANOVA - pooled MT1 principal components between populations							**Levene's test**			
		Sum of Squares	**df**	**Mean Square**	**F**	***p***	**Levene Statistic**	**df1**	**df2**	***p***
PC1	Between Groups	141.936	3	47.312	11.685	**.000**	2.016	3	38	.128
	Within Groups	153.860	38	4.049						
	Total	295.796	41							
PC2	Between Groups	43.022	3	14.341	3.173	**.035**	.831	3	38	.485
	Within Groups	171.755	38	4.520						
	Total	214.778	41							
PC3	Between Groups	33.461	3	11.154	10.256	**.000**	.144	3	38	.933
	Within Groups	41.328	38	1.088						
	Total	74.790	41							
PC4	Between Groups	6.850	3	2.283	1.670	.190	.537	3	38	.660
	Within Groups	51.948	38	1.367						
	Total	58.798	41							
PC5	Between Groups	.281	3	.094	.093	.964	.576	3	38	.635
	Within Groups	38.462	38	1.012						
	Total	38.743	41							

Table 7.1.38. Pairwise post-hoc comparisons of PC scores between pooled sex populations.

One-way ANOVA principal components MT1								
	Populations	**N**	**Mean**	**S.D.**	**S.E.**	**Pairwise post-hoc**		***p***
PC1	Black Earth	10	2.52	2.75	0.87	Black Earth	Jebel Moya	1.000
	Jebel Moya	4	2.61	2.80	1.40		Kerma	**.000**
	Kerma	11	-1.83	1.09	0.33		St. Johns	**.001**
	St. Johns	17	-0.92	1.77	0.43	Jebel Moya	Kerma	**.003**
	Total	42	0.00	2.69	0.41		St. Johns	**.018**
						Kerma	St. Johns	.806
PC2	Black Earth	10	1.14	1.53	0.48	Black Earth	Jebel Moya	.948
	Jebel Moya	4	0.07	2.49	1.25		Kerma	.999
	Kerma	11	0.76	2.58	0.78		St. Johns	.054
	St. Johns	17	-1.18	2.02	0.49	Jebel Moya	Kerma	.994
	Total	42	0.00	2.29	0.35		St. Johns	.868
						Kerma	St. Johns	.129
PC3	Black Earth	10	-0.48	1.04	0.33	Black Earth	Jebel Moya	1.000
	Jebel Moya	4	-0.62	1.10	0.55		Kerma	.849
	Kerma	11	-0.98	0.88	0.26		St. Johns	**.004**
	St. Johns	17	1.06	1.12	0.27	Jebel Moya	Kerma	.992
	Total	42	0.00	1.35	0.21		St. Johns	**.035**
						Kerma	St. Johns	**.000**
PC4	Black Earth	10	-0.52	0.95	0.30	Black Earth	Jebel Moya	.231
	Jebel Moya	4	0.92	1.22	0.61		Kerma	.582
	Kerma	11	0.25	1.24	0.38		St. Johns	.915
	St. Johns	17	-0.07	1.22	0.30	Jebel Moya	Kerma	.903
	Total	42	0.00	1.20	0.18		St. Johns	.562
						Kerma	St. Johns	.976
PC5	Black Earth	10	0.12	0.87	0.27	Black Earth	Jebel Moya	1.000
	Jebel Moya	4	-0.03	0.64	0.32		Kerma	.996
	Kerma	11	-0.11	1.13	0.34		St. Johns	1.000
	St. Johns	17	0.01	1.05	0.26	Jebel Moya	Kerma	1.000
	Total	42	0.00	0.97	0.15		St. Johns	1.000
						Kerma	St. Johns	1.000

Talus

Table 7.1.39. ANOVA of BV/TV between pooled sex populations.

ANOVA - pooled sex talus BV/TV							**Test of Homogeneity of Variances**			
		Sum of Squares	**df**	**Mean Square**	**F**	***p***	**Levene Statistic**	**df1**	**df2**	***p***
ACF	Between Groups	.059	3	.020	5.153	**.004**	.285	3	40	.836
	Within Groups	.152	40	.004						
	Total	.211	43							
PCF	Between Groups	.167	3	.056	13.414	**.000**	.465	3	40	.708
	Within Groups	.166	40	.004						
	Total	.333	43							
TH	Between Groups	.167	3	.056	16.983	**.000**	1.354	3	40	.271
	Within Groups	.131	40	.003						
	Total	.299	43							
TL	Between Groups	.160	3	.053	10.952	**.000**	1.334	3	40	.277
	Within Groups	.195	40	.005						
	Total	.355	43							
TC	Between Groups	.085	3	.028	6.976	**.001**	.116	3	40	.950
	Within Groups	.162	40	.004						
	Total	.247	43							
TM	Between Groups	.043	3	.014	4.351	**.010**	.459	3	40	.712
	Within Groups	.131	40	.003						
	Total	.173	43							

Table 7.1.40. Pairwise post-hoc comparisons of BV/TV between pooled sex populations.

Pooled sex Talus BV/TV pairwise post hoc comparisons									
Summary statistics						**Post Hoc**			
VOI	**Population**	**N**	**Mean**	**S.D**	**S.E.**	**type**	**pairwise comparison**		***p***
ACF	Black Earth	8	.361	.066	.023	Hochberg	Black Earth	Jebel Moya	.896
	Jebel Moya	8	.391	.078	.027			Kerma	.322
	Kerma	12	.307	.052	.015			St. Johns	.149
	St. Johns	16	.299	.057	.014		Jebel Moya	Kerma	**.028**
	Total	44	.329	.070	.011			St. Johns	**.008**
							Kerma	St. Johns	1.000
PCF	Black Earth	8	.487	.060	.021	Hochberg	Black Earth	Jebel Moya	.996
	Jebel Moya	8	.503	.080	.028			Kerma	**.003**
	Kerma	12	.376	.055	.016			St. Johns	**.000**
	St. Johns	16	.361	.064	.016		Jebel Moya	Kerma	**.001**
	Total	44	.414	.088	.013			St. Johns	**.000**
							Kerma	St. Johns	.990
TH	Black Earth	8	.554	.044	.016	Hochberg	Black Earth	Jebel Moya	1.000
	Jebel Moya	8	.555	.054	.019			Kerma	**.000**
	Kerma	12	.437	.060	.017			St. Johns	**.000**
	St. Johns	16	.420	.062	.016		Jebel Moya	Kerma	**.000**
	Total	44	.474	.083	.013			St. Johns	**.000**
							Kerma	St. Johns	.966
TL	Black Earth	8	.498	.046	.016	Hochberg	Black Earth	Jebel Moya	.758
	Jebel Moya	8	.541	.081	.029			Kerma	**.025**
	Kerma	12	.401	.070	.020			St. Johns	**.009**
	St. Johns	16	.394	.073	.018		Jebel Moya	Kerma	**.000**
	Total	44	.442	.091	.014			St. Johns	**.000**
							Kerma	St. Johns	1.000
TC	Black Earth	8	.461	.072	.025	Hochberg	Black Earth	Jebel Moya	.998
	Jebel Moya	8	.475	.074	.026			Kerma	**.040**
	Kerma	12	.378	.060	.017			St. Johns	**.023**
	St. Johns	16	.377	.057	.014		Jebel Moya	Kerma	**.011**
	Total	44	.410	.076	.011			St. Johns	**.006**
							Kerma	St. Johns	1.000
TM	Black Earth	8	.444	.064	.023	Hochberg	Black Earth	Jebel Moya	.970
	Jebel Moya	8	.465	.044	.016			Kerma	.127
	Kerma	12	.382	.053	.015			St. Johns	.449
	St. Johns	16	.402	.062	.016		Jebel Moya	Kerma	**.016**
	Total	44	.416	.063	.010			St. Johns	.080
							Kerma	St. Johns	.932

Table 7.1.41. ANOVA of Tb.Th between pooled sex populations.

ANOVA - pooled sex talus Tb.Th							**Test of Homogeneity of Variances**			
		Sum of Squares	**df**	**Mean Square**	**F**	***p***	**Levene Statistic**	**df1**	**df2**	***p***
ACF	Between Groups	.022	3	.007	5.104	**.004**	.041	3	40	.989
	Within Groups	.056	40	.001						
	Total	.078	43							
PCF	Between Groups	.061	3	.020	13.206	**.000**	1.063	3	40	.376
	Within Groups	.062	40	.002						
	Total	.123	43							
TH	Between Groups	.062	3	.021	19.005	**.000**	2.225	3	40	.100
	Within Groups	.044	40	.001						
	Total	.106	43							
TL	Between Groups	.060	3	.020	12.603	**.000**	.729	3	40	.541
	Within Groups	.064	40	.002						
	Total	.125	43							
TC	Between Groups	.043	3	.014	11.391	**.000**	.202	3	40	.895
	Within Groups	.050	40	.001						
	Total	.093	43							
TM	Between Groups	.023	3	.008	7.475	**.000**	.537	3	40	.659
	Within Groups	.040	40	.001						
	Total	.063	43							

Table 7.1.42. Pairwise post-hoc comparisons of Tb.Th between pooled sex populations.

Pooled sex talus Tb.Th pairwise post hoc comparisons									
Summary statistics						**Post Hoc**			
VOI	**Population**	**N**	**Mean**	**S.D**	**S.E.**	**type**	**pairwise comparison**		***p***
ACF	Black Earth	8	.296	.031	.011	Hochberg	Black Earth	Jebel Moya	.985
	Jebel Moya	8	.308	.041	.014			Kerma	.131
	Kerma	12	.255	.036	.010			St. Johns	.128
	St. Johns	16	.257	.040	.010		Jebel Moya	Kerma	**.022**
	Total	44	.273	.043	.006			St. Johns	**.020**
							Kerma	St. Johns	1.000
PCF	Black Earth	8	.340	.037	.013	Hochberg	Black Earth	Jebel Moya	1.000
	Jebel Moya	8	.336	.034	.012			Kerma	**.000**
	Kerma	12	.260	.032	.009			St. Johns	**.000**
	St. Johns	16	.260	.047	.012		Jebel Moya	Kerma	**.001**
	Total	44	.288	.053	.008			St. Johns	**.000**
							Kerma	St. Johns	1.000
TH	Black Earth	8	.353	.028	.010	Hochberg	Black Earth	Jebel Moya	.975
	Jebel Moya	8	.365	.019	.007			Kerma	**.000**
	Kerma	12	.284	.034	.010			St. Johns	**.000**
	St. Johns	16	.280	.039	.010		Jebel Moya	Kerma	**.000**
	Total	44	.310	.050	.007			St. Johns	**.000**
							Kerma	St. Johns	1.000
TL	Black Earth	8	.325	.033	.012	Hochberg	Black Earth	Jebel Moya	.804
	Jebel Moya	8	.349	.040	.014			Kerma	.060
	Kerma	12	.276	.033	.010			St. Johns	**.001**
	St. Johns	16	.254	.047	.012		Jebel Moya	Kerma	**.002**
	Total	44	.290	.054	.008			St. Johns	**.000**
							Kerma	St. Johns	.620
TC	Black Earth	8	.312	.037	.013	Hochberg	Black Earth	Jebel Moya	.710
	Jebel Moya	8	.335	.031	.011			Kerma	.276
	Kerma	12	.280	.034	.010			St. Johns	**.002**
	St. Johns	16	.253	.037	.009		Jebel Moya	Kerma	**.008**
	Total	44	.286	.046	.007			St. Johns	**.000**
							Kerma	St. Johns	.268
TM	Black Earth	8	.281	.037	.013	Hochberg	Black Earth	Jebel Moya	.384
	Jebel Moya	8	.310	.022	.008			Kerma	.775
	Kerma	12	.264	.033	.009			St. Johns	.094
	St. Johns	16	.247	.032	.008		Jebel Moya	Kerma	**.016**
	Total	44	.269	.038	.006			St. Johns	**.000**
							Kerma	St. Johns	.677

Table 7.1.43. ANOVA of DA between pooled sex populations.

ANOVA - pooled sex talus DA							**Test of Homogeneity of Variances**			
		Sum of Squares	**df**	**Mean Square**	**F**	***p***	**Levene Statistic**	**df1**	**df2**	***p***
ACF	Between Groups	.013	3	.004	.997	.404	.384	3	40	.765
	Within Groups	.172	40	.004						
	Total	.185	43							
PCF	Between Groups	.007	3	.002	1.447	.243	.947	3	40	.427
	Within Groups	.065	40	.002						
	Total	.072	43							
TH	Between Groups	.025	3	.008	5.974	**.002**	1.299	3	40	.288
	Within Groups	.057	40	.001						
	Total	.082	43							
TL	Between Groups	.012	3	.004	2.475	.075	1.407	3	40	.255
	Within Groups	.066	40	.002						
	Total	.078	43							
TC	Between Groups	.087	3	.029	6.459	**.001**	.442	3	40	.724
	Within Groups	.180	40	.004						
	Total	.267	43							
TM	Between Groups	.050	3	.017	2.998	**.042**	.848	3	40	.476
	Within Groups	.223	40	.006						
	Total	.273	43							

Table 7.1.44. Pairwise post-hoc comparisons of DA between pooled sex populations.

Pooled sex talus DA pairwise post hoc comparisons									
Summary statistics						**Post Hoc**			
VOI	**Population**	**N**	**Mean**	**S.D**	**S.E.**	**type**	**pairwise comparison**		***p***
ACF	Black Earth	8	.649	.067	.024	Hochberg	Black Earth	Jebel Moya	.700
	Jebel Moya	8	.693	.048	.017			Kerma	.664
	Kerma	12	.690	.079	.023			St. Johns	.996
	St. Johns	16	.663	.061	.015		Jebel Moya	Kerma	1.000
	Total	44	.673	.066	.010			St. Johns	.881
							Kerma	St. Johns	.858
PCF	Black Earth	8	.766	.042	.015	Hochberg	Black Earth	Jebel Moya	1.000
	Jebel Moya	8	.765	.031	.011			Kerma	.490
	Kerma	12	.736	.034	.010			St. Johns	.715
	St. Johns	16	.743	.046	.012		Jebel Moya	Kerma	.514
	Total	44	.749	.041	.006			St. Johns	.739
							Kerma	St. Johns	.998
TH	Black Earth	8	.831	.029	.010	Hochberg	Black Earth	Jebel Moya	**.012**
	Jebel Moya	8	.769	.036	.013			Kerma	.322
	Kerma	12	.799	.051	.015			St. Johns	1.000
	St. Johns	16	.830	.030	.007		Jebel Moya	Kerma	.423
	Total	44	.811	.044	.007			St. Johns	**.003**
							Kerma	St. Johns	.173
TL	Black Earth	8	.808	.026	.009	Hochberg	Black Earth	Jebel Moya	.171
	Jebel Moya	8	.762	.030	.011			Kerma	.123
	Kerma	12	.764	.052	.015			St. Johns	.132
	St. Johns	16	.766	.040	.010		Jebel Moya	Kerma	1.000
	Total	44	.772	.043	.006			St. Johns	1.000
							Kerma	St. Johns	1.000
TC	Black Earth	8	.750	.050	.018	Hochberg	Black Earth	Jebel Moya	**.001**
	Jebel Moya	8	.604	.088	.031			Kerma	.167
	Kerma	12	.682	.061	.018			St. Johns	**.044**
	St. Johns	16	.669	.067	.017		Jebel Moya	Kerma	.083
	Total	44	.675	.079	.012			St. Johns	.169
							Kerma	St. Johns	.996
TM	Black Earth	8	.699	.051	.018	Hochberg	Black Earth	Jebel Moya	**.039**
	Jebel Moya	8	.592	.069	.024			Kerma	.422
	Kerma	12	.640	.094	.027			St. Johns	.124
	St. Johns	16	.622	.070	.017		Jebel Moya	Kerma	.660
	Total	44	.636	.080	.012			St. Johns	.925
							Kerma	St. Johns	.989

Table 7.1.45. ANOVA of residual DA between pooled sex populations.

ANOVA - pooled sex talus residual DA							**Test of Homogeneity of Variances**			
		Sum of Squares	**df**	**Mean Square**	**F**	***p***	**Levene Statistic**	**df1**	**df2**	***p***
ACF	Between Groups	.007	3	.002	.483	.696	.326	3	36	.807
	Within Groups	.164	36	.005						
	Total	.171	39							
PCF	Between Groups	.007	3	.002	1.429	.250	1.176	3	36	.333
	Within Groups	.058	36	.002						
	Total	.065	39							
TH	Between Groups	.033	3	.011	7.831	**.000**	1.540	3	36	.221
	Within Groups	.051	36	.001						
	Total	.084	39							
TL	Between Groups	.012	3	.004	2.478	.077	.889	3	36	.456
	Within Groups	.059	36	.002						
	Total	.071	39							
TC	Between Groups	.057	3	.019	4.205	**.012**	1.576	3	36	.212
	Within Groups	.162	36	.004						
	Total	.219	39							
TM	Between Groups	.033	3	.011	1.998	.132	1.414	3	36	.254
	Within Groups	.199	36	.006						
	Total	.232	39							

Table 7.1.46. Pairwise post-hoc comparisons of residual DA between pooled sex populations.

Pooled sex talus residual DA pairwise post hoc comparisons									
Summary statistics						**Post Hoc**			
VOI	**Population**	**N**	**Mean**	**S.D**	**S.E.**	**type**	**pairwise comparison**		***p***
ACF	Black Earth	8	-.022	.066	.023	Hochberg	Black Earth	Jebel Moya	.905
	Jebel Moya	6	.014	.052	.021			Kerma	.894
	Kerma	10	.010	.083	.026			St. Johns	.997
	St. Johns	16	-.008	.062	.016		Jebel Moya	Kerma	1.000
	Total	40	-.003	.066	.010			St. Johns	.985
							Kerma	St. Johns	.985
PCF	Black Earth	8	.010	.042	.015	Hochberg	Black Earth	Jebel Moya	1.000
	Jebel Moya	6	.005	.030	.012			Kerma	.355
	Kerma	10	-.026	.031	.010			St. Johns	.710
	St. Johns	16	-.013	.046	.012		Jebel Moya	Kerma	.618
	Total	40	-.009	.041	.006			St. Johns	.920
							Kerma	St. Johns	.971
TH	Black Earth	8	.023	.031	.011	Hochberg	Black Earth	Jebel Moya	**.002**
	Jebel Moya	6	-.057	.039	.016			Kerma	.230
	Kerma	10	-.014	.053	.017			St. Johns	1.000
	St. Johns	16	.022	.028	.007		Jebel Moya	Kerma	.180
	Total	40	.001	.046	.007			St. Johns	**.001**
							Kerma	St. Johns	.129
TL	Black Earth	8	.033	.026	.009	Hochberg	Black Earth	Jebel Moya	.300
	Jebel Moya	6	-.009	.034	.014			Kerma	.109
	Kerma	10	-.014	.052	.016			St. Johns	.131
	St. Johns	16	-.008	.040	.010		Jebel Moya	Kerma	1.000
	Total	40	-.002	.043	.007			St. Johns	1.000
							Kerma	St. Johns	1.000
TC	Black Earth	8	.067	.052	.018	Hochberg	Black Earth	Jebel Moya	**.011**
	Jebel Moya	6	-.055	.101	.041			Kerma	.245
	Kerma	10	.002	.065	.020			St. Johns	.054
	St. Johns	16	-.013	.060	.015		Jebel Moya	Kerma	.485
	Total	40	.000	.075	.012			St. Johns	.713
							Kerma	St. Johns	.995
TM	Black Earth	8	.049	.052	.018	Hochberg	Black Earth	Jebel Moya	.340
	Jebel Moya	6	-.026	.056	.023			Kerma	.564
	Kerma	10	-.004	.102	.032			St. Johns	.138
	St. Johns	16	-.026	.068	.017		Jebel Moya	Kerma	.994
	Total	40	-.005	.077	.012			St. Johns	1.000
							Kerma	St. Johns	.978

Table 7.1.47. ANOVA of Tb.Sp between pooled sex populations.

ANOVA - pooled sex talus Tb.Sp							**Test of Homogeneity of Variances**			
		Sum of Squares	**df**	**Mean Square**	**F**	***p***	**Levene Statistic**	**df1**	**df2**	***p***
ACF	Between Groups	.057	3	.019	2.923	**.045**	.435	3	40	.729
	Within Groups	.261	40	.007						
	Total	.318	43							
PCF	Between Groups	.037	3	.012	3.304	**.030**	.324	3	40	.808
	Within Groups	.151	40	.004						
	Total	.188	43							
TH	Between Groups	.030	3	.010	3.588	**.022**	.429	3	40	.733
	Within Groups	.113	40	.003						
	Total	.143	43							
TL	Between Groups	.053	3	.018	4.697	**.007**	.219	3	40	.882
	Within Groups	.150	40	.004						
	Total	.202	43							
TC	Between Groups	.049	3	.016	4.548	**.008**	.377	3	40	.770
	Within Groups	.145	40	.004						
	Total	.195	43							
TM	Between Groups	.057	3	.019	7.619	**.000**	.064	3	40	.979
	Within Groups	.099	40	.002						
	Total	.155	43							

Table 7.1.48. Pairwise post-hoc comparisons of Tb.Sp between pooled sex populations.

Pooled sex talus Tb.Sp pairwise post hoc comparisons									
Summary statistics						**Post Hoc**			
VOI	**Population**	**N**	**Mean**	**S.D**	**S.E.**	**type**	**pairwise comparison**		***p***
ACF	Black Earth	8	.563	.092	.033	Hochberg	Black Earth	Jebel Moya	.995
	Jebel Moya	8	.584	.097	.034			Kerma	.054
	Kerma	12	.663	.073	.021			St. Johns	.659
	St. Johns	16	.612	.071	.018		Jebel Moya	Kerma	.201
	Total	44	.612	.086	.013			St. Johns	.965
							Kerma	St. Johns	.458
PCF	Black Earth	8	.476	.054	.019	Hochberg	Black Earth	Jebel Moya	.710
	Jebel Moya	8	.436	.077	.027			Kerma	.788
	Kerma	12	.510	.058	.017			St. Johns	.703
	St. Johns	16	.512	.059	.015		Jebel Moya	Kerma	.065
	Total	44	.491	.066	.010			St. Johns	**.039**
							Kerma	St. Johns	1.000
TH	Black Earth	8	.384	.048	.017	Hochberg	Black Earth	Jebel Moya	.992
	Jebel Moya	8	.399	.046	.016			Kerma	.064
	Kerma	12	.448	.058	.017			St. Johns	.081
	St. Johns	16	.442	.054	.014		Jebel Moya	Kerma	.256
	Total	44	.425	.058	.009			St. Johns	.326
							Kerma	St. Johns	1.000
TL	Black Earth	8	.420	.059	.021	Hochberg	Black Earth	Jebel Moya	.725
	Jebel Moya	8	.380	.054	.019			Kerma	.186
	Kerma	12	.481	.064	.019			St. Johns	1.000
	St. Johns	16	.422	.063	.016		Jebel Moya	Kerma	**.005**
	Total	44	.430	.069	.010			St. Johns	.515
							Kerma	St. Johns	.093
TC	Black Earth	8	.419	.054	.019	Hochberg	Black Earth	Jebel Moya	.876
	Jebel Moya	8	.450	.073	.026			Kerma	**.009**
	Kerma	12	.512	.065	.019			St. Johns	.843
	St. Johns	16	.448	.053	.013		Jebel Moya	Kerma	.160
	Total	44	.461	.067	.010			St. Johns	1.000
							Kerma	St. Johns	**.045**
TM	Black Earth	8	.415	.054	.019	Hochberg	Black Earth	Jebel Moya	.935
	Jebel Moya	8	.438	.041	.015			Kerma	**.002**
	Kerma	12	.503	.054	.016			St. Johns	1.000
	St. Johns	16	.421	.048	.012		Jebel Moya	Kerma	**.037**
	Total	44	.445	.060	.009			St. Johns	.971
							Kerma	St. Johns	**.001**

Table 7.1.49. ANOVA of residual Tb.Sp between pooled sex populations.

ANOVA - pooled sex talus residual Tb.Sp							**Test of Homogeneity of Variances**			
		Sum of Squares	**df**	**Mean Square**	**F**	***p***	**Levene Statistic**	**df1**	**df2**	***p***
ACF	Between Groups	.083	3	.028	4.593	**.008**	2.166	3	36	.109
	Within Groups	.218	36	.006						
	Total	.302	39							
PCF	Between Groups	.043	3	.014	3.929	**.016**	1.572	3	36	.213
	Within Groups	.130	36	.004						
	Total	.173	39							
TH	Between Groups	.040	3	.013	4.639	**.008**	.781	3	36	.512
	Within Groups	.103	36	.003						
	Total	.143	39							
TL	Between Groups	.048	3	.016	4.246	**.011**	.101	3	36	.959
	Within Groups	.137	36	.004						
	Total	.185	39							
TC	Between Groups	.053	3	.018	4.832	**.006**	.742	3	36	.534
	Within Groups	.132	36	.004						
	Total	.185	39							
TM	Between Groups	.051	3	.017	6.994	**.001**	.084	3	36	.969
	Within Groups	.088	36	.002						
	Total	.140	39							

Table 7.1.50. Pairwise post-hoc comparisons of residual Tb.Sp between pooled sex populations.

Pooled sex talus residual Tb.Sp pairwise post hoc comparisons									
Summary statistics						**Post Hoc**			
VOI	**Population**	**N**	**Mean**	**S.D**	**S.E.**	**type**	**pairwise comparison**		***p***
ACF	Black Earth	8	-.061	.085	.030	Hochberg	Black Earth	Jebel Moya	.996
	Jebel Moya	6	-.082	.129	.053			Kerma	**.031**
	Kerma	10	.049	.053	.017			St. Johns	.680
	St. Johns	16	-.015	.062	.016		Jebel Moya	Kerma	**.015**
	Total	40	-.018	.088	.014			St. Johns	.382
							Kerma	St. Johns	.261
PCF	Black Earth	8	-.017	.054	.019	Hochberg	Black Earth	Jebel Moya	.479
	Jebel Moya	6	-.071	.096	.039			Kerma	.630
	Kerma	10	.024	.041	.013			St. Johns	.716
	St. Johns	16	.017	.057	.014		Jebel Moya	Kerma	**.025**
	Total	40	-.001	.067	.011			St. Johns	**.025**
							Kerma	St. Johns	1.000
TH	Black Earth	8	-.039	.048	.017	Hochberg	Black Earth	Jebel Moya	1.000
	Jebel Moya	6	-.047	.066	.027			Kerma	.054
	Kerma	10	.030	.045	.014			St. Johns	.104
	St. Johns	16	.018	.056	.014		Jebel Moya	Kerma	**.047**
	Total	40	.000	.060	.010			St. Johns	.090
							Kerma	St. Johns	.992
TL	Black Earth	8	-.001	.057	.020	Hochberg	Black Earth	Jebel Moya	.711
	Jebel Moya	6	-.045	.068	.028			Kerma	.189
	Kerma	10	.063	.060	.019			St. Johns	1.000
	St. Johns	16	.001	.063	.016		Jebel Moya	Kerma	**.010**
	Total	40	.009	.069	.011			St. Johns	.552
							Kerma	St. Johns	.095
TC	Black Earth	8	-.033	.052	.019	Hochberg	Black Earth	Jebel Moya	.999
	Jebel Moya	6	-.020	.090	.037			Kerma	**.009**
	Kerma	10	.065	.061	.019			St. Johns	.865
	St. Johns	16	-.005	.051	.013		Jebel Moya	Kerma	.056
	Total	40	.005	.069	.011			St. Johns	.995
							Kerma	St. Johns	**.039**
TM	Black Earth	8	-.026	.053	.019	Hochberg	Black Earth	Jebel Moya	1.000
	Jebel Moya	6	-.022	.049	.020			Kerma	**.005**
	Kerma	10	.061	.048	.015			St. Johns	1.000
	St. Johns	16	-.020	.049	.012		Jebel Moya	Kerma	**.016**
	Total	40	-.001	.060	.009			St. Johns	1.000
							Kerma	St. Johns	**.002**

Table 7.1.51. ANOVA of log10 Conn.D between pooled sex populations.

ANOVA - pooled sex talus log10Conn.D							**Test of Homogeneity of Variances**			
		Sum of Squares	**df**	**Mean Square**	**F**	***p***	**Levene Statistic**	**df1**	**df2**	***p***
ACF	Between Groups	.033	3	.011	.882	.459	.480	3	40	.698
	Within Groups	.505	40	.013						
	Total	.538	43							
PCF	Between Groups	.384	3	.128	7.368	**.000**	1.396	3	40	.258
	Within Groups	.695	40	.017						
	Total	1.079	43							
TH	Between Groups	.248	3	.083	5.909	**.002**	1.387	3	40	.261
	Within Groups	.560	40	.014						
	Total	.809	43							
TL	Between Groups	.357	3	.119	7.130	**.001**	.814	3	40	.494
	Within Groups	.668	40	.017						
	Total	1.026	43							
TC	Between Groups	.202	3	.067	4.843	**.006**	.237	3	40	.870
	Within Groups	.555	40	.014						
	Total	.757	43							
TM	Between Groups	.257	3	.086	7.376	**.000**	.612	3	40	.611
	Within Groups	.464	40	.012						
	Total	.721	43							

Table 7.1.52. Pairwise post-hoc comparisons of log10 Conn.D between pooled sex populations.

Pooled sex talus log10Conn.D pairwise post hoc comparisons									
Summary statistics						**Post Hoc**			
VOI	**Population**	**N**	**Mean**	**S.D**	**S.E.**	**type**	**pairwise comparison**		***p***
ACF	Black Earth	8	.671	.095	.034	Hochberg	Black Earth	Jebel Moya	.984
	Jebel Moya	8	.633	.088	.031			Kerma	.995
	Kerma	12	.643	.120	.035			St. Johns	.991
	St. Johns	16	.700	.123	.031		Jebel Moya	Kerma	1.000
	Total	44	.667	.112	.017			St. Johns	.674
							Kerma	St. Johns	.711
PCF	Black Earth	8	.555	.091	.032	Hochberg	Black Earth	Jebel Moya	.847
	Jebel Moya	8	.628	.151	.053			Kerma	**.004**
	Kerma	12	.780	.102	.030			St. Johns	**.002**
	St. Johns	16	.781	.155	.039		Jebel Moya	Kerma	.089
	Total	44	.712	.158	.024			St. Johns	.060
							Kerma	St. Johns	1.000
TH	Black Earth	8	.542	.112	.040	Hochberg	Black Earth	Jebel Moya	.706
	Jebel Moya	8	.621	.064	.023			Kerma	**.003**
	Kerma	12	.750	.132	.038			St. Johns	**.014**
	St. Johns	16	.709	.130	.032		Jebel Moya	Kerma	.123
	Total	44	.674	.137	.021			St. Johns	.439
							Kerma	St. Johns	.931
TL	Black Earth	8	.611	.109	.038	Hochberg	Black Earth	Jebel Moya	.925
	Jebel Moya	8	.671	.100	.035			Kerma	.116
	Kerma	12	.753	.132	.038			St. Johns	**.001**
	St. Johns	16	.848	.147	.037		Jebel Moya	Kerma	.661
	Total	44	.747	.154	.023			St. Johns	**.018**
							Kerma	St. Johns	.308
TC	Black Earth	8	.729	.108	.038	Hochberg	Black Earth	Jebel Moya	1.000
	Jebel Moya	8	.745	.099	.035			Kerma	.991
	Kerma	12	.761	.118	.034			St. Johns	**.022**
	St. Johns	16	.887	.129	.032		Jebel Moya	Kerma	1.000
	Total	44	.798	.133	.020			St. Johns	**.049**
							Kerma	St. Johns	**.047**
TM	Black Earth	8	.787	.105	.037	Hochberg	Black Earth	Jebel Moya	1.000
	Jebel Moya	8	.784	.084	.030			Kerma	1.000
	Kerma	12	.792	.132	.038			St. Johns	**.008**
	St. Johns	16	.947	.099	.025		Jebel Moya	Kerma	1.000
	Total	44	.846	.130	.020			St. Johns	**.007**
							Kerma	St. Johns	**.003**

Table 7.1.53. ANOVA of residual log10 Conn.D between pooled sex populations.

ANOVA - pooled sex talus residual log10Conn.D							**Test of Homogeneity of Variances**			
		Sum of Squares	**df**	**Mean Square**	**F**	***p***	**Levene Statistic**	**df1**	**df2**	***p***
ACF	Between Groups	.022	3	.007	.596	.622	.251	3	36	.860
	Within Groups	.438	36	.012						
	Total	.460	39							
PCF	Between Groups	.347	3	.116	7.099	**.001**	2.128	3	36	.114
	Within Groups	.586	36	.016						
	Total	.932	39							
TH	Between Groups	.235	3	.078	5.924	**.002**	.522	3	36	.670
	Within Groups	.477	36	.013						
	Total	.712	39							
TL	Between Groups	.316	3	.105	7.629	**.000**	.409	3	36	.747
	Within Groups	.497	36	.014						
	Total	.813	39							
TC	Between Groups	.180	3	.060	4.851	**.006**	.612	3	36	.612
	Within Groups	.446	36	.012						
	Total	.626	39							
TM	Between Groups	.207	3	.069	6.551	**.001**	.375	3	36	.772
	Within Groups	.379	36	.011						
	Total	.586	39							

Table 7.1.54. Pairwise post-hoc comparisons of residual log10Conn.D between pooled sex populations.

Pooled sex talus residual log10Conn.D pairwise post hoc comparisons									
Summary statistics						**Post Hoc**			
VOI	**Population**	**N**	**Mean**	**S.D**	**S.E.**	**type**	**pairwise comparison**		***p***
ACF	Black Earth	8	.004	.082	.029	Hochberg	Black Earth	Jebel Moya	.997
	Jebel Moya	6	.034	.097	.039			Kerma	.998
	Kerma	10	-.018	.118	.037			St. Johns	.981
	St. Johns	16	.037	.121	.030		Jebel Moya	Kerma	.928
	Total	40	.016	.109	.017			St. Johns	1.000
							Kerma	St. Johns	.764
PCF	Black Earth	8	-.163	.073	.026	Hochberg	Black Earth	Jebel Moya	.553
	Jebel Moya	6	-.057	.189	.077			Kerma	**.003**
	Kerma	10	.066	.091	.029			St. Johns	**.001**
	St. Johns	16	.067	.140	.035		Jebel Moya	Kerma	.343
	Total	40	.002	.155	.024			St. Johns	.260
							Kerma	St. Johns	1.000
TH	Black Earth	8	-.150	.101	.036	Hochberg	Black Earth	Jebel Moya	.066
	Jebel Moya	6	.015	.091	.037			Kerma	**.002**
	Kerma	10	.069	.132	.042			St. Johns	**.009**
	St. Johns	16	.022	.117	.029		Jebel Moya	Kerma	.934
	Total	40	-.002	.135	.021			St. Johns	1.000
							Kerma	St. Johns	.889
TL	Black Earth	8	-.136	.094	.033	Hochberg	Black Earth	Jebel Moya	.297
	Jebel Moya	6	-.013	.126	.052			Kerma	**.047**
	Kerma	10	.020	.102	.032			St. Johns	**.000**
	St. Johns	16	.105	.132	.033		Jebel Moya	Kerma	.995
	Total	40	.018	.144	.023			St. Johns	.229
							Kerma	St. Johns	.389
TC	Black Earth	8	-.069	.100	.035	Hochberg	Black Earth	Jebel Moya	.961
	Jebel Moya	6	-.021	.128	.052			Kerma	.983
	Kerma	10	-.034	.084	.027			St. Johns	**.012**
	St. Johns	16	.091	.124	.031		Jebel Moya	Kerma	1.000
	Total	40	.011	.127	.020			St. Johns	.220
							Kerma	St. Johns	**.049**
TM	Black Earth	8	-.055	.095	.034	Hochberg	Black Earth	Jebel Moya	.974
	Jebel Moya	6	-.014	.125	.051			Kerma	.998
	Kerma	10	-.033	.104	.033			St. Johns	**.004**
	St. Johns	16	.109	.097	.024		Jebel Moya	Kerma	.999
	Total	40	.022	.123	.019			St. Johns	.093
							Kerma	St. Johns	**.009**

Table 7.1.55. PCA scores - talus. Variables contributing >.15 are in bold.

Importance of top five principal components – all talus VOIs						
		PC1	PC2	PC3	PC4	PC5
Standard deviation		3.45	2.64	1.53	1.22	1.16
Proportion of Variance		0.40	0.23	0.08	0.05	0.05
Cumulative Proportion		0.40	0.63	0.71	0.76	0.80
PC scores						
VOI	Properties	PC1	PC2	PC3	PC4	PC5
ACF	BV/TV	**-0.22**	0.08	0.18	-0.16	**0.25**
	Tb.Th	**-0.21**	-0.03	0.18	**-0.32**	0.10
	DA	0.05	-0.12	0.17	**-0.24**	**0.46**
	Res. Tb.Sp	0.15	**-0.23**	-0.16	-0.13	-0.13
	Res. Conn.D	0.01	**0.27**	-0.11	**0.37**	-0.07
PCF	BV/TV	**-0.27**	0.02	-0.06	0.02	0.02
	Tb.Th	**-0.26**	-0.09	-0.07	-0.02	-0.15
	DA	-0.04	-0.08	**0.27**	**-0.45**	**-0.23**
	Res. Tb.Sp	0.16	**-0.24**	0.04	0.03	**-0.26**
	Res. Conn.D	0.18	**0.23**	-0.05	0.04	**0.25**
TH	BV/TV	**-0.27**	0.00	-0.01	0.13	0.09
	Tb.Th	**-0.26**	-0.09	-0.08	0.10	0.06
	DA	0.09	-0.08	**0.37**	**0.22**	**-0.43**
	Res. Tb.Sp	**0.20**	**-0.20**	-0.11	-0.08	-0.06
	Res. Conn.D	0.10	**0.24**	-0.12	**-0.30**	0.04
TL	BV/TV	**-0.26**	0.03	-0.10	-0.02	-0.05
	Tb.Th	**-0.24**	-0.12	-0.19	0.01	-0.04
	DA	-0.10	-0.09	**0.28**	**-0.29**	**-0.21**
	Res. Tb.Sp	0.16	**-0.27**	-0.07	0.05	-0.03
	Res. Conn.D	0.13	**0.29**	0.04	-0.05	0.06
TC	BV/TV	**-0.27**	0.03	0.03	0.04	0.05
	Tb.Th	**-0.24**	-0.12	-0.13	0.03	0.07
	DA	0.00	-0.16	**0.40**	**0.32**	**0.25**
	Res. Tb.Sp	0.17	**-0.23**	-0.23	-0.04	0.00
	Res. Conn.D	0.06	**0.34**	0.08	-0.14	-0.13
TM	BV/TV	**-0.24**	0.04	-0.04	0.06	**-0.21**
	Tb.Th	**-0.23**	-0.12	-0.18	-0.06	-0.11
	DA	0.01	-0.18	**0.40**	**0.20**	0.13
	Res. Tb.Sp	0.15	**-0.26**	-0.20	-0.10	**0.21**
	Res. Conn.D	0.06	**0.34**	0.04	-0.04	-0.17

Table 7.1.56. ANOVA of PC scores between pooled sex populations.

ANOVA - talus all VOIs							**Levene's test**			
		Sum of Squares	**df**	**Mean Square**	**F**	***p***	**Levene Statistic**	**df1**	**df2**	***p***
PC1	Between Groups	258.014	3	86.005	15.060	**.000**	.183	3	36	.908
	Within Groups	205.593	36	5.711						
	Total	463.607	39							
PC2	Between Groups	48.067	3	16.022	2.575	.069	.377	3	36	.770
	Within Groups	223.982	36	6.222						
	Total	272.049	39							
PC3	Between Groups	29.313	3	9.771	5.657	**.003**	1.851	3	36	.155
	Within Groups	62.185	36	1.727						
	Total	91.498	39							
PC4	Between Groups	8.264	3	2.755	2.001	.131	.558	3	36	.646
	Within Groups	49.565	36	1.377						
	Total	57.829	39							
PC5	Between Groups	11.677	3	3.892	3.410	**.028**	.466	3	36	.708
	Within Groups	41.089	36	1.141						
	Total	52.766	39							

Table 7.1.57. Pairwise post-hoc comparisons of PC scores between pooled sex populations.

Pairwise comparisons of principal components of the talus								
	Populations	**N**	**Mean**	**S.D.**	**S.E.**	**Pairwise post-hoc**		***p***
PC1	Black Earth	8	-3.12	2.00	0.71	Black Earth	Jebel Moya	.992
	Jebel Moya	6	-3.87	2.92	1.19		Kerma	**.000**
	Kerma	10	2.02	2.44	0.77		St. Johns	**.000**
	St. Johns	16	1.75	2.33	0.58	Jebel Moya	Kerma	**.000**
	Total	40	.00	3.45	0.55		St. Johns	**.000**
						Kerma	St. Johns	1.000
PC2	Black Earth	8	-1.37	2.22	0.79	Black Earth	Jebel Moya	.640
	Jebel Moya	6	.54	3.00	1.22		Kerma	1.000
	Kerma	10	-1.04	2.22	0.70		St. Johns	.142
	St. Johns	16	1.13	2.58	0.65	Jebel Moya	Kerma	.774
	Total	40	.00	2.64	0.42		St. Johns	.997
						Kerma	St. Johns	.200
PC3	Black Earth	8	1.19	0.86	0.30	Black Earth	Jebel Moya	**.012**
	Jebel Moya	6	-1.17	0.79	0.32		Kerma	**.013**
	Kerma	10	-.87	1.21	0.38		St. Johns	.645
	St. Johns	16	.38	1.65	0.41	Jebel Moya	Kerma	.998
	Total	40	.00	1.53	0.24		St. Johns	.104
						Kerma	St. Johns	.132
PC4	Black Earth	8	.75	1.22	0.43	Black Earth	Jebel Moya	.144
	Jebel Moya	6	-.71	0.79	0.32		Kerma	.378
	Kerma	10	-.25	1.12	0.35		St. Johns	.662
	St. Johns	16	.05	1.28	0.32	Jebel Moya	Kerma	.968
	Total	40	.00	1.22	0.19		St. Johns	.688
						Kerma	St. Johns	.988
PC5	Black Earth	8	-.31	0.78	0.28	Black Earth	Jebel Moya	.462
	Jebel Moya	6	.66	1.31	0.54		Kerma	.326
	Kerma	10	.65	1.00	0.32		St. Johns	.999
	St. Johns	16	-.50	1.13	0.28	Jebel Moya	Kerma	1.000
	Total	40	.00	1.16	0.18		St. Johns	.157
						Kerma	St. Johns	.062

Appendix 7.2 Pairwise ANOVA

Table 7.2.1. Pairwise ANOVA and post-hoc comparisons between pooled sex populations – Achilles tendon.

ANOVA - Achilles tendon

		Sum of Squares	df	Mean Square	F	*p*	Levene Statistic	df 1	df 2	*p*
BV/TV	Between Groups	.167	3	.056	9.306	**.000**	1.877	3	63	.142
	Within Groups	.376	63	.006						
	Total	.543	66							
Tb.Th	Between Groups	.042	3	.014	9.785	**.000**	3.417	3	63	.023
	Within Groups	.090	63	.001						
	Total	.132	66							
DA	Between Groups	.037	3	.012	3.414	**.023**	2.552	3	63	.063
	Within Groups	.228	63	.004						
	Total	.265	66							
Tb.Sp	Between Groups	.113	3	.038	6.664	**.001**	.993	3	63	.402
	Within Groups	.355	63	.006						
	Total	.468	66							
Log10 Conn.D	Between Groups	.043	3	.014	1.111	.351	1.916	3	63	.136
	Within Groups	.806	63	.013						
	Total	.849	66							
Residual Tb.Sp	Between Groups	.112	3	.037	7.407	**.000**	1.020	3	63	.390
	Within Groups	.317	63	.005						
	Total	.428	66							
Residual DA	Between Groups	.034	3	.011	3.229	**.028**	2.132	3	63	.105
	Within Groups	.224	63	.004						
	Total	.258	66							
Residual Conn.D	Between Groups	.036	3	.012	1.250	.299	3.702	3	63	.016
	Within Groups	.602	63	.010						
	Total	.638	66							

Post-hoc

		N	Mean	S.D.	S.E.	Type	Pairwise comparisons		*p*
BV/TV	Black Earth	17	0.45	0.11	0.03	Hochberg	Black Earth	Jebel Moya	.993
	Jebel Moya	14	0.47	0.06	0.02			Kerma	**.000**
	Kerma	16	0.33	0.07	0.02			St. Johns	.125
	St. Johns	20	0.39	0.05	0.01		Jebel Moya	Black Earth	.993
	Total	67	0.41	0.09	0.01			Kerma	**.000**
								St. Johns	**.039**
							Kerma	Black Earth	**.000**

								Jebel Moya	**.000**
								St. Johns	.210
Tb.Th	Black Earth	17	0.31	0.05	0.01	Games-Howell	Black Earth	Jebel Moya	.951
	Jebel Moya	14	0.32	0.04	0.01			Kerma	**.018**
	Kerma	16	0.27	0.03	0.01			St. Johns	**.021**
	St. Johns	20	0.27	0.02	0.01		Jebel Moya	Black Earth	.951
	Total	67	0.29	0.04	0.01			Kerma	**.001**
								St. Johns	**.001**
							Kerma	Black Earth	**.018**
								Jebel Moya	**.001**
								St. Johns	.991
DA	Black Earth	17	0.72	0.07	0.02	Hochberg	Black Earth	Jebel Moya	.964
	Jebel Moya	14	0.74	0.07	0.02			Kerma	.772
	Kerma	16	0.75	0.06	0.01			St. Johns	**.018**
	St. Johns	20	0.78	0.04	0.01		Jebel Moya	Black Earth	.964
	Total	67	0.75	0.06	0.01			Kerma	.999
								St. Johns	.212
							Kerma	Black Earth	.772
								Jebel Moya	.999
								St. Johns	.402
Tb.Sp	Black Earth	17	0.42	0.09	0.02	Hochberg	Black Earth	Jebel Moya	.999
	Jebel Moya	14	0.43	0.06	0.01			Kerma	**.001**
	Kerma	16	0.53	0.09	0.02			St. Johns	.829
	St. Johns	20	0.45	0.06	0.01		Jebel Moya	Black Earth	.999
	Total	67	0.46	0.08	0.01			Kerma	**.005**
								St. Johns	.988
							Kerma	Black Earth	**.001**
								Jebel Moya	**.005**
								St. Johns	**.015**
log10 Conn.D	Black Earth	17	0.74	0.07	0.02	Hochberg	Black Earth	Jebel Moya	.974
	Jebel Moya	14	0.71	0.11	0.03			Kerma	.361
	Kerma	16	0.67	0.15	0.04			St. Johns	.959
	St. Johns	20	0.71	0.11	0.03		Jebel Moya	Black Earth	.974
	Total	67	0.71	0.11	0.01			Kerma	.894
								St. Johns	1.000
							Kerma	Black Earth	.361

								Jebel Moya	.894
								St. Johns	.853
Residual Tb.Sp	Black Earth	17	-0.02	0.08	0.02	Hochberg	Black Earth	Jebel Moya	1.000
	Jebel Moya	14	-0.03	0.07	0.02			Kerma	**.001**
	Kerma	16	0.08	0.08	0.02			St. Johns	.954
	St. Johns	20	0.00	0.05	0.01		Jebel Moya	Black Earth	1.000
	Total	67	0.01	0.08	0.01			Kerma	**.001**
								St. Johns	.935
							Kerma	Black Earth	**.001**
								Jebel Moya	**.001**
								St. Johns	**.007**
Residual DA	Black Earth	17	-0.02	0.07	0.02	Hochberg	Black Earth	Jebel Moya	.997
	Jebel Moya	14	-0.01	0.07	0.02			Kerma	.850
	Kerma	16	0.00	0.06	0.01			St. Johns	**.029**
	St. Johns	20	0.03	0.04	0.01		Jebel Moya	Black Earth	.997
	Total	67	0.00	0.06	0.01			Kerma	.994
								St. Johns	.157
							Kerma	Black Earth	.850
								Jebel Moya	.994
								St. Johns	.419
Residual Conn.D	Black Earth	17	0.01	0.06	0.01	Games-Howell	Black Earth	Jebel Moya	.997
	Jebel Moya	14	0.02	0.10	0.03			Kerma	.425
	Kerma	16	-0.04	0.13	0.03			St. Johns	.986
	St. Johns	20	0.01	0.09	0.02		Jebel Moya	Black Earth	.997
	Total	67	0.00	0.10	0.01			Kerma	.487
								St. Johns	.974
							Kerma	Black Earth	.425
								Jebel Moya	.487
								St. Johns	.638

Table 7.2.2. Pairwise ANOVA and post-hoc comparisons between pooled sex population - Calcaneocuboid.

ANOVA - Calcaneocuboid

		Sum of Squares	df	Mean Square	F	*p*	Levene Statistic	df 1	df 2	*p*
BV/TV	Between Groups	.253	3	.084	17.366	**.000**	1.094	3	60	.359
	Within Groups	.292	60	.005						
	Total	.545	63							
Tb.Th	Between Groups	.067	3	.022	11.646	**.000**	.693	3	60	.560
	Within Groups	.115	60	.002						
	Total	.182	63							
DA	Between Groups	.011	3	.004	1.476	.230	1.827	3	60	.152
	Within Groups	.152	60	.003						
	Total	.164	63							
Tb.Sp	Between Groups	.222	3	.074	10.108	**.000**	1.953	3	60	.131
	Within Groups	.440	60	.007						
	Total	.663	63							
log10 Conn.D	Between Groups	.220	3	.073	3.909	**.013**	.102	3	60	.959
	Within Groups	1.127	60	.019						
	Total	1.347	63							
Residual Tb.Sp	Between Groups	.247	3	.082	13.065	**.000**	1.097	3	60	.357
	Within Groups	.378	60	.006						
	Total	.625	63							
Residual DA	Between Groups	.014	3	.005	1.997	.124	.955	3	60	.420
	Within Groups	.143	60	.002						
	Total	.157	63							
Residual Conn.D	Between Groups	.263	3	.088	5.855	**.001**	.182	3	60	.908
	Within Groups	.897	60	.015						
	Total	1.160	63							

Post-hoc

		N	Mean	S.D.	S.E.	type	Pairwise comparisons		*p*
BV/TV	Black Earth	13	0.45	0.09	0.03	Hochberg	Black Earth	Jebel Moya	.163
	Jebel Moya	15	0.51	0.07	0.02			Kerma	**.002**
	Kerma	19	0.35	0.07	0.02			St. Johns	**.015**
	St. Johns	17	0.37	0.06	0.01		Jebel Moya	Black Earth	.163
	Total	64	0.41	0.09	0.01			Kerma	**.000**
								St. Johns	**.000**
							Kerma	Black Earth	**.002**
								Jebel Moya	**.000**
								St. Johns	.989
Tb.Th	Black Earth	13	0.36	0.05	0.01	Hochberg	Black Earth	Jebel Moya	.917
	Jebel Moya	15	0.37	0.05	0.01			Kerma	**.012**

	Kerma	19	0.31	0.04	0.01			St. Johns	**.002**
	St. Johns	17	0.30	0.04	0.01		Jebel Moya	Black Earth	.917
	Total	64	0.33	0.05	0.01			Kerma	**.000**
								St. Johns	**.000**
							Kerma	Black Earth	**.012**
								Jebel Moya	**.000**
								St. Johns	.983
DA	Black Earth	13	0.73	0.04	0.01	Hochberg	Black Earth	Jebel Moya	.617
	Jebel Moya	15	0.71	0.04	0.01			Kerma	.889
	Kerma	19	0.71	0.06	0.01			St. Johns	.243
	St. Johns	17	0.70	0.05	0.01		Jebel Moya	Black Earth	.617
	Total	64	0.71	0.05	0.01			Kerma	.995
								St. Johns	.994
							Kerma	Black Earth	.889
								Jebel Moya	.995
								St. Johns	.820
Tb.Sp	Black Earth	13	0.52	0.12	0.03	Hochberg	Black Earth	Jebel Moya	.212
	Jebel Moya	15	0.45	0.05	0.01			Kerma	**.023**
	Kerma	19	0.61	0.09	0.02			St. Johns	.944
	St. Johns	17	0.55	0.08	0.02		Jebel Moya	Black Earth	.212
	Total	64	0.54	0.10	0.01			Kerma	**.000**
								St. Johns	**.015**
							Kerma	Black Earth	**.023**
								Jebel Moya	**.000**
								St. Johns	.146
log10 Conn.D	Black Earth	13	0.48	0.12	0.03	Hochberg	Black Earth	Jebel Moya	.804
	Jebel Moya	15	0.55	0.15	0.04			Kerma	.653
	Kerma	19	0.55	0.14	0.03			St. Johns	**.009**
	St. Johns	17	0.65	0.14	0.03		Jebel Moya	Black Earth	.804
	Total	64	0.56	0.15	0.02			Kerma	1.00
								St. Johns	.177
							Kerma	Black Earth	.653
								Jebel Moya	1.00
								St. Johns	.194
Residual Tb.Sp	Black Earth	13	-0.01	0.11	0.03	Hochberg	Black Earth	Jebel Moya	**.035**
	Jebel Moya	15	-0.09	0.06	0.02			Kerma	**.024**
	Kerma	19	0.08	0.08	0.02			St. Johns	.991
	St. Johns	17	0.01	0.06	0.02		Jebel Moya	Black Earth	**.035**
	Total	64	0.00	0.10	0.01			Kerma	**.000**
								St. Johns	**.003**
							Kerma	Black Earth	**.024**
								Jebel Moya	**.000**
								St. Johns	.074
Residual DA	Black Earth	13	0.03	0.03	0.01	Hochberg	Black Earth	Jebel Moya	.345
	Jebel Moya	15	-0.01	0.05	0.01			Kerma	.791

	Kerma	19	0.00	0.06	0.01			St. Johns	.136
	St. Johns	17	-0.02	0.05	0.01		Jebel Moya	Black Earth	.345
	Total	64	0.00	0.05	0.01			Kerma	.967
								St. Johns	.999
							Kerma	Black Earth	.791
								Jebel Moya	.967
								St. Johns	.757
Residual Conn.D	Black Earth	13	-0.10	0.11	0.03	Hochberg	Black Earth	Jebel Moya	.237
	Jebel Moya	15	0.00	0.13	0.03			Kerma	.321
	Kerma	19	-0.01	0.12	0.03			St. Johns	**.001**
	St. Johns	17	0.09	0.13	0.03		Jebel Moya	Black Earth	.237
	Total	64	0.00	0.14	0.02			Kerma	1.00
								St. Johns	.205
							Kerma	Black Earth	.321
								Jebel Moya	1.00
								St. Johns	.079

Table 7.2.3. Pairwise ANOVA and post-hoc comparisons between pooled sex population – Calcaneal tuber.

ANOVA - Calcaneal tuber

		Sum of Squares	df	Mean Square	F	*p*	Levene Statistic	df1	df2	*p*
BV/TV	Between Groups	.122	3	.041	12.082	**.000**	4.840	3	64	.004
	Within Groups	.216	64	.003						
	Total	.338	67							
Tb.Th	Between Groups	.034	3	.011	6.654	**.001**	2.672	3	64	.055
	Within Groups	.111	64	.002						
	Total	.145	67							
DA	Between Groups	.018	3	.006	4.655	**.005**	.687	3	64	.563
	Within Groups	.081	64	.001						
	Total	.099	67							
Tb.Sp	Between Groups	.310	3	.103	9.877	**.000**	3.069	3	64	.034
	Within Groups	.670	64	.010						
	Total	.980	67							
log10 Conn.D	Between Groups	.267	3	.089	4.437	**.007**	.126	3	64	.944
	Within Groups	1.285	64	.020						
	Total	1.553	67							
Residual Tb.Sp	Between Groups	.326	3	.109	12.037	**.000**	1.224	3	64	.308
	Within Groups	.578	64	.009						
	Total	.904	67							
Residual DA	Between Groups	.020	3	.007	5.613	**.002**	.798	3	64	.500
	Within Groups	.076	64	.001						
	Total	.096	67							
Residual Conn.D	Between Groups	.318	3	.106	6.571	**.001**	.310	3	64	.818
	Within Groups	1.033	64	.016						
	Total	1.351	67							

Post-hoc

		N	Mean	S.D.	S.E.	type	Pairwise comparisons		*p*
BV/TV	Black Earth	16	0.39	0.08	0.02	Games-Howell	Black Earth	Jebel Moya	.982
	Jebel Moya	15	0.39	0.04	0.01			Kerma	**.003**
	Kerma	19	0.29	0.04	0.01			St. Johns	.077
	St. Johns	18	0.32	0.06	0.01		Jebel Moya	Black Earth	.982
	Total	68	0.35	0.07	0.01			Kerma	**.000**
								St. Johns	**.001**
							Kerma	Black Earth	**.003**
								Jebel Moya	**.000**
								St. Johns	.309
Tb.Th	Black Earth	16	0.36	0.06	0.01	Hochberg	Black Earth	Jebel Moya	.728
	Jebel Moya	15	0.34	0.03	0.01			Kerma	**.001**
	Kerma	19	0.30	0.03	0.01			St. Johns	**.008**
	St. Johns	18	0.31	0.04	0.01		Jebel Moya	Black Earth	.728
	Total	68	0.33	0.05	0.01			Kerma	.073

								St. Johns	.270
							Kerma	Black Earth	**.001**
								Jebel Moya	.073
								St. Johns	.992
DA	Black Earth	16	0.80	0.03	0.01	Hochberg	Black Earth	Jebel Moya	.215
	Jebel Moya	15	0.78	0.04	0.01			Kerma	.903
	Kerma	19	0.81	0.03	0.01			St. Johns	.339
	St. Johns	18	0.78	0.04	0.01		Jebel Moya	Black Earth	.215
	Total	68	0.79	0.04	0.00			Kerma	**.015**
								St. Johns	1.000
							Kerma	Black Earth	.903
								Jebel Moya	**.015**
								St. Johns	**.026**
Tb.Sp	Black Earth	16	0.62	0.13	0.03	Games-Howell	Black Earth	Jebel Moya	.793
	Jebel Moya	15	0.59	0.05	0.01			Kerma	**.009**
	Kerma	19	0.77	0.12	0.03			St. Johns	.733
	St. Johns	18	0.66	0.09	0.02		Jebel Moya	Black Earth	.793
	Total	68	0.67	0.12	0.01			Kerma	**.000**
								St. Johns	**.036**
							Kerma	Black Earth	**.009**
								Jebel Moya	**.000**
								St. Johns	**.022**
log10 Conn.D	Black Earth	16	0.32	0.13	0.03	Hochberg	Black Earth	Jebel Moya	.822
	Jebel Moya	15	0.38	0.13	0.03			Kerma	.322
	Kerma	19	0.23	0.16	0.04			St. Johns	.794
	St. Johns	18	0.38	0.14	0.03		Jebel Moya	Black Earth	.822
	Total	68	0.32	0.15	0.02			Kerma	**.020**
								St. Johns	1.000
							Kerma	Black Earth	.322
								Jebel Moya	**.020**
								St. Johns	**.013**
Residual Tb.Sp	Black Earth	16	-0.03	0.12	0.03	Hochberg	Black Earth	Jebel Moya	.467
	Jebel Moya	15	-0.09	0.07	0.02			Kerma	**.001**
	Kerma	19	0.10	0.10	0.02			St. Johns	.962
	St. Johns	18	-0.01	0.08	0.02		Jebel Moya	Black Earth	.467
	Total	68	0.00	0.12	0.01			Kerma	**.000**
								St. Johns	.087
							Kerma	Black Earth	**.001**
								Jebel Moya	**.000**
								St. Johns	**.007**
Residual DA	Black Earth	16	0.01	0.03	0.01	Hochberg	Black Earth	Jebel Moya	.074
	Jebel Moya	15	-0.02	0.04	0.01			Kerma	.960
	Kerma	19	0.02	0.03	0.01			St. Johns	.196
	St. Johns	18	-0.01	0.04	0.01		Jebel Moya	Black Earth	.074
	Total	68	0.00	0.04	0.00			Kerma	**.006**

								St. Johns	.995
							Kerma	Black Earth	.960
								Jebel Moya	**.006**
								St. Johns	**.019**
Residual Conn.D	Black Earth	16	-0.02	0.12	0.03	Hochberg	Black Earth	Jebel Moya	.184
	Jebel Moya	15	0.08	0.14	0.04			Kerma	.485
	Kerma	19	-0.09	0.14	0.03			St. Johns	.359
	St. Johns	18	0.06	0.11	0.03		Jebel Moya	Black Earth	.184
	Total	68	0.00	0.14	0.02			Kerma	**.002**
								St. Johns	.998
							Kerma	Black Earth	.485
								Jebel Moya	**.002**
								St. Johns	**.004**

Table 7.2.4. Pairwise ANOVA and post-hoc comparisons between pooled sex population – PTF anterior.

ANOVA - PTF anterior

		Sum of Squares	**df**	**Mean Square**	**F**	***p***	**Levene Statistic**	**df1**	**df2**	***p***
BV/TV	Between Groups	.144	3	.048	5.972	**.001**	.733	3	59	.536
	Within Groups	.476	59	.008						
	Total	.620	62							
Tb.Th	Between Groups	.082	3	.027	8.105	**.000**	1.880	3	59	.143
	Within Groups	.198	59	.003						
	Total	.279	62							
DA	Between Groups	.039	3	.013	1.551	.211	1.862	3	59	.146
	Within Groups	.489	59	.008						
	Total	.528	62							
Tb.Sp	Between Groups	.123	3	.041	4.503	**.007**	1.890	3	59	.141
	Within Groups	.537	59	.009						
	Total	.660	62							
log10 Conn.D	Between Groups	.255	3	.085	4.592	**.006**	.596	3	59	.620
	Within Groups	1.092	59	.019						
	Total	1.347	62							
Residual Tb.Sp	Between Groups	.124	3	.041	4.906	**.004**	1.519	3	59	.219
	Within Groups	.495	59	.008						
	Total	.619	62							
Residual DA	Between Groups	.055	3	.018	2.437	.073	1.816	3	59	.154
	Within Groups	.443	59	.008						
	Total	.498	62							
Residual Conn.D	Between Groups	.272	3	.091	5.891	**.001**	.773	3	59	.514
	Within Groups	.907	59	.015						
	Total	1.179	62							

Post-hoc

		N	Mean	S.D.	S.E.	type	Pairwise comparisons		p
BV/TV	Black Earth	13	0.52	0.11	0.03	Hochberg	Black Earth	Jebel Moya	1.000
	Jebel Moya	12	0.53	0.09	0.03			Kerma	**.014**
	Kerma	18	0.42	0.09	0.02			St. Johns	.088
	St. Johns	20	0.44	0.08	0.02		Jebel Moya	Black Earth	1.000
	Total	63	0.47	0.10	0.01			Kerma	**.007**
								St. Johns	**.047**
							Kerma	Black Earth	**.014**
								Jebel Moya	**.007**
								St. Johns	.959
Tb.Th	Black Earth	13	0.44	0.07	0.02	Hochberg	Black Earth	Jebel Moya	1.000
	Jebel Moya	12	0.43	0.06	0.02			Kerma	**.011**
	Kerma	18	0.37	0.04	0.01			St. Johns	**.001**
	St. Johns	20	0.35	0.06	0.01		Jebel Moya	Black Earth	1.000
	Total	63	0.39	0.07	0.01			Kerma	**.029**
								St. Johns	**.004**
							Kerma	Black Earth	**.011**
								Jebel Moya	**.029**
								St. Johns	.983
DA	Black Earth	13	0.71	0.06	0.02	Hochberg	Black Earth	Jebel Moya	.322
	Jebel Moya	12	0.64	0.09	0.03			Kerma	1.000
	Kerma	18	0.70	0.11	0.03			St. Johns	1.000
	St. Johns	20	0.70	0.08	0.02		Jebel Moya	Black Earth	.322
	Total	63	0.69	0.09	0.01			Kerma	.404
								St. Johns	.353
							Kerma	Black Earth	1.000
								Jebel Moya	.404
								St. Johns	1.000
Tb.Sp	Black Earth	13	0.52	0.11	0.03	Hochberg	Black Earth	Jebel Moya	.911
	Jebel Moya	12	0.48	0.07	0.02			Kerma	.122
	Kerma	18	0.60	0.11	0.03			St. Johns	1.000
	St. Johns	20	0.51	0.08	0.02		Jebel Moya	Black Earth	.911
	Total	63	0.53	0.10	0.01			Kerma	**.009**
								St. Johns	.925
							Kerma	Black Earth	.122
								Jebel Moya	**.009**
								St. Johns	**.042**
log10 Conn.D	Black Earth	13	0.47	0.11	0.03	Hochberg	Black Earth	Jebel Moya	.843
	Jebel Moya	12	0.53	0.11	0.03			Kerma	1.000
	Kerma	18	0.46	0.13	0.03			St. Johns	**.027**
	St. Johns	20	0.61	0.16	0.04		Jebel Moya	Black Earth	.843
	Total	63	0.52	0.15	0.02			Kerma	.758
								St. Johns	.465

							Kerma	Black Earth	1.000
								Jebel Moya	.758
								St. Johns	**.010**
Residual Tb.Sp	Black Earth	13	-0.01	0.11	0.03	Hochberg	Black Earth	Jebel Moya	.706
	Jebel Moya	12	-0.06	0.08	0.02			Kerma	.173
	Kerma	18	0.07	0.10	0.02			St. Johns	1.000
	St. Johns	20	-0.02	0.07	0.02		Jebel Moya	Black Earth	.706
	Total	63	0.00	0.10	0.01			Kerma	**.004**
								St. Johns	.837
							Kerma	Black Earth	.173
								Jebel Moya	**.004**
								St. Johns	**.036**
Residual DA	Black Earth	13	0.02	0.06	0.02	Hochberg	Black Earth	Jebel Moya	.083
	Jebel Moya	12	-0.06	0.11	0.03			Kerma	.978
	Kerma	18	0.00	0.09	0.02			St. Johns	.992
	St. Johns	20	0.01	0.08	0.02		Jebel Moya	Black Earth	.083
	Total	63	0.00	0.09	0.01			Kerma	.256
								St. Johns	.178
							Kerma	Black Earth	.978
								Jebel Moya	.256
								St. Johns	1.000
Residual Conn.D	Black Earth	13	-0.07	0.10	0.03	Hochberg	Black Earth	Jebel Moya	.444
	Jebel Moya	12	0.01	0.12	0.03			Kerma	1.000
	Kerma	18	-0.06	0.11	0.03			St. Johns	**.005**
	St. Johns	20	0.08	0.15	0.03		Jebel Moya	Black Earth	.444
	Total	63	0.00	0.14	0.02			Kerma	.567
								St. Johns	.513
							Kerma	Black Earth	1.000
								Jebel Moya	.567
								St. Johns	**.005**

Table 7.2.5. Pairwise ANOVA and post-hoc comparisons between pooled sex population – PTF central.

ANOVA - PTF central

		Sum of Squares	df	Mean Square	F	*p*	Levene Statistic	df1	df2	*p*
BVTV	Between Groups	.195	3	.065	8.043	**.000**	1.523	3	60	.218
	Within Groups	.485	60	.008						
	Total	.679	63							
Tb.Th	Between Groups	.111	3	.037	9.570	**.000**	1.132	3	60	.344
	Within Groups	.231	60	.004						
	Total	.342	63							
DA	Between Groups	.137	3	.046	5.234	**.003**	.083	3	60	.969
	Within Groups	.522	60	.009						
	Total	.659	63							
Tb.Sp	Between Groups	.034	3	.011	1.889	.141	1.551	3	60	.211
	Within Groups	.360	60	.006						
	Total	.394	63							
log10 Conn.D	Between Groups	.532	3	.177	9.837	**.000**	1.338	3	60	.270
	Within Groups	1.082	60	.018						
	Total	1.614	63							
Residual Tb.Sp	Between Groups	.036	3	.012	2.209	.096	1.392	3	60	.254
	Within Groups	.328	60	.005						
	Total	.364	63							
Residual DA	Between Groups	.154	3	.051	6.333	**.001**	.068	3	60	.977
	Within Groups	.485	60	.008						
	Total	.639	63							
Residual Conn.D	Between Groups	.523	3	.174	11.828	**.000**	2.438	3	60	.073
	Within Groups	.884	60	.015						
	Total	1.407	63							

Post-hoc

		N	Mean	S.D.	S.E.	type	Pairwise comparisons		*p*
BV/TV	Black Earth	13	0.59	0.12	0.03	Hochberg	Black Earth	Jebel Moya	.985
	Jebel Moya	13	0.62	0.08	0.02			Kerma	**.049**
	Kerma	18	0.50	0.07	0.02			St. Johns	**.008**
	St. Johns	20	0.49	0.09	0.02		Jebel Moya	Black Earth	.985
	Total	64	0.54	0.10	0.01			Kerma	**.006**
								St. Johns	**.001**
							Kerma	Black Earth	**.049**
								Jebel Moya	**.006**
								St. Johns	.989
Tb.Th	Black Earth	13	0.44	0.08	0.02	Hochberg	Black Earth	Jebel Moya	.899
	Jebel Moya	13	0.47	0.06	0.02			Kerma	.096
	Kerma	18	0.39	0.05	0.01			St. Johns	**.003**
	St. Johns	20	0.36	0.07	0.01		Jebel	Black Earth	.899

	Total	64	0.41	0.07	0.01		Moya	Kerma	**.005**
								St. Johns	**.000**
							Kerma	Black Earth	.096
								Jebel Moya	**.005**
								St. Johns	.761
DA	Black Earth	13	0.69	0.09	0.02	Hochberg	Black Earth	Jebel Moya	**.038**
	Jebel Moya	13	0.58	0.09	0.02			Kerma	.702
	Kerma	18	0.64	0.10	0.02			St. Johns	**.004**
	St. Johns	20	0.57	0.09	0.02		Jebel Moya	Black Earth	**.038**
	Total	64	0.62	0.10	0.01			Kerma	.437
								St. Johns	.997
							Kerma	Black Earth	.702
								Jebel Moya	.437
								St. Johns	.103
Tb.Sp	Black Earth	13	0.43	0.10	0.03	Hochberg	Black Earth	Jebel Moya	1.000
	Jebel Moya	13	0.43	0.05	0.01			Kerma	.324
	Kerma	18	0.49	0.08	0.02			St. Johns	.927
	St. Johns	20	0.46	0.07	0.02		Jebel Moya	Black Earth	1.000
	Total	64	0.45	0.08	0.01			Kerma	.216
								St. Johns	.828
							Kerma	Black Earth	.324
								Jebel Moya	.216
								St. Johns	.849
log10 Conn.D	Black Earth	13	0.50	0.08	0.02	Hochberg	Black Earth	Jebel Moya	.991
	Jebel Moya	13	0.47	0.15	0.04			Kerma	.438
	Kerma	18	0.59	0.13	0.03			St. Johns	**.001**
	St. Johns	20	0.70	0.15	0.03		Jebel Moya	Black Earth	.991
	Total	64	0.58	0.16	0.02			Kerma	.125
								St. Johns	**.000**
							Kerma	Black Earth	.438
								Jebel Moya	.125
								St. Johns	.056
Residual Tb.Sp	Black Earth	13	-0.01	0.10	0.03	Hochberg	Black Earth	Jebel Moya	.976
	Jebel Moya	13	-0.04	0.07	0.02			Kerma	.457
	Kerma	18	0.03	0.07	0.02			St. Johns	.981
	St. Johns	20	0.00	0.06	0.01		Jebel Moya	Black Earth	.976
	Total	64	0.00	0.08	0.01			Kerma	.096
								St. Johns	.589
							Kerma	Black Earth	.457
								Jebel Moya	.096
								St. Johns	.838
Residual DA	Black Earth	13	0.08	0.09	0.02	Hochberg	Black Earth	Jebel Moya	**.010**
	Jebel Moya	13	-0.04	0.09	0.03			Kerma	.519
	Kerma	18	0.03	0.09	0.02			St. Johns	**.001**
	St. Johns	20	-0.05	0.09	0.02		Jebel	Black Earth	**.010**

	Total	64	0.00	0.10	0.01		Moya	Kerma	.288
								St. Johns	1.000
							Kerma	Black Earth	.519
								Jebel Moya	.288
								St. Johns	.087
Residual Conn.D	Black Earth	13	-0.09	0.07	0.02	Hochberg	Black Earth	Jebel Moya	1.000
	Jebel Moya	13	-0.09	0.15	0.04			Kerma	.142
	Kerma	18	0.01	0.12	0.03			St. Johns	**.000**
	St. Johns	20	0.12	0.13	0.03		Jebel Moya	Black Earth	1.000
	Total	64	0.00	0.15	0.02			Kerma	.159
								St. Johns	**.000**
							Kerma	Black Earth	.142
								Jebel Moya	.159
								St. Johns	**.029**

Table 7.2.6. Pairwise ANOVA and post-hoc comparisons between pooled sex population – PTF posterior.

ANOVA - PTF posterior

		Sum of Squares	**df**	**Mean Square**	**F**	***p***	**Levene Statistic**	**df1**	**df2**	***p***
BV/TV	Between Groups	.190	3	.063	12.535	**.000**	2.157	3	60	.102
	Within Groups	.303	60	.005						
	Total	.493	63							
Tb.Th	Between Groups	.093	3	.031	13.045	**.000**	2.618	3	60	.059
	Within Groups	.142	60	.002						
	Total	.235	63							
DA	Between Groups	.051	3	.017	5.373	**.002**	2.148	3	60	.104
	Within Groups	.188	60	.003						
	Total	.239	63							
Tb.Sp	Between Groups	.087	3	.029	5.497	**.002**	2.026	3	60	.120
	Within Groups	.315	60	.005						
	Total	.402	63							
log10 Conn.D	Between Groups	.575	3	.192	15.733	**.000**	.960	3	60	.418
	Within Groups	.731	60	.012						
	Total	1.306	63							
Residual Tb.Sp	Between Groups	.088	3	.029	5.643	**.002**	2.127	3	60	.106
	Within Groups	.313	60	.005						
	Total	.401	63							
Residual DA	Between Groups	.055	3	.018	6.084	**.001**	2.330	3	60	.083
	Within Groups	.181	60	.003						
	Total	.236	63							
Residual Conn.D	Between Groups	.597	3	.199	17.305	**.000**	.857	3	60	.468
	Within Groups	.690	60	.011						
	Total	1.287	63							

Post-hoc

		N	Mean	S.D.	S.E.	type	Pairwise comparisons		*p*
BV/TV	Black Earth	15	0.53	0.10	0.03	Hochberg	Black Earth	Jebel Moya	.926
	Jebel Moya	12	0.55	0.06	0.02			Kerma	**.000**
	Kerma	17	0.42	0.04	0.01			St. Johns	**.004**
	St. Johns	20	0.44	0.07	0.02		Jebel Moya	Black Earth	.926
	Total	64	0.48	0.09	0.01			Kerma	**.000**
								St. Johns	**.000**
							Kerma	Black Earth	**.000**
								Jebel Moya	**.000**
								St. Johns	.952
Tb.Th	Black Earth	15	0.43	0.06	0.02	Hochberg	Black Earth	Jebel Moya	.990
	Jebel Moya	12	0.41	0.04	0.01			Kerma	**.000**
	Kerma	17	0.34	0.04	0.01			St. Johns	**.000**
	St. Johns	20	0.34	0.05	0.01		Jebel Moya	Black Earth	.990
	Total	64	0.38	0.06	0.01			Kerma	**.002**
								St. Johns	**.001**
							Kerma	Black Earth	**.000**
								Jebel Moya	**.002**
								St. Johns	1.000
DA	Black Earth	15	0.76	0.03	0.01	Hochberg	Black Earth	Jebel Moya	**.039**
	Jebel Moya	12	0.70	0.06	0.02			Kerma	.107
	Kerma	17	0.71	0.06	0.02			St. Johns	**.002**
	St. Johns	20	0.69	0.06	0.01		Jebel Moya	Black Earth	**.039**
	Total	64	0.71	0.06	0.01			Kerma	.989
								St. Johns	.985
							Kerma	Black Earth	.107
								Jebel Moya	.989
								St. Johns	.625
Tb.Sp	Black Earth	15	0.52	0.11	0.03	Hochberg	Black Earth	Jebel Moya	.384
	Jebel Moya	12	0.47	0.06	0.02			Kerma	.152
	Kerma	17	0.58	0.05	0.01			St. Johns	1.000
	St. Johns	20	0.51	0.06	0.01		Jebel Moya	Black Earth	.384
	Total	64	0.52	0.08	0.01			Kerma	**.001**
								St. Johns	.451
							Kerma	Black Earth	.152
								Jebel Moya	**.001**
								St. Johns	.058
log10 Conn.D	Black Earth	15	0.39	0.11	0.03	Hochberg	Black Earth	Jebel Moya	.079
	Jebel Moya	12	0.50	0.08	0.02			Kerma	**.003**
	Kerma	17	0.54	0.12	0.03			St. Johns	**.000**
	St. Johns	20	0.65	0.12	0.03		Jebel Moya	Black Earth	.079
	Total	64	0.53	0.14	0.02			Kerma	.934
								St. Johns	**.003**

							Kerma	Black Earth	**.003**
								Jebel Moya	.934
								St. Johns	**.022**
Residual Tb.Sp	Black Earth	15	0.00	0.11	0.03	Hochberg	Black Earth	Jebel Moya	.314
	Jebel Moya	12	-0.06	0.06	0.02			Kerma	.171
	Kerma	17	0.05	0.05	0.01			St. Johns	1.000
	St. Johns	20	-0.01	0.06	0.01		Jebel Moya	Black Earth	.314
	Total	64	0.00	0.08	0.01			Kerma	**.001**
								St. Johns	.405
							Kerma	Black Earth	.171
								Jebel Moya	**.001**
								St. Johns	.058
Residual DA	Black Earth	15	0.05	0.03	0.01	Hochberg	Black Earth	Jebel Moya	**.017**
	Jebel Moya	12	-0.02	0.07	0.02			Kerma	.067
	Kerma	17	0.00	0.06	0.01			St. Johns	**.001**
	St. Johns	20	-0.03	0.06	0.01		Jebel Moya	Black Earth	**.017**
	Total	64	0.00	0.06	0.01			Kerma	.973
								St. Johns	.995
							Kerma	Black Earth	.067
								Jebel Moya	.973
								St. Johns	.619
Residual Conn.D	Black Earth	15	-0.15	0.11	0.03	Hochberg	Black Earth	Jebel Moya	**.028**
	Jebel Moya	12	-0.02	0.08	0.02			Kerma	**.001**
	Kerma	17	0.01	0.12	0.03			St. Johns	**.000**
	St. Johns	20	0.12	0.11	0.03		Jebel Moya	Black Earth	**.028**
	Total	64	0.00	0.14	0.02			Kerma	.967
								St. Johns	**.004**
							Kerma	Black Earth	**.001**
								Jebel Moya	.967
								St. Johns	**.018**

Table 7.2.7. Pairwise ANOVA and post-hoc comparisons between pooled sex population – Plantar ligaments.

ANOVA - Plantar ligaments

		Sum of Squares	df	Mean Square	F	*p*	Levene Statistic	df1	df2	*p*
BV/TV	Between Groups	.142	3	.047	10.753	**.000**	1.549	3	55	.212
	Within Groups	.242	55	.004						
	Total	.383	58							
Tb.Th	Between Groups	.114	3	.038	19.416	**.000**	1.963	3	55	.130
	Within Groups	.107	55	.002						
	Total	.221	58							
DA	Between Groups	.041	3	.014	3.362	**.025**	.528	3	55	.665
	Within Groups	.221	55	.004						
	Total	.262	58							
Tb.Sp	Between Groups	.229	3	.076	5.385	**.003**	.582	3	55	.629
	Within Groups	.781	55	.014						
	Total	1.010	58							
log10 Conn.D	Between Groups	.160	3	.053	2.131	.107	.237	3	55	.870
	Within Groups	1.377	55	.025						
	Total	1.537	58							
Residual Tb.Sp	Between Groups	.247	3	.082	6.126	**.001**	.226	3	55	.878
	Within Groups	.738	55	.013						
	Total	.985	58							
Residual DA	Between Groups	.034	3	.011	3.293	**.027**	.266	3	55	.850
	Within Groups	.189	55	.003						
	Total	.223	58							
Residual Conn.D	Between Groups	.218	3	.073	3.592	**.019**	.421	3	55	.739
	Within Groups	1.112	55	.020						
	Total	1.329	58							

Post-hoc

		N	Mean	S.D.	S.E.	type	Pairwise comparisons		*p*
BV/TV	Black Earth	12	0.34	0.06	0.02	Hochberg	Black Earth	Jebel Moya	.900
	Jebel Moya	11	0.37	0.09	0.03			Kerma	**.001**
	Kerma	18	0.25	0.06	0.01			St. Johns	**.040**
	St. Johns	18	0.27	0.06	0.01		Jebel Moya	Black Earth	.900
	Total	59	0.30	0.08	0.01			Kerma	**.000**
								St. Johns	**.002**
							Kerma	Black Earth	**.001**
								Jebel Moya	**.000**
								St. Johns	.755
Tb.Th	Black Earth	12	0.38	0.05	0.01	Hochberg	Black Earth	Jebel Moya	.324
	Jebel Moya	11	0.34	0.06	0.02			Kerma	**.000**
	Kerma	18	0.27	0.03	0.01			St. Johns	**.000**
	St. Johns	18	0.29	0.04	0.01		Jebel	Black Earth	.324

	Total	59	0.31	0.06	0.01		Moya	Kerma	**.000**
								St. Johns	**.008**
							Kerma	Black Earth	**.000**
								Jebel Moya	**.000**
								St. Johns	.627
DA	Black Earth	12	0.67	0.07	0.02	Hochberg	Black Earth	Jebel Moya	.563
	Jebel Moya	11	0.71	0.06	0.02			Kerma	.410
	Kerma	18	0.71	0.06	0.01			St. Johns	**.015**
	St. Johns	18	0.75	0.06	0.02		Jebel Moya	Black Earth	.563
	Total	59	0.71	0.07	0.01			Kerma	1.000
								St. Johns	.641
							Kerma	Black Earth	.410
								Jebel Moya	1.000
								St. Johns	.517
Tb.Sp	Black Earth	12	0.72	0.15	0.04	Hochberg	Black Earth	Jebel Moya	.179
	Jebel Moya	11	0.61	0.09	0.03			Kerma	.894
	Kerma	18	0.76	0.12	0.03			St. Johns	.629
	St. Johns	18	0.78	0.11	0.03		Jebel Moya	Black Earth	.179
	Total	59	0.73	0.13	0.02			Kerma	**.008**
								St. Johns	**.002**
							Kerma	Black Earth	.894
								Jebel Moya	**.008**
								St. Johns	.997
log10 Conn.D	Black Earth	12	0.30	0.16	0.05	Hochberg	Black Earth	Jebel Moya	.220
	Jebel Moya	11	0.44	0.14	0.04			Kerma	.485
	Kerma	18	0.40	0.15	0.04			St. Johns	.999
	St. Johns	18	0.32	0.17	0.04		Jebel Moya	Black Earth	.220
	Total	59	0.36	0.16	0.02			Kerma	.982
								St. Johns	.304
							Kerma	Black Earth	.485
								Jebel Moya	.982
								St. Johns	.640
Residual Tb.Sp	Black Earth	12	-0.01	0.14	0.04	Hochberg	Black Earth	Jebel Moya	.086
	Jebel Moya	11	-0.13	0.11	0.03			Kerma	.925
	Kerma	18	0.03	0.11	0.03			St. Johns	.707
	St. Johns	18	0.05	0.11	0.03		Jebel Moya	Black Earth	.086
	Total	59	0.00	0.13	0.02			Kerma	**.004**
								St. Johns	**.001**
							Kerma	Black Earth	.925
								Jebel Moya	**.004**
								St. Johns	.998
Residual DA	Black Earth	12	-0.04	0.06	0.02	Hochberg	Black Earth	Jebel Moya	.889
	Jebel Moya	11	-0.01	0.05	0.01			Kerma	.493
	Kerma	18	0.00	0.06	0.01			St. Johns	**.020**

	St. Johns	18	0.03	0.06	0.02		Jebel Moya	Black Earth	.889
	Total	59	0.00	0.06	0.01			Kerma	.998
								St. Johns	.334
							Kerma	Black Earth	.493
								Jebel Moya	.998
								St. Johns	.508
Residual Conn.D	Black Earth	12	-0.08	0.14	0.04	Hochberg	Black Earth	Jebel Moya	**.029**
	Jebel Moya	11	0.10	0.14	0.04			Kerma	.227
	Kerma	18	0.03	0.12	0.03			St. Johns	.970
	St. Johns	18	-0.04	0.16	0.04		Jebel Moya	Black Earth	**.029**
	Total	59	0.00	0.15	0.02			Kerma	.804
								St. Johns	.098
							Kerma	Black Earth	.227
								Jebel Moya	.804
								St. Johns	.605

Table 7.2.8. Pairwise ANOVA and post-hoc comparisons between pooled sex population – MT1 base dorsal.

ANOVA - MT1 base dorsal

		Sum of Squares	**df**	**Mean Square**	**F**	***p***	**Levene Statistic**	**df1**	**df2**	***p***
BV/TV	Between Groups	.085	3	.028	7.425	**.000**	.833	3	49	.482
	Within Groups	.187	49	.004						
	Total	.272	52							
Tb.Th	Between Groups	.033	3	.011	12.436	**.000**	2.191	3	49	.101
	Within Groups	.044	49	.001						
	Total	.077	52							
DA	Between Groups	.062	3	.021	12.126	**.000**	.750	3	49	.528
	Within Groups	.083	49	.002						
	Total	.145	52							
Tb.Sp	Between Groups	.037	3	.012	4.899	**.005**	.490	3	49	.691
	Within Groups	.124	49	.003						
	Total	.161	52							
log10 Conn.D	Between Groups	.311	3	.104	9.521	**.000**	.463	3	49	.709
	Within Groups	.533	49	.011						
	Total	.844	52							
Residual Tb.Sp	Between Groups	.035	3	.012	4.745	**.006**	.474	3	49	.702
	Within Groups	.122	49	.002						
	Total	.157	52							
Residual DA	Between Groups	.063	3	.021	12.429	**.000**	.744	3	49	.531
	Within Groups	.082	49	.002						
	Total	.145	52							
Residual Conn.D	Between Groups	.337	3	.112	11.795	**.000**	.839	3	49	.479
	Within Groups	.466	49	.010						
	Total	.803	52							

Post-hoc

		N	Mean	S.D.	S.E.	type	Pairwise comparisons		*p*
BV/TV	Black Earth	15	0.45	0.07	0.02	Hochberg	Black Earth	Jebel Moya	1.00
	Jebel Moya	7	0.46	0.06	0.02			Kerma	**.002**
	Kerma	14	0.36	0.05	0.01			St. Johns	**.016**
	St. Johns	17	0.38	0.06	0.01		Jebel Moya	Black Earth	1.00
	Total	53	0.41	0.07	0.01			Kerma	**.010**
								St. Johns	**.048**
							Kerma	Black Earth	**.002**
								Jebel Moya	**.010**
								St. Johns	.954
Tb.Th	Black Earth	15	0.29	0.04	0.01	Hochberg	Black Earth	Jebel Moya	.935
	Jebel Moya	7	0.28	0.02	0.01			Kerma	**.000**
	Kerma	14	0.24	0.02	0.01			St. Johns	**.000**
	St. Johns	17	0.24	0.02	0.01		Jebel Moya	Black Earth	.935
	Total	53	0.26	0.04	0.01			Kerma	**.049**
								St. Johns	**.010**
							Kerma	Black Earth	**.000**
								Jebel Moya	**.049**
								St. Johns	.988
DA	Black Earth	15	0.80	0.04	0.01	Hochberg	Black Earth	Jebel Moya	.090
	Jebel Moya	7	0.75	0.03	0.01			Kerma	.668
	Kerma	14	0.78	0.04	0.01			St. Johns	**.000**
	St. Johns	17	0.71	0.05	0.01		Jebel Moya	Black Earth	.090
	Total	53	0.76	0.05	0.01			Kerma	.682
								St. Johns	.274
							Kerma	Black Earth	.668
								Jebel Moya	.682
								St. Johns	**.001**
Tb.Sp	Black Earth	15	0.39	0.06	0.01	Hochberg	Black Earth	Jebel Moya	1.00
	Jebel Moya	7	0.39	0.05	0.02			Kerma	**.007**
	Kerma	14	0.46	0.05	0.01			St. Johns	.874
	St. Johns	17	0.41	0.04	0.01		Jebel Moya	Black Earth	1.00
	Total	53	0.42	0.06	0.01			Kerma	**.034**
								St. Johns	.922
							Kerma	Black Earth	**.007**
								Jebel Moya	**.034**
								St. Johns	.081
log10 Conn.D	Black Earth	15	0.74	0.10	0.03	Hochberg	Black Earth	Jebel Moya	.484
	Jebel Moya	7	0.82	0.10	0.04			Kerma	.051
	Kerma	14	0.85	0.12	0.03			St. Johns	**.000**
	St. Johns	17	0.94	0.09	0.02		Jebel Moya	Black Earth	.484
	Total	53	0.84	0.13	0.02			Kerma	.993

								St. Johns	.086
							Kerma	Black Earth	.051
								Jebel Moya	.993
								St. Johns	.114
Residual Tb.Sp	Black Earth	15	-0.02	0.06	0.01	Hochberg	Black Earth	Jebel Moya	.998
	Jebel Moya	7	-0.03	0.06	0.02			Kerma	**.013**
	Kerma	14	0.04	0.04	0.01			St. Johns	.945
	St. Johns	17	0.00	0.05	0.01		Jebel Moya	Black Earth	.998
	Total	53	0.00	0.06	0.01			Kerma	**.021**
								St. Johns	.813
							Kerma	Black Earth	**.013**
								Jebel Moya	**.021**
								St. Johns	.092
Residual DA	Black Earth	15	0.04	0.04	0.01	Hochberg	Black Earth	Jebel Moya	.070
	Jebel Moya	7	-0.01	0.03	0.01			Kerma	.617
	Kerma	14	0.02	0.04	0.01			St. Johns	**.000**
	St. Johns	17	-0.05	0.05	0.01		Jebel Moya	Black Earth	.070
	Total	53	0.00	0.05	0.01			Kerma	.649
								St. Johns	.296
							Kerma	Black Earth	.617
								Jebel Moya	.649
								St. Johns	**.001**
Residual Conn.D	Black Earth	15	-0.11	0.09	0.02	Hochberg	Black Earth	Jebel Moya	.162
	Jebel Moya	7	-0.01	0.10	0.04			Kerma	**.012**
	Kerma	14	0.00	0.12	0.03			St. Johns	**.000**
	St. Johns	17	0.09	0.08	0.02		Jebel Moya	Black Earth	.162
	Total	53	0.00	0.12	0.02			Kerma	.999
								St. Johns	.113
							Kerma	Black Earth	**.012**
								Jebel Moya	.999
								St. Johns	.098

Table 7.2.9. Pairwise ANOVA and post-hoc comparisons between pooled sex population – MT1 base dorsal

ANOVA - MT1 base plantar

		Sum of Squares	df	Mean Square	F	*p*	Levene Statistic	df 1	df 2	*p*
BV/TV	Between Groups	.049	3	.016	5.387	**.003**	1.490	3	44	.230
	Within Groups	.132	44	.003						
	Total	.181	47							
Tb.Th	Between Groups	.027	3	.009	9.704	**.000**	1.787	3	44	.163
	Within Groups	.041	44	.001						
	Total	.069	47							
DA	Between Groups	.047	3	.016	3.731	**.018**	2.530	3	44	.069
	Within Groups	.186	44	.004						
	Total	.233	47							
Tb.Sp	Between Groups	.099	3	.033	4.387	**.009**	.340	3	44	.797
	Within Groups	.331	44	.008						
	Total	.430	47							
log10 Conn.D	Between Groups	.347	3	.116	6.817	**.001**	2.485	3	44	.073
	Within Groups	.746	44	.017						
	Total	1.093	47							
Residual Tb.Sp	Between Groups	.081	3	.027	4.120	**.012**	.504	3	44	.681
	Within Groups	.288	44	.007						
	Total	.369	47							
Residual DA	Between Groups	.052	3	.017	4.376	**.009**	1.904	3	44	.143
	Within Groups	.173	44	.004						
	Total	.225	47							
Residual Conn.D	Between Groups	.357	3	.119	8.965	**.000**	.703	3	44	.555
	Within Groups	.584	44	.013						
	Total	.941	47							

Post-hoc

		N	Mean	S.D.	S.E.	type	Pairwise comparisons		*p*
BV/TV	Black Earth	13	0.32	0.06	0.02	Hochberg	Black Earth	Jebel Moya	.993
	Jebel Moya	4	0.31	0.07	0.04			Kerma	**.002**
	Kerma	13	0.24	0.05	0.01			St. Johns	.158
	St. Johns	18	0.28	0.05	0.01		Jebel Moya	Black Earth	.993
	Total	48	0.28	0.06	0.01			Kerma	.212
								St. Johns	.935
							Kerma	Black Earth	**.002**
								Jebel Moya	.212
								St. Johns	.284
Tb.Th	Black Earth	13	0.27	0.04	0.01	Hochberg	Black Earth	Jebel Moya	1.00
	Jebel Moya	4	0.27	0.02	0.01			Kerma	**.005**
	Kerma	13	0.23	0.03	0.01			St. Johns	**.000**
	St. Johns	18	0.22	0.02	0.01		Jebel Moya	Black Earth	1.00
	Total	48	0.24	0.04	0.01			Kerma	.139

								St. Johns	**.024**
							Kerma	Black Earth	**.005**
								Jebel Moya	.139
								St. Johns	.906
DA	Black Earth	13	0.61	0.06	0.02	Hochberg	Black Earth	Jebel Moya	.987
	Jebel Moya	4	0.59	0.02	0.01			Kerma	.998
	Kerma	13	0.60	0.09	0.02			St. Johns	**.024**
	St. Johns	18	0.54	0.06	0.01		Jebel Moya	Black Earth	.987
	Total	48	0.58	0.07	0.01			Kerma	1.00
								St. Johns	.701
							Kerma	Black Earth	.998
								Jebel Moya	1.00
								St. Johns	.084
Tb.Sp	Black Earth	13	0.56	0.07	0.02	Hochberg	Black Earth	Jebel Moya	.869
	Jebel Moya	4	0.61	0.08	0.04			Kerma	.062
	Kerma	13	0.65	0.11	0.03			St. Johns	.994
	St. Johns	18	0.54	0.08	0.02		Jebel Moya	Black Earth	.869
	Total	48	0.58	0.10	0.01			Kerma	.968
								St. Johns	.614
							Kerma	Black Earth	.062
								Jebel Moya	.968
								St. Johns	**.008**
log10 Conn.D	Black Earth	13	0.73	0.14	0.04	Hochberg	Black Earth	Jebel Moya	.995
	Jebel Moya	4	0.69	0.01	0.01			Kerma	1.00
	Kerma	13	0.71	0.16	0.04			St. Johns	**.008**
	St. Johns	18	0.89	0.11	0.03		Jebel Moya	Black Earth	.995
	Total	48	0.78	0.15	0.02			Kerma	1.00
								St. Johns	**.043**
							Kerma	Black Earth	1.00
								Jebel Moya	1.00
								St. Johns	**.003**
Residual Tb.Sp	Black Earth	13	-0.01	0.06	0.02	Hochberg	Black Earth	Jebel Moya	1.00
	Jebel Moya	4	0.01	0.09	0.05			Kerma	.189
	Kerma	13	0.06	0.09	0.02			St. Johns	.817
	St. Johns	18	-0.04	0.09	0.02		Jebel Moya	Black Earth	1.00
	Total	48	0.00	0.09	0.01			Kerma	.790
								St. Johns	.867
							Kerma	Black Earth	.189
								Jebel Moya	.790
								St. Johns	**.007**
Residual DA	Black Earth	13	0.04	0.06	0.02	Hochberg	Black Earth	Jebel Moya	.866
	Jebel Moya	4	0.00	0.03	0.01			Kerma	.962
	Kerma	13	0.02	0.08	0.02			St. Johns	**.008**
	St. Johns	18	-0.04	0.05	0.01		Jebel Moya	Black Earth	.866
	Total	48	0.00	0.07	0.01			Kerma	.996

								St. Johns	.823
							Kerma	Black Earth	.962
								Jebel Moya	.996
								St. Johns	.082
Residual Conn.D	Black Earth	13	-0.08	0.12	0.03	Hochberg	Black Earth	Jebel Moya	1.00
	Jebel Moya	4	-0.06	0.07	0.03			Kerma	.999
	Kerma	13	-0.06	0.12	0.03			St. Johns	**.000**
	St. Johns	18	0.11	0.11	0.03		Jebel Moya	Black Earth	1.00
	Total	48	0.00	0.14	0.02			Kerma	1.00
								St. Johns	.069
							Kerma	Black Earth	.999
								Jebel Moya	1.00
								St. Johns	**.001**

Table 7.2.10. Pairwise ANOVA and post-hoc comparisons between pooled sex population – MT1 head dorsal.

ANOVA - MT1 head dorsal

		Sum of Squares	**df**	**Mean Square**	**F**	***p***	**Levene Statistic**	**df 1**	**df 2**	***p***
BV/TV	Between Groups	.163	3	.054	23.671	**.000**	2.159	3	53	.104
	Within Groups	.121	53	.002						
	Total	.284	56							
Tb.Th	Between Groups	.051	3	.017	20.934	**.000**	8.578	3	53	.000
	Within Groups	.043	53	.001						
	Total	.094	56							
DA	Between Groups	.031	3	.010	5.292	**.003**	1.816	3	53	.156
	Within Groups	.103	53	.002						
	Total	.134	56							
Tb.Sp	Between Groups	.040	3	.013	6.848	**.001**	1.199	3	53	.319
	Within Groups	.104	53	.002						
	Total	.145	56							
log10 Conn.D	Between Groups	.218	3	.073	4.152	**.010**	.130	3	53	.942
	Within Groups	.926	53	.017						
	Total	1.143	56							
Residual Tb.Sp	Between Groups	.034	3	.011	6.359	**.001**	1.871	3	53	.146
	Within Groups	.096	53	.002						
	Total	.130	56							
Residual DA	Between Groups	.031	3	.010	5.299	**.003**	1.821	3	53	.155
	Within Groups	.103	53	.002						
	Total	.134	56							
Residual Conn.D	Between Groups	.297	3	.099	7.127	**.000**	.255	3	53	.857
	Within Groups	.736	53	.014						
	Total	1.033	56							

Post-hoc

		N	Mean	S.D.	S.E.	type	Pairwise comparisons		p
BV/TV	Black Earth	17	0.49	0.06	0.01	Hochberg	Black Earth	Jebel Moya	.981
	Jebel Moya	9	0.48	0.04	0.01			Kerma	**.000**
	Kerma	13	0.38	0.04	0.01			St. Johns	**.000**
	St. Johns	18	0.38	0.05	0.01		Jebel Moya	Black Earth	.981
	Total	57	0.43	0.07	0.01			Kerma	**.000**
								St. Johns	**.000**
							Kerma	Black Earth	**.000**
								Jebel Moya	**.000**
								St. Johns	1.000
Tb.Th	Black Earth	17	0.30	0.04	0.01	Games-Howell	Black Earth	Jebel Moya	.094
	Jebel Moya	9	0.27	0.01	0.00			Kerma	**.000**
	Kerma	13	0.23	0.02	0.01			St. Johns	**.000**
	St. Johns	18	0.24	0.02	0.00		Jebel Moya	Black Earth	.094
	Total	57	0.26	0.04	0.01			Kerma	**.000**
								St. Johns	**.000**
							Kerma	Black Earth	**.000**
								Jebel Moya	**.000**
								St. Johns	.611
DA	Black Earth	17	0.75	0.03	0.01	Hochberg	Black Earth	Jebel Moya	**.002**
	Jebel Moya	9	0.69	0.06	0.02			Kerma	1.000
	Kerma	13	0.75	0.04	0.01			St. Johns	.677
	St. Johns	18	0.73	0.05	0.01		Jebel Moya	Black Earth	**.002**
	Total	57	0.74	0.05	0.01			Kerma	**.009**
								St. Johns	.058
							Kerma	Black Earth	1.000
								Jebel Moya	**.009**
								St. Johns	.902
Tb.Sp	Black Earth	17	0.38	0.04	0.01	Hochberg	Black Earth	Jebel Moya	1.000
	Jebel Moya	9	0.39	0.04	0.01			Kerma	.060
	Kerma	13	0.43	0.04	0.01			St. Johns	**.001**
	St. Johns	18	0.44	0.05	0.01		Jebel Moya	Black Earth	1.000
	Total	57	0.41	0.05	0.01			Kerma	.240
								St. Johns	**.018**
							Kerma	Black Earth	.060
								Jebel Moya	.240
								St. Johns	.869
log10 Conn.D	Black Earth	17	0.74	0.14	0.03	Hochberg	Black Earth	Jebel Moya	.129
	Jebel Moya	9	0.87	0.12	0.04			Kerma	**.009**
	Kerma	13	0.90	0.14	0.04			St. Johns	.424
	St. Johns	18	0.82	0.13	0.03		Jebel Moya	Black Earth	.129
	Total	57	0.82	0.14	0.02			Kerma	.989
								St. Johns	.924

							Kerma	Black Earth	**.009**
								Jebel Moya	.989
								St. Johns	.390
Residual Tb.Sp	Black Earth	17	-0.02	0.03	0.01	Hochberg	Black Earth	Jebel Moya	1.000
	Jebel Moya	9	-0.03	0.05	0.02			Kerma	.184
	Kerma	13	0.01	0.04	0.01			St. Johns	**.003**
	St. Johns	18	0.03	0.05	0.01		Jebel Moya	Black Earth	1.000
	Total	57	0.00	0.05	0.01			Kerma	.198
								St. Johns	**.008**
							Kerma	Black Earth	.184
								Jebel Moya	.198
								St. Johns	.756
Residual DA	Black Earth	17	0.02	0.03	0.01	Hochberg	Black Earth	Jebel Moya	**.002**
	Jebel Moya	9	-0.05	0.06	0.02			Kerma	1.000
	Kerma	13	0.01	0.04	0.01			St. Johns	.675
	St. Johns	18	0.00	0.05	0.01		Jebel Moya	Black Earth	**.002**
	Total	57	0.00	0.05	0.01			Kerma	**.009**
								St. Johns	.058
							Kerma	Black Earth	1.000
								Jebel Moya	**.009**
								St. Johns	.902
Residual Conn.D	Black Earth	17	-0.10	0.13	0.03	Hochberg	Black Earth	Jebel Moya	**.016**
	Jebel Moya	9	0.06	0.12	0.04			Kerma	**.000**
	Kerma	13	0.09	0.11	0.03			St. Johns	.106
	St. Johns	18	0.00	0.11	0.03		Jebel Moya	Black Earth	**.016**
	Total	57	0.00	0.14	0.02			Kerma	.982
								St. Johns	.804
							Kerma	Black Earth	**.000**
								Jebel Moya	.982
								St. Johns	.198

Table 7.2.11. Pairwise ANOVA and post-hoc comparisons between pooled sex population – MT1 head plantar.

ANOVA - MT1 head plantar

		Sum of Squares	df	Mean Square	F	*p*	Levene Statistic	df 1	df 2	*p*
BV/TV	Between Groups	.066	3	.022	8.050	**.000**	.415	3	49	.743
	Within Groups	.133	49	.003						
	Total	.199	52							
Tb.Th	Between Groups	.039	3	.013	11.273	**.000**	3.547	3	49	.021
	Within Groups	.056	49	.001						
	Total	.094	52							
DA	Between Groups	.032	3	.011	2.588	.064	1.528	3	49	.219
	Within Groups	.199	49	.004						
	Total	.231	52							
Tb.Sp	Between Groups	.048	3	.016	2.424	.077	3.753	3	49	.017
	Within Groups	.323	49	.007						
	Total	.371	52							
log10 Conn.D	Between Groups	.044	3	.015	.865	.466	1.326	3	49	.277
	Within Groups	.825	49	.017						
	Total	.869	52							
Residual Tb.Sp	Between Groups	.043	3	.014	2.212	.099	4.649	3	49	.006
	Within Groups	.315	49	.006						
	Total	.357	52							
Residual DA	Between Groups	.034	3	.011	2.883	**.045**	1.408	3	49	.252
	Within Groups	.193	49	.004						
	Total	.227	52							
Residual Conn.D	Between Groups	.060	3	.020	1.283	.291	1.315	3	49	.280
	Within Groups	.765	49	.016						
	Total	.825	52							

Post-hoc

		N	Mean	S.D.	S.E.	type	Pairwise comparisons		*p*
BV/TV	Black Earth	14	0.37	0.06	0.01	Hochberg	Black Earth	Jebel Moya	.988
	Jebel Moya	8	0.35	0.06	0.02			Kerma	**.000**
	Kerma	13	0.28	0.05	0.01			St. Johns	**.020**
	St. Johns	18	0.31	0.05	0.01		Jebel Moya	Black Earth	.988
	Total	53	0.32	0.06	0.01			Kerma	**.012**
								St. Johns	.302
							Kerma	Black Earth	**.000**
								Jebel Moya	**.012**
								St. Johns	.396
Tb.Th	Black Earth	14	0.30	0.05	0.01	Games-Howell	Black Earth	Jebel Moya	.213
	Jebel Moya	8	0.27	0.03	0.01			Kerma	**.002**
	Kerma	13	0.24	0.03	0.01			St. Johns	**.003**
	St. Johns	18	0.24	0.02	0.01		Jebel	Black Earth	.213

	Total	53	0.26	0.04	0.01		Moya	Kerma	.064
								St. Johns	.123
							Kerma	Black Earth	**.002**
								Jebel Moya	.064
								St. Johns	.896
DA	Black Earth	14	0.60	0.04	0.01	Hochberg	Black Earth	Jebel Moya	1.000
	Jebel Moya	8	0.59	0.08	0.03			Kerma	.109
	Kerma	13	0.65	0.08	0.02			St. Johns	.999
	St. Johns	18	0.60	0.06	0.01		Jebel Moya	Black Earth	1.000
	Total	53	0.61	0.07	0.01			Kerma	.184
								St. Johns	.997
							Kerma	Black Earth	.109
								Jebel Moya	.184
								St. Johns	.200
Tb.Sp	Black Earth	14	0.56	0.05	0.01	Games-Howell	Black Earth	Jebel Moya	1.000
	Jebel Moya	8	0.56	0.08	0.03			Kerma	.135
	Kerma	13	0.63	0.11	0.03			St. Johns	.721
	St. Johns	18	0.58	0.08	0.02		Jebel Moya	Black Earth	1.000
	Total	53	0.58	0.08	0.01			Kerma	.286
								St. Johns	.889
							Kerma	Black Earth	.135
								Jebel Moya	.286
								St. Johns	.463
log10 Conn.D	Black Earth	14	0.66	0.11	0.03	Hochberg	Black Earth	Jebel Moya	.917
	Jebel Moya	8	0.71	0.10	0.04			Kerma	.964
	Kerma	13	0.70	0.16	0.05			St. Johns	.520
	St. Johns	18	0.73	0.13	0.03		Jebel Moya	Black Earth	.917
	Total	53	0.70	0.13	0.02			Kerma	1.000
								St. Johns	1.000
							Kerma	Black Earth	.964
								Jebel Moya	1.000
								St. Johns	.977
Residual Tb.Sp	Black Earth	14	-0.02	0.05	0.01	Games-Howell	Black Earth	Jebel Moya	.989
	Jebel Moya	8	-0.03	0.09	0.03			Kerma	.195
	Kerma	13	0.05	0.11	0.03			St. Johns	.847
	St. Johns	18	0.00	0.07	0.02		Jebel Moya	Black Earth	.989
	Total	53	0.00	0.08	0.01			Kerma	.302
								St. Johns	.860
							Kerma	Black Earth	.195
								Jebel Moya	.302
								St. Johns	.480
Residual DA	Black Earth	14	-0.02	0.04	0.01	Hochberg	Black Earth	Jebel Moya	1.000
	Jebel Moya	8	-0.02	0.07	0.03			Kerma	.063
	Kerma	13	0.04	0.08	0.02			St. Johns	.992
	St. Johns	18	-0.01	0.06	0.01		Jebel Moya	Black Earth	1.000
	Total	53	0.00	0.07	0.01			Kerma	.179

								St. Johns	.999
							Kerma	Black Earth	.063
								Jebel Moya	.179
								St. Johns	.166
Residual Conn.D	Black Earth	14	-0.05	0.10	0.03	Hochberg	Black Earth	Jebel Moya	.725
	Jebel Moya	8	0.02	0.11	0.04			Kerma	.829
	Kerma	13	0.00	0.16	0.04			St. Johns	.318
	St. Johns	18	0.03	0.12	0.03		Jebel Moya	Black Earth	.725
	Total	53	0.00	0.13	0.02			Kerma	1.000
								St. Johns	1.000
							Kerma	Black Earth	.829
								Jebel Moya	1.000
								St. Johns	.985

Table 7.2.12. Pairwise ANOVA and post-hoc comparisons between pooled sex population – Talus ACF.

ANOVA - Talus ACF

		Sum of Squares	**df**	**Mean Square**	**F**	***p***	**Levene Statistic**	**df 1**	**df 2**	***p***
BV/TV	Between Groups	.101	3	.034	8.155	**.000**	2.192	3	57	.099
	Within Groups	.234	57	.004						
	Total	.335	60							
Tb.Th	Between Groups	.033	3	.011	8.371	**.000**	.733	3	57	.537
	Within Groups	.075	57	.001						
	Total	.108	60							
DA	Between Groups	.013	3	.004	1.150	.337	.185	3	57	.906
	Within Groups	.209	57	.004						
	Total	.222	60							
Tb.Sp	Between Groups	.114	3	.038	4.052	**.011**	.328	3	57	.805
	Within Groups	.535	57	.009						
	Total	.650	60							
log10 Conn.D	Between Groups	.040	3	.013	.938	.428	.147	3	57	.931
	Within Groups	.803	57	.014						
	Total	.843	60							
Residual Tb.Sp	Between Groups	.109	3	.036	4.229	**.009**	.312	3	57	.817
	Within Groups	.491	57	.009						
	Total	.601	60							
Residual DA	Between Groups	.012	3	.004	1.075	.367	.289	3	57	.833
	Within Groups	.210	57	.004						
	Total	.221	60							
Residual Conn.D	Between Groups	.043	3	.014	1.096	.358	.208	3	57	.891
	Within Groups	.747	57	.013						
	Total	.790	60							

Post-hoc

	N	**Mean**	**S.D.**	**S.E.**	**type**	**Pairwise comparisons**		***p***

BV/TV	Black Earth	13	0.36	0.08	0.02	Hochberg	Black Earth	Jebel Moya	.774
	Jebel Moya	9	0.39	0.07	0.02			Kerma	**.020**
	Kerma	20	0.29	0.05	0.01			St. Johns	**.036**
	St. Johns	19	0.29	0.06	0.01		Jebel Moya	Black Earth	.774
	Total	61	0.32	0.07	0.01			Kerma	**.001**
								St. Johns	**.002**
							Kerma	Black Earth	**.020**
								Jebel Moya	**.001**
								St. Johns	1.000
Tb.Th	Black Earth	13	0.30	0.04	0.01	Hochberg	Black Earth	Jebel Moya	.974
	Jebel Moya	9	0.31	0.04	0.01			Kerma	**.005**
	Kerma	20	0.25	0.03	0.01			St. Johns	**.020**
	St. Johns	19	0.26	0.04	0.01		Jebel Moya	Black Earth	.974
	Total	61	0.27	0.04	0.01			Kerma	**.001**
								St. Johns	**.005**
							Kerma	Black Earth	**.005**
								Jebel Moya	**.001**
								St. Johns	.996
DA	Black Earth	13	0.67	0.06	0.02	Hochberg	Black Earth	Jebel Moya	.957
	Jebel Moya	9	0.69	0.05	0.02			Kerma	.715
	Kerma	20	0.69	0.06	0.01			St. Johns	1.000
	St. Johns	19	0.66	0.06	0.01		Jebel Moya	Black Earth	.957
	Total	61	0.68	0.06	0.01			Kerma	1.000
								St. Johns	.884
							Kerma	Black Earth	.715
								Jebel Moya	1.000
								St. Johns	.475
Tb.Sp	Black Earth	13	0.59	0.11	0.03	Hochberg	Black Earth	Jebel Moya	1.000
	Jebel Moya	9	0.59	0.09	0.03			Kerma	**.022**
	Kerma	20	0.69	0.09	0.02			St. Johns	.664
	St. Johns	19	0.63	0.10	0.02		Jebel Moya	Black Earth	1.000
	Total	61	0.64	0.10	0.01			Kerma	.054
								St. Johns	.760
							Kerma	Black Earth	**.022**
								Jebel Moya	.054
								St. Johns	.376
log10 Conn.D	Black Earth	13	0.64	0.10	0.03	Hochberg	Black Earth	Jebel Moya	1.000
	Jebel Moya	9	0.65	0.10	0.03			Kerma	.999
	Kerma	20	0.62	0.12	0.03			St. Johns	.858
	St. Johns	19	0.68	0.13	0.03		Jebel Moya	Black Earth	1.000
	Total	61	0.65	0.12	0.02			Kerma	.986
								St. Johns	.987
							Kerma	Black Earth	.999
								Jebel Moya	.986

								St. Johns	.488
Residual Tb.Sp	Black Earth	13	-0.04	0.10	0.03	Hochberg	Black Earth	Jebel Moya	.994
	Jebel Moya	9	-0.06	0.11	0.04			Kerma	**.044**
	Kerma	20	0.05	0.09	0.02			St. Johns	.811
	St. Johns	19	0.00	0.08	0.02		Jebel Moya	Black Earth	.994
	Total	61	0.00	0.10	0.01			Kerma	**.020**
								St. Johns	.484
							Kerma	Black Earth	**.044**
								Jebel Moya	**.020**
								St. Johns	.391
Residual DA	Black Earth	13	-0.01	0.06	0.02	Hochberg	Black Earth	Jebel Moya	.977
	Jebel Moya	9	0.01	0.05	0.02			Kerma	.763
	Kerma	20	0.02	0.06	0.01			St. Johns	1.000
	St. Johns	19	-0.01	0.06	0.01		Jebel Moya	Black Earth	.977
	Total	61	0.00	0.06	0.01			Kerma	1.000
								St. Johns	.910
							Kerma	Black Earth	.763
								Jebel Moya	1.000
								St. Johns	.488
Residual Conn.D	Black Earth	13	-0.02	0.09	0.03	Hochberg	Black Earth	Jebel Moya	.967
	Jebel Moya	9	0.02	0.11	0.04			Kerma	1.000
	Kerma	20	-0.03	0.12	0.03			St. Johns	.682
	St. Johns	19	0.03	0.12	0.03		Jebel Moya	Black Earth	.967
	Total	61	0.00	0.11	0.01			Kerma	.935
								St. Johns	.999
							Kerma	Black Earth	1.000
								Jebel Moya	.935
								St. Johns	.506

Table 7.2.13. Pairwise ANOVA and post-hoc comparisons between pooled sex population – Talus PCF.

ANOVA - talus PCF

		Sum of Squares	df	Mean Square	F	*p*	Levene Statistic	df1	df2	*p*
BV/TV	Between Groups	.201	3	.067	15.786	**.000**	1.497	3	56	.225
	Within Groups	.238	56	.004						
	Total	.440	59							
Tb.Th	Between Groups	.067	3	.022	14.486	**.000**	1.364	3	56	.263
	Within Groups	.087	56	.002						
	Total	.154	59							
DA	Between Groups	.006	3	.002	1.112	.352	.535	3	56	.660
	Within Groups	.101	56	.002						
	Total	.107	59							
Tb.Sp	Between Groups	.066	3	.022	5.354	**.003**	.516	3	56	.673
	Within Groups	.229	56	.004						
	Total	.294	59							
log10 Conn.D	Between Groups	.341	3	.114	6.566	**.001**	1.750	3	56	.167
	Within Groups	.969	56	.017						
	Total	1.310	59							
Residual Tb.Sp	Between Groups	.071	3	.024	6.039	**.001**	.466	3	56	.707
	Within Groups	.219	56	.004						
	Total	.289	59							
Residual DA	Between Groups	.006	3	.002	1.147	.338	.437	3	56	.728
	Within Groups	.101	56	.002						
	Total	.107	59							
Residual Conn.D	Between Groups	.375	3	.125	8.183	**.000**	.869	3	56	.463
	Within Groups	.855	56	.015						
	Total	1.229	59							

Post-hoc

VOI		**N**	**Mean**	**S.D.**	**S.E.**	**type**	**Pairwise comparisons**		***p***
BV/TV	Black Earth	12	0.48	0.08	0.02	Hochber	Black	Jebel Moya	.985

	Jebel Moya	13	0.49	0.08	0.02	g	Earth	Kerma	**.001**
	Kerma	18	0.38	0.05	0.01			St. Johns	**.000**
	St. Johns	17	0.36	0.06	0.02		Jebel Moya	Black Earth	.985
	Total	60	0.42	0.09	0.01			Kerma	**.000**
								St. Johns	**.000**
							Kerma	Black Earth	**.001**
								Jebel Moya	**.000**
								St. Johns	.970
Tb.Th	Black Earth	12	0.33	0.04	0.01	Hochberg	Black Earth	Jebel Moya	.995
	Jebel Moya	13	0.33	0.04	0.01			Kerma	**.000**
	Kerma	18	0.26	0.03	0.01			St. Johns	**.000**
	St. Johns	17	0.26	0.05	0.01		Jebel Moya	Black Earth	.995
	Total	60	0.29	0.05	0.01			Kerma	**.000**
								St. Johns	**.000**
							Kerma	Black Earth	**.000**
								Jebel Moya	**.000**
								St. Johns	1.000
DA	Black Earth	12	0.77	0.04	0.01	Hochberg	Black Earth	Jebel Moya	.976
	Jebel Moya	13	0.76	0.03	0.01			Kerma	.834
	Kerma	18	0.76	0.04	0.01			St. Johns	.382
	St. Johns	17	0.75	0.05	0.01		Jebel Moya	Black Earth	.976
	Total	60	0.76	0.04	0.01			Kerma	1.000
								St. Johns	.877
							Kerma	Black Earth	.834
								Jebel Moya	1.000
								St. Johns	.971
Tb.Sp	Black Earth	12	0.49	0.08	0.02	Hochberg	Black Earth	Jebel Moya	.198
	Jebel Moya	13	0.43	0.06	0.02			Kerma	.840
	Kerma	18	0.52	0.05	0.01			St. Johns	.761
	St. Johns	17	0.52	0.06	0.02		Jebel Moya	Black Earth	.198
	Total	60	0.49	0.07	0.01			Kerma	**.006**
								St. Johns	**.004**
							Kerma	Black Earth	.840
								Jebel Moya	**.006**
								St. Johns	1.000
log10 Conn.D	Black Earth	12	0.57	0.11	0.03	Hochberg	Black Earth	Jebel Moya	.416
	Jebel Moya	13	0.66	0.14	0.04			Kerma	**.003**
	Kerma	18	0.75	0.11	0.03			St. Johns	**.001**
	St. Johns	17	0.77	0.16	0.04		Jebel Moya	Black Earth	.416
	Total	60	0.70	0.15	0.02			Kerma	.347
								St. Johns	.189
							Kerma	Black Earth	**.003**
								Jebel Moya	.347

								St. Johns	.999
Residual Tb.Sp	Black Earth	12	0.00	0.07	0.02	Hochberg	Black Earth	Jebel Moya	.097
	Jebel Moya	13	-0.06	0.07	0.02			Kerma	.926
	Kerma	18	0.02	0.05	0.01			St. Johns	.795
	St. Johns	17	0.03	0.06	0.01		Jebel Moya	Black Earth	.097
	Total	60	0.00	0.07	0.01			Kerma	**.003**
								St. Johns	**.002**
							Kerma	Black Earth	.926
								Jebel Moya	**.003**
								St. Johns	1.000
Residual DA	Black Earth	12	0.02	0.04	0.01	Hochberg	Black Earth	Jebel Moya	.952
	Jebel Moya	13	0.00	0.04	0.01			Kerma	.780
	Kerma	18	0.00	0.04	0.01			St. Johns	.358
	St. Johns	17	-0.01	0.05	0.01		Jebel Moya	Black Earth	.952
	Total	60	0.00	0.04	0.01			Kerma	1.000
								St. Johns	.913
							Kerma	Black Earth	.780
								Jebel Moya	1.000
								St. Johns	.981
Residual Conn.D	Black Earth	12	-0.14	0.10	0.03	Hochberg	Black Earth	Jebel Moya	.110
	Jebel Moya	13	-0.02	0.14	0.04			Kerma	**.000**
	Kerma	18	0.06	0.11	0.03			St. Johns	**.000**
	St. Johns	17	0.06	0.14	0.03		Jebel Moya	Black Earth	.110
	Total	60	0.00	0.14	0.02			Kerma	.370
								St. Johns	.331
							Kerma	Black Earth	**.000**
								Jebel Moya	.370
								St. Johns	1.000

Table 7.2.14. Pairwise ANOVA and post-hoc comparisons between pooled sex population – Talus head.

ANOVA - Talus head

		Sum of Squares	df	Mean Square	F	*p*	Levene Statistic	df1	df2	*p*
BV/TV	Between Groups	.392	3	.131	35.51	**.000**	.509	3	61	.677
	Within Groups	.224	61	.004						
	Total	.616	64							
Tb.Th	Between Groups	.126	3	.042	29.84	**.000**	.168	3	61	.917
	Within Groups	.086	61	.001						
	Total	.212	64							
DA	Between Groups	.038	3	.013	9.983	**.000**	2.779	3	61	.049
	Within Groups	.078	61	.001						
	Total	.117	64							
Tb.Sp	Between Groups	.110	3	.037	12.11	**.000**	1.419	3	61	.246
	Within Groups	.185	61	.003						
	Total	.295	64							
log10 Conn.D	Between Groups	.282	3	.094	5.065	**.003**	.008	3	61	.999
	Within Groups	1.134	61	.019						
	Total	1.416	64							
Residual Tb.Sp	Between Groups	.111	3	.037	13.17	**.000**	.761	3	61	.520
	Within Groups	.171	61	.003						
	Total	.282	64							
Residual DA	Between Groups	.042	3	.014	12.01	**.000**	1.829	3	61	.151
	Within Groups	.072	61	.001						
	Total	.114	64							
Residual Conn.D	Between Groups	.356	3	.119	8.526	**.000**	.112	3	61	.953
	Within Groups	.849	61	.014						
	Total	1.205	64							

Post-hoc

		N	Mean	S.D.	S.E.	type	Pairwise comparisons		*p*
BV/TV	Black Earth	11	0.55	0.05	0.01	Hochberg	Black Earth	Jebel Moya	.576
	Jebel Moya	16	0.59	0.07	0.02			Kerma	**.000**
	Kerma	19	0.42	0.06	0.01			St. Johns	**.000**
	St. Johns	19	0.41	0.06	0.01		Jebel Moya	Black Earth	.576
	Total	65	0.48	0.10	0.01			Kerma	**.000**
								St. Johns	**.000**
							Kerma	Black Earth	**.000**
								Jebel Moya	**.000**
								St. Johns	.997
Tb.Th	Black Earth	11	0.35	0.04	0.01	Hochberg	Black Earth	Jebel Moya	.431
	Jebel Moya	16	0.38	0.04	0.01			Kerma	**.000**
	Kerma	19	0.28	0.03	0.01			St. Johns	**.000**
	St. Johns	19	0.28	0.04	0.01		Jebel	Black Earth	.431

	Total	65	0.32	0.06	0.01		Moya	Kerma	**.000**
								St. Johns	**.000**
							Kerma	Black Earth	**.000**
								Jebel Moya	**.000**
								St. Johns	1.000
DA	Black Earth	11	0.83	0.03	0.01	Games-Howell	Black Earth	Jebel Moya	**.000**
	Jebel Moya	16	0.78	0.03	0.01			Kerma	.057
	Kerma	19	0.80	0.05	0.01			St. Johns	1.000
	St. Johns	19	0.83	0.03	0.01		Jebel Moya	Black Earth	**.000**
	Total	65	0.81	0.04	0.01			Kerma	.341
								St. Johns	**.000**
							Kerma	Black Earth	.057
								Jebel Moya	.341
								St. Johns	**.049**
Tb.Sp	Black Earth	11	0.39	0.04	0.01	Hochberg	Black Earth	Jebel Moya	.995
	Jebel Moya	16	0.38	0.05	0.01			Kerma	**.002**
	Kerma	19	0.47	0.06	0.01			St. Johns	**.007**
	St. Johns	19	0.46	0.06	0.01		Jebel Moya	Black Earth	.995
	Total	65	0.43	0.07	0.01			Kerma	**.000**
								St. Johns	**.000**
							Kerma	Black Earth	**.002**
								Jebel Moya	**.000**
								St. Johns	.994
log10 Conn.D	Black Earth	11	0.56	0.13	0.04	Hochberg	Black Earth	Jebel Moya	.654
	Jebel Moya	16	0.63	0.15	0.04			Kerma	**.003**
	Kerma	19	0.75	0.13	0.03			St. Johns	.101
	St. Johns	19	0.68	0.14	0.03		Jebel Moya	Black Earth	.654
	Total	65	0.67	0.15	0.02			Kerma	.083
								St. Johns	.847
							Kerma	Black Earth	**.003**
								Jebel Moya	.083
								St. Johns	.599
Residual Tb.Sp	Black Earth	11	-0.04	0.04	0.01	Hochberg	Black Earth	Jebel Moya	.865
	Jebel Moya	16	-0.06	0.05	0.01			Kerma	**.003**
	Kerma	19	0.04	0.06	0.01			St. Johns	**.010**
	St. Johns	19	0.03	0.06	0.01		Jebel Moya	Black Earth	.865
	Total	65	0.00	0.07	0.01			Kerma	**.000**
								St. Johns	**.000**
							Kerma	Black Earth	**.003**
								Jebel Moya	**.000**
								St. Johns	.999
Residual DA	Black Earth	11	0.03	0.03	0.01	Hochberg	Black Earth	Jebel Moya	**.000**
	Jebel Moya	16	-0.04	0.03	0.01			Kerma	**.024**
	Kerma	19	-0.01	0.04	0.01			St. Johns	1.000

	St. Johns	19	0.03	0.03	0.01		Jebel Moya	Black Earth	**.000**
	Total	65	0.00	0.04	0.01			Kerma	.235
								St. Johns	**.000**
							Kerma	Black Earth	**.024**
								Jebel Moya	.235
								St. Johns	**.011**
Residual Conn.D	Black Earth	11	-0.14	0.12	0.03	Hochberg	Black Earth	Jebel Moya	.081
	Jebel Moya	16	-0.02	0.13	0.03			Kerma	**.000**
	Kerma	19	0.09	0.11	0.03			St. Johns	**.010**
	St. Johns	19	0.01	0.11	0.03		Jebel Moya	Black Earth	.081
	Total	65	0.00	0.14	0.02			Kerma	.057
								St. Johns	.967
							Kerma	Black Earth	**.000**
								Jebel Moya	.057
								St. Johns	.273

Table 7.2.15. Pairwise ANOVA and post-hoc comparisons between pooled sex population – Trochlea lateral.

ANOVA - Trochlea lateral

		Sum of Squares	**df**	**Mean Square**	**F**	***p***	**Levene Statistic**	**df1**	**df2**	***p***
BV/TV	Between Groups	.316	3	.105	19.55	**.000**	.349	3	58	.790
	Within Groups	.312	58	.005						
	Total	.629	61							
Tb.Th	Between Groups	.115	3	.038	19.56	**.000**	1.384	3	58	.257
	Within Groups	.113	58	.002						
	Total	.228	61							
DA	Between Groups	.013	3	.004	2.418	.075	1.175	3	58	.327
	Within Groups	.104	58	.002						
	Total	.117	61							
Tb.Sp	Between Groups	.088	3	.029	9.130	**.000**	.253	3	58	.859
	Within Groups	.186	58	.003						
	Total	.274	61							
log10 Conn.D	Between Groups	.496	3	.165	9.989	**.000**	.135	3	58	.939
	Within Groups	.959	58	.017						
	Total	1.455	61							
Residual Tb.Sp	Between Groups	.093	3	.031	10.18	**.000**	.176	3	58	.912
	Within Groups	.177	58	.003						
	Total	.270	61							
Residual DA	Between Groups	.012	3	.004	2.304	.086	1.124	3	58	.347
	Within Groups	.105	58	.002						
	Total	.117	61							
Residual Conn.D	Between Groups	.507	3	.169	11.80	**.000**	.406	3	58	.750
	Within Groups	.830	58	.014						
	Total	1.337	61							

Post-hoc

VOI		N	Mean	S.D.	S.E.	type	Pairwise comparisons		*p*
BV/TV	Black Earth	14	0.50	0.07	0.02	Hochberg	Black Earth	Jebel Moya	.199
	Jebel Moya	15	0.56	0.08	0.02			Kerma	**.002**
	Kerma	15	0.40	0.07	0.02			St. Johns	**.001**
	St. Johns	18	0.39	0.07	0.02		Jebel Moya	Black Earth	.199
	Total	62	0.46	0.10	0.01			Kerma	**.000**
								St. Johns	**.000**
							Kerma	Black Earth	**.002**
								Jebel Moya	**.000**
								St. Johns	1.000
Tb.Th	Black Earth	14	0.33	0.05	0.01	Hochberg	Black Earth	Jebel Moya	.650
	Jebel Moya	15	0.35	0.05	0.01			Kerma	**.004**
	Kerma	15	0.27	0.03	0.01			St. Johns	**.000**
	St. Johns	18	0.25	0.05	0.01		Jebel Moya	Black Earth	.650
	Total	62	0.30	0.06	0.01			Kerma	**.000**
								St. Johns	**.000**
							Kerma	Black Earth	**.004**
								Jebel Moya	**.000**
								St. Johns	.619
DA	Black Earth	14	0.80	0.03	0.01	Hochberg	Black Earth	Jebel Moya	.309
	Jebel Moya	15	0.77	0.05	0.01			Kerma	.160
	Kerma	15	0.76	0.05	0.01			St. Johns	.103
	St. Johns	18	0.76	0.04	0.01		Jebel Moya	Black Earth	.309
	Total	62	0.77	0.04	0.01			Kerma	1.000
								St. Johns	.998
							Kerma	Black Earth	.160
								Jebel Moya	1.000
								St. Johns	1.000
Tb.Sp	Black Earth	14	0.42	0.06	0.02	Hochberg	Black Earth	Jebel Moya	.114
	Jebel Moya	15	0.37	0.05	0.01			Kerma	**.046**
	Kerma	15	0.48	0.06	0.02			St. Johns	1.000
	St. Johns	18	0.43	0.06	0.01		Jebel Moya	Black Earth	.114
	Total	62	0.43	0.07	0.01			Kerma	**.000**
								St. Johns	**.050**
							Kerma	Black Earth	**.046**
								Jebel Moya	**.000**
								St. Johns	**.047**
log10 Conn.D	Black Earth	14	0.62	0.12	0.03	Hochberg	Black Earth	Jebel Moya	.760
	Jebel Moya	15	0.68	0.13	0.03			Kerma	.053
	Kerma	15	0.75	0.12	0.03			St. Johns	**.000**
	St. Johns	18	0.85	0.14	0.03		Jebel	Black Earth	.760

	Total	62	0.73	0.15	0.02		Moya	Kerma	.600
								St. Johns	**.001**
							Kerma	Black Earth	.053
								Jebel Moya	.600
								St. Johns	.118
Residual Tb.Sp	Black Earth	14	0.00	0.06	0.01	Hochberg	Black Earth	Jebel Moya	**.050**
	Jebel Moya	15	-0.05	0.05	0.01			Kerma	.051
	Kerma	15	0.06	0.06	0.01			St. Johns	1.000
	St. Johns	18	0.00	0.06	0.01		Jebel Moya	Black Earth	**.050**
	Total	62	0.00	0.07	0.01			Kerma	**.000**
								St. Johns	**.025**
							Kerma	Black Earth	.051
								Jebel Moya	**.000**
								St. Johns	**.041**
Residual DA	Black Earth	14	0.03	0.03	0.01	Hochberg	Black Earth	Jebel Moya	.374
	Jebel Moya	15	0.00	0.05	0.01			Kerma	.178
	Kerma	15	-0.01	0.05	0.01			St. Johns	.114
	St. Johns	18	-0.01	0.04	0.01		Jebel Moya	Black Earth	.374
	Total	62	0.00	0.04	0.01			Kerma	.999
								St. Johns	.996
							Kerma	Black Earth	.178
								Jebel Moya	.999
								St. Johns	1.000
Residual Conn.D	Black Earth	14	-0.13	0.11	0.03	Hochberg	Black Earth	Jebel Moya	.235
	Jebel Moya	15	-0.04	0.13	0.03			Kerma	**.013**
	Kerma	15	0.01	0.11	0.03			St. Johns	**.000**
	St. Johns	18	0.12	0.13	0.03		Jebel Moya	Black Earth	.235
	Total	62	0.00	0.15	0.02			Kerma	.813
								St. Johns	**.003**
							Kerma	Black Earth	**.013**
								Jebel Moya	.813
								St. Johns	.085

Table 7.2.16. Pairwise ANOVA and post-hoc comparisons between pooled sex population – Trochlea central.

ANOVA - Trochlea central

		Sum of Squares	df	Mean Square	F	*p*	Levene Statistic	df1	df2	*p*
BV/TV	Between Groups	.169	3	.056	10.021	**.000**	1.204	3	58	.316
	Within Groups	.327	58	.006						
	Total	.496	61							
Tb.Th	Between Groups	.069	3	.023	13.559	**.000**	.441	3	58	.725
	Within Groups	.098	58	.002						
	Total	.166	61							
DA	Between Groups	.118	3	.039	9.789	**.000**	1.618	3	58	.195
	Within Groups	.233	58	.004						
	Total	.351	61							
Tb.Sp	Between Groups	.066	3	.022	6.099	**.001**	.205	3	58	.892
	Within Groups	.210	58	.004						
	Total	.276	61							
log10 Conn.D	Between Groups	.242	3	.081	6.946	**.000**	.721	3	58	.544
	Within Groups	.673	58	.012						
	Total	.914	61							
Residual Tb.Sp	Between Groups	.065	3	.022	6.203	**.001**	.721	3	58	.544
	Within Groups	.201	58	.003						
	Total	.266	61							
Residual DA	Between Groups	.100	3	.033	8.263	**.000**	1.624	3	58	.194
	Within Groups	.234	58	.004						
	Total	.334	61							
Residual Conn.D	Between Groups	.252	3	.084	8.136	**.000**	.955	3	58	.420
	Within Groups	.600	58	.010						
	Total	.852	61							

Post-hoc

		N	Mean	S.D.	S.E.	type	Pairwise comparisons		*p*
BV/TV	Black Earth	14	0.45	0.10	0.03	Hochberg	Black Earth	Jebel Moya	.621
	Jebel Moya	13	0.49	0.08	0.02			Kerma	**.009**
	Kerma	17	0.36	0.06	0.02			St. Johns	.057
	St. Johns	18	0.37	0.06	0.01		Jebel Moya	Black Earth	.621
	Total	62	0.41	0.09	0.01			Kerma	**.000**
								St. Johns	**.001**
							Kerma	Black Earth	**.009**
								Jebel Moya	**.000**
								St. Johns	.974
Tb.Th	Black Earth	14	0.31	0.05	0.01	Hochberg	Black Earth	Jebel Moya	.375
	Jebel Moya	13	0.34	0.04	0.01			Kerma	**.023**
	Kerma	17	0.27	0.04	0.01			St. Johns	**.002**
	St. Johns	18	0.25	0.04	0.01		Jebel	Black Earth	.375

	Total	62	0.29	0.05	0.01		Moya	Kerma	**.000**
								St. Johns	**.000**
							Kerma	Black Earth	**.023**
								Jebel Moya	**.000**
								St. Johns	.967
DA	Black Earth	14	0.74	0.05	0.01	Hochberg	Black Earth	Jebel Moya	**.000**
	Jebel Moya	13	0.61	0.08	0.02			Kerma	**.037**
	Kerma	17	0.68	0.06	0.01			St. Johns	**.009**
	St. Johns	18	0.67	0.06	0.01		Jebel Moya	Black Earth	**.000**
	Total	62	0.68	0.08	0.01			Kerma	**.035**
								St. Johns	.101
							Kerma	Black Earth	**.037**
								Jebel Moya	**.035**
								St. Johns	.997
Tb.Sp	Black Earth	14	0.44	0.07	0.02	Hochberg	Black Earth	Jebel Moya	1.000
	Jebel Moya	13	0.44	0.07	0.02			Kerma	**.005**
	Kerma	17	0.52	0.06	0.01			St. Johns	.980
	St. Johns	18	0.46	0.05	0.01		Jebel Moya	Black Earth	1.000
	Total	62	0.46	0.07	0.01			Kerma	**.003**
								St. Johns	.931
							Kerma	Black Earth	**.005**
								Jebel Moya	**.003**
								St. Johns	**.024**
log10 Conn.D	Black Earth	14	0.70	0.09	0.03	Hochberg	Black Earth	Jebel Moya	.643
	Jebel Moya	13	0.76	0.09	0.02			Kerma	.231
	Kerma	17	0.78	0.11	0.03			St. Johns	**.000**
	St. Johns	18	0.87	0.13	0.03		Jebel Moya	Black Earth	.643
	Total	62	0.79	0.12	0.02			Kerma	.995
								St. Johns	**.035**
							Kerma	Black Earth	.231
								Jebel Moya	.995
								St. Johns	.091
Residual Tb.Sp	Black Earth	14	-0.02	0.06	0.02	Hochberg	Black Earth	Jebel Moya	.993
	Jebel Moya	13	-0.03	0.07	0.02			Kerma	**.009**
	Kerma	17	0.05	0.05	0.01			St. Johns	.993
	St. Johns	18	-0.01	0.05	0.01		Jebel Moya	Black Earth	.993
	Total	62	0.00	0.07	0.01			Kerma	**.002**
								St. Johns	.805
							Kerma	Black Earth	**.009**
								Jebel Moya	**.002**
								St. Johns	**.028**
Residual DA	Black Earth	14	0.06	0.05	0.01	Hochberg	Black Earth	Jebel Moya	**.000**
	Jebel Moya	13	-0.06	0.08	0.02			Kerma	.082
	Kerma	17	0.00	0.06	0.01			St. Johns	**.015**

	St. Johns	18	-0.01	0.06	0.01		Jebel Moya	Black Earth	**.000**
	Total	62	0.00	0.07	0.01			Kerma	.056
								St. Johns	.204
							Kerma	Black Earth	.082
								Jebel Moya	.056
								St. Johns	.989
Residual Conn.D	Black Earth	14	-0.09	0.09	0.02	Hochberg	Black Earth	Jebel Moya	.246
	Jebel Moya	13	-0.01	0.09	0.02			Kerma	.079
	Kerma	17	0.00	0.10	0.03			St. Johns	**.000**
	St. Johns	18	0.08	0.12	0.03		Jebel Moya	Black Earth	.246
	Total	62	0.00	0.12	0.02			Kerma	.999
								St. Johns	.059
							Kerma	Black Earth	.079
								Jebel Moya	.999
								St. Johns	.097

Table 7.2.17. Pairwise ANOVA and post-hoc comparisons between pooled sex population – Talus PCF.

ANOVA - Trochlea medial

		Sum of Squares	**df**	**Mean Square**	**F**	***p***	**Levene Statistic**	**df1**	**df2**	***p***
BV/TV	Between Groups	.101	3	.034	9.231	**.000**	.182	3	56	.908
	Within Groups	.203	56	.004						
	Total	.304	59							
Tb.Th	Between Groups	.041	3	.014	11.552	**.000**	.288	3	56	.834
	Within Groups	.067	56	.001						
	Total	.108	59							
DA	Between Groups	.048	3	.016	2.535	.066	.083	3	56	.969
	Within Groups	.354	56	.006						
	Total	.402	59							
Tb.Sp	Between Groups	.085	3	.028	12.788	**.000**	.093	3	56	.964
	Within Groups	.124	56	.002						
	Total	.209	59							
log10 Conn.D	Between Groups	.272	3	.091	8.642	**.000**	.504	3	56	.681
	Within Groups	.587	56	.010						
	Total	.858	59							
Residual Tb.Sp	Between Groups	.081	3	.027	12.184	**.000**	.178	3	56	.911
	Within Groups	.123	56	.002						
	Total	.204	59							
Residual DA	Between Groups	.038	3	.013	2.071	.114	.190	3	56	.903
	Within Groups	.344	56	.006						
	Total	.382	59							
Residual Conn.D	Between Groups	.265	3	.088	9.858	**.000**	.570	3	56	.637
	Within Groups	.503	56	.009						
	Total	.768	59							

Post-hoc

		N	Mean	S.D.	S.E.	type	Pairwise comparisons		*p*
BV/TV	Black Earth	14	0.45	0.07	0.02	Hochberg	Black Earth	Jebel Moya	.907
	Jebel Moya	13	0.48	0.06	0.02			Kerma	**.003**
	Kerma	15	0.37	0.05	0.01			St. Johns	.092
	St. Johns	18	0.40	0.06	0.01		Jebel Moya	Black Earth	.907
	Total	60	0.42	0.07	0.01			Kerma	**.000**
								St. Johns	**.006**
							Kerma	Black Earth	**.003**
								Jebel Moya	**.000**
								St. Johns	.637
Tb.Th	Black Earth	14	0.29	0.04	0.01	Hochberg	Black Earth	Jebel Moya	.471
	Jebel Moya	13	0.31	0.04	0.01			Kerma	.059
	Kerma	15	0.26	0.03	0.01			St. Johns	**.004**
	St. Johns	18	0.25	0.03	0.01		Jebel Moya	Black Earth	.471
	Total	60	0.27	0.04	0.01			Kerma	**.000**
								St. Johns	**.000**
							Kerma	Black Earth	.059
								Jebel Moya	**.000**
								St. Johns	.957
DA	Black Earth	14	0.67	0.08	0.02	Hochberg	Black Earth	Jebel Moya	.071
	Jebel Moya	13	0.60	0.08	0.02			Kerma	.967
	Kerma	15	0.65	0.09	0.02			St. Johns	.407
	St. Johns	18	0.62	0.07	0.02		Jebel Moya	Black Earth	.071
	Total	60	0.64	0.08	0.01			Kerma	.332
								St. Johns	.886
							Kerma	Black Earth	.967
								Jebel Moya	.332
								St. Johns	.912
Tb.Sp	Black Earth	14	0.42	0.05	0.01	Hochberg	Black Earth	Jebel Moya	.998
	Jebel Moya	13	0.43	0.04	0.01			Kerma	**.000**
	Kerma	15	0.51	0.05	0.01			St. Johns	.999
	St. Johns	18	0.43	0.05	0.01		Jebel Moya	Black Earth	.998
	Total	60	0.45	0.06	0.01			Kerma	**.000**
								St. Johns	1.000
							Kerma	Black Earth	**.000**
								Jebel Moya	**.000**
								St. Johns	**.000**
log10 Conn.D	Black Earth	14	0.78	0.10	0.03	Hochberg	Black Earth	Jebel Moya	1.000
	Jebel Moya	13	0.79	0.09	0.02			Kerma	.998
	Kerma	15	0.80	0.12	0.03			St. Johns	**.000**
	St. Johns	18	0.93	0.10	0.02		Jebel Moya	Black Earth	1.000
	Total	60	0.83	0.12	0.02			Kerma	1.000

								St. Johns	**.002**
							Kerma	Black Earth	.998
								Jebel Moya	1.000
								St. Johns	**.002**
Residual Tb.Sp	Black Earth	14	-0.02	0.05	0.01	Hochberg	Black Earth	Jebel Moya	1.000
	Jebel Moya	13	-0.02	0.05	0.01			Kerma	**.000**
	Kerma	15	0.06	0.05	0.01			St. Johns	1.000
	St. Johns	18	-0.02	0.05	0.01		Jebel Moya	Black Earth	1.000
	Total	60	0.00	0.06	0.01			Kerma	**.000**
								St. Johns	1.000
							Kerma	Black Earth	**.000**
								Jebel Moya	**.000**
								St. Johns	**.000**
Residual DA	Black Earth	14	0.03	0.08	0.02	Hochberg	Black Earth	Jebel Moya	.169
	Jebel Moya	13	-0.04	0.07	0.02			Kerma	.998
	Kerma	15	0.02	0.09	0.02			St. Johns	.513
	St. Johns	18	-0.01	0.07	0.02		Jebel Moya	Black Earth	.169
	Total	60	0.00	0.08	0.01			Kerma	.372
								St. Johns	.966
							Kerma	Black Earth	.998
								Jebel Moya	.372
								St. Johns	.823
Residual Conn.D	Black Earth	14	-0.06	0.08	0.02	Hochberg	Black Earth	Jebel Moya	.840
	Jebel Moya	13	-0.02	0.09	0.02			Kerma	.827
	Kerma	15	-0.02	0.11	0.03			St. Johns	**.000**
	St. Johns	18	0.10	0.09	0.02		Jebel Moya	Black Earth	.840
	Total	60	0.00	0.11	0.01			Kerma	1.000
								St. Johns	**.003**
							Kerma	Black Earth	.827
								Jebel Moya	1.000
								St. Johns	**.002**

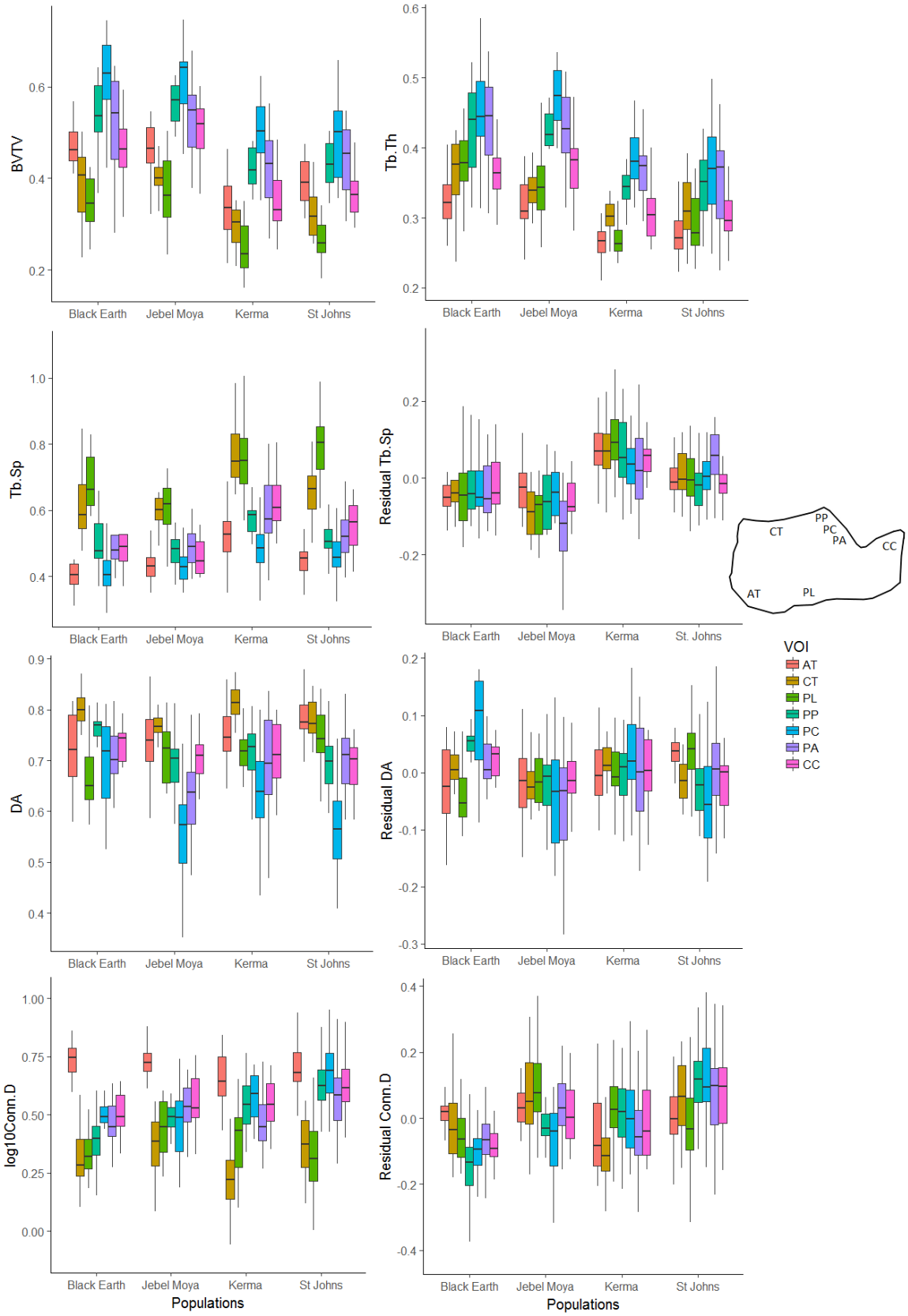

Figure 7.2.1. Boxplots of calcaneal trabecular properties in pooled sex populations. Achilles tendon (AT), calcaneal tuber (CT), plantar ligaments (PL), posterior talar facet (PP: posterior, PC: central, PA: anterior), calcaneocuboid (CC), dorsal base (BD), plantar base (BP), dorsal head (HD), plantar head (HP), talar head (TH), anterior calcaneal facet (ACF), posterior calcaneal facet (PCF), trochlea (lateral: TL, central: TC, medial: TM).

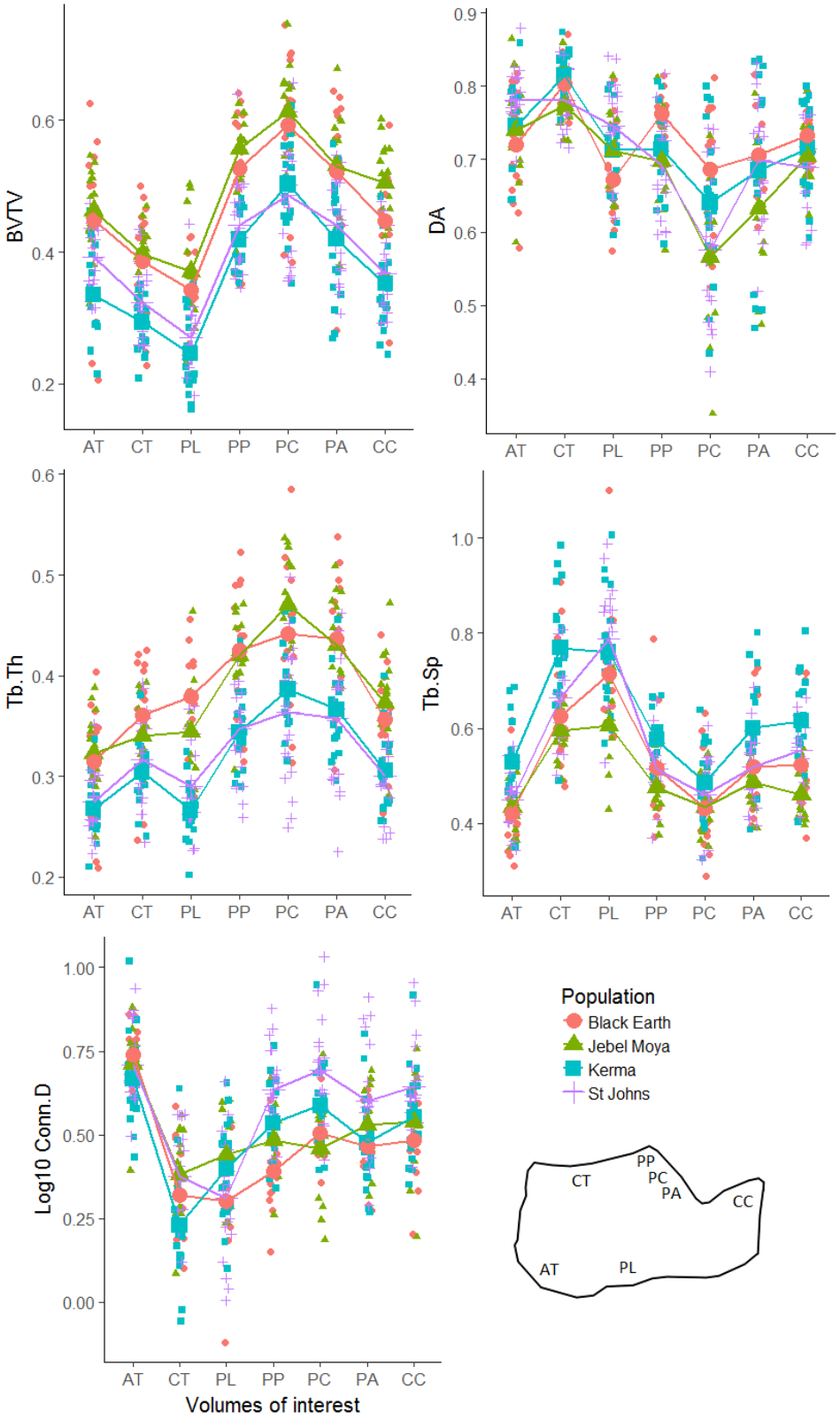

Figure 7.2.2. Line plots of calcaneal trabecular properties in pooled sex populations. Achilles tendon (AT), calcaneal tuber (CT), plantar ligaments (PL), posterior talar facet (PP: posterior, PC: central, PA: anterior), calcaneocuboid (CC), dorsal base (BD), plantar base (BP), dorsal head (HD), plantar head (HP), talar head (TH), anterior calcaneal facet (ACF), posterior calcaneal facet (PCF), trochlea (lateral: TL, central: TC, medial: TM).

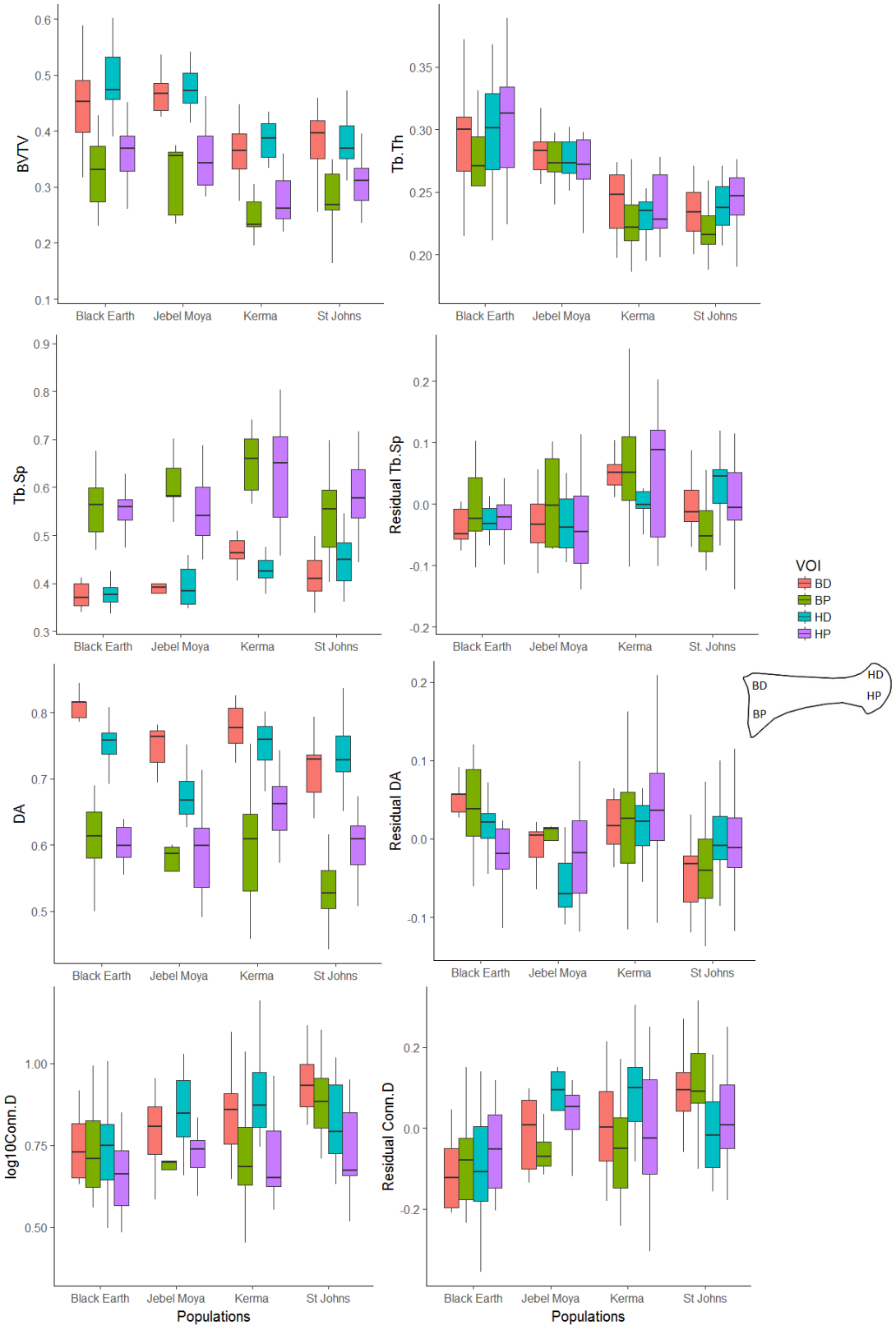

Figure 7.2.3. Boxplots of first metatarsal trabecular properties in pooled sex populations. Achilles tendon (AT), calcaneal tuber (CT), plantar ligaments (PL), posterior talar facet (PP: posterior, PC: central, PA: anterior), calcaneocuboid (CC), dorsal base (BD), plantar base (BP), dorsal head (HD), plantar head (HP), talar head (TH), anterior calcaneal facet (ACF), posterior calcaneal facet (PCF), trochlea (lateral: TL, central: TC, medial: TM).

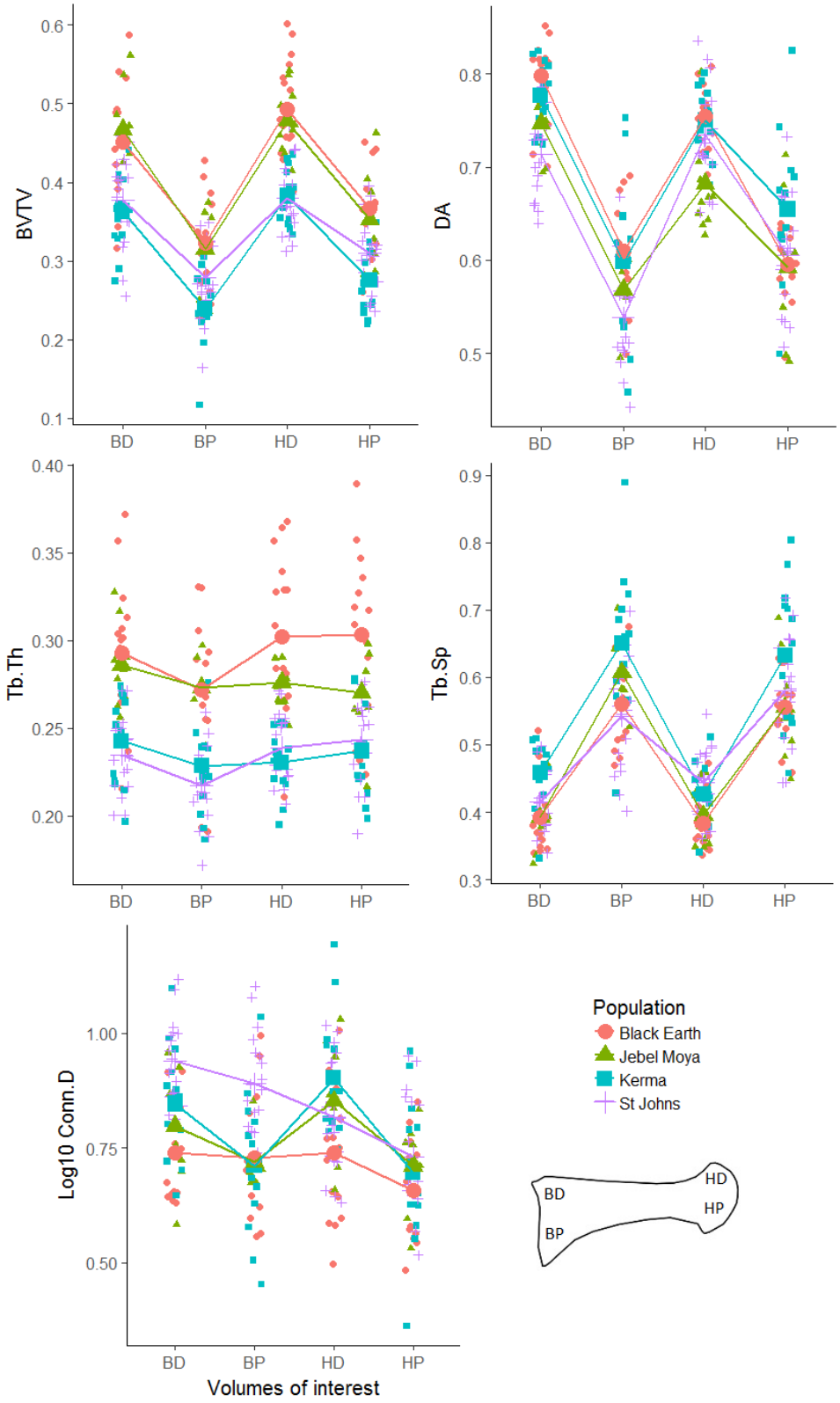

Figure 7.2.4. Line plots of first metatarsal trabecular properties in pooled sex populations. Achilles tendon (AT), calcaneal tuber (CT), plantar ligaments (PL), posterior talar facet (PP: posterior, PC: central, PA: anterior), calcaneocuboid (CC), dorsal base (BD), plantar base (BP), dorsal head (HD), plantar head (HP), talar head (TH), anterior calcaneal facet (ACF), posterior calcaneal facet (PCF), trochlea (lateral: TL, central: TC, medial: TM).

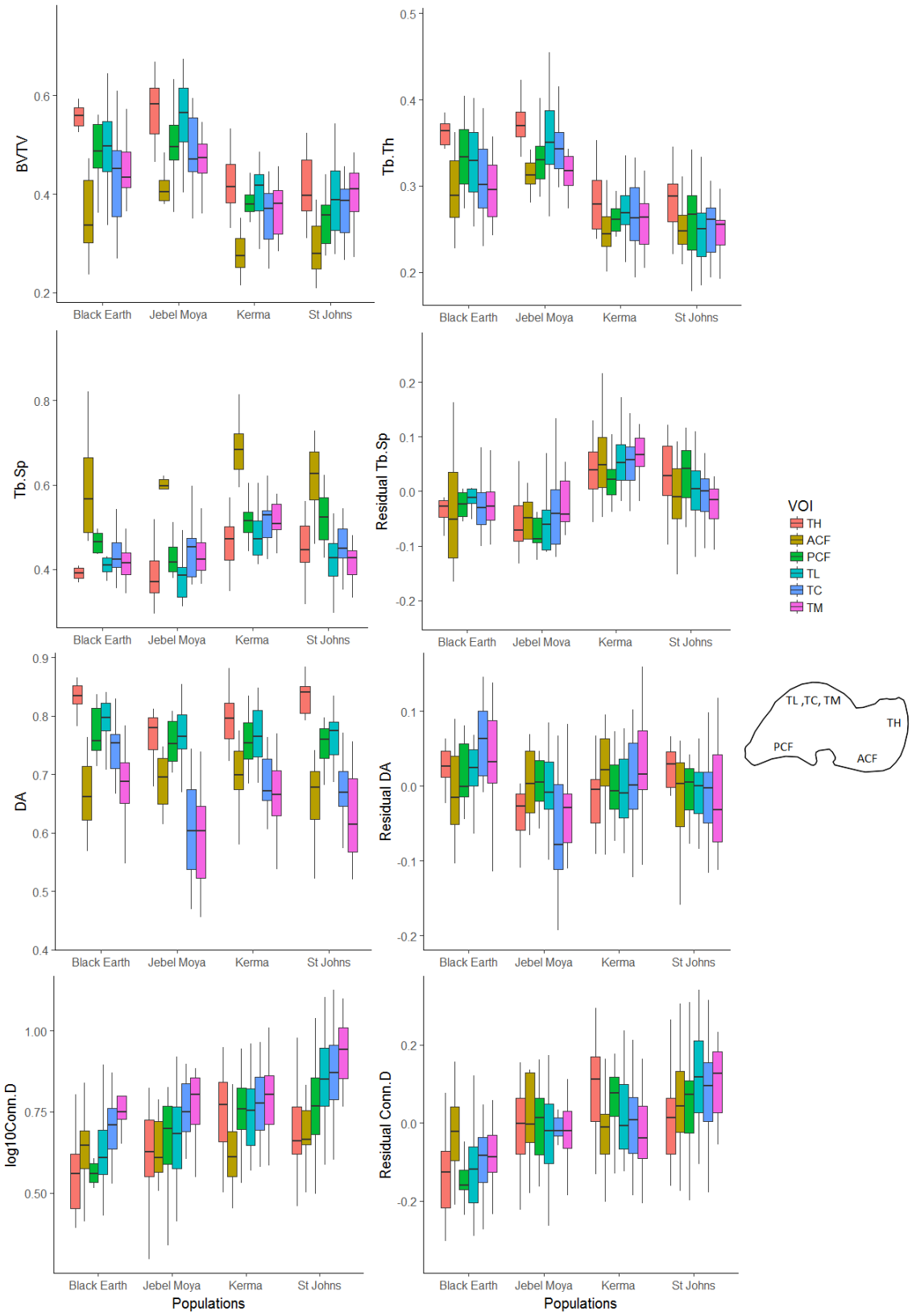

Figure 7.2.5. Boxplots of talar trabecular properties in pooled sex populations. Achilles tendon (AT), calcaneal tuber (CT), plantar ligaments (PL), posterior talar facet (PP: posterior, PC: central, PA: anterior), calcaneocuboid (CC), dorsal base (BD), plantar base (BP), dorsal head (HD), plantar head (HP), talar head (TH), anterior calcaneal facet (ACF), posterior calcaneal facet (PCF), trochlea (lateral: TL, central: TC, medial: TM).

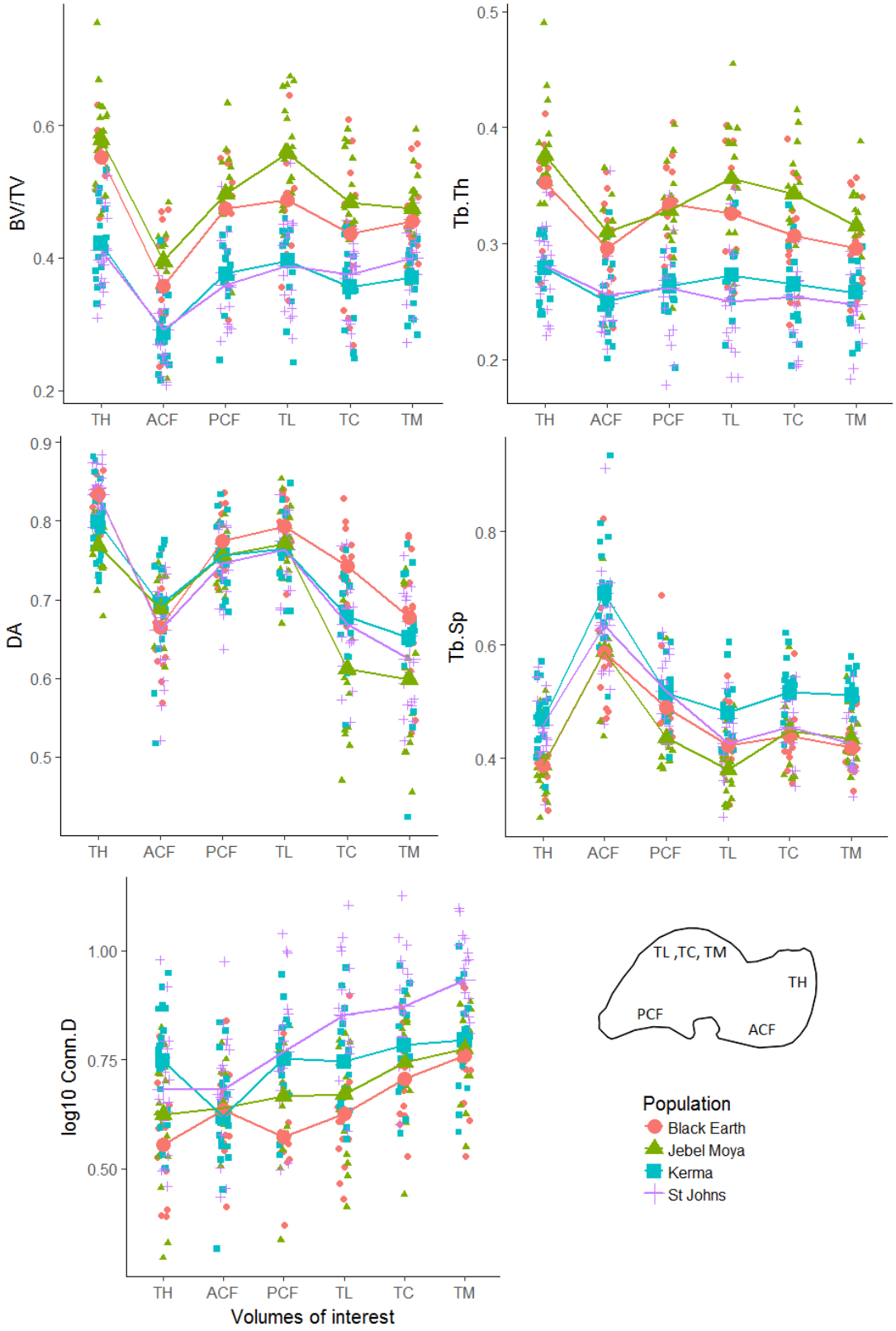

Figure 7.2.6. Lines plots of talar trabecular properties in pooled sex populations. Achilles tendon (AT), calcaneal tuber (CT), plantar ligaments (PL), posterior talar facet (PP: posterior, PC: central, PA: anterior), calcaneocuboid (CC), dorsal base (BD), plantar base (BP), dorsal head (HD), plantar head (HP), talar head (TH), anterior calcaneal facet (ACF), posterior calcaneal facet (PCF), trochlea (lateral: TL, central: TC, medial: TM).

Appendix 7.3 PCA of individual VOIs

Table 7.3.1. Summary statistics of PC1 to PC3 for all VOIs. Achilles tendon (AT), calcaneal tuber (CT), plantar ligaments (PL), posterior talar facet (PP: posterior, PC: central, PA: anterior), calcaneocuboid (CC), dorsal base (BD), plantar base (BP), dorsal head (HD), plantar head (HP), talar head (TH), anterior calcaneal facet (ACF), posterior calcaneal facet (PCF), trochlea (lateral: TL, central: TC, medial: TM).

	Calcaneus			**First metatarsal**			**Talus**		
	PC1	**PC2**	**PC3**	**PC1**	**PC2**	**PC3**	**PC1**	**PC2**	**PC3**
		AT			**BD**			**ACF**	
Standard deviation	1.60	1.12	1.02	1.59	1.30	0.80	1.56	1.30	0.87
Proportion of Variance	0.51	0.25	0.21	0.51	0.34	0.13	0.49	0.34	0.15
Cumulative Proportion	0.51	0.76	0.97	0.51	0.85	0.97	0.49	0.82	0.97
BV/TV	**-0.61**	0.17	0.02	**0.57**	-0.30	0.03	**-0.57**	0.33	0.06
Tb.Th	**-0.48**	**0.55**	0.00	**0.59**	0.08	0.38	**-0.41**	**0.56**	-0.26
DA	-0.09	-0.35	**0.88**	0.27	**0.48**	**-0.81**	0.29	**0.40**	**0.84**
Res. Tb.Sp	**0.58**	0.28	-0.04	-0.37	**0.56**	0.34	**0.56**	0.17	**-0.42**
Res. Conn.D	-0.25	**-0.68**	**-0.47**	-0.35	**-0.60**	-0.30	-0.33	**-0.63**	0.22
		CC			**BP**			**PCF**	
Standard deviation	1.59	1.32	0.79	1.46	1.38	0.92	1.62	1.20	0.92
Proportion of Variance	0.51	0.35	0.13	0.42	0.38	0.17	0.52	0.29	0.17
Cumulative Proportion	0.51	0.85	0.98	0.42	0.81	0.98	0.52	0.81	0.98
BV/TV	**-0.60**	0.19	-0.04	0.35	**-0.61**	0.07	**-0.59**	0.23	-0.03
Tb.Th	**-0.60**	-0.13	0.26	-0.10	**-0.69**	0.22	**-0.59**	-0.08	0.21
DA	-0.13	**-0.56**	**-0.81**	-0.29	-0.22	**-0.92**	-0.09	**-0.52**	**-0.83**
Res. Tb.Sp	**0.42**	**-0.50**	0.34	**-0.64**	0.15	0.26	0.31	**-0.62**	**0.44**
Res. Conn.D	0.29	**0.61**	-0.39	**0.61**	0.28	-0.17	**0.44**	**0.53**	-0.25
		CT			**HD**			**TH**	
Standard deviation	1.64	1.27	0.72	1.57	1.30	0.85	1.68	1.15	0.84
Proportion of Variance	0.54	0.32	0.10	0.49	0.34	0.14	0.56	0.26	0.14
Cumulative Proportion	0.54	0.86	0.97	0.49	0.83	0.97	0.56	0.83	0.97
BV/TV	**-0.54**	0.34	-0.01	**-0.62**	0.11	-0.07	**0.59**	0.00	-0.09
Tb.Th	-0.36	**0.60**	0.22	**-0.60**	-0.20	0.18	**0.56**	0.13	0.17
DA	0.34	**0.46**	**-0.81**	0.11	**-0.56**	**-0.78**	-0.20	**0.64**	**-0.69**
Res. Tb.Sp	**0.57**	0.06	0.35	0.39	**-0.47**	**0.55**	**-0.49**	0.23	**0.57**
Res. Conn.D	-0.37	**-0.56**	-0.40	0.30	**0.65**	-0.20	-0.24	**-0.72**	-0.39
		PA			**HP**			**TC**	
Standard deviation	1.56	1.31	0.83	1.51	1.33	0.92	1.49	1.24	0.97
Proportion of Variance	0.49	0.35	0.14	0.45	0.36	0.17	0.45	0.31	0.19
Cumulative Proportion	0.49	0.84	0.97	0.45	0.81	0.98	0.45	0.75	0.94
BV/TV	**-0.63**	0.03	-0.05	**0.60**	-0.26	0.20	**-0.62**	0.20	-0.09
Tb.Th	**-0.55**	0.35	0.13	0.35	**-0.63**	0.01	**-0.65**	-0.01	-0.23
DA	0.20	**0.49**	**-0.83**	-0.35	-0.07	**0.92**	-0.09	**-0.56**	**0.70**
Res. Tb.Sp	**0.50**	0.35	**0.46**	**-0.56**	-0.29	-0.34	0.30	**-0.46**	**-0.65**
Res. Conn.D	0.08	**-0.72**	-0.28	0.28	**0.67**	0.03	0.32	**0.66**	0.16
		PC						**TL**	
Standard deviation	1.65	1.21	0.82				1.69	1.15	0.86

Proportion of Variance	0.54	0.29	0.13	0.57	0.26	0.15
Cumulative Proportion	0.54	0.84	0.97	0.57	0.83	0.98
BV/TV	**-0.58**	0.18	-0.07	**-0.56**	-0.26	0.14
Tb.Th	**-0.58**	-0.13	0.16	**-0.56**	0.03	0.31
DA	-0.04	**-0.64**	**-0.76**	-0.32	0.34	**-0.87**
Res. Tb.Sp	0.37	**-0.55**	**0.49**	0.31	**0.70**	0.26
Res. Conn.D	0.43	**0.49**	-0.38	0.41	**-0.57**	-0.25
	PP			**TM**		
Standard deviation	1.65	1.20	0.84	1.51	1.30	0.96
Proportion of Variance	0.54	0.29	0.14	0.46	0.34	0.18
Cumulative Proportion	0.54	0.83	0.98	0.46	0.80	0.98
BV/TV	**-0.55**	-0.31	0.15	**0.65**	-0.04	0.11
Tb.Th	**-0.57**	0.04	0.33	**0.59**	-0.31	-0.20
DA	-0.32	0.38	**-0.84**	-0.17	-0.39	**0.86**
Res. Tb.Sp	0.30	**0.67**	0.32	**-0.45**	**-0.44**	**-0.46**
Res. Conn.D	0.41	**-0.56**	-0.25	-0.08	**0.75**	0.10
	PL					
Standard deviation	1.59	1.22	0.94			
Proportion of Variance	0.51	0.30	0.18			
Cumulative Proportion	0.51	0.80	0.98			
BV/TV	**-0.58**	0.30	0.08			
Tb.Th	**-0.43**	**0.55**	-0.28			
DA	0.18	0.39	**0.89**			
Res. Tb.Sp	**0.58**	0.20	-0.26			
Res. Conn.D	-0.34	**-0.64**	0.25			

Table 7.3.2. Summary statistics of ANOVAs for PC4 and PC5. Achilles tendon (AT), calcaneal tuber (CT), plantar ligaments (PL), posterior talar facet (PP: posterior, PC: central, PA: anterior), calcaneocuboid (CC), dorsal base (BD), plantar base (BP), dorsal head (HD), plantar head (HP), talar head (TH), anterior calcaneal facet (ACF), posterior calcaneal facet (PCF), trochlea (lateral: TL, central: TC, medial: TM).

PC4						**PC5**				
VOI	**Levene *p***	**F**	**df**	***p***	**Sig. Posthoc**	**Levene *p***	**F**	**df**	***p***	**Sig. Posthoc**
AT	.505	2.862	3, 63	**.044**		.412	.386	3, 63	.763	
CC	.505	.926	3, 60	.434		.963	.731	3, 60	.538	
CT	.036	.873	3, 64	.460		.660	1.447	3, 64	.237	
PA	.580	.621	3, 56	.621		.688	1.424	3, 56	.245	
PC	.081	.771	3, 60	.515		.964	1.605	3, 60	.198	
PP	.058	.687	3, 55	.564		.437	2.036	3, 55	.119	
PL	.344	.103	3, 53	.958		.614	2.020	3, 53	.122	
BD	.584	2.956	3, 46	**.042**	BE>K	.443	.359	3, 46	.783	
BP	.351	.339	3, 44	.797		.340	.608	3, 44	.613	
HD	.210	1.369	3, 53	.262		.197	2.057	3, 53	.117	
HP	.147	1.626	3, 46	.196		.785	2.315	3, 46	.088	
ACF	.213	4.304	3, 50	**.009**	BE>JM,K	.352	3.808	3, 50	**.016**	K>SJ
PCF	.934	.296	3, 48	.828		.637	.811	3, 48	.494	
TH	.053	1.603	3, 54	.199		.616	2.476	3, 54	.071	
TL	.253	1.263	3, 51	.297		.175	1.080	3, 51	.366	
TC	.099	1.622	3, 51	.196		.130	.895	3, 51	.450	
TM	.698	4.869	3, 49	**.005**	BE>K,SJ	.194	1.402	3, 49	.253	

Appendix 7.4 Plots of trabecular properties per sex

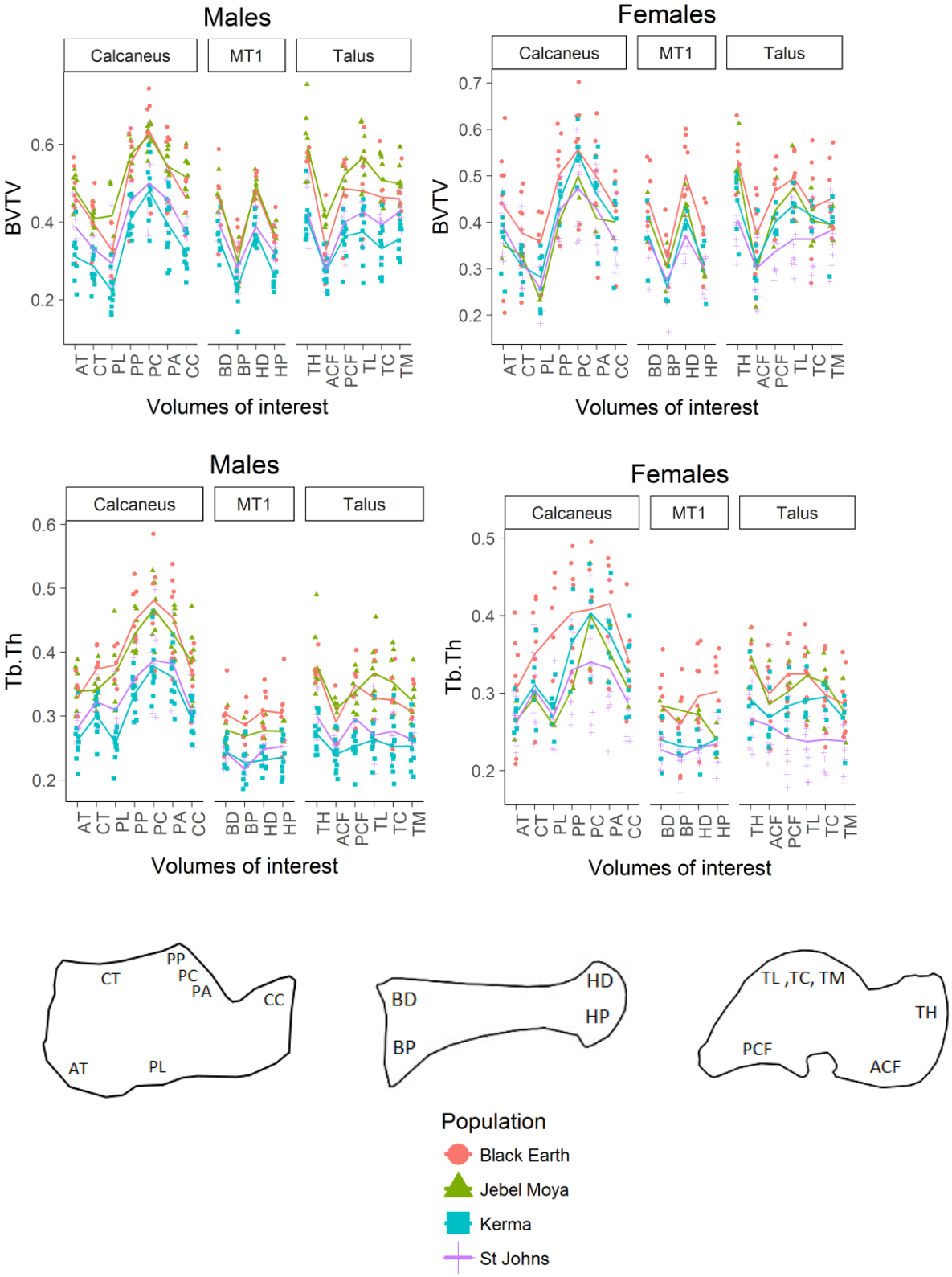

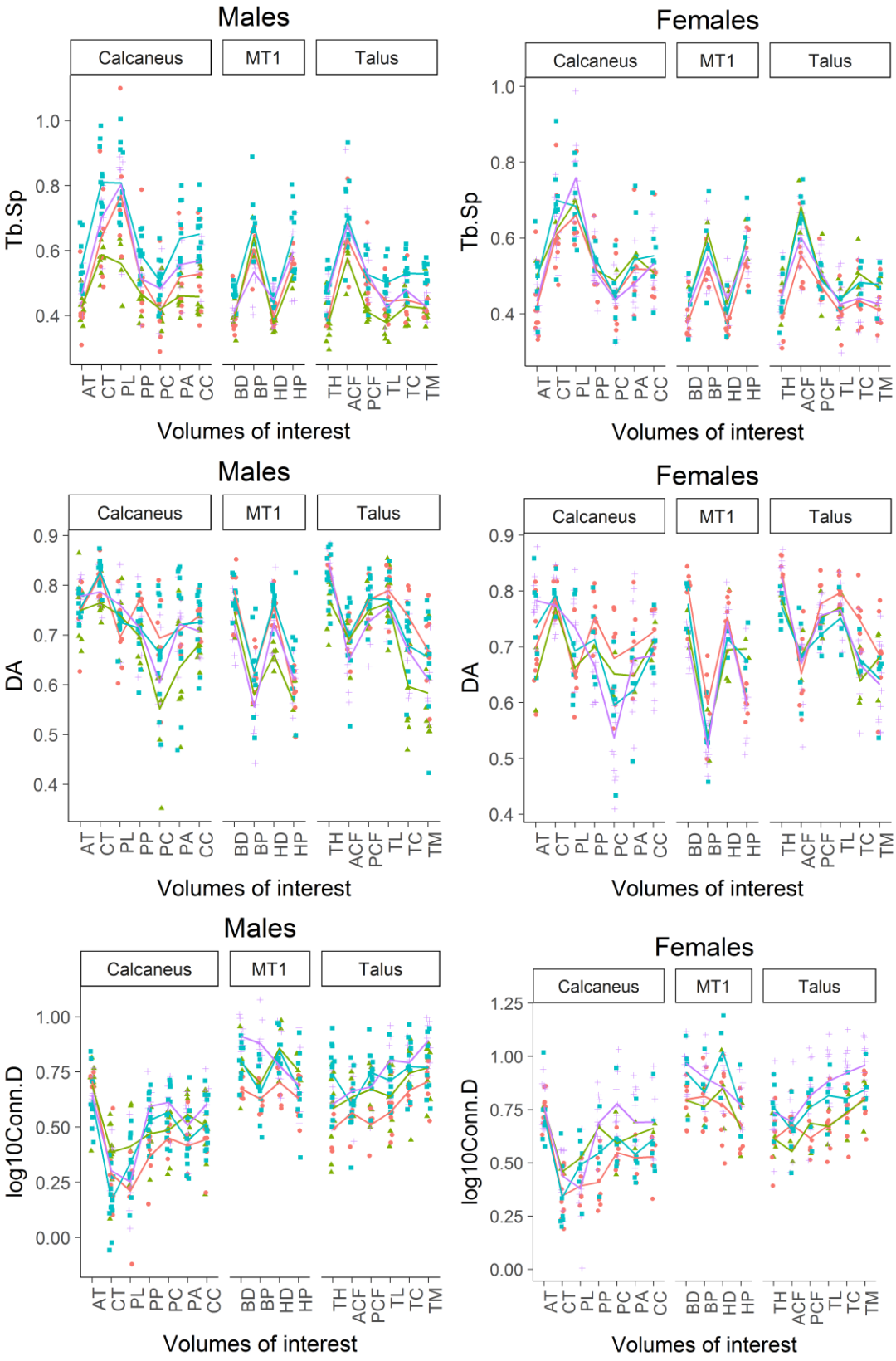
Males
Females
Calcaneus
MT1
Talus
Tb.Sp
DA
log10Conn.D
AT CT PL PP PC PA CC
BD BP HD HP
TH ACF PCF TL TC TM
Volumes of interest

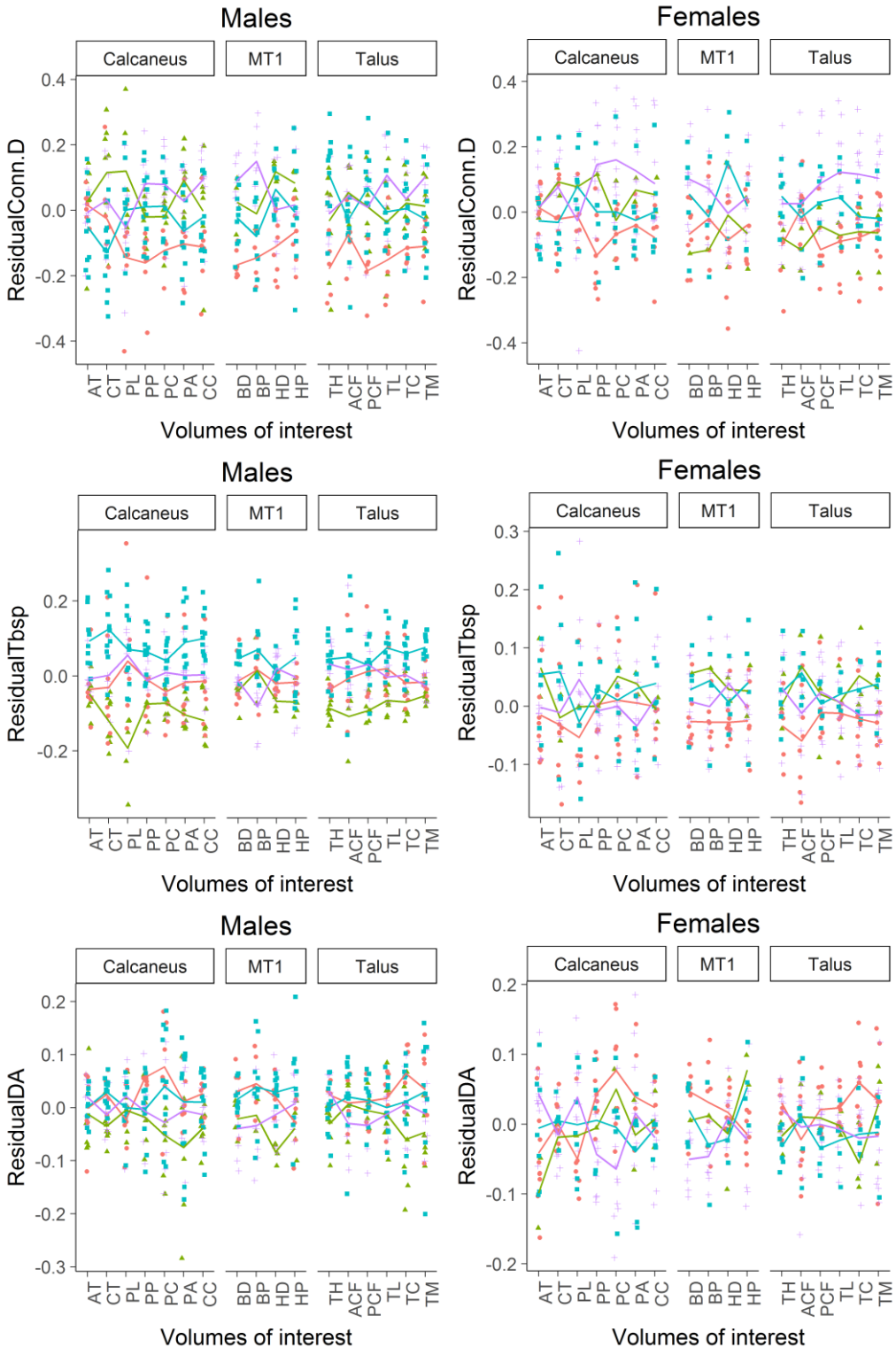

Figure 7.4.1. Plots of trabecular properties of males and females throughout the foot. Achilles tendon (AT), calcaneal tuber (CT), plantar ligaments (PL), posterior talar facet (PP: posterior, PC: central, PA: anterior), calcaneocuboid (CC), dorsal base (BD), plantar base (BP), dorsal head (HD), plantar head (HP), talar head (TH), anterior calcaneal facet (ACF), posterior calcaneal facet (PCF), trochlea (lateral: TL, central: TC, medial: TM).

Appendix 7.5 Controlling for age and body mass in Black Earth and St. Johns

Age categories are estimated for most individuals from the Black Earth and St. Johns populations. Residuals from a multiple regression between trabecular properties and body mass + age category are compared between the Black Earth and St. Johns. Boxplots of residual trabecular properties are presented in Figure 7.5.1. Summary statistics for the Welch's independent t-tests are presented in Table 7.5.1.

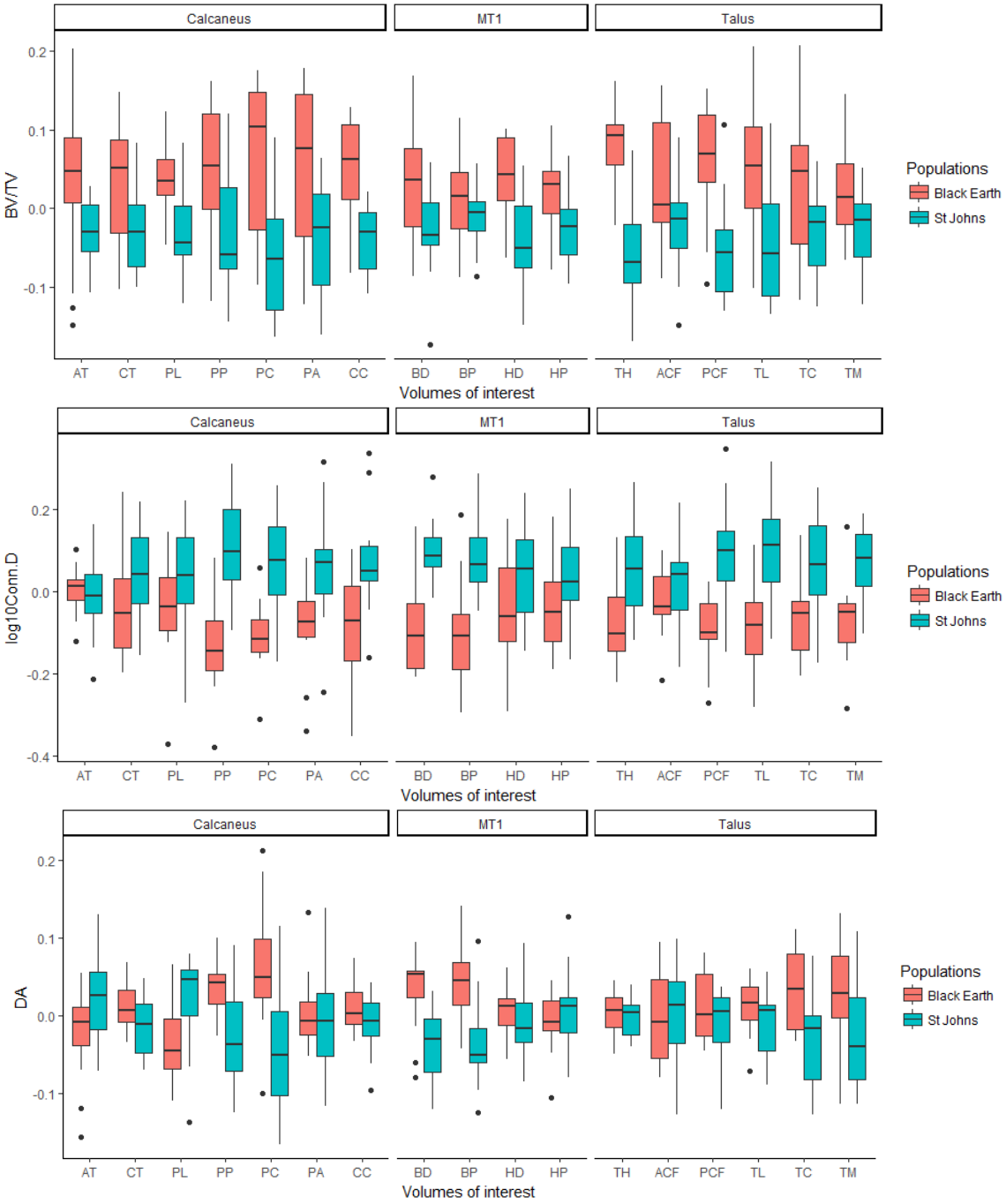

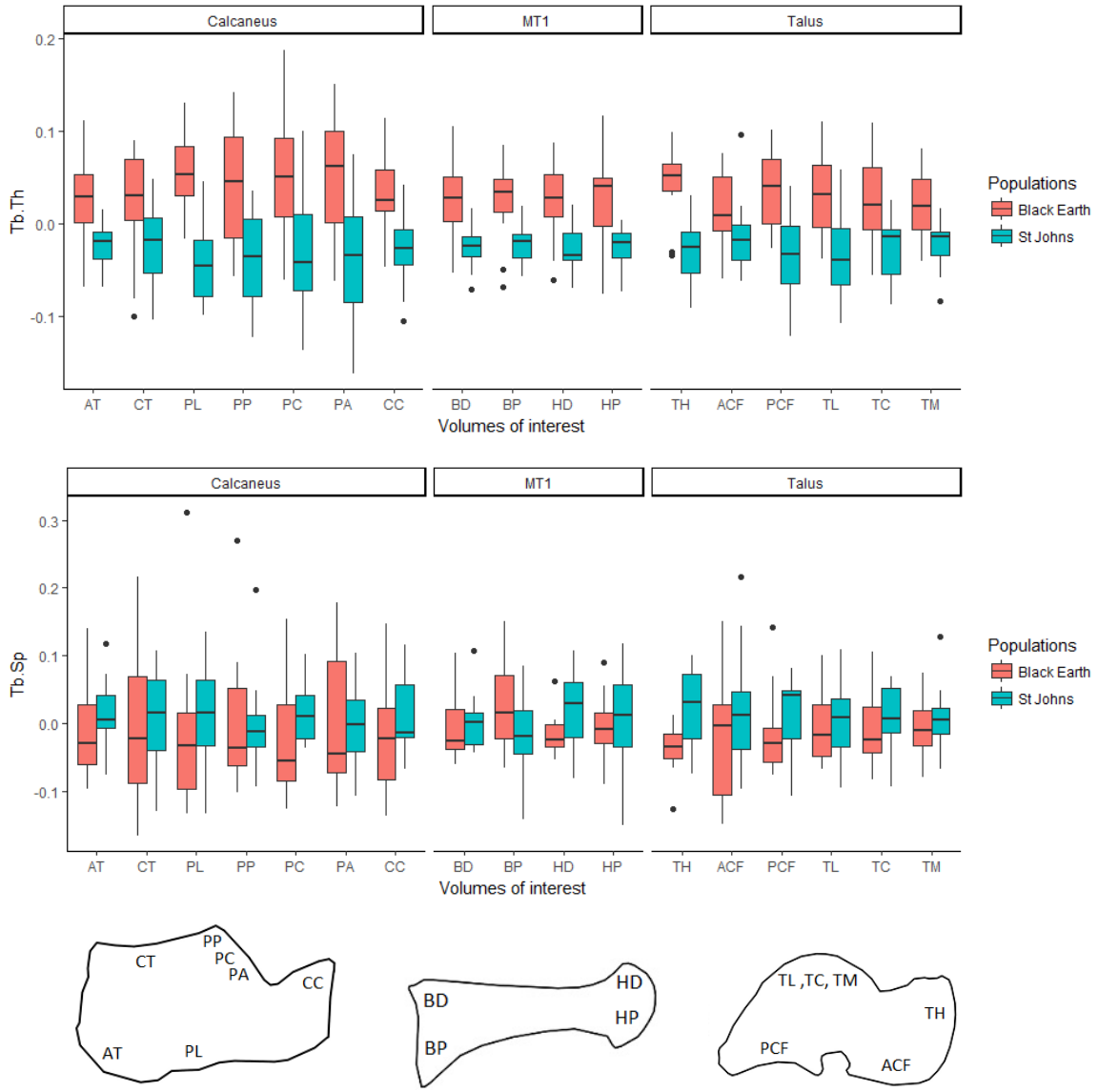

Figure 7.5.1. Boxplots of residuals from multiple regressions between trabecular properties and body mass and age category for the St. Johns and Black Earth populations. Achilles tendon (AT), calcaneal tuber (CT), plantar ligaments (PL), posterior talar facet (PP: posterior, PC: central, PA: anterior), calcaneocuboid (CC), dorsal base (BD), plantar base (BP), dorsal head (HD), plantar head (HP), talar head (TH), anterior calcaneal facet (ACF), posterior calcaneal facet (PCF), trochlea (lateral: TL, central: TC, medial: TM).

After controlling for the effects of body mass and age the Black Earth have significantly greater residual BV/TV and Tb.Th and significantly lower Conn.D compared to the St. Johns. Few significant differences are found between both populations in Tb.Sp. The Black Earth had significantly more anisotropic structures in the talar trochlea, the first metatarsal base, and in the posterior talar facet of the calcaneus. However, the St. Johns had more anisotropic trabeculae in the Achilles tendon and plantar ligaments (i.e. both calcaneal tensile VOIs). Interestingly, the St. Johns have significantly greater anisotropy in tensile VOIs, while the VOIs where Black Earth have greater anisotropy are all largely loaded in compression. However, an explanation for this observation is not obvious.

After correcting for the effects of age and body mass on trabecular properties in the Black Earth and St. Johns, the mobile Black Earth still show more robust trabecular structures consisting of high

BV/TV and Tb.Th, and low Tb.Sp and Conn.D. Correcting for the effects of age and body mass increased the number of significant differences between the two populations. This may indicate that removing the confounding factors of age and body mass enhances variation resulting from behaviour. However, these differences may also result from the fact that the residuals for this test were generated from regressions using only two populations rather than the four populations used to generate the residuals used in the rest of this thesis. To test this the analysis was run using residuals from regressions between body mass and trabecular properties without adding age to the regression. Results show exactly similar patterns of significant differences between the Black Earth and St. Johns both with and without controlling for the effects of age. Inspection of the multiple regression statistics shows that age category is often not a significant factor in the model. Similarly, adding sex into the multiple regression has no noticeable effects. Thus, age and sex do not have a significant effect in this analysis. This finding provides greater confidence in the results obtained from the analyses in this current chapter in which age could not be controlled for. However, it is recommended that future studies be carefully designed to be able to account for potential effects of age, sex, and body mass before behaviour is inferred.

Table 7.5.1. Test statistics for Welch's two sample t-test of residuals of trabecular properties between Black Earth and St. Johns. Significant results are in bold. Red indicates Black Earth has a significantly higher mean and blue indicates St. Johns has a significantly higher mean. Achilles tendon (AT), calcaneal tuber (CT), plantar ligaments (PL), posterior talar facet (PP: posterior, PC: central, PA: anterior), calcaneocuboid (CC), dorsal base (BD), plantar base (BP), dorsal head (HD), plantar head (HP), talar head (TH), anterior calcaneal facet (ACF), posterior calcaneal facet (PCF), trochlea (lateral: TL, central: TC, medial: TM).

variable	stats	AT	CT	PL	PP	PC	PA	CC	BD	BP	HD	HP	TH	ACF	PCF	TL	TC	TM
BV/TV	t	1.89	2.20	2.65	2.69	2.69	2.27	2.92	2.76	1.68	5.96	2.92	6.43	2.48	3.97	3.50	2.00	2.40
	df	22.55	27.06	23.08	25.28	21.51	21.17	18.22	25.29	20.67	29.71	25.57	24.34	19.83	21.08	27.30	21.08	26.92
	p	0.07	**0.04**	**0.01**	**0.01**	**0.01**	**0.03**	**0.01**	**0.01**	0.11	**0.00**	**0.01**	**0.00**	**0.02**	**0.00**	**0.00**	0.06	**0.02**
DA	t	-3.28	1.55	-2.52	4.09	3.61	0.48	1.78	4.55	3.47	1.08	-0.65	0.18	0.39	1.47	2.02	3.92	2.14
	df	25.53	26.93	22.82	24.25	25.79	27.50	25.57	26.45	25.27	22.11	25.12	23.82	26.32	23.93	26.41	25.60	27.97
	p	**0.00**	0.13	**0.02**	**0.00**	**0.00**	0.63	0.09	**0.00**	**0.00**	0.29	0.52	0.86	0.70	0.15	0.05	**0.00**	**0.04**
log10 Conn.D	t	1.05	-1.06	-0.79	-6.85	-4.57	-2.96	-3.17	-6.04	-3.61	-1.41	-1.62	-2.22	-1.11	-3.49	-4.50	-3.99	-4.14
	df	27.03	28.35	24.01	29.38	25.99	27.92	26.00	27.30	22.99	29.81	26.64	22.12	27.00	22.56	27.03	24.85	27.63
	p	0.30	0.30	0.44	**0.00**	**0.00**	**0.01**	**0.00**	**0.00**	**0.00**	0.17	0.12	**0.04**	0.27	**0.00**	**0.00**	**0.00**	**0.00**
Tb.Th	t	3.25	2.46	5.01	3.97	2.88	3.41	3.72	4.71	4.07	5.54	4.27	4.57	2.83	4.00	4.29	3.36	3.55
	df	21.21	28.11	22.49	25.84	23.88	25.28	21.25	20.17	15.86	21.71	16.27	19.73	24.04	23.96	27.89	26.30	25.57
	p	**0.00**	**0.02**	**0.00**	**0.00**	**0.01**	**0.00**	**0.00**	**0.00**	**0.00**	**0.00**	**0.00**	**0.00**	**0.01**	**0.00**	**0.00**	**0.00**	**0.00**
Tb.Sp	t	-0.88	-0.95	-0.80	0.37	-0.92	0.14	-0.90	-0.75	1.33	-3.53	-0.94	-3.69	-1.34	-1.12	-0.30	-0.74	-0.53
	df	27.95	27.19	18.93	22.50	21.38	21.12	20.52	25.38	25.55	23.32	23.19	24.87	25.53	22.21	26.97	25.85	27.00
	p	0.39	0.35	0.44	0.72	0.37	0.89	0.38	0.46	0.19	**0.00**	0.36	**0.00**	0.19	0.27	0.77	0.46	0.60

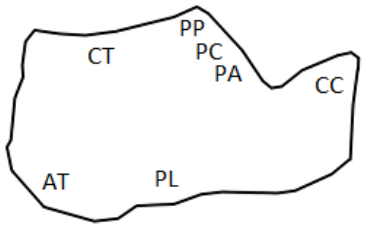

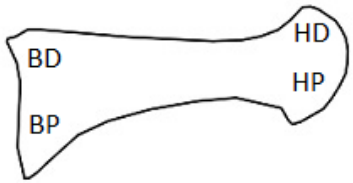

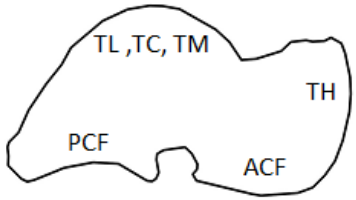

Appendix 8.

Appendix 8.1 Spearman correlations

Table 8.1.1. Pairwise Spearman correlations. Significant positive correlations are in green, significant negative correlations are in red. Calcaneocuboid (CC), plantar ligaments (PL), and posterior talar facet (PTF).

Pairwise Spearman's rho - CC

		Age	Body mass	BV/TV	Tb.Th	Tb.Sp	DA	Conn.D
Age	ρ		.965	.493	.934	.507		-.596
	p		.000	.014	.000	.012		.002
	N		19	24	24	24		24
BM	ρ	.965		.854	.881	.104		-.168
	p	.000		.000	.000	.673		.491
	N	19		19	19	19	19	19
BV/TV	ρ	.493	.854		.566	-.171	-.331	-.002
	p	.014	.000		.003	.405	.099	.993
	N	24	19		26	26	26	26
Tb.Th	ρ	.934	.881	.566		.585	.130	-.685
	p	.000	.000	.003		.002	.526	.000
	N	24	19	26		26	26	26
Tb.Sp	ρ	.507	.104	-.171	.585		.404	-.807
	p	.012	.673	.405	.002		.041	.000
	N	24	19	26	26		26	26
DA	ρ			-.331	.130	.404		-.338
	p			.099	.526	.041		.092
	N			26	26	26		26
Conn.D	ρ	-.596	-.168	-.002	-.685	-.807	-.338	
	p	.002	.491	.993	.000	.000	.092	
	N	24	19	26	26	26	26	

Pairwise Spearman's rho - PL

		Age	Body mass	BV/TV	Tb.Th	Tb.Sp	DA	Conn.D
Age	ρ		.965	.579	.919	.814	.697	-.867
	p		.000	.003	.000	.000	.000	.000
	N		19	24	24	24	24	24
BM	ρ	.965		.709	.868	.796	.360	-.830
	p	.000		.001	.000	.000	.130	.000
	N	19		19	19	19	19	19
BV/TV	ρ	.579	.709		.706	.357	.590	-.441
	p	.003	.001		.000	.074	.002	.024
	N	24	19		26	26	26	26
Tb.Th	ρ	.919	.868	.706		.811	.611	-.861
	p	.000	.000	.000		.000	.001	.000
	N	24	19	26		26	26	26
Tb.Sp	ρ	.814	.796	.357	.811		.350	-.907
	p	.000	.000	.074	.000		.080	.000
	N	24	19	26	26		26	26

DA	ρ	.697	.360	.590	.611	.350		-.374
	p	.000	.130	.002	.001	.080		.060
	N	24	19	26	26	26		26
Conn.D	ρ	-.867	-.830	-.441	-.861	-.907	-.374	
	p	.000	.000	.024	.000	.000	.060	
	N	24	19	26	26	26	26	

Pairwise Spearman's rho - PTF

		Age	Body mass	BV/TV	Tb.Th	Tb.Sp	DA	Conn.D
Age	ρ		.965	.582	.914	.709		-.854
	p		.000	.003	.000	.000		.000
	N		19	24	24	24		24
BM	ρ	.965		.698	.821	.518		-.677
	p	.000		.001	.000	.023		.001
	N	19		19	19	19		19
BV/TV	ρ	.582	.698		.741	.122	-.475	-.335
	p	.003	.001		.000	.551	.014	.094
	N	24	19		26	26	26	26
Tb.Th	ρ	.914	.821	.741		.638	-.143	-.831
	p	.000	.000	.000		.000	.485	.000
	N	24	19	26		26	26	26
Tb.Sp	ρ	.709	.518	.122	.638		.054	-.880
	p	.000	.023	.551	.000		.793	.000
	N	24	19	26	26		26	26
DA	ρ			-.475	-.143	.054		-.145
	p			.014	.485	.793		.481
	N			26	26	26		26
Conn.D	ρ	-.854	-.677	-.335	-.831	-.880	-.145	
	p	.000	.001	.094	.000	.000	.481	
	N	24	19	26	26	26	26	

Table 8.1.2. Listwise Spearman correlations. Significant positive correlations are in green, significant negative correlations are in red. N=19 for all correlations. Calcaneocuboid (CC), plantar ligaments (PL), and posterior talar facet (PTF).

Listwise Spearman's rho - CC

		Age	Body mass	BV/TV	Tb.Th	Tb.Sp	DA	Conn.D
Age	ρ		.965	.870	.891	.085		-.184
	p		.000	.000	.000	.731		.451
BM	ρ	.965		.854	.881	.104		-.168
	p	.000		.000	.000	.673		.491
BV/TV	ρ	.870	.854		.830	-.230	-.312	.054
	p	.000	.000		.000	.343	.194	.825
Tb.Th	ρ	.891	.881	.830		.231	-.346	-.379
	p	.000	.000	.000		.340	.147	.109
Tb.Sp	ρ	.085	.104	-.230	.231		.167	-.665
	p	.731	.673	.343	.340		.493	.002
DA	ρ			-.312	-.346	.167		.024
	p			.194	.147	.493		.923
Conn.D	ρ	-.184	-.168	.054	-.379	-.665	.024	
	p	.451	.491	.825	.109	.002	.923	

Listwise Spearman's rho - PL

Variable		Age	Body mass	BV/TV	Tb.Th	Tb.Sp	DA	Conn.D
Age	ρ		.965	.754	.891	.722	.487	-.828
	p		.000	.000	.000	.000	.034	.000
BM	ρ	.965		.709	.868	.796	.360	-.830
	p	.000		.001	.000	.000	.130	.000
BV/TV	ρ	.754	.709		.857	.433	.672	-.607
	p	.000	.001		.000	.064	.002	.006
Tb.Th	ρ	.891	.868	.857		.711	.577	-.801
	p	.000	.000	.000		.001	.010	.000
Tb.Sp	ρ	.722	.796	.433	.711		.168	-.842
	p	.000	.000	.064	.001		.491	.000
DA	ρ	.487	.360	.672	.577	.168		-.277
	p	.034	.130	.002	.010	.491		.251
Conn.D	ρ	-.828	-.830	-.607	-.801	-.842	-.277	
	p	.000	.000	.006	.000	.000	.251	

Listwise Spearman's rho - PTF

		Age	Body mass	BV/TV	Tb.Th	Tb.Sp	DA	Conn.D
Age	ρ		.965	.719	.872	.524		-.710
	p		.000	.001	.000	.021		.001
BM	ρ	.965		.698	.821	.518		-.677
	p	.000		.001	.000	.023		.001
BV/TV	ρ	.719	.698		.853	.077	-.811	-.274
	p	.001	.001		.000	.753	.000	.257
Tb.Th	ρ	.872	.821	.853		.482	-.693	-.694
	p	.000	.000	.000		.037	.001	.001
Tb.Sp	ρ	.524	.518	.077	.482		-.256	-.857

	p	.021	.023	.753	.037		.290	.000
DA	ρ			-.811	-.693	-.256		.225
	p			.000	.001	.290		.355
Conn.D	ρ	-.710	-.677	-.274	-.694	-.857	.225	
	p	.001	.001	.257	.001	.000	.355	

Appendix 8.2 Scatterplots of trabecular properties

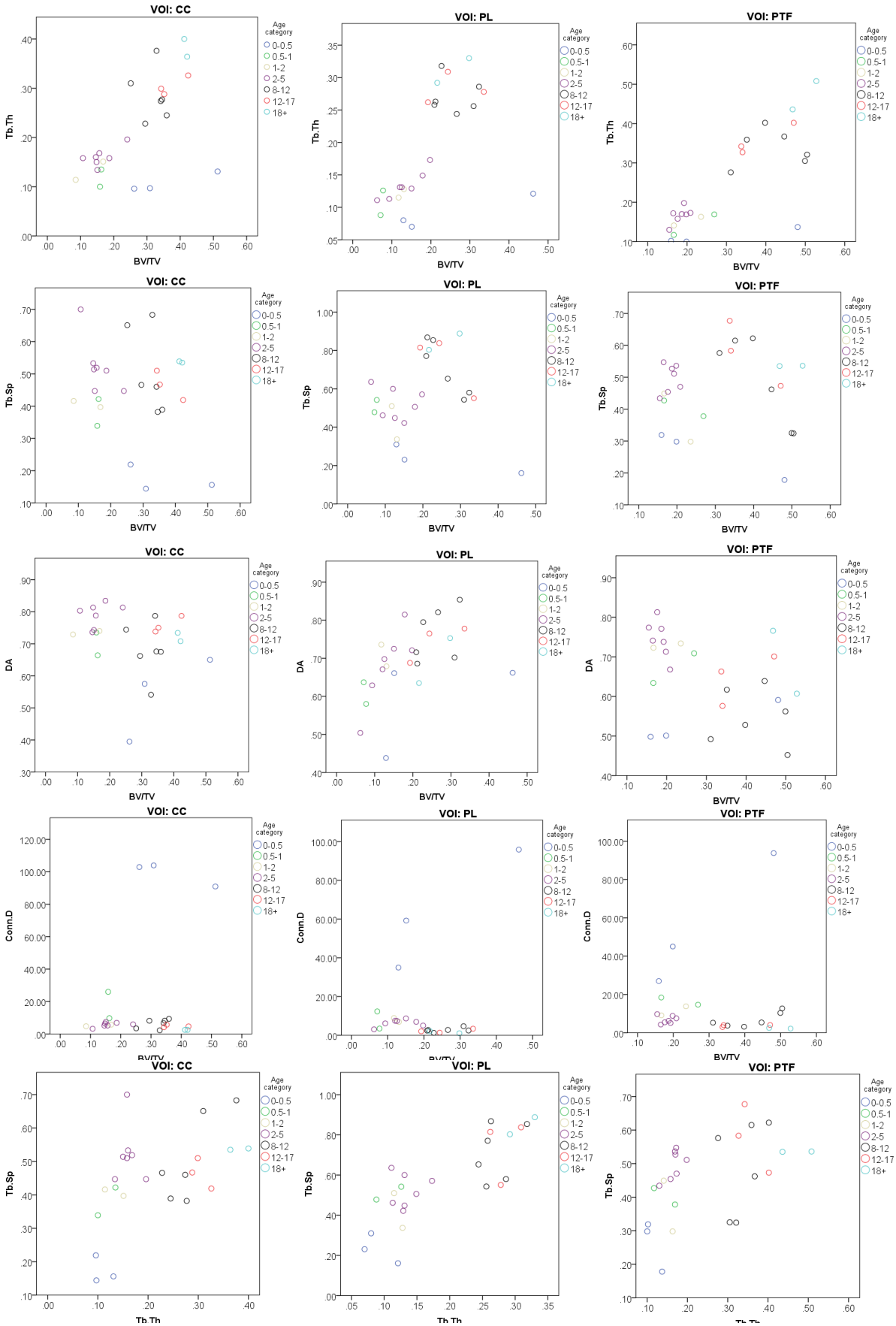

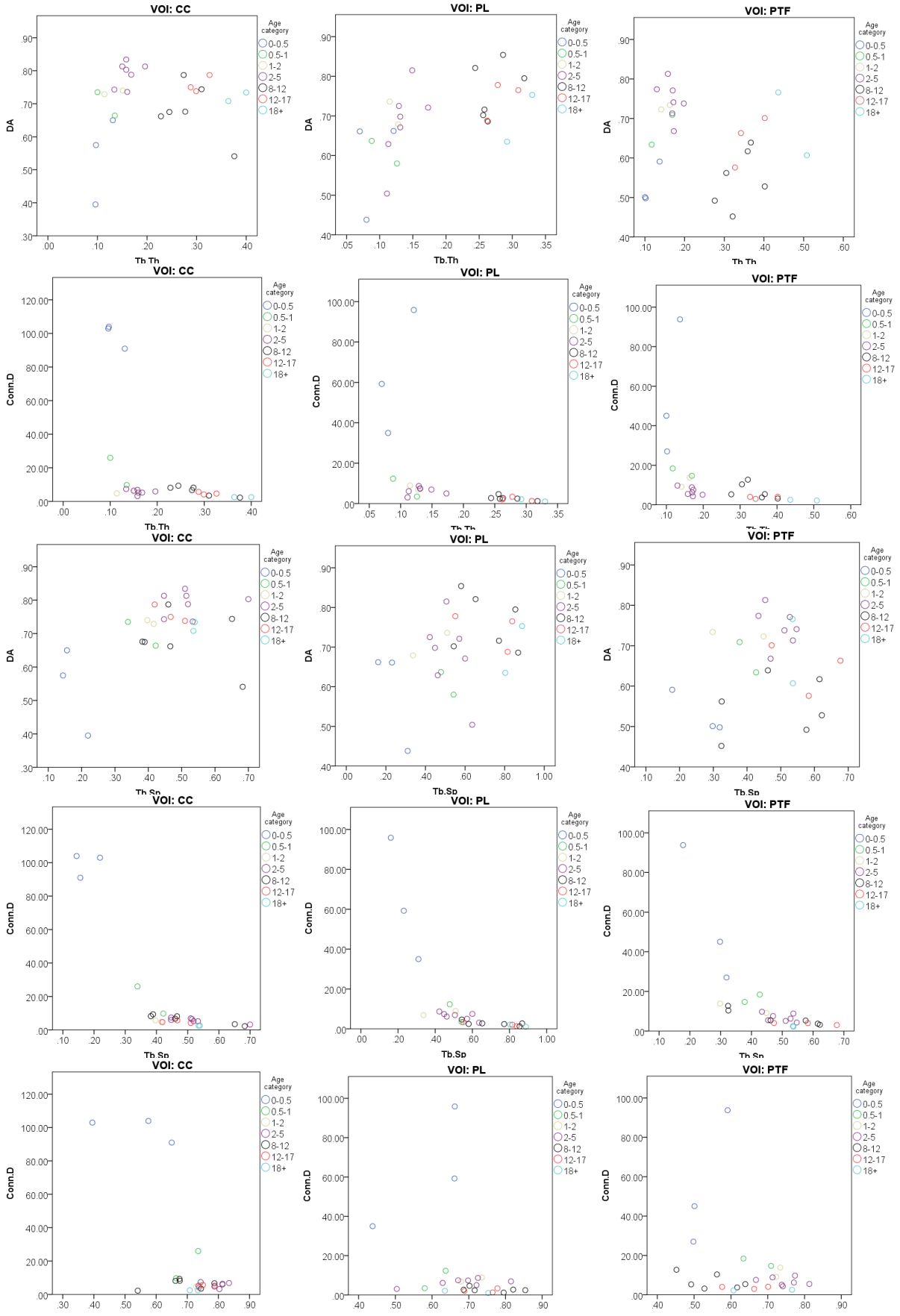

Figure 8.2.1. Scatterplots of trabecular properties in calcaneocuboid (CC), plantar ligaments (PL), and posterior talar facet (PTF) VOIs.

Appendix 8.3 Trabecular structure in the Norris Farms sample

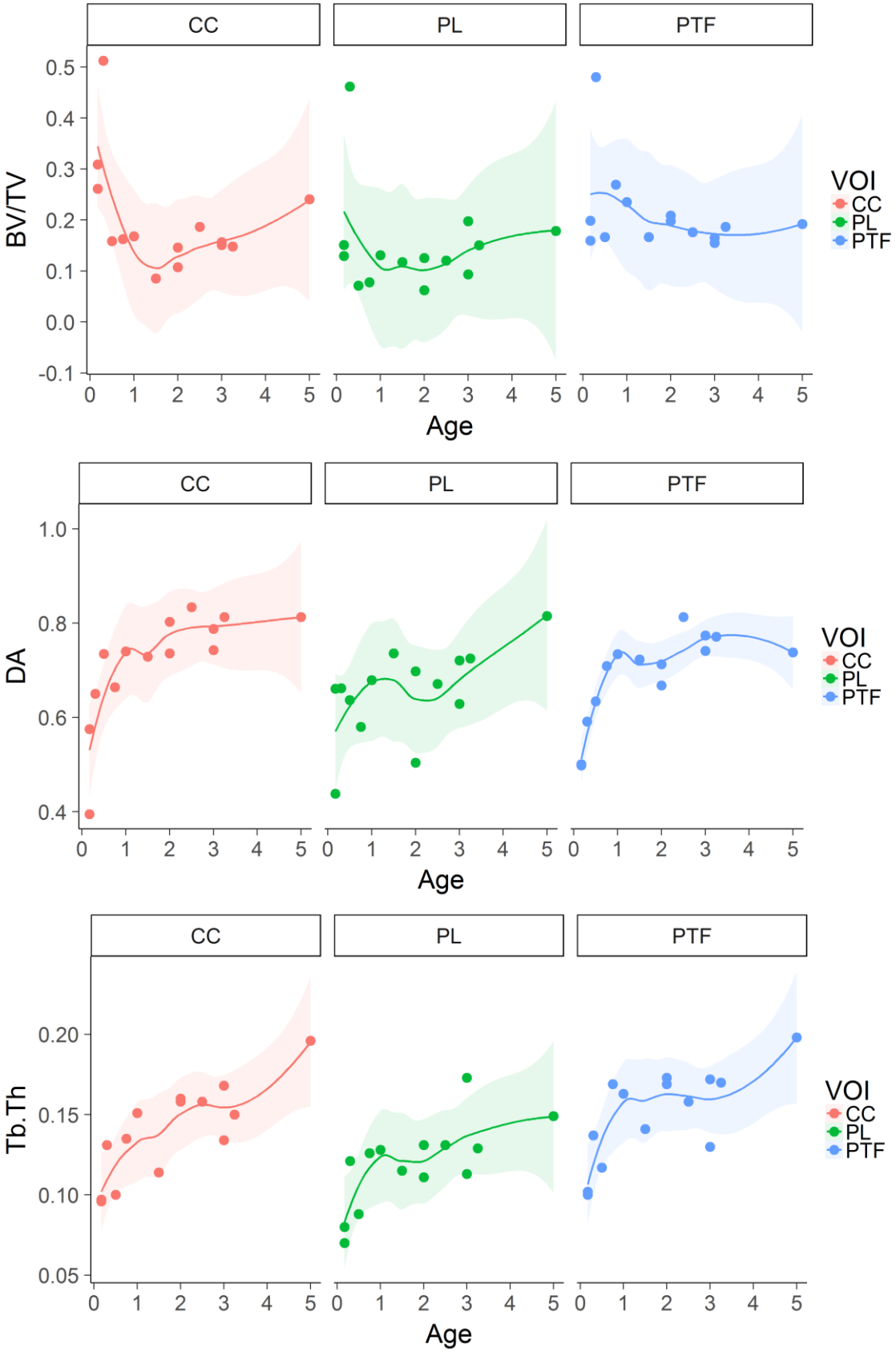

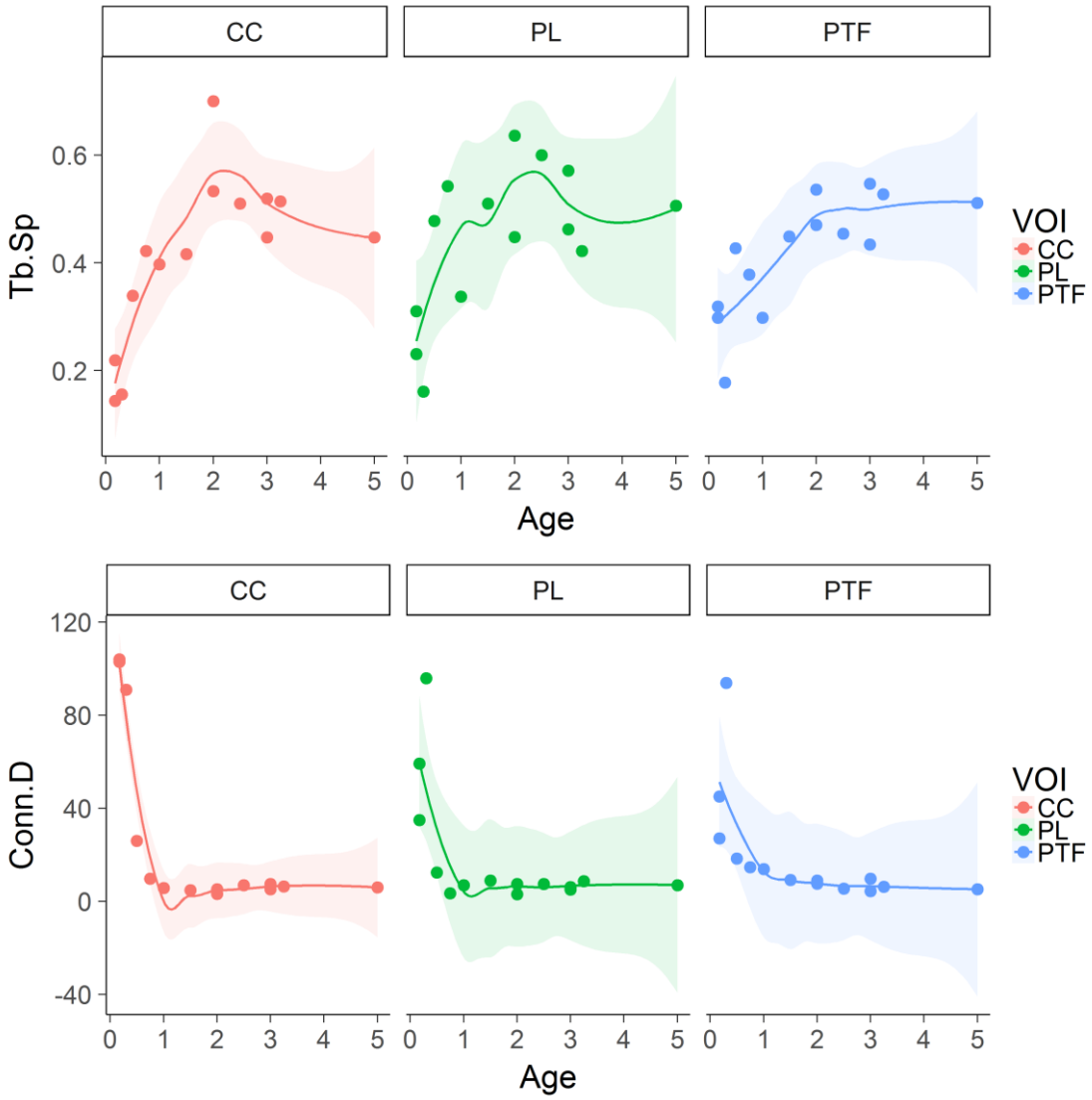

Figure 8.3.1. Trabecular bone properties plotted against age in the Norris Farms population. CC=calcaneocuboid, PL=plantar ligaments, PTF=posterior talar facet, n=14.

Appendix 8.4 Trabecular structure in the St. Johns sample

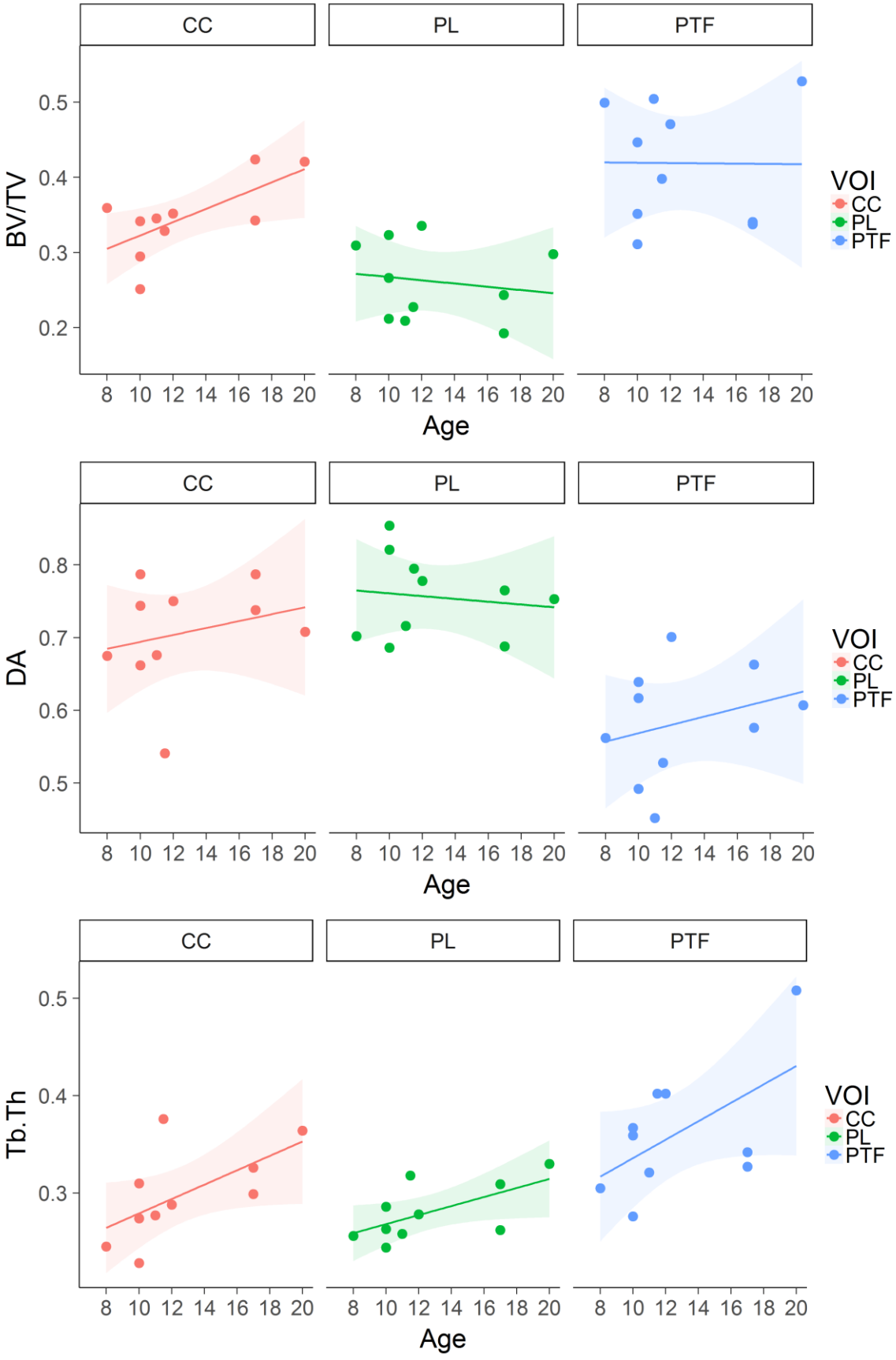

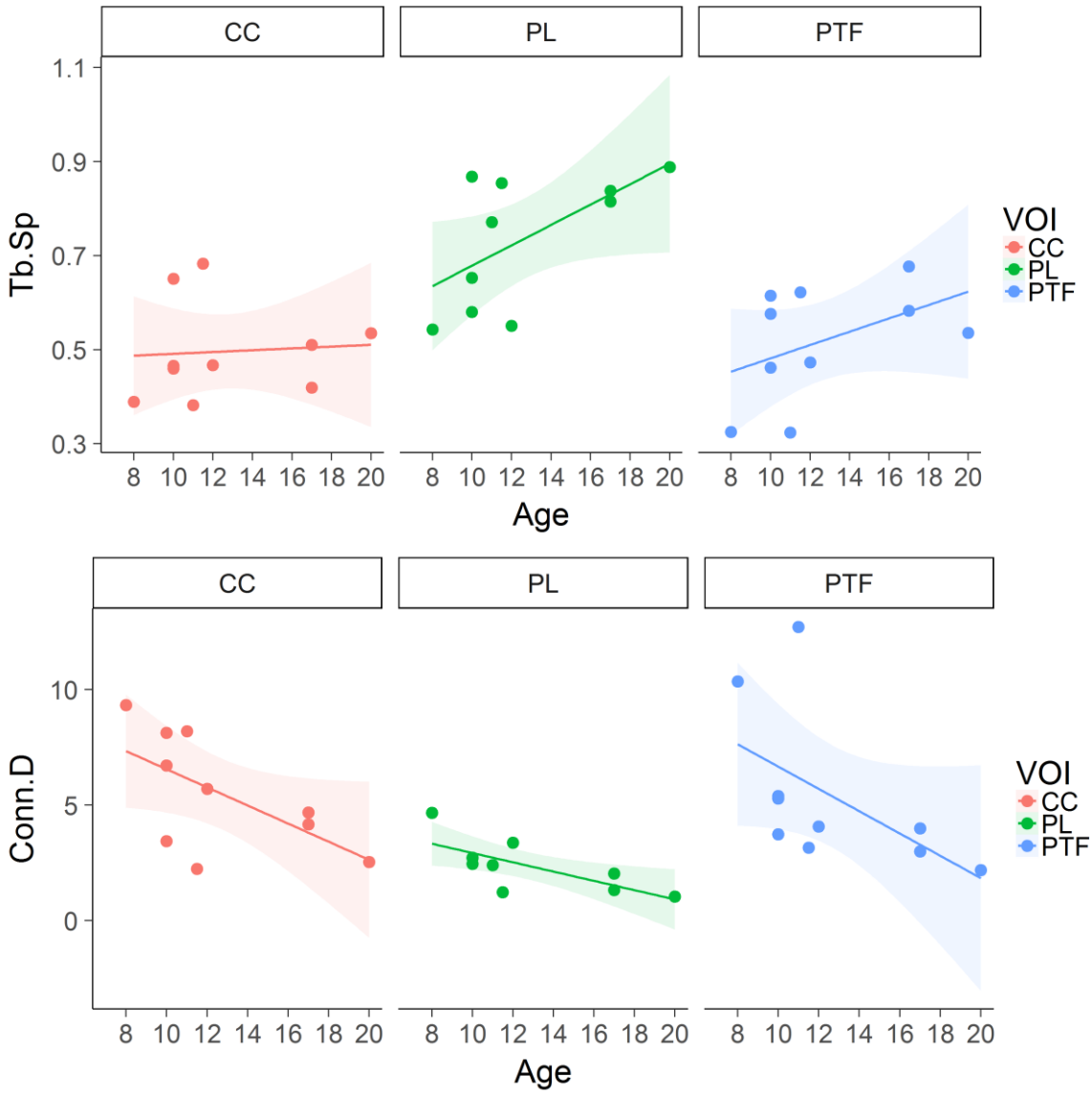

Figure 8.4.1. Trabecular bone properties plotted against age in the St. Johns population. CC=calcaneocuboid, PL=plantar ligaments, PTF=posterior talar facet, n=10.

Table 8.4.1. Regressions between age and trabecular properties in the St. Johns population. P values below .05 are accepted as significant and are presented in bold, n=10 for each VOI.

Variable	VOI	intercept	slope	R^2	t	*p*
BV/TV	CC	.234	.009	.456	2.588	**.032**
	PL	.289	-.002	.027	-.468	.653
	PTF	.421	.000	.000	-.027	.979
Tb.Th	CC	.205	.007	.375	2.193	.060
	PL	.222	.005	.384	2.236	.056
	PTF	.241	.009	.324	1.959	.086
Tb.Sp	CC	.472	.002	.005	.209	.840
	PL	.462	.022	.373	2.181	.061
	PTF	.340	.014	.210	1.456	.183
DA	CC	.647	.005	.065	.746	.477
	PL	.780	-.002	.017	-.374	.718
	PTF	.511	.006	.084	.859	.416
Conn.D	CC	10.475	-.392	.378	-2.207	.058
	PL	4.942	-.201	.519	-2.936	**.019**
	PTF	11.494	-.482	.306	-1.880	.097

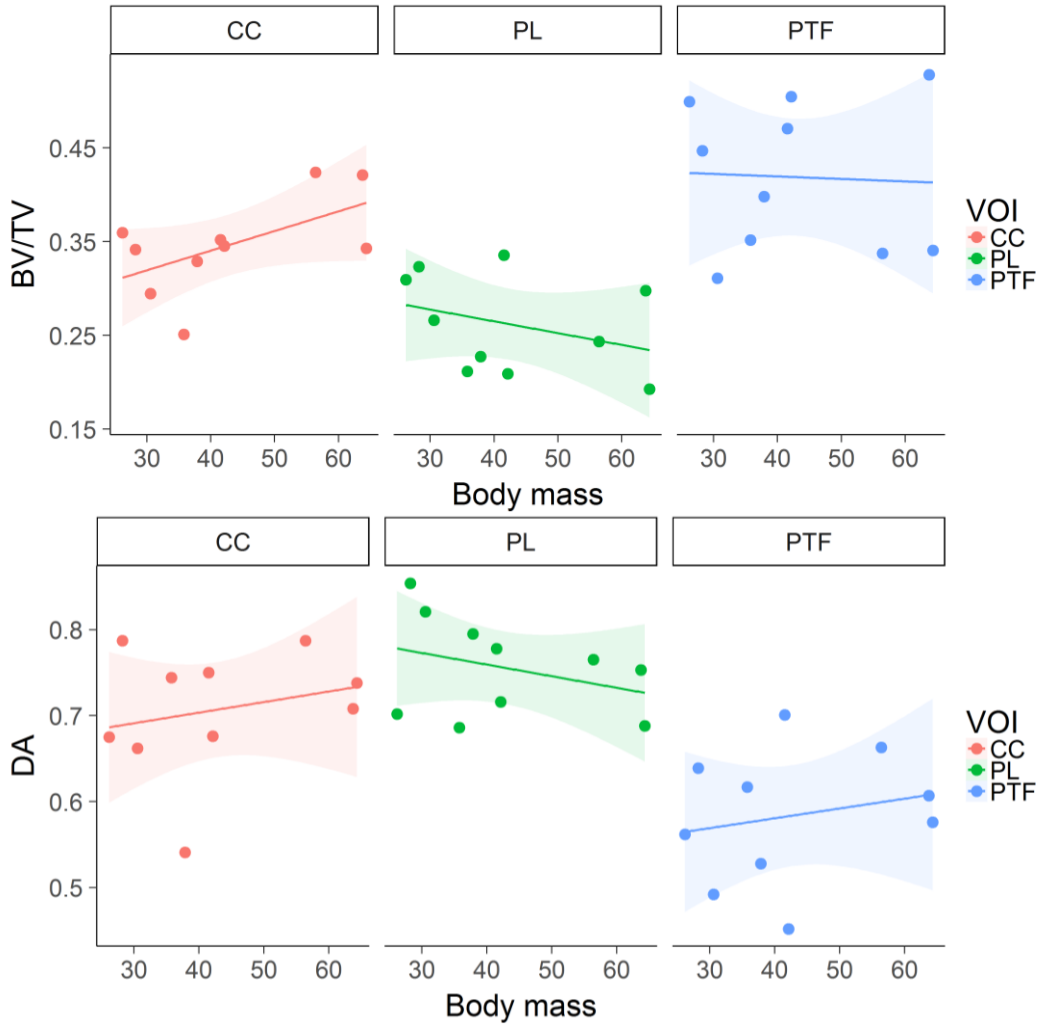

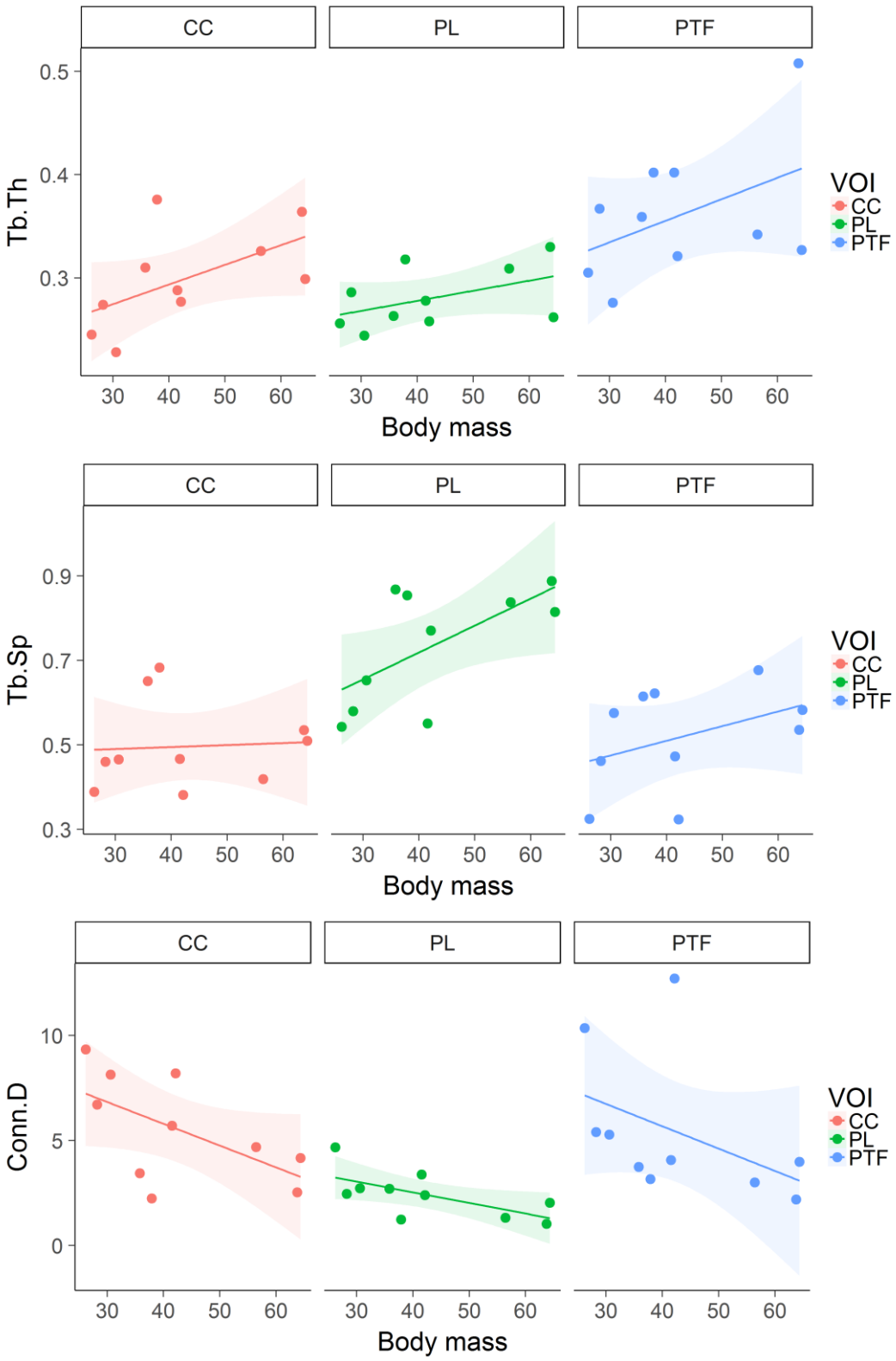

Figure 8.4.2. Trabecular bone properties plotted against body mass in the St. Johns population. CC=calcaneocuboid, PL=plantar ligaments, PTF=posterior talar facet, n=10.

Table 8.4.2. Regressions between body mass and trabecular properties in the St. Johns population. P values below 0.05 are accepted as significant and are presented in bold, n=10 for each VOI.

Variable	VOI	intercept	slope	R^2	t	*p*
BV/TV	CC	.257	.002	.331	1.990	.082
	PL	.315	-.001	.117	-1.028	.334
	PTF	.430	.000	.002	-.132	.898
Tb.Th	CC	.217	.002	.324	1.957	.086
	PL	.239	.001	.220	1.500	.172
	PTF	.272	.002	.203	1.430	.191
Tb.Sp	CC	.476	.000	.004	.184	.859
	PL	.464	.006	.418	2.396	**.043**
	PTF	.371	.003	.163	1.247	.248
DA	CC	.654	.001	.056	.690	.510
	PL	.814	-.001	.110	-.993	.350
	PTF	.535	.001	.043	.602	.564
Conn.D	CC	9.947	-.104	.344	-2.046	.075
	PL	4.560	-.051	.426	-2.437	**.041**
	PTF	9.931	-.106	.193	-1.382	.204